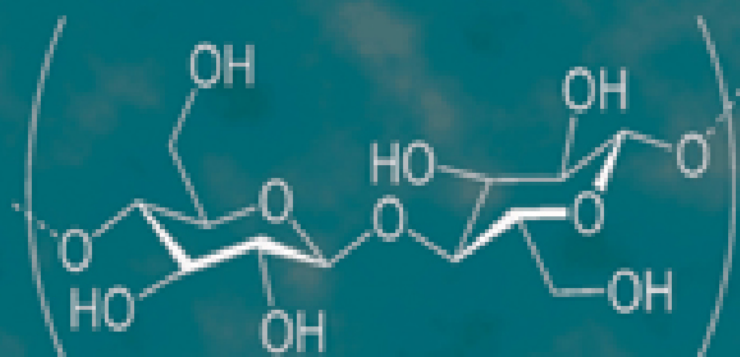


VOL
1

Handbook of Composites from Renewable Materials

STRUCTURE AND CHEMISTRY



Edited by **VIJAY KUMAR THAKUR**,
MANJU KUMARI THAKUR and **MICHAEL R. KESSLER**

 **Scrivener
Publishing**

WILEY

Handbook of Composites from Renewable Materials

Scrivener Publishing
100 Cummings Center, Suite 541J
Beverly, MA 01915-6106
www.scrivenerpublishing.com

Publishers at Scrivener
Martin Scrivener (martin@scrivenerpublishing.com)
Phillip Carmical (pcarmical@scrivenerpublishing.com)

Handbook of Composites from Renewable Materials

Edited by Vijay Kumar Thakur, Manju Kumari Thakur and Michael R. Kessler

Volume 1: Structure and Chemistry

ISBN: 978-1-119-22362-7

Volume 2: Design and Manufacturing

ISBN: 978-1-119-22365-8

Volume 3: Physico-Chemical and Mechanical Characterization

ISBN: 978-1-119-22366-5

Volume 4: Functionalization

ISBN: 978-1-119-22367-2

Volume 5: Biodegradable Materials

ISBN: 978-1-119-22379-5

Volume 6: Polymeric Composites

ISBN: 978-1-119-22380-1

Volume 7: Nanocomposites: Science and Fundamentals

ISBN: 978-1-119-22381-8

Volume 8: Nanocomposites: Advanced Applications

ISBN: 978-1-119-22383-2

8-volume set

ISBN 978-1-119-22436-5

Handbook of Composites from Renewable Materials

**Volume 1
Structure and Chemistry**

Edited by

**Vijay Kumar Thakur, Manju Kumari Thakur
and Michael R. Kessler**



WILEY

This edition first published 2017 by John Wiley & Sons, Inc., 111 River Street, Hoboken, NJ 07030, USA and Scrivener Publishing LLC, 100 Cummings Center, Suite 541J, Beverly, MA 01915, USA

© 2017 Scrivener Publishing LLC

For more information about Scrivener publications please visit www.scrivenerpublishing.com.

All rights reserved. No part of this publication may be reproduced, stored in a retrieval system, or transmitted, in any form or by any means, electronic, mechanical, photocopying, recording, or otherwise, except as permitted by law. Advice on how to obtain permission to reuse material from this title is available at <http://www.wiley.com/go/permissions>.

Wiley Global Headquarters

111 River Street, Hoboken, NJ 07030, USA

For details of our global editorial offices, customer services, and more information about Wiley products visit us at www.wiley.com.

Limit of Liability/Disclaimer of Warranty

While the publisher and authors have used their best efforts in preparing this work, they make no representations or warranties with respect to the accuracy or completeness of the contents of this work and specifically disclaim all warranties, including without limitation any implied warranties of merchantability or fitness for a particular purpose. No warranty may be created or extended by sales representatives, written sales materials, or promotional statements for this work. The fact that an organization, website, or product is referred to in this work as a citation and/or potential source of further information does not mean that the publisher and authors endorse the information or services the organization, website, or product may provide or recommendations it may make. This work is sold with the understanding that the publisher is not engaged in rendering professional services. The advice and strategies contained herein may not be suitable for your situation. You should consult with a specialist where appropriate. Neither the publisher nor authors shall be liable for any loss of profit or any other commercial damages, including but not limited to special, incidental, consequential, or other damages. Further, readers should be aware that websites listed in this work may have changed or disappeared between when this work was written and when it is read.

Library of Congress Cataloging-in-Publication Data

ISBN 978-1-119-22362-7

Cover image: Vijay Thakur

Cover design by Russell Richardson

Set in size of 11pt and Minion Pro by Exeter Premedia Services Private Ltd., Chennai, India

Printed in

10 9 8 7 6 5 4 3 2 1

To my parents and teachers who helped me become what I am today.

Vijay Kumar Thakur

Contents

Preface	xix
1 Carbon Fibers from Sustainable Resources	1
<i>Rafael de Avila Delucis, Veronica Maria de Araujo Calado, Jose Roberto Moraes d'Almeida and Sandro Campos Amico</i>	
1.1 Introduction	1
1.2 Lignin and Other Sustainable Resources	3
1.3 Carbon Fibers from Lignin	9
1.4 Carbon Fibers from Other Sustainable Resources	12
1.5 Concluding Remarks	15
References	15
2 Polylactic Acid Composites and Composite Foams Based on Natural Fibers	25
<i>A.A. Pérez-Fonseca, H. Teymoorzadeh, J.R. Robledo-Ortíz, R. González-Nuñez and D. Rodrigue</i>	
2.1 Introduction	25
2.2 PLA-Natural Fibers Composites	27
2.2.1 Morphology	28
2.2.2 Thermal Properties of PLA-Natural Fiber Composites	29
2.2.3 Mechanical Properties	32
2.3 PLA Composite Foams with Natural Fibers	36
2.3.1 Batch Processing	37
2.3.2 Extrusion	42
2.3.3 Injection Molding	46
2.4 Thermal Annealing of PLA Composites	51
2.5 Conclusions	55
References	55
3 Microcrystalline Cellulose and Related Polymer Composites: Synthesis, Characterization and Properties	61
<i>Djalal Trache</i>	
3.1 Introduction	61
3.2 Cellulose: Structure and Sources	63
3.2.1 Structure of Cellulose	63
3.2.2 Sources	64

3.3	Microcrystalline Cellulose	66
3.3.1	Introduction	66
3.3.2	Isolation of MCC	67
3.3.3	Types of MCC	71
3.3.3.1	Powdered MCC	71
3.3.3.2	Colloidal MCC	71
3.4	Characterization and Properties of Microcrystalline Cellulose	72
3.4.1	Chemical Structure	72
3.4.2	Morphology and Particle Size	73
3.4.3	Degree of Polymerization	74
3.4.4	Degree of Crystallinity	75
3.4.5	Thermal Stability	75
3.4.6	Mechanical Properties	77
3.4.7	Surface Chemistry	78
3.5	MCC-Based Composites	78
3.5.1	Classification of Polymer Composite Materials	79
3.5.2	Production and Properties of MCC-based Composites	80
3.6	Application of Composite Materials Based on MCC	83
3.7	Conclusions	84
	Acknowledgments	85
	References	85
4	Tannin-Based Foams: The Innovative Material for Insulation Purposes	93
	<i>Gianluca Tondi and Alexander Petutschnigg</i>	
4.1	First Tannin Foams and their Characterization	93
4.2	Formulation and Process Modifications	96
4.2.1	Hardeners	96
4.2.2	Furfuryl Alcohol	97
4.2.3	Aromatic Backbone	97
4.2.4	Blowing Agent	98
4.2.5	Catalyst	98
4.2.6	Additive for Improving Specific Properties	99
4.2.7	Process Modification	99
4.3	Composite Materials: Tannin-Based Panels	100
4.4	Conclusions	102
	References	102
5	Renewable Feedstock Vanillin-Derived Polymer and Composites: Structure Property Relationship	107
	<i>G. Madhumitha, Selvaraj Mohana Roopan, D. Devi Priya and G. Elango</i>	
5.1	Introduction	107
5.1.1	History of Vanillin	108
5.1.2	Occurrence	109
5.2	Vanillin Production	109
5.2.1	Vanillin Extraction <i>via</i> Natural Route	109
5.2.2	Biosynthesis of Vanillin	109
5.2.3	Chemical Synthesis of Vanillin	110

5.3	Some Common Applications of Vanillin	111
5.3.1	Food Production	111
5.3.2	Vanillin in Beverages	111
5.3.3	Cosmetics and Pharmaceutical Industries	111
5.3.4	Agriculture and Animal Feed	112
5.3.5	Other Industries	112
5.4	Vanillin-Derived Polymers	112
5.4.1	Poly Acetyl Polymers	113
5.4.2	Poly Esters Polymers	113
5.4.3	Polyaldimines	114
5.4.4	Poly Benzoxazines	118
5.4.5	ADMET and Thiol-ene Polymerization (Poly Alkenes)	118
5.4.5.1	ADMET Polymers	118
5.4.6	Epoxy Polymers	119
5.4.7	Tri-Ethyl-Benzyl-Ammonium Chloride (TEBAC)	119
5.5	Vanillin-Based Composites	119
5.6	Applications of Vanillin-Based Polymers and Composites	121
5.7	Conclusion	124
	References	125
6	Biomass-Based Formaldehyde-Free Bio-Resin for Wood Panel Process	129
	<i>Xiaobin Zhao</i>	
6.1	Introduction	129
6.1.1	Wood Composite	129
6.1.2	Biomass-Based Adhesives	130
6.2	Market Analysis of Biomass Based Adhesives	130
6.3	Bio-Based Adhesive Formulations	131
6.3.1	Starch-Based Adhesive	132
6.3.2	Lignin	132
6.3.3	Tannin	133
6.3.4	Soya Protein-Based Wood Adhesives	133
6.3.5	Biomimetic Adhesives	134
6.3.6	Liquefied Woody Biomass	134
6.3.7	Chicken Feather	135
6.3.8	Natural Fiber Modified with Adhesive Functions	135
6.4	Cambond Biomass Based Adhesives	135
6.4.1	Distiller's Dry Grain and Solubles (DDGS) as the Biomass	135
6.4.2	Algal Biomass	136
6.4.2.1	Macroalgae	136
6.4.2.2	Microalgae	136
6.4.3	Formulation of Cambond Biomass-Based Bio-Resin (DIGLUE and ALGLUE)	137
6.4.3.1	Materials and Methods	137
6.4.3.2	Preliminary Particle Board Preparation Method	137
6.4.3.3	Results and Discussion	138
6.5	Bio-composites Based on Cambond Bio-Resin	142
6.6	Final Remarks	145
	References	146

7	Bio-Derived Adhesives and Matrix Polymers for Composites	151
	<i>Mariusz Ł. Mamiński and Renata Toczyłowska-Mamińska</i>	
7.1	Introduction	151
7.2	Glycerol	152
7.3	Tannins	156
7.4	Lignin	159
7.5	Polysaccharides	165
7.5.1	Starch	165
7.5.2	Cellulose	167
7.5.3	Chitosan	169
7.6	Proteins	170
7.7	Oils	175
7.8	Microorganism-produced Biopolymers	177
7.8.1	Polyhydroxyalkonates (PHAs)	177
7.8.2	Poly(lactic Acid)	179
	References	182
8	Silk Biocomposites: Structure and Chemistry	189
	<i>Alexander Morin, Mahdi Pahlevan and Parvez Alam</i>	
8.1	Introduction	189
8.2	Spider Silk Protein	189
8.2.1	Types, Structures and Properties	189
8.2.2	Computational Research	192
8.2.3	Recombinant Spider Silk	194
8.3	<i>Bombyx mori</i> Silk	195
8.3.1	Structures and Chemistry	195
8.3.2	Physical Properties of <i>B. mori</i> Silk	198
8.3.3	Spectroscopy of Silks	200
8.3.4	Silk-Water Interactions	201
8.3.5	Degumming	203
8.4	Silk Biocomposites: Applications	205
8.4.1	Composite Textiles	205
8.4.2	Biomedical Composites and Biomaterials	205
8.4.3	Structural Biocomposites	207
	References	212
9	Isolation and Characterisation of Water Soluble Polysaccharide from <i>Colocasia esculenta</i> Tubers	221
	<i>Harshal Ashok Pawar, Pritam Dinesh Choudhary and Amit Jagannath Gavasane</i>	
9.1	Introduction	221
9.2	Materials and Methods	224
9.2.1	Collection of Plant Material	224
9.2.2	Isolation of Polysaccharide	224
9.2.3	Purification of Polysaccharide	224
9.2.4	Characterization of Polysaccharide	224
9.2.4.1	Organoleptic Evaluation	224
9.2.4.2	Preliminary Phytochemical Evaluation	225

9.2.5	Physicochemical Evaluation	225
9.2.5.1	Solubility	225
9.2.5.2	Powder Flow Characteristics	226
9.2.5.3	pH	227
9.2.5.4	Loss on Drying (LOD)	227
9.2.5.5	Specific Gravity	227
9.2.5.6	Swelling Capacity	227
9.2.5.7	Viscosity	228
9.2.6	Differential Scanning Colorimeter (DSC)	228
9.2.7	X-ray Powder Diffraction (XRD)	229
9.2.8	Estimation of Total Sugar Content	229
9.2.9	Identification of Gum Components by Thin Layer Chromatography	229
9.2.10	Investigation of Structure of the Polysaccharide	230
9.2.11	Rheological Study of <i>C. esculenta</i> Gum	230
9.3	Results and Discussion	230
9.4	Conclusions	238
	Acknowledgements	238
	References	238
10	Bio-Based Fillers for Environmentally Friendly Composites	243
	<i>Thabang H. Mokhothu and Maya J. John</i>	
10.1	Introduction	243
10.2	Bio-Based Fillers/Reinforcements	244
10.2.1	Benefits and Drawbacks of Bio-Based Fillers	244
10.2.2	Surface Modification of Natural Fibers	247
10.2.3	Extraction of Cellulose and/or Cellulose Nanowhiskers from Bio-Fillers	249
10.2.4	Lignin Bio-Fillers	254
10.2.5	Rice Husk Bio-Fillers	255
10.3	Bio-based Fillers Reinforced Biopolymer Composites	255
10.3.1	Natural Fiber Composites	255
10.3.2	Nano-Cellulose/Cellulose Whisker Composites	257
10.3.3	Lignin Composites	259
10.3.4	Rice Husk (RH) Composites	260
10.4	Applications of Bio-Based Composites	261
10.5	Summary	262
	References	264
11	Keratin-Based Materials in Biotechnology	271
	<i>Hafiz M. N. Iqbal and Tajalli Keshavarz</i>	
11.1	Introduction	271
11.2	Biopolymers	273
11.3	Classification of Biopolymers	273
11.4	Occurrence and Physicochemical Properties of Keratin	274
11.5	Keratin-based Biomaterials	276
11.6	Bio-composites	276

11.7	Properties of Bio-composites for Bio-medical Applications	278
11.7.1	Biocompatibility	278
11.7.2	Biodegradability	279
11.8	Biomedical and Biotechnological Applications	280
11.9	Potential Applications	281
11.9.1	Wound Healing	281
11.9.2	Tissue Engineering	281
11.9.3	Biosensors	282
11.10	Concluding Remarks	284
	References	284
12	Pineapple Leaf Fiber: A High Potential Reinforcement for Green Rubber and Plastic Composites	289
	<i>Taweechai Amornsakchai</i>	
12.1	Introduction	289
12.2	Structure of Pineapple Leaf and Pineapple Leaf Fiber	292
12.3	Conventional Methods of Fiber Extraction	293
12.3.1	Hand Scraping	293
12.3.2	Water Retting	293
12.3.3	Machine Decortication	293
12.4	The Novel Mechanical Grinding Method	293
12.4.1	Process Description	294
12.4.2	Characteristic of PALF and By-product	295
12.4.3	Advantages and Disadvantages of the Process	296
12.5	Potential Applications of PALF as Reinforcement for Polymer Matrix Composites	298
12.5.1	A Concept for Better Utilization of PALF in Composites	298
12.5.2	Rubber Reinforcement	298
12.5.3	Plastic Reinforcement	301
12.5.4	Other Types of Reinforcement	303
12.6	Concluding Remarks	304
	Acknowledgements	305
	References	305
13	Insights into the Structure of Proteins Adsorbed onto Bioactive Glasses	309
	<i>Klára Magyari, Adriana Vulpoi and Lucian Baia</i>	
13.1	Introduction	309
13.2	Bioactive Glasses as Renewable Materials	310
13.3	Proteins Structure	313
13.3.1	The Most Used Proteins in Testing the <i>In vitro</i> Interactions with Bioactive Glasses	315
13.4	Suitable Methods for Proteins Investigation	315
13.4.1	FTIR Spectroscopy on Proteins	315
13.4.1.1	FTIR Imaging Spectroscopy	315
13.4.1.2	FTIR Spectra of Proteins	317
13.4.1.3	Secondary Structure of Proteins Obtained by FTIR Spectra	318

13.4.2	Scanning Electron Microscopy (SEM) Coupled with Electron Energy Dispersive X-ray (EDX) Spectroscopy of Proteins	319
13.5	Interaction of Protein with Bioactive Glasses	320
13.5.1	Protein Adsorption onto Bioactive Glass Surfaces in Terms of Biocompatibility	321
13.5.2	Relation Between the Attached Proteins on Glass Surface and Bioactivity	325
13.5.3	Secondary Structure of Proteins Obtained from FT-IR Spectra	327
13.6	Summary	330
	Acknowledgements	331
	References	331
14	Effect of Filler Properties on the Antioxidant Response of Thermoplastic Starch Composites	337
	<i>Tomy J. Gutiérrez, Paula González Seligra, Carolina Medina Jaramillo, Lucía Famá and Silvia Goyanes</i>	
14.1	Introduction	337
14.2	Starch-Based Nanocomposites	338
14.2.1	Starch-Based Nanocomposites with Natural Antioxidant	339
14.2.2	Starch-Based Nanocomposites with Bactericidal Fillers	342
14.2.2.1	Starch/Zinc Oxide Nanocomposites	343
14.2.2.2	Starch/Titanium Oxide Nanocomposites	346
14.2.2.3	Starch/Silver Nanocomposites	349
14.2.3	Starch-based Nanocomposites with Natural Filler and Bactericidal Fillers	352
14.3	Regulatory Aspect	355
14.4	Conclusions and Outlook	357
	Acknowledgements	358
	References	358
15	Preparation and Application of the Composite from Chitosan	371
	<i>Chen Yu</i>	
15.1	Introduction	371
15.2	Composites from Chitosan and Natural Polymers	372
15.2.1	Composites from Chitosan and Collagen	372
15.2.2	Composites from Chitosan and Gelatin	374
15.2.3	Composites from Chitosan and Chondroitin Sulfate	374
15.2.4	Composites from Chitosan and Hyaluronic Acid	376
15.2.5	Composites from Chitosan and Heparin	378
15.2.6	Composites from Chitosan and Glucomannan	378
15.3	Composites from Chitosan and Synthetic Polymers	380
15.3.1	Composites from Chitosan and Polyurethanes	380
15.3.2	Composites from Chitosan and Poly (Lactic Acid)	383
15.3.3	Composites from Chitosan and Polyvinyl Alcohol	384
15.3.4	Composites from Chitosan and Poly(γ -Glutamic Acid)	386

15.4	Composites from Chitosan and Biomacromolecules	388
15.4.1	Composites from Chitosan and DNA or SiRNA	388
15.4.2	Composites from Chitosan and Peptides	391
15.4.3	Composites from Chitosan and Liposomes	393
15.5	Composites from Chitosan and Inorganic Components	394
15.5.1	Composites from Chitosan and Hydroxyapatite	395
15.5.2	Composites from Chitosan and Calcium Carbonate	396
15.5.3	Composites from Chitosan and Silicon Dioxide	397
15.5.4	Composites from Chitosan and Bioactive Glasses	398
15.5.5	Composites from Chitosan and Fe_3O_4	400
15.5.6	Composites from Chitosan and Gold Nanoparticles	404
15.5.7	Composites from Chitosan and Silver Nanoparticles	407
15.6	Composites from Chitosan and Carbon Materials	409
15.6.1	Composites from Chitosan and Activated Carbon	409
15.6.2	Composites from Chitosan and Carbon Nanotubes	410
15.6.3	Composites from Chitosan and Graphene	417
	Acknowledgments	420
	References	420
16	Overview on Synthesis of Magnetic Bio Char from Discarded Agricultural Biomass	435
	<i>Manoj Tripathi, N.M. Mubarak, J.N. Sahu and P.Ganesan</i>	
16.1	Introduction	436
16.2	Magnetic Bio Char	437
16.3	Synthesis of Magnetic Bio Char	438
16.3.1	Materials	438
16.3.2	Synthesis Techniques of Magnetic Bio Char	439
16.3.2.1	Synthesis of Magnetic Bio Char by Pyrolysis of Agriculture Waste	439
16.3.2.2	Synthesis of Magnetic Bio Char by Chemical Precipitation	440
16.3.2.3	Synthesis of Magnetic Bio Char by High Temperature Treatment of Agriculture Waste Char/Activated Carbon	442
16.3.2.4	Synthesis of Magnetic Bio Char by Encapsulation using Bio-Polymer	442
16.3.2.5	Synthesis of Magnetic Bio Char by Microwave Heating	444
16.3.2.6	Synthesis of Magnetic Bio Char Composites	446
16.4	Characteristics of Magnetic Bio Char	447
16.4.1	Surface Area Characteristics	448
16.4.2	Magnetic Characteristics	449
16.5	Applications of Magnetic Bio Char	450
16.6	Challenges and Future Scope of Magnetic Bio Char	452
16.7	Summary	452
	Acknowledgement	454
	References	454

17	Polyurethanes Foams from Bio-Based and Recycled Components	461
	<i>S.Gaidukovs, U.Cabulis and G.Gaidukova</i>	
17.1	Introduction	461
17.2	Experiments	464
17.2.1	Raw Materials	464
17.2.2	Polyol Synthesis	464
17.2.3	Characterization of Polyols	464
17.2.4	Preparation of Polyurethane Rigid Foams	465
17.2.5	Characterization of Rigid Polyurethane Foams	467
17.3	Results and Discussion	467
17.3.1	Characterization of Polyols	467
17.3.2	Formation of PU Rigid Foams	473
17.3.3	Cellular Structure of PU Rigid Foams	474
17.3.4	Compression Strength of PU Rigid Foams	475
17.3.5	FTIR of PU Rigid Foams	477
17.4	Conclusions	478
	Acknowledgements	479
	References	479
18	Biodegradable Polymers for Protein and Peptide Therapeutics: Next Generation Delivery Systems	483
	<i>Sathish Dyawanapelly, Nishant Kumar Jain, Sindhu KR, Maruthi Prasanna and Akhilesh Vikram Singh</i>	
18.1	Introduction	484
18.2	Protein Therapeutics and Their Challenges	484
18.2.1	Asparaginase	484
18.2.2	Adenosine Deaminase	485
18.2.3	Granulocyte Colony-Stimulating Factor	485
18.2.4	Anti-Tumor Necrosis Factor	485
18.2.5	Interferons	486
18.2.6	Growth Hormone Antagonist	486
18.2.7	Uricase	486
18.2.8	Erythropoiesis Stimulating Agent	487
18.3	Biodegradable Polymers for Conjugation	487
18.4	PEGylated Protein Therapeutics	488
18.4.1	Basic Features and Properties of PEG	488
18.4.2	Critical Factors for Protein PEGylation: PEG Structure and Size	491
18.4.3	Chemistry and Different Sites of PEGylation	491
18.4.3.1	PEGylation of Amine Group	492
18.4.3.2	PEGylation of Thiol Group	492
18.4.3.3	Disulfide Bridging PEGylation of Proteins	493
18.4.4	Enzymatic PEGylation	493
18.4.4.1	Proteins Modified by TGase PEGylation	493
18.4.5	PEGylation of Proteins Containing Unnatural Amino Acid	494
18.4.6	Non-Covalent PEGylation	494
18.4.7	Releasable of PEGylation	494
18.4.7.1	Aromatic Linkers (BE Series)	495

18.4.7.2	Synthetic BE Linkers	495
18.4.7.3	Aliphatic Linkers (Bicin Linkers)	495
18.4.7.4	B-alanine Linkers	495
18.4.8	Pharmacology of PEGylation	495
18.4.9	Emerging PEGylated Drugs	496
18.4.9.1	PEGylated hCH (ARX-201)	496
18.4.9.2	PEG-G-CSF (DA-3031)	496
18.4.9.3	PEG-IFN- α -2a (DA-3021)	496
18.4.9.4	PEG-GLP-1	496
18.4.9.5	PEG-Growth Hormone Releasing Factor (PEG-GRF)	496
18.4.9.6	PEG-Salmon Calcitonin	496
18.4.9.7	PEG-Uricase	496
18.4.9.8	PEG-arginine Deiminase (ADI)	498
18.4.10	Limitations of PEGylation	498
18.4.11	Emerging Techniques Alternative to PEGylation	498
18.5	Glycosylation of Proteins	498
18.5.1	Types of Glycosylation <i>In vivo</i>	499
18.5.2	Effect of Glycosylation on Proteins	499
18.5.3	Polysialic Acid (PSA)-Protein Conjugates	500
18.5.3.1	Polysialic Acid-catalase Conjugates	501
18.5.3.2	Polysialic Acid-asparaginase Conjugates	501
18.5.3.3	Polysialic Acid-insulin Conjugates	501
18.5.3.4	Polysialic Acid-single Chain Fv Fragment Conjugates	507
18.5.3.5	Polysialic Acid-cytokine Conjugates	507
18.5.3.6	Polysialic Acid-G-CSF Conjugates	507
18.5.3.7	Polysialic Acid-erythropoietin Conjugates	507
18.5.3.8	Polysialic Acid-IgG Fab Fragments Conjugate	508
18.6	Polyglycerols (PG)-Protein Conjugates	508
18.6.1	Polyglycerol-Ovalbumin Peptide Conjugates	508
18.6.2	Polyglycerol-Arginine-Glycine-Aspartic Acid (RGD) Peptide Conjugates	509
18.7	Dendrimer-Protein Conjugates	509
18.7.1	PAMAM-Trypsin and Trypsin Inhibitor Conjugates	513
18.7.2	PAMAM- α 4 β 1 Integrin Binding Peptide Conjugates	513
18.7.3	Porphyrin Dendrimer-Glucose Oxidase Conjugates	513
18.8	HESylation of Proteins	513
18.8.1	HES-Erythropoietin Mimetic Peptide (AGEM400 (HES)) Conjugate	514
18.8.2	HES-Anakinra Conjugates	514
18.8.3	HES-G-CSF Conjugates	515
18.9	Dextran-Protein Conjugates	515
18.9.1	Dextran-Asparaginase Conjugates	515
18.9.2	Dextran-Carboxypeptidase G ₂ Conjugates	515
18.9.3	Dextran-Uricase Conjugates	516
18.9.4	Dextran-Insulin Conjugates	516
18.9.5	Dextran-Hemoglobin Conjugates	522

18.10	Dextrin-Protein Conjugates	522
18.10.1	Dextrin-rhEGF Conjugates	522
18.10.2	Dextrin-Trypsin and Melanocyte Stimulating Hormone (MSH) Conjugates	523
18.10.3	Dextrin-Phospholipase A2	523
18.11	Hyaluronic Acid (HA)-Protein Conjugates	524
18.11.1	Hyaluronic Acid-Interferon α Conjugate	524
18.11.2	Hyaluronic Acid-hGH Conjugate	529
18.11.3	Hyaluronic Acid-Insulin Conjugate	529
18.11.4	Hyaluronic Acid-Trypsin	529
18.11.5	Hyaluronic Acid-EGF Conjugate	530
18.11.6	Hyaluronic Acid-Exendin 4 Conjugates	530
18.11.7	Hyaluronic Acid-anti-Flt1 Peptide Conjugates	530
18.11.8	Hyaluronic Acid-Superoxide Dismutase Conjugates	531
18.12	Some Other Polymer-Protein Conjugates	531
18.13	PASylation	531
18.14	Conclusion and Future Perspectives	532
	Abbreviations	532
	References	535
Index		543

Preface

The concept of green chemistry and sustainable development policy impose on industry and technology to switch raw material base from the petroleum to renewable resources. Remarkable attention has been paid to the environmental friendly, green and sustainable materials for a number of applications during the last few years. Indeed the rapidly diminishing global petroleum resources, along with awareness of global environmental problems, have promoted the way to switch towards renewable resources based materials. In this regards, bio-based renewable materials can form the basis for variety of eco-efficient, sustainable products that can capture and compete markets presently dominated by products based solely on petroleum based raw materials. The nature provides a wide range of the raw materials that can be converted into a polymeric matrix/ adhesive/ reinforcement applicable in composites formulation. Different kinds of polymers (renewable/nonrenewable) and polymer composite materials have been emerging rapidly as the prospective substitute to the ceramic or metal materials, due to their advantages over conventional materials. In brief, polymers are macromolecular groups collectively recognized as polymers due to the presence of repeating blocks of covalently linked atomic arrangement in the formation of these molecules. The repetitive atomic arrangements forming the macromolecules by forming covalent links are the building block or constituent monomers. As the covalent bond formation between monomer units is the essence of polymer formation, polymers are organic or carbon compounds of either biological or synthetic origin. The phenomenon or process of polymerization enables to create diverse forms of macromolecules with varied structural and functional properties and applications. On the other hand, composite materials, or composites, are one of the main improvements in material technology in recent years. In the materials science field, a composite is a multi-phase material consisting of two or more physically distinct components, a matrix (or a continuous phase) and at least one dispersed (filler or reinforcement) phase. The dispersed phase, responsible for enhancing one or more properties of matrix, can be categorized according to particle dimensions that comprise platelet, ellipsoids, spheres and fibers. These particles can be inorganic or organic origin and possess rigid or flexible properties.

The most important resources for renewable raw materials originate from nature such as wood, starch, proteins and oils from plants. Therefore, renewable raw materials lead to the benefit of processing in industries owing to the short period of replenishment cycle resulting in the continuous flow production. Moreover, the production cost can be reduced by using natural raw materials instead of chemical raw materials. The waste and residues from agriculture and industry have been also used as an alternative renewable resources for producing energy and raw materials such as chemicals, cellulose, carbon and silica. For polymer composites applications, an intensifying focus has been directed toward the use of renewable materials. Bio-based polymers are one of the most attractive candidates

in renewable raw materials for use as organic reinforcing fillers such as flex, hemp, pine needles, coir, jute, kenaf, sisal, rice husk, ramie, palm and banana fibres which exhibited excellence enhancement in mechanical and thermal properties. For green polymer composites composed of inorganic reinforcing fillers, renewable resources based polymers have been used as matrix materials.

Significant research efforts all around the globe are continuing to explore and improve the properties of renewable polymers based materials. Researchers are collectively focusing their efforts to use the inherent advantages of renewable polymers for miscellaneous applications. To ensure a sustainable future, the use of bio-based materials containing a high content of derivatives from renewable biomass is the best solution.

This volume of the book series “*Handbook of Composites from Renewable Materials*” is solely focused on the “*Structure and Chemistry*” of renewable materials. Some of the important topics include but not limited to: carbon fibers from sustainable resources; polylactic acid composites and composite foams based on natural fibres; composites materials from other than cellulosic resources; microcrystalline cellulose and related polymer composites; Tannin based foam; Renewable feedstock vanillin derived polymer and composites; silk biocomposites; bio-derived adhesives and matrix polymers; biomass based formaldehyde-free bio-resin; isolation and characterisation of water soluble polysaccharide; bio-based fillers; keratin based materials in biotechnology; structure of proteins adsorbed onto bioactive glasses for sustainable composite; effect of filler properties on the antioxidant response of starch composites; composite of chitosan and its derivate; magnetic biochar from discarded agricultural biomass; biodegradable polymers for protein and peptide conjugation; polyurethanes and polyurethane composites from bio-based/recycled components.

Several critical issues and suggestions for future work are comprehensively discussed in this volume with the hope that the book will provide a deep insight into the state-of-art of “Structure and Chemistry” of the renewable materials. We would like to thank the Publisher and Martin Scrivener for the invaluable help in the organisation of the editing process. Finally, we would like to thank our parents for their continuous encouragement and support.

Vijay Kumar Thakur, Ph.D.
University of Cranfield, U.K.

Manju Kumari Thakur, M.Sc., M.Phil., Ph.D.
Himachal Pradesh University, Shimla, India

Michael R. Kessler, Ph.D., P.E.
Washington State University, U.S.A.

Carbon Fibers from Sustainable Resources

Rafael de Avila Delucis¹, Veronica Maria de Araujo Calado²,
Jose Roberto Moraes d'Almeida³ and Sandro Campos Amico^{1*}

¹*Mining, Metallurgical and Materials Engineering Post-Graduate Program (PPGE3M),
Federal University of Rio Grande do Sul (UFRGS), Porto Alegre/RS, Brazil*

²*School of Chemistry, Federal University of Rio de Janeiro (UFRJ), Rio de Janeiro/RJ, Brazil*

³*Materials Engineering Department, Pontificia Universidade Catolica Rio de Janeiro (PUC-Rio),
Rio de Janeiro/RJ, Brazil*

Abstract

Carbon fibers (CF) combine unique properties that have enabled their growing use as reinforcement in polymeric composites. CF based on polyacrylonitrile (PAN) are widely in use today, even though the first attempt to produce these fibers in 1878 employed cotton and other materials. Ongoing and steady research for “green” precursors for CF from available natural resources is motivated by the high cost and generation of toxic products related to PAN- or pitch-based fibers. This chapter reviews some of the work being carried out on lignin and other natural resources (rayon, wood, cotton, jute, ramie, wool, chitin, chitosan, tar pitches and sea squirts). Due to its importance and wide availability, lignin, from hardwood or softwood, is discussed in detail, including the various extraction methods available. The processing for obtaining CF varies but, for polymeric precursors such as PAN or lignin, three basic steps are common: thermal extrusion and spinning, thermal stabilization, and carbonization. This chapter also describes the use of blends of lignin with polymers, such as PEG, PEO, PET/PP, PVA, PAN and PLA, as precursor for CF.

Keywords: Lignin, cellulose, natural fibers, wood, rayon, precursors

1.1 Introduction

Carbon fibers (CF) combine unique properties such as dimensional stability, high strength, high stiffness, low thermal expansion coefficient, biological compatibility and elevated fatigue resistance (Chand, 2000; Wazir & Kakakhel, 2009). Due to these and other features, these fibers have been used in composites to replace plastics, steel, and other engineering materials in sectors/applications such as military, aerospace, marine, automotive, civil construction, petrochemical, offshore structural components, biomedical, sporting goods, pressurized gas storage, as well as supercapacitors, lithium-ion batteries and flywheels (Fitzer, 1989; Momma *et al.*, 1996).

*Corresponding author: amico@ufrgs.br

In 2005, the value of the worldwide carbon fiber market amounted to around \$900 million, split into commercial grade (59%) and aerospace grade (41%). The numbers for 2015 reached \$2 billion, with a production increase of 122%, and a relative expansion in the commercial grade fiber (71%) in relation to the aeronautical grade (29%) (Zoltek, 2015). Thus, we are seeing a trend towards mass production of less specialized CF.

Even though CF based on polyacrylonitrile (PAN) are in wide use, the first attempt to produce these fibers, in 1878, was based on cotton, when Thomas Edison produced filaments for incandescent lamps (Edison, 1880). The production process for CF can be broadly divided into precursor production/isolation, fiber spinning, fiber stabilization, fiber carbonization and fiber graphitization (Edie, 1998). However, each stage has specific features depending on the nature of the precursor used and the required final properties of the CF (Edie, 1998; Zhang, 2014). Considerations when selecting a precursor/process include:

- a. Technical standpoint: Chemical composition of the precursor is vital; it should present a high carbon content, at least 92 wt% of anisotropic carbon (Frank *et al.*, 2014). Also, it should not melt during carbonization (Park & Heo, 2015).
- b. Economic standpoint: Compared with other artificial fibers (e.g., glass and polymeric fibers), CF are costly, which limits their use to a range of applications (Wu *et al.*, 2013). Moreover, as reported by Mainka *et al.*, (2015), more than 50% of the carbon fiber cost is related to the precursor, 15% to the oxidation process and 23% to the carbonization process. The price of the precursor is linked to its availability, as is its isolation process.
- c. Environmental standpoint: Preferably, processing should not result in toxic wastes, and the precursor should come from a sustainable resource.

Currently, due to the high mechanical strength of the fibers produced, PAN – a synthetic non-renewable petroleum-based precursor – is the main commercial precursor, representing about 90% of the total carbon fiber production. Pitch and viscose rayon are also widely used precursors for CF (Chand, 2000). Although these precursors present relatively proven technical efficiency (Mora *et al.*, 2002), they have drawbacks related to high cost and generation of toxic products during processing, e.g., hydrogen cyanide (HCN).

Thus, much of the current research regarding carbon fiber production focuses on defining alternative precursors, especially “green” ones from available natural resources. Indeed, the use of precursors from biomass that may lead to low price and eco-friendly CF could overcome the cited problems and increase the applications in which carbon fibers may be used. According to Langholtz *et al.*, (2014), this could increase biorefinery gross revenue by 30% to 300% and reduce carbon dioxide (CO₂) emissions.

In general, to be considered a potential candidate for carbon fiber production, a natural resource-based precursor must present high carbon content (Mavinkurve *et al.*, 1995), resistance to high temperature (Dumanli & Windle, 2012), not more than one carbon atom between the aromatic rings (Chand, 2000), a high degree of order,

orientation and flatness (Inagaki *et al.*, 1991; Inagaki *et al.*, 1992), simple release of non-carbon atoms and easy cyclization (Mavinkurve *et al.*, 1995; Huang, 2009), high molecular weight (Morgon, 2005), and ash content lower than 1000 ppm (0.01%) (Frank *et al.*, 2014). According to Chand (2000), in order to resist to high temperatures, the precursor should preferably be a heterocyclic aromatic polymer and the heteroatoms should not belong to the main molecule chain.

Forests, agricultural waste, crop residues, and wood chips, among others are all possible biomass sources (Agrawal *et al.*, 2014). Primarily lignin, cotton, wool, jute, and ramie are regarded as potential sustainable precursors for CF. Among them, lignin is largely cited because of its high availability and ecological appeal since it is obtained as an industrial waste from the cellulose pulping process. The cited natural resources and the chemical modifications required to make them appropriate for processing are further exploited below.

1.2 Lignin and Other Sustainable Resources

Lignin is responsible for a mass corresponding to 300,000 Mton in the biosphere, and is one of the most abundant materials in nature, second only to cellulose (Gregorová *et al.*, 2006). Both are sustainable and naturally occurring renewable polymers (Fengel & Wegener, 1989 (Voicu *et al.*, 2016). Its name comes from Latin *lignum*, meaning wood (Piló-Veloso, 1993). In its natural state, lignin is found in biological materials associated with carbohydrates such as cellulose and hemicellulose, and concentrated in intercellular spaces of all vascular plants, promoting the interconnection between anatomical characters (Evert, 2006). The estimated annual production of lignin reaches approximately 50 Mton (Thakur *et al.*, 2014), especially as a co-product of pulping, and more recently, as a by-product of cellulosic ethanol production in biorefineries (Thakur & Thakur, 2015).

Many different structures have been proposed for lignin, which are believed to depend not only on source (hardwood, softwood and grass plants), but also on plant age, environmental conditions and the extraction process used (Kraft, organosolv, alkali, and so on). The molecular structure of lignin from hardwood allows good spinning and slow stabilization, whereas for softwood lignin, stabilization is easier, but the lignin is not readily spoolable.

The lack of an effective method to isolate lignin, makes it difficult to fully elucidate its chemical structure. Nevertheless, the lignin structure has been cited in recent decades as a complex, three-dimensional, heteropolymeric, amorphous, cross-linked and highly branched structure. More specifically, polyether-phenylpropane is considered the major unit of lignin (Silva *et al.*, 2009), with carbon-carbon and ether linkages between monomeric units. Hydroxyl and methoxyl groups are often cited as substituents on the phenyl group.

Lignin has a carbon content greater than 60% (Mainka *et al.*, 2015) and it may be classified as a function of the pretreatment used to fractionate the lignocellulosic matrix or based on its chemical configurations. The methods applied for biomass pretreatment are broadly divided into physical, chemical, physico-chemical and biological and include steam explosion (Wang *et al.*, 2010), microbial

fermentation (Chang *et al.*, 2012), alkali pretreatment (Xu *et al.*, 2015), hydrolysis with diluted acid (Kim *et al.*, 2015), hydrothermal treatment with hot water (Pelaez-Samaniego *et al.*, 2015), microwave irradiation (Li *et al.*, 2015), ionic liquids pretreatment (Zhang *et al.*, 2015b), electron beam irradiation (Metreveli *et al.*, 2014), wet oxidation (Klinke *et al.*, 2002), supercritical fluid extraction (Assmann *et al.*, 2013) and organosolv pretreatment (Santos *et al.*, 2014).

It is out of the scope of this chapter to approach all chemical configurations wherein lignin is found artificially and for every pretreatment for the fractioning of lignocellulosic biomass. Instead, it will briefly discuss the main features of those lignins that are potential precursors for CF. The various configurations wherein lignin is found artificially are called technical lignins that, owing to processes carried out for the obtaining of the lignocellulosic raw material, may be classified into:

- a. Extracted lignins: Milled wood lignin (MWL), Milled wood enzyme lignin (MWEL), Cellulase enzyme lignin (CEL) and Braun's lignin.
- b. Residual lignins: Klason lignin and Willstaller lignin.
- c. Derived lignins: Thiolignins, Organosolv lignin, Kraft lignin and Sulfite lignin (lignosulfonates).

Depending on the method used, the obtained lignin will have distinct characteristics, leading to carbon fibers with particular properties for different applications. Some of them are discussed below.

Milled wood lignin (MWL), also called Björkman Milled Wood Lignin or Björkman Lignin, is obtained from sawdust-sized particles through extraction in aqueous *p*-dioxane (Björkman, 1956). The obtained lignin presents itself in its natural state (protolignin) (Ikeda, 2002), with a yield between 20 and 30% (Rencoret *et al.*, 2009; Goundalkar *et al.*, 2014). Increase in the milling extent increases the MWL yield and the lignin obtained becomes more representative of the original amount of lignin. However, severe chemical modification of the lignin may occur, including increase in carbonyl content and phenolic hydroxyl content (Bjorkman, 1957; Chang, 1975), decrease in molecular weight (Chang, 1975) as well as cleavage of aryl ether linkages (Gellerstedt & Northey, 1989), which is undesirable for CF production. A carbohydrate residue of approx. 10% remains in the obtained lignin, depending on plant species (Guerra *et al.*, 2006; Goundalkar *et al.*, 2014), and the final product, of high molecular weight, is not completely dissolved in commonly used solvents for lignin (El Hage, 2009; Bu *et al.*, 2011).

In order to increase the final purity, MWL is often transformed into Milled Wood Enzyme Lignin (MWEL) by enzymatic hydrolysis of the polysaccharides (Gellerstedt, 1992) and fractioned by a soluble solvent, obtaining Cellulase Enzyme Lignin (CEL) (Ikeda, 2002). According to Guerra *et al.*, (2006), the molecular weight decreases in the following order: MWEL, CEL and MWL, therefore possibly increasing the CF production capability.

Braun's lignin (BNL), or native lignin, is obtained by extraction in methanol. Samples are flour-sized particles and, after ethanol extraction, the lignin can be purified by washing in cold water and diethyl ether to remove foreign components (Hiltunen *et al.*, 2006). Compared to MWL, a lower yield (about 8%, depending of the degree

of milling) of a lower molecular weight lignin is obtained (Agrawal *et al.*, 2014), which is considered disadvantageous for CF production.

Classified as residual lignins, Willstätter lignin and Klason lignin are obtained by hydrolysis of soluble polysaccharides in water, which is performed by treating with sulfuric acid and hydrochloric acid, respectively. After the chemical reaction, the lignin is recovered as an insoluble residue. These methods for lignin isolation are mainly used for evaluating the lignin content (Goundalkar *et al.*, 2014; Santos *et al.*, 2014), because the obtained lignin presents a highly condensed structure (Rowell *et al.*, 2012) which prevents its use for the manufacturing of new products.

In general, derived lignins are byproducts of pulp and paper production processes. Differently from extracted or residual lignins, these technical lignins are not isolated with the intention of representing the lignin in its natural state (i.e., protolignins). Therefore, after isolation and purification, it is very important to evaluate the degree of carbohydrate contamination. These lignins have economic and environmental appeal because they are waste from industrial processes being produced on large scale, and are considered environmental pollutants. After the pulping process, this lignin is often burned for energy production but the total amount of lignin produced is 60% greater than what is actually needed for internal power supply (Sannigrahi *et al.*, 2010). This is often a bottleneck in the production process, thus favoring the insertion of lignin in other niches such as for CF production. In addition, according to Paananen & Sixta, (2015), pulping processes that use excess alkali generate a highly alkaline residual black liquor that is very difficult to use for incineration, requiring an extra step in the recovery procedure to reduce alkalinity.

Kraft lignin is produced in the most widespread chemical process in the industry. In general terms, this lignin is obtained by dissolution and degradation of the lignocellulosic raw material in an alkaline sodium sulphite solution, called “white liquor.” It has low molecular weight and high content of phenolic compounds (Sadeghifar *et al.*, 2012), which results in high reactivity and low potential to be used as CF precursor. On the other hand, the organosolv pulping process is considered the most environmental-friendly method for the fractioning of lignocellulosic materials, yielding value-added products (i.e., lignin and hemicelluloses) (Santos *et al.*, 2014). For García *et al.* (2011), the production process for organosolv lignin is sulphur-free, the yield is about 78% depending mainly on the process temperature (Astner *et al.*, 2015), and the derived lignin presents low molecular weight (El Mansouri & Salvadó, 2006).

The lignosulfonates, also called lignin sulfites, are the cellulosic waste from the sulfite pulping process. This process may be understood as a lignocellulosic matter treatment by immersion in an aqueous solution of sodium sulfite at high temperature. The lignosulfonates composition varies based on the extent of the lignin degradation and the number of sulfonic groups present (Gandini, 2008; Areskog *et al.*, 2010). Compared with Kraft lignin, it has lower α -cellulose content and higher molecular weight (Miao *et al.*, 2014).

Steam explosion lignins are obtained by defibrillation of lignocellulosic matter based on a treatment with steam at high temperature and pressure followed by the rapid release of pressure, obtaining about 50% yield (Martin-Sampedro *et al.*, 2011). The first CF obtained following the steam-explosion of lignin was reported by Sudo & Shimizu (1992). Treating lignin under such conditions, at very low pH, is considered

undesirable because of its structural complexity and thermal instability. Elevated temperatures convert lignin into an unwanted condensed, inert and insoluble material (El Mansouri *et al.*, 2011).

Besides lignin, other natural resources have been used for CF production such as viscose rayon, wool, cotton and bast fibers (Reinhardt *et al.*, 2013). Shells of some crustaceans, chitin and their products can also be useful for this purpose. All these resources have environmental appeal and are largely available.

Rayon may be considered an array of manufactured fibers composed of regenerated cellulose. According to Sixta *et al.*, (2013), more than 30% of the 4,2 Mton of dissolved wood pulps produced in the world annually were converted into rayon and its byproducts. It is mainly commercialized as four products, which are classified based on the fiber production method (Chen, 2014b), namely:

- a. Viscose rayon: Produced by reacting caustic soda with wood pulp to make alkali cellulose solution that is mixed with carbon disulfide to produce sodium cellulose xanthate, which is later dissolved in a weak caustic soda solution. This material is largely pure cellulose (X-ray crystallinity between 55 and 65%) with a low degree of polymerization (300–450) (Kadolph, 2001; Ruan *et al.*, 2004) that produces highly-oriented cellulose chains by wet-spinning (Siller *et al.*, 2014). Viscose rayon is the most important regenerated cellulose fiber, including when used for composite materials (Reinhardt *et al.*, 2013).
- b. Lyocell rayon: Produced by directly dissolving cellulose into N-methylmorpholine-N-oxide (NMMO) in order to reduce several side reactions and the amount of byproducts produced, as well as to effectively recover the high-cost solvents employed (Ruan *et al.*, 2004). Lyocell rayon fiber is among the new generation of regenerated cellulose fibers, due to its eco-friendly character. Lyocell fiber is commonly used in apparel application, paper industry, nonwoven fabrics manufacturing, blend production, etc. (Perepelkin, 2007; Singha, 2012) and its common composition is 50–60% NMMO, 20–30% water and 10–15% cellulose (Rosenau *et al.*, 2001).
- c. Cupro rayon: Produced by dissolving cellulose into a cuprammonium solution and then wet-spinning it to regenerate cellulose. This process, known as cuprammonium hydroxide process, requires the use of high-priced cotton cellulose and copper salts, so it is not competitive with viscose rayon, being produced in a much inferior amount (Gupta, 2007). Compared to Lyocell rayon, it is disadvantageous due to the production of highly toxic by-product waste and pollutants (Fink *et al.*, 2001). Compared to viscose rayon, it has a higher polymerization degree (Eichhorn & Young, 2001) and is useful in certain specialty markets.
- d. Acetate: This is a cellulose-derived fiber rather than a regenerated cellulose fiber. It is produced by acetylating cellulose using acetic anhydride and sulfuric acid. The resulting cellulose acetate is dissolved in acetone and dry-spun into fiber (Imura *et al.*, 2014). Cellulose acetate has very good handling and comfort properties (Rana *et al.*, 2014) and it

is generally directed for films, plastics, coatings, cellulose ethers and cellulose powder (Sixta *et al.*, 2013).

Currently, the world production of regenerated cellulose fiber is about 3 Mton per year, accounting for approximately 5% of the global man-made fiber production (Chen, 2014b; Pappu *et al.*, 2015). Because of this, much research has been directed towards investigating CF manufactured from rayon-based precursors (Plaisantin *et al.*, 2001). These precursors are still important nowadays because they are largely available, and have low cost and non-melting character (Li *et al.*, 2007).

Wood is commonly classified as a natural composite material, comprising fibers, parenchymas, vessels, ray cells, drilling plates and pits arranged in three different planes (Evert, 2006). However, only the fibrous cells are significantly used to produce carbon products (Tondi & Pizzi, 2009; Huang *et al.*, 2015).

At the ultrastructural level, wood fibers are built up of four layers, namely, middle lamella (mainly composed of lignin), primary wall, secondary wall and warty layer, which differ mainly in their microfibrils angle (Fengel & Wegener, 1989) (Singha and Thakur, 2009). The wood cell wall is chemically comprised of carbohydrates (65–75%) and lignin (18–35%). Elementary composition of the cell fibers from wood is carbon (≈ 50 wt%), oxygen (≈ 44 wt%), hydrogen (≈ 6 wt%) and other inorganic components (≈ 1 wt%) (Rowell *et al.*, 2012). Compared to other natural fibers, fibers from wood are considered short and fine, and their morphological characteristics are influenced by factors like planting area, genetic heritability, hormone production, seed origin, weather conditions and silvicultural management (Bendtsen, 1978; Pande, 2013).

Based on anatomical and morphological characteristics, it is possible to classify wood species into:

- a. Softwood: Wood species of the gymnosperm class. Its cell fibers are called tracheids that present mean length and width of about 2000–6000 μm and 20–40 μm , respectively (Dai & Fan, 2014). These anatomical elements represent over 90% of its volume (Wiedenhoeft, 2010).
- b. Hardwood: Wood species of the angiosperms dicotyledones class. It has a much more complex structure than softwood. Its axial system comprises various types of fibrous elements, vessel elements of distinct sizes and arrangements, and axial parenchyma in various patterns and amounts (Wiedenhoeft, 2010). Its fibers represent approximately 50% of the wood volume, with mean length and width of about 1000–2000 μm and 10–50 μm , respectively (Dai & Fan, 2014).

The methods employed for the defibration of wood are called pulping processes. They can be classified in:

- a. Mechanical pulping: The wood logs are lubricated by water and concomitantly pressed against one rotating stone. The friction between them causes two simultaneous mechanisms, the lignin concentrated in the intercellular spaces is softened, and the fibers are forced to separate from

each other (Hellström *et al.*, 2008; Hellström *et al.*, 2009). This procedure commonly presents about 92–96% yield (Biermann, 1996).

- b. Chemical pulping: The wood logs are chopped into chips and then treated under high pressure in the presence of chemicals. There are many routes, but the main methods are sulfite and Kraft sulfate (Lourençon *et al.*, 2015). The yield levels obtained are commonly around 40–45% (Biermann, 1996). These processes are traditionally employed to obtain cellulose for paper production but, as previously mentioned, they can be used for lignin production.

Wood is also vastly used as wood flour due to cost and environmental aspects related to the reuse of industrial waste. Wood flour may be defined as a finely ground wood derived from various wood planer shavings, chips, sawdust, and other clean waste wood from saw mills and other wood processing industries (Matuana & Stark, 2015) (Singha & Thakur, 2010).

Cotton has been used since around 5000 BC in India and the Middle East; its annual production is around 25,000 Mton with a growth trend of 2% per annum. Cotton is one of the main materials for textile applications because it combines considerable strength with good absorbency (Dochia & Sirghie, 2012). Cotton is composed of cellulose and hemicelluloses (about 95–97% wt%), along with proteins, pectoses, pigments and small levels of oils, waxes and mineral substances, reaching a crystallinity of about 70% (Chen, 2014a).

Jute is a largely available natural fiber, being second to cotton in amount produced, reaching an estimated annual production of more than 3 Mton (Faostat, 2012). It grows in Southern Asia and it is mostly produced in Bangladesh, India, China and Thailand (Zhou *et al.*, 2013). Jute fiber has been traditionally used for the manufacture of sacks, carpet, twines, and ropes, among others (Roy & Lutfar, 2012a; Chen, 2014b). However, it is also used as reinforcing material in the automotive, construction and packaging industries (Gon *et al.*, 2012). In comparison to other multicellular fibers, jute fibers are known for their greater lignin content. Del Rio *et al.*, (2009) evaluated their chemical composition as: holocellulose (81.6 wt%), Klason lignin (13.3 wt%), acid-soluble lignin (2.8 wt%), ash (1.0 wt%), hydrosolubles (1.0 wt%) and lipophilic extractives (~0.4 wt%).

Ramie, also known as “China grass,” is native to China, Japan and the Malay Peninsula, where it was reported in as early as 1300 AD, being used for a long period as a textile fiber. It represents the second most important fiber market in the world trade. In China, ramie is one of the main economic crops, reaching a production of 150 Mton of fibers per year, about 96–97% of the world production (Faostat, 2012). Although of tropical origin, ramie was successfully introduced in other environments, appearing suited to temperate conditions, giving satisfactory yields (Kipriotis *et al.*, 2015).

Currently, ramie fibers are used in many niches, including industrial sewing threads, fabrics for household furnishings, high-quality papers, packing materials, fishing nets, parachute fabrics, woven fire hoses, and clothing, among others (Sen & Reddy, 2011; Roy & Lutfar, 2012b). Mohanty *et al.*, (2000) reported ramie's main constituents as cellulose (68.676.2 wt%), hemicelluloses (13.116.7 wt%), lignin (~0.7 wt%), pectin (1.9 wt%) and wax (0.3 wt%).

Wool, the most commonly used animal fiber, is a textile material mainly composed of insoluble and tough fibrous proteins, such as keratins (Fortier *et al.*, 2012). In its natural state, keratin is present in the form of filaments, which are known as α -keratin fibers. These α -keratin fibers are aligned in the direction of the main fiber axis constituting macrofibrils of about 300 nm diameter, covered by a lipid membrane and linked by a intermacrofibrillar matrix called cell membrane complex (Mura *et al.*, 2015). From an economic point of view, wool demand has been growing in many countries, like China, USA, Japan, South Korea, Italy and UK (Kuffner & Popescu, 2012), and is used in many applications including household textiles, garment materials and accessories (Zhang *et al.*, 2015a). Elemental analysis of wool produces carbon (around 50 wt%), hydrogen (7 wt%), oxygen (22 wt%), nitrogen (16 wt%) and sulphur (5 wt%) (Popescu & Hoecker, 2007).

Chitin is produced from the exoskeleton of shrimp, crabs, squid, lobsters, crayfishes and cuttlefishes, as well from the bone plate of squid (Nwe *et al.*, 2014). Chitin is commonly obtained at laboratory, as well as industrial scale (Rinaudo, 2006). Chemically, it can be described as a linear polymer of β (1–4) linked 2-acetamido-2-deoxy-D-glucopyranose.

Among the polymers obtained from chitin, chitosan (N-deacetylated) is the most important, combining bioresorption, absence of cytotoxicity and low environmental impact during processing (Szymańska & Winnicka, 2015; Thakur & Thakur, 2014a). From the chemical standpoint, it is a linear binary copolymer of (1–4)-linked A-units and 2-amino-2-deoxy- β -D-glucopyranose (GlcN; D-unit) (Badawy & Rabea, 2011). Chitosan is considered more versatile than chitin due to its reactive amino groups at the C-2 positions, which are responsible for the chitosan polycationic nature in aqueous media (Sibaja *et al.*, 2015). Nevertheless, the physicochemical properties of this chitin product depend on its purification, which requires several steps, broadly referred as demineralization, deproteination, discoloration and deacetylation (Tajik *et al.*, 2008). To be considered a chitosan, the chitin needs to present a degree of deacetylation of about 50%. It is traditionally used as antioxidative agent, edible film, and plant fertilizer, among others (Nwe *et al.*, 2014; Trung & Bao, 2015).

1.3 Carbon Fibers from Lignin

After extraction, the lignin powder can be used to produce blends with other polymers, in resins and even for the production of carbon fiber, a very noble application first patented in 1969. The processing for obtaining CF varies but, for polymeric precursors such as PAN or lignin, three basic steps are common: thermal extrusion and spinning, thermal stabilization and carbonization. The graphitization step may also follow.

In the thermal extrusion step, the melting temperature or softening point must be inferior to the decomposition temperature of the lignin. This temperature is controversial in the literature. For Braun *et al.*, (2005), it is around 190 °C, for Kadla *et al.*, (2002) it is around 270 °C. Other researchers argue that degradation occurs within 200–500 °C (Brebú & Vasile, 2010). Above 400 °C, pyrolysis of lignin, decomposition reactions and condensation of aromatic rings occur. This variation may be related to different sources of lignin.

During thermostabilization, the glass transition temperature (T_g) increases and the thermoplastic lignin fiber becomes a thermoset. This step is necessary to promote infusibility of the fiber in the subsequent step (carbonization). The process is generally carried out in an oxidizing atmosphere, usually air due to its low cost (Hayashi *et al.*, 1995). The treatment consists of inserting oxygen cross-links between molecules and incorporating oxidized groups, justifying the increase in T_g (Braun *et al.*, 2005). This is one of the most expensive steps of the process and optimization studies have been carried out to minimize stabilization time and conversion costs, while ensuring the desired properties (Hayashi *et al.*, 1995), i.e., microwave-assisted plasma processing (White *et al.*, 2014).

Fiber quality is compromised if thermal stabilization is performed quickly (Edie, 1998), and low heating rate guarantees oxidation of the functional groups (Braun *et al.*, 2005). For high temperatures and low heating rates, T_g increases faster than the system temperature, keeping the material in the glassy state. For high heating rates, the reactions cannot maintain a T_g higher than the temperature of the system, leading to fiber melting (Braun *et al.*, 2005). It is also important to apply a tension to the fiber in order to limit relaxation of the polymer structure during heating (Edie, 1998). The thermal oxidation process of lignin is complex and still not fully understood (Braun *et al.*, 2005).

During the carbonization step, flat sheets of graphene with high carbon content are produced (Kadla *et al.*, 2002; Hayashi *et al.*, 1995). This step occurs in an inert atmosphere and most of the non-carbonaceous elements in the fiber are volatilized as gases, increasing the amount of carbon-carbon bonds and consequently improving the mechanical, electrical and thermal properties of the fiber (Edie, 1998). The mass loss in this step varies with the precursor, being within 48–51% for lignin (Kadla *et al.*, 2002). The maximum tensile strength is achieved at 1500 °C. Above this temperature, strength decreases even though modulus increases. A high carbonization rate causes structural defects to the fiber, while a low rate causes great loss of heteroatoms. Thus, process optimization is recommended (Huang, 2009).

To improve lignin spinning characteristics, some authors proposed modification of its structure, while others added plasticizers. In fact, lignin-based CF were first developed by Nippon Kayaku in 1969 (Otani *et al.*, 1969). The pilot process consisted of dry spinning lignin dissolved in an alkaline solution with polyvinyl alcohol as plasticizer. Because of the poor mechanical properties owing to lignin with many impurities, the process was terminated (Kadla *et al.*, 2002). In the 1970s, a similar process was patented by Mannsmann *et al.*, (1973), using an aqueous solution of lignin or lignin salts with the addition of polyethylene oxide (PEO) as plasticizer.

In order to obtain CF with good properties, the Oak Ridge National Laboratory suggested that the precursor should have a lignin content higher than 99%, with less than 500 ppm of carbohydrates, less than 5 wt% of volatiles, and less than 1000 ppm of ashes. Therefore, lignin extracted from many sources need to be purified prior to the whole process (Luo *et al.*, 2011), removing impurities that hinder the spooling process. In a recent paper, Nordström *et al.*, (2013a) proposed the use of a ceramic membrane to fractionate black liquor from hard and softwood, reducing the processing temperature.

The lignin molecule is very complex, with different groups, so it is a very hard task to align it in order to promote mechanical properties. Different treatments have been proposed to obtain lignin, such as hydrogenation (Sudo & Shimizu, 1992), acetylation

(Eckert & Abdullah, 2008; Zhang & Ogale, 2014), as well as esterification with octanoyl chloride (Lewis & Brauns, 1947) and lauroylchloride (Lewis *et al.*, 1943). The results were considered satisfactory by the authors, reducing the T_g of lignin and increasing the carbon content of the treated lignin and the CF.

The literature presents many papers about lignin-based CF. Some authors use pure lignin from hardwood and softwood (Braun *et al.*, 2005; Ruiz-Rosas *et al.*, 2010; Xiaojun *et al.*, 2010; Foston *et al.*, 2013; Teng *et al.*, 2013; Nordström *et al.*, 2013a; Nordström *et al.*, 2013b; Chatterjee *et al.*, 2014) others use a blend of lignin and polymers, such as Poly(ethylene glycol) - PEG (Lin *et al.*, 2012; Lin *et al.*, 2014), poly(ethylene oxide) - PEO (Schreiber *et al.*, 2014; Dallmeyer *et al.*, 2014a; Dallmeyer *et al.*, 2014b), poly(ethylene terephthalate)/poly(propylene) - PET/PP (Kubo & Kadla, 2005), Poly(vinyl alcohol) - PVA (Ago *et al.*, 2012; Lai *et al.*, 2014a; Lai *et al.*, 2014b), PAN (Maradur *et al.*, 2012; Xu *et al.*, 2013; Xu *et al.*, 2014; Hu *et al.*, 2014; Jin *et al.*, 2014a; Jin *et al.*, 2014b; Oroumei *et al.*, 2015), poly(lactic acid) - PLA (Thunga *et al.*, 2014; Wang *et al.*, 2015). The results are very promising.

Thus, there is a trend, in recent papers, to mix lignin with a polymer to improve the properties of lignin-based CF, especially related to their brittleness and mechanical properties. However, lignin-based CF with structural characteristics are still yet to be realized. An alternative is to manufacture lignin-based carbon mats by using melt-blown system or electrospinning. These techniques allow the production of carbon nanofibers to be used in high temperature processes (e.g., fireproofing fabrics), secondary structures of airplanes, car panels and hoods, boards for electronic devices, and the like. There are some papers in the literature that present very good results, especially related to the fiber spooling process (Ago *et al.*, 2012; Xu *et al.*, 2013; Lai *et al.*, 2014a; Dallmeyer *et al.*, 2014a; Dallmeyer *et al.*, 2014b; Schreiber *et al.*, 2014; Jin *et al.*, 2014a).

The overall challenges in this area include techniques to isolate and purify lignin, reduction in brittleness of lignin fiber, spinning rate during the extrusion process, heating rates inside the oven, carbon yield in the final fiber, and homogeneity of properties considering that lignin comes from different sources.

Carbon fiber that has modulus between 40 GPa and 200 GPa is classified as low modulus and costs less than \$22/kg. It can be used for nonstructural applications (Prince Engineering, 2015). For aerospace and military applications, ultra-high modulus (600–965 GPa) CF is required, and its price reaches \$55/kg (Prince Engineering 2015). The papers published since the 1990s generally show an evolution in mechanical properties of the produced CF. In their study, Sudo & Shimizu, (1992) obtained lignin CF extracted by steam-explosion of birch wood chips reaching CF yields of about 15.7–17.4% in relation to the starting material. The values reported were: $7.6 \pm 2.7 \mu\text{m}$ fiber diameter, $1.63 \pm 0.19\%$ elongation, $660 \pm 230 \text{ MPa}$ tensile strength and $40.7 \pm 6.3 \text{ GPa}$ modulus of elasticity.

Ten years later, Kadla *et al.*, (2002), using lignin from soft and hardwood extracted by Kraft and organosolv methods, respectively, published the following values: $63 \pm 7 \mu\text{m}$ fiber diameter, $1.25 \pm 0.26\%$ elongation, $339 \pm 53 \text{ MPa}$ tensile strength and $33 \pm 2 \text{ GPa}$ modulus of elasticity. Additionally, these authors performed thermal extrusions, with and without PEO, at temperatures between 130 and 240 °C, concluding that the glass transition temperatures (T_g) of the polymer blend with PEO decreased, all organosolv

lignin-PEO fibers fused together on thermostabilization, and that hardwood Kraft lignin-PEO fibers with high PEO content were not thermally stable.

Ten years after that, this same research group, through the study published by Qin & Kadla, (2012), analyzed three types of lignin-based CF using organosolv lignin, Kraft lignin and pyrolytic lignin (from bio-oil from wood flour) as precursors. In this case, the authors reported 49 ± 1 μm fiber diameter, 412 ± 39 MPa tensile strength and 41 ± 3 GPa modulus.

Many other important papers in this area have been published recently. For instance, Lin *et al.*, (2012) used lignin isolated from cedar wood by a H_2SO_4 solution, Zhang & Ogale, (2014) and Thunga *et al.*, (2014) employed softwood Kraft lignin, and Wang *et al.* (2015), hardwood Kraft lignin. For their lignin-based CF, Lin *et al.*, (2012) reported 11.5 ± 2.0 μm fiber diameter, $2.0 \pm 0.5\%$ elongation, 441 ± 100 MPa tensile strength and 23.0 ± 5.4 GPa modulus of elasticity.

For their lignin-based CF, Zhang & Ogale (2014) showed average tensile modulus and strength of 52 ± 2 GPa and 1.04 ± 0.10 GPa, respectively, and concluded that the fibers would be more reactive than those with a graphitic structure, which is beneficial for composites. On the other hand, Thunga *et al.*, (2014) presented CF with high lignin content. They reported around 0.95 μm elongation, 32.0 GPa tensile strength and 32.5 GPa modulus of elasticity. In their study, Zhang *et al.*, (2015) reported a mean strength of 258.6 GPa and modulus of 1.7 GPa. In this work, the authors produced PLA-based blends reinforced by their lignin-based CF and concluded that strength decreased with the increase in PLA content, while the opposite happened to tensile modulus. Their CF presented voids because of the volatilization of PLA during heating.

1.4 Carbon Fibers from Other Sustainable Resources

Cellulose-based CF were developed as early as the 1950s, and several types of natural-based materials can be used as precursors to manufacture commercial grade CF, or at least activated CF. Although traditional lignocellulosic fibers such as ramie, sisal and hemp were used in the past as cellulosic precursor fibers, these fibers are no longer important sources of CF (Chand, 2000; Huang, 2009) (Thakur & Thakur, 2014b). The main constraint of these and other cellulosic precursors that still hinders their use is their low carbon yield.

CF obtained from cellulose precursors amounts to only around 1–2% of the total carbon fiber production (Zhang *et al.*, 2006). However, due to the increasing demand for a more “green engineering” approach towards a sustainable development, there is a renovated interest in renewable cellulosic CF precursors (Dumanli & Windle 2012).

Rayon, i.e., regenerated cellulose, was the basis for the development of CF in the late 1950s, but the interest in its use declined after the development of PAN-based fibers because PAN allows higher carbon yields and the hot stretching process of rayon fibers is costly (Dumanli & Windle, 2012). Also, PAN-based CF show superior physical properties compared to rayon-based fibers. Tensile properties of rayon-based CF are typically 1.25 GPa for strength and 170 GPa for Young’s modulus (Dumanli & Windle, 2012). Rayon-based CF typically show a very irregular surface, and this could partially account for their comparatively poor mechanical properties (Wu & Pan, 2002), i.e., 2.47 GPa for tensile strength and 221 GPa for Young’s modulus (Naito *et al.*, 2008).

Recently, improvements in processing of rayon-based CF, especially regarding a controlled microstructural change throughout stabilization and carbonization processes, lead to a better set of properties although still very low compared to PAN-based fibers (Park & Heo, 2015). These fibers are, in fact, better tailored to be the source of activated CF for non-structural applications, such as gas absorption applications (Huang, 2009). Park & Heo, (2015) showed that, during pyrolysis, an amorphous structure is generated, destroying the previous crystalline order of the cellulosic precursor, which is later recovered with carbonization under tension. Karacan & Soy, (2013) showed that microstructural control should begin in the very first steps of the treatment process of rayon fibers. They reported that boric acid–phosphoric acid impregnation enhanced thermal stability and minimized volatile by-products during oxidation of the fibers. An increase in char yield was thus obtained. They also mentioned that hot stretching during graphitization influences both structure and properties of these fibers (Zhang *et al.*, 2014).

Lyocell is also a purely cellulosic fiber spun from wood or from cotton pulp (Carrillo *et al.*, 2004). Carbon fibers using Lyocell as a precursor were developed by Wu & Pan, (2002). These fibers are considered a very suitable precursor because they have homogeneous circular cross section, with an average diameter of $10.0 \pm 0.9 \mu\text{m}$, and a smooth surface. The process to produce CF is similar to that from rayon viscose. According to Kong *et al.*, (2012), a typical methodology would follow these processes: stabilization in air at about 150–200 °C, carbonization at 1000 °C using inert argon atmosphere, and graphitization with coke dust medium at about 2500 °C. Lyocell-based CF with a uniform diameter of $7.5 \pm 0.9 \mu\text{m}$ were successfully produced using a two-stage thermal treatment (i.e., low temperature in air + high temperature in nitrogen), obtaining better mechanical properties than rayon-based CF due to their greater degree of crystallinity, more round cross-sections and less defects (Peng *et al.*, 2003). The tensile strength of these fibers was, however, low (around 900 MPa) compared to common CF, but high enough to be used in several composite parts where low to medium strength requirements are needed.

Bocell is a new thin high-modulus regenerated cellulose fiber with average diameter of about 11.8 μm . It shows Young's modulus within 46.6–60 GPa (Mottershead *et al.*, 2007; Gindl *et al.*, 2008), higher than that presented by Lyocell (around 23.4 GPa) (Adusumali *et al.*, 2006). Also, Bocell is a high strength fiber, in the 1.17–2.6 GPa range (Mottershead *et al.*, 2007; Gindl *et al.*, 2008). These properties are due to the high molecular alignment obtained by spinning the liquid crystalline solution of cellulose in phosphoric acid (Boerstoele *et al.*, 2001). The high orientation of the final structure obtained at the graphitization step is very attractive and is related to the crystallite size of the cellulose precursor (Kong *et al.*, 2012). Currently, pyrolyzed fibers present a skin-core structure consisting of a highly graphitized skin and a less graphitized inner core. Using Raman spectroscopy, Kong *et al.*, (2012) indicated that the skin could show a modulus of 140 GPa, against 40 GPa for the core. Although this skin-core structure is detrimental to high-strength, high-modulus applications, Bocell-derived CF are very promising for medium to high strength structural applications.

Several other natural polymers have been investigated as possible precursors for CF. Khan *et al.*, (2007) and Khan *et al.*, (2009) studied silk fibers, which were first treated with iodine vapor at 100 °C for 12 h and heated from 25 to 800 °C in a multi-stage carbonization process. The process conditions were established based on the optimum

thermal degradation rate of silk. The carbon yield of the process reached 36 wt%, and fibers with smooth surfaces but with irregular cross sections were obtained. Iodine treated fibers showed better tensile properties than untreated fibers, presenting a tensile strength up to 12.6 gf. Silk fibers could, therefore, be an interesting precursor since the process temperatures are low compared to those usual for PAN-based fibers (Chand, 2000).

Prauchner *et al.*, (2005) used eucalyptus tar pitches to produce CF. A four-step production process was chosen, with a final carbonization step at 1000 °C under nitrogen atmosphere. The obtained fibers had smooth surfaces but large diameter ($27 \pm 2 \mu\text{m}$) and low mechanical properties (130 MPa of tensile strength and 14 GPa of Young's modulus). The authors suggested the use of these fibers as felts for electrical insulation. It could be highlighted that this precursor is a bio-pitch, available as a by-product of the charcoal industry, and abundant on many countries.

The use of waste wood as raw material to manufacture CF was described by Lin *et al.* (1995) and Okabe *et al.*, (2005). They processed wood powder to obtain a phenolic resin, and this resin was blended with high density polyethylene (HDPE). The phenolic-HDPE polymer blend was mechanically homogenized and the fibers were obtained by melt-spinning. These fibers were stabilized using an acid solution and then carbonized under inert atmosphere at 1000 °C. During carbonization, HDPE was removed and fibers as thin as 1 μm were obtained. However, the obtained fibers presented a steady fraction of mesopores and were considered worthy only as activated CF.

Another possible natural precursor for CF is chitosan. Bengisu & Yilmaz, (2002) studied the oxidation and pyrolysis of chitosan fibers. The process used a maximum pyrolysis temperature of 700 °C and reached a carbon yield of ~20%, but the tensile strength of the fibers was very low (591 MPa). The authors proposed to stretch the fibers during the final pyrolysis step to enhance their mechanical properties. Schreiber *et al.*, (2014) used chitosan blended with lignin to produce fibers. Polyethylene oxide was used to aid the electro-spinning of the fibers and it was later removed by a washing process. The obtained chitosan-lignin blended fiber showed homogeneous distribution of both components throughout the fiber, and was cited as a feasible carbon fiber precursor.

Wool fibers are also being investigated as possible precursor for CF (Hassan *et al.*, 2015). As with other renewable precursors, a low yield was obtained, varying from 16.7% for an untreated fiber to 25.8% for a chemically treated fiber. Stabilization of the fibers was obtained by pyrolysis at 800 °C, but the tensile properties of treated or untreated fibers was low, varying between 143 to 219 MPa. The CF obtained were also very brittle, with an average tensile strain of 0.5%. The very irregular surface and cross-section of the obtained fiber is perhaps responsible for its low mechanical properties.

For last, Kim *et al.*, (2001) showed that high crystalline native cellulose samples can be conveniently heat-treated to obtain graphite structures following a graphitization step at 2000 °C. A three-dimensional crystalline order was produced when cellulose obtained from the outer shell of sea squirt *Halocynthia roretzi* (sea pineapple). Long graphite microfibrillar units were also observed when cellulose from the green alga,

Cladophora wrightiana, was used as precursor, indicating that certain regions of the original cellulose microfibrils retained their morphology after graphitization.

1.5 Concluding Remarks

The use of sustainable resources as precursor for carbon fibers is an alternative way to obtain less expensive fibers and to promote their use in comparison to glass and polymeric fibers. Regenerated cellulose and lignins from industrial wastes are the most common precursors due to their low cost, high carbon content and abundance. However, others sources such as chitosan, wood, and wool, along with more traditional rayon, presented interesting results.

The mechanical properties of bio-based CF showed improvement in the last ten to twenty years. However, they are still far from the properties obtained for PAN- and pitch-based fibers. In this sense, it is important to further optimize the processing of these fibers, for example manufacturing lignin-based carbon mats by melt-blown systems or electrospinning viscose rayon-based carbon fibers during graphitization.

Also, many natural resources require chemical modification in order to make them appropriate for processing and there may be large variations in the final properties of the carbon fibers derived from renewable resources. These factors undermine their utilization and lead to their use in less-demanding sectors. Nevertheless, a great effort has been devoted to these green carbon fibers and many researchers are working on related subjects. Perhaps these fibers will achieve greater application with more commercial competitiveness in the not too distant future.

References

- Adusumali, R.B., Reifferscheid, M., Weber, H., Röder, T., Sixta, H., Gindl, W., Mechanical properties of regenerated cellulose fibres for composites, *Macromolecular Symposis*, 244, 119, 2006.
- Ago, M., Okajima, K., Jakes, J.E., Park, S., Rojas, O.J., Lignin-Based Electrospun Nanofibers Reinforced with Cellulose Nanocrystals. *Biomacromolecules*, 13, 918, 2012.
- Agrawal, A., Kaushik, N., Biswas, S., Derivatives and Applications of Lignin – An Insight. *The Scitech Journal*, 1, 30, 2014.
- Areskog, D., Li, J., Gellerstedt, G., Henriksson, G., Investigation of the Molecular Weight Increase of Commercial Lignosulfonates by Laccase Catalysis. *Biomacromolecules*, 11, 904, 2010.
- Assmann, N., Werhan, H., Ładosz, A., Von Rohr, P.R., Supercritical extraction of lignin oxidation products in a microfluidic device. *Chem. Eng. Sci.*, 99, 177, 2013.
- Astner, A.F., Young, T.M., Bozell, J.J., Lignin yield maximization of mixed biorefinery feedstocks by organosolv fractionation using Taguchi Robust Product Design. *Biomass Bioenergy*, 73, 209, 2015.
- Badawy, M.E.I., Rabea, E.I., A Biopolymer Chitosan and Its Derivatives as Promising Antimicrobial Agents against Plant Pathogens and Their Applications in Crop Protection. *Int. J. Carbohydr. Chem.*, 2011, 1, 2011.
- Bendtsen, B.A., Properties of wood from improved and intensively managed trees. *Forest Products Journal*, 28, 61, 1978.
- Bengisu, M., Yilmaz, E., Oxidation and pyrolysis of chitosan as a route for carbon fiber derivation. *Carbohydr. Polym.*, 50, 165, 2002.

- Biermann, C.J., Pulping Fundamentals, in: *Handbook of Pulping and Papermaking*, C.J. Biermann (Ed.), pp. 55–100, Elsevier, San Diego, 1996.
- Bjorkman, A., Lignin and lignin-carbohydrate complexes - extraction from wood meal with neutral solvents. *Ind. Eng. Chem.*, 49, 1395, 1957.
- Björkman, A., Studies on finely divided wood. Part I. Extraction of lignin with neutral solvents. *Sven. Papperstidn*, 13, 477, 1956.
- Boerstol, H., Maatman, H., Westerink, J.B., Koenders, B.M., Liquid crystalline solutions of cellulose in phosphoric acid. *Polymer*, 42, 7371, 2001.
- Braun, J.L.; Holtman, K.M.; Kadla, J.F., Lignin-Based carbon fibers: Oxidative thermostabilization of kraft lignin. *Carbon*, 43, 385, 2005.
- Brebu, M., Vasile, C., Thermal Degradation Of Lignin – A Review. *Cellul. Chem. Technol.*, 44, 353, 2010.
- Bu, L., Tang, Y., Gao, Y., Jian, H., Jian, J., Comparative characterization of milled wood lignin from furfural residues and corncob. *Chem. Eng. J.*, 175, 176, 2011.
- Carrillo, F., Colom, X., Sunol, J.J., Saurina, J., Structural FTIR analysis and thermal characterisation of lyocell and viscose-type fibres. *Eur. Polym. J.*, 40, 2229, 2004.
- Chand, D., Review Carbon fibers for composites. *J. Mater. Sci.*, 35, 1303, 2000.
- Chang, H.M., Cowling, E.B., Brown, W., Adler, E., Miksche, G., Comparative studies on cellulolytic enzyme lignin and milled wood lignin of sweetgum and spruce. *Holzforschung*, 29, 153, 1975.
- Chang, J., Cheng, W., Yin, Q., Zuo, R., Song, A., Zheng, Q., Wang, P., Wang, X., Liu, J., Effect of steam explosion and microbial fermentation on cellulose and lignin degradation of corn stover. *Bioresour. Technol.*, 104, 587, 2012.
- Chatterjee, S., Clingenpeel, A., McKenna, A., Rios, O., Johs, A., Synthesis and characterization of lignin-based carbon materials with tunable microstructure. *RSC Adv.*, 4, 4743, 2014.
- Chen, H., Chemical Composition and Structure of Natural Lignocellulose, in: *Biotechnology of Lignocellulose*, H. Chen (Ed.), pp. 25–71, Springer, Beijing, 2014a.
- Chen, J., Synthetic Textile Fibers: Regenerated Cellulose Fibers, *Textiles and Fashion*, R. Sinclair (Ed.), pp. 79–95, Woodhead, Sawston, 2014b.
- Dai, D., Fan, M., Wood fibres as reinforcements in natural fibre composites: structure, properties, processing and applications, in: *Natural Fibre Composites*, A. Hodzic, R. Shanks (Eds.), pp. 3–65, Woodhead, Sawston, 2014.
- Dallmeyer, I., Lin, L.T., Li, Y., Ko, F., Kadla, J.F., Preparation and Characterization of Interconnected, Kraft Lignin-Based Carbon Fibrous Materials by Electrospinning. *Macromol. Mater. Eng.* 299, 540, 2014a.
- Dallmeyer, I., Ko, F., Kadla, J.F., Correlation of Elongational Fluid Properties to Fiber Diameter in Electrospinning of Softwood Kraft Lignin Solutions. *Ind. Eng. Chem. Res.*, 53, 2697, 2014b.
- Del Río, J.C., Rencoret, J., Marques, G., Li, J., Gellerstedt, G., Jimenez-Barbero, J., Martínez, A.T., Gutiérrez, A., Structural Characterization of the Lignin from Jute (*Corchorus capsularis*) Fibers. *J. Agric. Food Chem.*, 57, 10271, 2009.
- Dochia, M., Sirghie, C., Cotton fibers, in: *Handbook of Natural Fibres: Types, Properties and Factors Affecting Breeding and Cultivation*, R.M. Kozłowski (Ed.), pp. 11–23, Woodhead, Sawston, 2012.
- Dumanli, A.G., Windle, A. H., Carbon fibres from cellulosic precursors: a review. *J. Mater. Sci.*, 47, 4236, 2012.
- R.C Eckert and Z. Abdullah, Carbon Fiber from Kraft Softwood Lignin, US Patent 20080317661, assigned to Weyerhaeuser Co, 2008.
- Edie, D.D., The effect of processing on the structure and properties of carbon fibers. *Carbon*, 36, 345, 1998.

- T.A Edison, Eletric lamp, US Patent 223898 A, assigned to Thomas Alva Edison, 1980.
- Eichhorn, S.J., Young, R.J., The Young's modulus of a microcrystalline cellulose. *Cellulose*, 8, 197, 2001.
- El Mansouri, N.E., Yuan, Q., Huang, F., Characterization of alkaline lignins for use in phenol-formaldehyde and epoxy resins. *Bioresources*, 6, 2647, 2011.
- El Mansouri, N.E., Salvadó, J., Structural characterization of technical lignins for the production of adhesives: Application to lignosulfonate, kraft, sodaanthraquinone, organosolv and ethanol process lignins. *Ind. Crops Prod.*, 24, 8, 2006.
- El Hage, R., Brosse, N., Chrusciel, L., Sanchez, C., Sannigrahi, P., Ragauskas, A., Characterization of milled wood lignin and ethanol organosolv lignin from miscanthus. *Polym. Degrad. Stab.*, 94, 1632, 2009.
- Evert, R.F. (Ed.), *Esau's Plant Anatomy: meristems, cells, and tissues of the plant body: their structure, function, and development*, John Wiley & Sons, New Jersey, 2006.
- Fitzer, E., Pan-based carbon fibers - present state and trend of the technology from the viewpoint of possibilities and limits to influence and to control the fiber properties by the process parameters. *Carbon*, 27, 621, 1989.
- Food and Agriculture Organization of the United Nations (FAOSTAT), <http://faostat.fao.org/site/567/default.aspx#ancor>, 2012.
- Foston, M., Nunnery, G.A., Meng, X., Sun, Q., Baker, F.S., Ragauskas, A., NMR a critical tool to study the production of carbon fiber from lignin. *Carbon*, 52, 65, 2013.
- Fengel, D., Wegener, G. (Ed.), *Wood Chemistry, Ultrastructure and Reactions*, Walter De Gruyter, Berlin, 1989.
- Fink, H.P., Weigel, P., Purz, H.J., Ganster, J., Structure formation of regenerated cellulose materials from NMMO-solution. *Prog. Polym. Sci.*, 26, 1473, 2001.
- Fortier, P., Sui, S., Kreplak, L., Nanoscale Strain-Hardening of Keratin Fibres. *PloS One*, 7, 1, 2012.
- Frank, E., Steudle, L.M., Ingildeev, D., Spörl, J.M., Buchmeiser, M.R., Carbon Fibers: Precursor Systems, Processing, Structure, and Properties. *Angew. Chem. Int. Ed.*, 53, 2, 2014.
- Gandini, A., Polymers from Renewable Resources: A Challenge for the Future of Macromolecular Materials. *Macromolecules*, 41, 9491, 2008.
- García, A., Alriols, M.G., Llano-Ponte, R., Labidi, J., Energy and economic assessment of soda and organosolv biorefinery processes. *Biomass Bioenergy*, 35, 516, 2011.
- Gellerstedt, G., Gel permeation chromatography, in: *Methods in Lignin Chemistry*. S.Y. Lin, C.W. Dence (Eds.), pp. 487–497, Springer-Verlag, Heidelberg, 1992.
- Gellerstedt, G., Northey, R.A., Analysis of birch wood lignin by oxidative-degradation. *Wood Sci. Technol.*, 23, 75, 1989.
- Gindl, W., Reifferscheid, M., Adusumalli, R.B., Weber, H., Röder, T., Sixta, H., Schöberl, T., Anisotropy of the modulus of elasticity in regenerated cellulose fibres related to molecular orientation. *Polymer*, 49, 792, 2008.
- Gon, D., Das, K., Paul, P., Maity, S., Jute Composites as Wood Substitute. *International Journal of Textile Science*, 1, 84, 2012.
- Goundalkar, M.J., Corbett, D.B., Bujanovic, B.M., Comparative Analysis of Milled Wood Lignins (MWLs) Isolated from Sugar Maple (SM) and Hot-Water Extracted Sugar Maple (ESM). *Energies*, 7, 1363, 2014.
- Gregorová, A., Košíková, B., Moravčíková, R., Stabilization effect of lignin in natural rubber. *Polym. Degrad. Stab.*, 31, 229, 2006.
- Guerra, A., Filpponen, I., Lucia, L.A., Argyropoulos, D.S., Comparative Evaluation of Three Lignin Isolation Protocols for Various Wood Species. *J. Agric. Food Chem.*, 54, 9696, 2006.
- Gupta, B.S., Manufactured Textile Fibers, in: *Kent and Riegel's Handbook of Industrial Chemistry and Biotechnology*, A. Hent (Ed.), pp. 431–498, Springer-Verlag, New York, 2007.

- Hassan, M.M., Schiermeister, L., Staiger, M.P., Thermal, chemical and morphological properties of carbon fibres derived from chemically pre-treated wool fibres, *RSC Advances*, 5, 55353, 2015.
- Hayashi, J., Nakashima, M., Kusakabe, K., Morooka, S., Mitsuda, S., Rapid stabilization of pitch fiber precursor by multi-step thermal oxidation. *Carbon*, 33, 1567, 1995.
- Hellström, L.M., Gradin, P.A., Carlberg, T., A method for experimental investigation of the wood chipping process. *Nord. Pulp Paper Res. J.*, 23, 339, 2008.
- Hellström, L.M., Isaksson, P., Gradin, P.A., Eriksson, K., An analytical and numerical study of some aspects of the wood chipping process. *Nordic Pulp Paper Res. J.*, 24, 225, 2009.
- Hiltunen, E., Alvila, L., Pakkanen, T.T., Characterization of Brauns' lignin from fresh and vacuum-dried birch (*Betula pendula*) wood. *Wood Sci. Technol.*, 40, 575, 2006.
- Hu, S., Zhang, S., Pan, N., Hsieh, Y., High energy density supercapacitors from lignin derived submicron activated carbon fibers in aqueous electrolytes. *J. Power Sources*, 270, 106, 2014.
- Huang, X. Fabrication and Properties of Carbon Fibers. *Materials*, 2, 2369, 2009.
- Huang, Y., Ma, E., Zhao, G., Thermal and structure analysis on reaction mechanisms during the preparation of activated carbon fibers by KOH activation from liquefied wood-based fibers. *Ind. Crops Prod.*, 69, 447, 2015.
- Ikeda, T., Holtman, K., Kadla, J.F., Chang, H.M., Jameel, H., Studies on the Effect of Ball Milling on Lignin Structure Using a Modified DFRC Method. *J. Agric. Food Chem.*, 50, 129, 2002.
- Imura, Y., Hogan, R.M.C., Jaffe, M., Dry spinning of synthetic polymer fibers, in: *Advances in Filament Yarn Spinning of Textiles and Polymers*. D. Zhang (Ed.), pp. 187–202, Elsevier, New Jersey, 2014.
- Inagaki, M., Sakamoto, K., Hishiyama, Y., Carbonization and graphitization of polyimide Upilex. *J. Mater. Res.*, 6, 1108, 1991.
- Inagaki, M., Ibuki, T., Takeichi, T., Carbonization Behavior of Polyimide Films with Various Chemical Structures. *J. Appl. Polym. Sci.*, 44, 521, 1992.
- Jin, J., Yu, B., Shi, Z., Wang, C., Chong, C., Lignin-based electrospun carbon nanofibrous webs as free-standing and binder-free electrodes for sodium ion batteries. *J. Power Sources*, 272, 800, 2014a.
- Jin, J., Shi, Z., Wang, C., Electrochemical Performance of Electrospun carbon nanofibers as free-standing and binder-free anodes for Sodium-Ion and Lithium-Ion Batteries, *Electrochim. Acta*, 141, 302, 2014b.
- Kadla, J.F., Kubo, S., Venditti R.A., Gilbert, R.D., Compere, A.L., Griffith, W., Lignin-based carbon fibers for composite fiber applications. *Carbon*, 40, 2913, 2002.
- Kadolph, S.J., *Textiles*, pp.600, Prentice Hall, 2001.
- Karacan, I., Soy, T., Structure and properties of oxidatively stabilized viscose rayon fibers impregnated with boric acid and phosphoric acid prior to carbonization and activation steps. *J. Mater. Sci.*, 48, 2009, 2013.
- Khan, M.M.R., Gotoh, Y., Morikawa, H., Miura, M., Fujimori, Y., Nagura, M., Carbon fiber from natural biopolymer: Bombyx mori silk fibroin with iodine treatment, *Carbon*, 45, 1035, 2007.
- Khan, M.M.R., Gotoh, Y., Morikawa, H., Miura, M., Graphitization behavior of iodine-treated *Bombyx mori* silk fibroin fiber. *J. Mater. Sci.*, 44, 4235, 2009.
- Kim, D.Y., Nishiyama, Y., Wada, M., Kuga, S., Graphitization of highly crystalline cellulose. *Carbon*, 39, 1051, 2001.
- Kim, J.Y., Hwang, H., Oh, S., Choi, J.W., Structural features of lignin-rich solid residues obtained from two-step acid-hydrolysis of Miscanthus biomass (*Miscanthus sacchariflorus* Benth.). *J. Ind. Eng. Chem.*, 30, 302, 2015.
- Kipriotis, E., Heping, X., Vafeiadakis, T., Kiprioti, M., Alexopoulou, E., Ramie and kenaf as feed crops. *Ind. Crops Prod.*, 68, 126, 2015.

- Klinke, H.B., Ahring, B.K., Schmidt, A.S., Thomsen, A.B., Characterization of degradation products from alkaline wet oxidation of wheat straw. *Bioresour. Technol.*, 82, 15, 2002.
- Kong, K., Deng, L., Kinloch, I.A., Young, R.J., Eichhorn, S.J., Production of carbon fibres from a pyrolysed and graphitized liquid crystalline cellulose fibre precursor. *J. Mater. Sci.*, 47, 5402, 2012.
- Kubo, S., Kadla, J.F., Lignin-based Carbon Fibers: Effect of Synthetic Polymer Blending on Fiber Properties. *J. Polym. Environ.*, 13, 97, 2005.
- Kuffner, H., Popescu, C., Wool fibres, in: *Handbook of Natural Fibres: Types, Properties and Factors Affecting Breeding and Cultivation*, R.M. Kozłowski (Ed.), pp. 171–195, Woodhead, Sawston, 2012.
- Lai, C., Kolla, P., Zhao, Y., Fong, H., Smirnova, A.L., Lignin-derived electrospun carbon nanofiber mats with supercritically deposited Ag nanoparticles for oxygen reduction reaction in alkaline fuel cells. *Electrochim. Acta*, 130, 431, 2014a.
- Lai, C., Zhou, Z., Zhang, L., Wang, X., Zhou, Q., Zhao, Y., Wang, Y., Wu, X., Zhu, Z., Fong, H., Free-standing and mechanically flexible mats consisting of electrospun carbon nanofibers made from a natural product of alkali lignin as binder-free electrodes for high-performance supercapacitors. *J. Power Sources*, 247, 134, 2014b.
- Langholtz, M., Downing, M., Graham, R.L., Baker, F., Compere, A., Griffith, W., Lignin-Derived Carbon Fiber as a Co-Product of Refining Cellulosic Biomass. *SAE Int. J. Mater. Manf.*, 7, 115, 2014.
- Lewis, H. F.; Brauns, F. E.; Buchanan, M. A., Lignin esters of mono- and dibasic aliphatic acids. *Ind. Eng. Chem.*, 35, 1113, 1943.
- H.F Lewis and F.E Brauns, Esters of lignin material, US 2429102, assigned to Mead Corp, 1947.
- Li, H., Qu, Y., Yang, Y., Chang, S., Xu, J., Microwave irradiation – A green and efficient way to pretreat biomass. *Bioresour. Technol.*, 199, 34, 2015.
- Li, H., Yang, Y., Wen, Y., Liu, L., A mechanism study on preparation of rayon based carbon fibers with (NH₄)₂SO₄/NH₄Cl/organosilicon composite catalyst system. *Compos. Sci. Technol.* 67, 2675, 2007.
- Lin, J., Kubo, S., Yamada, T., Koda, K., Uraki, Y., Chemical Thermostabilization for the Preparation of Carbon Fibers from Softwood Lignin. *BioResources*, 7, 5634, 2012.
- Lin, L., Yoshioka, M., Yao, Y., Shiraishi, N., Preparation and properties of phenolated wood/phenol/formaldehyde cocondensed resin. *J. Appl. Polym. Sci.*, 58, 1297, 1995.
- Lin, X., Zhou, M., Wang, S., Lou, H., Yang, D., Qiu, X., Synthesis, Structure, and Dispersion Property of a Novel Lignin-Based Polyoxyethylene Ether from Kraft Lignin and Poly(ethylene glycol). *ACS Sustainable Chem. Eng.*, 7, 1902, 2014.
- Lourençon, T.V., Hansel, F.A., Silva, T.A., Ramos, L.P., Muniz, G.I.B., Magalhaes, W.L.E., Hardwood and softwood kraft lignins fractionation by simple sequential acid precipitation. *Sep. Purif. Technol.*, 154, 82, 2015.
- Luo, J., Genco, J., Cole, B., Fort, R., Lignin recovered from the near-neutral hemicellulose extraction process as a precursor for carbon fibers. *Bioresources*, 6, 4566, 2011.
- Mainka, H., Täger, O., Körner, E., Hilfert, L., Busse, S., Edelmann, F.T., Herrmann, A.S., Lignin – An alternative precursor for sustainable and cost-effective automotive carbon fiber. *J. Mater. Res. Technol.*, 4, 283, 2015.
- Maradur, S.P., Kim, C.H., Kimb, S.Y., Kim, B., Kim, W.C., Yang, K.S., Preparation of carbon fibers from a lignin copolymer with polyacrylonitrile. *Synth. Met.*, 162, 453, 2012.
- Martin-Sampedro, R., Capanema, C.A., Hoeger, I., Villar, J.C., Rojas, O.J., Lignin Changes after Steam Explosion and Laccase-Mediator Treatment of Eucalyptus Wood Chips. *J. Agric. Food Chem.*, 59, 8761, 2011.

- Matuana, L.M., Stark, N.M., The use of wood fibers as reinforcements in composites, *Biofiber Reinforcements in Composite Materials*. O. Faruk, M. Sain (Eds.), pp. 648–688, Elsevier, Sawston, 2015.
- Mavinkurve, A., Visser, S., Pennings, J., An initial evaluation of poly(vinylacetylene) as a carbon fiber precursor. *Carbon* 33, 757, 1995.
- Metreveli, P.K., Metreveli, A.K., Kholodkova, E.M., Ponomarev, A.V., Effect of an electron beam on the subsequent pyrogenic distillation of lignin and cellulose. *Radiat. Phys. Chem*, 96, 167, 2014.
- Miao, Q., Chen, L., Huang, L., Tian, C., Zheng, L., Ni, Y., A process for enhancing the accessibility and reactivity of hardwood kraft-based dissolving pulp for viscose rayon production by cellulose treatment. *Bioresour. Technol.* 154, 109, 2014.
- Mohanty, A., Misra, M., Hinrichsen, G., Biofibres, biodegradable polymers and biocomposites: an overview. *Macromol. Mater. Eng.* 276, 1, 2000.
- Momma, T., Liu, X., Osaka, T., Ushio, Y., Sawada, Y., Electrochemical modification of active carbon fiber electrode and its application to double-layer capacitor. *J. Power Sources*, 60, 249, 1996.
- Mora, E., Blanco, C., Prada, V., Santamaría, R., Granda, M., Menéndez, R., A study of pitch-based precursors for general purpose carbon fibres. *Carbon*, 40, 2719, 2002.
- Morgon, P. (Ed.), *Carbon Fibers and Their Composites*, Taylor & Francis, Boca Raton, 2005.
- Mottershead, B., Eichhorn, S.J., Deformation micromechanics of model regenerated cellulose fibre-epoxy/polyester composites. *Compos. Sci. Technol.* 67, 2150, 2007.
- Mura, S., Greppi, G., Malfatti, L., Lasio, B., Sanna, V., Mura, M.E., Marceddu, S., Lugliè, A., Multifunctionalization of wool fabrics through nanoparticles: A chemical route towards smart textiles. *J. Colloid Interface Sci.* 456, 85, 2015.
- Naito, K., Tanaka, Y., Yang, J.M., Kagawa, Y., Tensile properties of ultrahigh strength PAN-based, ultrahigh modulus pitch-based and high ductility pitch-based carbon fibers. *Carbon*, 46, 189, 2008.
- Nordström, Y., Norberg, I., Sjöholm, E., Drougge, R., A New Softening Agent for Melt Spinning of Softwood Kraft Lignin. *J. Appl. Polym. Sci.*, 129, 1274, 2013a.
- Nordström, Y., Joffe, R., Sjöholm, E., Mechanical Characterization and Application of Weibull Statistics to the Strength of Softwood Lignin-Based Carbon Fibers. *J. Appl. Polym. Sci.*, 130, 3689, 2013b.
- Nwe, N., Furuike, T., Tamura, H., Isolation and Characterization of Chitin and Chitosan from Marine Origin. *Adv. Food Nutr. Res.* 72, 1, 2014.
- Okabe, K., Yao, T., Shiraishi, N., Oya, A., Preparation of thin carbon fibers from waste wood-derived phenolic resin. *J. Mater. Sci.*, 40, 3847, 2005.
- Oroumei, A., Fox, B., Naebe, M., Thermal and Rheological Characteristics of Biobased Carbon Fiber Precursor Derived from Low Molecular Weight Organosolv Lignin. *ACS Sustainable Chem. Eng.*, 3, 758–769, 2015.
- S Otani, Y Fukuoka, B Igarashi and K Sasaki, Method for producing carbonized lignin fiber, US3461082 A, assigned to Nippon Kayaku Kk, 1969.
- Paananen, M., Sixta, H., High-alkali low-temperature polysulfide pulping (HALT) of Scots pine. *Bioresour. Technol.* 193, 97, 2015.
- Pande, P.K., Influence of growth, wood anatomical properties and specific gravity on heartwood, sapwood and tension-wood in *Dalbergia sissoo* Roxb. *J. Indian Acad. Wood Sci.* 10, 16, 2013.
- Pappu, A., Patil, V., Jain, S., Mahindrakar, A., Haque, R., Thakur, V.K., Advances in industrial prospective of cellulosic macromolecules enriched banana biofibre resources: A review. *Int. J. Biol. Macromol.* 79, 449, 2015.

- Park, S.J., Heo, G.Y., Precursors and Manufacturing of Carbon Fibers, *Carbon Fibers*, S.J. Park (Ed.), pp. 31–66, Springer-Verlag, Dortrecht, 2015.
- Pelaez-Samaniego, M.R., Yadama, V., García-Perez, M., Lowell, E., Abundance and characteristics of lignin liquid intermediates in wood (*Pinus ponderosa* Dougl. ex Laws.) during hot water extraction. *Biomass Bioenergy* 81, 117, 2015.
- Peng, S., Shao, H., Hu, X., 2003. Lyocell Fibers as the Precursor of Carbon Fibers. *J. Appl. Polym. Sci.*, 90, 1941.
- Perepelkin, K.E., Lyocell fibres based on direct dissolution of cellulose in n-methylmorpholine n-oxide: Development and prospects. *Fibre Chem.* 39, 58, 2007.
- Perepelkin, K.E., Lyocell fibres based on direct dissolution of cellulose in N-methylmorpholine N-oxide: Development and prospects. *Fibre Chem.*, 39, 163, 2007.
- Piló-Veloso, D., Isolamento e análise estrutural de ligninas. *Quím. Nova*, 16, 435, 1993.
- Plaisantin, H., Pailler, R., Guette, A., Daudé, G., Pétraud, M., Barbe, B., Birot, M., Pillot, J.P., Olry, P., Conversion of cellulosic fibres into carbon fibres: a study of the mechanical properties and correlation with chemical structure. *Compos. Sci. Technol.* 61, 2063, 2001.
- Popescu, C., Hoecker, H., Hair: The most sophisticated biological composite material. *Chem. Soc. Rev.* 36, 1282, 2007.
- Prauchner, M.J., Pasa, V.M.D., Otani, S., Otani, C., Biopitch-based general purpose carbon fibers: Processing and properties. *Carbon*, 43, 591, 2005.
- Prince Engineering, <http://www.build-on-prince.com/carbon-fiber.html#sthash.TjU9kCmB.dpbs>, 2015.
- Qin, W., Kadla, J.F., Carbon Fibers Based on Pyrolytic Lignin. *J. Appl. Polym. Sci.*, 126, 203, 2012.
- Rana, S., Pichandi, S., Parveen, S., Fanguero, R., Regenerated Cellulosic Fibers and Their Implications on Sustainability, in: *Roadmap to Sustainable Textiles and Clothing*, S.S. Muthu (Ed.), Springer-Verlag, Singapore, 2014.
- Reinhardt, M., Kaufmann, J., Kausch, M., Kroll, L., PLA-viscose-composites with continuous fibre reinforcement for structural applications. *Procedia Mater. Sci.*, 2, 137, 2013.
- Rencoret, J., Marques, G., Gutiérrez, A., Nieto, L., Jiménez-Barbero, J., Martínez, A.T., Del Río, J.C., Isolation and structural characterization of the milled-wood lignin from *Paulownia fortunei* wood. *Ind. Crops Prod.*, 30, 137, 2009.
- Rinaudo, M., Chitin and chitosan: Properties and applications. *Prog. Polym. Sci.*, 31, 603, 2006.
- Rosenau, T., Potthast, A., Sixta, H., Kosma, P., The chemistry of side reactions and byproduct formation in the system NMMO/cellulose (Lyocell process). *Prog. Polym. Sci.*, 26, 1763, 2001.
- Rowell, R.M., Pettersen, R., Tshabalala, M.A., Cell Wall Chemistry, in: *Handbook of Wood Chemistry and Wood Composites*, R.M. Rowell (Ed.), pp. 33–74, Taylor & Francis, Boca Raton, 2012.
- Roy, S., Lutfar, L.B., Bast fibres: jute, in: *Handbook of Natural Fibres: Types, Properties and Factors Affecting Breeding and Cultivation*, R.M. Kozłowski (Ed.), pp. 24–46, Woodhead, Sawston, 2012a.
- Roy, S., Lutfar, L.B., Bast fibres: ramie, in: *Handbook of Natural Fibres: Types, Properties and Factors Affecting Breeding and Cultivation*, R.M. Kozłowski (Ed.), pp. 47–55, Woodhead, Sawston, 2012b.
- Ruan, D., Zhang, L., Zhou, J., Jin, H., Chen, H., Structure and Properties of Novel Fibers Spun from Cellulose in NaOH/Thiourea Aqueous Solution. *Macromol. Biosci.*, 4, 1105, 2004.
- Ruiz-Rosas, R., Bedia, J., Lallave, M., Loscertales, I.G., Barrero, A., Rodríguez-Mirasol, J., Cordero, T., The production of submicron diameter carbon fibers by the electrospinning of lignin, *Carbon*, 48, 695, 2010.
- Sadeghifar, H., Cui, C., Argyropoulos, D.S., Toward Thermoplastic Lignin Polymers. Part 1. Selective Masking of Phenolic Hydroxyl Groups in Kraft Lignins via Methylation and Oxypropylation Chemistries. *Ind. Eng. Chem. Res.*, 51, 16713, 2012.

- Sannigrahi, P., Pu, Y., Ragauskas, A., Cellulosic biorefineries—unleashing lignin opportunities. *Current Opinion in Environmental Sustainability*, 2, 383, 2010.
- Santos, P.S.B., Cademartori, P.H.G., Prado, R., Gatto, D.A., Labidi, J., Composition and structure of organosolv lignins from four eucalypt species. *Wood Sci. Technol.*, 48, 873, 2014.
- Schreiber, M., Vivekanandhan, S., Cooke, P., Mohanty, A.K., Misra, M., Electrospun green fibres from lignin and chitosan: a novel polycomplexation process for the production of lignin-based fibres, *J. Mater. Sci.*, 49, 7949, 2014.
- Sen, T., Reddy, H.J., Various industrial applications of hemp, kinaf, flax and ramie natural fibres. *International Journal of Innovation, Management and Technology*, 2, 192, 2011.
- Sibaja, B., Culbertson, E., Marshall, P., Boy, R., Broughton, R.M., Solano, A.A., Esquivel, M., Parker, J., De La Fuente, L., Auad, M.L., Preparation of alginate–chitosan fibers with potential biomedical applications. *Carbohydr. Polym.*, 134, 598, 2015.
- Siller, M., Ahn, K., Pircher, N., Rosenau, T., Potthast, A. Dissolution of rayon fibers for size exclusion chromatography: a challenge. *Cellulose*, 21, 3291, 2014.
- Silva, R., Haraguchi, S.H., Muniz, E.C., Rubira, A.F., Aplicações de fibras lignocelulósicas na química de polímeros e em compósitos. *Quim. Nova*, 32, 661, 2009.
- Singha, K., Importance of the Phase Diagram in Lyocell Fiber Spinning. *International Journal of Material Engineering*, 2, 10, 2012.
- Singha, A.S., Thakur, V.K., Study of mechanical properties of urea-formaldehyde thermosets reinforced by pine needle powder. *BioResources* 4, 292, 2009.
- Sixta, H., Iakovlev, M., Testova, L., Roselli, A., Hummel, M., Borrega, M., Van Heiningen, A., Froschauer, C., Schottenberger, H., Novel concepts of dissolving pulp production. *Cellulose*, 20, 1547, 2013.
- Singha, A.S., Thakur, V.K., Mechanical, Morphological, and Thermal Characterization of Compression-Molded Polymer Biocomposites. *Int. J. Polym. Anal. Charact.* 15, 87, 2010.
- Sudo, K., Shimizu, K., A New Carbon Fiber from Lignin. *J. Appl. Polym. Sci.* 44, 127, 1992.
- Szymańska, E., Winnicka, K., Stability of Chitosan—A Challenge for Pharmaceutical and Biomedical Applications. *Mar. Drugs*, 13, 1819, 2015.
- Tajik, H., Moradi, M., Rohani, S.M., Erfani, A.M., Jalali, F.S., Preparation of chitosan from brine shrimp (*Artemia urmiana*) cyst shells and effects of different chemical processing sequences on the physicochemical and functional properties of the product. *Molecules*, 13, 1263, 2008.
- Teng, N., Dallmeyer, I., Kadla, J.F., Incorporation of Multiwalled Carbon Nanotubes into Electrospun Softwood Kraft Lignin-Based Fibers. *J. Wood Chem. Technol.*, 33, 299, 2013.
- Thakur, V.K., Thakur, M.K., Recent Advances in Graft Copolymerization and Applications of Chitosan: A Review. *ACS Sustain. Chem. Eng.* 2, 2637, 2014a.
- Thakur, V.K., Thakur, M.K., Processing and characterization of natural cellulose fibers/thermoset polymer composites. *Carbohydr. Polym.* 109, 102, 2014b.
- Thakur, V.K., Thakur, M.K., Raghavan, P., Kessler, M.R., Progress in Green Polymer Composites from Lignin for Multifunctional Applications: A Review. *ACS Sustainable Chem. Eng.*, 2, 1072, 2014.
- Thakur, V.K., Thakur, M.K., Recent advances in green hydrogels from lignin: a review. *Int. J. Biol. Macromol.* 72, 834–847, 2015.
- Thunga, M., Chen, K., Grewell, D., Kessler, M.R., Bio-renewable precursor fibers from lignin/poly lactide blends for conversion to carbon fibers. *Carbon* 68, 159, 2014.
- Tondi, G., Pizzi, A., Tannin-based rigid foams: Characterization and modification. *Ind. Crops Prod.*, 29, 356, 2009.
- Trung, T.S., Bao, H.N.D., Physicochemical Properties and Antioxidant Activity of Chitin and Chitosan Prepared from Pacific White Shrimp Waste. *Int. J. Carbohydr. Chem.*, 2015, 1, 2015.

- Voicu, S.I., Condruz, R.M., Mitran, V., Cimpean, A., Miculescu, F., Andronesu, C., Miculescu, M., Thakur, V.K., Sericin Covalent Immobilization onto Cellulose Acetate Membrane for Biomedical Applications. *ACS Sustain. Chem. Eng.* 4, 1765, 2016.
- Wang, J., Yue, Z.B., Chen, T.H., Peng, S.C., Yu, H.Q., Chen, H.Z., Anaerobic digestibility and fiber composition of bulrush in response to steam explosion. *Bioresour. Technol.*, 101, 6610, 2010.
- Wang, S., Li, Y., Xiang, H., Zhou, Z., Chang, T., Zhu, M., Low cost carbon fibers from bio-renewable Lignin/Poly(lactic acid) (PLA) blends. *Compos. Sci. Technol.* 119, 20, 2015.
- Wazir, A.H., Kakakhel, L., Preparation and characterization of pitch-based carbon fibers. *New Carbon Materials*, 24, 83, 2009.
- White, T.L., Paulauskas, F.L., Bigelow, T.S., System to continuously produce carbon fiber via microwave assisted plasma processing, US 20140205511 A1, assigned to Ut-Battelle, 2014.
- Wiedenhoef, A., Structure and Function of Wood, in: *Wood handbook - Wood as an engineering material*, R.J. Ross (Ed.), pp. 1–16, Forest Products Laboratory, Wisconsin, 2010.
- Wu, H., Fan, S.W., Yuan, X.W., Chen, L.F., Deng J.L., Fabrication of carbon fibers from jute fibers by pre-oxidation and carbonization. *New Carbon Materials*, 28, 448, 2013.
- Wu, Q., Pan, D., A new cellulose based carbon fiber from a lyocell precursor, *Text. Res. J.*, 72, 405, 2002.
- Xiaojun, M., Guangjie, Z., Preparation of carbon fibers from liquefied wood. *Wood Sci. Technol.*, 44, 3, 2010.
- Xu, H., Yu, G., Mu, X., Zhang, C., DeRoussel, P., Liu, C., Li, B., Wang, H., Effect and characterization of sodium lignosulfonate on alkali pretreatment for enhancing enzymatic saccharification of corn stover. *Ind. Crops Prod.*, 76, 638, 2015.
- Xu, X., Zhou, J., Jiang, L., Lubineau, G., Chen, Y., Wu, X., Piere, R., Porous core-shell carbon fibers derived from lignin and cellulose nanofibrils. *Mater. Lett.*, 109, 175, 2013.
- Xu, X., Zhou, J., Jiang, L., Lubineau, G., Payne, S.A., Gutschmidt, D., Lignin-based carbon fibers: Carbon nanotube decoration and superior thermal stability. *Carbon*, 80, 91, 2014.
- Zhang, H., Guo, L., Shao, H., Hu, X., Nano-Carbon black filled lyocell fiber as a precursor for carbon fiber. *J. Appl. Polym. Sci.*, 99, 65, 2006.
- Zhang, M., Ogale, A.A., Carbon fibers from dry-spinning of acetylated softwood kraft lignin, *Carbon*, 69, 626, 2014.
- Zhang, Q., Zhang, W., Huang, J., Lai, Y., Xing, T., Chen, G., Jin, W., Liu, H., Sun, B., Flame retardance and thermal stability of wool fabric treated by boron containing silica sols. *Mater. Des.*, 85, 796, 2015a.
- Zhang, P., Dong, S.J., Ma, H.H., Zhang, B.X., Wang, Y.F., Fractionation of corn stover into cellulose, hemicellulose and lignin using a series of ionic liquids. *Ind. Crops Prod.*, 76, 688, 2015b.
- Zhang, X., Lu, Y., Xiao, H., Peterlik, H., Effect of hot stretching graphitization on the structure and mechanical properties of rayon-based carbon fibers, *J. Mater. Sci.*, 49, 673, 2014.
- Zhou, X., Ghaffar, S.H., Dong, W., Oladiran, O., Fan, M., Fracture and impact properties of short discrete jute fibre-reinforced cementitious composites. *Mater. Des.*, 49, 35, 2013.
- Zoltek™ Carbon Fiber, <http://zoltek.com/carbonfiber/the-future-of-carbon-fiber>, 2015.

Polylactic Acid Composites and Composite Foams Based on Natural Fibers

A.A. Pérez-Fonseca^{1,2}, H. Teymoorzadeh¹, J.R. Robledo-Ortíz³, R. González-Núñez²
and D. Rodrigue^{1*}

¹*Department of Chemical Engineering and CERMA, Université Laval, Quebec City, Canada*

²*Departamento de Ingeniería Química, Universidad de Guadalajara, Guadalajara, Jalisco, México*

³*Departamento de Madera, Celulosa y Papel, Universidad de Guadalajara, Las Agujas, Zapopan, Jalisco, México*

Abstract

Polylactic acid (PLA) is a well-known and commercially available biopolymer that can be produced from different sources. Although PLA has several advantages like good rigidity and strength, it also has some drawbacks like brittleness and low thermal stability. To improve the use of PLA, several avenues have been investigated but the addition of natural fibers (lignocellulosic materials) is an interesting way to get fully biodegradable materials using 100% bio-sourced components. Furthermore, to reduce weight for applications like material handling, packaging and automotive applications, weight reduction is highly important and can be achieved through foaming. In this chapter, a review of the literature is presented for PLA based composites and composite foams using different sources of natural reinforcement. In each case, the morphological, thermal, physical and mechanical properties are reported, discussed and compared. Finally, thermal annealing is presented as a way to control PLA crystallinity and modify the thermo-mechanical behavior of the final parts in terms of strength, rigidity and stability.

Keywords: Polylactic acid, natural fibers, composites, foams, processing, morphology, mechanical properties

2.1 Introduction

The high consumption of petroleum resources, solid waste disposal problems and emissions during incineration combined with increasing environmental regulations have led to increased interest in the development of compostable polymers compatible with the environment and not based on fossil fuels (Thakur & Thakur, 2014 a, b). One possible solution is to use bio-based materials containing a high content of derivatives from renewable biomass to ensure a sustainable future (Pilla, 2011) (Pappu *et al.*, 2015)

*Corresponding author: Denis.Rodrigue@gch.ulaval.ca

(Voicu *et al.*, 2016). Studies on polymer matrices being environmentally friendly focused on biopolymers like thermoplastic starch (TPS), polylactic acid (PLA), polycaprolactone (PCL) and polyhydroxybutyrate (PHB) (Nampoothiri *et al.*, 2010).

PLA is really the first viable thermoplastic that can be processed by conventional melt processing technologies and being produced at large industrial scale as well as being biodegradable (Rehmat *et al.*, 2012). An estimated annual production capacity of about 800,000 tons of polylactic acid (PLA) is expected for 2020 (Carus, 2012).

PLA is a linear aliphatic thermoplastic polyester made from 100% renewable resources like sugar, corn, potatoes, beet, etc. (Armentano *et al.*, 2013). PLA is actually the most used biopolymer in food packaging for short shelf-life products due to its high mechanical strength, easy processability, good transparency, availability and low cost (Arrieta *et al.*, 2014).

PLA can be produced by direct condensation of lactic acid or by a ring-opening polymerization of the cyclic lactide dimer, as presented in Figure 2.1. Condensation polymerization (polycondensation) is the least expensive method, and includes solution polycondensation and melt polycondensation. Nevertheless, it is difficult to obtain a solvent-free high molecular weight PLA from these routes (Garlota, 2001). In direct polycondensation, solvents and/or catalysts are used under high vacuum and temperature for water removal (Lasprilla *et al.*, 2012). The resulting polymer is a low/intermediate molecular weight polymer, which can be used directly or coupled with isocyanates, epoxides or peroxides to get a wide range of molecular weight (Gupta *et al.*, 2007). In order to increase molecular weight, chain-coupling agents are added, as these will mostly react with hydroxyl or carboxyl groups.

Ring-opening polymerization (ROP) is the most common route to achieve high molecular weight PLA. This process involves the ring opening of the lactic acid cyclic dimer (lactide) with a catalyst. The process comprises three steps: polycondensation, depolymerization and ring opening polymerization. This route requires additional purification steps that are relatively complex and expensive. Careful control of residence time and temperature, as well as catalyst type and concentration can control the ratio and sequence of D- and L-lactic acid units (Lasprilla *et al.*, 2012).

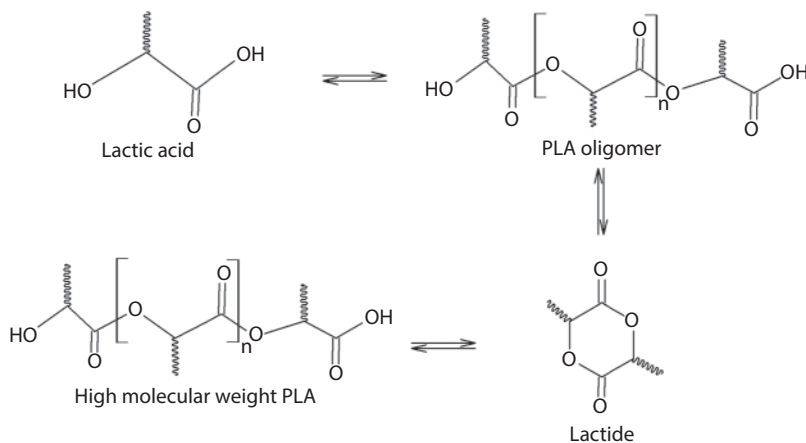


Figure 2.1 Condensation and ring opening PLA polymerization.

PLA can be amorphous or semi-crystalline depending on its stereochemistry and thermal history (Lim *et al.*, 2008). Its high brittleness, poor crystallization behavior and low gas barrier properties limits its current application (Rasal *et al.*, 2010). This is why several investigations were devoted to overcome these limitations. The most common ones are addition of particles, additives and plasticizers, as well as copolymerization and blending with other polymers.

Some studies focused on using plasticizers for PLA. The plasticizers must be miscible with the polymer matrix and stable at high temperature needed for processing and provide appropriate mechanical and barrier properties (Arrieta *et al.*, 2014). Martin & Averous (2001) used glycerol, citrate ester, polyethylene glycol (PEG) and oligomeric lactic acid (OLA) as plasticizers. They found that OLA and PEG gave the best results with 20% content. Decreases in T_g were from 58 to 8 and 12 °C, respectively. Oksman *et al.*, (2003) used triacetin (glycerol triacetate ester) as a plasticizer and found that the addition of 15% resulted in increased elongation at break, but lower tensile strength. Ljunberg & Wesslen, (2002) also used different plasticizers and reported T_g decreases of 10 °C at 25% for triacetin or tributyl citrate.

PLA has been copolymerized with a wide range of polyesters and different monomers by polycondensation of lactic acid, producing low molecular weight copolymers. Another possibility is via ring opening copolymerization of lactide with cyclic monomers like glycolide, ϵ -caprolactone, δ -valerolactone, trimethylene carbonate, as well as linear monomers like ethylene glycol producing high molecular weight copolymers (Rasal *et al.*, 2010). Arrieta *et al.*, (2013) prepared polylactic acid-polyhydroxybutyrate (PLA-PHB) blends for food packaging using two different plasticizers: poly(ethylene glycol) (PEG) and acetyl-tri-n-butyl citrate (ATBC) to improve on the natural brittleness of both biopolymers. The blends were disintegrated under composting conditions in less than one month, showing their biodegradable character. The ability of PHB to act as nucleating agent in PLA/PHB blends delayed PLA disintegration, while plasticizers increased it. Loureiro *et al.*, (2013) evaluated PLA/PHA blends and used different models to predict their tensile and flexural properties. It was shown that good adhesion between both phases was obtained, but at lower PHA contents (less than 30%) the experimental data deviates from the perfect adhesion models, suggesting a decreased adhesion between both polymers. The addition of PHA in the blend led to lower flexural modulus, but higher tensile modulus.

PLA degradation occurs via two main stages: hydrolytic and enzymatic degradation. Hydrolysis starts with the diffusion of water into the polymer and leads to random non-enzymatic chain scissions of the ester groups. The cleavage of ester linkages results in oligomers formation and lactic acid which can be assimilated by fungi and bacteria (Armentano *et al.*, 2013).

2.2 PLA-Natural Fibers Composites

During the last decades, the use of natural fiber to produce reinforced polymer composites has been attracting attention with the purpose of reducing the impact on the environment (Thomas & Pothan, 2009; Pilla, 2011) (Thakur & Kessler, 2015). Composites based on PLA and natural fibers have been the topic of several review papers (Yu *et al.*, 2006;

Sahari & Sapuan, 2011; Bajpai *et al.*, 2014). These reviews presented the development of bio-composites in terms of their mechanical properties, where the combination of natural fibers and PLA offers a sustainable development of economical and ecological technology. Due to increased environmental concern, the industries are looking for more ecologically friendly bio-based materials for interior and outdoor applications. This is why natural fiber-reinforced composites can have great potential (Baghei *et al.*, 2013). For PLA, the use of natural fibers as reinforcement can overcome some disadvantages such as thermal and mechanical instability at higher temperature due to its low softening point of around 60 °C which it is not suitable for high performance applications (Baheti *et al.*, 2013) and reduction of the brittle behavior of the composites (Pappu *et al.*, 2015).

2.2.1 Morphology

Figure 2.2 shows that the quality of the PLA-fiber interface is better compared with the interface of non-degradable polymers (polyethylene or polypropylene) for neat natural fibers. Nevertheless, the adhesion between PLA and fiber is not optimum. PLA is a polymer with polar oxygen atoms that could form hydrogen bonds with the hydroxyl groups of natural fibers (Baghaei *et al.*, 2013). Therefore, PLA-fiber interactions are expected to be much better than in most non-polar polymers which are generally hydrophobic. However, from the results reported in the literature it can be assumed that these hydrogen bonds only have a limited influence on the fiber/matrix adhesion or that interaction between the polar groups cannot occur during processing because of the macromolecular structure of cellulose, hemicellulose and lignin that are the main components of natural fibers (Bax & Mussig, 2008). Csikos *et al.*, (2015) used maleic anhydride grafted to PLA (MAPLA) to improve the fiber-matrix adhesion in PLA-wood (30% fiber) composites and observed that there was no trace of debonding

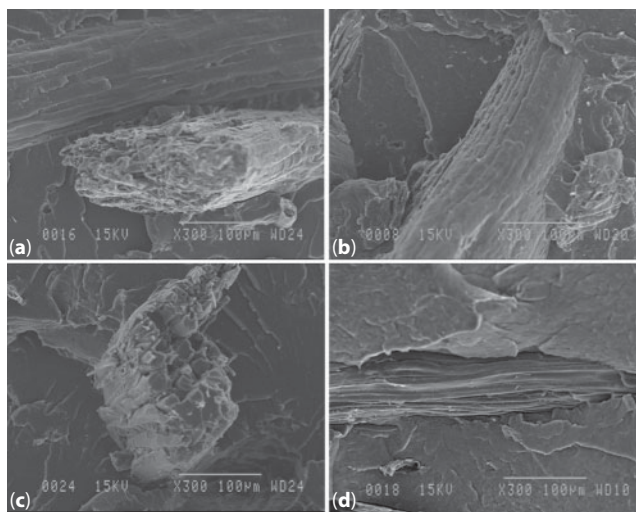


Figure 2.2 SEM micrographs of PLA composites: (a) agave, (b) coir, (c) pine, and (d) composite of HDPE + agave.

or pull-out in the composites containing coupling agents. Based on their results they reported that in composites containing MAPLA, fiber fracture was the dominating failure process. Faludi *et al.*, (2013) used 1,1-(methylenedi-4,1-phenylene) bismaleimide (DBMI) to improve interfacial adhesion between PLA and wood. They observed by SEM that debonding and fiber pull-out was very limited and the main deformation mechanism is the fiber fracture. Ma & Joo (2011) found that processing temperatures influence the fiber-matrix adhesion. For PLA-jute composites, voids were easily seen at processing temperatures of 200 and 210 °C indicating poor interfacial bonding, while no voids were observed at 220 °C.

2.2.2 Thermal Properties of PLA-Natural Fiber Composites

Adding fiber to PLA can have different effects depending on parameters such as processing conditions and type of fiber. Typical T_g values for neat PLA are around 60 °C (Lim *et al.*, 2013). For agave, coir and pine based composites, T_g values are similar to neat PLA (similar results reported by Mofokeng *et al.*, 2011), while by using flax or maple fibers the T_g decreased with the addition of fiber. Lee *et al.*, (2008) found a 2.5 °C decrease for composites with 40% wood and stated that T_g values are dependent on molecular characteristics and composition, as well as compatibility of the components in the amorphous matrix. Some authors have found increased T_g values due to fiber addition. Mathew *et al.*, (2006) worked with microcrystalline cellulose (MCC), cellulose fibers (CF) and wood flour (WF) at 25% showing increases from 54.1 °C (neat PLA) to 56.6, 57.5 and 58.3 °C, respectively. Chun & Husseinsyah (2013) prepared composites with corn cob and found increases from 57.7 to 58.3 and 59.3 °C for 20 and 40% fiber, respectively. They attributed this behavior to polymer relaxation that was delayed by the presence of reinforcements and lower chain mobility due to increased crystallinity.

PLA can exhibit a single or two endothermic melting peaks, and one exothermic crystallization peak as presented in Figure 2.3 (thermal treatment by annealing is discussed in Section 2.4). The appearance of these peaks is related to different factors

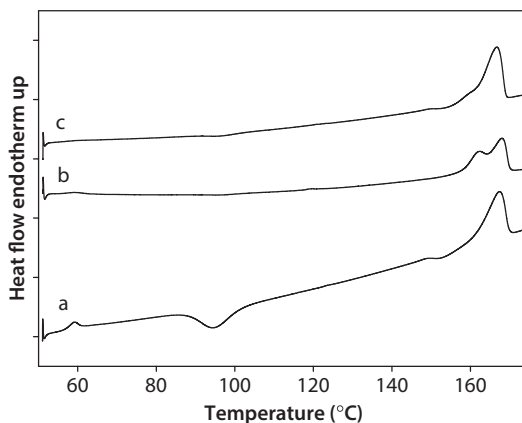


Figure 2.3 DSC thermograms of PLA-wood (maple) composites: (a) neat composite, (b) composite annealed at 105 °C for 2 minutes, and (c) composite annealed at 105 °C for 30 minutes.

Table 2.1 Transition temperatures (T_g , T_m and T_c) of PLA-natural fiber composites.

Samples	Fiber content (%)	T_g (°C)	T_m (°C)	T_c (°C)	Reference
PLA		59.9	167.2	96.0	Pérez-Fonseca <i>et al.</i> , (2015)
Agave	10	60.2	167.5	93.5	
	20	59.8	166.7	93.5	
	30	60.0	166.4	93.5	
Coir	10	61.0	167.2	94.0	
	20	60.6	167.0	94.0	
	30	60.3	166.8	92.0	
Pine	10	60.1	166.7	96.0	
	20	58.9	166.6	97.0	
	30	59.7	165.4	97.5	
PLA		62.0	170.0	99.0	Teymoorzadeh & Rodrigue (2014, 2015)
Maple	15	56.9	168.0	94.6	
	25	57.6	164.8	91.6	
	40	55.3	165.9	–	
Flax	10	59.0	166.0	95.0	
	25	60.0	168.0	95.0	
	40	60.0	167.0	93.0	

such as thermo-mechanical conditions, sample composition, nature of the filler, PLA molecular weight and the time-temperature history of the sample (Way *et al.*, 2012). The explanation for double melting includes the presence of two distinct lamellar populations or the possibility of melting-recrystallization-melting phenomena (molecular reorganization during the scan), or imperfect crystals changing into more stable structures via a melt recrystallization mechanism leading to a second endotherm at higher temperature (Shi & Dou, 2014). Usually, fiber addition (like any solid particles) causes a slight T_m reduction of the PLA matrix as reported for different natural fibers in Table 2.1. This reduction in T_m may be related to a lower molecular weight, but this may also be offset by the presence of fibers restricting PLA chain mobility (Harmaen *et al.*, 2014).

The crystallization peak of neat PLA is usually observed around 95 °C (Pantani *et al.*, 2010). As reported in Table 2.1, the crystallization temperature of PLA decreases with fiber addition, with the exception of pine fibers. When fibers are used as reinforcement, crystal formation can be initiated at different locations: fiber surface (heterogeneous crystallization or trans-crystallization) or defects in the composites (interface) depending on the fiber type (Mathew *et al.*, 2006). Reduced induction time for semi-crystalline polymers with fibers can also be associated with fiber surface roughness, which can play a key role at increasing crystal nuclei density (Arias *et al.*, 2013). On the other hand, increased crystallization temperature can be associated to the fibers acting as nucleation sites for crystallization or restricting the mobility of polymer chains. Mofokeng *et al.*, (2011) reported that increasing the amount of fibers made the immobilization effect dominant.

PLA can be semi-crystalline or totally amorphous, depending of the polymer backbone (Mohanty *et al.*, 2005). Through injection molding, PLA parts are usually amorphous because of the slow crystallization kinetics associated with this polymer. Only under suitable conditions, such as slow cooling rate or by addition of nucleating agents, can the samples can become crystalline (Perego *et al.*, 1996). Dong *et al.*, (2014) mentioned that fibers can play an important nucleation role to accelerate PLA crystallization and improve crystal growth rate. Nevertheless, some researchers reported lower crystallinity with fiber addition, which was related to the chemical composition of the fiber (Way *et al.*, 2012). Table 2.2 presents the crystallinity of PLA composites with different natural fibers. In some cases, even with the same fiber type, crystallinity increases or decreases with fiber addition. The differences between each case can be related to

Table 2.2 Crystallinity of PLA-natural fiber composites.

Samples	Fiber content (%)	Crystallinity (%)	Reference
PLA-agave	0	47.7	Pérez-Fonseca <i>et al.</i> , (2015)
	10	44.3	
	20	45.2	
	30	51.1	
PLA-coir	0	47.7	
	10	44.6	
	20	47.5	
	30	46.6	
PLA-pine	0	47.7	
	10	45.9	
	20	41.5	
	30	44.6	
PLA-bamboo	0	33.2	Lee & Wang (2006)
	30	23.5	
	0	55.7	Baghaei <i>et al.</i> , (2011)
PLA-hemp	10	35.5	
	20	32.1	
	35	32.0	
	45	30.7	
PLA-recycled cellulose	0	46.6	Huda <i>et al.</i> , (2005)
	30	43.8	
	30	40.6	
	30	28.4	
PLA-corn-cob	0	30.2	Chun & Husseinsyah (2013)
	20	24.1	
	40	20.5	

(Continued)

Table 2.2 Cont.

Samples	Fiber content (%)	Crystallinity (%)	Reference
PLA-coir	0	6.9	Dong <i>et al.</i> , (2014)
	5	9.5	
	10	10.3	
	20	8.8	
	30	12.1	
PLA-hemp	0	7.5	Sawpan <i>et al.</i> , (2011)
	10	21.0	
	20	27.5	
	30	27.5	
PLA-banana	0	46.6	Majhi <i>et al.</i> , (2010)
	30	24.0	

parameters like sample preparation, type of PLA (grade) and type of fibers (origin and treatment).

2.2.3 Mechanical Properties

Tensile Properties

The tensile properties of natural fiber composites are highly a function of fiber type and fiber-matrix compatibility (Singha & Thakur, 2008a–c). The hydrophilic character of natural fibers results in poor interfacial bonding with most polymers (Perez-Fonseca *et al.*, 2014). In most cases where tensile strength decreases with increasing fiber content, this is an indication of limited interfacial adhesion that leads to low stress transfer (Oskman *et al.*, 2003). Composites made with different natural fibers showed that tensile strength of PLA (60 MPa) decreased to 53, 55 and 47 MPa for agave, coir and pine (30% fiber), respectively. For composites with coir and pine, tensile strength decreased with fiber content, while for agave composites, a maximum value of 55 MPa at 20% of fiber was obtained. Haque *et al.*, (2009) prepared PP-palm and PP-coir composites and found that coir composites presented higher tensile strength than palm composites. This behavior was related to lower cellulose and higher lignin contents in coir. Because of higher lignin content, the fibers are more resilient and stronger. Majhi *et al.*, (2010) used banana fibers as PLA reinforcement and found that PLA tensile strength (49 MPa) decreases with fiber addition. For PLA composites, they found increased tensile strength with fiber content from 10% wt. to 30% wt. (27 to 35 MPa), while at 40% wt. the tensile strength decreased (32 MPa). Increases in tensile strength with fiber addition is mainly attributed to uniform stress transfer from the matrix to the fibers, while decreases are associated with poor interfacial adhesion between both phases. Chun & Husseinsyah (2013) prepared PLA-corn cob composites and reported decreases in tensile strength from 54 MPa (neat PLA) to 44, 38, 31 and 28 MPa for 10, 20, 30 and 40% filling, respectively. Bax & Mussig (2008) prepared PLA-cordenka and PLA-flax

composites and found that tensile modulus and tensile strength increased with fiber content. The PLA matrices used for the composites as reported in Table 2.3 have different tensile strength values (45 to 60 MPa), thus explaining the differences between the composite values reported. It is difficult to compare the values for the tensile modulus

Table 2.3 Tensile properties of PLA-natural fiber composites.

Samples	Fiber content (%)	Tensile strength (MPa)	Tensile modulus (MPa)	Reference (Processing method)
Agave	10	53.5	1.4	Pérez-Fonseca <i>et al.</i> , (2015) (injection)
	20	55.5	1.5	
	30	53.1	1.5	
Coir	10	58.6	1.3	
	20	56.8	1.4	
	30	54.7	1.6	
Pine	10	50.7	1.3	
	20	50.7	1.6	
	30	47.1	1.8	
Cordenka	10	50.0	3.3	Bax & Mussig (2008) (compression)
	20	51.0	4.0	
	30	57.0	4.9	
Flax	10	43.0	3.9	
	20	49.0	5.0	
	30	54.0	6.3	
Banana	10	27.0	2.7	Majhi <i>et al.</i> , (2010) (compression)
	20	30.0	2.9	
	30	35.0	3.0	
	40	32.0	3.1	
Banana/sisal	30	57.0	1.7	Asaithambi <i>et al.</i> , (2014) (injection)
Cotton	5	54.7	1.3	Way <i>et al.</i> , (2012) (injection)
	10	56.3	1.5	
	15	58.1	1.6	
	20	59.6	1.8	
	25	61.5	1.9	
Maple	5	58.1	1.6	
	10	59.7	1.9	
	15	60.8	2.1	
	20	61.8	2.4	
	25	62.6	2.5	

because very different values for neat PLA have been reported, from 1 GPa up to values above 3.5 GPa (Bax & Mussig, 2008; Majhi *et al.*, 2010; Way *et al.*, 2012). Nevertheless, fiber addition has the same effect for all the studies: higher fiber content leads to higher tensile modulus, at least for the range of conditions tested.

The mechanical properties of composites mostly depend on fiber/matrix adhesion in combination with the strength and modulus of both fiber and matrix. A requirement for the successful use of reinforcement properties in lignocellulosic materials is good interfacial bonding to ensure load transfer from the matrix to the reinforcement (Singha & Thakur 2009a–e). The modification of natural fibers with chemical treatments is known to enhance the fiber-matrix compatibility, even if chemical treatments can adversely affect the strength and modulus of the fiber itself (Sawpan *et al.*, 2011). Surface modification of natural fibers affects the crystalline regions of cellulosic materials, which affects the physical and chemical properties of the fibers, such as swelling, moisture absorbance, thermal behavior, water uptake, and chemical resistance (Singha & Thakur 2009a–e). Goriparthi *et al.*, (2012) prepared PLA/jute fiber composites and observed that fiber treatments had significant effects on the tensile strength and moduli of the composites that increased in the following order: trimethoxymethyl silane > 3-aminopropyl trimethoxysilane > peroxide > permanganate > alkalization > untreated. The treatment of jute fiber with trimethoxymethyl silane resulted in maximum tensile strength (35%) and moduli (38%) improvement. Csikos *et al.*, (2015) prepared PLA-wood (30%) composites with maleic anhydride grafted to PLA (MAPLA) at different content (5, 10, 15 and 20% vol.) and found that with increasing MAPLA content, tensile strength increased from 47.5 MPa for the composites without coupling agent to 56 MPa at 20% MAPLA. Rajesh & Ratna, (2014) studied the effect of alkali treatment (5, 10 and 15% NaOH) and bleaching (hydrogen peroxide) of jute fibers as reinforcement for PLA. They reported that alkaline treatment with 10% NaOH and bleaching increased the tensile strength of the composites by 7% compared to neat PLA. Isocyanates have also been used as compatibilizers in PLA based composites because they can react with hydroxyl or carboxyl groups to form stable chemical bonds between PLA and hydrophilic fillers. Yu *et al.*, (2015) used diisocyanates as compatibilizers for PLA-ramie composites (5% fiber) and found that tensile strength and modulus increased from 52.5 to 61.5 and 2900–3100 MPa, respectively. Zou *et al.*, (2012) treated sisal fibers by mercerization, silane, acetylation and permanganate to prepare composites with 10% fiber. They reported that tensile strength and tensile modulus increased from 75 MPa and 5.2 GPa for untreated fibers to 89, 92, 95 and 82 MPa, and 5.9, 6.6, 6.3 and 6.5 GPa, respectively (10, 20, 30 and 40% fiber). Arias *et al.*, (2012) prepared maleic anhydride grafted PLA (PLA-g-MA) in a twin-screw extruder using 2% wt. of maleic anhydride and 0.25% wt. of a peroxide initiator. They made PLA/flax/PLA-g-MA (80/20/20) composites and observed that tensile modulus and strength were very similar with or without maleic anhydride. But the addition of flax increased the tensile modulus by 50% and tensile strength by 10%, while the elongation at break decreased by about 50% for all the systems studied.

Impact Strength

The impact strength of a composite is controlled by several factors including toughness properties of the matrix and fiber, interfacial interaction and friction force required to

pull out the fibers from the matrix. For agave and coir composites, the impact strength was found to increase with fiber content. For neat PLA the impact strength is 30 J/m and adding 30% of coir or agave fibers increases the value to 40 J/m. For pine composites with the same PLA, a constant value was obtained with 10, 20 and 30% (around 30 J/m). This behavior can be related to the effect of fiber length where the agave and coir fibers used were much longer than pine. In fact, previous studies reported that composite impact strength can increase because of higher mechanical energy dissipated during failure (longer fiber pull-out distance) and possible fiber-fiber interaction (entanglements), as long as no fiber break-up occurs (Baghaei *et al.*, 2013). When longer fibers were introduced into PLA, the impact strength increased due to a high number of long fiber pull-outs (Tokoro *et al.*, 2008). Teymoorzadeh & Rodrigue (2015) prepared PLA-maple wood composites and found that neat PLA impact strength (16 J/m) was significantly increased to a maximum of 26.2 J/m (64% increase) at 40% wt. wood flour. Majhi *et al.*, (2010) worked with a virgin PLA exhibiting an impact strength of 21 J/m, but the incorporation of banana fibers resulted in lower values around 19 J/m for all fiber contents (20, 30 and 40% wt.). Jandas *et al.*, (2011) prepared PLA-banana fiber (BF) composites by compression molding. The virgin PLA used in their study had an impact strength of 24.7 J/m, but the addition of BF decreased the value depending on fiber loading. Incorporation of 10% wt. BF decreased impact strength to 41% whereas 20 and 30% wt. reduced to 38 and 23%, respectively. They reported that the best impact strength was at 30% wt. BF (19.1 J/m). Different to tensile and flexural properties, where it was reported that chemical treatments increased these properties, Goriparthi *et al.*, (2012) found that for treated composites (PLA-jute) the impact strength was lower than the untreated composites since fiber pull-out required more energy than fiber fracture and debonding. Although high impact strength of untreated composites can be attributed to more fiber pull-outs due to weak interfacial bonding, for treated composites, fiber fracture occurs instead of pull-outs, which required less energy. Oksman *et al.*, (2003) prepared PLA-flax composites with 40% fiber and triacetin (glycerol triacetate ester) used as a plasticizer for PLA. They found that impact strength was not affected with triacetin addition. Zou *et al.*, (2012) reported impact strength increases due to fiber mercerization from 2.25 kJ/m² (PLA-untreated sisal fiber) to 4.4 kJ/m² (PLA-treated sisal fiber). They attributed these results to the fact that mercerization improved the fiber surface adhesion by removing natural and artificial impurities. Owing to the decrease in spiral angle and the increase in molecular orientation after mercerization, closer packing of cellulose chain also leads to improved impact strength. The use of diisocyanates as coupling agents showed improvements in impact strength of 61% when compared to untreated composites. The increased impact strength of the composites was attributed to the fact that the diisocyanates improved the surface adhesion characteristics by producing a cross-link surface morphology compared to composites without diisocyanate (Yu *et al.*, 2015).

Flexural Properties

Fiber-matrix interactions without coupling agents are related to physical mechanisms based on mechanical anchoring associated to the porous surface of natural fibers (Pérez-Fonseca *et al.*, 2014). Similarly to tensile properties, fiber addition can decrease PLA flexural strength due to weak polymer-fiber interaction. Composites

made with PLA-agave, coir or pine fibers showed that PLA flexural strength (95 MPa) decreases due to fiber addition. However, for agave, the flexural strength increased with fiber content up to a maximum of 89 MPa (30% of fiber). In coir composites the flexural strength was almost constant between 10 and 30% fiber. On the other hand, in pine composites the values decreased with fiber content: 85, 80 and 73 MPa for 10, 20 and 30% of fiber, respectively. A good fiber-matrix interface lead to good load transfer and improved strength. Nevertheless, without coupling agents to improve interfacial adhesion, it is common that flexural strength decreases (Kim *et al.*, 2011; Way *et al.*, 2012). Awal *et al.*, (2015) prepared PLA-wood composites and found that the neat PLA flexural strength was higher than that of the PLA-wood composites, attributing this behavior to poor interfacial adhesion between wood fibers and PLA. Pérez-Fonseca *et al.* (2014) showed that pine fibers have low cellulose (50%) and high wax (19%) contents. Waxes on the fiber surface strongly influence the surface properties of cellulose-based materials. In some cases, it is recommended to treat the fibers to remove these non-cellulosic components and increase the accessibility of surface functional groups (Mohanty *et al.*, 2005). In addition, higher cellulose contents give more strength to the fibers (Perez-Fonseca *et al.*, 2014) as is the case for agave and coir fibers. Usually, the flexural modulus of composites increases due to fiber addition, as reported for PLA-agave, coir or pine fibers. The strength increased from 2300 MPa (neat PLA) to values around 3000 MPa (composites with 30% of each fiber). Shah *et al.*, (2008) prepared PLA-wood composites and showed that the addition of wood flour to the PLA matrix slightly reduced the flexural strength of PLA. On the other hand, the flexural modulus increased with wood content. While the flexural modulus for neat PLA was 3200 MPa, the addition of 40% wood increased to 6000 MPa. Yu *et al.*, (2015) showed that the addition of diisocyanates increased the flexural strength from 82 MPa (neat PLA) to 102 MPa (5% ramie fiber). Baghaei *et al.*, (2013) reported increases in flexural strength (from 40 to 120 MPa) and modulus (from 2.2 to 10 GPa) with hemp fiber addition. Ma & Joo (2011) prepared jute fiber samples using three processing temperatures (200, 210 and 220 °C) and reported that at higher temperature the flexural properties increased. For composites with 15% of fiber at 200 °C, the flexural modulus and strength were 2272 MPa and 39.5 MPa, while for 220 °C the values were 3709 MPa and 70.4 MPa. Dong *et al.*, (2014) used coir fiber as PLA reinforcement and found that alkali treatments produced slightly improved flexural strength while flexural modulus decreased. The alkali fiber treatment often leads to the removal of lignins and pectins from coir fibers, resulting in higher cellulose contents and improving the flexibility and elasticity of coir fibers (Gu *et al.*, 2009).

2.3 PLA Composite Foams with Natural Fibers

Generally, foaming polymer composites can be achieved using different blowing agents that can be classified as chemical and physical. Chemical blowing agents (CBA) are chemical substances added to the polymer matrix to create foam cells upon their decomposition under the effect of temperature. These materials are also divided into two categories: exothermic (azodicarbonamide) and endothermic (sodium bicarbonate). On the other hand, physical blowing agents (PBA) are compressed gases (nitrogen [N₂] and

carbon dioxide [CO_2] or liquids (water, low boiling point alcohols and light hydrocarbons). After the dissolution and homogenization of these gases inside the polymer matrix and under the induction of a thermodynamic instability such as pressure drop and/or increased temperature, foam cells are nucleated (Luebke, 2001). In physical foaming of polymers and composites, the cellular structure produced generally has cell sizes smaller than $10\text{ }\mu\text{m}$ and cell densities above 10^9 cells/cm^3 , which are also known as microcellular foams (Diaz-Costa, 2011). Compared to chemical blowing agents, physical blowing agents have no decomposition temperature; thus, lower processing temperatures are required to foam polymers, which results in more cost effective foam production. Low processing temperature also prevents the degradation of both polymer and fibers (Koyama, 2011).

Several techniques have been developed by which foamed PLA/lignocellulosic fiber-reinforced composites can be produced: batch, injection molding and extrusion. Through batch processes, physical blowing agents (supercritical gases such as CO_2) are mostly used to create the cellular structure inside the polymer matrix. However, via injection molding and extrusion, both chemical and physical blowing agents are available, but CBA are generally used for high density foams, while PBA are used for lower densities. Nevertheless, various parameters need to be controlled/measured to determine the properties of foamed PLA/lignocellulosic fiber-reinforced composites. For instance, the melt viscosity of the polymer matrix is an important factor influencing cell nucleation rate, cell growth and stabilization of the foamed structure (Cho *et al.*, 2013). Other factors such as process conditions (pressure, temperature, flow rate, equipment design), lignocellulosic fiber type and content, as well as fiber treatment (interfacial properties) are also affecting the final properties of these foams. In the following sections, the effects of these parameters are discussed in relation to the morphological, thermal and mechanical properties of foamed PLA/lignocellulosic fiber-reinforced composites.

2.3.1 Batch Processing

In batch foaming, the polymer samples are placed in a high-pressure chamber to be saturated with carbon dioxide (CO_2) or nitrogen (N_2) at ambient temperature. By a sudden thermodynamic instability obtained by releasing the pressure and heating the sample, the solubility of the gas into the polymer drops, leading to the nucleation of foam cells and their growth up to the final foam structure (Lee & Park, 2014). Processing parameters such as saturation pressure, temperature, time, pressure drop rate and cooling rates are known to control the final morphology of foamed composites (Neagu *et al.*, 2011). Several investigations have been devoted to batch foaming of PLA and PLA/lignocellulosic fiber composites, as is described next.

Matuana & Faruk (2010) produced foamed PLA and PLA/wood flour composites with a batch process and studied the effect of gas saturation pressure and foaming time on expansion ratio (ratio between the density of the unfoamed over the foamed one). They reported that by increasing the saturation pressure from 1.38 MPa to 5.52 MPa, the amount of CO_2 absorbed by PLA increased from 2.5% to 20%. They also showed that at low saturation pressure (1.38 MPa), as the saturation time increased from one day to 10 days, the amount of CO_2 absorbed by PLA increased from 2.5% to 5%. At low

saturation pressure (1.38–2.76 MPa) more uniform foam cells were obtained compared to higher saturation pressure (4.14–5.52 MPa) where inhomogeneous and collapsed structures were produced due to CO₂-induced crystallinity of PLA. Finally, they reported that at a saturation pressure of 2.76 MPa, a critical CO₂ concentration of 9.4% was achieved, resulting in a significant foam expansion ratio. In addition, they selected a low saturation pressure (2.76 MPa) and a saturation time of four days to foam PLA/wood flour composites having uniform and homogenous morphology. Compared to neat PLA, all foamed PLA/wood flour samples had finer average cell sizes. By increasing wood flour content from 0 to 40% wt., the void fraction decreased from 90% to 50%. Volume expansion was also affected by wood flour content, as it dropped from 80% to 18% for wood flour contents of 0 and 40% wt., respectively. They concluded that the addition of wood flour in PLA decreased the expansion ratio because the volume fraction of polymer decreases with increasing wood flour leading to lower amounts of CO₂ absorbed by the PLA matrix, therefore less foam cells are nucleated resulting in lower PLA expansion ratio.

Neagu *et al.*, (2011) produced composites of PLA and wood flour (1, 5 and 10% wt.) through a slurry process designed for paper production. Composite foams were manufactured via batch processing using supercritical CO₂, while the surface of the wood fibers was treated with butyl tetracarboxylic acid (CLWF) and butyl tetracarboxylic acid with an additional disodium hydrogen phosphate surfactant (SCWF). All the properties were measured in two directions, namely the transverse and the foaming directions. Wood fibers were oriented in-plane in layers perpendicular to the foaming direction and the foam microstructure was found to be inhomogeneous, as the formation of foam cells took place between the layered wood fiber networks. The expansion ratio was shown to decrease with increasing wood fiber content. As the wood fiber content increased, foam cells were produced that were elongated perpendicular to the foaming direction. It was observed that wood fiber decreased the average foam cell diameter from 0.27 mm to 0.14 mm at 0 and 10% wt. wood fiber, respectively. Increasing wood fiber content resulted in smaller cell diameters. For treated wood fibers, by increasing wood fiber content from 0 to 10% wt., cell diameter decreased from 0.22 to 0.17 and 0.14 mm in the transverse and foaming directions, respectively. For untreated wood fiber, increasing wood fiber content from 0 to 10% wt. decreased the cell diameter from 0.22 to 0.15 and 0.13 mm in the transverse and foaming directions, respectively. Generally, it was concluded that wood fiber treatment had no significant effect on cell morphology. Density also decreased from 0.32 to 0.18 g/cm³ for PLA/1% wt. untreated wood fiber. It then increased to 0.32 and 0.53 g/cm³ at fiber contents of 5 and 10% wt., respectively. For CLWF, PLA density first decreased from 0.32 g/cm³ at 0% wood fiber to 0.20 g/cm³ at 1% wt. wood fiber content, and then increased to 0.30 and 0.50 g/cm³ at 5 and 10% wt., respectively. For SCWF, density decreased from 0.32 at 0% wood fiber to 0.20 and 0.28 g/cm³ at 1 and 5% wt. wood fiber content, respectively. Cell density of PLA/untreated wood fiber increased from 2.8×10^4 to 4×10^4 and 5×10^4 cells/cm³ at fiber contents of 0, 1 and 5% wt., respectively. Increasing fiber content to 10% wt. resulted in lower cell density (4.1×10^4 cells/cm³). For PLA/CLWF, cell density increased from 2.8×10^4 to 4×10^4 cells/cm³. No significant difference in cell density was observed for different wood fiber contents; it remained almost constant at 4×10^4 cells/cm³. Average cell wall thickness of PLA/untreated wood

fiber decreased from 0.043 to 0.018, 0.022, and 0.039 mm at 0, 1, 5 and 10% wt. wood fiber, respectively. For PLA/CLWF composites, cell wall thickness decreased from 0.043 to 0.018 and 0.030 mm at wood fiber contents of 0, 1 and 5% wt., respectively. Further increasing fiber content to 10% wt. resulted in cell wall thickness of 0.043 mm. Both cell wall thickness and cell density increased with increasing wood fiber content. The results for compressive stiffness of PLA/untreated wood fiber in the transverse direction showed that stiffness increased from 95.2 to 140.3 and 366.3 MPa at fiber contents of 5 and 10% wt., respectively. On the other hand, in the foaming direction the only increased stiffness was seen for PLA/10% wt. wood flour composites, which increased from 39.4 to 187.9 MPa. For PLA/CLWF composites and in the transverse direction, stiffness increased from 95.2 to 137.4 and 396.9 MPa for fiber contents of 0, 5 and 10% wt., respectively. In the foaming direction, stiffness was only enhanced for fiber content of 10% wt. and increased from 39.4 to 111.8 MPa. It was clear that stiffness was higher in the transverse direction, as the wood fibers were mainly oriented in the plane of the preforms leading to stacked layers of fiber reinforcements. For PLA/SCWF composites however, in both the transverse and foaming directions, stiffness decreased at wood flour contents of 1 and 10% wt. In the transverse direction, stiffness decreased from 95.2 to 50.9 and 92.8 MPa at 0, 1 and 5% wt. wood fiber content, respectively. In the foaming direction stiffness also decreased from 39.4 to 23.1 and 25.9 MPa at wood fiber contents of 0, 1 and 10% wt., respectively. The most important factor in stiffness is the ability of the matrix to transfer stresses to the reinforcing fibers. Therefore, it was concluded that fiber treatment resulted in reduced adhesion between wood fiber and PLA, leading to lower stiffness.

Boissard *et al.*, (2012) manufactured microfibrillated cellulose-reinforced polylactic foamed biocomposites (PLA/MFC) through a wet mixing technique combined with supercritical CO₂ foaming. They studied the effect of composition on morphology, density and compression modulus of the foams. For this, two types of foamed composites were produced as preformed PLA/MFC composites through wet mixing and extruded PLA/MFC preforms. They also used an epoxy styrene-acrylic oligomer (Joncryl™ ADR-4368) to modify the melt elasticity. Based on the morphological investigations, limited expansion during foaming was obtained for foamed PLA composites reinforced with 1 and 5% wt. microfibrillated cellulose (MFC) compared to neat PLA. They related this behavior to the high rigidity of the MFC network, high cellulose degree of crystallinity, and poor interfacial adhesion between the fibers and the matrix providing voids/gaps/channels leading to blowing gas escape. The foaming expansion was shown to be five to six times greater in composites produced after extrusion than preformed composites. Electron microscopy images revealed homogenous cellular structures in neat PLA and the extruded composites. It was also shown that decreasing saturation temperature from 165 °C to 155 °C and depressurization rate from 14 bar/s to 4 bar/s resulted in reduced cell diameters and narrower cell size distributions. Therefore, they concluded that the optimum saturation temperature and depressurization rate to obtain homogenous cellular structures for both neat and MFC reinforced PLA are 155 °C and 4 bar/s, respectively.

In terms of cell coalescence, neat PLA foams from as-received PLA pellets showed more homogenous structures than the extruded neat PLA foams, which in turn showed better cellular homogeneity than PLA/MFC extruded composites. Using intrinsic

viscosity to estimate the viscosity average molecular weight for the different samples supported the aforementioned trends: addition of the chain extender increased the viscosity, melt strength and foamability of PLA. SEM images of the foamed samples revealed that chain extension led to more homogenous cellular structures of foamed PLA/MFC. Results of mechanical properties showed that the compression modulus of PLA/MFC increased from 20 to 50 MPa with increasing MFC content from 0 to 5% wt. Density was also increased from around 0.15 to 0.35 g/cm³ at MFC content of 0 and 5% wt., respectively. Therefore, higher compression modulus was partially the result of increased density of the cellular PLA/MFC. Density of chain extended neat PLA and PLA/MFC was found to be 60 to 75% lower in comparison with samples without chain extenders and decreased to 0.045 and 0.13 g/cm³ for 0 and 5% wt. MFC. Moreover, compression moduli decreased to 5.2 and 27.3 MPa for neat chain extended PLA and PLA/5% wt. MFC composites.

Ding *et al.*, (2013) investigated the effect of cellulose fiber type (micro- and nano-sized) and its content (0.5, 1, 3, 5 and 10% wt.) on the morphology and volume expansion ratio of foamed cellulose fiber reinforced PLA composites via batch foaming with CO₂ at a saturation pressure of 4.14 MPa. Scanning electron microscopy of the foamed neat PLA revealed a non-uniform cell structure with two different cell distributions: large cells close to the surface and small cells in the core region due to non-uniform heat transfer through the thickness. Compared to neat PLA, micro-sized cellulose fiber-reinforced PLA composites showed lower cell density and larger cell size. They explained that the rough fiber surface leads to crystal nucleation and transcrystallinity, resulting in non-uniform and large crystal sizes that negatively affect the uniformity of the cell morphology and high cell density. Moreover, decreased CO₂ solubility in PLA with the presence of cellulose fibers, faster gas loss after pressure release and during foaming due to poor interfacial adhesion between PLA and cellulose fibers, increased gas diffusion rate through the canals at the interface of PLA and fibers, and finally, increased melt strength due to fiber addition were the reasons attributed to lower cell density and larger cell sizes. On the other hand, nano-sized fiber composites showed more uniform cell size distribution with smaller cell sizes and increased cell density. They also reported that the large surface area of nano-sized fibers provided large interfacial area between the fibers and PLA, leading to effective heterogeneous nucleation. Moreover, crystallized PLA molecules around the fibers (during gas saturation) and stress-induced cell nucleation due to local pressure variations around the fibers or transcrystalline fibers contributed to increased cell density. They also related improvements in cell density and cell size to the increased viscosity and melt strength as a result of fiber addition and transcrystallinity during the solid-state foaming process. They also believed that nano-sized fibers with very high aspect ratios contributed to more fiber entanglement, acting as a gas barrier limiting gas diffusion rate and preventing cell coarsening. Considering better morphology of nano-sized fiber composites against micro-sized counterparts proved that the gas diffusion rate in the former case is lower due to high level of entanglement. The results of complex viscosity revealed that at similar fiber content, the melt viscosity of nano-sized fiber composites is significantly higher than for micro-sized fiber composites. The evaluation of the effect of fiber content showed that for both micro- and nano-sized fibers, cell densities increased and cell sizes decreased as the fiber content increased. The reason behind this trend is related

to the increase in both melt viscosity and heterogeneous nucleation at higher contents. They also reported that at higher fiber contents (10% wt.) for micro-size compared to nano-size composites (3% wt.), non-uniform cell size distribution was obtained. This can be explained by the difficulty of getting good fiber dispersion into PLA at higher contents, which can affect crystal formation. In addition, the expansion ratio of the micro-size fiber composites increased from 32 to 35 between 0.5 and 3% wt. which then decreased to 27 at 5% wt. fiber content. At 10% wt., the expansion ratio significantly decreased to 6.4. For nano-sized fiber composites, at low fiber content, the average expansion ratio remained close to 45, which was similar to neat PLA. Nevertheless, at 3% wt. fiber content, the expansion ratio decreased to 31. Lower expansion ratio of the PLA/fiber composites was associated with lower solubility, higher gas diffusion rate and higher melt viscosity of the composites compared to neat PLA. The best results for cell density and volume expansion were obtained for nano-sized fiber reinforced composites at 0.5 and 3% wt. fiber content. It is obvious that nano-sized fibers have large surface area and higher aspect ratio, preventing cell coalescence and thus allowing cells to grow larger favoring expansion ratio.

Cho *et al.*, (2013) prepared foamed nanocomposites of PLA/cellulose nanofiber (CNF) to study the effects of CNF content and saturation temperatures on foam morphology and properties. They also investigated the complex viscosity of the nanocomposites as a function of fiber content. They reported that the complex viscosity was higher for nanocomposites than for neat PLA and increased with increasing CNF content. Filler-filler interactions via hydrogen bonds as well as a good filler-matrix interfacial adhesion contributed to the increased viscosity. Furthermore, by increasing processing temperature from 145 to 165 °C, nanocomposites with different cell morphology were obtained. For instance, at 145 °C only a few cells were formed. But as the temperature increased to 165 °C, the cellular structure deteriorated since the viscosity was low and foam stabilization was limited. SEM images showed that increasing CNF content resulted in decreased cell size from 52.6 to 37.3, 32.9, and 26.7 μm at CNF contents of 0, 1, 2 and 5% wt., respectively. Cell density was also influenced by CNF content and increased from 0.56 to 1.21, 2.45 and 4.21×10^8 cells/cm³ at CNF contents of 0, 1, 2 and 5% wt., respectively. They also confirmed the effect of rheological properties and crystallinity on cellular morphology changes and proposed that gas solubility and diffusivity decreased with increasing degree of crystallinity, as gas molecules do not dissolve in crystallites. Foam densities were also affected by CNF content. As CNF content increased from 0 to 1 and 2% wt., the foam density decreased from 0.23 to 0.15, and 0.16 g/cm³, respectively. However, by increasing fiber content to 5% wt., the foam density increased to 0.25 g/cm³, which was attributed to reduced nucleation sites available due to fiber-fiber contact.

Rizvi *et al.*, (2011) produced PLA-chitin (PLA/C), PLA/nano-chitin (PLA/nC) and PLA/maleic anhydride compatibilized chitin (PLA/nC-MA) composites in a two-step batch foaming process using carbon dioxide with a constant saturation pressure of 4.14 MPa at four chitin contents (0, 1, 2 and 5% wt.). No porous morphology was detected via scanning electron microscopy for neat PLA samples. By evaluating foam density, it was concluded that solvent-induced crystallization of neat PLA in the presence of pressurized carbon dioxide hindered foam expansion, as crystalline domains do not absorb carbon dioxide. Conversely, scanning electron microscopy images of various

composites (PLA/C, PLA/nC, and PLA/nC-MA) showed that at 5% wt. chitin, uniform foam cell morphology was achieved. It was also shown that adding small amounts of chitin significantly decreased the density of the composites compared to neat PLA, and this behavior was associated with a reduction of composite viscosity in the presence of chitin. Overall, the results from various studies on batch foaming can lead to significant trends that can be explained by the different characteristics of PLA/lignocellulosic fiber composites. First, it can be concluded that the addition of fibers directly influence the morphology of the foamed composites (Matuana & Faruk, 2010; Rizvi *et al.*, 2011). That is to say, upon lignocellulosic fiber addition more uniform cell structures with narrower cell size distribution and smaller cell diameter are achieved. The addition of fiber decreased the cell size and increased the cell density (Ding *et al.*, 2013; Cho *et al.*, 2013; Neagu *et al.*, 2011). Furthermore, compressive properties such as compressive stiffness and modulus were improved by fiber addition. On the other hand, fiber reinforcement increased the density and decreased the expansion ratio of the composites (Ding *et al.*, 2013; Neagu *et al.*, 2011; Matuana & Faruk, 2010; Boissard *et al.*, 2012; Rizvi *et al.*, 2011). It is also believed that inhomogeneity in foam cell structures can be eliminated by the use of chain extenders (Boissard *et al.*, 2012). By optimization of processing conditions such as saturation pressure, time and temperature, morphological properties of the foamed samples can be improved. For instance, by increasing saturation pressure and temperature, cell size increased and cell density decreased (Boissard *et al.*, 2012). Moreover, lower saturation pressure seemed to be more effective in obtaining foamed composites with better foam cell uniformity. In addition, low saturation pressure combined with longer saturation time lead to more uniform foam cell distributions (Matuana & Faruk, 2010).

Finally, batch processing has some disadvantages such as long cycle time to effectively diffuse the blowing gas in the polymer matrix at ambient temperature, especially for thick parts. Also, it is a small and non-continuous production scale, which is not cost effective. Therefore, other techniques like continuous production of foamed composites are preferred for commodity applications (Lee & Park, 2014; Nofar & Park, 2014).

2.3.2 Extrusion

In extrusion, a physical blowing agent is injected under high pressure into an extruder to solve the gas molecules into a polymer melt. Due to the plasticizing effect of the dissolved gas, a uniform polymer/gas mixture flows along the extruder can be obtained with a low viscosity. At the die exit, a rapid pressure drop creates thermodynamic instability, leading to cell nucleation followed by cell growth (Nofar & Park, 2014). It has been shown that increasing blowing agent content can generate higher supersaturation, leading to improved cell nucleation and growth (Zhan, 2012). In the microcellular extrusion of PLA/lignocellulosic fiber composites, melt viscosity changes due to fiber addition is believed to be an important factor affecting foam nucleation, cell growth and cell stabilization (Matuana & Diaz, 2013), because fillers generally increase the melt viscosity (Cho *et al.*, 2013). In a study by Matuana & Diaz (2013) the effect of melt rheology and wood flour content on cell morphology of foamed PLA/wood flour composites through continuous extrusion was investigated. The authors produced composites with 20% wt. wood flour in PLA with different amounts (1.3–6%) of Epolene E-43 as

a rheology modifier to study the importance of polymer melt viscosity on composites foamability. The rheology modifier contents were chosen to get a MFI below, equal (matching point) or above the MFI of the unfilled PLA. SEM images clearly showed that homogeneous cell structures with an average cell size of approximately 10 μm were obtained when the MFI was close to the one of neat PLA. They concluded that 2% Epolene E-43 was enough to allow cell formation but not too high to prevent cell coalescence. The average cell size increased from 9.2 to 15.5 and 18.3 μm as the Epolene E-43 content increased from 2 to 4 and 6%, respectively. As the Epolene E-43 content increased to 4 and 6%, the cell structure started to deteriorate as large cracks were observed as well as cell coalescence. As the MFI of the composites increased above the matching point, the melt viscosity decreased, leading to insufficient melt strength, preventing the polymer melt to trap the growing bubbles, resulting in cell coalescence. It was also shown that by increasing the amount of Epolene E-43, the void fraction also decreased from 22 to 17 and 11% at 2, 4 and 6%, respectively. At 20% wt. wood flour, cell density decreased from 0.67×10^9 to 0.28×10^9 and 0.08×10^9 cells/ cm^3 at Epolene E-43 contents of 2, 4 and 6%, respectively. They also used Epolene E-43 contents of 0.3, 2 and 5% for composites containing 10, 20 and 40% wt. wood flour to investigate the effect of wood flour content on the cell morphology of PLA/wood flour composites. Compared to neat PLA foam, more uniform cell structure was obtained for composites with up to 20% wt. wood flour. As the wood flour content increased above 20% wt., foam cells began to deteriorate, producing large cells with irregular-shaped structures. By increasing wood flour content from 0 to 10, 20, 30 and 40% wt., cell density decreased from 1.46×10^9 to 1.02×10^9 , 0.67×10^9 and 0.26×10^9 cells/ cm^3 , respectively. They related this decrease to reduced polymer fraction, which dissolves the foaming gas. They also reported that cell nucleation at higher wood flour contents changed from homogeneous cell nucleation taking place in the polymer melt phase to heterogeneous nucleation at the interface between PLA and wood flour. This increased heterogeneous cell nucleation rate results in reduced overall nucleation rate, thus lowering cell density. Results of void fraction showed that between 0 and 20% wt. wood flour, void fraction remained unchanged at almost 20%. However, by increasing fiber content to 30% wt., void fraction decreased by approximately 15%. The results for cell diameters showed that increasing wood flour content from 0 to 20% wt. decreased the uniformity of the foam cells. In other words, at 0% wt. wood flour, more than 90% of the foam cells were below 10 μm . At wood flour content of 10–20% wt. similar cell size distribution, with about 60% being smaller than 10 μm and around 90% smaller than 15 μm , was obtained. However, by further increasing wood flour content beyond 20% wt., larger cells with less uniformity were obtained. The authors stated that higher wood flour contents provide sites for undissolved gas pockets leading to uncontrolled cell growth and overall deterioration of the cell morphology. It was also believed that wood flour can release some volatiles that can be detrimental to the foam cell structure. Finally, the average cell size increased from 7.4 μm at 0% wt. wood flour to 8.9, 9.3, and 11.3 μm at wood flour contents of 10, 20, and 30% wt.

Koyama *et al.*, (2011) prepared cellulose fiber (20% wt.) reinforced PLA foams via extrusion using CO_2 as the physical blowing agent. The effects of extrusion die temperature, PLA matrix type and cellulose on foam cell morphology was investigated. It was reported that increasing die temperature from 110 to 150 $^\circ\text{C}$ did not influence the foam

density of neat amorphous PLA as it remained at 0.9 g/cm^3 . However, by increasing the die temperature, the foam density of crystalline PLA increased from 0.1 to 0.9 g/cm^3 . Moreover, increasing the die temperature increased the foam density of amorphous and crystalline PLA composites. For instance the foam density of amorphous PLA/cellulose composites at 110°C was around 0.82 g/cm^3 , which was increased to 1.0 g/cm^3 at a die temperature of 150°C . It was also shown that the foam density of crystalline PLA/cellulose composites increased from 0.9 g/cm^3 at 130°C to 1.1 g/cm^3 at 145°C . However, it was believed that the sensitivity of foam density in pure crystalline PLA is much higher than that of amorphous and crystalline PLA composites. They reported that crystallization is useful to decrease the foam density of neat PLA, but it has less effect on the foam density of PLA composites. They also reported that the addition of cellulose fibers to PLA significantly increased foam density, which was associated with the higher density of the fibers as well as less polymer that could be foamed and restrictions on foam expansion imposed by cellulose fibers. The results for cell density also showed that, by increasing die temperature, cell density of both neat PLA and cellulose fiber composites increased. For example, by increasing the die temperature from 120 to 140°C , cell density increased from 2×10^5 to $3 \times 10^6 \text{ cells/cm}^3$ for amorphous neat PLA. In crystalline neat PLA the same increasing trend was observed, as cell density increased from 4×10^5 to $1 \times 10^6 \text{ cells/cm}^3$ with increasing die temperature from 115 to 145°C . The same increasing trend was obtained for cellulose-based composites. For crystalline PLA/cellulose fiber composites and by increasing the die temperature from 110 to 150°C , cell density was increased from 5×10^6 to $8 \times 10^7 \text{ cells/cm}^3$. Generally, cell density of PLA/cellulose fiber-reinforced composites was higher than neat crystalline and amorphous PLA foams. It was concluded that the addition of cellulose fibers significantly increased cell density. It was also reported that the crystallinity of neat crystalline PLA increased with decreasing die temperature. However, higher die temperature did not affect the crystallinity of cellulose-based composites. It was also reported that cellulose fiber addition can increase the crystallinity of PLA. Cell density increase in both neat crystalline PLA and crystalline PLA composites can be associated with the heterogeneous nucleating effect of crystalline domains and cellulose fibers, where the influence of the latter is more pronounced in the case of PLA composites. The results for complex shear viscosity also revealed that in both crystalline neat PLA and PLA/cellulose composites, viscosity decreased after extrusion foaming and further decreased with decreasing die temperature. The decrease in shear viscosity is due to PLA degradation induced by heating from the extrusion barrel, higher shear stress applied in the extruder at lower die temperature, and PLA hydrolysis. Based on the results from shear viscosity, it was shown that, as the shear viscosity decreased at lower die temperature, lower PLA melt strength can lead to cell coalescence, which in turns leads to lower cell density. Using SEM images, cracks were observed on the surface of neat crystalline PLA and composites at higher die temperature. These cracks are responsible for CO_2 gas loss from the extrudate resulting in a lower expansion ratio. Conversely, at lower die temperature, fewer cracks were observed on the extrudate surface of both neat PLA and composites due to a rapid solidification, creating an unfoamed skin layer. In this case, gas loss was significantly reduced leading to higher cell growth and lower foam density.

Zhan, (2012) manufactured foamed PLA composites using sugar beet pulp (TSBP) with a chemical blowing agent through continuous extrusion. Different CBA contents

(0.2, 0.5, 1 and 2 phr) were selected, while the TSBP content was kept constant at 20% wt. The effects of foaming temperature (130, 140, 150, and 160 °C) and screw speed on cell density, void fraction and cellular morphology were investigated. SEM images revealed that by increasing CBA content from 0.2 to 2 phr, cell size increased and large cells appeared in the core region. CBA content also significantly influenced the cell density as it decreased from 2.44×10^6 to 4.84×10^5 cells/cm³ by increasing CBA content from 0.2 to 2 phr. Reduced PLA melt strength was related to increased CBA content (plasticizing effect) leading to lower cell density. By increasing CBA content from 0.2 to 1 phr, void fraction increased from 20 to 37%. However, by further increasing CBA content to 2 phr, void fraction decreased to 27%. As the state of supersaturation is strongly dependent on CBA content, increasing CBA content can improve cell growth, leading to increased cell size and higher void fraction. On the other hand, excessive CBA content may increase the chance of cell coalescence. It is widely accepted that each polymer has a unique gas containment limit (saturation) that could result in gas escape through channels during foaming when overloaded. In the case of 2 phr CBA, the gas loss led to a sudden decrease in void fraction and formation of a large unfoamed area. SEM images also showed that increasing foaming temperature from 130 to 160 °C resulted in larger cells and cell coalescence. It was also noted that a foaming temperature of 140 °C was the optimum temperature to obtain fine-sized cells. By increasing the foaming temperature from 130 to 160 °C, cell density decreased from 2.21×10^6 to 7.28×10^5 cells/cm³. The void fraction was also increased from 30 to 42% by increasing the foaming temperature from 130 to 140 °C. Low viscosity and melt strength followed by low expansion pressure led to better cell growth and void fraction. The addition of 20% wt. TSBP increased the heterogeneous nucleation rate, which is dependent on the foaming temperature and pressure drop. Increasing the heterogeneous nucleation rate results in lower cell density. It was also shown that lowering temperature increased polymer melt strength, which is favorable in preventing cell coalescence. Therefore, the average cell density was higher at lower foaming temperature.

The effect of screw speed (40, 60, 80 and 100 rpm) for composites containing 1 phr CBA at a foaming temperature of 150 °C was also studied. It was reported that by increasing screw speed from 40 to 60 rpm, finer cells were obtained. As the screw speed was further increased to 100 rpm, cell coalescence was observed, since by increasing screw speed, the material residence time decreases, resulting in reduced CBA decomposition. Furthermore, increasing the screw speed enhanced the shear rate leading to more PLA shear-thinning. Therefore, melt viscosity decreased, which strongly increased cell coalescence and the formation of irregular-shaped cells. Increasing screw speed from 40 to 60 rpm resulted in increased cell density from 6.80×10^5 to 1.76×10^6 cells/cm³. But further screw speed increase to 100 rpm led to lower cell density (5×10^5 cells/cm³). The reason behind this is the decreased PLA melt strength with increasing screw speed contributes to cell coalescence followed by lower cell density. The results of void fraction showed that as the screw speed increased from 40 to 60 rpm, void fraction decreased from 43 to 40%. Further increase in screw speed (100 rpm) resulted in higher void fraction (43%).

Bergeret & Benezet (2011) reinforced PLA foams with two neat cellulose fibers of short (SFC) and micro (CMF) size at two contents (20 and 30% wt.) via extrusion with a chemical blowing agent. For each reinforcing fiber, two lengths were selected. It was

shown that the presence of cellulose fiber decreased the void content. For instance, the void contents for 20% wt. short cellulose fiber and 30% wt. micro-cellulose fiber reinforced foams were about 11 and 25% respectively, which were significantly lower than 43% for neat PLA foamed. Cell diameter was also affected by the addition of cellulose fiber as it decreased from 106 to 55 and 67 μm at 30% wt. of short cellulose fiber and micro cellulose fiber reinforced composites, respectively. They attributed this decrease to a higher number of nucleating sites due to fiber addition. On the other hand, cell density showed a different trend: cell density decreased from 6.98×10^5 to 3.67×10^5 cells/ cm^3 for neat PLA and PLA composites reinforced with 20% wt. short cellulose fiber of 130 μm length. However, for foamed composites with 20% wt. of short cellulose fiber (60 μm), cell density increased to 9.47×10^5 cells/ cm^3 . Furthermore, for micro-cellulose fiber foamed composites of 40 and 18 μm lengths, cell density first increased to 15.8×10^5 cells/ cm^3 and then decreased to 6.87×10^5 cells/ cm^3 . Cell wall thickness increased as a result of cellulose fiber addition. With the addition of 20% wt. of short and micro-cellulose fibers, cell wall thickness increased from 54.7 μm to the maximum of 172.1 μm and 109.3 μm , respectively. Compared to neat PLA foam, a decrease of the open-cell ratio was reported for fiber reinforced PLA composites. This is related to the presence of micro-holes between PLA and the fibers associated to low interfacial adhesion between both phases. The results for mechanical properties did not show any pronounced effects of fiber content and length. The yield stress and strain remained unchanged at about 20 MPa and 7% for neat foamed PLA and all the foamed composites. Moreover, micro-cellulose fiber treated with silane did not improve the mechanical properties of the foamed composites, as the yield stress and strain remained constant.

Generally, it was shown that the viscosity of a polymer melt plays an important role in the determination of the cell morphology and cell characteristics. This means that changes in melt viscosity induced by various parameters from the process conditions such as extrusion screw speed, die temperature, foaming temperature and fiber content all influence the cell size and cell density (Zhan, 2012; Koyama *et al.*, 2011). Moreover, fiber geometry such as length can significantly influence cell density (Bergeret & Benezet, 2011). Finally, similar to batch foaming, lignocellulosic fiber addition could also affect the cell morphology, since it correspondingly changes the heterogeneous nucleating rate of foam cells (Matuana & Diaz, 2013; Bergeret & Benezet, 2011).

2.3.3 Injection Molding

Compared to other polymer foaming techniques, injection molding offers advantages including low material costs, high dimensional stability, high energy efficiency and faster cycle time. Moreover, foam injection molding is known to produce better mechanical properties such as improved fatigue life, impact strength and toughness (Nofar & Park, 2014). In injection molding, both chemical and physical blowing agents can be used. In the former, the chemical blowing agent and PLA/lignocellulosic fiber reinforced pellets are dry blended prior to being injection molded to the desired shapes (Teymoorzadeh & Rodrigue, 2016). However, for physical blowing agents, supercritical gases such as carbon dioxide (CO_2) and nitrogen (N_2) are mostly used. Generally, the solubility of nitrogen is lower than carbon dioxide, but cell nucleation is higher in

the former. Due to the plasticizing effect of PBA, the melt viscosity of the polymer is reduced and processing can be done at lower temperatures, reducing energy use and processing costs. This temperature reduction is advantageous in foaming temperature-sensitive biopolymers such as PLA to limit degradation.

There are two types of microcellular injection molding: high-pressure and low-pressure. In the high-pressure injection molding (MuCell technology), the cavity is fully filled and void fractions of around 5–15% can be achieved. High-pressure injection molding is widely used in the production of structural foams since it can better control cell nucleation and cell coalescence in fixed molds, but the process has been modified with the addition of a mold-opening step. Through this technique, the mold cavity is pressurized prior to being fully filled with the polymer/gas mixture. Then, the mold is opened in the thickness direction leading to pressure drop in the cavity and cell nucleation occurs. It has been reported that foam cells obtained via this process are more uniform (cell distribution) with higher void fractions. In low-pressure injection molding, the mold cavity is only partially filled (short shot) and foamed samples with high void fractions (up to 40%) can be obtained. Compared to the MuCell technology, the control of cell nucleation, growth and coalescence is more difficult. Therefore, less uniform cell structures are obtained (Nofar & Park, 2014). Although foam injection molding has been widely used in the production of PLA parts for various applications, limited works have been focusing on the manufacture of PLA/lignocellulosic fiber composite foams. Here, the latest results on the morphological, thermal and mechanical properties of these materials are presented.

Pilla *et al.*, (2009) produced foamed flax fiber reinforced PLA at three different flax concentrations (1, 10 and 20% wt.) through a microcellular injection molding process. The effect of silane treatment was also investigated on the morphological, thermal and mechanical properties of these foamed composites. SEM images showed that the average cell diameter was larger in neat PLA than in PLA/flax composites. They concluded that the addition of flax fibers decreased cell size but increased cell nucleation, which limited the amount of supercritical fluid (nitrogen, N₂) required for cell growth. Furthermore, the presence of flax fibers resulted in increased viscosity, inducing strain-hardening that hindered cell growth and cell coalescence resulting in lower cell size. Compared to an average cell size of 8.4 μm for neat PLA, the cell sizes of PLA/flax composites decreased by about 11, 47 and 67% at 1, 10 and 20% wt. flax fiber, respectively. Increasing fiber concentrations increased cell density from approximately 2.5×10^7 cells/cm³ for neat PLA to 7×10^7 , 1.4×10^8 and 2.2×10^8 cells/cm³ at flax concentrations of 1, 10 and 20% wt., respectively. This behavior was again associated with heterogeneous cell nucleation leading to more uniformity in cell nucleation and growth. Moreover, the morphological analyses revealed that the silane treatment of flax fiber did not affect cell size and cell density of the foamed composites. The results of differential scanning calorimetry (DSC) for the first heating cycle showed that the addition of flax fiber enhanced the degree of crystallinity from 8% for neat PLA to 9, 16 and 27% at 1, 10 and 20% wt. flax content, respectively. The second heating cycle also resulted in increased degree of crystallinity from 8% for neat PLA to 11, 21 and 31% at 1, 10 and 20% wt. fiber concentration, respectively. Flax fibers were believed to act as crystallization nucleating agents, thereby increasing the degree of crystallinity with fiber addition, but the silane treatment did not show any significant effect on the foam crystallinity.

The weight reduction of neat PLA, PLA/1% flax/1% silane, PLA/10% flax/0% silane, PLA/1% flax/1% silane, and PLA/20% flax/1% silane was found to be similar (between 13 and 19%). Stress-strain curves for neat PLA and PLA/1% flax/1% silane showed necking. On the other hand, the other foamed samples presented a brittle mode of fracture. This is due to higher fiber loadings and the presence of a few large cells acting as stress concentration sites. The specific toughness and strain-at-break of foamed PLA/flax fiber composites remained unchanged (and similar to neat foamed PLA) at about 0.001 MPa/(kg/m³) and 4%, respectively. On the other hand, the specific tensile modulus increased by about 3, 10 and 22% for the foamed composites at 1, 10 and 20% wt. fiber loadings, respectively. Higher specific modulus for the composites is due to the higher modulus of flax fibers compared to PLA and to the restraining effect of fillers on polymer chain movements leading to increased stiffness. No significant effect of silane was reported on the specific toughness, strain-at-break and specific tensile modulus of foamed composites. Overall, specific toughness, strain-at-break, and specific tensile strength of the foamed composites were lower than their solid counterparts. However, for specific tensile modulus, no significant difference was seen for unfoamed and foamed PLA composites. Specific tensile strength of foamed composites with 1, 10 and 20% flax fiber decreased by about 4, 15 and 5%, respectively. The authors related this decrease in specific tensile strength to the presence of large voids in the composites acting as stress concentration sites, leading to lower mechanical properties. Unlike the unfoamed composites, the effect of silane treatment was more pronounced in foamed samples; i.e., the specific tensile strength was improved by a factor of 8 compared to the untreated fiber composites. The dynamic mechanical analysis showed that besides PLA/1% flax/1% silane, increasing flax concentration to 10 and 20% increased the storage modulus compared to the neat foamed PLA. Moreover, the storage modulus of the foamed samples was higher than their unfoamed counterparts due to the presence of foam cells. Based on $\tan \delta$ curves, Pilla *et al.*, (2009) reported that flax fiber addition did not change the glass transition temperature of PLA. However, the glass transition of the foamed composites was around 2–3 °C lower than for unfoamed samples. Silane treatment did not affect the glass transition. The area under the $\tan \delta$ curve decreased by about 3, 29 and 58% at 1, 10 and 20% wt. fiber content, showing that the damping energy is lower in foamed composites than for neat PLA foams. Moreover, the area under the $\tan \delta$ curve of foamed specimens was lower than their unfoamed counterparts, which is in agreement with toughness and strain-at-break results. This behavior can be associated to the formation of large voids.

Teymoorzadeh & Rodrigue, (2016) prepared foamed PLA/wood flour composites via injection molding (short shot) using azodicarbonamide as a chemical blowing agent. They investigated the effect of wood flour concentration (15, 25 and 40% wt.) and injection molding conditions on the morphological (cell density, cell diameter and skin thickness), mechanical (tensile, flexural and impact) and thermal properties (melting and crystallinity) of foamed PLA composites. Five different shot sizes (31, 33, 36, 38 and 43% of the total shot capacity of the injection molding: 114 cm³) were selected. Density reduction in neat foamed PLA was found to be controlled by the shot size, which decreased by around 25% for a 31% shot size. However, by further increasing the shot size to 43%, only 15–17% density reduction was obtained. This behavior was related to improved cell growth and the ability of foam cells to expand more freely

when less material is injected inside the mold cavity. For foamed PLA composites, density reduction decreased by increasing wood flour content from 8 to 6, and 3% at fiber concentrations of 15, 25 and 40% wt., respectively. Comparing the density reduction between foamed and unfoamed PLA composites revealed that foaming significantly led to 6–7% lower density. On the other hand, the density of foamed composites was about 13, 15 and 19% higher than for neat foamed samples at wood flour concentration of 15, 25 and 40% wt., respectively. SEM images showed that the addition of wood flour led to more uniform morphology with a narrower cell size distribution. It was also shown that, by increasing wood flour concentration from 15 to 40% wt., cell deterioration occurred that resulted in the formation of irregular-shaped foam cells. SEM images also revealed that as the injection molding shot size increased from 31 to 43%, foam cells became smaller. Furthermore, it was shown by SEM images that increasing shot size from 31 to 43% also increased the number of small cells. The results demonstrated that cell diameter decreased by about 54% by increasing shot size from 31 to 43%. Cell diameters in foamed PLA composites were significantly smaller than for neat foamed PLA. For instance, the cell diameter decreased from 0.1 to 0.06, and 0.04 mm at wood flour concentration of 15, 25 and 40% wt., respectively. This decrease was associated with the addition of wood flour, which increased heterogeneous nucleation and increased melt viscosity resulting in limited cell growth: the formation of a higher number of smaller cells. The results of cell density also revealed that increasing the shot size resulted in higher cell density. For instance, cell density increased from 0.5×10^7 to 3.7×10^7 cells/cm³ for shot sizes of 31 and 38%, respectively. It was also shown that a 38% shot size was optimum to achieve the best cell morphology. Nevertheless, wood flour addition resulted in lower cell density: from 3.7×10^7 to 0.3×10^7 cells/cm³ for foamed PLA with a shot size of 38% and foamed PLA/15% wt. wood flour, respectively. Skin thickness was also influenced by the shot size, which decreased from 270 to 50 μ m by increasing the shot size from 31 to 43%. This was attributed to a more effective foam cell nucleation and cell growth of the core region. Moreover, wood flour addition significantly increased the skin thickness from 270 to 600 μ m for neat foamed PLA with a 31% shot size and PLA/15% wt. wood flour, respectively. As the melt viscosity increased with wood flour addition, foam cell growth and gas diffusion was hindered. Therefore, thinner foam core and thicker unfoamed skin layer was obtained. However, by increasing wood flour concentration from 15 to 40% wt., skin thickness decreased from 600 to 250 μ m. It was believed that increasing wood flour beyond 15% wt. resulted in a more effective nucleating effect of the wood flour, which facilitated the formation of foam cells in the core region leading to thinner skins. The specific tensile strength of PLA decreased from 977 MPa/(g.cm⁻³) for unfoamed neat PLA to an average of 769 MPa/(g.cm⁻³) for foamed neat PLA samples (21% reduction). In addition, by increasing shot size from 31% to 40% the best specific tensile modulus and specific tensile strength of 850 MPa/(g.cm⁻³) and 32 MPa/(g.cm⁻³) were obtained. The best result for the elongation at break of foamed PLA was for a shot size of 38% that produced only a 17% decrease compared to the other shot sizes. On the other hand, specific flexural modulus was shown to be higher for foamed PLA samples compared to neat unfoamed PLA. For instance, the specific flexural modulus of foamed PLA with a 31% shot size increased by about 35% from 2364 MPa/(g.cm⁻³) to 3200 MPa/(g.cm⁻³). For the specific flexural strength, however, foamed PLA showed

lower strength compared to unfoamed PLA. Overall, compared to neat PLA, the average specific flexural modulus increased by about 22% and the specific flexural strength decreased by around 48%. Furthermore, by increasing the shot size from 31% to 43%, the specific flexural strength increased by about 37%. Specific impact strength also decreased from 28 to 19 J.m⁻¹/g.cm⁻³ for a shot size of 38% (32% reduction). On average, foaming decreased the specific impact strength of PLA by about 25%. This behavior is associated with the presence of foam cells acting as stress concentration regions and crack initiators. Wood flour reinforcement resulted in increased specific tensile modulus from 977 MPa/(g.cm⁻³) for neat PLA to 1389 MPa/(g.cm⁻³) and 1394 MPa/(g.cm⁻³) for the foamed composites with 25% and 40% wt. wood flour, respectively. It was believed that the higher modulus of wood flour compared to PLA and its restraining effect on PLA chain mobility both contributed to increase the specific tensile modulus. The specific tensile modulus for unfoamed PLA/wood flour composites also improved from 977 MPa/(g.cm⁻³) to 1492 MPa/(g.cm⁻³) at 40% wt. wood flour. In general, the average tensile modulus and strengths of the foamed composites were 13% and 28% lower than that of solid counterparts, respectively. This was attributed to the stress concentration behavior of foam cells under tensile loads. The elongation at break of PLA decreased from 6% to 3% and 1% for unfoamed and foamed PLA/wood flour composites, respectively. The presence of rigid wood flour particles hindered the motion of PLA molecules (lower deformation) leading to lower elongation at break. The average elongation at break of the unfoamed composites is about 160% higher than for foamed samples. So the presence of fillers and foam cells significantly reduced the elongation at break of PLA. On the other hand, the specific flexural modulus increased from 2364 MPa/(g.cm⁻³) to 5089 MPa/(g.cm⁻³) for foamed PLA/25% wt. wood flour composites. High strength to weight ratio of wood flour contributed to the increased flexural modulus of the foamed composites. But the average specific flexural modulus of the foamed composites was similar to the unfoamed samples. At constant fiber concentrations of 15% and 25% wt., the specific flexural modulus increased by about 5%. Impact strength of PLA was influenced by both wood flour and foaming by decreasing by about 15% and 3% for unfoamed and foamed PLA composites respectively, compared to neat PLA. The stress concentration effect of wood flour as well as its rigidity and brittleness contributed to lower impact strength. A 17% increase in impact strength was also reported as a result of foaming. Compared to neat foamed PLA, specific impact strength, specific flexural strength and specific tensile modulus of the foamed PLA composites were increased by about 26%, 5% and 64%, respectively at various wood flour concentrations. The maximum specific flexural modulus for the neat foamed PLA samples was about 3200 MPa/(g.cm⁻³), which increased by about 60% to reach 5089 MPa/(g.cm⁻³) for PLA/25% wt. wood flour. Furthermore, wood flour decreased the elongation at break of the foamed composites compared to neat foamed PLA. The results of thermal analysis showed no significant change in melting temperature as a result of foaming at various shot sizes. However, foaming led to a maximum of 19% increase in crystallinity for foamed samples at a shot size of 31%. Conversely, melting temperature decreased from 167 to 165 °C for neat unfoamed PLA and foamed PLA/wood flour composites, respectively. Crystallinity also decreased from 41% for solid PLA to 33% for foamed PLA/40% wt. wood flour. Compared to neat foamed PLA samples, crystallinity also decreased from 49% for

foamed PLA with a shot size of 31% to 33% for foamed PLA/40% wt. wood flour. Therefore, foaming and wood flour addition both decreased PLA crystallinity. On average, the crystallinity of the foamed composites is about 20% lower than for neat foamed samples. Moreover, the average crystallinity of foamed PLA composites is 16% lower than their solid counterparts due to the effect of wood and foam cells on restraining the mobility of PLA molecules.

As presented here, the same improvement in foam cell morphology was significantly observed by the addition of lignocellulosic fiber. For instance, adding both flax fiber and wood flour resulted in smaller cell size and higher cell density. Changes in PLA melt viscosity were also believed to alter the foam morphology. In addition, lignocellulosic reinforcement of foamed PLA composites led to increased specific tensile and flexural moduli. Moreover, changes in PLA crystallinity induced by fiber addition can potentially influence the morphology of foamed PLA composites (Pilla *et al.*, 2009; Teymoorzadeh & Rodrigue, 2016).

2.4 Thermal Annealing of PLA Composites

PLA main limitation is related to its mechanical and thermal properties not being stable at high temperature due to its low softening point of around 60 °C (Baheti *et al.*, 2013). To overcome this drawback, some studies focused on improving PLA crystallinity by thermal annealing, i.e., a post-processing treatment consisting in submitting the samples to a controlled temperature for a limited period. Mofokeng *et al.*, (2011) applied an annealing process after the extrusion of PLA/sisal composites. They placed the samples in an oven at 120 °C for 3 h for recrystallization and the samples were then dried in an oven at 85 °C followed by injection molding at 190 °C. They reported that PLA composites showed a better interaction between the fibers and PLA than other polymers like polypropylene (PP). However, the material lost its ability to sustain stresses as soon as the glass transition temperature was exceeded. Mathew *et al.*, (2006) treated neat PLA, PLA-cellulose and PLA-wood composites by heating for 3 days at 80 °C. The treatment improved the crystallinity of PLA, PLA-cellulose and PLA-wood from 19, 35 and 45% to 57, 53 and 52% respectively. At the same time, the dynamic modulus at 80 °C increased from 2.2, 46.7 and 24.5 MPa to 720, 2160 and 2150 MPa. Pantani & Sorrentino, (2013) prepared PLA samples by injection molding and kept the samples in an oven at 105 °C for 8 hours to increase crystallinity (maximum crystallinity reached of 30%) to study its effect on material degradation in a homemade respirometric system. Higher crystallinity was found to decrease the PLA degradation rate: amorphous samples reached 60% degradation in about 35 days, while semi-crystalline samples reached only 30% in 60 days. Perego *et al.*, (1996) submitted their samples to annealing by heating for 90 min at 105 °C. They used four PLA matrices with different molecular weights and reported that the enthalpy (ΔH) for annealed samples was much higher than for untreated samples with values from 8, 13, 8 and 3 J/g to 65, 59, 48 and 42 J/g.

Table 2.4 shows the effect of thermal annealing on PLA crystallinity and some natural fiber composites. The crystallinity for untreated PLA was 47.7% which increased to 51.5% after annealing. The crystallinity of the composites also increased due to

Table 2.4 Effect of annealing on the crystallinity of PLA-natural fiber composites.

Samples	Fiber content (%)	Crystallinity (%)	
		U	T
PLA		47.7	51.5
Agave	10	44.3	47.4
	20	45.2	51.1
	30	51.1	56.9
Coir	10	44.6	49.3
	20	47.5	48.9
	30	46.6	48.1
Pine	10	45.9	50.7
	20	41.5	51.8
	30	44.6	52.4

U: Composites without annealing; T: Composites with annealing.

Table 2.5 Minimum annealing time to enhance the storage modulus of PLA.

Annealing treatment temperature (°C)	Untreated sample	65	70	75	80	85	95	105	115
Minimum treatment time (min)	–	30	30	10	10	5	5	2	2
Storage modulus at 70 °C	39	1381	1301	1327	1347	1374	1273	1363	1171

annealing, but the level (2–9%) depends on fiber type and content. The maximum crystallinity level was achieved for PLA-agave composites (57%).

As previously mentioned, PLA is very susceptible to temperature. By thermal dynamical mechanical analysis, a sharp modulus reduction around 55–80 °C is associated with the matrix softening and the α -relaxation of the amorphous regions of PLA (Mathew *et al.*, 2006). As reported above, the storage modulus of PLA composites increases with fiber content. These increases are related to fiber reinforcement and the presence of an interface with the PLA matrix controlling stress transfer (Bledzki & Gassan, 1999). Thermal annealing at different temperatures (65–115 °C) and different times was evaluated for PLA-maple wood composites (75%–25% wt.). In Table 2.5, it can be observed that for temperatures between 105 and 115 °C with only 2 minutes of annealing, these conditions can improve the storage modulus. However, when the temperature decreases the time necessary to improve storage modulus increases. For example, at 65 °C the minimum time was 30 minutes. Figure 2.4 shows typical dynamic modulus improvement for PLA-maple wood flour composites due to annealing. It can be seen that at 85 °C and for different times, storage modulus loss above 55 °C was almost eliminated for annealed samples.

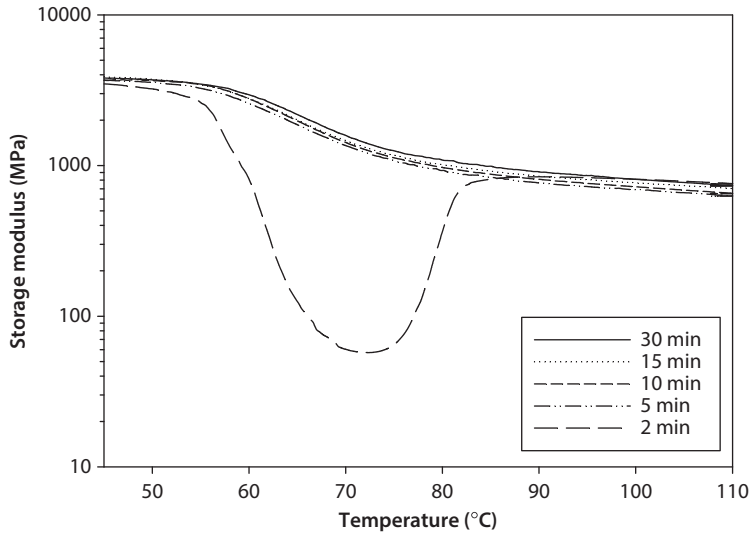


Figure 2.4 Storage modulus of PLA-wood composites at different annealing time (95 °C).

Table 2.6 Effect of annealing on the storage modulus of PLA-natural fiber composites.

Sample	Fiber content (%)	Dynamic modulus at 40 °C (MPa)		Dynamic modulus at 70 °C (MPa)		Temperature for 30% of the modulus at 40 °C (°C)	
		U	T	U	T	U	T
PLA	0	1278	1243	7	483	56	74
Agave	10	1511	1740	18	787	56	78
	20	1682	1715	49	871	58	94
	30	1990	1556	99	886	59	110
Coir	10	1401	1271	16	613	57	85
	20	1835	1454	30	848	56	110
	30	1704	1341	42	1053	58	110
Pine	10	1648	1175	11	628	55	78
	20	2171	1326	25	717	57	90
	30	1489	1416	7	793	57	110

Table 2.6 presents the storage modulus of composites treated by thermal annealing for one hour at 95 °C. It is clear that the values considerably increased (by around two orders of magnitude) when the temperature is 70 °C. In general, samples without treatment have 30% of the initial dynamic modulus (value at 40 °C) for temperatures around 55 °C, while for treated samples this value was reached at much higher temperatures (around 110 °C). Mathew *et al.*, (2006) also reported that heat treatment substantially improved the dynamic modulus and thermal stability of PLA-cellulose and PLA-wood

composites. This improvement means that the treated composites can be used at much higher temperatures than the untreated ones.

The impact strength of PLA can also be modified by annealing. Perego *et al.*, (1996) annealed PLA and observed that impact strength of amorphous PLA (26 J/m) increased up to 70 J/m (169%). PLA-agave composites showed increases of 52, 32 and 10% for 10, 20 and 30% fiber, respectively. In coir composites, the increases were 45, 40 and 5% for 10, 20 and 30% fiber, respectively. For pine composites with only 10% fiber the impact strength increased significantly (33%), while for 20 and 30% the increase was much less (12 and 3% respectively). Again, the results can be related to matrix crystallinity. As reported in Table 2.7, flexural and tensile modulus can increase or remain very similar after annealing while flexural and tensile strength decrease with annealing. Zhou *et al.*, (2013) studied the addition of high-density polyethylene (HDPE) and annealing treatment to isotactic polypropylene (PP) at different temperatures (80, 100, 120 and 130 °C) and found similar results. The impact strength was improved with annealing by 79, 179, 753, and 1107% respectively, compared to untreated PP. On the other hand, they found that annealing leads to lower elongation at break. The flexural moduli increased, showing that annealing and incorporation of HDPE exhibited

Table 2.7 Effect of annealing on the mechanical properties of PLA and PLA composites.

	Flexural strength (MPa)		Flexural modulus (MPa)		Tensile Strength (MPa)		Tensile modulus (MPa)		Impact strength (J/m)		
	U	T	U	T	U	T	U	T	U	T	
PLA	64	51	3650	4200	59	47	3550	4100	19	32	Perego <i>et al.</i> , (1996)
	97	83	3600	4100	55	54	3550	4050	22	55	
	100	113	3600	4150	58	59	3750	4050	25	70	
	106	119	3650	4150	59	66	3750	4150	26	66	
	95	79	2349	2555	60	59	1242	1285	30	49	
Agave	85	72	2716	2991	53	53	1388	1454	30	46	Pérez-Fonseca <i>et al.</i> , (2015)
	86	70	2846	3082	55	53	1524	1547	35	47	
	89	70	3007	3222	53	48	1541	1578	41	45	
Coir	92	72	2729	3105	59	55	1331	1304	30	44	
	88	73	2905	3223	57	52	1417	1438	34	48	
	91	73	3111	3317	55	52	1585	1540	41	43	
Pine	85	71	2653	2919	51	49	1347	1509	30	40	
	81	68	3100	3267	51	45	1644	1751	31	35	
	73	57	3029	3216	47	42	1865	1936	31	32	

substantial synergistic toughening effect with limited stiffening effect on PP. These have good potential to obtain excellent PP rigidity/toughness balance.

2.5 Conclusions

Composites based on PLA, foamed or not, are fully biodegradable materials when reinforced with sustainable and available natural/lignocellulosic fibers. These compounds can be found in various applications like the automotive, packaging and construction industries. These materials can be produced by standard thermoplastics processing techniques like extrusion, compression and injection molding. Nevertheless, processing conditions, mainly temperature, must be optimized to account for limitations related to thermo-mechanical degradation of both PLA and fibers.

This chapter presented the effect of fiber type, treatment and content on PLA and PLA foams. In general, the addition of lignocellulosic fibers significantly influence the morphology and mechanical properties of PLA, as well as processability through rheology changes (viscosity and elasticity). It was also shown that the mechanical behavior of PLA-based materials can be substantially modified by a simple thermal annealing since PLA is highly sensitive to crystallinity content.

Finally, PLA/lignocellulosic fiber composites can offer sustainability and biodegradability, which are two important properties when compared to petroleum-based resins reinforced with synthetic fibers like glass, boron and Kevlar. Nevertheless, there is still room for additional research to improve the overall properties and reduce costs with efficient processing.

References

- Ameli, A., Nofar, M., Jahani, D., Rizvi, G., Park, C.B., Development of high void fraction polylactide composite foams using injection molding: crystallization and foaming behaviors. *Chem. Eng. J.*, 262, 78, 2015.
- Ameli, A., Jahani, D., Nofar, M., Jung, P.U., Park, C.B., Development of high void fraction polylactide composite foams using injection molding: mechanical and thermal insulation properties. *Compos. Sci. Technol.*, 90, 88, 2014.
- Arias, A., Heuzey, M.C., Huneault, M.A., Thermomechanical and crystallization behavior of polylactide-based flax fiber biocomposites. *Cellulose*, 20, 439, 2013.
- Armentano, I., Bitinis, N., Fortunati, E., Mattioli, S., Rescignano, N., Verdejo, R., Lopez-Manchado, M.A., Kenny, J.M., Multifunctional nanostructured PLA materials for packaging and tissue engineering. *Prog. Polym. Sci.*, 38, 1720, 2013.
- Arrieta, M.P., Parres, F., López, J., Jiménez, A., Development of a novel pyrolysis-gas chromatography/mass spectrometry method for the analysis of poly(lactic acid) thermal degradation products. *J. Anal. Appl. Pyrol.*, 101, 150, 2013.
- Arrieta, M.P., López, J., Rayón, E., Jiménez, A., Disintegrability under composting conditions of plasticized PLA-PHB blends. *Polym. Degrad. Stabil.*, 108, 307, 2014.
- Asaithambi, B., Ganesan, G., Ananda-Kumar, S., Bio-composites: Development and Mechanical Characterization of Banana/Sisal Fibre Reinforced Poly Lactic Acid (PLA) Hybrid Composites. *Fibers Polym.*, 15, 847, 2014.

- Awal, A., Rana, M., Sain, M., Thermorheological and mechanical properties of cellulose reinforced PLA bio-composites. *Mech. Mater.*, 80, 87, 2015.
- Baghaei, B., Skrifvars, M., Berglin, L., Manufacture and characterisation of thermoplastic composites made from PLA/hemp co-wrapped hybrid yarn preregs. *Compos. Part. A.*, 50, 93, 2013.
- Baheti, V., Militky, J., Marsalkova, M., Mechanical properties of poly lactic acid composite films reinforced with wet milled jute nanofibers. *Polym. Compos.*, 34, 2133, 2013.
- Bajpai, P.K., Singh, I., Madaan, J., Development and characterization of PLA-based green composites: a review. *J. Thermoplast. Compos. Mater.*, 27, 52, 2012.
- Bax, B., Mussig, J., Impact and tensile properties of PLA/Cordenka and PLA/flax composites. *Compos. Sci. Technol.*, 68, 1601, 2008.
- Bergret, A., Benezet, J.C., Natural-fiber reinforced biofoams. *Int. J. Polym. Sci.*, 2011, 1, 2011.
- Bledzki, A.K., Gassan, J., Composites reinforced with cellulose based fibres. *Prog. Polym. Sci.*, 24, 221, 1999.
- Boissard, C.I.R., Bourban, P.A., Plummer, C.J.G., Neagu, R.C., Månson, J.A.E., Cellular biocomposites from polylactide and microfibrillated cellulose. *J. Cell. Plast.*, 48, 445, 2012.
- Carus, M., Nova-Institute, <http://news.bio-based.eu/growth-in-pla-bioplastics>, 2012.
- Chirayil, C.J., Mathew, L., Thomas, S., Review of recent research in nano cellulose preparation from different lignocellulosic fibers. *Rev. Adv. Mater. Sci.*, 37, 20, 2014.
- Cho, S.Y., Park, H.H., Yun, Y.S., Jin, H.J., Influence of cellulose nanofibers on the morphology and physical properties of poly(lactic acid) foaming by supercritical carbon dioxide. *Macromol. Res.*, 21, 529, 2012.
- Chun, K.S., Husseinsyah, S., Polylactic acid/corn cob eco-composites: Effect of new organic coupling agent. *J. Thermoplast. Compos.*, 27, 1667, 2013.
- Csikos, A., Faludi, G., Domján, A., Renner, K., Móczó, J., Béla, Pukánszky, Modification of interfacial adhesion with a functionalized polymer in PLA/wood composites. *Eur. Polym. J.*, 68, 592, 2015.
- Diaz-Acosta, C.A., Continuous microcellular foaming of polylactic acid/natural fiber composites. PhD thesis, Michigan State University, USA, 2011.
- Ding, W.D., Kuo, P.Y., Kuboki, T., Park, C.B., and Sain, M., Foaming of Cellulose Fiber Reinforced Polylactic Acid Composites: The Effect of Cellulose Fiber type and Content. Society of Plastics Engineers, 71th Annual Technical Conference, Paper #1591117, April 22–24, Cincinnati, Ohio, USA, 2013.
- Dong, Y., Ghataura, A., Takagi, H., Haroosh, H., Nakagaito, A., Lau, K.T., Polylactic acid (PLA) biocomposites reinforced with coir fibres: Evaluation of mechanical performance and multifunctional properties. *Compos. Part. A.*, 63, 76, 2014.
- Faludi, G., Dora, G., Renner, K., Móczó, J., Pukánszky, B., Improving interfacial adhesion in PLA/wood biocomposites. *Compos. Sci. Technol.*, 89, 77, 2013.
- Garlota, D., A Literature Review of Poly(Lactic Acid). *J. Polym. Environ.*, 9, 63, 2001.
- Goriparthi, B.K., Suman, K.N.S., Mohan-Rao, N., Effect of fiber surface treatments on mechanical and abrasive wear performance of polylactide/jute composites. *Compos. Part. A.*, 43, 1800, 2012.
- Gu, H., Tensile behaviours of the coir fibre and related composites after NaOH treatment. *Mater. Design.*, 30, 3931, 2009.
- Gupta, B., Revagade, N., Hilborn, J., Poly(lactic acid) fiber: an overview. *Prog. Polym. Sci.*, 34, 455, 2007.
- Haque, M., Hasan, M., Islam, S., Ali, E., Physico-mechanical properties of chemically treated palm and coir fiber reinforced polypropylene composites. *Biores. Technol.*, 100, 4903, 2009.
- Harmaen, S.H., Khalina, A., Azowa, I., Hassan, M.A., Tarmian, A., Jawaed, M., Thermal and Biodegradation Properties of Poly(lactic acid)/Fertilizer/Oil Palm Fibers Blends Biocomposites, *Polym. Compos.*, 36, 576, 2015.

- Huda, M.S., Mohanty, A.K., Drzal, L.T., Schut, E., "Green" composites from recycled cellulose and poly(lactic acid): Physico-mechanical and morphological properties evaluation. *J. Mater. Sci.*, 40, 4221, 2005.
- Huda, M.S., Drzal, L.T., Misra, M., Mohanty, A., Wood-fiber-reinforced poly(lactic acid) composites: evaluation of the physicomechanical and morphological properties *J. Appl. Polym. Sci.*, 102, 4856, 2006.
- Kim, K.W., Lee, B.H., Kim, H.J., Sriroth, K., Dorgan, J.R., Thermal and mechanical properties of cassava and pineapple flours-filled PLA bio-composites. *J. Therm. Anal. Calorim.*, 108, 1131, 2012.
- Koyama, R., Kuboki, T., Ding, W.D., Adhikary, K.B., Chen, N., and Park, C.B., Extrusion Foaming of Cellulose Fiber Reinforced Polylactic Acid Biocomposites. Annual Technical Conference of Society of Plastics Engineers, Paper #0370, 1–5 May, Boston, Massachusetts, USA, 2011.
- Lasprilla, A., Martinez, G., Lunelli, B., Jardini, A., Filho, R., Poly-lactic acid synthesis for application in biomedical devices. A review. *Biotechnol. Adv.*, 30, 321, 2012.
- Lee, P.C., Park, C.B., *Extrusion of high-density and low-density microcellular plastics*, S. T. Lee, C. B. Park (Ed.), pp. 436–486, Taylor & Francis Group, Florida, 2014.
- Lee, S.Y., Kang, I.A., Doh, G.H., Yoon, H.G., Park, B.D., Wu, Q., Thermal and Mechanical Properties of Wood Flour/Talc-filled Polylactic Acid Composites: Effect of Filler Content and Coupling Treatment. *J. Thermoplast. Compos.*, 21, 209, 2008.
- Lee, S.H., Wang, S., Biodegradable polymers/bamboo fiber biocomposite with bio-based coupling agent. *Compos. Part. A.*, 37, 80, 2006.
- Lim, L.T., Auras, R., Rubino, M., Processing technologies for poly(lactic acid). *Prog. Polym. Sci.*, 33, 820, 2008.
- Lim, J.S., Park, K., Chung, G.S., Kim, J.H., Effect of composition ratio on the thermal and physical properties of semicrystalline PLA/PHB-HHx composites. *Mater. Sci. Eng. C.*, 33, 2131, 2013.
- Ljunberg, N., Wesslen, B., The Effects of Plasticizers on the Dynamic Mechanical and Thermal Properties of Poly(Lactic Acid). *J. Appl. Polym. Sci.*, 86, 1227, 2002.
- Loureiro, N.C., Esteves, J.L., Viana, J.C., Ghosh, S., Development of polyhydroxyalkanoates/poly(lactic acid) composites reinforced with cellulosic fibers. *Compos. Part. B.*, 60, 603, 2014.
- Luebke, G., Advantage of the use of chemical blowing agents in wood-plastic composites, Blowing agents and foaming processes conference 2001, *Rapra Technology Limited*, Shropshire, 2001.
- Ma, H., Joo, C.W., Structure and mechanical properties of jute-poly(lactic acid) biodegradable composites. *J. Compos. Mater.*, 45, 1451, 2011.
- Majhi, S.K., Nayak, S.K., Mohanty, S., Unnikrishnan, L., Mechanical and fracture behavior of banana fiber reinforced polylactic acid biocomposites. *Int. J. Plast. Technol.*, 14, S57, 2010.
- Martin, O., Averous, L., Poly (lactid acid): plasticization and properties of biodegradable multi-phase systems. *Polymer*, 42, 6209, 2001.
- Mathew, A.P., Oksman, K., Sain, M., The effect of morphology and chemical characteristics of cellulose reinforcements on the crystallinity of polylactic acid. *J. Appl. Polym. Sci.*, 101, 300, 2006.
- Matuana, L.M., Faruk, O., Effect of gas saturation conditions on the expansion ratio of microcellular poly(lactic acid)/wood-flour composites. *EXPRESS Polym. Lett.*, 4, 621, 2010.
- Matuana, L., Diaz, C.A., Strategy to produce microcellular foamed poly(lactic acid)/wood flour composites in a continuous extrusion process. *Ind. Eng. Chem. Res.*, 52, 12032, 2013.
- Mofokeng, J.P., Luyt, A.S., Tabi, T., Kovacs, J., Abstract comparison of injection moulded, natural fibre-reinforced composites with PP and PLA as matrices. *J. Thermoplast. Compos. Mater.*, 25, 927, 2011.

- Plackett D., Södergård A., Polylactide-Based Biocomposites, in: *Natural Fibers, Biopolymers, and Biocomposites*. Mohanty, A., Misra, M., Drzal, L., (Ed.), pp 584–600, Taylor & Francis Group, Florida, 2005.
- Najafi, N., Heuzey, M.C., Carreau, P.J., Therriault, D., Park, C.P., Rheological and foaming behavior of linear and branched polylactides. *Rheol. Acta.*, 53, 779, 2014.
- Nampoothiri, K.M., Nair, N.R., John, R.P., An overview of the recent developments in polylactide (PLA) research. *Biores. Technol.*, 101, 8493, 2010.
- Neagu, R.C., Cuénoud, M., Berthold, F., Bourban, P.E., Gamstedt, E.K., Lindström, M., Månson, The potential of wood fibers as reinforcement in cellular biopolymers. *J. Cell. Plast.*, 48, 71, 2011.
- Nishino, T., Hirao, K., Kotera, M., Nakamae, K., Inagaki, H., Kenaf reinforced biodegradable composite. *Compos. Sci. Technol.*, 63, 1281, 2003.
- Nofar, M., Park, C.B., Poly(lactic acid) foaming. *Prog. Polym. Sci.*, 39, 1721, 2014.
- Oksman, K., Skrifvars, M., Selin, J.F., Natural fibres as reinforcement in polylactic acid (PLA) composites. *Compos. Sci. Technol.*, 63, 1317, 2003.
- Pantani, R., De Santis, F., Sorrentino, A., De Maio, F., Titomanlio, G., Crystallization kinetics of virgin and processed poly(lactic acid). *Polym. Degrad. Stabil.*, 95, 1148, 2010.
- Pantani, R., Sorrentino, A., Crystallization kinetics of virgin and processed poly(lactic acid). *Polym. Degrad. Stabil.*, 98, 1089, 2013.
- Pappu, A., Patil, V., Jain S., Mahindrakar, A., Haque, R., Thakur V.K., Advances in industrial prospective of cellulosic macromolecules enriched banana biofibre resources: A review. *Int. J. Biol. Macromol.*, 79, 449, 2015.
- Perego, G., Cella, G.D., Bastl, C., Effect of Molecular Weight and Crystallinity on Poly(lactic acid) Mechanical Properties. *J. Appl. Polym. Sci.*, 59, 37, 1996.
- Peinado, V., Garcia, L., Fernandez, A., Castell, P., Novel lightweight foamed poly(lactic acid) reinforced with different loadings of functionalised sepiolite. *Compos. Sci. Technol.*, 101, 17, 2014.
- Pérez-Fonseca, A.A., Robledo-Ortiz, J.R., Ramirez-Arreola, D.E., Ortega-Gudiño, P., Rodrigue, D., González-Núñez, R., Effect of hybridization on the physical and mechanical properties of high density polyethylene–(pine/agave) composites. *Mater. Design*, 64, 35, 2014.
- Pérez-Fonseca, A.A., Robledo-Ortiz, J.R., González-Núñez, R., Rodrigue, D., Effect of thermal annealing on the mechanical and thermal properties of polylactic acid/natural fibers composites, *J. Appl. Polym. Sci.*, submitted.
- Pilla, S., Handbook of Bioplastics and Biocomposites Engineering Applications, John Wiley & Sons, Inc. Hoboken, New Jersey, 2011.
- Pilla, S., Kramschuster, A., Lee, J., Auer, G.K., Gong, S., Turng, L.S., Microcellular and solid polylactide-flax fiber composites. *Compos. Interfaces.*, 16, 869, 2009.
- Rajesh, G., Ratna-Prasad, A.V., Tensile properties of successive alkali treated short jute fiber reinforced PLA composites. *Proc. Mater. Sci.*, 5, 2188, 2014.
- Rasal, R.M., Janorkar, A.V., Hirta, D.E., Poly(lactic acid) modifications. *Prog. Polym. Sci.*, 35, 338, 2010.
- Rahmat, A.R., Sin, L.T., Rahman, W.A., Polylactic Acid: PLA Biopolymer Technology and Applications, William Andrew Publishing, 2012.
- Rizvi, R., Cochrane, B., Naguib, H., Lee, P.C., Fabrication and characterization of melt-blended polylactide-chitin composites and their foams. *J. Cell. Plast.*, 47, 283, 2011.
- Sahari, J., Sapuan, S.M., Natural fibre reinforced biodegradable polymer composites. *Rev. Adv. Mater. Sci.*, 30, 166, 2011.
- Sawpan, M.A., Pickering, K.L., Fernyhough, A., Improvement of mechanical performance of industrial hemp fibre reinforced polylactide biocomposites. *Compos. Part. A*, 42, 310, 2011.
- Shah, B.L., Selke, S.E., Walters, M.B., Heiden, P.A., Effects of Wood Flour and Chitosan on Mechanical, Chemical, and Thermal Properties of Polylactide. *Polym. Compos.*, 29, 655, 2008.

- Shi, N., Dou, Q., Crystallization Behavior, Morphology, and Mechanical Properties of Poly(lactic acid)/Tributyl Citrate/Treated Calcium Carbonate Composites. *Polym. Compos.*, 35, 1570, 2014.
- Singha, A.S., Thakur, V.K., Synthesis and Characterization of Pine Needles Reinforced RF Matrix Based Biocomposites. *J. Chem.* 5, 1055, 2008a.
- Singha, A.S., Thakur, V.K., Mechanical, Morphological and Thermal Properties of Pine Needle-Reinforced Polymer Composites. *Int. J. Polym. Mater.* 58, 21, 2008b.
- Singha, A.S., Thakur, V.K., Synthesis and characterization of Grewia optiva fiber-reinforced PF-based composites. *Int. J. Polym. Mater.* 57, 1059, 2008c.
- Singha, A.S., Thakur, V.K., Morphological, thermal, and physicochemical characterization of surface modified pinus fibers. *Int. J. Polym. Anal. Charact.* 14, 271–289, 2009a.
- Singha, A.S., Thakur, V.K., Synthesis and characterizations of silane treated Grewia optiva fibers. *Int. J. Polym. Anal. Charact.* 14, 301–321, 2009b.
- Singha, A.S., Thakur, V.K., Chemical resistance, mechanical and physical properties of biofibers-based polymer composites. *Polym.-Plast. Technol. Eng.* 48, 736–744, 2009c.
- Singha, A.S., Thakur, V.K., Study of mechanical properties of urea-formaldehyde thermosets reinforced by pine needle powder. *BioResources* 4, 292–308, 2009d.
- Singha, A.S., Thakur, V.K., Fabrication and characterization of S. ciliare fibre reinforced polymer composites. *Bull. Mater. Sci.* 32, 49–58, 2009e.
- Teymoorzadeh, H., Rodrigue, D., Biocomposites of Flax Fiber and Polylactic Acid: Processing and Properties. *J. Renew. Mater.*, 2, 270, 2014.
- Teymoorzadeh, H., Rodrigue, D., Biocomposites of Wood Flour and Polylactic Acid: Processing and Properties. *J. Biobased. Mater. Bioenergy*, 9, 1, 2015.
- Teymoorzadeh, H., Rodrigue, D., Morphological, Mechanical, and Thermal Properties of Injection Molded PLA Foams/Composites based on Wood Flour, *J. Cell. Plast.*, submitted, 2016.
- Thomas, S., Pothan, L.A., *Natural Fiber Reinforced Composites: From Macro to Nanoscale*. Old City Publishing Philadelphia, PA, 2009.
- Thakur, V.K., Kessler, M.R., Self-healing polymer nanocomposite materials: A review. *Polymer* 69, 369, 2015.
- Thakur, V.K., Thakur, M.K., Processing and characterization of natural cellulose fibers/thermoset polymer composites. *Carbohydr. Polym.* 109, 102, 2014a.
- Thakur, V.K., Thakur, M.K., Recent Advances in Graft Copolymerization and Applications of Chitosan: A Review. *ACS Sustain. Chem. Eng.* 2, 2637, 2014b.
- Tokoro, R., Vu, D.M., Okubo, K., Tanaka, T., Fujii, T., Fujiura, T., How to improve mechanical properties of polylactic acid with bamboo fibers. *J. Mater. Sci.*, 43, 775, 2008.
- Voicu, S.I., Condruz, R.M., Mitran, V., Cimpean, A., Miculescu, F., Andronescu, C., Miculescu, M., Thakur, V.K., Sericin Covalent Immobilization onto Cellulose Acetate Membrane for Biomedical Applications. *ACS Sustain. Chem. Eng.* 4, 1765, 2016.
- Way, C., Wu, D.Y., Cram, D., Processing stability and biodegradation of polylactic acid (PLA), composites reinforced with cotton linters or maple hardwood fibres. *J. Polym. Environ.*, 21, 54, 2012.
- Yu, L., Dean, K., Li, L., Polymer blends and composites from renewable sources. *Prog. Polym. Sci.*, 31, 576, 2006.
- Yu, T., Hu, C., Chen, X., Li, Y., Effect of diisocyanates as compatibilizer on the properties of ramie/poly(lactic acid) (PLA) composites. *Compos. Part. A.*, 76, 20, 2015.
- Zhan, P., Investigation of poly(lactic acid) (PLA)/sugar beet pulp bioplastics: processing, morphology, properties and foaming application. M.Sc. thesis, department of mechanical and materials engineering, Washington State University, USA, 2012.
- Zou, H., Wang, L., Gan, H., Yi, C., Effect of Fiber Surface Treatments on the Properties of Short Sisal Fiber/Poly(lactic acid). Biocomposites. *Polym. Compos.*, 33, 1659, 2012.

Microcrystalline Cellulose and Related Polymer Composites: Synthesis, Characterization and Properties

Djalal Trache

*Education and Research Unit of Applied Chemistry, Ecole Militaire Polytechnique,
Algiers, Algeria*

Abstract

Aramide, glass and carbon have been widely used as reinforcement fibers. While the composites based on these fibers show favorable properties, such as heat resistance and high strength, they are difficult to recycle, expensive to produce and are not biodegradable. A trend has been prompted mainly due to many diverse economic, performance and environmental issues. Interest in microcrystalline cellulose (MCC) has been increasing exponentially. Owing to its excellent mechanical properties, remarkable reinforcing capability, high surface area and environmental benefits, this renewable nanomaterial has recently attracted the attention of scientists and researchers to develop green polymer composites. In addition, MCC exhibits a large capacity to allow grafting or tailoring of chemical species to improve the morphology, thermal and mechanical properties of resulting composites.

This chapter describes the isolation processes, characterization and properties of MCC based on chemical structure, molecular weight, morphology, crystallinity, and thermal and mechanical behaviors. Based on different characterizations, MCC shows tremendous potential use in engineering applications. Also discussed in this review is the context for inclusion of MCC fibers from natural sources in many fields such as pharmaceutical carriers, reinforcement, building materials and composites, automotive applications, and others. The improvement of environmental, physical, thermal and mechanical properties of MCC-based composite materials is explained as well.

Keywords: Microcrystalline cellulose, sources, properties, polymer, composite, applications

3.1 Introduction

Over the last two decades, remarkable attention has been paid to environmental, green and sustainable materials for a number of applications (La Mantia & Morreale, 2011; Abdul Khalil *et al.*, 2012; Fernandes *et al.*, 2013; Thakur, 2015a). Indeed, rapidly diminishing global petroleum resources, along with awareness of global environmental

Corresponding author: djalaltrache@gmail.com

Vijay Kumar Thakur, Manju Kumari Thakur and Michael R. Kessler (eds.), Handbook of Composites from Renewable Materials, (61–92) © 2017 Scrivener Publishing LLC

problems, have paved the way to switch towards renewable materials (Satyanarayana *et al.*, 2009; Ma *et al.*, 2011; Khalil *et al.*, 2012; Thakur & Thakur, 2014). In this regard, bio-based polymers can form the basis for a variety of eco-efficient, sustainable products that can capture and compete in markets presently dominated by products based solely on petroleum-based raw material (Ma *et al.*, 2011; Thakur & Thakur, 2014; Thakur, 2015a–b). Polymers have been rapidly emerging as the prospective substitute to ceramic or metal materials, due to their advantages over conventional materials (Mian & Hamad, 2013; Thakur, 2015b). They are low cost, flexible and easy to process (Wu *et al.*, 2016) (Lin *et al.*, 2011a) (Lin *et al.*, 2011b). However, for some specific applications, some mechanical properties of polymer materials are found to be insufficient (Thakur *et al.*, 2014 a–g). Many approaches have been used to overcome such drawbacks. In most of these applications, the properties of polymers are tailored using fibers and fillers to suit the mechanical requirements. Composite materials exhibit excellent mechanical and thermal properties compared to the conventional materials and show a high potential for future applications in diverse industries, including automotive applications, defense, building, packaging, aerospace, sporting goods, marine, medical and electronic fields to name a few (Singha & Thakur, 2008; Mian & Hamad, 2013; Thakur & Thakur, 2014; Pandey *et al.*, 2015; Thakur & Kessler, 2015).

Composite materials, or composites, are one of the main improvements in materials technology in recent years (Abdul Khalil *et al.*, 2012; Fernandes *et al.*, 2013; Thakur *et al.*, 2014a–d). In the materials science field, a composite is a multi-phase material consisting of two or more physically distinct components, a matrix (or a continuous phase) and at least one dispersed (filler or reinforcement) phase. The dispersed phase, responsible for enhancing one or more properties of matrix, can be categorized according to particle dimensions that comprise platelets, ellipsoids, spheres and fibers. These particles can be of inorganic or organic origin and possess rigid or flexible properties.

Fibers such as aramide, glass and carbon have been widely used as reinforcement fibers. While these composites demonstrate favorable properties such as heat resistance and high strength, they are difficult to recycle, do not biodegrade and are expensive to produce (Shanks *et al.*, 2004). Recently, it has been reported that there are further drawbacks to using carbon and glass fibers. They can lead to irritation of the skin, eyes, and upper respiratory tract. It is reported that long-term exposure to these materials causes cancer and lung scarring (i.e., pulmonary fibrosis) (Thakur, 2015b). From an economic standpoint, making products from carbon fiber-reinforced composites presents a high cost manufacturing process. There has been a trend towards including natural fibers into composites, prompted mainly due to economic, performance and environmental concerns (Spoljaric *et al.*, 2009; Sun *et al.*, 2014; Izzati Zulkifli *et al.*, 2015; Thakur, 2015a; Thakur, 2015b). Among such materials, cellulose-based composites have gained increasing attention from researchers and industrialists (Thakur *et al.*, 2012; Thakur *et al.*, 2013). Among the advantages of using cellulose fibers in polymer composites, the most important are cheapness, availability, biodegradability, renewability, high surface area, low density and excellent mechanical properties.

Cellulose, the most ubiquitous and abundant resource on the planet, is present in a wide range of living species including plants, marine animals, and some bacteria. It is the major structural component of plants and is gaining significance as a renewable resource to substitute petroleum feedstock (Khalil *et al.*, 2012) (Singha & Thakur, 2009, a–e). The annual production of cellulose is expected to be over

$7.5 \cdot 10^{10}$ tons (Habibi *et al.*, 2010). Regardless of the source, cellulose consists of a linear macromolecular chain composed of 1–4 linked β -D-anhydroglucopyranose units (Thakur & Thakur, 2014a). The repeating unit is a dimer of glucose, known as cellobiose. Cellulose microfibrils are composed of a crystalline cellulosic part and a less ordered amorphous part located at the surface and along their main axis (Mohamad Haafiz *et al.*, 2013a; Trache *et al.*, 2014). Upon contact with acid solutions amorphous regions are preferentially cleaved, whereas crystalline domains that have a higher resistance to acid attack (MCC) stay essentially intact. Crystalline cellulose is much stiffer and stronger than amorphous cellulose and cellulose itself, and is believed to be a better reinforcing agent than cellulose.

A prominent class of cellulosic reinforcing agent is microcrystalline cellulose (Ma *et al.*, 2011; Hoyos *et al.*, 2013; Mohamad Haafiz *et al.*, 2013b; Sun *et al.*, 2014; Izzati Zulkifli *et al.*, 2015). MCC has been extensively utilized especially in cosmetics, food, suspension stabilizers, and the defense and medical industries. Furthermore, MCC is used in polymer composites as a reinforcing agent. When compared with carbon, silica and glass fibers, MCC has many advantages: nontoxicity, little abrasion to equipment, low density, biodegradability, low cost, and renewability. Research is now being undertaken that incorporates MCC as filler in different polymer matrices to manufacture new products with improved properties at low price.

In this review we will cover microcrystalline cellulose—its sources, synthesis, morphology, thermal stability and mechanical properties, crystallinity and surface modification possibilities (especially when trying to enhance interfacial adhesion to a matrix). We will also focus on the production and properties of MCC-based polymer composites and their main applications.

3.2 Cellulose: Structure and Sources

3.2.1 Structure of Cellulose

Cellulose is considered to be the most abundant natural polymer and one of the most important renewable resources. Its empirical formula was determined in 1838 by Anselm Payen by isolating a white powder from plant tissue (Habibi *et al.*, 2010; Siqueira *et al.*, 2010). In 1839, he coined the term cellulose for the first time. The structure of cellulose was found late, in 1920, by Hermann Staudinger (Borges *et al.*, 2015). Several reviews have been already been published reporting the state of knowledge of this fascinating polymer so only some details are provided to avoid duplication (Klemm *et al.*, 2005; Habibi *et al.*, 2010; Siqueira *et al.*, 2010; Wertz *et al.*, 2010).

Cellulose is defined as a macromolecule, a nonbranched β (1,4) linked D glucopyranosyl units (anhydroglucose unit). The monomers are related together by condensation such that glycosidic oxygen bridges connect the sugar rings. In nature, cellulose chains have a degree of polymerization of roughly 15,000 glucopyranose units in native cellulose cotton and about 10,000 in wood cellulose (Azizi Samir *et al.*, 2005; Klemm *et al.*, 2005). These cellulose polymer chains are biosynthesized by enzymes, placed in a continuous fashion and combined to form microfibrils, long threadlike bundles of molecules stabilized laterally by hydrogen bonds between hydroxyl groups and oxygen of adjacent molecules. Depending on their origin, the microfibril diameters range from

about 2 to 20 nm for lengths that can reach several tens of microns (Klemm *et al.*, 2005). These microfibrils are highly ordered (crystalline) domains that alternate with less ordered (amorphous) domains.

There are four different polymorphs of cellulose: cellulose I, II, III, and IV. Cellulose I, native cellulose, is the form established in nature, and it took place in two allomorphs, I_α and I_β . Cellulose II, or regenerated cellulose, comes out after re-crystallization or mercerization with aqueous sodium hydroxide. The main difference between these two forms of cellulose lies in the layout of their atoms: cellulose I runs in a parallel direction, whereas the chains in cellulose II have antiparallel packing (Klemm *et al.*, 2005; Wertz *et al.*, 2010).

Cellulose III_I and III_{II} are produced by ammonia treatment of cellulose I and II, respectively, and with the modification of cellulose III, cellulose IV is finally obtained (Klemm *et al.*, 2005; Wertz *et al.*, 2010).

Within the framework of this survey, only native cellulose I is considered. This semi-crystalline fibrillar structure is the main source of MCC.

3.2.2 Sources

Cellulose-based materials have been conventionally used by human beings. However, in recent years, this natural polymer has received significant attention as a well-known sustainable and renewable feedstock for obtaining environmentally friendly technological and compatible product (Kalia *et al.*, 2011). The versatility of cellulose has been reevaluated as a functional and useful structural material. The environmental advantages of cellulose products have become even more noticeable. Cellulose is revered as a versatile feedstock for subsequent chemical modification in production of artificial cellulose-based products (films, threads) as well as of numerous of cellulose derivatives for their use in many fields such as cosmetics, composite materials, food, textiles, pharmaceuticals, and so forth.

The primary feature of cellulose is the accessible lignocellulosic material in forests, with wood (hardwoods, softwoods) as the main source (Abdul Khalil *et al.*, 2012). Cellulose can be even obtained from a variety of sources such as agriculture residues, annual and water plants (Kalia *et al.*, 2011; Abdul Khalil *et al.*, 2012; Wüstenberg, 2015). These include bast fibers (ramie, hemp, flax, jute, kenaf, nettle, mesta, urena), cereal straws (barley, oat, rice, corn, wheat) seed fibers (cotton, coir, milkweed, kapok), fruit fibers (coconut, oil palm), leaf fibers (sisal, pineapple, date-palm, abaca, curaua) and grasses (alfa, bamboo, bagasse). In addition to cellulose, these sources contain lignin, hemicelluloses, and a comparably small amount of extractives (Thakur & Singha, 2010; Pappu *et al.*, 2015). Cellulose can also be produced by other living organisms as well (Voicu *et al.*, 2016). For instance, the tunicate is a marine animal that secretes a tough cellulose sac called tunicin. Other cellulose producing organisms include different types of bacteria (*Acetobacter xylinum*, *Gluconacetobacter*, *Rhizobium*, *Agrobacterium*, *Sarcina*), algae (*Oocystis apiculata*, *Valonica ventricosa*) and some types of fungi (Kalia *et al.*, 2011; Abdul Khalil *et al.*, 2012; Wüstenberg, 2015). The content of cellulose strongly depends on its origin and the isolation process. Nowadays, cotton and wood are the raw materials for commercial production of cellulose. Figure 3.1 depicts how cellulose occurs in nature. Irrespective of its source, cellulose is a white fiber-like structure with a density of around 1.5 g/cm³. The composition of some cellulose sources is shown in Table 3.1.

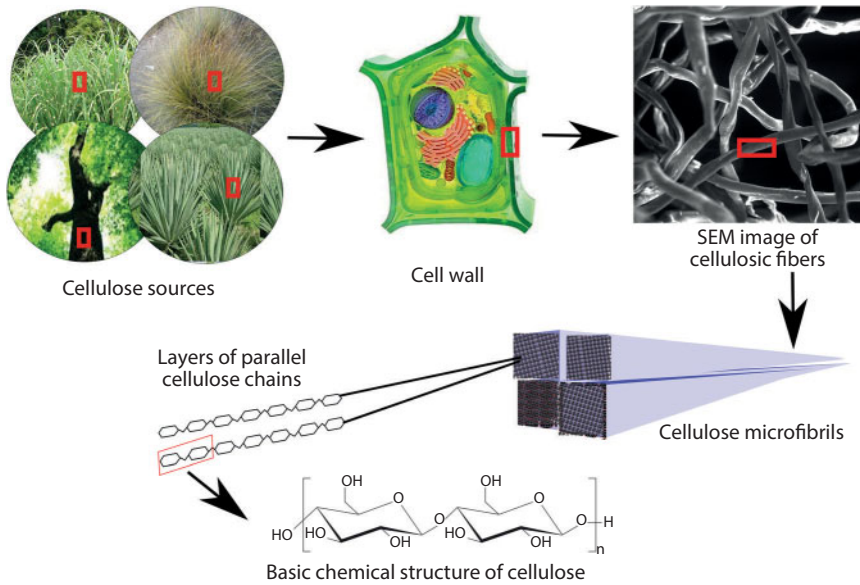


Figure 3.1 Structural levels of organization of cellulose from the sources to the molecules.

Table 3.1 Chemical composition of cellulose-containing materials.

Source	Composition (wt.%)			Reference
	Cellulose	Hemicellulose	Lignin	
Hardwood	43–47	25–35	16–24	Abdul Khalil <i>et al.</i> , 2012
Softwood	40–44	25–29	25–31	Abdul Khalil <i>et al.</i> , 2012
Cotton	93	3	–	Averous & Le Digabel, 2006
Coconut	32–43	0.15–0.25	40–45	Rosa <i>et al.</i> , 2009
Hemp	68	15	10	Mariano <i>et al.</i> , 2006
Alfa	43.6	22.7	21.5	Trache <i>et al.</i> , 2014
Rice hulls	30.98	32.68	16.21	Adel <i>et al.</i> , 2011
Bean hulls	51.87	26.50	10.42	Adel <i>et al.</i> , 2011
Jute	61–71	14–20	12–13	Alvarez <i>et al.</i> , 2006
Ramie	68.6–76.2	13.1–16.7	0.6–0.7	Goda <i>et al.</i> , 2006
Flax	71	18.6–20.6	2.2	Susan <i>et al.</i> , 2004
Sisal	65	12	9.9	Joseph <i>et al.</i> , 2003
Banana	63–64	19	5	Pendy <i>et al.</i> , 2015
Kenaf	44–72	19	9–19	Kalia <i>et al.</i> , 2011
Curaua	73.6	9.9	7.5	Claudio & Caraschi, 2003
Pineapple	73.4	7.1	10.5	Abdul Khalil <i>et al.</i> , 2006

3.3 Microcrystalline Cellulose

3.3.1 Introduction

MCC has a high potential to be utilized in several fields such as a water retainer and suspension stabilizer, in the pharmaceutical, cosmetics, and food industries, and particularly as reinforcement in the development of nanocomposites. Features like strength, crystallinity, fibrous nature, lightness, stiffness, water insolubility, biodegradability and renewability make MCC attractive for uses in diverse industrial applications (Ma *et al.*, 2011; Hoyos *et al.*, 2013; Mohamad Haafiz *et al.*, 2013b; Thoorens *et al.*, 2014; Sun *et al.*, 2014; Izzati Zulkifli *et al.*, 2015; Merci *et al.*, 2015).

MCC is a naturally occurring substance produced from purified, partially depolymerized cellulose, obtained by treating alpha cellulose, and prepared as a pulp from fibrous plant material with mineral acids (as shown in Figure 3.2). The microfibrils that compose the alpha cellulose are made up of paracrystalline and crystalline regions. The paracrystalline area is an amorphous mass of cellulose chains and the crystalline regions consist of tight bundles of microcrystals in a rigid linear arrangement. The crystallite domains are named cellulose crystallites and they are composed of cellulose chains due to hydrogen bonding and Van der Waals interactions. These crystallites have the same diameter order than that of the cellulose microfibrils (Leppänen *et al.*, 2009). The amorphous domains are more susceptible to hydrolysis so partial depolymerization by acid hydrolysis outcomes in more crystalline and shorter fragment, i.e., microcrystalline cellulose.

Interestingly, the discovery of MCC initiated from an unsuccessful experiment (Battista & Smith, 1962). The authors attempted to utilize a Waring blender to split up hydrolyzed cellulose into small particles in water. They supposed the sharp blades of the Waring blender would generate very small fragments of the aggregated microcrystals in the hydrolyzed cellulose, and the prepared microcrystalline fragments would settle out

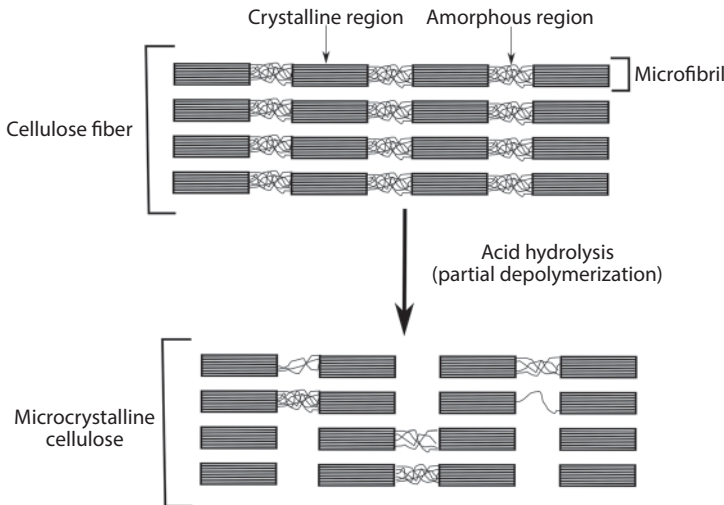


Figure 3.2 Schematic diagram of MCC separation during acid hydrolysis.

of water. Instead however, they obtained a stable colloidal suspension, which is recognized commercially as Avicel (Miao & Hamad, 2013).

Today, MCC is a commercially available material with over a half century of history and price of $\approx \$4/\text{kg}$, similar or less than some other engineering fillers (glass or aramid) (Kiziltas *et al.*, 2011). More than 5 decades later, MCC is produced globally by more than 10 providers (Thorens *et al.*, 2014). Industrial scale MCC is obtained through hydrolysis of cotton and wood cellulose by means of dilute mineral acids. Although wood is surely the most important industrial source of cellulose, competition from many sectors such as the furniture, pulp and paper, and building products industries, as well as the combustion of wood for energy, makes it challenging to provide all users with sufficient quantities of wood at reasonable prices. For this reason, cellulose fibers from other sources are expected to become of increasing interest. MCC can be produced from any material that is high in cellulose. Reports have demonstrated that MCC can be made from cereal straw (Jain *et al.*, 1993), bagasse and corn cob (Okhamafe *et al.*, 1995), bamboo (Ofoefule & Chukwu, 1999), sugar beet pulp (Hanna *et al.*, 2001), orange mesocarps (Ejikeme, 2008), jute (Jahan *et al.*, 2011), bacterial cellulose (De Oliveira *et al.*, 2011), rice and bean hulls (Adel *et al.*, 2011), hemp stalks and rice husks (Virtanen *et al.*, 2012), oil palm biomass (Mohamad Haafiz *et al.*, 2013a), fodder grass (Kalita *et al.*, 2013), and waste paper (Okwonna, 2013). Alfa grass (Trache *et al.*, 2014) and soybean hulls (Merci *et al.*, 2015) have also been investigated as potential sources of MCC. Microcrystalline cellulose obtained from diverse sources using various processes and conditions differ in surface area, crystallinity, moisture content, porous structure, molecular weight and particle size, etc.

3.3.2 Isolation of MCC

The manufacture of MCC starts from the hydrolysis process. Many processes like reactive extrusion, radiation-enzymatic, acid hydrolysis, and so forth have been reported in the literature. During the hydrolysis procedure, the originally tightly packed cellulose microcrystals are divided because the attached amorphous cellulose is dissolved. Examples of microcrystalline cellulose production are shown in Table 3.2.

Extrusion technology is a short-duration, high-temperature hydrolysis process with the advantage of high flexibility and nonexistence of effluents (Merci *et al.*, 2015). Extrusion processing can offer a continuous reactor environment for a combination of thermo-mechanical and chemical treatment of the lignocellulosic biomass with higher throughput and solid levels (Lamsa *et al.*, 2010). Therefore, this technology could be applied to the extraction of cellulose from lignocellulosic materials, employing a process with lower moisture content. United States Patent attributed to Hanna *et al.* describes the manufacture of MCC by reactive extrusion that the feedstock is provided through an extruder in the presence of basic aqueous solution so as to disintegrate the lignocellulosic complex into lignin, hemicelluloses and cellulose (Hanna *et al.*, 2001). Merci *et al.* produced MCC from soybean hulls employing a simple method based on reactive extrusion (Merci *et al.*, 2015). The procedure was based on two-step extrusion process; in the first step, the soybean hull was extruded with sodium hydroxide, followed by extrusion with sulfuric acid in the second step. These authors found that the

Table 3.2 Examples of microcrystalline cellulose preparation procedures.

Method	Raw material	Procedure	References
Chemical method	Unbleached wood pulp	Hydrolyzing pulp with a sufficient amount of active oxygen in an acidic environment in a one step process.	Schaible & Sherwood, 2003
	Paper grade pulp	Contracting a paper grade pulp with an alkali hydrolysis agent, washing the hydrolyzed pulp and contracting it with an acid hydrolysis agent.	Nguyen, 2006
	Hardwood (birch and aspen) and softwood (pine) bleached sulphate pulps Bagasse and rice straw pulps	Hydrochloric acid treatment, followed by disintegration in a ball mill, subsequently washed-off, dried at 80 °C and additionally ground.	Laka & Chernyavskaya, 2007 Ilindra & Dhake, 2008
		Treatment with 2.5 N hydrochloric acid at 85 °C for 15 min, then stirring for 10 min. The product is filtered, washed, dried and disintegrated in a grinder.	
	Orange mesocarp pulp	Treatment with 2.5 N hydrochloric acid at 105 °C for 15 min. The obtained component was filtered, washed and oven dried at 69 °C for 1 hour.	Ejikeme, 2008
	Cotton linter, flax fibers and kraft pulp	MCC was prepared by mild acid hydrolysis in 2.5 M solution of HCl at 105 °C for 1 h.	Leppänen <i>et al.</i> , 2009
	Rice hulls and bean hulls	Pretreatment with mineral acid in an autoclave at 120 °C for 90 min and 10% consistency, followed by filtration, washing and oven drying.	Adel <i>et al.</i> , 2011
	Gluconacetobacter xylinus and kenaf pulp	Hydrochloric acid treatment, followed by 10% sodium hydroxide. The obtained gels were precipitated using ethanol.	Keshk & Abu Haija, 2011
	Oil palm empty fruit bunch pulp	Treatment with 2.5 N hydrochloric acid at 105 °C for 30 min under constant agitation in the ratio of 1:20 pulp over liquor. The obtained product was filtered, washed and oven dried.	Mohamad Haafiz <i>et al.</i> , 2013
	Fodder grass pulp	Treatment with hydrochloric acid (2.5N) at 100 °C for 30 min. The extracted product was washed with water.	Kalita <i>et al.</i> , 2013

	Waste paper	Starting with soda pulping and de-inking process with NaClO/ H_2O_2 , followed by 15% sulfuric acid hydrolysis at 373 K for 30 min. The obtained product was filtered, washed and oven dried.	Okwonna, 2013
	Alfa grass	After pulping and bleaching, cellulose is suspended in an aqueous acid (2.5 mol/L) at 85 °C for 120 min with constant agitation in the ratio of 1:10 pulp over liquor. The degraded cellulose was filtered, washed and oven dried.	Trache <i>et al.</i> , 2014
Reactive-extrusion method	sugar beet pulp	The raw material is fed through an extruder in the presence of basic aqueous solution so as to break down the lignocellulosic complex	Hanna <i>et al.</i> , 2001
	soybean hulls	The procedure was based on two-step extrusion process; in the first step, the soybean hull was extruded with sodium hydroxide, followed by extrusion with sulfuric acid in the second step	Merci <i>et al.</i> , 2015
Radiation-enzymatic method	Spruce pulp	The process was based on the radiation degradation by means of an electron beam to initially depolymerize the pulp prior to enzymatic hydrolysis. The degraded cellulose was then processed by milling and drying.	Stupinska <i>et al.</i> , 2007

MCC produced was composed of short and rod shaped fibers, with a cellulose content of 83.79% and a crystallinity index of 70%.

Stupinska *et al.* have used a bleached dissolving pulp made from mountain spruce employing an environment-friendly, effective two-step radiation-enzymatic depolymerization process (Stupinska *et al.*, 2007). The process was grounded on the radiation degradation by means of an electron beam to initially depolymerize the pulp prior to enzymatic hydrolysis. The depolymerized cellulose pulp was further processed by milling and drying to form MCC. These authors found that the MCC obtained is characterized by a degree of polymerization of 150 and a crystallinity index of 64%.

Although enzymatic methods are desirable because glucose, a useful by-product, is produced, these methods are more expensive and give MCC products with lower crystallinity (Adel *et al.*, 2011). Thus acid hydrolysis is the conventional procedure of choice for producing MCC (Hanna *et al.*, 2001). The acid hydrolysis process is commonly used for MCC production because it requires shorter reaction time than other processes. It can be made by a continuous process rather than a batch-type process and it uses limited amount of acid and produces small particles of microcrystalline cellulose. Jahan *et al.* made MCC from jute fibers by: (1) performing cellulose extraction with formic acid/ peroxyformic acid at atmospheric pressure; (2) bleaching experiments carried out with sodium hydroxide and hydrogen peroxide; followed by acidic hydrolysis; and finally, (3) neutralized and dried (Jahan *et al.*, 2011). The authors mentioned that the yield of MCC was 48–52.8% on jute. The transmission electron microscopy (TEM) results demonstrated that the diameter of MCC samples was 15–40 nm and the crystallinity index obtained by X-ray diffraction was 73.9%. In another paper, De Oliveira *et al.* prepared MCC from bacterial cellulose (De Oliveira *et al.*, 2011). To achieve the synthesis of MCC, the authors used sulfuric acid at a reflux system under constant stirring. The hydrolyzed pulp was thoroughly washed with distilled water and was wetted with ethanol and dried in an oven. The MCC samples produced an average particle size between 70 and 90 μm , the crystallinity index determined by X-ray diffraction was 69% and a degree of polymerization (DP) of 250. A method for producing MCC from hemp plant was reported by Virtanen *et al.*, (Virtanen *et al.*, 2012). The principle of their method was to extract pure cellulose using different steps; starting with cutting the raw stems into pieces and boiling it in sodium hydroxide solution. The washing steps were performed in hot water and acetic acid several times. The obtained mass was then dried. MCC sample was prepared by acid hydrolysis to so called level-off degree of polymerization (LODP). The results revealed that the DP of MCC sample was 125 and the crystallinity index determined by X-ray diffraction was 791.3%. Recently, Mohamad Haafiz *et al.* isolated MCC from oil palm empty fruit bunch (Mohamad Haafiz *et al.*, 2013a). They first bleached the pulp using an oxygen-ozone-hydrogen peroxide bleaching sequence. MCC was made from oil palm fruit bunch pulp using an acid hydrolysis method based on original procedures reported by (Battista, 1950). The morphology of the hydrolyzed MCC showed a compact structure and a rough surface and crystallinity was evaluated as 87%. In another work carried out by Trache (Trache *et al.*, 2014) the desired MCC fibers were achieved by applying an acidic hydrolysis method using alfa grass fibers as feedstock. Dry cellulose, obtained by pulping and leaching of alfa fibers, was suspended in an aqueous hydrochloric acid under reflux conditions and gentle stirring. Several steps of neutralization and washing were performed. The resultant

alfa-MCC was transformed into fine powder by using a grinder. The obtained product after drying was snowy-white in appearance. The authors showed that the DP of MCC was 318 and the crystallinity index was 81%.

The MCC obtained from different sources have many features including biodegradability, biocompatibility, and unique chemical and reactive surface properties. Microcrystalline cellulose has great potential and is gaining interest in the fields of composites reinforcement as well as in pharmaceutical, and food industries.

3.3.3 Types of MCC

3.3.3.1 Powdered MCC

The common manufacturing process of powdered MCC comprises three stages: hydrolysis procedure as mentioned earlier, neutralizing and washing steps, and finally, drying and disintegration (Mohamad Haafiz *et al.*, 2013a; Trache *et al.*, 2014). The first stage in the widely used chemical process involves heating the purified pulp with a dilute mineral acid in water. This destroys the fibrous structure of cellulose, leaving fine microcrystals. The process continues to a leveling-off degree of polymerization. The wet-cake obtained is free of water and the dried crystalline cellulose agglomerate is recuperated and ground to get powdered grade MCC. Powdered MCC grade is odorless, tasteless, white, relatively free-flowing powder that is almost freed from inorganic and organic contaminants. It is crystalline in nature, chemically inert and insoluble in water. Its particles seem porous. This porosity permits the MCC particles to absorb huge amounts of water or oil onto the surface. It has potential application in many products including pharmaceuticals, foods and composite materials (Mohamad Haafiz *et al.*, 2013b; Thoorens *et al.*, 2014; Wüstenberg, 2015).

3.3.3.2 Colloidal MCC

For the preparation of colloidal MCC (gelled MCC) compounds, the washed hydrolyzed pulp is submitted to mechanical treatment under the action of friction and strong shear forces to split up the compact structure of the cellulose fiber agglomerates and to generate microcrystals (Imeson, 1997; Wüstenberg, 2015). Once this is achieved, the product is then capable to produce a stable dispersion in aqueous and other media. After the mechanical treatment step, the microcrystalline parts are co-processed with a hydrophilic dispersant, such as sodium carboxymethyl cellulose, alginates, guar gum or xanthan gum. The co-polymer forms a barrier which prevents the microcrystals aggregating through hydrogen bonding and also facilitates water uptake and dispersion when the powder is added to water. When colloidal grades of MCC are appropriately dispersed, the cellulose crystallites set up a three-dimensional network, with particle sizes less than 0.2 μm (Imeson, 1997; Wüstenberg, 2015). The swelling capacity of the soluble hydrocolloid supplies the dispersant function by helping in the dispersibility of the microcrystalline cellulose particles during reconstitution as well as in the stabilization of the obtaining colloidal dispersion. The good properties (thixotropy, elasticity, compatibility and viscosity) of colloidal MCC impart various desirable characteristics suitable in food application (Imeson, 1997; Wüstenberg, 2015). However, in

non-food-industries, cross-linked or gelled MCC is an outstanding binder for granules, tablets, or any compacted product (Wüstenberg, 2015).

3.4 Characterization and Properties of Microcrystalline Cellulose

To better understand the effect of MCC in composite materials, it is important to first investigate and analyze their physical properties and chemical structure. The MCC features depend on the origin of the cellulose and processing variables, such as reaction duration and temperature, mechanical agitation of the slurry, drying conditions, and so forth.

3.4.1 Chemical Structure

The chemical structure of MCC corresponds to the chemical composition of the native cellulose. The molecule is a linear unbranched chain of β -D-glucose monomers that is 1 \rightarrow 4 linked. The structural formula is $(C_6H_{10}O_5)_n$.

Fourier transform infrared spectrometer (FTIR) is an appropriate technique for investigating changes occurred by any chemical treatment. In this experiment, dried and powdered form samples were often blended with KBr and then compressed. The spectra of samples could be recorded in the range of 4000 to 400 cm^{-1} . For instance, the FTIR spectrum of commercial MCC can be seen in Figure 3.3 and its peak analysis is displayed in Table 3.3. The sample displayed two main domains as reported by Mohamad Haafiz (Mohamed Haafiz *et al.*, 2013a). These domains are displayed at high wavenumbers (3500–2800 cm^{-1}) and low wavenumbers (1700–650 cm^{-1}), respectively. FTIR spectroscopy showed the similarities between the MCC spectrum and the native cellulose reported in the literature (Jahan *et al.*, 2011; Adel *et al.*, 2011;

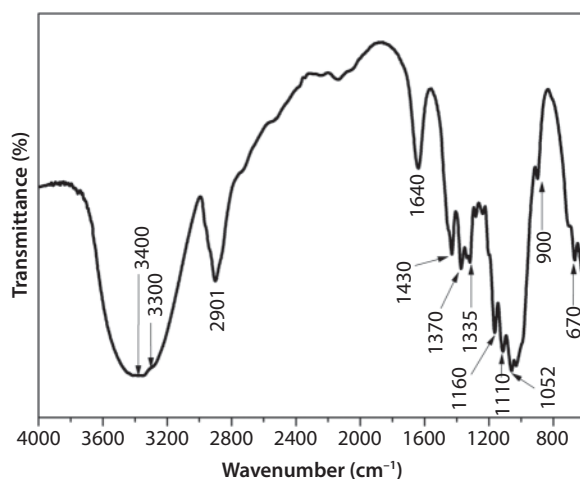


Figure 3.3 FTIR spectrum of commercial microcrystalline cellulose.

Table 3.3 FTIR peak analysis of MCC (Das *et al.*, 2010; Adel *et al.*, 2011; Mohamad Haafiz *et al.*, 2013a; Trache *et al.*, 2014).

IR region (cm ⁻¹)	Peak (cm ⁻¹)	Assignments
3500–2800	3400	Intra-molecular hydrogen bonding C(3)OH...O(5) C(6)O...(O)H
	3300	Inter-molecular hydrogen bonding C(3)OH...C(6)O
	2901	CH ₂ asymmetrical stretching
1700–650	1640	O–H bending of adsorbed water
	1430	O–H in-plane deformation
	1370	C–H bending
	1335	CH ₂ rocking
	1160	Anti-symmetrical bridge C–O–C stretching
	1110	A symmetric in-plane ring stretching
	1052	C–O stretching
	900	C–H rock vibration of cellulose (anomeric vibration, specific for β -glucosides)
	670	OH out-of-plane bending

Trache *et al.*, 2014) which is a demonstration that MCC samples preserve the chemical structure of its precursor.

According to previous research, the absence of peaks located in the range 1609–1509 cm⁻¹, which would correspond to c=c aromatic skeletal vibration, indicated the absence of lignin. The nonexistence absorption band in the domain 1740–1700 cm⁻¹, attributed normally to either the acetyl or uronic ester groups of hemicelluloses, showed the efficient removal of hemicelluloses. Analogous results have been reported by (Trache *et al.*, 2014) and (Jahan *et al.*, 2011) during production of MCC from alfa fibers and jute, respectively.

3.4.2 Morphology and Particle Size

MCC is known to have strong mechanical features, and it can therefore be utilized in the manufacture of high strength and low-abrasive products (Eichhorn & Young, 2001). It is even well accepted that the dimension of the microcrystalline cellulose are essential in yielding these mechanical features (Jahan *et al.*, 2011). The morphological structure of cellulose is intended to illustrate the arrangement of crystals into microfibrils, cell walls, tissues, layers, fibers or other cellulose morphologies. MCC occurs usually as fibers with a morphology differing from that of native cellulose. Depending upon the cellulose source and the method of fabrication, MCC exhibits similar morphologies but different dimensions. Experimental techniques such as scanning electron

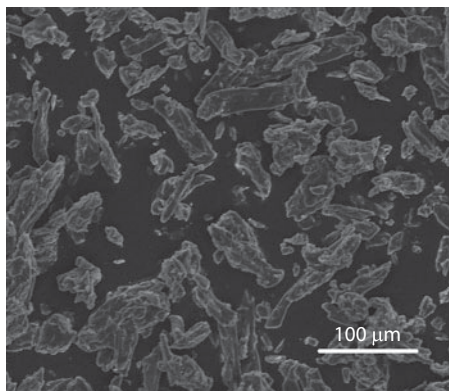


Figure 3.4 SEM graph of commercial microcrystalline cellulose.

microscopy (SEM), transmission electron microscopy (TEM), atomic force microscopy (AFM), and field-emission scanning electron microscopy (FE-SEM) have been used to study MCC and to measure the particles length (L) and their diameter (D).

Using SEM method, MCC showed particles size in micron range (Figure 3.4). The particles shapes were not isometric, but often looked like the morphology of their precursor. Trache *et al.* measured the diameter of commercial MCC (10–20 μm) and MCC fibers from alfa (5–10 μm) what is similar to its native cellulose (Trache *et al.*, 2014). The obtained fiber lengths of the MCC samples were in the same trend ranging from 20–200 μm . The MCC samples exhibited short fibers strands with rough surface. The SEM study of MCC extracted from fodder grass revealed individually organized rods with variable length and thickness in the range of 5–30 μm and 5–7 μm , respectively (Kalita *et al.*, 2013). Such rod like shape of the MCC from various lignocellulosic materials has been previously reported (Adel *et al.*, 2011). In another paper, the MCC from cotton was showed to be flat, with a convoluted, ribbon like structure looking like the structure of cellulose; but MCC from jute displayed flat, small rigid rod like morphology (Das *et al.*, 2010). Mohamad Haafiz reported in his work that MCC obtained from oil palm showed irregular shaped fibrils with a rough surface morphology (Mohamad Haafiz *et al.*, 2013a).

3.4.3 Degree of Polymerization

Naturally occurring cellulose has a degree of polymerization of about 10,000, which correspond to a molecular weight of about 2,000,000 g mol^{-1} . Depending on the method of extraction, cellulose polymer seems to have an average degree of polymerization of 300–3000 and consequently has average molecular weights of 50,000–500,000 g mol^{-1} . During hydrolysis process, owing to chain fracture, the molecular weight of MCC decreases with respect to that of the original cellulose and ranges between 30,000 and 50,000 g mol^{-1} . The degree of polymerization is usually less than 400 (Imeson, 1997; Wüstenberg, 2015). It is merely an identity test to differentiate MCC (DP<400) from powdered cellulose (DP>440). Thoorens reported that the source of the feedstock and the manufacture procedure more decisively affect the MCC features than DP (Thoorens *et al.*, 2014). For any producer, DP is merely a condition used to help guide the hydrolysis

of MCC, whereas for user DP is a manner to distinguish between MCC and powdered cellulose.

The determination of the degree of polymerization of cellulose is practically limited to two methods: viscometry and size exclusion chromatography (SEC) (Dupont & Martha, 2004; Lojewski *et al.*, 2011; Wüstenberg, 2015). Viscometric method is relatively the simplest and the most extensively applied technique to measure the DP, which is based on determining the intrinsic viscosity also recognized as the Staudinger index. The intrinsic viscosity conveys the reduced viscosity of a solution at an infinitely small concentration. This parameter can be computed by extrapolating the concentration of dilute solution to the value “zero.” The average molecular weight can be calculated according to Mark-Howink-Sakurada equation (Dupont & Martha, 2004). The common cellulose solvents used for this purpose are cupri-ethylenediamine and cadmium oxide. SEC method has been developed to provide a fast and highly reproducible method for this reason after derivatization of cellulose samples (Trache *et al.*, 2014). The DP of MCC is shown in Table 3.4 based on different sources.

3.4.4 Degree of Crystallinity

MCC is composed of both crystalline and amorphous domains, and measurement of degree of crystallinity could explain the behavior of the properties of the material. The proportion of crystalline regions in MCC is about 70% and the amorphous fraction is 30%. In comparison, a so-called cellulose powder as a fine-milled native cellulose fiber consists on average of 45% crystalline fraction and 55% amorphous regions. However, a wide range of degree of crystallinity of MCC has been reported, what could be elucidated by the different approaches employed to measure this parameter, including X-ray diffraction, solid state magnetic resonance and infrared spectroscopy, but also by the procedure of data manipulation and analysis. The methods details could be found in the literature (Kalita *et al.*, 2013; Trache *et al.*, 2014 and the references therein). Also, the degree of crystallinity depends on extraction process, source and origin of cellulose. However, the hydrolysis conditions have very little impact on the crystallinity index (Adel *et al.*, 2011; Thoorens *et al.*, 2014).

It is worth mentioning that an increase in crystallinity is associated to increases in the rigidity of the cellulose structure, which can engender higher tensile strength to fibers. This increase would be expected to increase the mechanical properties of composite materials (Rosa *et al.*, 2012). As shown in Table 3.4, compared to the raw cellulosic fibers, the degree of crystallinity of MCC samples is higher due to removal of amorphous domains by hydrolysis process, which prompts the hydrolytic cleavage of glycosidic bonds, finally liberating individual crystallites (Adel *et al.*, 2011; Trache *et al.*, 2014).

3.4.5 Thermal Stability

Cellulosic products are well known for undertaking fast thermal decomposition at low to moderate temperatures, namely below 400 °C. Study of the thermal stability of cellulose fibers is crucial in order to evaluate their applicability for composite technology, in which the processing temperature for thermoplastic polymers increases above 200 °C.

Table 3.4 Degree of polymerization, crystallinity, and thermal decomposition of MCC from different sources.

Source		DP	Crystallinity (%)	Temperature of decomposition (°C)	References
Cotton	Native cotton	2200	66.45	ND	Das <i>et al.</i> , 2010; Leppänen <i>et al.</i> , 2009
	MCC	165	79.8	330.0	Das <i>et al.</i> , 2010; Leppänen <i>et al.</i> , 2009
Coniferous kraft pulp	Native cellulose	1135	50	ND	Leppänen <i>et al.</i> , 2009
	MCC	150	63	ND	Leppänen <i>et al.</i> , 2009
Fodder grass	Native cellulose	ND	ND	353.0	Kalita <i>et al.</i> , 2013
	MCC	ND	80	377.5	Kalita <i>et al.</i> , 2013
Alfa	Native cellulose	844	59	332.7	Trache <i>et al.</i> , 2014
	MCC	318	73	351.3	Trache <i>et al.</i> , 2014
Jute	Native cellulose	ND	68.7	337.0	Jahan <i>et al.</i> , 2011
	MCC	ND	73.9	315.0	Jahan <i>et al.</i> , 2011
Bacterial-MCC		ND	85	320	Keshk & Abu Haija, 2011
Oil palm-MCC		ND	87	326	Mohamad Haafiz <i>et al.</i> , 2013a
Bagasse-MCC		158.4	ND	ND	Ilindra & Dhake, 2008
Wast paper-MCC		207	78.1	ND	Okwonna, 2013
Commercial MCC		294	81	353.1	Trache <i>et al.</i> , 2014

The thermal decomposition of cellulose-based fibers is significantly affected by their chemical composition and structure; hence, different cellulosic fibers exhibit various decomposition profiles. For example, recent studies have been performed to study the thermal stability of cellulosic fibers and the respective MCCs (Table 3.4). The higher temperature of decomposition obtained for MCCs reflects an improved thermal behaviors of the fibers. This can be assigned to removal of residual hemicellulose, lignin and some cellulose amorphous parts from the fibers during the MCC extraction process. Furthermore, as previously reported, the higher temperature of decomposition of MCC suggested that cellulose with higher crystallinity exhibited higher thermal stability (Keshk & Abu Haija, 2011; Kalita *et al.*, 2013; Trache *et al.*, 2014). Besides, the sulfuric acid hydrolyzed MCC showed lower thermal stability compared to the native cellulose (Table 3.4). Jahan *et al.* reported that the decrease in thermal stability of Jute MCC is caused by the introduction of sulfate groups into the outer surface of cellulose crystals during hydrolysis process of jute cellulose (Jahan *et al.*, 2011). In view of the above discussion, it was deduced that MCC present interesting thermal stability and will appropriate in the manufacture of biocomposites, food stabilizers and pharmaceutical compounds.

3.4.6 Mechanical Properties

Mechanical properties of MCC have been characterized using different methods such as Raman spectroscopy, tensile test and nanoindentation techniques. Eichhorn and Young estimated the Young's modulus of 25 GPa for distinct MCC particles based on the band shift of Raman spectra (Eichhorn & Young, 2001). In that experiment, MCC powder was inserted in epoxy and then distinct MCC particles were carefully chosen under the microscope. When applying forces on the cured epoxy beam, the deformation of the MCC particles was evaluated by examining the shift of the band of Raman at $1,095\text{ cm}^{-1}$. In another investigation, Edge *et al.*, (Edge *et al.*, 2000) studied the strength of compacted specimens of MCC with median size 50 and 90 μm , respectively. The samples were obtained by compressing MCC powders in a 25 mm diameter die at a load of 200 MPa. The tensile strengths of the specimens were 11.5 and 10.5 MPa for 50 and 90 μm samples, respectively. Das *et al.* extracted MCC particles from different sources like cotton, jute, newsprint and filter paper (Das *et al.*, 2010). The authors prepared MCC pellets that were subjected to nanoindentation test to determine their modulus values. The obtained modulus values were in the range 1.8–7.6 GPa. More recently, Adel *et al.* succeeded in preparing MCC from different sources such as rice and bean hulls by a simple mechanical process (Adel *et al.*, 2011). The measured tensile strength values, using tensile test, were 2.03 and 1.19 MPa for Rice and bean hulls, respectively. Hoyos *et al.* reported that micro-crystals of cellulose microfibrils present excellent mechanical properties with an elastic modulus of about 150 GPa, superior to glass fibers (85 GPa) and aramide fibers (65 GPa) modulus. Besides, impressive mechanical properties of MCC make it ideal candidate for the processing of polymer composites. With a surface area of several hundred square meters per gram ($270\text{--}380\text{ m}^2\text{ g}^{-1}$) (Virtanen *et al.*, 2012), it has at the potential to significantly reinforce polymers at low filler loadings.

3.4.7 Surface Chemistry

The foremost problems encountered with MCC reinforced polymer composites are due to the inherent incompatibility and dispersibility between the hydrophilic and highly polar cellulose fibers and the hydrophobic and non-polar polymer matrix. These not only hinder preparation of MCC reinforced polymer composites via the procedure of mixing MCC with polymer solution, but also affect the mechanical properties because of low interface bonding strength. To overcome these shortcomings, fiber surfaces can be modified using chemical, physical or physicochemical methods depending on the polymer matrices to be employed (Spoljaric *et al.*, 2009; Miao & Hamad, 2013; Dong *et al.*, 2013; Izzati Zulkifli *et al.*, 2015; Farid & Abad, 2015; Motokawa *et al.*, 2015). The MCC hydroxyl groups can be treated to produce several cellulose derivatives. Preferably, the modifications need to be restricted to the surface hydroxyl groups to conserve the structure and the integrity of these fibers and therefore their mechanical properties.

However, as clearly reported in the review paper by (Hubbe *et al.*, 2008), surface-treated cellulosic materials can have a negative effect on the cost of manufacturing processes of composites. The high surface area per unit mass of nanomaterials, which is their most attractive attribute, inappropriately becomes a disadvantage when they have to be modified because of the cost of the surface treatment.

3.5 MCC-Based Composites

Natural fiber, such as purified cellulose obtained from several natural raw materials, has great potential to substitute synthetic reinforcements such as glass fiber or fiber produced from petroleum-derived polymers utilized in polymer composites. For this purpose, many forms of cellulose including MCC, cellulose nanowhiskers and cellulose nanofibrils have been explored as reinforcements for different composites (Azizi Samir *et al.*, 2005; Spoljaric *et al.*, 2009; Habibi *et al.*, 2010; Siqueira *et al.*, 2010; Abdul Khalil *et al.*, 2012; Sun *et al.*, 2014; Izzati Zulkifli *et al.*, 2015; Thakur, 2015a; Thakur, 2015b). The development of composite materials is promptly emerging as multidisciplinary research area whose results could broaden the application of polymers to great benefit of several industries such as automotive, building materials, and household products (Mathew *et al.*, 2005). Polymer composites filled with MCC is a relatively new research area with respect to conventional filled polymers, and they possess some interesting properties such as high strength and stiffness combined with low density, high surface area, unique morphology, renewability and biodegradability. However, for reinforcement applications, MCC particles present some drawbacks: for example, poor wettability, moisture absorption, incompatibility with most of polymeric matrices and limitation of processing temperature (Spoljaric *et al.*, 2009; Dai *et al.*, 2014; Sun *et al.*, 2014; Izzati Zulkifli *et al.*, 2015). Indeed, cellulosic materials start to degrade near 220 °C, restricting the type of matrix that can be employed in association with cellulosic fillers.

Taking into account of MCC properties, the present section focuses on classification of polymer composites, MCC-based composites, their production processes and properties.

3.5.1 Classification of Polymer Composite Materials

Composites have existed for centuries, and there has been significant progresses owing to the booming of aviation industry in the mid-20th century plus the emergence of aerospace applications. Since then, several research works have been performed to find composite materials with improved properties (John & Sabu, 2012). Many industrial applications necessitate properties that are not found in individual materials; hence composites presenting better properties are needed.

According to the American Society for Testing and Materials (ASTM), composite materials are the combination of two or more different substances to form a new and useful engineering material, differing from the neat constituents from which they originated (Furtado *et al.*, 2012). Often, among the phases making a composite material, one is distinguished as being “reinforcement”: this is generally the strongest phase of the material. In most case, the reinforcement is geometrically distributed as distinct elements (particle, fibers) within the composite material (Mortensen, 2007; Furtado *et al.*, 2012; Thakur & Thakur, 2014). The other phase, the matrix material surrounds and bonds the reinforcement (Mortensen, 2007; Furtado *et al.*, 2012; Thakur & Thakur, 2014). Even though generally the weak phase, the matrix affects noticeably the properties of the composite material. Composite materials can be tailored to display a wide range of preferred properties. Several composites offer advantageous properties in terms of low weight, increased design flexibility, better damage tolerance, high strength, increased fracture toughness, increased impact resistance, superior corrosion resistance, increased chemical resistance, superior fatigue resistance and low coefficient of thermal expansion (Thakur *et al.*, 2014c). Composite materials are therefore classified according to the nature of their matrix (polymer, metal, ceramic and carbon) or by the type of reinforcement (fiber, flakes and particles) (Mortensen, 2007).

The polymeric matrices are widely used to produce materials for many industrial markets, since they show lower costs than other matrices. They present also low density and consequently light weight composites. Numerous polymers are used as matrix materials depending upon the applications (Mortensen, 2007; Furtado *et al.*, 2012; Thakur *et al.*, 2014c; Thakur *et al.*, 2014c; Thakur, 2015a). Some of the commercially important polymeric matrices include polyethylene, polypropylene, polyester, polystyrene, phenolic resins, amino resins, epoxy, polylactic acid and starch.

On the basis of reinforcement nature (Mortensen, 2007; Furtado *et al.*, 2012; Thakur & Thakur, 2014; Thakur *et al.*, 2014c), composites are divided into different categories: (a) particles reinforced composites, composed of macroscopic particles (fillers such as calcium carbonate, graphite, silica, quartz and metal powders) of one or more constituents dispersed into matrix; (b) fibrous reinforced composites; the reinforcement is used in the form of fibers and it may be natural (vegetal, animal and mineral) or synthetic (aramid, glass and carbon) fibers or combination of both; (c) laminated composites, composed of layers from at least two diverse constituents which are associated to form a laminate.

Composite materials are also classified into three different types (Akil *et al.*, 2011; Thakur & Thakur, 2014; Thakur *et al.*, 2014c), depending upon the renewable/non-renewable nature of the polymer matrix as well as the reinforcement, (a) totally renewable composite materials, in which both the matrix material and the reinforcing

materials comes from renewable resources; (b) partly renewable composite materials, in which either the reinforcing material or the matrix is obtained from renewable resources; (c) non-renewable composites, in which both the matrix material and the reinforcing materials comes from non-renewable resources. The polymer composites discussed in this review belong to the two former categories.

3.5.2 Production and Properties of MCC-based Composites

The (most probable) first publication on cellulose composites is attributed by Berglund (Berglund *et al.*, 1987) to Boldizar (Boldizar *et al.*, 2005). In 1987, the fabrication of thermoplastics reinforced with hydrolyzed pulp fibers was reported. The embrittlement caused by the hydrolytic process was proposed as a means to simplify the breakdown of the original fiber into fibrillar entities or nanofibers, suggesting the possibility to exploit their unusually high modulus and strength values to make composites. Recently, there is an increased use of MCC as the load-bearing component in developing new and inexpensive composite materials due to its attractive properties. As compared to other organic reinforcing fillers, MCC has several advantages, including a positive ecological, low density, low-energy consumption in producing, high sound attenuation, ease for recycling by combustion, and comparatively simple processability due to their non-abrasive nature, which engenders high filling levels, in turn resulting in noteworthy cost savings.

During the last two decades, the use of MCC from various sources such as cotton, wood, oil palm, sisal, bean hull, rice straw and so on for the preparation of high performance composite materials has been extensively investigated and reported. Both synthetic and natural polymers were tested as the matrices (Figure 3.5). Synthetic polymers such as polyethylene (Maskavs *et al.*, 1999), polypropylene (Ashori & Nourbakhsh, 2010; Izzati Zulkifli *et al.*, 2015), styrene butadiene rubber, poly-butadiene rubber (Bai & Li, 2009), nylon 6 (Kiziltas *et al.*, 2011), polyurethane (Wu *et al.*, 2008; Rafiee & Keshavarz, 2015), polyaniline (Da Silva *et al.*, 2015), polycaprolactone (Sabo *et al.*, 2013), epoxy resin (Xiao *et al.*, 2014), acrylic resin (Cataldi *et al.*, 2015a), poly 2-ethyl-2-oxazoline

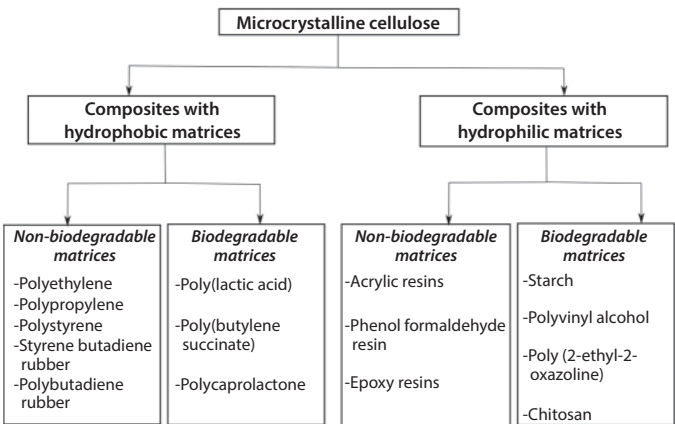


Figure 3.5 Synthetic and natural polymers used as matrix for MCC-based composites.

(Cataldi *et al.*, 2015b) have been used. Different biopolymers such as sodium carboxymethylcellulose (Laka *et al.*, 2003), starch (Ma *et al.*, 2008; Adel & El-Shinnawy, 2012), chitosan (Li *et al.*, 2012), polylactic acid (Mathew *et al.*, 2005; Mohamad Haafiz *et al.*, 2013b; Dai *et al.*, 2014), poly (3hydroxybutyrate) (El-Hadi, 2013), poly (vinyl alcohol) (Sun *et al.*, 2014) have also been employed as matrices.

Numerous processing methods including extrusion, solution casting, and *in-situ* polymerization have been reported (Dai *et al.*, 2014; Xiao *et al.*, 2014; Glowinska & Datta, 2015). The various processing methods of the polymer composites are dictated by several factors such as morphology of the MCC, degree of dispersion, interfacial characteristics, and eventual form and shape of the final product that is desired. Commonly used processing methods for MCC composites are listed in Table 3.5.

Many researchers have investigated the potential of MCC as reinforcement in composite materials. Laka *et al.* synthesized MCC from wood pulp and produced MCC/Na-carboxymethylcellulose composite by film casting of an aqueous mixture. The obtained results showed that the mechanical properties of the film had no modification

Table 3.5 Processing methods for MCC-based composites.

Processing method	Polymer matrix	References
Casting	Poly (lactic acid)	Petersson & Oksman, 2006; Mohamad Haafiz <i>et al.</i> , 2013b
	Nylon 6	Kiziltas <i>et al.</i> , 2011
	Epoxy resin	Xiao <i>et al.</i> , 2014
Extrusion	Starch	Ma <i>et al.</i> , 2008
	Starch/poly (butylene adipate-co-terephthalate)	Reis <i>et al.</i> , 2014
	Poly (lactic acid)	Dai <i>et al.</i> , 2014
	Polypropylene	Ashori & Nourbakhsh, 2010; Izzati Zulkifli <i>et al.</i> , 2015
	Poly (lactic acid)/Poly (butylenes succinate)	Chaiwutthinan <i>et al.</i> , 2015
Melt-processing	Poly (vinyl alcohol)	Sun <i>et al.</i> , 2014
	Nylon 6	Kiziltas <i>et al.</i> , 2014
	Acrylic resin	Cataldi <i>et al.</i> , 2015a
<i>In-situ</i> polymerization	Polyurethane	Hatakeyama <i>et al.</i> , 2012; Glowinska & Datta, 2015; Rafiee & Keshavarz, 2015
Layer-by-layer self-assembly	Polyaniline	Da Silva <i>et al.</i> , 2015

when the dry weight content was lower than 43%. However, the elastic modulus and tensile strength of the composite material augmented after that and reached peak values, 30% and 42%, respectively, at 70% of MCC content (Laka *et al.*, 2003). In a study performed by Mathew *et al.* biodegradable composites were obtained by injection process using poly (lactic acid) (PLA) as a matrix and MCC (10–25 %) as the reinforcement. Compared to neat PLA, the addition of MCC decreased the mechanical properties (elongation and tensile strength) of the composite materials as the content of MCC increased, while the storage modulus enhanced (Mathew *et al.*, 2005). In another investigation, Wu *et al.* produced MCC-based polyurethane composites by combining MCC with thermoplastic polyurethane elastomer in dimethylformamide followed by film casting. They found high tensile strength of 257 MPa for the composite, at 5 wt% MCC content, with respect to 39 MPa for individual polyurethane. The Young's modulus and strain-to-failure also enhanced from 3.9 to 12.9 MPa and 159 to 237%, respectively. These results could be attributed to many factors. First, the MCC fibers were swollen by dimethylformamide/lithium chloride mixture permitting the monomer to enter into the space within MCC, thus improving the adhesion at interface. Second, the hydrophilic nature of polyurethane facilitates the distribution of MCC in composites. Finally, there are hydrogen bonds and covalent bonds formed between MCC and polyurethane, which engender MCC not merely a filler, but a cross-linking agent in polyurethane.

In the paper presented by Ma *et al.* thermoplastic starch/MCC composites were fabricated by extrusion using various quantity of MCC. The authors deduced that MCC improved the elongation at break and tensile strength, and this was ascribed to the good interaction between the MCC and starch (Ma *et al.*, 2008). Spoljaric *et al.* studied polypropylene composites reinforced with MCC. They revealed that the glass transition temperature loss and storage modulus increased with MCC concentration due to efficient interactions between MCC and polypropylene (Spoljaric *et al.*, 2009). In the same context, maleic anhydride treated polypropylene was utilized as a compatibilizer for polypropylene/MCC/wood flour composites by Ashori (Ashori & Nourbakhsh, 2010). The obtained results demonstrated that MCC along with wood flour could be efficiently utilized as a reinforcing agent in thermoplastics.

Miao *et al.* have used MCC and castor oil for the production of polymer composite materials. They modified MCC via 4,4-methylnbis (phenyl isocyanate). The obtained results showed that the tensile strength of castor oil-based polyurethane was increased due to the formation of composites containing modified MCC particles (Miao *et al.*, 2012). On the other hand, Mohamad Haafiz *et al.* made PLA composites reinforced with MCC (1, 3 and 5%) using casting process. The authors showed that when the amount of MCC was increased, elongation at break and the tensile strength of the composites decreased, while the Young's modulus enhanced (Mohamad Haafiz *et al.*, 2013b).

Sun *et al.* established a feasible and efficient approach to the production of eco-friendly composites based on MCC synthesized from waste cotton fabrics and plasticized poly (vinyl alcohol) using melt processing. The waste-derived MCC was utilized as reinforcement to enhance melt-processability of poly (vinyl alcohol), using water and formamide as plasticizer (Sun *et al.*, 2014). The authors postulated that MCC and formamide can form intermolecular complexes with poly (vinyl alcohol) through hydrogen bonding and consequently confine the crystallization of poly (vinyl alcohol). In another study, Catalidi *et al.* used MCC as a natural reinforcement and a commercial

acrylic adhesive to prepare new thermoplastic polymer composites for the cultural heritage conservation field. The authors demonstrated that the introduction of MCC has led to an increase of the thermal expansion coefficient, an increase of the elastic modulus and creep stability with respect to the neat resin, and an enhancement of the fracture toughness due to the addition of MCC (Cataldi *et al.*, 2014).

More recently, Glowinska obtained bio-based polyurethane composites using bio-components such as, bio-glycol, modified natural oil-based polyol, and MCC using *in-situ* polymerization process. The author showed that the increase of MCC filler content decreased the tensile strength and elongation to break. Moreover, the incorporation of MCC improved the hardness of the eco-friendly composite materials (Glowinska & Datta, 2015). In the investigation of Rafiee and Keshavarz., MCC-based polyurethane composites have been produced. They reported that the incorporation of MCC in a polyurethane matrix improved the mechanical properties and the thermal stability significantly (Rafiee & Keshavarz, 2015). The study performed by Chaiwutthinan aimed to improve the brittleness and thermal stability of PLA by inclusion of poly (butylene succinate) (PBS) and MCC (Chaiwutthinan *et al.*, 2015). It was revealed that the incorporation of 5 parts by weight per hundred to 70/30 PLA/PBS blend improved the thermal stability. In addition, the obtained composite exhibited high impact strength with respect to the neat PLA, while the elongation at break was acceptable.

Finally, it is important to mention that high MCC loading is generally needed in composite materials in order to enhance the mechanical properties, mainly due to its larger size with respect to nanocellulosic materials, low intrinsic strength, and more notably, low aspect ratio.

3.6 Application of Composite Materials Based on MCC

A broad range of applications of MCC exists even with a high number of unknowns. MCC-reinforced materials can find multiple applications in market segments like construction industries (cements), automotive industries (dashboard, door panels, and instrument panels), packaging (boxes, cases, and pellets), and adhesives. Along with these applications, MCC-based materials are also being used in preparation of products for medicine and nanotechnology. Figure 3.6 shows the diverse potential applications of MCC-based materials (Spoljaric *et al.*, 2009; Ashori & Nourbakhsh, 2010; Mohamad Haafiz *et al.*, 2013b; Hoyos *et al.*, 2013; Cataldi *et al.*, 2014; Sun *et al.*, 2014; Thoorens *et al.*, 2014; Chaiwutthinan *et al.*, 2015; Silva *et al.*, 2015; Wüstenberg, 2015).

The development and the application of polymeric composites filled with MCC have attracted both scientific and industrial interest. Several scientific publications and experts revealed its potential even if the majority of the investigations focus on their mechanical properties as reinforcing agent and their tableting properties in the pharmaceutical industries. However, as for any nanoparticles, the most important challenge is related to their homogenous dispersion within a polymeric matrix. Reinforcement using MCC is widely used in diverse fields not only in hard composite but also in thin film. Therefore, its application could cover pretty much in every industry from material reinforcement for automotive to smart materials.

Cellulose reinforced composites for construction applications have been reported by several authors (Mohamed *et al.*, 2010; Peters *et al.*, 2010; Hoyos *et al.*, 2013), highlighting

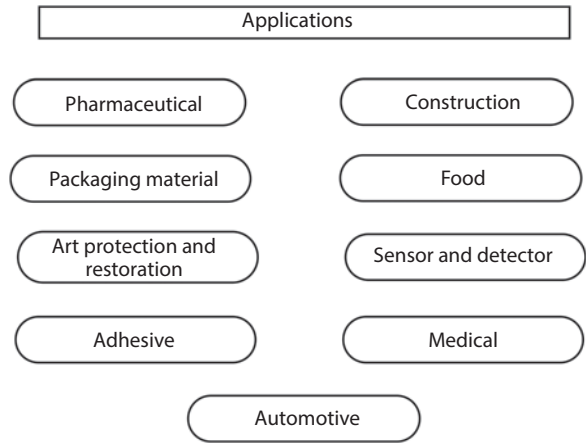


Figure 3.6 Potential applications of MCC-based materials.

their advantages such as low cost, low energy consumption during production, acceptable specific strength and stiffness, and high corrosion resistance. Current study has revealed that MCC-based composite materials have mechanical properties that permit their utilization as building materials. Hoyos *et al.* investigated the influence of MCC particles on mechanical properties and hydration process of cement composites. It was demonstrated that cement-based composites with MCC particles could be employed to elaborate precast pieces (Hoyos *et al.*, 2013).

Da Silva prepared an electrically conductive composite based on MCC modified with maleic anhydride and polyaniline (PANI) through a layer-by-layer-assembly technique (Da Silva *et al.*, 2015). The MCC/PANI composites showed high electrical conductivity with improved mechanical characteristics; they were tested as platforms for electrochemical trials. Furthermore, these composites can be used in many fields such as detectors, sensors, flexible electrodes, and eclectically conductive and papers and flexible films.

It therefore remains that the initial application of MCC is in the pharmaceutical industry as an excipient for the formulation of solid dosage forms, especially for tabletting due to outstanding dry binding properties (Thoorens *et al.*, 2014). MCC compacts well when subjected to low pressure to get tablets that are hard and stable, yet disintegrate rapidly. Moreover, it is stable, safe and physiologically inert. In the food industry (Wüstenberg, 2015), MCC has been utilized as a texturing agent, naturally derived stabilizer and fat replacer.

According to new applications of biocomposites, extensive work is currently being performed by several research laboratories and companies with MCC fiber and polymers to develop parts for diverse sectors like construction, medical, automotive industry, packaging, smart materials, foods and pharmaceuticals.

3.7 Conclusions

The current trend of developing new materials from renewable resources is driven not only by demand for alternative sources to petroleum and environmental concern, but

by the advancements happening in the materials science and technology fields as well. As an available natural biopolymer, cellulose is extensively distributed in every corner of the world; it is one of the most promising feedstocks for preparing nano-size reinforcement for wide range of applications. MCC-based polymer composites have drawn a lot of concern owing to their several advantages, such as low cost, availability, light weight, interesting mechanical properties, and at the same time are nontoxic, non-abrasive, can be simply tailored by chemical agents, and come from renewable sources, making their application more attractive.

The aim of this chapter was to demonstrate a comprehensive as well as state-of-art review of several aspects of MCC that are essential for further understanding of this material. Here the focus was on the synthesis and characterization. Different methods including pretreatment techniques and acid hydrolysis were depicted for preparing MCC from different sources. Furthermore, numerous properties of this material were considered including, chemical composition, crystallinity, morphology, thermal and mechanical properties.

We have reviewed the capabilities of MCC to improve on properties of some existing polymers; however, MCC's full potential has not been realized yet. MCC compatibility, dispersion, surface modification, and bonding with the polymer matrices are highlighted as major areas for research and development. Methods of fabrication and processing can be a key in opening new applications and reducing the cost of production as well. However, much interdisciplinary research and development is required in order to bring MCC products to successful commercialization.

Finally, it can be pointed out that this chapter is practical for students and scientists of both industry and academia interested in new opportunities to consider additional applications of MCC. New aspects, including cellulose technologies, comprise strategies, future aims, and perspectives of MCC research for different applications.

Acknowledgments

The author gratefully acknowledges the Ecole Militaire Polytechnique for the necessary facilities and encouragement for the accomplishment of this research.

References

- Abdul Khalil, H.P.S., Bhat, A.H., Ireana Yusra, A.F., Green composites from sustainable cellulose nanofibrils: A review. *Carbohydr. Polym.*, 87, 963, 2012.
- Abdul Khalil, H.P.S., Siti Alwani, M., Mohd Omar, A.K., Chemical composition, anatomy, lignin distribution and cell wall structure of Malaysian plant waste fiber. *BioResources*, 1, 220, 2006.
- Adel, A.M., Abd El-Wahab, Z.H., Ibrahim, A.A., Al-Shemy, M.T., Characterization of microcrystalline cellulose prepared from lignocellulosic materials. Part II: Physicochemical properties. *Carbohydr. Polym.*, 83, 676, 2011.
- Adel, A.M., El-shinnawy, N.A., Hypolipidemic applications of microcrystalline cellulose composite synthesized from different agricultural residues. *Int. J. Biol. Macromol.*, 51, 1091, 2012.
- Akil, H.M., Omar, M.F., Mazuki, A.A.M., Safiee, S., Ishak, Z.A.M., Abu Bakar, A., Kenaf fiber reinforced composites: A review. *Mater. Design*, 32(8–9), 4107, 2011.

- Ashori, A., Nourbakhsh, A., Performance properties of microcrystalline cellulose as a reinforcing agent in wood plastic composites. *Compos. Part A*, 41, 578, 2010.
- Alvarez, V., Rodriguez, E., Vázquez, A., Thermal degradation and decomposition of jute/vinylester composites. *J. Therm. Anal. Calorim.*, 85, 383, 2006.
- Averous, L., Le Digabel, F., Properties of biocomposites based on lignocellulosic fillers. *Carbohydr. Polym.*, 66, 480, 2006.
- Azizi Samir, M.A.S., Alloin, F., Dufresne, A., Review of research into cellulosic whiskers, their properties and their application in nanocomposites field. *Biomacromolecules*, 6(2), 612, 2005.
- Bai, W., Li, K., Partial replacement of silica with microcrystalline cellulose in rubber composites. *Compos. Part A*, 40, 1597, 2009.
- Battista, O.A., Smith, P.A., Microcrystalline cellulose. *J. Ind. Eng. Chem.*, 54(9), 20, 1962.
- Berglund, L.A., Cellulose-based nanocomposites, *Natural Fibers, Biopolymers, and Biocomposites*, A.K.Mohanty, M. Misra and L.T. Drzal (Eds), pp.807–832, CRC Press, Boca Raton, 2005.
- Boldizar, A., Klason, C., Kubat, J., Naslund, P., and Saha, P., Prehydrolyzed cellulose as reinforcing filler for thermoplastics. *Int. J. Polym. Mater.*, 11, 229, 1987.
- Borges, J.P., Canejo, J.P. *et al.*, Cellulose-based liquid crystalline composite systems, *Nanocellulose Polymer Nanocomposites: Fundamental and Applications*, V.K. Thakur (Ed.), pp. 215–235, Wiley-Scrivener, 2015.
- Cataldi, A., Dorigato, A., Deflorian, F., Pegoretti, A., Thermo-mechanical properties of innovative microcrystalline cellulose filled composites for art protection and restoration. *J. Mater. Sci.*, 49, 2035, 2013.
- Cataldi, A., Dorigato, A., Deflorian, F., Pegoretti, A., Innovative microcrystalline cellulose as lining adhesives for canvas. *Polym. Eng. Sci.*, 55, 1349, 2015a.
- Cataldi, A., Deflorian, F., Pegoretti, A., Poly 2-ethyl-2-oxazoline/microcrystalline cellulose composites for cultural heritage conservation: mechanical characterization in dry and wet state and application as lining adhesives of canvas. *Int. J. Adhes. Adhes.*, 62, 92, 2015b.
- Chaiwutthanan, P., Pimpan, V., Chuayjuljit, S., Leejarkpai, T., Biodegradable plastics prepared from poly(lactic acid), poly(butylene succinate) and microcrystalline cellulose extracted from waste-cotton fabric with a chain extender, 2015.
- Claudio, J., Caraschi, A.L.L., Characterization of curaua fiber. *Mol. Cryst. Liq. Cryst.* 353, 149, 2003.
- Da Silva, J.R.T., Farias, E.A.D.O., Filho, E.C.S., Eiras, C., Development and characterization of composites based on polyaniline and modified microcrystalline cellulose with anhydride maleic as platforms for electrochemical trials. *Colloid. Polym. Sci.*, 293, 1049, 2015.
- Dai, X., Xiong, Z., Na, H., Zhu, J., How does epoxidized soybean oil improve the toughness of microcrystalline cellulose filled polylactide acid composites? *Compos. Sci. Technol.*, 90, 9, 2013.
- Das, K., Ray, D., Bandypadhyay, N.R., Sengupta, S., Study of the properties of microcrystalline cellulose particles from different renewable resources by XRD, FTIR, nanoindentation, TGA and SEM. *J. Polym. Environ.*, 18, 355, 2010.
- De Oliveira, R.L., Barud, H.D.S., de Assunção, M.N., Meireles, C.D.S., Carvalho, G.O., Filho, G.R., Messaddeq, Y., Ribeiro, S.J.L., Synthesis and characterization of microcrystalline cellulose produced from bacterial cellulose. *J. Therm. Anal. Calorim.*, 106, 703, 2011.
- Dong, X., Dong, Y., Jiang, M., Wang, L., Tong, J., Zhou, J., Modification of microcrystalline cellulose by using soybean oil for surface hydrophobization. *Ind. Crops Prod.*, 46, 301, 2013.
- Edge, S., Steele, D.F., Chen, A., Tobyn, M.J., Staniforth, J.N., The mechanical properties of compacts of microcrystalline cellulose and silicified microcrystalline cellulose. *Int. J. Pharm.*, 2001, 67, 2000.
- Eichhorn, S.J., Young, R.J., The Young's modulus of microcrystalline cellulose. *Cellulose*, 8, 197, 2001.

- Ejikeme, P.M., Investigation of the physicochemical properties of microcrystalline cellulose from agricultural wastes I: orange mesocarp. *Cellulose*, 15, 141, 2008.
- El-Hadi, A.M., Influence of microcrystalline cellulose fiber (MCCF) on the morphology of poly (3-hydroxybutyrate) (PBH). *Colloid. Polym. Sci.*, 291, 743, 2013.
- Fernandes, E.M., Pires, R.A., Mano, J.F., Ries, P.L., Bionanocomposites from lignocellulosic resources: Properties, applications and future trends for their use in the biomedical field. *Prog. Polym. Sci.*, 38, 1415, 2013.
- Furtado, S.C.R., Silva, A.J. *et al.*, Natural fibre composites: automotive applications, *Natural Polymers, Volume 1: Composites*, M.J. John., T. Sabu (Eds.), pp.118–139, RSC Publishing, 2012.
- Glowinska, E., Datta, J., Structure, morphology and mechanical behaviour of novel bio-based polyurethane composites with microcrystalline cellulose. *Cellulose*, 2015.
- Goda, K., Sreekala, M.S., Gomes, A., Kaji, T., and Ohgi, J., Improvement of plant based natural fibers for toughening green composites–Effect of load application during mercerization of ramie fibers. *Compos. Part A*, 37, 2213, 2006.
- Habibi, Y., Lucia, L.A., Rojas, O. J., Cellulose nanocrystals: Chemistry, self assembly, and applications. *Chem. Rev.*, 110(6), 3479, 2010.
- Hanna, M., Blby, G., Miladinove, V., Production of microcrystalline cellulose by reactive extrusion, US Patent 6228213, assigned to University of Nebraska-Lincoln, 2001.
- Hatakeyama, H., Kato, Naomi, Nanbo, T., Hatakeyama, T., Water absorbent polyurethane composites derived from molasses and lignin filled with microcrystalline cellulose, 2012.
- Hoyos, C.G., Cristia, E., Vázquez, A., Effect of cellulose microcrystalline particles on properties of cement based composites. *Mater. Design*, 51, 810, 2013.
- Hubbe, M.A., Rojas, O.J., Lucia, L.A., Sain, M., Cellulosic nanocomposites: a review. *BioResources*, 3, 929, 2008.
- Illindra, A., Dhake, J.D., Microcrystalline cellulose from bagasse and rice straw. *Indian J. Chem. Technol.*, 15, 497, 2008.
- Imeson, A., Thickening and Gelling Agents for Food, pp. 180–198, Springer Science, 1997.
- Izzati Zulkifli, N., Samat, N., Zainuddin, N., Mechanical properties and failure modes of recycled polypropylene/microcrystalline cellulose composites. *Mater. Design*, 69, 113, 2015.
- Jahan, M.S., Saeed, A., He, Z., Ni, Y., Jute as raw materials for the preparation of microcrystalline cellulose. *Cellulose*, 18, 451, 2011.
- Jain, J. K., Dixit, V. K., Varma, K. C., Preparation of microcrystalline cellulose from cereal straw and its evaluation as a tablet excipient. *Indian J. Pharm. Sci.*, 45, 83, 1993.
- John., M.J., Sabu, T. (Eds.), *Natural Polymers, Volume 1: Composites*. RSC Publishing, 2012.
- Joseph, P.V., Joseph, K., Thomas, S., Pillai, C.K.S., Prasad, V.S., Groeninckx, G., Mariana, S. The thermal and utylenesites studies of short sisal fibre reinforced polypropylene composites. *Composites*, 34, 253, 2003.
- Kalia, S., Kaith, B.S., Kaur, I. (Eds.), *Cellulose Fibers: Bio- and Nano-Polymer Composites*. Springer, 2011.
- Kalita, R.D., Nath, Y., Ochubiojo, M.E., Buragohain, A.K., Extraction and characterization of microcrystalline cellulose from fodder grass; *Setaria glauca* (L) P. Beauv, and its potential as drug delivery vehicle for isoniazid, a first line antituberculosis drug. *Colloid. Surface B*, 108, 85, 2013.
- Keshk, S.M.A.S., Abu Haija, M., A new method for producing microcrystalline cellulose from *Gluconacetobacter xylinus* and kenaf. *Carbohydr. Polym.*, 84, 1301, 2011.
- Kiziltas, A., Gardner, D. J., Han, Y., Yang, H.Y., Dynamic mechanical behavior and thermal properties of microcrystalline cellulose (MCC)-filled nylon 6 composites. *Thermochim. Acta*, 519, 38, 2011.
- Kiziltas, A., Gardner, D. J., Han, Y., Yang, H.Y., Mechanical properties of microcrystalline cellulose (MCC) filled engineering thermoplastic composites. *J. Polym. Environ.*, 22, 365, 2013.

- Klemm, D., Heublein, B., Fink, H.P., Bohn, A., Cellulose: Fascinating Biopolymer and sustainable raw Materials. *Angew. Chem. Int. Ed.*, 44, 3358, 2005.
- La Mantia, F.P., Morreale, M., Green composites: A brief review. *Compos. Part A: Appl. S.*, 42(6), 579, 2011.
- Laka, M., Chernyavskaya, S., Obtaining microcrystalline cellulose from softwood and hardwood pulp. *BioResources*, 2(3), 583, 2007.
- Lamsal, B., Yoo, J., Brijwani, K., Alavi, S., Extrusion as a thermo-mechanical pretreatment for lignocellulosic ethanol. *Biomass Bioenerg.*, 34, 1703, 2010.
- Leppänen, K., andersson, S., Torkkeli, M., Knaapila, M., Kotelnikova, N., Serimaa, R., Structure of cellulose and microcrystalline cellulose from various wood species, cotton and flax studied by X-ray scattering. *Cellulose*, 16, 999, 2009.
- Lin, M.-F., Thakur, V.K., Tan, E.J., Lee, P.S., Surface functionalization of BaTiO₃ nanoparticles and improved electrical properties of BaTiO₃/polyvinylidene fluoride composite. *RSC Adv.* 1, 576, 2011a.
- Lin, M.-F., Thakur, V.K., Tan, E.J., Lee, P.S., Dopant induced hollow BaTiO₃ nanostructures for application in high performance capacitors. *J. Mater. Chem.* 21, 16500, 2011b.
- Li, C., Wang, X., Liu, L., Cui, J., Zhang, R., The effect of corn stalk microcrystalline cellulose on thermal and mechanical properties of chitosan composites. *Appl. Mech. Mater.*, 174, 1038, 2012.
- Ma, X., Chang, P.R., Yu, J., Properties of biodegradable thermoplastic pea starch/carboxymethyl cellulose and pea starch/microcrystalline cellulose composites. *Carbohydr. Polym.*, 72, 369, 2008.
- Ma, H., Zhou, B., Li, H., Li, Y., Ou, S., Green composite films composed of nanocrystalline cellulose and cellulose matrix regenerated from functionalized ionic liquid solution. *Carbohydr. Polym.*, 84, 383, 2011.
- Madrid, J.F., Abad, L.V., Modification of microcrystalline cellulose by gamma radiation-induced grafting. *Radiat. Phys. Chem.*, 115, 143, 2015.
- Mathew, A.P., Oksman, K., Sain, M., Mechanical properties of biodegradable composites from poly lactic acid (PLA) and microcrystalline cellulose. *J. Appl. Polym. Sci.*, 97, 2013, 2005.
- Mariano, P., Donatella, C., Irene, A., Zbigniew, K., Ewa, P., Functionalization, compatibilization and properties of polypropylene composites with hemp fibres. *Compos. Sci. Technol.*, 66, 2218, 2006.
- Maskavs, M., Kalnins, M., Reihmane, S., Laka, M., Chernyavskaya, S., Effect of water sorption of some mechanical parameters of composite systems based on low-density polyethylene and microcrystalline cellulose. *Mech. Compos. Mater.*, 35(1), 55, 1999.
- Merci, A., Urbano, A., Grossmann, M.V.E., Tischer, C.A., Mali, S., Properties of microcrystalline cellulose extracted from soybean hulls by reactive extrusion. *Food Res. Int.*, 73, 38, 2015.
- Miao, C., Hamad, W.Y., Cellulose reinforced polymer composites and nanocomposites: a critical review. *Cellulose*, 20, 221, 2013.
- Miao, S., Liu, Y., Wang, P., Zhang, S., Castor oil and microcrystalline cellulose based polymer composites with high tensile strength. *Adv. Mater. Res.*, 399(401), 1531, 2012.
- Mohamad Haafiz, M.K., Hassan, A., Zakaria, Z., Inuwa, I.M., Islam, M.S., Jawaid, M., Isolation and characterization of microcrystalline cellulose from oil palm biomass residue. *Carbohydr. Polym.*, 93, 633, 2013a.
- Mohamad Haafiz, M.K., Hassan, A., Zakaria, Z., Inuwa, I.M., Islam, M.S., Jawaid, M., Properties of polylactic acid composites reinforced with oil palm biomass microcrystalline cellulose. *Carbohydr. Polym.*, 98, 139, 2013b.
- Mohamed, M.A.S., Ghorbel, E., Wardah, G., Valorization of micro-cellulose fibers in self-compacting concrete, *Constr. Build. Mater.*, 24(12), 2473, 2010.
- Mortensen, A., *Concise Encyclopedia of Composite Materials*, pp. xvii–xxix, Elsevier, 2007.

- Motokawa, T., Makino, M., Enomoto-Rogers, Y., Kawaguchi, T., Ohura, T., Iwata, T., Sakaguchi, M., Novel method of the surface modification of the microcrystalline cellulose powder with poly(isobutyl vinyl ether) using mechanochemical polymerization. *Adv. Powder Technol.*, 2015. <http://dx.doi.org/10.1016/j.apt.2015.07.012>
- Nguyen, X.T., Process for preparing microcrystalline cellulose, US Patent 7005514, assigned to International Paper Company, 2006.
- Ofoefule, S. I., Chukwu, A., Application of blends of MCC–C issus gum in the formation of aqueous suspensions. *Boll. Chim. Farm.*, 138(5), 217, 1999.
- Okhamafe, A. O., Ejike, E. N., Akinrinola, F. F., Ubane-Ine, D., Aspect of tablet disintegrant properties of cellulose derived from Bagasse and Maize Cob. *W. Afr. J. Pharm.*, 9(1), 8, 1995.
- Okwonna, O.O., The effect of pulping concentration treatment on the properties of microcrystalline cellulose powder obtained from waste paper. *Carbohydr. Polym.*, 98, 721, 2013.
- Pandey, J.K., Takagi, H., Nakagaito, A.N., Kim, H.J.K. (Eds.), *Handbook of Polymer Nanocomposites*. Processing, Performance and Application. Springer, 2015.
- Pappu, A., Patil, V., Jain, S., Mahindrakar, A., Haque, R., Thakur, V.K., Advances in industrial prospective of cellulosic macromolecules enriched banana biofibre resources: A review. *Int. J. Biol. Macromol.*, 79, 449, 2015.
- Peters, S.J., Rushing, T.S., Landis, E.N., Cummins, T.K., Nanocellulose and microcellulose fibers for concrete. *Transp. Res. Rec. J. Transp. Res. Board*, 2142, 25, 2010.
- Petersson, L., Oksman, K., Biopolymer based nanocomposites: comparing layered silicates and microcrystalline cellulose as nanoreinforcement. *Compos. Sci. Technol.*, 66, 2187, 2006.
- Rafiee, Z., Keshavarz, V., Synthesis and characterization of polyurethane/microcrystalline cellulose bionanocomposites. *Prog. Org. Coat.*, 85, 190, 2015.
- Reis, M.O., Zanela, J., Olivato, J., Garcia, S., Yamashita, F., Grossmann, M.V.E., Microcrystalline cellulose as reinforcement in thermoplastic starch/poly (butylenes adipate-co-terephthalate) films. *J. Polym. Environ.*, 22, 545, 2013.
- Rosa, M., Chiou, B., Medeiros, E., Wood, D., Mattoso, L., Orts, W., Imam, S., Biodegradable composites based on starch/EVOH/glycerol blends and coconut fibers. *J. Appl. Polym. Sci.*, 111, 612, 2009.
- Rosa, S.M.L., Rehman, N., De Miranda, M.I.G., Nachtigall, S.M.B., Bica, C.I.D., Chlorine-free extraction of cellulose from rice husk and wisker isolation. *Carbohydr. Polym.*, 87, 1131, 2012.
- Sabo, R., Jin, L., Stark, N., Ibach, R.E., Effect of environmental conditions on the mechanical properties and fungal degradation of polycaprolactone/microcrystalline cellulose/wood flour composites. *BioResources*, 8(3), 3322, 2013.
- Satyanarayana, K.G., Arizaga, G.C.C., Wypych, F., Biodegradable composites based on lignocellulosic fibers—An overview. *Prog. Polym. Sci.*, 34, 982, 2009.
- Scabible, D., Sherwo, B., Treatment of pulp to produce microcrystalline cellulose, US Patent 0131957, assigned to Edward Mendell Co., Inc, 2003.
- Singha, A.S., Thakur, V.K., Synthesis and characterization of Pine needles reinforced RF matrix based biocomposites. *J. Chem.*, 5(S1), 1055, 2008.
- Singha, A.S., Thakur, V.K., Morphological, thermal, and physicochemical characterization of surface modified pinus fibers. *Int. J. Polym. Anal. Charact.* 14, 271, 2009a.
- Singha, A.S., Thakur, V.K., Synthesis and characterizations of silane treated Grewia optiva fibers. *Int. J. Polym. Anal. Charact.* 14, 3011, 2009b.
- Singha, A.S., Thakur, V.K., Chemical resistance, mechanical and physical properties of biofibers-based polymer composites. *Polym.-Plast. Technol. Eng.* 48, 736, 2009c.
- Singha, A.S., Thakur, V.K., Study of mechanical properties of urea-formaldehyde thermosets reinforced by pine needle powder. *BioResources* 4, 292, 2009d.

- Singha, A.S., Thakur, V.K., Fabrication and characterization of S. cilliare fibre reinforced polymer composites. *Bull. Mater. Sci.* 32, 49, 2009e.
- Siqueira, G., Bras, J., Dufresne, A., Cellulosic bionanocomposites: A review of preparation, properties and applications. *Polymer*, 2(4), 728, 2010.
- Shanks, R.A., Hodzic, A., Wong, S., Thermoplastic biopolyester natural fiber composites. *J. Appl. Polym. Sci.*, 91, 2113, 2003.
- Spoljaric, S., Genovese, A., Dhanks, R.A., Polypropylene-microcrystalline cellulose composites with enhanced compatibility and properties. *Compos. Part A*, 40, 791, 2009.
- Stupinska, H., Iller, E., Zimek, Z., Wawro, Z., Ciechanska, D., Kopania, E., Palenik, J., Milczarek, S., Steplewski, W., Krzyzanowska, G., An environment-friendly method to prepare microcrystalline cellulose. *Fibers Text. East. Eur.*, 15, 167, 2007.
- Sun, X., Lu, C., L, Y., Zhang, W., Zhang, X., Melt-processed poly(vinyl alcohol) composites filled with microcrystalline cellulose from waste cotton fabrics. *Carbohydr. Polym.*, 101, 642, 2013.
- Susan, W., Robert, S., Alma, H. Interfacial improvements in poly(3-hydroxybutyrate)-flax fibre composites with hydrogen bonding additives. *Compos. Sci. Technol.*, 64, 1321, 2003.
- Thakur, V.K. (Ed.), *Nanocellulose Polymer Nanocomposites: Fundamental and Applications*, Wiley-Scrivener, 2015a.
- Thakur, V.K. (Ed.), *Lignocellulosic Polymer composites: Processing, Characterization, and Properties*, Wiley-Scrivener, 2015b.
- Thakur, V.K., Kessler, M.R., Self-healing polymer nanocomposites materials: A review. *Polymer*, 69, 369, 2015a.
- Thakur, V.K., Thakur, M.K., Recent advances in green hydrogels from lignin: a review. *Int. J. Biol. Macromol.* 72, 833, 2015b.
- Thakur, V.K., Singha, A.S., Thakur, M.K., Green composites from natural fibers: Mechanical and chemical aging properties. *Int. J. Polym. Anal. Charact.*, 17, 401, 2012.
- Thakur, V.K., Singha, A.S., Thakur, M.K., Fabrication and physic-chemical properties of high-performance pine needles/green polymer composites. *Int. J. Polym. Mater.*, 62, 226, 2013.
- Thakur, V.K., Singha, A.S., KPS-initiated graft copolymerization onto modified cellulosic biofibers. *Int. J. Polym. Anal. Charact.*, 15, 471, 2010.
- Thakur, V.K., Thakur, M.K., Processing and characterization of natural cellulose fibers/thermoset polymer composites. *Carbohydr. Polym.*, 109, 102, 2013.
- Thakur, V.K., Thakur, M.K., Recent advances in graft copolymerization and applications of Chitosane: A review. *ACS Sustain. Chem. Eng.*, 2(12), 2637, 2014a.
- Thakur, V.K., Thakur, M.K., Gupta, R.K., Review: raw natural fiber-based polymer composites. *Int. J. Polym. Anal. Charact.*, 19, 256, 2014b.
- Thakur, V.K., Thakur, M.K. *et al.*, Green composites: an introduction, *Green Composites from Natural Resources*, V.K. Thakur (Ed.), pp. 1–10, CRC/Taylor & Francis, 2014c.
- Thakur, V.K., Thakur, M.K., Raghavan, P., Kessler, M.R., Progress in green polymer composites from lignin for multifunctional applications: A review. *ACS Sustain. Chem. Eng.*, 2(5), 1072, 2014d.
- Thakur, V.K., Thunga, M., Madbouly, S.A., Kessler, M.R., PMMA-g-SOY as a sustainable novel dielectric material. *RSC Adv.* 4, 18240, 2014e.
- Thakur, V.K., Vennerberg, D., Kessler, M.R., Green Aqueous Surface Modification of Polypropylene for Novel Polymer Nanocomposites. *ACS Appl. Mater.*, 6, 9349, 2014f.
- Thakur, V.K., Vennerberg, D., Madbouly, S.A., Kessler, M.R., Bio-inspired green surface functionalization of PMMA for multifunctional capacitors. *RSC Adv.* 4, 6677, 2014g.
- Thoores, G., Krier, F., Leclercq, B., Carlin, B., Evrard, B., Microcrystalline cellulose, a direct compression binder in a quality by design environment—A review. *Int. J. Pharm.*, 473, 63, 2013.

- Trache, D., Donnot, A., Khimeche, K., Benelmir, R., Brosse, N., Physico-chemical properties and thermal stability of microcrystalline cellulose isolated from Alfa fibres. *Carbohydr. Polym.*, 104, 223, 2013.
- Virtanen, T., Svedström, K., Andersson, S., Tervala, T., Torkkeli, M., Knaapina, M., Kotelnikova, N., Maunu, S.L., Serimaa, R., A physic-chemical utylenesitesn of new raw materials for microcrystalline cellulose manufacturing. *Cellulose*, 19, 219, 2011.
- Voicu, S.I., Condruz, R.M., Mitran, V., Cimpean, A., Miculescu, F., Andronescu, C., Miculescu, M., Thakur, V.K., Sericin Covalent Immobilization onto Cellulose Acetate Membrane for Biomedical Applications. *ACS Sustain. Chem. Eng.* 4, 1765, 2016.
- Wertz, J.L., Bédué, O. *et al.*, Cellulose Science and Technology, EPLF Press, Switzerland, 2010.
- Wu, Q., Henriksson, M., Liu, X., Berglund, L.A., A high strength utylenesites based on microcrystalline cellulose and polyurethane. *Biomacromolecules*, 8, 3687, 2007.
- Wu, H., Thakur, V.K., Kessler, M.R., Novel low-cost hybrid composites from asphaltene/SBS tri-block copolymer with improved thermal and mechanical properties. *J. Mater. Sci.* 51, 2394–2403, 2016.
- Wüstenberg, T., Cellulose and Cellulose Derivatives in the Food Industry, pp. 95–184, Wiley-VCH, 2015.
- Xiao, X., Lu, S., Qi, B., Zeng, C., Yuan, Z., Yu, J., Enhancing the thermal and mechanical properties of epoxy resins by addition of hyperbranched aromatic polyamide grown on microcrystalline cellulose fibers. *RSC Adv.*, 4, 14928, 2013.

Tannin-Based Foams: The Innovative Material for Insulation Purposes

Gianluca Tondi* and Alexander Petutschnigg

Dept of Forest Products Technology & Timber Construction, Salzburg University of Applied Sciences, Kuchl, Austria.

Abstract

Tannin-based foams are black porous materials which have the main advantage of being up to 100% natural, lightweight, fire-resistant and with a low thermal conductivity. These properties are the most important for building insulation purposes and therefore tannin foams have attracted significant market and industrial interest. Tannin foams are also a versatile material that can be produced with tailored properties modifying the formulation components and the process parameters; however the brittleness and the relatively weak mechanical properties suggested the need for a supporting material. For this reason, tannin-foam-based sandwich boards have been successfully produced with various wood and wood engineered side-layers such as HDF, particleboards and OSB. The production of these composite materials is nowadays industrially possible without the need of any external adhesive. An innovative and interesting product for the new generation of green insulation materials has been developed.

Keywords: Insulation material, green foam, formaldehyde-free, black panels, thermal conductivity, sandwich panels, industrial production

4.1 First Tannin Foams and their Characterization

The innovative materials presented in this chapter, namely the tannin-based foams (TBFs) are natural, light, fire-resistant and thermally insulating and hence they represent the ideal core layer of sandwich panels for building insulation. Nowadays it is possible to produce hundreds of interesting tannin foams according to the desired final properties, but the way to achieve this result was not always easy.

Today's tannin foams, indeed, are the result of several years of studies in which thousands of formulations and settings were tested and characterized in order to understand the material properties in detail. In Table 4.1 all the studies on this subject and the related findings are chronologically reported.

Initially the TBFs were prepared mixing tannin extract with formaldehyde, furfuryl alcohol, blowing agent and catalysts (Meikleham & Pizzi, 1994). The material obtained

*Corresponding author: gianluca.tondi@fh-salzburg.ac.at

Table 4.1 Chronological summary of the main findings in the study of tannin foams.

Authors	Year	Findings
Meikleham, Pizzi	1994	First tannin-based rigid foams.
Tondi, Pizzi	2008	Optimization and rough characterization of the foams.
Pizzi, Tondi, Celzard	2008	Chemical characterization of the first foams.
Celzard, Tondi, Pizzi	2009	Intrinsic properties of the first tannin foams.
Celzard, Tondi, Fierro	2009	First carbon derivate of the tannin foams.
Tondi, Pizzi	2009	First application opportunities: Absorber & Insulation.
Zhao, Celzard, Pizzi	2010	Physical characterization of the first foams.
Link, Tondi, Petutschnigg	2011	Formaldehyde-free tannin foams / Lightweight panels.
Basso, Pizzi, Celzard	2011	Formaldehyde-free tannin foams (room temperature).
Celzard, Amaral-Labat, Pizzi	2011	Details on fire properties of tannin foams.
Li, Pizzi, Celzard	2012	Additives for improving mechanical resistance/ elasticity.
Li, Pizzi, Celzard	2012	Study of different blowing agents.
Kolbitsch, Tondi, Petutschnigg	2012	Irradiation produced tannin foams (microwave & IR).
Lacoste, Pizzi, Celzard	2013	Pine tannin foams. Glyoxal foams.
Basso, Pizzi, Fierro	2013	Blowing agent and formaldehyde-free foams.
Zhou, Pizzi, Celzard	2013	Sandwich panels with tannin foam core.
Sanchez-M., Beltran-H., Rubio A.	2013	Optimization of the foams as absorber.
De Yuso, Pizzi, Celzard	2014	Quebracho tannin foams.
Scszurek, Fierro, Celzard	2014	Meringue tannin foams.
Basso, Giovando, Pizzi	2014	Alkaline tannin foams.
Cop, Lacoste, Pizzi, Sernek	2014	Spruce tannin foams.
Lagel, Pizzi, Celzard	2014	Replace phenol with chestnut tannin in phenolic foams.
Basso, Pizzi, Celzard	2014	Isocyanate-tannin foam in industrial plant.
Tondi, Oo, Petutschnigg	2015	IR spectroscopy for the characterization of tannin foams.
Lacoste, Celzard, Pizzi	2015	Acoustic studies on tannin foams.
Trey, Tondi, Johansson	2015	Semi-conductive tannin foams.
Lesacher, Link, Tondi	2015	Industrial tannin foams.
Tondi, Link, Van Doorslaer	2016	Lignin-furanic foams.

was the first prototype for acid- and alkali-catalysed tannin foams and therefore it was not subject to deep analysis.

Several years later, the studies of Meikleham & Pizzi were repeated and improved (Tondi & Pizzi, 2009). Various formulation modifications were tested to obtain a repeatable universal formulation that could produce lighter and more mechanically resistant TBFs. The black porous materials produced with this “milestone” formulation were then characterized in detail from the structural, mechanical and chemical perspective and for the purposes of this chapter they are referred to as “classic” tannin foams.

The “classic” TBFs are a porous material having almost only open-pores (92.5–96.9%) with bulk densities of 50 to 120 kg/m³ and with a surface area of around 1 m²/g. The features of the cells of the foams were dependent on the local density and on the position in the foam. Usually they had elongated shapes in the body of the sample, which rendered this material orthotropic. The cell diameter varied from ideally 0 to 2 mm but with average values between 100 to 400 µm (Tondi *et al.*, 2009a; Tondi *et al.*, 2009b; Zhao *et al.*, 2010a). Figure 4.1 shows an example of tannin foam and its tomographic elaboration. The physical properties of these materials are strongly dependent on density: the mechanical resistance of denser foams is linearly higher than lighter foams while permeability is higher for lighter foams (Celzard *et al.*, 2010; Zhao *et al.*, 2010b). The TBFs also showed strong insulating properties regarding electrical currents and they present particular resistance against water, solvents, acids and also against fire (Celzard *et al.*, 2011).

These outstanding physical properties are derived from the highly stable chemical structure. It was demonstrated that tannin, formaldehyde and furfuryl alcohol combine randomly, producing a multi-branched rigid co-polymer that resists thermal degradations particularly well because of the possibility of easy rearrangements of the aromatic moieties of the tannin-furanic network to more compacted carbonized structures (Tondi *et al.*, 2008a; Pizzi *et al.*, 2008; Tondi *et al.*, 2008b). These findings were also confirmed by the chemical and physical properties of the derived carbonized materials that will not be described in this chapter (Tondi *et al.*, 2009c; Tondi *et al.*, 2010).

Due to their water resistance and their remarkable fire behavior, the classic TBFs were analyzed for two main applications: i) Heavy-metal and organic pollutant absorber and ii) Insulation material. Interesting properties as heavy-metal complexing agents were discovered by Tondi *et al.*, (2009d) while the group of Sanchez-Martin *et al.*, (2013 a,b)

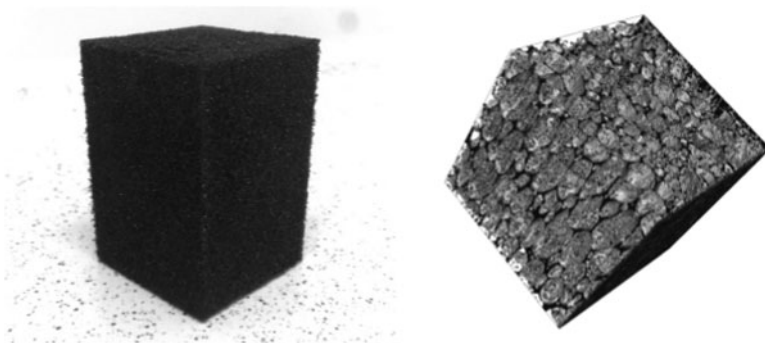


Figure 4.1 Classic tannin foam after production and skin removal (left); Tomographic elaboration (right).

focused successfully on the absorption of ionic pollutants as well as several pharmaceutical compounds in diluted water solutions. Even if the results of these experiments were highly satisfactory, much higher market potential was attracted when the TBFs were presented as insulation material (Tondi *et al.*, 2009e). Small samples of tannin foams measured with a lab-made static system for the measurement of the thermal conductivities showed outstanding λ -values between 0.023 and 0.030 W/m.K. Even if these values were never reached again with the transient plane-source method, this finding represented a great breakthrough for the future studies of tannin foams and acted as a strong catalyst for the tailored optimization of the foams.

After the first characterization experiments the material resulted already very attractive and therefore more than five years of study have been conducted to modify the component of the blend and the process in order to get more natural/sustainable and performing TBFs.

4.2 Formulation and Process Modifications

Thermosetting foams always consists of a subtle equilibrium between resin hardening and gas flowing. For this reason it is not really possible to produce new TBFs changing only one variable of the formulation. For example, if we increase the amount of a liquid component, the starting formulation will be less viscous and hence it will become solid later; if we apply a higher temperature, the polymerization and the blowing rate will be faster. Considering that it would be impossible to consider all the variables simultaneously, we classify the optimization studies according to the main formulation modification.

4.2.1 Hardeners

Once the classic TBFs were characterized it was evident that the restraining component of the formulation was the formaldehyde. When considering its use, particularly as insulation material for walls, formaldehyde had to be avoided because it was classified as carcinogenic molecule (IARC, 2006). Formaldehyde had the role of polymer hardener due to its feature of covalently combining with nucleophilic molecules that produce a reactive hydroxyl-methyl group which further combines with nucleophilic or hydroxyl-containing molecules. This unique chemistry cannot be easily replaced but the use of di-functional molecules like di-aldehydes that covalently cross-link in two positions was the more viable alternative. The simplest candidates for formaldehyde replacement were then glyoxal and glutaraldehyde, which have been successfully exploited for the production of formaldehyde-free pine TBFs (Lacoste *et al.*, 2013a). These glyoxal-containing products presented relatively large pores but comparable mechanical and thermal properties to the formaldehyde-containing ones. Two other approaches were considered for the complete elimination of the hardener. Basso *et al.* prepared formaldehyde-free TBFs, increasing the amount of furfuryl alcohol and blowing agent resulting in a less brittle material having on average slightly lower mechanical properties but also improved λ -values (0.038 W/m.K) (Basso *et al.*, 2011). Simultaneously the group of Link *et al.* prepared formaldehyde-free TBFs, applying external sources of energy



Figure 4.2 Formaldehyde-free tannin foam according to Link: Core layer (left); Sandwich panel (right).

(oven, press plate) to facilitate the hardening and the blowing. The so-made foams also presented slightly weaker mechanical properties with the main advantage of presenting higher homogeneity over the foam profile (Link *et al.*, 2011). Formaldehyde-free TBFs visually appear very similar to the classic ones and therefore it would be difficult to distinguish the two products just by looking at them (Figure 4.2). In order to overcome this aspect a simple spectroscopic method to evaluate the presence of formaldehyde in the structure of TBFs has recently been presented (Tondi *et al.*, 2015a).

4.2.2 Furfuryl Alcohol

This chemical represents the “engine” of the polymerization of the “classic” TBFs; its polymerization in acid environment is highly exothermic and the energy produced allows the curing of the resin and the evaporation of the blowing agent. This component was always considered essential for the production and for the structural stability of TBFs, but recently, a new concept for the TBFs has been developed to produce furan-free foams. It consists of the production of an emulsion of tannin foam by whisking a tannin water solution with a non-ionic emulsifier and a hardener (hexamethylenetetramine) followed by a hardening phase at higher temperature. The material made in this way presents very interesting intrinsic properties like a good homogeneity and low densities, but also weaker mechanical properties (Scszurek *et al.*, 2014; Celzard *et al.* 2015). Furan-free TBFs were produced also with alkaline catalyst but these will be described in more detail in the catalyst part (4.2.5).

4.2.3 Aromatic Backbone

The condensed tannin of mimosa (*Acacia mearnsii*) bark was the preferred backbone for the preparation of the classic TBFs due to its good water solubility and its moderate polymerization rate (Tondi *et al.*, 2013a). Several studies were conducted to exploit other extracts and the simplest, due to the chemical similarity, was the production quebracho-based tannin foams (De Yuso *et al.*, 2014). Even if the quebracho tree (*Schinopsis balansae*) is available only in some regions of South America, the high content of tannin in the tree and the high yield of the extraction process allows collection of a high amount of extract that is widely exploited for tannery purposes among others. This work showed that the quebracho TBFs are very similar to the mimosa ones but they present slightly larger cells, slightly improved mechanical properties but also slightly higher thermal

conductivities for low density foams. More challenging was the preparation of foams made of European trees extracts such as pine (*Pinus radiata*) and (*Picea abies*) spruce. These procyanidin/ prodelphinidin flavonoid extracts are way more reactive than the profisetinidin/prorobinetidin mimosa and quebracho and therefore, the polymerization/blowing equilibrium was completely different. Lacoste, (2013b) presented the pine tannin foams (with and without formaldehyde), which are characterized by slightly lower mechanical resistances and also lower densities and λ value. These TBFs were also tested for their acoustic properties, which showed considerably high performance especially as high-frequency insulators. Very recently, Cop prepared the tannin foams also with spruce extract, which presently are produced with lower proportion of extract but they still present very good homogeneity (Cop *et al.* 2015).

Even more challenging was producing foams out of much less reactive bio-resources. The hydrolyzable tannin of chestnut, for example was used in combination with phenol (30:70) and produced valuable phenolic foams with similar properties as the classic resolic foams, but more sustainable (Lagel *et al.*, 2014). By exploiting the external energy to produce the foams, it was possible to also synthesize stable lignin foams based on the spent-liquor of the magnefite pulping process (Tondi *et al.*, 2016). The latter are characterized by good homogeneities but higher densities and lower mechanical and thermal properties even if it has to be considered that this material is still in its starting phase.

4.2.4 Blowing Agent

Classic TBFs with different densities could be prepared by simply adding different amounts of diethyl ether. Due to the small amount of suitable chemicals with boiling point between 25 and 45 °C, the use of different solvents was studied only with pentane. The pentane-blown derived foams showed very low densities ($d = 30 \text{ kg/m}^3$) and consequent very low thermal conductivities (ca 0.037 W/m.K) but also larger cells (700 μm) (Li *et al.*, 2012a). Later, the same group discovered that stable tannin foams can be obtained also without blowing agent by adding a small amount of diisocyanate (Basso *et al.*, 2013). However, new blowing agents can be proposed as soon as the production temperature increases: ethanol, acetone and even water become suitable.

4.2.5 Catalyst

The catalyst for TBFs is the component that starts the whole polymerization/blowing process. Most of the TBFs were produced with a strong and concentrated organic acid, namely p-toluensulphonic acid. Several tests were also successful with other inorganic acid, like sulphuric acid, which is the main catalyst for the heat-supported foams and phosphoric acid that has been proven to increase the fire properties of the TBFs. However, the more challenging TBFs were the ones that were produced in alkaline environment with the support of external heat. These foams did not contain any furan and the tannins were copolymerized with hexamine or glutaraldehyde. The process of curing was much longer and the foams particularly brittle, but very interesting results were registered in terms of fire resistance because these materials showed instantaneous self-extinction (Basso *et al.*, 2014a).

4.2.6 Additive for Improving Specific Properties

Classic TBFs and their modifications involve a wide range of properties that can be tailored according to the final application for which the foams are prepared. However, some features of these materials were still not satisfactory and therefore there was the need to improve their properties by adding specific chemicals. The great majority of the modifications were carried out to improve the mechanical performances. More resistant TBFs were obtained by adding hyper-branched amino-esters and carbon fibers nanotubes. The compression resistances were increased 36.6% and 31.8% respectively (Li *et al.*, 2012b; Li *et al.*, 2013). The mechanical resistance was also enhanced by mixing the TBFs with isocyanates and polyurethane obtaining mechanical improvement up to 5 times (Li *et al.*, 2012c). The rigidity of “classic” TBFs implies also a high brittleness. The additions of glycerol, isocyanates and polyurethane were successfully tested for the production of more elastic materials (Li *et al.*, 2012d; Basso *et al.*, 2014b). Industrial production of isocyanate-tannin-furanic copolymer foams was also established and the so-produced materials have shown that low density and low thermal conductivities can be achieved with a copolymer in which each of the component is co-reacted (Basso *et al.* 2014c).

Recently, TBFs have also been modified to obtain semi-conductive electric properties by impregnating the foam with aniline that is then *in-situ* polymerized to polyaniline (Tondi *et al.*, 2015b) and also to achieve a more hydrophobic surface by IR beam treatments (Tondi *et al.*, 2015c). Figure 4.3. shows the details of a semi-conductive and a hydrophobic TBF.

4.2.7 Process Modification

The “classic” expansion at room temperature was the most-used process. However, nowadays it is proven that TBFs can also be produced at higher temperatures, saving some of the chemicals required: i) no formaldehyde nor other aldehydes and ii) lower amount of blowing agent or substances at higher boiling point (even water in some cases). The TBFs produced in the oven and in the press showed good homogeneity and good moisture absorption but lower mechanical properties (Link *et al.*, 2011). It was observed that the TBFs can blow also when radiative energy is used and the materials

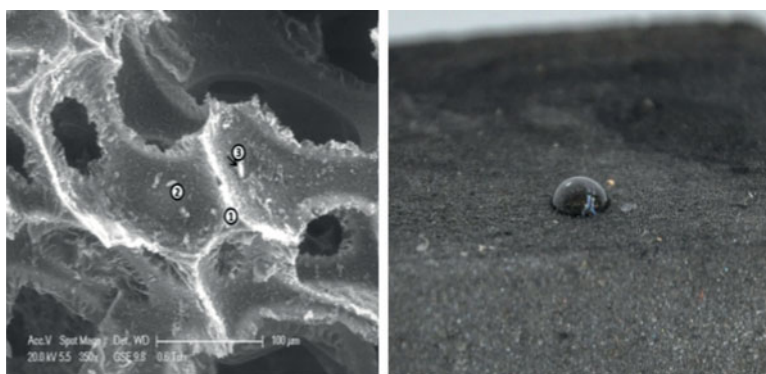


Figure 4.3 Polyaniline modified semi-conductive TBF SEM detail (left); IR modified tannin foam surface (right).



Figure 4.4 Microwave produced TBF sandwich panel (left); IR beam produced TBF (right).

made in this way require even less material, have fast production time and have even better fire resistance, but higher densities and lower homogeneity were registered (Kolbitsch *et al.*, 2012; Tondi *et al.*, 2013b). Examples of microwave and IR beam produced foams are reported in Figure 4.4.

As also mentioned in previous sub-chapters, the great versatility of the TBFs that can be produced with tailored properties is summarized in Table 4.2.

It can be observed that it is possible to modify the formulations in every single component and the physical properties can be modified according to the required specifications. It also appears evident that the ideal product is always the result of compromises. According to the required properties for specific applications, the formulation and the production process of TBFs can be tailored in order to get a suitable product. As an example, the lightweight foams cannot be very resistant and therefore it can be necessary to combine the properties of the TBFs with the ones of other materials to produce a more commercially attractive item.

4.3 Composite Materials: Tannin-Based Panels

TBFs are outstanding products because they simultaneously present the following four features: i) They are bio-based: ii) Lightweight iii) Fire resistant and iv) Thermally insulating. Consequently, it seems logical to exploit these foams in building construction. The weakest feature for this application is that they do not perform particularly well mechanically. Classic lightweight TBFs of around 50 kg/m^3 resist compression stresses of max 0.15 MPa but the use of additives like isocyanates enhance this resistance up to 0.3 MPa . Moreover, the brittleness of the material means that small spots of the surface can break and therefore the material results are not too easy to manage.

Easily transportable, formaldehyde-free, lightweight panels were produced using common paper and recycling paper as side-layer (Tondi *et al.*, 2015d). The composite obtained, without the need of any external adhesive, was much easier to handle because its surface was less brittle and hence it was directly applicable in the core compartment of the insulation walls. For special applications in which lightness need to be combined with good aesthetic appearance such as for ceiling and partition walls, melamine laminates were selected as side-layer.

Even more interesting were the composite materials for structural or semi-structural purposes. The combination of the tannin foams with more mechanically resistant panels such as wood, wood-based panels and plastic was the more obvious solution

Table 4.2 Summary of the tannin foams formulations and its properties. The classic formulation is compared with the maximum values registered in enhanced foams.

		Classic	Enhanced
Formulation	Tannin (%)	43.6	52.0 (Kolbitsch <i>et al.</i> , 2012)
	Furfuryl alcohol (%)	15.1	0.0 (Szscurek <i>et al.</i> , 2014; Basso <i>et al.</i> , 2014)
	Formaldehyde (%)	4.1	0.0 (Link <i>et al.</i> , 2011; Basso <i>et al.</i> , 2011)
	Blowing agent (%)	4.4	0.0 (Kolbitsch <i>et al.</i> , 2012)
	Catalyst (%)	11.3	3.4 (Szscurek <i>et al.</i> , 2014)
	Additives (%)	–	Several, 70 (Lagel <i>et al.</i> , 2014)
	Natural resources formulation (%)	58.7	90.7 (Szscurek <i>et al.</i> , 2014)
	Natural material in solid (%)	93.5	100.0 (Link <i>et al.</i> , 2011; Basso <i>et al.</i> , 2011)
Intrinsic properties	Density (kg/m ³)	50–120	35–150
	Homogeneity	Good	Very good
	Porosity (%)	92–98	–
	Cell dimensions (μm)	100–400	50–800
Physical properties	Mechanical resistance (MPa) ^a	0.3–0.45	0.85–0.9 (Li <i>et al.</i> , 2012)
	Elasticity	Brittle	Elastic (Li <i>et al.</i> , 2012)
	Fire resistance	Self-extinguish	Immediate self-extinguish (Basso <i>et al.</i> , 2014)
	Water absorption (%) ^a	300–350	700–750 (Link <i>et al.</i> , 2011)
	Thermal conductivity (W/m.K)	0.023–0.03 ^b	0.03–0.05

a = for a foam of 100 kg/m³

b = measured with lab-made instrument

μw = microwaves; IR = infrared beam; Mer = Meringues; Alk = Alkaline FF= Formaldehyde-free; Ch = Chestnut; PMDI = isocyanate; PU = Polyurethane TF = tannin foam; PTF = Phenol-tannin foam

to fill the mechanical performance required for the use of the TBFs in construction. Formaldehyde-free tannin-based composites were also produced without the need for any external adhesive, but just exploiting the distinguishing hardening behaviour of the formulation (Link *et al.*, 2011).

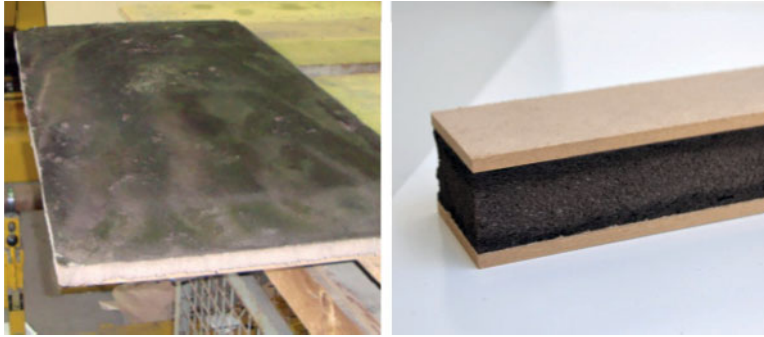


Figure 4.5 Industrially produced tannin foams: immediately after pressing (left); HDF sandwich panel (right).

High density fiberboards (HDF), particleboards, oriented strand boards (OSB) and plywood were used as side-layers for the preparation of various composites for structural or semi-structural applications like indoor walls, doors, windows and furniture. These materials showed improved mechanical properties due to the side layers: As an example, the composites with HDF and plywood as side layers registered a modulus of elasticity over 70 times higher than that of the foam itself. In another study the TBFs were glued with semi-synthetic adhesives to sandwich panels having wood, plywood and fiber-based supports as side layers. In this case the bending properties of the composites were compared with the single side-layer and no significant variations were observed (Zhou *et al.*, 2013).

4.4 Conclusions

In summary, the structural tannin-foam composites combine the good mechanical performances of the side-layer materials with the lightness, the high fire resistance and the good thermal and acoustic insulation properties of the natural tannin foams. These composites have attracted even more industrial interest when they have been produced in larger scale with common continuous presses (Tondi *et al.*, 2015e). In Figure 4.5, two industrially produced TBFs are presented. The possibility to industrially produce formaldehyde-free tannin foams represents a great potential in commercial applications of next-generation green buildings.

References

- Basso, M. C., Li, X., Fierro, V., Pizzi, A., Giovando, S., & Celzard, A. Green, formaldehyde-free, foams for thermal insulation. *Adv. Mater. Lett.*, 2(6), 378–382, 2011.
- Basso, M. C., Giovando, S., Pizzi, A., Celzard, A., & Fierro, V. Tannin/furanic foams without blowing agents and formaldehyde. *Ind. Crops Prod.*, 49, 17–22, 2013.
- Basso, M. C., Giovando, S., Pizzi, A., Lagel, M. C., & Celzard, A. Alkaline tannin rigid foams. *J. Renew. Mat.*, 2(3), 182–185, 2014a.

- Basso, M. C., Giovando, S., Pizzi, A., Pasch, H., Pretorius, N., Delmotte, L., & Celzard, A. Flexible-elastic copolymerized polyurethane-tannin foams. *J. Appl. Polym. Sci.*, 131(13), 2014b.
- Basso, M.C., Pizzi, A., Lacoste, C., Delmotte, L., Al-Marzouki, F.M., Abdalla, S., Celzard, A. MALDI-TOF and ¹³C NMR Analysis of fannin-furanic-polyurethane foams adapted for industrial continuous lines application. *Polymers*, 6, 2985–3004, 2014c.
- Celzard, A., Zhao, W., Pizzi, A., & Fierro, V. Mechanical properties of tannin-based rigid foams undergoing compression. *Mat. Sci. Eng.: A*, 527(16), 4438–4446, 2010.
- Celzard, A., Fierro, V., Amaral-Labat, G., Pizzi, A., & Torero, J. Flammability assessment of tannin-based cellular materials. *Polym. Degr. Stab.*, 96(4), 477–482, 2011.
- Celzard, A., Szczurek, A., Jana, P., Fierro, V., Basso, M. C., Bourbigot, S. & Pizzi, A. Latest progresses in the preparation of tannin-based cellular solids. *J. Cell. Plas.*, 51(1), 89–102, 2015.
- Čop, M., Laborie, M. P., Pizzi, A., & Sernek, M. Curing characterisation of spruce tannin-based foams using the advanced isoconversional method. *BioResources*, 9(3), 4643–4655, 2014.
- De Yuso, A. M., Lagel, M. C., Pizzi, A., Fierro, V., & Celzard, A. Structure and properties of rigid foams derived from quebracho tannin. *Mat. Des.*, 63, 208–212, 2014.
- Kolbitsch, C., Link, M., Petutschnigg, A., Wieland, S., & Tondi, G. Microwave produced tannin-furanic foams. *J Mat Sci Res*, 1(3), 84, 2012.
- IARC Working Group on the Evaluation of Carcinogenic Risks to Humans. Formaldehyde, 2-butoxyethanol and 1-tert-butoxypropan-2-ol. *IARC monographs on the evaluation of carcinogenic risks to humans/World Health Organization, International Agency for Research on Cancer*, 88, 1, 2006.
- Lacoste, C., Basso, M. C., Pizzi, A., Laborie, M. P., Garcia, D., & Celzard, A. Bioresourced pine tannin/furanic foams with glyoxal and glutaraldehyde. *Ind. crops Prod.*, 45, 401–405, 2013a.
- Lacoste, C., Basso, M. C., Pizzi, A., Laborie, M. P., Celzard, A., & Fierro, V. Pine tannin-based rigid foams: mechanical and thermal properties. *Ind. crops Prod.*, 43, 245–250, 2013b.
- Lagel, M. C., Pizzi, A., Giovando, S., & Celzard, A. Development and Characterisation of Phenolic Foams with Phenol-Formaldehyde-Chestnut Tannins Resin. *J. Renew. Mat.*, 2(3), 220–229, 2014.
- Li, X., Pizzi, A., Lacoste, C., Fierro, V., & Celzard, A. Physical properties of tannin/furanic resin foamed with different blowing agents. *BioResources*, 8(1), 743–752, 2012a.
- Li, X., Essawy, H. A., Pizzi, A., Delmotte, L., Rode, K., Le Nouen, D. & Celzard, A. Modification of tannin based rigid foams using oligomers of a hyperbranched poly (amine-ester). *J.Polym. Res.*, 19(12), 1–9, 2012b.
- Li, X., Basso, M. C., Fierro, V., Pizzi, A., & Celzard, A. Chemical modification of tannin/furanic rigid foams by isocyanates and polyurethanes. *Maderas*, 14(3), 257–265, 2012c.
- Li, X., Pizzi, A., Cangemi, M., Fierro, V., & Celzard, A. Flexible natural tannin-based and protein-based biosourced foams. *Ind. crops Prod.*, 37(1), 389–393, 2012d.
- Li, X., Srivastava, V. K., Pizzi, A., Celzard, A., & Leban, J. Nanotube-reinforced tannin/furanic rigid foams. *Ind. crops Prod.*, 43, 636–639, 2013.
- Link, M., Kolbitsch, C., Tondi, G., Ebner, M., Wieland, S., & Petutschnigg, A. Formaldehyde-free tannin based foams and their use as lightweight panels. *BioResources*, 6(4), 4218–4228, 2011.
- Meikleham, N. E., & Pizzi, A. Acid-and alkali-catalyzed tannin-based rigid foams. *J. Appl. Polym. Sci.*, 53(11), 1547–1556, 1994.
- Pizzi, A., Tondi, G., Pasch, H., & Celzard, A. Matrix-assisted laser desorption/ionization time-of-flight structure determination of complex thermoset networks: Polyflavonoid tannin-furanic rigid foams. *J. Appl. Polym. Sci.*, 110(3), 1451–1456, 2008.

- Sánchez-Martín, J., Beltrán-Heredia, J., Delgado-Regaña, A., Rodríguez-González, M. A., & Rubio-Alonso, F. Optimization of tannin rigid foam as adsorbents for wastewater treatment. *Ind. crops Prod.*, 49, 507–514, 2013a.
- Sanchez-Martin, J., Beltran-Heredia, J., Delgado-Regaña, A., Rodriguez-Gonzalez, M. A., & Rubio-Alonso, F. Adsorbent tannin foams: New and complementary applications in wastewater treatment. *Chem. Eng. J.*, 228, 575–582, 2013b.
- Szczurek, A., Fierro, V., Pizzi, A., Stauber, M., & Celzard, A. A new method for preparing tannin-based foams. *Ind. crops Prod.*, 54, 40–53, 2014.
- Tondi, G., Pizzi, A., Masson, E., & Celzard, A. Analysis of gases emitted during carbonization degradation of polyflavonoid tannin/furanic rigid foams. *Polym. Degr. Stab.*, 93(8), 1539–1543, 2008b.
- Tondi, G., & Pizzi, A. Tannin-based rigid foams: Characterization and modification. *Ind. crops Prod.*, 29(2), 356–363, 2009.
- Tondi, G., Pizzi, A., Pasch, H., Celzard, A., & Rode, K. MALDI-ToF investigation of furanic polymer foams before and after carbonization: Aromatic rearrangement and surviving furanic structures. *Eur. Polym. J.*, 44(9), 2938–2943, 2008.
- Tondi, G., Zhao, W., Pizzi, A., Du, G., Fierro, V., & Celzard, A. Tannin-based rigid foams: a survey of chemical and physical properties. *Biores. Technol.*, 100(21), 5162–5169, 2009a.
- Tondi, G., Blacher, S., Léonard, A., Pizzi, A., Fierro, V., Leban, J. M., & Celzard, A. X-ray microtomography studies of tannin-derived organic and carbon foams. *Microsc. Microanal.*, 15(05), 384–394, 2009b.
- Tondi, G., Fierro, V., Pizzi, A., & Celzard, A. Tannin-based carbon foams. *Carbon*, 47(6), 1480–1492, 2009c.
- Tondi, G., Oo, C. W., Pizzi, A., Trosa, A., & Thevenon, M. F. Metal adsorption of tannin based rigid foams. *Ind. crops Prod.*, 29(2), 336–340, 2009d.
- Tondi, G., Pizzi, A., & Olives, R. Natural tannin-based rigid foams as insulation for doors and wall panels. *Maderas*, 10(3), 219–227, 2009e.
- Tondi, G., Pizzi, A., Delmotte, L., Parmentier, J., & Gadiou, R. Chemical activation of tannin-furanic carbon foams. *Ind. crops Prod.*, 31(2), 327–334, 2010.
- Tondi, G., Thevenon, M. F., Mies, B., Standfest, G., Petutschnigg, A., & Wieland, S. Impregnation of Scots pine and beech with tannin solutions: effect of viscosity and wood anatomy in wood infiltration. *Wood sci. technol.*, 47(3), 615–626, 2013a.
- Tondi, G., Link, M., Kolbitsch, C., & Petutschnigg, A. Infrared-catalyzed synthesis of tannin-furanic foams. *BioResources*, 9(1), 984–993, 2013b.
- Tondi, G., Link, M., Oo, C. W., & Petutschnigg, A. A simple approach to distinguish classic and formaldehyde-free tannin based rigid foams by ATR FT-IR. *J. Spectr.*, 2015, 2015a.
- Tondi, G., Johansson, M., Leijonmarck, S., & Trey, S. Tannin based foams modified to be semi-conductive: Synthesis and characterization. *Progr. Org. Coat.*, 78, 488–493, 2015b.
- Tondi, G., & Petutschnigg, A. Hydrophobic tannin foams. *Int. Wood Prod. J.*, 2042645315Y-0000000007, 2015c.
- Tondi, G., Link, M., & Kolbitsch, C. Sandwich panels with 100% natural tannin furanic foam core. *For. Prod. J.*, 65, s33–s38, 2015d.
- Tondi, G., Link, M., Kolbitsch, C., Lesacher, R., Petutschnigg, A. Pilot plant up- scaling of tannin foams. *Ind. Crops Prod.*, 2015e.
- Tondi, G., Link, M., Kolbitsch, C., Gavino, J., Luckeneder, P., Petutschnigg, A., Herchl, R., Van Doorslaer, C. Lignin-based foams: Production process and characterization. *BioResources*, 2016.
- Zhao, W., Pizzi, A., Fierro, V., Du, G., & Celzard, A. Effect of composition and processing parameters on the characteristics of tannin-based rigid foams. Part I: cell structure. *Mat. Chem. Phys.*, 122(1), 175–182, 2010a.

- Zhao, W., Fierro, V., Pizzi, A., Du, G., & Celzard, A. Effect of composition and processing parameters on the characteristics of tannin-based rigid foams. Part II: Physical properties. *Mat. Chem. Phys.*, 123(1), 210–217, 2010b.
- Zhou, X., Pizzi, A., Sauget, A., Nicollin, A., Li, X., Celzard, A. & Pasch, H. Lightweight tannin foam/composites sandwich panels and the coldset tannin adhesive to assemble them. *Ind. Crops Prod.*, 43, 255–260, 2013.

Renewable Feedstock Vanillin-Derived Polymer and Composites: Structure Property Relationship

G. Madhumitha, Selvaraj Mohana Roopan*, D. Devi Priya and G. Elango

*Chemistry of Heterocycles & Natural Product Research Laboratory, Department of Chemistry,
School of Advanced Sciences, VIT University, Vellore, Tamilnadu, India*

Abstract

Bean or Pod of Vanilla Orchid is an origin for the isolation of vanillin. It can be synthesized via chemical and biological methods. Due to the potency and its application vanillin has been used in various industries such as beverages, perfumes, food, and pharmaceuticals. Natural source (vanillin) contains reactive functional groups (-CHO), which is useful to provide additional function from the target material. Also based on the environmental concerns, policies and financial incentives, various material science sectors have moved towards the use of such natural source in their product. In this chapter, we will describe the preparation and application of vanillin-derived polymers and composites.

Keywords: vanillin, natural source, polymer, composites, application

5.1 Introduction

Several plants contain various phyto constituents that are also secondary metabolites. In these plant metabolites one of the major composites is vanillin. Natural vanilla was extracted from vanilla orchid pods. This naturally extracted vanilla was a combination of many organic and inorganic natural compounds, among which vanillin has been considered as one of the compounds. Natural vanillin extract contains artificial vanilla flavoring solution; it was extracted by various extraction techniques. Each year more than 20,000 tons of flavoring and fragrance ingredient was extracted from vanillin (Fache *et al.*, 2015).

Natural vanillin, synthesized vanillin and ethyl vanillin were widely applied as dyeing and flavoring agents in various fields like nutrients, drinks, and pharmaceuticals. It can also be isolated from byproducts from paper industries. In petroleum-based industries vanillin requires few reaction steps for isolation (Kumar *et al.*, 2012; Lawrence *et al.*, 1997; Martin *et al.*, 1997; Gary *et al.*, 1977).

*Corresponding author: mohanaroopan.s@gmail.com, mohanaroopan.s@vit.ac.in

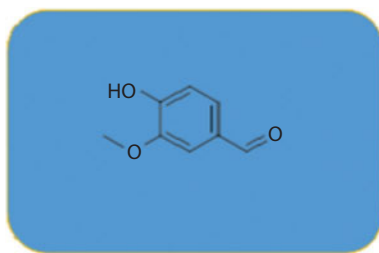


Figure 5.1 Structure of vanillin.

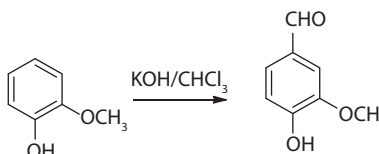


Figure 5.2 Synthesis vanillin from guaiacol.

Morphological appearance of vanillin is white crystalline powder that has melting point of 81 °C, vapor pressure of 0.33Pa, is less soluble in water and increasing solubility with increase in temperature. Vanillin is an organic compound that can also called 4-hydroxy-3-methoxybenzaldehyde. Vanillin is a perfumed aldehyde that belongs to the position of C_6-C_1 phenolic compounds. It contains a phenol group in structure, and also it contains methoxy group and aldehyde present in particular positions (Figure 5.1).

There are two types of vanillin, and ethyl vanillin was more expensive with stronger flavor due to the presence of ethoxy group ($-O-C_2H_5$) in the place of methoxy group ($-O-CH_3$). Vanillin was first synthesized from eugenol, lignin containing sulfite liquor, wood pulp byproduct (Gallage & Moller, 2015). Although various types of vanillin is isolated from lignin surplus, currently most artificial vanillin is produced via two steps from petrochemical originators such as vanillin, ethyl vanillin, guaiacol and glyoxylic acid.

In 2010, Universal trades of vanillin crossed 15,000,000 kg which is less than 1% solution obtained from vanilla pods. The production of vanilla beans and the separation of vanillin starting form vanilla pods was said to be a difficult and expensive process: making of 1 kg of vanillin involves roughly 500 kg of vanilla pods, consistent to the cross-pollination of more or less 40,000 vanilla orchid flowers (Gallage & Moller, 2015).

5.1.1 History of Vanillin

In 1858, Nicolas-Theodore Gobley was the first person to isolate pure compound of vanillin from vanilla extract (Gobley, 1858). German scientists Ferdinand Tiemann and Wilhelm Haarmann prepared vanillin from coniferyl in 1874 and Karl Reimer synthesized vanillin from guaiacol in 1876. Later on vanillin prepared as semi-synthetic method for eugenol from clove oil which is commercially available nowadays (Figure 5.2).

In the 1930s, vanillin was more available in society. Vanillin synthesized from clove oil extracted lignin containing waste, which contains wood pulp for paper industries. These paper industries were one of the main suppliers for semi-synthetic vanillin. In a world market 60% of a single pulp was supplied for vanillin. Today vanillin is also synthesized by two-step process from some chemicals which includes petrochemicals, guaiacol and glyoxylic acid (Gobley, 1858).

5.1.2 Occurrence

Vanillin is a flavored compound isolated from vanilla pods that contain 2% of a vanillin compound. Purest forms of vanillin were isolated from Vanillin pods by physical state of a white dust or frost. This vanillin is also isolated from a species named *Leptotes bicolor* and originates in Paraguay and southern Brazil. When vanillin is allowed to react with other chemicals which produces flavor of aroma, coffee, maple syrup. This vanillin was treated with other chemicals for the formation of various flavors like oatmeal, products of whole-grain, coffee, and maple syrup (Kermasha, 1995).

5.2 Vanillin Production

Vanillin is produced by three methods: natural production, biosynthesis, and chemical synthesis.

5.2.1 Vanillin Extraction via Natural Route

Vanillin is isolated from *Vanilla planifolia*, which is native to Mexico. The largest production of vanillin is said to be Madagascar. Vanillin contain from β -D-glucoside, in green pods but it does not contains aroma or odor flavor (Figure 5.3). After cultivation of vanilla seed pods, aroma was developed and after few months vanillin compound was synthesized by using natural production method.

5.2.2 Biosynthesis of Vanillin

Vanillin is also synthesized by using extract of *Vanilla planifolia* seed pods. Several biological pathways are utilized for synthesis of vanillin, like phenyl-propanoid pathway which can also be called vanillin pathway. In this phenyl-propanoid pathway

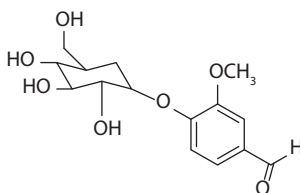


Figure 5.3 Natural production of vanillin.

L-phenylalanine was converted to a phenyl-alanine ammonia lyase (PAL) to form cinnamic acid (Dixon 2014). Finally vanillin synthase hydrates are synthesized using hydration reaction after that it forms double bond of ferulic acid which was followed by a retro-aldol elimination to produce vanillin and also it can synthesize other end products from vanilla like glucoside, p-hydroxybenzaldehyde which can act as a precursor for vanillin biosynthesis (Kaur & Chakraborty, 2012; Thakur *et al.*, 2013 a).

5.2.3 Chemical Synthesis of Vanillin

In the demand for vanilla aroma compound, vanillin was synthesized by chemical method. Vanillin was chemically first synthesized by eugenol and “Brown liquor.” This Brown liquor was isolated from by-product of the pulp industries. Many methods are available for the production of vanillin from guaiacol. In 1970 vanillin was synthesized by two-step process, first it was processed by glyoxylic acid and guaiacol. Next step is vanillylmandelic acid was transformed into 4-hydroxy-3-methoxyphenyl glyoxylic acid to form vanillin in oxidative decarboxylation (Figure 5.4).

Vanillin also produced by microbial conversions, like construction of vanillin from ferulic acid, eugenol and iso-eugenol, sugars and others substrates. Vanillin was mostly utilized in the polymer field. The mono aromatic compound present in vanillin is used for the preparation of polymer. Approaches to synthesize vanillin-based polymers can be classified into three groups. The first one is a direct mono functionalization of vanillin derivative with mono-aromatic monomer. The second one is the combination of two vanillin derivatives like di-functional and di-aromatic monomer present in the same group on both ends. The third one is said to be vanillin embedding derivative, which can also be called as a preexisting polymer. These approaches were engaged to prepare a wide range of polymers by two methods like step-growth or chain-growth polymerization (Fache *et al.*, 2015).

Precursors of vanillin like eugenol and iso-eugenol were applied by ADMET (acyclic diene metathesis) polymerization which was obtained for unsaturated poly ethers and carbonates with mass of 27,000 to 32,000 g/mol. ADMET approach is one of the very useful approaches in polymer synthesis, which includes activity and various functional groups (Firdaus *et al.*, 2013). Vanillin can be also utilized as cationic surfactants for the production of fine chemicals. Vanillin and vanillic acid are used as agents for anti-melanogenesis. This vanillin was selected as a core structure for the concise and cost-effective synthesis of ester derivatives that contain hydroxy substituted aryl moiety for their improved tyrosinase inhibitory activity. Vanillin derivatives have also been synthesized by incorporating heterocyclic piperazine ring to explore its role in tyrosinase inhibitory activity (Ashraf *et al.*, 2015).

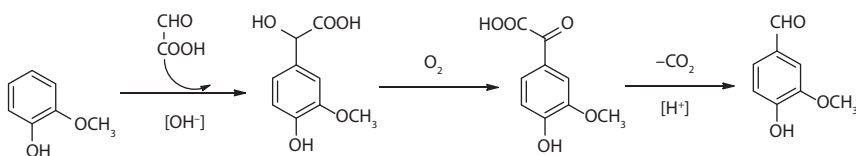


Figure 5.4 Chemical synthesis of vanillin.

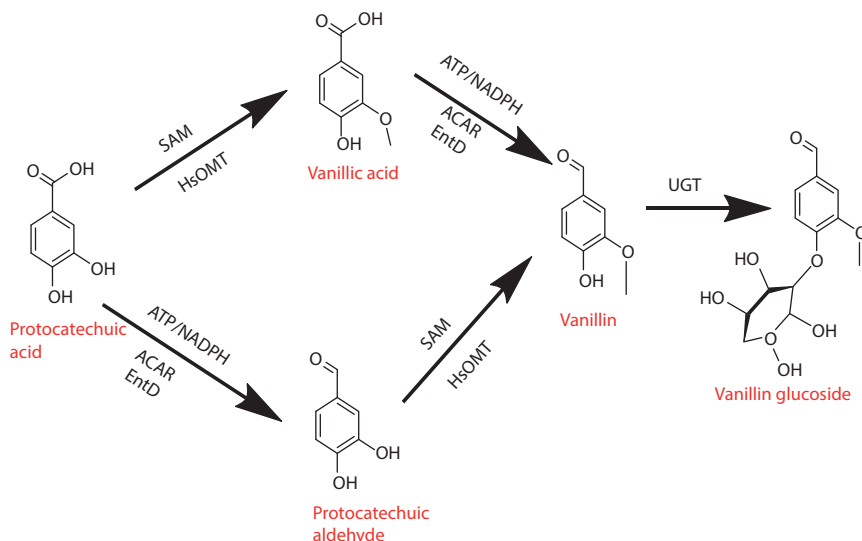


Figure 5.5 Synthesis of vanillin.

For vanillin synthesis one of the major requirements was said to be lignin wastes by depolymerization of lignosulfate. This was a less economic process of vanillin synthesis. Recently vanillin is manufactured by aromatic industries by various synthesis methods like bio-based synthesis, which also contains synthesis of polymer networks (Figure 5.5) (Fache *et al.*, 2015). On the overall decade vanillin prepared from lignin wastes can be used for synthesis of polymer and polymer composites. In the following sections, we mainly focus on synthesis of polymers and polymer composites with various applications for the vanillin compound (Silva *et al.*, 2009; Voith *et al.*, 2008; Brazinha *et al.*, 2011; Araujo *et al.*, 2010).

5.3 Some Common Applications of Vanillin

5.3.1 Food Production

Vanillin is mostly utilized in perfume and food industries as a flavor enhancer in chocolates, candies, biscuits, instant noodles and bread to improve flavor.

5.3.2 Vanillin in Beverages

It is also used as flavor enhancer in beverage industries, and is utilized for flavoring ice-creams.

5.3.3 Cosmetics and Pharmaceutical Industries

In cosmetics industries vanillin is utilized for the fragrances of creams, perfumes, etc. In pharmaceuticals industries it plays a major role as an intermediate for preparation of medicine.

5.3.4 Agriculture and Animal Feed

Vanillin also useful enhancement of flavor in the agriculture field by enhancing animal feeds, and is also used as masking agent by giving pleasant smell to feeds.

5.3.5 Other Industries

It was also used in candles, incense cones, shampoos, soaps, room sprays, body lotions and shower gels. Ethyl vanillin is regularly used because of its stronger aroma. Vanilla is also used to increase the aroma of paints and spring-cleaning products.

5.4 Vanillin-Derived Polymers

Polymers derived from renewable source are called as bio-polymers (Singha & Thakur, 2009a–d) (Thakur *et al.*, 2014a–e). Most bio-polymers are synthesized using industrial methods. Bio-based polymers are also said to be cycloaliphatic or aliphatic polymers, which are produced from triglycerides, cellulose and starch. Three renewable sources are used for bio-based monomers: polyphenols, lignins and liquid extracted from nutshell. Lignin is one of the most rich feedstock. It is an unstructured cross-linkage polymer making up woody biomass. Production of vanillin from lignin derivatives like lignosulfonates are commercialized. Many methods having the transformation from lignin to vanillin were identified. From the renewable resources most of the polymers and composites like triglycerides, 1, 3-propanediol, furfural, 2, 5-furandicarboxylic acid with various derivatives like lactic acid, levulinic acid was one of the simplest process. To synthesize polymeric compounds vanillin is one of the major renewable sources (Figure 5.6). Nowadays most researchers are focused on vanillin for synthesizing polymers (Amarasekara *et al.*, 2012; Thakur *et al.*, 2013a).

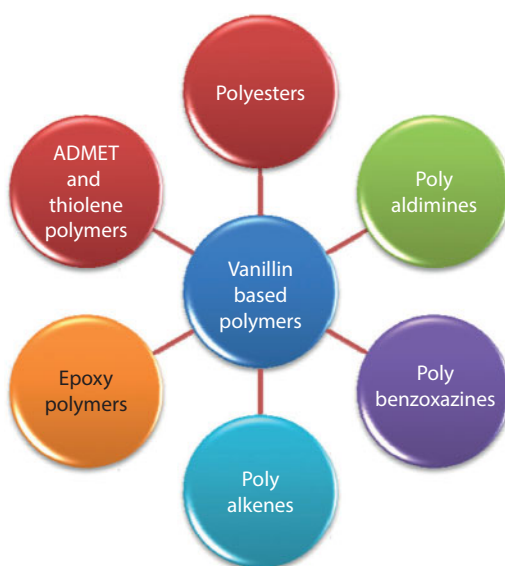


Figure 5.6 Vanillin based polymers.

5.4.1 Poly Acetyl Polymers

Polyoxymethylene (POM) is also known as polyacetal polymers. Vanillin contains two symmetrical biphenyl monomers, so it forms an acetal with 2, 3 butanediol catalyzed by *p*-toluene sulfonic acid in toluene (Figure 5.7). For the synthesis of acetyl polymer vanillin derivatives like di-aldehyde will react with tetraol monomers by the process known as acetalization. It comprises two steps as follows:

- Preparation of di-functional vanillin,
- Di-aldehyde monomers react with tetra functional alcohol to give poly acetyl polymer (Figure 5.8) (Pemba *et al.*, 2014).

5.4.2 Poly Esters Polymers

Poly ester is one of the categories of polymers that contain the functional group of vanillin which is also known as polyethylene terephthalate (PET). Natural polyesters are synthetic and biodegradable, but in the case of synthetic polyesters is not degradable. Poly esters are very important polymers in vanillin derivatives which play a major role of applications in clothing, food packing like, soft drinks and plastic bottles.

One of the most popular bio based synthones is said to be vanillin, which is highly utilized in Perkin reaction for the formation of acrylates. In Perkin reaction authors utilized the acetyl ferulic acid for the reduction mechanisms which was converted to acetyl di-hydro ferulic acid and further condensed to form polyester polymers (Mialon *et al.*, 2010). The mechanism behind this synthesis method is schematically represented in Figure 5.9.

These polyesters were also prepared from vanillic acid which can react with ester from monomers; these monomers will readily react in the presence of phenolic hydroxyls, to form polyesters as illustrated in Figure 5.10 (Long *et al.*, 1981; Thakur *et al.*, 2013b).

For the formation of vanillic acid, two monomers will react with poly esters by coupling reaction mechanisms. Most of the poly esters react with these two monomers like methyl vanillate derivative and methyl chloro acetate derivatives were shown in Figure 5.11 (Pang *et al.*, 2014).

Vanillin based polymers were prepared from vanillin was further acetalized with tri-methyloethane and then catalyzed with di-hydroxyl intermediate which react with oxalyl chloride to form a poly ester. The mechanisms of reaction are clearly illustrated in Figure 5.12 (Kwon *et al.*, 2013; Thakur *et al.*, 2013 c)

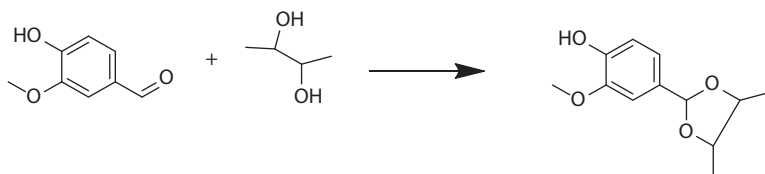


Figure 5.7 Poly acetyl polymer.

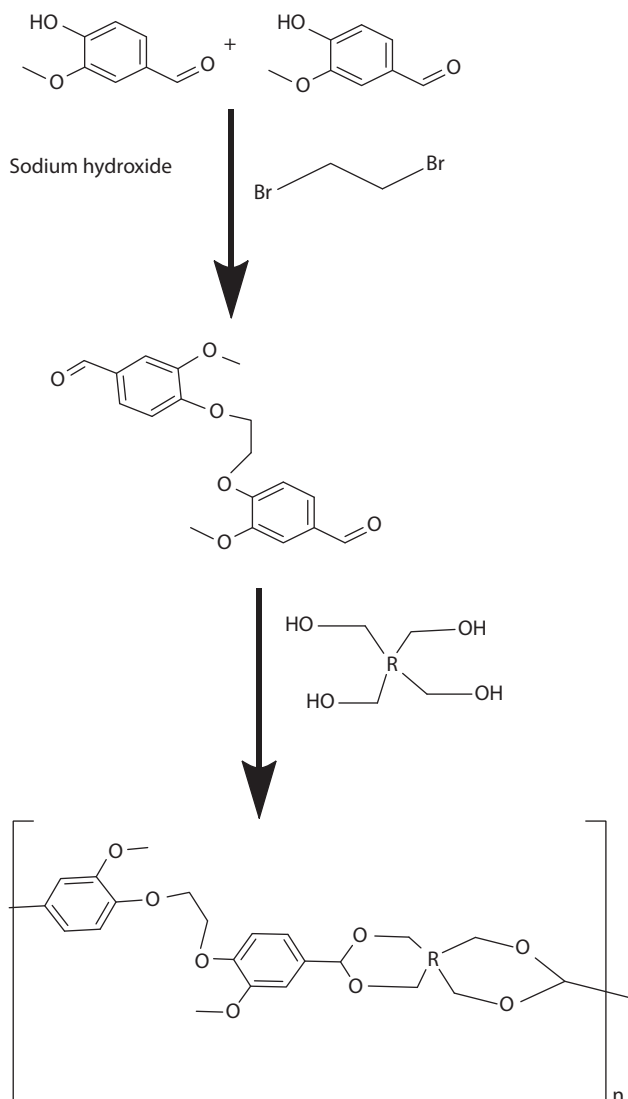


Figure 5.8 Poly acetyl polymer from vanillin derivatives.

5.4.3 Polyaldimines

An aldehyde and an amine that react to form secondary aldimines is known as a Schiff base. This Schiff base can alter by changing aldehyde group which can react with vanillin to form aldimines. This vanillin derivative can also react with chitosan free amino groups for the formation of aldimines in the presence of reducing agent sodium cyanoborohydride, as is clearly illustrated in Figure 5.13 (Jagadish *et al.*, 2012).

Mixture of vanillin and 1, 3-propanediamine will react with metals like Cu(II), Fe(II) and Co(II) to form cross-linked polymers. These types of polymers also called as

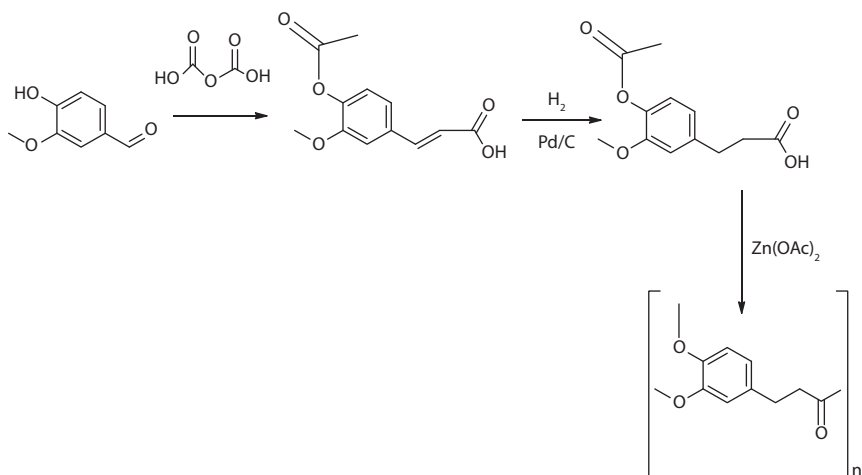


Figure 5.9 Poly ester from acrylates.

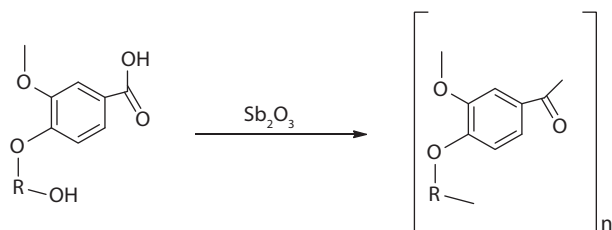


Figure 5.10 Poly ester from esterification.

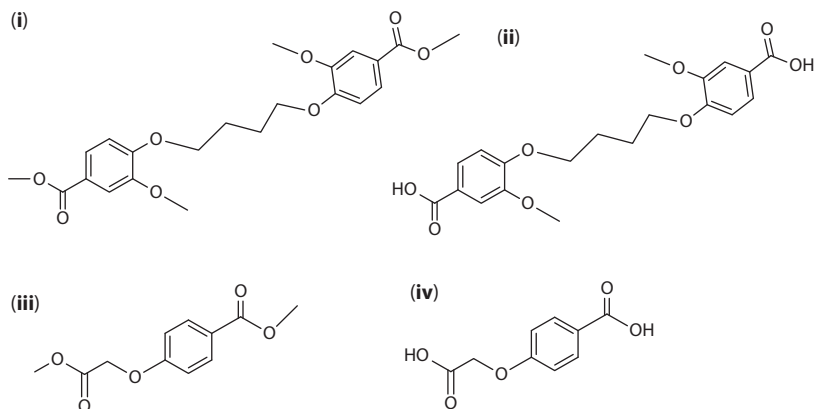


Figure 5.11 Methyl vanillate monomers.

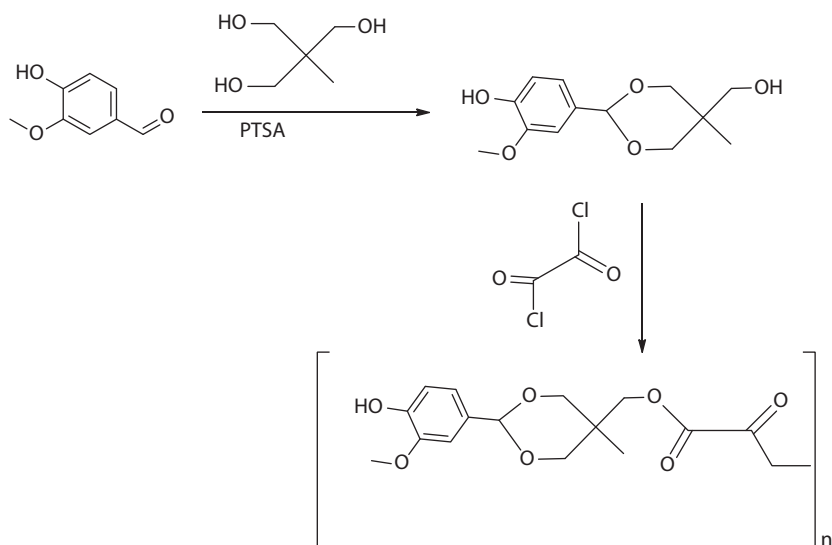


Figure 5.12 Poly ester of vanillin.

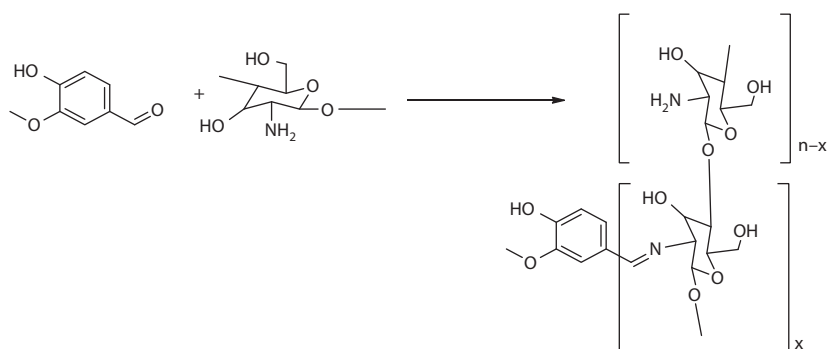


Figure 5.13 Poly aldimes in vanillin.

vanillin Schiff base polymers with various types of monomers like three di-vanillin Schiff base polymer, etc., (Amarasekara *et al.*, 2012).

Most of the natural polymers derived from chitin and chitosan have unfamiliar arrangement of mechanical, physical, chemical and biological properties. In the chemical aspect chitosan, it reacts with different type of aldehydes like 4-hydroxybenzaldehyde, 2-hydroxybenzaldehyde, vanillin, 3-thiophenecarboxaldehyde, and their polymers also form Schiff base polymers (Figure 5.14).

By two-step process vanillin cross-linked chitosan microspheres of PS (Pterostilbene) were prepared. Chitosan and vanillin underwent first step process to form the vanillin cross-linked CS (Chitosan) microspheres. Adding the PS to the above polymers gives rises to PS-loaded polymers (Zhang *et.al.* 2014). This same method is adopted for synthesizing the vanillinimine chitosan polymer loaded with resveratrol-loaded microspheres, shown in Figure 5.15 (Peng *et al.*, 2010; Thakur *et al.*, 2013c).

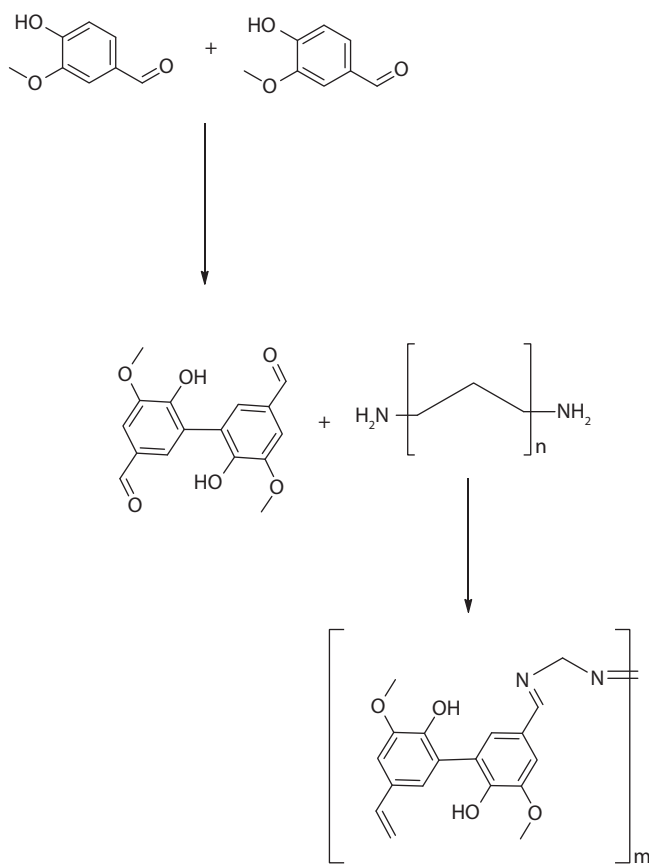


Figure 5.14 Di-vanillin Schiff base polymer.

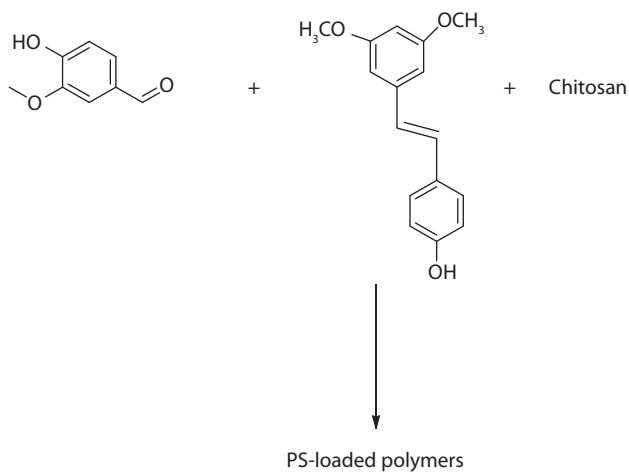


Figure 5.15 Vanillin cross-linked CS polymers.

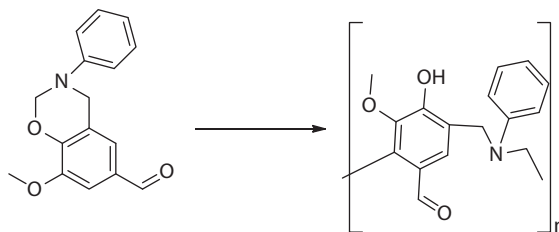


Figure 5.16 Polymer of vanillin-aniline.

5.4.4 Poly Benzoxazines

With the phenolic derivate, primary amine and formaldehyde can be used to synthesis the Poly benzoxazines (Ning & Ishida, 1994). Vanillin reacts with aniline then with paraformaldehyde in the presence of base to form a 8-Methoxy-3-phenyl-3,4-dihydro-2H-benzo[e][1,3]oxazine-6-carbaldehyde, monomers (Figure 5.16). To get polymer product, monomers were condensed with each other, based on this polymer benzoxazine-based surfactant was formed (Peng *et al.*, 2010).

Vanillin is prepared from the bis-benzoxazine monomers and ethylene di-amine, di-phenyl amino ethers, sulphones, methane. Here monomers were formed in Bis-benzoxazine polymers (Sini *et al.*, 2014).

5.4.5 ADMET and Thiol-ene Polymerization (Poly Alkenes)

The three type of polymerization reaction monomers were produced by vanillin and fatty acids. They are thiol-ene addition, poly condensation and ADMET (acyclic diene metathesis). These polymers were performed in following reactants carousel tube, thiols and AIBN which further react with monomers to form thiol-ene polymer.

5.4.5.1 ADMET Polymers

- One of the best reported methods for vanillin derived polymers were ADMET polymerization method. Ferulic acid can act as a precursor for the formation of vanillin derivatives which contains α , β -dienes resulting from oleic and erucic acid. It forms ADMET polymerization polymers with high potential applications.
- ADMET polymerization methods are a step-growth polymerization method, which was derived from condensate release.
- In this polymerization technique α , β -dienes, reacted to give linear polymers in a well-defined manner. These polymers are backbones of polyethylene.
- The mechanism of these polymerization cycles shows organization of an alkene bond to a transition metal alkylidene to form intermediate of metallacyclobutane
- It produces complex of alkylidene in active form, reacting with the monomers to form metallacyclobutane ring. The cycle reacts diene or coordination polymers to give ethylene by productive cleavage.
- ADMET is very easy approach to prepare polymers in highly improved activity and functional groups (Mutlu *et al.*, 2011).

- By using 1, 4 benzoquinone monomers ADMET polymers is synthesized poly condensation
- By combination or condensation of the thio-ene and ADMET polymers poly condensation was synthesized Figure 5.17 (Firdaus *et al.*, 2013).

5.4.6 Epoxy Polymers

Epoxy polymers can be produced by step or chain polymerization or by both mechanisms. Epoxy polymers prepared from epoxy monomers were synthesized using furans (Cho *et al.*, 2012; Hu *et al.*, 2014), 4-hydroxybenzoic acid (Fourcade *et al.*, 2013), cinnamic acid (Xin *et al.*, 2014), catechin (Nouailhas *et al.*, 2011), gallic acid (Aouf *et al.*, 2012), vanillic acid (Aouf *et al.*, 2013), eugenol (Qin *et al.*, 2014) and vanillin (Koike *et al.*, 2012; Pion *et al.*, 2013; Mohammed *et al.*, 2012; Bjorsvik *et al.*, 1999; Thakur *et al.*, 2012a).

5.4.7 Tri-Ethyl-Benzyl-Ammonium Chloride (TEBAC)

TEBAC polymers were prepared by two steps, first by removing phenolate ions from the organic solution. In another step epichlorohydrin was reacted with phenolate ions. These two mechanisms are like SN_2 and ring opening reactions. In ring opening reaction intermediate is chlorinated and the SN_2 mechanism to produce glycidylated product. In a chlorinated intermediate was reacting with phase transfer catalyst and NaOH aqueous solution. By the combine reaction of Tri-phenyl-butyl-phosphonium bromide, methoxyhydroquinone, Iso-PhoroneDi-Amine (IPDA), sodium hydroxide give rises to epoxy monomers. Vanillin derivatives are also can act as di-epoxy monomers (Figure 5.18). These monomers are used to from epoxy thermosets, resins (Fache *et al.*, 2015; Thakur *et al.*, 2012 b).

5.5 Vanillin-Based Composites

Organic-inorganic joined materials are most useful in polymer composites synthesis (Thakur & Thakur, 2014a, b). Composites are one of the important materials that

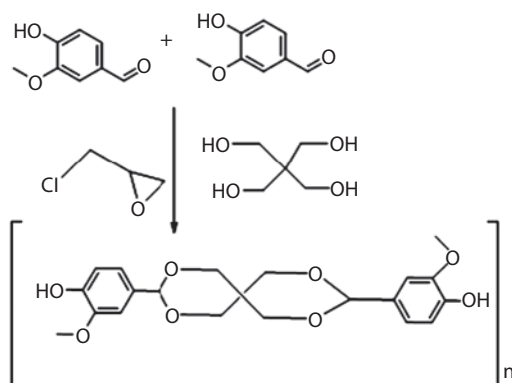


Figure 5.17 Thio-ene addition polymers.

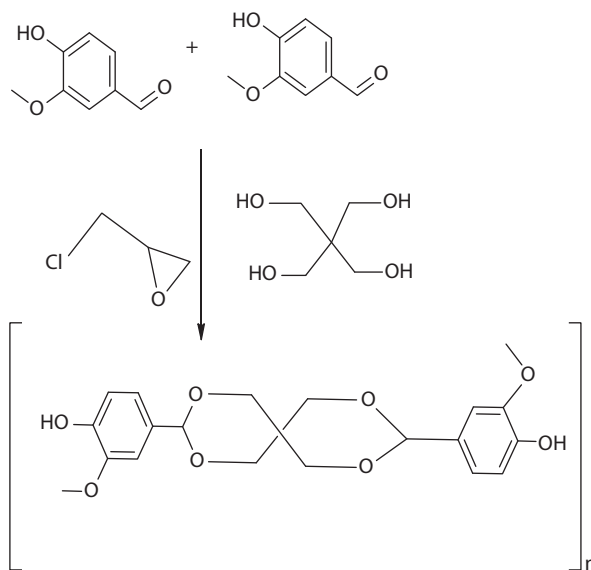


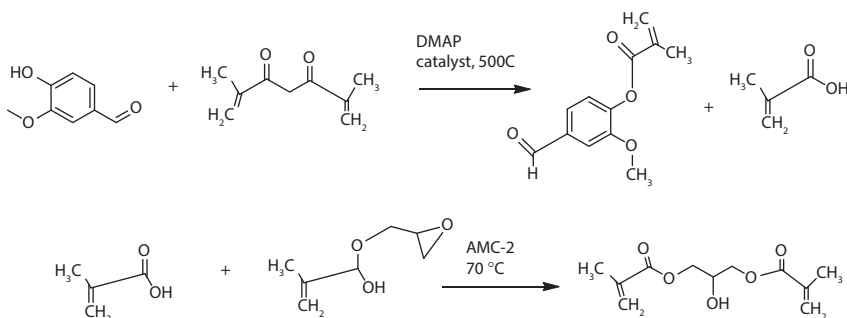
Figure 5.18 Epoxy polymers.

contain new properties and manipulating exclusive synergism between organic and inorganic consistent (Thakur & Kessler, 2015; Thakur & Thakur, 2015). Vanillin is a naturally occurring phenolic polymer, and is sustainable and valuable chemical feedstock. It has renewable materials like eugenol, guaiacol as bio-phenols (Low *et al.*, 1999). It reacts with paraformaldehyde and POSS (polyhedral oligomeric silsesquioxanes) to polibenzoxazine nano composites. These composites have superior properties to any other composites that were studied and reported. For renewable resources POSS-Pbz nanocomposites act as a package of microelectronics with high potency due to their thermal stability and dielectric properties with stability temperature (Periyasamy *et al.*, 2015).

Composites based films were produced by chitosan and vanillin. The vanillin and chitosan were prepared for different mole ratios to form composite films. The color of the film is yellow. SEM and TEM morphology shows that films are combined with emulsifiers or without emulsifiers. Composites also synthesized from PVA (poly vinyl alcohol), cellulose material from bacteria and vanillin. Film was synthesized using dilution of water with PVA and along adding vanillin in different concentration. The film consists of three layers, two outer layers and one inner layer. The inner layer consists of vanillin. Compared to the two outer most layer inner layers are very important ones (Stroescu *et al.*, 2015).

Epoxy compounds have probable high uses as composites and epoxy resins and are said to be bio-based aromatic ethers of diglycidyl. Certainly, both morphologies are similar to the recently studied petro-based epoxy monomers and also experienced as bisphenol replacements in terms of security and measurable performances (Fache *et al.*, 2014).

Petroleum-based vinyl ester resins were recycled to synthesis polymer composites. Vanillin has been utilized as a bio-based source in vinyl ester resins. Having an aromatic character, vanillin is also an essential aromatic compound which is used in flavor and fragrance companies. Vanillin has probable bio-based reactants, methacrylic anhydride



Scheme 5.1 Synthesis of methacrylated vanillin-glyceroldimethacrylate polymer.

and glycidyl methacrylate used to prepare nano composites. Vanillin-based vinyl ester resin useful for the commercially prepared polymer composites. This reaction has two steps: one is the vinyl ester resin taken 1:1 mole ratio, to form monomers and then synthesized monomers were react with a cross-linking agent glyceroldimethacrylate. Finally methacrylated vanillin-glyceroldimethacrylate (MVGDM) polymers (Scheme 5.1) were formed (Stanzione *et al.*, 2012; Thakur *et al.*, 2014 b).

Electrochemical behavior of vanillin containing acetylene black paste electrode improved with graphene-polyvinylpyrrolidone composite film. This polyvinylpyrrolidone can be useful to excellent to confirm that the graphene was dispersed uniformly with stability in nature, further it was spread in water to improve the stability of electrochemical reaction. Instead of allowing electron transfer directly from vanillin, acetylene black was reacted to amplify vanillin signal. Conventional carbon paste electrodes have poor signal compared to the signal for vanillin at the modified electrode, which has significantly better quality. The preparation conditions for the sensor, suitable operating conditions, calibration curve, detection limit and selectivity in vanillin detection are useful in electrochemical process. In the best conditions, vanillin based electrochemical behavior method to detect the lower range calibration method. It is the one of the best methods to easily prepare electrode, saving time and lowering cost. The graphene-polyvinylpyrrolidone nanocomposite was easily prepared through vanillin based composites. These composites are applied in various types of highly sensitive and stable electrochemical sensors (Deng *et al.*, 2015).

5.6 Applications of Vanillin-Based Polymers and Composites

Vanillin helps to construction of a bio-based compounds operating in the field of polymer. The non-existence of bio-based aromatic monomers essential subjected to identify the level of mechanical thermo properties. Vanillin as the preliminary point of the stage as one of the few mono aromatic bio based compounds. Definitely, vanillin is previously industrially produced by lignin depolymerization. Different oxidation states of three vanillin derivatives were selected as precursors to identify the depolymerization of lignin with several end products. In stabilized chemical formed by carboxylic acid moieties, amine, allyl, cyclic carbonates, alcohol etc., novel bio based epoxy monomers

were useful for PU, NIPU and polyester. The compounds of epoxy-functionalized were tested against bisphenol A-based epoxy resins, which can acts as a better alternative. The amine group contains compounds are non-aliphatic bio based on the hardeners of amine, useful also in epoxy or NIPU materials. The cyclic carbonate-functionalized compounds were having ideal properties of NIPU. Vanillin-derived methoxyhydroquinone products are highly remarkable and useful. Industrialization is possible to syntheses of the methoxyhydroquinone is very impact polymer properties.

Vanillin is derived from the wood and it is non- toxic and a well-known compound, known as building block in chemistry. It is industrially available. Its aromatic structure makes it particularly suitable for high performance thermosetting polymers. Vanillic acid derived polymer is very useful, di-epoxy monomer has very good thermo-setting properties and has high stability in very high temperature so it is used in the industry. It is known as DGEBA (Fache *et al.*, 2014). At 200 °C bis-benzoxazine monomers also have good adhesive strength, so it has potential application in industry (Sini *et al.*, 2014). For the anti-microbial activity vanillin and its composite materials are used because chitosan-vanillin films having good antimicrobial activity against *E.coli*. Due to this phenomenon these type films are used for food and cosmetic industries (Stroescu *et al.*, 2011).

Vanillin derivative is used for microcapsule preparation, in the encapsulation technology presents enormous applications in several industries, such as isolation of solvents, separation of organic compounds, protection of food ingredients, release of perfumes, removal of metal etc. One difficulty faced by perfume industry is to control the fragrances. By adopting the encapsulation process it is control fragrance from beginning to the end (Figure 5.19).

It is also useful for the textile industries, for long lasting fragrance release in the fabric aroma released impregnated with capsules containing perfume. Mainly vanillin films are used for encapsulation process. Micro capsule preparation is also used as vanillin derivative and poly sulfone polymer. Emulsion is a mixture of multiple immiscible fluids. In modest state, it has a two-phase system consisting of a disseminated phase and endless phase, alleviated by a surfactant. A surfactant ideally exists at the interphase of the two phases to reduce the interfacial tension and it helpful to stable

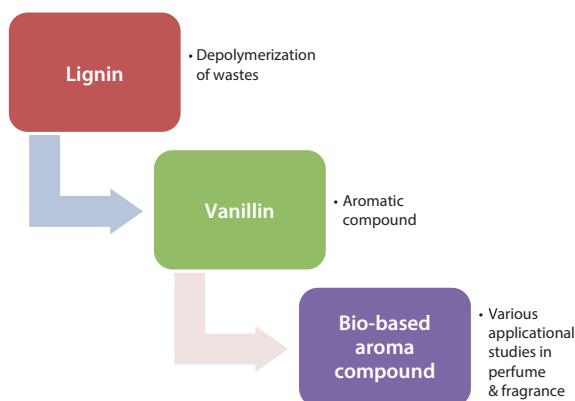


Figure 5.19 Vanillin use in perfume industries.

the regions. Vanillin derivatives used for quasi-stable mini-emulsion in the surfactant for industries. From the environment biopolymers freshly or directly extracted have the ability to produced microorganisms, and can also be prepared by chemical synthesis, vanillin based polymers are very good antioxidant agents. Carbon nanotubes are one of the derivatives of the carbon materials. They possess various mechanical and electro chemical properties, etc. Vanillin composites are used for the synthesis of PVN-MWNT (Multi-wall carbon Nano tubes), and these nanotubes are used for the electrochemical behavior of NO_2 in water samples. And it used for synthesis of various electrodes (Zhang *et al.*, 2014).

PVA (poly vinyl alcohol) coated with vanillin polymers with cyclo-dextrin complex is useful for electro spinning technique. In this complex cyclo-dextrin derivatives are used, for example, alpha cyclo-dextrin, beta cyclo-dextrin, gamma cyclo-dextrin. These three types of vanillin based complexes were used for the PVA nanowebs in electrospun encapsulation. It has higher thermal stability and prolonged shelf life, which is done by vanillin derivatives (Kayaci & Uyar, 2012).

Vanillin has unique aroma, anti-oxidative and anti-microbial property. It also used in production of beverages and medicine. The excessive ingestion of vanillin can cause various health effects. To avoid these effects vanillin coated films are used for the detection of vanillin. In this manner graphene was prepared chemically, it was coated with Au-Pd alloy nano particles electro deposited from graphene film, and then vanillin film also treated with graphene film to from a hybrid film. The prepared Au-Pd-graphene composite film has strong electro catalysis toward the oxidation of vanillin, thus vanillin produces a sensitive anodic peak at the Au-Pd-graphene modified GCE. The electrode also exhibits good stability and reproducibility, and it can be used by vanillin in real samples. Vanillin provides an example for making use of alloy nanoparticles to construct new sensors (Shang *et al.*, 2014; Thakur *et al.*, 2014 b).

Voltammetry determination of vanillin by using poly (Acid Chrome Blue k) modified carbon electrode to identify the catalytic ability of vanillin was studied and resulted in good electro catalytic ability to the oxidation of vanillin (Lou *et al.*, 2012).

Vanillin azo coumarin (VAC) was employed to find the presence of mercury in the brain cell imaging (Guha *et al.*, 2011).

Vanillin is a familiar ingredient in bakery products, like beverages, chocolate, cakes, confectioneries and desserts, etc. It also has various bioactive properties such as anti-clastogenic, anti-mutagenic, and antitumor. Vanillin also used for antimicrobial film. Antimicrobial effects of vanillin are also used for the paperboard of backer materials. In the solution of vanillin mixtures were intended for packing bakery products. It inhibited bacteria like *E. coli*, *S. aureus* and *B. cereus* (Rakchoy *et al.*, 2009).

From the natural source vanilla, vanillin was isolated due to antioxidant and anti-inflammatory properties. Anti-inflammatory is one of the unique properties of vanillin polymeric pro-drug of antioxidant, defined poly (Vanillin oxalate) (PVO). PVO reacts with H_2O_2 to from per-oxalate ester bonds, acid-responsive, acetyl linkages as a backbone. PVO indicated pH-dependent hydrolytic degradation kinetics, and its nanoparticles were able to rummage H_2O_2 . These nanoparticles contain H_2O_2 responsive per oxalate with the backbone of ester bonds. PVO nanoparticles exhibit high antioxidant activities and also having sifting H_2O_2 . It inhibits LPS-stimulated cells from generation of oxidants. PVO nanoparticles show better anti-inflammatory activity by varying the

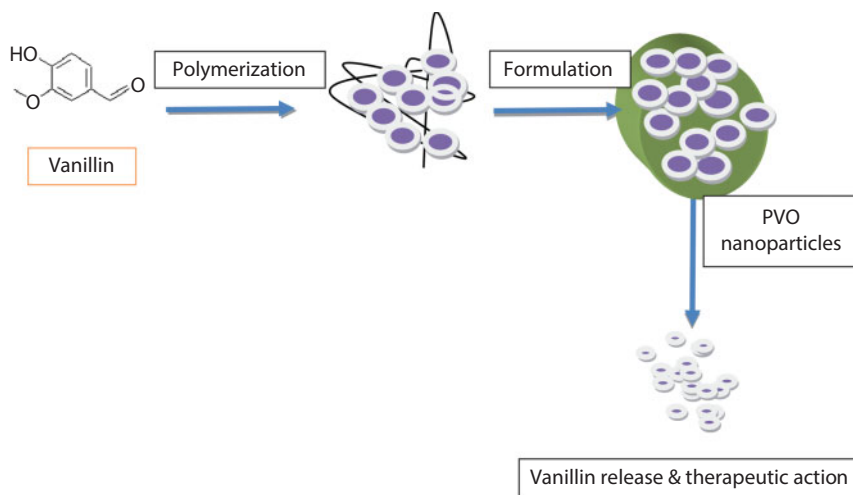


Figure 5.20 Therapeutical formulations of vanillin.

conditions of apoptosis to the communication of $\text{TNF-}\alpha$ and iNOS with addition of intravenously administered PVO nanoparticles expressively concentrated the APAP-induced acute hepatic injury, and also have excellent bio compatibility, anti-oxidant, and anti-inflammatory activity. PVO NPs have revisable oxidative stress for swelling diseases (Figure 5.20). Potential PVO NPs can be utilized to restore tissues undergoing oxidative stress by using a clinically relevant animal model by the various methods of drug delivery systems (Kwon *et al.*, 2013). Vanillin was said to be one of the best chemical intermediates in the pharmaceutical synthesis compared to other fine chemicals. Electrochemical deposition of poly vanillic acid on carbon paste electrode was done for testing the presence of ascorbic acids (AA) and dopamine (DA). It gives as a selective and sensitive detection of DA and AA present exclusively in other species. Poly vanillin is one of main application to determine AA and DA, most useful for the biological and chemical researchers. It also acts as an electrochemical sensor with excellent selectivity and high sensitivity (Manjunatha *et al.*, 2012).

Vanillin and its derivatives are also used for the anti-fungal activity against eighteen different organisms, such as *C. jejuni*, *E. coli*, *L. monocytogenes*, and *S. enterica*, *S. cerevisiae*, *Z. bailii*, *D. hansenii*, and *Z. rouxii*, etc. a number methods to inhibit the prokaryotic and eukaryotic microorganisms, but vanillin and its derivatives like guaiacol, 4-hydroxybenzaldehyde were useful for a reduction of antifungal activity (Fitzgerald *et al.*, 2005).

5.7 Conclusion

This book chapter deals about vanillin and vanillic acid derivatives preparation methods like chemical and biological methods. Chapter also deals about vanillin derived polymers and composites and its types with various applications like biosensor, anti-microbial, anti-fungal, electro chemical application also deals in this chapter. This

chapter facilitates the researchers focusing on polymers for synthesizing non-toxic polymer to the environment by using various production methods.

References

- Amarasekara, A.S., Razzaq, A., Vanillin-based polymers – part II: synthesis of schiff base polymers of divanillin and their chelation with metal ions. *ISRN. Polym. Sci.*, 2012, 1, 2012.
- Ashraf, Z., Rafiq, M., Seo, S.Y., Babar, M.M., Zaidi, N.S.S., Synthesis, kinetic mechanism and docking studies of vanillin derivatives as inhibitors of mushroom tyrosinase. *Bioorganic Med. Chem.*, 23, 5870, 2015.
- Aouf, C., Lecomte, J., Villeneuve, P., Dubreucq, E., Fulcrand, H., Chemoenzymatic functionalization of gallic and vanillic acids: synthesis of bio-based epoxy resins prepolymeres. *Green Chem.* 14, 2328, 2012.
- Aouf, C., Nouailhas, H., Fache, M., Caillol, S., Boutevin, B., Fulcrand, H., Multi-functionalization of gallic acid synthesis of a novel bio-based epoxy resin. *Eur. Polym. J.* 49, 1185, 2013.
- Araujo, J.D.P., Grande, C.A., Rodrigues, A.E., Vanillin production from lignin oxidation in a batch reactor. *Chem. Eng. Res. Des.* 88, 1024, 2010.
- Brazinha, C., Barbosa, D.S., Crespo, J.G., Sustainable recovery of pure natural vanillin from fermentation media in a single pervaporation step. *Green Chem.* 13, 2197, 2011.
- Bjorsvik, H.R., Minisci, F., Synthesis of vanillin by oxidation of lignosulfonates. *Org. Process. Res. Dev.* 3, 330, 1999.
- Cho, J.K., Lee, J.S., Jeong, J., Kim, B., Kim, S., Synthesis of carbohydrate biomass based furanic compounds bearing epoxide end group(s) and evaluation of their feasibility as adhesives. *J. Adhes. Sci. Technol.* 27, 2127, 2012.
- Deng, P., Xu, Z., Zeng, R., Ding, C., Electrochemical behavior and voltammetric determination of vanillin based on an acetylene black paste electrode modified with graphene-polyvinylpyrrolidone composite film. *Food Chem.* 180, 156, 2015.
- Fache, M., Boutevin, B., Caillol, S., Vanillin, a key-intermediate of bio based polymers. *European Poly. J.*, 68, 488, 2015.
- Fache, M., Auvergne, R., Boutevin, B., Caillol, S., New vanillin-derived diepoxy monomers for the synthesis of biobased thermosets. *European. Polym. J.* 67, 527, 2015.
- Fache, M., Darroman, E., Besse, V., Auvergne, R., Caillol, S., Boutevin, B., Vanillin, a promising biobased building-block for monomer synthesis. *Green Chem.* 16, 1987, 2014.
- Firdaus, M., Meier, A.R.M., Renewable co-polymers derived from vanillin and fatty acid derivatives. *European Poly. J.*, 49, 156, 2013.
- Fitzgerald, J.D., Stratford, M., Gasson, M.J., Narbad, A., Structure Function Analysis of the vanillin Molecule and Its Antifungal Properties. *J. Agric. Food Chem.* 53, 1769, 2005.
- Fourcade, D., Ritter, B.S., Walter, P., Schonfeld, R., Mulhaupt, R., Renewable resource-based epoxy resins derived from multifunctional poly(4- hydroxybenzoates). *Green Chem.* 15, 910, 2013.
- Gallage, N.J., Moller, B.L., Vanillin-Bioconversion and Bioengineering of the Most Popular Plant Flavor and Its De Novo Biosynthesis in the Vanilla Orchid. *Mol. Plant.*, 8, 40, 2015.
- Gary, L.M., Andrews, J., Bratz, W., Hanssen, O., Kelley, K., Perry, D., Ridgeway, A., "Preparation of vanillin from eugenol and sawdust". *J. Chem. Edu.* 54, 776, 1977.
- Gobley, N.T., Recherches sur le principe odorant de la vanille. *J. de. Pharma. Et. De. Chimie.* 34, 401, 1858.
- Guha, S., Lohar, S., Haui, I., Subhra, K.M., Das, D., Vanillin-coumarin hybrid molecule as an efficient fluorescent probe for trace level determination of Hg(II) and its application in cell imaging. *Talanta.* 85, 1658, 2011.

- Hu, F., La Scala, J.J., Sadler, J.M., Palmese, G.R., Synthesis and characterization of thermosetting furan-based epoxy systems. *Macromole.* 47, 3332, 2014.
- Jagadish, R.S., Divyashree, K.N., Viswanath, P., Srinivas, P., Raj, B., Preparation of N-vanillyl chitosan and 4-hydroxybenzyl chitosan and their physico-mechanical, optical, barrier, and antimicrobial properties. *Carbohydr. Polym.*, 87, 110, 2012.
- Kaur, B., Chakraborty, D., Biotechnological and molecular approaches for vanillin production: a review. *Appl. Biochem. Biotechnol.* 169, 1353, 2012.
- Kayaci, F., Uyar, T., Encapsulation of vanillin/cyclodextrin inclusion complex in electrospun polyvinyl alcohol (PVA) nanowebs: Prolonged shelf-life and high temperature stability of vanillin. *Food Chem.* 133, 641, 2012.
- Kumar, R., Sharma, P.K., Mishra, P.S., Review on the vanillin derivatives showing various Biological activities. *International. J. Pharma. Tech. Res.*, 4, 266, 2012.
- Kermasha, S., Goetghebeur, M., Dumont, J., "Determination of Phenolic Compound Profiles in Maple Products by High Performance Liquid Chromatography". *J. Agri. Food. Chem.* 43, 708, 1995.
- Koike, T., Progress in development of epoxy resin systems based on wood biomass in Japan. *Polym. Eng. Sci.* 52, 701, 2012.
- Kwon, J., Kim, J., Park, S., Khang, G., Kang, P.M., Lee, D., Inflammation responsive antioxidant nanoparticles based on a polymeric pro drug of vanillin. *Biomacromol.*, 14, 1618, 2013.
- Lawrence J.E., Formanek, K., Kientz, G., Mauger, F., Maureaux, V., Robert, G., Truchet, F., *Vanillin - Encyclopedia of Chemical Technology*. K. Othmer (4thEd), pp. 812–825, 24. New York: John Wiley & Sons, 1997.
- Long, W., Kordsachia, O., Preparation and Properties of available from vanillin and syringaldehyde polyesters. *Wood. Raw. Mater.*, 39, 107, 1981.
- Lou, S., Liu, X., Poly(Acid Chrome Blue K) Modified Glassy Carbon Electrode for the Determination of Vanillin. *Int. J. Electrochem. Sci.*, 2, 138. 6396, 2012.
- Low, H.Y., Ishida, H., Structural effects of phenols on the thermal and thermo oxidative degradation of polybenzoxazines. *Polym.* 40, 4365, 1999.
- Martin, B.H., Vanillin: Synthetic Flavoring from Spent Sulfite Liquor. *J. Chem. Edu.* 74, 1055, 1997.
- Manjunatha, J.G., Kumaraswamy, B.E., Deraman, M., Mamatha, G.P., Simultaneous voltammetric measurement of ascorbic acid and dopamine at poly (vanillin) modified carbon paste electrode: A cyclic voltammetric study. *Der. Pharma. Chemica.*, 4, 2489, 2012.
- Mialon, L., Pemba, A.G., Miller, S.A., Biorenewable polyethylene terephthalate mimics derived from lignin and acetic acid. *Green. Chem.*, 12, 1704, 2010.
- Mohammed, I.A., Hamidi, R.M., Synthesis of new liquid crystalline di-glycidyl ethers. *Molecules.* 17, 645, 2012.
- Mutlu, H., de Espinosa, L.M., Meier, M.A.R., Flavours and Fragrances: Chemistry, Bioprocessing and Sustainability. *Chem. Soc. Rev.*, 40, 1404, 2011.
- Ning, X., Ishida, H., Phenolic materials via ring-opening polymerization-synthesis and characterization of bisphenol-a based benzoxazines and their polymers. *J. Polym. Sci. A. Polym. Chem.* 32, 1121, 1994.
- Nouailhas, H., Aouf, C., Le Guerneve, C., Caillol, S., Boutevin, B., Fulcrand, H., Synthesis and properties of biobased epoxy resins. Part 1: Glycidylation of flavonoids by epichlorohydrin. *J. Polym. Sci. A. Polym. Chem.* 49, 2261, 2011.
- Pang, C., Zhang, J., G., Wang, Y., Gao, H., Ma, J., Renewable polyesters derived from 10-undecenoic acid and vanillic acid with versatile properties. *Polym Chem.*, 5, 2843, 2014.
- Peng, H., Xiong, H., Li, J., Xie, M., Liu, Y., Bai, C., Vanillin cross-linked chitosan microspheres for controlled release of resveratrol. *Food Chem.* 121, 23, 2010.

- Periyasamy, T., Asrafali, S.P., Muthuswamy, S., New benzoxazines containing polyhedral oligomeric silsesquioxane from eugenol, guaiacol and vanillin. *New J. Chem.*, 39, 1691, 2015.
- Pemba, A.G., Rostagno, M., Lee, T.A., Miller, S.A., Cyclic and spirocyclic polyacetal ethers from lignin-based aromatics. *Polym. Chem.*, 5, 3214, 2014.
- Pappu, A., Patil, V., Jain, S., Mahindrakar, A., Haque, R., Thakur, V.K., Advances in industrial prospective of cellulosic macromolecules enriched banana biofibre resources: A review. *International Journal of Biological Macromolecules.*, 79, 449-458, 2015.
- Pion, F., Reano, A.F., Ducrot, P.H., Allais, F., Chemo-enzymatic preparation of new bio-based bis- and trisphenols: new versatile building blocks for polymer chemistry. *RSC Adv.* 3, 8988, 2013.
- Qin, J., Liu, H., Zhang, P., Wolcott, M., Zhang, J., Use of eugenol and rosin as feedstocks for biobased epoxy resins and study of curing and performance properties. *Polym. Int.* 63, 760, 2014.
- Rakchoy, S., Suppakul, P., Jinkarn, T., Antimicrobial effects of vanillin coated solution for coating paperboard intended for packaging bakery products. *As. J. Food Ag-Ind.* 2, 138, 2009.
- Ran, Q.C., Gu, Y., Concerted reactions of aldehyde groups during polymerization of an aldehyde-functional benzoxazine. *J. Polym. Sci. A. Polym. Chem.* 49, 1671, 2011.
- Silva, B.D.E.A., Zabkova, M., Araujo, J.D., Cateto, C.A., Barreiro, M.F., Belgacem, M.N., An integrated process to produce vanillin and lignin based polyurethanes from Kraft lignin. *Chem. Eng. Res. Des.* 87, 1276, 2009.
- Sini, N.K., Bijwe, J., Varma, I.K., Renewable benzoxazine monomer from vanillin: synthesis, characterization, and studies on curing behavior. *J. Polym. Sci. Part. A. Polym. Chem.* 52, 7, 2014.
- Singha, A.S., Thakur, V.K., Physical, chemical and mechanical properties of Hibiscus sabdariffa fiber/polymer composite. *Int. J. Polym. Mater.* 58, 217, 2009a.
- Singha, A.S., Thakur, V.K., Mechanical, thermal and morphological properties of grewia optiva fiber/polymer matrix composites. *Polym.-Plast. Technol. Eng.* 48, 201, 2009b.
- Singha, A.S., Thakur, V.K., *Grewia optiva* Fiber Reinforced Novel, Low Cost Polymer Composites. *J. Chem.* 6, 71, 2009c.
- Singha, A.S., Thakur, V.K., Fabrication and Characterization of H. sabdariffa Fiber-Reinforced Green Polymer Composites. *Polym.-Plast. Technol. Eng.* 48, 482, 2009d.
- Shang, L., Zhao, F., Zeng, B., Sensitive voltammetric determination of vanillin with an AuPd nanoparticles_graphene composite modified electrode. *Food chem.* 151, 53, 2014.
- Stanzione, J.F., Sadler, J.M., La Scala, J.J., Renoc, K.H., Wool, R.P., Vanillin-based resin for use in composite applications. *Green Chem.* 14, 2346, 2012.
- Stroescu, M., Guzun, A.S., Jipa, I.M., Vanillin release from poly (vinyl alcohol)-bacterial cellulose mono and multilayer films. *J. Food. Engg.* 114, 153, 2015.
- Stroescu, M., Guzun, A.S., Isopencu, G., Jinga, S.I., Parvulescu, O., Dobre, T., Vasilescu, M., Chitosan-vanillin composites with antimicrobial properties. *Food Hydro.* 48, 62, 2011.
- Thakur, V.K., Thakur, M.K., Processing and characterization of natural cellulose fibers/thermoset polymer composites. *Carbohydr. Polym.* 109, 102, 2014a.
- Thakur, V.K., Thakur, M.K., Processing and characterization of natural cellulose fibers/thermoset polymer composites. *Carbohydrate Polymers.*, 109, 102, 2014b.
- Thakur, V.K., Thakur, M.K., Prasanth, R., and Michael, R. K., Progress in Green Polymer Composites from Lignin for Multifunctional Applications: A Review. *ACS Sustainable Chem. Eng.*, 2, 1072, 2014a.
- Thakur, V.K., Vennerberg, D., Kessler, M.R., Green Aqueous Surface Modification of Polypropylene for Novel Polymer Nanocomposites. *ACS Appl. Mater.* 6, 9349, 2014b.

- Thakur, M.K., Raju, K. G., Thakur, V.K., Surface modification of cellulose using silane coupling agent. *Carbohydrate Polymers.*, 111, 849, 2014c.
- Thakur, V.K., Thakur, M, K., Raju, K. G., Review: Raw Natural Fiber-Based Polymer Composites. *International Journal of Polymer Analysis and Characterization.*, 13, 8, 2014d.
- Thakur, V.K., Thakur, M.K., Gupta, R.K., Graft copolymers of natural fibers for green composites. *Carbohydrate Polymers.*, 104, 87, 2014e.
- Thakur, V.K., Thakur, M, K., Raju, K. G., Rapid synthesis of graft copolymers from natural cellulose fibers. *Carbohydrate Polymers* 98, 820, 2013a.
- Thakur, V.K., Thakur, M.K., Gupta, R.K., Development of functionalized cellulosic biopolymers by graft copolymerization. *International Journal of Biological Macromolecules.*, 62, 44, 2013b.
- Thakur, V.K., Thakur, M.K., Gupta, R.K., Synthesis of lignocellulosic polymer with improved chemical resistance through free radical polymerization. *International Journal of Biological Macromolecules.*, 61, 121, 2013c.
- Thakur, V.K., Singha, A.S., Thakur, M.K., Graft Copolymerization of Methyl Acrylate onto Cellulosic Biofibers: Synthesis, Characterization and Applications. *J. Polym. Environ.*, 20, 164, 2012a.
- Thakur, V.K., Singha, A.S., Thakur, M.K., In-Air Graft Copolymerization of Ethyl Acrylate onto Natural Cellulosic Polymers. *International Journal of Polymer Analysis and Characterization.*, 17, 1, 2012b.
- Van, A., Chiou, K., Ishida, H., Use of renewable resource vanillin for the preparation of benzoxazine resin and reactive monomeric surfactant containing oxazine ring. *Polym.* 55, 1443, 2014.
- Voitl, T., Rohr R.V.P., Oxidation of lignin using aqueous polyoxometalates in the presence of alcohols. *Chem. Sus. Chem.* 1, 763, 2008.
- Xin, J., Zhang, P., Huang, K., Zhang, J., Study of green epoxy resins derived from renewable cinnamic acid and dipentene: synthesis, curing and properties. *RSC Adv.* 4, 8525, 2014.
- Zhang, Y., Shi, X., Yu, Y., Zhao, S., Song, H., Chen, A., Shang, Z., Preparation and characterization of vanillin Cross-linked Chitosan Microspheres of Pterostilbene. *Interntional J. Polym. Anal. Charact.*, 19, 83, 2014.

Biomass-Based Formaldehyde-Free Bio-Resin for Wood Panel Process

Xiaobin Zhao

Cambond Limited, Cambridge, UK

Abstract

Bio-based composites have been widely used in green industry. Wood composites are vital components in the construction and furniture industry. They are made from bonding wood particles with synthetic adhesives such as urea/phenol/formaldehyde resins. There is a need for 'greener' sustainable, formaldehyde-free adhesives. Given the volume of adhesives used by industry (globally >25 million tonnes) the feedstock for the adhesives needs to be scalable and sustainable. Using renewable biomaterials to replace all or part of oil-based adhesives is reviewed in this chapter. In addition to the current development in this field, a new process that uses biomass from various sources to make formaldehyde-free adhesives has been developed. These 'green' resins can be alternatives to the existing urea-formaldehyde based synthetic resins for wood panel production.

Keywords: Wood composites, biomass based products, biomass based adhesives, bio-adhesives, green glue, wood panel

6.1 Introduction

6.1.1 Wood Composite

Bio-based composites have been widely used for making green bio-composites (Thakur *et al.*, 2014a-e). Wood is the most abundant renewable biomaterial in the world. Wood composites, such as fiberboard, plywood and particleboard, are vital components in the construction industry and in furniture manufacture. In 2013, global wood-based panel production surged to a new record high of 358 million cubic metres — up 7.8% from 2012 and 35% from 2009. Wood-based panels were the only product category that did not contract during the recent recession and their production has been growing steadily. This is due to rapid and consistent growth in the Asia-Pacific and Latin America and Caribbean regions, where production has increased by 59% and 23% respectively over the period 2009–2013 (FAO, 2015). In 2014, the production of wood composites was estimated about 76.8 million M³ and the value of the wood composites

Corresponding author: xzhao@cambond.co.uk

Vijay Kumar Thakur, Manju Kumari Thakur and Michael R. Kessler (eds.), Handbook of Composites from Renewable Materials, (129–150) © 2017 Scrivener Publishing LLC

worth about 22 billion euros in Europe (FAO, 2015). At present, petrochemical-based adhesives such as formaldehyde-based adhesives are predominantly used for production of wood composite panels and other bio-based composites (Singha & Thakur, 2009a–c; Wu *et al.*, 2016). Common formaldehyde-based resins are urea formaldehyde, melamine-formaldehyde and phenol-formaldehyde while other phenolic compounds (e.g. resorcinol) can also react with formaldehyde to provide polymers of the same type with differences in adhesive cost and reactivity (Singha & Thakur, 2010a–e). Wood-based panels, like particleboards (PB), fibreboards (e.g., medium density fibreboard-MDF), oriented strand boards (OSB), plywood (PW) etc., are produced by adhering together parts of wood in various sizes with these resins under heat and pressure. However, the oil-based wood adhesives are not sustainable in the long run. In addition, the emission of carcinogenic formaldehyde in the production and use of wood composite panels bonded with the UF resins has been a big concern in recent years. As a result, the California Air Resources Board (CARB) passed a regulation on limiting formaldehyde emission from wood-based products used and sold in California in April 2007. A national regulation of limiting formaldehyde emission, “formaldehyde standards for composite wood products act,” was signed into law on July 7, 2010. There is a trend to tighten the limit of formaldehyde emissions from wood panels in Europe and China (Cambridge CVP, 2015) and an urgent need for development of a formaldehyde-free wood adhesive from renewable materials (Grand View Research, 2015). In particular, given the volume of adhesives used by the wood panel industry (globally >25 million tonnes per year) the feedstock for the adhesives needs to be sustainable and ideally biodegradable (Von Dungen, 2014, Parker, 2014).

6.1.2 Biomass-Based Adhesives

Biomass-based adhesives (bio-based adhesives) are direct derivatives from renewable biomaterials and are predicted to be an area of growth within the bioproducts industry. There are a number of drivers to encourage both the adhesives and wood composites manufacturers to switch to bio-based adhesives:

- Reduce the generation of hazardous waste
- Lower chemical emissions and reduce waste disposal
- Lower insurance costs as a result of reduced risk
- Make savings on systems required for emissions control and reduction, release agents, or reduce the need for other processing
- Reserve oil and use less oil-based products and make economic development sustainable

6.2 Market Analysis of Biomass Based Adhesives

The global demand for adhesives and sealants has experienced different growth patterns since recovering from the last major recession 2008–2009. The volume of the global market reached more than 13 million tonnes and a value of € 34 bn (manufacturers’ level) in 2013 (Park, 2014).

The Europe-Middle East-Africa (EMEA) and the Asia-Pacific & Oceania regions generated the largest adhesives and sealants demand volumes in 2013. With equal shares of 35% they controlled 70% of the global market while the Americas maintained a share of 30%. The Americas suffered a longer recession (2007–2009) and maintained moderate growth after recovery (2–3% annually) (Association of the European Adhesive & Sealant Industry, 2014).

The history of adhesives is long. The early adhesives were bio-based using blood, collagen and starch. Later came the use of plant proteins in adhesives (Onusseit, 1993, Lambuth, 2003, Pöyry Management Consulting, 2010). These adhesives were very good when kept in dry conditions but when exposed to water, the durability decreased significantly. This problem was partially solved by heat curing of blood and casein adhesives (Vijayendran, 2010). In the beginning of the 20th century formaldehyde adhesives were developed; these adhesives had very good durability and could be used outdoors. The lack of durability of the bio-based adhesives made them fall behind. In recent years, however, the world has been made more aware of the environmental aspect of the synthetic adhesives. The raw materials used in the synthesis of these polymers are far from renewable and are often derived from natural oil or gas. Another aspect that has fuelled the research on renewable adhesives is that some of the raw material may be dangerous for humans and the environment – formaldehyde is considered as a priority pollutant. Carbohydrates can also be used in renewable adhesives. They are most often found in nature in the form of polysaccharides and are abundant in many plants. The low price of polysaccharides is due to their abundance as three-fourths of the dry weight of plants consists of this kind of carbohydrate. The idea of using renewable polymers in adhesives is beneficial to both industry and nature. By using renewable adhesives, the industry can be guaranteed of the supply of raw material and the environmental impact of producing and using these adhesives will decrease significantly.

According to a market research report (Global Information, 2015), the market for biobased adhesives is projected to reach \$1.24 billion by 2017, with predicted annual growth rates between 2010 and 2020 of 2.7% per annum. There is a higher market share in industries with tight regulation and largest volume use, such as packaging, construction, woodworking, transportation, shoe making, and paper products.

At present the majority of biobased adhesives are derived from starch (65% of all bio-based adhesives). The rest may come from plant oils (polyols, epoxies, polyamides and polyisoprene); lignins; tannins or proteins. Starch-based adhesives can be used in hot-melt or waterborne dispersions. Polyols are primarily used in polyurethane adhesives and sealants; and modified waxes are used as plasticizers in hot-melt (Wang, 2006).

It has been predicted that 15% of the \$3 trillion global chemical sales will be derived from biobased materials by 2025 (Imam, *et al.*, 2001, Gua, 2010)

6.3 Bio-Based Adhesive Formulations

Various natural resources including animal glues, fish glues, casein and vegetable protein glues, and blood albumen glues have been used for the wood industry. Several new technologies have been investigated to explore the adhesive potential of various

biomaterials, including tannins, lignins, carbohydrates, unsaturated oils, liquefied wood rice bran, soy protein and organisms (Danielson, 1998, Mansouri *et al.*, 2007, Kim, 2009). Soy protein isolates (SPI) gained much attention over the last century as bio-based and renewable materials. Much research has been conducted on the use of soy proteins as adhesives in the past 10 years (Huang & Li, 2008, Li *et al.*, 2004), with most of this work focused on improving water resistance through increasing the hydrophobicity of soy proteins via chemical modification (Liu & Li, 2002). Markets for soy protein products include applications in interior and exterior wood composite panels and new or emerging uses.

6.3.1 Starch-Based Adhesive

There have been many studies conducted on renewable adhesives using different types of starch. One example of a starch-based adhesive is a formulation based on starch and PVA. A cross-linking agent, hexamethoxymethylmelamine, was added to the formulation as well. In addition to PVA, a synthetic latex was added to the formulation which improved the moisture resistance. The solid content of the formulation was 27%. The samples were stored in an atmosphere of 93% relative humidity and tests showed that the de-bonding that occurred depended on failure in wood rather than failure of the adhesive joint (Imam *et al.*, 2001). Another example of starch-based adhesives is a formulation that combines starch and polymeric isocyanate. The solid content that gave rise to the best results was 50% and the viscosity was 200–300 mPas at 23 °C. The addition of polymeric isocyanates improved the water resistance of the adhesive when compared with the starch adhesive without polymeric isocyanates (Gua *et al.*, 2010).

6.3.2 Lignin

Lignin is one of the most abundant, renewable natural products on earth and technical lignins are produced in tremendous quantities every year as a by-product of the pulping process (Thakur & Thakur, 2014a, b). Extensive work has been conducted to include organosolv lignins and other lignins with their polymeric structure of phenolic units in PF resins (Danielson, 1998). Lignin-based wood adhesives have been prepared without formaldehyde substituted by non-volatile non-toxic aldehyde, namely glyoxal. The adhesives have been tested for application to wood panels such as particleboard. The adhesives yielded good IB strength and the panels comfortably pass the relevant international standard specifications for exterior-grade panels. The adhesives also showed sufficient reactivity to yield panels in press times comparable to those of formaldehyde-based commercial adhesives (Mansouri *et al.*, 2007). Particleboard without synthetic adhesive is the lignocellulosic-based panel where the lignocellulosic materials are bonded together without using synthetic adhesives (Anglès *et al.*, 2001). Processing parameters of making particleboard without synthetic adhesive, including appropriate hot pressing conditions and the type of lignocellulosic material, are able to trigger the reaction of the chemical constituents contained in the lignocellulosic itself, which together with the fibre cross-linking, to achieve the self bonding between particles (Hashim *et al.*, 2011; Pappu *et al.*, 2015).

6.3.3 Tannin

Tannin is an excellent renewable resource that can be used for replacing petroleum-derived phenolic compounds. The major species from which it can be obtained are Mimosa, Quebracho and Radiata Pine. It is mainly concentrated in the inner layer of the bark and has been used in the adhesive industry in Africa, South America and Oceania to obtain the low formaldehyde emission levels required for environmental-friendly adhesives. In the last decade several approaches to the problem of producing low formaldehyde emission wood panels using these wood adhesives have been developed. Moreover, hardeners cause formaldehyde emission even when tannin adhesives are used (Kim, 2009).

6.3.4 Soya Protein-Based Wood Adhesives

Since the 1930s, soybeans were widely used as wood adhesives, but the synthetic petroleum-based resins quickly replaced the soy-based adhesives after the 1960s (Liu & Li, 2004). In recent years, the emerging environmental and sustainability agendas have revived interest in these adhesives. Soybean is abundant, renewable and readily available (Thakur & Kessler, 2014a,b). Several soy-based adhesives have been developed in recent years (Liu & Li, 2006, Li *et al.*, 2004, Sun & Bian, 1999, Zhong *et al.*, 2003). While soy-based adhesives have many advantages such as easy handling and low press temperatures, the adhesives have low bonding strength and low water resistance (Hettiarachchy *et al.*, 1995, Zhang & Hua, 2007). Therefore modification of soy protein and its derivatives is required (Thakur *et al.*, 2016; Thakur *et al.*, 2014 d,e). Modifications of soy protein structures can be obtained by physical, chemical, and enzymatic treatments. One of the methods used to alter the protein structures is denaturation and disulfide bond cleavage of soy proteins through exposure to heat, acid/alkali, urea (Huang & Sun, 2000a), guanidine hydrochloride (GuHCL) (Zhong *et al.*, 2002), and sodium dodecyl sulfate (SDS) etc (Huang & Sun, 2000b). It was reported that soy proteins modified by alkali and trypsin resulted in improved bond strength and water resistance of adhesives compared to unmodified soy proteins (Hettiarachchy *et al.*, 1995). In alkali treatment, dispersion and unfolding of the protein structures are enhanced, which leads to better interaction of soy proteins with woody materials. The effects of soy proteins modified by surfactant such as sodium dodecyl sulfate (SDS) and sodium dodecylbenzene sulfonate (SDBS) on adhesive properties have been investigated (Huang & Sun, 2000b). This research showed that both SDS and SDBS-modified SPI adhesives had greater shear strength and water resistance than unmodified adhesives, specifically at 0.5 and 1% concentrations (Huang & Sun, 2000b). All these results were obtained from small pieces of veneer laminates in the laboratory and have not been consistently confirmed in a commercial plywood production where big multi-ply plywood panels are produced in several minutes.

The performance of soy-based adhesives can be improved by introducing cross-linking agents that form covalent linkages between polar functional groups such as amino groups and carboxylic acid groups of amino acid residues in soy proteins (Miller & Gerrard 2005, Wong, 1991). The cross-linking agents that are widely used for enhancing the adhesive performance contain epoxides, and aldehydes (Bjorksten,

1951, Lambuth, 1951). It was demonstrated that the soy proteins modified with aliphatic epoxides, which were used as cross-linking agents in protein-based adhesives, enhanced adhesive performance. Epoxidized soybean oil (ESO) and 1,2,7,8-diepoxyoctane as cross-linking agents were reported to prepare modified soy protein isolate (SPI) adhesives to obtain an improved water resistance (Sun *et al.*, 2008). Aldehydes can react with amino groups in soy proteins. Formaldehyde is known as a common and very strong cross-linking agent for soy-based adhesives. Formaldehyde provides improved water resistance and bonding strength (Ghorpasde *et al.*, 1995, Ly *et al.*, 1998, Park *et al.*, 2000, Wang *et al.*, 2007). Presently, one of the soy-based adhesive systems has been successfully used in the wood composites industry, especially for the manufacturing of interior plywood since 2004 (Liu & Li 2002, Liu & Li, 2004, Li *et al.*, 2004, Liu & Li, 2007, Huang & Li, 2008).

6.3.5 Biomimetic Adhesives

In recent years, researchers have been particularly fascinated by biotechnology, nanotechnology, biomimetics and nanofabrication (Lin *et al.*, 2011a,b) (Thakur *et al.*, 2012a,b). During those pursuits, humankind learned that wet adhesion contributes to the phenomenon of a mussel's ability to cling to wet surfaces (Bitton *et al.*, 2007, Waite, 2008). Mussel proteins, also called marine adhesive proteins (MAPs), mainly consist of 3,4-dihydroxyphenylalanine (DOPA), lysine, glycine, and serine or threonine. MAPs are known as strong and water-resistant adhesives, which have been introduced as functional groups of MAPs onto soy proteins (Liu & Li, 2002, Liu & Li, 2004) (Thakur *et al.*, 2014f, g). It was found that the modification of the soy proteins with a DOPA group and free mercapto (-SH) provided increased strength and water resistance to their adhesives for wood. Kymene® 557H, a commercial wet strength agent for paper, was used as a curing agent in a new soy-adhesive system. The SPI-Kymene adhesives presented very similar properties to phenol-formaldehyde (PF) resins, which were feasible to be used for exterior purposes (Li *et al.*, 2004). However, the new adhesive system was as yet impractical for mass production because SPI is too expensive as a raw material for wood adhesives. Soy flour is a much less expensive soybean product. Soy flour-Kymene adhesive has been commercialized for production of plywood since 2004 (Li & Liu 2007).

6.3.6 Liquefied Woody Biomass

Development of thermosetting resins from renewable raw materials has been used for partial replacement of phenol in phenol-formaldehyde resins. The thermochemical liquefaction technology, which was developed in the 1970s in Japan, applied successfully to the liquefaction of wood in the presence of phenols or alcohols with or without acidic catalysts, including sulfuric acid, phosphoric acid and so forth. The resulted liquid wood, commonly known as "liquefied or phenolated wood," has been proved effective raw material in the synthesis of phenol-formaldehyde resins. Despite the promising results of this technique, it has not found a broad application as the use of phenol as a liquefying reagent is associated with a number of drawbacks, including the difficulty

of recovering the phenol from the liquefied materials and the problem of toxicity (Lee *et al.*, 2002, Alma & Bastiirk, 2001).

6.3.7 Chicken Feather

Feather protein-based resins, which contained one part feather protein and two parts phenol, were formulated under the conditions of two feather protein hydrolysis methods (with and without presence of phenol during hydrolysis), two formaldehyde/phenol molar ratios (1.8 and 2.0), and three pH levels (9.5, 10.5, and 11.5). Southern pine fiberboard bonded with feather protein-based resins were fabricated and bending strength, bending stiffness, internal bonding strength, and percent thickness swell were evaluated. Results indicated that the test parameters all significantly affected resin quality. The resin formulated with feather protein hydrolyzed in the presence of phenol, using a F/P ratio of 2.0, and at a pH of 10.5 performed as well as the neat PF resin. Based on our findings, feather protein is a potential cost-effective material for the production of PF-type adhesive resins. Developing eco-materials from this waste source has caught the attention of the shoe manufacturers such as Nike (Jiang *et al.*, 2008).

6.3.8 Natural Fiber Modified with Adhesive Functions

In recent years, interest in using natural fibers in a number of applications, especially in biocomposites, has grown because they are eco-friendly, lightweight, combustible, non-toxic, low cost and easy to recycle. However, the lack of good interfacial adhesion and poor resistance to moisture absorption and chemicals make the use of natural fibers less attractive. Chemical treatment of the lignocellulosic fiber can stop the moisture absorption process, clean the fiber surface, chemically modify the surface or increase the surface roughness. The introducing of the silane-adhesive functionality to the surface of natural fibers is a promising process for improving physical and chemical properties of fibers (Singha & Thakur 2009, Singha *et al.*, 2009).

6.4 Cambond Biomass Based Adhesives

6.4.1 Distiller's Dry Grain and Solubles (DDGS) as the Biomass

In recent years, there have been concerted global efforts to develop biofuels and bio-renewable chemicals. Bioethanol and biodiesel from fatty acid methyl esters account for the vast majority of global biofuel production and use today, both of which are primarily made from agricultural commodities, e.g., grain, sugar cane/beet molasses, cassava, whey, potato and food/beverage waste for bioethanol production; vegetable oil for biodiesel production. In 2010, an estimated 142.5 million tonnes of grain was used globally for bioethanol production, representing 6.3% of global grain use (Licht, 2011). The by-product resulting from bioethanol fermentation process is known as "oil extracted" Distiller's Dry Grain and Solubles (DDGS) or "de-oiled" DDGS. These co-products typically have lower fat content than conventional DDGS, but slightly higher

concentrations of protein and other nutrients, hence they are mainly used as animal feed, which deliver limited commercial value.

6.4.2 Algal Biomass

Algae are a diverse group of eukaryotic photosynthetic organisms that constitute over 40,000 species. They can be single-celled (unicellular) or multicellular, such as seaweed. Microalgae have been described as nature's very own power cells and could provide alternatives to petroleum-based fuels without competing with crops. Algae can harvest the power of the sun through photosynthesis and convert this into biomass. Algal biomass is another type of material that is high in lipids, proteins, and carbohydrates that can be processed into fuels or other valuable co-products through chemical, biochemical, or thermochemical means (Zhao, 2010, BBSRC, 2014a). Algae have the added benefit of not competing for land and water with traditional food crops, as they can be grown on marginal lands and utilise brackish or waste water. Recently algae have attracted considerable interest globally as a potential feedstock for a bio-based economy. The industrial and research communities in the UK have much to offer in this space and UK companies and academics have laid the foundations for several now globally-used algal biotechnology and engineering advances (BBSRC, 2014b).

6.4.2.1 Macroalgae

Globally, macroalgae are both collected from the wild (e.g., in the UK, Ireland, Norway, the US and Chile) and cultivated (esp. in China, Indonesia and the Philippines), predominantly for food, feed, fertilisers, chemicals and cosmetics. In the UK, macroalgae are a traditional crop. They have been wild-harvested and used for food, feed and as fertilizer in coastal communities for centuries. Microalgae can be grown in large bioreactors and continually harvested unlike crops or macroalgae. They could be grown using the waste CO₂ from industrial processes, power stations or waste treatment plants. The oil they produce can then be converted into liquid fuel such as biodiesel. The ability of microalgae to capture industrial CO₂ emissions as their source of carbon for growth and be cultivated on non-agricultural land or in the sea reducing their competition with food crops for land, makes them an attractive proposition both economically and sustainably. Unfortunately, the culture of algae on a large commercial scale (mainly as biomass aquaculture for specialised products such as natural food colourants, omega-3 oils and antioxidants) has so far been restricted to sunny climates, and mainly to those species that are tolerant to extreme environments such as high light or saline conditions. A core of commercial activity is hence well established: Companies such as the Hebridean Seaweed Company, Bød Ayre, Mara, Irish Seaweed, Viking Fish Farms, and Seagreens harvest seaweeds from the wild and produce food and feed products as well as speciality chemicals and fertilizers (BBSRC, 2014b, Becker, 2007).

6.4.2.2 Microalgae

Microalgae are globally grown at significant scale for high value food, nutraceutical and cosmeceutical use, e.g., in Australia (>650 ha of open ponds for beta-carotene²¹), the US, China and Israel. Microalgal-derived biofuels are currently developed both through heterotrophic cultivation (e.g., Solazyme), and phototrophic growth (e.g., Algenol).

Due to increase in global population, and the move towards protein-rich diets, there is great need for protein for food and especially feed, and microalgal protein would be a logical potential replacement for the highly unsustainable feedstock such as fish-meal (Becker, 2007).

6.4.3 Formulation of Cambond Biomass-Based Bio-Resin (DIGLUE and ALGLUE)

A new generation of bio-resins that use both animal blood protein (Zhao, 2013) and biomass previously discarded or considered to be “low value” (i.e., de-oiled DDGS and full algal biomass) has been developed (Zhao, 2014a,b). This technology provides a green, cost-effective and scalable adhesive production process that has shown great potential in making no-added formaldehyde wood panel adhesives.

This new process (termed Biomass Cross-linking and Blocking – BCB technology) is based on our discovery that algae and DDGS biomass in aqueous medium can be cross-linked by isocyanate-containing cross-linking agents to form a water resistant polymeric network. At the same time, natural phenol groups in algae or hydroxyl groups from the biomass block the isocyanate functional groups to protect the isocyanate activities. The blocked isocyanate groups are believed to keep the adhesives stable in aqueous solution, and to be more stable than virgin isocyanates, leading to lower carbon dioxide generation. De-blocking of the isocyanate-phenol/alcohol conjugates will then take place during the heating phase of the wood composite manufacturing process to create strong wood-wood bonding effect.

6.4.3.1 *Materials and Methods*

DIGLUE was formulated by mixing DDGS with other additives to form a physical blend, which was subsequently milled into a fine powder. The particle size was controlled at greater than 100 mesh (Zhao, 2014a,b). ALGLUE was formulated by mixing dry algae mass collected from Lake Tai in China with other additives to form a physical blend, which was subsequently milled into a fine powder. The particle size was controlled at greater than 100 mesh (Zhao, 2014b). Standard urea formaldehyde resin and PMDI were obtained from a commercial source and used for board manufacturing as controls.

6.4.3.2 *Preliminary Particle Board Preparation Method*

100g of DIGLUE powder was added into 400g of distilled water and mixed using a homogeniser for 2 hours. PMDI was added to the glue (Table 6.1) and mixed for 30 minutes to obtain bio-resin ready for particleboard preparation. The calculated amount of DIGLUE bio-resin was weighed out according to Table 6.1 and the resin was added to 1000g of pine wood particles having moisture content of approximately 5% and mixed with a mechanical mixer. A $9 \times 9 \times 9$ inch wood fibre matrix forming box was centred on a $12 \times 12 \times 0.1$ inch stainless steel plate, which was covered with aluminium foil. The wood-adhesive mixture was slowly added into the forming box to achieve a uniform density of particles coated with bio-resin. The mixture was compressed by hand with a plywood board and the matrix-forming box was carefully removed so that the particle-board mat would not be disturbed. Then, the plywood board was removed, a piece of

Table 6.1 Sample compositions for preparation of the preliminary particleboard.

Sample no	Wood particle (g)	PMDI (g)	Urea-formaldehyde (g)	DIGLUE bio-resin (20%)(g)
1	1000	10	0	0
2	1000	50	0	0
3	1000	10	0	60
4	1000	10	0	80
5	1000	20	0	90
6	1000	30	0	90
7	1000	0	120	0

aluminium foil was placed on the mat, and another stainless steel plate was placed on top of the mat. The particleboard mat was then pressed to a thickness of $\frac{3}{4}$ inch using the following conditions: 120 psi for 10 minutes at a press platen temperature of 170 °C. The particleboard was trimmed to 5 × 5 inches to check the thickness swelling (TS) ratio and water absorption property (WAC%), which related to the cross-linking density of the wood composites. The particleboard sample compositions are shown in Table 6.1. Similarly, other particleboards were produced using urea-formaldehyde glue and PMDI as controls. The TS (%) and the water absorption capacity (WAC%) were measured according to the industrial standard by immersing the dry board specimen into water for 2 hours and 24 hours. The thickness increase and weight increase of the boards before and after 24 hours in water were measured and calculated to obtain the results.

Preparation of MDF and Particle Board with Programmed Board Pressing Process

This preparation was carried out in an MDF board manufacturer's R&D lab using programmed hot-pressing cycles set the pressing time at 68, 74, 83, 93, 143, 148, 158 and 180 seconds respectively. The density of the fibreboard was 860 kg/m³ and the thickness of the board was controlled at 8 mm. Hot press temperature was 220 °C. The pre-forming matrix was produced using the same procedure as described in the preliminary experiment. In this paper, a press time of 180 s was used for the process.

The DIGLUE solid/fibre ratio was set at 4.0%, 7.5%, 8.6% and 11.7%, while DIGLUE solid content was 30% and the PMDI content % in the fibre was varied from 1%, 1.875%, 2.15% to 2.93%. The internal bond (IB), surface soundness (SS), modulus of elasticity (MOE), modulus of rupture (MOR), water absorption capacity (WAC) and the thickness swelling (TS) of the produced MDF were tested according to international standards. Standard UF was used to make fibreboard as a control in which 11.7% glue/fibre was used for the process. Other process conditions were kept the same. Similarly, ALGLUE was used to make both fibreboard and particle board with the ratio of glue solid/wood fibre or particle at 4.0%.

6.4.3.3 Results and Discussion

Preliminary Results

In the preliminary study, the TS (%) and the WAC (%) of the pressed particleboard were measured to reflect the cross-linking network of the wood particle composites

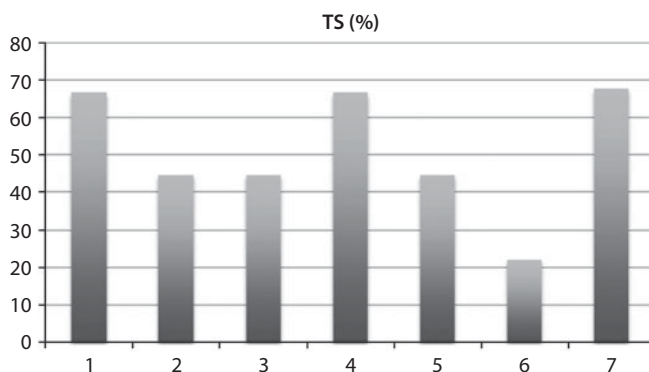


Figure 6.1 Thickness swelling (%) of the preliminary samples of particleboards.

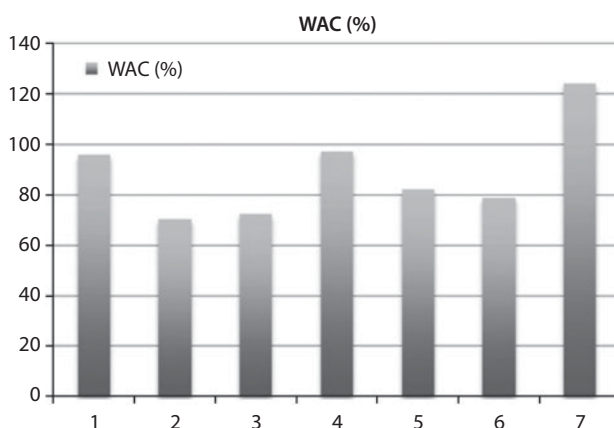


Figure 6.2 Water absorption capacity (WAC) of the preliminary samples of particle boards.

and the water resistance. In general, the higher thickness swelling and water absorption capacity indicates the lower degree of cross-linking network and less water resistance of the composites. The results are shown in Figure 6.1 and Figure 6.2.

From Figure 6.1 and Figure 6.2, it is seen that the higher amount of PMDI (5%) led to the lower TS (%) and WAC (%). This indicates the formation of a higher degree of cross-linked PMDI/wood fibre network. By introducing the bio-resin, the amount of PMDI used for wood fibre bonding can be markedly reduced (1–3%). This means the efficiency of PMDI binding capacity can be enhanced in the presence of DIGLUE while the high amount of urea-formaldehyde resin is required to get a similar degree of cross-linking using PMDI and DIGLUE system.

Preparation of MDF and Particle Board with a Programmed Hot-pressing Process

Based on the initial studies, MDF and particleboards were prepared using a programmed hot-pressing process set at different amounts of bio-resin in the wood fibres/particles. The characteristics of the MDF and particleboards produced by this way were analyzed and the results are shown in Figure 6.3 – Figure 6.9.

The test results, clearly demonstrate that the IB, SS, MOE, MOR, TS (%) at 2 hour and 24 hours, and WAC (%) are affected by the ratio of bio-resin/fibre. The same

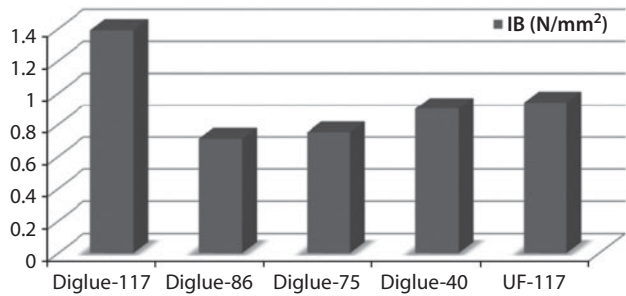


Figure 6.3 Test results of IB of MDF with different DIGLUE/Fibre ratio.

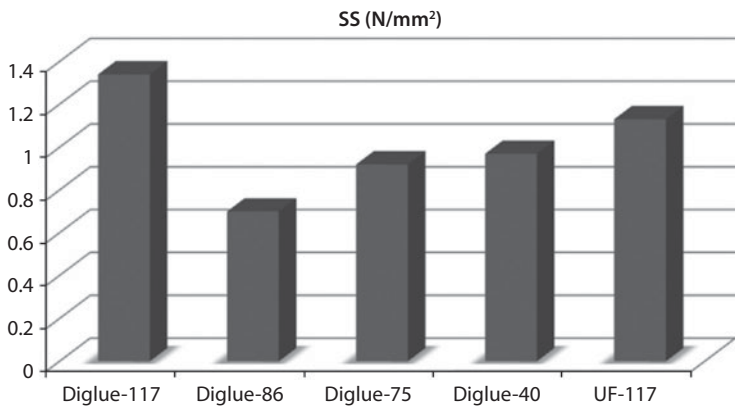


Figure 6.4 SS value of MDF with different DIGLUE/Fibre ratio.

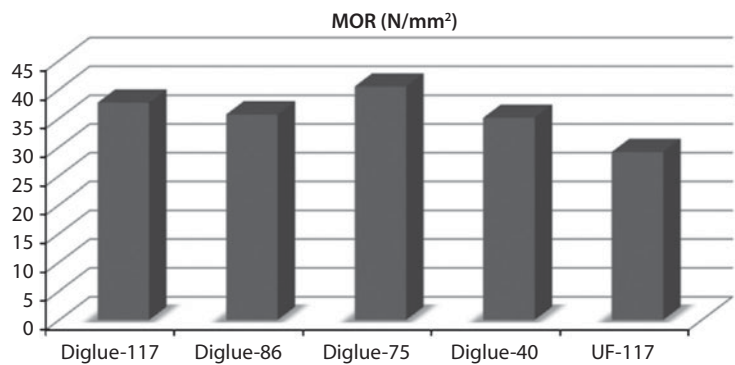


Figure 6.5 MOR Value of MDF with different DIGLUE/Fibre ratio.

amount of DIGLUE as the UF control added into the composites leads to the highest IB value while the 40 kg/m³ of the DIGLUE and ALGLUE can also obtain IB values above 0.6 N/mm² which meets the standard. Regarding the water resistance of MDF produced using DIGLUE and UF, the former has significantly higher water resistance than the latter. The UF composite in this sample does not have wax added to enhance the water resistance, which resulted in the highest water absorption capacity.

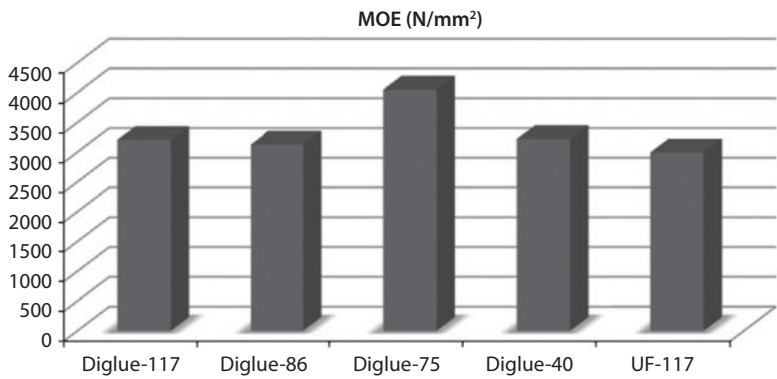


Figure 6.6 MOE value of MDF with different DIGLUE/Fibre ratio.

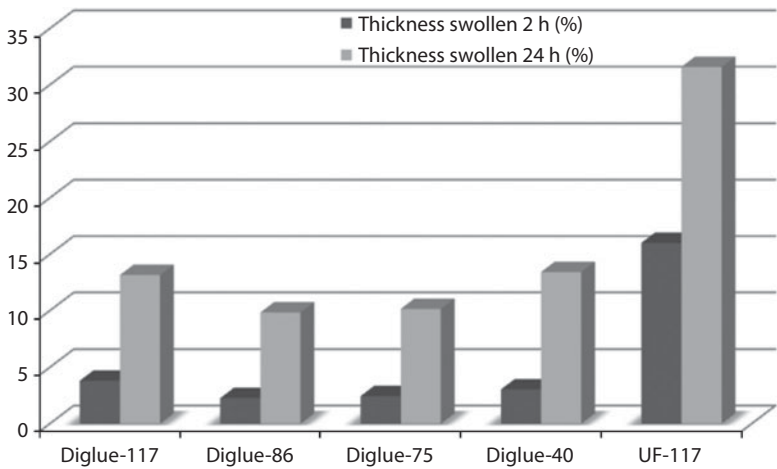


Figure 6.7 TS % of MDF with different DIGLUE/Fibre ratio.

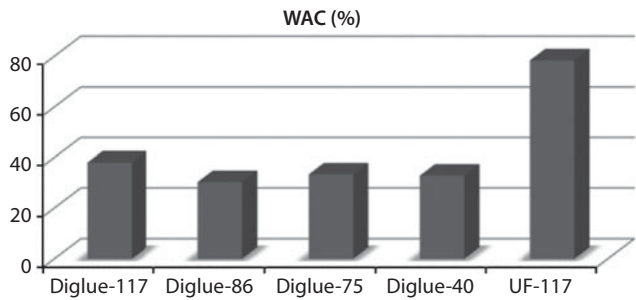


Figure 6.8 Water absorption capacity of MDF with different DIGLUE/Fibre ratio.

This study also shows that ALGLUE has similar bonding capability to DIGLUE. In this paper, only IB value of both MDF and particleboard was shown in Figure 6.9. Other parameters of the boards were tested and have met the world wide industrial standards.

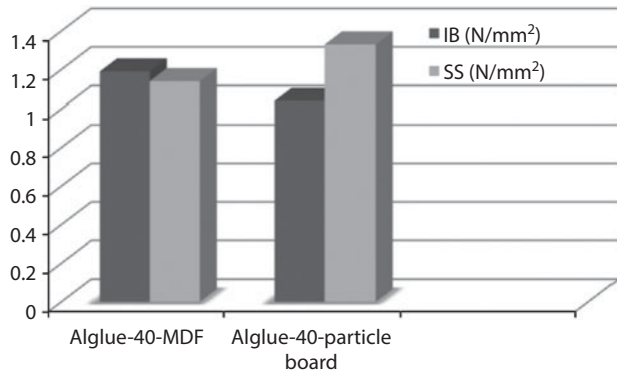


Figure 6.9 IB value of MDF with different ALGLUE/Fibre ratio.



Figure 6.10 Straw fibre based bio-composite beams using Cambond bio-resin.

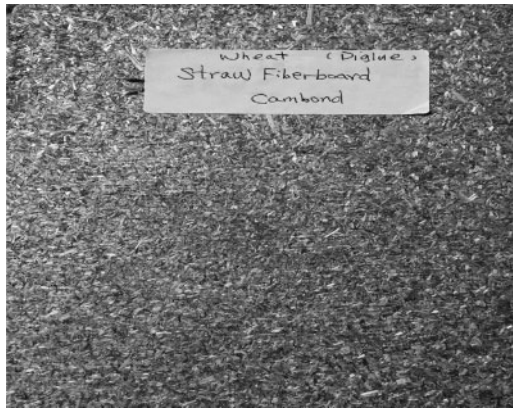


Figure 6.11 Straw Boards produced using Cambond bio-resin.

6.5 Bio-composites Based on Cambond Bio-Resin

Using Cambond biomass based glue, various bio-composite materials have been manufactured at large scale including straw beam (Figure 6.10) produced by extrusion process, straw boards with standard wood panel particleboard manufacturing process (Figure 6.11). In addition, straw fibres can also be produced as insulation materials



Figure 6.12 Straw boards for insulation and interior decoration.

and interior decoration boards for green construction with breathable properties (Figure 6.12).

Standard MDF, PB and OSB are manufactured using a continuous manufacturing process. The general steps used to produce fibreboard panels such as MDF include mechanical pulping of wood chips to fibres (refining), drying, blending fibres with resin and sometimes wax, forming the resinated material into a mat, and hot pressing. Typically a blowline system is used, in which the fibres are first blended with resin, wax, and other additives in a blowline, which is a duct that discharges the resinated fibres to the dryer. After drying, the fibres are separated from the gas stream by a fibre recovery cyclone and then conveyed to a dry fibre storage bin. The MDF panels are compressed to a density of 0.50 to 0.80 specific gravity (31–50 lb/ft³) by addition of Cambond bio-resin at 40 kg–80 kg/m³ based dry solid of glue. Additives such as wax and fire-retardants may be introduced during manufacturing to improve certain properties. Because the boards can be cut into a wide range of sizes and shapes, applications are many, including industrial packaging, displays, exhibits, toys and games, furniture and cabinets, wall paneling, molding, and door parts.

For particleboards and OSB, the top layers and core layers will be mixed with Cambond resin separately with similar glue/particle/chips ratio. For particleboard or chipboard manufacturing, the process is involved by mixing wood particles with resin to form the mix to be pressed into a mat. The mat formed is then hot-compressed under pressures and temperatures between 140 °C and 220 °C. This process sets and hardens the glue. The boards are then cooled, trimmed and sanded. The particleboards can then be sold as raw board or surface improved through the addition of a wood veneer or laminate surface. For OSB manufacturing, rather long strands of wood strips on the external layers are aligned to the panel's strength axis, while internal layers are perpendicular. OSB panels are engineered with multiple layered mats that are cross-aligned strands that become interweaved under the heat and pressure of the formation process. This process results in a structurally engineered wood panel that is stronger and has no



Figure 6.13 MDF produced using Cambond Bio-resin.



Figure 6.14 OSB produced using Cambond Bio-resin.

gaps or voids in the panels. All products produced meet current industrial standards with no-added formaldehyde in the boards (Figure 6.13–Figure 6.15).

Wood biocomposites engineered using biomass-based resins have advantages compared to those manufactured by formaldehyde-based resin, they have improved low carbon, low formaldehyde emissions and recyclability. The biomass is readily available (for example algae and Distiller's Dry Grains and Solubles - DDGS) and can be used in a manufacturing process that is simple, clean, free of toxic waste and releases 80% less CO_2 during manufacture. The biomass during growth can absorb large quantities



Figure 6.15 Particle boards produced using Cambond Bio-resin.

of CO₂ and the subsequent manufacturing process produces the formaldehyde-free adhesives in a significantly ‘greener’ process compared to the manufacture of conventional wood adhesives with 60% less energy consumption. The boards produced using the Cambond bio-resin are demonstrably ‘greener’ and more sustainable.

6.6 Final Remarks

In this chapter, a new generation of DDGS and algae biomass-based bio-resin has been developed which has no added formaldehyde. This novel resin system can clearly reduce the amount of PMDI used for MDF and particleboard preparation. This will significantly reduce the cost of production. In addition, no major process changes are required for using the novel resin, while it consumes less oil-based adhesives for green wood panel industry. Further works have been carried out for manufacturing of wood panels using optimized process conditions. In the future, the research on “green” adhesives focusing either on the replacement of even more petrochemical raw materials (e.g., formaldehyde) by other natural origin or the development of totally natural binder systems from even more natural products as to provide feasible and cost effective resin solutions based on regional plant species in each continent. As every country has its existing bio-industry manufacturing biomass such as DDGS and algae biomass as a result of bio-ethanol/biodiesel production, and there is also a world market drive to support and utilize environmentally friendly ‘green’ wood composite products. Rapid absorption of bio-resin technologies would be expected in wood panel manufacturing to help the industry meet its environmental and sustainability objectives. The ready availability of biomass and the marked alignment to ‘green’ products makes the world

greener, lowers the carbon footprint and help the industry to contribute to global (COP21) climate change objectives.

References

- Alma, M. H., Bastiirk, M. A., Co-condensation of NaOH catalyzed liquefied wood wastes, phenol, and formaldehyde for production of resol type adhesives. *Ind. Eng. Chem. Res.*, 40, 5036, 2001.
- Anglès, M.N., Ferrando, F., Farriol, X., Salvadó, J. "Suitability of steam exploded residual softwood for the production of binderless panels. Effect of the pre-treatment severity and lignin addition," *Biomass Bioenerg.* 21, 211–224, 2001.
- Association of the European Adhesive & Sealant Industry, *The European Adhesive and Sealant Industry Facts & Figures 2014*, 2014.
- BBSRC scoping study (a), 'Biofence' photobioreactor design and microalgal fermentation: 'Algal Research in the UK', Available at bbsrc.ac.uk/web/FILES/Reviews/algal_scoping_study_report.pdf. pp 19–20.
- BBSRC Algal Scoping Study (b); bbsrc.ac.uk/web/FILES/Reviews/algal_scoping_study_report.pdf.
- Becker, E.W., Microalgae as a source of protein. *Biotechnology Advances* 25, 207, 2007.
- Bitton, R., Berglin, M., Elwing, H., Colin, C., Delage, L., Potin, P., Bianco-Peled, H., The influence of halide-mediated oxidation on algae-born adhesives. *Macromol. Biosci.* 7, 1280, 2007.
- Bjorksten, J., Cross-linkages in protein chemistry. *Adv. Protein. Chem.*, 6, 343, 1951.
- Cambridge Venture Project (CVP) Report, Cambridge University Judge Business School (MBA Project), 2015.
- Danielson, B., Kraft Lignin in Phenol Formaldehyde Resin. *Licentiate Thesis*. Chalmers University of Technology, Göteborg, Sweden, p25, 1998.
- Food and Agricultural Organization of the United Nations (FAO), 2015. *Forestry Trade*. <http://faostat3.fao.org/home/E>. (Accessed December 2015)
- Gua, J., Zuob, Y., Zhang, Y., Tand, H., Zhu, L., Shen, J., Preparation of Plywood Using Starch Adhesives Modified with Isocyanate, *Applied Mechanics and Materials*, 26–28, 1065, 2010.
- Ghorpade, V.M., Li, H., Gennadios, A., Hanna, M.A., Chemically modified soy protein films. *Trans. ASAE*, 38, 1805, 1995.
- Grand View Research, *Bioadhesives Market Analysis By Source (Plant Based & Animal based), By Application (Packaging & Paper, Construction, Wood, Personal Care, Medical) And Segment Forecasts To 2022*, 2015.
- Hashim, R., Wan Nadhari, W. N. A., Sulaiman, O., Kawamura, F., Hiziroglu, S., Sato, M., Sugimoto, T., Tay, G.S., Tanaka, R. "Characterization of raw materials and manufactured binderless particleboard from oil palm biomass," *Mater. Design*, 32, 246–254, 2011.
- Hettiarachchy, N.S., Kalapathy, U., Myers, D.J., 1995. Alkali-modified soy protein with improved adhesive and hydrophobic properties. *J. Am. Oil Chem. Soc.*, 72(12), 1461.
- Huang, J., Li, K., A new soy flour-based adhesive for making interior type II plywood. *J. Am. Oil Chem. Soc.*, 85, 63–70, 2008.
- Huang, W., Sun, X., Adhesive properties of soy proteins modified by urea and guanidine hydrochloride. *J. Am. Oil Chem. Soc.*, 77(1), 101, 2000a.
- Huang, W., Sun, X., Adhesive properties of soy proteins modified by sodium dodecyl sulfate and sodium dodecylbenzene sulfonate. *J. Am. Oil Chem. Soc.*, 77(7), 705, 2000b.
- Imam, S.H., Gordon, S.H., Mao, L., Chen, L., Environmentally friendly wood adhesives from a renewable plant polymer: characteristics and optimization, *Polymer Degradation and Stability*, 73, 529, 2001.

- Jiang, Z., Qin, D., Hse, C-Y., Kuo, M., Luo, Z., Wang, G., Yu, Y., Preliminary study on chicken feather protein-based wood adhesives, *Journal of Wood Chemistry and Technology* 28, 240–246, 2008.
- Kim, S., Environment-friendly adhesives for surface bonding of wood-based flooring using natural tannin to reduce formaldehyde and TVOC emission, *Bioresource Technology*, 100, 744, 2009.
- Lambuth, A.L., Protein Adhesives for Wood, in: *Handbook of Adhesive Technology* 2nd edition, Pizzi, A., Mittal, K.L., (Ed.), Chapter 2, Marcel Dekker, Inc., 2003.
- Lambuth, A.L., Process for the preparation of epoxide modified adhesive compositions. US Patent 3,192,171, 1965.
- Lee, S. H., Teramoto, Y., Shiraishi, N., Resol type phenolic resin from liquefied phenolated wood and its application to phenolic foam. *J. Appl. Polym. Sci.*, 84, 468, 2002.
- Li, K., Peshkova, S., Geng, X., Investigation of soy protein-Kymene adhesive systems for wood composites. *J. Am. Oil Chem. Soc.*, 81, 487, 2004.
- Lin, M.-F., Thakur, V.K., Tan, E.J., Lee, P.S., Surface functionalization of BaTiO₃ nanoparticles and improved electrical properties of BaTiO₃/polyvinylidene fluoride composite. *RSC Adv.* 1, 576, 2011a.
- Lin, M.-F., Thakur, V.K., Tan, E.J., Lee, P.S., Dopant induced hollow BaTiO₃ nanostructures for application in high performance capacitors. *J. Mater. Chem.* 21, 16500, 2011b.
- Licht F.O., Feedstock use for biofuels – The outlook for 2011. *World Ethanol & Biofuels Report*, 9(17), 1, 2011.
- Liu, Y., Li, K., Chemical modification of soy protein for wood adhesives. *Macromol Rapid Commun.*, 23, 739, 2002.
- Liu, Y., Li, K., Modification of soy protein for wood adhesives using mussel protein as a model: the influence of a mercapto group. *Macromol Rapid Commun.*, 25, 1835, 2004.
- Liu, Y., Li, K., Development and characterization of adhesives from soy protein for bonding wood. *Int. J. Adhes Adhes.*, 27, 59, 2006.
- Ly, Y., Jane, J., Johnson, L.A., Soy proteins as biopolymers, D kaplan, (ed.) *Biopolymers from renewable resources*. Springer-Verlag, Heidelberg. pp 171–200, 1998.
- Mansouri, N. El., Pizzi, A., Salvadó, J., Lignin-based wood panel adhesives without formaldehyde, *Holz als Roh- und Werkstoff*, 65(1) 65, 2007.
- Market Research Report – 327985, Bioadhesive Market by Type (Plant Based, and Animal Based), by Application (Packaging & Paper, Construction, Wood, Personal Care, Medical, and Others) - Global Forecast to 2019, Global Information, 2015.
- Miller, A.G., Gerrard, J.A., The maillard reaction and food protein cross-linking. *Prog. Food Biopolym. Res.*, 1, 69, 2005.
- Onusseit, H., Starch in industrial adhesives, *Industrial Corps and Products*, 1, 141, 1993.
- Parker, B., Biobased adhesives: Markets and UK-based manufacturers, *InCrops Enterprise Hub*, 2014.
- Park, S.K., Bae, D.H., Rhee, K.C., Soy protein biopolymer cross-linked with glutaraldehyde. *J. Am. Oil Chem. Soc.*, 77(8), 879, 2000.
- Pappu, A., Patil, V., Jain, S., Mahindrakar, A., Haque, R., Thakur, V.K., Advances in industrial prospective of cellulosic macromolecules enriched banana biofibre resources: A review. *Int. J. Biol. Macromol.* 79, 449, 2015.
- Pöyry Management Consulting, D2.3 - Report on the “Assessment of the Bio-based Products Market Potential for Innovation” <http://www.biochem-project.eu/download/toolbox/innovation/06/Bio-based%20product%20market%20potential.pdf>, 2010.
- Singha, A.S., Thakur, V.K., Mechanical, Morphological, and Thermal Characterization of Compression-Molded Polymer Biocomposites. *Int. J. Polym. Anal. Charact.* 15, 87, 2010a.
- Singha, A.S., Thakur, V.K., Synthesis, Characterization and Study of Pine Needles Reinforced Polymer Matrix Based Composites. *J. Reinf. Plast. Compos.* 29, 700, 2010b.

- Singha, A.S., Thakur, V.K., Synthesis and Characterization of Short *Grewia optiva* Fiber-Based Polymer Composites. *Polym. Compos.* 31, 459, 2010c.
- Thakur, V.K., Singha, A.S., Natural fibres-based polymers: Part I—Mechanical analysis of Pine needles reinforced biocomposites. *Bull. Mater. Sci.* 33, 257, 2010d.
- Thakur, V.K., Singha, A.S., Physico-chemical and mechanical characterization of natural fibre reinforced polymer composites. *Iran. Polym. J.* 19, 3, 2010e.
- Singha, A.S., Thakur, V.K., Morphological, Thermal, and Physicochemical Characterization of Surface Modified *Pinus* Fibers, *International Journal of Polymer Analysis and Characterization*, 14(3), 271, 2009a.
- Singha, A.S., Thakur, V.K., Physical, chemical and mechanical properties of *Hibiscus sabdariffa* fiber/polymer composite. *Int. J. Polym. Mater.* 58, 217, 2009b.
- Singha, A.S., Thakur, V.K., Mechanical, thermal and morphological properties of *grewia optiva* fiber/polymer matrix composites. *Polym.-Plast. Technol. Eng.* 48, 201, 2009c.
- Singha, A. S., Thakur V.K., Mehta I. K., Shama Anjali, Khanna A. J., Rana R. K. & Rana, A.K., Surface-Modified *Hibiscus sabdariffa* Fibers: Physicochemical, Thermal, and Morphological Properties Evaluation, *International Journal of Polymer Analysis and Characterization*, 14 (8), 695, 2009.
- Sun, S., Wang, D., Zhong, Z., Yang, G., Adhesives from modified soy protein. US Patent 7,416,598 B2, 2008.
- Sun, X., Bian, K., Shear strength and water resistance of modified soy protein adhesives. *J. Am. Oil Chem. Soc.*, 76(8), 977, 1999.
- Thakur, V.K., Lin, M.-F., Tan, E.J., Lee, P.S., Green aqueous modification of fluoropolymers for energy storage applications. *J. Mater. Chem.* 22, 5951, 2012a.
- Thakur, V.K., Yan, J., Lin, M.-F., Zhi, C., Golberg, D., Bando, Y., Sim, R., Lee, P.S., Novel polymer nanocomposites from bioinspired green aqueous functionalization of BNNTs. *Polym. Chem.* 3, 962, 2012b.
- Thakur, V.K., Thakur, M.K., Raghavan, P., Kessler, M.R., Progress in green polymer composites from lignin for multifunctional applications: A review - *ACS Sustainable Chemistry & Engineering*, 1072, 2014a.
- Thakur, V.K., Thakur, M. K., Gupta, R.K., Review: raw natural fiber-based polymer composites, *International Journal of Polymer Analysis and Characterization* 19(3), 256, 2014b.
- Thakur, V.K., Thakur, M.K., Gupta, R.K., Graft copolymers of natural fibers for green composites. *Carbohydr. Polym.* 104, 87–93, 2014c.
- Thakur, V.K., Grewell, D., Thunga, M., Kessler, M.R., Novel Composites from Eco-Friendly Soy Flour/SBS Triblock Copolymer. *Macromol. Mater. Eng.* 299, 953, 2014d.
- Thakur, V.K., Thunga, M., Madbouly, S.A., Kessler, M.R., PMMA-g-SOY as a sustainable novel dielectric material. *RSC Adv.* 4, 18240, 2014e.
- Thakur, V.K., Vennerberg, D., Kessler, M.R., Green Aqueous Surface Modification of Polypropylene for Novel Polymer Nanocomposites. *ACS Appl. Mater.* 6, 9349, 2014f.
- Thakur, V.K., Vennerberg, D., Madbouly, S.A., Kessler, M.R., Bio-inspired green surface functionalization of PMMA for multifunctional capacitors. *RSC Adv.* 4, 6677, 2014g.
- Thakur, V.K., Thakur, M.K., Processing and characterization of natural cellulose fibers/thermoset polymer composites, *Carbohydrate polymers*, 109, 102–117, 2014a.
- Thakur, V.K., Thakur, M.K., Recent Advances in Graft Copolymerization and Applications of Chitosan: A Review. *ACS Sustain. Chem. Eng.* 2, 2637, 2014b.
- Thakur, V.K., Kessler, M.R., Free radical induced graft copolymerization of ethyl acrylate onto SOY for multifunctional materials. *Mater. Today Commun.* 1, 34, 2014a.
- Thakur, V.K., Kessler, M.R., Synthesis and characterization of AN-g-SOY for sustainable polymer composites. *ACS Sustain. Chem. Eng.* 2, 2454, 2014b.

- Vijayendran, B., *Biobased Chemicals: Technology, Economics and Markets* (white paper), 2010.
- Von Dungen, M., The European Adhesives and Sealants Market 2012–2015, the British Adhesives and Sealants Association. FEICA, 2014. www.feica.org/library/market-reports
- Wang, Y., Adhesive performance of soy protein isolate enhanced by chemical modification and physical treatment. Dissertation, Kansas State University, 2006.
- Waite, J.H., Surface chemistry – mussel power. *Nat. Mater.*, 7, 8, 2008.
- Wang, Y., Mo, X., Sun, S., Wang, D., Soy protein adhesion enhanced by glutaraldehyde cross-link. *J. Appl. Polym. Sci.*, 104, 130, 2007.
- Wong, S.S., Introduction. *Chemistry of protein conjugation and cross-linking*, Wong, S.S., (Ed.). CRC, Boca Raton, FL. p7, 1991.
- Wu, H., Thakur, V.K., Kessler, M.R., Novel low-cost hybrid composites from asphaltene/SBS tri-block copolymer with improved thermal and mechanical properties. *J. Mater. Sci.* 51, 2394–2403, 2016.
- Zhang, Z., Hua, Y., Urea-modified soy globulin proteins (7S and 11S): Effects of wettability and secondary structure on adhesion. *J. Am. Oil Chem. Soc.*, 84, 853, 2007.
- Zhao, X., Algae Treatment Agents and Application, Chinese Patent CN101125688, 2010.
- Zhao, X., Bioadhesives for Plywood, Process and Manufacturing, Chinese Patent, CN 201210258794.2, Assigned to Cambond Ltd., 2013.
- Zhao, X., Distilled Grain based bioadhesives, process, manufacturing and their uses, UK patent application GB1401275.1, assigned to Cambond Ltd., 2014a.
- Zhao, X., Algal biomass based bioadhesives, process, manufacturing and their uses, UK patent application GB1400267, assigned to Cambond Ltd., 2014b.
- Zhong, Z., Sun, X.S., Wang, D., Ratto, J.A., Wet strength and water resistance of modified soy protein adhesives and effect of drying treatment. *J. Poly. Environ.*, 11(4), 137, 2003.
- Zhong, Z., Sun, X.S., Fang, X., Ratto, J.A., Adhesive strength of guanidine hydrochloride-modified soy protein for fiberboard application. *Int. J. Adhes. Adhes.*, 22, 262–272, 2002.

Bio-Derived Adhesives and Matrix Polymers for Composites

Mariusz Ł. Mamiński* and Renata Toczyłowska-Mamińska

*Faculty of Wood Technology, Warsaw University of Life Sciences – SGGW
Warsaw, Poland*

Abstract

The concept of green chemistry and sustainable development policy impose on industry and technology to switch raw material base from the petroleum to renewable resources. The need for green products and manufacturing is a driving force of the research for the environmentally-friendly technologies. Thus, the employment of bio-based raw materials is an issue of the present and future times.

This chapter contains basic considerations on the use of glycerol, tannins, lignin, polysaccharides, proteins, vegetable oils, poly(hydroxyalkonates) and poly(lactide) as the potential components of bio-based polymeric materials. The main pathways and approaches to their conversion into adhesives and polymer matrices have been indicated.

Keywords: Bio-based adhesives, composites, matrix, renewable resources, polymer

7.1 Introduction

In the 21st century environmental policy, depleting fossil resources and increasing demand for greener products are the driving force of the search for the environmentally-friendly technologies merging with the concepts of green chemistry and sustainable development (Wu *et al.*, 2016). The development of novel materials for engineering employs the renewable resources as the alternatives to petroleum-based feedstock (Thakur & Kessler, 2015; Thakur & Thakur, 2015). Composites involving bioplastic or biomass-derived adhesives and matrices are the solutions of tomorrow. Matrix is the part of a composite that filler or reinforcing additive (e.g. fibers) is embedded within.

Nature provides a wide range of the raw materials that can be converted into a polymeric matrix or adhesive applicable in biocomposites formulation. The most abundant plant-derived feedstocks and resources from the microbial fermentation – poly (lactic acid) and poly(hydroxyalkanoates) are shown in Figure 7.1.

*Corresponding author: mariusz_maminski@sggw.pl

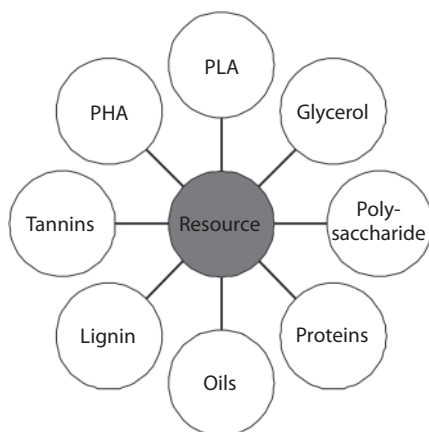


Figure 7.1 Bioresources for composites technology.

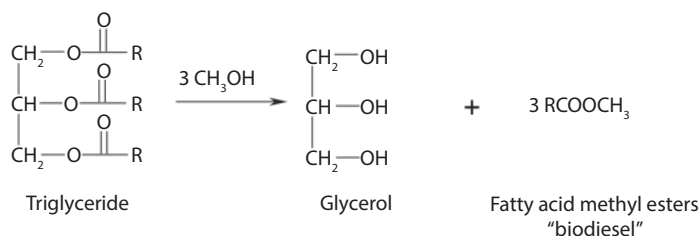


Figure 7.2 Scheme for transesterification of triglycerides with methanol. R – fatty acid residues $\text{C}_{12} - \text{C}_{20}$.

Due to a wide range of biomaterials chosen for the chapter, basics for chemical nature of these renewable resources, main directions of their utilization and fundamental pathways for their conversion into the polymers applicable as binders or composite matrices have been described. Wherever possible references to more comprehensive literature focused on a specific bioresource are given.

7.2 Glycerol

The production of biodiesel generates large amounts of crude glycerol that becomes a valuable raw material for polymer technology. The process of biodiesel production is based on the transesterification of triglyceride-rich vegetable oils with methanol (Figure 7.2). Rape oil in Europe, while soy, sunflower, palm or castor oils are the dominating feedstocks for biodiesel in South America. Global production of glycerol in 2025 is estimated on 6 million tons (Ciriminna *et al.*, 2014). Thus, the abundance and availability of this raw material is substantial and cannot be neglected.

The main pathways for glycerol to polymeric materials are depicted in Figure 7.3. The first transformation route is glycerol conversion into cyclic glycerol carbonate (4-hydroxymethyl-1,3-dioxolane-2-on) under alkaline conditions in the reaction with dimethyl carbonate (Rokicki *et al.*, 2005). Subsequently, the monomer can easily be

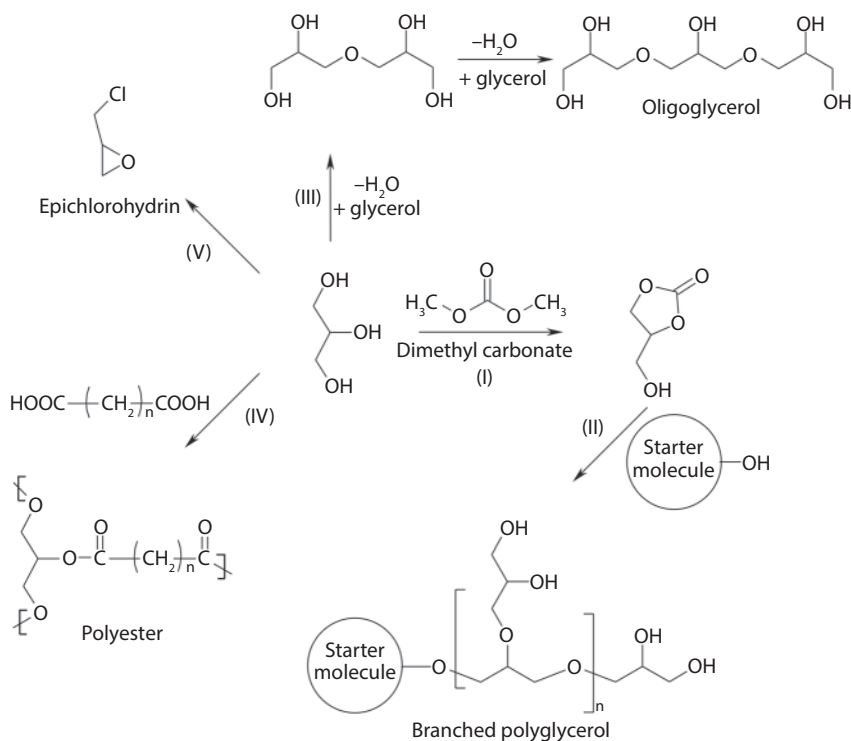


Figure 7.3 Reactions of conversion of glycerol to cyclic glycerol carbonate (I), branched polyglycerols (II), oligomeric glycerols (III), polyesters (IV) and epichlorohydrin (V).

converted into hyperbranched polyglycerols (HBPs) that have been recently employed in adhesive formulations (Mamiński *et al.*, 2011) and as the additives and modifiers in other engineering materials as well. The other routes are based on glycerol dehydration followed by oligomerization with linear oligoglycerols formation, polyesterification with aliphatic or aromatic dicarboxylic acids, and, last but not least, conversion to epichlorohydrin. Polyesters as well as oligo- and polyglycerols can be further functionalized or used directly as the components of polymeric systems (polyurethanes, epoxies, acrylates etc.).

The number of reports on the use of hyperbranched polyglycerols in adhesives is quite limited. The most recent works by Mamiński *et al.* (2011; 2012) deal with wood adhesives. One of the approaches regards the glycerol-derived hyperbranched polymers as the components of polyurethane adhesives.

A range of the HBPs of different core-structure and terminal functionality in the shell was used as polyols in the 2-component polyurethane adhesives (Figure 7.4). It was shown that gel times of the adhesives at 20 °C ranged between 1 and 9 minutes and were influenced by the HBP structure, functionality and isocyanate index. It was also proved that the presence of aromatic moieties and/or polyglycerol hydroxyl functionality about 6 were the key factors to provide bond line shear strength exceeding that of the wood (9–11 MPa).

An alternative direction for utilization of polyglycerols are polymeric matrices. Parzuchowski *et al.*, (2007) employed a hyperbranched polyglycerol bearing terminal

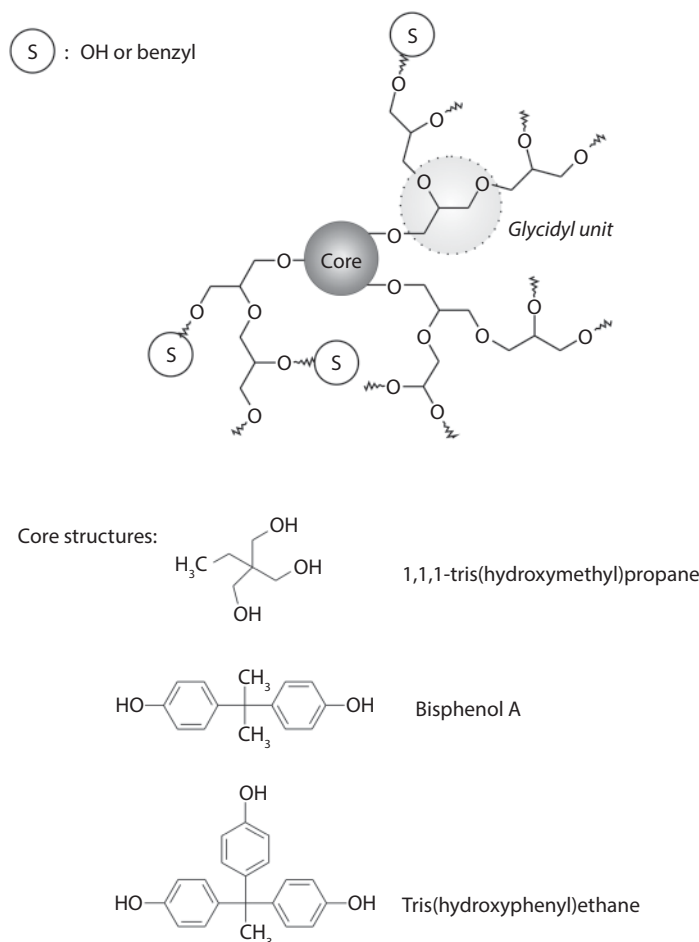


Figure 7.4 HBP backbone and core structures (Mamiński, 2013).

five-membered cyclic carbonate moieties as a modifier for the bisphenol A-based epoxy resin system cured with triethylenetetramine (TETA). It was proved that HBPs with terminal cyclic carbonates could be used as low viscosity tougheners for epoxies without the reduction in mechanical performance of the epoxy matrix.

More popular and widely investigated approach is the esterification of glycerol with carboxylic acids, so that polymer building blocks or macromonomers are obtained. The main areas of their utilization are adhesives, composites or biomedical applications.

Dai *et al.*, (2015) synthesized a series of polyols based on itaconic acid and glycerol. Subsequently, the polyesters were subjected to copolymerization with acrylated epoxidized soybean oils. The resultant thermosetting polymeric material exhibited great mechanical performance and durability against chemical and physical degradation. Hyperbranched poly(glycerol-co-diacid)s were developed by Whyatt, (2012). The polyesters were obtained by the polycondensation of glycerol with aliphatic dicarboxylic acids of variable chain length. The polymers exhibited a wide range of molecular weights varying between 4,160 and 445,000 Da and polydispersity indexes between 1.3

and 5.8 dependently on the reagents ratio. These materials are likely to become a basis for adhesives and composites.

The esters of glycerol with sebacic acid are recognized as biodegradable elastomeric materials (Tang *et al.*, 2006). In the work thermal and mechanical properties of a series of elastic polyesters were discussed. It was found that elongation at break, glass transition temperature, modulus of elasticity and tensile strength decreased with the decreasing content of glycerol. On the other hand, material susceptibility to biodegradation increased with increasing glycerol proportion. Tisserat *et al.*, (2012) showed that branched polyesters prepared from glycerol and citric acid might be a reliable and convenient material for biobased foams of excellent mechanical properties. Of note, the proposed microwave-assistance shortened processing time to ca. 60 seconds.

In general, glycerol polyesters with acids like citric, sebacic or adipic are known to be biodegradable and valuable polymers in the modern technology. But not only have glycerol esterifications with aliphatic dicarboxylic acids been shown to be convenient conversion routes. Some efforts have been made to develop aromatic polyesters. A polymeric matrix based on glycerol-phthalic/terephthalic acid for the natural fiber reinforced (0–10%) composite was prepared by the Miranda *et al.*, (2012). The composite materials were determined tensile strength to reach 2.2–3.0 MPa, Young's modulus 1098–2247 MPa and elongation at break 49.3–63.4%. Another concept that was positively verified in the course of experimental work is the esterification of glycerol with phthalic anhydride in order to obtain polyester polyols for polyurethanes (Velayutham *et al.*, 2009).

Besides the matrix applications, aromatic polyesters can be useful as hot-melt adhesives (Mamiński, 2013). A series of hydroxyl-terminated hyperbranched polyglycerols was subjected to melt-esterification with phthalic anhydride and sebacic acid (170 °C, 3 h, 100 mbar). The bond line shear strengths obtained in solid wood are shown in Table 7.1.

Table 7.1 Shear strengths of the hot-melt adhesive bond lines.

HBP		Acidic reagent	Reagents molar ratio	Bond line shear strength [N/mm ²]
Core	No. of terminal OHs			
bisphenol A	4	phthalic anhydride	1:3	1.20 ± 0.37
	4	phthalic anhydride	1:2	1.0 ± 0.11
bisphenol A	10	sebacic acid	1:2	0.12 ± 0.06
	10	phthalic anhydride	1:2	1.0 ± 0.15
	12	phthalic anhydride	1:3	2.70 ± 0.35
tris(hydroxyphenyl) ethane	13	phthalic anhydride	1:3	1.44 ± 0.12
reference*	–	–	–	2.45 ± 0.35

*commercial hot-melt

It has been demonstrated by the means of FTIR that hydroxyl groups of a hyper-branched polyglycerol can be effectively esterified. The performance of the bond line strongly depends on the components used – i.e., functionality and structure of polyglycerols as well as on the type of the acidic reagent. As found for the sebacic acid ester, flexible long-chain intermonomer linkages provided very low mechanical properties. The results indicate that that type of the polyesters can be considered as thermoplastic glycerol-derived binders for bio-based composites.

The other areas – not discussed here – for the use of glycerol derivatives in polymer technology are esters, alkyd resins and cellulosic films. Moreover, poly(glycerol sebacate)s are the materials widely used in the medical applications (Rai *et al.*, 2012), while poly(glycerol sebacate urethane)s are applied as biodegradable and biocompatible shape-memory matrices (Wu *et al.*, 2014).

Thus, it is apparent that the main ways of glycerol conversion into bio-based plastics or adhesives go either via esterification/polyesterification or via building up oligo- and polyglycerols that can be subsequently functionalized and used as macromonomers.

7.3 Tannins

That group is defined by two different classes of phenolic compounds naturally occurring in bark and wood: hydrolysable tannins and condensed tannins. The former group is phenols and their esters with simple sugars. Due to their low-molecular character and low reactivity, their practical and economical significance is limited. Unlike hydrolysable tannins, the importance of the latter group is much bigger. They attracted the attention of many research groups back in the 1950s. The annual production of the condensed tannins reaches 200,000 tons. Nowadays, tannins are mainly produced from wattle/mimosa (*Accacia*), quebracho (*Schinopsis*), pine (*Pinus*) or pecan (*Carya illinoensis*).

Two types of tannins can be differentiated: resorcinolic and phloroglucinolic (Figure 7.5). Both types are highly reactive toward formaldehyde, so the main area of their use is the adhesive technology. Due to the presence of dihydroxyl-substituted A ring in the phloroglucinolic tannin, its reactivity is even higher than that of the resorcinolic, so that phloroglucin-based adhesives are easily curable at ambient temperature, while resorcin-based ones need an increased temperature. Dependently on the botanic origin of a tannin, the proportion in resorcinolic-to-phloroglucinolic units varies which affects tannin reactivity. In general, the rate of reaction of tannin with formaldehyde is 10–50 times that for phenol. During the oil crisis in the 1970s, tannins were used as a

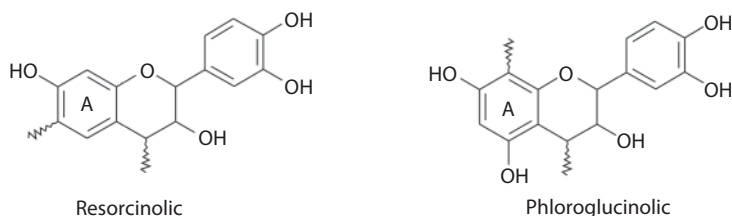


Figure 7.5 Substructures of condensed tannins.

renewable substitute for phenol. Tannin-formaldehyde adhesives were used in manufacturing of plywood, glue laminated beams and timber as well as for the exterior grade particleboards (Pizzi & Mittal, 2003).

An apparent drawback associated with the use of tannins in adhesives is their contamination with simple sugars that do not react with formaldehyde and do reduce mechanical properties of the bond line. As reported in the literature pine, pecan and mimosa bark tannins contain, respectively, 80%, 87% and 80% phenolic moieties, 5–8%, 0% and 3–6% hydrocolloid carbohydrate gum as well as 3–5%, 6.9% and 3–5% simple sugars (Pizzi, 1994). The effect can be weakened by co-condensation of tannins with amino resins or addition of amino resins upon glue formulating (Vázquez *et al.*, 2000; Bisanda *et al.*, 2003) which, due to substantial hydroxymethyl ($-\text{CH}_2\text{OH}$) groups content, work as the fortifying agents.

Since the environmental and health issues affect the development of adhesives and composites, it was necessary to substitute paraformaldehyde with other compounds able to act as cross-linkers for tannins (e.g., glyoxal) or develop formaldehyde-free strategies: employ tannin autocondensation ability or use alternative hardeners. The former approach regards tannin polycondensation under alkaline or acidic conditions where heterocyclic ring of a tannin opens following by subsequent condensation with another tannin molecule (Figure 7.6). A detailed discussion of the mechanism of the reaction,

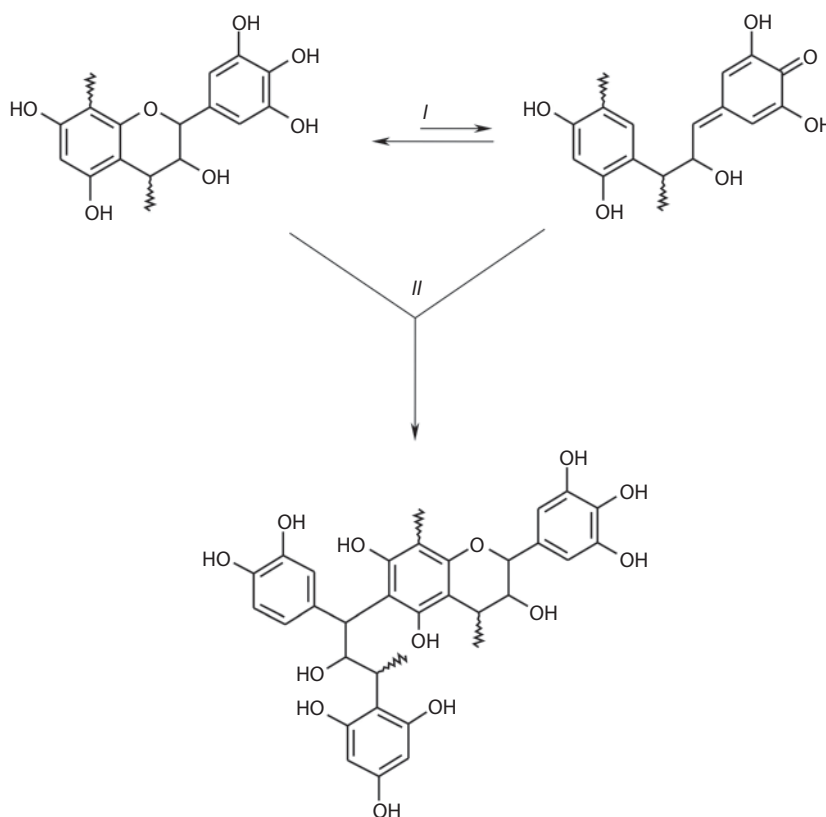


Figure 7.6 A simplified scheme for tannin autocondensation reaction: *I* – heterocyclic ring opening, *II* – secondary condensation.

its limitations and applicability can be found in the source reference (Meikleham *et al.*, 1994).

The other strategy for tannin cross-linking involves a number of compounds highly reactive toward tannins – e.g., tris(hydroxymethyl)nitromethane (Trosa & Pizzi, 2001), polyethyleneimine (Li *et al.*, 2004) or hexamethylenetetramine (hexamine, urotropine). The latter – in presence of highly reactive nucleophilic sites of tannin – is known to decompose into reactive imines and iminoaminomethylene bases (e.g., $\text{CH}_2=\text{N}-\text{CH}_2^+$) able to attack tannin molecule (Pichelin *et al.*, 2006). The approach was proved to be effective in the manufacturing of zero-emission wood-based panels.

Based on that chemistry, more complex adhesive systems have recently been investigated, too. Mansouri *et al.*, (2011) developed tannin/hexamine/glyoxylated lignin adhesive for plywood and particleboards. A scheme for the reaction sequence is presented in Figure 7.7. As reported the manufactured wood-based composites had met the requirements of the respective international standards.

More recently, a new type of adhesives based on tannin-sucrose chemistry was investigated by Zhao & Umemura (2014). What is interesting, under the heating treatment sucrose undergoes an *in situ* rearrangement to 5-hydroxymethylfurfural which subsequently reacts with a tannin. The results indicate that the new material entirely obtained from bioresources proved to be useful to manufacture particleboards that meet industrial standards (modulus of rupture and the modulus of elasticity in the range of 19.6–21.2 MPa and 4.6–5.0 GPa, respectively).

Not only are tannins predestinated to the adhesive applications. The other class of polymeric materials that much attention is paid to are foams. Today the majority of the foamed materials being exploited in packaging and insulation are petroleum-derived (polyolefins, phenolic and amino resins or petropolyol-based polyurethanes). For some time, due to an increasing demand on biosourced and sustainable products, an intensified research in the field of biobased foams has been observed. Foams occurred to be

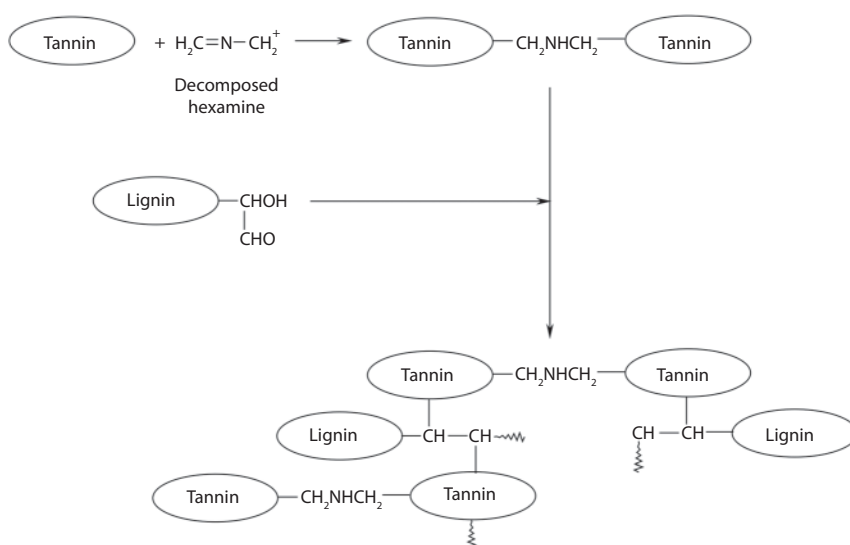


Figure 7.7 Schematic reaction between tannin and glyoxylated lignin in presence of hexamine.

an excellent field for the tannins to be employed. Tannin-derived foams proved to have great insulating properties as well as substantial resistance to chemicals. Moreover, they were found to be useful in the environmental applications like wastewater treatment or as sorbents (Sánchez-Martín *et al.*, 2013; Tondi *et al.*, 2009).

Quebracho, pine, and mimosa tannins or their mixtures were involved in rigid foam formulations (Martinez de Yuso *et al.*, 2014, Tondi & Pizzi 2009; Meikleham & Pizzi 1994). The chemistry of the system is based on the simultaneous acid-catalyzed exothermic reactions of (1) furfural with formaldehyde, (2) tannin with formaldehyde and (3) furfural autocondensation. The system is a self-blowing one where diethyl ether evaporates upon exothermic curing. An undoubted advantage of the procedure is its efficiency, since typical foam setting times do not exceed a few minutes. Produced foams exhibit densities ranging from 50 to 130 kg/m³, compression strength below 0.5 MPa as well as autoextinguish features and ease of density control by the amount of the blowing agent. However, in that case, control of foam stiffness/flexibility is not as easy as for polyurethanes and still remains a challenge.

The tannin-furfural-formaldehyde foams mentioned above gave way for further research in the field. Thus, that class of foams became a basis of the carbon-doped materials of enhanced thermal and electrical conductivities (Jana *et al.*, 2014). The best-performing material exhibited thermal conductivity 3.65 Wm⁻¹K⁻¹. The preparation procedure includes carbonization step which increases mechanical properties of the foams.

High reactivity of tannin-furfural-formaldehyde systems allowed the development of a range of sandwich-type lightweight composites with tannin-based foam in the core layer (Zhou *et al.*, 2013). Face layers were MDF, plywood or natural fibers, while tannin resin was the matrix. The sandwich panels exhibited good mechanical properties – the observed moduli of elasticity exceeded 6,500 MPa and bending strengths were higher than that of the plywood.

A number of published experimental works (Ramires & Frollini, 2012; Barbosa *et al.*, 2010; Ndazi *et al.*, 2006) as well as excellent and abundant review papers (Yan *et al.*, 2014; Satyanarayana *et al.*, 2009) on the use of tannin-based matrices for natural fiber composites indicate a significant potential of the approach in the future applications. Natural fibers of *Saccharum cilliare*, *Grewia optiva* and *Hibiscus sabdariffa* have also been reported to be convenient reinforcement for green composites (Thakur *et al.*, 2010; Singha & Thakur, 2010a-c; Singha & Thakur, 2009a-d; Singha & Thakur, 2008a, b).

The above considerations indicate that the tannins are a renewable feedstock of outstanding potential to be used in modern bio-based composites industry; however, economic conditions are still the crucial factor that limits their large-scale utilization today.

7.4 Lignin

Lignin – one of the major components of all woody plants – is a natural aromatic polymer. Two other components are cellulose and hemicelluloses. Lignin provides plants rigidity and strength necessary for growth. Its content varies between 19% and 35%wt (Dence & Lin, 1992). In industry huge amounts of low-value lignin-rich material are

generated during production of paper. Annual worldwide production of this by-product is estimated on 50 million tons (Suhas *et al.*, 2007). The prospective sources of additional lignins are production of cellulosic ethanol (0.5 kg lignin per 1 L ethanol) and biomass-derived products. However, only 1–2% of that quantity is processed into other products (Lora & Glasser, 2002). The rest of the material is a surplus which is burnt for energy production or considered waste. Thus, any developed lignin-derived product will increase the economics of an individual technology and will help to manage waste disposal as well.

As a raw material lignin exhibits some excellent features useful in chemical technology. These are: (1) presence of aromatic moieties providing good mechanical properties, (2) abundance of reactive functional groups allowing for easy grafting and chemical transformations, (4) small particle size and (5) hydrophobic or hydrophilic character determined by the origin. Representative structures of monomers present in lignin are depicted in Figure 7.8. These phenyl-propenoid building blocks constitute the skeleton of lignin macromolecules that contain various substituents, different intramonomer linkages and exhibit different degree of substitution. Common linkages' structures and their abundance in wood are shown in Figure 7.9 (Sjöström, 1993).

As it is widely known that lignin chemistry depends on the process of delignification, materials from different sources exhibit different structure, functionality and subsequently their usefulness is different for various purposes. Technical lignins generated from industry can be divided into two groups: (1) sulfur-containing (e.g., Kraft lignin and lignosulfonates) and (2) sulfur-free lignins (e.g. organosolv, soda, steam explosion and bioethanol hydrolysis lignins).

Upon delignification lignocellulosic material is subjected to the aggressive environment allowing for breaking down native lignin into fragments of lower molecular weight – typically 1,000 – 20,000 g/mol.

Water-soluble lignosulfonates with Mg, Na or NH_4^+ cations are yielded from acid-catalysed “sulfite process”. They are cross-linked polymers bearing both sulfonates and phenolic hydroxyl groups. 5%wt sulfur content limits wide applications of that type of lignin, so that it is mainly used for energy production (Doherty *et al.*, 2011).

“Kraft process” is based on strong alkaline hydrolysis (sodium hydroxide, sodium sulphide) of ether bonds in lignin. Obtained “Kraft lignin” bears aliphatic thiol groups and is hydrophobic. For sulfur content of 1–2%wt this type of lignin is used as a fuel in pulp mills.

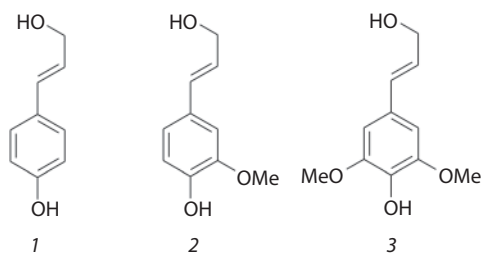


Figure 7.8 Phenylpropane units present in lignin: 1 – *p*-coumaryl alcohol, 2 – coniferyl alcohol, 3 – sinapyl alcohol.

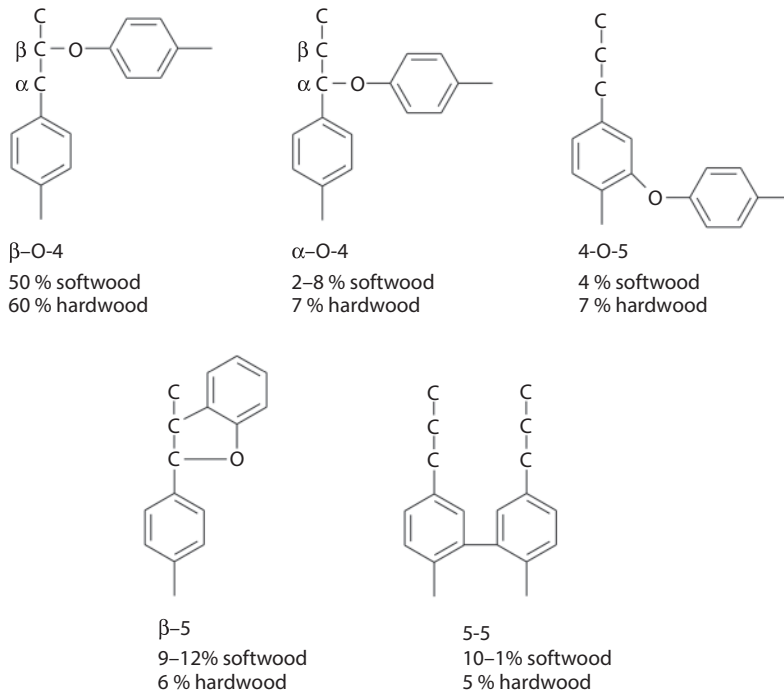


Figure 7.9 Intramonomer linkages in lignin and their abundance (Sjöström, 1993).

“Soda process” based on alkaline hydrolysis (sodium hydroxide) is becoming the main method used for delignification of non-wood materials (straws, hemp, kenaf, sisal etc.) The “soda lignin” is carboxyl-rich due to oxidation of aliphatic hydroxyl groups and contains no sulfur, so it is considered a good dispersant and a candidate for conversion into high value products.

Another type of commercially available lignin is “organosolv” from extraction with organic solvents (e.g., formic acid or ethanol). It contains no sulfur and has lower molecular weight and higher hydrophobicity. Genetic origin and extraction method determine the properties of a lignin. In consequence, the physical and chemical properties determine the purpose lignin can be used for and how can be processed. For instance, as reported in the literature molecular weight can vary from 800 g/mol for hardwood organosolv lignin to 3,000 g/mol for softwood Kraft lignin. The carboxyl groups abundance ranges from 3.6% to 13.6% for organosolv and soda lignin, respectively, while phenolic hydroxyl content varies between 2.6 and 5.1% for wheat straw soda lignin and soda bagasse lignin, respectively (Doherty *et al.*, 2011). Glass transition temperature T_g , which can be associated with crystallinity and degree of cross-linking, indicates viscoelastic region of the material. Due to variable chemical structure, functionality and molecular weight T_g may vary from 91–97 °C to 138–160 °C for lignin of different origin (Gargulak & Lebo, 2000).

Another type of lignin is called “bio-oil” obtained from pyrolysis in which about 70% of wood is converted into crude product. In the process defragmentation of lignin macromolecule takes place and low-molecular fractions are yielded (Sahaf *et al.*,

2014; Zhou *et al.*, 2014; Liaw *et al.*, 2013). The process results in formation of methyl-, methoxy- and vinyl-substituted phenols as well as carbonyl- and carboxyl-functionalized lignin oligomers. The applicability of the bio-oil in material science has not been widely recognized yet and remains open.

Thus, such wide range of chemical and physical properties makes lignin a reservoir of aromatic raw materials for polymer technology. Hence, two roles can be indicated for lignin: (1) low-molecular reagent in thermosetting or chemosetting materials and (2) thermoplastic polymer for matrix forming. Therefore, some types of lignin exhibit thermoplastic-like nature and can possibly be processed by extrusion, especially when grafted or plasticized with long-chain compounds providing reduced brittleness and decreased T_g . Such materials can be considered a prospective replacement for polyolefins. Other types of lignins – especially when water-soluble – can be used as components of adhesives.

In general, the direct use of lignin as a monomer or oligomer in the synthesis of resins (epoxy, polyurethane or phenolic) is limited by its low reactivity in comparison to phenol. In order to overcome that problem, lignin reactivity can be increased by: (1) hydroxymethylation, (2) demethylation, (3) phenolation at carbon α position or (4) epoxidation (Dence & Lin, 1992). The respective reactions of practical significance are shown in Figure 7.10. Other modification and functionalization reactions have been discussed in details in a review paper by Laurichesse & Avérous, (2014).

A modified lignin is a feasible substitute for phenol. In numerous works on lignin-phenol-formaldehyde (LPF) adhesives it was clearly demonstrated that substitution of 10 to 50% phenol for lignin allowed retention of mechanical properties of the bond lines. The environmental effect of using a renewable substitute for phenol can be additionally increased by the replacement of formaldehyde with other aldehydes – e.g., glyoxal (Mansouri *et al.*, 2007). The performance of the latter adhesive system was sufficient to meet international standards when applied for particleboards. Another option for the application of LPF resins is manufacturing of oriented strand boards (OSB) where the LPF adhesives were successfully used in the industrial scale.

A less recognized, but still effective, approach to lignin cross-linking in wood adhesives is the reaction with polyethyleneimines (PEI) as reported by Geng & Li, (2006). The composites produced with the use of lignin-PEI binder exhibit high water resistance and high shear strength even after a boiling water test.

An alternative approach to employing lignin in the field of adhesives is an *in situ* enzymatic oxidation by oxidoreductase – e.g., laccase and peroxidase. These enzymes can be used for the oxidation of wood components and subsequent bond formation. The chemistry is based on the oxidation of lignin, followed by the formation of phenoxy radicals and secondary cross-linking. The concept was evaluated on fiber- and particleboards (Felby *et al.*, 1997, Felby *et al.*, 2002). Though mechanical performance of the enzymatically bonded panels was close to those found for the reference bonded with urea-formaldehyde resin, the economic feasibility of the process is questionable. In Figure 7.11, laccase-mediated cross-linking of lignin model compound was shown (Bohlin *et al.*, 2005). A more recent excellent example of the use of laccase-treated lignin in an adhesive formulation can be found in the work by Ibrahim *et al.*, (2013). Adhesives based on the combinations of lignin with polyethyleneimine, chitosan and soy protein were investigated. Laccase-treated adhesive showed significant water resistance after two boiling water cycles and drying.

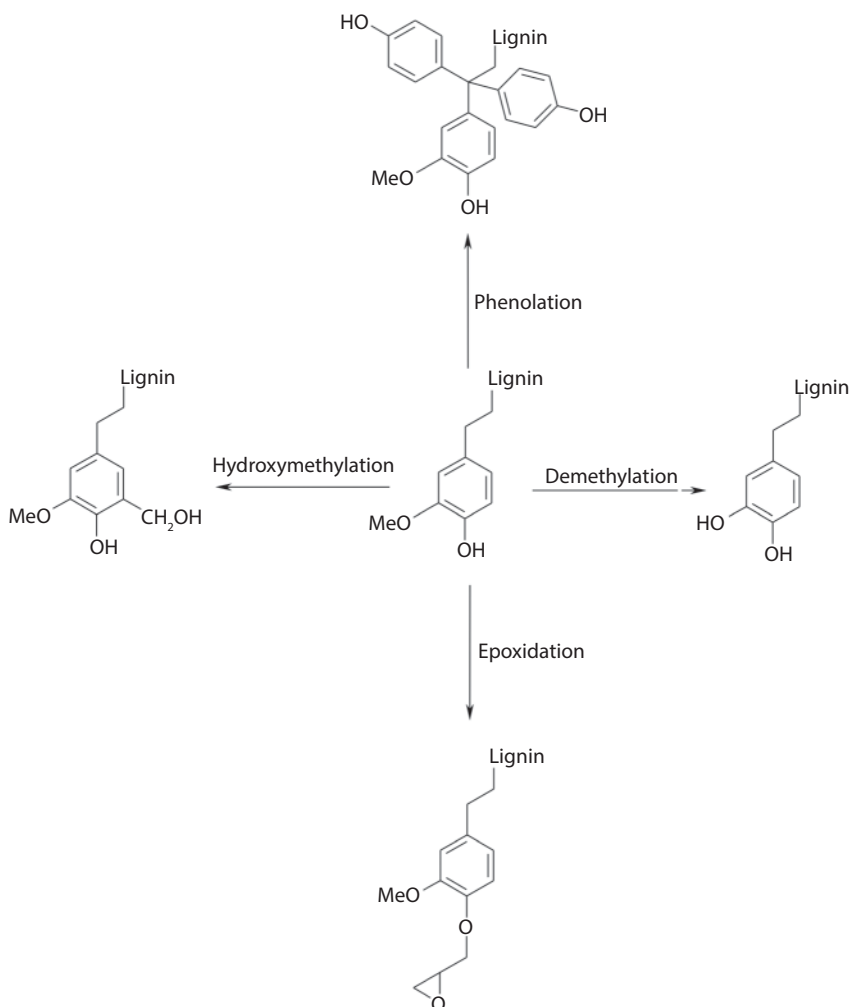


Figure 7.10 Lignin functionalization reactions.

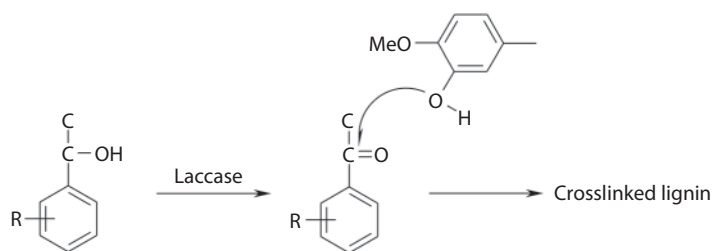


Figure 7.11 Laccase-mediated cross-linking of lignin model compound (Bohlin *et al.*, 2005).

The other option for lignin utilization are the components of polyurethanes. Since hydroxymethylated lignin possesses more active sites for isocyanate to attack, the combinations of lignin-isocyanate or lignin-PF-isocyanate with high lignin content were successfully employed for exterior-grade particleboard manufacturing (Chahar *et al.*, 2004).

Though lignin is a readily available renewable material and much effort has been done to develop lignin-based adhesives, its application in industrial scale is still limited due to low reactivity and poor repeatability of lignin quality.

Other applications of lignin are polymeric matrices. Detailed discussion on lignin applications in encapsulation agents, hydrogels, sorbents or carbon material precursors can be found in the comprehensive reviews dedicated to those fields (Thakur & Thakur, 2015; Norgren & Edlund, 2014; Duval & Lawoko, 2014; Thakur *et al.*, 2014a–d).

Epoxidation is an interesting pathway to extend the area of lignin application. When functionalized with epoxy groups, lignin can be used as a bio-derived component of the epoxy systems. Usually epoxidation with epichlorohydrin is performed on a methyloated or glyoxylated lignin instead of an original (Mansouri *et al.*, 2011). Epoxies are a versatile class of chemosetting polymers and they are very convenient materials for the composite matrices. Thus, a wide range of lignin-based epoxy matrices was developed: epoxidized lignin-poly(propylene oxide) (Hofmann & Glasser, 1993a,b), biodegradable lignin esters with caprolactone, ethylene succinate and polylactic acid (Hirose *et al.*, 2003; Hirose *et al.*, 2005).

Another type of chemosetting matrices lignin can be used for are foams. The modifications that increase the content of primary hydroxyls in a molecule (e.g., hydroxymethylation) – make the use of lignin in polyurethanes more efficient. However, as Hatakeyama and Hatakeyama (2010) state some types of lignin (Kraft from pulping, sulfine pulping and hydrolysis lignin from bioethanol plant) can be used without a pretreatment. It was demonstrated that after ready dissolution in glycols a lignin can be used directly in foam formulations and should not be neglected as a renewable feedstock. In the same work composites with bio-derived polyurethane matrix and wood powder (50–90% content) as a filler were reported and their thermal and mechanical performance was discussed. Recent studies regarded lignin-PMDI foams (Šercer *et al.*, 2010) or synthetic bio-based polyol system (Hatakeyama & Hatakeyama, 2010) were reported. A microwave-assisted synthesis of soft foams from kraft lignin with water as a blowing agent was shown by Cinelli *et al.*, (2013). Lignin nanoparticle-reinforced phenolic foams or rigid polyurethane foams from oxypropylated lignins are the other types of foams recently developed.

Thermoplastics are an important class of polymeric matrices since they are inherently prone to thermoforming and, further, when compounded with organic or inorganic filler, to form a composite material. Various types of lignin have been blended with other types of polymers so far. However, some limitations are to be overcome.

The main problem is to render a good compatibility between non-polar polymer and polar lignin. The modification is aimed at the reduction of abundance of hydroxyl groups. Typically performed modifications are alkylation or esterification with anhydrides. The approach greatly improves compatibility and leads to the blends exhibiting valuable properties. The use of anhydrides of various chain length is a tool to enhance compounding with polycaprolactone, polyethylene, polypropylene and poly(hydroxybutyrate). The weight fraction of lignin determines such properties like melting point, crystallinity or glass transition temperature. But it must be stressed that lignin polyesterification reactions are still a challenge, since, high hydroxyl functionality of lignin favors cross-linking which must be avoided for a thermoplastic material. Blending of lignin with thermoplastics like polyethylene, polypropylene, polyethylene

oxide, polyvinylchloride and polyethyleneterephthalate have successfully been carried out.

Graft-copolymerization gives a way to new thermoplastic materials. A number of lignin-grafted copolymers can be found in the literature, namely: lignin-polystyrene, lignin-poly(acrylic acid) or lignin-poly(vinyl acetate). These graft copolymers were proved to be useful as matrices for nanocomposites of great mechanical properties.

Sahaf *et al.*, (2013) analyzed the thermoplastic behavior of phenolic-rich bio-oil fraction. They showed that the material properties were tunable and as such may be useful in melt processing and adhesive technologies.

Fox & McDonald, (2010) have synthesized a series of industrial lignin-based thermoplastic polyesters with the properties comparable to those of polyolefins and polyethyleneterephthalate. It was also shown that polycondensation of triethanolamine and adipic acid with an industrial lignin was an efficient route to a new type of thermoplastic material (Sivasankarapillai & McDonald, 2011).

In conclusion to the issues mentioned above, it can be stated that the use of lignin in adhesive and polymer matrix applications is challenging. Although high content of reactive sites makes lignin an excellent platform for chemical modifications, the method of isolation and lignin origin strongly affect its macromolecular structure, so that elaborated protocols for conversion do not always work.

7.5 Polysaccharides

The most abundant polysaccharides naturally occurring in nature are cellulose and starch (Voicu *et al.*, 2016). The main source of cellulose is wood while cereals and potatoes are the main sources of starch. Both polysaccharides are produced in billions tones annually. That is why they have been being paid attention for years. The third polysaccharide of interest is chitosan – a fully or partially deacetylated product of chitin which is the main constituent of crustaceans shells. In general polysaccharides do not produce strong innate adhesive interactions, thus a proper conversion is required.

7.5.1 Starch

Starch macromolecule is built of α -D-glucose monomers, but linked in two types of chains: linear amylose and branched amylopectin. The fractions ratio depends on the starch botanic origin, namely amylase content is as follows: potato – 21%, corn – 28%, waxy corn – 3%, wheat – 28%, tapioca – 17%. Before starch is used as an adhesive, it needs to be gelatinized by heating, alkalia, acids or oxidation. However, due to the intrinsic properties of starch, it is not useful for most applications. Therefore, in order to extend its application area, starch is subjected to modifications. The main routes exploited today are: addition of new properties/functionalities and blending with other materials. The typical batch modifications used to be performed in tank reactors. The approach was inconvenient because of the cost, yields and difficulties with processing. Today, the reactive extrusion modification becomes a new solution (Moad, 2011). The mode has been reported effective for: (1) base-catalyzed hydroxypropylation with propylene oxide, (2) cross-linking with epichlorohydrin, (3) copolymerization with cyclic

lactones and (4) esterification with anhydrides, carboxylic acids and vinyl esters. Other conversions aimed at starch utilization in composites are as follows: coupling with agents improving compatibility with other polymers (isocyanates, anhydride plus peroxide, radical grafting, oxidation) and hydrolysis and glycolysis to produce low molecular products.

Since starch-based adhesives are weak when compared to the synthetic ones, it is necessary to strengthen them. As mentioned above, the most investigated routes are grafting and oxidation. The main directions of starch utilization are polyurethane adhesives and hot-melts. Starch degradation is an efficient route to raw materials useful for polyurethane binders. Desai *et al.*, (2003) proposed the approach where glycosides were transesterified with vegetable oils to yield biopolyols. More recent works confirm the efficiency of the use in wood adhesives (Gu *et al.*, 2010; Zhang *et al.*, 2015, Xu *et al.*, 2014). Besides polyurethanes, hot-melts are the area starch-derivates can be applied in. The first starch-based hot-melts adhesives were patented a decade ago. However, the recent starch conversions regard blends with lactic acid and propionate derivatives with glycerol for biodegradable hot melts applications (Inkinen *et al.*, 2008; Zhang *et al.*, 2014).

An alternative approach is oxidizing with formation of formyl and carboxyl groups followed by grafting with vinyl monomers and radical polymerization (Zhang *et al.*, 2015, Li *et al.*, 2015; Wang *et al.*, 2012). The approach revealed that the higher vinyl acetate/starch ratio was, the better dry and wet bond line performance was rendered. The idea of starch modification was shown in Figure 7.12.

Native starch is not thermoplastic, thus only after a proper conversion does it become thermoformable. Thermoplastic starch and its blends can be molded into a variety of products. According to Zhang *et al.*, (2008) the mechanical properties of thermoplastic

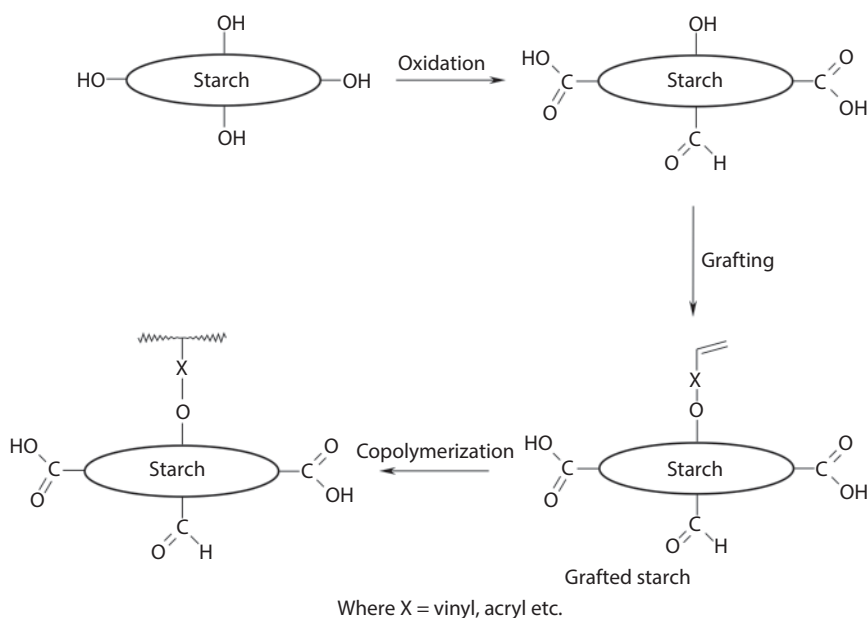


Figure 7.12 Starch oxidizing followed by grafting.

starch greatly depend on the origin and additives and they can vary in a wide range, namely, tensile strength 0.2–11 MPa, elongation at break 3–101% and elastic modulus 3–1050 MPa. The most common plasticizers are water, glycerol, glycols, sugars or urea, amides and amino acids. Other components of starch-based matrix composites are: non-biodegradable polymers like polyethylene, biodegradable (polyvinyl alcohol, polylactide, polycaprolactone, polypropylene carbonate, polylactic acid, poly-3-hydroxybutyrate), lignocelulosic fibers or nanoclays. Addition of polymers renders significantly improved mechanical properties, fibers improved stress transfer, while nanoclays increased both mechanical and thermal resistance. An undoubted advantage of the approach is an opportunity to control and tune thermomechanical properties of a blend.

7.5.2 Cellulose

As far as cellulose is concerned, many efforts have recently been made in cellulose fiber-based composites, nanocellulose and fiber treatments. The comprehensive review papers are available in the literature (Mokhothu & John, 2015; Lavoine *et al.*, 2015; Pappu *et al.*, 2015; Thakur *et al.*, 2014b; Thakur & Thakur, 2014b). Composites reinforcement with cellulose fibers is out of the scope of this chapter. Therefore, it is limited to the chemical conversion of cellulose to components of adhesives and composite matrices.

Cellulose is a biopolymer built of repeating units of β -D-glucose linked via ether linkages. Degree of polymerization of cellulose is up to 20,000. Its annual production exceeds 7.5×10^{10} tons (Habibi *et al.*, 2010). High hydroxyl functionality in a cellulose macromolecule provides strong intra- and intermolecular hydrogen bonds to give highly crystalline structure and lack of solubility in common solvents. Therefore, neat cellulose is not useful as a binder. Moreover, weak adhesive interactions between cellulose and non-polar matrix materials limit its applications. In order to overcome that shortcomings treatments are required. An improvement of compatibility with a variety of matrices can be achieved by reduction in hydroxyl group number – i.e., epoxidation, esterification with anhydride, acetylation (Ifuku *et al.*, 2007), silylation (Gousse *et al.*, 2004), carboxymethylation, oxidation or grafting with diisocyanates (Siqueira *et al.*, 2010). Main routes to cellulose derivatives are shown in Figure 7.13. The approach was proved to be effective in terms of compatibilization of cellulose fibers with non-polar matrices. However, for the matrix-formation purposes a soluble or thermoplastic cellulose is required.

Insolubility of cellulose can be overcome by a proper derivatization. Cellulose esters with aliphatic acid anhydrides (cellulose acetate, propionate, butyrate and their mixed esters) and ethers (ethylcellulose, carboxymethylcellulose, hydroxymethylcellulose) are the most important derivatives (Table 7.2) that are used either as adhesives or thermoplastics.

So-called “liquefied wood” is another cellulose-derived resource of the components for adhesives. It is a product of acid-catalyzed chemical degradation of cellulose in presence of phenol, glycols, glycerol or cyclic carbonates (Yamada & Ono, 1999). The solvolysis yields a mixture of cellulose and hemicelluloses degradation products that can be used as polyols for polyurethanes or reagents for phenol-formaldehyde resins,

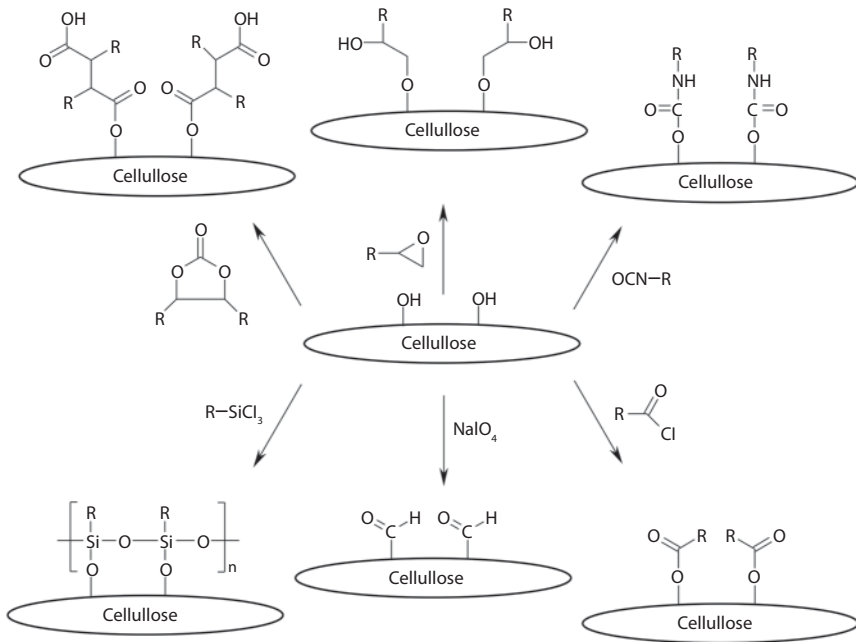


Figure 7.13 Common cellulose modifications.

Table 7.2 Most important cellulose derivatives and applications.

Material	Solubility	Application
hydroxyethyl cellulose	water	adhesive, paper products
carboxymethyl cellulose	water	thickener for adhesives
ethylcellulose	organic solvent	film forming, hot-melt adhesive
methyl cellulose	water	film forming, ceramics adhesive
cellulose acetate butyrate	organic solvent	hot-melt adhesive, solvent-borne adhesive
cellulose acetate	organic solvent	plastics, thermoforming

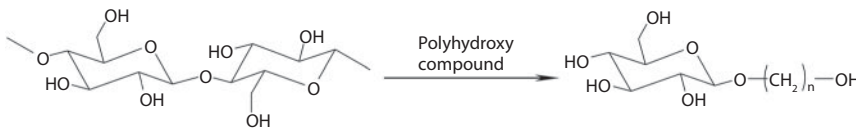


Figure 7.14 Solvolysis of cellulose.

aminoresins and epoxies (Kobayashi *et al.*, 2001) (Figure 7.14). Although large number of options for the use of cellulose in adhesives have been developed, the significance of cellulose-based binders is still lower than that of the starch-based ones.

Moldable thermoplastic derivatives of cellulose can be the basis of polymeric matrices for the bio-based composites, however, cellulose di- and triacetates have been dominating in this field for a long time. Another convenient approach to yield moldable and

castable form of cellulose is peroxide oxidation, which generates highly reactive formyl groups that can further be derived. Oxidized cellulose followed by cationization (e.g., with amines) was proved to be an efficient route to the thermoformable and castable celluloses (Sirviö *et al.*, 2014).

7.5.3 Chitosan

Chitin is a polysaccharide naturally comprising exoskeletons of crustaceans, mollusks and insects. A natural lack of solubility in aqueous solutions is an obstacle for chitin to be further processed. However, chitin deacetylated derivative – chitosan, poly[β -(1 \rightarrow 4)-2-amino-2-deoxy-d-glucopyranose], is readily soluble in diluted aqueous acid solutions of pH below 6.5 (e.g., p-toluene sulfonic, formic, acetic, 10-camphorosulfonic acids).

The deacetylation degree and molecular weight affect the properties of chitosan as well as its solubility and viscosity of the solutions. For the deacetylation degree ranging from 40% to 98%, the molecular weight range is 5×10^4 Da – 2×10^6 Da (Mourya *et al.*, 2008). Usually deacetylation is carried out under alkaline conditions or via enzymatic hydrolysis (Ryu *et al.*, 2015). The structural changes rendered from deacetylation are shown in Figure 7.15.

High molecular weight and high viscosity of solutions make chitosan a valuable component of wood adhesives (Umemura *et al.*, 2003) and polymer matrices like films, hydrogels, foams, fibers or membranes. Biocompatibility and biodegradability make chitosan especially useful matrix polymer in biomedical (tissue engineering, wound dressings, textiles etc.), environmental, food and packaging applications. Chitosan films inhibit microbial growth, thus they are dedicated to food packaging. Their mechanical properties are comparable to those of the cellulose films.

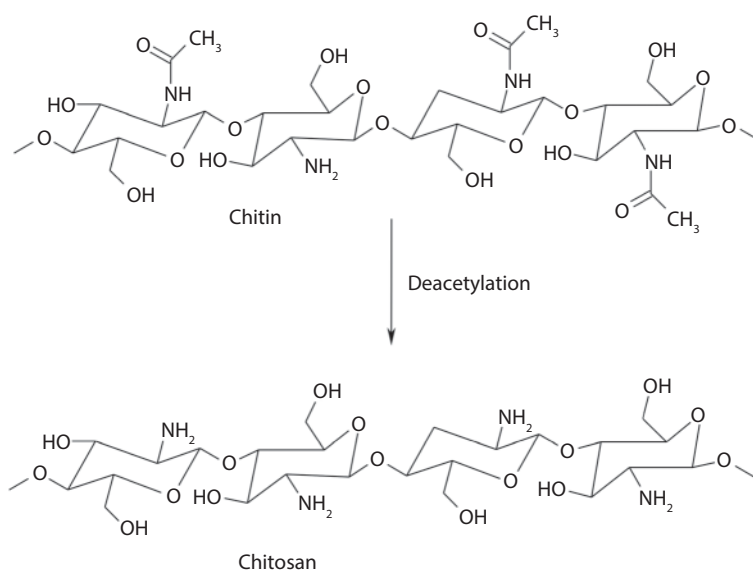


Figure 7.15 Deacetylation of chitin.

In order to obtain oligo- and monomers for chemical processing, high-molecular chitosan can be subjected to chitonolysis. The main routes to chitosan oligomers involve: (1) deamination with HNO_2 , (2) heating and (3) enzymes like chitosanase, pronase, pectinase, lipase or papain. Degrees of polymerization of products range from 1 to 40. But not only are these methods applicable for chitosan oligomerization. Other efficient procedures are based on chemoenzymatic and physical approaches (Mourya *et al.*, 2008).

Chitosan is an amendable compound with amine and hydroxyl functions. Thus, both in the form of high molecular polysaccharide and low molecular chitoooligomer, it is an excellent platform for further conversion. Many efforts have been made to modify chitosan. The most important functionalizations are: quaternization, N-acylation, N- or O-carboxyalkylation, and hydroxyalkylation. A wider scope of possible modifications can be found in the review paper by Mourya *et al.*, (2008). Another common type of chemical conversion of polysaccharides is a graft copolymerization. In order to graft vinyl or acrylic polymer or monomer, a free radical induced polymerization approach is undertaken. The route goes via generation of free radicals onto chitosan backbone and its further action as a macroinitiator. An extensive review of chitosan graft modifications was done by Thakur & Thakur, (2014a).

The number of chitosan-based material applications other than biomedical is limited. However, chitosan was proved to be a convenient component of biodegradable composite polyethylene-chitosan films exhibiting antifungal and antibacterial activity (Quiroz-Castilloa *et al.*, 2014; Martínez-Camacho *et al.*, 2010).

Though stretch, the significance of chitosan has recently been exposed in the domain of adhesives. Chitosan was successfully involved in the konjac glucomannan/chitosan/polypeptide thermosetting adhesive systems (Shang *et al.*, 2015), while methacrylate-modified chitosan was applied in the dentine bonding systems (Diolosa *et al.*, 2014).

These examples shown above indicate substantial potential of chitosan in the novel chitosan-based materials and composites. However, domain of biomedical applications still dominates.

7.6 Proteins

Chemical structure of proteins is very complex. The primary structure involves chains of amino acid residues linked with peptide bonds in a unique sequence, the secondary structure defines the spatial orientation (α -helix, β -sheet, globular) of the polypeptide chains linked with intra- and intermolecular hydrogen bonds, while tertiary structure is related with the overall geometry and shape of a protein. The diversity of macromolecules results from large number of possible combinations in the sequence of 20 common amino acids. In consequence, the structure and properties of proteins depend on their biological origin. Proteins are present in plants and animals. The main resources of proteins are cereals (soy, wheat, canola etc.) and animal tissue like tendons, hoof, horn, feather and epidermis. The peak for use of animal proteins (i.e., collagen) as an adhesive was from the years 1930 through 1960, until they were replaced with synthetic resins. Nowadays, the main bioresource of proteins for the material applications are crops. Animal proteins like casein, collagen, and albumin are not available in the

amounts sufficient to quench the demand of modern technology, thus their industrial significance is narrow.

The annual production of soy beans in the United States only reaches 220 million tons which makes 36% of global production. Soy beans contain 40% to 50% of proteins that are convenient raw material for further processing. Unlike soy, the more common crops in Europe are canola (*Brassica L.*), wheat (*Triticum L.*), maize (*Zea mays L.*) and leguminous pea (*Pisum sativum L.*). Their beans contain, respectively, 17–36 %, 12%, 7–12% and 14–39% of crude protein. Soy protein can be in the form of flour, concentrate and protein isolate (54%, 70% and 90% protein, respectively). The three most abundant amino acids in soy, maize and pea proteins are shown in Table 7.3 and their chemical structures in Figure 7.16.

Protein macromolecules are abundant in functional groups (amine, carboxyl, hydroxyl and thiol) that make them reactive toward many reagents. However, it is necessary to disintegrate their tertiary structure and open the macromolecule, so reactive sites are available for a reagent (Lépine *et al.*, 2015). The process is called denaturation and can be realized by the chemical or physical means. The former are acids, bases, urea or cationic agents. When alkaline treatment is applied, the unfolding of tertiary structure and hydrolysis of secondary and primary structures occur.

Large numbers of reactive sites in a molecule allows to readily cross-link protein, so that a polymer network is produced. When properly carried out, mechanical and physico-chemical properties of a polymer matrix can be improved. Cross-linking can be induced both by a number of physical (irradiation, heat) or chemical factors: aldehydes,

Table 7.3 Main aminoacids in soy, maize and pea proteins (Santoni & Pizzo, 2013).

Protein origin	Protein component		
	1st most abundant	2nd most abundant	3rd most abundant
soy	glutamic acid (18.7%)	aspartic acid (11.7%)	leucine (7.8%)
maize	glutamic acid (23.1%)	leucine (14.8%)	alanine (7.5%)
pea	glutamic acid (16.7%)	aspartic acid (11.5%)	arginine (8.7)

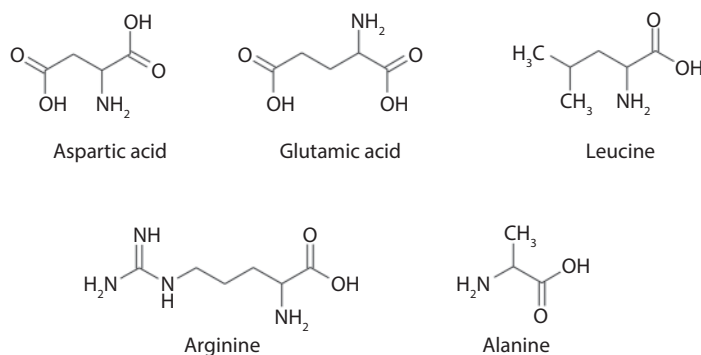


Figure 7.16 Structures of the main aminoacids present in soy, maize and pea proteins.

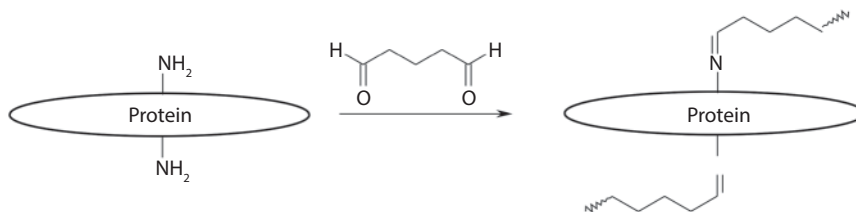


Figure 7.17 Protein cross-linking with glutaraldehyde.

acids, alcohols and ketones. An exemplary cross-linking reaction with an aldehyde was presented in Figure 7.17.

Using soybean isolates as adhesives is not new – the first patent is from 1923. In general, for feasible dispersing in water, the protein must be alkaline treated, so the uncoiled molecules expose polar moieties that contribute to the adhesive interactions with a substrate. The obvious drawbacks of soy glues are a-few-hours pot-life and dark-colored glue line because of alkali-induced wood degradation. The viscosity of the adhesive can be easily adjusted with water to the required value (500–30,000 mPas) depending on the purpose. Soy-based binders can be used for cold- or hot-bonding.

Recently, numerous new routes to soy-based adhesives have been reported. Thermosetting soybean-furfural resins were applied as adhesives for plywood (Lèpine *et al.*, 2015). An aqueous dispersion as a binder for particle boards was also investigated. Huang & Li, (2008) developed a soy protein-based adhesive cured with maleic anhydride-modified polyethyleneimine (Figure 7.18). The approach allowed formulation of adhesive to pass standardized boiling tests for the plywood. Typical bonding was performed at 160 °C for 2–6 minutes.

However, the solutions that have been successfully implemented in industry are formaldehyde-free 2-component soy-based adhesive systems cross-linked with poly-amidoamine epichlorohydrin resin (PAE). Protein content ranges from 43% to 65%. Cross-linking involves reaction between amine or carboxylic groups of protein with the azetidine cation of PAE (Figure 7.19). Recently, the third generation of these adhesives has entered the market. Reformulation allowed for lowering viscosities, so that they became applicable in flooring and wood-based composites like plywood, MDF and particleboard manufacturing. An additional advantage of the soy-based adhesives is their miscibility with synthetic amino resins, which renders reduction in formaldehyde emission.

Wheat gluten produced in amounts ca. 100,000 tons annually was demonstrated to be a valuable component of adhesives. In 2006 Krug and co-workers successfully developed protein-phenol-formaldehyde resins for wood based composites industry where phenol had been replaced for wheat protein. The manufactured MDF and particleboards met the requirements of the standards, so that scaling up of the solution was undertaken.

Proteins can be transformed into polymer matrices via two basic pathways: dry and wet forming. The dry processing requires the use of additives. When protein-rich mixture is subjected to thermoforming (molded, extruded or injected); in order to avoid protein degradation, it is required to add plasticizers. Then processing can be performed below protein decomposition temperature. At elevated temperatures and

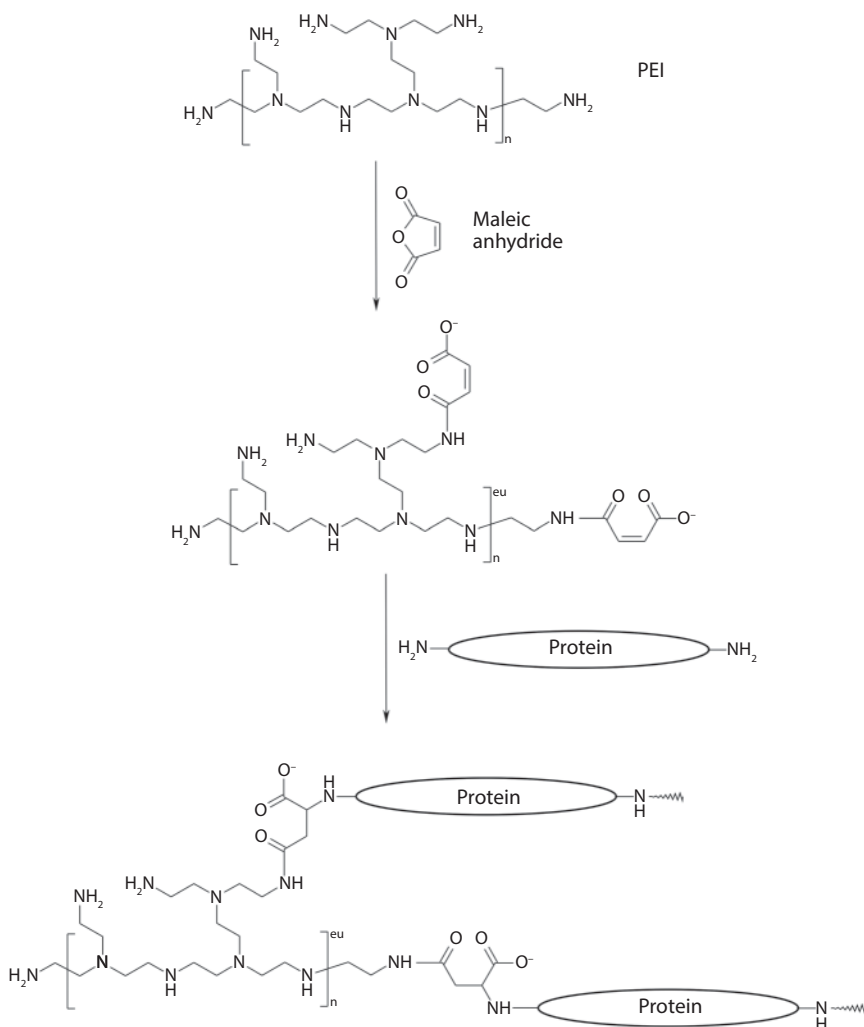


Figure 7.18 Soy protein curing with anhydride-modified polyethyleneimine (Huang & Li, 2008).

shear force a protein undergoes structural rearrangements like dissociation, unfolding and subsequent cross-linking. Proper formulation of the mixture allows to control final properties of the protein-based matrix, i.e., hydrophobicity, moduli, flexibility, glass transition temperature, crystallinity etc (Shi & Dumont, 2014).

Wet process involves forming by casting and drying. At the first step a protein is solubilized in an alkaline solution. This is a critical point, since it takes long time and its efficiency depends on the chemical composition and biological origin of the protein. Thus, the wet process is less convenient to perform than the dry method.

The maize protein-based films were widely described by Shi & Dumont, (2014). A raw material is zein – a protein isolated from maize. Film casting can be realized either from aqueous solutions or from zein-fatty acid emulsion. The latter approach significantly improves mechanical properties of the films. However, it was also shown that such systems are prone to phase separation with time (Lai *et al.*, 1997). In order to

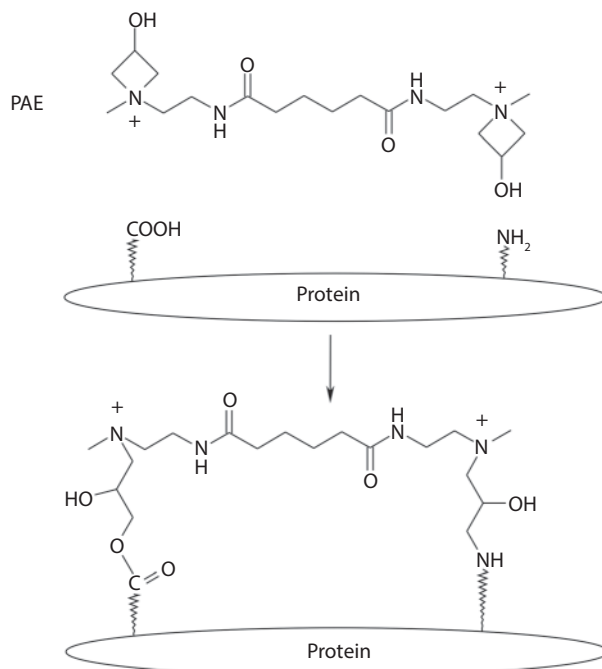


Figure 7.19 The chemistry of PAE-protein reactions.

overcome that inconvenience two pathways may be considered: (1) cross-linking with reactive plasticizer or (2) coating with a drying oil (e.g., flax oil) followed by curing with UV or γ -irradiation (Wang & Padua, 2005). Dependently on the forming method, additives and product form (sheet, slab etc.), the mechanical properties of the zein-based matrices range from 311 to 1967 MPa, 0.8–270% and 0.04–11.6 MPa, respectively, for modulus, elongation at break and tensile strength (Selling *et al.*, 2009; Oliviero *et al.*, 2010).

Main applications of the zein-based polymers are food packaging, tissue engineering, drug delivery and edible films when plasticized with sugars (Shi & Dumont, 2014). Though there are reports on the use of pea, canola and wheat proteins in matrix material preparation, their practical significance is limited.

In contrary to the above mentioned resources, soy protein utilization is much wider. Tens of examples of soy protein-based polymeric matrices can be found in a comprehensive and recent review by Koshy *et al.*, (2015). It has been shown that feedstock availability and environmentally benign character of the soy-based polymers make them useful in the composites with cellulose, starch, chitin and chitosan, as well as in the hybrid inorganic filler-reinforced composites and many more. Another advantage of soy proteins is a wide range of methods for composite preparation – namely: extrusion, compression molding, hot pressing, solvent casting, injection molding, impregnation or electrospinning.

Thus, it is apparent that that soy and other proteins produced in large quantities have potential to replace petroleum-derived feedstock in plastics and in composite materials as well.

7.7 Oils

Ancient people already revealed feasibility of drying oils as binders in varnishes and paints. In the last 20 years, when bioresources attract attention of industry and academia, the interest in oils returned. In general, oils can be divided into two main groups: edible (palm, rapeseed, sunflower, soybean etc.) and non-edible (cashew nut shell liquid, castor, tung, tall etc.). They are available in huge amounts from plants. A vegetable oil molecule is built of glycerol moiety and fatty acid residues (Figure 7.20). Typically, fatty acid residue has 14 to 22 carbons and 0 to 3 double bonds. The exact structure depends on the botanic origin.

Such structures possess two reaction sites (ester unit and C=C functions) that can be conveniently converted into monomers for polymer synthesis. The ester group can be transesterified to monoglycerides and then subjected to further reactions: (1) polycondensation, (2) esterification, (3) amidification and (4) thioesterification (Desroches *et al.*, 2012).

The other reaction sites are double bonds to give way for a range of modifications. Thus, it is apparent that the chemical structure of vegetable oils makes them an excellent platform for further multidirectional transformation into polymeric materials. Most important transformation routes are shown in Figure 7.21. The approaches have been widely reported as effective in the development of polymeric networks both in adhesives and polymer matrices.

Unmodified oils may undergo radical polymerization in the presence of oxygen from air. The higher unsaturated functionality of an oil, the easier auto-polymerization is. The degree of unsaturation is the factor that determines whether an oil is drying, semi-drying or non-drying and is expressed by the iodine number (the amount of iodine in mg to react with C=C bonds in 100g of oil): > 130, 100–130 and < 100, respectively. The unmodified vegetable oils have been demonstrated to act as co-monomers in radical polymerizations with vinyl and acrylic co-monomers to form plastics exhibiting a wide range of physico-mechanical properties (Xia & Larock, 2010).

The derivatized vegetable oils are convenient monomers for adhesives and matrix synthesis. The general pathways for conversion of oil into polyol can be indicated (Desroches *et al.*, 2012). These are: (1) double bond epoxidation followed by ring opening, (2) alcoholysis of epoxidized oil, (3) hydrogenation of epoxy groups, (4) epoxide opening with a diol, (5) carbonation of epoxide, (6) hydroformylation of double bonds and (7) addition of formaldehyde.

A widely used non-edible oil naturally suitable for polyurethanes is castor oil – a triglyceride of ricinoleic acid bearing OH group which is a site in the reactions with



Figure 7.20 General structure of vegetable oil.

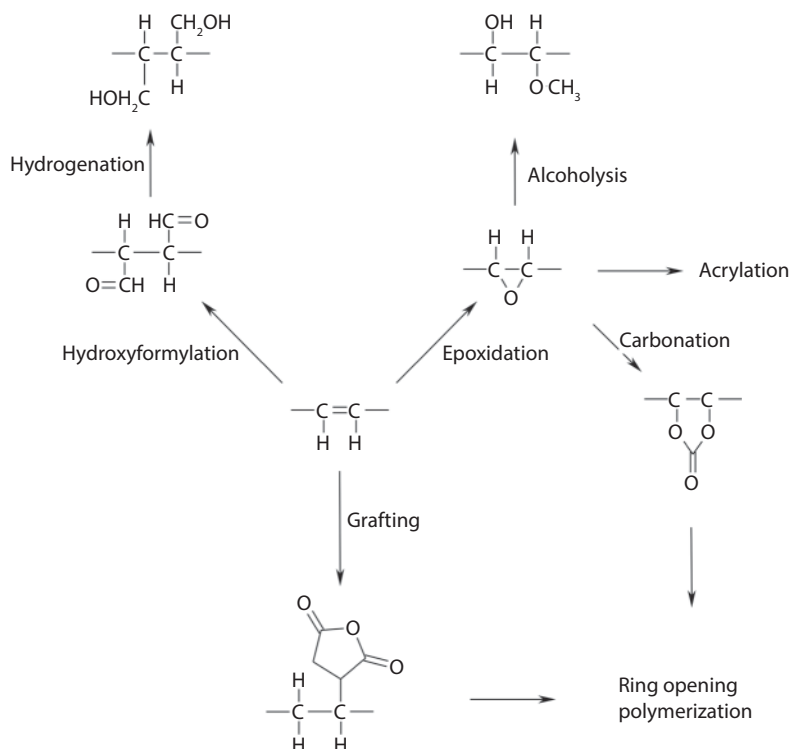


Figure 7.21 Pathways for transformation of double bond in oils.

isocyanates. The approaches like (1) direct reaction of the unmodified OH-bearing oil with diisocyanate (Silva *et al.*, 2010), (2) the use of polyester polyols obtained from castor oil and saccharide (Desai *et al.*, 2003) or (3) hydroxylation of double bond for increased hydroxyl functionality have been elaborated. But it is worth noting that the approaches are applicable to other vegetable oils (i.e., soybean oil), too.

Another oil of practical significance in adhesives is cashew nut shell liquid (CNSL) obtained from *Anacardium occidentale* (Figure 7.22). Phenol residue present in the molecule structure makes it a suitable substitute for phenol in the synthesis of phenol-formaldehyde resins. The concept has been implemented in practice.

Although the epoxidized soybean and linseed oils are commercially available, the research on other modifications and utilization pathways is being continued. The routes to functionalization of oils presented in Figure 7.21 allow development of thermo- and chemosetting polymer matrices. Parzuchowski *et al.*, (2007) investigated application of carbonated soybean oil as a toughener in epoxy matrix. Other examples of use of acrylated epoxidized soybean oil as the matrices for glass fiber- and natural fiber-reinforced composites or in foams are available in the literature, too.

For the detailed discussion on synthetic methods for oil-based polyesters, polyethers and polyamides reference to the reviews is advised (Xia & Larock, 2010; Miao *et al.*, 2014).

Minding all the routes indicated above, it seems clear that a wide variety of products can be yielded from the functionalized vegetable oils, and, it becomes much wider when possible subsequent derivatization is performed.

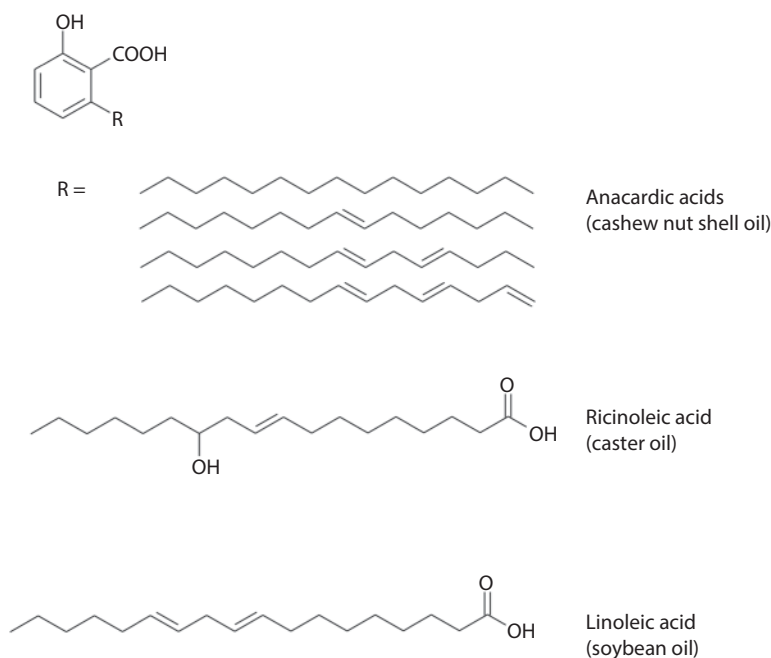


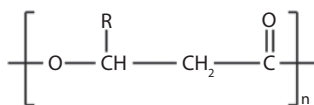
Figure 7.22 Main components of cashew nut shell liquid, castor oil and soybean oil.

7.8 Microorganism-produced Biopolymers

7.8.1 Polyhydroxyalkonates (PHAs)

One of the main concerns of the growing human population is huge amounts of non-degradable waste materials released to the environment. Most of them are well-known polyolefins and polyesters of petrochemical origin. They are consumed in the amount of 140 million tons per annum and it takes decades for them to decompose. For this reason an interest in producing environmentally-friendly biodegradable plastics has grown. An alternative for petroleum-derived plastics are the biopolymers synthesized by various organisms. Among them, the most widely produced microbial biopolymers are polyhydroxyalkanoates (PHA). PHAs are composed of 3-hydroxycarboxylic acid units forming linear polyesters. In Figure 7.23 general structure of PHAs is shown.

PHA are polyesters of hydroxyalkanoates synthesized in bacteria, yeast, plant and animal cells. PHA are produced as the constituent of the cell or they are accumulated inside the bacteria cell as the nutrient reserve and are degraded to carbon dioxide and water by the microorganisms synthesizing PHA depolymerases in a few months (Jendrossek, 2001). Well-known natural producer of storage PHA is *R. eutropha* which can store the amount of PHA equal to 90% of its dry weight. Non-storage PHA, having low molecular weight (e.g. poly(3hydroxybutyrate – P3HB), have been found in organisms' cell membrane, cytoplasm and cytoplasmic membrane (e.g. *E. coli*, *Bacillus megaterium*, *B. cereus*, *B. megaterium*). Storage PHAs are produced by gram-positive and gram-negative bacteria of 75 genera, mainly members of the family *Halobacteriaceae* of the *Archea*. This way they gain carbon and energy reserves. Storage PHA are of high molecular weight (50,000–1,000,000 Da) and can be composed of more than a



R =	C ₁	poly (3-hydroxybutyrate)	PHB
	C ₂	poly (3-hydroxyvalerate)	PHV
	C ₃	poly (3-hydroxyhexanoate)	PHH
	C ₄	poly (3-hydroxyheptanoate)	PHO
	C ₅	poly (3-hydroxyoctanoate)	
	[...]		
	C ₁₃	poly (3-hydroxyhexadecanoate)	PHHD

Figure 7.23 General structure and nomenclature of the PHAs.

hundred different monomer units. Produced PHA structure and properties depend on the organism (Ha & Cho, 2002). Among bacteria-produced PHAs over 150 different constituents have been identified. The most often are short-length PHAs containing 3-hydroxybutyrate units or medium-length PHAs bearing hydroxyoctanoate (HO) and hydroxydecanoate (HD) units (Anderson & Dawes, 1990).

They are divided into three groups with respect to the monomer size: short-length PHA – up to 5 monomer units, medium-length PHA with 6-14 monomer units and long-chain PHAs with more than 14 monomer units. Short-chain length PHAs like homopolymer PHB are stiff and brittle bioplastics. Their properties are similar to conventional plastics, which limits their use. Typical PHB elongation at break and modulus reach, respectively, 15% and above 1,000 MPa.

PHAs made of longer monomers like medium-length PHAs are similar to elastomers and rubbers in character. PHA copolymers of HB with long-chain monomers like hydroxyvalerate (HV), hydroxyhexanoate (HH), hydroxyoctanoate (HO) are flexible and tough materials used in many different products such as containers, bottles and food packaging. Water-resistant layers of paper, film or cardboard are produced from the latex of PHAs. PHB and copolymer P(HB-HV) was used in the diapers (Martini *et al.*, 1989). As PHAs' degradation products are 3-hydroxyacids naturally existing in the human body, they are also biocompatible, which makes them favorable material for biomedical applications like implants, gauzes, sutures, and drug delivery (capsules, tablets) (Zinn *et al.*, 2001; Chen & Wu, 2005 a,b).

Co-feeding upon biosynthesis results in heteropolymers with different monomers combinations (e.g. 3-hydroxybutyrate, 3-hydroxyvalerate, 3-hydroxyhexanoate or 4-hydroxybutyrate), so that, poly(3-hydroxybutyrate-co-3-hydroxyvalerate) can be produced. Modification of the quantity and type of the carbon source in the growth medium affects the composition of products (Steinbüchel & Schlegel, 1991). For example, presence of propionic or valeric acid yields the hydroxybutyrate/hydroxyvalerate copolymer. Natural producers of PHA, such as *R. eutropha*, are not efficient in industrial production due to long time to grow. For this reason fast-growing bacteria, such as

E.coli, has been genetically modified for efficient PHA homopolymers and copolymers production. Under optimal culturing conditions recombinant *E.coli* is able to store up to 85% of the cell dry weight. By changing glucose and fatty acid concentration in the medium, it is possible to change the copolymer composition (Lu *et al.*, 2004). It has been also shown that some bacteria strains, e.g., *A. eutrophus*, *Rhizobium* *Nocardia* can produce PHA from lower volatile fatty (Kalia *et al.*, 2000). However, the cost of PHA production by bacteria is high in comparison with petroleum-derived polymers. That is why many studies have been taken on PHA production in eukaryotic cells, e.g., yeasts. Unfortunately, PHA accumulation in *Saccharomyces cerevisiae* turned out to be very low, about 1% of dry weight. The other route of investigation, alternative to bacterial production, is PHA production by genetically engineered plants. (Bohmert *et al.*, 2000).

High molecular weight of bacterial PHB and other PHA makes their characteristics similar to conventional plastic like polypropylene. For matrix molding purposes PHAs and their co-polymers are blended with PLA or other thermoplastic materials (starch, polycaprolactone, poly(vinyl acetate) etc.).

PHAs are considered water insoluble, soluble in chlorinated solvents, relatively resistant to hydrolysis, resistant to UV, low resistant to acids and bases and weak adhesive in molten state. A molecule is built up of 600 to 35,000 hydroxy fatty acid units with a saturated alkyl group in the side chain (Khanna & Srivastava, 2005). Average molecular weight of a polymer is 1,000 to 10,000. Chemical structures of common PHAs are depicted in Figure 7.20. Depending on the chemical structure, the polymers exhibit elastomeric or thermoplastic properties. Thermal and mechanical properties of the commercial PHAs can vary in a wide range: melting points 160–176 °C, T_g from non-detectable to 125 °C, crystallinity 30 to 70%, elongation at break 2–1200% tensile strength 10–39 MPa and modulus 300–3800 MPa (Bugnicourt *et al.*, 2014). Most of the thermoforming processes are applicable to PHAs, i.e., injection molding, extrusion or blowing.

The features like biocompatibility, biodegradability, high crystallinity and insolubility in water make PHAs excellent renewable raw materials for a wide range of applications. They are used in the production of packaging materials, and disposable hygiene articles such as diapers. Their biodegradability allows using PHAs in, for example, drug delivery or long-term dosage of herbicides and hormones. They are also used in medicine as bone plates or vessel replacements, and synthesis of medicines. Depolymerized PHAs can be used for the production of bulk chemicals, especially “green solvents.”

7.8.2 Polylactic Acid

Poly(lactide) – PLA – is a popular biodegradable polymers is aliphatic polymer. It is produced via synthetic route (Figure 7.24) or by bacterial fermentation. PLA is a biopolymer of lactic acid produced by two-step process: (1) bacterial fermentation of starch-rich crops e.g. corn, rice, sugarcane, lignocellulosic biomass into lactic acid and (2) polymerization. The fermentation of lactic acid may be heterofermentative or homofermentative depending of the type of bacteria used for the process.

PLA can be produced in one-step process by recombinant *Escherichia coli* with the employment of transferase isolated from *Clostridium propionicum* and *Pseudomonas sp.* PMEL6-19 polyhydroksyalkanoate synthase 1 (Yang, 2010). By using the engineered

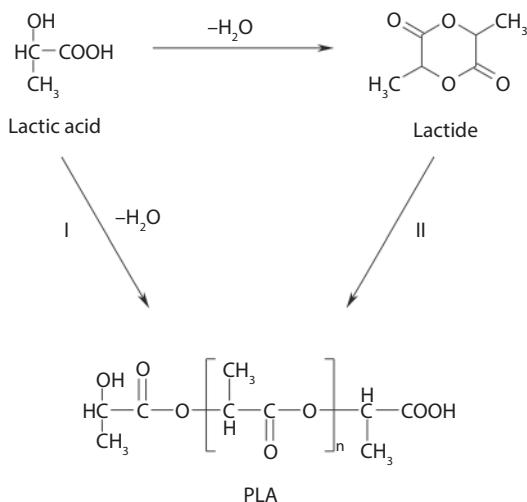


Figure 7.24 Synthetic route to PLA from lactic acid (I) and lactide (II).

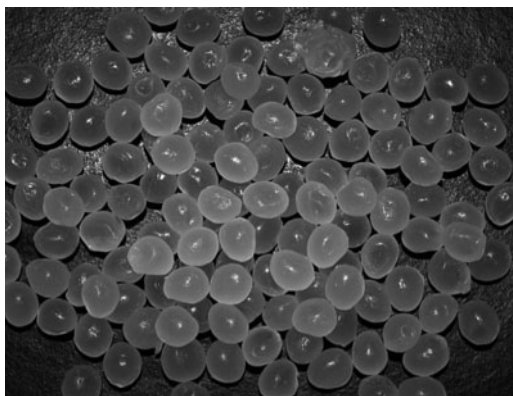


Figure 7.25 PLA pellets for thermoforming.

E. coli strain PLA homopolymer was produced from glucose up to 11%wt. Most lactic acid bacteria need complex growth medium composition with the addition of vitamins, amino acids, fatty acids, yeast extract, peptones, beef extract etc. for efficient growth and biological activity.

The synthesis of PLA is usually realized via two routes: (1) a condensation of lactic acid and (2) ring-opening polymerization of lactide. Direct PLA condensation is the cheapest method, but ring-opening polymerization allows for obtaining PLA of the highest purity. In direct condensation PLA of $M_w > 300,000$ is obtained. In ring-opening polymerization D-lactic acid or L-lactic acid are prepolymerized into low molecular weight PLA followed by a depolymerization to a mixture of lactide stereoisomers. Purified lactides are polymerized into PLA with molecular weight above 100,000.

The physical, mechanical and chemical properties like crystallinity, hardness or glass transition temperature of PLA depend on proportions of L-, meso- and D-isomers. For example, PLA with 93% L-stereoisomer content is semicrystalline, while PLA with 50–93% L-lactic acid is amorphous. In Figure 7.25, pelletized PLA for thermoforming is shown.

Besides many advantages of PLA like biodegradability, biocompatibility and unlimited accessibility, Gregorova & Wimmer, (2014) indicate some drawbacks, too. These are: high price, high brittleness and low compatibility with hydrophilic materials (fillers, substrates etc.). Most common pathways to overcome those shortcomings are: (1) plasticizing, (2) blending with other polymers and (3) derivatization/partial depolymerization. The treatments are aimed at the reduction in stiffness/brittleness, lowering melting point and increasing the abundance of polar groups that is necessary to improve and strengthen interactions with substrate in bonding and with fillers in matrices as well.

PLA is a convenient thermoplastic. Typical mold temperature is 120–210 °C depending on the grade. However, its high glass transition temperature (55–65 °C) needs to be lowered for some applications. Thus, PLA can be plasticized with, for example, triacetine, poly(ethylene glycol) or low molecular citrates. In order to improve processability and rheologic properties upon thermoforming, PLA is copolymerized or blended with poly(ethylene oxide), poly(vinyl acetate), poly(caprolactone) or poly(hydroxyalkonates). In biodegradable composites, PLA can work as a matrix for the reinforcing additives like carbon nanotubes, natural or synthetic fibers, microfibrillated cellulose, nanomaterials, wood flour and many others.

However, due to a small amount of hydrophilic groups in the macromolecule, the effect of the compounding is often ambiguous. For instance, the tensile strength of the PLA/wood flour (30 vol. %) composite decreased, while modulus of elasticity increased (Gregorova & Wimmer, 2014). The phenomena are explained by low interfacial adhesion between wood and PLA, and, on the other hand, the changes in PLA crystallinity. Thus, the weak interfacial interactions of PLA with a filler (natural or synthetic fibers, nanomaterials, lignocellulosics, etc.) is a problem to overcome. It was shown by Wu, (2009) that the use of maleic anhydride-grafted PLA as a matrix greatly improved adhesive interactions and compatibility between the filler and PLA by formation of ester bonds. Maleic anhydride was also found to be effective compatibilizer for the blends with thermoplastic starch. Other compatibilizers useful in blending with polyolefins are: glycidyl methacrylate and maleic anhydride-grafted polypropylene.

Another approach to increasing hydrophilicity is a controlled depolymerization of PLA (Figure 7.26). The procedure allows to yield PLA esters with lower molecular weights (Leibfarth *et al.*, 2012). The treatment was effective in transesterification of PLA with glycols, so that, after secondary esterification with succinic anhydride, the polyesters with Mw between 4,700 and 11,200 Da and glass transition temperature about 10 °C were obtained.

PLA is the material that attracted great attention in respect to use in biomedical applications. The properties that are especially important in medicine are compatibility with blood and tissues and non-toxic degradation. It is also bioresorbable (does not

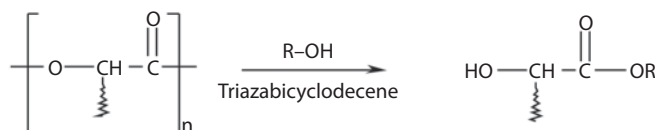


Figure 7.26 Transesterification of PLA with alcohol.

require mechanical removal) which creates the possibility of application of PLA in the production of medical implants, biodegradable sutures, resorbable prostheses, intravascular stents, suture anchors or in tissue engineering. Biodegradation allowed for using PLA as drug carriers in the form of microcapsules, microspheres, pellets and tablets. PLA-based composites are also used as substrates for skin grafts or in orthopedics (Vainionpaa *et al.*, 1989; Middleton & Tripton, 2000).

Biodegradation and food safety makes PLA great packaging material. It also has favorable physical properties such as high elastic modulus, transparency and high melting temperature. For these reasons PLA was used in the coated papers, disposable cutlery as well as in food and beverage containers. One of the common applications of PLA is films. Thin sheets of PLA are used for the production of packaging and waste bags biodegrading within 4-6 weeks.

Hence, poly(lactide) seems to be a potential, versatile, valuable and environmentally benign green matrix polymer useful in a number of applications. However, before it is commercialized in adhesives and composites areas, the issues of high price, weak interfacial interactions and mechanical performance need to be overcome.

References

- Anderson, A.J., Dawes, E.A., Occurrence, metabolism, metabolic role and industrial use of bacteria polyhydroxyalkanoates. *Microbiol. Rev.*, 54, 450, 1990.
- Barbosa Jr., V., Ramires, E.C., Razera, I.A.T., Frollini, E., Biobased composites from tannin-phenolic polymers reinforced with coir fibers. *Ind. Crops Prod.*, 32, 305, 2010.
- Bisanda, E.T.N., Ogola, W.O., Tesha, J.V. Characterization of tannin resin blends for particle board applications. *Cement. Concrete Comp.*, 25, 593, 2003.
- Bohlin, C., Persson, P., Gorton, L., Lundquist, K., Jönsson, L.J., Product profiles in enzymic and non-enzymic oxidations of the lignin model compound erythro-1-(3,4-dimethoxyphenyl)-2-(2-methoxyphenoxy)-1,3-propanediol. *J. Mol. Catal. B: Enzym.* 35, 100, 2005.
- Bohmert, K., Balbo, I., Kopka, J., Mittendorf, V., Narath, C., Poirier, Y., Tischendorf, G., Trethewey, R.N., Willmitzer, L. Transgenic Arabidopsis plants can accumulate polyhydroxybutyrate to up to 4% of their fresh weight. *Planta*, 211, 841, 2000.
- Bugnicourt, E., Cinell, P., Lazzeri, A., Alvarez, V., Polyhydroxyalkanoate (PHA): Review of synthesis, characteristics, processing and potential applications in packaging. *eXPRESS Polym. Lett.*, 8, 791, 2014.
- Chahar, S., Dastidar, M.G., Choudhary, V., Sharma, D.K., Synthesis and characterisation of polyurethanes derived from waste black liquor lignin. *J. Adhes. Sci. Technol.*, 18, 169, 2004.
- Chen, G.Q., Wu, Q., Microbial production and applications of chiral hydroxyalkanoates. *Appl. Microbiol. Biotechnol.*, 67, 592, 2005a.
- Chen, G.Q., Wu, Q., The application of polyhydroxyalkanoates as tissue engineering materials. *Biomaterials*, 26, 6565, 2005b.
- Cinelli, P., Anguillesi, I., Lazzeri, A., Green synthesis of flexible polyurethane foams from liquefied lignin. *Eur. Polym. J.*, 49, 1174, 2013.
- Ciriminna R., Della Pina C., Rossi, M., Pagliaro, M., Understanding the glycerol market. *Eur. J. Lipid Sci. Technol.*, 116, 1432, 2014.
- Dai, J., Ma, S., Wu, Y., Han, J., Zhang, L., Zhu, J., Liu, X., Polyesters derived from itaconic acid for the properties and bio-based content enhancement of soybean oil-based thermosets. *Green Chem.*, 17, 2383, 2015.

- Dence, C.W., Lin, S.Y., General structure features of lignin, in: *Methods in lignin chemistry*, S.Y. Lin., C.W. Dence (Eds.), pp. 3–17, Springer-Verlag, Berlin, 1992.
- Desai, S.D., Patel, J.V., Sinha, V.K., Polyurethane adhesive system from biomaterial-based polyol for bonding wood. *Int. J. Adhes. Adhes.*, 23, 393, 2003.
- Desroches, M., Escouvois, M., Auvergne, R., Caillol, S., Boutevin, B., From vegetable oils to polyurethanes: Synthetic routes to polyols and main industrial products. *Polym. Rev.*, 52, 38, 2012.
- Diosolá, M., Donati, I., Turco, G., Cadenaro, M., Di Lenarda, R., Breschi, L., Paoletti, S., Use of methacrylate-modified chitosan to increase the durability of dentine bonding systems. *Biomacromolecules*, 15, 4606, 2014.
- Doherty, W.O.S., Mousavioun, P., Fellows, C.M., Value-adding to cellulosic ethanol: Lignin polymers. *Ind. Crops Prod.*, 33, 259, 2011.
- Duval, A., Lawoko, M., A review on lignin-based polymeric, micro- and nano-structured materials, *React. Funct. Polym.*, 85, 78, 2014.
- Felby, C., Hassingboe, J., Lund, M., Pilot-scale production of fiberboards made by laccase oxidized wood fibers: board properties and evidence for cross-linking of lignin. *Enzym. Microb. Technol.*, 31, 736, 2002.
- Felby, C., Pedersen, L.S., Nielsen, B.R., Enhanced autocondensation of wood fibers using phenol oxidases. *Holzforschung*, 51, 281, 1997.
- Fox, S.C., McDonald, A.G., Chemical and Thermal Characterizaion of three Industrial Lignins and their Corresponding Lignin Esters. *BioResources*, 5, 990, 2010.
- Gargulak, J.D., Lebo, S.E., Commercial use of lignin-based materials. *ACS Symp. Ser.* 742, 304, 2000.
- Geng, X., Li, K., Investigation of wood adhesives from kraft lignin and polyethyleneimine. *J. Adhes. Sci. Technol.*, 8, 847, 2006.
- Gousse, C., Chanzy, H., Cerrada, M.L., Fleury, E., Surface silylation of cellulose microfibrils: Preparation and rheological properties. *Polymer*, 45, 1569, 2004.
- Gregorova, A., Wimmer, R., Filler-matrix compatibility of poly(cactic acid) based composites, in: *Poly(lactic Acid: Synthesis, properties and applications*, V. Piemonte (Ed.), pp. 97–119, Nova Science Publications, Inc., New York, 2014.
- Gu, J.Y., Zuo, Y.F., Zhang, Y.H., Tan, H.Y., Zhu, L.B., Shen, J., Preparation of plywood using starch adhesives modified with isocyanate. *Appl. Mech. Mater.*, 26–28, 1065, 2010.
- Ha, C.S., Cho, W.J., Miscibility, properties and biodegradability of microbial polyester containing blends. *Prog. Polym. Sci.*, 2002, 27, 759, 2002.
- Habibi, Y., Lucia, L.A., Rojas, O.J., Cellulose nanocrystals: Chemistry, self assembling, and applications. *Chem. Rev.*, 110, 3479, 2010.
- Hatakeyama, H., Hatakeyama, T., Lignin Structure, Properties, and Applications. *Adv. Polym. Sci.*, 232, 1, 2010.
- Hirose, S., Hatakeyama, T., Hatakeyama, H., Synthesis and thermal properties of epoxy resins from ester- carboxylic acid derivative of alcoholysis lignin. *Macromol. Symp.*, 197, 157, 2003.
- Hirose, S., Hatakeyama, T., Hatakeyama, H., Curing and glass transition of epoxy resins from ester-carboxylic acid derivatives of mono- and disaccharides and alcoholysis lignin. *Macromol. Symp.* 224, 343, 2005.
- Hofmann, K., Glasser, W.G., Engineering plastics from lignin. 21. Synthesis and properties of epoxidized lignin-poly(propylene oxide) copolymers. *J. Wood Chem. Technol.*, 13, 73, 1993a.
- Hofmann, K., Glasser, W.G., Engineering plastics from lignin. 22. Cure of lignin-based epoxy resins. *J. Adhes.*, 40, 229, 1993b.
- Huang, J., Li, K., A New soy flour-based adhesive for making interior type II plywood. *J. Am. Oil Chem. Soc.*, 85, 63, 2008.

- Ibrahim, V., Mamo, G., Gustafsson P.-J., Hatti-Kaul, R., Production and properties of adhesives formulated from laccase modified Kraft lignin. *Ind. Crops Prod.*, 45, 343, 2013.
- Ifuku, S., Nogi, M., Abe, K., Handa, K., Nakatsubo, F., Yano, H., Surface modification of bacterial cellulose nanofibers for property enhancement of optically transparent composites: Dependence on acetyl-group DS. *Biomacromolecules*, 8, 1973, 2007.
- Inkinen, S., Stolt, M., Sodergard, A., Stability studies on blends of a lactic acid-based hot melt adhesive and starch. *J. Appl. Polym. Sci.*, 110, 2467, 2008.
- Jana, P., Fierro, V., Pizzi, A., Celzard, A., Biomass-derived, thermally conducting, carbon foams for seasonal thermal storage. *Biomass Bioenerg.*, 67, 312, 2014.
- Jendrossek, D., Microbial degradation of polyhydroalkanoates. *Annu. Rev. Microbiol.*, 56, 403, 2002.
- Kalia, V.C., Raizada, N., Sonakya, V., Bioplastics. *J. Sci. Ind. Res.*, 59, 433, 2000.
- Khanna, S., Srivastava, A.K., Recent advances in microbial polyhydroxyalkanoates. *Process Biochem.*, 40, 607, 2005.
- Kobayashi, M., Hatano, Y., Tomita, B., Viscoelastic properties of liquefied wood/epoxy resin and its bond strength. *Holzforschung*, 55, 667, 2001.
- Koshy, R., Mary, S.K., Thomas, S., Pothan, L.A., Environment friendly green composites based on soy protein isolate. A review. *Food Hydrocolloid.*, 50, 174, 2015.
- Krug, D., Tobisch, S., Hepp, W., Gozzi, A., New low-emissive resins for moisture-resistant-bonded wood-based panels. *5th European Wood-Based Panel Symposium*, 4–6 October, Hannover, Germany, 2006.
- Lai, H.M., Padua, G.W., Wei, L.S., Properties and microstructure of zein sheets plasticized with palmitic and stearic acids. *Cereal Chem.*, 74, 83, 1997.
- Laurichesse, S., Avérous, L., Chemical modification of lignins: Towards biobased polymers, *Prog. Polym. Sci.*, 39, 1266, 2014.
- Lavoine, N., Desloges, I., Dufresne, A., Bras, J., Microfibrillated cellulose - Its barrier properties and applications in cellulosic materials: A review. *Carbohydr. Polym.*, 90, 735, 2012.
- Leibfarth, F.A., Moreno, N., Hawker, A.P., Shand, J.D., Transforming polylactide into value-added materials. *J. Polym. Sci. Pol. Chem.*, 50, 4814, 2012.
- Lépine, E., Riedl, B., Wang, X.-M., Pizzi, A., Delmotte, L., Hardy, J.-M., Da Cruz, M.J.R., Synthesis of bio-adhesives from soybean flour and furfural: Relationship between furfural level and sodium hydroxide concentration. *Int. J. Adhes. Adhes.*, 63, 74, 2015.
- Li, K., Geng, X., Simonsen, J., Karchesy, J., Novel wood adhesives from condensed tannins and polyethylenimine. *Int. J. Adhes. Adhes.*, 24, 327, 2004.
- Li, Z., Wang, J., Li, C., Gua, Z., Li, C., Hong, Y., Effects of montmorillonite addition on the performance of starch-based wood adhesive. *Carbohydr. Polym.*, 115, 394, 2015.
- Liaw, S.-S., Zhou, S., Wu, H., Garcia-Perez, M., Effect of pretreatment temperature on the yield and properties of bio-oils obtained from the auger pyrolysis of Douglas fir wood. *Fuel*, 103, 672, 2013.
- Liu, Y., and K. Li. Preparation and characterization of demethylated lignin-polyethylenimine adhesives. *J. Adhes.*, 82, 593, 2006.
- Lora, J.H., Glasser, W.G., Recent industrial applications of lignin: A sustainable alternative to nonrenewable materials. *J. Polym. Environ.*, 10, 39, 2002.
- Mamiński, M. *Applicability of hyperbranched polyglycerols as components of wood adhesives*. WULS Press, Warsaw, 2013 (in Polish).
- Mamiński, M., Parzuchowski, P., Trojanowska, A., Dziejewski, Sz., Fast-curing polyurethane adhesives derived from environmentally friendly hyperbranched polyglycerols - the effect of macromonomer structure. *Biomass Bioenerg.*, 35, 4461, 2011.
- Mamiński, M., Szymański, R., Parzuchowski, P., Antczak, A., Szymona, K., Hyperbranched polyglycerols with bisphenol A core as glycerol-derived components of polyurethane wood adhesives. *BioResources*, 7, 1440, 2012.

- Manosuri, H.R., Navarrete, P., Pizzi, A., Tapi-Lingua, S., Benjelloun, B., Pasch, H., Rigolet, S., Synthesis-resin-free wood panel adhesives from mixed low molecular mass lignin and tannin. *Eur. J. Wood. Prod.*, 69, 221, 2011.
- Mansouri, N.E., Yuan, Q., Huang, F., Synthesis and characterization of kraft lignin-based epoxy resins. *Bioresources*, 6, 2492, 2011.
- Mansouri, N.-E., Pizzi, A., Salvado, J., Lignin-based wood panel adhesives without formaldehyde. *Holz Roh Werkst.*, 65, 65, 2007.
- Martinez de Yuso, A., Lagel, M.C., Pizzi, A., Fierro V., Celzard A., Structure and properties of rigid foams derived from quebracho tannin. *Mater. Design*, 63, 208, 2014.
- Martínez-Camacho, A.P., Cortez-Rocha, M.O., Ezquerro-Brauer, J.M., Graciano-Verdugo, A.Z., Rodríguez-Félix, F., Castillo-Ortega, M.M., Yépiz-Gómez, M.S., Plascencia-Jatomea, M., Chitosan composite films: Thermal, structural, mechanical and antifungal properties. *Carbohydr. Polym.*, 82, 305, 2010.
- F. Martini, L. Perazzo, P. Vietto, Sheets materials of HB polymers, US Patent 4 826493, 1989.
- Meikleham, N.E., Pizzi, A., Acid- and alkali-catalyzed tannin-based rigid foams. *J. Appl. Polym. Sci.*, 53, 1547, 1994.
- Meikleham, N., Pizzi, A., Stephanou, A., Induced accelerated autocondensation of polyflavonoid tannins for phenolic polycondensates. I. ^{13}C -NMR, ^{29}Si -NMR, X-ray, and polarimetry studies and mechanism. *J. Appl. Polym. Sci.*, 54, 1827, 1994.
- Miao, A.S., Wang, P., Su, Z., Hang, S., Vegetable-oil-based polymers as future polymeric biomaterials. *Acta Biomater.*, 10, 1692, 2014.
- Middleton, J.C., Tripton, A.J., Synthetic biodegradable polymers as orthopedic devices, *Biomaterials*, 21, 2335, 2000.
- Miranda, C.S., Fiuza, R.P., Oliveira, J., Carvalho, R.F., Guimarães, D.H., Jose, N.M., Thermal, mechanical and morphological properties of composites developed from glycerol and dicarboxylic acids reinforced with piassava fiber. *Macromol. Symp.*, 319, 74, 2012.
- Moad, G., Chemical modification of starch by reactive extrusion. *Prog. Polym. Sci.*, 36, 218, 2011.
- Mokhothu, T.H., John, M.J., Review on hygroscopic aging of cellulose fibres and their biocomposites. *Carbohydr. Polym.*, 131, 337, 2015.
- Mourya, V.K., Inamdar, N.N., Chitosan-modifications and applications: Opportunities galore. *React. Funct. Polym.*, 68, 1013, 2008.
- Ndazi, B., Tesha, J.V., Karlsson, S., Bisanda, E.T.N., Production of rice husks composites with Acacia mimosa tannin-based resin. *J. Mater. Sci.* 41, 6978, 2006.
- Norgren, M., Edlund, H., Lignin: Recent advances and emerging applications. *Curr. Opin. Colloid In.*, 19, 409, 2014.
- Oliviero, M., Di Maio, E., Iannace, S., Effect of molecular structure on film blowing ability of thermoplastic zein. *J. Appl. Polym. Sci.*, 115, 277, 2010.
- Pappu, A., Patil, V., Jain, S., Mahindrakar, A., Haque, R., Thakur, V.K., Advances in industrial prospective of cellulosic macromolecules enriched banana biofibre resources: A review. *Int. J. Biol. Macromol.*, 79, 449, 2015.
- Parzuchowski, P.G., Kizlińska, M., Rokicki, G., New hyperbranched polyether containing cyclic carbonate groups as a toughening agent for epoxy resin. *Polymer*, 48, 1857, 2007.
- Pichelin, F., Nakatani, M., Pizzi, A., Wieland, S., Despres, A., Rigolet, S. Structural beams from thick wood panels bonded industrially with formaldehyde-free tannin adhesive. *Forest. Prod. J.*, 56, 31, 2006.
- Pizzi, A., Natural phenolic adhesives I: Tannin, in: *Handbook of adhesive technology*, A. Pizzi, K.L. Mittal (Eds.), pp. 347–358, Marcel Dekker, New York, 2003.
- Pizzi, A., *Advanced Wood Adhesives Technology*, pp.149–215, Marcel Dekker, New York, 1994.
- Quiroz-Castillo, J.M., Rodríguez-Félix, D.E., Grijalva-Monteverde, H., del Castillo-Castro, T., Plascencia-Jatome, M., Rodríguez-Félix, F., Herrera-Franco, P.J., Preparation of extruded

- polyethylene/chitosan blends compatibilized with polyethylene-graft-maleic anhydride. *Carbohydr. Polym.*, 101, 1094, 2014.
- Rai, R., Tallawi, M., Grigore, A., Boccaccini, A.R., Synthesis, properties and biomedical applications of poly(glycerol sebacate) (PGS): A review. *Prog. Polym. Sci.*, 37, 1051, 2012.
- Ramires, E.C., Frollini, E., Tannin-phenolic resins: synthesis, characterization, and application as matrix in biobased composites reinforced with sisal fibers. *Compos. Part B-Eng.*, 43, 2851, 2012.
- Rokicki, G., Rakoczy, P., Parzuchowski, P., Sobiecki, M., Hyperbranched aliphatic polyethers obtained from environmentally benign monomer: glycerol carbonate. *Green Chem.*, 7, 529, 2005.
- Ryu, J.H., Hong, S., Lee, H., Bio-inspired adhesive catechol-conjugated chitosan for biomedical applications: A mini review. *Acta Biomater.* 2015. (in press)
- Sahaf, A., Laborie, M.-P. G., Englund, K., Garcia-Perez, M., McDonald, A.G., Rheological properties and tunable thermoplasticity of phenolic rich fraction of pyrolysis bio-oil. *Biomacromolecules*, 14, 1132, 2013.
- Sánchez-Martín, J., Beltrán-Heredia, J., Delgado-Regaña, A., Rodríguez-González, M.A., Rubio-Alonso, F., Optimization of tannin rigid foam as adsorbents for wastewater treatment. *Ind. Crop Prod.*, 49:507, 2013.
- Santoni, I., Pizzo, I., Evaluation of alternative vegetable proteins as wood adhesives. *Ind. Crops Prod.*, 45, 148, 2013.
- Satyanarayana, K.G., Arizaga, G.G.C., Wypych, F., Biodegradable composites based on lignocellulosic fibers-An overview. *Prog. Polym. Sci.*, 34, 982, 2009.
- Selling, G.W., Woods, K.K., Biswas, A., Willett, J.L., Reactive extrusion of zein with glyoxal. *J. Appl. Polym. Sci.*, 113, 1828, 2009.
- Šercer, M., Raos, P., Rujnić-Sokele, M., Thermal properties of bio- and synthetic-based PUR foams. *Int. J. Mater. Form. 3: Suppl. 1*, 535, 2010.
- Shang, J., Liu, H., Qi, C., Guo, K., Tran, V.C. Evaluation of curing and thermal behaviors of konjac glucomannan-chitosan-polypeptide adhesive blends. *J. Appl. Polym. Sci.*, 132, 42202, 2015.
- Shi, W., Dumont, M.-J., Review: bio-based films from zein, keratin, pea, and rapeseed protein feedstocks. *J. Mater. Sci.*, 49, 1915, 2014.
- Silva, B.B.R., Santana, R.M.C., Forte, M.M.C., A solventless castor oil-based PU adhesive for wood and foam substrates. *Int. J. Adhes. Adhes.*, 30, 559, 2010.
- Singha, A.S., Thakur, V.K., Fabrication and study of lignocellulosic *Hibiscus sabdariffa* fiber reinforced polymer composites. *BioResources*, 3, 1173, 2008a.
- Singha, A.S., Thakur, V.K., Synthesis and characterization of *Grewia optiva* fiber-reinforced PF-based composites. *Int. J. Polym. Mater.*, 57, 1059, 2008b.
- Singha, A.S., Thakur, V.K., Fabrication and characterization of S. ciliare fibre reinforced polymer composites. *B. Mater. Sci.*, 32, 49, 2009a.
- Singha, A.S., Thakur, V.K., Physical, chemical and mechanical properties of Hibiscus sabdariffa fiber/polymer composite. *Int. J. Polym. Mater.*, 58, 217, 2009b.
- Singha, A.S., Thakur, V.K., Mechanical, thermal and morphological properties of *Grewia optiva* fiber/polymer matrix composites. *Polym. Plast. Technol. Eng.*, 48, 201, 2009c.
- Singha, A.S., Thakur, V.K., *Grewia optiva* fiber reinforced novel, low-cost polymer composites. *Journal of Chemistry*, 6, 71, 2009d.
- Singha, A.S., Thakur, V.K., Mechanical, morphological, and thermal characterization of compression-molded polymer biocomposites. *Int. J. Polym. Anal. Ch.*, 15, 87, 2010.
- Singha, A.S., Thakur, V.K., Synthesis, Characterization and Study of Pine Needles Reinforced Polymer Matrix Based Composites. *J. Reinf. Plast. Compos.* 29, 700, 2010b.
- Singha, A.S., Thakur, V.K., Synthesis and Characterization of Short *Grewia optiva* Fiber-Based Polymer Composites. *Polym. Compos.* 31, 459, 2010c.

- Siqueira, G., Bras, J., Dufresne, A., New process of chemical grafting of cellulose nanoparticles with a long chain isocyanate. *Langmuir*, 26, 402, 2010.
- Sirviö, J.A., Anttila, A.-K., Pirttilä, A.M., Liimatainen, H., Kilpeläinen, I., Niinimäki, J., Horm, O., Cationic wood cellulose films with high strength and bacterial anti-adhesive properties. *Cellulose*, 21, 3573, 2014.
- Sivasankarapillai, G., McDonald, A.G., Synthesis and properties of lignin-highly branched poly (ester-amine) polymeric systems. *Biomass Bioenerg.*, 35, 919, 2011.
- Sjöström, E., *Wood Chemistry Fundamentals and Applications*. Academic Press, Inc., San Diego, 1993.
- Steinbuchel, A., Schlegel, H.G., Physiology and molecular genetics of poly(α -hydroxyalkanoic acid) synthesis in *Alcaligenes eutrophus*. *Mol. Microbiol.*, 5, 535, 1991.
- Suhas, P.J.M., Ribeiro C.M.M.L., Lignin - from natural adsorbent to activated carbon: A review. *Bioresour. Technol.*, 98, 2301, 2007.
- Tang, J., Zhang, Z., Song, Z., Chen, L., Hou, X., Yao, K., Synthesis and characterization of elastic aliphatic polyesters from sebacic acid, glycol and glycerol. *Eur. Polym. J.*, 42, 3360, 2006.
- Thakur, V.K., Singha, A.S., Kaur, I., Nagarajarao, P., Liping, Y., Silane functionalization of *Saccharum cilliare* fibers: thermal, morphological, and physicochemical study, *Int. J. Polym. Anal. Ch.*, 15, 397, 2010.
- Thakur, V.K., Kessler, M.R., Self-healing polymer nanocomposite materials: A review. *Polymer* 69, 369, 2015.
- Thakur, V.K., Thakur, M.K., Recent advances in green hydrogels from lignin: a review. *Int. J. Biol. Macromol.* 72, 834, 2015.
- Thakur, V.K., Thakur, M.K., Recent advances in graft copolymerization and applications of chitosan: A review. *ACS Sustainable Chem. Eng.*, 2, 2637, 2014a.
- Thakur, V.K., Thakur, M.K., Processing and characterization of natural cellulose fibers/thermoset polymer composites. *Carbohydr. Polym.*, 109, 102, 2014b.
- Thakur, V.K., Thakur, M.K., Raghavan, P., Kessler, M.R. Progress in green polymer composites from lignin for multifunctional applications: A review. *ACS Sustainable Chem. Eng.*, 2, 1072, 2014a.
- Thakur, V.K., Thakur, M.K., Gupta, R.K., Review: Raw Natural Fiber-Based Polymer Composites. *Int. J. Polym. Anal. Ch.*, 19, 256, 2014b.
- Thakur, V.K., Thakur, M.K., Gupta, R.K., Graft copolymers of natural fibers for green composites. *Carbohydr. Polym.* 104, 87, 2014c.
- Thakur, V.K., Vennerberg, D., Madbouly, S.A., Kessler, M.R., Bio-inspired green surface functionalization of PMMA for multifunctional capacitors. *RSC Adv.* 4, 6677, 2014d.
- Tissarat, B., Selling, G.W., Byars, J.A., Stuff, A., Instrumental physical analysis of microwaved glycerol citrate foams. *J. Polym. Environ.*, 20, 291, 2012.
- Tondi, G., Oo, C.W., Pizzi, A., Trosa, A., Thevenon, M.F., Metal adsorption of tannin based rigid foams. *Ind. Crops Prod.*, 29, 336, 2009.
- Tondi, G., Pizzi, A., Tannin-based rigid foams: Characterization and modification. *Ind. Crops Prod.*, 29, 356, 2009.
- Tondi, G., Zhao, W., Pizzi, A., Dub, G., Fierro, V., Celzard, A., Tannin-based rigid foams: A survey of chemical and physical properties. *Bioresour. Technol.*, 100, 5162, 2009.
- Trosa, A., Pizzi, A. A no-aldehyde emission hardener for tannin-based wood adhesives for exterior panels. *Holz Roh Werkst.*, 59, 266, 2001.
- Umemura, K., Inoue, A., Kawai, S. Development of new natural polymer-based wood adhesives I: dry bond strength and water resistance of konjac glucomannan, chitosan, and their composites. *J. Wood Sci.*, 49, 221, 2003.
- Vainionpää, S., Rokkanen, P., Tormala, P., Surgical applications of biodegradable polymers in human tissues. *Prog. Polym. Sci.*, 14, 679, 1989.

- Vázquez, G., González, J., Antorrena, G., Eucalyptus globulus plywoods prepared with tannin phenol-formaldehyde adhesives obtained under various extraction conditions. *Holz Roh Werkst.*, 59, 451, 2000.
- Velayutham, T.S., Abd Majid, W.H., Ahmad, A.B., Kang, G.Y., Gan, S.N., Synthesis and characterization of polyurethane coatings derived from polyols synthesized with glycerol, phthalic anhydride and oleic acid. *Prog. Org. Coat.*, 66, 367, 2009.
- Voicu, S.I., Condruz, R.M., Mitran, V., Cimpean, A., Miculescu, F., Andronesu, C., Miculescu, M., Thakur, V.K., Sericin Covalent Immobilization onto Cellulose Acetate Membrane for Biomedical Applications. *ACS Sustain. Chem. Eng.* 4, 1765, 2016.
- Wang, Q., Padua, G.W., Properties of zein films coated with drying oils. *J. Agric. Food Chem.*, 53, 3444, 2005.
- Wang, Z., Li, Z., Gu, Z., Hong, Y., Cheng, L., Preparation, characterization and properties of starch-based wood adhesive. *Carbohydr. Polym.*, 88, 699, 2012.
- Wu, T., Frydrych, M., O'Kelly, K., Chen, B., Poly (glycerol sebacate urethane)-cellulose nanocomposites with water-active shape-memory effects. *Biomacromolecules*, 2014, 15, 2663, 2014.
- Wu, C.-S., Renewable resource-based composites of recycled natural fibers and maleated polylactide bioplastic: Characterization and biodegradability. *Polym. Degrad. Stabil.*, 94, 1076, 2009.
- Wu, H., Thakur, V.K., Kessler, M.R., Novel low-cost hybrid composites from asphaltene/SBS tri-block copolymer with improved thermal and mechanical properties. *J. Mater. Sci.* 51, 2394–2403, 2016.
- Xia, Y., Larock, R.C., Vegetable oil-based polymeric materials: synthesis, properties, and applications. *Green Chem.*, 2010. 12, 1893, 2010.
- Xu, W.B., Shi J.Y., Wang S.M., Study on heat aging properties of starch based aqueous polymer isocyanate adhesive for wood. *Adv. Mater. Res.*, 933, 138, 2014.
- Yamada, T., Ono, H., Rapid liquefaction of lignocellulosic waste by using ethylene carbonate. *Bioresource Technol.*, 70, 61, 1999.
- Yan, L., Chouw, N., Jayaraman, K., Flax fibre and its composites - a review. *Compos. Part B-Eng.*, 56, 296, 2014.
- Yang, T.H., Kim, T.W., Kang, H.O., Lee, S.H., Lee, E.J., Lim, S.C., Oh, S.O., Song, A.J., Parl, S.J., Lee, S.Y., Biosynthesis of polylactic acid and its copolymers using evolved propionate CoA transferase and PHA synthase. *Biotechnol. Bioengineer.*, 105, 150, 2010.
- Zhang, Y., Longlong, D., Gu, J., Tan, H., Zhu, L., Preparation and properties of a starch-based wood adhesive with high bonding strength and water resistance. *Carbohydr. Polym.*, 115, 32, 2015.
- Zhang, Z., Macquarrie, D.J., Clark, J.H., Matharu, A.S., Chemical modification of starch and the application of expanded starch and its esters in hot melt adhesive. *RSC Adv.*, 4, 41947, 2014.
- Zhang, Y., Liu, Z., Han, J.H., Starch-based edible films, in: *Environmental-Compatible Food Packaging*, E. Chiellini (Ed.), pp. 108–136, Woodhead Publishing, Cambridge, 2008.
- Zhao, Z., Umemura, K., Investigation of a new natural particleboard adhesive composed of tannin and sucrose. *J. Wood Sci.*, 60, 269, 2014.
- Zhou, S., Pecha, B., van Kuppevelt, M., McDonald, A.G., Garcia-Perez, M., Slow and fast pyrolysis of Douglas-fir lignin: Importance of liquid-intermediate formation on the distribution of products. *Biomass Bioenerg.*, 66, 398, 2014.
- Zhou, X., Pizzi, A., Sauget, A., Nicollina, A., Li, X., Celzard, A., Rode, K., Pasch, H., Lightweight tannin foam/composites sandwich panels and the coldset tannin adhesive to assemble them. *Ind. Crops Prod.*, 43, 255, 2013.
- Zinn, M., Witholt, B., Egli, T., Occurrence, synthesis and medical application of bacterial polyhydroxyalkanoate. *Adv. Drug Rev.*, 53, 5, 2001.

Silk Biocomposites: Structure and Chemistry

Alexander Morin, Mahdi Pahlevan and Parvez Alam*

Laboratory of Paper Coating and Converting, Centre for Functional Materials, Abo Akademi University, Turku, Finland

Abstract

Spider dragline silks are often considered archetypal biomacromolecular materials as they are architecturally complex nanocrystalline polymer composites with properties of toughness far exceeding that of steel. In this chapter, we delve into the finer details of spider dragline, as well as other types of silk. We bring to light the structural basis for the mechanical function of silks, and as such, emphasise the relevance of silk biomechanics in advanced polymer and composites engineering design.

Keywords: Silk, Spider, *Bombyx mori*, nanocrystals, structural hierarchy

8.1 Introduction

Silk is an attractive material since it has enormous capacity for mechanical absorption, is biocompatible and has superior chemical resistance. Concurrently, silk is renewable, sustainable and biodegradable. It has found use in a plethora of textile and biomedical applications, and the idea for its utility within the framework of structural composites is gaining popularity. This chapter aims to elucidate the qualities of silk that make it an excellent natural fibre for use in structural (natural fibre) composites, and will furthermore highlight the most recent advances in silk biocomposites research. We begin by describing the physical structures and chemical compositions of spider silks and silk-worm silks, after which we consider their utility as biocomposite materials.

8.2 Spider Silk Protein

8.2.1 Types, Structures and Properties

There are around 40,000 known species of spiders, each producing several distinct silk proteins; half of which are typically used for catching prey (Römer & Scheibel,

*Corresponding author: parvez.alam@abo.fi

2008). Silk proteins are produced from a wide range of glands, ducts and spigots and have evolved for specific application. As a consequence each type of silk has specific mechanical properties. The orb weaving spider (*Nephila Clavipes*), for example, is one of the most studied spider species and produces up to 7 types of silk protein.

Dragline silk is the strongest and toughest type of silk and it is used primarily for the web frame and radial threads. Spiders may extrude this type of silk as a ‘lifeline’ when escaping predatory attack. Dragline silk is produced from the major ampullate glands. Some dragline silks exhibit tensile strengths exceeding 4 GPa (Teulé *et al.*, 2012), which is comparable to man-made fibres such as Nylon and Kevlar, Table 8.1. Dragline can also extend up to 33% of its original length when subjected to load. Flagelliform silk is used for capture spiral threads and is produced in the flagellate gland. This silk is typically weaker than dragline silk (1 GPa). Flagelliform silk fibres are nevertheless extremely elastic and can strain to *c.a.* 3 times their original length, making them suitable for absorbing energy on prey capture. For instance when an insect collides with a very high kinetic energy, flagelliform silk fibres are able to absorb the impact energy of prey without fracturing.

There are other types of silk producing glands such as the piriform gland, which produces silk that is used primarily in web scaffolding, connecting joints and in the connection of the web frame to surrounding materials. The minor ampullate gland produces silk used for temporary frames to stabilise and support draglines, whilst concurrently providing a template for the flagelliform silk fibres. Other types of silk are depicted in Figure 8.1 (Eisholdt *et al.*, 2011).

Spider silk proteins are rich in nonpolar and hydrophobic amino acids such as glycine and alanine, exhibiting a modular structure of repeat protein sequences in their large core domains that are flanked by non-repetitive, conserved N- and C-terminal regions. Spider silk proteins comprise 150–500 amino acids with a molecular weight commonly at *ca.* 250–320 kDa depending on the type of silk or the species of spider. Repeat units in the protein sequence can be further subdivided into shorter amino acid motifs and non-repetitive (NR) regions are in the amino- and carboxyl termini of the proteins. Amino acid motifs are formed by large-scale hydrogen bonding between protein strands and create the secondary structure of a protein strand, which can be categorised into four distinct motifs; highly crystalline alanine rich beta-sheet stacks

Table 8.1 Generalised silk mechanical properties compared against synthetic material properties (from Römer & Scheibel, 2008).

Material	Density[g.cm ⁻³]	Strength[GPa]	Elasticity[%]	Toughness[MJ.m ⁻³]
MA silk	1.3	1.1	27	180
Flag silk	1.3	0.5	270	150
Insect silk	1.3	0.6	18	70
Nylon 6.6	1.1	0.95	18	80
Kevlar 49	1.4	3.6	2.7	50
Carbon fibre	1.8	4	1.3	25
Steel	7.8	1.5	0.8	6

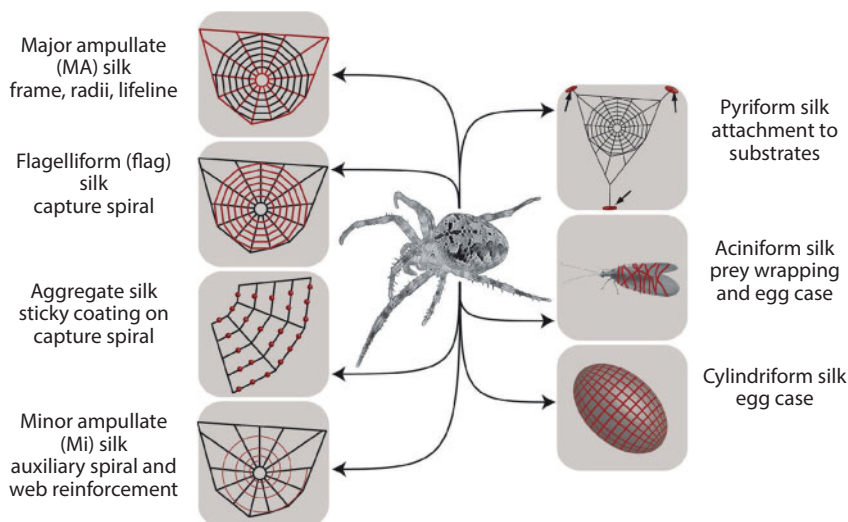


Figure 8.1 Schematic overview of different silk types produced by female orb weaving spiders (*Araneae*). Each silk type (highlighted in red) is tailored for a specific purpose. (Eisholdt *et al.* 2011). Reproduced with the permission of Elsevier.

of A_n or $G(A_n)$, GPGXX motifs that form elastic beta-turn spirals, GGX, and spacers (Keten & Buehler 2010b, Hinman *et al.*, 2011, Cranford & Buehler 2012, Spiess *et al.*, 2010). The motifs account for the functionality of silk protein; for example, dragline silk contains GGX and GA_n motifs. The GGX (X is typically of alanine, tyrosine, leucine or glutamine) motif is the main group giving dragline silk a moderate elasticity, forming an amorphous 3_1 helical structure. Contrarily, alanine rich GA_n or A_n domains form beta sheet stacks that are highly crystalline and develop outstanding strength in the silk strands.

Dragline silk consists of cross-linking antiparallel and parallel beta-sheet crystals that form an array of hydrogen bonds, all within a semi-amorphous glycine rich amorphous matrix. These nanocrystals are no larger than a few nanometres and make up at least 10–15% volume fraction of the silk (Römer & Scheibel, 2008, Fu *et al.*, 2009, Hardy *et al.* 2008). Furthermore, the zip-like structure of beta sheets increases their strength and improves their self-healing properties. The minimum number of alanine groups to create a beta sheet is 3 alanine groups, but stable beta sheets require at least 6 alanine groups, however, there is no mechanical improvement beyond 8 monomer units (Römer & Scheibel 2008, Pahlevan *et al.*, 2014).

The high elasticity of flagelliform silks originates from the secondary structures of the silk protein. According to Raman spectroscopic data, flagelliform dope is in a highly disordered state within the flagelliform gland and furthermore, compared to dragline silk, flagelliform silk does not display structural reorganisation and alignment through the spinning process (Teulé *et al.*, 2012). During the process of self-assembly, repeat units in flagelliform silks form from a combination of specific structural amino acid motifs, which create their secondary structures. The main structural feature of flagelliform silk is GPGGX where X can be Ala, Val, Ser or Tyr. This develops into a repeating unit which forms type II beta-turns and the resulting series of consecutive (up to

63 times before interruption by GGX) beta-turns are thought to form a beta-spiral (Hayashi & Lewis 1998). GGX form 3_1 helices which are also present in dragline silk. The GGX motif is attached to a spacer. There is no definitive explanation for the role of spacers in the protein; however, the presence of mostly negatively charged amino acid (Asp, Glu) in spacers suggests that there is a purpose for spacers, albeit currently unknown. This modular structure creates a spring-like structure within the protein secondary structure, which accounts for the high elasticity of flagelliform silk.

Spider silk also has the unique ability to super-contract. Hydration is an important factor in the elasticity of flagelliform silk allowing for the plasticisation of flagelliform silk. This is reported to increase the capture success in some species by two fold. Absorption of water leads to shrinkage and tightening of the silk thread, which stabilises the structure by forcing hydrophobic amino acids into a packed array. This is achieved by weakening the hydrogen bonds between the spirals with alternating X5(Ser)/X5(Tyr/Val). Although hydration decreases the stiffness of dragline silk, it concurrently allows flagelliform silk to stretch more easily with reduced breakage (Hayashi & Lewis, 1998). Spiders can also naturally maintain hydration of flagelliform silks using wet, non-fibrous aggregate gland secretions to coat the silk surface.

The spinning process of spider silk starts with highly concentrated, unfolded protein dope which is secreted and stored in the spinning glands. The process is highly dependent on the surrounding environmental conditions and requires accurate control over environmental elements such as pH, ionic concentration, water content in the spinning glands and ducts. The highly concentrated protein dope (up to 50 % w/v) is stored primarily as random coil structures in the gland, which later self-assemble when passing through the spinning duct (Hijirida *et al.*, 1996).

Initially the dope passes through an ion exchange channel wherein phase separation takes place. The process involves ion exchange between chaotropic sodium and chloride ions by kosmotropic potassium and phosphate, and water extraction during passage along the duct. There are two theories addressing the mechanism of silk fibre assembly; one proposes that the spinning dope has a liquid crystalline behaviour and it can be considered as the reason for the formation of intermolecular interactions such as van der Waals and hydrogen bonds between neighbouring molecules. Following this stage, by losing the solvent the dope will find its assembled configuration at steady state and will be drawn out of the spinning duct. Alignment of the proteins in solution increases by an increase in flow rate; therefore stiffer, stronger, but less extensible fibres are developed through the formation of aligned beta sheet crystalline regions (Hardy *et al.*, 2008, Chen *et al.*, 2006). The second theory is based on micellar organisation of the protein prior to elongation to form the thread assembly. Mechanical factors such as reeling speed and shear stresses in the drawing of silk can further adjust the amorphous-crystalline segmentation of silk protein.

8.2.2 Computational Research

Several computational studies have been carried out to better understand the mechanical performance of spider silks. Detailed atomistic simulations are important for complex protein folding procedures and for providing mechanistic insights at the molecular level where such information is difficult to obtain through experimentation (Caflisch &

Paci 2005, Shea & Brooks III 2001). A plethora of studies focus on discerning the nano-structural features of spider silk using replica exchange molecular dynamics REMD (Bratzel & Buehler 2012, Ketten & Buehler 2010b, Bratzel & Buehler 2011, Alam 2013), or group interaction modelling (GIM) (Porter *et al.*, 2005, Foreman *et al.*, 2008, Alam 2014) and finite element simulations (Cetinkaya *et al.*, 2011, Cetinkaya *et al.*, 2011b, Tarakanova & Buehler 2012). The vast majority of computational studies focus on the effects of dimension and geometry, and of the energetics within crystalline segments in spider silk proteins (Cetinkaya *et al.*, 2011, Ketten *et al.*, 2010a, Nova *et al.*, 2010, Sintya & Alam 2016, Pahlevan *et al.*, 2014), the size of which is a critical determinant to failure in dragline silk. Computational modelling can provide insights on mechanical performance during self-assembly and loading stress and self-healing mechanisms. For instance, the mechanisms dragline silk experience when subjected to pulling forces can be categorised in four stages; the first stage (I) is related to shear resistance that is instigated from weak hydrogen bonds within amorphous regions. The second stage (II) concerns unfolding of the soft protein matter. This is followed by nanocrystal resistance giving rise to the breaking of hydrogen bonds (III). Finally, frictional resistance to sliding and self-healing takes place (IV) (Cranford & Buehler 2012). Hydrogen bonding interlock (Alam 2015) and self-healing (Alam 2014b) are most prominent between the nanocrystalline regions, proving considerable intermolecular resistance to shearing. On stretching, the β -sheet nanocrystals will be forcibly oriented towards the loading direction and will reinforce the part-extended fibre, which improves cohesion between the strands and permits greater stretching of the amorphous regions. Finally, the proteins comprised of two crystalline segments tend to fold to smaller dimensions than proteins with a single longer crystalline segment. The consequence is a higher strain to failure for proteins with two crystals as compared to the single crystal proteins. Recently, it has been shown that the third phase of silk, the semi-crystalline phase, can self-assemble at beta-sheet interfaces (Sintya & Alam 2016), Figure 8.2, which has considerable implications for energy transfer from soft to hard matter and *vice versa*, and may further explain why silk is able to absorb significant mechanical energy. Strong interfacial bonds such as these are less likely to fail prematurely are thus critical parameters in any composite system (Singha & Thakur 2009).

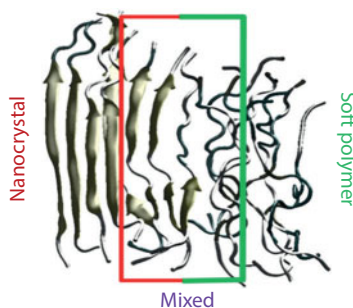


Figure 8.2 Semi-crystalline domains form at interfaces between beta-sheets and amorphous matter. For further information see Sintya & Alam (2016).

8.2.3 Recombinant Spider Silk

Due to the cannibalistic nature of spiders, it is extremely difficult to farm spiders for their silks. Nevertheless, recent advances in recombinant silk engineering have encouraged further manufacture and application of this material (Schacht & Scheibel 2014). The mechanical properties, biocompatibility and functionalisation of recombinant silk by biotechnological methods has given rise to numerous silk-based materials suitable for a wide range of biomedical applications such as implant coatings (Zeplin 2014), scaffolds for tissue engineering (Zhu *et al.*, 2015, Lewicka *et al.*, 2012), wound dressing devices (Baoyong *et al.*, 2010) and drug delivery systems (Lammel *et al.*, 2011) (Hardy *et al.*, 2013).

Due to an increased demand for high mechanical performance spider silk proteins, several approaches for the production of recombinant spider silk proteins are currently being employed. Each method has its own pros and cons; however, the main objective is to produce as long and repetitive spidroins as possible. The first limitation involves the difficulty in determining the complete cDNA sequences of spider silk gene. Here, inaccurate cDNA sequences provide limited information on gene size or the number of repeating units. Furthermore, sequencing of repetitive proteins causes problems i.e., genetically unstable deprived tRNA pools and undesired mRNA secondary structures, as well as limitations related to insolubility of the final product that may result in proteolysis (Zhou *et al.*, 2001).

To overcome these difficulties, several approaches have been considered, such as codon optimisation, different gene construction and host systems. Prokaryotic and eukaryotic hosts such as bacteria, yeast, plants, insect cells, mammalian cells, and even transgenic animals have been tested. Each method has its own limitations considering production cost and simplicity, expression levels and risk of host derived contaminations (Widhe *et al.*, 2012).

Gram-negative enterobacterium *Escherichia coli* (*E. coli*) is, for example, widely used for silk gene expression in large scale production. It is however complicated by different codon usage, unstable DNA fragments, insolubility and low protein yield. Other methods also suffer from various operational shortcomings, like gram positive bacteria which can be simpler to secrete protein. However, there are greater precautions required in using gram-negative *E.coli* due to its pathogenic nature. Yeast can produce longer protein chains with minimised truncation; however unwanted glycosylation may increase allergic reactions. Expression of the spidroin gene in plants like tobacco allow for cheaper and more efficient protein production, but lower yield and possible traces of toxic substances, which in turn can cause allergic reactions. There are several reports on expression in mammalian cells (e.g., Lazaris *et al.*, 2002); however, no protein longer than 60 kDa has yet been expressed. Mammalian cell lines are also prone to infections. Furthermore, spider silk genes have been expressed in the milk glands of transgenic goats and mice. While the initial results from this research were promising, lower concentrations of soluble protein in the milk prohibited further efficient purification for thorough analysis (Römer & Scheibel 2008).

The expression and production of spidroin is followed by purification, artificial spinning and processing into solid structures. Purification often involves precipitation or lyophilisation of protein, followed by solubilisation with various solvents like

urea, guanidine hydrochloride, LiBr, hexafluoroisopropanol (HFIP), or formic acid. Thereafter, the material can be processed to different formats (Widhe *et al.*, 2012).

The process of self-assembly of recombinant silk takes place by dehydration or solvent removal to increase stability and beta sheet content; however, aqueous forms of recombinant silk can be processed to different mechanically, chemically and thermally stable scaffolds such as fibre, mesh, film and foam. Spinning of recombinant silk proteins into fibre is managed using methods such as wet spinning, hand drawing, spinning via microfluidic devices, and electrospinning. Dry/wet spinning or hand drawing methods yield μm scale thread diameters, while nm scale thread diameters can be manufactured through electrospinning. Films are produced by casting and dip/spin coating, while silk hydrogels may be manufactured through contact with an aqueous solution. Freeze-drying hydrogels, gas foaming or salt leaching methods are used to prepare silk foams. Electro spraying or precipitation through addition reaction between a poor solvent and a silk solution to obtain silk spheres and silk capsules is possible by protein adsorption at the interface of an emulsion of water in oil. After processing the proteins, they are usually treated by sterilisation techniques such as autoclaving, filtration or with alcohol or aqueous solutions of kosmotropic salts (e.g., potassium phosphate) to induce β -sheet development within the material (Schacht & Scheibel 2014).

8.3 *Bombyx mori* Silk

8.3.1 Structures and Chemistry

Silks from worms are classified into mulberry and non-mulberry depending upon the food source for the worm. One of the most utilised and domesticated species of mulberry silkworms is *Bombyx mori* (Kundu *et al.*, 2014). They use silk as a protective layer for their larva by spinning cocoons with a considerable number of fibres, reaching up to 1500 meters in length, Figure 8.3.

Silk is produced by the epithelial cells of special glands and is stored in the lumen until it is secreted to build a cocoon (Gamo *et al.*, 1977). The secretion of silk filament begins at the end of 5th instar stage, which is the last phase before the larva undergoes metamorphosis. During previous instars, silk is stored in an aqueous solution and does not form threads. Thread formation is based upon the spinning process, which leads to



Figure 8.3 *Bombyx mori* cocoons covered with silk fibres.

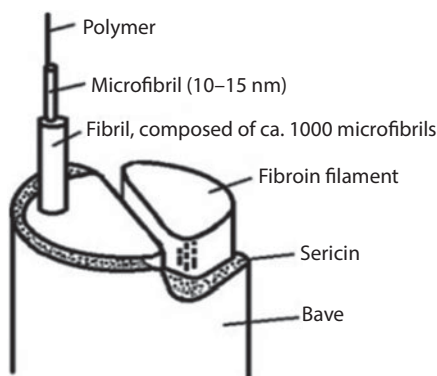


Figure 8.4 Structural components of silk fibre (Ude *et al.*, 2014). Reproduced by permission of Elsevier.

Table 8.2 Percentage distribution of amino acids in silk fibroin and sericin (Ude *et al.*, 2014).

Amino acid	Fibroin [%]	Sericin [%]	Amino acid	Fibroin [%]	Sericin [%]
Glycine	42.8	8.8	Glutamic acid	1.7	10.1
Alanine	32.4	4.0	Serine	14.7	30.1
Leucine	0.7	0.9	Threonine	1.2	8.5
Isoleucine	0.9	0.6	Phenylalanine	1.2	0.6
Valine	3.0	3.1	Tyrosine	11.8	4.9
Arginine	0.9	4.2	Proline	0.6	0.5
Histidine	0.3	1.4	Methionine	0.2	0.1
Lysine	0.5	5.5	Tryptophan	0.5	0.5
Aspartic acid	1.9	16.8	Cystine	0.1	0.3

the synthesis of continuous filaments (Nagaraju, 2015). As shown in Figure 8.4, silk fibres are composed of two main polymers (Sobajo *et al.*, 2008):

1. Fibroin – conserved repeat sequences, the main constituent protein of silk,
2. Sericin – glue-like protein which cements silk fibres (fibroin) together.

Besides sericin and fibroin, minor substances are present in silk such as wax matter (0.4–0.8%), carbohydrates (1.2–1.6%), inorganic matter (0.7%) and pigment (0.2%) (Gulrajani, 1988). The percentage distribution of amino acids within the main silk proteins is provided in Table 8.2 (Ude *et al.*, 2014). Silks as well as other fibrous proteins (e.g., collagen) possess repetitive primary sequences, which in turn leads to homogeneity in secondary structures and the development of β -sheets. This type of structure exhibits high mechanical properties in contrast to globular proteins such as regulatory or catalytic ones (Altman *et al.*, 2003).

Fibroin constitutes the inner core of silk fibres and makes up 70–80% of the total molecular weight (Zhou *et al.*, 2001). Silkworm silk thread consists of two fibroin filaments, each of 10–14 μm , which form the fibre core. Fibroin, in turn, is built up of smaller

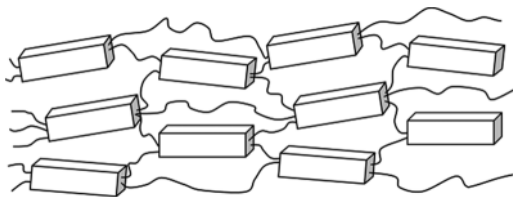


Figure 8.5 Crystalline (blocks) and amorphous (lines) domains of silk fibroin.

filaments, fibrils and microfibrils (Figure 8.4), which form a hierarchical structure of silk. Silk fibroin includes two polypeptide chains - 26kDa (light chain) and 370 kDa (heavy chain) linked by disulfide bridges, which are attached to the C-terminal parts of H-chain (Yamaguchi *et al.*, 1989). Moreover, H-L complex binds P25-glycoprotein (30 kDa) via hydrophobic interactions, which enables the formation of micellar units, crucial for transportation of fibroin through the gland lumen before spinning into fibres (Vepari & Kaplan, 2007), (Inoue *et al.*, 2000). X-ray diffraction shows that fibroin consists of non-crystalline and crystalline parts, where crystalline regions are aligned with the fibre axis (Figure 8.5). Crystalline regions, which contribute to the superior mechanical properties of silk, are built up of H-chains, while L-chains have little strengthening role in the fibres. H-chains are distributed among 12 hydrophobic and 11 hydrophilic domains separated by short linkages (Vollrath and Porter, 2009).

X-ray diffraction analysis has also revealed that the most favourable conformation for heavy chains are pleated β -sheets, while light chains consist of non-repetitive sequences that occupy marginal locations in a fibre. Heavy chain sequences are less complex and include 2377 repeats of Gly-X motif. GX is a fundamental part of the β -sheet and comprises the crystalline regions of the protein, which provides stiffness and strength in the fibre. Here, X is a variable that can be represented by 5 amino acids (with different probabilities): Ala (64%), Ser (22%), Tyr (10%), Val (3%), Thr (1.3%). No other amino acids are present in the repeat (Zhou *et al.*, 2001). More than 70% of H-chain is composed of two hexapeptides GAGAGS and GAGAGY which are found in the amount of 433 and 120 copies, respectively.

Sericin is a glue-like protein which surrounds fibroin filaments and holds it together. It constitutes 25–30% of the total molecular weight of silk. The molecular weight of sericin varies from 10 to 400 kDa, depending on the extraction method. For example, extraction of the polymer using hot water results in *c.a.* 24 kDa molecules, whereas enzyme extraction yields *c.a.* 50 kDa molecules (Rawar & Padamwar, 2004). The fraction of sericin differs along the layers of cocoon and is more predominant in the outermost layer, where the fibroin fraction is lower. It is an extremely hydrophilic protein with unique properties that are beneficial for the development of cocoons. These include: oxidation resistance, antibacterial properties, UV resistance and ease of moisture absorption and release. Two major genes, Ser1 and Ser2, encode a 38 amino acid sequence of the molecule, which is thought to be the primary structure responsible for the mechanical strength of sericin: SSTGS-SSNTD-SNSNS-VGSST-SGGSS-TYGYS-SNSRD-GSV.

It may be noticed from the sequence that almost 50% of all amino acids are serine (Ser). Since sericin is responsible for agglutinating fibroins, it must be able to produce as much intermolecular bonding as possible. This task of adhesion is made possible by the high concentrations of Ser molecules. Serine is a relatively small amino acid which

is predominant in both the interior and at the surface of the protein and is able to easily develop high levels of H-bonds. It is also the main amino acid responsible for hydrogen bonding in turns and helices (Gray and Matthews, 1984). In an unfolded state sericin consists of 35% β -sheets and 62% random coil with no α -helical structures. In a folded state α -helical motives are formed, Figure 8.6, and β -sheets connect through polar zipper interactions, where H-bonds between polar amino acids of Ser rich motifs are abundant (Kundu *et al.*, 2008). Beside serine, other amino acids which have a potential for H-bonds formation are present in the molecule. Amongst them are asparagine, glycine and threonine.

Sericin is easily degraded under heat and in an alkaline environment, which occurs during routine purification methods. Thus, most treatments with protein are performed in the native state. Secondary structures can be altered using ethanol or water, both of which change the properties of the sericin. The underlying process involves changes in molecular orientation which can make the protein more solid, thus presenting opportunities for its wider application. Here, β -sheets aggregate and enhance structural stability as well as resistance to water dissolution (Tremoto *et al.*, 2007).

8.3.2 Physical Properties of *B. mori* Silk

Since silk is considered to be one of the toughest natural materials, its physical and mechanical properties are of high interest to scientists and engineers. Fibroin is a particularly attractive polymer because it constitutes 80% of the mechanical performance of silks. Fibroin tensile properties have thus been reported in a number of studies (Table 8.3). The mechanical properties of β -sheet crystallites have moreover been researched through simulations. Young's moduli (Table 8.2) comparisons between fibroin and crystallites reveal little difference, which suggests that fibroin mechanics is

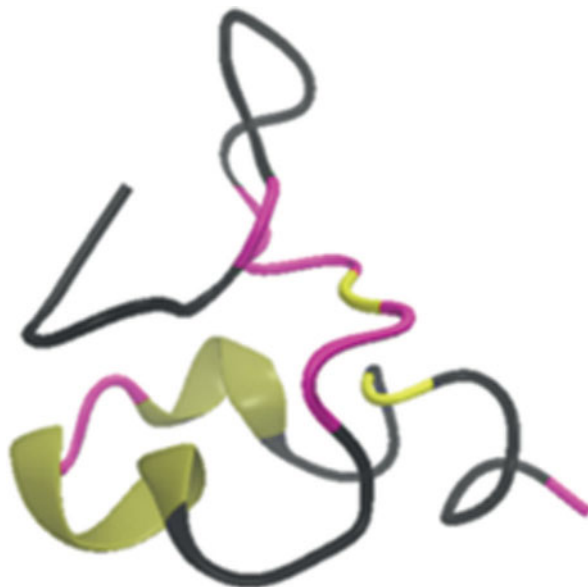


Figure 8.6 Sericin molecule in folded state. Brown regions correspond to α -helices, yellow – β -sheets.

Table 8.3 Mechanical properties of silk compounds.

	Ultimate strength	Breaking strain	Toughness	Young's modulus
<i>B.mori</i> silk	500–600 MPa	19%	70 MJ m ⁻³ (X.L., 2014)	5–12 GPa
<i>B.mori</i> silk (without sericin)	610–690 MPa	4–16%	–	15–17 GPa
<i>B.mori</i> silk fibroin	300–740 MPa (J.S., 2003)	4–26% (Z.S., 2002)	70–78 MJ m ⁻³ (Z.S., 2002)	10–18 GPa (C.V., 2007)
β -sheets crystallites	–	–	–	16–17 GPa (P.M.C., 1994)

strongly guided by its crystallites. In addition, the crystallinity of *B. mori* silk is 40% (Du *et al.*, 2010), while the same value for fibroin varies between 27–55%, according to different sources (Pan *et al.*, 2014). Other studies (Perez-Rigueiro *et al.*, 2000) reveal that silk loses mechanical strength and stiffness when its sericin content is high (Table 8.2) (Liu & Zhang, 2014), (Sirichaisit *et al.*, 2003), (Shao & Vollrath, 2002), (Vepari & Kaplan, 2007), (Cunnif *et al.*, 1994)). Both these results reinforce the idea that the crystalline structures govern the strength and stiffness of fibres while toughness and elasticity are influenced by the amorphous regions.

Although native silk exhibits outstanding mechanical performance, its properties can be altered by different processing methods. For example, heat is considered to induce the formations of β -sheets, and thermal effects on silk are indubitably of high importance. During heating, silk loses bound water molecules, and the mobility of the amorphous regions increases a little prior to crystallisation. This is known as the glass transition (T_g) and equals 451 K (178 °C) in amorphous structures such as fibroin solutions or as obtained from silk glands (Hu *et al.*, 2007). However, the glass transition of fibroin in ordered structures such as fibres can be as high as 220–230 °C (Yuan *et al.*, 2010). The following table (Table 8.4) provides the main thermal transitions in *B.mori* silk.

Sericin also experiences specific changes under heat. It obtains gelling properties because high temperatures increase the solubility of random coils by converting them to β -sheets. Larger numbers of sheets correlates with decreased solubility of the entire molecule as it leads to gel formation (Huddar, 1985). Moreover, sericin easily undergoes a gel-sol transition at 50–60 °C and returns back to a gel when cooling (Zhu *et al.*, 1996).

Table 8.5 shows main chemical properties of silk polymers such as the isoelectric point and solubility (Voegeli *et al.*, 1993), (Timar-Balazsy and Eastop, 2012). Fibroin dissolves at 100 °C over 170 min, and at temperatures >100 °C less time is required for dissolution. However, no dissolution occurs at 95 °C, but rather fibres tend to swell (Xu *et al.*, 2005), which is the reason for why fibroin can be processed at 95 °C without alteration to its own molecular structure. Both sericin and fibroin are insoluble in water at room temperature, and require either hot water or hot acid/alkaline solutions (Moreas *et al.*, 2010).

Table 8.4 Thermal transitions in *Bombyx mori* silk (Kundu, 2014).

Thermal process	Temperature, °C
Water evaporation	30–120
Glass transition	175–179
Crystallisation	212–220
Thermal degradation	227–297

Table 8.5 Chemical properties of *B.mori* silk polymers.

	Sericin	Fibroin
Isoelectric point, pH	4.0(V.R.,1993)	2.8(A.T-B., 2012)
Solubility	Hot water, hot acidic/alkaline solutions	Hot water (>100 °C), hot acidic/alkaline solutions

8.3.3 Spectroscopy of Silks

Studies on the tensile strength of *B. mori* silk fibres showed correlation between the mechanical performance of a material and its Raman spectra intensity (Leffevre *et al.*, 2009). Stretching of the fibres up to 9% causes a decrease in amide I and amide III, which reflects a C=O stretching vibration and N-H in-plane bending/C-N stretching vibration, respectively. This has been connected to a decreased orientation of protein chains along the fibre axis. Since Raman spectroscopy elucidates the most information on β -sheets, disorientation of the crystalline part may be a reason for such behaviour. Although it was thought that elongation aligns fibres along the axis, the latter results elucidated the opposite hypothesis. This might be explained in terms of a reorganisation of amorphous silk matter, which induces disorientation of β -sheets and makes them align more perpendicularly to the fibre axis. A shift toward lower wavenumbers may refer to changes in peptide bonding during stretching.

Since on elongation, no shifts can be detected in the amide I band, deformation does not affect carbonyl groups. One hypothesis is that C=O groups are already aligned perpendicular to the fibre axis, and as such are insensitive to elongation. It is interesting to note that disorientation of the structure disappears when the fibre undergoes post-stretching relaxation, proving a degree of reversibility is possible, most probably as a function of stress relaxation.

FTIR (Fourier transform infrared spectroscopy) is another spectroscopy method used for identifying secondary structures. Three regions are most common for silks: amide I, amide II and amide III, which reflect specific functional groups. Amide I depends on the secondary structures relating to the protein backbone. It is caused mainly by C=O stretching vibrations and to a lesser extent, by NH in-plane bending, CN stretching vibration and CNN deformations. The amide I band provides information about H-bonds and bonding with donors such as H₂O/H⁺ from the same or other molecules (Hu *et al.*, 2008). Amide II is caused by CN stretching vibrations and NH in-plane bending. Downshifts of amide II and upshifts of amide I peaks provide information about water loss. Amide III depends upon NH bending and CN stretching vibration and, to a lesser extent, on C=O in-plane bending and C-C stretching vibration (Cai & Singh, 1999).

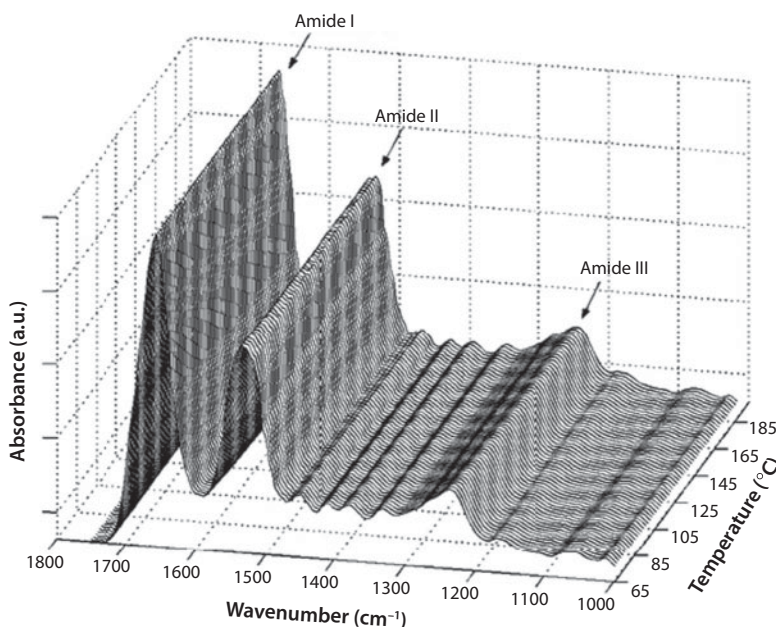


Figure 8.7 Typical FTIR spectra for silk. Reprinted with permission from Hu *et al.* (2008). Copyright 2008 American Chemical Society.

Numerous FTIR spectroscopy studies of silks have been performed under heating between 65 to 165 °C. A typical FTIR spectrum for silks under heat is presented in Figure 8.7. Each region is associated with certain structures. For amide I/II, the 1600–1640 cm^{-1} peak is formed from β -sheets. Random coils and α -helices relate to the 1640–1660 cm^{-1} peak regions and the 1660–1690 cm^{-1} peak arises from turns. For the amide III band, which varies from 1200 to 1350 cm^{-1} , the 1280–1320 cm^{-1} peak relates to α -helices while 1200–1240 cm^{-1} relates to β -sheets. Pure turns and random coils are responsible for the 1260–1280 and 1240–1260 cm^{-1} peaks, respectively (DeOlivera *et al.*, 1994). A peak at 1515 cm^{-1} is normally observed in the amide II region when solvent molecules are excluded from Tyr residues, which contribute to β -sheets interfaces and function as turns (Fabian *et al.*, 1994, Backmann *et al.*, 1996).

8.3.4 Silk-Water Interactions

Water molecules can interact with polymers in different ways and may be present as either unbound or bound water molecules. Unbound water molecules have the same temperature transition as bulk water, which is why it is also called freezing water or free water, since it does not exhibit tight interactions with the polymer (Hodge *et al.*, 1996). Bound water is strongly connected with the polymer molecule and can act as a plasticiser. The latter can also be interpreted as a mobility enhancer because it decreases intermolecular friction thus allowing for more conformational variability (Hu *et al.*, 2007). Recent studies (Mortimer *et al.*, 2013) report on how different environments affect silk fibre tensile properties. Samples were subjected to three conditions; vacuum, humid cycle and ambient conditions. There was no significant difference detected in

the breaking stress between samples though there was a difference noted in the breaking strain between samples. For all samples, vacuum treatment led to lower strain values than ambient conditions. This can be explained by the loss of water which increases the attractive forces between separate protein chains in the non-crystalline regions of silk (Hu *et al.*, 2008, Volltrath & Edmonds, 1989).

Other studies were devoted to regenerated fibroin films (RFF) exposed to moisture rich environments (Yin *et al.*, 2010). RFF are amorphous and are brittle in character. Water treatment increases the formation of β -sheets, which is responsible for the crystalline structure, thus enhancing the stiffness of the films (Hu *et al.*, 2011). As a result, the material acquires a rubber-like look and is able to stretch to almost 3 times its original length. However, no significant changes in tensile properties before and after treatment are reported.

Since films are usually placed in humidity chambers, the interactions occur between polymer and water vapour. Current research shows that water vapour penetrates fibroin and alters its properties (Hirai *et al.*, 2001). Logarithmic measurements reveal a direct correlation between the elongation of films and the amount of water per unit volume of the polymer (Figure 8.8).

Here, elongation of the film (cm/cm) is along the ordinate, while the abscissa is the mass of water in the polymer (gr/gr). This data also makes evident that a small fraction of water is sufficient to soften films, which increases gradually with the level of humidity. Water vapour first penetrates into loose amorphous regions of fibroin and then into the dense aggregated parts. A scheme of water penetration into fibroin is provided in Figure 8.9, where S1 is the amorphous region and S2 is the aggregated region of fibroin. When softening reaches a certain level, the material undergoes a glass-rubber transition. This process means an increase of mobility of molecular segments.

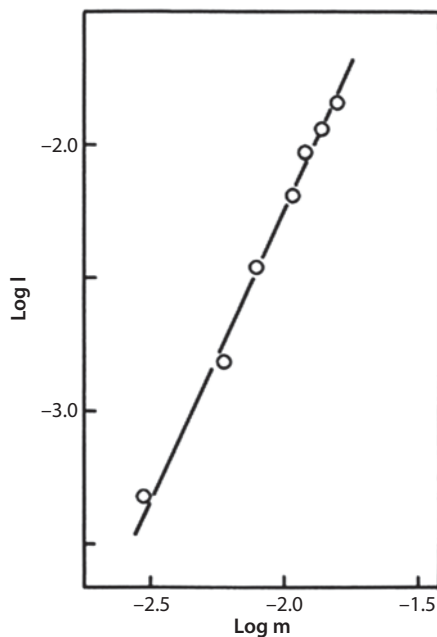


Figure 8.8 Correlation between elongation and water vapour portion in the polymer (Hirai *et al.*, 2001). Reproduced by permission of Elsevier.

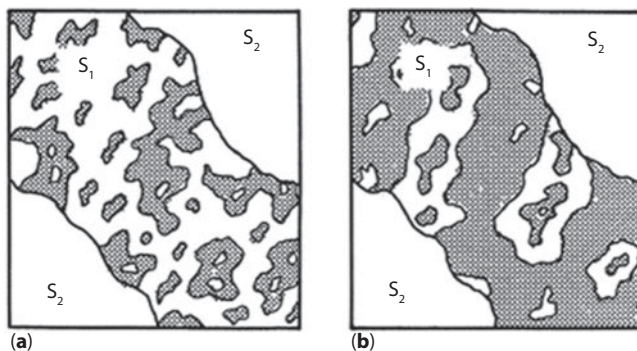


Figure 8.9 Shadowed areas reflect the softened parts of the polymer (Hirai *et al.*, 2001). Reproduced by permission of Elsevier.

Interactions between silk and water are of importance when it comes to understanding and manipulating the mechanical properties of the proteins. In the work of (Mo *et al.*, 2009) NIR was used to elucidate structural changes in the temperature-dependent transitions of both dry and wet regenerated fibroin films. In dry samples, peak areas at 4580 and 4530 cm^{-1} were used to estimate the content of helical structures and β -sheets, respectively. After temperature treatment, no significant variations were measured, meaning there is a lack of structural modification within the silk fibroin. Other studies also reinforce the current understanding in that no β -sheets are formed during heating, although fibroin can be plasticised by water (Hu *et al.*, 2007). However, wet fibroin films show some changes when heated: 4605 cm^{-1} peak decreased dramatically while 4525 cm^{-1} peak raised (Figure 8.10), implying internal changes in the β -sheet structure. Formation of β -sheets induced stronger H-bonding between N-H and C=O groups. In turn, this led to increased interactions between hydrophilic peptides in helical structures and random coils. This can be explained as hydrogen bond alignment ($\text{C=O} \cdots \text{H-N}$) along β -sheet peptides, which restricts stretching of amide and carboxyl bonds. Surprisingly, breakage of H-bonds between water and peptides was also noticed to occur at 60°C which indicates that bound water becomes free after heating. In essence, β -sheets are formed during the dissociation of hydrogen bonds between water molecules and peptides followed by a re-association of these bonds between peptides, thus making stronger H-bonds. It also causes the insolubility of fibroin in water. Hu and co-workers also revealed plasticisation can occur by freezing the water.

8.3.5 Degumming

Degumming is a process of sericin removal from silk fibres. It is actively used in the textile industry and other fields where fibroin purification is required. Today, several methods of degumming are being practiced: boiling in water with and without soap treatment, enzymatic degumming and treatment in acidic solution (Ho *et al.*, 2012). It has been shown that degumming detrimentally changes silk properties (Altman *et al.*, 2003), and that the extent of such changes varies as a function of the duration of treatment and the nature of the treatment agent. For example, silks lose 20–25% of their weight, which is estimated to be equal to the sericin fraction. Removal of sericin also

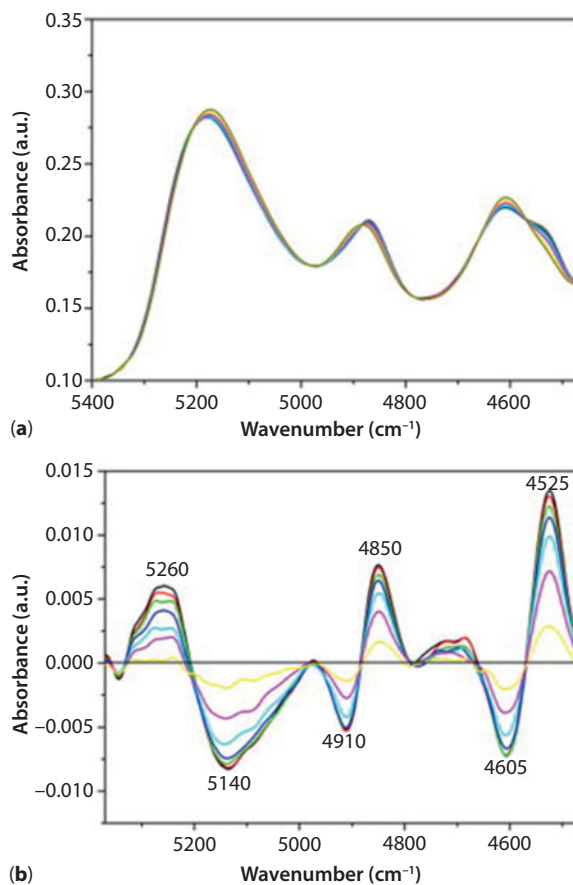


Figure 8.10 NIR spectra of wet fibroin film (a) and spectra difference (b) (Mo *et al.*, 2009). Reproduced by permission of Elsevier.

leads to decrement of the fibre diameter. Nevertheless, degummed fibres still have superior mechanical properties, which are in turn related to the twisted nature of fibres. When sericin is removed, fibroins will be aligned towards the loading direction, which decreases friction between the fibres. This in turn increases the load bearing capacity and fibre elasticity improves (Mahmoodi *et al.*, 2010). The soap method (as well as enzyme and acid treatments) causes undesirable effects (MacIntosh *et al.*, 2008) such as decreases in tensile strength, damage to the protein molecules and bond breakage. For example, all treatment agents with the exception of enzymes increase the elongation properties of fibroin, though initial moduli are reduced (Khan *et al.*, 2010). It is also important to highlight that tensile properties do not represent the actual mechanical properties of the core fibroin fibres since different fractions of sericin may be present after the degumming process (Jiang *et al.*, 2006) due to incomplete processing (Hardy & Scheibel, 2009). Microscopy techniques and image analysis are useful means by which means one can define the level of purification as well as the fibroin conditions for further processing.

It has been reported that regenerated filaments have a lower tensile strength than natural fibres. Therefore, there should be a component which lacks regenerated filaments

yet is present in natural silk. This component must be responsible for differences in the mechanical properties. In addition, regardless of the amount of sericin, filaments have no cracks, which would normally affect the mechanical properties. Stress-strain curves illustrate that the breaking strength of filaments with sericin content is 50% higher than for pure fibroin filaments. Strain shows the same correlation. A possible explanation is that sericin increases the β -sheet crystal content while excess sericin contributes to the increased tenacity of silk filaments (Ki *et al.*, 2007). Nevertheless, sericin is normally removed from silks in order to satisfy commercial requirements of the materials. It has been shown that production of up to 1600 tons of pure silk is a source for 250–300 tons of sericin per year (Gulrajani, 2015). If this amount is recycled and used for other purposes, it may have enormous social and economic benefits. Polymer grafting techniques, shown to have advantageous effects on natural cellulosic fibres (Singha *et al.* 2008, Thakur & Singha 2011b; Thakur *et al.*, 2016; Thakur & Thakur, 2014a,b) may also be a means by which silk fibre properties can be improved.

8.4 Silk Biocomposites: Applications

8.4.1 Composite Textiles

Silk has been used as a textile for over 4000 years. The main reason for this is the length of silk filaments. Since cocoons are made up of single fibres which reach up to 1500 m, and as such continuous threads can be easily obtained. However, sericin has been shown to spoil the commercial properties of silk such as luster, and is hence removed from fibroin during manufacture. This process is performed in hot water and is known as degumming. Then, cocoon filaments are fixed together from one end, and the resultant thread is wound using a moving reel (Ude *et al.*, 2014). Silk reeling may be performed in two different ways: direct and indirect reeling. Direct reeling has traditionally been the main method used in the textiles industry. Cocoons are placed in hot water under reel. Silk filaments then are passed through a small hole in a wooden design before being fixed upon a reel after which the reel starts turning. Indirect methods differ such that silk threads are first spun on a small reeling machine and then re-reeled on a larger one. This technique is used in modern processes as better quality textiles can be produced (Zhao *et al.*, 2005).

8.4.2 Biomedical Composites and Biomaterials

The first application of silks in medicine was as sutures for wounds (Omenetto & Kaplan, 2010). At that time it was the most efficient way of closing wounds since silk has excellent mechanical and biodegradable properties. Nevertheless to a point, there have been limited biomedical applications for silk in eye, lip or intraoral surgery. The primary reason is that sericin, comprising *c.a.* 20 wt% of silk, caused allergic reactions and other side-effects. Virgin silk is an allergen causing a Type I allergic response (Kurosaki *et al.*, 1999). In other cases silk sutures gave rise to delayed responses; including asthma and malfunctions in IgE regulation. Thorough purification of silk fibre from its sericin content opened up channels to a new range of applications in the biomedical field. For

example, pure fibroin films are used for *in vivo* wound healing and improve the healing speed while lowering inflammatory responses as compared to conventional techniques (Sugihara *et al.*, 2000). Although sericin was identified to be an allergenic compound some researchers still find the biomedical applications promising. Sericin can undergo specific processing with other substances to eliminate its adverse side-effects. For example, when sericin solution is gelled with ethanol without any chemical modifications and then dried, it can be used for wound dressing. Here, infrared analysis reveals a β -sheet meshwork, which provides gel with anti-swelling properties and higher absorption. Recent studies where gel film was used as matrix for fibroblast cultures reveal that sericin gel does not give rise to cytotoxicity and additionally had low adhesion, thus permitting its application as wound dressing (Teramoto *et al.*, 2007). Today, many other properties of sericin have been elucidated including antibacterial, anti-apoptotic, anti-inflammatory (Aramwit *et al.*, 2013), UV-resistance (Dash *et al.*, 2008) and immunogenicity (Aramwit & Sangcakul, 2007). Moreover, sericin suppresses lipid peroxidation (Kato *et al.*, 1998) and exhibits anti-tumor properties (Kaewkorn *et al.*, 2012). Hence, certain processing techniques can improve sericin properties and allows it to be a competitive candidate for pharmaceutical and biotechnological applications (Mitrana *et al.*, 2015).

Silk biomaterials may also be applied as scaffolds for tissue engineering. These scaffolds are used to support tissues *in vitro* prior to implantation into the organism. The function of the matrix is to support cell attachment, growth and development. A key quality in such scaffolds is matrix degradation through proteolytic activity in the organism into biocompatible fragments that can be further metabolised by cells. In addition to biodegradability, silk-based scaffolds exhibit excellent tensile properties which make them useful in load bearing applications (Altman *et al.*, 2002). Here, silk fibroin provides both mechanical and biological advantage. Fibroin is also used to construct artificial blood vessels which have benefits over polyurethane vessels in respect of their mechanical properties (Lovett *et al.*, 2008). Moreover, regenerated fibroin can be used as an effective drug carrier for controlled delivery. The attachment of therapeutic proteins to fibroin improves a range of properties, which in turn enhances the delivery process. Other advantages include; thermal stability, high circulation lifetime and reduced antigenicity. Usually, a combination of fibroin with certain biomolecules is most effective. These include; glucose oxidase, L-ASNase lipase and phenylalanine ammonia-lyase (Zhang *et al.*, 2012).

Spider silk has not been utilised at a large scale in biomedical applications, however recent advances in the production of silk recombinantly increases the demand for the production of silk based biomaterials at the laboratory scale. Natural spider silk has been used for wound dressing and sutures, and has been tested to observe local tissue reaction. There were no instant macroscopic signs of inflammation, however after two weeks; there were signs of inflammatory reactions and spider silk tended to degrade over the period of study. A similar study on recombinant silk has been conducted and promising results were reported; no inflammatory reaction and quicker wound healing. Silk-based biocomposites can take advantage of the mechanical performance of spider silk while adding other functionalities (Alam 2015b). Recombinant spider silks are mostly intended to be used in biomedical applications that require the material to be biocompatible. Biocompatibility can be referred to using various terms and conditions and there is no specific definition for it, however, the main issue is in preventing unacceptable inflammatory reactions in the host tissue. The term can be subdivided to (1) biosafety

which refers to appropriate local response and absence of cytotoxicity in the material and (2) biofunctionality which ensures desired performance of implanted material.

Several studies (Widhe *et al.*, 2010, Wohlrab *et al.*, 2012, Widhe *et al.*, 2013) have employed recombinant silk proteins as scaffolds for cell culture, for ease of fabrication into film, foam, fibre and mesh matrices with various dimensionalities, microstructures and nano-topographies. These substrates show good cell growth and adhesion as well as providing 3D culturing conditions for foam and fibre based matrices which are favourable to the environment of extracellular matrices. Electro-spun recombinant silk together with collagen as a composite (Zhu *et al.*, 2015) has high tensile strength and elasticity, and a similar performance to pure collagen matrices in supporting cell proliferation. Furthermore, Lewicka *et al.*, (2012) reported the successful use of recombinant silks as synthetic matrices for culturing neural stem cells, and the results show similar performance when compared to the golden standard coating of embryonic NSCs with the mechanical advantage of silk protein as well as biosafety and three-dimensionality. An *et al.*, (2015) further confirmed that spider silk MaSp1 provides proper surface charge and substrate stiffness to support neuron regenerative growth for primary rat cortical neurons. Recombinant silk also has been tested as wound dressing on second-degree burn wounds in SD rats and the results were on par with commercially used collagen. Controlled drug delivery by artificial silk is reported in several studies (Hofer *et al.*, 2012, Hardy *et al.*, 2013); where the drug is essentially adsorbed onto silk particles by electrostatic attraction and the drug is encapsulated in an all-aqueous process under ambient conditions. The concluding transport processes are then driven by concentration gradients.

8.4.3 Structural Biocomposites

Silk biocomposites can be combined in diverse forms including; matrix-particles, matrix-fibres, multilayers, wovens and a plethora of other arrangements. Silks and other natural filaments (Thakur & Singha 2010a, 2010b, 2011, Singha & Thakur 2008, 2009b) show great promise for use in matrix-fibres structural composites. With such materials, the matrix transfers load from fibre to fibre via shear stresses at fibre interfaces. Therefore, strong bonding between the fibres and the matrix is critical. Fundamentally, if interfacial properties are poor, structural biocomposites will be mechanically weak and may not be useful in e.g., load bearing situations. Molecular interactions between different parts of a composite can be altered through either physical or chemical treatments. The result is typically improved adhesion between matrix and fibre, and this enhances the mechanical performance of the entire material (Luo & Netravali, 1999). For example, silane is shown to increase tensile and stiffness of jute-epoxy composites (Gassan & Bledzki, 1999), and maleic anhydride treatment improves the tensile strength of both sisal and hemp (Mishra *et al.*, 2000). Silk possesses amphiphilic properties and as such it has both hydrophobic and hydrophilic groups. When manufacturing reinforced composites with polymer as a matrix, hydrophilic characteristics can cause poor interactions with the polymer. The reason is that most polymers which are used for scaffolding fibres are hydrophobic, and dissimilarity in the chemical interactions creates incompatibility and prevents efficient fibre-polymer interactions. Moreover, tight connections between fibres may lead to agglomerations, which prevent the equal distribution of fibres along the length of filament (Matuana *et al.*, 2001, Saheb & Jog, 1999, Keener *et al.*, 2004).

Table 8.6 Critical differences between glass and natural fibres that may affect the selection processes for green composites. Here NF refers to natural fibre (Wambua *et al.*, 2003).

Property	Glass fibres	Natural fibres
Cost	Low, but higher than NF	Low
Density	Twice higher of NF	Low
Renewability/ Recyclability	No	Yes
Distribution	Wide	Wide
Energy Consumption	High	Low
Carbon neutrality	No	Yes
Health risk when inhaled	Yes	No
Disposal	Yes	No

A primary function of composites is as structural materials which are commonly used in the construction, aerospace engineering, automobile industries. For decades, glass fibres have been major components in such composites since they have high tensile properties and are relatively low in cost. However, alongside an increasing concern for the environment, eco-friendly composite technologies aim to supplement glass fibres in composites. Natural fibres are one of the main alternatives as they exhibit outstanding mechanical and biodegradable properties. Though glass fibres have many advantages, they concurrently have certain drawbacks, Table 8.6, which makes them less suitable for green composites technology than natural fibres (Wambua *et al.*, 2003).

Currently, some of the predominant candidate natural fibres showing potential as replacements to synthetic fibres are hemp, flax, jute and kenaf. Although raw natural fibres possess less mechanical strength than synthetic analogues, certain processing techniques can enhance their tensile values, Table 8.7 (Perez-Rigueiro *et al.*, 2000, Craven *et al.*, 2000, Bledzki & Gassan, 1999). In addition, they possess other advantageous qualities over conventional fibre composites such as biodegradability and recyclability. Fibres in the form of continuous filaments often provide the best replacements as reinforcing materials. Silk is a single fibre which exists in nature in continuous filamentous form. In comparison to plant and synthetic fibres, silk has several advantages (Shah *et al.*, 2014):

1. natural flame resistance
2. low density
3. moderate strength
4. unparalleled toughness
5. favourable raw material in terms of ecological impact
6. continuous length
7. high compressibility.

Another advantage of silks is in the geometry of the fibre cross-section. Plant fibre yarns are circular in cross-section whereas silk yarns are lenticular, which yields a different width to thickness ratio and increases the fibre packing density by inter yarn compaction (Lewin, 2007). Lenticular shapes of silk fibres can be subdivided into

Table 8.7 Tensile values of natural and synthetic fibres (Shah *et al.*, 2014).

Material	Density (kg/cm ³)	Tensile strength (MPa)	Young's modulus (GPa)	Elongation at failure (%)	Source
B.mori silk	1.3–1.8	650–750	16	18–20	(J.P-R.,2000)
Spider silk	1.3	1300–2000	30	28–30	(J.P.C.,2000)
Flax	1.5	345–1035	50	2.7–3.2	(A.K.B.,1999)
Hemp	1.48	690	70	1.6	(A.K.B.,1999)
Jute	1.3	393–773	26.5	1.5–1.8	(A.K.B.,1999)
Coir	1.2	175	4.0–6.0	10.0	(A.K.B.,1999)
Sisal	1.5	155–635	9.2–22.0	2.0–2.5	(A.K.B.,1999)
Cotton	1.5–1.6	287–597	5.5–12.5	7.0–8.0	(A.K.B.,1999)
E-glass	2.7	1200	73	2.5	(A.K.B.,1999)
Carbon	1.8	4000	131	2.8	(A.K.B.,1999)
Kevlar49	1.44	3600–4100	131	2.8	(J.P.C.,2000)

concave and convex cross-sections. These essentially slot into each other and provide additional lateral support.

The mechanical properties of silk cocoons were first investigated to elucidate tensile values for individual filaments. The thicknesses of silk fibres were measured as being within the range of 2–4 μm (Zhao *et al.*, 2005). Since sericin covers fibroin fibres, it absorbs part of the energy while loading. Shear stress accumulates at the fibres ends, which is why length is also of high importance. It has furthermore been shown that the critical length decreases when Young's modulus and shear modulus of the polymer increase. A thicker sericin layer requires a larger length of stress transfer. Therefore, the maximum shear stress is higher for thinner sericin layers (Ho *et al.*, 2012). Hydrogen bonds are important contributors to molecular stability. These are likely to be affected during the degumming process. Water penetrates into the amorphous regions of a molecule and weakens the inter- and intra-molecular bonds. It leads to the increased displacement of chain segments in a protein, and the elongation at break is increased (Perez-Rigueiro *et al.*, 2000). Mechanical properties of silk vary somewhat both before and after processing. Since sericin is usually removed from fibroin, the diameter of fibres can change dramatically. Fine silk fibres have higher tensile strength and breaking energy, however elongation at break does not change with fibre diameter (Tsukada *et al.*, 1996).

It has been shown that incorporation of waste silk fabric at 1wt% into epoxy resin (Araldite HY960) improves its stiffness in terms of tensile strength and elongation at break (Cheung & Lau, 2006). Silk fibroin was mixed together with polyvinyl alcohol to produce hydrogels, where elongation at break and strength increased as the polymer content increased (Li *et al.*, 2002). Studies showed that polyester poly ϵ -caprolactone together with silk fibroin give rise to reinforced films. The optimal mechanical properties were with 35–45wt% content of fibroin (Qiao *et al.*, 2009). However there is currently no research on the mechanical properties of materials composed of only of silk protein mixtures.

Many attempts have been made to produce silk-based composites. All of them vary in regards to structure and function. Here, several examples of silk composites are briefly described:

1. Silk fibroin fibres were combined with nanotubes, both SWNT (single walls nanotubes) and MWNT (multi walls nanotubes) to produce novel high stiffness or high strength composites. Fibroin acted as the matrix over which SWNT nanotubes were spread. Fibroin was shown to form β -sheets and random coils (Khare and Bose, 2005). Interestingly, the Young's modulus increased by 46%, however, other mechanical values decreased dramatically due to the poor alignment and distribution of SWNT along the fibroin (Ayutsede *et al.*, 2006). The combination of silk with MWNT produced composites with improved tensile strength and Young's modulus, however the elongation at break failed to increase (Kim *et al.*, 2008). The combination of silk fibroins and MWNT showed high resistance to washing and sonication due to large number of hydrogen bonds produced between the fibres and carboxylic acids, which tubes walls were coated with (Kang & Jin, 2007).
2. Films composed of fibroin and polyethylene oxide showed high tensile strength and elongation at break. Fabrication was performed in a humid environment to enable β -sheet formation in the fibroin. The ratio of fibroin to polyethylene oxide was 98:2. An increase in synthetic polymer volume demonstrated higher elongation values at the expense of strength (Jin *et al.*, 2004)
3. Silks can be combined together with biodegradable polymers with an aim towards biodegradable disposal. Fibroins with polylactic acid demonstrated increased tensile strength and elongation at break although hydrophilicity decreased. Synthesis included humidification for 48 hours which made hydrogen bonds the major interaction forces between polymers (Hu *et al.*, 2007)
4. The combination of silks with other natural fibres is a promising field. For example, collagen was combined with *B. mori* fibroin to produce films. Although the number of H-bonds increased due to the presence of collagen in the films, the mechanical properties were lower when compared to pure fibroin (Hu, 2006). Collagen-fibroin hydrogel was shown to form efficient multi-pore scaffolds for cell cultures, allowing cells to adhere to the matrix, migrate and proliferate actively. Here, sericin improved the biocompatibility of collagen-based scaffolds, which made these hydrogels good matrices for tissue engineering (Mitrana *et al.*, 2015).
5. Cellulose has been shown to be good material to combine with fibroin for making composite materials. Infrared spectroscopy revealed hydrogen bonds between fibroin and cellulose and an abundance of β -sheet rich crystalline domains. These composites showed improved mechanical performance in comparison to pure fibroin (Freddi *et al.*, 1995)

Ashby charts can be used to better understand the tensile properties of silks in comparison to other materials (Ashby & Cebon, 1992). The charts provide a representation

of materials screening based on performance indices using a bubble chart. As shown in Figure 8.11, the abscissa represents the Young's modulus in GPa while the ordinate represents tensile strength in MPa. From the Ashby's charts we can see that silkworm silk possesses better strength than soft tissues, mineralised tissues and wood-like materials. It also exceeds some engineering materials in terms of strength; such as stones, bricks, foams, elastomers and polymers. Therefore, silks are unique in terms of mechanics over both engineering and natural materials. Moreover, these charts are a reflection of the raw silk properties, and further processing can improve its performance.

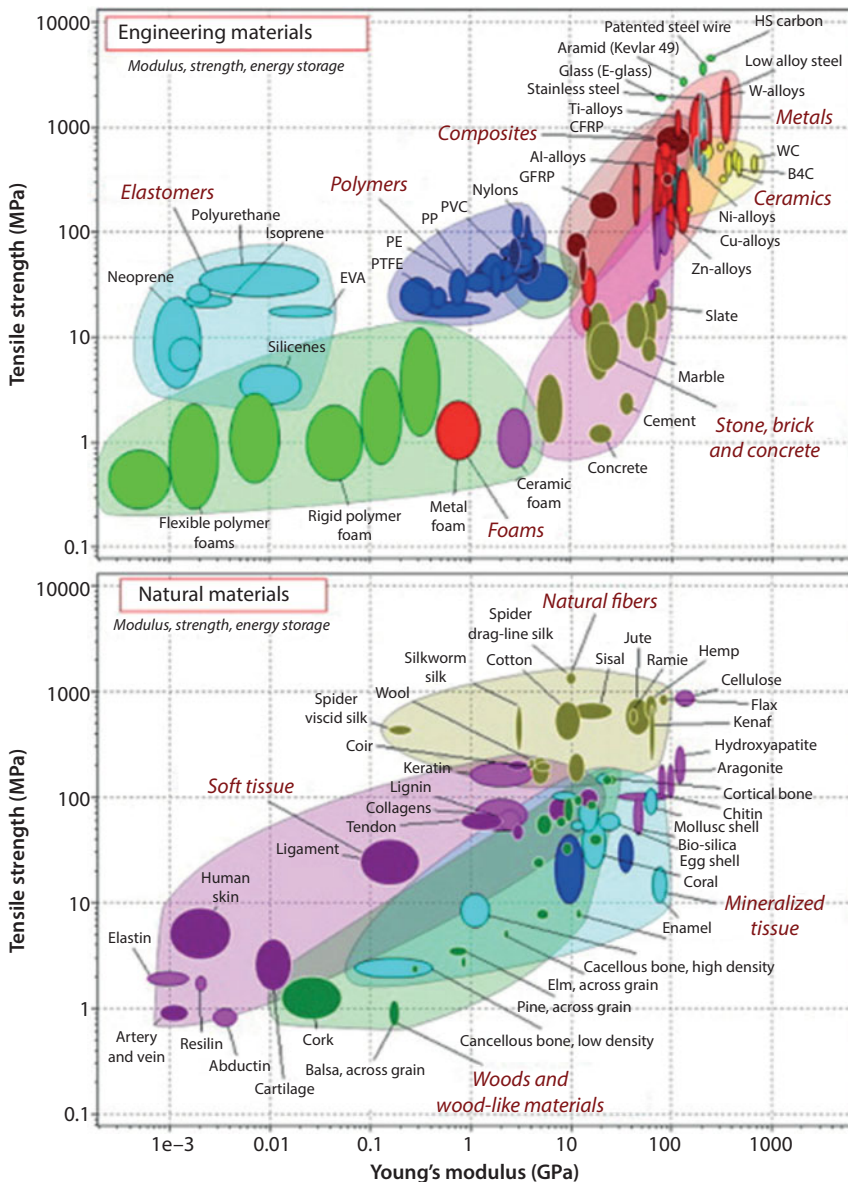


Figure 8.11 Ashby's chart for engineering and natural materials (Shah, 2014). Reproduced by permission from Elsevier.

References

- Alam, P. Biomimetic insights: structure-toughness relations in spider silk nanocrystals; *Adv. Mater. Res.*, Vol. 622–623, pp. 1799–1802, 2013.
- Alam, P. Protein unfolding versus beta-sheet separation in spider-silk nanocrystals; *Advances in Natural Sciences: Nanoscience and Nanotechnology*; Institute of Physics Publishing, Vol. 5(1), 015015(6), 2014.
- Alam, P. Chapter 13: Structural Organisation and Biomimesis of Nature's Polymer Composites; *New Developments in Polymer Composites Research*; Ed. Laske, S., pp. 325–379, Nova Science Publishers Inc., 2014b. ISBN 978-1-62948-340-5
- Alam, P. Chapter 10: Mechanical Properties of Bio-Nanostructured Materials; *Handbook of Mechanical Nanostructuring* Vol. 1; Ed. Aliofkhazraei, M., pp. 211–231, Wiley-VCH, 2015.
- Alam, P. Chapter 14: Biomimetic Composite Materials Inspired by Wood; *Wood Composites*; Ed. Ansell, M. P., pp. 357–394, Elsevier (Woodhead Publishing imprints), 2015b.
- Altman, G., F. Diaz, C. Jakuba, T. Calabro, R. Horan, and J. Chen *et al.* Silk-based biomaterials. *Biomaterials*, 24(3):401–416, 2003.
- Altman, G., R. Horan, H. Lu, J. Moreau, I. Martin, J. Richmond, and D. Kaplan. Silk matrix for tissue engineered anterior cruciate ligaments. *Biomaterials*, 23(20):4131–4141, 2002.
- An, B., Hinman, M. B., Holland, G. P., Yarger, J. L., & Lewis, R. V. Inducing β -Sheets Formation in Synthetic Spider Silk Fibers by Aqueous Post-Spin Stretching. *Biomacromolecules*, 12, 2375–2381, 2011.
- An, B., Tang-Schomer, M., Huang, W., He, J., Jones, J., Lewis, R., *et al.* Physical and biological regulation of neuron regenerative growth and network formation on recombinant dragline silks. *Biomaterials*, 48, 137–146, 2015.
- Aramwit, P., and A. Sangcakul. The Effects of Sericin Cream on Wound Healing in Rats. *Biosci. Biotech. Bioch.* 71(10):2473–2477, 2007.
- Aramwit, P., P. Towiwat, and T. Srichana. An Investigation of the Anti-Inflammatory Potential of Silk Sericin. *Adv Sci Lett*, 19(12):3615–3619, 2013.
- Ashby, M., and D. Cebon. *Materials selection in mechanical design*. Oxford: Pergamon Press, 1992.
- Ataollahi, S., S. Taher, R. Eshkoo, A. Ariffin, and C. Azhari. Energy absorption and failure response of silk/epoxy composite square tubes: Experimental. *Compos. Part B-Eng*, 43(2):542–548, 2012.
- Ayutsede, J., M. Gandhi, S. Sukigara, H. Ye, C. Hsu, Y. Gogotsi, and F. Ko. Carbon Nanotube Reinforced Bombyx mori Silk Nanofibers by the Electrospinning Process. *Biomacromolecules*, 7(1):208–214, 2006.
- Backmann, J., C. Schultz, H. Fabian, U. Hahn, W. Saenger, and D. Naumann. Thermally induced hydrogen exchange processes in small proteins as seen by FTIR spectroscopy. *Proteins*. 24(3):379–387, 1996.
- Baoyong, L., Jian, Z., Denglong, C., & Min, L. Evaluation of a new type of wound dressing made from recombinant spider silk protein using rat models. *Burns*, 36, 891–896, 2010.
- Bledzki, A., and J. Gassan. Composites reinforced with cellulose based fibres. *Prog. Polym. Sci.* 24(2):221–274, 1999.
- Bourmaud, A., and C. Baley. Rigidity analysis of polypropylene/vegetal fibre composites after recycling. *Polym. Degrad. Stabil.* 94(3):297–305, 2009.
- Bratzel, G., & Buehler, M. J. Molecular Mechanics of Silk Nanostructures Under Varied Mechanical Loading. *Biopolymers*, 97, 408–417, 2011.
- Bratzel, G., & Buehler, M. J. Sequence-structure correlations in silk: Poly-Ala repeat of N. clavipes MaSp1 is naturally optimized at a critical length scale. *Journal of the Mechanical Behavior of Biomedical Materials*, 7, 30–40, 2012.

- Caflich, A., & Paci, E. Molecular Dynamics Simulations to Study Protein Folding and Unfolding. In J. B. Kieffer (Ed.), *Protein Folding Handbook* (pp. 1143–1169), 2005.
- Cai, S., and B. Singh. Identification of beta-turn and random coil amide III infrared bands for secondary structure estimation of proteins. *Biophys. Chem.* 80(1):7–20, 1999.
- Case, D., T. Cheatham, T. Darden, H. Gohlke, R. Luo, and K. Merz *et al.* The Amber biomolecular simulation programs. *J. Comput. Chem.*, 26(16):1668–1688, 2005.
- Cetinkaya, M., Xiao, S., & Gräter, F. Bottom-up computational modeling of semi-crystalline fibers: from atomistic to continuum scale. *Physical Chemistry Chemical Physics*, 13, 10426–10429, 2011.
- Cetinkaya, M., Xiao, S., & Gräter, F. Effects of crystalline subunit size on silk fiber mechanics. *Soft Matter*, 7, 8142–8148, 2011.
- Charlet, K., C. Baley, C. Morvan, J. Jernot, M. Gomina, and J. Breard. Characteristics of Hermé's flax fibres as a function of their location in the stem and properties of the derived unidirectional composites. *Compos. Part A – Appl. S.* 38(8):1912–1921, 2007.
- Chen, X., Shao, Z., & Vollrath, F. The spinning processes for spider silk. *Soft Matter*, 2, 448–451, 2006.
- Cheng, Y., L. Koh, D. Li, B. Ji, M. Han, and Y. Zhang. On the strength of beta-sheet crystallites of Bombyx mori silk fibroin. *J. Roy. Soc. Interface*, 11(96), 2014.
- Cheung, H., and A. Lau. Mechanical Performance of Silk-Based Structural Composites. *Key. Eng. Mat.* 326–328; 457–460, 2006.
- Cranford, S. W., & Buehler, M. J. *Biomaterialomics* (1st ed.). Springer, 2012.
- Craven, J., R. Cripps, and C. Viney. Evaluating the silk/epoxy interface by means of the Microbond Test. *Compos. Part A – Appl. S.* (7):653–660, 2000.
- Cunniff, P., S. Fossey, M. Auerbach, J. Song, D. Kaplan, and W. Adams *et al.* Mechanical and thermal properties of dragline silk from the spider Nephila clavipes. *Polym. Adv. Technol.*, 5(8):401–410, 1994.
- Dash, R., M. Mandal, S. Ghosh, and S. Kundu. Silk sericin protein of tropical tasar silkworm inhibits UVB-induced apoptosis in human skin keratinocytes. *Mol. Cell. Biol.* 311(1–2): 111–119, 2008.
- DeOliveira, D., W. Trumble, H. Sarkar, and B. Singh. Secondary Structure Estimation of Proteins Using the Amide III Region of Fourier Transform Infrared Spectroscopy: Application to Analyze Calcium-Binding-Induced Structural Changes in Calsequestrin. *Appl. Spectrosc.* 48(11):1432–1441, 1994.
- Du, N., Z. Yang, X. Liu, Y. Li, and H. Xu. Structural Origin of the Strain-Hardening of Spider Silk. *Adv. Funct. Mater.* 21(4):772–778, 2010.
- Eisholdt L, Smith A, Scheibel T. Decoding the secrets of spider silk. *Materials Today*, 14(3): 80–86, 2011.
- Fabian, H., C. Schultz, J. Backmann, U. Hahn, W. Saenger, H. Mantsch, and D. Naumann. Impact of Point Mutations on the Structure and Thermal Stability of Ribonuclease T1 in Aqueous Solution Probed by Fourier Transform Infrared Spectroscopy. *Biochem.* 33(35):10725–10730, 1994.
- Faruk, O., A. Bledzki, H. Fink, and M. Sain. Biocomposites reinforced with natural fibers: 2000–2010. *Prog. Polym. Sci.* 37(11):1552–1596, 2012.
- Foreman, J. P., Porter, D., Behzadi, S., & Jones, F. R. A model for the prediction of structure–property relations in cross-linked polymers. *Polymer*, 49, 5588–5595, 2008.
- Freddi, G., M. Romano, M. Massafra, and M. Tsukada. Silk fibroin/cellulose blend films: Preparation, structure, and physical properties. *J. Appl. Polym. Sci.* 56(12):1537–1545, 1995.
- Fu, C., Shao, Z., & Vollrath, F. Animal silks: their structures, properties and artificial production. *Chemical Communications*, 43, 6515–6529, 2009.
- Gamo, T., T. Inokuchi, and H. Laufer. Polypeptides of fibroin and sericin secreted from the different sections of the silk gland in Bombyx mori. *Insect Biochem.* 7(3):285–295, 1977.

- Gassan, J., and A. Bledzki. Effect of cyclic moisture absorption desorption on the mechanical properties of silanized jute-epoxy composites. *Angew. Makromol. Chem.*, 272(1): 17–23, 1999.
- Grant, J., B. Pickup, M. Sykes, C. Kitchen, and A. Nicholls. A simple formula for dielectric polarisation energies: The Sheffield Solvation Model. *Chem. Phys. Lett.* 441(1–3):163–166, 2007.
- Gray, T., and B. Matthews. Intrahelical hydrogen bonding of serine, threonine and cysteine residues within α -helices and its relevance to membrane-bound proteins. *J. Mol. Biol.* 175(1):75–81, 1984.
- Gulrajani, M. Degumming of Silk. *Silk dyeing printing and finishing*, pp. 63–95. New Dehli: Hauz Khas, 1988.
- Gulrajani, M. Sericin: A Bio-Molecule of Value. In 20 the Congress of the International Sericultural Comission, pp. 21–29. Bangalore, 2015.
- Hardy, J. G., Leal-Egana, A., & Scheibel, T. R. Engineered Spider Silk Protein-Based Composites for Drug Delivery. *Macromolecular Bioscience*, 13, 1431–1437, 2013.
- Hardy, J. G., Römer, L. M., & Scheibel, T. R. Polymeric materials based on silk proteins. *Polymer*, 49, 4309–4327, 2008.
- Hardy, J., and T. Scheibel. Silk-inspired polymers and proteins. *Biochim. Soc. Trans.*, 37(4): 677–681, 2009.
- Harris, B. *Engineering Composite Materials*. London: The Institute of Materials, 1999.
- Hayashi, C. Y., & Lewis, R. V. Evidence from Flagelliform Silk cDNA for the Structural Basis of Elasticity and Modular Nature of Spider Silks. *J. Mol. Biol.*, 275, 773–784, 1998.
- Hijirida, D., Do, K., Michal, C., Wong, S., Zax, D., & Jelinski, L. ¹³C NMR of Nephila clavipes major ampullate silk gland. *Biophysical Journal*, 71, 3442–3447, 1996.
- Hirai, Y., J. Ishikuro, and T. Nakajima. Some comments on the penetration of water vapor into regenerated silk fibroin. *Polymer*, 42(12):5495–5499, 2001.
- Ho, M., H. Wang, K. Lau, J. Lee, and D. Hui. Interfacial bonding and degumming effects on silk fibre/polymer biocomposites. *Compos. Part B-Eng.* 43(7):2801–2812, 2012.
- Hodge, R., T. Bastow, G. Edward, G. Simon, and A. Hill. Free Volume and the Mechanism of Plasticization in Water-Swollen Poly(vinyl alcohol). *Macromolecules*, 29(25):8137–8143, 1996.
- Hofer, M., Winter, G., & Myschik, J. Recombinant spider silk particles for controlled delivery of protein drugs. *Biomaterials*, 33, 1554–1562, 2012.
- Hu, K. Biocompatible Fibroin Blended Films with Recombinant Human-like Collagen for Hepatic Tissue Engineering. *J. Bioact. Compat. Pol.* 21(1):23–37, 2006.
- Hu, K., Q. Lv, F. Cui, L. Xu, Y. Jiao, and Y. Wang *et al.* A Novel Poly(L-lactide) (PLLA)/Fibroin Hybrid Scaffold to Promote Hepatocyte Viability and Decrease Macrophage Responses. *J. Bioact. Compat. Pol.* 22(4):395–410, 2007.
- Hu, X., D. Kaplan, and P. Cebe. Effect of water on the thermal properties of silk fibroin. *Thermochim. Acta*, 461(1–2):137–144, 2007.
- Hu, X., D. Kaplan, and P. Cebe. Dynamic Protein-Water Relationships during β -Sheet Formation. *Macromolecules*, 41(11):3939–3948, 2008.
- Hu, X., K. Shmelev, L. Sun, E. Gil, S. Park, P. Cebe, and D. Kaplan. Regulation of Silk Material Structure by Temperature-Controlled Water Vapor Annealing. *Biomacromolecules*. 12(5):1686–1696, 2011.
- Huang, J., R. Valluzzi, E. Bini, B. Vernaglia, and D. Kaplan. Cloning, Expression, and Assembly of Sericin-like Protein. *J. Biol. Chem.* 278(46):46117–46123, 2003.
- Huddar, P. A study of natural and synthetic compound with reference to chemistry of formation of silk in silkworm (PhD Thesis). University of Pune, 1985.
- Inoue, S., K. Tanaka, F. Arisaka, S. Kimura, K. Ohtomo, and S. Mizuno. Silk Fibroin of Bombyx mori Is Secreted, Assembling a High Molecular Mass Elementary Unit Consisting of H-chain, L-chain, and P25, with a 6:6:1 Molar Ratio. *J. Biol. Chem* 275(51):40517–40528, 2000.

- Jiang, P., H. Liu, C. Wang, L. Wu, J. Huang, and C. Guo. Tensile behavior and morphology of differently degummed silkworm (*Bombyx mori*) cocoon silk fibres. *Mater. Lett.* 60(7):919–925, 2006.
- Jin, H., J. Park, R. Valluzzi, P. Cebe, and D. Kaplan. Biomaterial Films of *Bombyx Mori* Silk Fibroin with Poly(ethylene oxide). *Biomacromolecules*, 5(3):711–717, 2004.
- Joseph, K., and L. de Carvalho. Jute/cotton woven fabric reinforced polyester composites: effect of hybridization. *International Symposium on Natural Polymers and Composites*, pp. 454–459, 2000.
- Kaewkorn, W., N. Limpeanchob, W. Tiyafoonchai, S. Pongcharoen, and M. Sutheerawattananonda. Effects of silk sericin on the proliferation and apoptosis of colon cancer cells. *Biol. Res.* 45(1):45–50, 2012.
- Kang, M., and H. Jin. Electrically conducting electrospun silk membranes fabricated by adsorption of carbon nanotubes. *Colloid. Polym. Sci.* 285(10):1163–1167, 2007.
- Kato, N., S. Sato, A. Yamanaka, H. Yamada, N. Fuwa, and M. Nomura. Silk Protein, Sericin, Inhibits Lipid Peroxidation and Tyrosinase Activity. *Biosci. Biotech. Bioch.*, 62(1):145–147, 1998.
- Kawahara, Y., M. Shioya, and A. Takaku. Mechanical properties of silk fibers treated with methacrylamide. *J. Appl. Polym. Sci.* 61(8):1359–1364, 1996.
- Keener, T., R. Stuart, and T. Brown. Maleated coupling agents for natural fibre composites. *Compos. Part A – Appl. S.* 35(3):357–362, 2004.
- Keten, S., & Buehler, M. J. Nanostructure and molecular mechanics of spider dragline silk protein assemblies. *Journal of the Royal Society Interface*, 7, 1709–1721, 2010b.
- Keten, S., Xu, Z., Britni, I., & Markus, B. J. Nanoconfinement controls stiffness, strength and mechanical toughness of beta-sheet crystals in silk. *Nature Materials*, 9, 359–367, 2010a.
- Khan, M., M. Tsukada, Y. Gotoh, H. Morikawa, G. Freddi, and H. Shiozaki. Physical properties and dyeability of silk fibers degummed with citric acid. *Bioresource Technol.* 101(21):8439–8445, 2010.
- Khare, R., and S. Bose. Carbon nanotube based composite. *J. Miner. Miner. Charact. & Eng.* 4(1):31–46, 2005.
- Ki, C., J. Kim, H. Oh, K. Lee, and Y. Park. The effect of residual silk sericin on the structure and mechanical property of regenerated silk filament. *Int. J. Biol. Macromol.* 41(3):346–353, 2007.
- Kim, H., W. Park, Y. Kim, and H. Jin. Silk fibroin films crystallized by multiwalled carbon nanotubes. *Int. J. Mod. Phys. B.* 22:1807–1812, 2008.
- Kundu, B., N. Kurland, S. Bano, C. Patra, F. Engel, V. Yadavalli, and S. Kundu. Silk proteins for biomedical applications: Bioengineering perspectives. *Prog. Polym. Sci.* 39(2):251–267, 2014.
- Kundu, S. *Silk biomaterials for tissue engineering and regenerative medicine*. Amsterdam: Woodhead Publishing, 2014.
- Kundu, S., B. Dash, R. Dash, and D. Kaplan. Natural protective glue protein, sericin bioengineered by silkworms: Potential for biomedical and biotechnological applications. *Prog. Polym. Sci.* 33(10):998–1012, 2008.
- Kurosaki, S., H. Otsuka, M. Kunitomo, M. Koyama, R. Pawankar, and K. Matumoto. Fibroin allergy. IgE mediated hypersensitivity to silk suture materials. *Nippon Ika Daigaku Zasshi*, 66(1):41–44, 1999.
- Lammel, A., Schwab, M., Hofer, M., Winter, G., & Scheibel, T. Recombinant spider silk particles as drug delivery vehicles. *Biomaterials*, 32, 2233–2240, 2011.
- Lazaris A, Arcidiacono S, Huang Y, Zhou JF, Duguay F, Chretien N, Welsh EA, Soares JW, Karatzas CN. Spider silk fibers spun from soluble recombinant silk produced in mammalian cells. *Science*, 295(5554):472–6, 2002.
- Leffevre, T., F. Paquet-Mercier, S. Lesage, M. Rousseau, S. Bedard, and M. Pezolet. Study by Raman spectromicroscopy of the effect of tensile deformation on the molecular structure of *Bombyx mori* silk. *Vibr. Spectrosc.* 51(1):136–141, 2009.

- Lewicka, M., Hermanson, O., & Rising, A. U. Recombinant spider silk matrices for neural stem cell cultures. *Biomaterials*, 33, 7712–7717, 2012.
- Lewin, M. *Handbook of fiber chemistry*. Boca Raton: CRC/Taylor & Francis, 2007.
- Li, M., S. Lu, Z. Wu, K. Tan, N. Minoura, and S. Kuga. Structure and properties of silk fibroin-poly(vinyl alcohol) gel. *Int. J. Biol. Macromol.* 30(2): 89–94, 2002.
- Ling, S., Z. Qi, B. Watts, Z. Shao, and X. Chen. Structural determination of protein-based polymer blends with a promising tool: combination of FTIR and STXM spectroscopic imaging. *Phys. Chem. Chem. Phys.*, 16(17):7741, 2014.
- Liu, X., and K. Zhang. Silk Fiber - Molecular Formation Mechanism, Structure-Property Relationship and Advanced Applications. C. Lesieure, *Oligomerization of Chemical and Biological Compounds* (1st ed.), 2014.
- Lovett, M., C. Cannizzaro, G. Vunjak-Novakovic, and D. Kaplan. Gel spinning of silk tubes for tissue engineering. *Biomaterials*. 29(35):4650–4657, 2008.
- Luo, S., and A. Netravali. Mechanical and thermal properties of environment-friendly “green” composites made from pineapple leaf fibers and poly(hydroxybutyrate-co-valerate) resin. *Polym. Composite*. 20(3):367–378, 1999.
- MacIntosh, A., V. Kearns, A. Crawford, and P. Hatton. Silk-based biomaterials for tissue engineering. *Top. Tiss. Eng.* 4, 2008.
- Mahmoodi, N., M. Arami, F. Mazaheri, and S. Rahimi. Degradation of sericin (degumming) of Persian silk by ultrasound and enzymes as a cleaner and environmentally friendly process. *J. Clean. Product*. 18(2):146–151, 2010.
- Manfredi, L., E. Rodriguez, M. Wladyka-Przybylak, and A. Vazquez. Thermal degradation and fire resistance of unsaturated polyester, modified acrylic resins and their composites with natural fibres. *Polym. Degrad. Stab.* 91(2):255–261, 2006.
- Matuana, L., J. Balatinez, R. Sodhi, and C. Park. Surface characterization of esterified cellulosic fibers by XPS and FTIR Spectroscopy. *Wood Sci. Technol.* 35(3):191–201, 2001.
- Mishra, S., J. Naik, and Y. Patil. The compatibilising effect of maleic anhydride on swelling and mechanical properties of plant-fiber-reinforced novolac composites. *Compos. Sci. Technol.* 60(9):1729–1735, 2000.
- Mitrana, V., M. Albu, E. Vasile, A. Cimpean, and M. Costache. Dose-related effects of sericin on preadipocyte behavior within collagen/sericin hybrid scaffolds. *Prog. Nat. Sci. – Mater. Int.* 25(2):122–130, 2015.
- Mo, C., P. Wu, X. Chen, and Z. Shao. The effect of water on the conformation transition of Bombyx mori silk fibroin. *Vibr. Spectrosc.* 51(1):105–109, 2009.
- Mohanty, A., M. Khan, and G. Hinrichsen. Surface modification of jute and its influence on performance of biodegradable jute-fabric/Biopol composites. *Compos. Sci. Technol.* 60(7):1115–1124, 2000.
- Mondal, M., K. Trivedy, and S. Kumal. The silk proteins, sericin and fibroin in silkworm, Bombyx mori Linn.,-a review. *Caspian J. Env. Sci.* 5(2):63–76, 2007.
- Moraes, M., G. Nogueira, R. Weska, and M. Beppu. Preparation and Characterization of Insoluble Silk Fibroin/Chitosan Blend Films. *Polymers*. 2(4):719–727, 2010.
- Mortimer, B., D. Drodge, K. Dragnevski, C. Siviour, and C. Holland. *In situ* tensile tests of single silk fibres in an environmental scanning electron microscope (ESEM). *J. Mater. Sci.* 48(14): 5055–5062, 2013.
- Nagaraju, J. SilkSatDB-A Silkworm Microsatellite Database. Cdfe.org.in., 2015. Retrieved 2004, from <http://www.cdfe.org.in/SILKSAT/index.php?f=silkbio>
- Nova, A., Keten, S., Pugno, N. M., Redaelli, A., & Buehler, M. J. Molecular and Nanostructural Mechanisms of Deformation, Strength and Toughness of Spider Silk Fibrils. *Nano Letters*, 10, 2626–2634, 2010.

- Oksman, K. Mechanical properties of natural fibre mat reinforced thermoplastic. *Appl. Compos. Mater.* 7:403–414, 2000.
- Omenetto, F., and D. Kaplan. New Opportunities for an Ancient Material. *Science*. 329(5991): 528–531, 2010.
- Pahlevan, M., Toivakka, M., & Alam, P. Electrostatic charges instigate ‘concertina-like’ mechanisms of molecular toughening in MaSp1 (spider silk) proteins. *Materials Science and Engineering C*, 41, 329–334, 2014.
- Pan, H., Y. Zhang, H. Shao, X. Hu, X. Li, F. Tian, and J. Wang. Nanoconfined crystallites toughen artificial silk. *J. Mater. Chem. B*, 2(10):1408, 2014.
- Perez-Rigueiro, J., C. Viney, J. Llorca, and M. Elices. Mechanical properties of single-brin silk-worm silk. *J. Appl. Polym. Sci.* 75(10):1270, 2000.
- Porter, D., Vollrath, F., & Shao, Z. Predicting the mechanical properties of spider silk as a model nanostructured polymer. *The European Physical Journal E*, 16, 199–206, 2005.
- Pracella, M., D. Chionna, I. Anguillesi, Z. Kulinski, and E. Piorkowska. Functionalization, compatibilization and properties of polypropylene composites with Hemp fibres. *Compos. Sci. Technol.* 66(13):2218–2230, 2006.
- Qiao, X., W. Li, K. Sun, S. Xu, and X. Chen. Nonisothermal crystallization behaviors of silk-fibroin-fiber-reinforced poly(E- μ -caprolactone) biocomposites. *J. Appl. Polym. Sci.* 111(6):2908–2916, 2009.
- Rawar, A., and M. Padamwar. Silk sericin and its applications: A review. *J. Sci. Ind. Res. India*. 63:323–329, 2004.
- Römer, L., & Scheibel, T. The elaborate structure of spider silk: Structure and function of a natural high performance fiber. *Prion*, 2, 154–161, 2008.
- Saheb, D., and J. Jog. Natural fiber polymer composites: A review. *Adv. Polym. Tech.* 18(4):351–363, 1999.
- Salavatian, M., and L. Smith. An investigation of matrix damage in composite laminates using continuum damage mechanics. *Compos. Struct.* 131:565–573, 2015.
- Schacht, K., & Scheibel, T. Processing of recombinant spider silk proteins into tailor-made materials for biomaterials applications. *Current Opinion in Biotechnology*, 29, 62–69, 2014.
- Shah, D. Natural fibre composites: Comprehensive Ashby-type materials selection charts. *Mater. Design*. 62:21–31, 2014.
- Shah, D., D. Porter, and F. Vollrath. Opportunities for silk textiles in reinforced biocomposites: Studying through-thickness compaction behaviour. *Compos. Part A-Appl. Sci.* 62:1–10, 2014.
- Shao, Z., and F. Vollrath. Materials: Surprising strength of silkworm silk. *Nature*. 418(6899):741–741, 2002.
- Shea, J.-E., & Brooks III, C. L. From folding theories to folding proteins: a review and assessment of simulation studies of protein folding and unfolding. *Annual Review of Physical Chemistry*, 52, 499–535, 2001.
- Singha A.S.S., Sharma A. and Thakur V.K. X-ray diffraction, morphological, and thermal studies on methylmethacrylate graft copolymerised *Saccharum ciliare* fibre. *International Journal of Polymer Analysis and Characterisation*, 13:447–462, 2008.
- Singha A.S. and Thakur V.K. Mechanical, morphological and thermal properties of pine needle reinforced polymer composites. *International Journal of Polymeric Materials*, 58:21–31, 2008.
- Singha A.S. and Thakur V.K. Fabrication and characterisation of *H. sabdariffa* fibre-reinforced green polymer composites. *Polymer-Plastics Technology and Engineering*, 48:482–487, 2009.
- Singha A.S. and Thakur V.K. Synthesis, characterisation and analysis of Hibiscus sabdariffa fibre reinforced polymer matrix based composites. *Polymers and Polymer Composites*, 17(3):189–194, 2009b.

- Sintya, E. and Alam, P. Self-assembled semi-crystallinity at parallel beta-sheet nanocrystal interfaces in clustered MaSp1 (spider silk) proteins; *Materials Science and Engineering C: Materials for Biological Applications* Vol. 58, pp. 366–371, 2016.
- Sirichaisit, J., V. Brookes, R. Young, and F. Vollrath. Analysis of Structure/Property Relationships in Silkworm (*Bombyx mori*) and Spider Dragline (*Nephila edulis*) Silks Using Raman Spectroscopy. *Biomacromolecules*. 4(2):387–394, 2003.
- Sobajo, C., F. Behzad, X. Yuan, and A. Bayat. Silk: A Potential Medium for Tissue Engineering. *Open Access J. Plast.Surg.* 8(47), 2008.
- Spiess, K., Lammel, A., & Scheibel, T. Recombinant Spider Silk Proteins for Applications in Biomaterials. *Macromolecular Bioscience*, 10, 998–1007, 2010.
- Sugihara, A., K. Sugiura, H. Morita, T. Ninagawa, K. Tubouchi, and R. Tobe *et al.* Promotive Effects of a Silk Film on Epidermal Recovery from Full-Thickness Skin Wounds. *P. Soc. Exp. Biol. Med.* 225(1):58–64, 2000.
- Tarakanova, A., & Buehler, M. J. A Materiomics Approach to Spider Silk: Protein Molecules to Webs. *JOM*, 64, 2012.
- Teramoto, H., A. Kakazu, K. Yamauchi, and T. Asakura. Role of Hydroxyl Side Chains in *Bombyx mori* Silk Sericin in Stabilizing Its Solid Structure. *Macromolecules*. 40(5):1562–1569, 2007.
- Teramoto, H., T. Kameda & T. Yasushi. Preparation of Gel Film from *Bombyx mori* Silk Sericin and Its Characterization as a Wound Dressing. *Bioscience, Biotechnology, and Biochemistry* 72(12):3189–3196, 2008.
- Teulé, F., Addison, B., Cooper, A., Ayon, J., Henning, R., Benmore, C., *et al.* Combining flagelliform and dragline spider silk motifs to produce tunable synthetic biopolymer fibers. *Biopolymers*, 97, 418–431, 2012.
- Thakur V.K. and Singha A.S. Natural fibres-based polymers: Part I – mechanical analysis of pine needles reinforced biocomposites. *Bulletin of Materials Science*, 33(3):257–264, 2010a.
- Thakur V.K. and Singha A.S. Physico-chemical and mechanical characterisation of natural fibre reinforced polymer composites. *Iranian Polymer Journal*, 19(1):3–16, 2010b.
- Thakur V.K. and Singha A.S. Physico-chemical and mechanical behaviour of cellulosic pine needle based biocomposites. *International Journal of Polymer Analysis and Characterisation*, 16:390–398, 2011.
- Thakur V.K. and Singha A.S. Rapid synthesis, characterisation, and physicochemical analysis of biopolymer-based graft copolymers. *International Journal of Polymer Analysis and Characterisation*, 16:153–164, 2011b.
- Thakur, V.K., Thakur, M.K., Processing and characterization of natural cellulose fibers/thermoset polymer composites. *Carbohydr. Polym.* 109, 102–117, 2014a.
- Thakur, V.K., Thakur, M.K., Recent Advances in Graft Copolymerization and Applications of Chitosan: A Review. *Acs Sustain. Chem. Eng.* 2, 2637–2652, 2014b.
- Thakur, M.K., Thakur, V.K., Gupta, R.K., Pappu, A., Synthesis and Applications of Biodegradable Soy Based Graft Copolymers: A Review. *ACS Sustain. Chem. Eng.* 4, 1–17, 2016.
- Timar-Balazsy A., and D. Eastop. *Chemical principles of textile conservation*. Oxford [England]: Butterworth-Heinemann, 2012.
- Tsukada, M., M. Obo, H. Kato, G. Freddi, and F. Zanetti. Structure and dyeability of *Bombyx mori* silk fibers with different filament sizes. *J. Appl. Polym. Sci.* 60(10):1619–1627, 1996.
- Ude, A., R. Eshkoor, R. Zulkifili, A. Ariffin, A. Dzuraidah, and C. Azhari. *Bombyx mori* silk fibre and its composite: A review of contemporary developments. *Mater. Design.* 57:298–305, 2014.
- Vepari, C., and D. Kaplan. Silk as a biomaterial. *Prog. Polym. Sci.* 32(8–9):991–1007, 2007.
- Voegeli, R., J. Meier, and R. Blust. Sericin silk protein: unique structure and properties. *Cosmet. Tolieteries*. 108:101–108, 1993.
- Vollrath, F., and D. Edmonds. Modulation of the mechanical properties of spider silk by coating with water. *Nature*. 340(6231):305–307, 1989.

- Vollrath, F., and D. Porter. Silks as ancient models for modern polymers. *Polymer*, 50(24):5623–5632, 2009.
- Wambua, P., J. Ivens, and I. Verpoest. Natural fibres: can they replace glass in fibre reinforced plastics?. *Compos. Sci. Technol.* 63(9):1259–1264, 2003.
- Widhe, M., Bysell, H., Nystedt, S., Nystedt, S., Schenning, I., Malmsten, M., *et al.* Recombinant spider silk as matrices for cell culture. *Biomaterials*, 31, 9575–9585, 2010.
- Widhe, M., Johansson, J., Hedhammar, M., & Rising, A. Current Progress and Limitations of Spider Silk for Biomedical Applications. *Biopolymers*, 97, 468–478, 2012.
- Widhe, M., Johansson, U., Hillerdahl, C.-O., & Hedhammar, M. Recombinant spider silk with cell binding motifs for specific adherence of cells. *Biomaterials*, 34, 8223–8234, 2013.
- Wohlrab, S., Müller, S., Schmidt, A., Neubauer, S., Kessler, H., Leal-Egaña, A., *et al.* Cell adhesion and proliferation on RGD-modified recombinant spider silk proteins. *Biomaterials*, 33, 6650–6659, 2012.
- Xu, Y., Y. Zhang, H. Shao, and X. Hu. Solubility and rheological behavior of silk fibroin (*Bombyx mori*) in N-methyl morpholine N-oxide. *Int. J. Biol. Macromol.* 35(3–4):155–161, 2005.
- Yamaguchi, K., Y. Kikuchi, T. Takagi, A. Kikuchi, F. Oyama, K. Shimura, and S. Mizuno. Primary structure of the silk fibroin light chain determined by cDNA sequencing and peptide analysis. *J. Mol. Biol.* 210(1):127–139, 1989.
- Yang, L., C. Tan, M. Hsieh, J. Wang, Y. Duan, and P. Cieplak *et al.* New-Generation Amber United-Atom Force Field. *J. Phys. Chem. B*, 110(26):13166–13176, 2006.
- Yin, J., E. Chen, D. Porter, and Z. Shao. Enhancing the Toughness of Regenerated Silk Fibroin Film through Uniaxial Extension. *Biomacromolecules*, 11(11):2890–2895, 2010.
- Yuan, Q., J. Yao, L. Huang, X. Chen, and Z. Shao, Z. Correlation between structural and dynamic mechanical transitions of regenerated silk fibroin. *Polymer*, 51(26):6278–6283, 2010.
- Zeplin, P. H., Maksimovikj, N. C., Jordan, M. C., Nickel, J., Lang, G., Leimer, A. H., *et al.* Spider Silk Coatings as a Bioshield to Reduce Periprosthetic Fibrous Capsule Formation. *Adv. Funct. Mater.*, 24, 2658–2666, 2014.
- Zhang, H., L. Li, F. Dai, H. Zhang, B. Ni, and W. Zhou *et al.* Preparation and characterization of silk fibroin as a biomaterial with potential for drug delivery. *J. Trans. Med.* 10(1):117, 2012.
- Zhao, H., X. Feng, S. Yu, W. Cui, and F. Zou, F. Mechanical properties of silkworm cocoons. *Polymer*, 46(21):9192–9201, 2005.
- Zhou, C., F. Confalonieri, M. Jacquet, R. Perasso, Z. Li, and J. Janin. Silk fibroin: Structural implications of a remarkable amino acid sequence. *Protein*, 44(2):19–122, 2001.
- Zhou, Y., Wu, S., & Conticello, V. P. Genetically Directed Synthesis and Spectroscopic Analysis of a Protein Polymer Derived from a Flagelliform Silk Sequence. *Biomacromolecules*, 2, 111–125, 2001.
- Zhu, B., Li, W., Lewis, R. V., Segre, C. U., & Wang, R. E Spun Composite Fibers of Collagen and Dragline Silk Protein: Fiber Mechanics, Biocompatibility, and Application in Stem Cell Differentiation. *Biomacromolecules*, 16, 202–213, 2015.
- Zhu, L., M. Arai, and K. Hirabayashi. Sol-gel transition of sericin. *J. Sericult. Sci. Japan.*, 65(4): 270–274, 1996.

Isolation and Characterisation of Water Soluble Polysaccharide from *Colocasia esculenta* Tubers

Harshal Ashok Pawar*, Pritam Dinesh Choudhary and Amit Jagannath Gavasane

Dr. L. H. Hiranandani College of Pharmacy, Ulhasnagar, Maharashtra, India

Abstract

Colocasia esculenta (*C. esculenta*) is a fast growing plant largely cultivated for consumption of both leaves and tubers. The present investigation deals with isolation, purification and characterisation of the water soluble polysaccharide from *C. esculenta* tubers. The polysaccharide extraction was based on chopping, soaking of the tubers, water dissolution, filtration and precipitation with acetone. The polysaccharide obtained from *C. esculenta* tubers was characterized by using physicochemical and chromatographic procedures, as well as FTIR, ¹³C NMR and ¹H NMR spectroscopy. The results indicated that the polysaccharide has four sugar moieties namely α -(1 \rightarrow 4)-D-Glucopyranose, α -(1 \rightarrow 6)-D-Glucopyranose, β -D-Galactopyranose and β -D-Arabinopyranose. The rheological studies indicated that the *C. esculenta* gum (1%, w/v) solution possesses pseudoplastic flow. Due to ready availability, neutral nature and good swelling ability, *C. esculenta* tuber polysaccharide can be used as a novel herbal excipient in the development of sustained and controlled release drug delivery system.

Keywords: *Colocasia esculenta*, polysaccharides, NMR, FTIR, tubers, glucopyranose, TLC

9.1 Introduction

Today there is an increasing awareness in replacing synthetic polymers with natural polymers for different applications (Thakur & Thakur, 2014a–c). Biological macromolecules enriched resources are rapidly emerging as sustainable, cost effective and environmental friendly materials for several industrial applications (Pappu A. *et al.*, 2015; Singha & Thakur, 2010a–d). Polysaccharides are biopolymers that have unique properties along with an enormous diversity in their structure. A large amount of polysaccharides are biosynthetically formed by many organisms including animals, plants, algae, fungi and microorganisms as macromolecules due to their ability for structure formation by interactions that are supramolecular of variable types (Thakur *et al.*, 2016; Thakur & Kessler, 2015; Thakur & Thakur, 2015). The recent attention of the whole world towards renewable and sustainable resources has resulted in many unique and

*Corresponding author: hapkmk@rediffmail.com, harshal.dlhhcop@gmail.com

ground-breaking research activities. Polysaccharides, which possess different options for use and application, are by far the most important renewable resources (Voicu *et al.*, 2016; Wu *et al.*, 2016). From the viewpoint of a chemist, the unique structure of polysaccharides combines with many promising properties like hydrophilicity, biocompatibility, biodegradability (in the original state), stereoregularity, polyfunctionality and multichirality. Polysaccharides, including gums and mucilages that are found in abundance in nature and constitute a vast class of macromolecules showcasing a wide range of physicochemical properties, are widely used recently in medicine and pharmacy (Clifford *et al.*, 2002). In recent years polysaccharides of natural origin have been widely used in various pharmaceutical applications like diluent, oral liquid thickeners, protective colloids in suspensions, gelling agents in gels and bases in suppository, binder, disintegrant in tablets, etc. (Zatz & Kushla, 1989). They are also used in textiles, cosmetics, paints and paper making (Jania *et al.*, 2009). These natural polymers are readily available, biocompatible, cheap and are preferred over synthetic and semi synthetic excipients due to their low cost, easy availability, lack of toxicity and non-irritant nature (Whistler, 1996; Giriraj *et al.*, 2002; Kakrani & Jain, 1981). The approach of characterization of pharmaceutical excipients using a material science has helped the designing of drug formulations thus obtaining a desired set of properties. It has thus become increasingly apparent that there is an important relationship between the excipients properties and the dosage forms containing those excipients. Preformulation studies showed the influence of the properties of the excipients on stability, bioavailability and the process by which the dosage forms are prepared. There is a need to acquire more information and use of standards for excipients characterization.

Colocasia esculenta is the edible variety that is most widely cultivated and consumed in Southeast Asia and also known by the names like *Arbi*, *Arvi* and *Eddoe*. Taro is also grown throughout the humid tropics and is widely used throughout the world: Africa, Asia, the West Indies, and South America. The corms and tubers of several genera of the family *Araceae* are commonly known as Taro. A wide range of chemical compounds including flavonoids, β -sitosterol, and steroids have been isolated from this species. Phytochemical studies on the *Colocasia esculenta* extracts have shown the presence of anthocyanins like pelargonidin-3-glucoside, cyanidin-3-glucoside and cyanidin-3-rhamnoside. These moieties possess antioxidant activities as evident from previous studies. (Noda Y *et al.*, 2002; Cambie, R. C. & Ferguson, 2003; Kowalczyk, E., Kopff A *et al.*, 2003). The juice of leaf of the plant acts as a stimulant, styptic, rubefacient, and is useful in internal haemorrhages, adenitis, otalgia and buboes. The juice of the corm has properties like demulcent, laxative and anodyne. The leaves of *Colocasia esculenta* have been studied to possess anthelmintics, anti-diabetic and anti-inflammatory action (Lin & Huang, 1993). Its edible leaves and tubers are traditionally used for hepatic ailments (Tuse T.A. *et al.*, 2009). *Colocasia esculenta* (L) Schott of the family *Araceae* is a perennial herbaceous plant cultivated annually. Kirtikar and Basu have summarised morphology of this plant in their study. It is a tall herb, is tuberous or has a stout short caudex, flowering and leafing is together. Leaves of this plant are simple, with a stout petiole, lamina peltate, ovate-cordate or sagittate-cordate. The spadix is shorter than the petiole and much shorter than the spathe; the appendix is much shorter than the inflorescence. Stem above ground, or slightly swollen at the base of the leaf-sheaths,

arising from a hard tapering rhizome or in cultivated forms a tuberous rhizome suckers and stolons sometimes present (Kirtikar KR & Basu BD., 2005). The large green leaves are often described as 'elephant ear' due to their large size and shape. The tuberous roots contain starch and is the main edible part of the crop. The leaves of *Colocasia esculenta* are also used as a leafy vegetable. *Colocasia esculenta* leaves have been reported to be rich in nutrients including minerals and vitamins such as calcium, phosphorous, iron, vitamin C, thiamine riboflavin and niacin (Lewu M.N. *et al.*, 2009)

Awasthi and Singh have studied ayurvedic implications of *Colocasia esculenta* plant. Among various edible aroids commercially cultivated in India, *Colocasia esculenta* has noteworthy dietary significance, including multiple uses in the form of various culinary preparations of its corm and edible stem. Fresh edible leaves of *Colocasia esculenta* form rich source of protein, ascorbic acid, dietary fibres and some nutritionally important minerals. Tender leaves of *Colocasia esculenta* are used as a vegetable. Leaf juice is applied over scorpion sting or snake bite and also given for food poisoning of plant origin (Ayurveda identified ailments viz.). The plant is also reported to be used in cases of vata and pitta, constipation, stomatitis, alopecia, haemorrhoids and general weakness (Awasthi CP & Singh AB, 2000; Devarkar V.D. *et al.*, 2011).

Earlier research showed the presence of water soluble gum or mucilage (Crabtree & Baldry, 1982; Moy, Wang & Nakayama, 1977; Allen & Allen, 1933) in Taro gum. Sustained release formulations of Metoprolol Succinate using Taro gum were prepared and evaluated. 32 full optimization procedure was adopted (Soumya M, *et al.*, 2014). Another researcher discusses formulation and evaluation of Mucoadhesive matrix tablets using gum Taro. Matrix tablets of Domperidone. This study showed mucoadhesive property and release retardant potential of taro gum dependent on its concentration in the formulation of gastro retentive mucoadhesive matrix tablets (Gurpreet Arora *et al.*, 2011). Chukwu and Udeala studied the effective property of *Colocassia esculenta* gum in drugs that are poorly compressible like paracetamol and metronidazole tablet formulations. The polysaccharide gum obtained from the corms of *Colocassia esculenta* was evaluated comparatively with established binders like acacia and methylcellulose in the formulation of poorly compressible drugs (Chukwu K. I. & Udeala O. K, 2000). However, only limited attention was given on structure and rheological behaviour of taro polysaccharide. El-Mahdy and El-Sebaiy reported a preliminary study on the viscosities and molecular weight profiles of several different mucilages including taro gum. Glucose was identified as the major sugar constituent in the taro gum, along with smaller fractions of galactose and fructose. In yet another study, gum was extracted from taro corms (*Colocasia esculenta*) with a low-temperature extraction (4 °C) and purification procedure (Hui Lin & Alvin S. Huang. 1993). In the acid hydrolysates of the taro gum extracted by Hui and Alvin, D-galactose was identified as the main component by HPLC (61.6%), followed by D-glucose (19.7%) and D-arabinose (16.2%). Smaller quantities of galacturonic acid and proteins were also found in the gum. It was also observed that neither pH nor ionic strength of the gum solution had significant effect on viscosity of the polymer.

The main aim of this article is to shed light on the structural features, rheological behaviour and also physicochemical properties of *C. esculenta* polysaccharide extracted from *C. esculenta* tubers at room temperature.

9.2 Materials and Methods

9.2.1 Collection of Plant Material

Fresh tubers of *Colocasia esculenta* were collected from local market of Ambernath, district Thane, Maharashtra, India. Plant was authenticated by Dr. Rajendra. D. Shinde, Associate Professor, Blatter Herbarium; St. Xavier's College, Mumbai, India and was identified as *Colocasia esculenta* (L.) Schott belonging to family *Araceae*. The specimen matches with Blatter Herbarium specimen number 19033 of H. Santapau.

9.2.2 Isolation of Polysaccharide

Fresh tubers were washed and peeled to separate dirt and other unwanted materials from its surface. These were then sliced into small pieces and blended in a blender with little purified water at room temperature for 30 minutes. The resultant slurry was then passed through muslin cloth to get a slimy solution. Material retained on the muslin cloth was discarded. Acetone was added, twice the amount of the filtrate to precipitate the polysaccharide. The polysaccharide was separated using muslin cloth and dried overnight at 40 °C in a hot air oven. Dried polysaccharide was pulverised using ceramic mortar and pestle and gum powder was passed through 100# sieve. The polysaccharide thus obtained was stored at room temperature in double layered plastic pouches and then was placed in an air tight container till further use.

9.2.3 Purification of Polysaccharide

This is an important step to ensure that the polysaccharide obtained is of its pure form. Any impurity in the polysaccharide would result in erroneous results in detecting the structural components of the water soluble polysaccharide. The obtained polysaccharide was purified by dissolving the dried polysaccharide in water and reprecipitating it using acetone. The precipitated polysaccharide was separated using muslin cloth and again dried overnight at 40 °C in a hot air oven. This procedure was repeated three times to obtain pure polysaccharide. The polysaccharide thus obtained was stored at room temperature in double layered plastic pouches and then was placed in an air tight container till further use.

9.2.4 Characterization of Polysaccharide

The polysaccharide obtained after purification was subjected to organoleptic evaluation, preliminary phytochemical evaluation and physicochemical evaluations like solubility, powder flow characteristics, pH, Loss on drying, specific gravity, swelling capacity, viscosity. The polysaccharide was also evaluated for total sugar content, differential scanning calorimeter, X-ray diffraction (XRD) and thin layer chromatography (TLC). Structural investigation was done using ¹H NMR and ¹³C NMR.

9.2.4.1 Organoleptic Evaluation

Organoleptic evaluation of purified and sieved gum was carried out. The colour, odour, taste, shape and texture were noted.

9.2.4.2 Preliminary Phytochemical Evaluation

Preliminary phytochemical screening was carried out on hot water extract of *C. esculenta* polysaccharide (Khandelwal, 2012). The extract was prepared by adding dried extracted polysaccharide to distilled water and heating till the water boils. This is then cooled to room temperature and filtered using a wattman filter paper. The filtrate thus obtained is termed as hot water extract of *C. esculenta* polysaccharide. This extract was then subjected to Molisch's test, Fehling's test, Iodine test and Biuret test.

Molisch's test is a sensitive chemical test for detection of presence of carbohydrates, based on the mechanism of dehydration of the carbohydrate by sulphuric acid or hydrochloric acid to produce an aldehyde, which then condenses with two molecules of phenol (here α naphthol) to form a red- or purple-colored compound. For this test equal quantities of *C. esculenta* extract was mixed with α naphthol in a test tube. Concentrated Sulphuric acid was then added slowly to this mixture from the sides of the test tube.

Fehling's test is a test for reducing sugars and non-reducing sugars. For this test, a mixture of Fehling A and Fehling B reagents (1:1) was taken in a test tube. To this mixture, same quantity of *C. esculenta* extract was added. This was then heated on a water bath for about 5 minutes.

The Iodine test is used to test for the presence of starch. Iodine solution was prepared by dissolving it in an aqueous solution of potassium iodide. The iodine reacts with the starch, producing a purple-black colour. For this test 1 ml of *C. esculenta* extract was taken in a test tube. To this extract equal quantity of purified water was added to dilute it followed by two drops of Iodine solution.

The biuret test is a chemical test specifically used for detecting the presence of peptide bonds. If peptide bonds are present, a copper (II) ion forms violet-colored coordination complexes in an alkaline solution. To 1 ml of *C. esculenta* extract equal volume of Biuret reagent was added. Colour of the solution was observed.

Ruthenium red test is identification test for mucilages. For this test 1 ml of ruthenium red reagent was taken in a watch glass. To this small quantity of powder polysaccharide was added and mixed. After some time the powder was mounted on a glass slide and observed under an optical microscope for any pink coloration.

9.2.5 Physicochemical Evaluation

Knowing physical and chemical properties of the extracted polysaccharide is of great importance. It gives us an overview of the possible properties it may exhibit. It also helps in designing the application of the extracted polysaccharide.

9.2.5.1 Solubility

Solubility of a polysaccharide is an important parameter that helps to determine its applicability. Solubility of the polysaccharide was determined in different solvents like water, acetone, chloroform, ethanol, methanol, di-methyl sulfoxide (DMSO) and ether as given in Indian Pharmacopoeia 1996 (IP, 1996).

9.2.5.2 Powder Flow Characteristics

The powder flow properties were evaluated using the standard procedure available in literature (Alalor, Augustine & Avbunudiogba, 2014). It includes:

Bulk density-Bulk density of a granulation is dependent primarily on the particle size, particle size distribution and particle shape. It indirectly indicates measure of granule flow and determines the die fill volume. Granules that have a high bulk density require relatively lower die fill volume than those having small bulk density. 5 g of gum was taken into 25 mL dry measuring cylinder and initial bulk volume was noted. Reading was taken in triplicate. The following equation was used to calculate bulk density of the polysaccharide powder:

$$\text{Bulk density} = \frac{\text{mass}}{\text{bulk volume}}$$

Tapped density-The above cylinder was tapped 100 times to get tapped volume. Reading was taken in triplicate. The following equation was used to calculate Tapped density of the polysaccharide powder:

$$\text{Tapped density} = \frac{\text{mass}}{\text{tapped volume}}$$

Carr's index-Carr's index indicates the compressibility of a powder. It also gives an indication of flowability of the powder. The Carr's index for purified *C. esculenta* polysaccharide was calculated by using the following formula:

$$\text{Carr's index} = \frac{\text{tapped density} - \text{bulk density}}{\text{tapped density}} \times 100$$

Angle of repose-Angle of Repose is a characteristic related to interparticulate friction or resistant to movement between particles. Angle of Repose was calculated using fixed funnel method. Five gram of gum was taken and passed through a short stem funnel on a paper. The diameter and height of the powder heap was noted. Readings were taken in triplicate. The following equation was used to calculate Angle of Repose.

$$\text{Angle of repose} = \tan^{-1} \frac{\text{height}}{\text{radius}}$$

Hausner ratio-The Hausner ratio is a number that is related to the flowability of a powder or granular material. A Hausner ratio greater than 1.25 is considered to be an indication of poor flowability. It is also related to Carr's index. The following equation was used to calculate Hausner ratio.

$$\text{Hausner's ratio} = \frac{\text{tapped density}}{\text{bulk density}}$$

9.2.5.3 *pH*

pH of the extracted polysaccharide is an important parameter to be studied. It gives an idea about functional groups present in the polysaccharide. It also guides us for better extraction methods and better application of the extracted polysaccharide. For example, if the polymer is acidic in nature it can be successfully used in formulating gastroresistant dosage forms (Jain A, Gupta Y, Jain SK. 2007; Das S, Deshmukh R, Jha A K., 2010). Also hydrolysis method for the polysaccharide can be chosen on basis of its pH. pH of 1% (w/v) gum dispersion in water was checked after stirring for 5 minutes using a digital pH meter whose electrode was set at neutral before immersing the electrode into the dispersion. Triplicate measurements were made.

9.2.5.4 *Loss on Drying (LOD)*

This is a widely used test method to determine the moisture content of a sample. Moisture content analysis of natural products is very important as they have greater tendency for microbial growth. The more moisture, the more the natural product will tend to grow microbes. Here hot air oven method is used to determine moisture content of the extracted polysaccharide. One gram gum sample was heated in a hot air oven at 105°C till constant weight was observed. The loss in moisture content was then calculated by the following equation.

$$\% \text{LOD} = \frac{\text{weight of water in sample}}{\text{weight of dry sample}} \times 100$$

9.2.5.5 *Specific Gravity*

Specific gravity is an important property related to density and viscosity of the polysaccharide. Knowledge of the specific gravity of a particular polysaccharide will allow determination of a fluid's characteristics compared to a standard, usually water, at a specified temperature. As it is a ratio, it is dimensionless. Specific gravity of the gum was determined using Skoog and West's method (1963) using a pycnometer (Skoog, 1963). One percent solution of gum was prepared and poured into a dry calibrated pycnometer. It was capped and weighed at room temperature. Similarly weight of pycnometer with water was noted at room temperature. Specific gravity was obtained by following equation:

$$\text{Specific gravity} = \frac{\text{weight of water}}{\text{weight of gum solution}}$$

9.2.5.6 *Swelling Capacity*

The swelling capacity of a polymer is determined by the amount of liquid material that can be absorbed. Swelling in water is one of the important fundamental properties of all polysaccharides and is also a factor in determining its specific utilization. Swelling capacity of the extracted polymer was determined. One gram finely ground polymer

was introduced into a 25 mL measuring cylinder. This was tapped 200 times and initial volume was noted. Water was added up to 25 mL. The cylinder was shaken intermittently every 10 minutes for 1 hour. It was then allowed stand for 24 hours at room temperature. The volume occupied by the polymer, including any sticky mucilaginous portion, was noted as final volume. (Pendyala V *et al.*, 2010)

Swelling capacity was calculated as per following formula:

$$\text{Swelling capacity} = \frac{\text{Final volume}}{\text{Initial volume}}$$

9.2.5.7 Viscosity

Viscosity is the resistance to flow of a liquid system. It is increased in colloidal suspensions by the thickening of the liquid phase as a result of liquid absorption and consequent swelling of the dispersed colloid. Ostwald's viscometer was used for determining viscosity of the gum solution (0.1% w/v). 0.1 gram gum was kept for hydration in 25 mL water for 24 hours. This gum solution was then made up to 100 mL with water and homogenised using high speed homogeniser at 10,000 revolutions per minute (rpm) for 10 minutes to form a homogenised mixture. Viscosity of this solution was determined using water as reference. 10 mL of water was taken and time taken for water to move between the marks was noted. 10 mL of the homogenised polysaccharide solution was taken and time taken for solution to move between the marks was noted. Viscosity of the polysaccharide solution was calculated using following equation:

$$\frac{\text{time 1}}{\text{viscosity 1}} = \frac{\text{time 2}}{\text{viscosity 2}}$$

where,

time 1 and viscosity 1 are time taken to move between the marks and viscosity of water; time 2 and viscosity 2 are time taken to move between the marks and viscosity of homogenised polysaccharide solution.

9.2.6 Differential Scanning Colorimeter (DSC)

Differential scanning calorimetry or DSC is a thermoanalytical technique in which the difference in the amount of heat required to increase the temperature of a sample and reference is measured as a function of temperature. Throughout the experiment, both the sample material and reference material are maintained at nearly the same temperature. The result of a DSC experiment is a curve of heat flux versus temperature or versus time. Differential scanning calorimetry can be used to measure a number of characteristic properties of a sample. It is possible using this technique to observe crystallization and fusion events as well as glass transition temperatures (T_g). DSC is widely used for examining the polymeric materials thus determining their thermal transitions. The thermal transitions that are observed can be utilized to compare materials, although the transitions do not uniquely identify composition. DSC was performed using a 10 mg sample from 30 °C to 305 °C at a heating rate of 10 °C/min in a synthetic air atmosphere using DSC-SEIKO SII nanotechnology. Nitrogen was used as purge gas.

9.2.7 X-ray Powder Diffraction (XRD)

It is one of the most powerful techniques for material structure analysis, providing information about the structure of a material at atomic level. XRD can be used to determine the crystallinity by comparing the integrated intensity of the background pattern to that of the sharp peaks. Semicrystalline behaviour is shown by many polymers, i.e., part of the material forms an ordered crystallite by folding of the molecule. A single polymer molecule can be very well folded into two different, adjacent crystallites, thus forming a tie between the two crystallite forms. Diffraction pattern of powdered *C. esculenta* polysaccharide was recorded with an X-ray powder diffractometer. X-ray diffraction was performed at room temperature (30 °C) with a diffractometer; make, Bruker AXS D8 advance; configuration, vertical, Theta/2 Theta geometry; X-ray source - Cu, wavelength 1.5406 Å; detector, Si(Li) PSD; voltage, 40 kV; current 35 mA; step time 32.8 seconds.

9.2.8 Estimation of Total Sugar Content

Total polysaccharide content was determined using phenol sulphuric acid method (Harshal & Priscilla, 2011; Krishnaveni, Balasubramanian & Sadasivam, 1984; Dubois, Gilles, Hamilton, Rebers & Smith, 1956). In hot acidic medium polysaccharide is dehydrated to hydroxyl furfural. This forms a coloured product with phenol and has absorption maximum at 488 nm.

Preparation of blank solution-To 1 mL of distilled water 1 mL 5% phenol was added followed by 5mL of concentrated H_2SO_4 .

Preparation of standard solution-A stock solution of glucose (100 µg/mL) was prepared in distilled water. Aliquots from this solution were taken to obtained sugar concentration of 60–100 µg/mL. 1 mL of 5% phenol solution was added to 1 mL of sugar solution followed by 5mL of concentrated H_2SO_4 . The absorbance was measured after standing for 10 minutes at 488 nm against blank.

Estimation of polysaccharide in *C. esculenta* Gum (test preparation) – 100 mg gum powder was treated with 5 mL 2.5 N HCl and boiled on a water bath for 3 hours. Solid sodium carbonate was added to the resultant cooled solution after 3 hours till the effervescence ceased. Volume was made up to 100 mL with distilled water. The hydrolysed gum solution was then centrifuged and 1 mL supernatant was diluted to 10 mL to get a solution of concentration 100 µg/mL. 1 mL of this diluted solution was added to 1mL of 5% phenol solution. This was followed by 5mL of concentrated H_2SO_4 . The absorbance of the resultant solution was measured after 10 minutes at 488 nm against blank using UV-Visible spectrophotometer. The experiment was carried out in triplicate.

9.2.9 Identification of Gum Components by Thin Layer Chromatography

Thin layer chromatography (TLC) is a chromatography technique used to separate non-volatile mixtures. Study of separation of the components of a polysaccharide can be helpful in determining and confirming presence of different sugars in it. For this purpose hydrolysed sample of the polysaccharide is used. 0.5 gram of the polysaccharide was hydrolysed by boiling it in 20 mL of 10% hydrochloric acid for three hours. This solution was cooled and centrifuged at 3000 rpm for 10 minutes. The supernatant

was decanted in an evaporating dish and concentrated to get thick black mass. Small amount of the black mass was dissolved in water and used as test sample for TLC.

TLC of the hydrolysed gum was performed on precoated silica gel GF 254 plates (stationary phase) using mixture of 1-propanol, ethyl acetate and water in the ratio 4:0.5:0.5 as mobile phase. Glucose and galactose were used as a standard. Detection was done by dipping dried developed TLC plate in 10% v/v solution of H_2SO_4 in methanol. The plate was then heated in a hot air oven at 110°C for 1 hour. The R_f values of the spots were calculated and compared with R_f of pure standard and also values reported in literature (Agnieszka, Grażyna, Magdalena, Helena & Ireneusz, 2009).

9.2.10 Investigation of Structure of the Polysaccharide

Optical spectroscopy is used for semiquantitative methods for the functional groups determination. It can also be used in determining the conformation of structural features of pure polysaccharides. FTIR spectroscopy yields “fingerprint” spectra usable as structural evidence. IR spectrum of the polysaccharide was taken using a Fourier transform infrared spectrometer (FTIR, SHIMADZU). *C. esculenta* gum was ground with potassium bromide (KBr) powder and then pressed using KBr press forming 1 mm pellets for FTIR measurement.

The most powerful tool for polysaccharide analysis is NMR spectroscopy. It helps in establishing a relation between different bondages and number of carbon and hydrogen atoms, thus helping in predicting structures taking into account results from IR spectra and other related spectroscopic methods. Nuclear magnetic resonance spectra were obtained using a Bruker Advance III, 400 MHz NMR spectrometer. Gum hydrolysate was prepared by boiling gum in 10% H_2SO_4 solution for 3 hours followed by neutralizing using barium hydroxide and then filtering and concentrating the filtrate to a thick black mass. Sample was prepared by dissolving this hydrolysate in D_2O . Both ^1H NMR and ^{13}C NMR were obtained.

9.2.11 Rheological Study of *C. esculenta* Gum

Rheological behaviour dependent on time can be very useful in a wide range of industrial applications like foods, paints, coatings, pharmaceuticals and cosmetics. For example, it is highly desirable to have a formulation that is thick and has high viscosity texture at rest but becomes liquid-like and easily pourable after shaking, regaining its high viscosity shortly after it is again brought to rest. Rheological studies were performed using Brookfield viscometer. 1% w/v solution of the gum was prepared in 50 mL beaker and after 48 hours of soaking dial readings were taken using Brookfield viscometer at different rpm for 5 minutes using spindle no.2. Viscosity of the gum solution at different rpm was calculated. Graphs were plotted of shear stress against shear rate and viscosity against shear rate.

9.3 Results and Discussion

The results of organoleptic evaluation of the isolated polysaccharide are summarised in Table 9.1. Being odourless and tasteless, the extracted polysaccharide can be easily

Table 9.1 Organoleptic characteristics of purified *C. esculenta* gum.

Colour	Odour	Taste	Shape	Texture
Buff colour	Odourless	Tasteless	Regular	Smooth

Table 9.2 Preliminary phytochemical tests of *C. esculenta* gum.

Test	Observation	Inference
Molisch's test	A violet ring appears at the junction of the two liquids.	Carbohydrate present
Fehling's test	Formation of brownish-red precipitate.	Reducing sugar present
Iodine test	Appearance of deep blue colour	Starch present
Biuret test	No violet purple colouration	Proteins may be absent
Ruthenium red test	No pink colouration	Mucilage absent

Table 9.3 Physicochemical evaluation.

Parameters		Results
Solubility		Forms viscous colloidal solution in hot water, insoluble in acetone, ethanol, methanol, DMSO and ether.
Powder characteristics	Bulk density	0.5455 g/cc
	Tapped density	0.7692 g/cc
	Angle of repose	16.189°
	Carr's index	29.082
	Hausner's ratio	1.41
pH		6.88
Loss on drying		15.6% w/w
Specific gravity (1% w/v solution)		0.9937 g/ml
Swelling capacity		10.67 folds
Viscosity (0.1% w/v, in water)		0.93 cP

incorporated in different oral preparations. The yield of the polysaccharide from *C. esculenta* was found to be 10%-13% w/w when extracted at room temperature. Preliminary phytochemical screening (Table 9.2) showed presence of carbohydrates, reducing sugars, starch and absence of proteins in the polysaccharide. Absence of proteins shows purity of the extracted polysaccharide.

The results of physicochemical evaluation are summarised in Table 9.3. The extracted polymer showed poor flow properties as can be seen from the powder characteristics. Table 9.4 and Table 9.5 gives experimental considerations of Carr index, Hausner ratio and Angle of Repose as given in US Pharmacopoeia (USP, Chapter 1174-Powder flow; Carr, 1965). The Carr index and Hausner ratio of the *C. esculenta* polysaccharide corresponds to poor flow property of the polysaccharide powder. The pH value of 1% solution of *C. esculenta* was found to be near to neutral on the acidic

Table 9.4 Experimental considerations for compressibility Index and Hausner Ratio.

Compressibility index (%)	Flow character	Hausner ratio
≤10	Excellent	1.00–1.11
11–15	Good	1.12–1.18
16–20	Fair	1.19–1.25
21–25	Passable	1.26–1.34
26–31	Poor	1.35–1.45
32–37	Very poor	1.46–1.59
>38	Very, very poor	>1.60

Table 9.5 Experimental considerations for Angle of Repose.

Flow property	Angle of repose (degrees)
Excellent	25–30
Good	31–35
Fair- aid not needed	36–40
Passable- may hang up	41–45
Poor- must agitate, vibrate	46–55
Very poor	56–65
Very, very poor	>66

side (pH 6.88). This indicates that it would not cause irritation to mucous membrane of buccal cavity and gastrointestinal tract and could be used in development of buccal and oral dosage forms. The extracted polysaccharide showed excellent swelling property. Swelling capacity of the polysaccharide was found to be 10.67 folds. This signifies that the extracted polysaccharide can be successfully used as a thickening agent, gelling agent and disintegrant.

The DSC of *C. esculenta* polysaccharide is represented in Figure 9.1. The extracted polysaccharide exhibited broad endothermic peak at about 107.7 °C due to loss of free or bound water present in the polysaccharide. It can thus be concluded that the glass transition temperature (T_g) of the polymer may be above 305 °C and hence the polymer would be stable at normal operational temperatures.

The standard curve of glucose for phenol sulphuric acid method for determination of total polysaccharide content of *C. esculenta* gum is shown in Figure 9.2. The calibration curve was found to be linear in the range 60–100 µg/mL and showed correlation coefficient of 0.9936 indicating good linearity. The regression equation was used for calculating total polysaccharide content of the gum isolate by taking average of three determinations. The total polysaccharide content of *C. esculenta* gum isolate was found to be 86.24% (w/w).

The X-ray diffraction pattern of the gum powder showed four sharp peaks at 15.210°, 17.251°, 18.099°, 23.218° (Figure 9.3). This indicates gum *C. esculenta* is partly amorphous and partly crystalline.

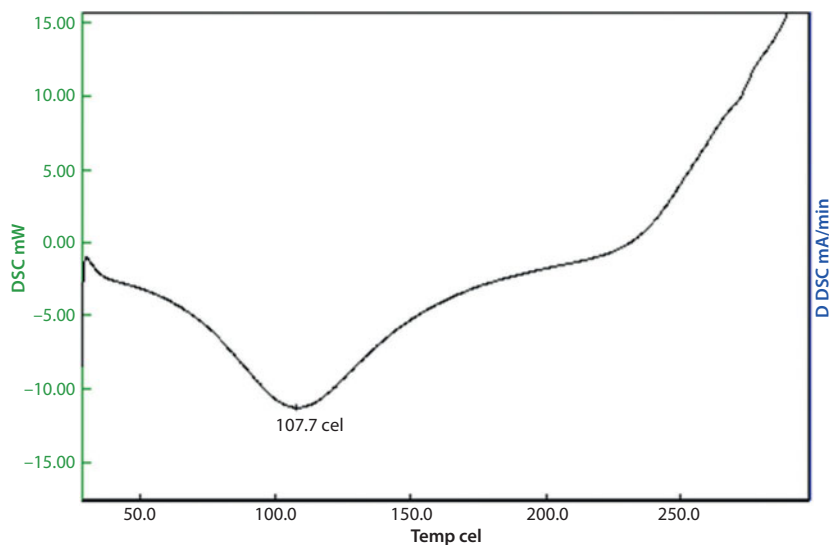


Figure 9.1 DSC thermogram of *C. esculenta* gum.

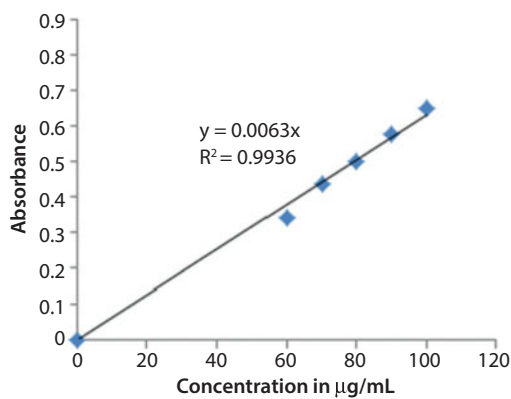


Figure 9.2 Standard curve of glucose.

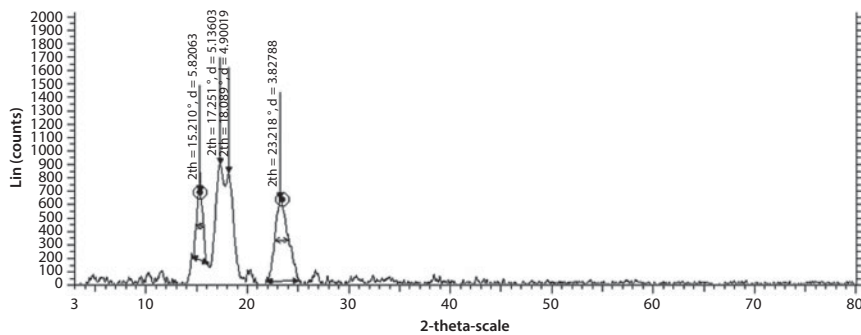


Figure 9.3 X-ray diffraction pattern of *C. esculenta* gum.

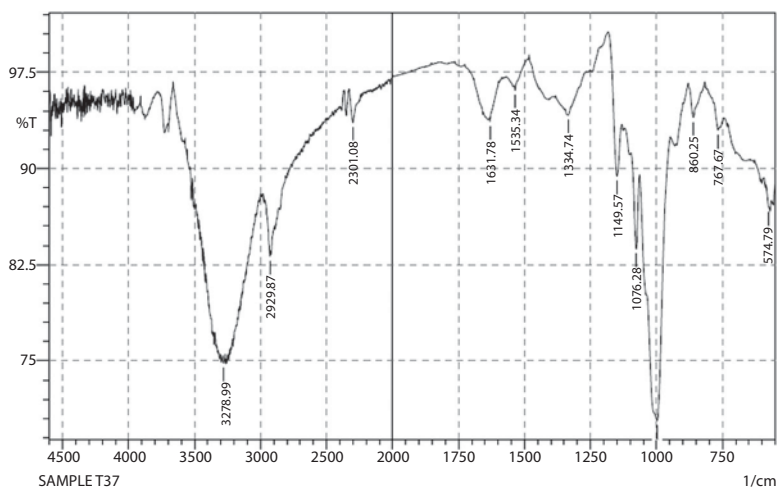


Figure 9.4 FTIR spectrum of *C.esculenta* gum.

TLC of the hydrolysate showed spots corresponding to glucose and galactose standard and reported R_f values (R_f glucose-0.63, R_f galactose- 0.58). TLC also showed spot corresponding to reported R_f value of arabinose (R_f 0.70) (Agnieszka, *et al.*, 2009). From the TLC study it can be said that the isolated polysaccharide may contain glucose, galactose and arabinose subunits in its polymeric structure.

A FTIR spectrum of purified polysaccharide is depicted in Figure 9.4. The absorbances of two ester carbonyl stretches at 1535.34 cm^{-1} and 1631.78 cm^{-1} indicated small amount of protein content. This signifies purity of the extracted gum (Hui & Alvin, 1993). The peak at 1149.57 cm^{-1} corresponds to bending vibrational modes of C-O, present in the pyranose ring, while the peaks 1076.28 cm^{-1} and 999.13 cm^{-1} is a characteristic contribution of C-OH bending (Savitha, Parvathy, Susheelamma, *et al.*, 2006). The broad bands around 2929.87 cm^{-1} and 3278.99 cm^{-1} are attributed to C-H stretching and to O-H stretching vibration, respectively (Yuen, Choi, Phillips, *et al.*, 2009).

^1H NMR spectra of the gum is shown in Figure 9.5 and Table 9.6 shows chemical shifts (in ppm) and the corresponding carbon atoms for ^1H NMR signals of *C. esculenta* gum. In the anomeric region four distinct signals of α -(1 \rightarrow 4)-D-Glucopyranose, α -(1 \rightarrow 6)-D-Glucopyranose, β -D-Galactopyranose and β -D-Arabinopyranose were observed. ^{13}C NMR spectrum of the gum is represented in Figure 9.6 and Table 9.7 shows corresponding carbon moieties. ^{13}C NMR spectra showed two signals for α and β anomeric atoms each. Taro gum contains starch, i.e., combination of amylose { α -(1 \rightarrow 4)-D-Glucopyranose} and amylopectin { α -(1 \rightarrow 4)-D-Glucopyranose and α -(1 \rightarrow 6)-D-Glucopyranose}(Hatada & Kitayama, 2006). Hence it can be concluded that the α anomeric atoms are from α -(1 \rightarrow 4)-D-Glucopyranose and α -(1 \rightarrow 6)-D-Glucopyranose units.

Viscosity of a polymer solution depends solely on the concentration and the molecular weight of the dissolved polysaccharide. By measuring the viscosity of the polysaccharide solution, we should be able to get an idea about its molecular weight. Viscosity techniques are very popular because they are experimentally simple. But, however are

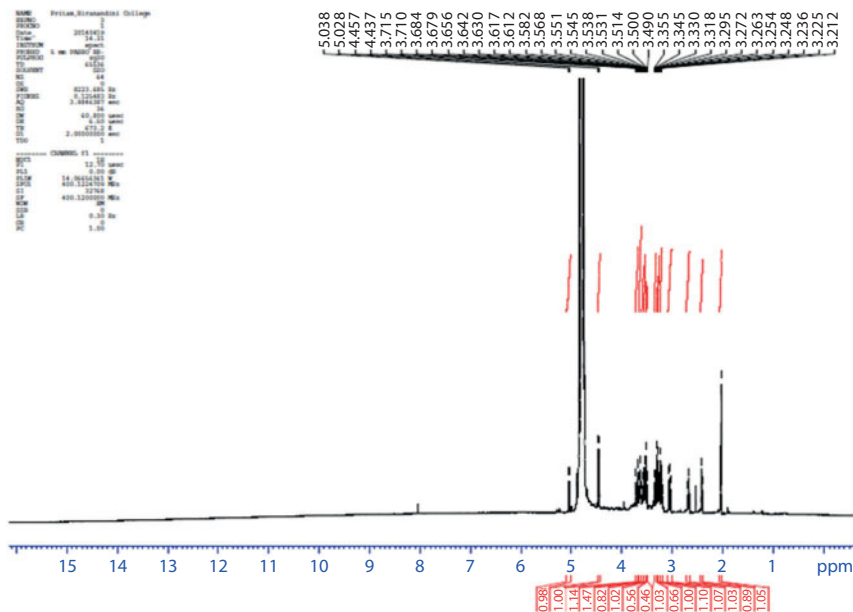


Figure 9.5 ¹H NMR spectra of *C. esculenta* gum, in D₂O.

Table 9.6 Chemical shifts (in ppm) and the corresponding carbon atoms for ¹H NMR signals of *C.esculenta* gum.

Chemical shift (ppm)	Corresponding moiety
5.028	H-1 (α) {α-d-sugar moieties}
5.038	
4.437	H-1 (β) {β-d-sugar moieties}
4.457	
3.318	H-2 to H-6
3.330	
3.345	
3.355	
3.490	
3.500	
3.514	
3.531	
3.538	
3.545	
3.551	
3.568	
3.582	
3.612	
3.617	
3.630	
3.642	

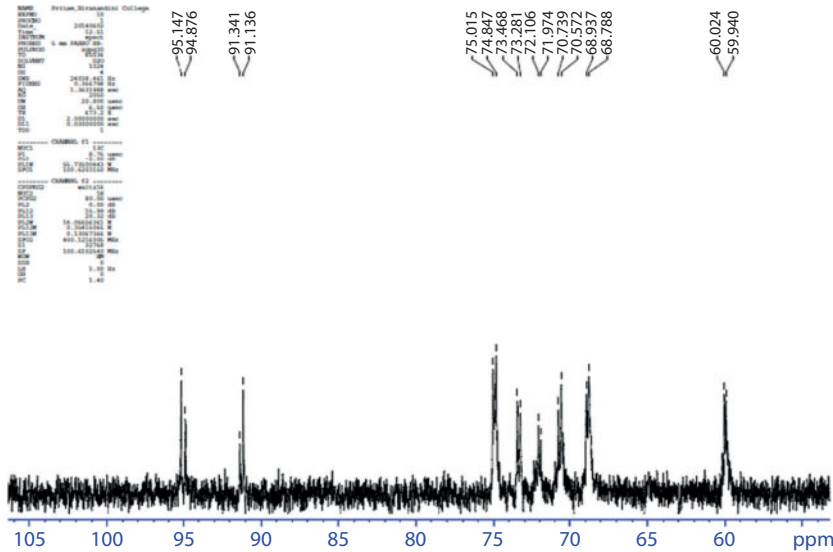


Figure 9.6 ^{13}C NMR spectra of *C. esculenta* gum, in D_2O .

Table 9.7 Chemical shifts (in ppm) and the corresponding carbon atoms for ^{13}C NMR signals of *C.esculenta* gum.

Chemical shift (ppm)	Corresponding C-atom (moiety)
95.147 94.876	C1 (β)
91.341 91.136	C1 (α)
75.015 74.847 73.468 73.281 72.106 71.974 70.739 70.572 68.937 68.788	C2 to C5
60.024 59.940	CH_2OH

less accurate and the molecular weight, the viscosity average molecular weight thus determined is less precise. A Newtonian fluid is one in which the viscosity is independent of the shear rate. In non-Newtonian fluids, the shear stress/strain rate relation is not linear. Typically the viscosity drops at high shear rates — a phenomenon known as shear thinning. Shear-thinning fluids also are called pseudoplastic fluids. The rheological properties of *C. esculenta* gum were studies by plotting rheograms. Figure 9.7 shows rheogram of shear stress versus shear rate. It was found that the curve obtained from

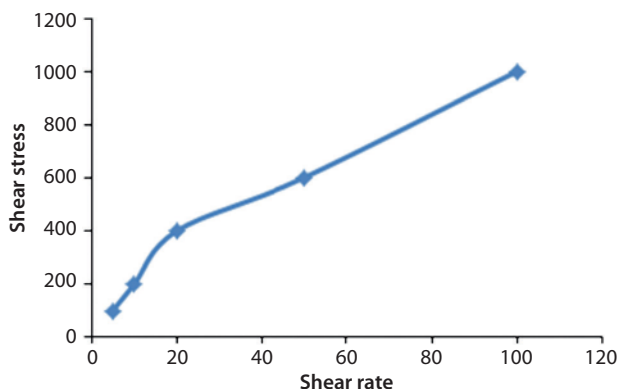


Figure 9.7 Rheogram of shear stress versus shear rate.

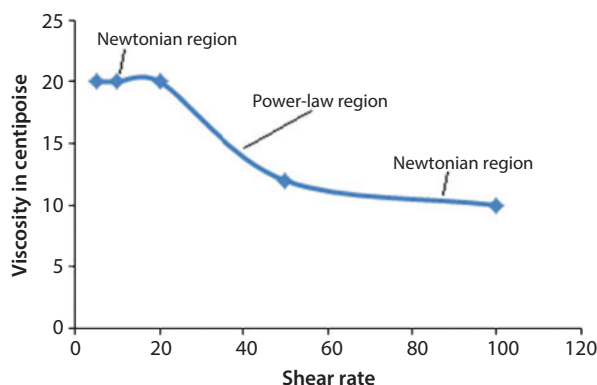


Figure 9.8 Rheogram of viscosity versus shear rate.

measurement at decreasing shear rate super imposed on that obtained from measurements taken at increasing shear rate. Absence of hysteresis loop indicates that there is no structural breakdown or modification of the polymer during stress conditions.

Figure 9.8 shows rheograms of viscosity versus shear rate. It was found that viscosity decreases with increasing shear rate. The gum solution showed shear thinning flow which makes it easy to handle under high shear. The gum solution exhibited Newtonian behaviour at extreme shear rates, both at low as well as high shear rates. The regions where the viscosity seems to be constant are known as Newtonian regions and the region between these extremes is known as Power-Law region. From this it can be concluded that beyond the Power-Law region the effective viscosity of the polymer solution would indefinitely decrease with increase in shear rate (Shankar, 2010).

The applications of any natural gum are dependent on its viscosity and rheological properties. For any polymer to be used in slow release hydrophilic matrix systems, it should possess certain characteristics like fast hydration of the polymer, high gel strength and should be stable during the shelf life of the product. The results indicated that the polysaccharide isolated from *C. esculenta* tubers possess pseudoplastic flow and good swelling capacity. *C. esculenta* tuber polysaccharide hydrates quickly and swells rapidly and forms a thick viscous gel around it. This rheological behaviour of

polysaccharide confirmed its suitability in the development of sustained and controlled release drug delivery systems.

9.4 Conclusions

Natural polymers can be used extensively due to their non-toxic nature and abundant availability in nature. Attempts have been made to isolate *C. esculenta* polysaccharide at room temperature and characterize its physicochemical properties as well as elucidate its structure. Physicochemical properties showed poor flow properties and presence of reducing sugars in the extracted polysaccharide. Structural elucidation and phytochemical tests showed presence of α -(1 \rightarrow 4)-D-Glucopyranose, α -(1 \rightarrow 6)-D-Glucopyranose, β -D-Galactopyranose and β -D-Arabinopyranose. Rheological study indicated pseudoplastic behaviour of polysaccharide at 1% w/v concentration. *C. esculenta* polysaccharide was found to have excellent swelling capacity. Due to ready availability, neutral nature and good swelling ability, *C. esculenta* tuber polysaccharide can be used as a novel herbal excipient in the development of sustained release and controlled release drug delivery system. It can also be used as a successful disintegrant. In addition, it can also be used in pharmaceutical preparations like suspensions, emulsion, gels, etc.

Acknowledgements

Authors are very much thankful to Dr. P.S. Gide, Principal of Hyderabad Sindh National Collegiate Boards (HSNCB's) Dr. L. H. Hiranandani College of Pharmacy, Ulhasnagar for his continuous support, guidance and encouragement.

References

- Agnieszka Skalska-Kamińska, Grażyna Matysik, Magdalena Wójciak-Kosior, Helena Donica & Ireneusz Sowa, *Annales Universitatis Mariae Curie – Skłodowska Lublin – Polonia*, Vol. Xxii, N 4, 2 Section DDD, 2009.
- Allen, O. N. & Allen, E. K., *The manufacture of poi from taro in Hawaii: with special emphasis upon its fermentation*, Bulletin 70, Hawaii Agricultural Experiment Station, Honolulu, Hawaii, 1933.
- Awasthi, C.P. and Singh, A. B., Nutritional quality evaluation of edible leaves of some promising Colocasia and Alocasia collections, *Ind. J. Agric. Res.* 34(2), 117–121, 2000.
- C. A. Alalor, J. A. Avbunudiogba, K. Augustine, Isolation And Characterization Of Mucilage Obtained From *Colocasia Esculenta*, *International Journal of pharma and bio sciences*, 4 (1), 25–29, 2014.
- Cambie, R. C. & Ferguson, L. R. *Potential functional foods in the traditional Maori diet*, Mutation Research, Fundamental and Molecular Mechanisms of Mutagenesis. 523–524: 109–117, 2003.
- Carr, R. L., Evaluating Flow Properties of Solids. *Chem. Eng.* 72, 163–168, 1965.
- Chukwu K. I., Udeala O. K., Binding effectiveness of Colocassia esculenta gum in poorly compressible drugs-paracetamol and metronidazole tablet formulations. *Boll. Chim. Farm.* 139 (2), 89–97, 2000.

- Clifford, S.C., S.K. Arndt, M. Popp and H.G. Jones, Mucilages and polysaccharides in Ziziphus species (Rhamnaceae): localization, composition and physiological roles during drought-stress. *Journal of Experimental Botany*, 53(366): 131–138, 2002.
- Crabtree, J. & Baldry, J., The use of taro products in bread making. *Journal of Food Technology*, 17, 771–7, 1982.
- D. A. Skoog, D.M. West, *Fundamentals of Analytical Chemistry*, 4th ed., Holt-Rinehart and Winston, Philadelphia, New York, pp. 880, 1963.
- Das S, Deshmukh R, Jha A K., Role of natural polymers in the development of multiparticulate systems for colon drug targeting. *Syst. Rev. Pharm.* 1:79–85, 2010.
- Devarkar V.D., Marathe V.R., Chavan D.P., *Dietary and medicinal significance of wild vegetables from Osmanabad region*, Maharashtra (India), Life Sciences Leaflets 11:317–332, 2011.
- Dubois. M, Gilles. K. A, Hamilton. J. K., Rebers. P.A. and Smith. F, Colorimetric method for determination of sugars and related substances. *Analytical. Chemistry*, 26, p. 350, 1956.
- El-Mahdy, A. R. & El-Sebaiy, L. A., Preliminary studies on the mucilages extracted from okra fruits, taro tubers, jaw's mellow leaves and fenugreek seeds. *Food Chem.* 14, 237119, 1984.
- Giriraj Kulkarni, Gowthamarajan K, Satish Kumar & Suresh B., Gums And Mucilages Therapeutic And Pharmaceutical Applications. *Natural Product Radiance*, 1(3), 10–17, 2002.
- Gurpreet Arora, Karan Malik, Inderbir Singh, Formulation and Evaluation of Mucoadhesive Matrix Tablets of Taro Gum: Optimization Using Response Surface Methodology, *Polimery w Medycynie*, 2, 41, 2011.
- Gurpreet Arora, Karan Malik, Inderbir Singh, Formulation and Evaluation of Mucoadhesive Matrix Tablets of Taro Gum: Optimization Using Response Surface Methodology. T. 41, Nr 2, 2011.
- H. K. Kakrani and N. K. Jain, A study on investigated as drug retarding agents, each presenting a binding properties of guggal gum. *Indian Journal Hospital Different Approach to the Matrix System*, vol. 18, Based on the Pharmacist, no. 3, 100–102, 1981.
- Harshal A. Pawar, Priscilla M. D., Spectrophotometric estimation of total polysaccharides in Cassia tora gum. *Journal of Applied Pharmaceutical Science*, 3, 93–95, 2011.
- Hatada & Kitayama, NMR Spectroscopy of Polymers. *Springer Laboratory Manuals in Polymer Science*, 2006.
- Hui Lin & Alvin S. Huang, Chemical composition and some physical properties of a water-soluble gum in taro (*Colocasia esculenta*), *Food Chemistry*, Elsevier Science, (48) 403–409, 1993.
- Indian Pharmacopoeia, Ministry of Health and Family Welfare, Government of India, Controller of Publication, New Delhi, vol. 556, pp. A100–A111, 1996.
- Jain A, Gupta Y, Jain SK., Perspectives of biodegradable natural polysaccharides for Site-Specific drug delivery to the colon. *J Pharm Pharmaceut Sci.* 10:86–128, 2007.
- Jania, G.K., D.P. Shahb, V.D. Prajapatia and V.C. Jainb, Gums and mucilages: versatile excipients for pharmaceutical formulations, *Asian Journal of Pharmaceutical Sciences*, 4(5):309–323, 2009.
- Khandelwal. K. R., Practical pharmacognosy, techniques and experiments, Ed. 22, Nirali publication, India, 2012.
- Kirtikar KR, Basu BD, *Indian Medicinal Plants*. Dehradun: International Book Distributors, 4:2615, 2005.
- Kowalczyk, E., Kopff, A., Fijalkowski, P. Niedworok, J., Blaszczyk, J., Kedziora, J., Effects of anthocyanins on selected biochemical parameters in rats exposed to cadmium, *Acta Biochimica Polonica*. 50, 543–548, 2003.
- Krishnaveni. S, Theymoli Balasubramanian and Sadasivam. S., Sugar Distribution in Sweet Stalk Sorghum. *Food Chemistry*, 15, p. 229, 1984.
- Lewu, M.N., Adebola, P.O. and Afolayan, A. J., Effect of cooking on the proximate composition of the leaves of some accessions of *Colocasia esculenta* (L.) Schott in KwaZulu- Natal province of South Africa. *African J of Biotechnology*. 8(8), 1619–1622, 2009.

- Lin H., Huang A. S., Chemical composition and some physical properties of a water-soluble gum in taro (*Colocasia esculenta.*). *Food Chemistry*, 48 (4), 403–409, 1993.
- Moy, J. H., Wang, N. T. S. & Nakayama, T. O. M., Dehydration and processing problems of taro. *Journal of Food Science*, 42, 917, 1977.
- Noda, y., kaneyuki, T., Mori, a. & Packer, l Antioxidant activities of pomegranate fruit extract and its anthocyanidins: Delphinidin, cyanidin, and pelargonidin. *Journal of Agricultural Food Chemistry*. 50: 166–171, 2002.
- Pappu A. *et al.*, Advances in Industrial Prospective of Cellulosic Macromolecules Enriched Banana biofibre resources: A Review; *International Journal of Biological Macromolecules*, 79: 449–458, 2015.
- Pendyala, V.; Baburao, C.; Chandrasekhar, K. B., Studies of some physicochemical properties of *Leucaena leucocephala* bark gum. *J. Adv. Pharm. Technol. Res.* 1(2), 253–259, 2010.
- R. Shankar Subramanian, *Non-Newtonian Flows*, Non-Newtonian Flows-Clarkson University Book, Department of Chemical and Biomolecular Engineering, Clarkson University, 2010.
- S.N. Yuen, S.M. Choi, D.L. Phillips, Raman and FTIR spectroscopic study of carboxymethylated non-starch polysaccharides. *Food Chemistry*, 114 1091–1098, 2009.
- Savitha Prashanth, M. R. and Parvathy, K. S. and Susheelamma, N. S. and Harish Prashanth, K. V. and Tharanathan, R. N. and Cha, A. and Anilkumar, G., *Galactomannan esters. A simple, cost-effective method of preparation and characterization.* *Food Hydrocolloids*, 20 (8). pp. 1198–1205, 2006.
- Singha, A.S., Thakur, V.K., Mechanical, Morphological, and Thermal Characterization of Compression-Molded Polymer Biocomposites. *Int. J. Polym. Anal. Charact.* 15, 87, 2010a.
- Singha, A.S., Thakur, V.K., Synthesis, Characterization and Study of Pine Needles Reinforced Polymer Matrix Based Composites. *J. Reinf. Plast. Compos.* 29, 700, 2010b.
- Thakur, V.K., Singha, A.S., Natural fibres-based polymers: Part I—Mechanical analysis of Pine needles reinforced biocomposites. *Bull. Mater. Sci.* 33, 257, 2010c.
- Singha, A.S., Thakur, V.K., Synthesis and Characterization of Short *Grewia optiva* Fiber-Based Polymer Composites. *Polym. Compos.* 31, 459, 2010d.
- Thakur, V.K., Singha, A.S., Physico-chemical and mechanical characterization of natural fibre reinforced polymer composites. *Iran Polym J* 19, 3, 2010e.
- Soumya M, Chowdary YA, Swapna VN, Prathyusha ND, Geethika R, Jyostna B, Krishna Mohan KS., Preparation and optimization of sustained release matrix tablets of metoprolol succinate and taro gum using response surface methodology. *Asian J. Pharm.*, 8:51–7, 2014.
- Thakur, V.K., Thakur, M.K., Processing and characterization of natural cellulose fibers/thermoset polymer composites. *Carbohydr. Polym.* 109, 102–117, 2014a.
- Thakur, V.K., Thakur, M.K., Recent Advances in Graft Copolymerization and Applications of Chitosan: A Review. *ACS Sustain. Chem. Eng.* 2, 2637–2652, 2014b.
- Thakur, V.K., Thakur, M.K., Recent trends in hydrogels based on psyllium polysaccharide: a review. *J. Clean. Prod.* 82, 1–15, 2014c.
- Thakur, V.K., Kessler, M.R., Self-healing polymer nanocomposite materials: A review. *Polymer* 69, 369–383, 2015.
- Thakur, V.K., Thakur, M.K., Recent advances in green hydrogels from lignin: a review. *Int. J. Biol. Macromol.* 72, 834–847, 2015.
- Thakur, M.K., Thakur, V.K., Gupta, R.K., Pappu, A., Synthesis and Applications of Biodegradable Soy Based Graft Copolymers: A Review. *ACS Sustain. Chem. Eng.* 4, 1–17, 2016.
- Tuse T.A., Harle U.N., Bore V.V., Hepatoprotective activity of *Colocasia antiquorum* against experimentally induced liver injury in rats. *Malaysian J Pharma Sci.* Vol 7, No. 2, 99–112, 2009.
- US Pharmacopoeia, Chapter 1174, Powder flow. http://www.pharmacopeia.cn/v29240/usp29nf24s0_c1174.html

- Voicu, S.I., Condruz, R.M., Mitran, V., Cimpean, A., Miculescu, F., Andronescu, C., Miculescu, M., Thakur, V.K., Sericin Covalent Immobilization onto Cellulose Acetate Membrane for Biomedical Applications. *ACS Sustain. Chem. Eng.* 4, 1765, 2016.
- Whistler, R.L., Industrial gums, *Drug-release retarding polymers are the key performers*. Academic Press, 2 Ed, London, 1996.
- Wu, H., Thakur, V.K., Kessler, M.R., Novel low-cost hybrid composites from asphaltene/SBS tri-block copolymer with improved thermal and mechanical properties. *J. Mater. Sci.* 51, 2394–2403, 2016.
- Zatz, J.L. and G.P. Kushla, *Pharmaceutical dosage forms-Disperse systems*, M. M. Reiger and G.S. Banker, Ed; Marcel Dekker Inc., New York, 2: 508, 1989.

Bio-Based Fillers for Environmentally Friendly Composites

Thabang H. Mokhothu^{1*} and Maya J. John^{1,2}

¹CSIR Materials Science and Manufacturing, Polymers and Composites Competence Area,
Port Elizabeth, South Africa

²Department of Chemistry, Faculty of Science, Nelson Mandela Metropolitan University,
Port Elizabeth, South Africa

Abstract

The use of bio-based fillers as alternative replacement for synthetic fillers has been dictated by increasing ecological concerns as well as depleting petroleum resources. The other aspect is a growing need for eco-friendly, renewable and sustainable products. In recent years, natural fibers have gained attention as suitable reinforcements in polymeric matrices because they are biodegradable, low cost, environmentally friendly and renewable. Furthermore, they possess high specific strength and can be effectively used for composites in various applications. This chapter will give an overview of the different types of bio-based fillers (natural fibers, lignin, cellulose and rice husk) used in biopolymer matrices. The application of these green composites in the industrial area will also be discussed.

Keywords: Applications, bio-fillers, biodegradability, biopolymers, cellulose

10.1 Introduction

The development of biodegradable and recyclable materials from renewable resources such as natural fibers and biopolymers have drawn attention as they are found to be suitable replacements for petroleum-based materials (Dong *et al.*, 2014; Mokhothu *et al.*, 2011; Tanobe *et al.*, 2014). This is due to increasing pressure from the consumer and environmental legislations on finding suitable replacement for petroleum-based materials (Thakur & Kessler, 2014a,b). Industrial sectors such as automotive, packaging and aerospace are forced to seek eco-friendly and sustainable materials. Industrial ecology, green chemistry, sustainability and eco-efficiency have put pressure on these industries to introduce renewable and eco-friendly materials (Deka *et al.*, 2013). The advantages of using sustainable and eco-friendly materials is influenced by environmental benefits

*Corresponding author: TMokhothu@csir.co.za

such as reduction of global warming gases, global sustainability, cost effectiveness and sustainable economy (Voicu *et al.*, 2016; Wu *et al.*, 2016). Accordingly, a number of articles and review papers have been published on bio-based composites derived from natural fibers and biopolymers as suitable alternatives to replace petroleum based composites (Azwa & Yousif, 2013; Azwa *et al.*, 2013; Deka *et al.*, 2013; John & Thomas, 2008a; Majeed *et al.*, 2013; Mohanty *et al.*, 2000; Mtibe *et al.*, 2015; Terzopoulou *et al.*, 2015; Thakur *et al.*, 2014a; Thakur *et al.*, 2014b; Thakur *et al.*, 2012; Xie *et al.*, 2010). The extensive ongoing research on bio-based composites produced from renewable resources suggests a unique opportunity to expand the potential and availability of numerous natural resources for the development of biodegradable and/or recyclable biocomposites (Thakur *et al.*, 2016).

10.2 Bio-Based Fillers/Reinforcements

Natural fibers such as plant fibers and cellulose based fibers are the most commonly used bio-fillers which are available worldwide for reinforcing various types of polymer matrices (Singha & Thakur, 2009a–e). In addition, bio-fillers obtained from agricultural waste such as sugarcane bagasse, soy protein, wheat straw and rice husk, groundnut shell, coconut husk and cotton stalk are also used to reinforce polymers because of their abundance and as an economical solution for waste management (Thakur and Kessler, 2014a,b; Thakur *et al.*, 2014a–e). In this chapter, bio-based fillers such as natural fibers, cellulose (extracted from agro-waste), lignin (obtained from bio-refineries) and rice husk (obtained from rice milling) will be discussed.

10.2.1 Benefits and Drawbacks of Bio-Based Fillers

Bio-based fillers such as natural fibers (NFs) have received extensive attention as an alternative replacement for traditional synthetic fillers because of their attractive properties such as biodegradability, low cost and density, renewability, negligible carbon dioxide (CO₂) emissions, and high specific strength. Further, the prominent feature of natural fibers is that they are cheaper than synthetic fibers and have low environmental and health hazards during production when compared to glass fibers. Another advantage is that NFs can be used for developing better acoustic and thermal insulator nonwoven materials because of their hollow and lignocellulosic nature. Natural fibers such as sugarcane bagasse, hemp, jute, sisal, flax, curaua and those shown in Figure 10.1 are known to have high tensile strength and can be effectively used for composites in numerous applications. Other types of bio-fillers that are renewable and abundant in nature are rice husks and lignin. Lignin is the third most available natural polymers in nature after cellulose and hemicellulose while rice husk is one of the by-products (20%) from rice milling.

Another point of interest for these types of NFs mentioned above is that they contain 40–90% cellulose which can be extracted and used for reinforcing as cellulose fibers and/or cellulose nanowhiskers (Figure 10.2). The extracted cellulose fibers and/or cellulose nanowhiskers are then used to reinforce a wide variety of polymer matrices to enhance their mechanical properties. Interestingly, there is also a growing trend in

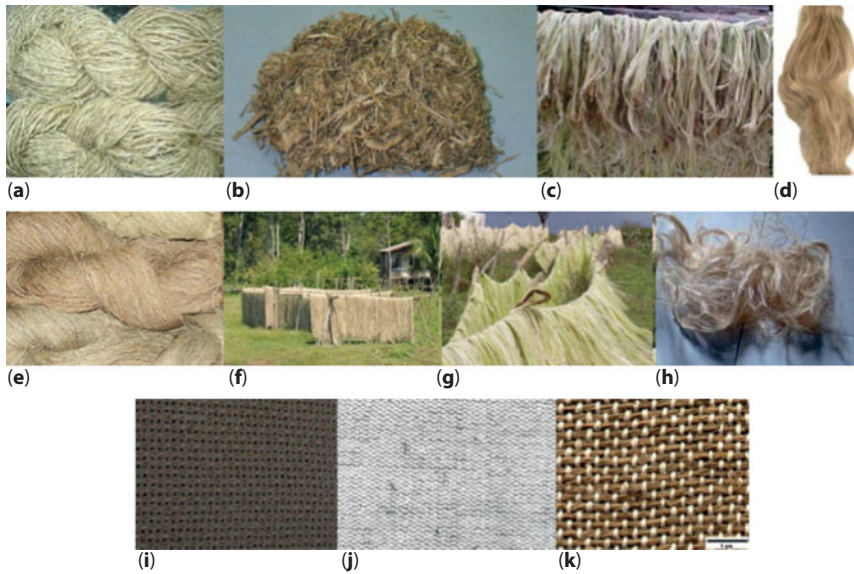


Figure 10.1 Lignocellulosic (LC) reinforcements (a) Banana; (b) sugarcane bagasse; (c) curaua; (d) flax; (e) hemp; (f) jute; (g) sisal; (h) kenaf. Woven lignocellulosic fabric used for reinforcing polymer composites. (i) Jute fabric; (j) ramie-cotton fabric. (k) jute-cotton fabric. Reprinted from Majeed *et al.*, (2013), Copyright 2013 and Satyanarayana *et al.*, (2009), Copyright 2009, with permission from Elsevier.

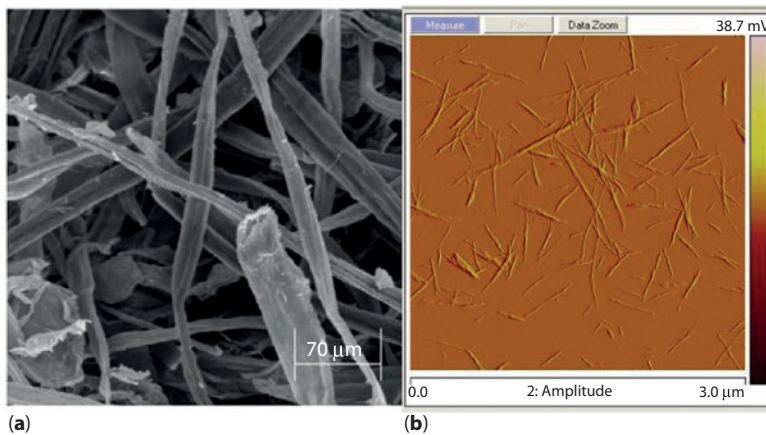


Figure 10.2 (a) SEM micrograph of bleached cellulose. Reprinted from Pereira *et al.*, (2011), Open Access and (b) AFM image of cellulose nanowhiskers (CNWs). Reprinted from Mtibe *et al.*, (2015a), Copyright 2014, with permission from Elsevier.

the application of cellulose and/or cellulose nanowhiskers extracted from agro-based natural resources such as rice husk; sugarcane bagasse; wheat straw; maize stalk and pineapple. Cellulose is considered an almost unlimited source of raw material in the expanding demand for biocompatible and environmentally friendly products (Fatah *et al.*, 2014). Also, cellulose provides stability and strength to fibers and it is the main structural component in the fiber (Reddy & Yang, 2005). The quantity of cellulose in a fiber has direct impact on the usefulness of the fiber for numerous applications,

properties and economics of fiber production. For example, for applications like paper and textiles, fibers possessing higher cellulose content would be applicable, while higher hemicellulose content fractions would be preferably used for fabricating ethanol and other fermentation products, because of the ease of hydrolyzing hemicellulose to fermentable sugars.

Natural fibers do not cause any environmental complications associated with the discarding of most synthetic-based fillers. Hence, they are used in the fabrication of hybrid composites and biocomposites due to biodegradable characteristics contrary to synthetic reinforced composites. Conversely, the main disadvantages of bio-based fillers in composite materials are their poor compatibility with polymer matrices and their hydrophilic nature, which result in relative high tendency of moisture sorption (Deka *et al.*, 2013; Majeed *et al.*, 2013; Satyanarayana *et al.*, 2009; Tanobe *et al.*, 2014). These disadvantages lead to poor mechanical properties which declines the dimensional stability of composites. Nevertheless, in literature, various types of chemical treatments are reported on natural fiber modification to enhance their adhesion compatibility with polymer matrices and also to reduce moisture uptake. The hydrophilic hydroxyl group from the fiber surface is modified by means of different chemical treatments such as benzylation; acetylation; alkali; silane; maleated coupling agents; isocyanates; acrylation, permanganates, and many more have been reported (John & Anandjiwala, 2008b; Kumar *et al.*, 2011; Saw *et al.*, 2013; Zhu *et al.*, 2013). These chemical treatments are centered on the application of reagent functional groups that are able to react with the functional groups in the fiber structure and therefore, altering their composition. The modification promotes fiber compatibility with polymer matrices and most importantly reduces moisture absorption. Further, the chemical modification does not only modify the fibers but also improves their strength and in composite materials increases their mechanical properties (Satyanarayana *et al.*, 2009; Saw *et al.*, 2013).

The reason behind the increasing interest in the application of lignocellulosic fibers in composite materials is basically driven by their properties in comparison with those of synthetic fibers depicted in Table 10.1. Further, a list of several merits emphasizing the reasons for the selection of these raw materials in composites often cited in literature are summarized in Table 10.2. Moreover, there's a steadily expanding market on the utilization of lignocellulose fibers, with North American market projected to expand from \$155 million in 2000 to \$ 1.38 billion in 2025 (Liu *et al.*, 2007; Satyanarayana *et al.*, 2009). On the other hand, the global market growth for natural fiber composites is

Table 10.1 Comparison of some specific properties and cost of lignocellulosic fibers and synthetic fibers. Reprinted from Satyanarayana *et al.*, (2009), Copyright 2009, with permission from Elsevier.

Fiber	Specific gravity	Specific tensile strength/GPa	Specific tensile modulus/GPa	Cost	Energy content/GJ/tons
Plant fiber	0.6–1.2	1.60–2.95	10–130	200–1000	4
Glass	2.6	1.35	30	1200–1800	30
Kevlar	1.4	2.71	90	7500	25
Carbon	1.8	1.71	130	12500	130

Table 10.2 Merit list of the use of lignocellulosic fibers incorporated composites. Reprinted from Satyanarayana *et al.*, (2009), Copyright 2009, with permission from Elsevier.

Meets minimum recycle content requirements
Non-brittle fracture on impact
Lower processing energy requirements
Same performance for lower weight
Low-cost-less than the base resin
Stronger (25–30%) for the same weight
Reduced molding cycle time-up to 30%
Fully and easily recyclable
High notched impact-up to $2 \times$ base resin
High flex modulus-up to $5 \times$ base resin
High tensile modulus-up to $5 \times$ base resin
Low mold shrinkage
Easily colored
Good sound abatement capability
Better energy management characteristics
More shatter resistant
Low thermal expansion coefficient
Natural appearance
Non-abrasive to machinery

predicted to reach \$5.83 billion by 2019, at a Compound Annual Growth Rate (CAGR) of 12.31% between 2014 and 2019 (<http://www.marketsandmarkets.com/PressReleases/natural-fiber-composites.asp>).

These figures highlight the importance of technology and economic features of natural fibers leading to sustainable development, since these fibers can lead to the manufacturing of high durable consumer products that are more recyclable.

10.2.2 Surface Modification of Natural Fibers

Chemical modification of natural fiber surface is considered as a technique to optimize the fiber interface to reduce poor interfacial properties between the polymer matrix and fiber, which often minimizes their potential as reinforcing agents because of the hydrophilic nature of natural fibers. Application of chemical treatment is found to activate hydroxyl groups (OH) or introduce new moieties that can effectively interconnect with the matrix (Brigida *et al.*, 2010; Li *et al.*, 2007; Mwaikambo & Ansell, 2002; Razak *et al.*, 2014; Thakur & Singha, 2010; Van de Weyenberg *et al.*, 2006). For example, FTIR studies on kenaf fiber surface modification using hydrogen peroxide, before and after bleaching treatment were investigated by Razak *et al.*, (2014) (Figure 10.3a). The results revealed a change in the chemical composition of kenaf fiber after bleaching that resulted in an increase in the surface roughness of the fiber and created a good interlink

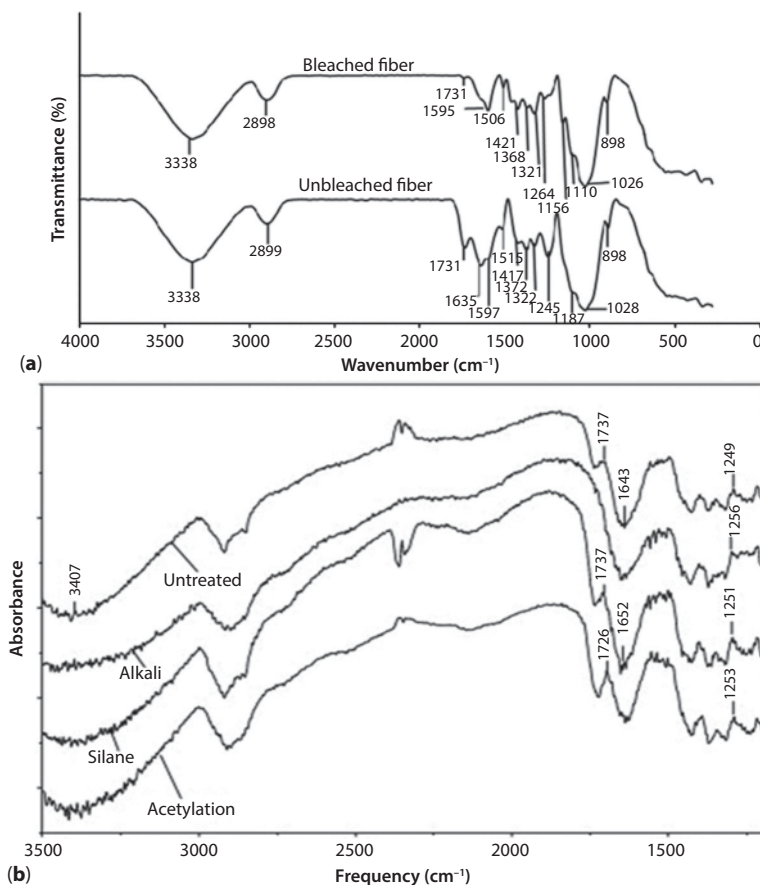


Figure 10.3 FTIR spectra of (a) bleached and unbleached kenaf fiber. Reprinted from Razak *et al.*, (2014), Open Access and (b) chemically-treated hemp fiber. Reprinted from Kabir *et al.*, (2012), Copyrights 2011, with permission from Elsevier.

with the PLA matrix. In this study, they found that after kenaf fiber bleaching, there was a decrease in peak intensities (3338, 2898, 2899 and 1738 cm^{-1} , related to $-\text{OH}$, $\text{C}-\text{H}$ and ester carbonyl of acetyl, feruloyl and p-coumaryl groups in lignin respectively) as compared to unbleached fiber, and this was ascribed to the removal of lignin. This was substantially confirmed by the disappearance of the vibration peak at 1245 cm^{-1} ascribed to $\text{C}-\text{O}$ vibration. Similar results were observed by Kabir *et al.* in the investigation of chemically-treated hemp fiber reinforced sandwich composites (Figure 10.3b). In their case, the peak intensity of the broad $-\text{OH}$ stretching peak of untreated fibers at 3407 cm^{-1} was increased upon chemical treatments such as acetylation; silane and alkali treatments and the band was shifted to 3419, 3386 and 3434 cm^{-1} respectively. This was attributed to the decrease of hydrogen bonding in cellulosic hydroxyl groups, thereby increasing $-\text{OH}$ concentration. This indicated the decrease in hydrophilic nature of the fiber with respect to fiber treatment. The removal of hemicelluloses from the fiber surface was observed from disappearance of the $\text{C}=\text{O}$ stretching in the acetyl groups of hemicelluloses of the unmodified fiber.

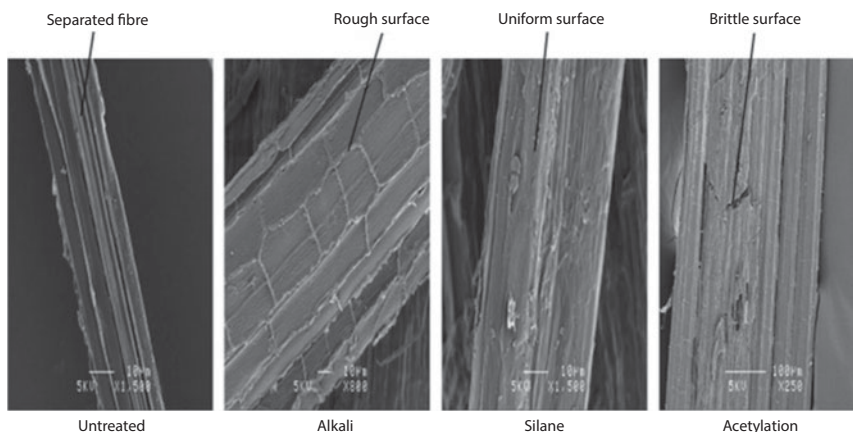


Figure 10.4 SEM micrograph of the untreated and treated hemp fibers. Reprinted from Kabir *et al.*, (2012), Copyrights 2011, with permission from Elsevier.

Again fiber modification does not only alter the chemical composition of the fibers but further changes the surface morphology of the fibers, thereby resulting in distinguishable morphology of unmodified and modified fibers predominantly in terms of their degree of smoothness and coarseness (Figure 10.4). Hence, studies on fiber surface topography provide important information on the degree of interfacial adhesion that would occur between the fiber and the polymer when utilized as a reinforcement (treated or untreated) in polymers (Edeerozey *et al.*, 2007). A great number of studies were performed on silane, alkaline, acetylated fibers and other treatments (e.g., NFs treated with maleated coupling agents) (Bilba & Arsene, 2008; Correa *et al.*, 2007; Jähn *et al.*, 2002; Spinace *et al.*, 2009; Sreekala & Thomas, 2003) and their morphological characteristics were co-related with their mechanical performance.

Chemical treatments are synthetic and usually use toxic chemicals; hence it would be ideal to use treatments that can maintain the biodegradability and renewable character of NFs. Another area of interest is to enhance the use of environmentally friendly chemicals for surface modification of NFs by application of coupling agents from natural products. Biological coupling agents such as fungi (Gulati & Sain, 2006), lignin (Thielemans *et al.*, 2002), chitin and chitosan (Shah *et al.*, 2005) and shellac (Ray *et al.*, 2006) have been used for fiber modification. The application of these natural coupling agents was found to improve and increase the adhesion between the fiber and the matrix as well as their mechanical properties. In addition, the use of natural coupling agents' show similar morphological characteristics as chemically treated fibers such as the elimination of impurities from the fiber surface as depicted in Figure 10.5.

10.2.3 Extraction of Cellulose and/or Cellulose Nanowhiskers from Bio-Fillers

Cellulose is the most abundant renewable and sustainable raw material that can be extracted from natural fibers, animal and agricultural/forest crops or residues (Chirayil *et al.*, 2014; Fatah *et al.*, 2014). The two main subcategories of cellulose that can be

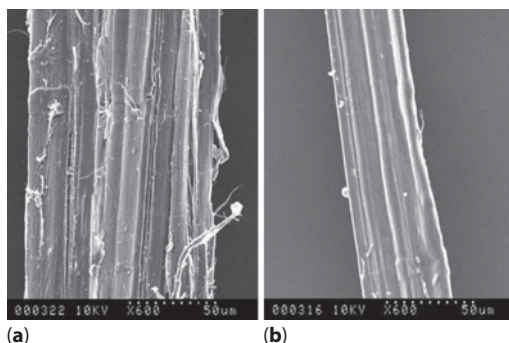


Figure 10.5 SEM picture of an (a) untreated and (b) *Ophiostoma ulmi* treated hemp fiber bundle. Reprinted from Gulati & Sain (2006), Copyrights 2006, with permission from Springer.

extracted are cellulose nanofibrils (CNFs) and cellulose nanocrystals (CNCs). Cellulose nanofibrils can be referred to as nanofibrillated cellulose (NFC) or microfibrillated cellulose (MFC) depending on their extraction method and size, while cellulose nanocrystals can be referred to as cellulose nanowhiskers, or nanocrystal cellulose (NCC). Diverse methods such as chemical treatment, chemo-mechanical and mechanical treatment are utilized for the extraction of cellulose from lignocellulosic fibers (Hoeger *et al.*, 2013; Kumar *et al.*, 2014; Motaung & Mokhena, 2015; Nair *et al.*, 2014; Rezende *et al.*, 2011; Sun *et al.*, 2004; Wang *et al.*, 2012). The chemical extraction of cellulose is mostly done by acid hydrolysis followed by alkaline pulping process (Battagazzore *et al.*, 2014; Pereira *et al.*, 2011) while in other cases alkaline hydrolysis followed by acid hydrolysis (Gbenga & Fatimah, 2014). Typical example of chemical treatments and cellulose extraction processes are depicted in Figure 10.6. During the hydrolysis process, lignin is completely removed by the reagents. It has been observed that the properties of composites reinforced with CNCs depend on the properties of nanocellulose which in turn is influenced by the extraction methods and original source of cellulose. For that reason, extensive characterization of CNCs extracted from various sources is an important pre-requisite before its application in biocomposites. For instance, Table 10.3 shows different extraction methods from various natural fibers and corresponding physical properties.

Acid hydrolysis is the most used treatment to isolate microfibrils from different cellulosic sources, which allows dissolution of amorphous domains and expose crystalline domains. The crystalline domains exhibit a rod-like shape with proportions depending on the basis of cellulose and preparation. Figure 10.7 and Table 10.4 show geometrical attributes of cellulose nanocrystals derived from different natural fibers. Cellulose nanocrystals are considered as ultimate candidates for production of nanocomposites because of their reinforcing capability and impressive mechanical properties (Samir *et al.*, 2005; Hubbe *et al.*, 2008). With an elastic modulus of 145 GPa, they have the potential to reinforce polymers at low filler loadings (Šturcová *et al.*, 2005). Scientific publications show reinforcing potential of cellulose even though most of the studies focus on the liquid self-ordering and mechanical properties (Kalia *et al.*, 2011). On the contrary, as in the case of any nanoparticle, the major obstacle is associated to their homogeneous dispersion within the polymer matrix.

Table 10.3 Physical properties of extracted cellulose from various extraction processes.

Fiber type	Sample	Extraction method	χ_c /%	T_{max} /°C	References
Sugarcane bagasse	Raw	–	51	380	(Motaung & Mokhena, 2015)
	Nanocellulose	Chemical + mechanical fibrillation	80	470	
Sugarcane bagasse	Raw	–	35.6	363	(Kumar <i>et al.</i> , 2014)
	CNCs	Acid hydrolysis	72.5	300	
Wheat Straw	Raw	–	–	304	(Nuruddin <i>et al.</i> , 2013)
	MFC	Microfibrillated cellulose (MFC)	–	355	
Oil palm empty fruit bunch	Raw	–	58.09	330	(Fatah <i>et al.</i> , 2014)
	MFC	Chemo-mechanical	80.42	326	
Maize stalk	Raw	–	53.8	–	(Mtibe <i>et al.</i> , 2015a)
	CNCs	Acid hydrolysis	72.6	–	
Rice husk	Raw	–	46.8	–	(Johar <i>et al.</i> , 2012)
	CNCs	Acid hydrolysis	59.0	–	
Mengkuang leaves (<i>pandanus tectorius</i>)	Raw	–	55.1	200	(Sheltami <i>et al.</i> , 2012)
	Alkali treated	Alkali treatment	60.2	250	
	Bleached	Bleaching	69.5	250	

T_{max} , maximum thermal degradation and crystallinity index respectively

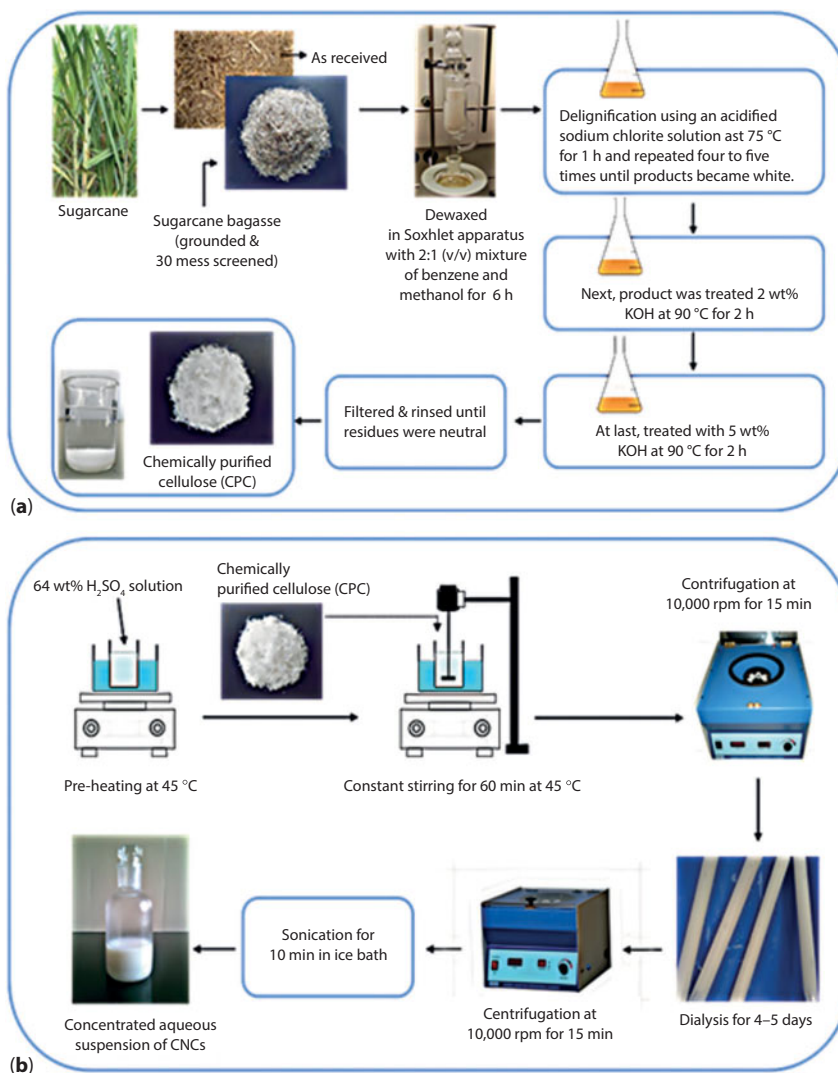


Figure 10.6 Schematic representation of chemical treatments: (a) Isolation of chemically purified cellulose (CPC) from sugarcane bagasse; (b) Extraction of cellulose nanocrystals (CNCs) from chemically purified cellulose (CPC). Reprinted from Kumar *et al.*, (2014), Open Access.

Cellulose nanofibers have the capability to be utilized in the production of micro- and nanopapers. Various research studies have investigated the application of mechanical grinding technique to extract CNFs (from various sources) with high tensile modulus and tensile strength (Mtibe *et al.*, 2015; Qing *et al.*, 2013; Wang *et al.*, 2013; Yousefi *et al.*, 2013). Researchers at the Council for Scientific and Industrial Research (CSIR) investigated the comparative properties of micro and nanopapers extracted from maize stalk (Mtibe *et al.*, 2015a). In this study, CNF-based nanopapers were prepared by chemical treatment followed by mechanical blending and grinding using supermasscolloider. The obtained nanopapers exhibited tensile strength of 95.6 MPa and tensile modulus of 8.8 GPa, while Qing *et al.*, (2013), reported a tensile modulus and tensile strength

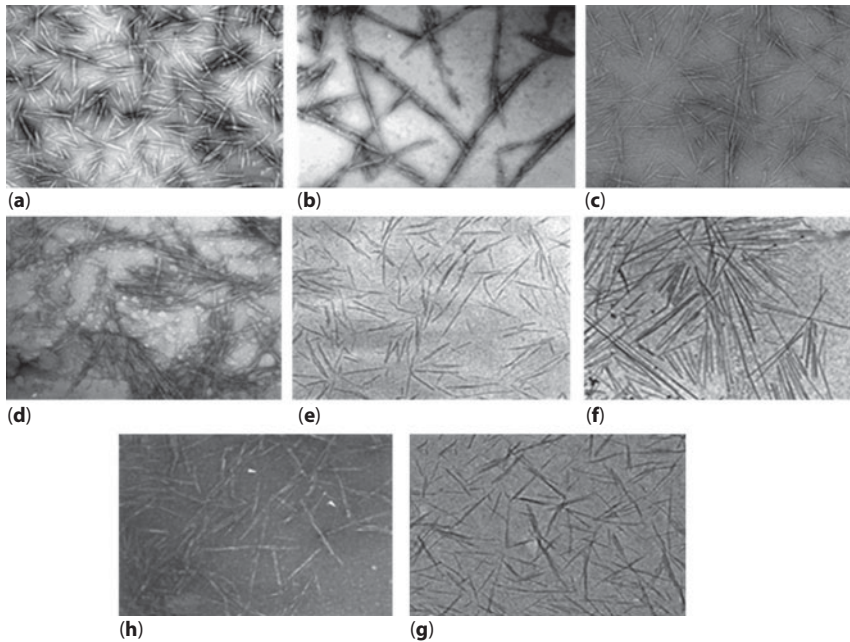


Figure 10.7 Transmission electron micrographs from dilute suspension of cellulose nanocrystals from: (a) ramie, (b) bacterial, (c) sisal, (d) microcrystalline cellulose, (e) sugar beet pulp, (f) tunicin, (g) wheat straw, and (h) cotton. Reprinted from Kalia *et al.*, (2011), Open Access.

Table 10.4 Geometrical characteristics of cellulose nanocrystals from various sources: length (L), cross section (D), and aspect ratio (L/D). Reprinted from Kalia *et al.*, (2011), Open Access.

Source	L/nm	D/nm	L/D
Acacia pulp	100–250	5–15	–
Alfa	200	10	20
Algal (<i>Valonia</i>)	>1000	10–20	∞
Bacterial	100–several 1000	5–10 \times 30–50	–
Banana rachis	500–1000	5	–
Bio-residue from wood bioethanol products	Several 100	10–20	–
Capim dourado	300	4.5	67
Cassava bagasse	360–1700	2–11	–
<i>Cladophora</i>	–	20 \times 20	–
Coconut husk fibers	80–500	6	39
Cotton	100–300	5–15	10
Cottonseed linter	170–490	40–60	–
Curaua	80–70	6–10	13–17
Date palm tree (rachis/leaflets)	260/180	6.1	43/30

(Continued)

Table 10.4 Cont.

Source	L/nm	D/nm	L/D
Eucalyptus wood pulp	145	6	24
Flax	100–500	10–30	15
Grass Zoysia	200–700	10–60	–
Hemp	Several 1000	30–100	–
Luffa cylindrical	242	5.2	47
MCC	150–300	3–7	–
Mulberry	400–500	20–40	–
Pea hull	240–400	7–12	34
Ramie	150–250	6–8	97, 131, 132
Recycled pulp	100–1800	30–80	–
Sisal	100–500	3–5	60/43
	215	5	
Sweet beet pulp	210	5	42
Sugarcane bagasse	200–310	2–6	64
Tunicin	100–several 1000	10–20	67
Wheat straw	150–300	5	45
Wood	100–300	3–5	50

of about 7 GPa and 123 MPa respectively for nanopapers prepared from bleaching process of eucalyptus Kraft pulp. In another study (Yousefi *et al.*, 2013), nanopapers extracted from bacterial cellulose and canola straw exhibited Young's modulus and tensile strength of 17.3 GPa and 185 MPa respectively. Also waste corrugated paper pulp was used to extract cellulose nanopapers by oven drying and hot pressing method (Wang *et al.*, 2013). The nanopapers showed tensile strength of about 152 MPa and tensile modulus of 6.7 GPa. From the above mentioned studies, highly networked and transparent CNFs having the highest toughness were obtained. The CNFs exhibited high thermal stability in comparison to micro and nanopapers prepared from CNCs.

10.2.4 Lignin Bio-Fillers

Lignin is the one of the most abundant renewable resource present in nature, after cellulose and hemicellulose, which is produced in large quantities in the paper, pulp and cellulosic ethanol industries (Agarwal *et al.*, 2014; Frigerio *et al.*, 2014; Setua *et al.*, 2000). Further, lignin is India's second most abundant biomass resource and also available in powdered form (Setua *et al.*, 2000). Lignin is a biopolymer made up of complex group of phenolic polymers that offers rigidity and strength to woody cell walls of different plants (Benko *et al.*, 2014; Thakur *et al.*, 2014c). Lignin together with hemicellulose assists in joining plant cells, making a composite with outstanding strength and elasticity. In general, lignin is light weight, brittle and stiff; however, there are limited studies on its application as a bio-filler in the field of composites. Lignin obtained from

bio-refineries or paper (about 2%) is used in applications such as adhesive and asphalts; isolation of chemicals, production of lignin based polyurethane, phenol replacement in phenol-formaldehyde formulations and other polymers like polyvinyl alcohol (PVA), polyethylene oxide (PEO), polyethylene chloride (PVC), polypropylene (PP) and their blends. However, there are limited studies in the application of lignin in blend systems (Agarwal *et al.*, 2014). In addition, lignin is characterized as one of the most complex structure in nature which limits its application as reinforcement. This has hindered the successful application of lignin from laboratory scale to an industrial scale (Thakur *et al.*, 2014).

10.2.5 Rice Husk Bio-Fillers

Rice husk (RH) is one of the most abundant by-products of rice with a wide aspect ratio range (Arjmandi *et al.*, 2015; Rahman *et al.*, 2010). Rice husk is separated from rice grain during the milling process. Additionally, it is reported in literature that about 0.23 tons of RH is formed from every ton of rice produced (Arjmandi 2015). Rice husk is made up of major components such as cellulose (22–35%), lignin (20–31%), hemicellulose (18–25%), and ash (17% of which 94% is silica). Rice husk produces two types of ash that can be used as fillers in polymer matrices, that is black rice husk ash (BRHA) and white rice husk ash (WRHA). It is reported that the WRHA consists of approximately 95% silica content while BRHA approximately 54% and 44% of substantial carbon content (Arjmandi *et al.*, 2015; Lim *et al.*, 2012). A variety of applications have been proposed for the exploitation of rice husk because of their unique properties such as low bulk density (90–150 kg m⁻³); durability; high availability; unique composition and resistance to weathering. Rice husks have great potential to be used as an insulating material in applications such as production of panel boards, activated carbon, and supplementary cementing material. Rice husk contains a large portion of cellulose which can be extracted for application of cellulose reinforced composites and a suitable candidate for reinforcement in biocomposites. Various studies have been reported in literature on the use of rice husks as reinforcement in polymer matrices such as polyethylene, vinylester, and polypropylene; however, there are limited reports on the use of rice husk in biodegradable polymers (Atuanya *et al.*, 2013; Dimzoski *et al.*, 2008; Rahman *et al.*, 2010).

10.3 Bio-Based Fillers Reinforced Biopolymer Composites

10.3.1 Natural Fiber Composites

For decades, traditional manufacturing techniques have been utilized to manufacture synthetic fiber reinforced polymer composites (Faruk *et al.*, 2014; Miao & Hamad, 2013). Manufacturing techniques such as extrusion, injection and compression molding were utilized to prepare conventional composites. On the other hand, due to increasing demand of eco-friendly and sustainable materials, these techniques through innovation and high-tech technology have been altered to cater for bio-based materials with an advantage of being renewable and biodegradable over traditional materials. These

techniques assist with embedding natural fibers in biopolymer matrices which hold the fibers together. This stabilizes and provides support to the composite formation, transfers the shear forces amongst the mechanically high-quality fibers, and preserves them against radiation and other aggressive media (Faruk *et al.*, 2014). On the other side, natural fiber composites produced by resin transfer molding (RTM), compression molding and pultrusion are implemented with thermosets matrix. For instance, Oksman, (2001) researched on the utilization of high quality natural fibers as reinforcements for composites produced by RTM processing technique. The results from mechanical testing showed that epoxy composite containing 50% of flax fiber had a stiffness of about 40 GPa compared to the stiffness in pure epoxy of 3.2 GPa. Furthermore, incorporation of flax resulted in an increase of tensile strength by 71%. This indicated that RTM was a suitable processing technique to produce high quality natural fiber composites. The incorporation of natural fibers in polymer matrices is directly dependent on the processing techniques, and the performance of reinforcement is influenced by the geometrical properties such as size distribution, shape and size. Another important aspect of natural fibers in bio-based composites is their performance and the quality of the final product.

The reinforcement of natural fibers in biopolymers such as polycaprolactone (PCL); polylactic acid (PLA); poly(3-hydroxybutyrate) (PHB); poly(ethylene oxide) (PEO); poly(butylene succinate) (PBSu), polyhydroxyalkanoate (PHA) and other biopolymers have been investigated (Barkoula *et al.*, 2010; John *et al.*, 2007; Liu *et al.*, 2009; Oksman *et al.*, 2003; Yu *et al.*, 2010). The advantage of these biopolymers is their various applications such as packaging materials; implants; fibers, mulch films and bottles. In addition, the particular polymers can be synthesized from monomers that are derived from renewable resources. Therefore, these biopolymers are potential replacements of petroleum based thermoplastics in a wide range of applications. For instance, Yu *et al.*, (2010) investigated the effect of surface treatment on the properties of PLA/ramie composites. Surface treatment was carried out by alkali and silane treatment on ramie fibers and the composites were prepared by two-roll mill followed by hot pressing. It was seen that incorporation of ramie fibers into PLA improved the tensile properties compared to neat PLA. Again, surface modified composites showed further improvements on the tensile properties with a maximum strength of 68.8 ± 1.7 MPa (NaOH treated composites) while a maximum of 64.2 ± 0.7 MPa was registered for silane treated composites. The improvement in the mechanical properties was associated with better compatibility and bonding at the interface between the PLA and ramie fibers. Similar improvements were observed for impact, flexural and dynamic mechanical properties. Researchers have investigated the properties of flax fiber reinforced with PLA and PP composites prepared by extrusion and compression molding (Oksman *et al.*, 2003). Comparative studies between PLA/flax composites and PP/flax composites have been conducted. From preliminary results, it was observed that PLA/flax (50%) composites had higher mechanical properties than PP/flax composites. Significant improvements in flexural modulus (3.4 GPa) and tensile strength (60 MPa) were observed as compared to the counterpart (1.6 GPa and 30 MPa). Meanwhile, Ochi, (2008), examined the biodegradability of unidirectional PLA/kenaf composite prepared by molding technique. The composites achieved flexural and tensile strength of 254 MPa and 223 MPa respectively. The biodegradability results showed that the weight of the composite decreased

by 38% after four weeks of exposure in a garbage-processing machine. Biodegradation studies on biocomposites such as PLA/PCL/jute (Goriparthi *et al.*, 2012), Ecoflex/kenaf (Mokhothu *et al.*, 2011), PBS/jute (Liu *et al.*, 2009), PLA/kenaf (Yussuf *et al.*, 2010) and PHBV/flax (Barkoula *et al.*, 2010) were examined using different biodegradation methods. The investigations showed that the presence of bast fibers can improve the biodegradation behavior of the prepared biocomposites because of the lignocellulosic nature of the fibers which can degrade in short period. In addition, it is well reported in literature that reinforcing biopolymers with natural fibers resulted in improved mechanical properties. Table 10.5 summarizes some important properties achieved by fiber reinforced composites prepared from various methods.

10.3.2 Nano-Cellulose/Cellulose Whisker Composites

Reinforcing of biopolymers with cellulose nanowhiskers is in large part driven by the opportunity to utilize the theoretically predicted strength and stiffness of cellulose crystals in load-bearing composites. Although the strength and modulus of cellulose crystals is challenging to determine (Eichhorn *et al.*, 2010), several studies have used numerical simulations and theoretical calculations to evaluate the axial modulus of a cellulose crystal to be around 58–180 GPa (Bergensträhle *et al.*, 2007; Eichhorn & Davies, 2006; Tanaka & Iwata, 2006). Several studies have also shown and reported on cellulose fibers exhibiting better reinforcing potential than carbon and glass fibers in thermoset matrices (De & Murty, 1984; Miao & Hamad, 2013). This is because cellulose fibers are flexible than brittle carbon and glass fibers and are less damaged during processing (Hamad, 2013). Cellulose has gained a great deal of interest as one of the reinforcements in a variety of polymer matrices due to their attractive and unique properties such as light weight; high aspect ratio; abundance; renewability; biocompatibility and biodegradability. Furthermore, due to increasing demand of renewable and sustainable materials, significant efforts have been put to place into manufacturing of high multifunctional and/or high performance cellulose based composites. In this regard, the amount of publications on cellulose nanocomposites has escalated exponentially over the past decade (Figure 10.8).

Mtibe *et al.*, (2015b) investigated the extraction of cellulose nanowhiskers (CNWs) from flax fibers that were incorporated in poly(furfuryl alcohol) (PFA) bio-resin; the cellulose nanowhiskers were obtained through acid hydrolysis and sonicated for dispersion in the preparation of PFA/CNWs composites by *in situ* polymerization. The extracted CNWs exhibited fiber length ranging from 200–400 nm and 10–16 nm with an aspect ratio between 20 and 25. The incorporation of 2% CNWs in PFA showed improvement in the mechanical properties of PFA/CNWs composite with tensile strength increasing by about 12% and the elongation at break followed the same trend. This was attributed to strong interfacial bonding between CNWs and PFA via hydrogen bonding. Furthermore, a shift in the glass transition temperature to high temperatures was observed from the thermo-mechanical properties. This was attributed to a restriction in chain mobility as a result of improved interaction due to reinforcement. In another study, Motaung & Mokhena, (2015) prepared cellulose reinforced poly(ethylene oxides) composite obtained by mechanical fibrillation of sugarcane bagasse (SB). The SB fibers were mechanically fibrillated by means of a supermasscolloider before chemical

Table 10.5 Mechanical properties of natural fiber reinforced biopolymer composites.

Matrix/Fiber	Processing method	Modification	Tensile strength/MPa	Tensile modulus/GPa	Strain at break/%	Flexural strength/MPa	Flexural modulus/GPa	References
PLA/kenaf	Compression molding	–	60.95 ± 1.41	5.73 ± 1.20	1.48 ± 0.05	–	–	(Taib <i>et al.</i> , 2010)
PLA/hemp	Injection molding	–	72.1	~ 2.0–2.5	52	~ 90–100	~ 6–7	(Song <i>et al.</i> , 2013)
		Silane coupling agent	~ 72–74	~ 2.2–2.4	~ 65–70	~ 100–105	~ 5.8–6.0	
PHBV-Ecoflex/jute	Injection molding	–	35.2 ± 1.3	7.0 ± 0.26	0.8 ± 0.0	–	–	(Bledzki & Jaskiewicz, 2010)
PHBV-Ecoflex/abaca		–	28.0 ± 1.3	4.4 ± 0.06	0.9 ± 0.1	–	–	
PLA/hemp Polyester/hemp	Injection molding Compression molding	Alkali	75.5	8.18	–	–	6.33	(Sawpan, 2010)
		Alkali	62.1	13.35	–	–	6.11	
		Alkali + Silane	83	14.4	–	–	6.7	
PCL/kenaf	Extrusion and compression molding	–	–	6.1	~ 10–20	–	–	(Pan <i>et al.</i> , 2008)
Epoxy/ArcticFlax	RTM	–	280 ± 15	35 ± 3	0.9	–	–	(Oksman, 2001)

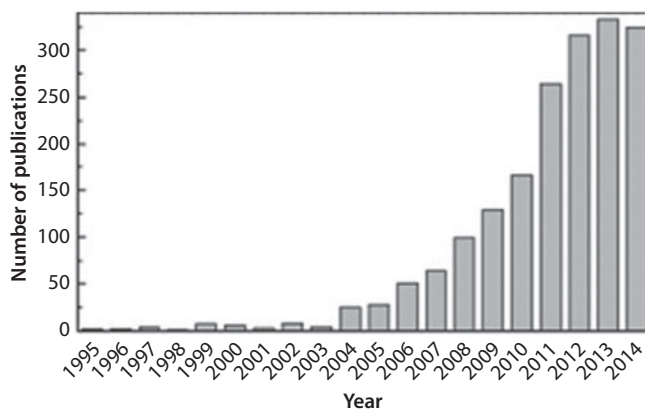


Figure 10.8 Number of publications in the area of cellulose nanocomposites. Reprinted from Lee *et al.*, (2014), Open Access.

treatment and acid hydrolysis process and the composites were prepared by solution casting method. Reinforcing PEO with CNFs resulted in PEO/CNFs (95/5) biocomposites with high crystallinity index of 92% and 80% according to the XRD deconvolution and peak height methods. The mechanical properties of the composites at low filler loading (5%) showed improved properties, with tensile strength of about 5.0 MPa and tensile modulus of about 0.70 MPa compared to neat PEO with tensile strength of 4.3 MPa and tensile modulus of 0.43 MPa. The improvement was attributed to good interaction between the polymer and the filler as well as the increased stiffness brought by the CNFs. Strong reinforcing effects at low loadings of nanocellulose were displayed and explained by Favier *et al.*, 1995a; and Favier *et al.*, 1995b. Nanocellulose whiskers extracted from tunicate were used to reinforce styrene and butyl acrylate copolymer latex with a loading content of up to 6%. It was reported that even at low filler loadings, the nanocomposites exhibited significantly higher mechanical properties than the neat polymer. The authors assigned the improvement to the formation of rigid nanocellulose whiskers network within the nanocomposites as a result of percolation of nanocellulose. Similar observation and explanations were reported on starch film reinforced with homogenized cellulose microfibrils obtained from potato pulp (Dufresne & Vignon, 1998). From the above discussed studies, it can be derived that nanocellulose is a promising reinforcement material for renewable and sustainable bio-based composites and due to their attractive properties such as stiffness and strength as well as biodegradability character, nanocellulose have a potential to replace traditional or synthetic fillers.

10.3.3 Lignin Composites

Lignin is characterized by a wide range of functional groups that are able to meet industrial needs (Thakur & Thakur, 2014a-c). For instance, sulphur-free lignins are receiving increasing attention because of their versatility and can be heat-processed without producing irritating odors commonly released by commercial Kraft lignin (Thakur *et al* 2014a-e). Moreover, sulphur-free lignins are cost efficient, renewable and abundant. They can be used in the application of thermoplastic and thermosets in conjunction

with epoxy, isocyanate and phenol resins (Bertini *et al.*, 2012; Frigerio *et al.*, 2014). A large number of research (Agarwal *et al.*, 2014; Frigerio *et al.*, 2014; Kosikova *et al.*, 2003; Kramarova *et al.*, 2007; Setua *et al.*, 2000), review (Thakur *et al.*, 2014) and patents (Benko *et al.*, 2014; Boutsicaris, 1984) have focused on the application of lignin as bio-based filler for rubber composites to replace carbon black and also as a filler for polymers and blends for sustainable and renewable materials (Bertini *et al.*, 2012; Mousavioun *et al.*, 2012). Research on reinforcement of nitrile rubber (NBR) with lignin has been reported and improved thermal stability of lignin-NBR composites was observed as opposed to phenol and carbon black filled composites (Agarwal *et al.*, 2014). Further, the lignin-rubber composites exhibited slightly higher modulus at 100% elongation with higher elongation and tear strength than neat NBR. However, the tensile strength was found to be lower, this was attributed to vulcanization deficiency caused by the addition of lignin which impaired the tensile strength. Interestingly, lignin-NBR composites exhibited highly effective antibacterial activity, which may suggest a potential application in waste management. In other research, sulphur-free lignin was used to reinforce styrene butadiene rubber (SBR) (Frigerio *et al.*, 2014); a strong reduction in mechanical properties was observed as compared to carbon black reinforced SBR. This is due to the primary factors such as shape of the particles and size, tendency of lignin to agglomerate, chemical nature and dispersibility which minimises the ability of lignin to be used as a filler. Contrary the presence of hexamethylenetetramine (HMT) in lignin-SBR composites showed increased tensile strength and the values were similar to carbon black composites.

Degradation studies were performed on lignin reinforced poly(hydroxybutyrate) (PHB) composites, which were prepared via melt extrusion (Mousavioun *et al.*, 2012). The lignin-PHB composites were buried in garden soil for 12 months. The degradation studies showed that 40 wt.% of mass was lost from neat PHB within 12 months, while in the case of PHB filled with 10 wt.% lignin, only 12 wt.% mass loss was attained during the same period. This was attributed to biochemical defense effect of lignin against the attack of micro-organisms on PHB. The results proposed that lignin created strong hydrogen bonds with PHB in the buried samples and reduced the degradation rate of PHB and this prevented rapid degradation of the blends.

10.3.4 Rice Husk (RH) Composites

Several reports on the relevance of rice husk as potential reinforcement in biopolymers such as poly(lactic acid) (PLA) have been documented in papers and in review papers. The influence of processing methods on the physical, thermal, mechanical and morphological properties was evaluated from the prepared biocomposites. Research on the mechanical and moisture properties of maleic anhydride (MAPP) modified rice husk powder reinforced PLA composites were reported. The composites were prepared by melt mixing method (Hua *et al.*, 2011). The authors reported that increasing rice husk powder content increased the tensile strength and the maximum bearable tension of the composites. On the other hand, the water absorption was found to increase after 24 hours of immersion whereas for composites modified with MAPP significant reduction in moisture absorption was observed. It was also reported that modification with MAPP improved the adhesion between PLA and the rice husk powder, which led to

increased mechanical properties. In addition, most recently, several research groups have focused on the influence of surface modification of mechanical, physical and morphological properties of RH fiber reinforced composites and a recent review has summarized several studies (Arjmandi *et al.*, 2015; Dimzoski *et al.*, 2008; Farah Dina *et al.*, 2014; Mohammadi-Rovshandeh *et al.*, 2014; Tran *et al.*, 2014). In the study on effects of alkaline and silane treatment of rice and wheat husks reinforced composites (Tran *et al.*, 2014), it was reported that both alkali and silane composites had higher bending moduli and stresses than unmodified composites and those modified with silane alone. It was further reported that rice and wheat filled composite after alkaline modification showed high sensitivity to moisture absorption and lower surface energies. But in the case of silane modified rice husk reinforced composites treated after alkaline treatment, a decrease in the moisture absorption was observed. Furthermore, the biocomposites showed increased thermal stability and higher mechanical properties. It was explained that, in the case of alkaline treated composites, the alkaline treatment cleaned the surface of husk and activated the hydroxyl groups (-OH) on the surface of the husks. Therefore, these activated -OH groups reacted more easily with silane functional groups than those on the surface of untreated husks. In another work (Mohammadi-Rovshandeh *et al.*, 2014), bleached rich husk (BRH) and rice husk (RH) were incorporated in PLA and prepared by melt mixing method followed by compression molding. It was found that BRH-PLA composites attained superior charpy impact strength, hardness and modulus compared to those filled with RH. This was ascribed to the removal of lignin through bleaching from RH, which promoted better mechanical interlocking between BRH and PLA. Furthermore, improvements in the crystallization behavior and reduction of the glass transition temperature (T_g from 47 to 31 °C) was observed for BRH filled biocomposites.

10.4 Applications of Bio-Based Composites

The development of biocomposites for industrial application is mainly dependent on performance and sustainability of the products. Hence, there is a growing trend in research all over the world, which is focusing on the overall performance of natural fiber composites. The utilization of bio-based composites in industrial application includes food packaging, automotive, construction, cosmetics, aerospace as well as electrical and electronics (Saba *et al.*, 2014).

Fiber reinforced polymer composites are utilized in construction as structural panels and building sections; further, the use of fiber reinforced composites has also developed into economically and sustainable feasible construction materials for load bearing elements in bridges and buildings over the past decades. Significant achievements have been obtained in civil engineering applications such as safety, economy and functionality of construction since the use of fiber reinforced polymer composites. The advantage of bio-based composites is their high strength to density ratio, excellent corrosion resistance and good mechanical properties. However, fiber reinforced composites show anisotropic behavior and their mechanical properties might be affected by environmental conditions and the rate of loading (Nicolae *et al.*, 2008). This is because (i) fibers have low stiffness in the transverse direction (ii) fibers are susceptible to moisture

sorption which result in swelling of the fibers and leads to debonding with the matrix and (iii) high fiber loadings can results in agglomeration which reduces stress transfer between the fiber and the matrix. On the other hand, several studies have investigated the application of natural fibers such as coir (Saravanan & Sivaraja, 2012), hemp (Jarabo *et al.*, 2012), flax (Yan & Chouw, 2013) and jute (Chakraborty *et al.*, 2013) as reinforcement in cement based material for building applications. From the aforementioned studies, it was observed that reinforcing of cement with natural fibers enhanced the physical and mechanical properties of the cement mortar.

The advantage of using natural fiber reinforced composites in aerospace over traditionally used components such as carbon fiber, metal alloys and hybrid laminates is that natural fibers offer high specific strength and stiffness. Natural fibers further offer; (i) efficient design of complex shapes that are aerodynamic than metal, (ii) reduction in fuel consumption and emission due to lower weight, (iii) renewable because they are biodegradable in nature and (iv) have no corrosion problem, which can reduce air-line maintenance cost. Research work on the development of composites from woven fabric and phenolic matrices was reported by CSIR research group (John *et al.*, 2008c). The research focused on developing flax-phenolic sandwiched panels for use as commercial panels for cabin interior for aerospace application. The research work focused on issues such as fiber-matrix adhesion and mechanical strength besides compliance to meet with airworthiness standards. The investigated flax fiber-phenolic sandwiched honeycomb panels showed a promising potential to be used for aerospace applications in the near future.

The use of natural fiber-based composites in the automotive sector is basically driven by a key strategy known as light-weighting, which helps increase transportation energy efficiency and fuel economy while maintaining safety standards (<http://energy.gov/eere/amo/advanced-manufacturing-office>). A reduction (10%) in a car's weight can improve the fuel economy by 6–8% or the range of a battery powered car can be increased by 10%. Therefore, the use of natural fiber in automotive components can be projected to escalate steadily with increasing model expansion. In addition, major car manufacturing industries all over the world now use bio-based filler reinforced composites in miscellaneous applications as listed in Table 10.6 (Faruk *et al.*, 2014). The biggest region for automotive application is Europe while North America is the biggest region for the use of NFs in construction and building applications. Environmental concerns are driving creation of natural fiber composites suitable for assorted new applications. Conversely, in order to enlarge other markets such as new materials for sporting goods, consumer goods and commercial construction, composites need to attain reliability standards, high-quality performance and serviceability.

10.5 Summary

The application of bio-based fillers as reinforcements in biopolymer based composites was reviewed. The increasing demand for renewable and sustainable bio-based materials was addressed from the point of view of performance, surface treatment, sustainability, biodegradability, structure, cost efficiency and application. Various types of

Table 10.6 Automotive models, manufacturer and components using natural fiber composites. Reprinted from Faruk *et al.*, (2014), Copyrights 2014, with permission from Wiley.

Model	Manufacturer	Components
A2, A3, A4, A4 Avant, A6, A8, Roadstar, Coupe	Audi	Seat back, side and back door panel, boot lining, hat rack, spare tire lining
C5	Citroen	Interior door paneling
3, 5, 7 series	BMW	Door panels, headliner panel, boot-lining, seat back, noise insulation panels, molded foot well linings
Eco Elise	Lotus	Body panels, spoiler, seats, interior carpets
Punto, Brava, Marea, Alfa Romeo 146, 156	Fiat	Door panel
Astra, Vectra, Zafira	Opel	Instrumental panel, headliner panel, door panels, pillar cover panel
406	Peugeot	Front and rear door panels
2000 and others	Rover	Insulation, rear storage shelf/panel
Raum, Brevis, Harrier, Celsior	Toyota	Door panels, seat backs, floor mats, spare tire cover
Golf A4, Passat Variant, Bora	Volkswagen	Door panel, seat back, boot-lid finish panel, boot-liner
Space star, Colt	Mitsubishi	Cargo area floor, door panels, instrumental panels
Clio, Twingo	Renault	Rear parcel shelf
Mercedes A, C, E, S class, Trucks, EvoBus (exterior)	Daimler-Benz	pillar cover panel, glove box, instrumental panel support, insulation, molding rod/apertures, seat backrest panel, trunk panel, seat surface/backrest, internal engine cover, engine insulation, sun visor, bumper, wheel box, roof cover
Pilot	Honda	Cargo area
C70, V70	Volvo	Seat padding, natural foams, cargo floor tray
Cadillac Deville, Chevrolet TrailBlazer	General Motors	Seat backs, cargo area floor
L3000	Saturn	Package trays and door panel
Mondeo CD 162, Focus, freestar	Ford	Floor trays, door panels, B-pillar, boot liner

bio-based fillers were discussed in this chapter to address the wide availability of the fillers with potential properties such as low cost; high specific strength; light weight; negligible CO₂ emissions; improved energy recovery; flexibility for manufacturing and above all environmentally friendliness. It is worth pointing out that the use of bio-based fillers may reduce the production cost with additional advantages of generating lower waste and less use of energy. Bio-based fillers such as lignin, cellulose, rice husks and various natural fibers are at the forefront of revolutionizing materials mainly focusing on eco-efficiency, green chemistry, sustainability, industrial ecology and biodegradability, which may guide the development of novel materials. However, the success of green composites is dependent on the appropriate processing techniques; filler loading; modification of fibers to enhance filler-matrix interactions and improved loadbearing properties for long-term durability. Furthermore, another important aspect of bio-fillers in bio-based composites is their performance and the quality of the final product which is influenced by the geometrical properties such as size distribution and shape.

References

- Agarwal, K., Prasad, M., Sharma, R., Setua, D.K., Novel bio-degradable lignin reinforced NBR composites. *Int. J. Energ. Eng.*, 4, 47, 2014.
- Atuanya, C., Olaitan, S., Azeez, T., Akagu, C., Onukwuli, O., Menkiti, M., Effect of rice husk filler on mechanical properties of polyethylene matrix composite. *Int. J. Cur. Res. Rev.*, 5, 111, 2013.
- Arjmandi, R., Hassan, A., Majeed, K., Zakaria, Z., Rice husk filled polymer composites. *Cellulose*, 25, 35, 2015.
- Azwa, Z., Yousif, B., Thermal degradation study of kenaf fibre/epoxy composites using thermo gravimetric analysis. *Proceedings of the 3rd Malaysian Postgraduate Conference (MPC 2013)*, pp. 256–264, Education Malaysia, 2013.
- Azwa, Z., Yousif, B., Manalo, A., Karunasena, W., A review on the degradability of polymeric composites based on natural fibres. *Mater. Design*, 47, 424, 2013.
- Barkoula, N., Garkhail, S., Peijs, T., Biodegradable composites based on flax/polyhydroxybutyrate and its copolymer with hydroxyvalerate. *Ind. Crop. Prod.*, 31, 34, 2010.
- Battegazzore, D., Bocchini, S., Alongi, J., Frache, A., Rice husk as bio-source of silica: preparation and characterization of PLA-silica bio-composites. *RSC Advances*, 4, 54703, 2014.
- Benko, D.A., Hahn, B.R., Cohen, M.P., Dirk, S.M., Cicotte, K.N., Functionalized lignin, rubber containing functionalized lignin and products containing such rubber composition. US Patents 8664305, 2014.
- Bergensträhle, M., Berglund, L. A., Mazeau, K., Thermal response in crystalline I β cellulose: a molecular dynamics study. *J. Phys. Chem. B*, 111, 9138, 2007.
- Bertini, F., Canetti, M., Cacciamani, A., Elegir, G., Orlandi, M., Zoia, L., Effect of ligno-derivatives on thermal properties and degradation behavior of poly (3-hydroxybutyrate)-based biocomposites. *Polym. Degrad. Stabil.*, 97, 1979, 2012.
- Bilba, K., Arsene, M.A., Silane treatment of bagasse fiber for reinforcement of cementitious composites. *Compos. Part A-Appl. S.*, 39, 1488, 2008.
- Bledzki, A., Jazskiewicz, A., Mechanical performance of biocomposites based on PLA and PHBV reinforced with natural fibres—A comparative study to PP. *Compos. Sci. Technol.*, 70, 1696, 2010.
- Boutsicaris, S.P., Lignin reinforced synthetic rubber. US Patents 4477612, 1984.
- Brígida, A., Calado, V., Gonçalves, L., Coelho, M., Effect of chemical treatments on properties of green coconut fiber. *Carbohydr. Polym.*, 79, 832, 2010.

- Chakraborty, S., Kundu, S. P., Roy, A., Basak, R. K., Adhikari, B., Majumder, S., Improvement of the mechanical properties of jute fibre reinforced cement mortar: A statistical approach. *Constr. Build. Mater.*, 38, 776, 2013.
- Chirayil, C. J., Mathew, L., Thomas, S., Review of recent research in nano cellulose preparation from different lignocellulosic fibers. *Rev. Adv. Mater. Sci.*, 37, 20, 2014.
- Correa, C., Razzino, C., & Hage, E. Role of maleated coupling agents on the interface adhesion of polypropylene—wood composites. *J. Thermoplast. Compos.*, 20, 323, 2007.
- De, S., Murty, V., Short fiber-rubber composites. *Polym. Eng. Rev.*, 4, 313, 1984.
- Deka, H., Misra, M., Mohanty, A., Renewable resource based “all green composites” from kenaf biofiber and poly (furfuryl alcohol) bioresin. *Ind. Crop. Prod.*, 41, 94, 2013.
- Dimzoski, B., Bogoeva-Gaceva, G., Srebrenkoska, V., Avella, M., Gentile, G., Errico, M., Preparation and characterization of poly (lactic acid)/rice hulls based biodegradable composites. *J. Polym. Eng.*, 28, 369, 2008.
- Dong, Y., Yan, Y., Zhang, S., Li, J., wood/polymer nanocomposites prepared by impregnation with furfuryl alcohol and nano-SiO₂. *BioResources*, 9, 6028–6040, 2014.
- Dufresne, A., Vignon, M.R., Improvement of starch film performances using cellulose microfibrils. *Macromolecules*, 31, 2693, 1998.
- Edeerozey, A.M., Akil, H. M., Azhar, A., Ariffin, M.Z., Chemical modification of kenaf fibers. *Mater. Lett.*, 61, 2023, 2007.
- Eichhorn, S., Davies, G., Modelling the crystalline deformation of native and regenerated cellulose. *Cellulose*, 13, 291, 2006.
- Eichhorn, S., Dufresne, A., Aranguren, M., Marcovich, N., Capadona, J., Rowan, S., Weder, C., Thielemans, W., Roman, M., Renneckar, S., Review: current international research into cellulose nanofibres and nanocomposites. *J. Mater. Sci.*, 45, 1, 2010.
- Farah Dina, A., Zaleha, S., Noor Najmi, B., Nor Azowa, I., The influence of alkaline treatment on mechanical properties and morphology of rice husk fibre reinforced polylactic acid. *Adv. Mater. Res.*, 911, 17, 2014.
- Faruk, O., Bledzki, A.K., Fink, H.P., Sain, M., Progress report on natural fiber reinforced composites. *Macromol. Mater. Eng.*, 299, 9, 2014.
- Fatah, I.Y.A., Khalil, H., Hossain, M.S., Aziz, A.A., Davoudpour, Y., Dungani, R., Bhat, A., Exploration of a chemo-mechanical technique for the isolation of nanofibrillated cellulosic fiber from oil palm empty fruit bunch as a reinforcing agent in composites materials. *Polymers*, 6, 2611, 2014.
- Favier, V., Canova, G.R., Cavaillé, J.Y., Chanzy, H., Dufresne, A., Gauthier, C., Nanocomposite materials from latex and cellulose whiskers. *Polym. Advan. Technol.*, 6, 351, 1995a.
- Favier, V., Chanzy, H., Cavaillé, J., Polymer nanocomposites reinforced by cellulose whiskers. *Macromolecules*, 28, 6365, 1995b.
- Frigerio, P., Zoia, L., Orlandi, M., Hanel, T., Castellani, L., Application of sulphur-free lignins as a filler for elastomers: Effect of hexamethylenetetramine treatment. *BioResources*, 9, 1387, 2014.
- Gbenga, B.L., Fatimah, O.F., Investigation of α -cellulose content of sugarcane scrappings and bagasse as tablet disintegrant. *J. Basic Appl. Sci.*, 10, 142, 2014.
- Goriparthi, B.K., Suman, K., Nalluri, M.R., Processing and characterization of jute fiber reinforced hybrid biocomposites based on polylactide/polycaprolactone blends. *Polym. Compos.*, 33, 237, 2012.
- Gulati, D., Sain, M., Fungal-modification of natural fibers: a novel method of treating natural fibers for composite reinforcement. *J. Polym. Environ.*, 14, 347, 2006.
- Hamad, W.Y., *Cellulosic materials: fibers, networks and composites*. Springer Science and Business Media, 2013.
- Hoeger, I.C., Nair, S.S., Ragauskas, A.J., Deng, Y., Rojas, O.J., Zhu, J., Mechanical deconstruction of lignocellulose cell walls and their enzymatic saccharification. *Cellulose*, 20, 807, 2013.

- Hua, J., Zhao, Z.M., Yu, W., Wei, B.Z., Hydroscopic and mechanical properties performance analysis of rice husk powder/PLA composites. *Adv. Mater. Res.*, 230, 1231, 2011.
- Hubbe, M.A., Rojas, O.J., Lucia, L.A., Sain, M., Cellulosic nanocomposites: a review. *BioResources*, 3, 929, 2008.
- Jähn, A., Schröder, M., Fütting, M., Schenzel, K., Diepenbrock, W., Characterization of alkali treated flax fibres by means of FT Raman spectroscopy and environmental scanning electron microscopy. *Spectrochim. Acta A.*, 58, 2271, 2002.
- Jarabo, R., Monte, M. C., Blanco, A., Negro, C., Tijero, J., Characterisation of agricultural residues used as a source of fibres for fibre-cement production. *Ind. Crop. Prod.*, 36, 14, 2012.
- Johar, N., Ahmad, I., Dufresne, A., Extraction, preparation and characterization of cellulose fibres and nanocrystals from rice husk. *Ind. Crop. Prod.*, 37, 93, 2012.
- John, M.J., Thomas, S., Biofibres and biocomposites. *Carbohydr. Polym.*, 71, 343, 2008a.
- John, M.J., Anandjiwala, R.D., Pothan, L.A., Thomas, S., Cellulosic fibre-reinforced green composites. *Compos. Interface.*, 14, 751, 2007.
- John, M.J., Anandjiwala, R.D., Recent developments in chemical modification and characterization of natural fiber-reinforced composites. *Polym. Compos.*, 29, 187, 2008b.
- John, M.J., Anandjiwala, R., Wambua, P., Chapple, S., Klems, T., Doecker, M., Goulain, M., Erasmus, L., Bio-based structural composite materials for aerospace applications. South African International Aerospace Symposium, 2008c.
- Kabir, M., Wang, H., Lau, K., Cardona, F., Aravinthan, T., Mechanical properties of chemically-treated hemp fibre reinforced sandwich composites. *Compos. Part B-Eng.*, 43., 159, 2012.
- Kalia, S., Dufresne, A., Cherian, B.M., Kaith, B., Avérous, L., Njuguna, J., Nassiopoulos, E., Cellulose-based bio-and nanocomposites: A review. *Int. J. Polym. Sci.*, 35, 2011.
- Kosikova, B., Alexy, P., Gregorova, A., Use of lignin products derived from wood pulping as environmentally desirable component of composite rubber materials. *Wood Res.*, 48, 62, 2003.
- Kramarova, Z., Alexy, P., Chodák, I., Špirk, E., Hudec, I., Košíková, B., Gregorova, A., Šúri, P., Feranc, J., Bugaj, P., Biopolymers as fillers for rubber blends. *Polym. Adv. Technol.*, 18, 135.
- Kumar, A., Negi, Y.S., Choudhary, V., Bhardwaj, N.K., Characterization of cellulose nanocrystals produced by acid-hydrolysis from sugarcane bagasse as agro-waste. *J. Mater. Phys. Chem.*, 2, 1, 2014.
- Kumar, R., Obrai, S., Sharma, A., Chemical modifications of natural fiber for composite material. *Der Chemica Sinica*, 2, 219, 2011.
- Lee, K.-Y., Aitomäki, Y., Berglund, L.A., Oksman, K., Bismarck, A., On the use of nanocellulose as reinforcement in polymer matrix composites. *Compos. Sci. Technol.*, 105, 15, 2014.
- Li, X., Tabil, L.G., Panigrahi, S. Chemical treatments of natural fiber for use in natural fiber-reinforced composites: a review. *J. Polym. Environ.*, 15, 25, 2007.
- Lim, S.L., Wu, T.Y., Sim, E.Y.S., Lim, P.N., Clarke, C., Biotransformation of rice husk into organic fertilizer through vermicomposting. *Ecol. Eng.*, 41, 64, 2012.
- Liu, L., Yu, J., Cheng, L., Yang, X., Biodegradability of poly (butylene succinate)(PBS) composite reinforced with jute fibre. *Polym. Degrad. Stabil.*, 94, 90, 2009.
- Liu, W., Thayer, K., Misra, M., Drzal, L.T., Mohanty, A.K., Processing and physical properties of native grass-reinforced biocomposites. *Polym. Eng. Sci.*, 47, 969, 2007.
- Majeed, K., Jawaid, M., Hassan, A., Bakar, A.A., Khalil, H.A., Salema, A.A., Inuwa, I., Potential materials for food packaging from nanoclay/natural fibres filled hybrid composites. *Mater. Design*, 46, 391, 2013.
- Market and markets, 2015. <http://www.marketsandmarkets.com/PressReleases/natural-fiber-composites.asp>
- Miao, C., Hamad, W.Y., Cellulose reinforced polymer composites and nanocomposites: a critical review. *Cellulose*, 20, 2221, 2013.

- Mohammadi-Rovshandeh, J., Pouresmaeel-Selakjani, P., Davachi, S.M., Kaffashi, B., Hassani, A., Bahmeyer, A., Effect of lignin removal on mechanical, thermal, and morphological properties of polylactide/starch/rice husk blend used in food packaging. *J. Appl. Polym. Sci.*, 131, 2014.
- Mohanty, A., Misra, M., Hinrichsen, G., Biofibres, biodegradable polymers and biocomposites: an overview. *Macromol. Mater. Eng.*, 276–277, 1, 2000.
- Mokhothu, T., Guduri, B., Luyt, A., Kenaf fiber-reinforced copolyester biocomposites. *Polym. Compos.*, 32, 2001, 2011.
- Motaung, T.E., Mokhena, T.C., Effects of mechanical fibrillation on cellulose reinforced poly(ethylene oxide). *Mater. Sci. Appl.*, 6, 713, 2015.
- Mousavioun, P., George, G.A., Doherty, W.O., Environmental degradation of lignin/poly(hydroxybutyrate) blends. *Polym. Degrad. Stabil.*, 97, 1114, 2012.
- Mtibe, A., Liganiso, L.Z., Mathew, A.P., Oksman, K., John, M.J., Anandjiwala, R.D., A comparative study on properties of micro and nanopapers produced from cellulose and cellulose nanofibres. *Carbohydr. Polym.*, 118, 1, 2015a.
- Mtibe, A., Mandlevu, Y., Liganiso, L.Z., Anandjiwala, R.D., Extraction of cellulose nanowhiskers from flax fibres and their reinforcing effect on poly(furfuryl) alcohol. *J. Biobased Mater. Bioeng.*, 9, 309, 2015b.
- Mwaikambo, L.Y., Ansell, M.P., Chemical modification of hemp, sisal, jute, and kapok fibers by alkalization. *J. Appl. Polym. Sci.*, 84, 2222, 2002.
- Nair, S.S., Zhu, J., Deng, Y., Ragauskas, A.J., Characterization of cellulose nanofibrillation by micro grinding. *J. Nanopart. Res.*, 16, 1, 2014.
- Nicolae, T., Gabriel, O., Dorina, I., Ioana, E., Vlad, M., Cătălin, B., Fibre reinforced polymer composites as internal and external reinforcements for building elements. *Bul. Inst. Polit. Iași*, 54, 2008.
- Nuruddin, M., Tcherbi-Narteh, A., Hosur, M., Chowdhury, R.A., Jeelani, S., Gichuhi, P., Cellulose microfibrils extracted from wheat straw: A novel approach. *45th ISTC*, 2013.
- Ochi, S., Mechanical properties of kenaf fibers and kenaf/PLA composites. *Mech. Mater.*, 40, 446, 2008.
- Oksman, K., High quality flax fibre composites manufactured by the resin transfer moulding process. *J. Reinf. Plast. Comp.*, 20, 621, 2001.
- Oksman, K., Skrifvars, M., Selin, J.-F., Natural fibres as reinforcement in polylactic acid (PLA) composites. *Compos. Sci. Technol.*, 63, 1317, 2003.
- Pan, P., Zhu, B., Dong, T., Serizawa, S., Iji, M., Inoue, Y., Kenaf fiber/poly (ϵ -caprolactone) biocomposite with enhanced crystallization rate and mechanical properties. *J. Appl. Polym. Sci.*, 107, 3512, 2008.
- Pereira, P.H.F., Voorwald, H.C.J., Cioffi, M.O.H., Mullinari, D.R., Da Luz, S.M., Da Silva, M.L.C.P., Sugarcane bagasse pulping and bleaching: Thermal and chemical characterization. *BioResources*, 6, 2471, 2011.
- Qing, Y., Sabo, R., Zhu, J., Agarwal, U., Cai, Z., Wu, Y., A comparative study of cellulose nanofibrils disintegrated via multiple processing approaches. *Carbohydr. Polym.*, 97, 226, 2013.
- Rahman, M.R., Islam, M.N., Huque, M.M., Hamdan, S., Ahmed, A.S., Effect of chemical treatment on rice husk (RH) reinforced polyethylene (PE) composites. *BioResources*, 5, 869, 2010.
- Ray, D., Sengupta, S., Rana, A., Bose, N.R., Static and dynamic mechanical properties of vinyl-ester resin matrix composites reinforced with shellac-treated jute yarns. *Ind. Eng. Chem. Res.*, 45, 2722, 2006.
- Razak, N.I.A., Ibrahim, N.A., Zainuddin, N., Rayung, M., Saad, W.Z., The influence of chemical surface modification of kenaf fiber using hydrogen peroxide on the mechanical properties of biodegradable kenaf fiber/poly (lactic acid) composites. *Molecules*, 19, 2957, 2014.
- Reddy, N., & Yang, Y. Biofibers from agricultural byproducts for industrial applications. *TRENDS Biotechnol.*, 23, 22, 2005.

- Rezende, C.A., De Lima, M.A., Maziero, P., Ribeiro deAzevedo, E., Garcia, W., Polikarpov, I., Chemical and morphological characterization of sugarcane bagasse submitted to a delignification process for enhanced enzymatic digestibility. *Biotechnol. biofuels*, 4(1), 1–19, 2011.
- Saba, N., Tahir, P.M., Jawaaid, M., A review on potentiality of nano filler/natural fiber filled polymer hybrid composites. *Polymers*, 6, 2247, 2014.
- Samir, M.A.S.A., Alloin, F., Dufresne, A., Review of recent research into cellulosic whiskers, their properties and their application in nanocomposite field. *Biomacromolecules*, 6, 612, 2005.
- Saravanan, R., Sivaraja, M., Durability studies on coir reinforced bio-composite concrete panel. *Eur. J. Sci. Res.*, 81, 220, 2012.
- Satyanarayana, K.G., Arizaga, G.G., Wypych, F., Biodegradable composites based on lignocellulosic fibers—An overview. *Prog. Polym. Sci.*, 34, 982, 2009.
- Saw, S.K., Purwar, R., Nandy, S., Ghose, J., Sarkhel, G., Fabrication, characterization, and evaluation of luffa cylindrica fiber reinforced epoxy composites. *BioResources*, 8, 4805, 2013.
- Sawpan, M. A., Mechanical performance of industrial hemp fibre reinforced polylactide and unsaturated polyester composites. PhD thesis, The University of Waikato, 2010.
- Setua, D., Shukla, M., Nigam, V., Singh, H., Mathur, G., Lignin reinforced rubber composites. *Polym. Compos.*, 21, 988, 2000.
- Shah, B.L., Matuana, L.M., Heiden, P.A., Novel coupling agents for PVC/wood-flour composites. *J. Vinyl Addit. Techn.*, 11, 160, 2005.
- Sheltami, R.M., Abdullah, I., Ahmad, I., Dufresne, A., Kargarzadeh, H., Extraction of cellulose nanocrystals from mengkuang leaves (*Pandanus tectorius*). *Carbohydr. Polym.*, 88, 772, 2012.
- Singha, A.S., Thakur, V.K., Morphological, thermal, and physicochemical characterization of surface modified pinus fibers. *Int. J. Polym. Anal. Charact.* 14, 271, 2009a.
- Singha, A.S., Thakur, V.K., Synthesis and characterizations of silane treated Grewia optiva fibers. *Int. J. Polym. Anal. Charact.* 14, 301, 2009b.
- Singha, A.S., Thakur, V.K., Physical, chemical and mechanical properties of Hibiscus sabdariffa fiber/polymer composite. *Int. J. Polym. Mater.* 58, 217, 2009c.
- Singha, A.S., Thakur, V.K., Mechanical, thermal and morphological properties of Grewia optiva fiber/polymer matrix composites. *Polym.-Plast. Technol. Eng.* 48, 201, 2009d.
- Singha, A.S., Thakur, V.K., *Grewia optiva* Fiber Reinforced Novel, Low Cost Polymer Composites. *J. Chem.* 6, 71, 2009e.
- Song, Y., Liu, J., Chen, S., Zheng, Y., Ruan, S., Bin, Y., Mechanical properties of poly (lactic acid)/hemp fiber composites prepared with a novel method. *J. Polym. Environ.*, 21, 1117, 2013.
- Spinace, M.A., Lambert, C.S., Fermoselli, K.K., De Paoli, M.-A., Characterization of lignocellulosic curaua fibres. *Carbohydr. Polym.*, 77, 47, 2009.
- Sreekala, M., Thomas, S., Effect of fibre surface modification on water-sorption characteristics of oil palm fibres. *Compos. Sci. Technol.* 63, 861, 2003.
- Šturcová, A., Davies, G.R., Eichhorn, S.J., Elastic modulus and stress-transfer properties of tunicate cellulose whiskers. *Biomacromolecules*, 6, 1055, 2005.
- Sun, J., Sun, X., Sun, R., Su, Y., Fractional extraction and structural characterization of sugarcane bagasse hemicelluloses. *Carbohydr. Polym.*, 56, 195, 2004.
- Taib, R. M., Ramarad, S., Ishak, Z.A.M., Todo, M., Properties of kenaf fiber/polylactic acid biocomposites plasticized with polyethylene glycol. *Polym. Compos.*, 31, 1213, 2010.
- Tanaka, F., Iwata, T., Estimation of the elastic modulus of cellulose crystal by molecular mechanics simulation. *Cellulose*, 13, 509, 2006.
- Tanobe, V.O., Flores-Sahagun, T.H., Amico, S.C., Muniz, G.I., Satyanarayana, K., Sponge gourd (*luffa cylindrica*) reinforced polyester composites: Preparation and properties. *Defence Sci. J.*, 64, 273, 2014.

- Terzopoulou, Z.N., Papageorgiou, G.Z., Papadopoulou, E., Athanassiadou, E., Alexopoulou, E., Bikiaris, D.N., Green composites prepared from aliphatic polyesters and bast fibers. *Ind. Crop. Prod.*, 68, 60, 2015.
- Thakur V.K., Singha A.S., KPS-initiated graft copolymerization onto modified cellulosic biofibers. *Int. J. Polym. Anal. Charact.*, 15, 485, 2010.
- Thakur V.K., Singha A.S., Thakur M.K., Green composites from natural fibers: Mechanical and chemical aging properties *Int. J. Polym. Anal. Charact.*, 17, 407, 2012.
- Thakur V.K., Thakur M.K., Processing and characterization of natural cellulose fibers/thermoset polymer composites. *Carbohydr. Polym.*, 109, 117, 2014a.
- Thakur, V.K., Thakur, M.K., Recent Advances in Graft Copolymerization and Applications of Chitosan: A Review. *ACS Sustain. Chem. Eng.* 2, 2637, 2014b.
- Thakur, V.K., Thakur, M.K., Recent trends in hydrogels based on psyllium polysaccharide: a review. *J. Clean. Prod.* 82, 1., 2014c
- Thakur, V.K., Thakur, M.K., Gupta, R.K., Graft copolymers of natural fibers for green composites. *Carbohydr. Polym.* 104, 87, 2014a.
- Thakur V.K., Thakur M.K., Gupta R.K., Review: Raw natural fiber-based polymer composites *Int. J. Polym. Anal. Charact.*, 19, 271, 2014b.
- Thakur V.K., Thakur M.K., Raghavan P., Kessler M.R., Progress in green polymer composites from lignin for multifunctional applications: A review. *ACS Sustainable Chem. Eng.*, 2, 1092, 2014c.
- Thakur, V.K., Grewell, D., Thunga, M., Kessler, M.R., Novel Composites from Eco-Friendly Soy Flour/SBS Triblock Copolymer. *Macromol. Mater. Eng.* 299, 953–958, 2014d.
- Thakur, V.K., Thunga, M., Madbouly, S.A., Kessler, M.R., PMMA-g-SOY as a sustainable novel dielectric material. *RSC Adv.* 4, 18240–18249, 2014e.
- Thakur, V.K., Kessler, M.R., Free radical induced graft copolymerization of ethyl acrylate onto SOY for multifunctional materials. *Mater. Today Commun.* 1, 34, 2014a.
- Thakur, V.K., Kessler, M.R., Synthesis and characterization of AN-g-SOY for sustainable polymer composites. *ACS Sustain. Chem. Eng.* 2, 2454, 2014b.
- Thakur, M.K., Thakur, V.K., Gupta, R.K., Pappu, A., Synthesis and Applications of Biodegradable Soy Based Graft Copolymers: A Review. *ACS Sustain. Chem. Eng.* 4, 1, 2016.
- Thielemans, W., Can, E., Morye, S., Wool, R., Novel applications of lignin in composite materials. *J. Appl. Polym. Sci.*, 83, 323, 2002.
- Tran, T.P.T., Bénézet, J.-C., Bergeret, A., Rice and Einkorn wheat husks reinforced poly (lactic acid)(PLA) biocomposites: Effects of alkaline and silane surface treatments of husks. *Ind. Crop. Prod.*, 58, 124, 2014.
- US Department of Energy, Energy efficiency and renewable energy: Advanced manufacturing office, 2015. <http://energy.gov/eere/amo/advanced-manufacturing-office>
- Van de Weyenberg, I., Truong, T.C., Vangrimde, B., Verpoest, I., Improving the properties of UD flax fibre reinforced composites by applying an alkaline fibre treatment. *Compos. Part A-Appl. S.* 37, 1368, 2006.
- Voicu, S.I., Condruz, R.M., Mitran, V., Cimpean, A., Miculescu, F., Andronescu, C., Miculescu, M., Thakur, V.K., Sericin Covalent Immobilization onto Cellulose Acetate Membrane for Biomedical Applications. *ACS Sustain. Chem. Eng.* 4, 1765, 2016.
- Wang, H., Li, D., Zhang, R., Preparation of ultralong cellulose nanofibers and optically transparent nanopapers derived from waste corrugated paper pulp. *BioResources*, 8, 1374, 2013.
- Wang, Q., Zhu, J., Gleisner, R., Kuster, T., Baxa, U., McNeil, S., Morphological development of cellulose fibrils of a bleached eucalyptus pulp by mechanical fibrillation. *Cellulose*, 19, 1631, 2012.
- Wu, H., Thakur, V.K., Kessler, M.R., Novel low-cost hybrid composites from asphaltene/SBS triblock copolymer with improved thermal and mechanical properties. *J. Mater. Sci.* 51, 2394, 2016.
- Xie, Y., Hill, C.A., Xiao, Z., Militz, H., Mai, C., Silane coupling agents used for natural fiber/polymer composites: A review. *Compos. Part A-Appl S.*, 41, 806, 2010.

- Yan, L., Chouw, N., Experimental study of flax FRP tube encased coir fibre reinforced concrete composite column. *Constr. Build. Mater.*, 40, 1118, 2013.
- Yousefi, H., Faezipour, M., Hedjazi, S., Mousavi, M.M., Azusa, Y., Heidari, A.H., Comparative study of paper and nanopaper properties prepared from bacterial cellulose nanofibers and fibers/ground cellulose nanofibers of canola straw. *Ind. Crop. Prod.*, 43, 732, 2013.
- Yu, T., Ren, J., Li, S., Yuan, H., Li, Y., Effect of fiber surface-treatments on the properties of poly (lactic acid)/ramie composites. *Compos. Part A-Appl. S.*, 41, 499, 2010.
- Yussuf, A., Massoumi, I., Hassan, A., Comparison of polylactic acid/kenaf and polylactic acid/rise husk composites: the influence of the natural fibers on the mechanical, thermal and biodegradability properties. *J. Polym. Environ.*, 18, 422, 2010.
- Zhu, J., Zhu, H., Njuguna, J., Abhyankar, H., Recent development of flax fibres and their reinforced composites based on different polymeric matrices. *Materials*, 6, 5171, 2013.

Keratin-Based Materials in Biotechnology

Hafiz M. N. Iqbal^{1,2*} and Tajalli Keshavarz^{2*}

¹*School of Engineering and Science, Tecnologico de Monterrey, Campus Monterrey, Monterrey, N.L., Mexico*

²*Applied Biotechnology Research Group, Department of Life Sciences, Faculty of Science and Technology, University of Westminster, London, United Kingdom*

Abstract

This chapter focuses on the application of keratin as a potential biomaterial candidate in biotechnology at large and composites in particular. Among the natural polymers, keratins are interesting candidates for the preparation of keratin-based composites and other products with novel characteristics in variety of bio- and non-bio-sectors. Owing to its chemical structure, natural abundance, bioactivity, renewability, non-toxicity and effectiveness as a biopolymer, keratin processes several complementary properties that positions it well in the materials sector in the modern world. In this context, utilisation of raw keratin from chicken feathers and other sources such as nails, horns, hooves, hair and wool, for the development of added-value materials-based products, is an original concept providing extensive opportunities for experimentation, interdisciplinary and/or multidisciplinary scientific research. Among these, keratin-based composites/blends, (hydro)-gels, thin films, nano- and/or micro-particles, and 3-D scaffolds are of supreme importance. To address the petroleum-based global issues, researchers have been redirecting their interests to the engineering of bio-based biomaterials for potential applications in different sectors of the modern world including cosmetics, pharmaceuticals and other biotechnological/biomedical applications. Keratin has a unique role to play in these sectors.

Keywords: Keratin, biomaterial, bio-composites, green technology, applications

11.1 Introduction

In recent years, there has been a great interest in bio-derived and/or bio-based biomaterials due to their potential as alternative polymeric materials to the traditional petroleum-based synthetic counterparts (Voicu *et al.*, 2016; Wu *et al.*, 2016). Research is underway around the world on the development of ‘greener’ technologies. In recent decades, extensive efforts have been made around the globe, by different scientists, to develop new high-performance materials-based innovative products (Iqbal *et al.*, 2014a; 2014b). The principle of ‘going green’ has directed this search towards eco-friendly materials. Words like renewability, recyclability and

*Corresponding authors: hafiz.iqbal@my.westminster.ac.uk; t.keshavarz@westminster.ac.uk

sustainability are emphasised in growing environmental awareness (Thakur *et al.*, 2016). The divergence from non-renewable to renewable materials is becoming the centre of interest for research in industrial communities around the globe. The fact is that environmental legislation is the driving force behind the development of these materials (Mohanty *et al.*, 2000). Owing to the limited or no disposal methods, ecological influence, and persistency within the ecosystem the traditional plastic-based wastes from the petroleum-based resources are considered critically (Pappu *et al.*, 2015). Moreover, the currently available petroleum-based resources are finite and becoming increasingly costly. Originally petroleum-based plastics were designed to be durable and were synthesized from petrochemical resources, mainly crude oil. The shortage of synthetic raw materials and the depletion of petroleum resources has pushed up prices in essential sectors worldwide including energy, materials, and medical (Mani & Bhattacharya, 2001). The dearth and price hike of petroleum-based synthetic materials have resulted in the strong demand for renewable resources, i.e., bio-derived and/or bio-based materials. Such materials should ease disputes on eco-pollution and reliance on fossil resources (Mani & Bhattacharya, 2001; Huda *et al.*, 2005). So focus has been shifted to polymers originating from bio-based renewable sources, which are often biocompatible and biodegradable (Plackett *et al.*, 2003). In this background, to address the growing ecological issues where petroleum-based resources are unsustainable researchers have been directing their interests to develop novel bio-based composite materials for target applications in different industries (Srubar *et al.*, 2012; Iqbal *et al.*, 2014c; 2015a). On the other hand, bio-polymers have a number of advantages over petroleum-based polymers, such as being renewable, abundant and biodegradable while also providing competitive mechanical properties.

From the last several years, there has been an increasing research interest for the development of novel materials with multifunctional characteristics, including high toughness, stiffer, lighter-weight material, specific strength, low density, and good thermo-mechanical properties, for a variety of industrial and biotechnological applications (Thakur & Thakur, 2014a-c; Thakur *et al.*, 2014a-e). To compensate the demand for better performance, extensive research has been devoted to bio-polymers and different polymer based green composites (Iqbal *et al.*, 2015b). Research is underway on the commercial development of 'greener' polymer technologies; new multifunctional materials with high performance at affordable costs. To meet the structural and design challenges, the selection of materials calls for a compromise between conflicting visions that are often non-commensurate, and any improvement in one is at conflict with the other (Ashby, 2000).

Environmental friendly, eco-efficiency and green engineering are guiding the next generation of processes and products (Markarian, 2008). Bio-based polymers are moving into the mainstream applications changing the dynamics of 21st century materials. Biopolymers, bio-based and biodegradable are the words that are becoming more important in the world of industrial plastics. These materials have not only been a dynamic factor for the research scientists from the materials-based community, but also they provide potential opportunities for improving the living standard (Nair & Laurencin, 2007). Before going into details, these words need to be distinguished with respect to their meaning. Generally speaking, a bio-based polymer is the term

used to describe a variety of materials. However, they fall into two principal categories (Christophe & Coszach, 2000).

- i. **Bio-based polymers** are produced by biological systems such as micro-organisms and/or plants. They are also called polymeric biomolecules, biological polymers, or simply biopolymers.
- ii. **Bio-derived polymers** are chemically synthesised, but their building-blocks are derived from biological monomers such as amino acids.

11.2 Biopolymers

Polymers that are produced by biological systems such as microbial organisms, plants and/or animals through metabolic-based engineering reactions are called biopolymers or simply natural polymers. Carbohydrates, keratin and polyhydroxyalkanoates (PHAs) are all counted as biopolymers (Stevens, 2001). As compared to the synthetic polymers, still, there are many issues including technical and processing that need to be addressed before the widespread use of bio-sustainable biopolymers is possible (Singha & Thakur, 2008a–c). A significant barrier to the widespread application of biopolymers in different sector is that their mechanical properties tend to compare unfavourably with existing petroleum-based polymers. For example, strength values are lower than those of the synthetic plastics so a component made from biopolymers would need to be thicker to compensate for lower mechanical properties. These shortcomings may be overcome by several means like grafting, blending and reinforcement with other suitable polymers. For example, keratin graft composites with cellulose (keratin-g-cellulose), improve or impart new characteristics including decrease fragility, increase mechanical strength and modulate the hydrophobic-hydrophilic characteristics of the pristine keratin (Iqbal *et al.*, 2015b).

11.3 Classification of Biopolymers

Polymeric materials come from a variety of sources, ranging from familiar synthetic ones (petroleum-based) such as polystyrene to natural biopolymers such as cellulose, proteins, and microbial-based polyesters that are fundamental to biological structure and function (Wollerdorfer & Bader, 1998; Pandey *et al.*, 2010). A wider spectrum of such materials has been categorised accordingly based on their derivation. However, biopolymers or bio-based polymeric materials can be classified into three main categories.

- Category 1:** Polymers that are isolated from the biomass, for example, cellulose and keratin.
- Category 2:** Polymers that are chemically synthesised using renewable bio-based monomers, for example, poly lactic acid (PLA).
- Category 3:** Polyssmers that are produced by genetically modified species, for example, PHAs.

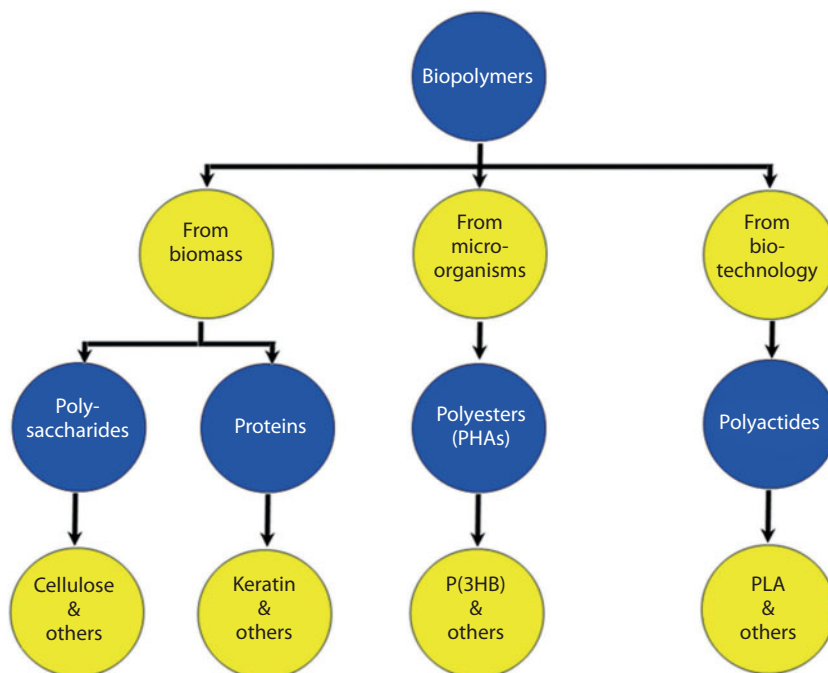


Figure 11.1 Illustrates a classical summary of biopolymers (Reproduced from Iqbal, 2015).

11.4 Occurrence and Physicochemical Properties of Keratin

The word “keratin” derives from a Greek word “kera” which means horn. From the historical point of view, in 1905, a United States patent was issued revealing a lime-based process to isolate keratin from animal hoofs (Jillian & Van Dyke, 2010). The word “keratin” first appeared in the scientific literature in 1950s. Since then many research-based methods have been developed, with the aim to extract keratin mainly using oxidative and reductive approaches (Khosa & Ullah, 2013). Initially, these technologies were applied to extract keratin from animal-based sources such as horns, hooves, chicken feathers and, finally human hairs (Jillian & Van Dyke, 2010). Owing to the structural stability due to the hydrogen bonding density, hydrophobic interactions, and disulphide bonds, the above mentioned keratin-rich sources are difficult to degrade. This is also because of the presence of polypeptide into super coiled chains which are tightly packed in α -helix (α -keratin) or β -sheet (β -keratin) (Kreplak *et al.*, 2004; Brandelli, 2008; Brandelli *et al.*, 2015). A range of compositional and structural components of keratin is shown in Figure 11.2.

In nature, chicken feather is perhaps the most abundant and easily available keratinous biopolymer (Khosa & Ullah, 2013). A typical feather is diagrammed in Figure 11.3. Globally, chicken feathers from butchery account for more than five million tons/year (Aluigi *et al.*, 2011; Ghosh & Collie, 2014). Unfortunately, this potential material is being thrown away as landfill disposal. Therefore, from the ecological and commercial point of view, it is also desirable to develop cost-effective and eco-friendly treatment methods to process such an abandoned material into value-added products (Wang & Cao, 2012).

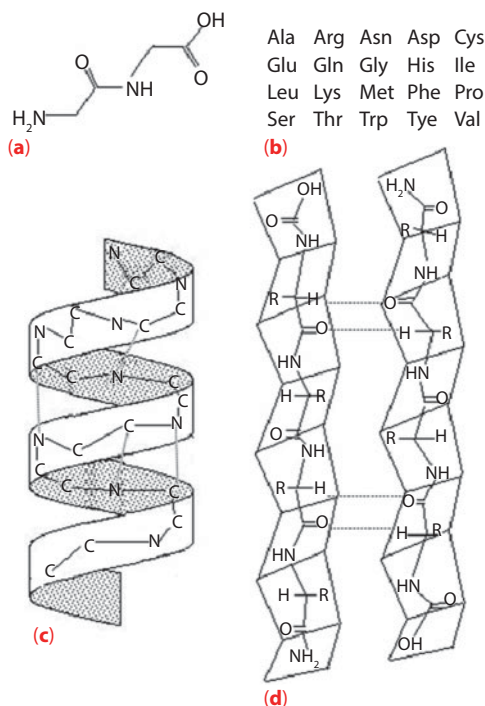


Figure 11.2 Schematic diagram of different components of cellulose and keratin; (a) polypeptide single unit; (b) amino acid sequence; (c) α -helix, and (d) β -Sheets conformations of keratin.

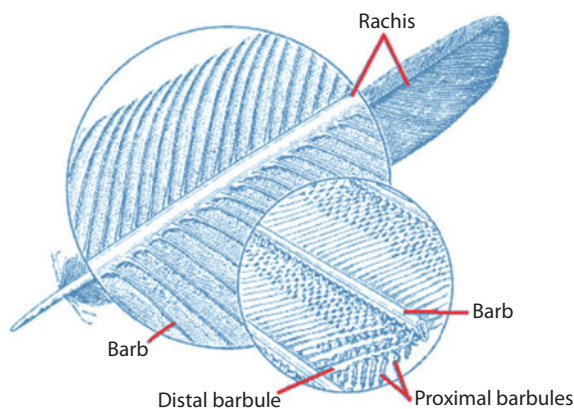


Figure 11.3 A typical feather (Reproduced from Iqbal, 2015).

From the chemistry point of view, the availability of many functional groups in the keratin structure makes it a potential candidate to react and link with other suitable materials under appropriate reaction environment. For example, di-sulphide, amino, thiol, phenolic and carboxylic are among potential functional groups. It is generally considered that under reducing reaction conditions the above mentioned functional groups, in the keratin, make its surface positive, and thus solubilisation occurs (Khosa & Ullah, 2013). Owing to its non-toxic nature, bio-degradability, bio-compatibility

and recyclability like features it is considered among versatile biopolymers that can be modified into a range of value-added products (Aluigi *et al.*, 2011; Ullah *et al.*, 2011; Khosa & Ullah, 2013). Apart from its minor usage in low grade products, the ever increasing scientific knowledge about such a resourceful material “keratin” suggests its outstanding and emerging consumption in cosmeceutical, pharmaceutical, biotechnological and biomedical applications (Brandelli, 2008; Brandelli *et al.*, 2010; 2015; Khosa & Ullah, 2013).

11.5 Keratin-based Biomaterials

Over the past few years, the growing research interests to develop keratin-based biomaterials are mainly due to the unique properties of keratin that play a critical role in the fabrication process. From the last few decades, novel physicochemical, thermo-mechanical and biological characteristics of keratin have been emerging fundamentals for biomaterials-based research institutes and industrial organisations. So far, plenty of scientific work has been done and published by several scientists on the development and characterisation of keratin and keratin-based novel products e.g., keratin-based composites/blends, (hydro)-gels, thin films, nano- and/or micro-particles, and 3-D scaffolds are of supreme importance. In many cases, the above-mentioned novel keratin-based materials are shown to possess multi-functional characteristics along with an excellent compatibility features. Recently, we have discovered novel enzyme-based methods for modulating the physicochemical, thermo-mechanical and biological characteristics of keratin to develop bio-composites with novel characteristics that pristine keratin fails to demonstrate on its own (Iqbal *et al.*, 2015b). Later on, laccase was also employed as a green catalyst to develop natural phenol grafted keratin-EC based bio-composites via surface dipping and incorporation technique. This work clearly demonstrated that the selection of various natural phenols that includes caffeic acid, gallic acid, *p*-4-hydroxybenzoic acid and thymol can uniquely determine the antibacterial potential of these newly developed novel bio-composites (Iqbal, 2015; Iqbal *et al.*, 2015a). Figure 11.4 illustrates a graphical representation of development and novel characteristics of phenol-g-keratin-EC-based bio-composites. Similarly, Verma and co-workers had reported construction, characterisation and biocompatibility of human hair-based keratin scaffolds for *in vitro* tissue engineering applications.

11.6 Bio-composites

A composite is a material that comprises two or more distinct polymers in order to obtain tailor-made characteristics or to improve or impart ideal properties (specific strength, thermal properties, surface properties, bio-compatibility, and bio-degradability) that individual counterparts fail to demonstrate on their own (Singha & Thakur, 2009a-e). Whereas, composites comprising various biologically derived phase(s) are described as bio-composites (Fowler *et al.*, 2006; Auras *et al.*, 2011). A broad definition of bio-composites is composite materials made up of natural or bio-derived polymers

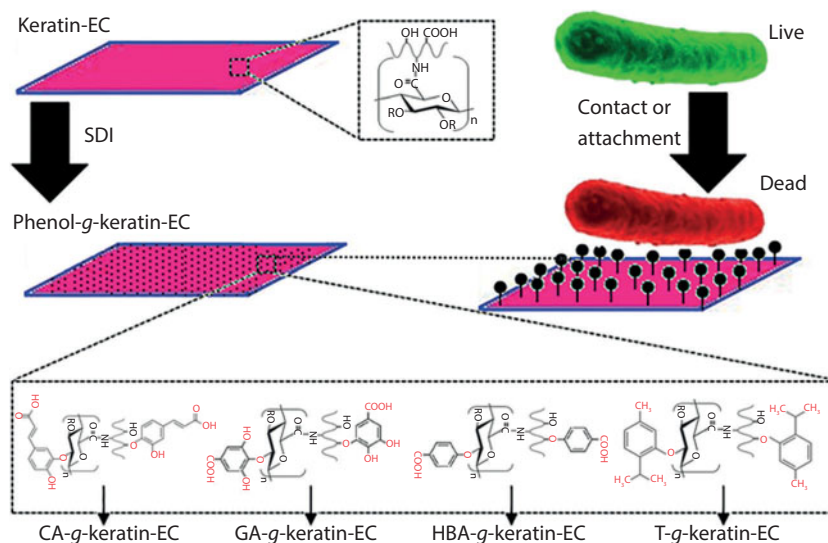


Figure 11.4 Development and novel characteristics of phenol-g-keratin-EC-based bio-composites (Reproduced from Iqbal *et al.*, 2015a).

(John & Thomas, 2008). A wider spectrum of methodological approaches has been identified to alter/modify polymers properties to make them useful for potential applications. For example, chemical-based, photochemical, plasma-induced, free radical-based and enzyme-based grafting are amongst emerging techniques (Mitomo *et al.*, 1995; Kim *et al.*, 2002; Grøndahl *et al.*, 2005; Lao *et al.*, 2007; 2010; Thakur *et al.*, 2013a; 2013b; 2014b; 2014c; Iqbal *et al.*, 2014a; 2015c; 2015d).

Fully sustainable bio-composite made up of bio/natural materials, and biodegradable polymers termed as green composites, are the centre of focus due to environmental concerns and legislations. Recently, bio-based composite materials have been engineered for target applications in different sectors such as bio-based packaging, bio-medical, pharmaceutical, textiles, paper and others (Klemm *et al.*, 2001; Grunert & Winter, 2002; Svensson *et al.*, 2005; Czaja *et al.*, 2006; Srubar *et al.*, 2012; Iqbal *et al.*, 2013; Iqbal, 2015). However, with an increasing scientific knowledge, environmental awareness, wasteful protection and de-protection steps, the use and removal of synthetically produced petroleum-based polymers or composite structures are considered more critically. Bio-based materials that are derived from renewable resources having an accepted level of recyclability and a triggered biodegradability, along with commercial and environmental viability, are described as sustainable bio-based products. It means that the materials would remain stable in their intended lifetime but would degrade after disposal in suitable environment (Iqbal *et al.*, 2015a; 2015e). The “green bio-composites” consist of biocompatible and biodegradable biopolymers (Mohanty *et al.*, 2002). Sustainability requirement is changing the dynamics of the materials industry, offering new opportunities and prospects. Innovations in the bio-plastic industry are providing new approaches which are eco-friendly and eco-efficient to alternate and/or compete the in practice and ongoing synthetic plastics. The sustainability concept is shown in Figure 11.5.

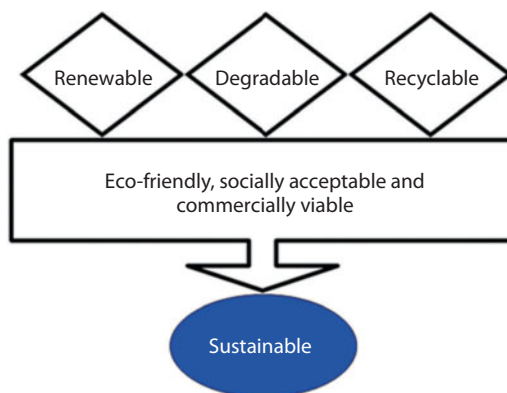


Figure 11.5 Concept of “sustainability” (Reproduced from Iqbal, 2015).

11.7 Properties of Bio-composites for Bio-medical Applications

11.7.1 Biocompatibility

A unifying property of biomaterials is biocompatibility. The ultimate goal of biocompatible materials in regenerative medicine is to assist in the reconstruction of any tissue or organ *in situ* from scratch. Such interpretation of biocompatibility may seem futuristic, but is, in fact, much closer than one would expect. Throughout the history, the idea of inserting foreign objects into the human body has developed steadily. *In vitro* cell studies are ideal extensions of biomaterials-based research as they allow direct observation of cell interaction with the test composites (Iqbal, 2015). It is generally recognised that cell interaction with a test surface is a simplification of physiological conditions that usually involves full immersion of the cell in a culture environment. Although, *in vitro* growth of cells on a surface cannot be expected to fully reflect *in vivo* responses, it is, nonetheless, a widely used approach for studying biomaterial surface effects on cell functionality (Ratner, 2004). The versatility of *in vitro* cell studies is affirmed by the vast amount of well-established techniques. Apart from the typical biochemical quantification methods, new microscopic-based techniques are emerging steadily owing to their wider coverage and depiction of cell morphology in relation to biomolecules.

It is often considered necessary to match, as much as possible, the physicochemical and mechanical characteristics of the support biomaterials surrounding tissues. Prior to the design and/or development of bio-composite biomaterials their physicochemical, mechanical, morphological, and toxicological characteristics must be evaluated carefully, and critically with regard to the biomedical-based applications. Over the past few years, substantial efforts have been made to prepare bio-composites with novel characteristics, while retraining the anticipated bulk features, with an aim to optimise both *in vitro* and *in vivo* performances. It has also been reported in literature that apart from materials chemistry, surface topography and hydrophobic/hydrophilic characteristics also have an important influence on the cell regulation, adhesion,

proliferation, alignment and orientation behaviour (Brown *et al.*, 1998; Ng & Swartz, 2003; Garcia *et al.*, 2007; Rhee & Grinnell, 2007; Iqbal, 2015). However, there are several factors, e.g., materials composition and chemistry, surface charge, and reaction conditions that need to be considered with regard to cell-matrix interactions (Iqbal *et al.*, 2015a).

As far as the use of tools and materials in medicine are concerned, owing to the emergence of novel green technologies, the benefits of carefully selected and crafted materials have been well established. Over the last 50 years, innovative devices such as joint replacements, pacemakers, lenses, cochlear implants, artificial heart valves, and blood vessels have significantly extended the lifetime and life quality of patients (Ratner, 2004). These devices are termed “implantable medical devices,” and the materials suitable for producing them are termed “biomaterials.” Although highly successful in several clinical applications, the design of such materials is far from its optimum (Whitesides, 2005). Consequently, the anticipation and inspiration for further research in biomaterials with novel characteristics intensifies. The interdisciplinary research area is more active and innovative than ever, and ranges from physics and chemistry through to molecular and cell biology and medicine.

11.7.2 Biodegradability

Biodegradation is mainly caused by the biological action of microorganisms, promoted by their complex enzyme systems and can occur under both aerobic and anaerobic environments, leading to a partial or complete removal of the target material from the environment. Moreover, towards the end of a degradation process the surface wearing off/down of the target material occurred due to the free H_2O uptake contents, followed by cracking and finally transformation to water and CO_2 . Figure 11.6 illustrates a schematic representation of various steps involved in the degradation of phenol grafted keratin-EC based bio-composite. Several researchers have examined the biodegradability of aliphatic homo- and co-polyesters-based materials under various environments such as soil, freshwater, and seawater (Rizzarelli *et al.*, 2004; Tokiwa & Calabia 2004; Lenz & Marchessault 2005; Volova *et al.*, 2010; Boyandin *et al.*, 2012; Iqbal *et al.*, 2015a).

As shown above in Figure 11.1, biodegradable polymers are mainly classified as biomass-based agro-polymers. As described earlier, in practice, most of the traditional petrochemical-based polymers are persistent in nature and thus are not biodegradable by

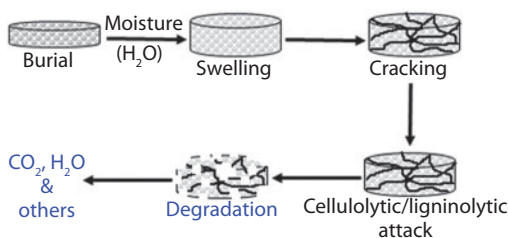


Figure 11.6 A schematic representation of proposed mechanism of soil burial degradation cycle (Reproduced from Iqbal *et al.*, 2015a).

nature. In this context, biodegradable biopolymers or bio-based polymers, contribute significantly to the sustainable development with low or no adverse ecological impact. Therefore, it is more important to consider the biodegradability features while designing and a product must be engineered from “cradle-to-cradle” approach. Moreover, the choice of the designed materials relates to the intended biotechnological and biomedical applications. In recent years, with increasing scientific knowledge and consciousness researchers are now trying to develop recyclable and degradable products from the renewable resources, which is also a part of the “going green” concept (Iqbal, 2015).

11.8 Biomedical and Biotechnological Applications

The use of biopolymers and/or their potential bio-composites such as keratin-based bio-composites for biotechnological applications has many advantages such as bio-compatibility, biodegradability, renewability, sustainability, and non-toxicity. In recent years, a wide spectrum of (bio)-polymers-based bio-composites have been engineered for target applications in both bio- and non-bio sectors of the modern world. Some of the major examples include keratin, cellulose and many others. All of the aforementioned biopolymers are characterised and well organised/developed into value-added structures, and thus can provide a proper route to emulate bio-systems — a biomimetic approach. Herein, Figure 11.7 illustrates an overview of the potential routes of biopolymers for various applications that includes both biotechnological and biomedical sectors.

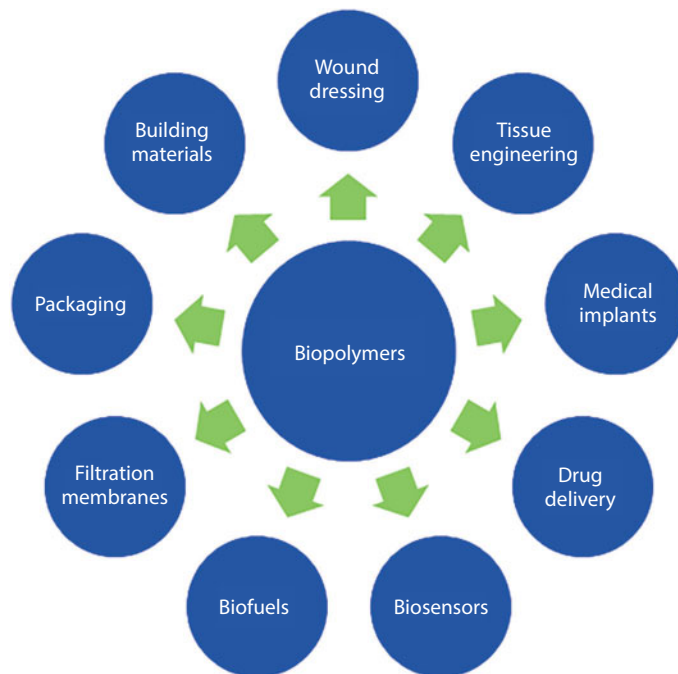


Figure 11.7 Use of biopolymers for various biomedical and biotechnological based applications.

11.9 Potential Applications

11.9.1 Wound Healing

Wound healing is an intricate process where the damaged skin needs to be repaired either by itself or through external aid. Driven by the major factors mentioned above, there is an urgent need for advanced wound care products. A superlative dressing must provide a suitable environment, to the wound surfaces, for an efficient and maximal healing rate (Iqbal, 2015). Apart from the basic covering function, in practice, dressings are being developed to facilitate infection free wound healing. Owing to scientific awareness and ever increasing demands of legislative authorities the characteristics of (i) haemostatic, (ii) absorption of exudates, (iii) provision and maintenance of a suitable environment (moisture, water and adequate gaseous exchange), (iv) functional adhesion, (v) painlessness, and (vi) cost-effectiveness have been recognised and considered more critically (Iqbal, 2015). In recent years, various medical and cosmetic applications of cellulose based bio-composites have drawn plenty of research attention in this field. Various potentials of cellulose originate from its unique properties such as strength, high liquid absorbency, biocompatibility, biodegradability and non-toxic nature. These characteristics make it an ideal option for specific demands of skin repair.

A well organised and structured composite materials can be obtained using polymers from a wider range of materials, such as cellulose and its derivatives (Kim *et al.*, 2001; Canejo *et al.*, 2008), PLA (Yang *et al.*, 2005), collagen (Buttafoco *et al.*, 2006), polyurethanes (Zhuo *et al.*, 2008), and keratin (Iqbal *et al.*, 2015a; 2015b). Another approach reported by Wang & Chen (2011) suggests a suitable method to prepare all-cellulose composites with characteristics for biomedical applications. Cellulose nanowhiskers are able to develop a porous network through their unique hydrogen bonding system with the host polymer matrix. Moreover, by analysing the controlled release of a model molecule such as bovine serum albumin from these nano-composites, these authors demonstrated their great potential as drug delivery systems, thus providing a useful option for skin tissue repair, and wound dressings. Beyond the improvement of the typical properties, composites can include additional properties, for instance, antibacterial characteristics. The incorporation of antibacterial agents such as phenols (Iqbal *et al.*, 2015a), silver nanoparticles (Son *et al.*, 2006) or polypeptides (Miao *et al.*, 2011) to kill bacterial pathogens has also been reported. Son *et al.*, (2006) have described the production of composites using cellulose acetate/silver nitrate that exhibited a strong antimicrobial activity which is necessary when considering wound dressing applications.

11.9.2 Tissue Engineering

Tissue engineering (TE) is an interdisciplinary arena that applies the principles of engineering and biological (biomedical) disciplines to develop suitable alternatives that maintain, improve, or restore biological function of a tissue (Iqbal, 2015). It has also been used in repair, regeneration, maintenance and/or enhancing the functional replacement of tissues such as skin, muscle, cartilage, bone, blood vessels etc. for clinical use (MacArthur & Oreffo, 2005). So far major developments in this multidisciplinary field have already provided substantial implementation strategies with innovative tissue

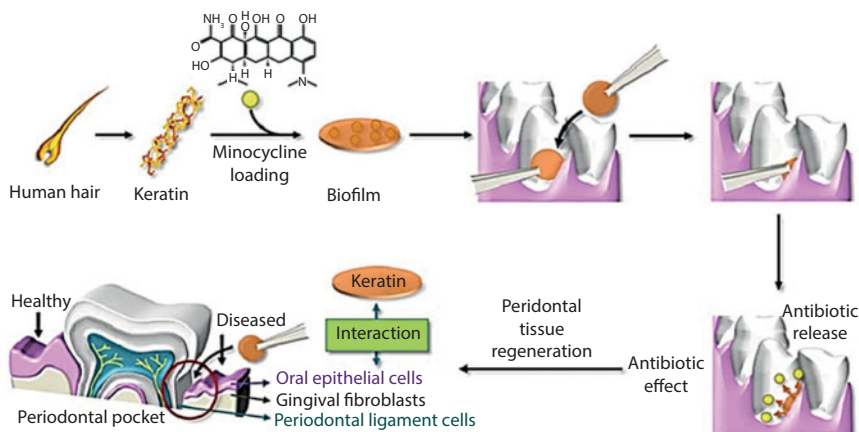


Figure 11.8 A schematic description of intrapocket antibiotic-eluting human hair keratin-based film for periodontal tissue regeneration (Reproduced from Lee *et al.*, 2015 with permission).

replacement. From the historical point of view, a detailed description about the TE history is given in the NSF report published in 2003 (Viola *et al.*, 2003).

Recent advances in the biomaterials have generated/shaped breakthrough opportunities to engineer tissues in the laboratory. Apart from biocompatibility and non-toxicity, the biodegradability of extracellular matrices is also recognised as a requisite property for TE. In recent years, substantial research efforts have been made in developing bio-materials including composites, blends, micro/nano-scale fibres and/or scaffolds etc. with novel functionalities for cell seeding, proliferation and differentiation prior to regenerate functional tissue or a whole organ. However, the final product's success strongly depends on two major factors *i.e.*, (i) cellular adhesion and (ii) cellular growth onto the target material's surface. Since the cell-surface interaction is fully understood at a cellular level, thus novel biomaterials or biomaterials-based products with new/improved functionalities can be easily developed (Kumari *et al.*, 2001).

Very recently, Lee & co-workers investigated the potent characteristics of the antibiotic loaded keratin-based biofilms for the treatment of chronic periodontitis. In the same study, they have also proposed that antibiotic eluting keratin-based biofilms are highly suitable candidates for biomedical type applications (Lee *et al.*, 2015). Figure 11.8 illustrates a schematic description of intra-pocket antibiotic-eluting keratin-based biofilm for periodontal tissue regeneration. In an earlier study, Li *et al.*, (2013) had also demonstrated the usefulness of keratin for preparing hydroxyapatite (HA)–keratin incorporated electro-spun poly(L-lactic acid) composites (Figure 11.9). This research also gave the feasibility and novel strategy to incorporate such bioactive molecules as suitable substrates for bone tissue regeneration applications.

11.9.3 Biosensors

Biosensors are sensors in which recognition processes rely on utilisation of biochemical mechanisms. They are typically comprised on two main parts *i.e.*, (i) bio-functional

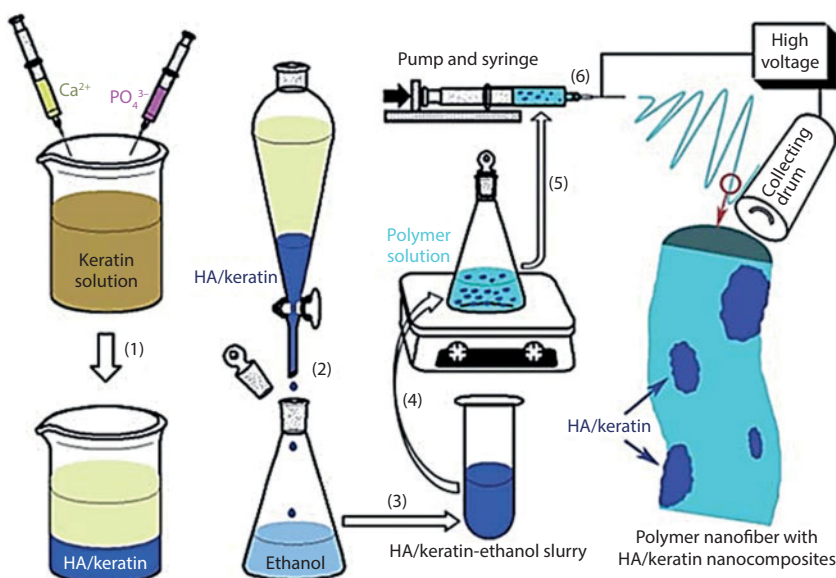


Figure 11.9 A schematic of the strategy to introduce HA-keratin nanocomposites into polymer nanofibers by the electrospinning process. (1) HA-keratin nanocomposites were synthesized by adding calcium and phosphate ions into a keratin solution; (2) HA-keratin was dispersed and washed by ethanol several times to replace water completely; (3) the HA-keratin-ethanol slurry was collected by centrifugation; (4) HA-keratin-ethanol was dispersed into the polymer solution homogeneously; (5) and (6) polymer solution was electrospun into polymer nanofibers with HA-keratin nanocomposites (Reproduced from Li *et al.*, 2013 with permission from The Royal Society of Chemistry).

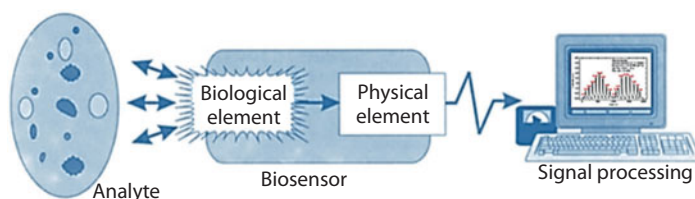


Figure 11.10 Conceptual diagram of a biosensor. The interaction of the analyte with the biological element is designed to produce an effect measured by the physical element, which converts the information into measurable values, for example electrical signals (adapted with modification from Kubik *et al.*, 2005).

membrane, also known as biological element, and responsible for sampling, and (ii) a physical element, often called transducer, and mainly responsible for the transmission of the sampling results for further processing (Vo-Dinh *et al.*, 2001; Thévenot *et al.*, 2001). A typical biosensor is diagrammed in Figure 11.10. Biosensors have been broadly used in various sectors including environmental, food, and medical. Various parameters that include response time, sensitivity, selectivity, reproducibility, and aging are strongly dependent on the characteristics of the sensing membrane and ultimately can affect the performance of a sensor. Owing to the detection criteria, particularly for gases at low concentration and some other biological substances, sensitivity is one of the critical properties.

11.10 Concluding Remarks

To date, several efforts have been made to develop novel biomaterials using pristine keratin extracted from various resources. However, there is still much left to alternate the traditional petrochemical-based materials by degradable and eco-friendly biomaterials. Therefore, in recent years, many researchers have redirected their interests in developing biomaterials with novel characteristics for targeted applications in different bio- and non-bio sectors. In this context, an effective exploitation of biotechnology and *in situ* modifications of various materials including keratin can lead to the development of eco-friendly products with new/improved multifunctional properties for potential applications in cosmeceuticals, pharmaceuticals, biotechnological and/or biomedical sectors of the modern world. Moreover, to address the challenges of green chemistry, laccase-assisted grafting processes are simple, eco-friendly and provide energy saving reactions. In addition to non-toxic nature and other benefits of laccase, its use as a biocatalyst, for grafting purposes, offer a possibility to replace the hazardous solvent-based techniques.

References

- Aluigi, A., Tonetti, C., Vineis, C., Tonin, C., Mazzuchetti, G., Adsorption of copper (II) ions by keratin/PA6 blend nanofibres. *Eur. Polym. J.*, 47, 1756–1764, 2011.
- Ashby, M. F., Multi-objective optimization in material design and selection. *Acta Mater.*, 48, 359–369, 2000.
- Auras, R. A., Lim, L. T., Selke, S. E., Tsuji, H. Eds., *Poly (lactic acid): synthesis, structures, properties, processing, and applications* (Vol. 10). John Wiley & Sons, 2011.
- Boyandin, A. N., Prudnikova, S. V., Filipenko, M. L., Khrapov, E. A., Vasil'ev, A. D., Volova, T. G., Biodegradation of polyhydroxyalkanoates by soil microbial communities of different structures and detection of PHA degrading microorganisms. *Appl. Biochem. Microbiol.*, 48(1), 28–36, 2012.
- Brandelli, A., Bacterial keratinases: useful enzymes for bioprocessing agroindustrial wastes and beyond. *Food Bioproc. Technol.*, 1, 105–116, 2008.
- Brandelli, A., Daroit, D. J., Riffel, A., Biochemical features of microbial keratinases and their production and applications. *Appl. Microbiol. Biotechnol.*, 85(6), 1735–1750, 2010.
- Brandelli, A., Sala, L., Kalil, S. J., Microbial enzymes for bioconversion of poultry waste into added-value products. *Food Research Int.*, 73, 3–12, 2015.
- Brown, R. A., Prajapati, R., McGrouther, D. A., Yannas, I. V., Eastwood, M., Tensional homeostasis in dermal fibroblasts: mechanical responses to mechanical loading in three-dimensional substrates. *J. Cell. Physiol.*, 175, 323–332, 1998.
- Buttafoco, L., Kolkman, N. G., Engbers-Buijtenhuijs, P., Poot, A. A., Dijkstra, P. J., Vermes, I., Feijen, J. Electrospinning of collagen and elastin for tissue engineering applications. *Biomater.*, 27(5), 724–734, 2006.
- Canejo, J. P., Borges, J. P., Godinho, M. H., Brogueira, P., Teixeira, P. I., Terentjev, E. M., Helical twisting of electrospun liquid crystalline cellulose micro-and nanofibers. *Adv. Mater.*, 20(24), 4821–4825, 2008.
- Christophe, J., Coszach, P., PLA: A potential solution to plastic waste dilemma. *Macromol. Symp.*, 153, 287–303, 2000.
- Czaja, W., Krystynowicz, A., Bielecki, S., Brown Jr, R. M., Microbial cellulose-the natural power to heal wounds. *Biomater.*, 27(2), 145–151, 2006.

- Fowler, P. A., Hughes, J. M., Elias, R. M., Biocomposites: technology, environmental credentials and market forces. *J. Sci. Food Agr.*, 86(12), 1781–1789, 2006.
- Garcia, Y., Collighan, R., Griffin, M., Pandit, A., Assessment of cell viability in a three-dimensional enzymatically cross-linked collagen scaffold. *J. Mater. Sci.: Mater. Med.*, 18(10), 1991–2001, 2007.
- Ghosh, A., Collie, S. R., Keratinous materials as novel absorbent systems for toxic Pollutants. *Defence Sci. J.*, 64(3), 209–221, 2014.
- Grunert, M., Winter, W.T., Nanocomposite of cellulose acetate butyrate reinforced with cellulose nanocrystals. *J. Polym. Environ.*, 10, 28–30, 2002.
- Grøndahl, L., Chandler-Temple, A., Trau, M., Polymeric grafting of acrylic acid onto poly (3-hydroxybutyrate-co-3-hydroxyvalerate): Surface functionalization for tissue engineering applications. *Biomacromol.*, 6(4), 2197–2203, 2005.
- Huda, M. S., Drzal, L. T., Misra, M., Mohanty, A. K., Williams, K., Mielewski, D. F. A study on biocomposites from recycled newspaper fiber and poly (lactic acid). *Ind. Eng. Chem. Res.*, 44(15), 5593–5601, 2005.
- Iqbal, H. M. N., Development of biocomposites with novel characteristics through enzymatic grafting. PhD Thesis, University of Westminster, London, UK, 2015.
- Iqbal, H. M. N., Kyazze, G., Keshavarz, T., Advances in the valorization of lignocellulosic materials by biotechnology: an overview. *BioRes.*, 8(2), 3157–3176, 2013.
- Iqbal, H. M. N., Kyazze, G., Locke, I. C., Tron, T., Keshavarz, T. Development of bio-composites with novel characteristics: Evaluation of phenol-induced antibacterial, biocompatible and biodegradable behaviours. *Carbohydr. Polym.*, 131, 197–207, 2015c.
- Iqbal, H. M. N., Kyazze, G., Locke, I. C., Tron, T., Keshavarz, T. Poly (3-hydroxybutyrate)-ethyl cellulose based bio-composites with novel characteristics for infection free wound healing application. *Int. J. Biological. Macromol.*, 81, 552–559, 2015d.
- Iqbal, H. M. N., Kyazze, G., Locke, I. C., Tron, T., Keshavarz, T., *In-situ* development of self-defensive antibacterial biomaterials: phenol-g-keratin-EC based bio-composites with characteristics for biomedical applications. *Green Chem.*, 17, 3858–3869, 2015a.
- Iqbal, H. M. N., Kyazze, G., Locke, I. C., Tron, T., Keshavarz, T. Development of novel antibacterial active, HaCaT biocompatible and biodegradable CA-g-P(3HB)-EC biocomposites with caffeic acid as a functional entity. *eXPRESS Polym. Lett.*, 9, 764–772, 2015e.
- Iqbal, H. M. N., Kyazze, G., Tron, T., Keshavarz, T., “One-pot” synthesis and characterisation of novel P (3HB)–ethyl cellulose based graft composites through lipase catalysed esterification. *Polym. Chem.*, 5(24), 7004–7012, 2014a.
- Iqbal, H. M. N., Kyazze, G., Tron, T., Keshavarz, T., A preliminary study on the development and characterisation of enzymatically grafted P (3HB)-ethyl cellulose based novel composites. *Cellulose.*, 21(5), 3613–3621, 2014b.
- Iqbal, H. M. N., Kyazze, G., Tron, T., Keshavarz, T., Laccase-assisted grafting of poly (3-hydroxybutyrate) onto the bacterial cellulose as backbone polymer: Development and characterisation. *Carbohydr. Polym.*, 113, 131–137, 2014c.
- Iqbal, H. M. N., Kyazze, G., Tron, T., Keshavarz, T., Laccase-assisted approach to graft multifunctional materials of interest: keratin-EC based novel composites and their characterisation. *Macromol. Mater. Eng.*, 300, 712–720, 2015b.
- Jillian, G. R. M., Van Dyke, M. E., A review of keratin-based biomaterials for biomedical applications. *Materials*, 3, 999–1014, 2010.
- John, M. J., Thomas, S., Biofibres and biocomposites. *Carbohydr. Polym.*, 71, 343–364, 2008.
- Khosa, M. A., Ullah, A. A sustainable role of keratin biopolymer in green chemistry: a review. *J. Food Proc. Beverages.*, 1(1), 8, 2013.
- Kim, H. S., Waksman, R., Cottin, Y., Kollum, M., Bhargava, B., Mehran, R., Mintz, G. S., Edge stenosis and geographical miss following intracoronary gamma radiation therapy for in-stent restenosis. *J. Am. College Cardiol.*, 37(4), 1026–1030, 2001.

- Kim, H. W., Chung, C. W., Kim, S. S., Kim, Y. B., Rhee, Y. H., Preparation and cell compatibility of acrylamide-grafted poly(3-hydroxyoctanoate). *Int. J. Biol. Macromol.*, 30(2), 129–135, 2002.
- Klemm, D., Schumann, D., Udhardt, U., Marsch, S., Bacterial synthesized cellulose—artificial blood vessels for microsurgery. *Prog. Polym. Sci.*, 26(9), 1561–1603, 2001.
- Kreplak, L., Doucet, J., Dumas, P., Briki, F., New aspects of the α -helix to β -sheet transition in stretched hard α -keratin fibers. *Biophys. J.*, 87(1), 640–647, 2004.
- Kumari, T. V., Vasudev, U., Kumar, A., Menon, B. Cell surface interactions in the study of biocompatibility. *Trends Biomater. Artificial Org.*, 15, 37–41, 2001.
- Lao, H. K., Renard, E., Langlois, V., Vallée-Rehel, K., Linossier, I., Surface functionalization of PHBV by HEMA grafting via UV treatment: Comparison with thermal free radical polymerization. *J. Appl. Polym. Sci.*, 116(1), 288–297, 2010.
- Lao, H. K., Renard, E., Linossier, I., Langlois, V., Vallée-Rehel, K., Modification of poly(3-hydroxybutyrate-co-3-hydroxyvalerate) film by chemical graft copolymerization. *Biomacromol.*, 8(2), 416–423, 2007.
- Lee, H., Hwang, Y. S., Lee, H. S., Choi, S., Kim, S. Y., Moon, J. H., Bae, H., Human hair keratin-based biofilm for potent application to periodontal tissue regeneration. *Macromol. Res.*, 23(3), 300–308, 2015.
- Lenz, R. W., Marchessault, R. H., Bacterial polyesters: biosynthesis, biodegradable plastics and biotechnology. *Biomacromol.*, 6(1), 1–8, 2005.
- Li, J. S., Li, Y., Liu, X., Zhang, J., Zhang, Y., Strategy to introduce an hydroxyapatite–keratin nanocomposite into a fibrous membrane for bone tissue engineering. *J. Mater. Chem. B.*, 1(4), 432–437, 2013.
- MacArthur, B. D. Oreffo, R. O., Bridging the gap. *Nature*, 433, 19, 2005.
- Mani, R., Bhattacharya, M., Properties of injection moulded blends of starch and modified biodegradable polyesters. *Eur. Polym. J.*, 37(3), 515–526, 2001.
- Markarian, J., Biopolymers present new market opportunities for additives in packaging. *Plastics, Add. Compound.*, 10(3), 22–25, 2008.
- Miao, J., Pangule, R. C., Paskaleva, E. E., Hwang, E. E., Kane, R. S., Linhardt, R. J., Dordick, J. S., Lysostaphin-functionalized cellulose fibers with antistaphylococcal activity for wound healing applications. *Biomater.*, 32(36), 9557–9567, 2011.
- Mitomo, H., Watanabe, Y., Yoshii, F., Makuuchi, K., Radiation effect on polyesters. *Radiation Phy. Chem.*, 46(2), 233–238, 1995.
- Mohanty, A. K., Misra, M., Hinrichsen, G., Biofibres, biodegradable polymers and biocomposites: an overview. *Macromol. Mater. Eng.*, 276(1), 1–24, 2000.
- Nair, L. S., Laurencin, C. T., Biodegradable polymers as biomaterials. *Prog. Polym. Sci.*, 32(8), 762–798, 2007.
- Ng, C. P., & Swartz, M. A., Fibroblast alignment under interstitial fluid flow using a novel 3-D tissue culture model. *Am. J. Physiology-Heart Circul. Physiol.*, 284(5), H1771–H1777, 2003.
- Pandey, J. K., Ahn, S. H., Lee, C. S., Mohanty, A. K., Misra, M., Recent advances in the application of natural fiber based composites. *Macromol. Mater. Eng.*, 295(11), 975–989, 2010.
- Pappu, A., Patil, V., Jain, S., Mahindrakar, A., Haque, R., Thakur, V. K. Advances in industrial prospective of cellulosic macromolecules enriched banana biofibre resources: A Review. *Int. J. Biol. Macromol.*, 79, 449–458, 2015.
- Plackett, D., Andersen, T. L., Pedersen, W. B., Nielsen, L., Biodegradable composites based on L-poly lactide and jute fibres. *Comp. Sci. Technol.*, 63(9), 1287–1296, 2003.
- Ratner, B. D., Hoffman, A. S., Schoen, F. J., Lemons, J. E., *Biomaterials science: an introduction to materials in medicine*. Academic press, 2004.
- Rhee, S., Grinnell, F., Fibroblast mechanics in 3D collagen matrices. *Adv. Drug Delivery Rev.*, 59(13), 1299–1305, 2007.

- Rizzarelli, P., Puglisi, C., Montaudo, G., Soil burial and enzymatic degradation in solution of aliphatic co-polyesters. *Polym. Degrad. Stab.*, 85(2), 855–863, 2004.
- Singha, A.S., Thakur, V.K., Synthesis and Characterization of Pine Needles Reinforced RF Matrix Based Biocomposites. *J. Chem.* 5, 1055–1062, 2008a.
- Singha, A.S., Thakur, V.K., Mechanical, Morphological and Thermal Properties of Pine Needle-Reinforced Polymer Composites. *Int. J. Polym. Mater.* 58, 21–31, 2008b.
- Singha, A.S., Thakur, V.K., Synthesis and characterization of Grewia optiva fiber-reinforced PF-based composites. *Int. J. Polym. Mater.* 57, 1059–1074, 2008c.
- Singha, A.S., Thakur, V.K., Synthesis and characterizations of silane treated Grewia optiva fibers. *Int. J. Polym. Anal. Character.* 14, 301–321, 2009a.
- Singha, A.S., Thakur, V.K., Morphological, thermal, and physicochemical characterization of surface modified pinus fibers. *Int. J. Polym. Anal. Character.* 14, 271–289, 2009b.
- Singha, A.S., Thakur, V.K., Fabrication and characterization of S. ciliare fibre reinforced polymer composites. *Bull. Mater. Sci.* 32, 49–58, 2009c.
- Singha, A.S., Thakur, V.K., Study of mechanical properties of urea-formaldehyde thermosets reinforced by pine needle powder. *BioResources* 4, 292–308, 2009d.
- Singha, A.S., Thakur, V.K., Chemical resistance, mechanical and physical properties of biofibers-based polymer composites. *Polym.-Plast. Technol. Eng.* 48, 736–744, 2009e.
- Son, W. K., Youk, J. H., Park, W. H., Antimicrobial cellulose acetate nanofibers containing silver nanoparticles. *Carbohydr. Polym.*, 65(4), 430–434, 2006.
- Srubar, W. V., Pilla, S., Wright, Z. C., Ryan, C. A., Greene, J. P., Frank, C. W., Billington, S. L., Mechanisms and impact of fiber–matrix compatibilization techniques on the material characterization of PHBV/oak wood flour engineered biobased composites. *Composit. Sci. Technol.*, 72(6), 708–715, 2012.
- Stevens, M. M., Biomaterials for bone tissue engineering. *Mater. Today*, 11(5), 18–25, 2008.
- Svensson, A., Nicklasson, E., Harrah, T., Panilaitis, B., Kaplan, D. L., Brittberg, M., Gatenholm, P., Bacterial cellulose as a potential scaffold for tissue engineering of cartilage. *Biomater.*, 26(4), 419–431, 2005.
- Thakur, V. K., Thakur, M. K. Processing and characterization of natural cellulose fibers/thermoset polymer composites. *Carbohydr. Polym.*, 109, 102–117, 2014a.
- Thakur, V.K., Thakur, M.K., Recent trends in hydrogels based on psyllium polysaccharide: a review. *J. Clean. Prod.* 82, 1–15, 2014b.
- Thakur, V.K., Thakur, M.K., Recent Advances in Graft Copolymerization and Applications of Chitosan: A Review. *ACS Sustain. Chem. Eng.* 2, 2637–2652, 2014bc.
- Thakur, V. K., Thakur, M. K., Gupta, R. K. Graft copolymers from natural polymers using free radical polymerization. *Int. J. Polym. Anal. Character.*, 18(7), 495–503, 2013a.
- Thakur, V. K., Thakur, M. K., Gupta, R. K. Synthesis of lignocellulosic polymer with improved chemical resistance through free radical polymerization. *Int. J. Biol. Macromol.*, 61, 121–126, 2013b.
- Thakur, V. K., Thakur, M. K., Gupta, R. K. Review: raw natural fiber-based polymer composites. *Int. J. Polym. Anal. Character.*, 19(3), 256–271, 2014a.
- Thakur, M. K., Gupta, R. K., Thakur, V. K. Surface modification of cellulose using silane coupling agent. *Carbohydr. Polym.*, 111, 849–855, 2014b.
- Thakur, V. K., Thakur, M. K., Gupta, R. K. Graft copolymers of natural fibers for green composites. *Carbohydr. Polym.*, 104, 87–93, 2014c.
- Thakur, V.K., Grewell, D., Thunga, M., Kessler, M.R., Novel Composites from Eco-Friendly Soy Flour/SBS Triblock Copolymer. *Macromol. Mater. Eng.* 299, 953–958, 2014d.
- Thakur, V.K., Thunga, M., Madbouly, S.A., Kessler, M.R., PMMA-g-SOY as a sustainable novel dielectric material. *RSC Adv.* 4, 18240–18249, 2014e.

- Thakur, M.K., Thakur, V.K., Gupta, R.K., Pappu, A., Synthesis and Applications of Biodegradable Soy Based Graft Copolymers: A Review. *ACS Sustain. Chem. Eng.* 4, 1–17, 2016.
- Thévenot, D. R., Toth, K., Durst, R. A., Wilson, G. S., Electrochemical biosensors: recommended definitions and classification. *Biosens. Bioelect.*, 16(1), 121–131, 2001.
- Tokiwa, Y., Calabia, B. P., Review degradation of microbial polyesters. *Biotechnol. Lett.*, 26(15), 1181–1189, 2004.
- Ullah, A., Wu, J., Feather fiber-based thermoplastics: effects of different plasticizers on material properties. *Macromol. Mater. Eng.*, 298(2), 153–162, 2013.
- Wang, Y. X., Cao, X. J., Extracting keratin from chicken feathers by using a hydrophobic ionic liquid. *Proc. Biochem.*, 47(5), 896–899, 2012.
- Wang, Y., Chen, L., Impacts of nanowhisker on formation kinetics and properties of all-cellulose composite gels. *Carbohydr. Polym.*, 83, 1937–1946, 2011.
- Whitesides, G. M., Nanoscience, nanotechnology, and chemistry. *Small*, 1(2), 172–179, 2005.
- Viola, J., Lal, B., Grad, O., The emergence of tissue engineering as a research field. *National Science Foundation, Arlington, VA*, 2003.
- Vo-Dinh, T., Cullum, B. M., Stokes, D. L., Nanosensors and biochips: frontiers in biomolecular diagnostics. *Sens. Actuators B: Chem.*, 74(1), 2–11, 2001.
- Wollerdorfer, M., Bader, H., Influence of natural fibres on the mechanical properties of biodegradable polymers. *Ind. Crop. Prod.*, 8(2), 105–112, 1998.
- Volova, T. G., Boyandin, A. N., Vasiliev, A. D., Karpov, V. A., Prudnikova, S. V., Mishukova, O. V., Gitelson, I. I., Biodegradation of polyhydroxyalkanoates (PHAs) in tropical coastal waters and identification of PHA-degrading bacteria. *Polym. Degrad. Stab.*, 95(12), 2350–2359, 2010.
- Voicu, S.I., Condruz, R.M., Mitran, V., Cimpean, A., Miculescu, F., Andronescu, C., Miculescu, M., Thakur, V.K., Sericin Covalent Immobilization onto Cellulose Acetate Membrane for Biomedical Applications. *ACS Sustain. Chem. Eng.* 4, 1765–1774, 2016.
- Wu, H., Thakur, V.K., Kessler, M.R., Novel low-cost hybrid composites from asphaltene/SBS tri-block copolymer with improved thermal and mechanical properties. *J. Mater. Sci.* 51, 2394–2403, 2016.
- Yang, F., Murugan, R., Wang, S., Ramakrishna, S., Electrospinning of nano/micro scale poly (L-lactic acid) aligned fibers and their potential in neural tissue engineering. *Biomater.*, 26(15), 2603–2610, 2005.
- Zhuo, H., Hu, J., Chen, S., Yeung, L., Preparation of polyurethane nanofibers by electrospinning. *J. Appl. Polym. Sci.*, 109(1), 406–411, 2008.

Pineapple Leaf Fiber: A High Potential Reinforcement for Green Rubber and Plastic Composites

Taweechai Amornsakchai

*Center of Sustainable Energy and Green Materials, Faculty of Science, Mahidol University,
Phuttamonthon Nakhon Pathom, Thailand*

*Center of Excellence for Innovation in Chemistry, Faculty of Science, Mahidol University,
Phuttamonthon Thailand*

*Polymer Science and Technology Program, Department of Chemistry, Faculty of Science, Mahidol
University, Phuttamonthon Thailand*

Abstract

Pineapple is grown worldwide and after every second or third fruit, the field is “knocked down,” and a new growing cycle begins. The residues left in the field are pineapple leaves and stems. Pineapple leaves are sources of high quality natural fiber which has long been used in crafts and textile but are still left underutilized. Considering the present situation, its availability and mechanical properties, pineapple leaf fiber (PALF) has many potential applications. Recently our research group has developed a method to extract short and fine PALF from leaf waste. PALF was used to reinforce different types of rubbers to produce rubber composites with very high stretching stress at low elongations. Rubber reinforcements using hybrid or combination of PALF/silica and PALF/carbon black were also studied and very promising results were obtained. For plastic reinforcement, both PALF and non-fibrous material (NFM) were tested on polypropylene in order to fully utilize the leaf waste. The use of PALF and NFM also offers a new way to ‘greening’ plastic composites for performance and cost effectiveness. In the last part, it is shown that nonwoven mats made from either whole ground pineapple leaves or PALF can be used as reinforcements for unsaturated polyester and acrylic resin.

Keywords: Plant fibers, lignocellulosic fibers, biocomposites, green composites, hybridization, mechanical properties, reinforced rubbers, reinforced plastics

12.1 Introduction

Natural fibers have been an important part of human life since very long ago. They have been largely replaced by synthetic fibers in modern society (Singha & Thakur, 2008a–e). However, over the past decades, the problems of climate changes and other

Corresponding author: taweechai.amo@mahidol.ac.th

Vijay Kumar Thakur, Manju Kumari Thakur and Michael R. Kessler (eds.), Handbook of Composites from Renewable Materials, (289–308) © 2017 Scrivener Publishing LLC

environmental problems, resources depletion and high oil prices have driven every industry and society to move toward greener low carbon and more sustainable society (Thakur *et al.*, 2014a–e). One of the many possible solutions is to use naturally abundant cellulosic fibers. These fibers have been studied and also put into real applications especially as reinforcement for composites in the automotive industry. There are numerous studies (see for examples: Singha & Thakur, 2008; Thakur & Singha, 2010; Thakur *et al.*, 2012) and excellent reviews (Bledzki & Gassan, 1999; Faruk *et al.*, 2012; Koronis *et al.*, 2013; Thakur & Thakur, 2014a–c; Pappu *et al.*, 2015; Pickering *et al.*, 2015) that deal with the use of natural fibers in polymer matrix composites. There are several advantages of using natural fibers when compared with glass fiber (Wambua *et al.*, 2003; Joshi *et al.*, 2004; Pickering *et al.*, 2015). Natural fiber composites are also regarded as carbon storage or carbon sink (Pervaiz & Sain, 2003). Although natural fibers have some disadvantages such as poor adhesion to matrix, high moisture adsorption and low upper processing temperatures, which limit the choice of matrices, studies have shown that some of these can be modified or improved (Bledzki & Gassan, 1999; Faruk *et al.*, 2012; Koronis *et al.*, 2013; Pickering *et al.*, 2015; Thakur & Singha, 2010b; Thakur *et al.*, 2012b; Thakur *et al.*, 2013).

There are so many different types of natural fibers that have been studied as seen in the above reviews. These fibers may be obtained from plants that grow naturally or purposely cultivated for the fibers. In addition, natural fibers can be obtained from agricultural wastes. Examples of the latter are pineapple leaf, banana, coir and bagasse. Considering land use, energy input and carbon footprint for the production of the fiber, it can be easily envisaged that agricultural wastes are the most suitable sources. With further consideration of availability and mechanical properties of the fibers, it will become clear later that pineapple leaf waste is very attractive and should be given much more attention. Thus, this chapter is devoted to the pineapple leaf fiber.

Pineapple is one of the most common fruits with worldwide annual production of about 25 million metric tons on approximately 1 million Hectare (FAO stat, 2013). Pineapples are grown mostly in Latin America and Asia. It is an important crop for many countries such as Thailand, Brazil, The Philippines, Costa Rica, Indonesia and China. The pineapple plant belongs to *Ananas* genus and is an herbaceous perennial. The plant has a short, stout stem and a rosette of waxy, strap-like leaves. The height and spread can vary but are in the range of two and a half to five feet and three to four feet, respectively. There are 30–40 leaves per plant and this could weigh up to 1.0–1.5 kg.

Despite being perennial, commercial growers do have different practices in the cultivation. Generally, after every second or third fruit or even the first fruit in some places, depending on grower practice, the field is “knocked down,” and a new growing cycle begins. The residues left in the field are pineapple leaves and stems. Figure 12.1 displays a typical pineapple field in Uthai Thani province, Central Thailand and the way farmer manages their pineapple field after the fruits were harvested and the field is ready for the knocked down. Mature suckers are cut, pruned and kept for sell or planting. The rest in the field are chopped down and sun-dried before tillage to start the next planting. In part, this provides organic matter to the soil but there are also chances that the chopped leaves will be rotten and produce methane.

It is known for a long time that pineapple leaves are sources of high quality natural fiber and have long been used for many different types of crafts. Table 12.1 compares



Figure 12.1 A typical pineapple field in Uthai Thani province, Central Thailand (top); After the last crop, farmer retrieves mature suckers, prunes and keeps them for planting (middle); The rest of the field are chopped down and sun-dried (bottom).

Table 12.1 Properties of some natural fibers and some synthetic fibers (Satyanaraya *et al.*, 1982; Susheel *et al.*, 2009).

Fibers	Density (g/cm ³)	Young's modulus (GPa)	Tensile strength (MPa)	Elongation at break (%)
Ramie	1.5	61.4–128	400–938	1.2–3.8
PALF	1.44	34.5–82.5	413–1627	1.6
Flax	1.5–3	27.6	450–1100	2.7–3.2
Jute	1.3–1.45	13–26.5	393–773	7–8
Hemp	–	–	690	1.6
Sisal	1.45	9.4–22	468–640	3–7
Cotton	1.5–1.6	5.5–12.6	287–800	7–8
Coir	1.15	4–6	131–175	15–40
E-glass	2.5	70	2000–3500	2.5
S-glass	2.5	86	4570	2.8
Aramid	1.4	63–67	3000–3150	3.3–3.7
Carbon	1.7	230–240	4000	1.4–1.8

mechanical properties of PALF with other natural fibers and some synthetic fibers. It is seen that modulus and strength of PALF are relatively high and compare very well with glass fiber in terms of specific properties. However, it should be noted that variations in the reported modulus and strength of PALF do exist (Mukherjee & Satyanarayana, 1986; Nabi Saheb & Jog, 1999). PALF properties also depend on the plant varieties (Sena Neto *et al.*, 2013). Over the past recent years, there have been many attempts in using the fiber as reinforcement in polymer matrix composites. There are several reviews on the topic (Asim *et al.*, 2015; Mishra *et al.*, 2004; Sapuan *et al.*, 2011). Other use such as fiber substitution for paper making industry has also been reported (Laftah & Abdul Rahaman, 2015). However, pineapple leaf waste is still left underutilized.

So far there have been many reviews on the use of pineapple leaf fiber (PALF) in polymer matrix composites (Asim *et al.*, 2015; Mishra *et al.*, 2004; Sapuan *et al.*, 2011). All of these reviews were based on PALF obtained with conventional methods. This will not be repeated here. Rather the recently developed method of fiber extraction would be presented and this would complement the already available reviews. In addition, the utilization of this new type of PALF as reinforcement in polymer matrix composites would be presented.

12.2 Structure of Pineapple Leaf and Pineapple Leaf Fiber

Cross-section of pineapple leaf is shown in Figure 12.2. In addition to fiber bundle which is of interest to us, the leaf also consists of an epidermis, palisade parenchyma and spongy mesophyll (Abdul Khalil *et al.*, 2006). Fibers can be found both in vascular tissue (fibrovascular bundles) (A) and mesophyll (mesophyll fiber bundles) (B). High magnification images show that both types of fiber have similar appearance, i.e., varying size and shape and thick wall. Elementary fiber has average diameter of approximately 4–5 μm . Fiber wall consists of primary wall and three sub-layers (Abdul Khalil *et al.*, 2006).

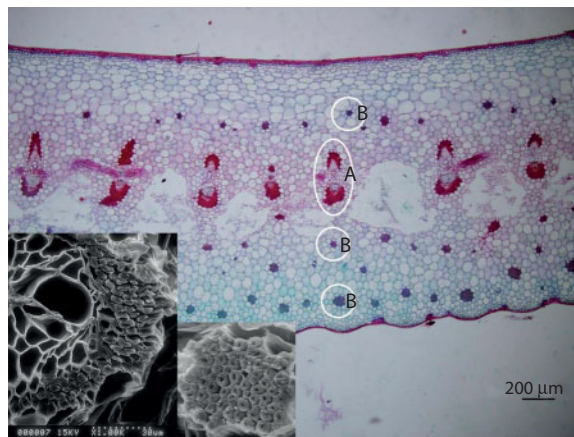


Figure 12.2 Optical micrograph of transverse section of pineapple leaf showing fibrovascular bundles (A) and mesophyll fiber bundles (B). High magnification images of regions A and B obtained with a scanning electron microscope are shown at lower left corner.

12.3 Conventional Methods of Fiber Extraction

Conventional methods for fiber extraction are hand (manual) scraping, water retting and machine decortication. These methods provide long fibers used mainly for hand craft and textile applications. Brief description of each method is given below.

12.3.1 Hand Scraping

Hand scraping is the most primitive method for the extraction of pineapple leaf fiber. Hard objects like broken ceramic plate, coconut shell, seashells or metal are used to scrape away the soft tissue to expose clean fiber. The fiber is then washed and dried. This method is slow, inefficient and laborious. It is still in use mostly for handcraft textile.

12.3.2 Water Retting

This method employs the activity of micro-organisms and water to dissolve or eat away the soft tissues surrounding fiber bundles in the leaves. The waxy cover of the leaves is scratched (by hand or machine) or crushed to produce several breaks for easy access of retting microbes. Chemicals may be added to speed up the process (Banik *et al.*, 2011). After a certain period of time, fiber can be easily separated, washed and dried.

12.3.3 Machine Decortication

To speed up the fiber production, a machine was developed. Many different designs of decorticating machine or simply decorticator have been developed. (See for example Reeves, 1949; Waldo, 1956). These machines were primarily invented and used for other fiber bearing plants such as sisal, abaca and hemp but can be modified to suit pineapple leaves. The essential part of the machine consists of a drum or roller with a number of rigid blades equally spaced on the periphery of the drum. The drum is rotated at high speed with its blades moving pass a fixed back plate to simulate the action of scraping and shearing action of manual scraping. This is called wiper drum. In certain designs, two pairs of rollers running at different tangential velocities are used for the purpose (Almassy, 1962). Since pineapple leaf fiber industry is rather small compared to that of sisal, only small decorticating machine was developed and the most popular type have only a small rotating drum. The diagram of the operation principle is shown in Figure 12.3.

12.4 The Novel Mechanical Grinding Method

There are several problems with conventional fiber extraction methods if pineapple leaf waste is going to be used in large scale. Only long, mature and undamaged straight leaves can be used with a decorticating machine. Thus a new concept that can accept all types of leaves is needed. Recently a novel and simple mechanical grinding method for fiber extraction has been introduced. The method is suitable for producing short and fine fiber for plastic and rubber reinforcements.

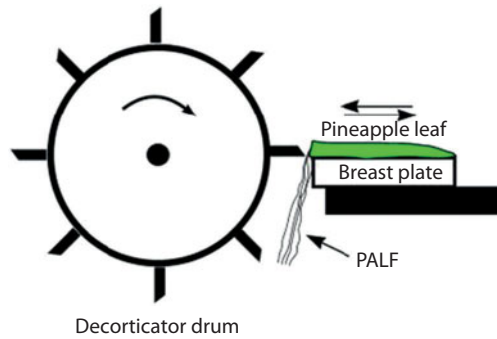


Figure 12.3 Operation principle of a decortivating machine.

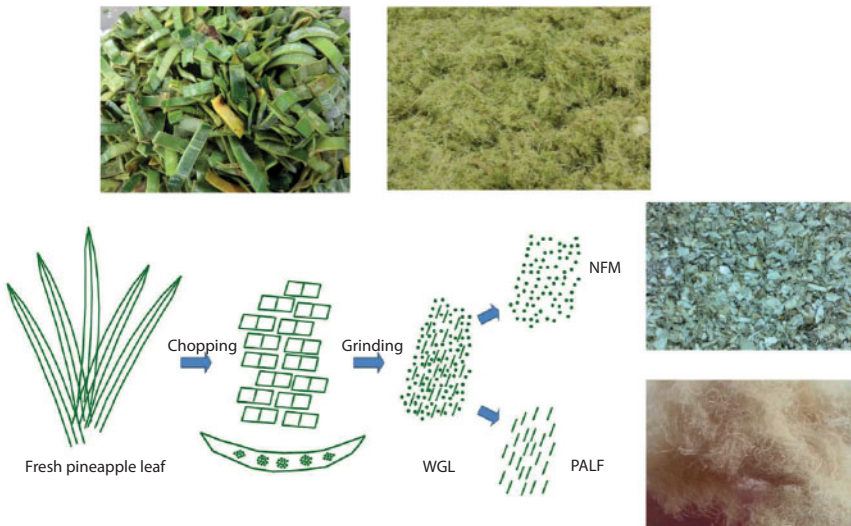


Figure 12.4 Schematic diagram of the new process for short PALF production.

12.4.1 Process Description

Fresh pineapple leaves are cut or chopped across their length to a fixed length of approximately 6 mm. These are then ground with suitable grinding machine such as a disk mill or a stone grinder. Soft tissue would be ground into paste while fiber bundles would be broken into finer fibers with the same starting length. The paste is then dried. The dried loose clumps, which may be called whole ground leaves (WGL), are then broken into loose particles and sieved to separate out the fiber. Generally, PALF would tangle and form loose wool-like structure on the sieve. Non-fibrous material (NFM), being rather particulate in shape, is going through the sieve.

Alternatively, WGL, while still wet, can be pressed into a mat or sheet-like form. The mat is then dried to give WGL nonwoven mat. Similar mat can be made from PALF which is called PALF nonwoven mat. NFM, being particulate, cannot form a mat on its own.

Figure 12.4 displays diagram of the process and different types of products made from pineapple leaf waste, respectively. Figure 12.5 displays the photographs of different



Figure 12.5 Loose PALF (top); nonwoven mat (middle); close-up appearance of nonwoven mats of PALF (bottom left) and WGL (bottom right).

types of the products that can be made according to this novel method, i.e., loose PALF, nonwoven mats of WGL and PALF.

It should be emphasized again that the grinding method could accept all types of leaves including pineapple crown provided they are neither rotten nor too dry. It has been shown that PALF obtained from grinding of dried leaves does not give as good reinforcement as that obtained from fresh leaves (Kengkhetkit & Amornsakchai, 2012).

12.4.2 Characteristic of PALF and By-product

PALF is a composite in itself. It is a bundle with a number of elementary fibers bound together with hemicellulose and lignin. PALF obtained with conventional methods are large fiber bundles. Figure 12.6 displays a broken end of hand scraped PALF. The bundle is seen to be composed of many small elementary fibers of about 3 microns. To demonstrate this point, cut end of hand scraped PALF is washed with 10% NaOH solution. The elementary fibers can now be seen more clearly (Figure 12.6, right).

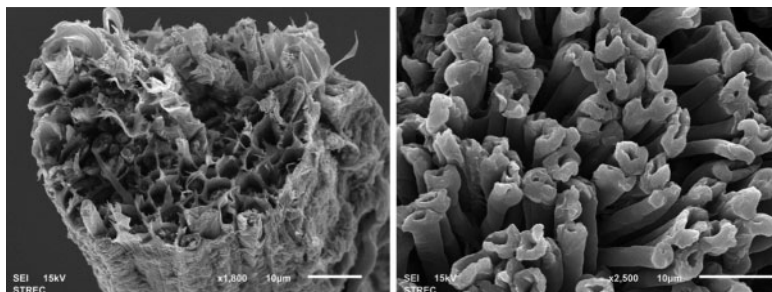


Figure 12.6 Broken end of hand scraped PALF (left) and end of hand scraped PALF after being washed with 10% NaOH solution (right).

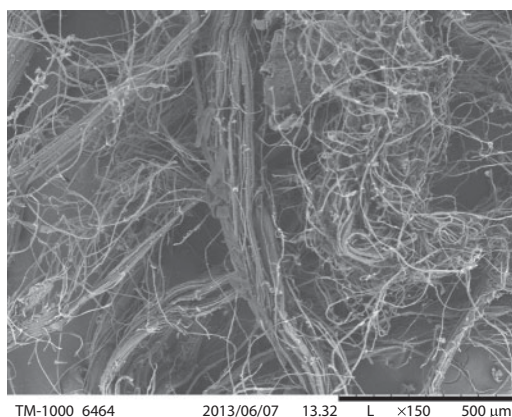


Figure 12.7 Scanning electron micrograph of PALF obtained by grinding method.

PALF obtained with the new process shown in Figure 12.3 are smaller than that obtained with conventional methods. Pictures of the PALF taken with a scanning electron microscope are shown in Figure 12.7. It is apparent that the new fiber extraction process can give PALF with the size as small as 3 microns and high fraction of small diameter fiber (Kengkhetkit & Amornsakchai, 2012). Further processing of PALF can be carried out to provide very high fraction of pineapple leaf microfiber (PALMF) with even greater cellulose content.

NFM is particulate with variety of irregular shapes. Mostly, the particle has a platelet shape. Figure 12.8 displays an optical image of NFM.

Table 12.2 compares size, size distribution and fiber yield obtained from different extraction methods. Table 12.3 displays compositions of WGL, PALF and NFM.

12.4.3 Advantages and Disadvantages of the Process

The process described above has several advantages when compared with conventional fiber extraction methods. While long, straight and perfect leaves are required for conventional method, the new method can accept all types of leaves including



Figure 12.8 Optical image of NFM.

Table 12.2 Size of PALF and fiber yield obtained from different extraction methods (modified from Kengkhetkit & Amornsakchai, 2012).

Extraction methods	Range of diameter (μm)	Average diameter (μm)	Fiber yield* (%)
Retting	5–272	37.86	1.17
Scraping	5–169	39.51	1.38
Grinding	3–138	13.22	2.75
Grinding of Dried Leaf	5–194	41.60	3.01

*Percentage by weight of dry fiber based on fresh leaf. Water content in fresh leaf is approximately 80%.

Table 12.3 Composition of ground pineapple leaves (WGL), PALF and NFM.

Composition	Percentage*	Dry matter	Lignin	Hemicellulose	Cellulose
Whole Ground Leaves	100	90.38	4.57	34.38	46.65
Fibrous Material (Pineapple Leaf Fiber)	21.4 ± 1.4	92.43	1.98	19.80	70.98
Non-Fibrous Material	78.6 ± 1.4	89.37	7.70	36.53	43.69

*Weight percentage of dried materials based on dried leaf.

pineapple crown provided they are neither rotten nor too dry. This means that most waste leaves in the field can be utilized. The method provides high quality PALF with uniform length and finer diameter than that prepared with conventional methods. The process also give greater fiber yield and allows greater flexibility in producing intermediate products with varying contents of NFM and PALF to adjust the cost performance ratio (see Section 12.5.3). Most importantly, the process can be scaled up for industrial production of the fiber.

12.5 Potential Applications of PALF as Reinforcement for Polymer Matrix Composites

12.5.1 A Concept for Better Utilization of PALF in Composites

It is known that some natural fibers have high mechanical properties close to that of glass fiber (see Table 12.1). Thus, it is often presented that natural fiber could be as good as glass fiber. However, natural fiber is only mechanically comparable to glass fiber in the longitudinal direction. Glass fiber is isotropic while natural fiber is highly anisotropic. Natural fiber is much weaker than glass fiber in the transverse direction. In addition, natural fiber is very easy to bend and kink while glass fiber is relatively stiff and straight. These facts explain why it is very difficult for natural fiber filled plastics to compete with glass fiber-filled plastics. Therefore, in order to get the most out of natural fiber, or PALF in this particular case, it is important that we have the fiber straight and aligned. This can be easily formed using a two-roll mill into a thin thermoplastic or rubber preregs (or preforms) (Figure 12.9) which can then be assembled in different ways (such as uniaxial, angle-ply or cross-ply) to form thicker sheet.

Composite examples given in the following sections, except that in the last one, were prepared according to the above concept, i.e., uniaxial composite. Mechanical properties were measured in the longitudinal direction unless explicitly stated otherwise.

12.5.2 Rubber Reinforcement

Normally different types of particulate filler are used to adjust properties of rubber matrix composites (Donnet & Custodero, 2005). Certain fillers increase, not only the modulus, but also the strength, of the rubber composites. These are known as reinforcing fillers and a good example of this is carbon black. However, short fiber has been studied and used as reinforcement in the rubber industry for a very long time, though its use is rather limited and not as widely practiced as carbon black and other particulate fillers. Inclusion of short fiber improves green strength, provides dimensional stability prior to cure, and also improves mechanical properties of the vulcanizate (Foldi, 1992). With proper fiber orientation, the general characteristic of the rubber's stress-strain curve changes considerably. Stress or what is conventionally called modulus at low elongation increases sharply and significantly. Fiber-reinforced rubber composites allow materials with high anisotropy to be produced. This unique characteristic can only be obtained from fiber reinforcement, but not from particulate fillers. Such property is useful in many applications where large deformation is undesirable (Lee, 1996).

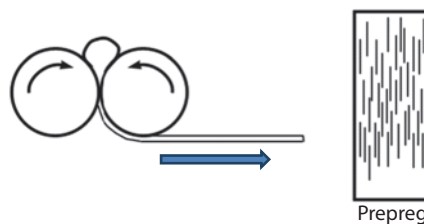


Figure 12.9 Formation of uniaxially aligned PALF reinforced polymer prepreg on a two-roll mill.

The fibers used or studied are, for example, cotton linters, cellulose, polyester and nylon (Foldi, 1992; Ashida, 1996; Lee, 1996; Agarwal *et al.*, 2002; Lopez Manchado & Arroyo, 2002; Rajesh *et al.*, 2004; Mathew & Narayanankutty, 2009). Many types of natural fibers have also been studied for rubber reinforcement. These includes jute, sisal, flax, coir, oil palm, bamboo, silk, pineapple leaf fiber (PALF) and grass (Chakraborty *et al.*, 1982; Ismail *et al.*, 1997; Geethamma *et al.*, 1998; Ismail *et al.*, 2002; Jacob *et al.*, 2004; Lopattananon *et al.*, 2006; De *et al.*, 2004). Not until recently have short fibers for rubber reinforcement gained more popularity and become more commercially accessible (Du Pont, 2015; RheinChemie, 2015; Finite Fiber, 2015). For applications that require exceptional properties, aramid fiber is the focus. Despite being widely studied, the use of natural fibers for rubber reinforcement is still not widely practiced. This is probably because the properties obtained thus far were not very satisfactory and especially the very low elongation at break.

The use of natural fiber for rubber reinforcement is, however, still very attractive given current resource and climate problems. As shown in Table 12.1, PALF has much greater specific mechanical properties than other natural fibers. Its mechanical properties are close to that of aramid fiber. Therefore, with greater than ever interest in using bio-derived products, greener rubber composites with superior properties can be expected.

Rubber products generally have to be either deformed to much great extent than plastic composites or deformed repeatedly. As such, large defects presence in the material can be detrimental. For rubber, the critical size of failure initiation sites has been estimated at about 50 μm (Setua & De, 1985; Akhtar *et al.*, 1986) and this is smaller than the size of most natural fibers. It is thus not surprising that natural fiber reinforced rubbers fail at relatively low strains (Chakraborty *et al.*, 1982; Setua & De, 1984; Agarwal *et al.*, 2002; Rajesh *et al.*, 2004).

Short and fine PALF prepared according to the method presented in Section 12.4 has diameter as small as 3 μm and an average diameter of approximately 18 μm . This PALF was thought to be fine enough for effective rubber reinforcement and this has led to the first report on its use for the reinforcement of acrylonitrile butadiene rubber (NBR) (Wisittanawat *et al.*, 2014a). PALF is preferentially aligned in order to get the best effect as already stated previously. A very large improvement in low strain moduli was obtained but the composite failed at relatively low strain. It was also found that resorcinol formaldehyde adhesion promoter could improve the low strain modulus but did not affect the elongation at break. The still low elongation at break could be responsible by some of large PALF presence.

To get around the low elongation at break, hybrid filler system of PALF and silica was utilized (Wisittanawat *et al.*, 2014b). It was proposed that if the rubber matrix's tear strength could be improved with silica, then the elongation at break of the composite should be improved. Indeed, remarkable improvement in elongation at break has been achieved with the hybrid filler system as shown in Figure 12.10 (Wisittanawat *et al.*, 2014b). The use of hybrid silica also increases the stress in the initial part of the stress-strain curve. However, it was found that addition of silica could interfere with the function of the resorcinol adhesion promoter.

A subsequent report has shown that reinforcing carbon black can also be used as hybrid filler with PALF (Prukkaewkanjana *et al.*, 2015). Rubber composites with very

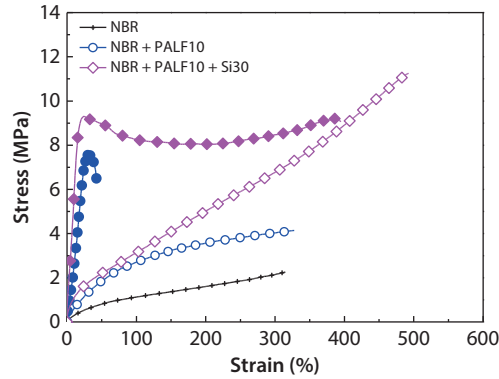


Figure 12.10 Stress-strain curves of unfilled NBR (—), PALF-NBR (○), PALF/Silica-NBR (◆) (modified from Wisittanawat *et al.*, 2014b).

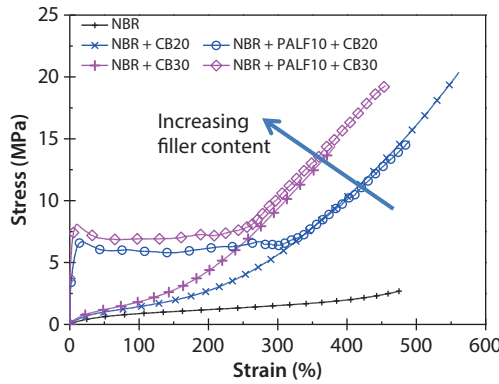


Figure 12.11 Stress-strain curves of PALF/CB-NBR (modified from Prukkaewkanjana *et al.*, 2015).

high modulus at low strain, high tensile strength and very high elongation at break could be prepared. The composites displayed high tensile strength due to an upturn in stress at high elongations (Figure 12.11). The results indicate that property of the composite in the low strain region is determined by PALF while that in the high strain region is determined by carbon black (Prukkaewkanjana *et al.*, 2015). Similar behavior was also observed in hybrid filler system of silica and PALF with slight modification of curing system from that used in Wisittanawat *et al.*, 2014b, to increase the cure time (Prukkaewkanjana, 2015).

PALF can, in principle, be used to reinforce any type of rubber. The effectiveness of reinforcement may, however, be varied depending on the characteristic of the rubber. The effect in natural rubber (NR) is slightly lesser than in NBR since NR is non-polar (Wongpreedee & Amornsakchai, 2015).

To summarize, PALF can be used effectively to reinforce rubber to provide rubber composites with very high stretching stress at low strains. The best effect is obtained in hybrid composites that have high extension to break and, at the same time, allow further control of the modulus at low strains. Such improved performance will certainly be beneficial in product design and use of rubbers. It is noted worthy that this behavior cannot be obtained from particulate fillers. The effect is much greater than using other

types of cellulose such as Kraft pulp (Lopez Manchado & Arroyo, 2002), microcrystalline cellulose (Bai & Li, 2009), soft wood fiber (Lopattananon *et al.*, 2011) and cellulose nanowhisker (Visakh *et al.*, 2012) at similar loading.

12.5.3 Plastic Reinforcement

The introduction of short natural fiber into plastic matrix has been studied for a long time and early information regarding this can be found in many reviews (Karnani *et al.*, 1997, Mishra *et al.*, 2004, Sapuan *et al.*, 2011). As pointed out in Section 12.5.1, the best effect of short fiber reinforcement will be obtained when fibers are straight and aligned. When the molten composite is forced to flow during processing, the fiber will tend to align along the flow streamlines. Thus a certain degree of fiber orientation can be expected after processing. Most reports so far relied on injection molding technique, which provides limited orientation of the fiber. Few reports paid attention to get the fiber fully aligned for the best effect. Yet, only limited improvement was obtained due to the low aspect ratio of the fiber (Chattopadhyay *et al.*, 2009).

Recently it was reported, using the concept discussed above, that preferentially aligned PALF-polypropylene (PP) composites can be successfully prepared. PALF can be directly used without the need of any surface modification. Since this PALF has very high aspect ratio, great improvement in mechanical properties was obtained (Kengkhetkit & Amornsakchai, 2012; Kengkhetkit & Amornsakchai, 2014). Figure 12.12

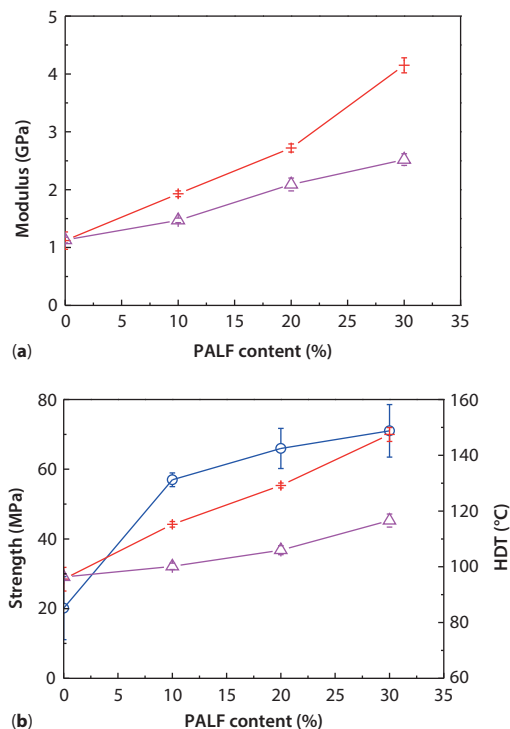


Figure 12.12 (a) Flexural modulus (+) and 1% secant modulus (Δ) of PALF-PP composites; (b) Flexural strength (+), tensile strength (Δ) and HDT (●) of PALF-PP composites (modified from Kengkhetkit & Amornsakchai, 2014).

displays flexural and tensile properties and heat distortion temperature (HDT) of the composites. The improvement in heat distortion temperature (HDT) for 30% PALF composite was very impressive with the value of about 148 °C.

For some matrices, mechanical properties of uniaxial PALF reinforced composite can be improved further if matrix orientation is present. Kalapakdee & Amornsakchai studied uniaxial PALF reinforced polypropylene based thermoplastic elastomer (Santoprene). It was found that after forming uniaxial prepreg, the matrix can display high crystalline orientation (Kalapakdee & Amornsakchai, 2014). If compression temperature for forming thicker part is not too high to cause complete melting, the crystalline orientation in the starting prepreg could be retained. As a result, the composite displays greater modulus than that compressed at high temperature.

PALF constitutes only approximately 20% of WGL (see Table 12.3) and the rest is NFM. It was thought that this NFM could be used as filler for plastic. This has led (Kengkhetkit & Amornsakchai, 2014) to explore the concept of using every part of these dried ground leaves or zero waste. PP composites filled with WGL, PALF and NFM were tested and very satisfactory results were obtained. NFM provided relatively good reinforcement which was better than expected. This was partly due to the platelets structure of NFM. The reinforcing performance for PP is in the order PALF>WGL>NFM (Figure 12.13). Mechanical properties of these composites could be adjusted with a maleic anhydride-grafted polypropylene compatibilizer. This concept allows the cost-performance ratio and also 'greening' level to be easily adjusted to match the requirements. In principle, these materials (PALF, WGL and NFM) can be used to reinforce any type of plastic.

Attempts have been made to produce test products from PALF-PP and PALF-NFM composites. Compound pellets can be produced according to normal factory operating procedure. Photographs of some test products are shown in Figure 12.14.

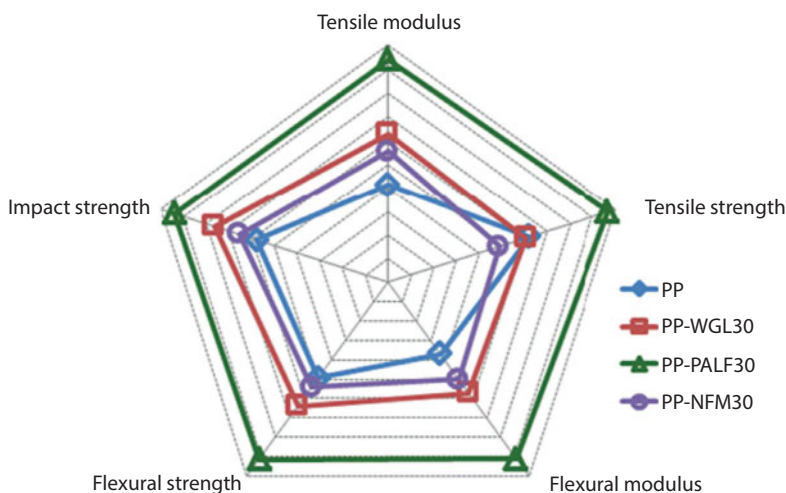


Figure 12.13 Radar plot of performance of PALF-PP, WGL-PP and NFM-PP composites (modified from Kengkhetkit & Amornsakchai, 2014).



Figure 12.14 Test products injected from different composites: Heavy duty carrying handle from PALF-PP (top); general plastic utensils (middle) and makeup brush handles (bottom) from NFM-PP composites.

12.5.4 Other Types of Reinforcement

The type of reinforcements presented in sections 12.5.1 and 12.5.2 are those with preferential alignment due to processing method. A different form of reinforcement, i.e., nonwoven mat, can also be prepared from PALF and WGL as shown in Figure 12.5. These can be used for the formation of composite structures with different types of resins. In the most simplest form, it can be used in a similar manner as one would use chopped strand mat of glass fiber. The mat can be used in any of glass fiber fabrication methods. Figure 12.15 displays the use of WGL nonwoven mat for the construction of boat and table-chair set.

PALF and WGL nonwoven mats can also be impregnated with appropriate resin to produce semi-finished mat ready for subsequent processing and manufacturing of finished products. Example of this type of resin is Acrodur® from BASF, which has been successfully used with flax (Khalfallah *et al.*, 2014a; Khalfallah *et al.*, 2014b). Figure 12.16 displays the photographs of PALF nonwoven mat being applied in the process.



Figure 12.15 Fabrication of a boat and table-chair set using WGL nonwoven mat in combination with glass chopped strand mat.



Figure 12.16 Preparation of semi-finished mat from PALF nonwoven mat and water based acrylic resin (Acrodur®) using brushing technique.

12.6 Concluding Remarks

Pineapple leaf waste contains high quality fibers, PALF. The fiber has been tested as reinforcement in various types of polymer matrix composites, i.e., rubber, thermoplastic and thermoset. It thus has promising potential as an alternative green reinforcement for polymers. However, the level of properties, especially strength, improvement depends on PALF size. With the novel method proposed, fine PALF can be obtained and this would widen the range of its applications further. Interesting application is uniaxial reinforcement for rubber and thermoplastic matrices. The former provides rubber composites with very high stretching stress at low strains. The best effect in rubber reinforcement is obtained through hybridization with conventional particulate reinforcing fillers. For plastics, fine PALF provides very impressive improvements in flexural strength and heat distortion temperature. In addition, the uses of WGL and NFM in plastic allow the cost-performance ratio and also 'greening' level to be easily adjusted to match the requirements. This should be very attractive as it will be a zero waste process. This concept can also be applied to produce nonwoven mat for resin reinforcement. It should be noted that examples of application given are for illustration and can be applied to other polymer matrices. In addition, appropriate surface modifications can be applied to improve the composite performance.

Acknowledgements

The author would like to express his gratitude to the support of the Thailand Textile Institute (TTTI), National Research Council of Thailand (NRCT) and Center of Excellence for Innovation in Chemistry (PERCH-CIC) for the financial support of the projects. A special thank you is also extended to Dr. Nanthaya Kengkhetkit, Mr. Ukrit Wisittanawat, Miss Kontapond Prukkaewkanjana and Miss Budsaraporn Surajarusarn whose works have formed an important part of this review.

References

- Abdul Khalil, H.P.S., Siti Alwani, M., Mohd Omar, A.K., Chemical composition, anatomy, lignin distribution, and cell wall structure of Malaysian plant waste fibers. *Bioresources*, 1, 220, 2006.
- Agarwal, K., Satua, D.K., Mathur, G.N., Short fibre and particulate-reinforced rubber composites. *Defence Sci. J.*, 52, 337, 2002.
- Akhtar, S., Bhowmick, A.K., De, P.P., De, S.K., Tensile rupture of short fiber filled thermoplastic elastomer. *J. Mater. Sci.*, 21, 4179, 1986.
- Ashida, M., Composites of polychloroprene rubber with short fibres of poly(ethylene terephthalate) and nylon, in: *Short Fiber-Polymer Composites*, J.R. White and S.K. De (Eds.), pp. 116–143, Woodhead Publishing, Cambridge, 1996.
- Asim, M., Abdan, K., Jawaid, M., Nasir, M., Dashtizadeh, Z., Ishak, M.R., Hoque, M.E., A Review on Pineapple Leaves Fibre and Its Composites. *Int. J. Polym. Sci.*, ID. 950567, 2015.
- Bai, W., Li, K., Partial replacement of silica with microcrystalline cellulose in rubber composites. *Compos. Part A-Appl. S.*, 40, 1597, 2009.
- Banik, S., Nag, D., Debnath, S., Utilization of pineapple leaf agro-waste for extraction of fibre and the residual biomass for vermicomposting. *Indian J. Fibre Text.*, 36, 172, 2011.
- Bledzki, A.K., Gassan, J., Composites reinforced with cellulose based fibres. *Prog. Polym. Sci.*, 24, 221, 1999.
- Chakraborty, S.K., Setua, D.K., De, S.K., Short jute fiber reinforced carboxylated nitrile rubber. *Rubber Chem. Technol.*, 55, 1286, 1982.
- Chattopadhyay, S.K., Khandal, R.K., Uppaluri, R., Ghoshal, A.K., Influence of varying fiber lengths on mechanical, thermal, and morphological properties of MA-g-PP compatibilized and chemically modified short pineapple leaf fiber reinforced polypropylene composites. *J. Appl. Polym. Sci.*, 113, 3750, 2009.
- De, D., De, D., Adhikari, B., The effect of grass fiber filler on curing characteristics and mechanical properties of natural rubber. *Polym. Adv. Technol.*, 15, 708, 2004.
- Donnet, J.B., Custodero, E., Reinforcement of Elastomers by Particulate Fillers, in: *Science and Technology of Rubber*, 3rd ed., J.E. Mark, B. Erman and F.R. Eirich (Eds.), pp. 367–400, Elsevier Academic Press, San Diego, 2005.
- DuPont, Kevlar®Engineered Elastomer, 2015. <http://www.dupont.com/products-and-services/fabrics-fibers-nonwovens/fibers/brands/kevlar/products/kevlar-engineered-elastomer.html>
- E. Almassy, Decorticating machine and process, US Patent 3050788, 1962.
- FAOSTAT, Food and Agriculture Organization of the United Nations, statistics division, 2013. <http://faostat3.fao.org/download/Q/QC/E>.
- Faruk, O., Bledzki, A.K., Fink, H.-P., Sain, M., Biocomposites reinforced with natural fibers: 2000–2010. *Prog. Polym. Sci.*, 37, 1552, 2012.
- Finite Fiber, 2015. <http://www.finitefiber.com/>

- Foldi, A.P., Short-Fibre-Reinforced Rubber: A New Kind of Composite, in: *Composite applications: the role of matrix, fibre, and interface*, T.L. Vigo and B.J. Kinzig (Eds.), pp. 133–177, VCH, New York, 1992.
- Geethamma, V.G., Mathew, K.T., Lakshminarayanan, R., Thomas, S., Composite of short coir fibers and natural rubber: effect of chemical modification, loading and orientation of fiber. *Polymer*, 39, 1483, 1998.
- Ismail, H., Rosnah, N., Rozman, H.D., Effects of various bonding systems on mechanical properties of oil palm fiber reinforced rubber composites. *Eur. Polym. J.*, 33, 1231, 1997.
- Ismail, H., Edyham, M.R., Wirjosentono, B., Bamboo fiber filled natural rubber composites: the effects of filler loading and bonding agent. *Polym. Test.*, 21, 139, 2002.
- Jacob, M., Thomas, S., Varughese, K.T., Mechanical properties of sisal/oil palm hybrid fiber reinforced natural rubber composites. *Compos. Sci. Technol.*, 64, 955, 2004.
- Joshi, S.V., Drzal, L.T., Mohanty, A.K., Arora S., Are natural fiber composites environmentally superior to glass fiber reinforced composites?. *Compos. Part A-Appl. S.*, 35, 371, 2004.
- J.S. Reeves, Decorticating Machine, US Patent 2490157, 1949.
- Kalapakdee, A. and Amornsakchai, T., Mechanical properties of preferentially aligned short pineapple leaf fiber reinforced thermoplastic elastomer: Effects of fiber content and matrix orientation. *Polym. Test.*, 37, 36, 2014.
- Karnani, R., Krishnan, M., Narayan, R., Biofiber-reinforced polypropylene composites. *Polym. Eng. Sci.*, 37, 476, 1997.
- Khalfallah, M., Abbès, B., Abbès, F., Guo, Y.Q., Marcel, V., Duval, A., Vanfleteren, F., Rousseau, F., Innovative flax tapes reinforced Acrodur biocomposites: A new alternative for automotive applications. *Mater. Des.*, 64, 116, 2014.
- Khalfallah, M., Marcel, V., Duval, A., Abbès, B., Abbès, F., Guo, Y.Q., Vanfleteren, F., Rousseau, F., Flax/Acrodur® sandwich panel: an innovative eco-material for automotive applications. *JEC Compos. Mag.*, 89, 73, 2014.
- Kengkhetkit, N. and Amornsakchai, T., Utilisation of pineapple leaf waste for plastic reinforcement: 1. A novel extraction method for short pineapple leaf fiber. *Ind. Crops Prod.*, 40, 55, 2012.
- Kengkhetkit, N. and Amornsakchai, T., A new approach to “Greening” plastic composites using pineapple leaf waste for performance and cost effectiveness. *Mater. Des.*, 55, 292, 2014.
- Koronis, G., Silva, A., Fontul, M., Green composites: A review of adequate materials for automotive applications. *Compos. Part B-Eng.*, 44, 120, 2013.
- Laftah, W.A., Abdul Rahaman, W.A.W., Chemical pulping of waste pineapple leaves fiber for kraft paper production. *J. Mater Res. Technol.*, 4, 254, 2015.
- Lee, M.C.H., Design and applications of short fibre reinforced rubbers, in: *Short Fiber-Polymer Composites*, J.R. White and S.K. De (Eds.), pp. 192–209, Woodhead Publishing, Cambridge, 1996.
- Lopattananon, N., Panawarangkul, K., Sahakaro, K., Ellis, B., Performance of pineapple leaf fiber–natural rubber composites: The effect of fiber surface treatments. *J. App. Polym. Sci.*, 102, 1974, 2006.
- Lopattananon, N., Jitkalong, D., Seadan, M., Hybridized reinforcement of natural rubber with silane-modified short cellulose fibers and silica. *J. Appl. Polym. Sci.*, 120, 3242, 2011.
- Lopez Manchado, M.A. and Arroyo M., Short fibers as reinforcement of rubber compounds. *Polym. Compos.*, 23, 666, 2002.
- Mathew, L. and Narayanankutty, S.K., Nanosilica as dry bonding system component and as reinforcement in short nylon-6 fiber/natural rubber composite. *J. Appl. Polym. Sci.*, 112, 2203, 2009.
- Mishra, S., Mohanty, A.K., Drzal, L.T., Misra, M., Hinrichsen G., A Review on pineapple leaf fibers, sisal fibers and their biocomposites. *Macromol. Mater. Eng.*, 289, 955, 2004.

- Mukherjee, P.S. and Satyanarayana, K.G., Structure and properties of some vegetable fibres Part 2 Pineapple fibre (*Anannus Comosus*). *J. Mater. Sci.*, 21, 51, 1986.
- Nabi Saheb, D., Jog, J.P., Natural fiber polymer composites: A review. *Adv. Polym. Technol.*, 18, 351, 1999.
- Pappu, A., Patil, V., Jain, S., Mahindrakar, A., Haque, R., Thakur, V.K., Advances in Industrial Prospective of Cellulosic Macromolecules Enriched Banana biofibre resources: A Review; *Int. J. Biol. Macromol.*, 79, 449, 2015.
- Pervaiz, M. and Sain, M.M., Carbon storage potential in natural fiber composites. *Resour. Conserv. Recy.*, 39, 325, 2003.
- Pickering, K.L., Aruan Efendy, M.G., Le, T.M., A review of recent developments in natural fibre composites and their mechanical performance. *Compos. Part A-Appl. S.*, in press, 2015. <http://dx.doi.org/10.1016/j.compositesa.2015.08.038>.
- Prukkaewkanjana, K., *Short pineapple leaf fiber and particulate filler hybrid reinforced rubber composites*, Master Thesis, Mahidol University, 2015.
- Prukkaewkanjana, K., Thanawan, S., Amornsakchai, T., High performance hybrid reinforcement of nitrile rubber using short pineapple leaf fiber and carbon black. *Polym. Test.*, 45, 76, 2015.
- Rajesh, C., Unnikrishanan, G., Purushothaman, E., Thomas, S., Cure characteristics and mechanical properties of short nylon fiber-reinforced nitrile rubber composites. *J. Appl. Polym. Sci.*, 92, 1023, 2004.
- RheinChemie Additives, Fiber dispersions, 2015. <http://www.rheinchemie-additives.com/products/rubber-4/polymer-bound-chemicals-2/fiber-dispersions?lang=en>
- Sapuan, S.M., Mohamed, A.R., *et al.*, Pineapple leaf fibres and PALF-reinforced polymer composites, *Cellulose fibres: Bio- and Nano-Polymer Composites*, S. Kalia, B.S. Kaith and I. Kaur (Eds.), pp. 325–343, Springer-Verlag, Berlin, 2011.
- Satyanarayana, K.G., Pillai, C.K.S., Pillai, S.G.K., Sukumaran, K., Structure property studies of fibers from various parts of the coconut tree. *J. Mater. Sci.*, 17, 2453, 1982.
- Sena Neto, A.R., Araujo, M.A.M., Souza, F.V.D., Mattoso, L.H.C., Marconcini, J.M., Characterization and comparative evaluation of thermal, structural, chemical, mechanical and morphological properties of six pineapple leaf fiber varieties for use in composites. *Ind. Crops Prod.*, 43, 529, 2013.
- Setua, D.K. and De, S.K., Short silk fibre reinforced nitrile rubber composites. *J. Mater. Sci.*, 19, 983, 1984.
- Setua, D.K. and De, S.K., Effect of short fibers on critical cut length in tensile failure of rubber vulcanizates. *J. Mater. Sci.*, 20, 2653, 1985.
- Singha, A.S. and Thakur, V.K., Synthesis and characterization of pine needles reinforced RF matrix based biocomposites. *J. Chem.*, 5 (S1), 1055, 2008a.
- Singha, A.S., Thakur, V.K., Effect of Fibre Loading on Urea-formaldehyde Matrix Based Green Composites. *Iran. Polym. J.* 17, 861, 2008b.
- Singha, A.S., Thakur, V.K., Synthesis and characterization of *Grewia optiva* fiber-reinforced PF-based composites. *Int. J. Polym. Mater.* 57, 1059, 2008c.
- Singha, A.S., Thakur, V.K., Mechanical, Morphological and Thermal Properties of Pine Needle-Reinforced Polymer Composites. *Int. J. Polym. Mater.* 58, 211, 2008d.
- Singha, A.S., Thakur, V.K., Fabrication and Study of Lignocellulosic Hibiscus Sabdariffa Fiber Reinforced Polymer Composites. *Bioresources* 3, 1173, 2008e.
- Susheel, K., Kaith, B.S., Inderjeet, K., Pretreatments of natural fibers and their application as reinforcing material in polymer composites - a review. *Polym. Eng. Sci.*, 49, 1253, 2009.
- Thakur, V.K. and Singha, A.S., KPS-Initiated Graft Copolymerization onto Modified Cellulosic Biofibers. *Int. J. Polym. Anal. Ch.*, 15 (8), 471, 2010.

- Thakur, V.K. and Singha, A.S., Mechanical and water absorption properties of natural fibers/polymer biocomposites, *Polym-Plast. Technol.*, 49 (7), 694, 2010.
- Thakur, V.K., Singha, A.S., Thakur, M.K., Green composites from natural fibers: Mechanical and chemical aging properties. *Int. J. Polym. Anal. Ch.*, 17 (6), 401, 2012.
- Thakur, V.K., Singha, A.S., Thakur, M.K., Surface Modification of Natural Polymers to Impart Low Water Absorbency. *Int. J. Polym. Anal. Ch.*, 17 (2), 133, 2012.
- Thakur, V.K., Singha, A.S., Thakur, M.K., Fabrication and Physico-Chemical Properties of High-Performance Pine Needles/Green Polymer Composites, *Int. J. Polym. Mater.*, 62 (4), 226, 2013.
- Thakur, V.K., Thakur, M.K., Recent Advances in Graft Copolymerization and Applications of Chitosan: A Review. *ACS Sustain. Chem. Eng.* 2, 2637, 2014a.
- Thakur, V.K., Thakur, M.K., Processing and characterization of natural cellulose fibers/thermoset polymer composites. *Carbohydr. Polym.*, 109, 102, 2014b.
- Thakur, V.K., Thakur, M.K., Recent trends in hydrogels based on psyllium polysaccharide: a review. *J. Clean. Prod.* 82, 1, 2014c.
- Thakur, V.K., Thakur, M.K., Gupta, R.K., Review: Raw Natural Fiber-Based Polymer Composites. *Int. J. Polym. Anal. Ch.*, 19 (3), 256, 2014a.
- Thakur, V.K., Thakur, M.K., Raghavan, P., Kessler, M.R., Progress in green polymer composites from lignin for multifunctional applications: A review. *ACS Sustainable Chem. Eng.*, 2 (5), 1072, 2014b.
- Thakur, V.K., Thakur, M.K., Gupta, R.K., Graft copolymers of natural fibers for green composites. *Carbohydr. Polym.* 104, 87–93, 2014c.
- Thakur, V.K., Grewell, D., Thunga, M., Kessler, M.R., Novel Composites from Eco-Friendly Soy Flour/SBS Triblock Copolymer. *Macromol. Mater. Eng.* 299, 953–958, 2014d.
- Thakur, V.K., Thunga, M., Madbouly, S.A., Kessler, M.R., PMMA-g-SOY as a sustainable novel dielectric material. *RSC Adv.* 4, 18240–18249, 2014e.
- Visakh, P.M., Thomas, S., Oksman, K., Mathew, A.P., Crosslinked natural rubber nanocomposites reinforced with cellulose whiskers isolated from bamboo waste: Processing and mechanical/thermal properties. *Compos. Part A-Appl. S.*, 43, 735, 2012.
- Wambua, P., Ivens, J., Verpoest, I., Natural fibres: can they replace glass in fibre reinforced plastics? *Compos. Sci. Technol.*, 63, 1259, 2003.
- W.G. Waldo, Decorticating apparatus, US Patent 2753600, 1956.
- Wisittanawat, U., Thanawan, S., Amornsakchai T., Mechanical properties of highly aligned short pineapple leaf fiber reinforced - nitrile rubber composite: Effect of fiber content and bonding agent. *Polym. Test.*, 35, 20, 2014.
- Wisittanawat, U., Thanawan, S., Amornsakchai, T., Remarkable improvement of failure strain of preferentially aligned short pineapple leaf fiber reinforced nitrile rubber composites with silica hybridization. *Polym. Test.*, 38, 91, 2014.
- Wongpreedee, T. and Amornsakchai, T., Synchrotron X-ray diffraction study of pineapple leaf fiber reinforced natural rubber composites during stretching. *Suranaree J. Sci. Technol.*, in press, 2015.

Insights into the Structure of Proteins Adsorbed onto Bioactive Glasses

Klára Magyari, Adriana Vulpoi and Lucian Baia*

*Faculty of Physics & Institute of Interdisciplinary Research in Bio-Nano-Sciences,
Babes-Bolyai University, Cluj-Napoca, Romania*

Abstract

When biomaterials come in contact with the organism fluids, the blood proteins saturate the surface of the material by rapidly covering it within a time frame of seconds to minutes. The characteristics of both adsorbing proteins and exposed surfaces may influence the adsorption dynamics and structural conformation, these properties affecting the cell response in terms of adhesion, migration, proliferation and growth of self-assembled and renewed material. The purpose of this work is to describe the interaction of the most abundant proteins in plasma with sol-gel and melt-derived bioactive glasses using different spectroscopic and microscopic techniques. Our interest was to reveal the influence of the adsorbed proteins on the glass surface, and try to understand any changes induced with regard to the ability of this kind of materials to renew themselves when implanted in live tissues.

Keywords: Renewable materials, bioactive glasses, FT-IR; SEM; EDX, biocompatibility

13.1 Introduction

One significant characteristic of renewable materials is biodegradability, namely, the capability of decaying through the action of living organisms. In the case of biomaterials this property is very important as it may exclude additional surgery, thereby gaining time, money and last but not least is a benefit for patients. This property of biodegradability of the bioactive glasses represents a great advantage. After implantation of bioactive glasses, bone regeneration occurs by physicochemical dissolution or by cellular activity, or by combination of both (Knabe and Ducheyne, 2008).

Protein adsorption is an important process that should be deeply understood in many biomedical applicative approaches. For instance, when a biomaterial comes in contact with a protein containing solution, its surface is almost instantly covered with protein, the absorbed layer modulating the further interaction of the material with the surrounding environment (Brash, 2000).

*Corresponding author: lucian.baia@phys.ubbcluj.ro

Although protein adsorption is an intensively studied subject_lately, how a protein interacts with a surface is still not completely elucidated (Hlady and Buijs, 1996; Nakanishi *et al.*, 2001; Wahlgren and Arnebrant, 1991). The most common characteristics of the adsorbed proteins are the following: the extent of adsorbed protein onto the surface, spatial organization of the adsorbed proteins (monolayer versus aggregates), conformation (secondary and tertiary structure), orientation (direction of the protein with respect to the surface), and biological activity (interaction with small molecules, other proteins, or cells) (Tronic, 2012).

In the case of implanted biomaterials, the protein adsorption has a crucial role on inflammation effect having the capacity of controlling biocompatibility (Tronic, 2012), cell adhesion (Velzenberger *et al.*, 2008), cell differentiation and clotting (Onuchic and Wolynes, 2004; Wu *et al.*, 2008). In solution, the proteins possess the ability to self-assembly into a highly ordered secondary and tertiary structure (Onuchic and Wolynes, 2004), while when they absorb to a surface, their structure changes depending on both protein and surface properties. Among the protein parameters that influence its adsorption, one can include the structure, size, and structural stability (Norde, 2008), while as surface properties one can include the hydrophobicity and surface chemistry (Ostuni *et al.*, 2001). Since the surfaces usually possess different chemical particularities, they have different free energy sites where the protein may *bind*, and therefore, is not possible to predict the interaction of proteins with certain surface. When a surface of material is brought in contact with a multiple proteins containing solution, a weak interaction of highly concentrated proteins with the surface may happen; moreover, proteins may undergo surface exchange, the small proteins from the surface may be displaced by larger proteins that have higher surface affinity (Norde and Giacomelli, 2000; Tronic, 2012).

As mentioned, the proteins adsorbed on a surface dictate the further interaction of the surface with the surrounding environment. The amount of adsorbed protein, the conformation/orientation on the surface, and the biological activity are important factors that justify the use or developing/adapting of a large variety of techniques for studying characteristics of the adsorbed proteins on bioactive surfaces (Gruian *et al.*, 2015).

13.2 Bioactive Glasses as Renewable Materials

Bioactive glasses and glass ceramics are attractive biomaterials for bone repair and regeneration due to their ability to bind with bone in living organism (Hench, 2006). The mechanism for bone bonding is due to carbonate apatite like layer which is formed on the glass surface after implantation in living organisms, as first step of biodegradation process (Kokubo and Takadama, 2006). The bone bonding ability of a material can be evaluated by following the formation of apatite phase on the material surface during the immersion in simulated body fluids (SBF). Thus, this method predicts the *in vitro* bioactivity of a material. The first application of bioactive glasses was used as implant for middle ear, followed by application in periodontology and endodontology (Boccaccini *et al.*, 2010; Chen *et al.*, 2006). In recent years, great potential has been attributed to the application of bioactive glass in tissue engineering (Chen *et al.*, 2006; Fu *et al.*, 2011; Jones, 2013; Wu *et al.*, 2014).

Since the discovery of Bioglass® 45S5 by Hench in 1969, great potential has been attributed to the application of this kind of biomaterials as renewable materials for bone regeneration (Gerhardt and Boccaccini, 2010). The mechanisms of bioactivity and bone bonding capability of bioactive glass have been intensively studied (Kokubo and Takadama, 2006; Rahaman *et al.*, 2011).

In vivo, this surface of inorganic reactions and ion-exchange phenomena are combined with protein adsorption, but not necessarily driven by the inorganic reaction meaning that serum proteins have a major effect on the properties of the surface reaction layer and that bone bonding and bone tissue ingrowths is the result of multiple organic-inorganic/inorganic-organic, parallel and sequential reactions at the biomaterial-tissue interface (de Bruijn *et al.*, 2008).

Figure 13.1 show the steps that occur once the bioactive glasses are in contact with biological fluids. These processes lead to the formation of new bone that may be considered a renewed material.

The first part of this reaction scheme, mainly the formation of biologically equivalent hydroxyapatite (HA) can be reproduced *in vitro* by immersion of bioactive glasses in SBF that mimics the ion concentrations from blood plasma (Figure 13.2a) (Kokubo and Takadama, 2006). As depicted in Figure 13.2b, the *in vitro* surface reactions include ion leaching/exchange, dissolution of the glass network and precipitation, and growth of a calcium-deficient carbonated apatite (HCA) surface layer.

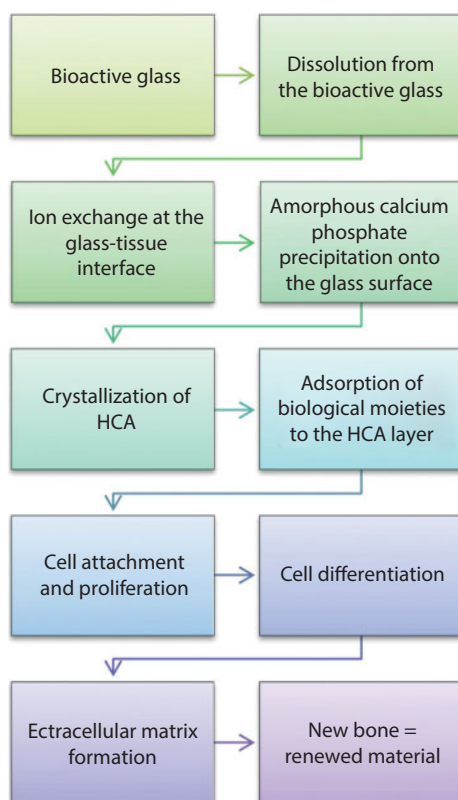


Figure 13.1 Reaction sequence of bioactive glasses when are in contact with biological fluids.

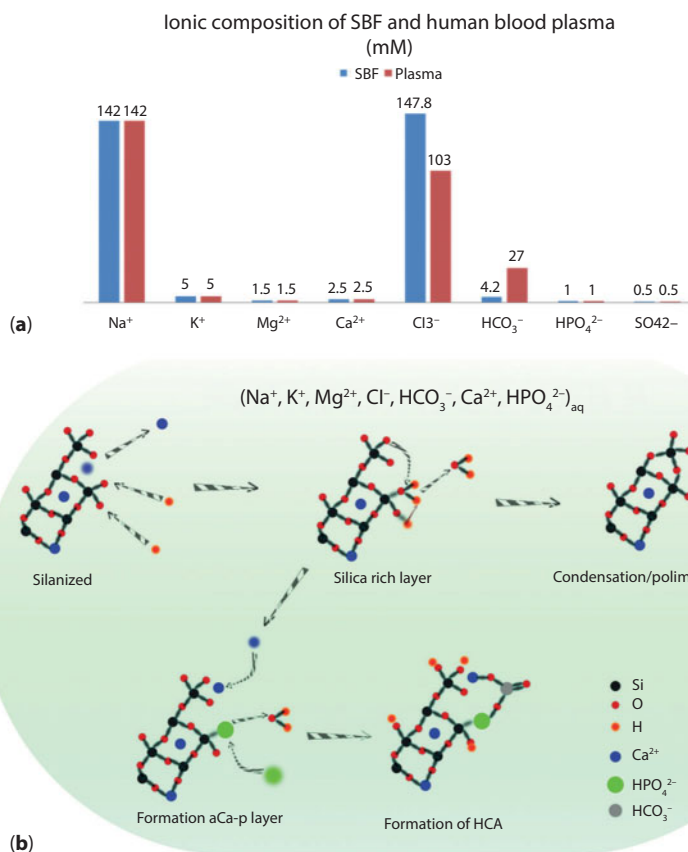


Figure 13.2 The well-known ion composition of SBF versus Human blood plasma (a) together with schematic illustration of apatite layer formation on bioactive glasses in body fluids (b).

Several types of bioactive glass were developed in time such as conventional silicates, phosphate-based glasses and borate-based glasses. With this extension, the applicability of the bioactive glasses becomes wider. The original Bioglass[®] was produced by melt quenching method, which involved melting of high-purity oxides (SiO₂, Na₂CO₃, CaCO₃ and P₂O₅) in platinum crucible at 1370 °C (Jones, 2008). In 1991 Li *et al.*, (Li *et al.*, 1991) developed the bioactive glass prepared by sol-gel method, which has great advantages compared to the melt-processed glass, i.e., higher surface area and porosity, and lower production price. The apatite layer formation on the sol-gel derived glasses is more rapid than on any melt derived glass (Jones, 2008; Li *et al.*, 1991). The sol-gel process consists in the hydrolysis and polycondensation of alkoxide precursors. The most common silica precursor for a silicate-based glass is tetraethyl orthosilicate (TEOS). As TEOS is insoluble in water, for the hydrolysis reaction a catalyst is necessary, usually acidic such as HNO₃, HCl etc. (Sinkó, 2010). Other components of glass are added one by one to the sol, either as alkoxides or as salts. Generally, phosphate is incorporated by adding *triethyl* phosphate (TEP), and the calcium by adding calcium nitrate tetrahydrate (Ca(NO₃)₂·3H₂O) (Vallet-Regi *et al.*, 2003). The sol undergoes polycondensation forming a gel from a time period of several hours to a few days. The sol-gel process can

be accelerated using the two-step catalyzing process by adding a solution with basic pH, i.e., ammonia solution, in the sol after acid catalyzed hydrolysis reaction (Riti *et al.*, 2015), reducing the time needed for the gel formation to few minutes. The gel is then aged for a few days, dried to remove the used solvents, and thermally treated in order to remove organic residues and other unneeded reaction byproducts.

Phosphate and borophosphate glasses are usually obtained by a conventional melt-quenching technique. The sol-gel synthesis of pure phosphate glasses is difficult, because condensed polyphosphates cannot be obtained via the hydrolysis and condensation of usual sol-gel precursors such as $\text{PO}(\text{OEt})_3$ or H_3PO_4 (Livage *et al.*, 1992). A possible route of synthesis is to use alkyl phosphates such as $\text{OP}(\text{OR})_x(\text{OH})_{3-x}$ ($x = 1, 2$) (Carta *et al.*, 2005; Carta *et al.*, 2008). The phosphate based glasses advantage is high solubility, which can be tailored by varying the composition and their chemical similarity to the inorganic phase of human bone (Ahmed *et al.*, 2004; Hoppe *et al.*, 2011; Magyari *et al.*, 2015b). With addition of B_2O_3 in the phosphate network, the glasses become bioresorbable, thus it can be broken down and absorbed by the body, becoming thus a renewable material. However, their poor mechanical properties limit their use in biomedical applications.

13.3 Proteins Structure

Prior discussions regarding the interaction between proteins and bioactive glasses, a brief introduction to protein structure is given. Proteins are linear biological polymers with monomeric units of amino acids that interact with each other giving rise to a molecule with a three-dimensional structure (Gallagher). From 20 different amino acids, each distinguished by group identity “R” one can build up an infinite number of sequences of protein macromolecules. The amino acids are linked covalently by $-\text{CO}-\text{NH}-$ peptide bonds. These bonds are generated by the removal of a water molecule as a result of the changes that occur between the amino groups and the carboxyl groups from one of the two amino acids involved in the reaction (Figure 13.3). The peptide chain is known as the backbone, and the “R” groups are known as side chains.

There are four distinct levels of protein structures: primary, secondary, tertiary and quaternary. The amino acid sequences make up the primary structure of proteins. The secondary structure of proteins refers to the local region of the polypeptide chain conformation, which is dependent on hydrogen bonds. There are three basic types of protein secondary structure as follow: α -helices, β -sheets and connective elements between them, β -loops (Latour Jr, 2005). In the α -helix structure the polypeptide backbone follows a single spiral chain (Figure 13.4a). It is stabilized by hydrogen bonds between backbone amino and carbonyl groups and those in the next turn of the helix, represented as

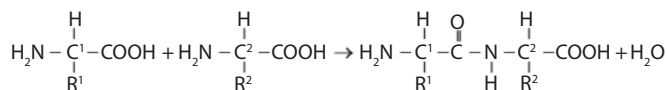


Figure 13.3 The peptide formation by linking two amino acids.

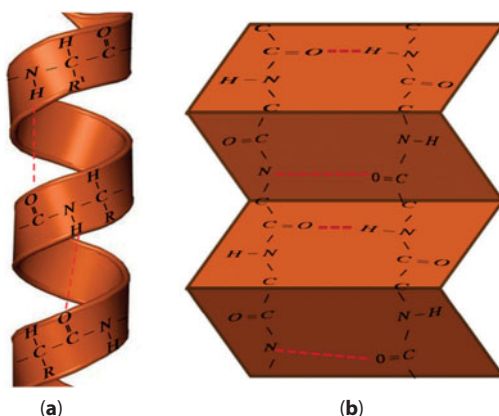


Figure 13.4 Secondary structure of proteins: α -helix (a) and β -sheet (b).

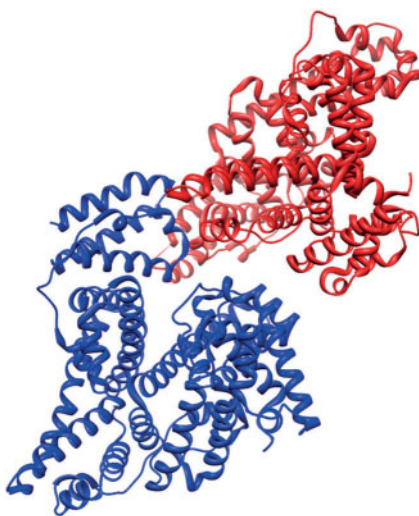


Figure 13.5 Quaternary structures of bovine serum albumin. The two monomers are coloured in red and blue, respectively. The crystal structure of bovine serum albumin dimer obtained by X-ray crystallography (4F5S from Protein Data Bank).

C=O and H-N groups. The β -sheet structure is also stabilized by hydrogen bonds linking together different segments from the protein structure (Figure 13.4b).

Tertiary structures are different combinations of secondary structures, resulting from hydrogen bonding, ionic and hydrophobic interactions, salt bridges and disulfide bonds within chains. Most of the proteins are composed of subunits that consist of two or more polypeptide chains. These subunits of protein are arranged and positioned to form the quaternary structures of the protein (Figure 13.5). They are stabilized by hydrophobic interaction between the nonpolar side chains at the contact regions of the subunits with additional stabilizing forces including interaction between side chains of the subunits and electrostatic interactions between ionic groups of opposite charges (Chinn and Slack, 2000).

13.3.1 The Most Used Proteins in Testing the *In vitro* Interactions with Bioactive Glasses

In this subchapter will be described the interaction of bioactive glasses with the most abundant proteins from human blood plasma, i.e. albumin, fibrinogen and hemoglobin.

Albumin is a small serum protein, being the most widespread protein in the blood in concentrations of about 40 mg/ml (Gelamo & Tabak, 2000). This protein is considered non-adhesive (Tronic, 2012), its main function being to maintain the osmotic blood pressure (Gelamo & Tabak, 2000). Albumin has the property to bind hydrophobic ligands (for example fatty acids, warfarin, steroids, or anesthetics), transporting them throughout body parts through blood (Gelamo & Tabak, 2000). Because of its high concentration and smaller size, albumin is most probably one of the first proteins that are adsorbed to the biomaterial's surface after immersion in body fluids (Wertz & Santore, 2001). Therefore, to understand its behavior after adsorption to a surface is important to characterize the interaction of a material with albumin containing SBFs.

Fibrinogen is a fibrous protein from human blood in a concentration of 2–4 mg/mL (Bai *et al.*, 2009). This 340 kDa dimeric protein has an important role in blood coagulation and thrombosis, and is adsorbed instantly on the surface of an implanted material. The adsorption of fibrinogen onto the surface of a certain material may be an indicator about the biocompatibility of that biomaterial (Magyari *et al.*, 2012; Vanea and Simon, 2011).

Hemoglobin is a globular protein contained in the red blood cells. It has the molecular mass of 64.5 kDa and the role of oxygen carries from the lungs to the rest of the body in order to sustain cellular functions that further lead to soft (skin, muscle) or hard (bone) tissues wound healing (Gruian *et al.*, 2012a). The subunits of hemoglobin protein chains contain a Fe^{2+} ion chelated by four nitrogen atoms called heme group. One type of hemoglobin is methemoglobin, when Fe^{2+} ions are replaced with Fe^{3+} ions, and is present in a 1% concentration in human blood. The structure of methemoglobin consists mostly of α helices, connected by short loop and turn segments (Cai and Singh, 2004; Gruian *et al.*, 2012a).

13.4 Suitable Methods for Proteins Investigation

13.4.1 FTIR Spectroscopy on Proteins

13.4.1.1 FTIR Imaging Spectroscopy

Infrared (IR) spectroscopy is definitely one of the most important analytical investigation methods available to researchers from our days (Stuart, 2004). It is a technique that analyses the vibrations of the atoms that build up a bond inside a molecule, and generally, the IR spectrum is obtained by passing IR radiation through a sample and determining the fraction of the incident radiation absorbed at a particular energy that corresponds to the frequency of a vibration of a sample molecule part. This spectroscopic technique is one of the consecrated methods used for structural determination of small molecules. Thus, it is a valuable tool used for investigating protein structures, molecular mechanisms of protein reactions and protein folding, unfolding or misfolding (Barth, 2007).

The classic Fourier transformed infrared spectroscopy (FT-IR) requires sample preparation before measurements, for example, samples should be embedded in KBr pellets. However, the pressure used in pellets yielding may induce conformational changes in the protein structure (Lin *et al.*, 2004). In order to avoid the above mentioned drawback the FT-IR imaging technique can be an excellent alternative tool that can be successfully used in protein investigation. Another main advantage for involving FT-IR imaging method consists in the fact that there is no need of any sample labeling technologies, the errors induced during the samples preparation being thus eliminated. Therefore, FT-IR imaging proves to be a very versatile method in biological tissue (Bi *et al.*, 2006; Kazarian & Chan, 2013; Petibois *et al.*, 2006) and biomaterials surface observation as well as in the understanding of the interaction between them (Boskey & Pleshko Camacho, 2007; Magyari *et al.*, 2012; Steiner *et al.*, 2007). Moreover, it provides the possibility of using point by point mapping technique, the obtained result being a spatial distribution of a certain vibration (Figure 13.6). The spatial distribution can be achieved by sequential recording of a series of FT-IR spectra, followed by spectroscopic map reconstruction (Steiner, 2008). Nevertheless, it may be also considered that the final spectrum represents the average signal from the imaged area. The imaged area is micrometric in size and depends on the device performance. One of the disadvantages

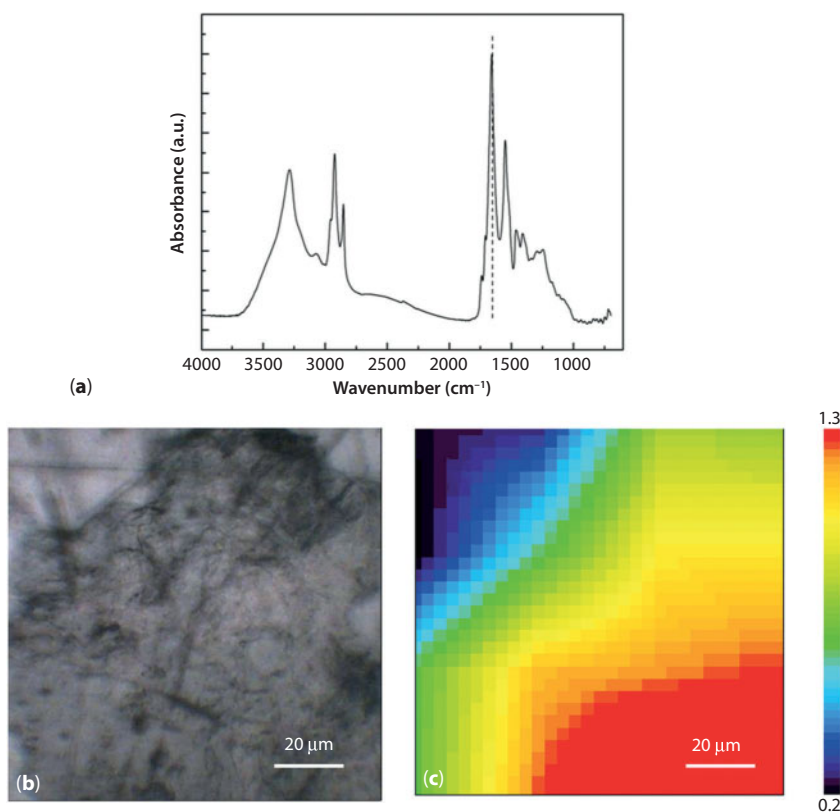


Figure 13.6 FT-IR spectra of the BSA (a); optical image of the sample area (b) and distribution of the 1650 cm^{-1} vibrational band (c). The right side image represents the IR band intensity. Note that the images were recorded in the same area.

of this method is that small molecules, such as proteins, cannot be detected as individual entities. Depending on the nature of the investigated samples FT-IR image can be recorded in transmission, reflection or total attenuated reflection (ATR) mode. Considering that the penetration depth of the incident radiation of this technique is around 1 μm , it appears optimal for being used in acquiring spectral information originated from the surface of the sample.

13.4.1.2 FTIR Spectra of Proteins

FT-IR spectra of proteins exhibit several absorption signals originating from the amide groups (Figure 13.7). The peptide groups, which are repeated units of proteins, have 9 characteristic bands named amides (A, B, I, II, III, IV, V, VI and VII). The signals corresponding to amide A ($\sim 3300\text{ cm}^{-1}$) and amide B ($\sim 3070\text{ cm}^{-1}$) arise mainly from the Fermi resonance between the first overtone of the amide II and the N-H stretching vibrations. The most intense signals of the FT-IR spectra of proteins are given by amide I, amide II and amide III. The amide I absorption signals ($\sim 1650\text{ cm}^{-1}$) arise mainly from C=O stretching vibrations with minor contributions from C-H out of phase stretching and N-H in-plane bending vibrations. The amide II band ($\sim 1550\text{ cm}^{-1}$) originates from both N-H bending and C-N stretching vibrations with smaller contributions from C=O in-plane bending, C=C and C-N stretching vibrations (Figure 13.7). The amide III signal ($1400\text{--}1200\text{ cm}^{-1}$) results from C-N stretching and N-H bending vibrations coupled with slight involvements of C=O in-plane bending and C=C stretching vibrations (Barth, 2007; Magyari *et al.*, 2012). The signal given by amide IV ($625\text{--}767\text{ cm}^{-1}$) is mainly associated with C-N torsion and N-H out-of-plane vibration modes. The amide V ($640\text{--}800\text{ cm}^{-1}$), amide VI ($537\text{--}606\text{ cm}^{-1}$) and amide VII ($\sim 200\text{ cm}^{-1}$) involve out of plane motions of the molecules (Cooper & Knutson, 1995).

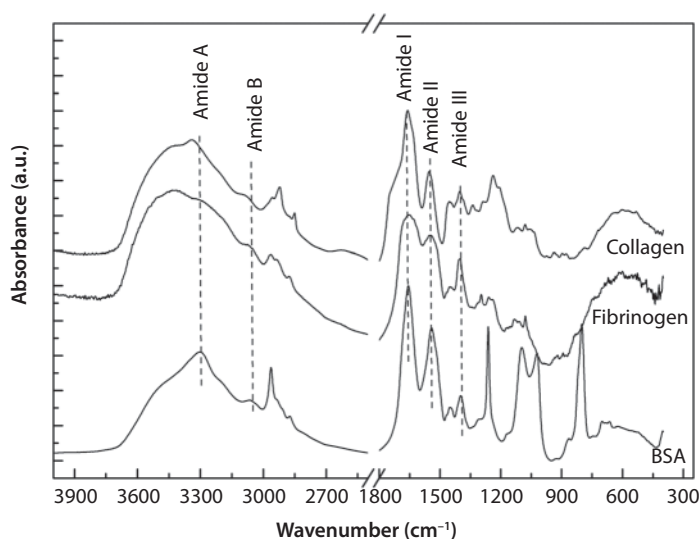


Figure 13.7 FTIR spectra of BSA, fibrinogen and collagen.

13.4.1.3 Secondary Structure of Proteins Obtained by FTIR Spectra

Protein secondary structure is mostly assessed by analyzing amide I and II, both components being sensitive to changes in protein secondary structure. However, the signals recorded from the amide I are the most sensitive ones. The amide I vibration signal within the FT-IR spectra of proteins and peptides is a convolution of a series of overlapped components, corresponding to different secondary structure elements characteristic for this kind of molecules (Chittur, 1998). By amide I band deconvolution, the obtained components can be assigned to specific types of secondary structures based on the correlations between crystallographic structures of proteins and their FTIR spectra (Dong *et al.*, 1990). Therefore, the content of the α -helix, β -sheet, β -turn and random structure may be approximated by deconvolution of the large amide I absorption band using the Gaussian line function, but not before establishing the number of components and their wavenumber with the aid of secondary derivate procedure (Tunc *et al.*, 2005). Additionally, the obtained values can be correlated with the previously reported ones and with the known protein structure (Figure 13.8). Prior to deconvolution, linear baseline subtraction must be performed in the amide I interval. In general, the absorbance in the 1649–1658 cm^{-1} spectral range is associated with the presence of α -helix structure. The β -sheet vibrations have been shown raise signals in the 1618–1641 cm^{-1} and 1674–1695 cm^{-1} spectral domains (Barth, 2007), while the band around 1636 cm^{-1} can appear as consequence of β -sheet structure overlapping with other loops and/or turns structures (Severcan & Haris, 2003). The absorption bands between 1662 and 1686 cm^{-1} can be attributed to β -turn structures, while bands between 1640 and 1648 cm^{-1} can be due to random coil vibrations (Barth, 2007; Schwinte *et al.*, 2001). The secondary structure composition can be determined from the areas of the corresponding components and their fraction from the total area (Figure 13.9).

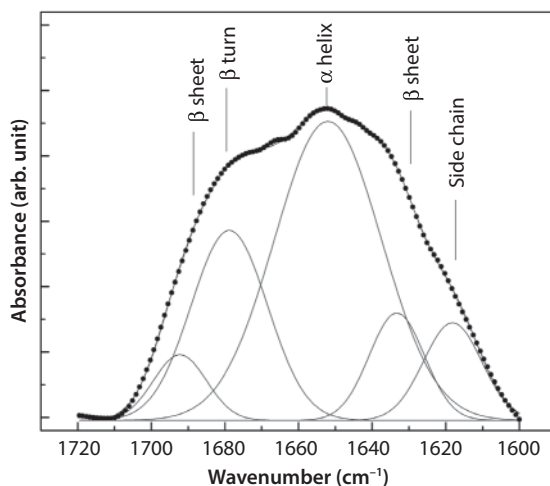


Figure 13.8 Deconvolution of the amide I (1700–1600 cm^{-1}) absorption band of the lyophilized fibrinogen (Reproduced from Reference (Magyari *et al.*, 2015a) with permission of John Wiley & Sons).

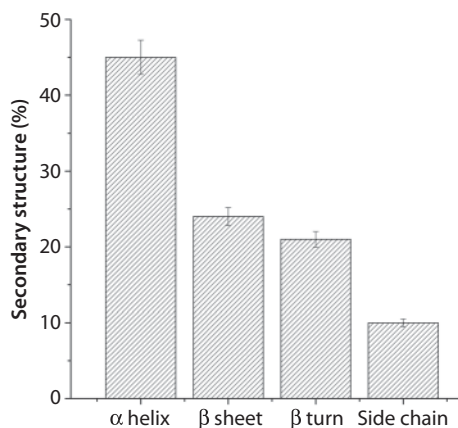


Figure 13.9 Distribution of secondary structure in lyophilized fibrinogen.

13.4.2 Scanning Electron Microscopy (SEM) Coupled with Electron Energy Dispersive X-ray (EDX) Spectroscopy of Proteins

It is worth noting the importance of scanning electron microscopy (SEM) as a semi-quantitative tool for observing protein layers adsorbed on biomaterials. For a better understanding of several biological functions, the visualization of nanometric structures of the proteins is mandatory (Brash, 2000; Hlady and Buijs, 1996; Nakanishi *et al.*, 2001), and electron microscopy is one of the most important tool for performing such observations (Ogura, 2012; Tronic, 2012; Velzenberger *et al.*, 2008; Wahlgren and Arnebrant, 1991).

SEM may supply knowledge about the conformation or the activity of proteins on a surface, being sensitive also to low protein surface coverage. This technique can be used for relatively rapid semi-quantitative characterization at high spatial resolution when compared to other characterization techniques such as X-ray photoelectron spectroscopy (XPS) (Lopez *et al.*, 1993).

The corresponding SEM images contrast of different proteins layers may be influenced by the thinness of the adsorbed protein layer that may further be related to the molecular weight and shape of the protein (Lopez *et al.*, 1993). The capability to differentiate protein ad-layers, based on appearance, may facilitate the interpretation of diverse adsorbed proteins. Multiple types of protein especially if adsorbed from a multi-component solution, may form complex patterns on a materials surface. Moreover, with the aid of SEM technique is possible the detection of non-uniformities in proteins coverage and other macromolecules (Lopez *et al.*, 1993).

Electron energy dispersive X-ray (EDX) spectroscopy coupled with SEMs is able to provide information about elemental composition of the material, after its examination by SEM. Thus, scanning electron microscopy together with energy dispersive X-ray spectrometry (SEM/EDX) is a versatile elemental microanalysis method capable to detect and quantify almost all elements from the periodic table, with the exception of hydrogen, helium and lithium (Newbury & Ritchie, 2013). High quality SEM and EDX data is very effective at showing critical microscopic properties of biomaterials.

13.5 Interaction of Protein with Bioactive Glasses

Adsorption of proteins is a key event whenever a material is introduced into a biological fluid. The application range of biomaterials is restricted due to the protein adsorption. It is known that blood proteins are rapidly adsorbed on the surface of the biomaterial when it is inserted into the body and then cellular attachment, proliferation and migration occur (Latour Jr, 2005; Wang *et al.*, 2012). Thus, the protein adsorption process is important for long-term performance of the implants since the cells that interact with the implant will be reacting primarily with the adsorbed protein layer (Chittur, 1998; Latour Jr, 2005).

The proteins adsorption investigation is important for two main reasons, namely: (i) to better understand the adsorption process and the influence of the material's surface properties on the protein adsorption process and (ii) to modify the surface by controlling the specific/non-specific protein adsorption in order to obtain a more compatible surface, and the cellular response controlled by the adsorbed protein layer (Latour Jr, 2005). For these, the adsorbed protein should not lose its conformational structure and biological functions. However, several studies have shown that the proteins conformation changes upon adsorption onto a material surface, affecting thus the material's biocompatibility and further the cellular response (Magyari *et al.*, 2012; Roach *et al.*, 2005; Vanea *et al.*, 2010; Wang *et al.*, 2012). Protein adsorption involves van der Waals, hydrophobic and electrostatic interactions, together with hydrogen bonding, thus is a very complex process. The difficulty of the problem is that the protein adsorbed on the biomaterial surface leads to changes in structural conformations with the extent of variations that are dependent on the protein stability and protein-surface interaction (Roach *et al.*, 2005; Yaseen *et al.*, 2010).

The protein-biomaterial interaction was studied by using various proteins such as fibrinogen (Magyari *et al.*, 2012; Martins *et al.*, 2003; Roach *et al.*, 2005; Vanea *et al.*, 2010), bovine serum albumin (Magyari *et al.*, 2010; Mavropoulos *et al.*, 2011; Nabian *et al.*, 2011; Ponta *et al.*, 2014; Roach *et al.*, 2005), methemoglobin (Gruian *et al.*, 2012b; Gruian *et al.*, 2013; Vulpoi *et al.*, 2012) etc. on various surfaces such as silica surface (Steiner *et al.*, 2007; Tunc *et al.*, 2005), bioactive glass (Lin *et al.*, 2011; Magyari *et al.*, 2015a; Ponta *et al.*, 2014; Vulpoi *et al.*, 2012), titanium dioxide (Yang *et al.*, 2007), HA (Mavropoulos *et al.*, 2011; Yang *et al.*, 2007) etc.

Since the protein-surface interactions radically influence the biocompatibility of a material, and serum albumin and fibrinogen are the two main components of blood plasma, these two proteins are most commonly used in studies of interaction between proteins and bioactive glasses. The main function of serum albumin is to transport metabolites in blood (Gelamo & Tabak, 2000) and it is considered that it reduces considerably the acute inflammatory response of the body to biomaterials (He & Carter, 1992). The human albumin was replaced in many studies with the cheaper bovine serum albumin (BSA), due to the structural homology of the two proteins (76%) (He & Carter, 1992). Fibrinogen is one of the key components in the plasma and it plays a central role in the mechanism of coagulation and thrombosis. It is a dimeric fibrous protein containing two sets of three polypeptide chains (α , β and γ). The simplest fibrinogen model comprises three spherical regions connected by two narrow rods (Yang *et al.*, 2007). The ratio of human serum albumin and fibrinogen is normally 10:1 (Lousinian *et al.*, 2008).

In several papers hemoglobin is also used as model protein in studies of adsorption onto bioactive glasses (Gruian *et al.*, 2012b; Gruian *et al.*, 2013; Ponta *et al.*, 2013; Vulpoi *et al.*, 2012). It is a major component of red blood cells. Its secondary structure consists mainly in α helices, connected by short loop and turns segments (Cai & Singh, 2004).

13.5.1 Protein Adsorption onto Bioactive Glass Surfaces in Terms of Biocompatibility

The first rapid test performed with the purpose of excluding non-biocompatible materials is to evaluate the BSA and/or fibrinogen adsorption efficiency on a material surface (Magyari *et al.*, 2012; Steiner *et al.*, 2007; Tunc *et al.*, 2005; Vanea *et al.*, 2010). If the blood proteins are adsorbed onto the material's surface and their secondary structure is preserved after adsorption, then the samples blood compatibility can be predicted. Thus, after immersion in protein solution, the FT-IR spectra of the studied material must show the presence of two absorption signals originating from the amide I (at 1650 cm^{-1}) and amide II (at 1550 cm^{-1}) vibrations that denote the protein adsorption on the surface (Figure 13.8). However, it must be considered that in the amide I spectral region also appear some water characteristic absorption signals (Sarawade *et al.*, 2007). Therefore, the obtained FT-IR spectra after protein adsorption must be compared with the spectra of samples before adsorption. The amide I/amide II intensity ratio can be used in order to follow the orientation changes of proteins (Lenk *et al.*, 1991; Roach *et al.*, 2005). This is possible because the dipole moment of the amide I and amide II are approximately perpendicular to each other, hence the changes of the ratio between these bands indicates the proteins conformational changes induced by their adsorption to a solid surface (Lenk *et al.*, 1991; Roach *et al.*, 2005). By using this method it has been shown that the network defects of glass and glass ceramic samples affect the secondary structure of BSA when adsorbed on their surfaces (Veres *et al.*, 2016).

The surface properties, including porosity and material composition, influence the protein adsorption. For example, the addition of silver in bioactive glass is aimed to minimize a potential microbial contamination by controlled release of silver ions/nanoparticles. The presence of silver may also influence the blood protein adsorption onto the used silver containing material that may have effect on the material's biocompatibility. In order to eliminate the influence of porosity on the adsorption process and to follow only the silver oxide influence on the protein adsorption, the conventional melt quenching preparation method was chosen for preparing the samples (Magyari *et al.*, 2014) and such an example of investigation is now presented. The FT-IR spectra illustrated in Figure 13.10 show that the optimal silver oxide concentration in the investigated bioactive glass system is 0.5 mol%, result reinforced by other performed analyses such as electron paramagnetic resonance (EPR and atomic force microscopy (AFM) (Magyari *et al.*, 2014).

To follow the surface changes after protein adsorption SEM images were also recorded. In Figure 13.11 are represented the SEM images of $x\text{MoO}_3 \cdot (100-x)[2\text{-SiO}_2 \cdot \text{CaO} \cdot 0.3\text{P}_2\text{O}_5]$ ($x = 0, 3, 5$ and 10%) samples before and after BSA adsorption (Ponta *et al.*, 2014). The aim of this investigation was to evaluate the efficiency of glasses containing molybdenum in the biomedical field. Molybdenum has been proven effective in the treatment

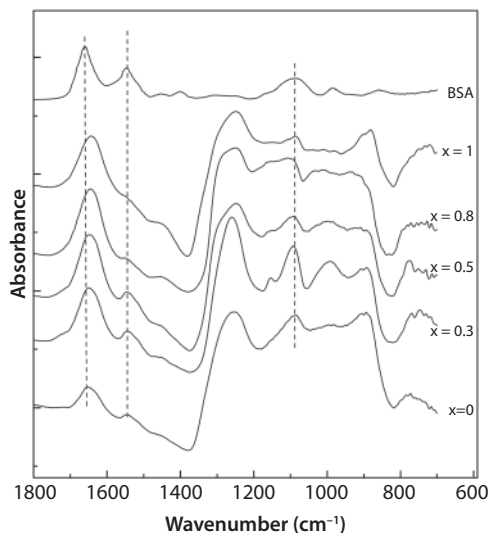


Figure 13.10 FT-IR spectra of the $60\text{P}_2\text{O}_5 \cdot 20\text{CaO} \cdot (20-x)\text{Na}_2\text{O} \cdot \text{Ag}_2\text{O}$ glass samples after BSA adsorption (Reproduced from Reference (Magyari *et al.*, 2014) with permission from the Royal Society of Chemistry).

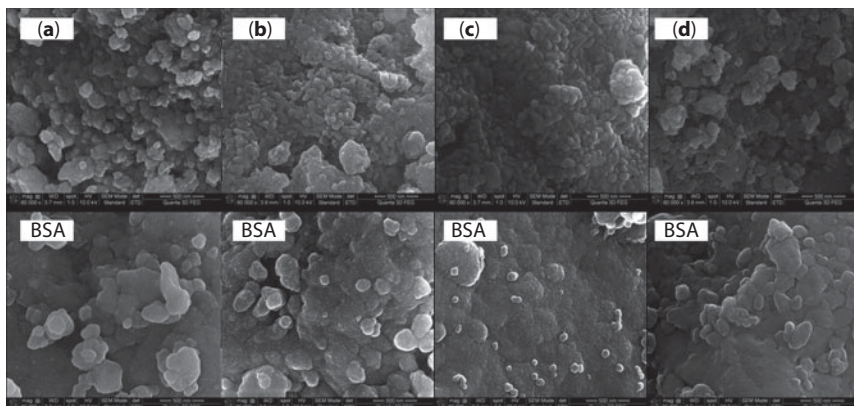


Figure 13.11 SEM images of $x\text{MoO}_3 \cdot (100-x)[2\text{-SiO}_2 \cdot \text{CaO} \cdot 0.3\text{P}_2\text{O}_5]$ samples with different MoO_3 content, before and after BSA adsorption, and SBF immersion: 0 mol% (a), 3 mol% (b), 5 mol% (c) and 10 mol% (d) (Reproduced from Reference (Ponta *et al.*, 2014) with permission of John Wiley & Sons).

of amyotrophic lateral sclerosis, Parkinson's diseases, diabetes (Stankov *et al.*, 2007) and Alzheimer's (Hille *et al.*, 2011). In the SEM images one can see that proteins cover the sample surface (Figure 13.9), thus, molybdenum content does not negatively influence the sample's biocompatibility, more than that it improves the biocompatibility performance. Taking into account the results obtained by X-ray diffraction (XRD), EPR, FT-IR and XPS it was stated that calcium molybdate crystals have a positive effect on the biological performance of silicate bioactive glasses (Ponta *et al.*, 2014).

By modifying the material's surface a higher biocompatibility can be created, but this surface alteration influences the protein adsorption. Grafting the surface by chemical

bonding represents an alternative solution to minimize structural changes of adsorbed proteins. As coupling agents can be used, for example origosinalnes (Thakur *et al.*, 2014a; Williams & Blanch 1994), vinyl monomers (Thakur *et al.*, 2014b), glutaraldehyde (Gruian *et al.*, 2015), butyl acrylate (Thakur *et al.*, 2013), etc.

Functional organosilanes with covalent attachment to glass substrate can be used for immobilizing antibodies and cellular receptors (Verne *et al.*, 2009). The silanes can form a uniform monolayer on the surface, trying to flatten the surface and allowing thus the attachment of biomolecules. In the SEM images depicted in Figure 13.12 one can see that after surface functionalization with 3-aminopropyl-triethoxylane (APTS) the surface becomes flatten, and after fibrinogen adsorption the proteins become also visible (Magyari *et al.*, 2015a). The EDX analysis confirmed the surface modification by means of elemental composition (Figure 13.13). The appearance of nitrogen and the increase of the C/Si ratio confirm the bioactive glass surface functionalization with APTS, while fibrinogen adsorption is indicated by the occurrence of nitrogen and the increase of the oxygen-silicon elemental ratio.

A possible approach to provide available sites for protein immobilization and to chemically functionalize the surface for protein attachment without losing their conformational functionality is the surface modification with a protein coupling agent (Gruian *et al.*, 2013; Williams & Blanch, 1994). Gruian *et al.*, (Gruian *et al.*, 2012a) reported that if bioactive glass surface is functionalized with glutaraldehyde (GA) the protein denaturalization is lower compared with the case when the protein is adsorbed directly on the bioactive glass surface.

In another study (Gruian *et al.*, 2012b) it was reported that GA offer more steady and precise points for protein bonding to the bioactive glass surface. When the material

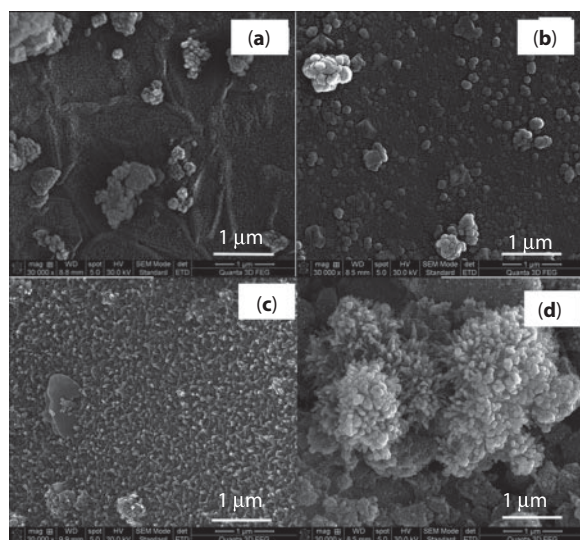


Figure 13.12 SEM images of $60\text{SiO}_2 \cdot 32\text{CaO} \cdot 8\text{P}_2\text{O}_5$ samples before (a), after surface functionalization with APTS (b), after fibrinogen adsorption on bioactive glass (c), and after fibrinogen adsorption on the functionalized sample (d) (Reproduced from Reference (Magyari *et al.*, 2015a) with permission of John Wiley & Sons).

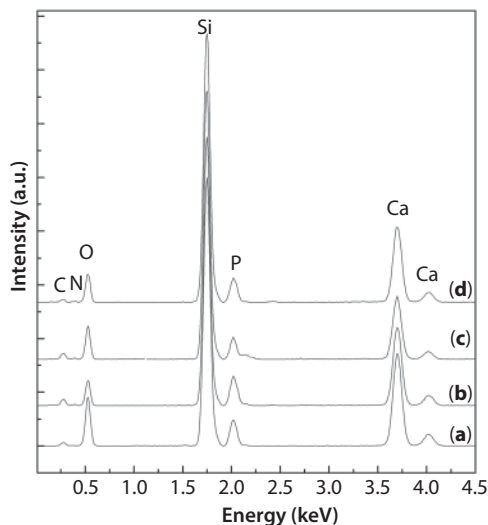


Figure 13.13 EDX spectra of $60\text{SiO}_2 \cdot 32\text{CaO} \cdot 8\text{P}_2\text{O}_5$ samples before surface modification (a), after surface modification with APTS (b), after fibrinogen adsorption on bioactive glass sample (c) and after fibrinogen adsorption on functionalized sample (d) (Reproduced from Reference (Magyari *et al.*, 2015a) with permission of John Wiley & Sons).

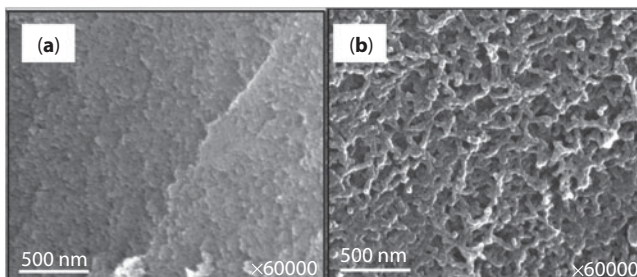


Figure 13.14 SEM images of the bioactive glass without GA (a) and with GA (b), after immersion in protein solution (Reproduced from (Gruian *et al.*, 2012b) with permission of Elsevier).

surface was not treated with GA, the protein attached to all free sites from the surface, some of the molecules being poorly attached. This statement sustained by SEM images (Figure 13.14), a more organized arrangement of the protein layer being observed when the surface is treated with GA. Moreover, GA can lead to the polymerization of hemoglobin, leading to organization of the protein molecules in chain structures of a few hundred nanometer (Figure 13.14), and as a consequence, it was concluded that GA improves the stability of the protein attachment, but reduces the amount of the adsorbed proteins (Gruian *et al.*, 2013).

It was also reported that the stability of the attached proteins is also influenced by the ionic strength of the protein solution, more protein remaining bounded to the surface after ultrasonication, when the bioactive glasses (treated or non-treated with GA) were immersed in a protein solution with lower salt content (10 mM NaCl) than in a higher one (500 mM NaCl), as can be observed in Figure 13.15.

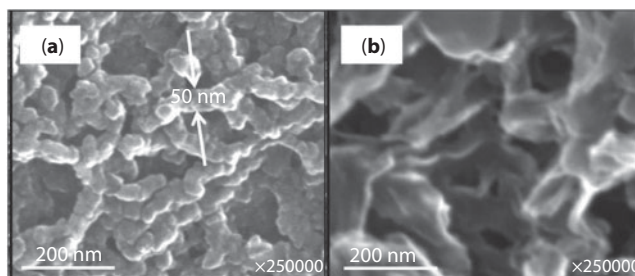


Figure 13.15 SEM images of bioactive glass with GA, after immersion in protein solution with 10 mM NaCl (a) and 500 mM NaCl (b) (Reproduced from (Gruian *et al.*, 2012b) with permission of Elsevier).

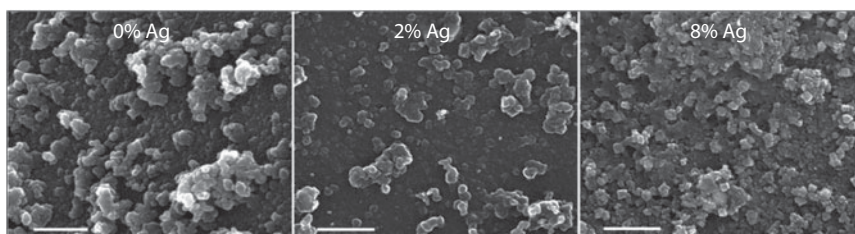


Figure 13.16 Surface morphology of protein-loaded bioactive glass substrates with different silver content (shown in the top of each image), according to SEM images (scale bars=500 nm) (Reprinted with permission from Gruian, C., *et al. J Phys Chem B*, 2013, 117(51): p. 16558–64. Copyright © 2013 American Chemical Society).

Using SEM images (Figure 13.16) it was also demonstrated that silver content from biomaterials can influence the hemoglobin immobilization. This may be happening as a result of the interaction between the thiol groups from hemoglobin structure and the silver ions from the bioactive glass (Gruian *et al.*, 2013). It was also shown that with increasing the silver content, the stability of the material-protein bond decreases. After ultrasonication only, 43%, 33%, and 31% respectively of the initially adsorbed protein remained attached on the samples with 0, 2, and 8% silver content. This may be happening due to the fact that proteins have the tendency to agglomerate around the positively charged ions (Gruian *et al.*, 2013).

13.5.2 Relation Between the Attached Proteins on Glass Surface and Bioactivity

Modifying the surface by controlled protein adsorption in order to obtain a more compatible surface, accordingly, it may alter the bioactivity of the investigated biomaterial. It is accepted that following the self-assembling of a carbonated HA layer on the surface of a material immersed in simulated body fluid (SBF) represents an easy *in vitro* way to predict the *in vivo* bioactivity of biomaterials after implantation.

Fibrinogen adsorption is one of the initial events that occur when biomaterials come into contact with the blood. Therefore, testing the initial adsorption of fibrinogen onto material surface can be a good strategy to get a biocompatible material. Considering that the fibrinogen does not cover the surface completely (Roach *et al.*, 2005), the FT-IR

imaging used for ‘visualization’ of material’s surface after fibrinogen adsorption and SBF immersion brings a useful information on this matter. For this reason one of our goal was trying to understand the effect of the fibrinogen attached on the bioactive glass surface during the apatite like phase formation (Magyari *et al.*, 2012). The obtained results confirm that the fibrinogen doesn’t attach to the entire surface and in the first part of the immersion period (three days) the HA layer grows significantly where the surface is not covered with fibrinogen (Figure 13.17). After two weeks, the HA layer extends and covers the entire surface of the biomaterial, even the fibrinogen adsorbed parts.

The inorganic ion concentration in SBF solution prepared according to Kokubo’s protocol is similar to those from human blood plasma (see Figure 13.2a). On the other hand, human blood plasma contains also several organic compounds including proteins. Having in mind this aspect, there were performed some studies (Magyari *et al.*, 2015a; Vanea *et al.*, 2010) in which *in vitro* bioactivity was evaluated in SBF solution enriched with proteins such as BSA (SBFA) or fibrinogen. Following the HA layer development on different surfaces it was found that when the sample’s surface is firstly covered with fibrinogen the formation of an apatite phase is more noticeable. It was also reported that the apatite presents a slower growth in the first immersion days of biomaterials in albumin containing SBF solution, this difference being overcome after two weeks. Exemplifications of previous remarks are given in Figure 13.18, where are compared the relative intensities of FT-IR absorption bands at 564 and 467 cm^{-1} related

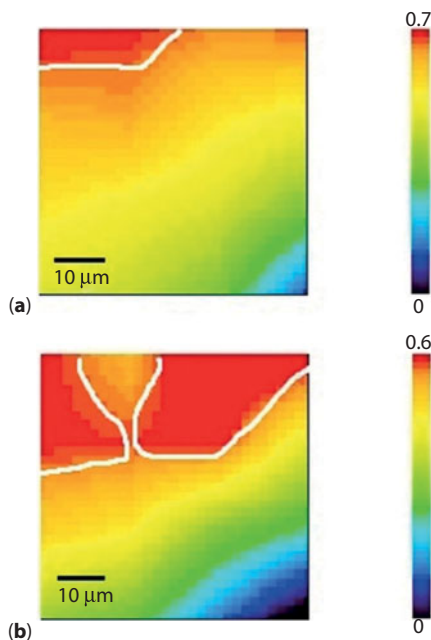


Figure 13.17 Distribution of (a) 1050 cm^{-1} PO_4^{3-} and (b) 1550 cm^{-1} amide II vibrational bands recorded after the fibrinogen attachment on the glass surface and immersion in SBF for 3 days. The right side image represents the IR band intensity. Note that the images were recorded from the same area (Reproduced from (Magyari *et al.*, 2012) with permission of Elsevier).

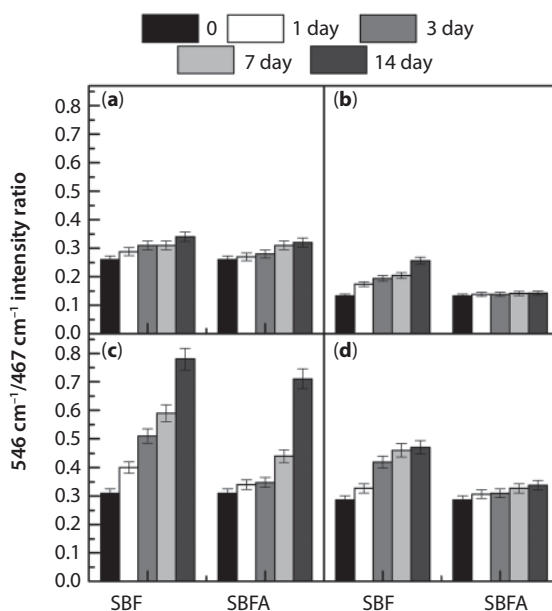


Figure 13.18 The $546\text{ cm}^{-1}/467\text{ cm}^{-1}$ intensity ratio of FT-IR spectra of $60\text{SiO}_2\cdot 32\text{CaO}\cdot 8\text{P}_2\text{O}_5$ sample (a), surface functionalized with APTS (b), fibrinogen adsorbed (c), and surface modified sample (d) after immersion in SBF and SBFA for different days (Reproduced from Reference (Magyari *et al.*, 2015a) with permission of John Wiley & Sons).

to stretching vibrations of the phosphate groups with Si-O-Si bending vibration signals. This comparison could be made only if considering the silicon content from the sample constant.

The obtained SEM images confirm the above mentioned results (Figure 13.19). The apatite layer is visible in both cases starting from the first day of immersion in albumin containing SBF. The previously attached fibrinogen remains uncovered by apatite in the first days, but it is gradually covered with increasing immersion time. When the glass sample was previously treated with APTS and adsorbed fibrinogen, after two weeks submerging in SBF, the adsorbed fibrinogen is fully covered by HA. This may be a consequence of the development of an BSA and apatite-like coating on the surface, but it is worth mentioning also the assumption that BSA may be able to dislocate some of the previously adsorbed fibrinogen ones (Pegueroles *et al.*, 2012).

13.5.3 Secondary Structure of Proteins Obtained from FT-IR Spectra

After the attachment of proteins onto surfaces, an important question that arises is related to the extent of the proteins secondary structure, if it is or not affected and if yes, in what manner and which amount. As it was mentioned in Section 4.1.3, the FT-IR spectroscopy is one of the methods that can be successfully involved for estimation of secondary structure of proteins. In the following example the results obtained from BSA adsorption onto a melt derived phosphate-based glasses with silver oxide content are presented (Magyari *et al.*, 2014). A deconvolution of the amide I signal recorded from a

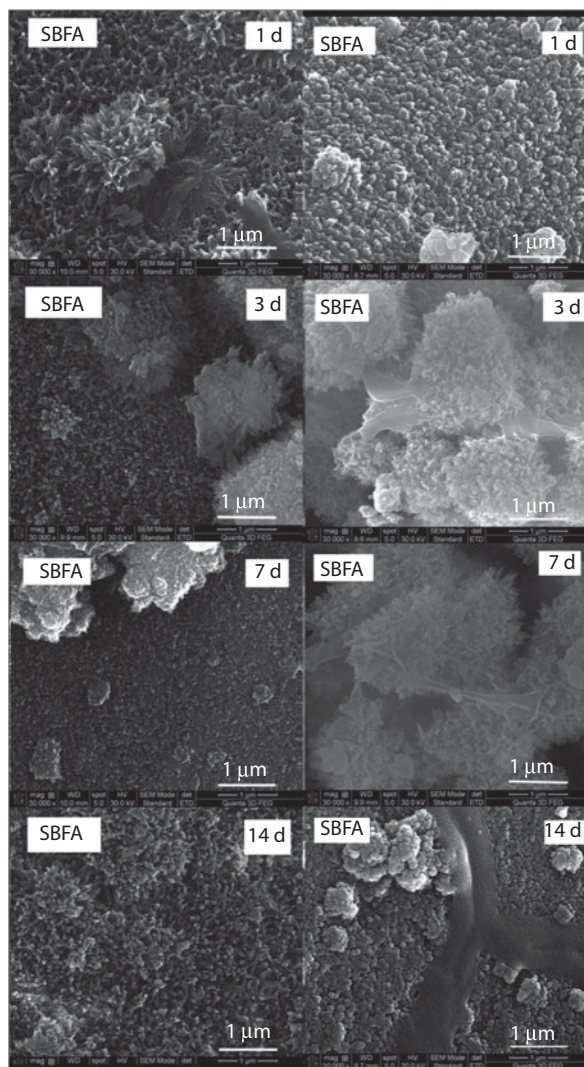


Figure 13.19 SEM images of $60\text{SiO}_2 \cdot 32\text{CaO} \cdot 8\text{P}_2\text{O}_5$ fibrinogen adsorbed sample (first column) and surface modified samples with APTS and fibrinogen (second column), after immersion in SBF with albumin (Reproduced from Reference (Magyari *et al.*, 2015a) with permission of John Wiley & Sons).

lyophilized BSA was performed assuming five components, while for the adsorbed BSA six components were considered (Figure 13.20). The new band at 1608 cm^{-1} attributed to the adsorbed protein may be due to the existence of β -sheet aggregation or amino acid side chain residues (Nafisi *et al.*, 2011). The helical structure of lyophilized BSA obtained by deconvolution of amide I band was estimated to be $60 \pm 5\%$ (Magyari *et al.*, 2014) from all present protein structure (Figure 13.21). This obtained value can be reasonably compared with the 66% value reported previously in the literature (Moriyama *et al.*, 2008). It was found that after adsorption onto glass surface, the BSA preserves its secondary structure on the samples with 0.5 mol% Ag_2O , indicating that this silver oxide content is the optimal concentration in the investigated bioactive glasses.

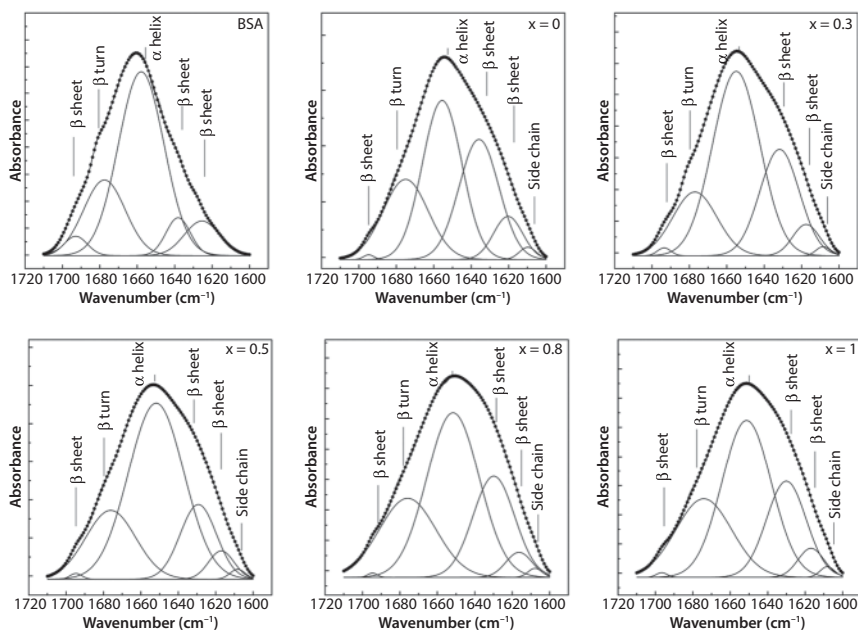


Figure 13.20 Deconvolution of the amide I (1700–1600 cm^{-1}) absorption band of the lyophilized BSA, before and after its adsorption on the bioactive $60\text{P}_2\text{O}_5\cdot 20\text{CaO}\cdot (20-x)\text{Na}_2\text{O}\cdot x\text{Ag}_2\text{O}$ glass samples' surface (Reproduced from Reference (Magyari *et al.*, 2014) with permission from the Royal Society of Chemistry).

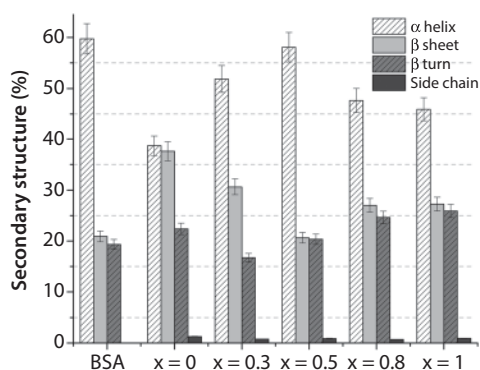


Figure 13.21 Distribution of secondary structure in lyophilized and adsorbed BSA onto $60\text{P}_2\text{O}_5\cdot 20\text{CaO}\cdot (20-x)\text{Na}_2\text{O}\cdot x\text{Ag}_2\text{O}$ glass samples' surface (Reproduced from Reference (Magyari *et al.*, 2014) with permission from the Royal Society of Chemistry).

Considering that fibrinogen has a key role in blood coagulation, its conformational changes after adsorption on material surface were intensively studied in order to predict the material's blood compatibility (Magyari *et al.*, 2015a; Steiner *et al.*, 2007; Vanea *et al.*, 2010). Thus, if the α -helix content obtained after adsorption on the material's surface is close to the native one and the β -sheet/ β -turn ratio increases, it can be considered that the investigated material is blood compatible, as obtained on aluminosilicates (Vanea *et al.*, 2010) and silicate glasses (Magyari *et al.*, 2015a). In Figure 13.22

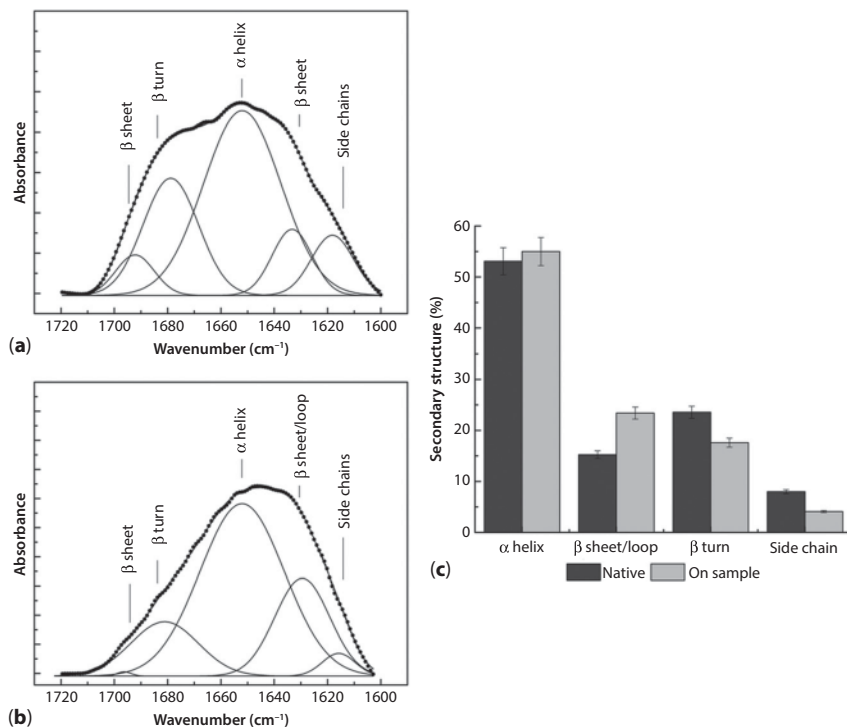


Figure 13.22 Deconvolution of the amide I (1700–1600 cm⁻¹) absorption band of lyophilized fibrinogen before (a) and after adsorption on the 45SiO₂·24.5CaO·6P₂O₅·24.5K₂O bioactive glass surface (b). Distribution of α -helix, β -sheet and β -turn secondary structures in lyophilized and adsorbed fibrinogen onto glass sample (c).

it is presented the deconvolution of the amide I absorption band of the lyophilized fibrinogen before and after adsorption on the 45SiO₂·24.5CaO·6P₂O₅·24.5K₂O bioactive glass surface. The secondary structure of fibrinogen after adsorption on glass surface evidenced only minor changes reflected in small increase of β -sheet structure and a corresponding decrease of β -turns. The appearance of these conformational changes may be caused by the electrostatic and hydrogen bonding interaction that result in alterations of the protein secondary structure. Upon adsorption the β -sheet component increases while the β -turn component decreases, which signifies that fibrinogen undergoes conformational changes toward superior β -sheet/ β -turn ratios, behavior that is a good indicative of the biocompatibility of the analyzed material.

13.6 Summary

Bioactive glasses represent an important biomaterial class usable in surgery as renewable materials. These materials after implant have a stimulatory effect on bone tissue formation, inducing enhanced osteoblastic differentiation. The bioactive glass bonds to living bone through the bonelike apatite layer, which is formed on the glass surface when it interacts with blood plasma. The apatite formation is accelerated by calcium

ion dissolved from the bioactive glass as a first step in the material transformation sequence. The proteins contained in the blood plasma (such as serum albumin, fibrinogen and hemoglobin) play an important role with regard to biomaterials biocompatibility, because by modifying the materials surface, the proteins may enhance the biocompatibility of the biomaterial with the living tissue and thus they optimize the implant.

Imaging techniques as SEM and FTIR combined with their spectroscopic counterparts prove to be viable methods in evaluation of the first events that may take place after bioactive glasses come in contact with body fluids. Moreover, the sequence and the duration of these events are strongly dependent on the material composition and surface structures, playing an important role in further acceptance or rejection of the implants by the living organism.

Acknowledgements

This work was supported by a grant of the Romanian National Authority for Scientific Research and Innovation, CNCS – UEFISCDI, project number PN-II-RU-TE-2014-4-1597. The authors would like to thank Prof. Dr. Viorica Simon for her precious advices and help given us during the chapter writing and to the PhD student Mihai Rusu for his contribution in realizing Figure 13.2.

References

- Ahmed I, Lewis M, Olsen I, Knowles JC, Phosphate glasses for tissue engineering: Part 1. Processing and characterisation of a ternary-based P_2O_5 -CaO- Na_2O glass system. *Biomaterials*, 25, 491, 2004.
- Bai ZJ, Filiaggi MJ, Dahn JR, Fibrinogen adsorption onto 316L stainless steel, Nitinol and titanium. *Surface Science* 603, 839, 2009.
- Barth A, Infrared spectroscopy of proteins *Biochimica et Biophysica Acta* 1767:1073–1101, 2007.
- Bi X, Yang X, Bostrom MP, Camacho NP, Fourier transform infrared imaging spectroscopy investigations in the pathogenesis and repair of cartilage. *Biochimica et Biophysica Acta*, 1758, 934, 2006.
- Boccaccini AR, Erol M, Stark WJ, Mohn D, Hong Z, Mano JF, Polymer/bioactive glass nanocomposites for biomedical applications: A review. *Composites Science and Technology*, 70, 1764, 2010.
- Boskey A, Pleshko Camacho N, FT-IR imaging of native and tissue-engineered bone and cartilage. *Biomaterials*, 28, 2465, 2007.
- Brash JL, Exploiting the current paradigm of blood-material interactions for the rational design of blood-compatible materials. *Journal of Biomaterials Science, Polymer Edition*, 11, 1135, 2000.
- Cai SW, Singh BR, A distinct utility of the amide III infrared band for secondary structure estimation of aqueous protein solutions using partial least squares methods. *Biochemistry*, 43, 2541, 2004.
- Carta D, Pickup DM, Knowles JC, Smith ME, Newport RJ, Sol-gel synthesis of the P_2O_5 -CaO- Na_2O - SiO_2 system as a novel bioresorbable glass. *Journal of Materials Chemistry*, 15, 2134, 2005.

- Carta D, Qiu D, Guerry P, Ahmed I, Abou Neel EA, Knowles JC, Smith ME, Newport R J, The effect of composition on the structure of sodium borophosphate glasses. *Journal of Non-Crystalline Solids*, 354, 3671, 2008.
- Chen QZ, Thompson ID, Boccaccini AR, 45S5 Bioglass-derived glass-ceramic scaffolds for bone tissue engineering. *Biomaterials*, 27, 2414, 2006.
- Chinn JA, Slack SM, *Biomaterials: Protein-Surface Interactions*, CRC Press LLC, 2000.
- Chittur KK, FT-IR/ATR for protein adsorption to biomedical surface. *Biomaterials*, 19, 357, 1998.
- Cooper EA, Knutson K, *Physical Methods to Characterize Pharmaceutical Proteins, Fourier Transform Infrared Spectroscopy Investigations of Protein Structure*. Springer Science - Business Media, New York, 1995.
- de Bruijn JD, Shankar K, Yuan H, Habibovic P, *Bioceramics and their Clinical Applications, Osteoinduction and its Evaluation*. Woodhead Publishing Limited and CRC Press LLC, Cambridge, 2008.
- Dong A, Huang P, Caughey W, Protein secondary structures in water from second-derivative amide I infrared spectra. *Biochemistry*, 29, 3303, 1990.
- Fu Q, Saiz E, Rahaman MN, Tomsia AP, Bioactive glass scaffolds for bone tissue engineering: state of the art and future perspectives. *Materials Science and Engineering C*, 31, 1245, 2011.
- Gallagher W, FTIR Analysis of Protein Structure http://www.chemu.wcedu/Chem455_S05/Pages/Manuals/FTIR_of_proteins.pdf
- Gelamo EL, Tabak M, Spectroscopic studies on the interaction of bovine (BSA) and human (HSA) serum albumins with ionic surfactants. *Spectrochimica Acta Part A: Molecular and Biomolecular Spectroscopy*, 56, 2255, 2000.
- Gerhardt LC, Boccaccini AR, Bioactive Glass and Glass-Ceramic Scaffolds for Bone Tissue Engineering. *Materials*, 3, 3867, 2010.
- Gruian C, Vanea E, Simon S, Simon V, FTIR and XPS studies of protein adsorption onto functionalized bioactive glass. *Biochimica et Biophysica Acta*, 1824, 873, 2012a.
- Gruian C, Vanea E, Steinhoff H-J, Simon S, *Handbook of Bioceramics and Biocomposites, Glass-Ceramics: Fundamental Aspects Regarding the Interaction with Proteins*. Springer International Publishing, 2015.
- Gruian C, Vulpoi A, Steinhoff HJ, Simon S, Structural changes of methemoglobin after adsorption on bioactive glass, as a function of surface functionalization and salt concentration. *Journal of Molecular Structure*, 1015, 20, 2012b.
- Gruian C, Vulpoi A, Vanea E, Oprea B, Steinhoff HJ, Simon S, The attachment affinity of hemoglobin toward silver-containing bioactive glass functionalized with glutaraldehyde. *Journal of Physical Chemistry B*, 117, 16558, 2013.
- He XM, Carter DC, Atomic structure and chemistry of human serum albumin. *Nature*, 358, 209, 1992.
- Hench LL, The story of Bioglass. *Journal of Material Science: Materials in Medicine*, 17, 967, 2006.
- Hille R, Nishino T, Bittner F, Molybdenum enzymes in higher organisms. *Coordination Chemistry Reviews*, 255, 1179, 2011.
- Hlady VV, Buijs J, Protein adsorption on solid surfaces. *Current Opinion in Biotechnology*, 7, 72, 1996.
- Hoppe A, Guldal NS, Boccaccini AR, A review of the biological response to ionic dissolution products from bioactive glasses and glass-ceramics. *Biomaterials*, 32, 2757, 2011.
- Jones JR, *Bioceramics and their Clinical Applications, Bioactive Glasses*. Woodhead Publishing Limited and CRC Press LLC, Cambridge, 2008.
- Jones JR, Review of bioactive glass: from Hench to hybrids. *Acta Biomaterialia*, 9, 4457, 2013.

- Kazarian SG, Chan KL, ATR-FTIR spectroscopic imaging: recent advances and applications to biological systems. *The Analyst*, 138, 1940, 2013.
- Knabe C, Ducheyne P, *Bioceramics and their Clinical Applications, Cellular Response to Bioactive Ceramics*. Woodhead Publishing Limited and CRC Press LLC, Cambridge, 2008.
- Kokubo T, Takadama H, How useful is SBF in predicting in vivo bone bioactivity?. *Biomaterials*, 27, 2907, 2006.
- Latour Jr RA, *Encyclopedia of Biomaterials and Biomedical Engineering, Biomaterials: Protein-Surface Interaction*, Taylor & Francis, New York, 2005.
- Lenk TJ, Horbett TA, Ratner BD, Infrared Spectroscopic Studies of Time-Dependent Changes in Fibrinogen Adsorbed to Polyurethanes. *Langmuir*, 7, 1755, 1991.
- Li R, Clark AE, Hench L, An Investigation of Bioactive Glass Powders by Sol-gel Processing. *Journal of Applied Biomaterials*, 2, 231, 1991.
- Lin S, Van den Bergh W, Baker S, Jones JR, Protein interactions with nanoporous sol-gel derived bioactive glasses. *Acta Biomaterialia*, 7, 3606, 2011.
- Lin SY, Wei YS, Hsieh TE, Li MJ, Pressure dependence of human fibrinogen correlated to the conformational alpha-helix to beta-sheet transition: an Fourier transform infrared study microspectroscopic study. *Biopolymers*, 75, 393, 2004.
- Livage J, Barbour P, Vandenborre MT, Schmutz C, Taulelle F, Sol-gel synthesis of phosphates. *Journal of Non-Crystalline Solids*, 147–148, 18, 1992.
- Lopez GP, Biebuyck AH, Harter R, Kumar A, Whitesides GM, Fabrication and Imaging of Two-Dimensional Patterns of Proteins Adsorbed on Self-Assembled Monolayers by Scanning Electron Microscopy. *Journal of the American Ceramic Society*, 115, 10774, 1993.
- Lousinian S, Kalfagiannis N, Logothetidis S, Albumin and fibrinogen adsorption on boron nitride and carbon-based thin films. *Materials Science and Engineering: B*, 152, 12, 2008.
- Magyari K, Baia L, Popescu O, Simon S, Simon V, The anchoring of fibrinogen to a bioactive glass investigated by FT-IR spectroscopy. *Vibrational Spectroscopy*, 62, 172, 2012.
- Magyari K, Baia L, Vulpoi A, Simon S, Popescu O, Simon V, Bioactivity evolution of the surface functionalized bioactive glasses. *Journal of biomedical materials research B: Applied biomaterials*, 103, 261, 2015a.
- Magyari K, Gruian C, Varga B, Ciceo-Lucacel R, Radu T, Steinhoff HJ, Varo G, Simon V, BaiaL, Addressing the optimal silver content in bioactive glass systems in terms of BSA adsorption. *Journal of Materials Chemistry B*, 2, 5799, 2014.
- Magyari K, Popescu O, Simon V, Interface processes between iron containing aluminosilicate systems and simulated body fluid enriched with protein. *Journal of materials science Materials in medicine*, 21, 1913, 2010.
- Magyari K, Stefan R, Vulpoi A, Baia L, Bioactivity evolution of calcium-free borophosphate glass with addition of titanium dioxide. *Journal of Non-Crystalline Solids*, 410, 112, 2015b.
- Martins MCL, Wang D, Ji J, Feng L, Barbosa MA, Albumin and fibrinogen adsorption on PU-PHEMA surfaces. *Biomaterials*, 24, 2067, 2003.
- Mavropoulos E, Costa AM, Costa LT, Achete CA, Mello A, Granjeiro JM, Rossi AM, Adsorption and bioactivity studies of albumin onto hydroxyapatite surface. *Colloids and Surfaces B: Biointerfaces*, 83, 1, 2011.
- Moriyama Y, Watanabe E, Kobayashi K, Harano H, Inui E, Takeda K, Secondary Structural Change of Bovine Serum Albumin in Thermal Denaturation up to 130 °C and Protective Effect of Sodium Dodecyl Sulfate on the Change. *Journal of Physical Chemistry B*, 112, 16585, 2008.
- Nabian N, Jahanshahi M, Rabiee SM, Synthesis of nano-bioactive glass-ceramic powders and its *in vitro* bioactivity study in bovine serum albumin protein. *Journal of Molecular Structure*, 998, 37, 2011.

- Nafisi S, Bagheri Sadeghi G, PanahYab A, Interaction of aspirin and vitamin C with bovine serum albumin. *Journal of photochemistry and photobiology B, Biology*, 105, 198, 2011.
- Nakanishi K, Sakiyama T, Imamura K, REVIEW On the Adsorption of Proteins on Solid Surfaces, a Common but Very Complicated Phenomenon. *Journal of Bioscience and Bioengineering*, 91, 233, 2001.
- Newbury DE, Ritchie NWM, Is Scanning Electron Microscopy/Energy Dispersive X-ray Spectrometry (SEM/EDS) Quantitative?. *Scanning*, 35, 141, 2013.
- Norde W, My voyage of discovery to proteins in flatland ...and beyond. *Colloids and Surfaces B: Biointerfaces*, 61, 1, 2008.
- Norde W, Giacomelli CE, BSA structural changes during homomolecular exchange between the adsorbed and the dissolved states. *Journal of Biotechnology*, 79, 259, 2000.
- Ogura T, *High-Contrast Observation of Unstained Proteins and Viruses by Scanning Electron Microscopy*. PLOS ONE, 7, e46904, 2012.
- Onuchic JN, Wolynes PG, *Theory of Protein Folding*. Current opinion in structural biology, 14, 70, 2004.
- Ostuni E, Chapman RG, Holmlin RE, Takayama S, Whitesides GM, A Survey of Structure-Property Relationships of Surfaces that Resist the Adsorption of Protein. *Langmuir*, 17, 5605, 2001.
- Pegueroles M, Tonda-Turo C, Planell JA, Gil FJ, Aparicio C, Adsorption of fibronectin, fibrinogen, and albumin on TiO_2 : time-resolved kinetics, structural changes, and competition study. *Biointerphases*, 7, 48, 2012.
- Petibois C, Gouspillou G, Wehbe K, Delage JP, Deleris G, Analysis of type I and IV collagens by FT-IR spectroscopy and imaging for a molecular investigation of skeletal muscle connective tissue. *Analytical and Bioanalytical Chemistry*, 386, 1961, 2006.
- Ponta O, Ciceo-Lucacel R, Vulpoi A, Radu T, Simon S, Molybdenum effect on the structure of SiO_2 -CaO- P_2O_5 bioactive xerogels and on their interface processes with simulated biofluids. *Journal of Biomedical Materials Research Part A*, 102, 3177, 2014.
- Ponta O, Gruian C, Vanea E, Oprea B, Steinhoff HJ, Simon S, Nanostructured biomaterials/biofluids interface processes: Titanium effect on methaemoglobin adsorption on titanosilicate microspheres. *Journal of Molecular Structure*, 1044, 2, 2013.
- Rahaman MN, Day DE, Bal BS, Fu Q, Jung SB, Bonewald LE, Tomsia AP, Bioactive glass in tissue engineering. *Acta biomaterialia*, 7, 2355, 2011.
- Riti PI, Vulpoi A, Simon V, Effect of pH dependent gelation time and calcination temperature on silica network in SiO_2 -CaO and SiO_2 -MgO glasses. *Journal of Non-Crystalline Solids*, 411, 76, 2015.
- Roach P, Farrar D, Perry CC. Interpretation of Protein Adsorption: Surface-Induced Conformational Changes. *Journal of the American Chemical Society*, 127, 8168, 2005.
- Sarawade PB, Kim J-K, Kim H-K, Kim H-T, High specific surface area TEOS-based aerogels with large pore volume prepared at an ambient pressure. *Applied Surface Science*, 2, 254, 574, 2007.
- Schwinte P, Voegel J-C, Picart C, Haikel Y, Schaaf P, Szalontai B, Stabilizing Effects of Various Polyelectrolyte Multilayer Films on the Structure of Adsorbed/Embedded Fibrinogen Molecules: An ATR-FTIR Study. *Journal of Physical Chemistry B*, 105, 11906, 2001.
- Severcan F, Haris PI, Fourier Transform Infrared Spectroscopy Suggests Unfolding of Loop Structures Precedes Complete Unfolding of Pig Citrate Synthase. *Biopolymers*, 69, 440, 2003.
- Sinkó K, Influence of Chemical Conditions on the Nanoporous Structure of Silicate Aerogels. *Materials*, 3, 704, 2010.
- Stankov MJ, Markovic SU, Antunovic I, odorovic M, Djurdevic P, Compounds of Mo, V and W in biochemistry and their biomedical activity. *Journal of Trace Elements in Medicine and Biology*, 21, 8, 2007.

- Steiner G, *Biomedical Imaging: Principles and Applications, Infrared and Raman Spectroscopy Imaging*, John Wiley and Son: 273–303, 2008.
- Steiner G, Tunc S, Maitz M, Salzer R, Conformational Changes during Protein Adsorption. FT-IR Spectroscopic Imaging of Adsorbed Fibrinogen Layers. *Analytical Chemistry*, 79, 1311, 2007.
- Stuart B, *Infrared Spectroscopy: Fundamentals and applications*. Wiley, 2004.
- Thakur MK, Gupta RK, Thakur VK, Surface modification of cellulose using silane coupling agent. *Carbohydrate polymers*, 111, 849, 2014a.
- Thakur VK, Thakur MK, Gupta RK, Development of functionalized cellulosic biopolymers by graft copolymerization. *International journal of biological macromolecules*, 62, 44, 2013.
- Thakur VK, Thakur MK, Gupta RK, Graft copolymers of natural fibers for green composites. *Carbohydrate polymers*, 104, 87, 2014b.
- Tronic EH, Surface Analysis of Adsorbed Proteins: A Multi-Technique Approach to Characterize Surface Structure. Doctoral dissertation, University of Washington, 2012.
- Tunc S, Maitz MF, Steiner G, Vazquez L, Pham MT, Salzer R, *In situ* conformational analysis of fibrinogen adsorbed on Si surfaces. *Colloids and Surfaces B, Biointerfaces*, 42, 219, 2005.
- Vallet-Regi M, Ragel CV, Salinas AJ, Glasses with Medical Applications. *European Journal of Inorganic Chemistry*, 6, 1029, 2003.
- Vanea E, Magyari K, Simon V, Protein attachment on aluminosilicates surface studied by XPS and FTIR spectroscopy. *Journal of Optoelectronics and Advanced Materials*, 12, 1206, 2010.
- Vanea E, Simon V, XPS study of protein adsorption onto nanocrystalline aluminosilicate microparticles. *Applied Surface Science*, 257, 2346, 2011.
- Velzenberger E, Pezron I, Legeay G, Nagel M-D, El Kirat K, Probing fibronectin-surface interactions: a multitechnique approach. *Langmuir*, 24, 11734, 2008.
- Veres R, Trandafir DL, Magyari K, Simon S, Barbos D, Simon V, Gamma irradiation effect on bioactive glasses synthesized with polyethylene-glycol template. *Ceramics International*, 42, 1990, 2016.
- Verne E, Vitale-Brovarone C, Bui E, Bianchi CL, Boccaccini AR, Surface functionalization of bioactive glasses. *Journal of Biomedical Materials Research Part A*, 90, 981, 2009.
- Vulpoi A, Gruian C, Vanea E, Baia L, Simon S, Steinhoff H J, Goller G, Simon V, Bioactivity and protein attachment onto bioactive glasses containing silver nanoparticles. *Journal of Biomedical Materials Research Part A*, 100, 1179, 2012.
- Wahlgren M, Arnebrant T, Protein adsorption to solid surfaces. *Trends in Biotechnology*, 9, 201, 1991.
- Wang K, Zhou C, Hong Y, Zhang X, A review of protein adsorption on bioceramics. *Interface Focus*, 2, 259, 2012.
- Wertz CF, Santore MM, Effect of surface hydrophobicity on adsorption and relaxation kinetics of albumin and fibrinogen: Single-species and competitive behavior. *Langmuir*, 17, 3006, 2001.
- Williams RA, Blanch HW, Covalent immobilization of protein monolayers for biosensor applications. *Biosensors and Bioelectronics*, 9, 159, 1994.
- Wu S, Liu X, Yeung KWK, Liu C, Yang X, Biomimetic porous scaffolds for bone tissue engineering. *Materials Science and Engineering: R: Reports*, 80, 1, 2014.
- Wu Y, Zhang M, Hauch KD, Horbett TA, Effect of adsorbed von Willebrand factor and fibrinogen on platelet interactions with synthetic materials under flow conditions. *Journal of Biomedical Materials Research Part A*, 85, 829, 2008.
- Yang Q, Zhang Y, Liu M, Ye M, Zhang Y, Yao S, Study of fibrinogen adsorption on hydroxyapatite and TiO₂ surfaces by electrochemical piezoelectric quartz crystal impedance and FTIR-ATR spectroscopy. *Analytica Chimica Acta*, 597, 58, 2007.
- Yaseen M, Zhao X, Freund A, Seifalian AM, Lu JR, Surface structural conformations of fibrinogen polypeptides for improved biocompatibility. *Biomaterials*, 31, 3781, 2010.

Effect of Filler Properties on the Antioxidant Response of Thermoplastic Starch Composites

Tomy J. Gutiérrez¹, Paula González Seligra², Carolina Medina Jaramillo^{2,3},
Lucía Famá^{2*} and Silvia Goyanes^{2*}

¹Composite Materials Group, Institute of Materials Science and Technology (INTEMA) (CONICET-UNMdP), Faculty of Engineering, National University of Mar del Plata and National Research Council (CONICET), Mar del Plata, Argentina

²Universidad de Buenos Aires. Facultad de Ciencias Exactas y Naturales, Departamento de Física, Laboratorio de Polímeros y Materiales Compuestos (LPM&C). Instituto de Física de Buenos Aires (IFIBA-CONICET). Ciudad Universitaria (1428), Ciudad Autónoma de Buenos Aires, Argentina

³Institute of Technology in Polymer and Nanotechnology, UBA-CONICET, Faculty of Engineering, University of Buenos Aires, Buenos Aires, Argentina

Abstract

In this chapter we will analyze different starch based nanocomposites employing two types of GRAS filler: natural filler or bactericidal filler. In one case, the filler would be acting as a mechanical reinforcement and introducing a tortuous path to the antioxidant diffusion while on the other, the filler itself has antioxidant property. In the last case, the influence of the filler dispersion into the matrix and its interface in the antioxidant efficiency of the composite will be discussed. Starch based composites with natural antioxidants, as well as with natural (cellulose and clay) and/or bactericidal nanofillers such as zinc oxide, titanium dioxide and silver nanoparticles, will be the focus of the discussion.

Keywords: Thermoplastic starch composites, natural antioxidants, natural fillers, bactericidal fillers

14.1 Introduction

Since several decades there has been great interest in science by raise awareness industries to invest in natural polymers materials in order to substitute traditional synthetics (Thakur & Kessler, 2014a,b). In this sense, biodegradable polymers such as cellulose, lignocellulose, hemicellulose, chitosan, pectin and starch, among others (Famá *et al.*, 2007; Thakur *et al.*, 2013a,b; Thakur 2014 *et al.*, 2014a,b; Anthony *et al.*, 2015; Patel, 2015; González Seligra *et al.*, 2016).

*Corresponding authors: lfama@df.uba.ar; goyanes@df.uba.ar

Polysaccharide-based biodegradable polymers, cellulose, starch specifically, reduce the use of materials made from petroleum (Thakur & Thakur, 2014a–c; Singha & Thakur, 2009a–d). Nonetheless, these matrixes used to form films have demonstrated poor mechanical properties, which are enhanced with the incorporation of several fillers such as cellulose, clays, inorganic nanoparticles, etc (Voicu *et al.*, 2016; Thakur *et al.*, 2016). Among another of the alternatives that frequently have been employed to improve the properties of films based on starch, it have the incorporation of bioactive substances as the antioxidant compounds, which have been “generally recognized as safe” (GRAS). In the same way, these food additives have allowed the development of active and functional films, since these possess beneficial effects on health. In addition, the antioxidant fillers that are conveyed through films based on starch, they achieve enhance the quality and safety of food, thus extending the useful-life of them. Nevertheless, the addition of antioxidant compounds may be limited by the hydrophobic characteristics of some of these substances. However, this drawback can be remedied with the addition of encapsulation materials, thus allowing produce films with bioactive activity with controlled release effect. Finally, in following chapter will be analyzed some legal aspects of this type of thermoplastic materials.

14.2 Starch-Based Nanocomposites

Today, the development of new and improved packaging concepts are based on extending the shelf-life of food, as well as they must also be environmentally friendly. Nonetheless, traditional packaging is based on polymers derived from petroleum, but these materials are not renewable, are expensive and may create pollution (García *et al.*, 2015). As an alternative the use of biodegradable polymers, with special emphasis on starches, has been proposed. Starches are cheap, plentiful, renewable and nontoxic (Tharanathan, 2003; Sorrentino *et al.*, 2007; Talja *et al.*, 2007). However, the properties of the starch based films such as water sensitivity, mechanical resistance, and barrier properties are not as good as films of synthetic polymers (Famá *et al.*, 2005; Famá *et al.*, 2006; Flores *et al.*, 2007; Hansen & Plackett, 2008; García *et al.*, 2009a; Dhakal & Zhang, 2012; Gutiérrez *et al.*, 2014a,b; Gutiérrez *et al.*, 2015). So that the starch can compete with synthetic polymers, these problems must be solved. One solution for this problem is to incorporate natural fillers into starch matrices, which could increase the mechanical properties, thermal stability, and water resistance of starch based films (Wang *et al.*, 2009; Famá *et al.*, 2009; Majdzadeh-Ardakani *et al.*, 2010; Aouada *et al.*, 2011). Table 14.1 shows the advantages and disadvantages of starch based films compared to films based on polymers derived from petroleum. In particular, organic and inorganic fillers are two of the more common fillers used in the development of biodegradable compounds (García *et al.*, 2009b; Famá *et al.*, 2010; Thakur *et al.*, 2010; García *et al.*, 2011; Müller *et al.*, 2011; Famá *et al.*, 2012; Sadegh-Hassani & Nafchi, 2014; Thakur & Thakur, 2014). As such, the ingredients cheapest of the composite materials are the fillers. In addition, the fillers often modify the mechanical and physicochemical properties of starch based films. Fillers depending on the application gives specific terms, such as smoke suppressors, nucleating agents, and UV stabilizers among others (Shalaby & Latour, 1997; Chawla, 1998; Medeiros *et al.*, 2001, 2002; Ray & Okamoto, 2003). Nanocomposite fillers can provide multiple advantages even if added in small amounts (Dufresne *et al.*, 2010; Famá *et al.*, 2011; Famá *et al.*, 2012; Morales *et al.*, 2015).

Table 14.1 Advantages and disadvantages of starch based films compared to films based on polymers derived from petroleum.

Type of material	Advantages	Disadvantages
Starch based films	Cheap, easy to obtain, and biodegradable.	Poor mechanical properties, high sensitivity, low permeability to gases.
Starch based films plus natural fillers	Intelligent and active films are obtained. Lower physicochemical and mechanical properties. Biodegradable.	Possible migration of the fillers on foods.
Films based on materials derived from petrochemicals	Low permeability to gases. Properties widely known.	Non biodegradable and highly polluting.

14.2.1 Starch-Based Nanocomposites with Natural Antioxidant

In recent years there has been upsurge in active packaging for food and pharmaceutical industries; mainly regarding to the development of packaging with antimicrobial or bactericidal activity, as well as with controlled release of antioxidants (Voicu *et al.*, 2016; Wu *et al.*, 2016). The incorporation of components that present these characteristics on thermoplastic materials also generates other effects due to the changes in the film microstructure, which for example, can change mechanical and barrier properties, as well, sensory properties such as opacity, color and texture (Silva-Weiss *et al.*, 2013; Pappu *et al.*, 2015).

Antioxidant use in polymeric matrices is a common practice in active packaging; however, the presence of synthetic antioxidants in foods is questioned because of potential risks; and strict legal controls are needed. The alternative focus that has been studied is the use of natural antioxidants such as tocopherol, plant extracts, and essential oils of herbs and spices. Generally, these antioxidants have as primary compounds a great number of polyphenols that are characterized by the presence of more than one phenol group for molecule (Gómez-Estaca *et al.*, 2014) and, based on the active compounds of the antioxidants, they can behave as hydrophilic or hydrophobic, granting special characteristics to the material which are applied. In this sense, the application of antioxidants in thermoplastic materials generates different behavior depending on both the matrix and the type of antioxidant used. Thus, most authors focus their study on the effect and antioxidant capacity of a material, in its mechanical behavior and permeability to water vapor properties, as they are important for its use as packaging or coatings in food and drugs.

The behavior of the polymers with the addition of antioxidants leads to changes in strain and stress at break, as well as in barrier properties.

Ghasemlou *et al.*, (2013) investigated hydrophobic antioxidants and observed that an increase in *Mentha pulegium* essential oils content from 1% to 2% (v/v) when it is incorporated into starch films caused a reduction in tensile strength ($p < 0.05$), but no significant differences were observed ($p > 0.05$) with concentrations from 2% to 3% (v/v). In contrast, the strain at break values of the film improved when the amount of *Avishan shirazi* and *Mentha pulegium* increased from 1% to 3% (v/v). The authors

attributed these results to the complex structures formed between the lipids and the starch polymers, which reduces the cohesion of the starch network forces, decreasing subsequently the resistance of the films to breakage (Jiménez *et al.*, 2013a). The addition of *Avishan shirazi* or *Mentha pulegium* improved the barrier properties of starch films, decreasing WVP up to 50% with respect to the control sample. According to Ghasemlou *et al.*, (2013), the lower WVP of the starch films with either *Avishan shirazi* or *Mentha* may be due to the hydrogen and covalent interactions between the starch network and these polyphenolic compounds.

The incorporation of hydrophilic antioxidants also leads to modifications of mechanical and barrier properties. For example, Reis *et al.*, (2015) studied the effect of the addition of mango pulp and yerba mate extracts into cassava starch films in order to test them as packaging for palm oil (Figure 14.1). The authors observed that the extracts decreased WVP of cassava starch films; due to the presence of insoluble fibers, which reduce the free space in the polymeric matrix, obstructing water vapor passage through the surfaces of films. Besides, the authors showed that mechanical properties were also altered, depending on the concentrations of mango pulp and yerba mate extracts incorporated. Compared to control, the elongation reductions ranged from 1.33% to 27.43%. A possible explanation is that free sugars naturally present in mango pulp and yerba mate, as glucose, fructose and sucrose, acted as plasticizers. Tensile strength was reduced from 33.50% to 259.59% compared with the control.

Medina Jaramillo *et al.*, (2015) reported the effect of the incorporation of yerba mate extract as antioxidant at different concentrations (5 wt.% and 20 wt.%) in cassava starch films on the antioxidant activity and physicochemical properties of the developed films. The authors observed decreases of WVP in the composites containing the extract compared to that of the matrix, being 50% lower in the case of the highest concentration of the antioxidant, as well as decreases in both Young's modulus and tensile strength values and a significant increase in the strain at break.



Figure 14.1 Cassava starch active films containing mango and yerba mate extracts tested as packaging for palm oil. From Reis *et al.*, (2015).

Kechichian *et al.*, (2010) reported the behavior of cassava starch films with the addition of different antioxidants such as: clove and its derivatives components, cinnamon, pepper, orange essential oil, coffee, honey and propolis, showing decreases in WVP and stress at break. Contrary to the expectable, the authors also observed decreases in the strain at break with respect to the matrix.

The antioxidant compounds from natural sources such as polyphenols, tocopherols, carotenoids etc., could be used to increase the stability of foods by preventing lipid peroxidation and also for protecting oxidative damage in living systems by scavenging oxygen radicals (López-Córdoba *et al.*, 2013). However, stability, bioactivity, bioavailability and unpleasant taste of most phenolic compounds limit their applications (Fang & Bhandari, 2010). Among other specific disadvantages of some antioxidant compounds, it may indicate:

1. Some flavonoids (isoflavones) and phenols have limited solubility into lipophilic systems (Viskupicova *et al.*, 2010).
2. Many polyphenols (quercetin, myricetin, taxifolin, procyanidines, salicin, thymol, and eugenol), terpenes and carotenoids are astringent and present an unpleasant flavor.
3. Some antioxidants such as ferulic acid are highly volatile, thus cannot inhibit oxidation at high temperatures for long periods of time (Nyström *et al.*, 2007).
4. Several vitamins (C, E, K) and some phytochemicals (phenols, flavonoids) are sensitive to UV-B, UV-C light and oxygen, limiting their use since most foods are exposed to such conditions (Durand *et al.*, 2010).

In this sense, some technologies of encapsulation can effectively alleviate these deficiencies. Starch based films can be regarded as encapsulating systems able to offer protection against the environment (temperature and light), improving solubility and controlling compounds release. In addition, encapsulating systems are more efficient than a direct application of the additive on the food surface, because edible films and coatings delay the migration of the agents away from the surface, helping to maintain a high concentration of bioactive compounds where necessary (Quirós-Sauceda *et al.*, 2014).

Frequently, starch derivatives and/or hydrocolloids such as cyclodextrins, sodium caseinate, carrageenan, calcium alginate and chitosan are widely used to encapsulate antioxidant.

On other hand, Partanen *et al.*, (2002) reported the benefits of cyclodextrin encapsulation of caraway fruit oil extract with maltodextrin and starch derivate. The inclusion complex seemed to protect volatile substances more efficiently during storage, whereas microcapsules with modified starches (such as wall material) were more heat tolerant. The release and thermal stability were assessed on dry samples. During rapid heating, cyclodextrin microcapsules protected the volatile substances from evaporation up to 100 °C. The protection properties of the maltodextrin microcapsules seemed to depend on the encapsulated molecules (160 °C for limonene and 120 °C for carvone). This indicates that the capsule contributes for the stabilization of bioactive compounds and prevents from degradation. In this context, edible coatings and films can protect the additives during the duration in such critical conditions (Ayala-Zavala *et al.*, 2008).

Bonilla *et al.*, (2013) used hydrophobic antioxidants such as essential oils (thyme and basil), and other components with antioxidant activity such as α -tocopherol (liposoluble antioxidant) and citric acid to incorporate into a wheat starch matrix, as well as chitosan as encapsulating agent. All evaluated systems exhibited antioxidant capacity being greater for the sample containing α -tocopherol, but the physicochemical properties of this material were affected. For thyme oil only a slight decrease in the strain at break was observed, however, films containing basil essential oil or α -tocopherol showed increases in the elastic modulus and stress at break. Although the incorporation of α -tocopherol or citric acid had a tendency to decrease WVP, essential oils had no significant impact in that parameter. In the case of citric acid it can be explained by its cross-linking effect, since a more closed matrix is formed, thus inhibiting the transfer of water molecules. The polymer phase separation induced in the films containing α -tocopherol, which enhances the tortuosity index for mass transport in the matrix may also explain the observed decrease in the WVP values (Perez-Gago & Krochta, 2001).

The effect of the addition of oleic acid and/or α -tocopherol in the properties of corn starch/sodium caseinate composite films was studied by Jimenez *et al.*, (2013b). Mechanical properties showed a decrease in the stress and an increase in the extensibility due to the presence of lipids that limit the formation of bonds between starch macromolecules due to its interaction with lipid molecules, leading to a material with more strain at break (Jimenez *et al.*, 2013a). Regarding the water vapor permeability (WVP), in principle there was a decrease in this property due to the increase in the hydrophobicity of the films; however, a slight increase thereof was observed over time due to the inhibition of the aggregation phenomenon, preventing hydrogen bond formation (Jimenez *et al.*, 2013a).

Hwang *et al.*, (2013) showed in starch/PLLA composites that the addition of α -tocopherol leads to an increase in the stress at break, without generating significant changes in the strain at break. The authors associated these results to the presence of the antioxidant which contributes to the compatibility between the chains of both polymers.

Chang-Bravo *et al.*, (2015) incorporated extract of propolis as antioxidant with carrageenan as encapsulate into a corn starch matrix film. These materials exhibited greater strain at break, as well as decreases in stress at break and Young's modulus. Figure 14.2 shows an illustration of the characteristics of encapsulated polyphenolic capsules produced by various encapsulation processes (Fang & Bhandari, 2010).

14.2.2 Starch-Based Nanocomposites with Bactericidal Fillers

In light of the recent concern for the advent of stronger and more resistant microbial attacks in foodstuffs, inorganic nanofillers have been a significant focus of investigation due to their potential activity against a wide range of microorganisms, such as bacteria, and fungi (Maneerat & Hayata 2006; Tayel *et al.*, 2011; Mohanty *et al.*, 2012; Rhim *et al.*, 2013; Kahrilas *et al.* 2014), and also because they are considered nontoxic for human body (AshaRani *et al.*, 2008; Jaberzadeh *et al.*, 2013; Fowler *et al.*, 2015). For these reasons, there has been ever increasing effort in the incorporations of inorganic nanofillers, in particular metallic and metallic oxide nanoparticles, into polysaccharide matrices to develop packaging materials in order to enhance their effectiveness in the food quality with improved convenience for final use (Chawengkijwanich & Hayata,

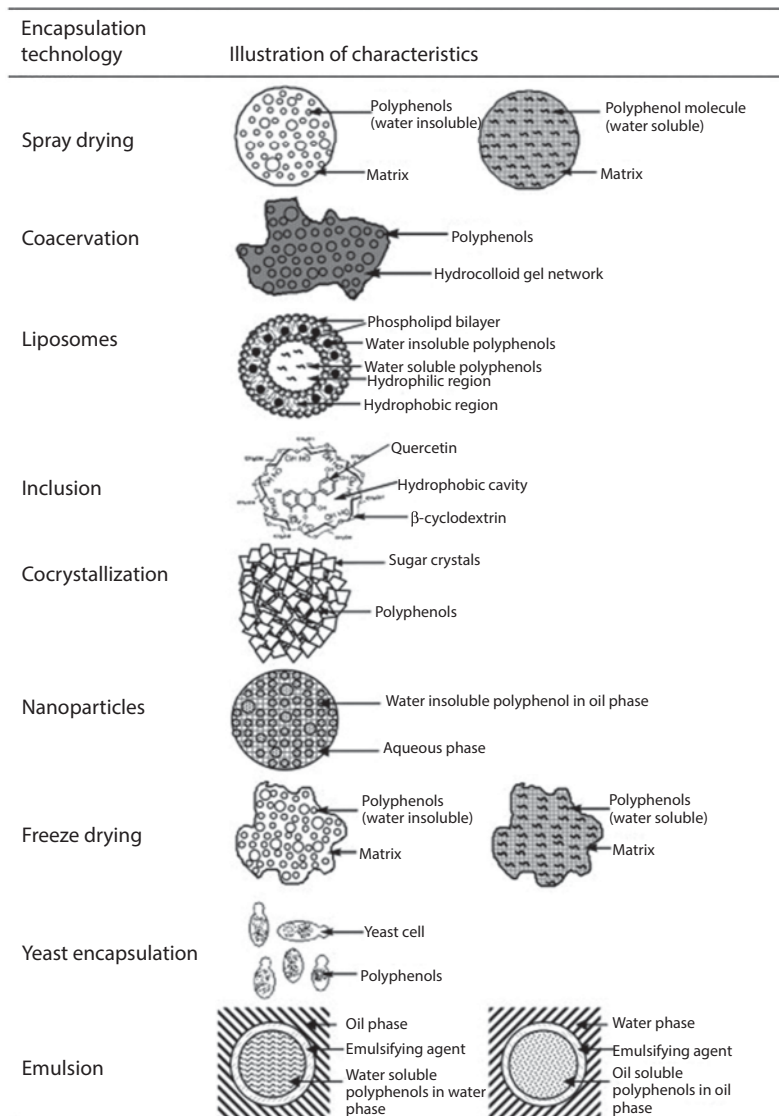


Figure 14.2 Illustration of the characteristics of encapsulated polyphenolic capsules produced by various encapsulation processes. From Fang & Bhandari (2010).

2008; Yoksan & Chirachanchai, 2010; Kanmani & Rhim, 2014; Metak, 2015). Among the antibacterial metallic nanoparticles in the literature, includes: titanium dioxide, zinc oxide and silver (Table 14.2). The exclusive and superlative physicochemical properties of these metallic nanoparticles also contribute to the great interest to use them into starch materials to be applied on food industries like a new technology.

14.2.2.1 Starch/Zinc Oxide Nanocomposites

Zinc oxide (ZnO) is a semiconductor material (n-type semiconductor) with a characteristic direct and band gap energy of 3.37 eV. It has been found highly attractive

Table 14.2 Mechanisms of action and characteristics of titanium dioxide, zinc oxide and silver nanoparticles. From Dizaj *et al.* (2014).

Type of nanoparticles	Proposed mechanism of antimicrobial action	Main characteristics as antimicrobial agent	References
Ag-NP	Ion release; induction of pits and gaps in the bacterial membrane; interact with disulfide or sulphydryl groups of enzymes that lead to disruption of metabolic processes. DNA loses its replication ability and the cell cycle halts at the G ₂ /M phase owing to the DNA damage (in the case of Ag ₂ O).	High antimicrobial activity against both bacteria and drug resistant bacteria, antifungal activity on spore producing fungal plant pathogens, high stability, nontoxicity.	Buzea <i>et al.</i> (2007), Pal <i>et al.</i> (2007), Egger <i>et al.</i> (2009), Yun <i>et al.</i> (2013), Iavicoli (2013).
ZnO-NP	ROS generation on the surface of the particles; zinc ion release, membrane dysfunction; and nanoparticles internalization into cell.	Photocatalytic activity; high stability; bactericidal effects on both Gram positive and Gram negative bacteria; antibacterial activity against spores which are resistant to high temperature and high pressure.	Ravishankar Rai <i>et al.</i> (2011), Saraf (2013), Liu <i>et al.</i> (2014), Azam <i>et al.</i> (2011), Cioffi <i>et al.</i> (2012), Rasmussen <i>et al.</i> (2010).
TiO ₂ -NP	Oxidative stress via the generation of ROS; lipid peroxidation that cause to enhance membrane fluidity and disrupt the cell integrity.	Suitable photocatalytic properties; high stability; effective antifungal for fluconazole resistant strains.	Allahverdiyev <i>et al.</i> (2011), Cioffi <i>et al.</i> (2012), Haghghi (2013), Carré (2014).

because of its remarkable application potential, for example, in solar cells, sensors, displays, gas sensors, varistors, piezoelectric devices, electroacoustic transducers, photodiodes and UV light emitting devices, gas sensors, UV absorbers, antireflection coatings, antibacterial materials, among others (Chen *et al.*, 2009; Ma *et al.*, 2009; Dastjerdi & Montazer, 2010).

In recent years nanostructures of ZnO, including particles and rods, have received increasing attention due to lower cost, white appearance and UV blocking property, compared to other metallic nanoparticles. Zinc oxide nanoparticles (ZnO-NP) are used to reinforce polymeric nanocomposites because of their very large surface area, crystalline structure and excellent mechanical properties. Another fundamental characteristic is their strong antimicrobial activity allowing them to use as antimicrobial agent (Lin *et al.*, 2009; Dastjerdi & Montazer, 2010; Shankar *et al.*, 2015). Nanosized particles of ZnO have more pronounced antimicrobial activities than large particles, since the small size and high surface to volume ratio of nanoparticles allow for better interaction with bacteria.

One cause of the antibacterial function could be the induction of intercellular reactive oxygen species, a strong oxidizing agent harmful to bacterial cell. ZnO-NP has been known to generate hydrogen peroxide (H_2O_2), which damage the cell membrane of bacteria. In addition, these nanoparticles may release Zn^{2+} ions, which could penetrate through the cell wall of bacteria and react with interior components that finally affects on viability of the cells (Nafchi *et al.*, 2012; Shankar *et al.*, 2015).

The antimicrobial activity of ZnO-NP is dependent on the cell wall structure of the bacteria. The thin peptidoglycan layer of Gram negative cell wall is sandwiched between an inner cytoplasmic cell membrane and a bacterial outer membrane, while Gram positive bacteria possess only one cytoplasmic membrane with a thick cell wall consisting of multilayers of peptidoglycan (Paisoonsin *et al.*, 2013).

Several authors have studied the effects of ZnO nanoparticles on both bacteria, Gram-positive and Gram negative. Tayel *et al.* (2011) showed that Gram positive bacteria were more sensitive than Gram negative bacteria to ZnO-NP.

In the last years, many researchers investigated the effect of ZnO-NP in polymer matrix composites. To develop these nanocomposites, there is a fundamental problem to solve: the agglomeration of the particles that occur due to the high surface energy of ZnO. There are different alternatives to prevent the formation of agglomerative nanoparticles as for example the modification of ZnO-NP surface or the use of capping agent.

Shahabi-Ghahfarrokhi *et al.*, (2015a) studied the influence of commercial ZnO nanoparticles in kefir bionanocomposite on the structure through SEM micrographs, showing that there was a lack of good affinity between ZnO-NP and kefir. However, Shankar *et al.*, (2015) prepared ZnO nanoparticles by reacting zinc nitrate or zinc acetate with sodium hydroxide and showed that, in the presence of capping agent (CMC), nanofillers were uniformly distributed in gelatin/ZnO-NP nanocomposites, and no aggregation of particles was observed.

In addition, because of their excellent mechanical properties, ZnO nanoparticles were used as reinforcement in various materials with polymer matrix (Chandramouleeswaran *et al.*, 2007; Li *et al.*, 2009; Ashraf *et al.*, 2015).

The incorporation of ZnO-NP in starch matrix composites can improve their mechanical properties and provide antibacterial properties, expanding the range of application

in food packaging, medical and pharmaceutical uses. Starch/ZnO nanocomposites were developed from different sources of starch, such as pea and sago, looking for improvements in these properties. ZnO nanoparticles were encapsulated by starch (Ma *et al.*, 2009) and by CMC (Yu *et al.* 2009) for better stabilization and dispersion in Pea starch matrix. In both studies, it was found evenly dispersion of ZnO-NP on the polymeric matrix. In another study, Rahman *et al.*, (2013) concluded, through FTIR analysis, that the interaction between starch and the ZnO nanorod was physical in nature, because after adding nanofiller in starch matrix, new functional groups was not observed.

The better the interaction between ZnO and starch is, the greater the transfer of the nanoparticle mechanical properties to the matrix. The incorporation of nanofiller caused an increase in the tensile yield strength and Young's modulus in starch based composites (Ma *et al.*, 2009; Yu *et al.*, 2009).

Antimicrobial activity was also studied in starch nanocomposites. Alebooyeh *et al.*, (2012) studied antimicrobial properties of sago starch films with ZnO nanorod by agar diffusion method. The authors demonstrated that the inhibition zone against *E. coli* O157:H7 increase by increasing ZnO nano rods contents, indicating that nanocomposites have antimicrobial activity against these microorganisms. According to this research, when the nanofillers have a rod shape, there is another possible mechanism of the antibacterial activities of the ZnO, the nanorods could act as needle and easily penetrates through cell wall, enhancing the attack on bacteria.

Nafchi *et al.*, (2012) studied the effect of sago starch film reinforced with ZnO-NP on the growth of *Staphylococcus aureus*. The results showed excellent antimicrobial activity against these bacteria. Furthermore, the inhibition zone of nanocomposites was increased by increasing ZnO-NP contents. As in previous works, SEM micrographs had shown good dispersion of nanofillers in continuous starch phase.

Ma *et al.*, (2009) study the structure and mechanical and permeability properties of nanocomposites formed by ZnO nanoparticles stabilized by soluble starch (ZnO-NP) as filler in a glycerol plasticized pea starch matrix. Increases in the tensile yield strength and Young's modulus when the concentration of filler varied from 0 to 4 wt.% and a decrease in WVP. The authors attributed these improvements to the interaction between ZnO-NP and starch matrix which provoked well dispersion of the filler in the matrix (Figure 14.3).

14.2.2.2 Starch/Titanium Oxide Nanocomposites

Titanium dioxide (TiO_2) is attractive in a wide range of industries because of its unique properties. It is chemically inert, thermally stable, poorly soluble, antibacterial from its

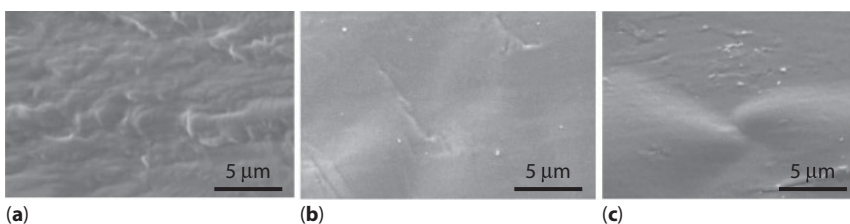


Figure 14.3 SEM micrograph of the fracture surfaces of starch/ZnO-NP composites with different concentration of filler: (a) 0 wt.%, (b) 1 wt.%, and (c) 3 wt.%. From Ma *et al.* (2009).

photoirradiation effect and resistant to corrosion; it also has broadband UV filter properties, high level of hardness, high refractive index, low cost, and it is one of the whitest chemicals that exist (Patil *et al.*, 2014). Furthermore, it is nonflammable; nontoxic for animals and humans, and it was approved by the U.S. Food and Drug Administration (FDA) (Abdullah & Kamarudin, 2015; Fowler *et al.*, 2015).

It occurs in nature in five forms, being the three more frequently used: rutile (tetragonal structure), anatase (octahedral structure) and brookite (orthorhombic structure). Among these, the most commercialized and manufactured as fine particles are rutile structure (80–92% TiO₂) and anatase structure (>94%), (Abdullah & Kamarudin, 2015) which are mostly used as pigments and catalysts.

TiO₂ rutile pigment has high light scattering properties, thereby imparting whiteness. It has been investigated to be applying for several industries, including adhesives, printing inks, coated fabrics and textiles, ceramics, floor coverings, roofing materials, water treatment agents, among others. However, for years now, rutile pigment has also been preferred to use as coating in packaging industries, acting as a white pigment because of its brightness and opacity when it is incorporated into a cover (TZMI, 2014; Abdullah & Kamarudin, 2015).

Like rutile, anatase is a more commonly occurring modification of titanium dioxide. It has been widely employed in research and development of solar cell, sewage disposal, antibacterial materials, and selfcleaning materials, because of its high photocatalytic activity (Melhem *et al.*, 2013; Wei *et al.*, 2015).

Titanium dioxide is the most important in terms of global production inorganic pigment. The global demand for TiO₂ has increased greatly as increases in the standard of living are compared over the last few years, according to the web page of University of York (2013), having a tendency to grow, being some of the producers with most capacity: DuPont, Made-in-China.com™, Cristal, Tronox, Huntsman and Ishihara Sangyo Kaisha (TZMI, 2014). Among the lots of uses of titanium dioxide, coating paints, paper and plastics takes the most proportions (University of York, 2013). Much smaller amounts of this metal are used as a semiconductor and to catalyze the photodecomposition of water into hydrogen and oxygen (Wist *et al.*, 2002; Bonilla *et al.*, 2013; Shahid *et al.*, 2015).

Due to its nontoxic characteristic, for years it was required for use in food contact materials and environmental industries, inactivating a wide variety of microorganisms in many applications in packaging industry (Singh *et al.*, 2003; Chawengkijwanich & Hayata, 2008; Patil *et al.*, 2014; Song *et al.*, 2014; Lin *et al.*, 2015). Bactericidal and fungicidal effect of TiO₂ on *E. coli*, *Salmonella choleraesuis*, *Vibrio parahaemolyticus*, *Listeria monocytogenes*, *Pseudomonas aeruginosa*, *Staphylococcus aureus*, *Diaporthe actinidiae* and *Penicillium expansum* have been reported (Wist *et al.*, 2002; Chawengkijwanich & Hayata, 2008; Lan *et al.*, 2013; Ammendolia *et al.*, 2014; Othman *et al.*, 2014; Bogdan *et al.*, 2015).

In particular, it is growing the applications of TiO₂ nanoparticles (TiO₂-NP) in the agricultural and food industries. These nanofillers have been used as a photocatalyst in food packaging film to preserve fruits and vegetables and as reinforced of biodegradable polymers nanocomposites to be applied on biotechnological food industries (Maneerat & Hayata 2006; Chawengkijwanich & Hayata, 2008; Zhou *et al.*, 2009; Song *et al.*, 2014; Lin *et al.*, 2015).

Different studies about TiO_2 -NP reported that they range of size which obviously depends on their obtaining method, is <100 nm (Yang *et al.*, 2004; Yun *et al.*, 2012; Song *et al.*, 2014; Chang *et al.*, 2014; Wang *et al.*, 2014).

TiO_2 -NP are used for the production of composites as coatings because it can confer mechanical properties such as high hardness and wear resistance mainly due to their large surface (Chaudhry *et al.*, 2008), making them an attractive material for the development of products that are in continuous exposure to movement or abrasion.

They also are of great importance as a white pigment for its dispersion properties. In a very recent research Song *et al.*, (2014) demonstrated that through the use of TiO_2 nanoparticles with starch it was possible to have a systematic approach to detect, characterize and quantify nanoparticles in food products. They also managed to quantify nanofiller in food by inductively coupled plasma optical emission spectrometry.

Among these researches, few focus on the use of TiO_2 -NP in thermoplastic starch (TPS) materials (TPS/ TiO_2 -NP). Composites based on tapioca starch containing different concentrations of this filler (1 wt.%, 3 wt.%, 5 wt.% and 7 wt.%) were studied by Nuryetti & Nasikin (2012). They showed that the prepared nanocomposites had similar energy gap range as semiconductors were effective as barriers for UV wavelength range. According to electrical conductivity behavior, the authors found that composites presented percolation thresholds when concentrations of the oxide were between 3 wt.% and 5 wt.%. Precisely, 5 wt.% is the concentration of TiO_2 -NP previously used by Follain *et al.*, (2006) to investigate their effect on the mechanical properties of TPS based nanocomposites. They observed an increase of the strength with the addition of the filler, while a decrease in strain at break occurred. They attributed that behavior to the strong interactions between starch and fillers.

Recently, Wang *et al.*, (2014) investigated the mechanical response of TiO_2 nanoparticles (0 wt.%, 0.5 wt.%, 1 wt.%, 2 wt.%, 3 wt.% or 4 wt.%) encapsulated by starch, as filler in a glycerol plasticized corn starch matrix. Synthesized TiO_2 -NP with starch revealed sizes of approximately 20 nm. Starch could form complexes with metal ions due to their high number of functional groups (hydroxyl and glucoside groups), improving the stability of TiO_2 -NP in water and preventing further aggregation of the filler. The authors revealed no residual granules of starch in the continuous thermoplastic starch phase, and tested the distribution of TiO_2 nanoparticles in the matrix detecting an evenly dispersion in the matrix, founding agglomerates of the filler in the composites with higher TiO_2 -NP concentration. In that investigation, increments about 4 times and one order of magnitude in the tensile yield strength and Young's modulus were obtained due to the interaction between TiO_2 -NP and starch matrix.

The structure of amylose/halloysite (HNT)/ TiO_2 -NP were investigated by Zheng *et al.*, (2015). They demonstrated great dispersion of TiO_2 nanoparticles which led to great photocatalytic activity, spatially effective for the photodegradation/removal of methylene blue and the persistent organic pollutant 4-nitrophenol under UV irradiation.

In the last years, some studies on starch with TiO_2 -NP have been made based on the incorporation of the filler to reinforce and increase the compatibility of starch polymers blends (Hejri *et al.*, 2012; Sreekumar *et al.*, 2012; Yun *et al.*, 2012; Fei *et al.*, 2013; Liu *et al.*, 2015). According to Liu *et al.*, (2015) 0.6% of TiO_2 -NP into high amylose starch/polyvinyl alcohol (PVA) blend based films led to the best tensile strength and water

resistance but decreases the strain at break. The results of the antimicrobial activities of the nanocomposites showed that there were inhibitory zones around the circular film disc when TiO_2 -NP were incorporated. Similarities in the mechanical behavior of starch/PVA/ TiO_2 -NP nanocomposites were reported by Sreekumar *et al.*, (2012) & Yun *et al.*, (2012) with the addition of 1 wt.% till 15 wt.% of the filler. The authors also observed increments in crystallinity and decreases in the degree of swelling in water. Yun *et al.*, (2012) demonstrated the photocatalytic degradability of the films containing TiO_2 showing photocatalytic activity under UV and visible light irradiation. When TiO_2 -NP were incorporated on starch/poly (ϵ -caprolactone) (PCL) composites the formation of hydrogen bonds and C-O-Ti bonds between the filler and the matrix generated an improvement in the interfacial interactions between the hydrophilic biopolymer (starch) and the hydrophobic one (PCL), leading to decreases on crystallinity degree and crystallization rate of the composites and increases on their mechanical properties and water resistance (Fei *et al.*, 2013).

14.2.2.3 Starch/Silver Nanocomposites

The action of silver (Ag) against bacteria, fungi and yeasts as well as the possible applications of silver polymeric nanocomposites were also discussed. Silver is an economical metal and highly toxic for microbes but not for humans when they are well treated (AshaRani *et al.*, 2008; Božanić *et al.*, 2011), so a number of products containing this element are available in the market due to its broad spectrum of antimicrobial activity (Sharma *et al.*, 2009; Latif *et al.*, 2015). It is well known that silver compounds, such as silver sulfadiazine, have been used to prevent the growth of bacteria and on the damaged skin (Božanić *et al.*, 2011). According to “The Global Source” (The Global Source, 2015), silver mine production grew year after year, being 5% higher in 2014 than the previous year.

Silver is present in these materials either in ionic (Ag^+) or metallic form (AgO). The antimicrobial function of this metal is mainly attributed to the action of both Ag^+ and AgO in nanoparticles form (Ag-NP). In particular, the antimicrobial mechanism of action of silver ions is (a) the penetration of ions in microbial cell wall and subsequent binding with phospholipids of cytoplasmic membrane, (b) binding of silver ions with bacterial DNA and subsequent disruption of DNA replication, (c) impairing the ability of ribosomes to transcribe messenger RNA, (d) inactivation of cytochrome b by binding with sulfhydryl group (Latif *et al.*, 2015). Silver nanoparticles represent the most sought after nanomaterial. This is mainly due to their unique electric (Haw, 2003; Liu *et al.*, 2010), optical (Vodnik *et al.*, 2008), catalytic (Salehi-Khojin *et al.*, 2013; Sharma *et al.*, 2009) and, particularly, antimicrobial properties (Panáček *et al.*, 2006; Hwang *et al.*, 2012), which are well established and extensively investigated mainly in require their entrapment on various matrices (Dallas *et al.*, 2011). Among their significant physicochemical properties, Ag-NP have attracted considerable interest in biological studies because of their good biocompatibility, relatively large surface area, potential antibacterial characteristics and environmentally friendliness (Rhim *et al.*, 2013).

The reduction or stopping of the microorganisms growing in biofilms due to the action of Ag-NP has been demonstrated in a number of studies (Sondi & Salopek-Sondi, 2004; Ibrahim, 2015; Franci *et al.*, 2015).

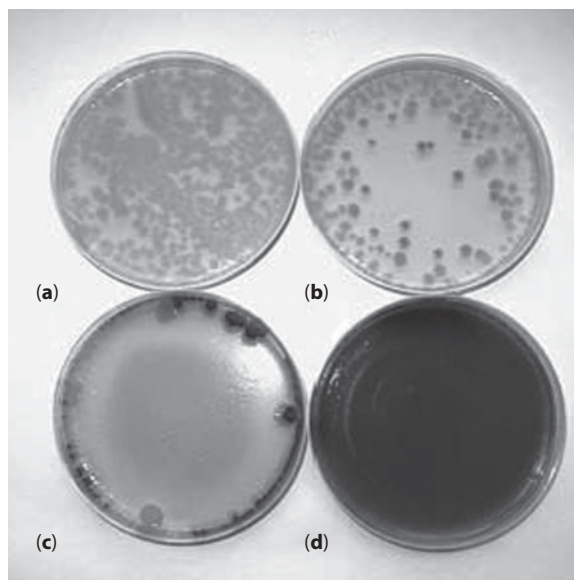


Figure 14.4 Photograph of Luria–Bertani medium plates containing different concentrations of Ag-NP: (a) 0, (b) 10, (c) 20, and (d) 50 $\mu\text{g cm}^{-3}$. From Sondi & Salopek-Sondi (2004).

The antimicrobial activity of silver nanoparticles against *E. coli* was investigated as a model for Gram negative bacteria by Sondi & Salopek-Sondi (2004). Figure 14.4 shows bacteriological tests performed in Luria–Bertani medium on solid agar plates and in liquid systems supplemented with different concentrations of Ag-NP. The authors observed that the presence of these particles (concentration of 10 $\mu\text{g cm}^{-3}$) inhibited 70% of bacterial growth. The size of bacterial colonies grown on plates with more than 20 $\mu\text{g cm}^{-3}$ of nanoparticles was significantly reduced and the colonies were mostly located at the edges of the agar plates.

Nonetheless, it is known that, at high concentrations, Ag-NP can be toxic, causing environmental damage (AshaRani *et al.*, 2009; Božanić *et al.*, 2011). In order to control or end this problem a large number of stabilizers, such as, surfactants, proteins, peptides, polymers, oligonucleotides, carbohydrates, plant extracts and organic solvents have been used to synthesize silver nanoparticles in order to obtain the desired shape silver nanomaterials and, also, to decrease the size of the filler (Sharma *et al.*, 2009; Liu *et al.*, 2011; Khan *et al.*, 2013). In such way, formation of Ag-NP in polysaccharide gels, which served both as reducing agents and stabilizers, has been of great interest (Manno *et al.*, 2008; Li *et al.*, 2015; Wang *et al.*, 2015; Yakout *et al.*, 2015).

In most research starch was used as “green” capping agent in the synthesis of silver nanoparticles, demonstrating a perfect combination for Ag-NP antibacterial activity against *E. coli* (Wang *et al.*, 2013; Kahrilas *et al.*, 2014; Salunke *et al.*, 2014; Taheri *et al.*, 2014), *S. typhi* (Mohanty *et al.*, 2012), *P. aeruginosa* (Raji *et al.*, 2012; Kahrilas *et al.*, 2014), *S. aureus* (Mohanty *et al.*, 2012; Kahrilas *et al.*, 2014), *S. flexneri* (Mohanty *et al.*, 2012), *S. epidermidis* (Raji *et al.*, 2012; Taheri *et al.*, 2014), *M. smegmatis* (Mohanty *et al.*, 2012), *Bacillus megaterium* (Wang *et al.*, 2013), *Bacillus subtilis* (Wang *et al.*, 2013; Kahrilas *et al.*, 2014), *Klebsiella pneumonia* (Kahrilas *et al.*,

2014), *P. aeruginosa* (Mohanty *et al.*, 2012) and *Janthinobacterium lividum* (Kahrilas *et al.*, 2014).

Many studies have shown that Ag-NP coated with starch are most commonly spherical with average size distributions in the range of 10–30 nm (Mohanty *et al.*, 2012; Raji *et al.*, 2012; Khan *et al.*, 2013; Ayala-Valencia *et al.*, 2013; Kahrilas *et al.*, 2014). In this sense, synthesized silver nanoparticles were one of the most common filler to perform polymeric film nanocomposites to use as antimicrobial food packaging (Incoronato *et al.*, 2010; Llorens *et al.*, 2012; Kanmani & Rhim, 2014; Metak, 2015), eliminating up to 90% the growth of microorganisms in food due to the strong antimicrobial activity of Ag-NP against a wide range of microorganisms: bacteria, viruses, and fungi, as well as to their high temperature stability and low volatility (Kumar & Münstedt, 2005). Although starch has been widely used as stabilizer agent in the synthesis of silver nanoparticles to improve their dispersion in polymeric based nanocomposites, few works to date have focused on the use of starch as compound of the matrix.

Sago starch with silver nanoparticles nanocomposites were developed as a material for the prevention of microbial growth (Božanić *et al.*, 2011). The authors demonstrated that when Ag-NP was incorporated into the starch matrix, a change in the morphology of the nanocomposites took place, presenting a relatively smooth surface. SEM analysis showed bright spots (nanoparticles) well dispersed in the biopolymer matrix. In other way, in this research antimicrobial activity of sago starch/Ag-NP nanocomposites was investigated. During the film formation part of Ag-NP was trapped in the water present in the starch system, which enabled partial oxidation into active Ag⁺ species. Due to oxidation of silver and its release into the water environment, the starch/Ag-NP films showed strong activity against *Staphylococcus aureus*, *Escherichia coli* and *Candida albicans*.

Bactericidal effect of silver nanowires incorporated into waxy corn starch films by a simple and green hydrothermal route were investigated by Valodkar *et al.*, (2010a). These nanocomposites showed inhibition against *Staphylococcus aureus* and *Escherichia coli*. The authors explained this fact to the antibacterial activity of the starch stabilized aqueous solution of Ag-NP against both Gram positive and negative bacteria. In that research it also observed increase in thermal stability and great conductivity as the concentration of Ag-NP, due to better compatibility of the starch with the filler and uniform distribution of the nanoparticles. Biodegradable nanocomposites based on potato starch glycerol reinforced by colloidal Ag-NP from an *in situ* growing process via a green chemistry approach were prepared by Cheviron *et al.*, (2014). The authors demonstrated that the use of soluble starch as stabilizer agent worked well for a correct dispersion of the nanofiller into the starch matrix. This behavior was because the soluble starch presence in the nanoparticles allowed their great dispersion the matrix due to their similar chemical structure and the high molar mass polymer chains of the starch.

As it is well known, the good dispersion of Ag nanoparticles in a starch matrix is a key point to optimize the physicochemical properties of starch/Ag-NP nanocomposites. Khachatryan *et al.*, (2013) investigated the effect of silver nanoparticles on the mechanical properties of nanocomposites based on dialdehyde starch. Although well dispersed of the filler in the matrix and with crystalline characteristics was observed by these authors (Figure 14.5), the decomposition of the composites occurred in slightly smaller temperatures than that of the matrix.

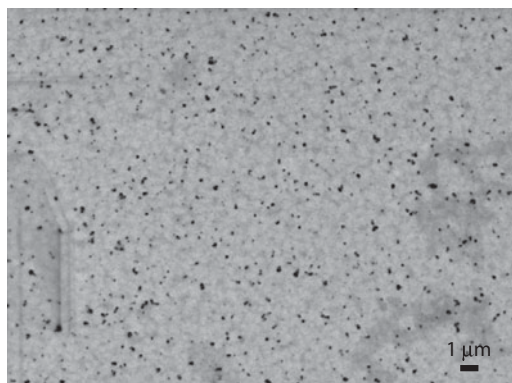


Figure 14.5 SEM image of the fracture surfaces of dialdehyde starch/Ag-NP nanocomposite. From Khachatryan *et al.* (2013).

Likewise, Yoksan & Chirachanchai (2010) observed that the use of low concentrations of Ag-NP (obtained by γ -ray irradiation reduction of silver nitrate in a chitosan solution) in a starch matrix led not markedly differences in tensile strength and strain at break respect to the matrix. Only high filler content achieved a slightly improvement in those parameters. In the case of the elastic modulus, a slight increase was obtained for all composites. In addition, composites slightly increased WVP. The authors explained this behavior to the obstruction of intermolecular hydrogen bond formation between starch molecules by Ag-NP, which caused their incompatibility to the matrix and adsorption of water vapor at the hydrophilic sites of starch.

14.2.3 Starch-based Nanocomposites with Natural Filler and Bactericidal Fillers

The use of natural fillers to improve physiochemical properties of starch films has been frequently investigated. They are generally used to form composite materials to reduce costs, since they usually are cheap with respect to synthetic materials. Among the several natural fillers used as reinforcing fillers in biopolymers based on starch found in the literature, cellulose and clay are striking for their important effects on starch nanocomposites properties (Averous, 2004; Orts *et al.*, 2005; Lu *et al.*, 2006; Zhao *et al.*, 2008; Alemdar & Sain, 2008; Dufresne *et al.*, 2010; Rodney *et al.*, 2015).

Cellulose can be considered as a string of cellulose crystallites, linked along the chain axis by amorphous domains (Klemm *et al.*, 2005; Dufresne *et al.*, 2010). Their structure consists of a predominantly crystalline cellulosic core which is covered with a sheath of paracrystalline polyglucosan material surrounded by hemicelluloses (Sarkanen & Ludwig, 1971; Meshitsuka & Isogai, 1996; Thakur & Singha, 2013; Thakur, 2013; Thakur & Thakur, 2014). It has low cost, availability, renewability, light weight, nanoscale dimension, low density and coefficient of thermal expansion, non-toxicity, unique morphology, sustainability and green issues. The properties of these biomaterials continue stimulating the development of structural materials different to petroleum derivatives (Spence *et al.*, 2011; Khalil *et al.*, 2015; Shahabi-Ghahafarrokh *et al.*, 2015b; Thakur *et al.*, 2013c).

Cellulose nanofibrils have been the most studied organic reinforcement in starch based nanocomposites, due to their remarkable mechanical properties. The affinity between starch and cellulose due to their similarity in structural can be exploited, not only to enhance the mechanical properties of composites, but also to produce biodegradable materials (Averous, 2004; Zhao *et al.*, 2008; Dufresne *et al.*, 2010).

In starch based nanocomposites, the mechanical properties are strongly related to moisture content and humidity conditions and the addition of nanofibrils on nanocomposites can reduce water uptake.

In a study of glycerol plasticized starch nanocomposites reinforced with cellulose nanofibrils from wheat straw, Alemдар & Sain (2008) found that the addition of 10 wt.% of cellulose nanofibrils improved the tensile strength and Young's modulus of the composites. Nanocomposites based on wheat starch plasticized with glycerol and reinforced with cellulose nanofibrils extracted from ramie fibers by acid hydrolysis (Lu *et al.*, 2006) showed improvement in water resistance, good dispersion, good adhesion between components, an increase in Young's modulus (from 56 to 480 MPa), and improvement in tensile strength (from 2.8 to 6.9 MPa) with increasing filler content from 0 to 40 wt.%.

On other hand, the addition of cellulose microfibrils extracted from cotton, softwood, or bacterial cellulose at low concentrations to wheat or potato starch blended with pectin has a significant effect on their mechanical properties (Orts *et al.*, 2005). Young's modulus of wheat starch nanocomposites reinforced with cotton nanofibrils increased by 5 times with the addition of only 2.1 wt.% of nanofibrils.

Likewise, strong interactions between cellulose nanofibers prepared from cottonseed linters and between the filler and the glycerol plasticized starch matrix were reported to play a key role in reinforcing properties (Lu *et al.*, 2005).

More recently, Rodney *et al.*, (2015) demonstrated that the addition of 5% (v/v) of tea tree fiber as filler (tea tree leaf, tea tree branch and tea tree trunk) improved the tensile strength of tapioca starch composites up to 34.39% in the first case, 82.80% in tea tree branch reinforced starch composites and 203.18% in the last composite.

On the other hand, spite that cellulose hasn't oxidant activity, recently Bumbudsanpharoke *et al.*, (2015) used cellulose as support for incorporating gold nanoparticles, and they found an antioxidant effect in that nanocomposite due to the addition of Au nanoparticles which were bioreduced to Au⁰ from Au³⁺. According to the authors these results suggests the possible application of the material for antioxidant food packaging.

Also, Sonkaew *et al.*, (2012) evaluated antioxidant activity of curcumin on cellulose based films, founding an antioxidant effect on the developed films due to the presence of curcumin. However, the effect on the mechanical properties of these nanocomposites have not been evaluated, therefore, it is interesting its future study.

Clays such as montmorillonite, muscovite, talcum, kaolinite, hectrite, and saponite are other alternatives to use as reinforced starch composites. They have been frequently used as pristine layered silicates, which are combined with biopolymeric materials as starch to form nanocomposites reinforced (Ray & Okamoto, 2003), thus improving the mechanical properties, resistance to water uptake, thermal resistance and water vapor permeability of natural biopolymeric nanocomposite materials based on starch (Huang & Yu, 2006; Chiou *et al.*, 2007; Magalhães & Andrade, 2009; Dufresne *et al.*, 2010). Likewise, the clays have been modified by different ways in order to improve its

adhesiveness, compatibility, dispersion and orientation within the polymeric matrix (De Carvalho *et al.*, 2001; Shen *et al.*, 2002; Fischer, 2003; Wan *et al.*, 2003).

Nanoclay also has demonstrated significant antimicrobial activity against *Escherichia coli*, *Staphylococcus aureus* and *Candida albicans*. For this reason, these films have been suggested for food industry applications (Egger *et al.*, 2009; Chandrasekaran *et al.*, 2011, Xie *et al.*, 2011).

On the other hand, clays usually contain hydrated sodium or potassium ions (Giannelis, 1996) and in this state these silicates are miscible only with hydrophilic polymers such as starches (Pandey *et al.*, 2005; Ray & Okamoto, 2003). Nonetheless, the majority of the starch clay nanocomposites have poor dispersion, which is an important property in creating high performance materials (Chung *et al.*, 2010). For this reason, the incorporation of chitosan as a compatibilizer has improved the dispersion of nanoclays, because chitosan is a natural polysaccharide that is compatible with the starch matrix, in addition to allowing the cation exchange clay-chitosan. In the same way, starches have also been modified in order to improve the dispersion of the clays.

Moreover, often the effect on the increase in mechanical properties has been remarkable to filler concentrations from 5–8% (Park *et al.*, 2003; Huang & Yu, 2006). Likewise, a higher elastic modulus has been found in films from waxy maize starch with clay aggregates (Chiou *et al.*, 2005). This could be explained by the low amylose content, since lack of amylose implies a lower number of cross-links bonds between amylose and clay, leading to a lower elastic modulus.

Another of the recent applications which has had the clays in the starch based polymeric systems is the controlled migration of Ag nanoparticles, which have antioxidant properties and antimicrobial (Rhim *et al.*, 2006; Fernández *et al.*, 2010; Valodkar *et al.*, 2010b; Abreu *et al.*, 2015). Others nanoparticles such as Cu, Zn, Mg, etc. have also been incorporated into starch based films through the ion exchange, which occurs in clays. These films are a predominant application of inorganic biocides (Ohashi *et al.*, 1998; Whilton *et al.*, 1998; Patakfalvi & Dékány, 2004; Patil *et al.*, 2005). According to Abreu *et al.*, (2015), the incorporation of Ag nanoparticles vehicled through clay has shown to improve the mechanical properties and gas permeability of the systems evaluated. Even the addition of Ag nanoparticles not significantly affect the color and opacity of the films based on starch. For this reason, the authors concluded that these types of nanocomposites have great potential to be used as nanostructured packaging material, which ensures the food quality and safety.

Nonetheless, one of the controversies of this type of system has been reported by Avella *et al.*, (2005), who showed that the migration of metals from biodegradable starch/clay nanocomposite films used for pakaging of vegetable samples was minimal. Although the authors suggest that more studies are needed to arrive to testify that this type of metals does not affect the sensory quality of food, and neither has detrimental effects on the health of consumers.

Varaprasad *et al.*, (2016) successfully fabricated antibacterial cellulose fibers by utilizing nano zinc oxide. The author synthesized ZnO by precipitation technique and then impregnated effectively over cellulose fibers through sodium alginate matrix (ZnO–SACNF) (Figure 14.6). They observed an effective bonding interaction between the compounds, as well as a feasibility of the fabricated fibers for longer duration utility

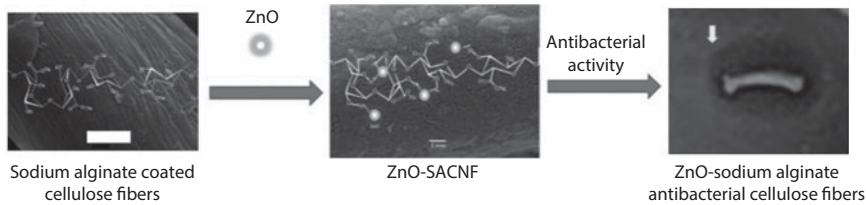


Figure 14.6 Schematic diagram of nano zinc oxide–sodium alginate antibacterial cellulose fibers. From Varaprasad *et al.* (2016).

without any significant damage or breakage. The antibacterial studies against *E. coli* revealed the excellent bacterial devastation property of ZnO-SACNF.

14.3 Regulatory Aspect

Considering the new tendencies to introduce the nanotechnology in the food industry, the Regulation (EC) No 1935/2004¹ and the Regulation (EC) No 450/2009² of the European Parliament and of the Council on materials and articles intended to come into contact with food introduces specific provisions concerning “active” packaging which extends the shelf life of food, or provides information on its freshness. All materials used to package food must satisfy Regulation requirements.

Only a few EU legal acts incorporate a nanomaterial definition No 1169/2011³ and 10/2011⁴ on food information to consumers and plastic food contact materials, respectively, and No 1223/2009⁵ and 528/2013⁶ on cosmetic and biocidal products, respectively. Interestingly, the definition in two former regulations is different from the one in the two latter definitions. In 2011 the European Commission published a Recommendation on the definition of a nanomaterial (2011/696/EU⁷). A draft law on

¹ Regulation (EC) No 1935/2004 of the European Parliament and the Council of 27 October 2004 on materials and articles intended to come into contact with food and repealing Directives 80/590/EEC and 89/109/EEC. *Official Journal of the European Union* L 138/4.

² Commission Regulation (EC) No 450/2009 of the Commission of the European Communities of 29 May 2009 on active and intelligent materials and articles intended to come into contact with food. *Official Journal of the European Union* L 135/3.

³ Regulation (EU) No 1169/2011 of the European Parliament and of the Council of 25 October 2011 on the provision of food information to consumers, amending Regulations (EC) No 1924/2006 and (EC) No 1925/2006. *Official Journal of the European Union* L 304, 18–63.

⁴ Commission Regulation (EU) No 10/2011 of 14 January 2011 on plastic materials and articles intended to come into contact with food. *Official Journal of the European Union* L12(1), 1–89.

⁵ Regulation (EC) No 1223/2009 of the European Parliament and of the Council of 30 November 2009 on cosmetic products. *Official Journal of the European Union* L342, 59–209.

⁶ Regulation (EU) No 528/2013 of the European Parliament and of the Council of 22 May 2012 concerning the making available on the market and use of biocidal products. *Official Journal of the European Union* L167, 1–121.

⁷ Recommendations Commission Regulation (EU) of 18 October 2011 on the definition of nanomaterial (2011/696/EU). *Official Journal of the European Union* L 275/38.

novel food (COM/2013/0435⁸) also provides a legal basis to regulate nanomaterials or the application of nanotechnology in food products (Peters *et al.*, 2014).

The use of metallic nanofiller in food package materials may present potential risks because metal particles can migrate during contact with food unacceptable quantities. In this sense EC normative requires that the food contact materials be safe and do not transfer their components into the foodstuff improperly, and thus prevent damage on both human health and the environment. Two types of migration limits have been established by EC: one, that applies to all substances that can migrate from the packaging to the product, consists on an overall migration limit of 60 mg (of substances)/kg (of food); and other that consists on a specific migration limit which applies individual authorized substances and a toxicological evaluation.

According to the uses and restrictions of the Code of Federal Regulations of the U.S. Food and Drug Administration (FDA) on food products, titanium dioxide quantity does not exceed 1% by weight of the food. Different directives introduce rules on disposal, monitoring and surveillance and programs for the reduction of pollution, with the aims to prevent and progressively reduce pollution caused by waste from the titanium dioxide industry. Titanium nitride is authorized in the EU for its use as additive or polymer production aid in plastic food contact materials (EU Regulation 1183/2012⁹).

The GRAS Substances (SCOGS¹⁰) Database, which allows access to opinions and conclusions from reports on the safety of Generally Recognized As Safe (GRAS) food substances published that there is no evidence in the available information on zinc oxide that demonstrates, or suggests reasonable grounds to suspect, a hazard to the public. The available information of that database indicates that a wide margin exists between present intake levels of zinc salts and those that have been reported to produce noticeably harmful effects.

The “Risk assessment status” query of silver nanoparticles was retrieved from a very limited number of studies, for example, being synthetic amorphous silica in food. Risk assessments are made very carefully because of the uncertainties in both the hazard and the human exposure data. Only a few EU legal acts incorporate a nanomaterial definition on food information to consumers and plastic food contact materials, respectively. Non EU countries have rather adopted a broader approach which builds mainly on guidance for industry. In the case of the safety, health and environmental effects of nanosilver, levels in blood and organs depend both on the dose and on the size of the silver nanomaterials used. Some excretion of silver can occur via feces. Finally, human toxicity of nanosilver has been considering as low (Peters *et al.*, 2014).

The food additive silicon dioxide may be safely used in food when it is used in an amount not to exceed 2% by weight of the food in only those foods in which the additive has been demonstrated to have an anticaking effect (FDA). The use of silicon dioxide in a direct form, which means that it can be added directly to food, is currently

⁸ Regulation of the European Parliament and of the Council (EC) on novel foods COM/2013/0894. *European Commission* Brussels, 18.12.2013.

⁹ Commission Regulation No 1183/2012 of 30 November 2012 amending and correcting Regulation (EU) No 10/2011 on plastic materials and articles intended to come into contact with food. *Official Journal of the European Union* L 338/11.

¹⁰ Select Committee on GRAS Substances (SCOGS), 2013. Opinion: Zinc oxide. From <http://www.fda.gov/Food/IngredientsPackagingLabeling/GRAS/SCOGS/ucm261016.htm>

regulated under several Regulations (21 CFR¹¹). As an indirect use, silicon dioxide can also be employed in the manufacture of coatings and polymers that are then used as components of food packaging materials. There are many FDA clearances for the indirect use of silicon dioxide under 21 CFR 175, 176, I 77 and 178. Regarding the safety of the silicates, the Committee on GRAS Substances (SCOGS) stated that there is no scientific evidence that demonstrates or suggests reasonable grounds to suspect a hazard to the public when silica is used at current levels, and provides further support that silicon dioxide is GRAS when added either directly or indirectly to food.

14.4 Conclusions and Outlook

Health and environmental concerns associated the advent of stronger and more resistant microbial attacks in foodstuffs as well to the synthetics packaging used in the food industry could be minimized by the use of alternative ecofriendly materials that provide biodegradability and potential activity against microorganisms. These materials must also have such features that preserve or improve the properties of a packaging. In this chapter a review of the most important recent results of starch based nanocomposites containing GRAS filler was exposed. On the one hand, the effect of bactericidal fillers such as titanium dioxide, zinc oxide and silver on starch materials was analyzed; and on the other hand, natural filler such as cellulose and clay nanoparticles plus natural antioxidants as additives on starch materials was explored. Finally, the influence of encapsulate the natural antioxidant or antimicrobial to use as additive in polymer composites was discussed.

Practically, all studies evaluated have shown that regardless of the nanofiller used (organic or inorganic), the mechanical properties of composites improve showing materials more resistant to possible impacts or cracks at the time of being used to coat or package food products. Among this advantage, inorganic nanofillers have attracted considerable interest in bionanotechnology because they have better mechanical properties than natural nanoparticles, as well as they can provide a value added because they present potential antibacterial characteristics by antonomasia. The most frequent nanofillers used to reinforce starch matrix in food industry are natural because they are mostly compatible with the starch, while metallic nanofillers need several processes with reducing agents and/or stabilizers to achieve good dispersion into a polymer matrix. When nanofillers without antimicrobial or antioxidant characteristics are used it is necessary to add any additive to the composition to form a product that can transmit these properties. However, often the addition of antioxidant compounds may be limited by their hydrophobic characteristics. It is shown that this drawback can be remedied encapsulating the additives. Several studies demonstrated that the incorporation of antimicrobial in encapsulation way produce films with bioactive activity with controlled release effect, living more efficient materials to a direct application on food surfaces, delaying the migration of the agents away from the surface, maintaining a high concentration of bioactive compounds and being able to control where they are

¹¹ FDA. US. Food and Drug Administration, 2015. CFR - Code of Federal Regulations. Food and Drug. Food and Drug Administration Department of Health and Human Services, Code of Federal Regulations, 1, Title 21, C 1. (2015).

needed. Starch nanocomposites with encapsulated antimicrobials also improve water vapor barrier and mechanical properties but increase oxygen permeability and decrease gloss and transparency of the films.

The requirements with regard to the use of packaging materials, such as that food contact materials be safe and do not transfer their components into the foodstuff have also been described. Unacceptable quantities of metallic nanofiller in food package materials may present potential risks. There is still not enough scientific data to prove health problems associated with the use of the mentioned inorganic fillers; however there is no doubt that a greater effort in the search for possible unintended effects is necessary.

The possibility of incorporating coatings or packaging with antibacterial effects on food products is one of the most promising forms to promote active packaging technologies. From this perspective, it is clear that starch nanocomposite containing both, natural nanofiller (plus antioxidant and/or antimicrobial) and inorganic filler, will act as coating or packaging to food products with an “added value”.

It is important to note that most of the literature research mentioned in this chapter conducted their investigations at a laboratory scale because antibacterial efficiency may be influenced by interfering substances that inhibit antibacterial action. In view of the observed beneficial effects on the exposed materials in laboratory scale, the scaleup of the production of these materials is expectable in order to allow them to be turned into marketable products, resulting a very good opportunity for new preservation trends.

Acknowledgements

The authors would like to thank the Consejo Nacional de Investigaciones Científicas y Técnicas (CONICET PIP 2014-2016 Project 11220120100508CO), University of Buenos Aires (2014-2017 Project 20020130100495BA) and PICT-2012-1093.

References

- Abdullah, N., Kamarudin, S.K., Titanium dioxide in fuel cell technology: An overview. *J. Power Sources*, 278, 109, 2015.
- Abreu, A.S., Oliveira, M., de Sá, A., Rodrigues, R.M., Cerqueira, M.A., Vicente, A.A., Machado, A.V., Antimicrobial nanostructured starch based films for packaging. *Carbohydr. Polym.*, 129, 127, 2015.
- Alebooyeh, R., Nafchi, A.M., Jokar, M., The Effects of ZnO nanorods on the characteristics of sago starch biodegradable films. *J. Chem. Health Risks*, 2, 13, 2012.
- Alemdar, A., Sain, M., Biocomposites from wheat straw nanofibers: Morphology, thermal and mechanical properties. *Compos. Sci. Technol.*, 68, 557, 2008.
- Allahverdiyev A.M., Abamor E.S., Bagirova, M., Rafailovich, M., Antimicrobial effects of TiO₂ and Ag₂O nanoparticles against drug-resistant bacteria and leishmania parasites. *Future Microbiol.*, 6, 933, 2011.
- Ammendolia, M.G., Iosi, F., De Berardis, B., Guccione, G., Superti, F., Conte, M.P., Longhi, C., *Listeria monocytogenes* behaviour in presence of non-UV-irradiated titanium dioxide nanoparticles. *PLOS one*, 9, e84986, 2014.

- Anthony, R., Xiang, Z., Runge, T., Paper coating performance of hemicellulose-rich natural polymer from distiller's grains. *Prog. Org. Coat.*, 89, 240, 2015.
- Aouada, F.A., Mattoso, L.H.C., Longo, E., New strategies in the preparation of exfoliated thermoplastic starch-montmorillonite nanocomposites. *Ind. Crop. Prod.*, 34, 1502, 2011.
- AshaRani, P.V., Low Kah Mun, G., Hande, M.P., Valiyaveetil, S., Cytotoxicity and genotoxicity of silver nanoparticles in human cells. *ACS Nano*, 3, 279, 2009.
- Asharani, P.V., Wu, Y.L., Gong, Z., Valiyaveetil, S., Toxicity of silver nanoparticles in zebrafish models. *Nanotechnology*, 19, 255102, 2008.
- Ashraf, M., Abd E, Ahmed M. Synthesis of ZnO nanoparticles and studying its influence on the antimicrobial, anticorrosion and mechanical behavior of polyurethane composite for surface coating. *Dyes and Pigments*, 121, 282, 2015.
- Avella, M., De Vlieger, J.J., Errico, M.E., Fischer, S., Vacca, P., Volpe, M.G., Biodegradable starch/clay nanocomposite films for food packaging applications. *Food Chem.*, 93, 467, 2005.
- Averous, L., Biodegradable multiphase systems based on plasticized starch: A review. *J. Macromol. Sci. Polym. Rev. C*, 44, 231, 2004.
- Ayala-Valencia, G., Cristina de Oliveira Vercik, L., Ferrari, R., Vercik, A., Synthesis and characterization of silver nanoparticles using water-soluble starch and its antibacterial activity on *Staphylococcus aureus*. *Starch-Stärke*, 65, 931, 2013.
- Ayala-Zavala, J., Del Toro Sánchez, L., Álvarez Parrilla, E., González Aguilar, G., High relative humidity in package of fresh cut fruits and vegetables: advantage or disadvantage considering microbiological problems and antimicrobial delivering systems. *J. Food Sci.*, 73, R41, 2008.
- Azam, A., Ahmed, A.S., Oves, M., Khan, M.S., Habib, S.S., Memic, A., Antimicrobial activity of metal oxide nanoparticles against Gram-positive and Gram-negative bacteria: a comparative study. *Int. J. Nanomedicine*, 7, 6003, 2011.
- Bogdan, J., Jackowska-Tracz, A., Zarzyńska, J., Pławińska-Czarnak, J., Chances and limitations of nanosized titanium dioxide practical application in view of its physicochemical properties. *Nanoscale Res. Lett.*, 10, 1, 2015.
- Bonilla, J., Talón, E., Atarés, L., Vargas, M., Chiralt, A., Effect of the incorporation of antioxidants on physicochemical and antioxidant properties of wheat starch-chitosan films. *J. Food Eng.*, 118, 271, 2013.
- Božanić, D.K., Djoković, V., Dimitrijević-Branković, S., Krsmanović, R., McPherson, M., Nair, P. S., Georges, M. K., Radhakrishnan, T., Inhibition of microbial growth by silver-starch nanocomposite thin films. *J. Biomat. Sci.-Polym. E*, 22, 2343, 2011.
- Bumbudsanpharoke, N., Choi, J., Park, I., Ko, S., Facile biosynthesis and antioxidant property of nanogold-cellulose fiber composite. *J. Nanomater.*, 2015, 1, 2015.
- Buzea, C., Pacheco, I.I., Robbie, K., Nanomaterials and nanoparticles: sources and toxicity. *Biointerphases*, 2, MR17, 2007.
- Carré, G., Hamon, E., Ennahar, S., Estner, M., Lett, M.-C., Horvatovich, P., Gies, J.-P., Keller, V., Keller, N., Andre, P., TiO₂ photocatalysis damages lipids and proteins in *Escherichia coli*. *Appl. Environ. Microbiol.*, 80, 2573, 2014.
- Chandramouleeswaran, S., Mhaske S.T., Kathe, A.A., Varadarajan, P.V., Prasad, V., Vigneshwaran N., Functional behaviour of polypropylene/ZnO-soluble starch nanocomposites. *Nanotechn.*, 18, 385702, 2007.
- Chandrasekaran, G., Han, H.K., Kim, G.J., Shin, H. J., Antimicrobial activity of delaminated aminopropyl functionalized magnesium phyllosilicates. *Appl. Clay Sci.*, 53, 729, 2011.
- Chang-Bravo, L., López-Córdoba, A., Martino, M., Biopolymeric matrices made of carrageenan and corn starch for the antioxidant extracts delivery of Cuban red propolis and yerba mate. *Reactive and Functional Polymers*, 85, 11, 2015.
- Chang, Q., Wang, Y., Cerneaux, S., Zhou, J.E., Zhang, X., Wang, X., Dong, Y., Preparation of microfiltration membrane supports using coarse alumina grains coated by nano TiO₂ as raw materials. *J. Eur. Ceram. Soc.*, 34, 4355, 2014.

- Chaudhry, Q., Scotter, M., Blackburn, J., Ross, B., Boxall, A., Castle, L., Aitken, R., Watkins, R., Applications and implications of nanotechnologies for the food sector. *Food Addit. Contam.*, 25, 241, 2008.
- Chawengkijwanich, C., Hayata, Y., Development of TiO₂ powder-coated food packaging film and its ability to inactivate *Escherichia coli* *in vitro* and in actual tests. *Int. J. Food Microbiol.*, 123, 288, 2008.
- Chawla, K.K. (Ed.), *Composite Materials, Science and Engineering*, New York: Springer, New York, USA, 1998.
- Chen, Y.W., Qiao, Q., Liu, Y.C., Yang, G.L., Size-Controlled Synthesis and Optical Properties of Small-Sized ZnO Nanorods. *J. Phys. Chem. C*, 113, 7497, 2009.
- Cheviron, P., Gouanvé, F., Espuche, E., Green synthesis of colloid silver nanoparticles and resulting biodegradable starch/silver nanocomposites. *Carbohydr. Polym.*, 108, 291, 2014.
- Chiou, B.-S., Wood, D., Yee, E., Imam, S.H., Glenn, G.M., Orts, W.J., *Polym. Eng. Sci.*, 47, 1898, 2007.
- Chiou, B.-S., Yee, E., Glenn, G.M., Orts, W.J., Rheology of starch–clay nanocomposites. *Carbohydr. Polym.*, 59, 467, 2005.
- Chung, Y.L., Ansari, S., Estevez, L., Hayrapetyan, S., Giannelis, E.P., Lai, H.M., Preparation and properties of biodegradable starch–clay nanocomposites. *Carbohydr. Polym.*, 79, 391, 2010.
- Cioffi, N., Rai, M., Nano-antimicrobials, *Synthesis and Characterization of Novel Nano Antimicrobials*, N. Cioffi, M. Rai (Eds.), Springer, Berlin Heidelberg, 2012.
- Dallas, P., Sharma, V.K., Zboril, R., Silver polymeric nanocomposites as advanced antimicrobial agents: classification, synthetic paths, applications, and perspectives. *Adv. Colloid Interfac.*, 166, 119, 2011.
- De Carvalho, A.J.F., Curvelo, A.A.S., Agnelli, J.A.M., A first insight on composites of thermoplastic starch and kaolin. *Carbohydr. Polym.*, 45, 189, 2001.
- Dhokal, H.N., Zhang, Z., Polymer matrix composites: moisture effects and dimensional stability, in: *Wiley encyclopedia of composites*, L. Nicolais and A. Borsachiello (Eds.), Wiley, New York, 2012.
- Dizaj, S.M., Lotfipour F., Barzegar-Jalali, M., Zarrintan, M.H., Adibkia, K., Antimicrobial Activity of the Metals and Metal Oxides Nanoparticles, *Mater. Sci. Eng. C*, 44, 278, 2014.
- Dastjerdi, R., Montazer, M., A review on the application of inorganic nano-structured materials in the modification of textiles: Focus on anti-microbial properties. *Colloids. Surf. B*, 79, 5, 2010.
- Dufresne, A., Medeiros, E.S., Orts, W.J., Starch-based nanocomposites. Bertolini A (Ed), *Starch: Characterization, properties, and applications*, LLC Boca Raton. p. 250, 2010.
- Durand, L., Habran, N., Henschel, V., Amighi, K., Encapsulation of ethylhexyl methoxycinnamate, a light-sensitive UV filter, in lipid nanoparticles. *J. Microencapsul.*, 27, 714, 2010.
- Egger, S., Lehmann, R.P., Height, M.J., Loessner, M.J., Schuppler, M., Antimicrobial properties of a novel silver-silica nanocomposite material. *Appl. Environ. Microb.*, 75, 2973, 2009.
- Famá, L., Bittante, A.M.B.Q., Sobral, P.J.A., Goyanes, S., Gerschenson, L.N., Garlic powder and wheat bran as fillers: their effect on the physicochemical properties of edible biocomposites. *Mat. Sci. Eng. C*, 30, 853, 2010.
- Famá, L., Flores, S.K., Gerschenson, L., Goyanes, S., Physical characterization of cassava starch biofilms with special reference to dynamic mechanical properties at low temperatures. *Carbohydr. Polym.*, 66, 8, 2006.
- Famá, L., Gañan, P., Bernal, C., Goyanes, S., Biodegradable starch nanocomposites with low water vapor permeability and high storage modulus. *Carbohydr. Polym.*, 87, 1989, 2012.
- Famá, L., Gerschenson, L., Goyanes, S., Starch-vegetable fiber composites to protect food products. *Carbohydr. Polym.*, 75, 230, 2009.

- Famá, L., Gerschenson, L., Goyanes, S., Influence of storage time at room temperature in physicochemical properties of tapioca starch edible films. *Carbohydr. Polym.*, 70, 265, 2007.
- Famá, L., Pettarin, V., Goyanes, S., Bernal, C.R., Starch based nanocomposites with improved mechanical properties. *Carbohydr. Polym.*, 83, 1226, 2011.
- Famá, L., Rojas, A.M., Goyanes, S., Gerschenson, L., Mechanical properties of tapioca-starch edible films containing sorbates. *LWT - Food Sci. Technol.*, 38, 631, 2005.
- Flores, S., Famá, L., Rojas, A.N., Goyanes, S., Gerschenson, L., Physicochemical properties of tapioca-starch edible films. Influence of gelatinization and drying technique. *Food Res. Int.*, 4, 257, 2007.
- Fang, Z., Bhandari, B., Encapsulation of polyphenols-a review. *Trends Food Sci. Technol.*, 21, 510, 2010.
- Fei, P., Shi, Y., Zhou, M., Cai, J., Tang, S., Xiong, H., Effects of nano-TiO₂ on the properties and structures of starch/poly (ϵ -caprolactone) composites. *J. Appl. Polym. Sci.*, 130, 4129, 2013.
- Fernández, A., Soriano, E., Hernández-Muñoz, P., Gavara, R., Migration of antimicrobial silver from composites of polylactide with silver zeolites. *J. Food Sci.*, 75, E186, 2010.
- Fischer, H., Polymer nanocomposites: From fundamental research to specific applications. *Mat. Sci. Eng. C.*, 23, 763, 2003.
- Follain, N., Joly, C., Dole, P., Roge, B., Mathlouthi, M., Quaternary starch based blends: Influence of a fourth component addition to the starch/water/glycerol system. *Carbohydr. Polym.*, 63, 400, 2006.
- Fowler, B.A., Prusiewicz, C.M., Nordberg, M., Metal Toxicology in Developing Countries, in: *Handbook on the Toxicology of Metals* (4th Ed.), M. Nordberg, B.A. Fowler and M. Nordberg (Eds.), Vol. I General Considerations, pp. 529-545, Elsevier B.V., London, 2015.
- Franci, G., Falanga, A., Galdiero, S., Palomba, L., Rai, M., Morelli, G., Galdiero, M., Silver Nanoparticles as Potential Antibacterial Agents. *Molecules*, 20, 8856, 2015.
- García, N.L., Famá, L., D'Accorso, N.B., & Goyanes, S., Biodegradable Starch Nanocomposites. In: Kumar TV and Kumari TM (Eds.), *Eco-friendly Polymer Nanocomposites*, Springer India, pp. 17-77, 2015.
- García, N.L., Famá, L., Dufresne, A., Aranguren, A., Goyanes, S., A comparison between the physico-chemical properties of tuber and cereal starches. *Food Res. Int.*, 42, 976, 2009a.
- García, N.L., Ribba, L., Dufresne, A., Aranguren, M., Goyanes, S., Physico mechanical properties of biodegradable starch nanocomposites. *Macromol. Mater. Eng.*, 294, 169, 2009b.
- García, N.L., Ribba, L., Dufresne, A., Aranguren, M., Goyanes, S., Effect of glycerol on the morphology of nanocomposites made from thermoplastic starch and starch nanocrystals. *Carbohydr. Polym.*, 84, 203, 2011.
- Ghasemlou, M., Aliheidari, N., Fahmi, R., Shojaei-Aliabadi, S., Keshavarz, B., Cran, M.J., Khaksar, R., Physical, mechanical and barrier properties of corn starch films incorporated with plant essential oils. *Carbohydr. Polym.*, 98, 1117, 2013.
- Giannelis, E.P., Polymer layered silicate nanocomposites. *Adv. Mater.*, 8, 29, 1996.
- Gómez-Estaca, J., López-de-Dicastillo, C., Hernández-Muñoz, P., Catalá, R., Gavara, R., Advances in antioxidant active food packaging. *Trends Food Sci. Tech.*, 35, 42, 2014.
- González Seligra, P., Medina Jaramillo, C., Famá, L., Goyanes, S., Biodegradable and non-retrogradable eco-films based on starch-glycerol with citric acid as cross-linking agent. *Carbohydr. Polym.*, 138, 66, 2016.
- Gutiérrez, T.J., Pérez, E., Guzmán, R., Tapia, M.S., Famá, L., Physicochemical and functional properties of native and modified by cross-linking, dark-cush-cush yam (*Dioscorea trifida*) and cassava (*Manihot esculenta*) starch. *J. Polym. Biopol. Phys. Chem.*, 2(1), 1, 2014a.
- Gutiérrez, T.J., Tapia, M.S., Pérez, E., Famá, L., Edible films based on native and phosphorylated 80:20 waxy:normal corn starch. *Starch/Stärke*, 66, 1, 2014b.

- Gutiérrez, T.J., Pérez, E., Guzmán, R., Tapia, M.S., Famá, L., Structural and mechanical properties of native and modified cush-cush yam and cassava starch edible films. *Food Hydrocolloid.*, 45, 211, 2015.
- Haghighi, F., Roudbar Mohammadi, S., Mohammadi, P., Hosseinkhani, S., Shipour, R., Antifungal Activity of TiO_2 nanoparticles and EDTA on *Candida albicans* Biofilms. *Infect. Epidemiol. Med.*, 1, 33, 2013.
- Hansen, N.M.L., Plackett, D., Sustainable films and coatings from hemicelluloses: a review. *Biomacromolecules*, 9, 1494, 2008.
- Haw, M., Holographic data storage: The light fantastic. *Nature*, 422, 556, 2003.
- Hejri, Z., Ahmadpour, A., Seifkordi, A.A., Zebajad, S.M., Role of nano-sized TiO_2 on mechanical and thermal behavior of starch/poly (vinyl alcohol) blend films. *International Congress on Nanoscience and Nanotechnology (ICNN)*, 8, 215, 2012.
- Huang, M., Yu, J., Structure and properties of thermoplastic corn starch/montmorillonite biodegradable composites. *J. Appl. Polym. Sci.*, 99, 170, 2006.
- Hwang, I.S., Hwang, J.H., Choi, H., Kim, K.J., Lee, D.G., Synergistic effects between silver nanoparticles and antibiotics and the mechanisms involved. *J. Med. Microbiol.*, 61, 1719, 2012.
- Hwang, S.W., Shim, J.K., Selke, S., Soto-Valdez, H., Matuana, L., Rubino, M., Auras, R., Migration of α -tocopherol and resveratrol from poly(L-lactic acid)/starch blends films into ethanol. *J. Food Engineer.*, 116, 814, 2013.
- Iavicoli, I., Fontana, L., Leso, V., Bergamaschi, A., The Effects of Nanomaterials as Endocrine Disruptors. *Int. J. Mol. Sci.*, 14, 16732, 2013.
- Ibrahim, H.M.M., Green synthesis and characterization of silver nanoparticles using banana peel extract and their antimicrobial activity against representative microorganisms. *J. Radiation Res. Appl. Scie.*, 8, 265, 2015.
- Incoronato, A.L., Buonocore, G.G., Conte, A., Lavorgna, M., Del Nobile, M.A., Active systems based on silver-montmorillonite nanoparticles embedded into bio-based polymer matrices for packaging applications. *J. Food Protect.*, 73, 2256, 2010.
- Jabberzadeh, A., Moaveni, P., Tohidi Moghadam, H.R., Zahedi, H., Influence of Bulk and Nanoparticles Titanium Foliar Application on some Agronomic Traits, Seed Gluten and Starch Contents of Wheat Subjected to Water Deficit Stress. *Not Bot Horti Agrobo*, 41, 201, 2013.
- Jiménez, A., Fabra, M. J., Talens, P., Chiralt, A., Phase transitions in starch based films containing fatty acids. Effect on water sorption and mechanical behavior. *Food Hydrocolloid.*, 30, 408, 2013a.
- Jiménez, A., Fabra, M. J., Talens, P., Chiralt, A., Physical properties and antioxidant capacity of starch–sodium caseinate films containing lipids. *J. Food Engineer.*, 116, 695, 2013b.
- Kahrilas, G.A., Haggren, W., Read, R.L., Wally, L.M., Fredrick, S.J., Hiskey, M., Prieto, A.L., Owens, J.E., Investigation of antibacterial activity by silver nanoparticles prepared by microwave-assisted green syntheses with soluble starch, dextrose, and arabinose. *ACS Sustainable Chem. Eng.*, 2, 590, 2014.
- Kanmani, P., Rhim, J.W., 2014. Nano and nanocomposite antimicrobial materials for food packaging applications. *Prog. Nanomat. Food Packag.*, 34.
- Kechichian, V., Ditchfield, C., Veiga-Santos, P., Tadini, C.C., Natural antimicrobial ingredients incorporated in biodegradable films based on cassava starch. *LWT - Food Sci. Technol.*, 43, 1088, 2010.
- Khachatryan, K., Khachatryan, G., Fiedorowicz, M., Para, A., Tomasik, P., Formation of nano-metal particles in the dialdehyde starch matrix. *Carbohydr. Polym.*, 98, 568, 2013.
- Khalil, H.A., Bhat, A.H., Bakar, A.A., Tahir, P.M., Zaidul, I.S.M., Jawaid, M., Cellulosic Nanocomposites from Natural Fibers for Medical Applications: A Review, in: *Handbook of*

- Polymer Nanocomposites. Processing, Performance and Application*, J.K. Pandey, H. Takagi and Nakagaito (Eds.), pp. 475-511, Springer, Berlin Heidelberg, 2015.
- Khan, Z., Singh, T., Hussain, J.I., Obaid, A.Y., AL-Thabaiti, S.A., El-Mossalamy, E.H., Starch-directed green synthesis, characterization and morphology of silver nanoparticles. *Colloid. Surfaces B*, 102, 578, 2013.
- Klemm, D., Heublein, B., Fink, H.-P., Boh, A., Cellulose: Fascinating biopolymer and sustainable raw material. *Angew. Chem. Int. Ed.*, 44, 3358, 2005.
- Kumar, R., Münstedt, H., Silver ion release from antimicrobial polyamide/silver composites. *Biomater.*, 26, 2081, 2005.
- Lan, Y., Lu, Y., Ren, Z., Mini review on photocatalysis of titanium dioxide nanoparticles and their solar applications. *Nano Energy*, 2, 1031, 2013.
- Latif, U., Al-Rubeaan, K., Saeb, A.T., A review on antimicrobial chitosan-silver nanocomposites: A roadmap toward pathogen targeted synthesis. *Int. J. Polymer. Mat. and Polymer. Biomater.*, 64, 448, 2015.
- Li, J.H., Hong, R.H., Li, M.Y., Li, H.Z., Zheng, Y., Ding, J., Effects of ZnO nanoparticles on the mechanical and antibacterial properties of polyurethane coatings. *Prog. Org. Coat.*, 64, 504, 2009.
- Li, Y.F., Gan, W.P., Jian, Z.H.O.U., Lu, Z.Q., Chao, Y.A.N.G., Ge, T.T., Hydrothermal synthesis of silver nanoparticles in Arabic gum aqueous solutions. *T. Nonferr. Metal. Soc.*, 25, 2081, 2015.
- Lin, W., Xu, Y., Huang, C., Ma, Y., Shannon, K., Chen, D., Huang, Y., Toxicity of nano- and micro-sized ZnO particles in human lung epithelial cells. *J Nanopart. Res.*, 11, 25, 2009.
- Lin, B., Luo, Y., Teng, Z., Zhang, B., Zhou, B., Wang, Q., Development of silver/titanium dioxide/chitosan adipate nanocomposite as an antibacterial coating for fruit storage. *LWT - Food Sci. Technol.*, 63, 1206, 2015.
- Liu, C.J., Burghaus, U., Besenbacher, F., Wang, Z.L., Preparation and characterization of nanomaterials for sustainable energy production. *ACS nano.*, 4, 5517, 2010.
- Liu, Y., Liu, X., Wang, X., Biomimetic synthesis of gelatin polypeptide-assisted noble-metal nanoparticles and their interaction study. *Nanoscale Res. Lett.*, 6, 22, 2011.
- Liu, Q., Zhang, M., Fang, Z., Rong, X., Effects of ZnO nanoparticles and microwave heating on the sterilization and product quality of vacuum packaged Caixin. *J. Sci. Food Agric.*, 94, 2547, 2014.
- Liu, C., Xiong, H., Chen, X., Lin, S., Tu, Y., Effects of nano-tio₂ on the performance of high-amylose starch based antibacterial films. *J. Appl. Polym. Sci.*, 132, 42339, 2015.
- Llorens, A., Lloret, E., Picouet, P.A., Trbojevich, R., Fernandez, A., Metallic-based micro and nanocomposites in food contact materials and active food packaging. *Trends Food Sci. Technol.*, 24, 19, 2012.
- López-Córdoba, A., Deladino, L., Martino, M., Effect of starch filler on calcium-alginate hydrogels loaded with yerba mate antioxidants. *Carbohydr. Polym.*, 95, 315, 2013.
- Lu, Y., Weng, L., Cao, X., Biocomposites of plasticized starch reinforced with cellulose crystallites from cottonseed. *Macromol. Biosci.*, 5, 1101, 2005.
- Lu, Y., Weng, L., Cao, X., Morphology, thermal and mechanical properties of ramie crystallites-reinforced plasticized starch biocomposites. *Carbohydr. Polym.*, 63, 198, 2006.
- Ma, X., Chang, P.R., Jang, J., Yu, J., Preparation and properties of glycerol plasticized-pea starch/zinc oxide-starch bionanocomposites. *Carbohydr. Polym.*, 75, 472, 2009.
- Magalhães, N.F., Andrade, C.T., Thermoplastic corn starch/clay hybrids: Effect of clay type and content on physical properties. *Carbohydr. Polym.*, 75, 712, 2009.
- Majdzhadeh-Ardakani, K., Navarchian, A.H., Sadeghi, F., Optimization of mechanical properties of thermoplastic starch/clay nanocomposites. *Carbohydr. Polym.*, 79, 547, 2010.
- Maneerat, C., Hayata, Y., Antifungal activity of TiO₂ photocatalysis against *Penicillium expansum* in vitro and in fruit tests. *Int. J. Food Microbiol.*, 107, 99, 2006.

- Manno, D., Filippo, E., Di Giulio, M., Serra, A., Synthesis and characterization of starch-stabilized Ag nanostructures for sensors applications. *J. Non-Cryst. Solids*, 354, 5515, 2008.
- Medeiros, E.S., Tocchetto, R.S., Carvalho, L.H., Conceicao, M.M., Souza, A.G., Nucleating effect and dynamic crystallization of a polypropylene/attapulgit. *J. Therm. Anal. Calorim.*, 67, 279, 2002.
- Medeiros, E.S., Tocchetto, R.S., Carvalho, L.H., Santos, I.M.G., Souza, A.G., Nucleating effect and dynamic crystallization of a polypropylene/talc system. *J. Therm. Anal. Calorim.*, 66, 523, 2001.
- Medina Jaramillo, C., González Seligra, P., Goyanes, S., Bernal, C., Famá, L., Biofilms based on cassava starch containing extract of yerba mate as antioxidant and plasticizer. *Starch-Stärke*, 67, 780, 2015.
- Melhem, H., Simon, P., Wang, J., Di Bin, C., Ratier, B., Leconte, Y., Herlin-Boime, N., Makowska-Janusik, M., Kassiba, A., Bouclé, J., Direct photocurrent generation from nitrogen doped TiO₂ electrodes in solid-state dye-sensitized solar cells: Towards optically-active metal oxides for photovoltaic applications. *Sol. Energ. Mat. Sol. C.*, 117, 624, 2013.
- Meshitsuka, G., Isogai, A., Chemical Structures of Cellulose, Hemicelluloses and Lignin. In: *Chemical Modification of Lignocellulosic Materials*, D.-N.S. Hon (Ed.), Marcel Dekker Inc, New York, NY, 1996.
- Metak, A.M., Effects of nanocomposite based nano-silver and nano-titanium dioxide on food packaging materials. *Int. J. Appl. Sci. Technol.*, 5, 26, 2015.
- Mohanty, S., Mishra, S., Jena, P., Jacob, B., Sarkar, B., Sonawane, A., An investigation on the antibacterial, cytotoxic, and antibiofilm efficacy of starch-stabilized silver nanoparticles. *Nanomedicine*, 8, 916, 2012.
- Morales, N.J., Candal, R., Famá, L., Goyanes, S., Rubiolo, G.H., Improving the physical properties of starch using a new kind of water dispersible nano-hybrid reinforcement. *Carbohydr. Polym.*, 127, 291, 2015.
- Müller, C., Laurindo, J., Yamashita, F., Effect of nanoclay incorporation method on mechanical and water vapor barrier properties of starch-based films. *Ind. Crop. Prod.*, 33, 605, 2011.
- Nafchi, A.M., Alias, A.K., Mahmud, S., Robal, M., Antimicrobial, rheological, and physico-chemical properties of sago starch films filled with nanorod-rich zinc oxide. *J. Food. Eng.*, 113, 511, 2012.
- Nuryetti, H.H., Nasikin, M., Structure, energy band gap and electrical conductivity of tapioca/metal oxide composite. *J. Chem. Chem. Eng.*, 6, 911, 2012.
- Nyström, L., Achrenius, T., Lampi, A., Moreau, R., Piironen, V., A comparison of the antioxidant properties of steryl ferulates with tocopherol at high temperatures. *Food Chem.*, 101, 947, 2007.
- Ohashi, F., Oya, A., Duclaux, L., Beguin, F., Structural model calculation of antimicrobial and antifungal agents derived from clay minerals. *Appl. Clay Sci.*, 12, 435, 1998.
- Orts, W.J., Shey, J., Imam, S.H., Glenn, G.M., Guttman, M.E., Revol, J.-F., Application of cellulose microfibrils in polymer nanocomposites. *J. Polym. Environ.*, 13, 301, 2005.
- Othman, S.H., Abd Salam, N.R., Zainal, N., Kadir Basha, R., Talib, R.A., Antimicrobial activity of TiO₂ nanoparticle-coated film for potential food packaging applications. *Int. J. Photoenergy*, 2014, 1, 2014.
- Paisoonsin, S., Pornsunthorntawe, O., Rujiravanit, R. Preparation and characterization of ZnO-deposited DBD plasma-treated PP packaging film with antibacterial activities. *Appl. Surf. Sci.*, 273, 824, 2013.
- Pal, S., Tak, Y.K., Song, J.M., Does the antibacterial activity of silver nanoparticles depend on the shape of the nanoparticle? A study of the gram-negative bacterium Escherichia coli. *Appl. Environ. Microbiol.*, 73, 1712, 2007.
- Panáček, A., Kvitek, L., Prucek, R., Kolar, M., Večeřová, R., Pizúrová, N., Sharma, V.K., Nevěčná, T., Zboril, R., Silver colloid nanoparticles: synthesis, characterization, and their antibacterial activity. *J. Phys. Chem. B*, 110, 16248, 2006.

- Pandey, J.K., Kumar, A.P., Misra, M., Mohanty, A.K., Drzal, L.T., Palsingh, R., Recent advances in biodegradable nanocomposites. *J. Nanosci. Nanotechnol.*, 5, 497, 2005.
- Park, H.M., Lee, W.K., Park, C.Y., Cho, W.J., Ha, C.S., Environmentally friendly polymer hybrids Part I. Mechanical, thermal, and barrier properties of thermoplastic starch/clay nanocomposites. *J. Mat. Sci.*, 38, 909, 2003.
- Partanen, R., Ahro, M., Hakala, M., Kallio, H., Forssell, P., Microencapsulation of caraway extract in β -cyclodextrin and modified starches. *Eur. Food Res. Technol.*, 214, 242, 2002.
- Patakfalvi, R., Dékány, I., Synthesis and intercalation of silver nanoparticles in kaolinite/DMSO complexes. *Appl. Clay Sci.*, 25, 149, 2004.
- Patel, A.K., Chitosan: Emergence as potent candidate for green adhesive market. *Biochem. Eng. J.*, 2015. <http://dx.doi.org/10.1016/j.bej.2015.01.005>.
- Pappu, A., Patil, V., Jain, S., Mahindrakar, A., Haque, R., Thakur, V.K., Advances in industrial prospective of cellulosic macromolecules enriched banana biofibre resources: A review. *Int. J. Biol. Macromol.* 79, 449, 2015.
- Patil, A.J., Muthusamy, E., Mann, S., Fabrication of functional protein–organoclay lamellar nanocomposites by biomolecule-induced assembly of exfoliated aminopropyl-functionalized magnesium phyllosilicates. *J. Mater. Chem.*, 15, 3838, 2005.
- Patil, M.A., Parikh, P.A., Investigation on likely effects of Ag, TiO_2 , and ZnO nanoparticles on sewage treatment. *B. Environ. Contam. Tox.*, 92, 109, 2014.
- Perez-Gago, M. B., Krochta, J. M., Drying Temperature Effect on Water Vapor Permeability and Mechanical Properties of Whey Protein–Lipid Emulsion Films. *J. Agric. Food Chem.*, 48, 2687, 2000.
- Peters, R., Brandhoff, P., Weigel, S., Marvin, H., Bouwmeester, H., Aschberger, K., ..., Mech, A., Inventory of Nanotechnology applications in the agricultural, feed and food sector. External Scientific Report, CFT/EFSA/FEED/2012/01. EFSA supporting publication EN-621, 1 2014.
- Quirós-Sauceda, A.E., Ayala-Zavala, J.F., Olivas, G.I., González-Aguilar, G.A., Edible coatings as encapsulating matrices for bioactive compounds: a review. *J. Food Sci. Tech. Mys.*, 51, 1674, 2014.
- Rahman, M.A., Mahmud, S., Alias, S.K., Mohd Nor, A., Effect of Nanorod Zinc Oxide on Electrical and Optical Properties of Starch-based Polymer Nanocomposites. *J. Phys. Sci.*, 24, 17, 2013.
- Raji, V., Chakraborty, M., Parikh, P.A., Synthesis of starch-stabilized silver nanoparticles and their antimicrobial activity. *Particul. Sci. Technol.*, 30, 565, 2012.
- Rasmussen, J.W., Martinez, E., Louka, P., Wingett, D.G., Zinc oxide nanoparticles for selective destruction of tumor cells and potential for drug delivery applications. *Expert Opin. Drug Deliv.*, 7, 1063, 2010.
- Ravishankar Rai, V., Jamuna Bai, A., Nanoparticles and their potential application as antimicrobials, in: *Science Against Microbial Pathogens: Communicating Current Research and Technological Advances*, A. Méndez-Vilas (Ed.), Formatex Research Center, USA, 2011.
- Ray, S.S., Okamoto, M., Polymer/layered silicate nanocomposites: A review from preparation to processing. *Prog. Polym. Sci.*, 28, 15391, 2003.
- Reis, L.C.B., Oliveira de Souza, C., Alves da Silva, J.B., Martins, A.C., Nunes, I.L., Druzian, J.I., Active biocomposites of cassava starch: The effect of yerba mate extract and mango pulp as antioxidant additives on the properties and the stability of a packaged product. *Food Bioprod. Process.*, 94, 382, 2015.
- Rhim, J.W., Hong, S.I., Park, H.M., Perry, K.W., Preparation and characterization of chitosan-based nanocomposite films with antimicrobial activity. *J. Agr. Food Chem.*, 54, 5814, 2006.
- Rhim, J.W., Wang, L.F., Hong, S.I., Preparation and characterization of agar/silver nanoparticles composite films with antimicrobial activity. *Food Hydrocolloid.*, 33, 327, 2013.
- Rodney, J., Sahari, J., Kamal, M., Shah, M., Sapuan, S.M., Thermochemical and mechanical properties of tea tree (*Melaleuca alternifolia*) fibre reinforced tapioca starch composites. *e-Polymers*, 15, 401, 2015.

- Sadegh-Hassani, F., Nafchi, A.M., Preparation and characterization of bionanocomposite films based on potato starch/halloysite nanoclay. *Int. J. Biol. Macromol.*, 67, 446, 2014.
- Salahi-Khojin, A., Jhong, H.R.M., Rosen, B.A., Zhu, W., Ma, S., Kenis, P.J., Masel, R.I., Nanoparticle silver catalysts that show enhanced activity for carbon dioxide electrolysis. *J. Phys. Chem. C*, 117, 1627, 2013.
- Salunke, G.R., Ghosh, S., Kumar, R.S., Khade, S., Vashisth, P., Kale, T., Chopade, S., Pruthi, V., Kundu, G., Bellare, J.R., Chopade, B.A., Rapid efficient synthesis and characterization of silver, gold, and bimetallic nanoparticles from the medicinal plant *Plumbago zeylanica* and their application in biofilm control. *Int. J. Nanomed.*, 9, 2635, 2014.
- Saraf, R., Cost effective and Monodispersed Zinc Oxide Nanoparticles Synthesis and their Characterization. *Int. J. Adv. Appl. Sci.*, 2, 85, 2013.
- Sarkanen, K.V., Ludwig, C.H., *Lignins-occurrence, formation, structure and reactions*, Wiley Interscience, New York, 1, 1971.
- Shahabi-Ghahfarrokhi, I., Khodaiyan, F., Mousavi, M., Preparation of UV-protective kefir/nano-ZnO nanocomposites: Physical and mechanical properties. *Int. J. Biol. Macromol.*, 72, 41, 2015a.
- Shahabi-Ghahfarrokhi, I., Khodaiyan, F., Mousavi, M., Yousefi, H., Preparation and characterization of nanocellulose from beer industrial residues using acid hydrolysis/ultrasound. *Fiber.Polym.*, 16, 529, 2015b.
- Shahid, M., McDonagh, A., Kim, J.H., Shon, H.K., Magnetised titanium dioxide (TiO₂) for water purification: preparation, characterisation and application. *Desalin. Water Treat.*, 54, 979, 2015.
- Shalaby, W.S., Latour, R.A., *Handbook of Composites*, S.T. Peters (Ed.), Springer, Berlin, 1997.
- Shankar, S., Teng, X., Li, G., Rhim, J., Preparation, characterization, and antimicrobial activity of gelatin/ZnO nanocomposite films. *Food Hydrocolloid*, 45, 264, 2015.
- Sharma, V.K., Yngard, R.A., Lin, Y., Silver nanoparticles: green synthesis and their antimicrobial activities. *Adv. Colloid Interfac.*, 145, 83, 2009.
- Shen, Z., Simon, G.P., Cheng, Y.B., Comparison of solution intercalation and melt intercalation of polymer-clay nanocomposites. *Polymers*, 43, 4251, 2002.
- Silva-Weiss, A., Ihl, M., Sobral, P.J.A., Gómez-Guillén, M.C., Bifani, V., Natural Additives in Bioactive Edible Films and Coatings: Functionality and Applications in Foods. *Food Eng. Rev.*, 5, 200, 2013.
- Singha, A.S., Thakur, V.K., *Grewia optiva* Fiber Reinforced Novel, Low Cost Polymer Composites. *J. Chem.*, 6, 71, 2009a.
- Singha, A.S., Thakur, V.K., Physical, chemical and mechanical properties of Hibiscus sabdariffa fiber/polymer composite. *Int. J. Polym. Mater.*, 58, 217, 2009b.
- Singha, A.S., Thakur, V.K., Mechanical, thermal and morphological properties of *grewia optiva* fiber/polymer matrix composites. *Polym.-Plast. Technol. Eng.*, 48, 201, 2009c.
- Singha, A.S., Thakur, V.K., Fabrication and Characterization of H. sabdariffa Fiber-Reinforced Green Polymer Composites. *Polym.-Plast. Technol. Eng.*, 48, 482, 2009d.
- Singh, R.P., Pandey, J.K., Rutot, D., Degée, P., Dubois, P., Biodegradation of poly (ε-caprolactone)/starch blends and composites in composting and culture environments: the effect of compatibilization on the inherent biodegradability of the host polymer. *Carbohydr. Res.*, 338, 1759, 2003.
- Song, X., Li, R., Li, H., Hu, Z., Mustapha, A., Lin, M., Characterization and quantification of zinc oxide and titanium dioxide nanoparticles in foods. *Food Bioprocess Tech.*, 7, 456, 2014.
- Sonkaew, P., Sane, A., Suppakul, P., Antioxidant activities of curcumin and ascorbyl dipalmitate nanoparticles and their activities after incorporation into cellulose-based packaging films. *J. Agr. Food Chem.*, 60, 5388, 2012.
- Sorrentino, A., Gorrasi, G., Vittoria, V., Potential perspectives of bionanocomposites for food packaging applications. *Trends Food Sci. Technol.*, 18, 84, 2007.

- Spence, K., Habibi, Y., Dufresne, A., Nanocellulose-based composites, *Cellulose fibers: bio-and nano-polymer composites*, K. Susheel, B.S. Kaith and I. Kaur (Eds.), pp. 179–213, Springer, Berlin Heidelberg, 2011.
- Sreekumar, P.A., Al-Harathi, M.A., De, S.K., Reinforcement of starch/polyvinyl alcohol blend using nano-titanium dioxide. *J. Compos. Mater.*, 46, 3181, 2012.
- Taheri, S., Baier, G., Majewski, P., Barton, M., Förch, R., Landfester, K., Vasilev, K., Synthesis and antibacterial properties of a hybrid of silver-potato starch nanocapsules by miniemulsion/polyaddition polymerization. *J. Mater. Chem. B*, 2, 1838, 2014.
- Talja, R.A., Helén, H., Roos, Y.H., Jouppila, K., Effect of various polyols and polyol contents on physical and mechanical properties of potato starch-based films. *Carbohydr. Polym.*, 67, 288, 2007.
- Tayel, A.A., El-Tras, W.F., Moussa, S., El-Baz, A.F., Mahrous, H., Salem, M.F. Brimer, L., Antibacterial action of zinc oxide nanoparticles against food borne pathogens. *J. Food Safety*, 31, 211, 2011.
- Thakur, V.K., *Green composites from natural resources*, pp. 419, CRC Press Taylor & Francis, 2013 2013. ISBN, 9781466570696
- Thakur, V.K., Singha, A.S., *Biomass-based Biocomposites*, pp. 386, Smithers Rapra, 2013. ISBN 978147359803.
- Thakur, V.K., Singha, A.S., Mehta, I.K., Renewable resource-based green polymer composites: analysis and characterization. *Int. J. Polym. Anal. Charact.*, 15, 137, 2010.
- Thakur, V.K., Thakur, M.K., Gupta, R.K., Graft Copolymers from Natural Polymers Using Free Radical Polymerization. *Int. J. Polym. Anal. Charact.*, 18, 495, 2013a.
- Thakur, V.K., Thakur, M.K., Gupta, R.K., Synthesis of lignocellulosic polymer with improved chemical resistance through free radical polymerization. *Int. J. Polym. Anal. Charact.*, 61, 121, 2013b.
- Thakur, V.K., Thakur, M.K., Gupta, R.K., Rapid synthesis of graft copolymers from natural cellulose fibers. *Carbohydr. Polym.*, 98, 820, 2013c.
- Thakur, M.K., Gupta, R.K., Thakur, V.K., Surface modification of cellulose using silane coupling agent. *Carbohydr. Polym.*, 111, 849, 2014a.
- Thakur, V.K., Thakur, M.K., Gupta, R.K., Graft copolymers of natural fibers for green composites. *Carbohydr. Polym.*, 104, 87, 2014b.
- Thakur, V.K., Thakur, M.K., Processing and characterization of natural cellulose fibers/thermoset polymer composites. *Carbohydr. Polym.*, 109, 102, 2014a.
- Thakur, V.K., Thakur, M.K., Recent Advances in Graft Copolymerization and Applications of Chitosan: A Review. *ACS Sustain. Chem. Eng.* 2, 2637, 2014b.
- Thakur, V.K., Thakur, M.K., Recent trends in hydrogels based on psyllium polysaccharide: a review. *J. Clean. Prod.* 82, 1, 2014c.
- Thakur, V.K., Kessler, M.R., Free radical induced graft copolymerization of ethyl acrylate onto SOY for multifunctional materials. *Mater. Today Commun.* 1, 34–41, 2014a.
- Thakur, V.K., Kessler, M.R., Synthesis and characterization of AN-g-SOY for sustainable polymer composites. *ACS Sustain. Chem. Eng.* 2, 2454–2460, 2014b.
- Thakur, M.K., Thakur, V.K., Gupta, R.K., Pappu, A., Synthesis and Applications of Biodegradable Soy Based Graft Copolymers: A Review. *ACS Sustain. Chem. Eng.* 4, 1–17, 2016.
- Tharanathan, R.N., Biodegradable films and composite coatings: Past, present and future. *Trends Food Sci. Technol.*, 14, 71, 2003.
- The Global Source. The silver institute, 2015. <https://www.silverinstitute.org/site/supply-demand/silver-production/>
- TZMI, TZ Minerals International PTY Ltd. ABN 99 003 492 519, Press Release, 2014. <http://www.tzmi.com/sites/default/files/pdf/Press%20Release%20-%20TiO2%20Pigment%20Annual%20Review%202014.pdf>
- University of York. The Essential Chemical Industry, Titanium Dioxide, 2013. <http://www.essentialchemicalindustry.org/chemicals/titanium-dioxide.html>

- Uraki, Y., Sugiyama, Y., Koda, K., Kubo, S., Kishimoto, T., Kadla, J.F., Thermal mobility of β -O-4-type artificial lignin. *Biomacromolecules*, 13, 867, 2012.
- Valodkar, M., Sharma, P., Kanchan, D.K., Thakore, S., Conducting and antimicrobial properties of silver nanowire-waxy starch nanocomposites. *Int. J. Green Nanotech. Phys. Chem.*, 2, 10, 2010a.
- Valodkar, M., Bhadoria, A., Pohnerkar, J., Mohan, M., Thakore, S., Morphology and antibacterial activity of carbohydrate-stabilized silver nanoparticles. *Carbohydr. Res.*, 345, 1767, 2010b.
- Viskupicova, J., Danihelova, M., Ondrejovic, M., Liptaj, T., Sturdik, E., Lipophilic rutin derivatives for antioxidant protection of oil-based foods. *Food Chem.*, 123, 45, 2010.
- Vodnik, V.V., Božanić, D.K., Bibić, N., Šaponjić, Z.V., Nedeljković, J.M., Optical properties of shaped silver nanoparticles. *J. Nanosci. Nanotechnol.*, 8, 3511, 2008.
- Voicu, S.I., Condruz, R.M., Mitran, V., Cimpean, A., Miculescu, F., Andronescu, C., Miculescu, M., Thakur, V.K., Sericin Covalent Immobilization onto Cellulose Acetate Membrane for Biomedical Applications. *ACS Sustain. Chem. Eng.* 4, 1765, 2016.
- Wan, C., Qiao, X., Zhang, Y., Zhang, Y., Effect of different clay treatment on morphology and mechanical properties of PVC-clay nanocomposites. *Polym. Test.*, 22, 453, 2003.
- Wang, C.R., Yan, X.Z., Yu, L.L., Fang, R., Preparation and properties of glycerol plasticized-corn starch/titanium dioxide-starch bionanocomposites. *Adv. Mat. Res.*, 997/480, 2014.
- Wang, J., Dong, Z., Huang, J., Li, J., Liu, K., Jin, J., Ma, J., Synthesis of Ag nanoparticles decorated multiwalled carbon nanotubes using dialdehyde starch as complexant and reductant for antibacterial purposes. *RSC Advances*, 3, 918, 2013.
- Wang, L.S., Wang, C.Y., Yang, C.H., Hsieh, C.L., Chen, S.Y., Shen, C.Y., Wang, J.J., Huang, K.S., Synthesis and anti-fungal effect of silver nanoparticles-chitosan composite particles. *Int. J. Nanomed.*, 10, 2685, 2015.
- Wang, X., Zhang, X., Liu, H., Wang, N., Impact of pre-processing of montmorillonite on the properties of melt-extruded thermoplastic starch/montmorillonite nanocomposites. *Starch-Stärke*, 61, 489, 2009.
- Wei, X., Liu, J., Liu, X.W., Ultrafine dice-like anatase TiO_2 for highly efficient dye-sensitized solar cells. *Sol. Energ. Mat. Sol. C*, 134, 133, 2015.
- Whilton, N.T., Burkett, S.L., Mann, S., Hybrid lamellar nanocomposites based on organically functionalized magnesium phyllosilicate clays with interlayer reactivity. *J. Mater. Chem.*, 8, 1927, 1998.
- Wist, J., Sanabria, J., Dierolf, C., Torres, W., Pulgarin, C., Evaluation of photocatalytic disinfection of crude water for drinking-water production. *J. Photoch. Photobio. A*, 147, 241, 2002.
- Wu, H., Thakur, V.K., Kessler, M.R., Novel low-cost hybrid composites from asphaltene/SBS triblock copolymer with improved thermal and mechanical properties. *J. Mater. Sci.* 51, 2394, 2016.
- Xie, A.G., Cai, X., Lin, M.S., Wu, T., Zhang, X.J., Lin, Z.D., Tan, S., Long-acting antibacterial activity of quaternary phosphonium salts functionalized few-layered graphite. *Mater. Sci. Eng. B*, 176, 1222, 2011.
- Yakout, S.M., Mostafa, A.A., A novel green synthesis of silver nanoparticles using soluble starch and its antibacterial activity. *Int. J. Clin. Exp. Med.*, 8, 3538, 2015.
- Yang, H., Zhu, S., Pan, N., Studying the mechanisms of titanium dioxide as ultraviolet-blocking additive for films and fabrics by an improved scheme. *J. Appl. Polym. Sci.*, 92, 3201, 2004.
- Yoksan, R., Chirachanchai, S., Silver nanoparticle-loaded chitosan-starch based films: Fabrication and evaluation of tensile, barrier and antimicrobial properties. *Mater. Sci. Eng. C*, 30, 891, 2010.
- Yu, J., Yang, J., Liu B., Ma, X., Preparation and characterization of glycerol plasticized-pea starch/ZnO-carboxymethylcellulose sodium nanocomposites. *Bioresour. Technol.*, 100, 2832, 2009.
- Yun, Y.H., Youn, Y.N., Yoon, S.D., Lee, J.U., Preparation and physical properties of starch-based nanocomposite films with the addition of titanium oxide nanoparticles. *J. Ceram. Process. Res.*, 13, 59, 2012.

- Yun, H., Kim, J.D., Choi, H.C., Lee, C.W., Antibacterial Activity of CNT-Ag and GO-Ag Nanocomposites Against Gram-negative and Gram-positive Bacteria. *Bull. Korean Chem. Soc.*, 34, 3261, 2013.
- Zhao, R., Torley, P., Halley, P.J., Emerging biodegradable materials: Starch- and protein-based bio-nanocomposites. *J. Mat. Sci.*, 43, 3058, 2008.
- Zheng, P., Du, Y., Chang, P.R., Ma, X., Amylose-halloysite-TiO₂ composites: Preparation, characterization and photodegradation. *Appl. Surf. Sci.*, 329, 256, 2015.
- Zhou, J.J., Wang, S.Y., Gunasekaran, S., Preparation and characterization of whey protein film incorporated with TiO₂ nanoparticles. *J. Food Sci.*, 74, N50, 2009.

Preparation and Application of the Composite from Chitosan

Chen Yu

School of Materials Science and Engineering, Beijing Institute of Technology, Beijing, China

Abstract

Chitosan (CS) is a kind of marine polymer that can be extracted from the shells of various shellfish including crabs and prawns. It has versatile properties, such as biodegradability, biocompatibility, hemostatic behavior and promotion of wound healing. Chitosan is also a very versatile material that can be readily chemical modified. Chitosan has been widely used in different fields. However, there are also many disadvantages for chitosan and its derivatives, such as lower mechanical property not prominent performance. In the current chapter, we want to introduce the method for preparation of the composite based on chitosan, such as the composite of chitosan/natural polymers, chitosan/synthetic polymers, chitosan/biomacromolecules, chitosan/inorganic components, chitosan/carbon materials, etc. By the way, we also want to introduce the progress for the application of the above composite in different fields, such as medical materials, environmental protection, agriculture, etc.

Keywords: Chitosan, composite, natural polymers, synthetic polymers, biomacromolecules, inorganic components, carbon materials

15.1 Introduction

Chitosan is a linear copolymer comprised of two monomeric units namely N-acetyl-2-amino-2-deoxy-d-glucose (N-acetylated groups) and 2-amino-2-deoxy-d-glucose residues (N-deacetylated groups, amino groups) (Figure 15.1). It is obtained by deacetylation of chitin, a polysaccharide widely distributed in the exoskeleton of insects, crustaceans and fungi. Chitosan polymers are renewable semi-synthetically derived amino-polysaccharides that have unique structures, highly sophisticated functionality, multidimensional properties and a wide range of applications in biomedical and other industrial areas (Dash *et al.*, 2011).

Chitosan is a natural polymer with numerous reactive groups for chemical activation, gel-forming capability, high adsorption capacity, chelating and complexing properties, biodegradability, adsorbable bioactivity and ecological safety. In addition, it is nontoxic and innately biocompatible to living tissues as well as having bioadhesivity, antimicrobial

Corresponding author: cylsy@163.com

Vijay Kumar Thakur, Manju Kumari Thakur and Michael R. Kessler (eds.), Handbook of Composites from Renewable Materials, (371–434) © 2017 Scrivener Publishing LLC

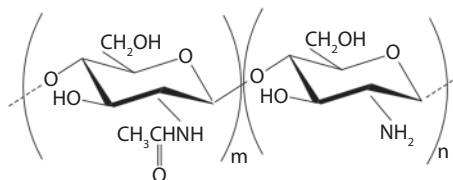


Figure 15.1 The structure of chitosan.

activity (bacteria, fungi, viruses) and antitumor activity (Thakur & Thakur, 2014a–c). These features highlight the suitability and extensive applications of chitosan or its derivatives in different fields, including drug delivery, tissue engineering, wound healing, gene therapy, agriculture, environmental protection, chemical detection, biosensor, etc. (Anitha *et al.*, 2014; Younes & Rinaudo, 2015). They can be easily processed into different forms such as membranes, sponges, gels, scaffolds, microparticles, nanoparticles and nanofibers (Cheung *et al.*, 2015; Thakur & Kessler, 2015; Thakur & Thakur, 2015; Thakur & Thakur, 2014a–c).

Besides that, there are still many disadvantages for chitosan or its derivatives, which confine their wide application. For example, their mechanical properties are weak and crisp, their antibacterial properties are limited, and their degradability and adsorption capacity are decided by their structures, and so on. Compositing of chitosan with other different components, including natural or synthetic polymers, biomacromolecules, inorganic components, can promote the properties of chitosan and combining the advantages of different components. It has been widely studied. In the current chapter, different patterns for preparation and application of the composite based on chitosan or its derivatives will be focused.

15.2 Composites from Chitosan and Natural Polymers

Due to their renewable nature, eco-efficiency, sustain ability and industrial ecology of natural polymers, and the intrinsically antibacterial activity, biodegradability, and biocompatibility of many natural polymers, composites prepared from chitosan or its derivatives and natural polymers have been well studied (Thakur *et al.*, 2016; Pappu *et al.*, 2015; Voicu *et al.*, 2016). The composites prepared from chitosan/chitosan derivatives (Hein *et al.*, 2008), chitosan/starch or its derivatives (Appelqvist & Debet, 1997), chitosan/cellulose or its derivatives (Popa & Breaban, 1995), chitosan/alginate or its derivatives (Hu *et al.*, 2015) have been well studied. In recent years, as outstanding properties of other natural polymers, including collagen, gelatine, chondroitin sulphate, hyaluronic acid, heparin, and so on, the composites prepared between them and chitosan or its derivatives have attracted more and more attention, especially in the fields of biomedical materials. Then we'll focus on the progress on the preparation and application of the above novel natural composites.

15.2.1 Composites from Chitosan and Collagen

Collagen is a protein of extracellular matrix that consists of three helical polypeptide chains, representing 90% organic matter of bone tissue, and is the major component of

cartilage and connective tissue of animals. Collagen is the most frequently used biomaterial due to its excellent property of physiology and physicochemical support for cell adhesion and proliferation (Wang *et al.*, 2015). Collagen possesses excellent biocompatibility and biodegradability and comprises the repetitive array of receptor-recognition motifs essential for cell interaction via specific collagen-binding $\beta 1$ integrins, such as GFOGER motif (G: glycine; F: phenylalanine; O: hydroxyproline; E: glutamate and R: arginine). Consequently, collagen-based scaffolds should not only mechanically support the native tissue during repair, but also play an important role in providing essential signals to influence cell activity (Martinez *et al.*, 2015). However, the structure of collagen may be broken when it was extracted. The fast degradation and low mechanical property make it difficult to be a carrier of seed cells for tissue engineering. Therefore, it seems interesting to develop composite collagen-chitosan scaffolds in order to improve the biostability of collagen (Cheng *et al.*, 2015), and create more suitable biomimetic microenvironments for cells compared to those provided by pure chitosan matrices.

Kumar *et al.* prepared collagen-chitosan scaffolds of different compositions by using emulsion air-drying method (Kumar *et al.*, 2012). The scaffolds prepared with 10–30 wt% of chitosan to collagen showed better mechanical properties than pure collagen scaffold. The composite scaffolds are biocompatible and show adequate physical and structural characteristics to support fibroblast attachment and proliferation. The above results demonstrate this kind of scaffold is a good substrate for biomedical application.

Besides the scaffolds, the composites prepared from collagen and chitosan can also be used to fabricate the ultrafine fibers to mimic the native extracellular matrix (ECM). Chen *et al.* prepared the collagen-chitosan complex single fibers and fibrous membrane from electrospun (Chen *et al.*, 2009). The mechanical study results showed that the ratio of collagen to chitosan in fibers would affect the tensile behaviour of the fibers and the fibrous membrane. During the electrospinning process, if the draw ratio that was applied was higher, fibers with a smaller diameter had higher strength but lower ductility could be prepared. For the electrospun single fibers, the fibers demonstrated excellent tensile ductility at chitosan content of 10% and 20% and the highest tensile strength and Young's modulus at chitosan content from 40% to 60%. For the fibrous membrane prepared from electrospun, the ultimate tensile strength of it was decreased with the increase of chitosan content in fibers. By the way, the changing trend for the ultimate tensile elongation is similar to that of the single fiber. The above producing method of the fibers with the desired mechanical properties is useful to prepare the tissue engineering scaffolds fitting for various requirements. Moreover, as good bioactivity of the collagen and chitosan composites, they can also be deposited on other fibers to promote the properties of the fibres. Huang *et al.* alternatively deposited the chitosan with positive charge and Type I collagen with negative charge on the surface of cellulose acetate (CA)/polycaprolactone (PCL) nanofibrous matrix via layer-by-layer (LBL) self-assembly technique (Huang *et al.*, 2015). It was found that the above composited nanofibrous matrices with LBL structure could accelerate cell migration, promote the higher cell attachment, proliferation, spreading and migration of cells in comparison to the unmodified ones. Besides, the degradation rate of LBL structured nanofibrous mats were faster than that of cellulose/PCL matrix *in vivo*. Moreover, it was found that the LBL modified nanofibrous mats showed complete re-epithelialization and regeneration to all the skin appendages. They revealed significantly higher wound recovery rate.

15.2.2 Composites from Chitosan and Gelatin

As a denatured collagen, gelatin exhibits quick *in vivo* degradation velocity, well cell adhesion properties and good tissue compatibility. Gelatin is an attractive material for cartilage tissue engineering. However, the bio-products prepared from gelatin are crisp, easy to be dissolved in water and easy to be deteriorated, which confined its application. Recently, modification of gelatin by compositing with chitosan materials to avoid the disadvantages of gelatin has gained much attention in biomedical applications such as tissue engineering scaffolds and drug carriers.

Han *et al.* prepared a layered gelatin-chitosan hydrogel with graded composition structure via photo cross-linking reaction to mimic the multi-layered gradient structure of the cartilage-bone interface tissue and simulate the polysaccharide/collagen composition of the natural tissue (Han *et al.*, 2015). The hydrogel showed well swelling ratio, the pore size and inter connectivity, as well as compressive mechanical properties, with which exhibiting a graded transition from the surface layer to the inner layer in the hydrogels. The results of the *in vitro* cytotoxicity assay showed that the hydrogel had good cytocompatibility and the *in vivo* repair results. The above gradient gelatin-chitosan hydrogel showed remarkable recovery for osteochondral defect, especially for the hydrogel loading transforming growth factor- β 1. So it has good application potential for osteochondral repair.

Pezeshki-Modaress *et al.* prepared the bead-free gelatin/chitosan composite nanofibrous mats through the electrospinning process (Pezeshki-Modaress *et al.*, 2015). The gelatin/chitosan blends nanofibrous with mean fiber diameter ranging from 163 to 344 nm and standard deviation of the fiber diameter ranging from 152 to 386 nm could be obtained, and the structure parameters were depending on the electrospinning conditions. The human dermal fibroblast cells could be attached and spread completely on the surface of the electrospun gelatin/chitosan nanofibrous scaffold. The above nanofibrous scaffolds could be used as for skin tissue engineering.

Beside to be used as biomedical materials, the composite prepared from chitosan and gelatine could also be used in many different fields. Recently, Konuklu *et al.* prepared chitosan-gelatin microcapsules containing one of two fatty acids, namely decanoic and caprylic acids, through the complex coacervation method following with being cross-linked by glutaraldehyde (Konuklu & Paksoy, 2015). It was found that the prepared microcapsules showed ideal thermal energy storage properties. Given the biodegradable, biocompatible, and nontoxic properties of gelatin and chitosan, they could be used as temperature-controlled packaging and transport materials in food package applications. Cui *et al.* prepared the porous chitosan/gelatin composite material with interpenetrating polymer networks (IPN) structure by using genipin as the cross-linker (Cui *et al.*, 2015). The above porous material displays pH-sensitive and rapidly response in adsorption and desorption of acid orange II dye from aqueous solution, which indicates that it could be used as a recyclable adsorbent in removal or separation of anionic dyes as changing of environmental pH condition.

15.2.3 Composites from Chitosan and Chondroitin Sulfate

Chondroitin sulfate, a glycosaminoglycan, is an important component of connective tissues and the extracellular matrix (Muzzarelli *et al.*, 2012). Chondroitin

sulfate is composed of alternating units of β -1,3-linked glucuronic acid and (β -1,4)-N-acetylgalactos amine (GalNAc), and it is sulfated in either the 4 or 6 position of the GalNAc residues (Kirker *et al.*, 2002). Chondroitin sulfate has biocharacteristics that include the binding and modulation of cytokines and growth factors, and it is involved in the adhesion, migration, proliferation, and differentiation of cells (Lee *et al.*, 2004). Chondroitin sulfate has been used to treat diseases related to ligaments, such as osteoarthritis. Moreover, chondroitin sulfate is a water-soluble biopolymer with an anionic nature that can polyelectrolyte interact with chitosan. The network structures formed through the polyelectrolyte complex between chondroitin sulphate and chitosan have an interesting pH-responsive, they can be used to construct the hydrogels, films, microparticles and so on.

Lopes *et al.* developed a physical hydrogel formed from polyelectrolyte complex of chitosan and chondroitin sulfate to act as a potential device for the controlled release of theophylline (TH) (Lopes *et al.*, 2013). According to the results of *in vitro* release of chondroitin sulfate and TH at pH 2 and 8, it was found that the release of both chondroitin sulfate and TH had strong pH dependence. A high fraction of TH was released from the hydrogel samples when they were swollen under acid conditions. The fractions of chondroitin sulfate and TH released from the hydrogel samples at pH 8 were very close. In addition, the mechanical and structural properties of the chitosan/ chondroitin sulfate /TH hydrogels were also affected by the variation of the pH of the swelling media. Fajardo *et al.* prepared a new type of dual-network hydrogel from chitosan and chondroitin sulphate (Fajardo *et al.*, 2013). Firstly, chitosan and chondroitin sulfate were chemically cross-linked with glycidyl methacrylate (MBA) through a free radical reaction. Subsequently, physically cross-linked networks were formed by immersion of the chemical hydrogels in chitosan or chondroitin sulphate stock solutions. And then the dual-network hydrogels could be formed. The process was shown in Figure 15.2. It was found that the morphologies and liquid uptake capacities of the chemical hydrogels were changed by the formation of a secondary network by polyelectrolyte complexation.

Wang *et al.* modified the collagen (Col)-chitosan (CS) membrane by a hot dehydrogenation cross-linking method (Wang *et al.*, 2012). Chondroitin sulfate was composited with Col-CS membrane and carbodiimide was added for further crossing modification. And then Col-CS-Chondroitin sulphate composite membrane was prepared. It was found that the carbodiimide modification technology and the introduction of

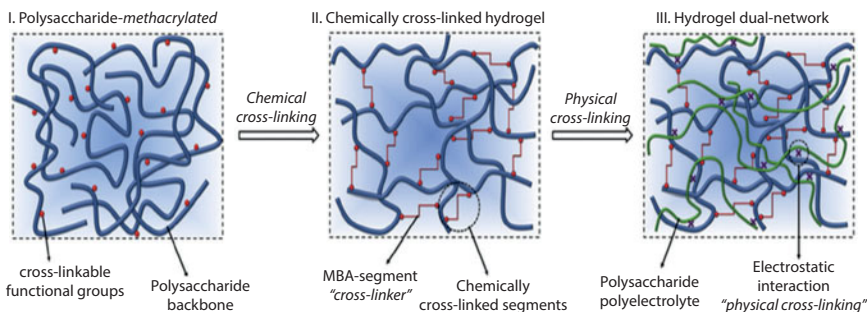


Figure 15.2 Formation of the dual-network hydrogel from chitosan and chondroitin sulfate (Fajardo *et al.*, 2013).

chondroitin sulphate improved the tensile strength, degradation and antienzymolysis ability of the composite membrane than that of Col-CS membrane. The good biocompatibility, mechanical properties, digestion resistance, and wound healing property of the above composite membrane make it a potential skin scaffold for tissue engineering or wound dressing.

Based on the electrostatic complexation of two oppositely-charged polysaccharides, chitosan and chondroitin sulphate, Santo *et al.* proposed a new formulation of nanoparticles (NPs) (Santo *et al.*, 2012). As it can act as controlled release system for encapsulated and/or adsorbed bio-macromolecules, the above nanoparticulate complex seems an especially promising delivery platform. By the way, it also provide a molecular, mechanical and physiological milieu similar to that found in the native ECM. As the interactions between the polysaccharides and the entrapped proteins mimic the interactions between chondroitin sulphate and proteins in the ECM, these nanoparticulate carriers are particularly promising for protein entrapment. The prepared spherical non-cytotoxic NPs exhibited high encapsulation efficiency for physiological levels of growth factors and a controlled protein release profile for over 1 month. Moreover, it was also found that these NPs can be uptaken by human adipose-derived stem cells (hASCs), depending on the concentration of NPs in the culture medium and incubation time. When the platelet lysates-loaded NPs were used to replace the bovine serum for *in vitro* hASCs culture, the viability and proliferation of hASCs was not compromised. This means the versatility of the developed NPs can also be used in the future as intracellular carriers for bioactive agents, such as nucleotides, besides acting as a protein delivery system. The release of platelet lysates from the above NPs also found to be effective for the enhancement of *in vitro* osteogenic differentiation of hASCs, as shown by the increased levels of mineralization, suggesting not only the effective role of the delivery system but also the role of platelet lysates as an osteogenic supplement for bone tissue engineering and regenerative medicine applications.

15.2.4 Composites from Chitosan and Hyaluronic Acid

Hyaluronic acid (HA, $pK_a = 2.9$) is a naturally occurring linear polysaccharide with a repeating disaccharide structure, consisting of 2-acetamide-2-deoxy- β -D-glucose and β -D-glucuronic acid residues, linked by alternating (1–3) and (1–4) glycoside bonding. It has high molecular weight. HA is a component of extracellular matrix of all higher animals including skin, cartilage, and connective tissue, which influences several cellular functions, such as migration, adhesion, and proliferation. It was recently reported that HA could increase osteoblastic bone formation *in vitro*. Recent biomedical applications of HA include as a component for drug delivery applications, tissue engineering, scaffolds for wound healing, ophthalmic surgery, implant materials and arthritis treatments (Krishna *et al.*, 2015). As negative charges distributed on the skeleton of HA, it is easy to form the polyelectrolyte complex with chitosan or its derivatives in the patterns of hydrogels, scaffold microparticles to improve the properties of them.

Zhao *et al.* developed a simple and green process to fabricate the HA/CS complex colloidal particles through electrostatic interactions (Zhao *et al.*, 2015). The process was shown in Figure 15.3. It was found that both the complex and the corresponding emulsion have good cytocompatibility. Furthermore, papain was introduced into the

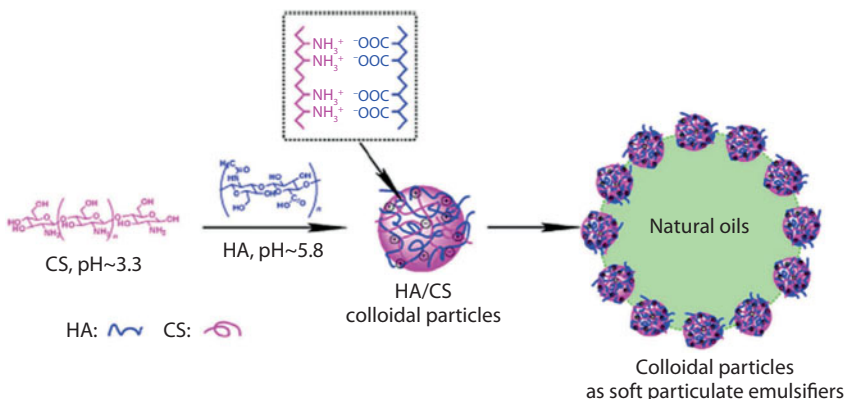


Figure 15.3 The formation and the oil-in-water interfacial behavior of HA/CS complex colloidal particles (Zhao *et al.*, 2015).

complex systems to form the papain/HA/CS complexes in a compact form to protect the enzyme and even cause an increase in the enzymatic activity, which showed great application potential as enzyme carriers.

Nath *et al.* prepared the chitosan–hyaluronic acid polyelectrolyte complex scaffold through the polyelectrolyte complex (PEC) of the opposite charges (Nath *et al.*, 2015). By the way, to increase the stability and longer degradation of the scaffold, free amino groups in chitosan were cross-linked with different amounts of genipin. After being immobilized of the bone morphogenetic protein-2 (BMP-2) in the chitosan–hyaluronic acid PEC by electrostatic attraction, the BMP-2 release profile with quite high loading efficacy could be achieved. It showed prolonged and sustained release properties to BMP-2. In addition, the study results indicated that released BMP-2 facilitated osteogenesis greatly, both at initial and later stage, which is a key factor for bone regeneration.

The conventional therapy used in clinic for the treatment of osteoarthritis is intra-articular injection of hyaluronic acid, which requires repeated, frequent injections. To extend the visco supplementation effect of hyaluronic acid, Kaderli *et al.* used stabilize unmodified HA and reacylated CS with the addition of different salts and formulation buffers to facilitate the transparent, homogeneous hydrogels (Kaderli *et al.*, 2015). The addition of CS to the HA hydrogels was found to reduce HA degradation during autoclaving in a dose dependent manner when calcium ions were used.

Postsurgical peritoneal adhesions are very common and serious complication after surgery. Postsurgical peritoneal adhesions may cause chronic pain, infertility, and even lethal bowel obstruction. HA has also been used for adhesion prevention and commercialized. However, due to its extremely high water absorbing properties and enzymatic degradation, HA hydrogels often exhibit very rapid erosion and degradation behaviors *in vivo*. Li *et al.* reported a class of injectable, biodegradable, flexible and non-toxic hydrogel prepared from aldehyde hyaluronic acid (A-HA) and N, O-carboxymethyl chitosan (NOCC), with being cross-linked by the Schiff base between the aldehyde groups in A-HA and amino groups of NOCC (Li *et al.*, 2014). The highly porous three dimensional hydrogel can supported the growth and proliferation of the cells encapsulated in

the hydrogels. But it was not favorable for the attachment of fibroblasts to the surface, suggesting that the above hydrogel can be developed for adhesion prevention. *In vivo* applications of the hydrogel on adhesion prevention indicated that the hydrogel was effective in reducing the formation of intraperitoneal adhesions after surgery.

15.2.5 Composites from Chitosan and Heparin

Heparin (HP) (Sarah *et al.*, 2015) is a linear biopolymer that consists of sulfated D-glucosamine units, joined in alternating sequence by (1, 4)-glycosidic linkages, to either D-glucuronic or L-iduronic acid. HP is an anionic polysaccharide. At specific conditions of pH, it could form polyelectrolyte complexes with cationic polymers. HP presents many applications in medical and pharmaceutical areas. It acts indirectly in the blood coagulation mechanism, stimulates cellular growth and has antibacterial effects.

Bueno *et al.* complexed N,N-dimethyl chitosan (DMC) and HP via PEC interaction (Bueno *et al.*, 2015). The PEC efficiently protected the HP in simulated gastric fluid condition in which HP is degraded. On the other hand, in simulated intestinal fluid PEC promoted the releasing of $80 \pm 1.5\%$ of loaded HP. So, the PEC based on DMC/HP could release HP of high molecular weight (14,000 g/mol) at pH close to physiological condition, then it has potential for act as an efficient vehicle for HP drug-carrier.

As good biocompatibility and blood compatibility of the CS-HP composites, they could be widely used in the tissue engineering. In order to improve the antithrombogenic property of chitosan, He *et al.* used heparin to composite with chitosan, and then prepared homogeneous CS-HP composite films and porous scaffolds under simple and mild conditions (He *et al.*, 2010). The composite matrices showed good mechanical properties, as well as improved blood compatibility and endothelial cell compatibility. They are promising candidates for blood contacting tissue engineering. Yu *et al.* developed a three-dimensional, macroporous composite CS-HP artificial extracellular matrix (AECM) by an interpolyelectrolyte complex method following with lyophilization (Yu *et al.*, 2008). It was found that the EDC/NHS-cross-linked CS-HP composite AECMs showed excellent biocompatibility according to the results of the *in vitro* cytotoxic test, which suggested that the above AECMs might be a good candidate to be used as scaffold-guided tissue engineering.

15.2.6 Composites from Chitosan and Glucomannan

Konjac glucomannan (KGM) is a neutral polysaccharide derived from the tuber of *Amorphophallus konjac* C. Koch. KGM is consisted of α -glucose and α -mannose by linking through β -1,4-linkage (Zhang *et al.*, 2014). It is composed of D-glucose and D-mannose units in the molar ratio 1:1.6 to 1:1.69. By the way, it is found that there are some branching points at the C-3 position of the mannoses. An acetyl group is attached to 1 per 19 sugar residues. It is widely accepted that the presence of this group gives good solubility of the konjac glucomannan in aqueous solution. KGM can be prepared to films or blend membranes, which can be used in many fields, such as chemical engineering, food and biomaterials. Composite of KGM with CS can promote its antibacterial property, bioactivity and mechanical properties. Du *et al.* prepared the KGM/CS composite blend films, and then they were irradiation modified (Du *et al.*, 2013). The KGM/CS

blend films prepared through irradiation showed good antibacterial effects against *E. coli*, *S. aureus* and *P. aeruginosa*. Antibacterial activity of the blend films was increased with increasing of the content of chitosan. At the same time, antibacterial activity against *E. coli* and *P. aeruginosa* also increased after the irradiation. Due to the intense intermolecular hydrogen bonds between the KGM and CS, the tensile strength of the film was prominently improved compared to the CS film. In addition, it showed good compatibility. Nie *et al.* prepared the bicomponent nanofibrous scaffolds of KGM and chitosan from their dilute acidic solution, and it was found that the average fiber diameter was decreased from 350nm to 180nm with the increase in chitosan content (Nie *et al.*, 2011). The cell culture results showed that bone mesenchymal stem cells could be adhered preferentially to the KGM/chitosan nanofibrous scaffolds than the bulk films. Meanwhile, the addition of KGM could improve the biocompatibility of chitosan material.

By reacting with sodium periodate, KGM can be oxidized. Simultaneously, the carbon-carbon bonds of the cisdiol group in KGM molecular chain will be cleaved to generate reactive aldehyde functions, which can develop chemical cross-linking action with gelatin, CS, proteins, and some drugs possessing primary amino group or aliphatic amino functions via Schiff's or imino bonds linkage between free amino groups and the aldehyde groups of oxidized polysaccharide. Yu *et al.* used dialdehyde konjac glucomannan (DAK) as macromolecular cross-linking agent for chitosan (CS) (Yu *et al.*, 2007) to prepare the hydrogels. The cross-linking structure could be formed through the Schiff-base reaction between the aldehyde groups of DAK and the amino groups of CS chains within 2–5 min. It was found that the swelling, morphology, mechanical, and drug release properties of the hydrogels could be regulated and controlled by varying the amount of oxidized KGM. Korkiatithaweechai *et al.* used sodium periodate oxidized KGM (OKG) to cross-linked with CS via imine bonds ($-C=N-$) (Korkiatithaweechai *et al.*, 2011). Then they evaluated the release profiles of diclofenac sodium (DFNa) from the CS/OKG polymer matrices. It was found that the composite prepared at 1:2:1 (w/w/w) ratio of CS:OKG:DFNa and at room temperature for 3 hours gave the highest encapsulation efficiency of $95.6 \pm 0.6\%$ and resulted in a minimal release of DFNa ($<1\%$ over 2 h) in simulated gastric fluid (pH 1.2) and a significantly improved sustained release in simulated intestinal fluid (pH 7.4) with $\sim 6\%$ and 19% release over 8 and 24 h, respectively, and the properties were 15- and 5-fold lower than that of the two commercial DFNa preparations, Diclosian and Voltaren. So the above composite is fitted to be used as a model for long term controllable release of drug in intestine (at least 3 days).

By the carboxymethylation of KGM, carboxymethyl konjac glucomannan (CKGM), an anionic polymer, can be produced. It has good biocompatibility, water solubility, bioactivity and excellent polyelectrolyte complex gelation ability when interacted with chitosan or its derivatives. Wang *et al.* prepared CKGM/CS nanocapsules spontaneously by electrostatic complexation, and then used it for immobilizing of L-asparaginase (Wang *et al.*, 2008). The process of the preparation does not degenerate the enzyme and the immobilized enzyme has better stability and activity in contrast to the native enzyme. The particle size was in a range 100–300 nm when both the concentrations of CKGM and CS were 0.01% and the encapsulation efficiency reached 68.0%. The matrix has semi-permeability to allow the product and substrate to pass through and to keep L-asparaginase in the matrix to prevent leaking. Du *et al.* prepared the CKGM/CS composite beads via electrostatic interaction (Du *et al.*, 2006). It was found that the

swelling rate of the beads was higher in the alkaline medium (7.4) than in the acid medium (5.2). Then the pH-sensitive release properties of bovine blood proteins (BSA) from the CKGM/CS beads were studied, it was found that the amount of BSA released at medium condition was relatively low, only about 65% of protein released within 3 h. However, during the same length of time, the amounts of BSA released was increased to 81% and 73% at pH 1.2 and pH 7.4, respectively.

15.3 Composites from Chitosan and Synthetic Polymers

A wide variety of synthetic polymers can be prepared with variations in main chain as well as side chains. As their structure can be designed and the properties can be controlled, they can show variegated properties and application potentials. Compositing of the synthetic polymers with chitosan or its derivatives can improve the properties of chitosan, such as mechanical properties, thermal stability, functional properties, and so on. The above composites have been widely studied and applied. In the current section, we'll introduce some of the most representative and widely applied composites from chitosan and synthetic polymers.

15.3.1 Composites from Chitosan and Polyurethanes

Polyurethanes (PU) are an important division of synthetic polymers that have been extensively used in biomedical applications and various industries for their attractive physical properties and good biocompatibility. Especially as a class of biomedical polymers, polyurethanes have been widely used in making aortic grafts, pacing leads insulation, heart valves, intra-aortic balloons, indwelling catheters, etc. Besides such traditional applications, development of biodegradable PUs for novel biomedical applications, including controlled release (CR) systems of the active ingredients, temporary scaffolds, ligament reconstruction prostheses, etc., have been investigated extensively. In recently years, using chitosan to prepare the composite of PUs to promote its bioactivity and biocompatibility has been well studied.

There are different ways to prepare the composite of chitosan and polyurethanes:

1. The CS/PU composite polymer can be prepared through the traditional step-growth polymerization technique. Zia *et al.* prepared the PU prepolymer by reacting of poly(ϵ -caprolactone) with 2,4-toluene diisocyanate firstly (Zia *et al.*, 2014). Then the above prepolymer was extended with different mole ratios of chitosan and 1,4-butanediol and the composite polymer was prepared. Barikani used different mass ratios of dimethylol propionic acid and chitosan as the chain extender to the aqueous polyurethane dispersions synthesized through the reaction of poly(ϵ -caprolactone) and isophorone diisocyanate (Barikani *et al.*, 2010). The thermal stability of polyurethane can be improved through incorporation of chitosan. The hydrophilicity of the polyurethanes would be reduced as the increasing amount of dimethylol propionic acid and chitosan chain extender.

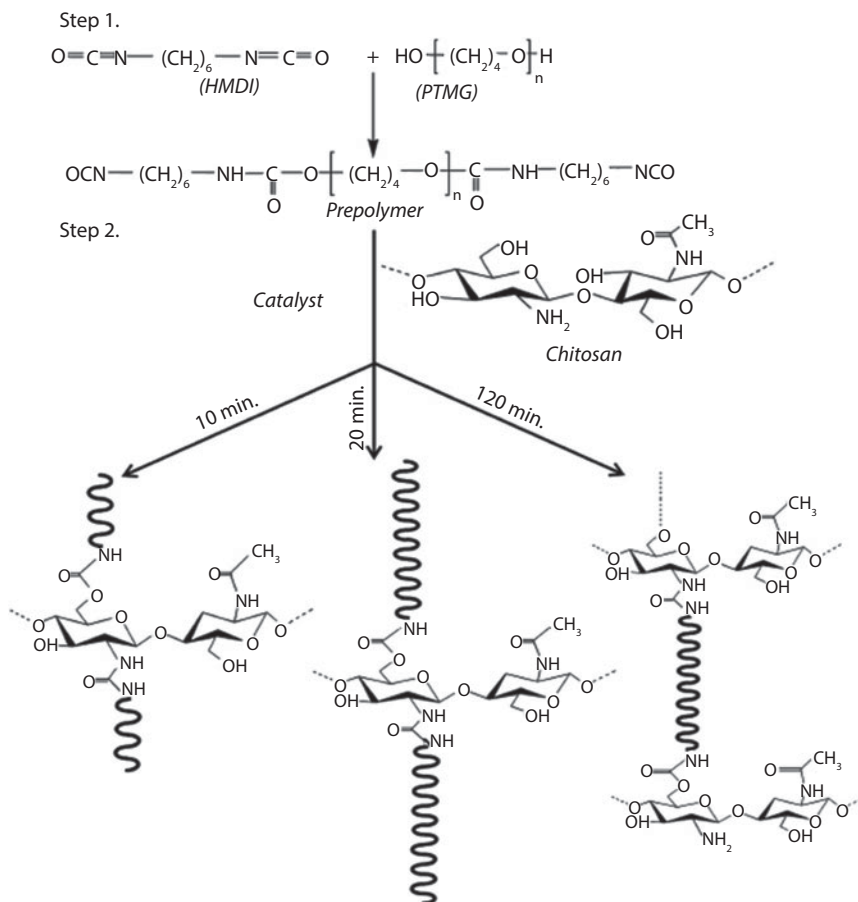


Figure 15.4 Scheme of the reaction showing time dependent chain length of grafted species and subsequent cross-linking between CS molecules at a higher degree of substitution (Mahanta *et al.*, 2015).

2. Isocyanate-terminated polyurethane can also be grafted on to the skeleton of the chitosan molecules to prepare the CS/PU composite polymer. Mahanta *et al.* grafted the isocyanate-terminated prepolymer on to the chitosan molecules (Mahanta *et al.*, 2015). Various degrees of substitutions with varying chain length, which was dependent by time, were obtained to control the hydrophilic nature of the polymer. Network structure was developed through cross-linking of chitosan molecules with polyurethane bridges. The process is shown in Figure 15.4. The above graft copolymers exhibited sustained release of drug and, thereby, overcome the burst release observed in pure CS.
3. Several studies have investigated on the preparation of full- and semi-interpenetrating polymer networks (IPNs and semi-IPNs) from PU and CS. Yu *et al.*, blended 6-O-carboxymethyl chitosan (6-OCC) with waterborne polyurethanes (WPU) with ester or ether soft segments (Yu *et al.*, 2006). After the polymeric chains of 6-OCC were respectively cross-linked with glutaraldehyde or cross-linked/grafted with ethylene

glycol diglycidyl ether (EGDE), the 6-OCC/WPU semi-IPN membranes was prepared. Cross-linking and grafting changed the miscibility of the 6-OCC/WPU semi-IPN membranes, resulted in their different tensile strength and modulus. Sullad *et al.* prepared the CS/PU semi-IPN microspheres through the water-in-oil emulsion cross-linking method by using glutaraldehyde as a cross-linker (Sullad *et al.*, 2015). Two widely used different types of water-soluble cardiovascular drugs in terms of plasma half-life and chemical structures, i.e., calcium dobesilate and isoxsuprine hydrochloride, were loaded into the composite microspheres. Their controlled release characteristics in acidic and alkaline pH conditions were investigated, it was found that these formulations are fit to be used as oral dosage forms.

Polyurethanes are widely used as cardiovascular biomaterials due to their excellent good biocompatibility and mechanical properties. However, protein adsorption, surface induced thrombosis and cytocompatibility are three serious problems when PU is used as implantable material. And the intrinsic inert property of PU is not fit for endothelial cell growth. Hence, it is necessary that the antithrombogenicity and biocompatibility of PU should be enhanced through modification. Xu *et al.* immobilized CS onto the surface of waterborne PU through the assembly of polyelectrolyte in aqueous emulsion, then a series of core-shell ionic complex aqueous emulsion, PU-c-CS, were prepared (Xu *et al.*, 2010). The corresponding films exhibited good mechanical properties. The PU-c-CS films exhibited very low cytotoxicity and supported the adhesion and growth of the human umbilical vein endothelial cells. The adsorption of the bovine serum albumin was significantly decreased for the PU-c-CS films. Furthermore, the test results of prothrombin time and activated partial thromboplastin time demonstrated that antithrombogenicity of the materials were effectively improved. Hence, the above composite is a new candidate for implantable materials. Lin *et al.* immobilized the water-soluble chitosan (WSC)/dextran sulfate (DS) onto the surface of thermoplastic polyurethane (TPU) membrane after ozone-induced graft polymerization of poly(acrylic acid) (PAA) (Lin *et al.*, 2005). It was found that the blood compatibility of TPU membranes was improved by immobilizing WSC/DS onto the surface. When WSC/DS-immobilizing TPU membrane is contacted with blood, the coagulation time is considerably prolonged, and platelet adhesion and protein adsorption are effectively reduced.

The ability of molecules, and in particular macromolecules, to mend broken bonds *in situ* is perhaps one of the most interesting phenomena that spark a lot of scientific interest. The recent exciting study results from Ghosh *et al.* showed that the composite prepared from chitosan and polyurethanes could be molecular level self-repaired as initiating of UV lighting (Ghosh & Urban, 2009; Ghosh *et al.*, 2012). They developed the heterogeneous PU networks based on oxolane substituted derivative of chitosan (OXO-CS) or oxetane substituted derivative of chitosan (OXE-CS), which upon reaction with hexamethylene diisocyanate (HDI) and polyethylene glycol (PEG) form heterogeneous OXO-CS-PU or OXE-CS-PU networks. The choice of these components was driven by their ability to serve specific functions. OXE-CS or OXO-CS provide the cleavage of a constrained four-membered ring (OXE) or five-membered ring (OXO)

and UV sensitivity through CS, and PU networks provide desirable heterogeneity through polyurethane and polyurea components.

15.3.2 Composites from Chitosan and Poly (Lactic Acid)

The poly (lactic acid) (PLA) can be produced from renewable resources such as starch via fermentation processes. It belongs to the family of aliphatic polyester commonly made from lactic acid. PLA is a biodegradable thermoplastic polymeric material with high strength, high modulus, low toxicity, excellent biocompatibility and bio-absorbability *in vivo*. However the degradation rate of PLA was reduced by its low hydrophilicity and high crystallinity. The disadvantages including poor toughness, uncontrolled degradation rate, strong hydrophobicity and local inflammatory response confined the direct application of PLA (Niu *et al.*, 2013).

However, effective compositing CS with PLA at a highly miscible level is still a challenge due to the following two main difficulties (Zhang & Cui, 2012): (1) It is impossible to blend CS with PLA by the melting processing technique because CS has a high glass transition temperature and will possibly start to decompose before melting, (2) PLA can normally only be dissolved in some organic solvents, while CS can only be dissolved in very few kinds of dilute acidic aqueous solutions. It is thus hard to find the suitable co-solvent for CS and PLA. So there is great challenge for preparation the homogeneous composite of CS and PLA.

The chemical composition of PLA provides a hydrophobic nature and linear structure which contributes to an excellent spinability process during electrospinning. The combination of CS and PLA as electrospun fiber has been reported for the development of new biomaterials for wound healing and tissue engineering at different configurations, like blend, co-spun and coaxial fibers. Hardiansyah *et al.* prepared the CS/PLA nanofibers via the blend electrospinning process by developing a new solvent system to prepare CS-blended PLA solution, in which ethanol was added to make chitosan/HAc (aq) and PLA/CHCl₃ miscible. The above composite nanofibers exhibited both noncytotoxicity to L-929 cells and antibacterial activity against *Eschericia Coli*, making them promising to be used for biomedical applications (Hardiansyah *et al.*, 2015). Siqueira *et al.* evaluated the influence of PLA/CS electrospun fibers as support for lipase immobilization (Siqueira *et al.*, 2015). It was found that the addition of chitosan to the composition of PLA nanofibers did not change the hydrophobicity / hydrophilicity of the support's surface significantly, but it had a considerable importance on the immobilization of lipase as well as in the reusability of the composite nanofibers.

CS and PLA can also be used to prepare the composite membrane. The introducing of the PLA is intended to reinforce the chitosan membrane. By the way, using of CS in the CS/PLA membrane can promote the antibacterial property and biocompatibility of it. Ferreira *et al.* developed a simple and optimized method for the preparation of CS/PLA composite membrane through solvent casting by using a common solvent, hexafluor-2-propanol. The visible phase separation could not be observed during the process (Ferreira *et al.*, 2014). Ku *et al.* prepared a CS/PLA multilayered membrane which was composed by the chitosan mesh as outer layers and nanoporous CS/PLA membrane as the middle layer (Ku *et al.*, 2009). The chitosan fibrous mesh outer membranes present a highly biocompatible and rough surface for ease of cell adherence.

The CS/PLA membrane could provide mechanical strength to the membrane, thereby preventing epithelial invasion. By the way, the CS/PLA membrane was applied as a local delivery carrier for growth factors. The above multilayered membrane properly functioned as mechanically stable and biocompatible barriers for guided tissue regeneration. The PLA and the chitosan exhibited interesting qualities in the field of bioactive packaging, due to excellent mechanical and moisture barrier properties associated with liquid water resistance of PLA films and antimicrobial properties of chitosan films. Sebastien *et al.* developed the CS/PLA composite membranes through a solution mixing and a membrane casting procedure (Sebastien *et al.*, 2006). It was found that the composite membranes show a great advantage in preventing the surface growth of mycotoxinogen strains because of their antifungal activity. So they are potential to be used as food packaging materials. Zhu *et al.* developed a new entrapment strategy to modify the PLA membrane with chitosan and chitosan-amino acid derivatives (Zhu *et al.*, 2002). The composite membrane possesses an ECM-like surface to promote cell adhesion, growth and chondrogenesis.

As adjustable degradability of the CS/PLA composite microparticles, they were good candidate as the carrier of the functional molecules, including drugs, DNA, RNA, and so on. Messai *et al.* surface modified the pre-formed PLA particles with various chitosans. Then the above composite particles were used as the DNA carrier for gene transfection (Messai *et al.*, 2005). The above biodegradable carriers could interact with DNA in acidic or neutral media. Dev *et al.* prepared CS/PLA composite nanoparticles through the emulsion method (Dev *et al.*, 2010). At the same time, the hydrophilic antiretroviral drug Lamivudine was loaded into the nanoparticles. The *in-vitro* drug release studies showed that drug release rate was lower in the acidic pH compared with alkaline pH. This may due to repulsion between cationic groups present in the polymeric nanoparticles and H⁺ ions. So such nanoparticles can provide sustained release at neutral pH (intestine) and then entrap and protect the drugs at stomach environment (acidic pH). The above PLA/CS nanoparticles are a potential carrier system for controlled delivery of anti-HIV drugs.

15.3.3 Composites from Chitosan and Polyvinyl Alcohol

Polyvinyl alcohol (PVA) is a synthetic, water soluble polymer with excellent emulsifying, film forming, and adhesive properties (Kanatt *et al.*, 2012). It also imparts good flexibility, tensile strength, biodegradability and biocompatibility, and hence has been widely used as biomaterial. Although PVA presents a promising application, simple PVA lacks biological activity. It cannot act as a matrix for stimulating cell migration and proliferation. As introducing of CS, the biological properties of PVA products could be promoted (He & Xiong, 2012) and the application fields of it could be expanded.

Zang *et al.* modified PVA with 3-aminopropyl triethoxysilane. After it was activated by glutaraldehyde, the chemically cross-linked beads were formed with chitosan. The corresponding catalase immobilized activated beads exhibited about 1400 U/g_{support} higher activity than the control group. The thermal stability of catalase was also enhanced after immobilization. Moreover, the immobilized catalase retained more than 90% of its original activity after being used nine times (Zang *et al.*, 2012).

PVA can be composited in the membrane of CS to enhance its mechanical property. Mishra *et al.* coated the CS/PVA composite membrane on Titanium (Ti) metal, which can

be used for orthopaedic implants (Mishra *et al.*, 2014). The composite membrane showed considerable improvement in mechanical properties comprising CS and PVA membrane on Ti metal. It could effectively and efficiently shield the high mechanical properties of Ti metal in physiological conditions. The scratch tests performed on the coated specimens also found a good adhesion of the composite membrane on the Ti metal surface.

By the way, there are some interesting properties for composite membrane of CS and PVA. Zarghami *et al.* used glutaraldehyde (GA) as cross-linker to cross-link the blended CS/PVA. And then a self-supported ion imprinted membrane (IIM) adsorbent via the solution casting method using copper ions as template was prepared (Zarghami *et al.*, 2015). The Adsorption behavior of Cu (II) ions on IIM was examined. The reusability of the adsorptive Cu (II) imprinted membranes was confirmed after five sorption-regeneration cycles. Liao *et al.* recently prepared a novel polymer composite electrolyte membrane consisting of quaternized polyvinyl alcohol (Q-PVA) and quaternized chitosan nano-particles (Q-chitosan) (Liao *et al.*, 2015). Incorporation of Q-chitosan nano-particles into the Q-PVA matrix results not only in an increased ion-exchange capacity but also a decreased polymer crystallinity and higher free volume hole density, which significantly enhance ion conduction. In addition, the resulting nano-composite exhibited an inhibited in-plane swelling ratio without sacrificing the alkali uptake level. The mechanism was shown in Figure 15.5. When it was used in a direct alcohol alkaline fuel cell, the maximum power density of $73 \text{ mW} \cdot \text{cm}^{-2}$ was achieved at the optimum conditions, which is higher than most data in the literature. The above Q-PVA/Q-chitosan nano-composite is a promising electrolyte for fuel cell and battery applications. Palana *et al.* also found that the PVA/CS/montmorillonite (MMT) composite membranes can

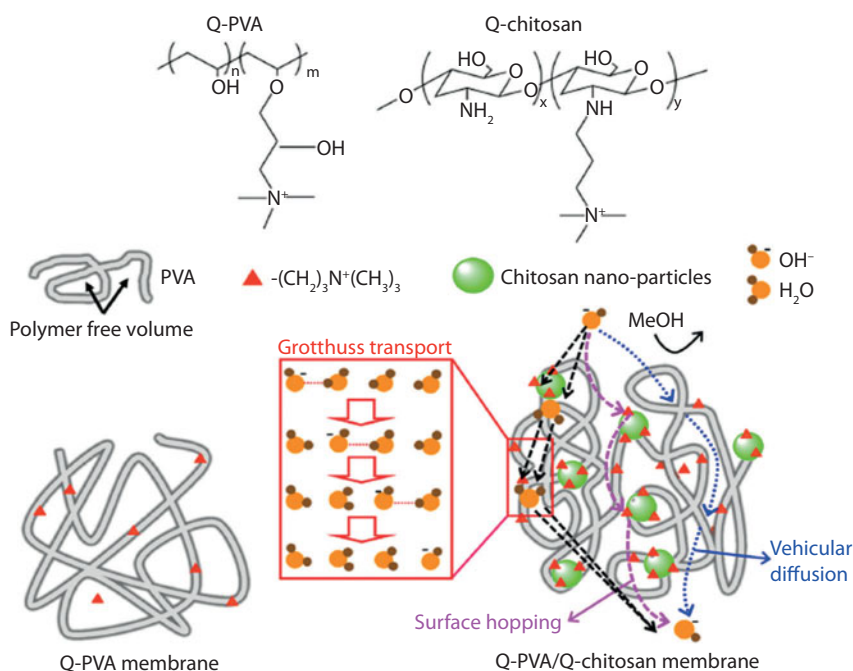


Figure 15.5 Illustration of super hydroxide-conducting pathway in the polymer electrolyte consisting of Q-PVA and Q-chitosan, which is synthesized to enhance anion hopping and diffusion property (Liao *et al.*, 2015).

improve the proton conductivity than the PVA/MMT membrane (Palani *et al.*, 2014). The introduction of CS into the composite membrane could assist in proton transfer and also improve the thermal stability.

PVA has excellent fiber forming property. Blending CS with PVA can increase the electrospinnability of chitosan solution and avoid the disadvantages for electrospinning of chitosan. The combination of the satisfied morphological structure and super-fine diameters of a CS/PVA nanofibrous mat, and containing a high content of CS at the same time, is an inevitable prerequisite to fabricate a high performance CS-containing nanofibrous mat which can be appropriated for a wide variety of applications (Askari *et al.*, 2014; Qu *et al.*, 2014). Charernsriwilaiwat *et al.* prepared the CS-ethylenediaminetetraacetic acid (EDTA)/PVA composite nanofiber mats by electrospinning (Charernsriwilaiwat *et al.*, 2012). It was found that the above CS-EDTA/PVA nanofiber showed satisfactory antibacterial activity against both gram-negative and gram-positive bacteria. An *in vivo* wound healing test showed that the CS-EDTA/PVA nanofiber mats showed better performance in decreasing acute wound size during the first week after tissue damage than gauze. They are promising to be used as wound dressing materials.

15.3.4 Composites from Chitosan and Poly(γ -Glutamic Acid)

Poly(γ -glutamic acid) (γ -PGA) is a kind of polyamino acid which is composed by D-glutamic acid and L-glutamic acid via the linkage of the γ -glutamine bond. They can be synthesized chemically or produced microbially. Their molecular weights are in the range of $1 \times 10^6 \sim 1 \times 10^7$. γ -PGA could be degraded to the monomer of glutamic acid in human body, which is essential for human body. By the way, γ -PGA bears good biocompatibility, low immunogenicity and non-poisonous. As the segments of amino acid in γ -PGA, the affinity of it with the cell could be promoted. Then the scaffold prepared from γ -PGA could adhere with the seed cells easily, and then the bioactivity could be promoted. By the way, as the wide range of the molecular weight of γ -PGA, the degradation rate of the corresponding tissue engineering scaffold could be adjusted by changing the degree of the polymerization of γ -PGA and the cross-linking degree of the network structure.

At the acid conditions, chitosan could be transferred to the cationic polyelectrolyte via interaction of the $-\text{NH}_2$ with H^+ . Then it could interact with Poly(γ -glutamic acid) through the polyelectrolyte complex and the novel CS/ γ -PGA composite could be formed (Antunes *et al.*, 2011). As good hydrophilicity of γ -PGA, introducing of it in the composite could promote the swelling property of the CS products. By the way, complexing of CS with γ -PGA could adjust the degradation rate of γ -PGA products. Moreover, the above polyelectrolyte complex could show very interesting pH responsibility (Park *et al.*, 2013).

Via the polyelectrolyte complex between CS and γ -PGA, the multi-functional composite microparticles could be prepared as the carrier of the bioactive molecules. Liu *et al.* coated the lysozymes with γ -PGA and further rewrapped with chitosan to prepare the lysozyme-loaded CS/ γ -PGA composite nanosystems for loading and controlling the release of lysozymes (Liu *et al.*, 2013). The loading efficiency and loading content could reach 76% and 40%, respectively. The *in vitro* release testing results

showed that the release of lysozyme was slow and presented a two-stage programmed release. The *in vitro* antibacterial testing indicated the above composite nanoparticles had outstanding antibacterial activity. An obvious assembly of bacterial cells and composite nanoparticles could be observed during the process of coin cubation. Sun *et al.* constructed the CS/ γ -PGA composite microparticles to use as the delivery systems of antimicrobial peptides and nitric oxide (Sun *et al.*, 2015). Using ionic complexation between the negatively charged polyelectrolyte γ -PGA and the positively charged antimicrobial peptides LL-37, γ -PGA /LL-37 microparticles with negative zeta potentials were produced firstly. Then γ -PGA/LL-37 composite microparticles were rewrapped by CS to obtain LL-37 loaded CS/ γ -PGA composite microparticles. Nitric oxide (NO), a diatomic free radical that has an important function in the natural immune system response to infection, was further loaded in microparticles by the reaction of NO and LL-37 loaded CS/ γ -PGA composite microparticles under high NO pressure. The composite particles could sustain release NO and LL-37 at pH 7.4 *in vitro*.

As the outstanding properties of CS and γ -PGA, their composite can be prepared to scaffolds for tissue engineering. Zhang *et al.* formed CS/PGA three-dimensional (3-D) scaffolds by electrostatic interaction (Zhang *et al.*, 2013; Yan *et al.*, 2013). Autologous adipose-derived stem cells (ASCs) were expanded and seeded on CS/PGA scaffolds. It was found that the CS/PGA scaffolds could effectively support ASCs adherence, proliferation and chondrogenic differentiation. The scaffolds seeded with ASCs could promote the regeneration of hyaline cartilage, repair a full thickness articular cartilage defect over 12 weeks. This novel CS/PGA polyelectrolyte complex possesses great potential as a scaffold for cartilage tissue engineering. Fang *et al.* homogeneously absorbed the PGA within the porous chitosan microspheres via polyelectrolyte complex (Fang *et al.*, 2014). Compared with microspheres fabricated from chitosan, the porous composite microspheres could efficiently promote chondrocyte attachment and proliferation. After being injected subcutaneously for 8 weeks, it was found that the composite microspheres loaded with chondrocytes were found to produce significant more cartilaginous matrix than chitosan microspheres, which indicate that these novel composite microspheres could be used as injectable cell carriers for cartilage tissue engineering.

Stimuli-responsive materials have attracted much attention due to their possible applications in biomedicine, such as probing biomolecules or delivering drugs. As the positive charges and negative charges were coexisted in the composite prepared from CS and γ -PGA, they can show very interesting stimuli-responsive properties. Yu *et al.* cross-linked the carboxymethyl chitosan (CM-CS)/ γ -PGA conjugates with fluorescence with genipin (Yu *et al.*, 2012). It was found that the genipin-conjugated polymers were sensitive to the oxidation product of glucose, gluconic acid and hydrogen peroxide (H_2O_2). The above polymers could be self-aggregated into nanoparticles and the fluorescent emissions were quenched under the stimulus of gluconic acid and H_2O_2 . BSA could be loaded in the self-aggregated nanoparticles and the incorporated BSA could be slowly released from the nanoparticles, in the presence of 25 or 50 mM gluconic acid. The result indicated that the above composites may be potential used as a stimuli-responsive material for optical sensing and protein delivery purposes.

15.4 Composites from Chitosan and Biomacromolecules

Besides composites of chitosan with different kinds of polymers, they can also composite with the different biomacromolecules, including DNA, RNA, protein, peptides, liposomes, etc. As good bioactivities of the above biomacromolecules, combining with them could promote the bioactivities and functionalities of chitosan. The above composites are widely used as biomedical materials.

15.4.1 Composites from Chitosan and DNA or SiRNA

Gene therapy is an effective method for the treatment of human disorders by the introduction of genetic material into specific target cells of a patient, where production of the encoded protein will occur. During the last ten years, gene delivery research has developed very rapidly due to its huge potential as a future therapeutic strategy for clinical applications to treat many inheritable or acquired diseases by substituting missing genes, replacing defective genes, or silencing unwanted gene expression. Gene therapy is currently being used in many different health problems such as AIDS, cancer, and cardiovascular diseases. However, naked therapeutic genes are rapidly degraded by nucleases, nonspecificity to the target cells, showing poor cellular uptake, and low transfection efficiency are the main problems that limit the development of the gene therapy (Kim *et al.*, 2007). Many researches are working in the field of finding safe and efficient gene delivery carriers, as they are one of the prerequisites for the success of gene therapy (Mao *et al.*, 2010). And a wide variety of vectors to deliver therapeutic genes into the desired target cells have been studied.

An ideal gene-delivering carrier should bear the property of transport genetic without any toxicity and immune responses. It must be capable of protecting the DNA or SiRNA before it reaches its target. To do so, the system must be small enough to allow internalization into cells and passage to the nucleus, it must have flexible tropisms for applicability in a range of disease targets, and it must be capable of escaping endosome-lysosome processing and of following endocytosis (Jayakumar *et al.*, 2010).

At present, major gene delivery systems use either viral or non-viral vectors. The most common viral vectors used today are herpes simplex virus, retrovirus, adenovirus, lentivirus and adeno-associated virus, each having its own characteristics (Oligino *et al.*, 2000). Viral vectors are very efficient for *in vivo* transfection, as well as immunization, for high transfection rate and a rapid transcription of the foreign material inserted in the viral genome. Their major drawbacks include possible toxicity, poor target specificity, immunogenicity, low capacity to incorporate foreign DNA sequences to their genome, the risk of causing insertional mutagenesis, viral wild-type mutations, inflammatory potential, and potential oncogenic effects. Therefore, viral-based vectors urgently need to be reassessed with regard to their safety for human gene therapy.

Non-viral vectors have attracted increasing attention due to such advantages as ease of synthesis, unrestricted gene materials size, minimal host immune response against the vector, stable in storage, easy to produce in large quantities in addition to potential benefits in terms of safety (Remaut *et al.*, 2007). Non-viral vectors include complexes of the negatively charged plasmid with cationic polymers, cationic liposomes, and nanoparticles. Although cationic liposomes show low immunogenicity, they are

not fit for gene therapy due to their relatively low transfection efficiency and the toxicity (Deshpande *et al.*, 1998).

Non-viral systems based on cationic polymers containing several amine groups in their backbone have been used extensively as gene carriers. They can provide well defined physicochemical properties, unlimited DNA packaging capacity, and a high degree of molecular diversity that allows extensive modifications to overcome extracellular and intracellular obstacles of gene delivery. Though the efficiency of gene delivery by cationic polymers is still relatively low, DNA/ cationic polymers complexes are more stable than cationic lipids (De Smedt *et al.*, 2000). An ideal polymeric carrier should hide from the host surveillance systems, form a stable complex with nucleic acids to maintain its stability in a biological solution, and deliver the therapeutic nucleic acid to the desired cell population by recognizing a specific characteristic on the cell surface. After being localized within the cells, the carrier should deliver the complexes to the vicinity of the targets, provide appropriate functionalities to escape from the endocytotic pathways, perform decomplexation (or unpacking) in response to a certain intracellular environment, such as pH or redox potential, and actively transport the nucleic acids to the target (Jeong *et al.*, 2007). The cationic polymers that has been investigated include poly(L-lysine), poly(L-histidine)-graft-poly(L-lysine), poly(D,L-lactide-coglycolide) (PLGA), poly(ethylene imine) (PEI), polyamidoamine dendrimers, polybrene, tetraminofullerene, etc. Natural polymers that have been tried include chitosan and its derivatives, gelatin, collagen, etc (Tahara *et al.*, 2008).

In 1995, Murnper *et al.* first reported that a kind of complex from chitosan and DNA with size of 150–500nm could be obtained by precipitation through the self-aggregation, it is potential to be used for the carrier of gene therapy (Murnper *et al.*, 1995). Up to now, chitosan has become one of good candidate for gene delivery system because positively charged chitosan can be complexed with negatively charged plasmid DNA (pDNA), siRNA and oligonucleotides by ionic interactions. Chitosan-based carriers are one of the important non-viral vectors that have attracted more and more attentions as a safe delivery system for gene materials (Hejazi & Amiji, 2003). Chitosan has beneficial qualities such as reduced cytotoxicity compared to other polymers, low immunogenicity, excellent biocompatibility, as well as a high positive charge density. Also, the mucoadhesive property of chitosan potentially permits a sustained interaction between the macromolecule being “delivered” and the membrane epithelia, promoting more efficient uptake and it has the ability to open intercellular tight junctions, facilitating its transport into the cells (Illum *et al.*, 2001).

Various gene delivery systems based on chitosan have been described such as DNA or SiRNA-chitosan nanospheres, self-assembling polymeric and permanent oligomeric chitosan/DNA or SiRNA complexes, etc. Recently, Yan *et al.* prepared a novel type of Tat tagged and folate modified N-succinyl-chitosan (Tat-Suc-FA), then it was self-assembled with DNA to form the Tat-Suc-FA/DNA composite nanoparticles for gene delivery (Yan *et al.*, 2015). Zeng *et al.* prepared the CS/poly(D, L-lactide-co-glycolide) (PLGA) composite nanoparticles (NPs) for plasmid DNA (pDNA) delivery by a spontaneous emulsion diffusion method (Zeng *et al.*, 2011). The effectiveness of pDNA-loaded CS/PLGA nanoparticles in slicing Hepatitis B virus (HBV) gene and in expressing the indicative enhanced Green Fluorescent Protein (eGFP) was examined in HepG2.2.15 cells. CS/PLGA NPs exhibited much higher loading efficiency than unmodified PLGA

NPs. EGFP expression indicated that pDNA-loaded CS/PLGA NPs could be more effectively taken up by the cells than plain-PLGA NPs. The HBV gene-silencing efficiency of CS/PLGA NPs was higher than those of plain-PLGA NPs and naked pDNA.

However, gene delivery efficiency of chitosan is significantly influenced by formulation related parameters, including degree of deacetylation of chitosan, negative/positive (N/P) charge ratio, the molecular weight of chitosan, chitosan sale form, plasmid concentration, adding of the additives and the pH of the culture medium, etc. Koping-Hoggard *et al.* combined fluorescence-labeled T4 DNA with six different chitosan oligomers (6-, 8-, 10-, 12-, 14- and 24-mers) (Koping-Hoggard *et al.*, 2003). It was found that charge ratio (+/-), chitosan chain length and solvent properties (pH and ionic strength) could affect the structure and stability of the complexes. It was found gene transfection efficiencies *in vitro* and *in vivo* were related to the physical shape and stability of the complexes. Only the 24-mer formed stable complexes could give a high level of gene expression comparable to that of high molecular weight ultra pure chitosan *in vitro* and *in vivo*. Cifani *et al.* obtained chitosan/DNA complexes using chitosan of 50 kDa and an N/P ratio of 10, they found that the *in vitro* transfection efficiencies of the complexes could be improved as the increased stabilization of them (Cifani *et al.*, 2015). These preparations showed reproducible transfection efficiencies *in vitro* in HEK293 cells and could be stable up to 3 months at 4 °C. Santos-Carballal *et al.* investigated the biological responses of self-assembled CS-micro RNA (miRNA) nano complexes produced with a range of (+/-) charge ratios (from 0.6 to 8) using chitosans with various molecular weight and degrees of acetylation to MCF-7 breast cancer cells cultured *in vitro* (Santos-Carballal *et al.*, 2015). It was found that chitosan could induce the base-stacking of miRNA in a concentration dependent manner. The complexes formed by low degree of acetylation chitosans are highly stable, none of the molecular weight. Furthermore, CS-miRNA nano complexes with degree of acetylation 12% and 29% were biologically active, which showed successful down regulation of target mRNA expression in MCF-7 cells.

In the opinion of clinic application, the transfection efficiency of the pure chitosan as the carrier of gene transfection is lower, and the specificity is also very weak. Chemical modification of chitosan is the important route to promote the transfection efficiency and specificity of chitosan. As there are abundant groups with high reactivity on the skeleton of chitosan, it is easy to promote the complexing ability and stability between chitosan and plasmid DNA via chemical modification. According to the requirement, the specific ligand or antibody can be conjugated with chitosan to promote the targeting effects of the carrier and increase the efficiency of gene transfection. Up to now, the mainly used modification methods including to increase the hydrophilicity, hydrophobicity, pH sensitivity, or conjugating with the specific ligand, etc. Sajomsang *et al.* prepared a series of methylated N-pyridylmethyl chitosan chlorides (M-PyMeCSCs) derivatives (Sajomsang *et al.*, 2014). It was found that M-PyMeChCs are able to form a complete complex formation with DNA since there is an N/P ratio of 5. The N-pyridinium positions of M-PyMeCSCs are related to transfection efficiency and cytotoxicity. Nam *et al.* used low molecular weight water soluble O-carboxymethyl chitosan (OCMCS), branched low molecular weight poly(ethyleneimine) (bPEI), and targeting ligand (epitope type, HER-2/neu) to prepare the OCMCS/bPEI/targeting ligand (HPOCP) targeting ligand-modified polyamphoteric copolymer (Nam *et al.*, 2016). It

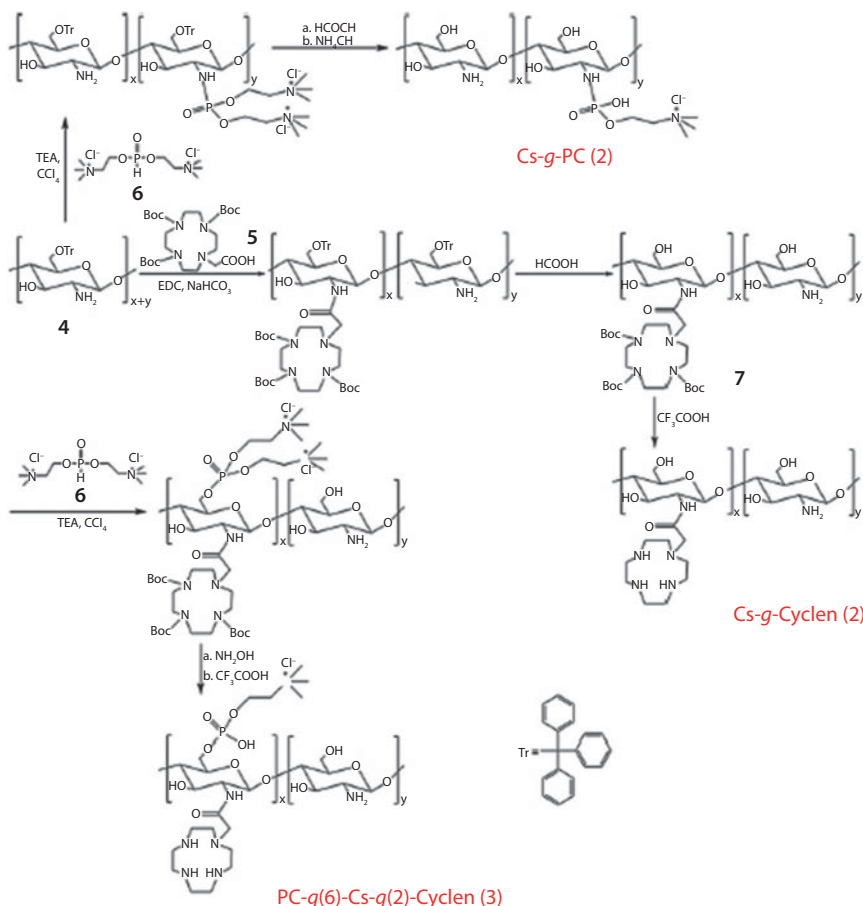


Figure 15.6 The synthesis routes of CS-g-Cyclen (1), CS-g-PC (2), and PC-g(6)-CS-g(2)-Cyclen (3) (Li *et al.*, 2015).

was found that HPOCP copolymer is a good candidate for a targeting gene (pDNA or siRNA) carrier in gene therapy, because of its high gene binding capability, high gene transfection efficiency, high cellular uptake efficiency and low cytotoxicity.

Li *et al.* prepared macrocyclic polyamine and phosphorylcholine grafted chitosan (PC-g(6)-CS-g(2)-Cyclen) via the process showed in Figure 15.6 (Li *et al.*, 2015). Compared with macrocyclic polyamine grafted chitosan (CS-g-Cyclen) and phosphorylcholine grafted chitosan (CS-g-PC), It was found that PC-g(6)-CS-g(2)-Cyclen could more efficiently bind and protect plasmid DNA. In addition, three polymer/DNA complexes showed 10~14 fold higher transfection efficiency and 5.1~15.1 fold greater uptake activity in 293T cells as compared to chitosan/DNA complex, in which PC-g(6)-CS-g(2)-Cyclen demonstrated the highest transfection activity.

15.4.2 Composites from Chitosan and Peptides

Peptides are biological polymer of amino acid linked by peptide (amide) bonds. Peptides have been widely used in medicine and biotechnology. They can regulate most

physiological processes, acting at some sites as neurotransmitters or growth factors and at others as endocrine or paracrine signals. Compositing of peptides with chitosan could promote the bioactivities of the derivate of chitosan, so it is attracted more and more attentions in recent years.

As good reactivity of the 2-NH₂ of chitosan, peptide can be conjugated to the skeleton of chitosan or its derivatives. Karagozlu *et al.* conjugated the tripeptides which consist of tryptophan (W), methionine (M) and glutamine (Q) with chitosan oligomers (COS) (Karagozlu *et al.*, 2014). It was found that QMW-COS and WMQ-COS are bioactive compounds which can inhibit HIV-induced cytopathic effects via exerting their effects on HIV entry stage. Zhu *et al.* coupled collagen peptides (COPs) on the backbone of quaternized carboxymethyl chitosan (QCMC) (Zhu *et al.*, 2014). It was found that the introduction of COPs into the QCMC could improve its hydrogen peroxide-scavenging activity and cell viability as increasing the degree of substitution and concentration. Therefore, the above composite product is beneficial to the process of the wound-healing.

The peptide conjugated chitosan can also be used to prepare other products, including micelle, microparticles, etc.

According to the requirment of the targeting delivery, Chen *et al.* prepared a homing peptide-(TNYLFSPNGPIA, TNYL) modified chitosan-g-stearate (CS) polymer micelle (named T-CS) (Chen *et al.*, 2015). The T-CS displayed specific binding affinity to EphB4, which is a member of the Eph family of receptor tyrosine protein kinases. The amphiphilic polymer T-CS can gather into micelles by themselves in an aqueous environment with nano-scaled size (82.1 ± 2.8 nm) and a low critical micelle concentration value ($91.2 \mu\text{g/L}$). The drug encapsulation efficiency for loading of the hydrophobic drug doxorubicin (DOX) could reach 86.43%. The cellular uptake and antitumor activity of the T-CS-based drug delivery system could be significantly enhanced in EphB4-positive cells due to increased endocytosis mediated by the targeting molecule TNYL. Both *in vitro* and *in vivo* tests showed the tumor-specific delivery due to the active-targeting modification. The above results demonstrate that the T-CS micelles are a potential candidate for active-targeting drug delivery.

Recently, Wang *et al.* developed a vasoactive peptide modified chitosan nanoparticles that could enhance drug accumulation and penetration in lung metastasis and subcutaneous tumor (Wang *et al.*, 2014). The platinum (IV) compound, a kind of bioreductively sensitive drug which could become cisplatin in intracellular reductive environments, and bradykinin-potentiating peptide (BPP) containing 9 amino acid residues, a kind of vasoactive peptide, are covalently linked with chitosan nanoparticles with a diameter of 120 nm. It was demonstrated that BPP-decorated chitosan nanoparticles decrease the tumor interstitial fluid pressure and increase the tumorous vascular permeability in tumor-bearing mice, both of which improve the penetration of nanoparticles in tumor tissues. The tumor inhibition examinations and *in vivo* bio-distribution demonstrate that the BPP-decorated nanoparticle formulation has more superior efficacy in enhancing drug accumulation in tumor, restraining tumor growth and prolonging the lifetime of tumor-bearing mice than non-decorated nanoparticle formulation and free drug. Meanwhile, the drug accumulation in the lung with metastasis for the chitosan nanoparticles with and without BPP decoration is 10-fold larger than that of free cisplatin. This work found a new way on the design of provascular nanoparticular drug delivery systems for cancer treatment.

15.4.3 Composites from Chitosan and Liposomes

Liposomes are vesicles composed of one or more phospholipid bilayers. They can carry a variety of molecules with therapeutical potential (water-soluble or not) and can enable the delivery of drugs in a sustained and predictable manner (Diebold *et al.*, 2007; Liu *et al.*, 2015). Indeed, since the first description of liposomes in 1965, numerous clinical trials have been achieved in the delivery of antibiotic, anti-fungal, anti-cancer drugs, gene medicines, anti-inflammatory drugs and anesthetics. These lipidic objects were the first nanomedicine delivery systems to make the transition from concept to clinical application. As chitosan can be widely used in drug delivery, incorporating of CS into the liposomes based drug delivery system is expected to overcome the disadvantages of the long term degradation/destabilization of the drug by the lipid bilayer.

Billard *et al.* entrapped the phosphatidylcholine liposomes within a chitosan physical hydrogel, which was only constituted of polymer and water, to construct a “liposome-in-hydrogel” system (Billard *et al.*, 2015). The pattern is shown in Figure 15.7. The incorporation of liposome did not prevent the formation of the gel. Ulteriorly, the delayed-release properties of this “hybrid” system were studied by using carboxy-fluorescein (CF) as a model water soluble molecule to be encapsulated in liposomes, and then they were incorporated into the chitosan hydrogel. Intensive washings of hydrogels revealed a delayed release of CF molecule encapsulated in liposomes for the “liposome-in-hydrogel” system (cumulated release of ca 70%) comparing with the system where CF was free in hydrogels (cumulated release of ca 85%).

Peptides and proteins have low stability. Thus, encapsulating of them in liposomes would promote the stability and safety. Compositing of them with chitosan further could promote the bioactivity and functionality. Degim *et al.* developed a chitosan gel formulation containing liposomes loaded with epidermal growth factor (EGF) (Degim *et al.*, 2011). Then their effects on the healing of second-degree burn wounds in rats were evaluated by histochemical and histological, immune histochemical methods with EGF-loaded liposome formulations and EGF gel as comparasion. It was found that the chitosan gel formulation with EGF-containing liposome could significant increases the cell proliferation and epithelisation rate compared with the other groups.

In the liposomes/chitosan composite, the pH sensitive delivering properties of the chitosan system could also be kept. And then they can show interesting pH sensitive sustained releasing property to drug. Caddeo *et al.* developed a hybrid system made of liposomes coated with sodium tripolyphosphate cross-linked chitosan (as shown in Figure 15.8) (Caddeo *et al.*, 2016). The use of a protective three-dimensional polyelectrolyte shell layer was expected to allow circumventing possible damage of both the vesicles

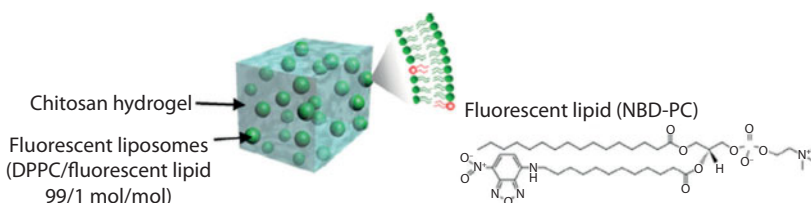


Figure 15.7 The pattern of liposome-in-hydrogel system (Billard *et al.*, 2015).

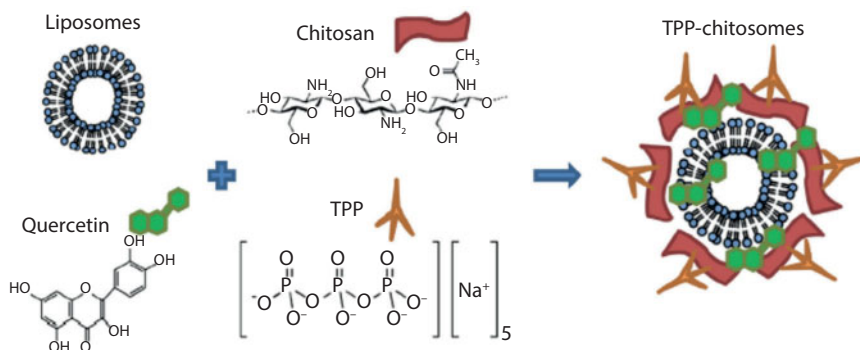


Figure 15.8 Cross-linked chitosan/liposome hybrid system (Caddeo *et al.*, 2016).

and the incorporated drug due to the acidic pH of the stomach. From *in vitro* tests, it was found that this system provided resistance to acidic conditions, and promoted the release in alkaline pH, mimicking the intestinal environment. Deng *et al.* coated the Cyclosporine A (CsA) liposomes (CL) with amphiphilic N-Octyl-N-Arginine-Chitosan (OACS) (Deng *et al.*, 2015). It was found through the release experiment that OACS could slow down drug release and protect its degradation in the stomach. *In-situ* single pass perfusion proved that the absorption of OACS-CL at the jejunum was enhanced about 22 and 3 times compared with commercial preparation of CsA suspensions and microemulsions (Tianke), respectively.

Recently, ternary complexes of cationic liposomes, cationic polymer and pDNA, named lipopolyplexes, have been developed as the second-generation non-viral vectors. Wang *et al.* developed the lipopolyplexes formed by combining N-[1-(2,3-dioleoyloxy)propyl]-N,N,N-trimethylammonium chloride (DOTAP) as cationic liposomes, CS (low molecular weight, 50–190 kDa; deacetylation, 75–85%) and pDNA via non-covalent conjugation (Wang *et al.*, 2012). They designed and constructed two types of ternary complexes, including DOTAP/CTS/pDNA (DOTAP was added to CTS/pDNA complex), and CTS/DOTAP/pDNA (CTS was added to DOTAP/pDNA complex). The new lipopolyplexes showed high transfection efficiency with a significant improvement of GFP gene expression 36~50-fold over CTS/pDNA polyplex and 4.8~10-fold over the control of DOTAP/pDNA lipoplex in Hep-2 and Hela cells, and luciferase gene expression 70~120-fold than CTS/pDNA control and 2~3-fold than DOTAP/pDNA control in Hep-2 cells, respectively.

15.5 Composites from Chitosan and Inorganic Components

Chitosan or its derivatives were also used to composite with different inorganic components, including clay (Huang *et al.*, 2015; Grigoriadi *et al.*, 2015; Wang *et al.*, 2014), such as kaolin, halloysite, montmorillonite, palygorskite, sepiolite, vermiculite, mica, illite, rectorite, hydrotalcite, etc., or inorganic active substance containing calcium or silicon (Mota *et al.*, 2012), inorganic polymer (Ng *et al.*, 2012; Kikuchi *et al.*, 1987) such as polyaluminum chloride, polyferric chloride, polyferric silicate sulfate and

so on. Among them, the composite prepared by chitosan or its derivatives and the inorganic components composed by calcium or silicon, such as hydroxyapatite, CaCO_3 , SiO_2 , bioactive glasses and different kinds of nanoparticles has attracted more and more attentions for their good bioactivity and wide application prospects.

15.5.1 Composites from Chitosan and Hydroxyapatite

Hydroxyapatite ($\text{Ca}_{10}(\text{PO}_4)_3\text{OH}$, HAp) has been widely used due to its compatibility with synthetic and natural polymers as polysaccharides, chemical similarity to bone and good biocompatibility in the physiological environment. It has been widely used to create the functional biomaterial for medical and veterinary application (Pighinelli *et al.*, 2013). HAp has been used as a biocompatible and osteoconductive substitute in the field of orthopedic surgery. However, HAp is hard to be shaped in the specific forms required for bone substitution due to its brittleness and hardness. By the way, when being used for the treatment of bone defects, HAp powders are easily migrated from the implanted sites. Therefore, novel composites of HAp and organic polymers that can improve the weak mechanical properties of HAp have become of great interest (Yamaguchi *et al.*, 2001).

In addition to the good biocompatibility, biodegradability of chitosan, it is flexible and has a high resistance upon heating due to the intramolecular hydrogen bonds formed between amino and hydroxyl groups. A composite biomaterial prepared from HAp and chitosan therefore is expected to show good biodegradability and biocompatibility together with sufficient mechanical strength for orthopedic use. Moreover, the composite made from chitosan and hydroxyapatite could be used to deliver osteoinductive factors like osteoblasts cultured from the bone-marrow aspirate, or bone-marrow aspirate, or BMP-2. Then it would be an effective material to repair bone defects (Mukherjee *et al.*, 2003).

Different preparation methods of HAp/chitosan composites have been reported, such as coating chitosan on the surface of HAp particles (Mattioli Belmonte *et al.*, 1995) and mixing of a HAp powder in a chitosan solution (Ito, 1991). Yamaguchi *et al.* prepared chitosan/hydroxyapatite (HAp) composites with a homogeneous nanostructure through co-precipitation method (Yamaguchi *et al.*, 2001). The growth of the HAp crystallites is considered to begin at nucleation sites, most probably forming the complexes with amino groups on chitosan with calcium ions. The composites were found to be mechanically flexible, and this flexibility has been improved further by heating at 120 °C for 20 min in an autoclave with saturated steam pressure. When HAp particles in the HAp/CS composites were prepared by mechanical mixing, a more extreme heterogeneity of pore structure and low compressive strength were observed because the homogeneous dispersion of HAp within the composites was difficult to accomplish due to particle agglomeration (Venkatesna & Kim, 2010). Kim *et al.* developed homogeneously dispersed chitosan/nano-sized hydroxyapatite composite scaffolds by using the alginate (AG) solution with a pH higher than 10 as a dispersant for the nano-HAp powders accompanying with the freezing dry (Kim *et al.*, 2015). The nano-HAp/chitosan composite scaffolds containing alginate demonstrated uniform pore structure even with a nano-HAp content of 70 wt.%. The even pore morphology contributed to an increase in the compressive strength and elastic modulus of composite scaffolds, which

increased as a function of nano-HAp content. Higher content of the HAp also helped develop more differentiation and mineralization of the MC3T3-E1 cells on the composite scaffolds.

In recently years, based on chitosan/hydroxyapatite composites, different functional components were also included to promote the properties of CS/HAp composites. Icaritin (ICA) is a kind of Chinese medicine. Chen *et al.* *in-situ* prepared the organic-inorganic hybrid CS/nano-HAp/ICA composite microspheres by high voltage static micro-capsule forming device (Chen *et al.*, 2015). The ICA loaded microspheres take on a sustained release behavior, which can be not only ascribed to electrostatic interaction between positive amine groups ($-NH_2$) of CS and reactive negative hydroxyl ($-OH$) of ICA, but also depended on the homogeneous dispersion of HAp nanoparticles inside CS organic matrix. The composite microspheres could provide a suitable microenvironment for osteoblast attachment and proliferation. The above ICA loaded hybrid microspheres are promising to be used in a bone repairing drug delivery systems.

In the last decades, HAp has also been widely used as an effective absorbent in the long-term disposal of heavy metals because of its low water solubility, high sorption capacity and low cost. Porous HAp provides a large surface area for the adsorption of heavy metal ions and accelerates the rates of ion exchange via porous channels. Besides, the amine groups in CS can form complexes with various heavy metal ions or different anions. The homogenous HAp/CS composite particles, especially the composites with porous structure, have also been used as the absorbents for heavy metal ions (Lei *et al.*, 2015) or anions (Kalimuthu & Natrayasamy, 2015) removal from aqueous solution.

15.5.2 Composites from Chitosan and Calcium Carbonate

Calcium carbonate ($CaCO_3$) is a kind of inorganic minerals widely distributed in nature. The crystal of it is easy to be characterized, and the crystal morphology of it can be controlled during the process of biomineralization. So $CaCO_3$ is a kind of commonly used model minerals for laboratory research. The special crystal structure formed under inducing of chitosan has been of concern for a very long time.

The shell is an attractive target for the design of organic/inorganic hybrid materials by mimicking biomineralization processes. The preparation of layered organic/inorganic composites with controlled structures based on calcium carbonate and chitosan may lead to the developing of new materials similar to the structure of the shell with high function and high performance as well as environmental benignity. Many studies have focused on control over the crystal habit, shape, morphology, and size of $CaCO_3$ on the chitosan matrices. Kato carried out crystallization of $CaCO_3$ on the chitosan matrices from a supersaturated aqueous solution of $CaCO_3$ in the presence of the soluble acidic macromolecules, and then the layered organic/inorganic composites with controlled structures based on $CaCO_3$ could be prepared (Kato, 2000). The thickness and crystal form of $CaCO_3$ layer could be controlled by the conditions. Zhang *et al.* performed the crystal growth of calcium carbonate on a chitosan substrate using a supersaturated calcium carbonate solution, by using various additives, such as polyacrylic acid (PAA) and 6-aminocaproic acid (6AA) (Zhang & Gonsalves, 1995). It was found that polyacrylic acid could promote the nucleation of calcium carbonate crystals and modify the surface of chitosan-film.

Hu *et al.* prepared the three-dimensional CaCO_3 /chitosan composite by the method of *in-situ* precipitation (Hu *et al.*, 2006). It could be observed through SEM that the particles of orbicular were distributed orbicularly on the cross section and its size was about 5~10 μm . It was found through the mechanical test that the bending strength of the composite could be increased to maximum value (~113MPa) as mass content of CaCO_3 at 10%, and the flexural modulus was 2.6 GPa at that time.

Sambudi *et al.* composited the CaCO_3 nanoparticles in electrospunchitosan/poly(vinyl alcohol) (PVA) nano-fibres as a reinforcing agent to increase the mechanical properties (Sambudi *et al.*, 2015). Besides the above simple composite, Zhang *et al.* fabricated a nanofibrous network-like CaCO_3 -Chitosan (CaCO_3 -CS NFs) composite in a controllable and simple approach based on electrolysis induced biomineralization (Zhang *et al.*, 2012). During the formation of the CaCO_3 -CS composite coating, chitosan played a important role as a structure-directing agent. The as-formed CaCO_3 -CS NFs were observed to be covered by multiple small nanoparticles with an average diameter of ~25 nm. These uniform nanoparticles were aligned along the surface of NFs, and constructing a 3D hierarchically interlaced network. It was found that the composite coating of CaCO_3 -CS NFs featuring high mechanical strength, loose 3D assembly, interconnected pores and large surface area, possess excellent cytocompatibility, greatly facilitating cell adhesion and proliferation.

15.5.3 Composites from Chitosan and Silicon Dioxide

As porous structure, certain chemical inertness, higher specific surface areas and thermal stability of nano- SiO_2 , it has been widely used as a supporter to improve the mechanical properties of polymer. It was found from the previous studies and SiO_2 can be well distributed in the matrix of chitosan and the compatability of them is very good. As complexing of SiO_2 , it could not only increase the specific surface areas and density of chitosan, but also promote the chitosan's mechanical property.

Al-Sagheer *et al.* prepapred the Chitosan/ SiO_2 hybrid composites films by sol-gel process using tetraethoxysilane (TEOS) as precursor (Al-Sagheer & Muslim, 2010). It was found that compositing of SiO_2 could promote the thermal stability and mechanical property of the composite at the same time.

Copello *et al.* prepared the chitin hydrogel/ SiO_2 and chitosan hydrogel/ SiO_2 hybrid mesoporous materials through the sol-gel method by using tetraethoxysilane (TEOS) as the SiO_2 precursor (Copello *et al.*, 2011). Then they were used as biosorbents for four dyes (Erythrosine B, Remazol Black B, Gentian Violet and Neutral Red). The use of the polysaccharides in the form of hydrogels showed full compatibility with the ethanol release from TEOS. SiO_2 composited in the network could improve the adsorption properties and mechanical behavior of the absorbents. It was found that chitin can be used to replace chitosan considering the efficiency and lower cost of chitin. By the way, it was found that the adsorption was pH dependent.

Sun *et al.* prepared underwater superoleophobic composite films containing hydrophilic SiO_2 nanoparticles and chitosan on glass substrates by a simple dip-coating method (Sun & Li, 2014). It was found that more hydrophilic SiO_2 powders accumulated on the surfaces of composite films as the increase of the volume ratio of hydrophilic SiO_2 -ethanol suspension to chitosan solution, leading to a significant increase of underwater oleophobicity.

Yuan *et al.* prepared the silicone oxide (SiO_2)-deposited doxorubicin (DOX)-loaded stearic acid-g-chitosan (CS-SA/ SiO_2 /DOX) nanoparticles through the sol-gel reaction under mild conditions by using TEOS as a silica precursor (Yuan *et al.*, 2012). Cross-linking by silica resulted in CS-SA/ SiO_2 /DOX nanoparticles with a mesoporous structure; the sizes of mesopores could be changed at different SiO_2 -deposited ratios. Compared with normal DOX-loaded CS-SA (CS-SA/DOX) micelles, CS-SA/ SiO_2 /DOX showed a more rapid drug release rate *in vitro* and could enter into the cells more easily.

15.5.4 Composites from Chitosan and Bioactive Glasses

Recently, silica based bioactive glasses (BG), a bioactive material composted by $\text{Na}_2\text{O}/\text{CaO}/\text{SiO}_2/\text{P}_2\text{O}_5$, have received many attentions due to their possible to be used in bone tissue engineering (Pon-On *et al.*, 2014). BG scaffolds have been shown to have excellent biocompatibility, osteoconductivity and ability integrate with the surrounding bone tissue *in vivo* by forming a calcium phosphate layer which bonds with living bone. The potential for utilizing their three-dimensional (3-D) structures to improve the mechanical properties and to provide enhanced biological response has received much attention. In recent decades a number of BG materials of different chemical make-up have been developed, and to design BG-based bone repair materials with a degradation rate matching that of bone in growth has become possible. Biocomposite of BG and organic material (biopolymers and synthetic polymers) has been synthesized for bone tissue engineering applications.

Chitosan is a kind of usually used biopolymers to composite with BG. Caridade *et al.* found that the composite membranes of CS with bioglass showed good flexibility; by the way, it could induce the precipitation of apatite upon immersion in stimulate body fluid, following with the biomineralization process (Caridade *et al.*, 2012). Jebahi *et al.* evaluated the *in-vivo* curative effect of CS/BG composite. The CS/BG composite was implanted in the femoral condyles of ovariectomized rats (Jebahi *et al.*, 2014). Superoxide dismutase, glutathione peroxidase and catalase activities significantly increased in ovariectomized group implanted with CS/BG composite (OVX-BG-CS) comparing to ovariectomized group implanted with bioactive glass (OVX-BG). A significant decrease of thiobarbituric acid-reactive substances was observed after implantation of CS/BG. The histomorphometric analysis showed that osteoblast number, osteoblast surface/bone surface and bone/tissue volume were significantly higher in (OVX-BG-CS) group than in OVX-BG group. On the other hand, Ca and P ion concentrations in the implanted micro environment was increased, and it could lead to the formation/deposition of Ca-P phases. Trace elements such as Sr and Fe could be detected in the newly formed bone and involved in bone healing. The above results suggested that CS/BG composites could be clinically used as a therapeutic and implantable material.

As for the simple composite of the chitosan and BG through the mixing process, a nonuniform degradation of physical mixture of organic-inorganic biomaterials increases their risk of failure. Recently, Ravarian *et al.* developed an alternative method for the preparation of a porous and bioactive chitosan for bone tissue engineering applications (Ravarian *et al.*, 2015). To achieve this aim chitosan was first functionalized with

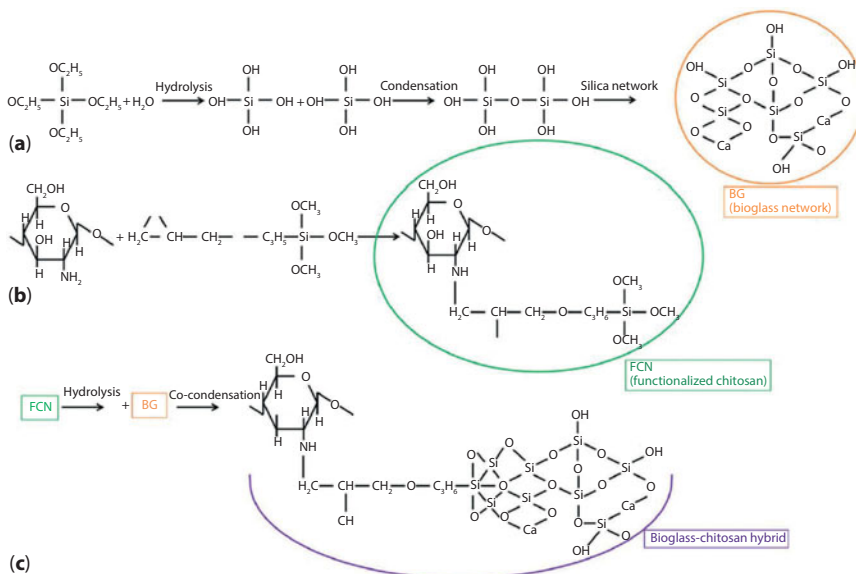


Figure 15.9 The mechanism of reaction between chitosan and bioglass. (a) hydrolysis and condensation of tetraethyl orthosilicate, (b) functionalization of chitosan with GPTMS, (c) formation of bioglass-chitosan hybrid (Ravarian *et al.*, 2015).

γ -glycidyloxypropyl trimethoxysilane (GPTMS) to promote the chemical bonding of this biopolymer to bioglass during sol-gel method (As shown in Figure 15.9). It was hypothesized that this nano-scale interaction had a significant impact on their physico-chemical properties such as mechanical, degradation and biological properties. Additionally, sodium bicarbonate was used as foaming agent to create porosity in the structure of chitosan–bioglass hybrids and eliminate the application of toxic chemicals.

Yang *et al.* [1] initially prepared a CS fibre 3D porous scaffold by needle-punching, and then deposited BG on the scaffold by dip-coating. Finally, a chitosan/bioglass (CS/BG) 3D porous scaffold was constructed (Yang *et al.*, 2014). The process was shown in Figure 15.10. The CS/BG 3D porous scaffold has an interconnected macroporous structure with high porosity, which could provide enough space for cell ingrowth and transport of nutrients. The lower water uptake capacity of the CS/BG 3D porous scaffold than the CS fibre 3D porous scaffold could counteract the swelling behaviour of CS and improve the stability of the scaffold structure. The CS/BG 3D porous scaffold possessed good mechanical properties, with an elastic modulus of 0.46 ± 0.02 GPa and a compression strength of 7.68 ± 0.38 MPa, which are well-matched to those of trabecular bone. *In vitro* cell assay results demonstrated that the CS/BG 3D porous scaffold showed good biocompatibility for facilitating the attachment, spread and proliferation of human bone marrow stromal cells (hBMSCs).

Moreover, BG can also be used for loading and delivering biomolecules such as chemical drugs and siRNA. The mesoporous structures, preparation methods, and even the dissolution of BG are extremely important for influencing biomolecule delivery. Combining with the outstanding property for drug delivering and gene transfection of chitosan or its derivatives, there is wide adjustable range for CS/BG composite using in the field of drug releasing and gene therapy. Recently, Luo *et al.* used the

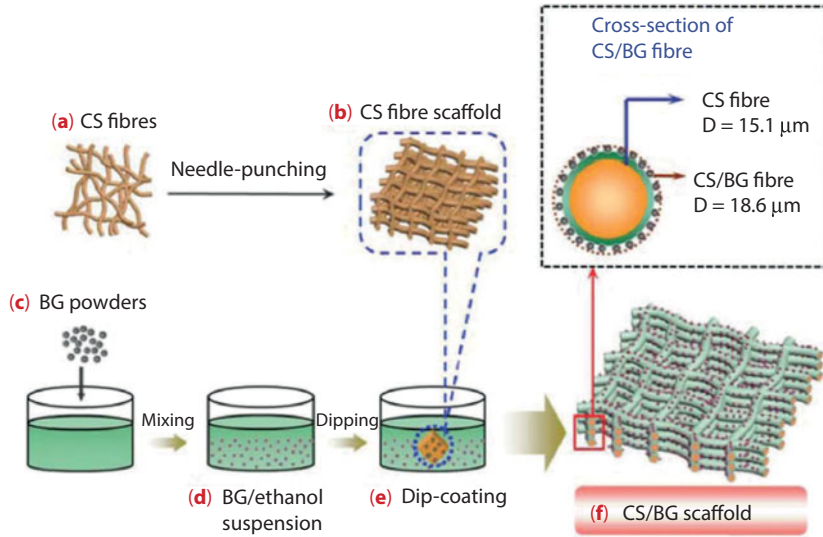


Figure 15.10 Construction of the CS/BG 3D porous scaffold: (a) CS fibres used as original materials; (b) preparation of CS fibre 3D porous scaffold by needle-punching; (c) BG powders; (d) formation of a BG/ethanol suspension by addition of BG powders into ethanol; (e) preparation of a CS/BG 3D porous scaffold by dip-coating; (f) CS/BG 3D porous scaffold; and (g) a cross-section of the CS/BG fibre (Yang *et al.*, 2014).

mesoporous bioglass (MBG) with a suitable size to evaluate the influence of complexes CS-PCL-mPEG/pOGP on the gene transfection in different types of cell lines (Luo *et al.*, 2015). Where CS-PCL-mPEG is a kind of amphiphilic derivate of chitosan, including PEG as a hydrophilic segment and polycaprolactone (PCL) as a hydrophobic one. By the way, osteogenic growth peptide (OGP), containing the osteogenic growth peptide and green fluorescent protein fusion gene, was chosen as a model gene, which can induce differentiation of osteoblasts. It was found that MBG/CS-PCL-mPEG condenses and dissociates the OGP more effectively, and MBG/CS-PCL-mPEG exhibits enhanced gene transfection efficiency. These results suggest that MBG has an enhanced impact on the polymer gene vectors.

15.5.5 Composites from Chitosan and Fe_3O_4

Owing to the unique properties, such as large surface-to-volume ratio, high surface area, superparamagnetism, good biocompatibility, easy separation under external magnetic fields and low toxicity, Fe_3O_4 nanoparticles have enormous potential in the fields such as biomedical and bioengineering usage, immobilization of biomaterials, bioseparation, food analysis, and environmental treatment (Xu *et al.*, 2014). Especially for the Fe_3O_4 nanoparticles with diameter less than 20 nm, which show good superparamagnetism, can be magnetized under the effect of the external magnetic field. While the external magnetic field is disappeared, the magnetic of the particles would be disappeared at the same time. The nanoparticles could not be permanent magnetized and they can show the targeting property under the effect of the external magnetic field. As the specific surface area effect of the Fe_3O_4 nanoparticles with superparamagnetism, they are easy

to composite with other molecule to form the magnetic nano composite material, and the application fields of them could be widen further.

Since the bare Fe_3O_4 nanoparticles often have poor stability and dispersity, various modification methods have been used to improve the solubility and biocompatibility of Fe_3O_4 nanoparticles. As good biocompatibility and bioactivity of the chitosan, and the positive charges were distributed on the skeleton of chitosan at the acid condition, chitosan could be used to composite with Fe_3O_4 nanoparticles to prepare the $\text{Fe}_3\text{O}_4/\text{CS}$ magnetic nano composite material. The defects of the Fe_3O_4 nanoparticles can be conquered. At the same time, the functions of them could be promoted as good reactivity of chitosan. So the resulting modified Fe_3O_4 nanoparticles would be extensively used for various applications.

There are two main methods for preparation of the $\text{CS}/\text{Fe}_3\text{O}_4$ magnetic composite:

1. Two step- method

Fe_3O_4 nanoparticles were synthesized first, and then is was coated by chitosan via different methods, including the precipitation method, reverse suspension cross-linking method, high voltage electrostatic method, ionic gelation method and spray-drying process, etc. For example, Denkbass *et al.* used the suspension cross-linking technique to prepare the magnetic chitosan microspheres (Denkbass *et al.*, 2002). In a typical procedure, a 4% chitosan solution was prepared using a 5% aqueous acetic acid solution containing a certain amount of dry magnetic material. It was then added into the dispersion medium composed of mineral oil, petroleum ether and Tween-80 as emulsifier. The above dispersion medium was stirred at 1000–2000 rpm at room temperature for ten minutes. Then glutaraldehyde was added into the above medium for cross-linking. Finally, the magnetic chitosan microspheres were collected using a magnet and washed to afford the final product. Qin *et al.* prepared the magnetic Fe_3O_4 nano particles by co-precipitation method of Fe^{2+} and Fe^{3+} (Qin *et al.*, 2015). Then the chitosan coated magnetic nano composites were prepared via ionic gelation of chitosan with tri-polyphosphate (TPP).

2. Permeating method

Another method is using the chitosan microparticle, membrane, fibre or hydrogel as the substrate, and the Fe^{2+} , Fe^{3+} ions are permeated into the chitosan substrate, after being *in situ* synthesized at the alkaline condition to afford $\text{CS}/\text{Fe}_3\text{O}_4$ magnetic composite. Or the Fe_3O_4 nanoparticles can be doped into the substrate of chitosan directly. For example, recently Karaca *et al.* doped the Fe_3O_4 nanoparticles into chitosan films by the solution casting technique (Karaca *et al.*, 2015). Seyed Dorraji *et al.* prepared the chitosan hollow fibers first, and then it was cross-linked by immersing in glutaraldehyde bath (Seyed Dorraji *et al.*, 2015). Then the iron ions (Fe II and III) were permeated into the chitosan hollow fibers and the products were washed with deionized water. After that, the chitosan hollow fibers with iron ions were soaked in the NaOH (3M) solution for 12 h at 60 °C to achieve $\text{Fe}_3\text{O}_4\text{-CS}$ nano composite hollow fibers.

As good biocompatibility and superparamagnetism of Fe_3O_4 /CS magnetic nano composite material, it is the good candidate as the carrier of the targeting drug delivery system with good prospective to be used for the treatment of the tumour and amaemia. For example, Ding *et al.* prepared the novel CS cross-linked carboxymethyl- β -cyclodextrin (CM- β -CD) polymer modified Fe_3O_4 magnetic nanoparticles (CS-CDpoly-MNPs), and then it was used for delivering hydrophobic anticancer drug 5-fluorouracil (5-Fu) (Ding *et al.*, 2015). CM- β -CD being grafted on the Fe_3O_4 nanoparticles (CDpoly-MNPs) could enhance the adsorption capacities of nanoparticles because of the inclusion abilities of its hydrophobic cavity with insoluble anticancer drugs through host-guest interactions. The size and physicochemical profiles of the fabricated nanocarriers could be controlled by changing the initial mass ratio of CS/5-Fu/CM- β -CD during the fabrication process. A reasonably high encapsulation efficiency ($97.6 \pm 1.3\%$) of 5-Fu could be gained in these chitosan based magnetic nanocarriers. Moreover, the free carboxymethyl groups could enhance the bonding interactions between anticancer drugs and the covalently linked CDpoly-MNPs. *In vitro* release studies revealed that the release behaviors of CS-CDpoly-MNPs carriers were pH dependent and showed a swelling and diffusion controlled release property. By the way, as the three-dimensional space needed for the cells growth and the process of metabolism can be provided by chitosan, combining with the good magnetic response function of Fe_3O_4 nanoparticles, the above composite could well simulate the growing environment of the chondrocyte, and is suitable for magnetic therapy. This has become a hotspot for study in orthopedics (Bhowmick *et al.*, 2015).

As free enzymes are easily inactivated and difficult to recover for reuse, developing the effective strategies to immobilise enzymes while retaining catalytic activity is the essential way for the utilisation of enzymes in biocatalysis, particularly at an industrial scale. Enzyme immobilisation increases significantly the number of times that a biocatalyst can be reused, leading to a reduction in the processing costs. Furthermore, enzyme immobilisation widens the use of enzyme reactions to a range of non-physiological environments. Enzymes immobilised in the presence of Fe_3O_4 nanoparticles show the advantage of be effectively and easily recovered through application of magnetic fields (Costa-Silva *et al.*, 2015), so it was drawn more and more attentions. As -OH and - NH_2 distributed on the skeleton of the chitosan were easy to be chemical modified, chitosan coated Fe_3O_4 nanoparticles showed good perspective for immobilizing of the enzymes (Pospiskova & Safarik, 2013). Wang *et al.* prepared magnetic Fe_3O_4 @chitosan nanoparticles through a simple *in situ* co-precipitation method (Wang *et al.*, 2015). Then the lipase from *Thermomyces lanuginosus* was covalent immobilized in the prepared Fe_3O_4 @chitosan nanoparticles by chemical conjugation after electrostatic entrapment (CCEE) (as shown in Figure 15.11). The immobilization product with the highest enzyme loading of 16.8 mg/g-support and the highest immobilization efficiency of 75% could be obtained. The immobilized enzyme showed higher activities, good reusability and higher thermal stability over the range of tested pH and temperature. Ascorbyl palmitate synthesis with immobilized lipase was carried out in tert-butanol at 50 °C, and a conversion of 52% could be achieved after being reacted for 12 h. From the above results, it was concluded that the immobilization of lipase onto magnetic chitosan nanoparticles by the CCEE method is a simple and efficient way for preparation of stable lipase. The immobilized enzyme has promising industrial applications.

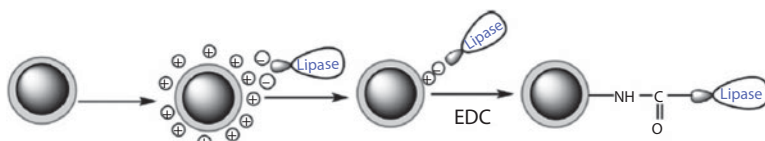


Figure 15.11 Immobilization of lipase on the Fe_3O_4 @chitosan nanoparticles (Wang *et al.*, 2015).

Efficient extraction of the active constituent is one of the most important study fields in the food industry and study on the biological products. It is also one of most difficult steps for the above process. As for using of Fe_3O_4 /CS magnetic composite materials in the process of separation and recovery of the protein, the reaction conditions, such as the pH value, ionic strength and dielectric constant of the mixture solution, are not need to be adjusted, which can avoid the losing of the protein. Then the separating time of the protein can also be saved, and the recovery rate and the purity of the protein can also be promoted (Shen *et al.*, 2014; Podzus *et al.*, 2009).

For Fe_3O_4 /CS magnetic nano composite material, as it good properties of non-toxicity, biodegradability, obvious treatment effects, not causing secondary pollution, it has become one of the main developing directions of the novel water treatment chemicals.

Since heavy metals have the potential to be hazardous and carcinogenic, their release into the environment leads to serious environmental, aesthetic, and health threats. So the removal of heavy metals from waste water has become a hot topic in recent years. However, waste water containing heavy metals are difficult to be removed because of their inert properties; by the way, as the heavy metals is usually low concentration in waste water, the conventional methods, such as coagulation and flocculation, adsorption on activated carbons, membrane filtration, reverse osmosis, ion exchange, chemical oxidation, ozonation and electrochemical techniques, etc., is unfavorable to be applied at a large scale for the high cost and low efficiency to remove trace amounts of contaminants. Chitosan can be used as an efficient adsorbent to recover heavy metals owing to the presence of functional groups such as $-\text{OH}$ and $-\text{NH}_2$, which could complex with the heavy metals. However, due to the presence of large amounts of hydrogen bonding within CS, the adsorption capacity becomes weaker. Furthermore, in the regeneration process of chitosan, acid is generally used; however, the application of acid is unsustainable and not environmentally-friendly. To overcome these limitations, metal oxides immobilized chitosan hybrid composites can be a suitable candidate (Haldorai *et al.*, 2015). In all of metal oxides, Fe_3O_4 nanoparticles have been found to be highly efficient for metal ion removal through the interaction of electrostatic attraction and ligand exchange reactions. Using an external magnetic field, adsorbents can be easily removed from wastewater. Coating CS on the surface of Fe_3O_4 nanoparticles, can combine the good properties of the above two materials, by the way, it can avoid the aggregation of the nanoparticles. Several researchers have reported the preparation of Fe_3O_4 /CS composites for metal ion adsorption. For example, Wang *et al.* removed the Cu (II) by the using the superparamagnetic chitosan microparticles (Wang *et al.*, 2013). Dodi *et al.* synthesized the core-shell iron oxide encapsulated by cross-linked chitosan for Cu (II) adsorption (Dodi *et al.*, 2012). Tran *et al.* used magnetite-chitosan composites to remove the Pb(II) and Ni(II) (Tran *et al.*, 2010).

The Fe_3O_4 /chitosan nanocomposite also showed good adsorption to dye molecules. Xiang *et al.* prepared the Fe_3O_4 /chitosan/ TiO_2 nanocomposite, which showed promising applications for adsorption and degradation of organic pollutants in waste water (Xiang *et al.*, 2015). Under the optimal condition, degradation rate of methyl blue by the Fe_3O_4 /chitosan/ TiO_2 nanocomposites was 93%. After multi-run experiments, it was found that the reused Fe_3O_4 /chitosan/ TiO_2 nanocomposites could still keep high photocatalytic performance. As the addition of magnetic Fe_3O_4 nanoparticles into the waste water, the nanocomposites can be separated from the water by assisting of an external magnetic field. Compared with the conventional photocatalytic materials, Fe_3O_4 /chitosan/ TiO_2 could serve as a sensitive, facile, recyclable, non-toxic and cost-effective photocatalysts for treatment of waste water.

By the way, as the non-toxicity, antimicrobial activity and sterilization of the Fe_3O_4 /chitosan nanocomposite, and the ability of removing impurity contents in the water, application of it for purification of the drinking water also attracts more and more attentions recently (Mohseni-Bandpi *et al.*, 2015).

15.5.6 Composites from Chitosan and Gold Nanoparticles

In the field of nanotechnology, gold nanoparticles have attracted great attentions due to their unique optical, electronic, chemical, thermal, biological properties and their potential catalytic applications in various fields such as physics, chemistry, biology, medicine, material science and other interdisciplinary fields (Panyala *et al.*, 2009). Chitosan and its derivatives can be used to synthesize of gold nanoparticles (Leiva *et al.*, 2015). Spano and coworkers reported the *in situ* formation of gold nanoparticles in hydrogel-type chitosan films loaded with chloroauric acid (HAuCl_4) (Spano *et al.*, 2012). The preparation of colloidal gold nanoparticles (AuNPs) stabilized in a chitosan matrix by reducing Au III to Au 0 with different organic acids (i.e., acetic, malonic, or oxalic acid) in aqueous chitosan has also been reported (Di Carlo *et al.*, 2012). The authors demonstrated that varying the acid nature tuned the gold precursor (HAuCl_4) reduction rate and modified the resultant metal nanoparticle morphology.

Biocompatible gold nanoparticles composited with specific targeting biomolecules/drugs play an important role in the diagnosis and therapy of several incurable diseases or biosensor. As the bioactivity and functional properties of chitosan and its derivatives, the nanocomposites prepared from chitosan and gold nanoparticles (CS/GNPs) have been paid much attention and been widely studied.

Due to the unique quality of high conductivities, large specific area, good biocompatibility, and a favorable microenvironment, gold nanoparticles (AuNPs) have attracted considerable attention in the area of analytical electrochemistry for preparation the biosensor with enhanced performance. For the application of the biosensor based on AuNPs, the stability of immobilization interfaces is very important. Via the derivatives of chitosan, the stability of AuNPs can be increased, and then the performance of the biosensor can also be promoted. Xiang *et al.* dispersed gold nanoparticles (GNPs) in chitosan hydrogel and the above composite was formed as a film to modify the glassy carbon electrode (Xiang *et al.*, 2015). Then it was oxidized by NaCl solution and used as a platform for the immobilization of capture antibody (Ab_1) for biorecognition. After being incubated in *Salmonella* suspension and horseradish peroxidase (HRP)

conjugated secondary antibody (Ab_2) solution, a sandwich electrochemical immunosensor for detection of *Salmonella* was prepared. GNPs played a very important role to amplify the electrochemical signal. The immunosensor exhibited the linear response range from 10 to 10^5 CFU/mL. In addition, the immunosensor was used to detect *Salmonella* in real-to-life samples and satisfactory results were obtained. Recently, Li *et al.* prepared a thiol graphene-thiol chitosan-gold nanoparticles (thGP-thCTS-AuNPs) nanocomposites film for the immobilization of AuNPs (Li *et al.*, 2015). Then it was deposited on glassy carbon electrode (GCE) and the porous structure could be formed. The introduction of thCTS and thGP provided a biocompatible environment with a large specific surface area for the further immobilization, and AuNPs facilitated the electron transfer. The above film exhibited improved conductivity and good biocompatibility, to construct immunosensor free label for detection of carcinoembryonic antigen (CEA).

Recently, the integration of metallic nanoparticles with UV-visible spectrometry has provided new analytical approach for the selective and sensitive detection of various metal ions in various environmental and biological samples. Among nanoparticles, AuNPs-based UV-visible spectrometric assays have recently attracted increasing attention in colorimetric sensors due to their fantastic physico-chemical properties, high extinction coefficient ($10^8 \text{M}^{-1}\text{cm}^{-1}$) and the rational design of their surface chemistry which play a important role in the aggregation of AuNPs induced by target analytes through covalent and non-covalent bonding (Saha *et al.*, 2012). Mehta *et al.* added chitosan dithiocarbamate (CSDTC) derivative into AuNPs solution to obtain the chitosan dithiocarbamate functionalized gold nanoparticles (CSDTC-AuNPs) (Mehta *et al.*, 2015). It was found that the Cd^{2+} ion was quickly induced the aggregation of CSDTC-AuNPs at PBS pH 8.0, yielding a red-shift in the surface plasmon resonance (SPR) peak from 523 to 685 nm accompanying the color change from red to blue, which facilitates development of a simple and selective colorimetric method for detection of Cd^{2+} ion. The method showed good linearity with concentration of Cd^{2+} in the range of 50–500 μM , and the detection limit was found to be 63 nM. CSDTC-AuNPs was applied to determine Cd^{2+} ion in water samples (drinking, tap, canal, river and industrial effluent).

CS/AuNPs composite nanoparticles are also very good carrier for drug deliver. Madhusudhan *et al.* used the carboxymethyl chitosan (CMC), which acted as a capping and reducing agent, to prepare the CMC/AuNPs composite nanoparticles (Madhusudhan *et al.*, 2014). The AuNPs capped with CMC exhibited stability in a wide range of pH and electrolyte concentration. Further, the cytotoxic drug Doxorubicin (DOX) was immobilized on the surface of the nanoparticles through the non-covalent interactions between the amino group of DOX and the carboxylic group of CMC. The DOX loaded gold nanoparticles could be effectively absorbed by cervical cancer cells compared to free DOX and their uptake could be further increased at acidic conditions induced by nigericin, an ionophore that causes intracellular acidification. Efficient uptake of DOX loaded gold nanoparticles at physiological pH and response at intracellular acidic pH make them an ideal pH-triggered drug delivery system to target cancers.

Gold nanoparticles can absorb near-infrared (NIR) light and then convert the absorbed light energy into heat due to their longitudinal surface plasmon resonance; NIR light can be transmitted into the deep tissues without damaging normal biological

tissues. This is called as photothermal effect of AuNPs. In addition, the controlled release of drugs from conjugates into tumor tissue could be induced by the NIR light irradiation. Therefore, AuNPs or its derivatives have been used to NIR photoactivated cancer therapy. As good properties for tumor targeting, delivery of therapeutic drugs, genes and proteins from chitosan or its derivatives, combining with their good properties of highly stable, biocompatible, biodegradable, abundant in nature and inexpensive, the composite of CS/AuNPs showed outstanding application potential in the fields of cancer therapy. Duan *et al.* conjugated the thiol-modified chitosan with gold nanorods, and DOX was covalently conjugated with derivatives of chitosan to form a prodrug (Duan *et al.*, 2014). Under conditions of low light intensity and short exposure time, the above prepared nanocarriers exhibited enhanced antitumor activity and reduced toxicity against tumor cells based on a combination of drug release therapeutic with photothermal effects.

Yang *et al.* recently developed a layer-by-layer assembled chitosan-gold nanorods (Chit-Au NRs) siRNA delivery system for gene silencing and photothermal therapy. Chit-Au NRs/siRNA were found to accumulate in high levels in tumor tissue (Yang *et al.*, 2015). The delivery system was able to inhibit the oncogene expression (pyruvate kinase isozyme M2) in MDA-MB-231 triple negative breast cancer cells, resulting in suppression of cell proliferation and migration. Moreover, the anticancer efficacy was further enhanced through gold nanorods-mediated photothermal ablation. The synergistic therapeutic properties of Chit-AuNRs/siRNA enable effective suppression of cancer growth.

Computed tomography (CT) technique has been widely used clinically because of unlimited penetration depth and high spatial resolution. AuNPs can be used as a CT contrast agent with low toxicity, high X-ray absorption coefficient, and slow clearance in the body. It could overcome the drawbacks of the traditional iodine-based CT contrast agent, which has renal toxicity and fast excretion. Polymer composited AuNPs can increase the targeting effects of the AuNPs, so it could promote the properties to be used as the CT contrast agent. After the chitosan was modified by tumor cell-specific targeting ligands and composited with the AuNPs, the sensitive and stable labeled nanoparticles could be used for cancer cell targeting imaging (Zhang *et al.*, 2015). Sun *et al.* used the biocompatible glycol chitosan (GC) as a reducing agent and a stabilizer of AuNPs (Sun *et al.*, 2014). The prepared GC/AuNPs composite nanoparticles were used as a CT contrast agent and the tomographic images of tumor in the tumor xenografted animal model. They showed excellent stability, biocompatibility, and enhanced tumor accumulation, which was inherited from GC on the surface.

The light-weight, good mechanical properties, corrosion resistance as well as low elastic modulus make Ti used in production of biomedical implants such as prosthodontic implants and hip prosthesis. But titanium can suffer from electrochemical reactions that occur in the body fluid leading to structure and mechanical degradation of the alloy and account as a major factor limiting the orthopedic implants. Surface modification of implantable Ti materials is usually required to increase biocompatibility, overcome damage and to resist the physiological reaction between the surrounding tissue and implants. Farghali *et al.* investigated the highly uniform bionanocomposite film composed of gold nanoparticles (AuNPs) and chitosan (CS) synthesized by electrodeposition method on surface corrosion resistance of Ti (Farghali *et al.*, 2015). It was found

that the combination of the antibacterial effect and high biocompatibility of chitosan and strong adsorption ability of AuNPs make AuNPs/CS bionanocomposite potential candidate for modifying biomaterial surfaces for medical implantation applications.

15.5.7 Composites from Chitosan and Silver Nanoparticles

Among metal nanoparticles, silver nanoparticles (AgNPs) have attracted much attention due to their potential as antimicrobial agent. AgNPs systems present several advantages that make them very interesting for a use as antimicrobial agents. They possess a very high activity against a broad range of parasites and microbes, even when low doses are used (full growth inhibition of bacteria can occur at only a few mg/ml). At these doses, silver presents very little systemic toxicity toward humans, and is relatively inexpensive and available (Benjamin & Francesco, 2015). They are widely applied in many biological and medical fields such as biosensors, wound healing, treat burns and cancer therapeutics. Several AgNPs based composites have demonstrated enhanced performance through the stabilization and support of nanoparticles. Regarding silver-based nanocomposites, CS/AgNPs nanocomposites represent an emerging group of bionano structured hybrid materials because of its biocompatibility and biodegradability.

Recently, Scaao *et al.* prepared a series of lactose-modified chitosan (Chitlac)/tripolyphosphate/silver nanoparticles (AgNPs) macroscopic hydrogels by means of a custom-made technique based on a slow ionotropic gelation of chitosan, and then the soft pliable membranes with good biocompatibility could be obtained (Scaao *et al.*, 2015). UV-Vis and TEM analyses demonstrated the time stability and the uniform distribution of AgNPs in the gelling mixture. By the way, the swelling studies indicated the hydrophilic behavior of membrane. A thorough investigation on bactericidal properties of the material pointed out the synergistic activity of chitosan and AgNPs to reduce the growth of *S. aureus*, *E. coli*, *S. epidermidis*, *P. aeruginosa* strains and to break apart mature biofilms. The above bioactive membranes show great promise for the treatment of non-healing wounds. Liu *et al.* prepared non-precipitation chitosan/silver nanoparticles (AgNPs) in 1% acetic acid aqueous solution from chitosan colloidal gel with various contents of silver nitrate via electron beam irradiation (EBI) (Liu *et al.*, 2015). Then the continuous and uniform CS/PVA/AgNPs nanofibres were prepared by electrospinning technique using eco-friendly solvent. The green EBI process was achievable to gain CS solution from CS gel and large-production of AgNPs from Ag^+ . It was observed that AgNPs dispersed uniformly in the CS/PVA nanofibres, which remained utilization of nanoparticles to the utmost extent. Furthermore, the properties of PVA/CS nanofibres were improved greatly by AgNPs loaded. These hybrid nanofibres mats showed good mechanical property and antibacterial activity toward *E. coli* bacteria and *S. aureus*, and latter bacteria was the more sensitive microbe against antimicrobial disk when the concentration of AgNPs was only 0.5 wt%. The resultant hybrid nanofibres provide a steady and prolonged silver ion release.

Although the highly antibacterial effect of AgNPs has been widely described, their mechanism of action is yet to be fully elucidated. Some scientists considered that the AgNPs would be transferred to Ag^+ with good antibacterial property when it was dispersed in water (Park *et al.*, 2009; Liu *et al.*, 1998). Some researchers attributed the effective antibacterial ability of AgNPs to its ultra-fine size and large specific surface

area. Then AgNPs could enter the inside of the bacterial cell easily going through the cell membrane, and then it was transferred to Ag^+ to destroy the inner structure of the cell. But recently Kumar-Krishnan *et al.* prepared chitosan-silver (CS/Ag) nanocomposites either in the form of nanoparticles (AgNPs) or as ionic dendritic structures (Ag^+) by a simple and environmentally friendly *in situ* chemical reduction process (Kumar-Krishnan *et al.*, 2015). The antibacterial activity of the resulting nanocomposites in the form of films is studied against two bacteria, gram-positive *Staphylococcus aureus* and gram-negative *Escherichia coli*. The results showed that in contrast to CS/ Ag^+ ion films, the CS/AgNPs composites films (average particle size less than 10 nm) showed a significantly higher antibacterial potency. The composites containing 1 wt.% of silver nanoparticles and about of 2 wt.% of silver ions exhibit a maximum antibacterial activity. The above results indicate that there is particular antibacterial mechanism for AgNPs.

By observing from SEM, Choi *et al.* found that the sphaeroid and hexagon AgNPs could be absorbed by the cell and then caused the disappearing of the cell membrane (Choi *et al.*, 2008). But other research (Choi *et al.*, 2009) found that the integrity of the cell membrane of the bacterial cell would be disturbed by the AgNPs with high concentration, which maybe the main reason for the death of the cell. The mechanism be widely known is that AgNPs could be absorbed on the membrane of the cells, and then it would enter the inner of the cell and interact with the sulfhydryl group of L-cysteine. Finally the intracellular enzyme would be caused to lose activity (Gordon *et al.*, 2010; Su *et al.*, 2009). It was found that the AgNPs with particle size lower than 5 nm could enter the inside of the bacterial cell easily and prevent translating of the transcriptase for hereditary substance. The Ag^+ transformed from AgNPs would cause the leaking of substantial proteins, reducing sugar and K^+ , and the exhausting of the membrane potential and ATP. Finally the cell would be caused to death (Dibrov *et al.*, 2002).

By the way, the chitosan/AgNPs composite is also good candidate for sensor or detection. Detection of mercury is important since mercury is a toxic pollutant. It is one of the major water contaminants which is highly carcinogenic and toxic to the cells. Among the various sensors the colorimetric sensors based on the change of color on addition of mercury have attracted much attention due to the technique being simple, economic and reliable. Recently, Nivethaa *et al.* found that the UV-Vis spectra of the chitosan-silver nanocomposite showed a decrease in intensity and a blue shift on interaction with mercury, which confirming the composite could be used as a colorimetric sensor for the detection of mercury (Nivethaa *et al.*, 2015). The limit of detection was found to be about 7.2×10^{-8} M. As high specificity and the sensitivity of the environmental friendly and non-toxic nanocomposite to detect very low concentrations of mercury, the system is a perspective one. Chen *et al.* synthesized the AgNPs with stable and narrow size distribution in the range of 15–25 nm under microwave irradiation, with quaternized chitosan (QCS) being used as reducing and stabilizing agent (Chen *et al.*, 2015). Then the above QCS/AgNPs composite was used as the substrate of surface enhanced Raman scattering (SERS). As QCS was coated on the surface of Ag core, it could avoid aggregation of AgNPs and creating hot spots, in turn, providing superior amplification of SERS. The above substrate was used for trace detection of tricyclazole and Sudan I, the usually used food contaminants. It was found that tricyclazole and Sudan I could be rapidly and sensitively detected with the limit of detection as low as

50 ppb and 10 ppm, respectively. The results show possibilities for practical applications of QCS/AgNPs composite in residue analysis of food contaminants with SERS technique.

15.6 Composites from Chitosan and Carbon Materials

Carbon can be existed in a variety of forms: carbon aerogels, activated carbon, carbon nanotubes, mesoporous carbon, diamond and grapheme (Liu *et al.*, 2015). As their advantages of the chemical and physical properties, such as light weight, superior mechanical properties and/or thermal conductivity, and low coefficient of thermal expansion, etc. (Huang *et al.*, 2014), the composites prepared from chitosan and carbon materials have also been widely studied in recently years.

15.6.1 Composites from Chitosan and Activated Carbon

Activated carbon (AC) is obtained through heat treatment of various natural precursors (coal, peat, coconut and wood). A physical thermal oxidation (pyrolysis followed by an oxidation by steam), or a chemical one (impregnation by a mineral agent followed by a pyrolysis), enable to develop an AC with high-specific surface, going from 500 to 2,000 m²/g (Venault *et al.*, 2010). The internal structure of AC is constituted by micropores (diameter of pores lower than 2 nm) and mesopores (between 2 and 50 nm). Activated carbon has been widely used as an adsorbent due to its large surface area and high porosity. However, there some disadvantages for the remove process of the activated carbon process, especially to the heavy metals, such as a limited temperature range for optimal operation, slow sorption kinetics and low regeneration rate of used activated carbon. Chitosan can also entrap various compounds through chemically or physically effects due to the presence of amine and hydroxyl groups that can serve as the chelating and reaction sites. However, it is hard to directly apply raw chitosan for absorbent because of its disadvantages, such as solubility in acidic conditions, swelling, and unsatisfactory mechanical properties.

Composites prepared from chitosan and AC could combine the good absorption properties of two matrixes and avoid their disadvantages. They have attracted more and more attentions recently. Ge *et al.* prepared a novel activated carbon-chitosan complex adsorbent (ACCA) via the cross-linking of glutaraldehyde and activated carbon-(NH₂-protected) chitosan complex under microwave irradiation (Ge & Fan, 2011). It was found that ACCA has higher adsorption capacity for Cd²⁺ and Pb²⁺ than chitosan. A thermodynamic study reveals that the adsorption is an exothermic and spontaneous physical process. The adsorbed Pb²⁺ and Cd²⁺ could be desorbed efficiently, and ACCA is recyclable. The above composite can be used as the effective and low-cost adsorbents in the removal of heavy metal ions from waste waters. Auta *et al.* used the renewable waste tea activated carbon (WTAC) to coalesce with chitosan to form the (CS/WTAC) composite adsorbent. And the adsorptive capacities for Acid blue 29 (AB29) and Methylene blue dye (MB) were compared with that of the cross-linked chitosan beads (CCB) through batch and fixed-bed studies. After five cycles of adsorbents desorption test, more than 50% CS/WTAC adsorption efficiency was retained while CCB only

had <20% adsorption efficiency. The results revealed that CS/WTAC composite is a promising adsorbent for treatment of cationic and anionic dyes in effluent waste waters (Auta & Hameed, 2013).

For the real applications, both domestic sewage and industrial waste water are often a mixture of many compounds containing organic and inorganic pollutants, such as heavy metals and aromatic compounds. The interactions of these compounds may mutually inhibit or mutually enhance adsorption capacity. Simultaneous adsorption of various inorganic and organic pollutants has increasingly attracted attention. The composite prepared from CS and AC can remove inorganic and organic pollutants from aqueous solutions simultaneously. Huang *et al.* investigated the simultaneous adsorption of phenol and Cr (VI) from aqueous solution by CS/AC composite membrane cross-linked by epichlorohydrin (Huang *et al.*, 2014). It was found that the composite could remove phenol and Cr (VI) simultaneously in a pH range of 2–5. The removals of phenol and Cr (VI) reached up to 95% when phenol and Cr (VI) concentrations were less than 50 mg/L and 200 mg/L, respectively. The presence of phenol reduced Cr(VI) adsorption, while the presence of Cr (VI) had no obvious effect on phenol adsorption. Liu *et al.* found that CS/AC composite can be used for simultaneous adsorption of Cu^{2+} and aniline from aqueous solution in a wide pH range, and no obvious competitive adsorption existed between aniline and Cu^{2+} (Liu *et al.*, 2015).

Because of its effective adsorption properties, AC could be used to remove in appropriate odors caused by wounds. Venault *et al.* used the vapor-induced phase separation process to prepare the chitosan-AC composite hydrogels. The rheometric property and mechanical property of the composite hydrogels were studied (Venault *et al.*, 2011). It was found that AC could enhance the mechanical properties of matrices. The above composite hydrogels showed great potential for medical applications.

AC is one of the most promising supports for enzyme immobilization because of its large surface area, high adsorption efficiency. However, the enzyme with a begin surrounding microenvironment cannot be provided by simple physical adsorption between enzyme and activated carbon due to low surface OH groups density on activated carbon. Composite of the chitosan on the surface of AC could improve the surface biocompatibility and increase the surface functional groups density of AC. Xue *et al.* immobilized *Pseudomonas cepacia* lipase (PSL) onto composite of CS/AC with CS coating on the surface of AC (Xue *et al.*, 2014). The immobilized lipase PSL/CS/AC catalyst exhibited enhanced catalytic activity for resolving racemic 1-phenyl-3-buten-1-ol compared to free PSL and PSL immobilized on sole activated carbon or chitosan. The higher catalytic performance was derived by the more surface active sites exposed by the PSL/CS/AC immobilized lipase. Moreover, the immobilized lipase PSL/CS-AC catalyst possessed of high thermal stability, reusability and storage stability.

15.6.2 Composites from Chitosan and Carbon Nanotubes

Carbon nanotubes (CNTs) are a kind of novel carbon materials which was discovered by Iijima in 1991 (Iijima, 1991). CNTs generated huge research interest from many areas of science and engineering due to their remarkable physical and chemical properties, such as high aspect ratio, high strength and high stiffness but very low density (Liew *et al.*, 2015). Carbon nanotubes can be divided into single-walled or multi-walled

structures. The single-walled carbon nanotube (SWCNT) is prepared by rolling a single graphene sheet seamlessly to obtain a cylinder with a diameter of 1 nm and length of order of centimeters. Similar to the basal plane separation in graphite, the multi-walled carbon nanotube (MWCNT) is an array of such cylinders formed separated and concentrically by 0.35 nm with diameters from 2 to 100 nm and lengths of tens of microns.

CNTs have been considered as ideal reinforcing fillers for polymer matrixes to achieve multifunctions and high performance, because of their high aspect ratios, nanometer size, and more importantly, their extraordinary mechanical strength and high thermal and electrical conductivity. The composites based on chitosan or its derivatives and CNTs have also been well studied.

There are many methods to prepare the CS/CNTs composite, including solution blending method, electrochemical deposition method, electrostatic spinning method, electrostatic self-assembly method, sol-gel method, surface deposition cross-linking method and covalent grafting method, etc. There are great difference for the properties and applications of the composites prepared from different method.

Among them, solution blending method is the most simple and commonly used method for preparation of CS/CNTs composite. The MWCNTs could be functionalized by refluxing in the solution of concentrated nitric or acid sulfuric acid to increase the hydroxyl and carboxylic groups, which can form strong hydrogen bonds and polyelectrolyte interactions with the chitosan matrix. Wang *et al.* prepared the chitosan/MWCNTs nanocomposites by a simple solution-evaporation method (Wang *et al.*, 2005). Firstly, the MWCNTs were homogenized suspended in an ultrasonic bath for 60 min, then the chitosan and acetic acid were added to the MWCNTs suspension, and the mixture was shaken for 1 h to dissolve the chitosan. The solutions were then stirred using a mechanical homogenizer at 18000rpm for 30 min, followed by being sonicated for 20 min to remove the bubbles. After being dried, the uniform nanocomposite thin films with an average thickness of 0.08 mm could be prepared. It was found that the homogeneous dispersion of MWCNTs in the matrix dramatically improved the mechanical properties of the chitosan. When compared to those of neat chitosan, for the nanocomposites incorporation of only 0.8 wt % MWCNTs, the tensile modulus and strength of the composites are greatly improved by about 93% and 99%, respectively.

Layer-by-layer self-assembly is another kind of usually used method for preparation of CS/CNTs composite. The advantage of this method is that the content of the CNTs in the films is higher, and the thickness of the composite films could be controlled. Pan *et al.* coated multilayer films containing tin disulfide (SnS_2) nanoparticles, chitosan and single-walled carbon nanotubes on glassy carbon electrodes through the layer-by-layer assembly technique (Pan *et al.*, 2013). After the bare GCE was lightly polished with alumina and sonicated in 1:1 nitric acid, acetone, and double-distilled water for 10 min, respectively, it was electrochemical pretreated by cycling from a potential -0.2 to $+1.6$ V at a scan rate of 100 mV/s in a 1.0 M H_2SO_4 solution. Then the pretreated electrode was rinsed with water and alternatively immersed into positively charged CS- SnS_2 and negatively charged SWCNTs. The assembly time for each layer was 30 min, and the electrode was well rinsed with double-distilled water after each assembly. The above multilayer films were stable, selective, and reproducible. And the modified electrodes could be used as a new sensor for the simultaneous detection of different neurotransmitters. Trigueiro *et al.* used the LBL technique to prepare multi-component hybrid

thin films by successive adsorptions of MWCNTs that were highly dispersed in chitosan and cellulose nanocrystal suspensions (Trigueiro *et al.*, 2014). The nanotubes are densely packed in each multilayer, forming a random network. Electrostatic interactions and hydrogen bonds between the negatively charged sulfate ester groups on the nanocrystal surfaces and NH_3^+ groups of chitosan were the driving forces for the buildup of the multilayered carbon nanotube thin films. The surface morphology of the LBL films revealed a relatively good dispersion of the MWCNT without the formation of large aggregates in each layer and a high density and uniform distribution of cellulose nanocrystal. It was revealed through the electrochemical characterization that a decrease in two orders of magnitude in the film resistance as the number of bilayers increased from 5 to 20, which is a consequence of an increase in the amount of conductive material (MWCNT). The thin films with up to 20 bilayers exhibited transmittance higher than 90% in the visible range.

Liu *et al.* used the surface-deposition and cross-linking method to prepare the chitosan surface modifying product of carbon nanotubes (Liu *et al.*, 2005). The MWCNTs were dispersed in acetic acid solutions of chitosan, and the blend were treated under an ultrasonic field. During this step, chitosan macromolecules were adsorbed on the surface of the MWCNTs, which acting as polymer cationic surfactants to stabilize the MWCNTs, and then the MWCNTs could be stably dispersed in acidic aqueous solutions. Subsequently, the diluted ammonia solution was added dropwise to the MWCNTs-CS dispersions. With increasing of the pH value of the system, the ionized chitosan would be deionized and become non-dissolvable in aqueous media, and thus it would be deposited on the surface of carbon nanotubes to form a chitosan coating layer. Then the glutaraldehyde was introduced to the system to cross-link the surface-deposited chitosan. After being collected by centrifugation and washed with diluted acetic acid to remove the uncross-linked and adsorbed chitosan, the final product could be afforded. The process was showed in Figure 15.12. As the pristine structures of the carbon nanotubes were not recomposed under those treatments, the unique properties of the pristine carbon nanotubes had not been compromised after the modification.

Up to now, the composites of CS/CNTs were mainly used to design different forms of bio electrochemical devices, including electrochemical sensor and biosensor, to promote the bioactivity and photoelectric property of these electrochemical devices. Besides that, they can also be used in the aspects of antibacterial fibres, gene therapy and drug delivery.

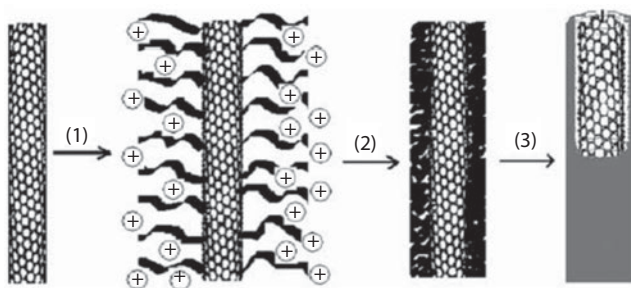


Figure 15.12 The process of the surface-deposition and cross-linking method (Liu *et al.*, 2005).

Because of their excellent electro catalytic activities, such as in the electrochemical oxidation of nicotinamide adenine dinucleotide hydrogen (NADH), dopamine hydrochloride (DA), ascorbic acid (AA), and epinephrine (NE), and promoting the electron-transfer reaction of redox protein, CNTs have been widely used for electro analytical applications.

CS/CNTs composites are considered as one of the most ideal candidates for electrode in the electrochemical field. It shows good electrochemical property and stronger absorption and ion exchanging effects to many electrochemical active substances. It can decrease the over potential of redox reactions. After the CS/CNTs furnished electrode was used, the sensitivity, selectivity and stability of the electrode are usually promoted. Janegitz *et al.* used the functionalized carbon nanotubes paste electrode (CNPE) modified with cross-linked chitosan to determine the Cu(II) in industrial waste water, natural water and human urine samples by linear scan anodic stripping voltammetry (LSASV) (Janegitz *et al.*, 2009). Under the optimal experimental conditions, the voltammetric response was linearly dependent on the Cu(II) concentration in the range from 7.90×10^{-8} to 1.60×10^{-5} mol/L with a detection limit of 1.00×10^{-8} mol/L. The samples analyses were evaluated using the proposed sensor and a good recovery of Cu(II) was obtained with results in the range from 98.0% to 104%. Jiang *et al.* developed a novel chitosan-carboxylated multiwall carbon nanotube modified glassy carbon electrode (Jiang *et al.*, 2005). It exhibited fast response towards nitrite with a linear range of 5×10^{-7} to 1×10^{-4} mol/L and a detection limit of 1×10^{-7} mol/L. The proposed method was successfully applied in the detection of nitrite in real samples. Recently, Salimi *et al.* used a nanocomposite containing chitosan and multi walled carbon nanotubes for immobilization of electrodeposited MnOx nanoflakes using combination of applied potentiostatic (0.6 V) and cyclic voltammetric (0.3–0.6 V) techniques (Salimi *et al.*, 2015). The modified electrode showed excellent electro catalytic activity toward oxidation of chromium (III) at natural pH solutions, and then cyclic voltammetry and hydrodynamic amperometry could be applied as measuring techniques for chromium detection. The developed sensor was applied for the detection of Cr (III) in real samples with satisfactory results.

Gholivand described a method to construct a novel electrochemical warfarin sensor based on covalent immobilization of CdS-quantum dots (CdS-QDs) onto carboxylated multiwalled carbon nanotubes/chitosan (CS) composite film on the surface of a glassy carbon electrode (Gholivand & Mohammadi-Behzad, 2015). The modified electrode was used to detect the concentration of warfarin with a wide linear range of 0.05–80 μ M and a detection limit (S/N = 3) of 8.5 nM. The sensor showed optimum anodic stripping response within 90 s at an accumulation potential of 0.75 V. This electrode presented the advantages of reasonable stability, repeatability, reproducibility and easy fabrication. It was successfully applied for the monitoring of warfarin in real samples with satisfactory results.

Using of the CS/CNTS furnished electrode in the biosensor mainly includes detecting of the important molecules in the bio-system and the direct electron transfer to the protein molecules (Zhao *et al.*, 2002). Specifically, (1) The furnished electrode could improve the reversibility of the redox reaction of the biomolecules, decrease the over potential and detect several kinds of molecules at the same time; (2) CNTs could transfer the electrons directly. This is mainly because that the higher surface activity

caused by the surface deficiency of CNTs is beneficial to the electron transfer between the enzymes and CNTs. By the way, the special nano structure of the CNTs could act as the molecular wire to transfer the electrons to the redox reaction center of enzymes. Liu *et al.* entrapped the glucose oxidase (GOD) in the composite of carbon nanotubes/chitosan to form a biosensor (Liu *et al.*, 2005). The electron transfer rate of GOD is greatly enhanced to 7.73 s^{-1} in the system, which is more than one-fold higher than that of flavin adenine dinucleotide adsorbed on the carbon nanotubes (3.1 s^{-1}). This can be attributed to the available approaching of active site for GOD to electrode of the conformational changes of GOD in the system. The GOD/CNTs/CS/GC electrode shows better ability to keep the bioactivity of GOD. So it can be used as an amperometric biosensor for glucose detection taking ferrocene monocarboxylic acid as the mediator. It displays higher sensitivity of $0.52 \mu\text{A}/\text{mM}$ and better stability. It was found that there was nearly no decrease of the catalytic current to glucose after keeping the biosensor for 15 days at 4°C .

Recently, Chen *et al.* developed a sensitive amperometric acetylcholinesterase (AChE) biosensor for detection of pesticide residues based on the nanocomposite film of tin oxide (SnO_2) nanoparticles, multi-walled carbon nanotubes and chitosan, with immobilization of AChE and Nafion (Chen *et al.*, 2015). Incorporating MWCNTs and SnO_2 into 0.2 % CS solution can enhance the electrochemical response, promote electron transfer, and improve the microarchitecture of the electrode surface. Because of the synergistic effects of the MWCNTs, SnO_2 , and CS, the biosensor exhibited excellent performance in the merits of good stability, good reproducibility, high sensitivity, wide linear response range, and short response time. The above biosensor was proven to be a feasible quantitative method for ultrasensitive detection of chlorpyrifos residues in vegetables and fruits.

Carbon nanotubes have attracted increasing attention as potential delivery vehicles for intracellular transport of drug molecules, nucleic acids and proteins due to their unique properties such as their high surface area-to-volume ratio. One of the intrinsic properties of CNTs is their strong optical absorbance in the near-infrared (NIR) region, which was reported to enhance thermal destruction of cancerous cells during NIR laser irradiation, revealing the great application promise of CNT-based drug delivery vehicles in cancer therapy by combining chemotherapy with physical therapy such as photothermal therapy. However, the application of CNTs in cancer therapy was usually constrained by the cytotoxicity caused by their hydrophobic surface, as well as their lack of solubility in aqueous medium. Functionalization of CNTs with CS through surface adsorption could increase their dispersibility in the solution. Dong *et al.* used low-molecular-weight chitosan conjugated transactivator of transcription (TAT) peptide for noncovalent functionalization of MWCNTs, in order to provide a more efficient drug delivery vehicle for cancer therapy (Dong *et al.*, 2015). It was found that TAT-CS-conjugated MWCNTs (MWCNTs-TC) were essentially nontoxic with perfect water solubility, and they were more efficient in terms of cancer-targeted intracellular transport both *in vitro* and *in vivo* as compared with chitosan-modified MWCNTs (MWCNTs-CS), suggesting the great application potential in cancer therapy.

By the way, carbon nanotubes have the promise for gene transfection because CNTs possess the capacity to penetrate into the target cells as well as the innately large aspect ratios for cargo molecule loading. However, the initial results demonstrated that the

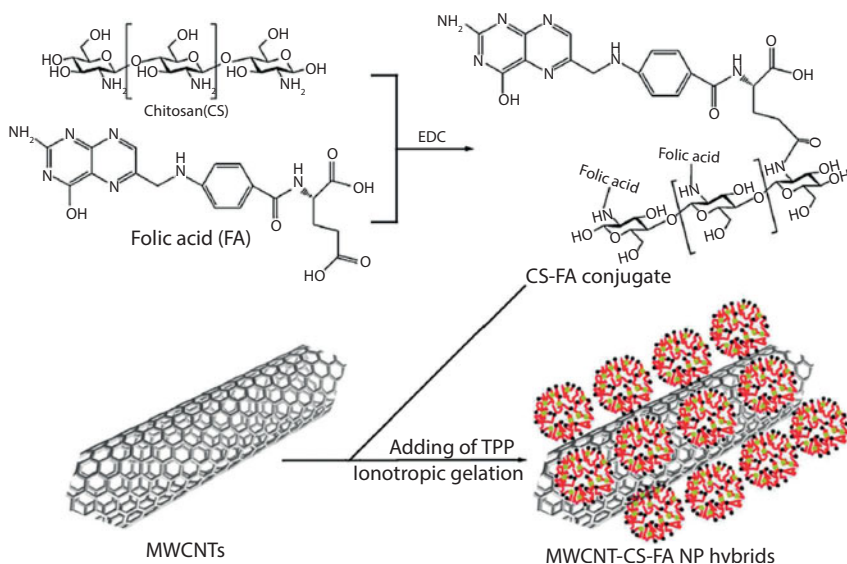


Figure 15.13 The process for synthesis of MWCNT-CS-FA NP hybrids (Liu *et al.*, 2013).

uptake of pristine CNTs into mammalian cells is poor, which results in little transport efficiency. Liu *et al.* functionalized the MWCNTs of different length with chitosan-folic acid nanoparticles (CS-FA NPs) through ionotropic gelation process (Liu *et al.*, 2013). The process was shown in Figure 15.13. The non-functionalized MWCNTs and MWCNT-CS-FA NPs all can deliver the plasmid DNA of enhanced green fluorescent protein (pEGFP-N1) into Hela and MCF-7 cells and the exogenous GFP gene was expressed. It was found that the surface functionalization of MWCNTs with CS-FA NPs increases the transfection efficiency and decreases the cytotoxicity as well.

Carbon nanotube has unique high mechanical properties compared to any other materials and it is also considered as a suitable biomaterial for tissue engineering. Venkatesan *et al.* developed a novel chitosan/MWCNT composite scaffold by freezing and lyophilisation method to mimic the function of extracellular matrix of bone (Venkatesan *et al.*, 2012). It was found that the porosity of scaffolds and water uptake ability were increased with increasing of the amount of MWCNT. The cell proliferation, alkaline phosphatase, protein content and mineralization of the composite scaffolds were higher than chitosan scaffold due to the addition of MWCNT. Based on biological and physiochemical properties of composite scaffold, it is a promising biomaterial for bone tissue engineering.

Huang *et al.* [1] prepared the CNT/chitosan composite fibers via the coagulation and hydrodynamic focusing method (Huang *et al.*, 2011). It was found through the physical property tests that the CNT/chitosan composites had superior electrical conductivity and tensile strength compared with those of chitosan alone. *In vitro* cell culture assays revealed that CNT/chitosan composites were not cytotoxic. With laminin (LN) coating onto fiber surfaces, cell adhesion ratio increased significantly from 3.5% to 72.2%. Experimental results showed that PC12 grown on LN-coated CNT/chitosan fibers *in vitro* extend longitudinally oriented neurites in a manner similar to that of native

peripheral nerves. Combining with the inherent electrical properties of CNTs, oriented CNT/chitosan fibers have a potential use as nerve conduits in nerve tissue engineering.

Mimicking biological function has become a promising way to design advanced functional materials and devices for sensing and actuation. As the electromechanical actuation properties of carbon nanotubes, they have become the unique material enabling the conversion of electrical stimulus to mechanical displacement. The introduction of the highly conductive CNTs could significantly enhance the polymer nanocomposite's electrical, mechanical, thermal, and interface properties, thus providing a suitable material for novel artificial muscle-like actuator investigations (Lu & Chen, 2011). Because chitosan is effective for the stabilization of CNTs, Hu *et al.* prepared high weight fraction single-walled carbon nanotube-chitosan composite films, which showed electromechanical actuation properties with motion controlled by low alternating voltage stimuli in atmospheric conditions, through simple solution blending and casting method (Hu *et al.*, 2010). It is very interesting that the displacement output imitated perfectly the electrical input signal in terms of frequency (<10 Hz) and waveform. It is believed that the vibrations are mostly controlled by thermal expansion and contraction of the polymer matrix, which is caused by periodically heating when an alternating current is passed through the CNT conductive network. Operational reliability was confirmed by stable vibration testing in air for more than 3000 cycles. On the other hand, they constructed a highly stable, high speed full solid chitosan/CNT bimorph electrochemical composite actuator, as shown in Figure 15.14. (Lu & Chen, 2010). For the high weight fraction of CNTs in a uniform chitosan/CNT composite electrode, the conductivity of the composite electrode could reach as high as 34.25 S cm^{-1} , which was made use for reinforcing the electrochemical charging and discharging property of the bimorph structure. The bending actuation performance of the composite strip could reach 2 mm/s high speed actuation performance under 3 V low voltage stimulation. This performance is higher than most traditional ionic polymer metal composite actuator strips. Most important, no heavy metal element is needed here, which is important for biomedical and haptic interface applications. Ozarkar *et al.* prepared the stable SWCNT/chitosan composite fibers of $50 \pm 2 \text{ }\mu\text{m}$, which can respond to an applied electric voltage, through the method of heat-set and solution

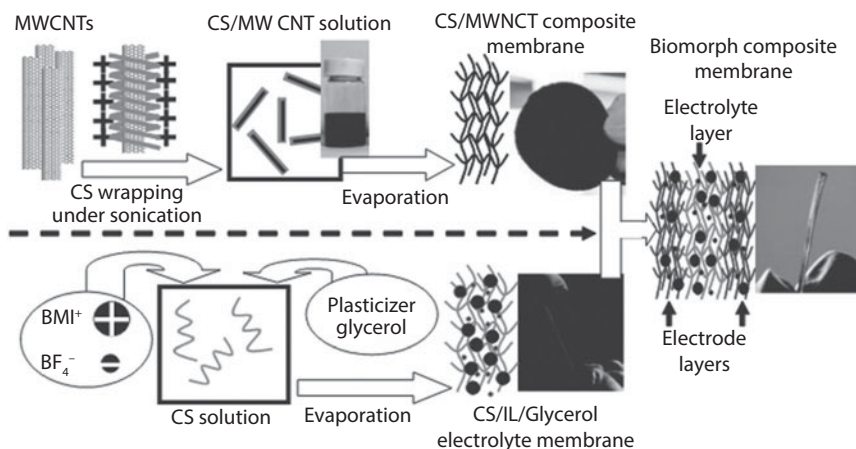


Figure 15.14 Scheme of preparation of the composite actuator (Lu & Chen, 2010).

spun (Ozarkar *et al.*, 2008). The composite fibers exhibited a significant increase in the mechanical properties, which was caused by the strong interaction of carboxylic functional groups of functionalized SWCNTs with the chitosan matrix. The functionalized carbon nanotubes also showed better stability during the electric field response. A significant reduction in response time was observed as increasing of the concentration of functionalized carbon nanotubes. The unique actuation performance of the carbon nanotube-chitosan composite, coupled with low driven voltage, tunable vibration, reliable operation, ease of fabrication and good biocompatibility, shows the great possibility for implementation of actuators for artificial muscle, microelectromechanical systems (MEMS), and biomimetic applications.

15.6.3 Composites from Chitosan and Graphene

Graphene is a single layer two-dimensional carbon material arranged in a honeycomb lattice composed by sp_2 bonded carbon. It has outstanding electronic, optical, electrochemical, mechanical and thermal properties. The intrinsic low weight and excellent thermal stability makes graphene an ideal filler to replace hydroxides and metal oxides with high weight densities for reinforcing polymers (Han *et al.*, 2011). Graphene oxide (GO) obtained by the oxidation of graphene contains a wide range of oxygen functional groups both on the basal planes and at the edges of GO sheets, such as $-COOH$, and $-OH$. These functional groups allow GO to participate in a wide range of bonding interactions. Preparation of graphene-based polymers has been widely investigated because of the impressive benefits of graphene.

As the surface functional groups of the GO, it could composite with the protonated amino group of chitosan or its derivatives through the electrostatic self-assembly technique. This has become one of the research hotspots of novel functional polymers. Wen *et al.* prepared the graphene oxide/chitosan composite membrane with a thickness of several hundred nanometers through an interfacial self-assembly process (Wen *et al.*, 2015). The surface morphology of synthesized membrane can be further tuned through adjusting the concentration of the chitosan solution.

Despite the favorable properties, the loss of structural integrity and the poor mechanical strength limit the applications of chitosan. Pan *et al.* prepared the graphene oxide/chitosan nanocomposite films through a simple solution casting method (Pan *et al.*, 2011). It was found that the mechanical properties of the nanocomposite were significantly promoted without sacrificing the optical transparency. The nanocomposite films containing 1 wt% GO sheets are strong and ductile. The Young's modulus, tensile strength, and elongation at break are found to increase by 51% and 93% and 41%, respectively, which are much higher than those of neat chitosan films. The simultaneous improvement of toughness and strength could be attributed to the homogeneous dispersion and unidirectional alignment of GO sheets in the chitosan matrix (as shown in Figure 15.15 a), the strong hydrogen bond between GO sheets containing abundant hydroxyl and carboxylic groups and chitosan matrix (as shown in Figure 15.15b), as well as the high specific surface area and the two-dimensional geometry of GO. Lim *et al.* prepared graphene oxide with large area of about $7000 \mu m^2$ and small area of less than $50 \mu m^2$, respectively (Lim *et al.*, 2012). Then the small area GO and large area GO were reduced by sodium hydroxide. By using a simplistic drop-casting technique,

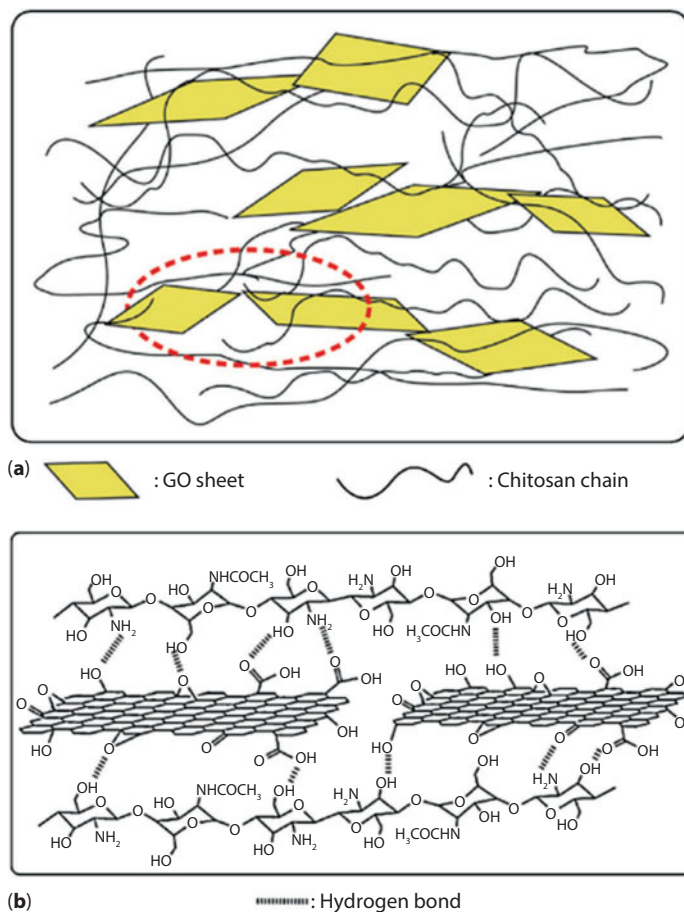


Figure 15.15 (a) Scheme for possible microstructure present in GO/chitosan nanocomposites; (b) formation of hydrogen bonds between GO sheets and chitosan chains (Pan *et al.*, 2011).

the reduced GO (rGO) with small area and large area were incorporated into a chitosan matrix respectively to produce a composite thin film. By study the mechanical strength of the composite film and the glass transition temperature (T_g), it was found that chitosan/large area rGO or GO displayed superior tensile and thermal properties. This is because large area graphene sheets restricted the mobility of the chitosan polymeric chains, resulting in increased thermal and tensile stability of the composite films. These composite materials with excellent tensile, thermal and antimicrobial properties find real-life applications in the physical, chemical, electrical, mechanical and bioengineering fields. Sayyar *et al.* prepared conducting biocompatible hydrogels using lactic acid and chitosan as the matrix (Sayyar *et al.*, 2015). Graphene was used as a filler to improve the conductivity and mechanical properties of the hydrogels. The addition of graphene to the polymer matrix can significant improve the mechanical strength of the hydrogels, with the addition of just 3 wt% graphene resulting in tensile strengths increasing by over 200%. The excellent dispersion of graphene nanosheets in the chitosan/lactic acid matrix and the strong hydrogen bond interactions and could be found. These graphene composites showed large improvements in the mechanical properties

and conductivity but retained the swellability and processability of the polymer matrix resulting in a robust, conducting material that could be extrusion-printed into three-dimensional scaffolds. It was found that the fibroblast cells showed good adhesion and growth on the surfaces of the hydrogel. These chitosan-graphene composites show great potential for use as conducting substrates for the growth of electro-responsive cells in tissue engineering.

The chitosan/GO composite can also be used as the carrier of the drug delivery. Justin *et al.* investigated the drug release performance of the chitosan nanocomposites containing varying drug loading ratios and GO contents (Justin *et al.*, 2014). It was found that the nanocomposite with 2 wt % GO provided the optimal combination of drug-loading capacity and mechanical properties. It offered a faster and a more substantial release of drug than chitosan as well as a slower biodegradation rate, owing to the abundant oxygenated functional groups, hydrophilicity and large specific surface area of GO sheets. The nanocomposite also demonstrated pH sensitivity of drug release, releasing 48% less drug in an acidic condition than in a neutral environment. Wen *et al.* grafted linear PEG-carboxylic acid and folic acid to the amine group on chitosan via the carbodiimide chemistry (Wen *et al.*, 2015). Then the above product was further conjugated to the carboxylic acid groups on GO. The prepared FA-PEG-CS/GO nanocomplexes exhibited high solubility and stability in both PBS solution and DMEM cell medium. TEM showed a unique layered structure of GO in the composite, which is suitable for anticancer drug DOX·HCl loading through π - π interaction. Importantly, tumor pH (pH 5.5) induced faster *in vitro* release of DOX than at pH 7.4. Thus, the above product may be potential carriers for controlled and targeted drug release.

The pristine GO is not good for electrochemical application due to its aggregation of nanosheets in bulk. To further increase the sensitivity of GO modified electrodes for electrochemical analysis, the well exfoliation of GO nanosheets is proved to be crucial (Tang *et al.*, 2015). CS is advantageous as a dispersion agent by constructing hydrogen bonds and electrostatic interactions with the corresponding substrates, so it can be used to stabilize exfoliated GO nanosheets for electrode modification (Zhang *et al.*, 2014; Fang *et al.*, 2010). The CS/GO composite modified acetylene black paste electrode was successfully employed for the simultaneous detection of both *p*-nitrophenol (*p*-NP) and *o*-nitrophenol (*o*-NP) with a detection limit of 0.08 and 0.2 μ M, respectively. The corresponding linear detection range was determined as 0.1~80 for *p*-NP and 0.4~80 μ M for *o*-NP (Deng *et al.*, 2014). The glassy carbon electrode (GCE) modified with CS/GO composite was sensitive in the electrochemical determination of ascorbic acid, 4-aminophenol, dopamine and uric acid (Yin *et al.*, 2010; Han *et al.*, 2010). Si *et al.* used the CS/GO composite to modify the glassy carbon electrode for the determination of copper (II) (Si *et al.*, 2015). The sensor showed a linear dynamic range from 1.0×10^{-9} to 1.5×10^{-8} mol/L for copper (II) with a limit of detection of 4.3×10^{-10} mol/L at a signal-to-noise ratio of three.

Chitosan can physically or chemically entrap various metal ions due to the presence of amine and hydroxyl groups that can serve as the chelating and reaction sites. It is a promising starting material for chelating resins. However, chitosan is only soluble in acidic solutions and is not easy to disperse in water, the non-solubility of chitosan in water has been a stumbling block in its appropriate utilization of heavy metal ions removal (Pillai *et al.*, 2009). Graphene oxide contains a wide range of oxygen functional

groups both on the basal planes and at the edges of GO sheets, such as -COOH, and -OH. These functional groups are essential for the high sorption of heavy metal ions, and allows GO to participate in a wide range of bonding interactions. What is more, the presence of these functional groups can provide potential advantages for using GO as a new adsorbent in water treatment because the polar oxygenous functional groups can improve GO's hydrophilicity strongly (Compton *et al.*, 2010). The composite prepared from chitosan and GP can combine the good properties of them, and the adsorption properties of them would be promoted further. Li *et al.* prepared the sulfydryl-functionalized graphene oxide (GO-SH) firstly (Li *et al.*, 2015). Then it was used to self-assemble with chitosan via an electro static interaction and the chitosan/sulfydryl-functionalized graphene oxide composite (CS/GO-SH) was prepared. It was found that the self-assembly of chitosan with GO-SH sheets changed the blocky structure of the CS to the loosely packed structure. These could further increase the specific surface area, facilitate the contact of metal ions and active adsorption sites as well as benefit the rapid equilibrium adsorption during the process. CS/GO-SH exhibited an extremely high adsorbing ability for metal ions such as Cu (II), Pb (II), and Cd (II). Moreover, in the ternary metal ion system, the results demonstrated that CS/GO-SH is an effective adsorbent when various ions exist simultaneously. Ge *et al.* prepared a novel triethylenetetramine modified graphene oxide/chitosan composite (TGOCS) by microwave irradiation (MW) method (Ge & Ma, 2015). Adsorption of Cr (VI) on the composite was studied. The experimental results indicated that the product obtained by MW had higher yield and uptake than one obtained by the conventional. The uptake of TGOCS for Cr (VI) was higher than that of the recently reported adsorbents. The maximum uptake of Cr (VI) with 20 mg TGOCS at 303 K was 219.5 mg/g at pH 2. The adsorption was a fast process which could reach 85% of maximal uptake in 20 min. By the way, the adsorbent could be recyclable. The chitosan/graphene oxide composite can also be used as the absorbent of dyes (Du *et al.*, 2014) and proteins (Li *et al.*, 2015; Ding *et al.*, 2015).

Acknowledgments

This work was supported by the Youth Talent Plan of Beijing City (YETP1163), the Combination Project of Guangdong Province (2013A090100005) and the “Yangfan” Innovative Research Team Project of Guangdong Province.

References

- Al-Sagheer, F., Muslim, S. Thermal and mechanical properties of chitosan/SiO₂ hybrid composites. *J. Nanomater.*, 490679, 2010.
- Anitha, A., Sowmya, S., Sudheesh Kumar, P. T., Deepthi, S., Chennazhi, K. P., Ehrlich, H., Tsurkanc, M., Jayakumar, R. Chitin and chitosan in selected biomedical applications. *Prog. Polym. Sci.*, 39, 1644–1667, 2014.
- Antunes, J. C., Pereira, C. L., Molinos, M., Ferreira-da-Silva, F., Dessi, M., Gloria, A., Ambrosio, L., Goncalves, R. M., Barbosa, M. A. Layer-by-layer self-assembly of chitosan and poly(γ -glutamic acid) into polyelectrolyte complexes. *Biomacromolecules*, 12, 4183–4195, 2011.

- Appelqvist, I. A. M., Debet, M. R. M. Starch-biopolymer interactions-a review. *Food Rev. Int.*, 13(2), 163–224, 1997.
- Askari, M., Rezaei, B., Shoushtari, A. M., Noorpanah, P., Abdouss, M., Ghani, M. Fabrication of high performance chitosan/polyvinyl alcohol nanofibrous mat with controlled morphology and optimised diameter. *Can. J. Chem. Eng.*, 92, 1008–1015, 2014.
- Auta, M., Hameed, B. H. Coalesced chitosan activated carbon composite for batch and fixed-bed adsorption of cationic and anionic dyes. *Colloids Surfaces B*, 105, 199–206, 2013.
- Barikani, M., Honarkar, H., Barikani, M. Synthesis and characterization of chitosan-based polyurethane elastomer dispersions. *Monatsh. Chem.*, 141, 653–659, 2010.
- Benjamin, L. O., Francesco, S. Antibacterial activity of silver nanoparticles: A surface science insight. *Nano Today*, 10(3), 339–354, 2015.
- Bhowmick, A., Saha, A., Pramanik, N., Banerjee, S., Das, M., Kundu, P. P. Novel magnetic antimicrobial nanocomposites for bone tissue engineering applications. *RSC Adv.*, 5(32), 25437–25445, 2015.
- Billard, A., Pourchet, L., Malaise, S., Alcouffe, P., Montebault, A., Ladavière, C. Liposome-loaded chitosan physical hydrogel: Toward a promising delayed-release biosystem. *Carbohydr. Polym.*, 115, 651–657, 2015.
- Bueno, P. V. A., Souza, P. R., Follmann, H. D. M., Pereira, A. G. B., Martins, A. F., Rubira, A. F., Muniz, E. C. N. N-Dimethyl chitosan/heparin polyelectrolyte complex vehicle forefficient heparin delivery. *Int. J. Biol. Macromol.*, 75, 186–191, 2015.
- Caddeo, C., Díez-Sales, O., Pons, R., Carbone, C., Ennas, G., Puglisi, G., Fadda, A. M., Manconi, M. Cross-linked chitosan/liposome hybrid system for the intestinal delivery of quercetin. *J. Colloid Interf. Sci.*, 461, 69–78, 2016.
- Caridade, S. G., Merino, E. G., Alves, N. M., Mano, J. F. Bioactivity and viscoelastic characterization of chitosan/bioglass composite membranes. *Macromol. Biosci.*, 12, 1106–1113, 2012.
- Di Carlo, G., Curulli, A., Toro, R., Bianchini, C., De Caro, T., Padeletti, G., Zane, D., Ingo, G. Green synthesis of gold–chitosan nanocomposites for caffeic acid sensing. *Langmuir*, 28 (12), 5471–5479, 2012.
- Charernsriwilaiwat, N., Rojanarata, T., Ngawhirunpat, T., Opanasopit, P. Electrospun chitosan/polyvinyl alcohol nanofibre mats for wound healing. *Int. Wound J.*, 11(2), 215–222, 2012.
- Chen, D. F., Sun, X., Guo, Y. M., Qiao, L., Wang, X. Y. Acetylcholinesterase biosensor based on multi-walled carbon nanotubes-SnO₂-chitosan nanocomposite. *Bioprocess. Biosyst. Eng.*, 38, 315–321, 2015.
- Chen, F. Y., Yan, J. J., Yi, H. X., Hu, F. Q., Du, Y. Z., Yuan, H., You, J., Zhao, M. D. TNYL peptide functional chitosan-g-stearate conjugate micelles for tumor specific targeting. *Int. J. Nanomed.*, 9, 4597–4608, 2014.
- Chen, J. D., Pan, P. P., Zhang, Y. J., Zhong, S. N., Zhang, Q. Q. Preparation of chitosan/nano hydroxyapatite organic-inorganic hybrid microspheres for bone repair. *Colloids Surfaces B*, 134, 401–407, 2015.
- Chen, K. H., Shen, Z. G., Luo, J. W., Wang, X. Y., Sun, R. C. Quaternized chitosan/silver nanoparticles composite as a SERS substrate for detecting triclazole and Sudan I. *Appl. Surf. Sci.*, 351, 466–473, 2015.
- Chen, M. M., Huang, Y. Q., Cao, H., Liu, Y., Guo, H., Chen, L. S., Wang, J. H., Zhang, Q. Q. Collagen/chitosan film containing biotinylated glycol chitosan nanoparticles for localized drug delivery. *Colloids Surfaces B*, 128, 339–346, 2015.
- Chen, Z. G., Wei, B., Mo, X. M., Lim, C. T., Ramakrishna, S., Cui, F. Z. Mechanical properties of electrospun collagen–chitosan complex single fibers and membrane. *Mat. Sci. Eng. C-Mater.*, 29, 2428–2435, 2009.
- Cheung, R. C. F., Ng, T. B., Wong, J. H., Chan, W. Y. Chitosan: An update on potential biomedical and pharmaceutical applications. *Mar. Drugs*, 13, 5156–5186, 2015.

- Choi, O., Deng, K. K., Kim, N. J., Ross, L., Surampalli, R. Y., Hu, Z. Q. The inhibitory effects of silver nanoparticles, silver ions, and silver chloride colloids on microbial growth. *Water Res.*, 42, 3066–3074, 2008.
- Choi, O. K., Hu, Z. Q. Nitrification inhibition by silver nanoparticles. *Water Sci. Technol.*, 9(59), 1699–1702, 2009.
- Compton, O.C., Nguyen, S.T. Graphene oxide, highly reduced graphene oxide, and graphene: versatile building blocks for carbon-based materials. *Small*, 6(6), 711–723, 2010.
- Costa-Silva, T. A., Marques, P. S., Souza, C. R. F., Said, S., Oliveira, W. P. Enzyme encapsulation in magnetic chitosan-Fe₃O₄ microparticles. *J. Microencapsul.*, 32(1), 16–21, 2015.
- Cifani, N., Chronopoulou, L., Pompili, B., Martino, A. D., Bordi, F., Sennato, S., Domenico, E. G. D., Palocci, C., Ascenzioni, F. Improved stability and efficacy of chitosan/pDNA complexes for gene delivery. *Biotechnol. Lett.*, 37, 557–565, 2015.
- Copello, G. J., Mebert, A. M., Raineri, M., Pesenti, M. P., Diaz, L. E. Removal of dyes from water using chitosan hydrogel/SiO₂ and chitin hydrogel/SiO₂ hybrid materials obtained by the sol-gel method. *J. Hazard. Mater.*, 186, 932–939, 2011.
- Cui, L., Xing, Z. H., Guo, Y., Liu, Y., Zhao, J. C., Zhang, C. J., Zhu, P. Fabrication of interpenetrating polymer network chitosan/gelatin porous materials and study on dye adsorption properties. *Carbohydr. Polym.*, 132, 330–337, 2015.
- Dash, M., Chiellini, F., Ottenbrite, R. M., Chiellini, E. Chitosan-A versatile semi-synthetic polymer in biomedical applications. *Prog. Polym. Sci.*, 36, 981–1014, 2011.
- De Smedt, S. C., Demeester, J., Hennink, W. E. Cationic polymer based genedelivery systems. *Pharm. Res.-Dordr.*, 17, 113–126, 2000.
- Degim, Z., Celebi, N., Alemdaroglu, C., Devci, M., Ozturk, S., Ozogul, C. Evaluation of chitosan gel containing liposome-loaded epidermal growth factor on burn wound healing. *Int. Wound J.*, 8, 343–354, 2011.
- Deng, J., Zhang, Z. H., Liu, C. Y., Yin, L. F., Zhou, J. P., Lv, H. X. The studies of N-octyl-N-arginine-chitosan coated liposome as an oral delivery system of Cyclosporine A. *J. Pharm. Pharmacol.*, 67, 1363–1370, 2015.
- Deng, P. H., Xu, Z. F., Li, J. H. Simultaneous voltammetric determination of 2-nitrophenol and 4-nitrophenol based on an acetylene black paste electrode modified with a graphene-chitosan composite. *Microchim. Acta*, 181, 1077–1084, 2014.
- Denkbas, E. B., Kilicay, E., Birlikseven, C., Ozturk, E. Magnetic chitosan microspheres: preparation and characterization. *React. Funct. Polym.*, 50, 225–232, 2002.
- Deshpande, D., Blezinger, P., Pillai, R., Duguid, J., Freimark, B., Rolland, A. Target specific optimization of cationic lipid-based systems for pulmonary gene therapy. *Pharm. Res.-Dordr.*, 15, 1340–1347, 1998.
- Dev, A., Binulal, N. S., Anitha, A., Nair, S. V., Furuike, T., Tamura, H., Jayakumar, R. Preparation of poly(lactic acid)/chitosan nanoparticles for anti-HIV drug delivery applications. *Carbohydr. Polym.*, 80, 833–838, 2010.
- Dibrov, P., Dzioba, J., Gosink, K. K., Hase, C. C. Chemiosmotic mechanism of antimicrobial activity of Ag⁺ in *Vibrio cholerae*. *Antimicrob. Agents Ch.*, 46, 2668–2670, 2002.
- Diebold, Y., Jarrin, M., Saez, V., Carvalho, E. L. S., Orea, M., Calonge, M., Seijo, B., Alonso M. J. Ocular drug delivery by liposome–chitosan nanoparticle complexes (LCS-NP). *Biomaterials*, 28, 1553–1564, 2007.
- Ding, X. Q., Wang, Y. Z., Wang, Y., Pai, Q., Chen, J., Huang, Y. H., Xu, K. J. Preparation of magnetic chitosan and graphene oxide-functional guanidinium ionic liquid composite for the solid-phase extraction of protein. *Analytica Chimica. Acta*, 861, 36–46, 2015.
- Ding, Y. L., Shen, S. Z., Sun, H. D., Sun, K. N., Liu, F. T., Qi, Y. S., Yan, J. Design and construction of polymerized-chitosan coated Fe₃O₄ magnetic nanoparticles and its application for hydrophobic drug delivery. *Mat. Sci. Eng. C-Mater.*, 48, 487–498, 2015.

- Dodi, G., Hritcu, D., Lisa, G., Popa, M. I. Core-shell magnetic chitosan particles functionalized by grafting: Synthesis and characterization. *Chem. Eng. J.*, 203, 130–141, 2012.
- Dong, X., Liu, L. X., Zhu, D. W., Zhang, H. L., Leng, X. G. Transactivator of transcription (TAT) peptide–chitosan functionalized multiwalled carbon nanotubes as a potential drug delivery vehicle for cancer therapy. *Int. J. Nanomed.*, 10, 3829–3841, 2015.
- Du, D. J., Sun, J. K., Li, Y. H., Yang, X. X., Wang, X. H., Wang, Z. H., Xia, L. H. Highly enhanced adsorption of congo red onto graphene oxide/chitosan fibers by wet-chemical etching off silica nanoparticles. *Chem. Eng. J.*, 245, 99–106, 2014.
- Du, J., Dai, J., Liu, J. L., Dankovich, T. Novel pH-sensitive polyelectrolyte carboxymethyl Konjacglucomannan-chitosan beads as drug carriers. *React. Funct. Polym.*, 66, 1055–1061, 2006.
- Du, X. Z., Yang, L. X., Ye, X., Li, B. Antibacterial activity of konjac glucomannan/chitosan blend films and their irradiation-modified counterparts. *Carbohydr. Polym.*, 92, 1302–1307, 2013.
- Duan, R. P., Zhou, Z. M., Su, G. H., Liu, L. R., Guan, M., Du, B., Zhang, Q. Q. Chitosan-coated gold nanorods for cancer therapy combining chemical and photothermal effects. *Macromol. Biosci.*, 14, 1160–1169, 2014.
- Fang, J. J., Zhang, Y., Yan, S. F., Liu, Z. W., He, S. M., Cui, L., Yin, J. B. Poly(L-glutamic acid)/chitosan polyelectrolyte complex porous microspheres as cell microcarriers for cartilage regeneration. *Acta Biomater.*, 10, 276–288, 2014.
- Fang, M., Long, J., Zhao, W. F., Wang, L. W., Chen, G. H. pH-responsive chitosan-mediated graphene dispersions. *Langmuir*, 26, 16771–16774, 2010.
- Fajardo, A. R., Fávoro, S. L., Rubira, A. F., Muniz, E. C. Dual-network hydrogels based on chemically and physically cross-linked chitosan/chondroitin sulphate. *React. Funct. Polym.*, 73, 1662–1671, 2013.
- Farghali, R. A., Fekry, A. M., Ahmed, R. A., Elhakim, H. K. A. Corrosion resistance of Ti modified by chitosan–gold nanoparticles for orthopedic implantation. *Int. J. Biol. Macromol.*, 79, 787–799, 2015.
- Ferreira, C. S., Caridade, S. G., Mano, J. F., Alves, N. M. Homogeneous poly(L-lactic acid)/chitosan blended films. *Polym. Adv. Technol.*, 25, 1492–1500, 2014.
- Ge, H. C., Fan, X. H. Adsorption of Pb^{2+} and Cd^{2+} onto a novel activated carbon-chitosan complex. *Chem. Eng. Technol.*, 34, 1745–1752, 2011.
- Ge, H. C., Ma, Z. W. Microwave preparation of triethylenetetramine modified graphene oxide/chitosan composite for adsorption of Cr(VI). *Carbohydr. Polym.*, 131, 280–287, 2015.
- Gholivand, M. B., Mohammadi-Behzad, L. An electrochemical sensor for warfarin determination based on covalent immobilization of quantum dots onto carboxylated multiwalled carbon nanotubes and chitosan composite film modified electrode. *Mat. Sci. Eng. C-Mater.*, 57, 77–87, 2015.
- Ghosh, B., Chellappan, K. V., Urban, M. W. UV-initiated self-healing of oxolane-chitosan-polyurethane (OXO-CHI-PUR) networks. *J. Mater. Chem.*, 22, 16104, 2012.
- Ghosh, B., Urban, M. W. Self-repairing oxetane-substituted chitosan polyurethane networks. *Science*, 323, 1458–1460, 2009.
- Gordon, O., Slenters, T. V., Brunetto, P. S., Villaruz, A. E., Sturdevant, D. E., Otto, M., Landmann, R., Fromm, K. M. Silver coordination polymers for prevention of implant infection: thiol interaction, impact on respiratory chain enzymes, and hydroxyl radical induction. *Antimicrob. Agents Ch.*, 54, 4208–4218, 2010.
- Grigoriadi, K., Giannakas, A., Ladavos, A. K., Barkoula, N. M. Interplay between processing and performance in chitosan-based clay nanocomposite films. *Polym. Bull.*, 72(5), 1145–1161, 2015.
- Haldorai, Y., Rengaraj, A., Ryu, T., Shin, J., Huh, Y. S., Han, Y. Y. Response surface methodology for the optimization of lanthanum removal from an aqueous solution using a Fe_3O_4 /chitosan nanocomposite. *Mat. Sci. Eng. B-Solid.*, 195, 20–29, 2015.

- Han, D. L., Yan, L. F., Chen, W. F., Li, W. Preparation of chitosan/graphene oxide composite film with enhanced mechanical strength in the wet state. *Carbohydr. Polym.*, 83, 653–658, 2011.
- Han, D. X., Han, T. T., Shan, C. S., Ivaska, A., Niu, L. Simultaneous determination of ascorbic acid, dopamine and uric acid with chitosan-graphene modified electrode. *Electroanal.*, 22, 2001–2008, 2010.
- Han, F. X., Yang, X. L., Zhao, J., Zhao, Y. H., Yuan, X. Y. Photo-cross-linked layered gelatin-chitosan hydrogel with graded compositions for osteochondral defect repair. *J. Mater. Sci.-Mater. Med.*, 26, 160, 2015.
- Hardiansyah, A., Tanadi, H., Yang, M. C., Liu, T. Y. Electrospinning and antibacterial activity of chitosan-blended poly(lactic acid) nanofibers. *J. Polym. Res.*, 22, 59, 2015.
- Hejazi, R., Amiji, M. Chitosan-based gastrointestinal delivery systems. *J. Control. Release*, 89, 151–165, 2003.
- He, Q., Ao, Q., Gong, K., Zhang, L. H., Hu, M., Gong, Y. D., Zhang, X. F. Preparation and characterization of chitosan–heparin composite matrices for blood contacting tissue engineering. *Biomed. Mater.*, 5, 055001, 2010.
- He, Z. Q., Xiong, L. Z. Evaluation of physical and biological properties of polyvinyl alcohol/chitosan blend films. *J. Macromol. Sci. B*, 51, 1705–1714, 2012.
- Hein, S., Wang, K., Stevens, W. F., Kjems, J. Chitosan composites for biomedical applications: status, challenges and perspectives. *Mater. Sci. Tech.-Lond.*, 24(9), 1053–1061, 2008.
- Hu, Q. L., Chen, Z. K., Chen, L., Shen, J. C. Preparation of CaCO_3 /chitosan three-dimensional composite material via *in-situ* precipitation. *Chem. J. Chinese U.*, 27(3), 575–578, 2006.
- Hu, Y., Chen, T., Dong, X. Y., Mei, Z. N. Preparation and characterization of composite hydrogel beads based on sodium alginate. *Polym. Bull.*, 72(11), 2857–2869, 2015.
- Hu, Y., Chen, W., Lu, L. H., Liu, J. H., Chang, C. R. Electromechanical actuation with controllable motion based on a single-walled carbon nanotube and natural biopolymer composite. *ACS Nano*, 4(6), 3498–3502, 2010.
- Huang, R., Li, W. Z., Lv, X. X., Lei, Z. J., Bian, Y. Q., Deng, H. B., Wang, H. J., Li, J. Q., Li, X. Y. Biomimetic LBL structured nanofibrous matrices assembled by chitosan/collagen for promoting wound healing. *Biomaterials*, 53, 58–75, 2015.
- Huang, R. H., Yang, B. C., Liu, Q., Liu, Y. P. Multifunctional activated carbon/chitosan composite preparation and its simultaneous adsorption of phenol and Cr(VI) from aqueous solutions. *Environ. Prog. Sustain.*, 33(3), 814–823, 2014.
- Huang, Y., Ouyang, Q. B., Zhang, D., Zhu, J., Li, R. X., Yu, H. Carbon materials reinforced aluminum composites: A review. *Acta Metall. Sin. (Engl. Lett.)*, 27(5), 775–786, 2014.
- Huang, Y. C., Huang, J. C., Cai, J. H., Lin, W. S., Lin, Q. X., Wu, F. C. Y., Luo, J. W. Carboxymethyl chitosan/clay nanocomposites and their copper complexes: Fabrication and property. *Carbohydr. Polym.*, 134, 390–397, 2015.
- Huang, Y. C., Hus, S. H., Kuo, W. C., Chang-Chien, C-L., Cheng, H., Huang, Y. Y. Effects of laminin-coated carbon nanotube/chitosan fibers on guided neurite growth. *J. Biomed. Mater. Res. Part A*, 99A, 86–93, 2011.
- Iijima, S. Helical microtubules of graphitic carbon. *Nature*, 354(6348), 56–58, 1991.
- Illum, L., Gill, I. J., Hinchcliffe, M., Fisher, A. N., Davis, S. S. Chitosan as a novel nasal delivery system for vaccines. *Adv. Drug Deliver. Rev.*, 51, 81–96, 2001.
- Ito, M. *In vitro* properties of a chitosan-bonded hydroxyapatite bone-filling paste. *Biomaterials*, 12, 41–45, 1991.
- Janegitz, B. C., Junior, L. H. M., Filho, S. P. C., Faria, R. C., Fatibello-Filho, O. Anodic stripping voltammetric determination of copper (II) using a functionalized carbon nanotubes paste electrode modified with cross-linked chitosan. *Sensor. Actuat. B*, 142(1), 260–266, 2009.
- Jayakumar, R., Chennazhi, K. P., Muzzarelli, R. A. A., Tamura, H., Nair, S. V., Selvamurugan, N. Chitosan conjugated DNA nanoparticles in gene therapy. *Carbohydr. Polym.*, 79, 1–8, 2010.

- Jebahi, S., Oudadesse, H., Saleh, G. B., Saoudi, M., Mesadhi, S., Rebai, T., Keskes, H., Feki, A., Feki, H. Chitosan-based bioglass composite for bone tissue healing: Oxidative stress status and antiosteoporotic performance in a ovariectomized rat model. *Korean J. Chem. Eng.*, 31(9), 1616–1623, 2014.
- J. Jeong, S. Kim., T. Park., Molecular design of functional polymers for gene therapy, *Prog. Polym. Sci.*, 32, 1239–1274, 2007.
- Jiang, L. Y., Wang, R. X., Li, X. M., Jiang, L. P., Lu, G. H. Electrochemical oxidation behavior of nitrite on a chitosan-carboxylated multiwall carbon nanotube modified electrode. *Electrochem. Commun.*, 7(6), 597–601, 2005.
- Justin, R., Chen, B. Q. Characterisation and drug release performance of biodegradable chitosan-graphene oxide nanocomposites. *Carbohydr. Polym.*, 103, 70–80, 2014.
- Kaderli, S., Boulocher, C., Pillet, E., Watrelot-Virieux, D., Rougemont, A. L., Roger, T., Viguier, E., Gurny, R., Scapozza, L., Jordan, O. A novel biocompatible hyaluronic acid–chitosan hybrid hydrogel for osteoarthritis therapy. *Int. J. Pharm.*, 483, 158–168, 2015.
- Kalimuthu, P., Natrayasamy, V. Synthesis and applications of eco-magnetic nano-hydroxyapatitechitosan composite for enhanced fluoride sorption. *Carbohydr. Polym.*, 134, 732–739, 2015.
- Kanatt, S. R., Rao, M. S., Chawla, S. P., Sharma, A. Active chitosan-polyvinyl alcohol films with natural extracts. *Food Hydrocolloid.*, 29, 290–297, 2012.
- Karaca, E., Şatır, M., Kazan, S., Açıkgöz, M., Öztürk, E., Gürdağ, G., Ulutaş, D. Synthesis, characterization and magnetic properties of Fe₃O₄ doped chitosan polymer. *J. Magn. Magn. Mater.*, 373, 53–59, 2015.
- Karagozlu, M. Z., Karadeniz, F., Kim, S. K. Anti-HIV activities of novel synthetic peptide conjugatedchitosan oligomers. *Int. J. Biol. Macromol.*, 66, 260–266, 2014.
- Kato, T. Polymer/calcium carbonate layered thin-film composites. *Adv. Mater.*, 12, 1543–1546, 2000.
- Kikuchi, Y. Macromolecular complexes consisting of polyaluminum chloride, glycol chitosan, and poly (potassium vinyl sulfate). *Nippon Kagaku Kaishi.*, (9), 1734–1740, 1987.
- Kim, H. L., Jung, G. Y., Yoon, J. H., Han, J. S., Park, Y. J., Kim, D. G., Zhang, M. Q., Kim, D. J. Preparation and characterization of nano-sizedhydroxyapatite/alginate/chitosan composite scaffolds for bone tissue engineering. *Mat. Sci. Eng. C-Mater.*, 54, 20–25, 2015.
- Kim, T., Jiang, H., Jere,D., Park, I., Cho, M., Nah, J., Choi, Y., Akaike, T., Cho,C., Chemical modification of chitosan as a gene carrier *in vitro* and *in vivo*, *Prog. Polym. Sci.*, 32, 726–753, 2007.
- Kirker, K. R., Luo, Y., Nielson, J. H., Shelby, J., Prestwich, G. D. Glycosaminoglycan hydrogel films as bio-interactive dressings for wound healing. *Biomaterials*, 23, 3661–3671, 2002.
- Koping-Hoggard, M., Melnikova, Y. S., Varum, K. M., Lindman, B., Artursson, P. Relationship between the physical shape and the efficiency of oligomeric chitosan as a gene delivery system *in vitro* and *in vivo*. *J. Gene. Med.*, 5, 130–141, 2003.
- Korkiatithaweechai, S., Umsarika, P., Praphairaksit, N., Muangsin, N. Controlled release of diclofenac from matrix polymer of chitosan and oxidized konjac glucomannan. *Mar. Drugs*, 9, 1649–1663, 2011.
- Konuklu, Y., Paksoy, H. O. The preparation and characterization of chitosan-gelatin microcapsules and microcomposites with fatty acids as thermal energy storage materials. *Energy Technol.*, 3, 503–508, 2015.
- Krishna, A. S., Radhakumary, C., Sreenivasan, K. Calcium ion modulates protein release from chitosan-hyaluronic acid poly electrolyte gel. *Polym. Eng. Sci.*, 55(9), 2089–2097, 2015.
- Ku, Y., Shim, I. K., Lee, J. Y., Park, Y. J., Rhee, S. H., Nam, S. H., Park, J. B., Chung, C. P., Lee, S. J. Chitosan/poly(L-lactic acid) multilayered membrane for guided tissue regeneration. *J. Biomed. Mater. Res. A*, 90A(3), 766–772, 2009.

- Kumar, B. S., Aigal, S., Ramesh, D. V. Air-dried 3D-collagen–chitosan biocomposite scaffold for tissue engineering application. *Polym. Composite.*, 33(11), 2029–2035, 2012.
- Kumar-Krishnan, S., Prokhorov, E., Hernandez-Iturriaga, M., Mota-Morales, J. D., Vazquez-Lepe, M., Kovalenko, Y., Sanchez, I. C., Luna-Barcenas, G. Chitosan/silver nanocomposites: Synergistic antibacterial action of silver nanoparticles and silver ions. *Eur. Polym. J.*, 67, 242–251, 2015.
- Lee, J. E., Kim, K. E., Kwon, I. C., Ahn, H. J., Lee, S. H., Cho, H., Kim, H. J., Seong, S. C., Lee, M. C. Effects of the controlled-released TGF- β 1 from chitosan microspheres on chondrocytes cultured in a collagen/chitosan/glycosaminoglycan scaffold. *Biomaterials*, 25, 4163–4173, 2004.
- Lei, Y., Guan, J. J., Chen, W., Ke, Q. F., Zhang, C. Q., Guo, Y. P. Fabrication of hydroxyapatite/chitosan porous materials for Pb(II) removal from aqueous solution. *RSC Adv.*, 5, 25462–25470, 2015.
- Leiva, A., Bonard, S., Pino, M., Saldías, C., Kortaberria, G., Radic, D. Improving the performance of chitosan in the synthesis and stabilization of gold nanoparticles. *Eur. Polym. J.*, 68, 419–431, 2015.
- Li, G. B., Xue, Q., Feng, J. J., Sui, W. P. Electrochemical biosensor based on nanocomposites film of thiol graphene–thiol chitosan/nano gold for the detection of carcinoembryonic antigen. *Electroanalysis*, 27, 1245–1252, 2015.
- Li, L., Wang, N., Jin, X., Deng, R., Nie, S. H., Sun, L., Wu, Q. J., Wei, Y. Q., Gong, C. Y. Biodegradable and injectable *in situ* cross-linking chitosan–hyaluronic acid based hydrogels for postoperative adhesion prevention. *Biomaterials*, 35, 3903–3917, 2014.
- Li, L., Zhao, F. F., Zhao, B. J., Zhang, J., Li, C., Qiao, R. Z. Chitosan grafted with phosphorylcholine and macrocyclic polyamine as an effective gene delivery vector: preparation, characterization and *in vitro* transfection. *Macromol. Biosci.*, 15, 912–926, 2015.
- Li, X. Y., Han, Y., Ling, Y. Z., Wang, X. Y., Sun, R. C. Assembly of layered silicate loaded quaternized chitosan/reduced graphene oxide composites as efficient absorbents for double-stranded DNA. *ACS Sustainable Chem. Eng.*, 3, 1846–1852, 2015.
- Li, X. Y., Zhou, H. H., Wu, W. Q., Wei, S. D., Xu, Y., Kuang, Y. F. Studies of heavy metal ion adsorption on Chitosan/Sulfhydryl functionalized graphene oxide composites. *J. Colloid Interf. Sci.*, 448, 389–397, 2015.
- Liao, G. M., Yang, C. C., Hu, C. C., Pai, Y. L., Lue, S. J. Novel quaternized polyvinyl alcohol/quaternized chitosan nano-composite as an effective hydroxide-conducting electrolyte. *J. Membrane Sci.*, 485, 17–29, 2015.
- Liew, K. M., Lei, Z. X., Zhang, L. W. Mechanical analysis of functionally graded carbon nanotube reinforced composites: A review. *Compos. Struct.*, 120, 90–97, 2015.
- Lim, H. N., Huang, N. M., Loo, C. H. Facile preparation of graphene-based chitosan films: Enhanced thermal, mechanical and antibacterial properties. *J. Non-Cryst. Solids*, 358, 525–530, 2012.
- Liu, Q., Yang, B. C., Zhang, L. J., Huang, R. H. Simultaneous adsorption of aniline and Cu^{2+} from aqueous solution using activated carbon/chitosan composite. *Desalin. Water Treat.*, 55, 410–419, 2015.
- Liu, X. H., Zhang, Y. Y., Ma, D. M., Tang, H., Tan, L., Xie, Q. J., Yao, S. Z. Biocompatible multi-walled carbon nanotube–chitosan–folic acid nanoparticle hybrids as GFP gene delivery materials. *Colloids Surfaces B*, 111, 224–231, 2013.
- Liu, Y., Nie, C. Y., Liu, X. J., Xu, X. T., Sun, Z., Pan, L. K. Review on carbon-based composite materials for capacitive deionization. *RSC Adv.*, 5, 15205–15225, 2015.
- Liu, Y., Sun, Y., Xu, Y. X., Feng, H., Fu, S. D., Tang, J. W., Liu, W., Sun, D. C., Jiang, H., Xu, S. C. Preparation and evaluation of lysozyme-loaded nanoparticles coated with poly- γ -glutamic acid and chitosan. *Int. J. Biol. Macromol.*, 59, 201–207, 2013.

- Liu, Y. J., Liu, D. D., Zhu, L., Gan, Q., Le, X. Y. Temperature-dependent structure stability and *in vitro* release of chitosan-coated curcumin liposome. *Food Res. Int.*, 74, 97–105, 2015.
- Liu, Y. N., Liu, Y., Liao, N. N., Cui, F. H., Park, M., Kim, H. Y. Fabrication and durable antibacterial properties of electropunchitosan nanofibers with silver nanoparticles. *Int. J. Biol. Macromol.*, 79, 638–643, 2015.
- Liu, Y. Y., Tang, J., Chen, X. Q., Xin, J. H. Decoration of carbon nanotubes with chitosan. *Carbon.*, 43(15): 3178–3180, 2005.
- Liu, Z. M., Stout, J. E., Boldin, M., *et al.* Intermittent use of copper-silver ionization for legionella control in water distribution systems: a potential option in buildings housing individuals at low risk of infection. *Clin. Infect. Dis.*, 1(26), 138–140, 1998.
- Liu, Y., Wang, M. K., Zhao, F., Xu, Z. A., Dong, S. J. The direct electron transfer of glucose oxidase and glucose biosensor based on carbon nanotubes/chitosan matrix. *Biosens. Bioelectron.*, 21, 984–988, 2005.
- Lin, W. C., Yu, D. G., Yang, M. C. Blood compatibility of thermoplastic polyurethane membrane immobilized with water-soluble chitosan/dextran sulphate. *Colloids Surfaces B*, 44, 82–92, 2005.
- Lopes, L. C., Fajardo, A. R., Piai, J. F., Rubira, A. F., Muniz, E. C. Incorporation of theophylline in a chitosan/chondroitin sulphate hydrogel matrix: *in vitro* release studies and mechanical properties according to pH changes. *J. Appl. Polym. Sci.*, 128(5), 3417–3424, 2013.
- Lu, L. H., Chen, W. Biocompatible composite actuator: a supramolecular structure consisting of the biopolymer chitosan, carbon nanotubes, and an ionic liquid, *Adv. Mater.*, 22, 3745–3748, 2010.
- Lu, L. H., Chen, W. Supramolecular self-assembly of biopolymers with carbon nanotubes for biomimetic and bio-inspired sensing and actuation. *Nanoscale.*, 3, 2412–2420, 2011.
- Luo, J., Ling, Y., Li, X., Yuan, B., Yu, F., Xie, W. H., Chen, X. F. Combining amphiphilic chitosan and bioglass for mediating cellular osteogenic growth peptide gene. *RSC Adv.*, 5, 79239–79248, 2015.
- Madhusudhan, A., Reddy, G. B., Venkatesham, M., Veerabhadram, G., Kumar, D. A., Natarajan, S., Yang, M. Y., Hu, A., Singh, S. S. Efficient pH dependent drug delivery to target cancer cells by gold nanoparticles capped with carboxymethyl chitosan. *Int. J. Mol. Sci.*, 15, 8216–8234, 2014.
- Mahanta, A. K., Mittal, V., Singh, N., Dash, D., Malik, S., Kumar, M., Maiti, P. Polyurethane-grafted chitosan as new biomaterials for controlled drug delivery. *Macromolecules.*, 48, 2654–2666, 2015.
- Mao, S. R., Sun, W., Kissel, T. Chitosan-based formulations for delivery of DNA and siRNA. *Adv. Drug Deliver. Rev.*, 62, 12–27, 2010.
- Martinez, A., Blanco, M. D., Davidenko, N., Cameron, R. E. Tailoring chitosan/collagen scaffolds for tissue engineering: Effect of composition and different cross-linking agents on scaffold properties. *Carbohydr. Polym.*, 132, 606–619, 2015.
- Mattiolibelmonte, M., Biagini, G., Muzzarelli, R. A. A., Castaldini, C., Gandolfi, M. G., Krajewski, A., Ravaglioli, A., Fini, M., Giardino, R. Osteoinduction in the presence of chitosan-coated porous hydroxyapatite. *J Bioact. Compat. Pol.*, 10(3), 249–257, 1995.
- Mehta, V. N., Basu, H., Singhal, R. K., Kailasa, S. K. Simple and sensitive colorimetric sensing of Cd²⁺ ion using chitosandithiocarbamate functionalized gold nanoparticles as a probe. *Sensors Actuat. B-Chem.*, 220, 850–858, 2015.
- Messai, I., Lamalle, D., Munier, S., Verrier, B., Ataman-Onal, Y., Delair, T. Poly(D,L-lactic acid) and chitosan complexes: interactions with plasmid DNA. *Colloid. Surface. A.*, 255, 65–72, 2005.
- Mishra, S. K., Kannan, S. Development, mechanical evaluation and surface characteristics of chitosan/polyvinyl alcohol based polymer composite coatings on titanium metal. *J. Mech. Behave. Biomed.*, 40, 314–324, 2014.

- Mohseni-Bandpi, A., Kakavandi, B., Kalantary, R. R., Azari, A., Keramati, A. Development of a novel magnetite-chitosan composite for the removal of fluoride from drinkingwater: adsorption modeling and optimization. *RSC Adv.*, 5(89), 73279–73289, 2015.
- Mota, J., Yu, N., Caridade, S. G., Luz, G. M., Gomes, M. E., Reis, R. L., Jansen, J. A., Walboomers, X. F., Mano, J. F. Chitosan/bioactive glass nanoparticle composite membranes for periodontal regeneration. *Acta Biomater.*, 8(11), 4173–4180, 2012.
- Mukherjee, D. P., Tunkle, A. S., Roberts, R. A., Clavenna, A., Rogers, S., Smith, D. An animal evaluation of a paste of chitosan glutamate and hydroxyapatite as a synthetic bone graft material. *J. Biomed. Mater. Res. B.*, 67B(1), 603–609, 2003.
- Murnper, R. J., Wang, J., Claspell, J. M., Rolland, A. P. Novel polymeric condensing carriers for gene delivery. *Proc. Int. Symo. Contol. Rel. Bioact. Mater.*, 22(3), 178–198, 1995.
- Muzzarelli, R. A. A., Greco, F., Busilacchi, A., Sollazzo, V., Gigante, A. Chitosan, hyaluronan and chondroitinsulfate in tissue engineering for cartilage regeneration: a review. *Carbohydr. Polym.*, 89(3), 723–739, 2012.
- Nam, J. P., Nah, J. W. Target gene delivery from targeting ligand conjugated chitosan-PEI copolymer for cancer therapy. *Carbohydr. Polym.*, 135, 153–161, 2016.
- Nath, S. D., Abueva, C., Kim, B., Lee, B. T. Chitosan-hyaluronic acid polyelectrolyte complex scaffold-cross-linked with genipin for immobilization and controlled release of BMP-2. *Carbohydr. Polym.*, 115, 160–169, 2015.
- Ng, M., Liana, A. E., Liu, S., Lim, M., Chow, C. W. K., Wang, D. S., Drikas, M., Amal, R. Preparation and characterisation of new-polyaluminumchloride-chitosan composite coagulant. *Water Res.*, 46(15), 4614–4620, 2012.
- Nie, H. R., Shen, X. X., Zhou, Z. H., Jiang, Q. S., Chen, Y. W., Xie, A., Wang, Y., Han, C. C. Electrospinning and characterization of konjac glucomannan/chitosan nanofibrous scaffolds favoring the growth of bone mesenchymal stem cells. *Carbohydr. Polym.*, 85, 681–686, 2011.
- Niu, X. F., Wang, L. Z., Chen, P., Li, X. M., Zhou, G., Feng, Q. L., Fan, Y. B. Emulsion self-assembly synthesis of chitosan/poly(lactic-co-glycolic acid) stimuli-responsive amphiphiles. *Macromol. Chem. Phys.*, 214, 700–706, 2013.
- Nivethaa, E. A. K., Narayanan, V., Stephen, A. Synthesis and spectral characterization of silver embedded chitosan matrix nanocomposite for the selective colorimetric sensing of toxic mercury. *Spectrochimica Acta A.*, 143, 242–250, 2015.
- Oligino, T. J., Yao, Q., Ghivizzani, S. C., & Robbins, P. Vector systems for gene transfer to joints. *Clin. Orthopedics.*, 379, S17–S30, 2000.
- Ozarkar, S., Jassal, M., Agrawal, A. K. pH and electrical actuation of single walled carbon nanotube/chitosan composite fibers. *Smart Mater. Struct.*, 17, 055016, 2008.
- Palani, P. B., Abidin, K. S., Kannan, R., Sivakumar, M., Wang, F. M., Rajashabala, S., Velraj, G. Improvement of proton conductivity in nanocomposite polyvinyl alcohol (PVA)/chitosan (CS) blend membranes. *RSC Adv.*, 4, 61781–61789, 2014.
- Pan, Y., Zhang, Y. Z., Li, Y. Layer-by-layer self-assembled multilayer films of single-walled carbon nanotubes and tin disulfide nanoparticles with chitosan for the fabrication of biosensors. *J. Appl. Polym. Sci.*, 128(1), 647–652, 2013.
- Pan, Y. Z., Wu, T. F., Bao, H. Q., Li, L. Green fabrication of chitosan films reinforced with parallel aligned graphene oxide. *Carbohydr. Polym.*, 83:1908–1915, 2011.
- Panyala, N. R., Maria, P. M. E., Havel, J. Gold and nano-gold in medicine: overview, toxicology and perspectives. *J. Appl. Biomed.*, 7(2), 75–91, 2009.
- Pappu, A., Patil, V., Jain, S., Mahindrakar, A., Haque, R., Thakur, V. K., Advances in industrial prospective of cellulosic macromolecules enriched banana biofibre resources: A review. *Int. J. Biol. Macromol.*, 79, 449–458, 2015.
- Park, B. G., Kang, H. S., Lee, W., Kim, J. S., Son, T. Reinforcement of pH-responsive γ -poly(glutamic acid)/chitosan hydrogel for orally administrable colon-targeted drug delivery. *J. Appl. Polym. Sci.*, 127(1), 832–836, 2013.

- Park, H. J., Kim, J. Y., Kim, J., Lee, J. H., Hahn, J. S., Gu, M. B., Yoon, J. Silver-ion-mediated reactive oxygen species generation affecting bactericidal activity. *Water Res.*, 4(43), 1027–1032, 2009.
- Pezeshki-Modaress, M., Zandi, M., Mirzadeh, H. Fabrication of gelatin/chitosan nanofibrous scaffold: process optimization and empirical modelling. *Polym. Int.*, 64, 571–580, 2015.
- Pighinelli, L., Kucharska, M. Chitosan-hydroxyapatite composites. *Carbohydr. Polym.*, 93, 256–262, 2013.
- Pillai, C., Paul, W., Sharma, C. P., Chitin and chitosan polymers: Chemistry, solubility and fiber formation. *Prog. Polym. Sci.*, 34(7), 641–678, 2009.
- Podzus, P. E., Daraio, M. E., Jacobo, S. E. Chitosan magnetic microspheres for technological applications: preparation and characterization. *Physica B.*, 404(18), 2710–2712, 2009.
- Pon-On, W., Charoenphandhu, N., Teerapornpuntakit, J., Thongbunchoo, J., Krishnamra, N., Tang, I-M. Mechanical properties, biological activity and protein controlled release by poly(vinyl alcohol)-bioglass/chitosan-collagen composite scaffolds: A bone tissue engineering applications. *Mat. Sci. Eng. C-Mater.*, 38, 63–72, 2014.
- Pospiskova, K., Safarik, I. Low-cost, easy-to-prepare magnetic chitosan microparticles for enzymes immobilization. *Carbohydr. Polym.*, 96(2), 545–548, 2013.
- Popa, V. I., Breaban, I. G. Cellulose as a component of biodegradable composites. *Cell.Chem. Technol.*, 29(5), 575–587, 1995.
- Qin, H., Wang, C. M., Dong, Q. Q., Zhang, L., Zhang, X., Ma, Z. Y., Han, Q. R. Preparation and characterization of magnetic Fe_3O_4 -chitosan nanoparticles loaded with isoniazid. *J. Magn. Magn.Mater.*, 381, 120–126, 2015.
- Qu, L. J., Guo, X. Q., Tian, M. W., Lu, A. Antimicrobial fibers based on chitosan and polyvinyl-alcohol. *Fiber.Polym.*, 15(7), 1357–1363, 2014.
- Ravarian, R., Craft, M., Dehghani, F. Enhancing the biological activity of chitosan and controlling the degradation by nanoscale interaction with bioglass. *J. Biomed. Mater. Res. Part A*, 103A, 2898–2908, 2015.
- Remaut, K., Sanders, N.N., De Geest, B.G., Braeckmans, K., Demeester, J., De Smedt, S.C., Nucleic acid delivery: where material sciences and bio-sciences meet. *Mater. Sci. Eng. R.*, 58 (118), 117–161, 2007.
- Sacco, P., Travan, A., Borgogna, M., Paoletti, S., Marsich, E. Silver-containing antimicrobial membrane based on chitosan-TPP hydrogel for the treatment of wounds. *J. Mater. Sci. Mater. Med.*, 26, 128, 2015.
- Saha, K., Agasti, S. S., Kim, C., Li, X., Rotello, V.M., Gold nanoparticles in chemical and biological sensing. *Chem. Rev.*, 112, 2739–2779, 2012.
- Sajomsang, W., Gonil, P., Ruktanonchai, U. R., Petchsangsa, M., Opanasopit, P., Puttipipatkachorn, S. Effect of N-pyridinium positions of quaternized chitosan on transfection efficiency in gene delivery system. *Carbohydr.Polym.*, 104, 17–22, 2014.
- Salimi, A., Pourbahram, B., Mansouri-Majd, S., Hallaj, R. Manganese oxide nanoflakes/multi-walled carbon nanotubes/chitosan nanocomposite modified glassy carbon electrode as a novel electrochemical sensor for chromium (III) detection. *Electrochim.Acta.*, 156, 207–215, 2015.
- Sambudi, N. S., Sathyamurthy, M., Lee, G. M., Park, S. B. Electrospun chitosan/poly(vinyl alcohol) reinforced with CaCO_3 nanoparticles with enhanced mechanical properties and biocompatibility for cartilage tissue engineering. *Compos. Sci. Technol.*, 106, 76–84, 2015.
- Santo, V. S., Gomes, M. E., Mano, J. F., Reis, R. L. Chitosan-chondroitin sulphate nanoparticles for controlled delivery of platelet lysates in bone regenerative medicine. *J. Tissue Eng. Regen. Med.*, 6, s47–s59, 2012.
- Santos-Carballal, B., Aaldering, L. J., Ritzefeld, M., Pereira, S., Sewald, N., Moerschbacher, B. M., Götte, M., Goycoolea, F. M. Physicochemical and biological characterization of chitosan microRNA nanocomplexes for gene delivery to MCF-7 breast cancer cells. *Sci. Rep.*, 5, 13567, 2015.

- Sarah, M., Mandana, M., Tima, K., Maryam, M. Anti-inflammatory effects of heparin and its derivatives: a systematic review. *Adv. Pharmacol.Sci.*, 507151, 2015.
- Sayyar, S., Murray, E., Thompson, B. C., Chung, J., Officer, D. L., Gambhir, S., Spinks, G. M., Wallace, G. G. Processable conducting graphene/chitosan hydrogels for tissue engineering. *J. Mater. Chem. B-Solid.*, 3, 481–490, 2015.
- Sebastien, F., Stephane, G., Copinet, A., Coma, V. Novel biodegradable films made from chitosan and poly(lactic acid) with antifungal properties against mycotoxinogen strains. *Carbohydr. Polym.*, 65, 185–193, 2006.
- Seyed Dorraji, M. S., Mirmohseni, A., Carraro, M., Gross, S., Simone, S., Tasselli, F., Figoli, A. Fenton-like catalytic activity of wet-spun chitosan hollow fibers loaded with Fe_3O_4 nanoparticles: batch and continuous flow investigations. *J. Mol. Catal. A-Chem.*, 398, 353–357, 2015.
- Shen, M., Yu, Y. J., Fan, G. D., Chen, G., Jin, Y. M., Tang, W. Y., Jia, W. P. The synthesis and characterization of monodispersed chitosan-coated Fe_3O_4 nanoparticles via a facile one-step solvothermal process for adsorption of bovine serum albumin. *Nanoscale Res. Lett.*, 9, 296, 2014.
- Siqueira, N. M., Garcia, K. C., Bussamara, R., Both, F. S., Vainstein, M. H., Soares, R. M. D. Poly (lactic acid)/chitosan fiber mats: Investigation of effects of the support on lipase immobilization. *Int. J. Biol. Macromol.*, 72, 998–1004, 2015.
- Si, Y. X., Liu, J., Wang, A. M., Niu, S. Y., Wan, J. A chitosan-graphene electrochemical sensor for the determination of copper (II). *Instrum. Sci. Technol.*, 43, 357–368, 2015.
- Spano, F., Massaro, A., Blasi, L., Malerba, M., Cingolani, R., Athanassiou, A. *In situ* formation and size control of gold nanoparticles into chitosan for nanocomposite surfaces with tailored wettability. *Langmuir*, 28(8), 3911–3917, 2012.
- Su, H. L., Chou, C. C., Hung, D. J. 2009. The disruption of bacterial membrane integrity through ROS generation induced by nanohybrids of silver and clay. *J. Biomaterials*, 30, 5979–5987.
- Sullad, A. G., Manjeshwar, L. S., Aminabhavi, T. M. Blend microspheres of chitosan and polyurethane for controlled release of water-soluble antihypertensive drugs. *Polym. Bull.*, 72, 265–280, 2015.
- Sun, I. C., Na, J. H., Jeong, S. Y., Kim, D. E., Kwon, I. C., Choi, K., Ahn, C. H., Kim, K. Biocompatible glycol chitosan-coated gold nanoparticles for tumor-targeting CT imaging. *Pharm. Res.*, 31, 1418–1425, 2014.
- Sun, L., Li, M. Preparation and properties of chitosan- SiO_2 composite films with underwater superoleophobicity. *ACTA Polym.Sin.*, 6, 822–830, 2014.
- Sun, Y., Liu, Y., Liu, W., Lu, C. J., Wang, L. Chitosan microparticles ionically cross-linked with poly(γ -glutamic acid) as antimicrobial peptides and nitric oxide delivery systems. *Biochem. Eng. J.*, 95, 78–85, 2015.
- Tahara, K., Sakai, T., Yamamoto, H., Takeuchi, H., Kawashima, Y. Establishing chitosan coated PLGA nanosphere platform loaded with widevariety of nucleic acid by complexation with cationic compound for genedelivery. *Int. J. Pharm.*, 354, 210–216, 2008.
- Tang, J., Zhang, L. L., Han, G. Q., Liu, Y., Tang, W. H. Graphene-chitosan composite modified electrode for simultaneous detection of nitrophenol isomers. *J. Electrochem. Soc.*, 162 (10), B269–B274, 2015.
- Thakur, V. K., Kessler, M. R. Self-healing polymer nanocomposite materials: A review. *Polymer*, 69(9), 369–383, 2015.
- Thakur, V. K., Thakur, M. K. Recent advances in green hydrogels from lignin: A review. *Int. J. Biol. Macromol.*, 72, 834–847, 2015.
- Thakur, V. K., Thakur, M. K. Recent advances in graft copolymerization and applications of chitosan: A review. *ACS Sustain. Chem. Eng.*, 2(12), 2637–2652, 2014a.
- Thakur, V. K., Thakur, M. K. Recent trends in hydrogels based on psyllium polysaccharide: A review. *J. Clean. Prod.*, 82(1), 1–15, 2014b.

- Thakur, V.K., Thakur, M.K., Processing and characterization of natural cellulose fibers/thermoset polymer composites. *Carbohydr. Polym.* 109, 102–117, 2014c.
- Thakur, M.K., Thakur, V.K., Gupta, R.K., Pappu, A., Synthesis and Applications of Biodegradable Soy Based Graft Copolymers: A Review. *ACS Sustain. Chem. Eng.* 4, 1–17, 2016.
- Tran, H.V., Tran, L.D., Nguyen, T.N. Preparation of chitosan/magnetite composite beads and their application for removal of Pb (II) and Ni (II) from aqueous solution. *Mat. Sci. Eng. C-Mater.*, 30, 304–310, 2010.
- Trigueiro, J. P. C., Silva, G. G., Pereira, F. V., Lavall, R. L. Layer-by-layer assembled films of multi-walled carbon nanotubes with chitosan and cellulose nanocrystals. *J. Colloid Interf. Sci.*, 432, 214–220, 2014.
- Venault, A., Bouyer, D., Pochat-Bohatier, C., Faur, C. Modeling the mass transfers during the elaboration of chitosan-activated carbon composites for medical applications. *AIChEJ.*, 56(6), 1593–1609, 2010.
- Venault, A., Vachoud, L., Bouyer, D., Pochat-Bohatier, C., Faur, C. Rheometric study of chitosan/activated carbon composite hydrogels for medical applications using an experimental design. *J. Appl. Polym. Sci.*, 120, 808–820, 2011.
- Venkatesna, J., Kim, S. K. Chitosan composites for bone tissue engineering-an overview, *Mar. Drugs*, 8, 2252–2266, 2010.
- Venkatesan, J., Ryu, B., Sudha, P. N., Kim, S. K. Preparation and characterization of chitosan-carbon nanotube scaffolds for bone tissue engineering. *Int. J. Biol. Macromol.*, 50, 393–402, 2012.
- Voicu, S.I., Condruz, R.M., Mitran, V., Cimpean, A., Miculescu, F., Andronescu, C., Miculescu, M., Thakur, V.K., Sericin Covalent Immobilization onto Cellulose Acetate Membrane for Biomedical Applications. *ACS Sustain. Chem. Eng.* 4, 1765–1774, 2016.
- Wang, B., Zhang, S. B., Cui, S. H., Yang, B. L., Zhao, Y. N., Chen, H. Y., Hao, X. M., Shen, Q., Zhou, J. T. Chitosan enhanced gene delivery of cationic liposome via non-covalent conjugation. *Biotechnol. Lett.*, 34, 19–28, 2012.
- Wang, C., Xie, X. D., Huuangu, X., Liang, Z., Zhou, C. R. A quantitative study of MC3T3-E1 cell adhesion, morphology and biomechanics on chitosan-collagen blend films at single cell level. *Colloids Surfaces B*, 132, 1–9, 2015.
- Wang, C.Y., Yang, C.H., Huang, K. S., Yeh, C.S., Wang, A.H.J., Chen, C.H. Electrostatic droplets assisted *in situ* synthesis of superparamagnetic chitosan microparticles for magnetic-responsive controlled drug release and copper ion removal. *J. Mater. Chem. B*, 1, 2205–2212, 2013.
- Wang, K. J., Dan, N. H., Xiao, S. W., Ye, Y. C., Dan, W. H. Preparation and characterization of collagen-chitosan-chondroitin sulfate composite membranes. *J. Membrane Biol.*, 245, 707–716, 2012.
- Wang, Q., Zhang, J. P., Mu, B., Fan, L., Wang, A. Q. Facile preparation of magnetic 2-hydroxypropyltrimethyl ammonium chloride chitosan/Fe₃O₄/halloysite nanotubes microspheres for the controlled release of ofloxacin. *Carbohydr. Polym.*, 102, 877–883, 2014.
- Wang, R., Xia, B., Li, B. J., Peng, S. L., Ding, L. S., Zhang, S. Semi-permeable nanocapsules of konjac glucomannan-chitosan for enzyme immobilization. *Int. J. Pharm.*, 364, 102–107, 2008.
- Wang, S. F., Shen, L., Zhang, W. D., Tong, Y. J. Preparation and mechanical properties of chitosan/carbon nanotubes composites. *Biomacromolecules*, 6(6), 3067–3072, 2005.
- Wang, X., Yang, C. C., Zhang, Y. J., Zhen, X., Wu, W., Jiang, X. Q. Delivery of platinum(IV) drug to subcutaneous tumor and lung metastasis using bradykinin-potentiating peptide-decorated chitosan nanoparticles. *Biomaterials*, 35, 6439–6453, 2014.
- Wang, X. Y., Jiang, X. P., Li, Y., Zeng, S., Zhang, Y. W. Preparation Fe₃O₄@chitosan magnetic particles for covalent immobilization of lipase from *Thermomyces lanuginosus*. *Int. J. Biol. Macromol.*, 75, 44–50, 2015.

- Wen, H. Y., Yin, C. J., Du, A. B., Deng, L. L., He, Y. S., He, L. J. Folate conjugated PEG–chitosan/graphene oxide nanocomplexes as potential carriers for pH-triggered drug release. *J. Control. Release*, 213, E44–E45, 2015.
- Wen, X. F., Han, D., Meng, H., Zhang, J. W., Cai, Z. Q., Qian, Y., Chen, T. 2015. Preparation and surface morphology control of self-assembled graphene oxide/chitosan composite membrane. *Sci. Adv. Mater.*, 7(6), 1083–1089, 2015.
- Xiang, C. L., Li, R., Adhikari, B., She, Z., Li, Y. X., Kraatz, H. B. Sensitive electrochemical detection of Salmonella with chitosan-gold nanoparticles composite film. *Talanta*, 140, 122–127, 2015.
- Xiang, Y., Wang, H., He, Y., Song, G. W. Efficient degradation of methylene blue by magnetically separable Fe_3O_4 /chitosan/ TiO_2 nanocomposites. *Desalin. Water Treat.*, 55, 1018–1025, 2015.
- Xu, D., Wu, K., Zhang, Q. H., Hu, H. Y., Xi, K., Chen, Q. M., Yu, X. H., Chen, J. N., Jia, X. D. Synthesis and biocompatibility of anionic polyurethane nanoparticles coated with adsorbed chitosan. *Polymer*, 51, 1926–1933, 2010.
- Xu, J. K., Zhang, F. F., Sun, J. J., Sheng, J., Wang, F., Sun, M. Bio and Nanomaterials Based on Fe_3O_4 . *Molecules*, 19, 21506–21528, 2014.
- Xue, P., Su, W. G., Ye, W. J., Zhao, T. S., Lai, X. Y. Pseudomonas cepacia lipase immobilized onto chitosan-coated activated carbon: an efficient catalyst for transesterification enantiomer resolution of (R,S)-1-Phenyl-3-buten-1-ol. *Asian J. Chem.*, 26(17), 5619–5622, 2014.
- Yamaguchi, I., Tokuchi, K., Fukuzaki, H., Koyama, Y., Takakuda, K., Monma, H., Tanaka, J. Preparation and microstructure analysis of chitosan/hydroxyapatite nanocomposites. *J. Biomed. Mater. Res. Part A*, 55(1), 20–27, 2001.
- Yan, C. Y., Gu, J. W., Hou, D. P., Jiang, H. Y., Wang, J., Guo, Y. Z., Katsumi, H., Sakane, T., Yamamoto, A. Synthesis of Tat tagged and folate modified N-succinyl-chitosan self-assembly nanoparticles as a novel gene vector. *Int. J. Biol. Macromol.*, 72, 751–756, 2015.
- Yan, S. F., Zhang, K. X., Liu, Z. W., Zhang, X., Gan, L., Cao, B., Chen, X. S., Cui, L., Yin, J. B. 2013. Fabrication of poly(L-glutamic acid)/chitosan polyelectrolyte complex porous scaffolds for tissue engineering. *J. Mater. Chem. B*, 1, 1541–1551.
- Yang, J., Long, T., He, N. F., Guo, Y. P., Zhu, Z. A., Qin, F. K. Fabrication of a chitosan/bioglass three-dimensional porous scaffold for bone tissue engineering applications. *J. Mater. Chem. B*, 2, 6611–6618, 2014.
- Yang, Z. Z., Liu, T. F., Xie, Y., Sun, Z. R., Liu, H. M., Lin, J. F., Liu, C. J., Mao, Z. W., Nie, S. N. Chitosan layered gold nanorods as synergistic therapeutics for photothermal ablation and gene silencing in triple-negative breast cancer. *Acta Biomater.*, 25, 194–204, 2015.
- Yin, H. S., Ma, Q., Zhou, Y. L., Ai, S. Y., Zhu, L. S. Electrochemical behavior and voltammetric determination of 4-aminophenol based on graphene–chitosan composite film modified glassy carbon electrode. *Electrochim. Acta.*, 55 (23), 7102–7108, 2010.
- Younes, I., Rinaudo, M. Chitin and chitosan preparation from marine sources. structure, properties and applications. *Mar. Drugs*, 13, 1133–1174, 2015.
- Yu, H. Q., Lu, J., Xiao, C. B. Preparation and properties of novel hydrogels from oxidized konjac glucomannan cross-linked chitosan for *in vitro* drug delivery. *Macromol. Biosci.*, 7, 1100–1111, 2007.
- Yu, S. H., Mi, F. L., Shyu, S. S., Tsai, C. H., Peng, C. K., Lai, J. Y. Miscibility, mechanical characteristic and platelet adhesion of 6-O-carboxymethyl chitosan/polyurethane semi-IPN membranes. *J. Membrane Sci.*, 276, 68–80, 2006.
- Yu, S. H., Wu, S. J., Tang, D. W., Ho, Y. C., Mi, F. L., Kuo, T. H., Sung, H. W. Stimuli-responsive materials prepared from carboxymethyl chitosan and poly(γ -glutamic acid) for protein delivery. *Carbohydr. Polym.*, 87, 531–536, 2012.
- Yu, S. H., Wu, Y. B., Mi, F. L., Shyu, S. S. Polysaccharide-based artificial extracellular matrix: preparation and characterization of three-dimensional, macroporous chitosan, and heparin composite scaffold. *J. Appl. Polym. Sci.*, 109, 3639–3644, 2008.

- Yuan, H., Bao, X., Du, Y. Z., You, J., Hu, F. Q. Preparation and evaluation of SiO_2 -deposited stearic acid-g-chitosan nanoparticles for doxorubicin delivery. *Int. J. Nanomed.*, 7, 5119–5128, 2012.
- Zang, J. J., Jia, S. Y., Liu, Y., Wu, S. H., Zhang, Y. B. A facile method to prepare chemically cross-linked and efficient polyvinyl alcohol/chitosan beads for catalase immobilization. *Catal. Commun.*, 27, 73–77, 2012.
- Zarghami, S., Mohammadi, T., Kazemimoghadam, M. Adsorption behavior of Cu(II) ions on cross-linked chitosan/polyvinyl alcohol ion imprinted membrane. *J. Disper. Sci. Technol.*, 36, 190–195, 2015.
- Zeng, P., Xu, Y., Zeng, C. H., Ren, H., Peng, M. L. Chitosan-modified poly(d,l-lactide-co-glycolide) nanospheres for plasmid DNA delivery and HBV gene-silencing. *Int. J. Pharm.*, 415, 259–266, 2011.
- Zhang, C., Chen, J. D., Yang, F. Q. Konjac glucomannan, a promising polysaccharide for OCDDS. *Carbohydr. Polym.*, 104, 175–181, 2014.
- Zhang, G. N., Li, J. R., Shen, A. G., Hu, J. M. Synthesis of size-tunable chitosan encapsulated gold-silver nanoflowers and their application in SERS imaging of living cells. *Phys. Chem. Chem. Phys.*, 17, 21261–21267, 2015.
- Zhang, L. L., Han, G. Q., Liu, Y., Tang, J., Tang, W. H. Immobilizing haemoglobin on gold/graphene-chitosan nanocomposite as efficient hydrogen peroxide biosensor. *Sensor. and Actuat. B-Chem.*, 197, 164–171, 2014.
- Zhang, S. K., Gonsalves, K. E. Chitosan-calcium carbonate composites by a biomimetic process. *Mater. Sci. Eng.*, 3, 117–124, 1995.
- Zhang, W., Liu, T., Hu, X. L., Gong, J. M. Novel nanofibrous composite of chitosan- CaCO_3 fabricated by electrolytic biomineralization and its cell biocompatibility. *RSC. Adv.*, 2, 514–519, 2012.
- Zhao, D. H., Wei, W., Zhu, Y., Sun, J. H., Hu, Q., Liu, X. Y. Stable emulsions prepared by self-assembly of hyaluronic Acid and chitosan for papain loading. *Macromol. Biosci.*, 15, 558–567, 2015.
- Zhao, Y. D., Zhang, W. D., Chen, H., Luo, Q. M., Li, S. F. Y. Direct electrochemistry of horseradish peroxidase at carbon nanotube powder microelectrode. *Sensor. Actuat. B.*, 87(1), 168–172, 2002.
- Zhang, K. X., Zhang, Y., Yan, S. F., Gong, L. L., Wang, J., Chen, X. S., Cui, L., Yin, J. B. Repair of an articular cartilage defect using adipose-derived stem cells loaded on a polyelectrolyte complex scaffold based on poly(L-glutamic acid) and chitosan. *Acta Biomater.*, 9, 7276–7288, 2013.
- Zhang, Z., Cui, H. F. Biodegradability and biocompatibility study of poly(chitosan-g-lactic acid) scaffolds. *Molecules*, 7, 3243–3258, 2012.
- Zhu, H. G., Ji, J., Lin, R. Y., Gao, C. Y., Feng, L. X., Shen, J. C. Surface engineering of poly(D,L-lactic acid) by entrapment of chitosan-based derivatives for the promotion of chondrogenesis. *J. Biomed. Mater. Res.*, 62(4), 532–539, 2002.
- Zhu, X. M., Zhou, X. Y., Yi, J. Y., Tong, J., Wu, H., Fan, L. H. Preparation and biological activity of quaternized carboxymethylchitosan conjugated with collagen peptide. *Int. J. Biol. Macromol.*, 70, 300–05, 2014.
- Zia, K. M., Anjum, S., Zuber, M., Mujahid, M., Jamil, T. Synthesis and molecular characterization of chitosan based polyurethane elastomers using aromatic diisocyanate. *Int. J. Biol. Macromol.*, 66, 26–32, 2014.

Overview on Synthesis of Magnetic Bio Char from Discarded Agricultural Biomass

Manoj Tripathi^{1,2*}, N.M. Mubarak^{3,4*}, J.N. Sahu^{4,5,6,7*} and P. Ganesan¹

¹*Department of Mechanical Engineering, Faculty of Engineering, University of Malaya, Kuala Lumpur, Malaysia*

²*Department of Applied Science, Dev Bhoomi Institute of Technology, Dehradun, India*

³*Department of Chemical Engineering, Faculty of Engineering and Science, Curtin University of Technology, Sarawak, Malaysia*

⁴*Department of Chemical Engineering, Faculty of Engineering, University of Malaya, Kuala Lumpur, Malaysia*

⁵*Department for Management of Science and Technology Development, Ton Duc Thang University, Ho Chi Minh City, Vietnam*

⁶*Faculty of Applied Sciences, Ton Duc Thang University, Ho Chi Minh City, Vietnam*

⁷*Petroleum and Chemical Engineering, Faculty of Engineering, Universiti Teknologi Brunei, Brunei Darussalam*

Abstract

Agricultural waste biomass is present in a large quantity in most of the countries have considered to be a suitable material for many applications because of their abundance, degradability and low cost. Agricultural wastes have been successfully converted into bio char by means of pyrolysis or other thermochemical conversion techniques. The bio char obtained from agricultural wastes are highly porous and thus are very useful in the adsorption applications. Moving one step ahead these bio char materials have been doped with magnetic medium to convert them in magnetic bio char as magnetic separation technology is an efficient technology for the separation of magnetic materials which is used for many applications in environmental technology, analytical chemistry and mining, medicine, diagnostics and cell biology. These magnetic bio char materials, with the combination of high porosity along with optimized magnetic properties have been successfully utilized in the adsorption of heavy metals, various organic and inorganic chemicals including phenol, tetracycline etc. The major advantage of magnetic bio char is that the magnetic bio char even with low BET surface area and low total pore volume can exhibit high adsorption capacity because more metal ions per unit surface area of magnetic bio char can be adsorbed easily. Moreover, the sorption of magnetic bio char from the aqueous solution is very simple and effective and thus neutralizes the issue of secondary pollution. It can be re-used after the regeneration, thus making the whole adsorption process economically viable and more environment friendly. Bio-polymer based magnetic bio char has tremendous applications in biomechanical engineering and medical

*Corresponding authors: jayanarayansahu@tdt.edu.vn, jay_sahu@yahoo.co.in; tripmanoj@gmail.com; mubarak.yaseen@gmail.com, mubarak.mujaawar@curtin.edu.my

Vijay Kumar Thakur, Manju Kumari Thakur and Michael R. Kessler (eds.), Handbook of Composites from Renewable Materials, (435–460) © 2017 Scrivener Publishing LLC

science since it can serve the purpose of drug carrier very efficiently in magnetic drug delivery systems which is utilized in the treatment of cancer and other diseases. Magnetic bio char with so many potential applications has been synthesized by a number of researchers using different techniques, and different combination of agricultural waste/activated carbon and chemicals. In this chapter we have discussed the various synthesizing techniques which have been adopted by the researchers to prepare magnetic bio char. The BET surface area and magnetic characteristics along with their potential applications and future scope of the magnetic bio char have also been given a notice in the present chapter.

Keywords: Activated carbon, agricultural waste, magnetic adsorption, magnetic bio char synthesis, magnetic bio char characteristics

16.1 Introduction

Agricultural waste materials are potential renewable sources of energy and there is an increasing trend towards the utilization of agricultural wastes to obtain various energy rich by-products such as bio-oil and bio char (Thakur *et al.*, 2014a; Thakur, 2013; (Thakur & Kessler, 2014a,b). Bio char is the solid residue remaining after the thermo-chemical conversion of the agricultural wastes. Bio char is a high heating value product which is sometimes comparable to the coal (Nizamuddin *et al.*, 2016) making it suitable to be used as fuel. Bio char has a high carbon content and has the ability to sequester the carbon in the soil for a very long time therefore it is utilized in soil procurement. Moreover, it provides renewable bio energy and mitigating the global warming and environment climate change issues (Tripathi *et al.*, 2015b). Other than this, bio char's porous structure, large specific surface area, enriched surface functional groups, high adsorption capacity, high chemical and mechanical stability and increased surface reactivity (Li *et al.*, 2009) 436A which ensures its applicability as a potential micro porous adsorbent. Extensive studies have shown that activated carbon synthesized by the agricultural wastes can adsorb various bio-resistant organic pollutants from the aqueous system (Achak *et al.*, 2009). Activated carbon (Di Natale *et al.*, 2013), silica gel (Cao *et al.*, 2014) and zeolite (Badillo-Almaraz *et al.*, 2003) have been widely used for the water purification but due their high generation cost researchers have drawn their attention towards the dead biomass and agricultural wastes such as sunflower leaves (Benaïssa & Elouchdi, 2007), sugarcane bagasse (Khoramzadeh *et al.*, 2013), pine cone (Mahmoodi *et al.*, 2011) guava leaf (Mahmoodi *et al.*, 2011) oil palm shell (Tripathi *et al.*, 2015a) etc. Although activated carbon contains high surface area and relatively high adsorption properties but the high cost involved with its production is still a challenge for the manufacturers. Commercially available activated carbons are expensive because they are produced from the non-renewable and costlier materials such as coal. This makes the activated carbon production not only expensive as well as creates the environment related problems too. Therefore, researchers are trying to develop new low cost material which is not only eco-friendly but also has high surface area and adsorption properties (Pappu *et al.*, 2015). Bio char, prepared from the agricultural wastes and dead biomass material is another class of activated carbon which sees off the challenges related to the activated carbons up to a very high extent. Agricultural wastes due to their low cost and high abundance offers a very high potential to be converted into bio char and get utilized as adsorbent for heavy metals and chemicals for water purification and chemical

industries. From various studies made on the adsorption of different heavy metals and pollutants, it has been found that the pristine bio char made from the thermochemical conversion of agricultural waste materials has a lower heavy metal adsorption capacity. Therefore, modification/activation such as functionalization and surface oxidization etc., have been applied to these synthesized bio char materials (Xue *et al.*, 2012) (Zhang *et al.*, 2011b). Modification in the bio char improves its chemical, physical and sorption behavior. USEPA also has considered the AC adsorption as one of the best available technologies for the organic compound removal process (Adams & Watson, 1996).

16.2 Magnetic Bio Char

Applications of bio char made from the agricultural waste is being successfully explored in various areas such as agriculture, purification and chemical industries. Adsorption of heavy metals from the bio char has been discussed by a number of researchers mentioning a very high degree of heavy metal removal. Although, agriculture based bio char shows very good sorption properties but it is extremely difficult to separate bio char from the aqueous solutions. Separation of these particles from the aqueous solution requires filtration and centrifugation which are tedious processes and also it limits magnetic bio char in their practical applications of wastewater treatment. After the completion of the sorption process a good adsorbent material should be renewable and it must be separable from the aqueous solution. Exhausted bio char contains pollutants and heavy metals so there should be an efficient technique that can avoid the secondary pollution by collecting the pollutant-laden adsorbent from the aqueous solution (Zhang *et al.*, 2015). Reuse of adsorbents and recovery of metals are big challenges and have been major research focuses worldwide for many years. A convenient and economical regeneration method can reduce not only the cost of transportation but also the amount of wasted metal-loaded adsorbents. To overcome this problem a new type of bio char has been developed by introducing the magnetic medium (e.g., Fe_2O_3 or $\gamma\text{-Fe}_2\text{O}_3$) to the synthesized adsorbent (i.e., bio char) by the process of chemical co-precipitation. This modified bio char is termed as magnetic bio char (MB). One of the major advantages of the use of magnetic bio char is that after the adsorption of the pollutants the magnetic bio char can effectively be separated by applying the magnetic separation technique (Chen *et al.*, 2011). Moreover, the combined magnetic medium offer the potential to add the function of bulk magnetic sorbent (Wiatrowski *et al.*, 2009) which includes strong sorption affinity to phosphate (Zeng *et al.*, 2004), selenium (López de Arroyabe Loyo *et al.*, 2008), and organic arsenic with magnetic iron oxide (Lim *et al.*, 2009). However, the loading of magnetic medium on to the bio char increases the cost of the sorbent but the increased cost can be compensated with the renewability of the sorbent. Magnetic bio char is recognized as highly efficient cost effective and more environment friendly sorbent for various types of pollutants and heavy metal removal. Magnetic bio char even with the modest surface area can exhibit good adsorption capacity (Mohan *et al.*, 2015). It is easy to manipulate the magnetic adsorbents by using a small external magnetic field which makes the recovery process more easy and simple. Some impurities like grease may cause carbon fouling and frequent separation/regeneration treatments may be required. Easy isolation and washing, followed by re-dispersion are the other benefits of magnetic separation process (Mohan *et al.*, 2014).

Magnetic biochar is recognized as a multifunctional substance for environmental purposes because of its high carbon storage capacity and greenhouse gas reduction ability. It is increasingly becoming very interesting material because it is a good absorbing material for metallic toxins and pollutants. Moreover, it has a wide range of applications in agricultural purposes such as soil nutrient improvement, increase of vegetation growth, improvement of soil fertility, and raising the soil cation exchange capacity (DeLuca *et al.*, 2009). Agricultural waste and dead biomass derived magnetic biochar is being used for adsorption of organic pollutant.

A wide range of applications of magnetic bio char has already been practiced (Thakur *et al.*, 2012a; Thakur & Thakur, 2015). Magnetic drug delivery also is an active field of interest for the researchers working in the biomedical field. The basic idea behind magnetic drug delivery systems is to inject a magnetically susceptible material coated with a drug-laden matrix and then to use an externally placed magnet to guide the drug matrix to the targeted site. Targeting is effected with a magnet of sufficient strength and focus to retain the particles in a flow field (Widder *et al.*, 1978).

16.3 Synthesis of Magnetic Bio Char

16.3.1 Materials

The state of science of magnetic biochar is that a biomass is synthetically mixed with a magnetic chemical solution and then it is converted into char by the thermochemical conversion process. The first step in synthesizing a magnetic bio char is to select the materials. Biomass is a biological solid product which can be either organic or non-organic which is derived from living or recently living organisms (Thakur *et al.*, 2016; Wu *et al.*, 2016). Various types of wastes such as agricultural waste, waste paper, animal manure, sludge and industrial wastes are also treated as biomass since these waste materials are also a mixture of organic and non-organic compounds. These biomass materials have been successfully converted into the bio char. The quality and characteristics of the magnetic biochar hugely depends upon the raw biomass used for its synthesis, therefore it is extremely important to select the appropriate biomass for the production of the magnetic bio char. Ease of availability, functional groups associated with the biomass, toxicity and economic aspects are few parameters used to select a biomass for the magnetic bio char production. A deep look into the literature has confirmed that there are different combinations of biomass and magnetic medium that have been used for the preparation of magnetic bio char. Most of the researchers have selected iron based materials such as FeCl_3 , Fe_2O_3 or Fe_3O_4 as the magnetic medium. Studies have shown that heavy metals present in the water have a tendency to accumulate on the metal oxy-hydroxides and clay minerals containing Fe, Cu, Al, Co and other metals (Wang *et al.*, 2015b). Therefore, many metals based bio char are also frequently used in the water purification process. Cobalt and nickel have also been used for the preparation of magnetic bio char as they have the extra edge of having magnetic properties also. The use of iron based compounds is preferred more because iron has higher magnetic properties as compared to nickel or cobalt and the use of iron makes the magnetic bio char cost effective also. Few agricultural waste and chemical mediums which have been utilized to synthesize the magnetic bio char for different applications are listed in Table 16.1.

Table 16.1 Various agricultural waste and magnetic medium combinations used for the synthesis of magnetic bio char for different applications.

Waste material	Magnetic medium	Application	Reference
Orange peel	Fe_2O_3	Pollutants and phosphate removal	(Chen <i>et al.</i> , 2011)
Coconut powdered activated carbon	CuFe_2O_4	Acid orange II (AO7) adsorption	(Zhang <i>et al.</i> , 2007)
Cotton wood	$\gamma\text{-Fe}_2\text{O}_3$	Arsenic removal	(Zhang <i>et al.</i> , 2013)
EFB	FeCl_3	Zn^{2+} removal	(Mubarak <i>et al.</i> , 2013)
Paper mill sludge	FeSO_4	Pentachlorophenol removal	(Devi & Saroha, 2014)
Rice hull	$\text{Fe}(\text{acac})_3/\text{ZnS}$	Pb(II) removal	(Yan <i>et al.</i> , 2015)
Pine wood	$\gamma\text{-Fe}_2\text{O}_3$	Arsenic removal	(Wang <i>et al.</i> , 2015b)
Corn stalk	Fe_3O_4 (nano)	Treatment of crystal violet polluted water	(Sun <i>et al.</i> , 2015)
Oak bark	$\text{FeSO}_4/\text{Fe}_2(\text{SO}_4)_3$	Cd and Pb removal	(Mohan <i>et al.</i> , 2014)
Saccharum spontaneum	$\text{Fe}^{+2}/\text{Fe}^{+3}$	Pb removal	(Mohan <i>et al.</i> , 2015)
Eucalyptus leaves	$\text{FeCl}_3/\text{FeSO}_4$	Pb removal	(Wang <i>et al.</i> , 2015a)
Eucalyptus leaves	$\text{FeCl}_3/\text{FeSO}_4$	Cr, Ni, Cu removal	(Wang <i>et al.</i> , 2014)
Kans grass	$\text{FeCl}_3/\text{FeSO}_4$	As (III, V) removal	(Baig <i>et al.</i> , 2014)

16.3.2 Synthesis Techniques of Magnetic Bio Char

Magnetic bio char is compound material composed of a magnetic medium (mostly iron based) impregnated over the highly carbonaceous bio char. There are in various techniques for the synthesis of magnetic bio char. These techniques are described one by one in the following sections:

16.3.2.1 Synthesis of Magnetic Bio Char by Pyrolysis of Agriculture Waste

In this method the magnetic chemical solution is mixed into the agricultural waste in a pre-decided ratio. The magnetic medium is allowed to mix and settle down into the agricultural waste properly and once the magnetic component is impregnated to the agricultural waste biomass, this magnetic component loaded biomass is dried and then finally the dried magnetic component loaded biomass is pyrolyzed under the appropriate process conditions to get the magnetic bio char. A schematic diagram for a typical procedure for the synthesis of magnetic bio char from the agricultural waste using single step pyrolysis technique is shown in Figure 16.1.

Wang *et al.* prepared a magnetic bio char from pine wood using the same technique mentioned above (Wang *et al.*, 2015b). $\gamma\text{-Fe}_2\text{O}_3$ was selected to be the magnetic medium for this study. Hematite treated pine wood was pyrolyzed at the temperature of 600 °C

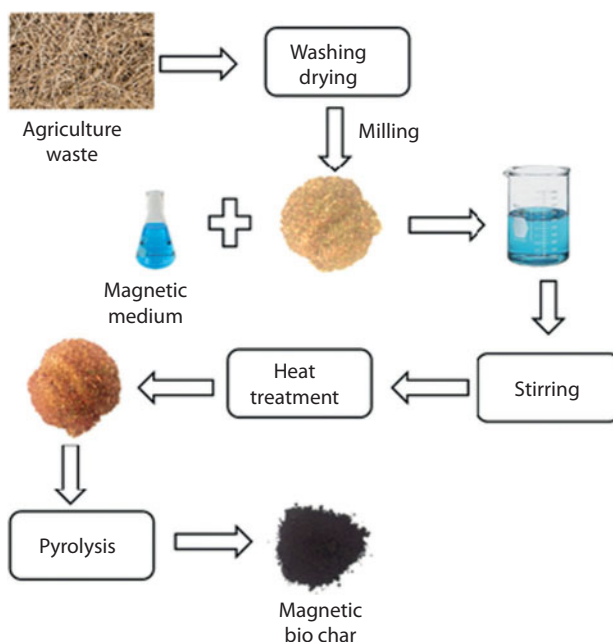


Figure 16.1 Synthesis of magnetic bio char by pyrolysis technique using agricultural waste.

for one hour under the N_2 atmosphere to get the magnetic bio char. In another study, Reddy and Lee (Harikishore Kumar Reddy & Lee, 2014) synthesized magnetic bio char by the impregnation of $Fe(NO_3)_3$ and $Co(NO_3)_2$ on the pine bark followed by the drying (at $70^\circ C$) and pyrolysis of the impregnated pine bark at $950^\circ C$ for 2 h under N_2 atmosphere. Few other researchers have also adopted this method to produce magnetic bio char from different biomass materials using different biomass and magnetic medium for their study (Zhang *et al.*, 2013) (Wang *et al.*, 2015b) (Ruthiraan *et al.*, 2015).

16.3.2.2 Synthesis of Magnetic Bio Char by Chemical Precipitation

Synthesis of magnetic bio char by the precipitation or co-precipitation is a two-step process. In the first step the selected agricultural waste material is converted into bio char either by pyrolysis or by any other thermochemical technique. Once the bio char is produced, the next step is alkaline precipitation of ferrous and ferric salts in the on the synthesized bio char. Afterwards, the aqueous suspension is heated for a definite time at a fixed temperature to get the magnetic bio char. The alkaline used for this process are generally NaOH, KOH, $NH_3 \cdot H_2O$ etc. A schematic representation of the magnetic bio char synthesis using an agricultural waste (Eucalyptus leaves) is shown in Figure 16.2. Figure 16.2 is taken from a published work by Wang *et al.* (Wang *et al.*, 2014) with the permission to reuse it from Elsevier.

Wang *et al.* synthesized a magnetic bio char by this two-step method using Eucalyptus leaves as the biomass waste material. Bio char was prepared by the carbonization of Eucalyptus leaves at $400^\circ C$ for 1 h after drying it at $120^\circ C$. Afterwards, precipitation of iron oxides from $FeCl_3 \cdot 6H_2O$ and $FeSO_4 \cdot 7H_2O$ by the alkaline 10M-NaOH aqueous

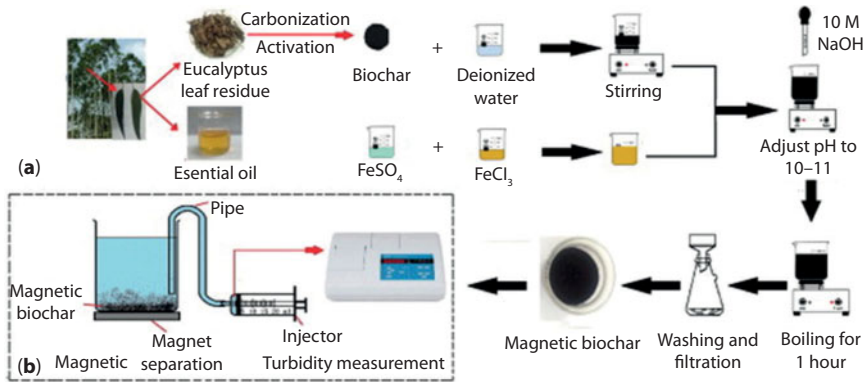


Figure 16.2 Schematic representation of magnetic bio char synthesis from agricultural waste by the chemical precipitation technique (Wang *et al.*, 2014) with permission of Elsevier.

Table 16.2 Bio char sources, reagents and alkaline medium along with the drying conditions to synthesize magnetic bio char using the chemical precipitation technique.

Bio char source	Reagent	Alkaline medium	Heat treatment		Reference
			Temp (°C)	Time (h)	
Coconut powder	CuCl_2 & FeCl_3	NaOH	98–100	2	(Zhang <i>et al.</i> , 2007)
Paper mill sludge	$\text{FeSO}_4 \cdot 7 \text{H}_2\text{O}$	NaBH_4	95	–	(Devi & Saroha, 2014)
Oak wood	FeSO_4 & $\text{Fe}_2(\text{SO}_4)_3$	NaOH	50	overnight	(Mohan <i>et al.</i> , 2014)
Eucalyptus leaves	FeCl_3 & FeSO_4	NaOH	70	12	(Wang <i>et al.</i> , 2015a)
Kans grass	FeCl_3 & FeSO_4	$\text{NH}_3 \cdot \text{H}_2\text{O}$	60	24	(Baig <i>et al.</i> , 2014)
Commercial activated carbon	FeCl_3 & FeSO_4	NaOH	60	24	(Castro <i>et al.</i> , 2009)
Bamboo	$\text{Fe}(\text{NO})$, $\text{Zn}(\text{NO}_3)_2$, $\text{Ni}(\text{NO}_3)_2$	NH_4OH	180	2	(Wu <i>et al.</i> , 2006)
Commercial activated carbon	FeCl_3 & FeSO_4	NaOH	100	3	(Oliveira <i>et al.</i> , 2002)
Commercial activated carbon	$\text{Co}(\text{NO}_3)_2$, $\text{Fe}(\text{NO}_3)_2$	NaOH	80	12	(Ai <i>et al.</i> , 2010)

solution was made. Magnetic bio char was obtained by the heat treatment of the filtrate product at 70 °C for 12 h (Wang *et al.*, 2014). Similar approach was for the synthesis of magnetic bio char have been adopted by different researchers with different combinations of biomass waste, magnetic medium and alkaline to precipitate the iron oxides. Table 16.2 summarizes the details of conversion of biomass waste into magnetic bio char using chemical precipitation method.

Tian *et al.*, (2011) prepared the magnetic wheat straw without converting it to the bio char. The modification of the wheat straw into the magnetic wheat straw was done by the *in-situ* chemical co-precipitation of iron oxides from FeCl_3 and FeSO_4 by $\text{NH}_3 \cdot \text{H}_2\text{O}$ followed by the heat treatment of the filtrate at 70 °C for 4 h on the non-heat treated wheat straw. As mentioned earlier a number of agricultural waste materials have been tested for their suitability as a magnetic bio char material. We have summarized the material and process conditions involved in the synthesis of magnetic bio char in Table 16.2. Table 16.2 describes the various bio char sources used for the synthesis of magnetic bio char, reagents and alkaline medium used to precipitate iron oxide along with the drying conditions.

16.3.2.3 *Synthesis of Magnetic Bio Char by High Temperature Treatment of Agriculture Waste Char/Activated Carbon*

In another approach to produce magnetic bio char is based on the impregnation of iron or nickel salts on the agriculture waste char or activated carbon and then heating this iron or nickel loaded agricultural waste char at a high temperature to get the magnetic bio char. The difference between this method and the previous method, discussed in Section 7.3.2.1 is that in the present technique, the agriculture waste is first converted into bio char before the impregnation with the magnetic medium and then the impregnated bio char is pyrolyzed at high temperature under the inert atmosphere while in the previous method, magnetic medium is impregnated directly on the agriculture waste biomass (not on the bio char) followed by the pyrolysis. Heating temperature and atmosphere required for the heat treatment is depends upon the salts used in the process. It has been observed that the magnetic bio char synthesized at high temperatures, shows a high absorption capacity as compared to their magnetic bio char synthesized at low temperatures which is due to the larger surface area high level of micro porosity developed within the magnetic bio char on the high temperature treatment.

Wang *et al.* dropped a solution of $\text{Ni}(\text{NO}_3)_2 \cdot 6\text{H}_2\text{O}$ into excess NaOH which produced an inorganic liquid system of NaNO_3 , NaOH and $\text{Ni}(\text{OH})_2$. Ethanol solution was added drop by drop to this inorganic liquid system. Thereafter, solvent evaporation was done at 60 °C followed by the carbonization of dried sample at 600 °C to obtain magnetic bio char. In one other approach, rice husk was carbonized by multilevel heating from 400 to 750 °C. The rice husk carbon was modified with HNO_3 at 80 °C for 3 h. This modified rice husk carbon was dispersed in $\text{Fe}(\text{NO}_3)_3$ and dried at 750 °C for 3 h in the presence of nitrogen to enable the formation of nano-particles of Fe_3O_4 (Yang *et al.*, 2008). Few other methods to synthesize the magnetic bio char by the heat treatment of impregnated bio char and activated carbons are described in Table 16.3.

16.3.2.4 *Synthesis of Magnetic Bio Char by Encapsulation using Bio-Polymer*

Another technique that is employed to synthesize the magnetic bio char is the encapsulation of bio char/activated carbon with magnetic particle in the presence of some suitable bio-polymer. Magnetic bio char synthesized by this approach can also be used in medical application such as drug delivery system for the treatment of cancer and other

Table 16.3 Description of the synthesis procedure of magnetic bio char by the heat treatment of impregnated bio char/activated carbon.

Description of method employed	Reference
A solution of $\text{Fe}(\text{NO}_3)_3$ in ethanol was dropped into the activated carbon followed by its drying at 90 °C for 2 h. Ethylene glycol was then impregnated over the dried sample and heat treated under nitrogen environment between 350 °C to 450 °C for 2 h.	(Yang <i>et al.</i> , 2008)
Anthracite coal, coal tar and $\text{Ni}(\text{NO}_3)_2 \cdot 9\text{H}_2\text{O}$ were mixed followed by its extrusion in the cylinders of 1 cm length. These cylinders were carbonized in N_2 atmosphere at 600 °C for 45 min. Samples were heat treated in N_2 atmosphere with heating rate 10 °C/min followed by the steam activation for 3 h.	(Zhang <i>et al.</i> , 2011a)
Chitosan microspheres was initially dried and then immersed in $(\text{NH}_4)_3[\text{Fe}(\text{C}_2\text{O}_4)_3]$ solution for 24 h. Chitosan microspheres were then filtered and dried at 60 °C for 12 h followed by the carbonization of dried $(\text{NH}_4)_3[\text{Fe}(\text{C}_2\text{O}_4)_3]$ treated chitosan microspheres in Ar atmosphere between 700 °C to 1000 °C for 4 h.	(Zhu <i>et al.</i> , 2008)
A solution of $\text{Fe}(\text{NO}_3)_3$ in ethanol was dropped into the activated carbon followed by its drying at 90 °C for 2 h. Dried sample was then impregnated by ethylene glycol. Afterwards, the impregnated activated carbon was heated between 250 °C to 450 °C for 2 h.	(Fuertes & Tartaj, 2006)
$\text{Fe}(\text{NO}_3)_3$ was impregnated over the commercial activated carbon and dried at 90 °C. Filtered sample was heated to 700 °C in the Ar environment followed by the flow of benzene vapor through rating tube and agitation for 30 min in the rotation tube in the argon–benzene flow.	(Schwickardi <i>et al.</i> , 2006)
Powdered coal was mixed to Fe_3O_4 and mixture was compressed to cylinders followed by carbonization at 600 °C for 45 min. The resulting chars were then activated at a temperature from 850 °C to 940 °C in 30 °C increments	(Yang <i>et al.</i> , 2010)
An aqueous solution of sucrose and $\text{Ni}(\text{NO}_3)_2$ was impregnated over the activated carbon and heated at 600 °C for 2 h in the N_2 atmosphere	(Gorria <i>et al.</i> , 2006)

diseases. Recently researchers have synthesized polymer based modified magnetic bio char by the incorporation of bio char and polymer (mostly bio-polymer) into the suitable magnetic medium for different adsorption and medical related applications. Studies on polymer based magnetic bio char have revealed that alginate/polyurethane composite foams have with improved mechanical properties and are highly efficient in selective adsorption of Pb-ions. These bio-polymers having various functionalities, large surface area and porosities are found to be stable in many organic solvents, which make them an apt material for the environment related applications.

The most common polymer used for the synthesis is alginate. Alginate, also called algin or alginic acid and having the chemical formula $(\text{C}_6\text{H}_8\text{O}_6)_n$, is an anionic polysaccharide

distributed widely in the cell walls of brown algae. Alginates are non-branched co-polymer salts having 1 \rightarrow 4 links of β -D-mannuronic acid and α -L-guluronic acids. On reaction with the divalent cations, these alginates produce gels which are thermally irreversible. It has been used for a long time for the biomedical applications as a biomolecule immobilization material. It also can be used as metal chelator since it has been successfully used as chelating agent for poly-hydroxy- or poly-carboxylic acid or a mixture of these two acids (Park *et al.*, 2007). Chitosan is another commonly used bio-polymer for magnetic bio char synthesis. Chitosan is a linear polysaccharide composed of randomly distributed β -linked D-glucosamine and N-acetyl-D-glucosamine. It is a non-toxic polymer and is the most common drug delivery carrier or functional excipient of the active compound being delivered (Ai *et al.*, 2011; Kean & Thanou, 2010). Chitosan contains positively charged ions, since chitosan has a significant amount of free amino groups present in it. The positively charged chitosan reacts with many negative species and makes the formation of chitosan composite microspheres easier. These chitosan composite microspheres can be converted into carbon composite microsphere by their carbonization (Zhu *et al.*, 2008).

Rocher *et al.*, (2008) synthesized the magnetic bio char using alginate bio-polymer. Activated carbon was mixed with sodium alginate and a ferrofluid consisting of maghemite (γ -Fe₂O₃) nanoparticles with the coating of citrate ions dispersed in aqueous solution. The resulting suspension was then added dropwise to calcium chloride (Rocher *et al.*, 2008). Liu *et al.* (2008) in the process of synthesizing magnetic cellulose used immediate dispersion of cellulose into a pre-cooled mixture of NaOH urea and water. The fiber after washing and drying was drawn into FeCl₃ solution. Afterwards, the fiber was treated with NaOH for 20 min to get cellulose/Fe₂O₃ composite (Liu *et al.*, 2008). Luo and Zhang synthesized transparent cellulose bends by an immediate dispersion of wood cellulose into a mixture solution of NaOH/urea/H₂O and then added γ -Fe₂O₃ and a very small amount of activated carbon to this transparent cellulose. NaOH was used as alkaline medium. The filtrate was dried at 75 °C for 2.5 h to obtain the magnetic cellulose (Luo & Zhang, 2009). Few other approaches followed to synthesize magnetic fiber/ polymer based magnetic char is described in Table 16.4.

16.3.2.5 Synthesis of Magnetic Bio Char by Microwave Heating

Heating by using the microwave irradiation has attracted many researchers in the recent past because the microwave can provide heating up to molecular level which is uniform in nature and results in fast thermal reactions (Ania *et al.*, 2007; Liu *et al.*, 2010; Zhang-Steenwinkel *et al.*, 2005). Microwave heating has many advantages over conventional heating; it is more controllable (Kappe, 2004) energy (Gronnow *et al.*, 2005) and cost (Mašek *et al.*, 2013) efficient and hence in many cases it is being considered as a potentially attractive alternative to “conventional” pyrolysis. The thermal conversion of the bio material requires a uniform heating to maintain the overall quality of the bio char. The heating process should also be fast to reduce the production cost. Microwave heating can be used to heat the bio-materials fast and uniformly throughout the bulk. Moreover, microwave heating provides the facility to recycle the carbon which in turn allows it to be reused many times. Microwave heating is seen to increase the surface area and micro and meso pores of carbon which ultimately increase its capacity to adhere more contaminants thus adding to the value of product (Ania *et al.*,

Table 16.4 Descriptions of the synthetization of magnetic bio char by encapsulation technique using bio-polymer.

Description of method employed	Reference
Sudden dispersion of cellulose was made in the pre cooled mixture of NaOH, ure and water. γ -Fe ₂ O ₃ and activated carbon was added to it and NaCl was dropwise added to this suspension. The beads were cross-linked by epichlorohydrin (C ₃ H ₅ ClO) and then heated at 75 °C.	(Luo & Zhang, 2009)
A homogeneous gel of activated charcoal, acrylamide, ferric oxide and methylenebisacrylamide with water, (CH ₃) ₂ NCH ₂ CH ₂ N(CH ₃) ₂ and (NH ₄) ₂ S ₂ O ₈ was formed. The gel was oven dried at 80 °C for overnight. Dried sample was milled to get it in powder form.	(Al-Dujaili <i>et al.</i> , 1979)
Activated carbon, alginate solution and citrate stabilized ferrofluid were mixed. The suspension from the solution was dropped into calcium chloride solution	(Lin <i>et al.</i> , 2005)
Charcoal and magnetically stable ferric oxide were mixed and this mixture was entrapped in a polyacrylamide gel. This combination then passed through lyophilisation followed by particle size reduction through micronisation.	(Dawes & Gardner, 1978)
Sodium alginate solution was mixed to activated carbon and the viscous solution was extruded on calcium chloride followed by allowing the beads to harden and then washing.	(Annadurai <i>et al.</i> , 2002)
Charcoal and BaFe ₂ O ₄ micro particles were mixed with bovine serum albumin solution. This solution was emulsified in n-butanol – castor oil – glutaraldehyde in continuous phase	(Ithakissios & Kubiawicz, 1977)
Solution containing sodium alginate and activated carbon was dropped into CaCl ₂ . The product was then washed and dried at 60 °C overnight. Dried sample was soaked into sodium alginate and treated with CaCl ₂ resulting in the formation of a coating on the surface with alginate gel.	(Park <i>et al.</i> , 2007)

2004). The heat generation mechanism is the main difference between microwave heating devices and conventional heating devices (Ania *et al.*, 2005). In the conventional mode of heating, thermal energy is passed to the material by the heat source located outside the carbon bed through conduction or convection mechanism. When we use conduction or conventional mode of heating, there is always a temperature gradient in the material until the state of thermal equilibrium is achieved. On the other hand, in microwave heating, the microwave radiation penetrates the material and the microwave energy is converted to heat energy. In this way heat is generated throughout the bulk of the material. This can reduce the processing time and the overall quality is improved (Benaddi *et al.*, 2000; Huidobro *et al.*, 2001). Mubarak *et al.* (2014) synthesized a highly porous magnetic bio char using this technique. They used ferric chloride hexahydrate (FeCl₃·6H₂O) solution as the magnetic medium and empty fruit bunch

(EFB) as the biomass based material. $\text{FeCl}_3 \cdot 6\text{H}_2\text{O}$ was impregnated into the powdered EFB in different ratio and mixed properly. Magnetic component loaded EFB was then undergone through the pyrolysis under the specified pyrolysis conditions to get the magnetic bio char. Rather than using the conventional heating, the researchers used the microwave pyrolysis because of many advantages of microwave pyrolysis over the conventional heating.

The factors which affect the properties and performance of the magnetic bio char include the impregnation ratio of magnetic component and the pyrolysis conditions. Mubarak *et al.*, (2014) discussed the effect of process parameters viz. microwave power and radiation time on the properties of synthesized magnetic bio char using microwave pyrolysis and by performing a statistical analysis found an optimum pyrolysis condition for the production of magnetic bio char. The study revealed that the process parameters have a significant role not only on the magnetic bio char yield but also on its properties. In the same study impregnation ration of the magnetic medium also seen to affect the magnetic bio char yield and its properties. Therefore, it is very essential to choose correct pyrolysis parameters and impregnation ratio while producing the magnetic bio char.

16.3.2.6 *Synthesis of Magnetic Bio Char Composites*

Magnetic bio char composites mostly are prepared by iron based oxides but composites materials are also been successfully used to magnetize the bio char. One of the major advantages of magnetic bio char composite is that these materials are tunable to optimize the magnetic properties as per the requirement. Magnetic bio char composites supposed to have certain properties such as the magnetic component in the composite should be chemically stable, inexpensive, easily available and most importantly non-toxic. The bio mass material and magnetic component used to synthesize the magnetic bio char composite must be chemically and physically interactive with each other.

Magnetic properties of magnetic bio char are very important to be known as these will be used to do the regeneration process of these materials. A wide range of magnetic materials have been used to synthesize the magnetic bio char with desired magnetic properties. In the run of finding some material to magnetize the bio char, researchers have found that spinel ferrite which has a general formula AFe_2O_4 ($\text{A} = \text{Mn}, \text{Zn}, \text{Ni}, \text{Co}, \text{Fe}, \text{etc.}$) can be used successfully to serve the purpose. Cobalt ferrite (CoFe_2O_4) having partial inverse spinel structure has been found to have a combination of high anisotropy and moderate saturation magnetization along with tunable coercivity (Harikishore Kumar Reddy & Lee, 2014). Magnetic bio char synthesized from these composites contains the variable valance of iron, which provides a very attractive structural stability and magnetic properties to it. These excellent properties have attracted many researchers to draw their attention to synthesize spinel ferrite based magnetic composites. Insertion of these magnetic composites into the bio char results in the better adsorption performance and improved magnetic properties. Many bio char based ferrite composites have already been synthesized and they have shown a good adsorption ability and found to be effective for

in wastewater treatment. Ai *et al.*, (2011) produced activated carbon/cobalt ferrite/alginate composite beads by an ionic polymerization route. Sodium alginate powder was dissolved in deionized water to form a transparent viscous solution and then activated carbon/cobalt ferrite was added to it. This solution was then dropwise added to CaCl_2 and the magnetic beads were finally washed with distilled water to get magnetic bio char.

A simple route to prepare anatase titania coated magnetic porous carbon was suggested by Ao *et al.* (Ao *et al.*, 2008b). Activated carbon was dried at 90 °C for 2 h after filling it to a solution of $\text{Fe}(\text{NO}_3)_3$ in $\text{CH}_3\text{CH}_2\text{OH}$. Dried sample was then impregnated with $\text{OH}-\text{CH}_2-\text{CH}_2-\text{OH}$ (ethylene glycol) followed by heating between 350 °C to 450 °C for 2 h in N_2 atmosphere. This magnetic activated carbon was then dispersed in titania sols under ultrasonic for 1 h to obtain titania coated magnetic activated carbon. In another work Yan *et al.*, (2015) prepared bio char from slow pyrolysis of rice hull and then by treating it to ferric acetylacetonate synthesized a magnetic bio char. Afterwards they coated this magnetic bio char with ZnS nanocrystals. The synthesized ZnS nanocrystal coated magnetic bio char showed a high degree of Pb(II) adsorption from the water.

Ai *et al.*, (2010) synthesized activated carbon/ CoFe_2O_4 composite by a facile refluxing route in alkaline solution. Solution of $\text{Fe}(\text{NO}_3)_3 \cdot 9\text{H}_2\text{O}$ and $\text{Co}(\text{NO}_3)_2 \cdot 6\text{H}_2\text{O}$ in distilled water was quickly poured in boiling suspension of activated carbon in NaOH solution, followed by heating at 100 °C for 2 h. Magnetic meso pore carbon (MMPC) was synthesized by Kondo *et al.*, (2010) from coconut shell activated carbon by impregnating it with $\text{Fe}(\text{NO}_3)_3$ solution and heating the product at 800 °C for 1 h. In an alternative procedure $\text{Fe}(\text{NO}_3)_3$, $\text{Zn}(\text{NO}_3)_2$ and $\text{Fe}(\text{NO}_3)_2$ were mixed in aqueous ammonia and then the mixture was mixed into bamboo charcoal and followed by the heat treatment at 180 °C for 2 h (Wu *et al.*, 2006).

16.4 Characteristics of Magnetic Bio Char

A number of researchers have synthesized and characterized the magnetic bio char. Magnetic bio char basically is a bio char material which has been magnetized using one of the existing techniques. Like bio char magnetic bio char also mostly is composed of carbon. The carbon content of magnetic bio char has been reported in much literature and it has been found to vary in the range of 55% to 70%. Although for the adsorption purpose high carbon percentage is not as important as high surface area properties, still more carbon content in magnetic bio char is desirable because it gives stability to the material. Carbon percentage in magnetic oak wood char and magnetic oak bark char have been found to be 56.14% and 69.02% respectively (Mohan *et al.*, 2014). A very low carbon percentage (10.28%) was observed in a magnetic bio char synthesized by EFB (Mubarak *et al.*, 2014).

Among different analyzed properties of magnetic bio char, the main characteristics on which the performance of the magnetic bio char hugely depends are their surface area properties and the magnetic properties. The following section discusses these characteristics one by one.

16.4.1 Surface Area Characteristics

Magnetic bio char is generally a highly porous material with high surface area and large pore volume. The surface characteristics of magnetic bio char depend upon many factors such as agricultural waste material which has been selected to synthesize the material, synthesis technique and the chemical and thermal treatment through which the material goes. The BET surface area of magnetic bio char is one of the most important property as it mostly is used for the adsorption of different kinds of metals or organic or non-organic chemicals. Higher BET surface area of the magnetic char is appreciated. Mubarak *et al.*, (2014) reported that BET surface area of the magnetic bio char depends upon the process parameters during its synthesis. A sharp increase in the BET surface area of magnetic bio char (from 250 m²/g to 890 m²/g) synthesized from the EFB was reported on increasing the microwave power from 600 W to 900 W while with the same microwave power range pore volume was reported to increase from 0.25 cm³/g to 0.68 cm³/g. Further increase in the microwave power reduced the BET surface area as well as pore volume of the magnetic bio char.

Since the iron oxide is less porous than activated carbon so the increase in the magnetic content, generally reduce the BET surface area of the magnetic bio char. Oliveira *et al.*, (2002) reported that the BET surface area and total pore volume of activated carbon based magnetic bio char to be 658 m²/g and 0.172 cm³/g while for untreated activated carbon these values were 933 m²/g and 0.264 cm³/g respectively.

Although much literature is available that suggests that the incorporation of magnetic particles in the bio char or activated carbon results in the lowering of BET surface area and pore volume, but few reports are available that claim that introduction of magnetic medium to activated carbon improves the BET surface area and total pore volume. In a typical example Nguyen *et al.*, (2011) reported that BET surface area and total pore volume of Fe₃O₄-activated carbon was observed to be 999.68 m²/g and 1.036 cm³/g while these values for the parent activated carbon were 999.53 m²/g and 1.004 cm³/g respectively. In another work Mohan *et al.*, (2014) reported a reduction in BET surface area of magnetic oak bark char from 25.4 m²/g to 8.8 m²/g on treating with magnetic medium. Although in the same published research work the BET surface area of magnetic wood bio char have been reported to increase its BET surface area from 2.04 m²/g to 6.1 m²/g.

Much research show a very high BET surface area and pore volume for the magnetic bio char materials, however very low BET surface area and pore volume for magnetic oak wood char (6.1 m²/g and 0.59 cm³/g) and magnetic oak bark char (8.8 m²/g and 0.81 cm³/g) was reported by Mohan *et al.*, (Mohan *et al.*, 2014). The authors claim that even the BET surface area and pore volumes of the synthesized magnetic bio char not very high still the adsorption capacity is more/ comparable to the many other bio char materials. As the magnetic bio char adsorb more metal ions per unit surface area as compared to un-magnetized bio char so magnetic bio char even with the low BET surface area and total pore volume can show high adsorption capacities. Bio char swelling in water is the main reason for the high metal ion remediation by the magnetic bio char. When these magnetic bio char are kept in solution they takes up the water from it and open up more pores or adsorption site which

were not available in BET surface area measurement when it was dry thus enhancing the adsorption capacity even with low BET surface properties (Mohan *et al.*, 2011; Mohan *et al.*, 2012).

16.4.2 Magnetic Characteristics

Magnetic properties determine the behavior of magnetic materials. The stability of the magnetic materials is represented by hysteresis loop, which is a curve of magnetization plotted against the magnetic field. This curve gives the saturation magnetization (M_s) magnetic coercivity (H_c) as well as the remnant magnetization (M_r) value of the material. These properties are very important while utilizing these materials in adsorption or drug delivery applications. Generally these properties are expected to be optimized for a better performance of the magnetic material for the efficient and effective regeneration process. Also, the optimized magnetic properties will ensure the better performance of magnetic material in drug delivery applications. The magnetization is dependent upon the type and the nature of the bio char which has been used to synthesize the magnetic bio char (Mohan *et al.*, 2014).

The lower H_c values of the magnetic bio char the more advantageous for the adsorption applications because the lower H_c value of magnetic bio char imply that they can be separated easily by a magnet or an applied magnetic field. Moreover, the low remnant magnetization values of the magnetic bio char are required for their re-dispersion in the solution after separation process is over (Nguyen *et al.*, 2011). The high value of saturation magnetization indicates that the material has more capability to carry the magnetic behavior within it, which is required for targeted drug delivery carrier materials. Saturation magnetization (M_s), coercive field (H_c) and remnant magnetization (M_r) of few magnetic bio char materials are listed in Table 16.5.

Table 16.5 Saturation magnetization, coercive field and remnant magnetization of magnetic bio char materials.

Material	(M_s) emu/g	(M_r) emu/g	(H_c) Oe	Reference
Fe ₃ O ₄ -activated carbon	6.2	1.1	108	(Nguyen <i>et al.</i> , 2011)
Fe ₂ MnO ₄ -activated carbon	6.2	0.85	108	(Nguyen <i>et al.</i> , 2011)
Titania coated γ -Fe ₃ O ₄ -activated carbon	40.23	2.32	45.27	(Ao <i>et al.</i> , 2008a)
Rice husk based based magnetic bio char	2.78	–	–	(Yang <i>et al.</i> , 2008)
Magnetic activated carbon	9.5	0.2	1.75	(Ao <i>et al.</i> , 2009)
Titania coated magnetic activated carbon	6.45	0.17	12.55	(Ao <i>et al.</i> , 2009)
iron oxide based CNT magnetic composite	27.2	0.87	48	(Ma <i>et al.</i> , 2013)
Activated carbon/CoFe ₂ O ₄ composite	7.6	1.4	–	(Ai <i>et al.</i> , 2010)

16.5 Applications of Magnetic Bio Char

Different types of agricultural waste materials are being processed for their better utilization in different sectors mainly due to their abundance and low cost (Thakur *et al.*, 2014b; Voicu *et al.*, 2016). Moreover, the use of these waste materials helps in the reduction of greenhouse gasses and other harmful emissions (Thakur *et al.*, 2013b; Thakur *et al.*, 2013d; Wu *et al.*, 2016). Synthesis of magnetic bio char or magnetic activated carbon has recently become a focus in the activated carbon industry, metallurgy, environmental, agriculture, chemical, and pharmaceutical areas. The intrinsic properties of magnetic bio char advocates it for its suitability in wastewater treatment include porous structure, high surface area. Moreover, the presence of various abundant functional groups can also be considered to be an extra advantage of magnetic bio char. Although, due to the high carbon content it can sequester the carbon in the soil for a very long time and it can reduce the rate of degradation of nutrients from the soil, most of the researchers are more attracted towards the high adsorption capacity of it (Thakur *et al.*, 2013c). Activated carbons are known to be very effective adsorbents. Magnetically treated agricultural wastes usually exhibit high adsorption not only for various kinds of organic compounds, noble and heavy metals but it has been successfully used for the adsorption of radionuclides and xenobiotics (Safarik *et al.*, 2011). It has shown a high degree of adsorption of different metals and other pollutants. Pb (II), Cd²⁺, Zn, As and many other harmful heavy metals have been successfully and effectively removed from the water using magnetic bio char. As we have discussed earlier the ability to recapture the magnetic bio char from the aqueous solution makes it more environment friendly and its ability to be re-used improves the cost efficiency.

Activated carbon/iron oxide magnetic composites for the adsorption of contaminants in water show no serious reduction in the BET surface area or in the porosity of the activated carbon due to the presence of the iron oxides in the composite was noticed. The composites have showed improved adsorption capacities for phenol, chloroform, chlorobenzene and drimaren red dye in aqueous solution and, more importantly, after the regeneration, no reduction in adsorption capacity was observed (Oliveira *et al.*, 2002). Moreover, when the magnetic bio char is synthesized with the nano-iron oxide particles, these iron nano-particles present in the magnetic bio char can also generate free radicals by the reaction with peroxides. These free radicals are toxic to the microorganisms, which enables the magnetic bio char to be used as disinfectants in the water purification industry and could be additional value added by-product from biorefineries (Battin *et al.*, 2009).

The carbon microspheres in the magnetic bio char actually combine the advantages of larger surface area and good magnetic reparability in the magnetic bio char. Magnetic carbon with porous microspheres show excellent adsorption capacity for phenol and nitrobenzene as model pollutants. Moreover, the phenol and the nitrobenzene that has been adsorbed by magnetic activated carbon or magnetic bio char can be effectively released, which is the additional advantage with the magnetic bio char. Generally, powdered magnetic bio char has higher removal efficiency in practical industrial applications. Nowadays, polymeric adsorbents containing superparamagnetic nano magnets are used for the magnetic separation of bio-compounds, and they have also proved to be a cost-effective way of removing transuranic elements from nuclear waste streams. A suitable polymer and activated carbon/bio char combined with iron oxides can extend its functionality (Ai *et al.*, 2011).

A recent study by Rocher *et al.*, (2008) developed a clean and safe process for the water treatment by synthesizing a low cost adsorbent using activated carbon mixed with alginate beads containing and magnetic iron oxide nanoparticles. $\text{Cu}_2\text{Fe}_2\text{O}_4$ -activated carbon composite particles have been found to successfully speed up the pyrolysis process of the adsorbed dye. Besides, almost all the adsorption capacity was regained after the regeneration process implying that this activated carbon based magnetic composite can be used for many cycles very effectively (Zhang *et al.*, 2007).

The use of bio-polymers, which are the bio-degradable polymers, in the biomedical applications is not new (Thakur *et al.*, 2014d; Thakur *et al.*, 2014e). These bio-polymers can be produced by the natural fibres like starch, cellulose and sugar. These bio-polymers have a wide range of potential uses in biomedical field because these have a better biocompatibility and non-toxic behaviour (Pappu *et al.*, 2015; Thakur & Thakur, 2014).

Due to their bio-degradability characteristic these bio-polymers have extensively been studied and afterwards successfully used in the tissue engineering (Thakur *et al.*, 2013e; Thakur *et al.*, 2013f). Biomedical engineers/scientists have successfully developed techniques to grow real skin cells by the use of the living cell and the carrier bio-polymer (Thakur *et al.*, 2012b). This application of bio-polymers can be seen as of huge importance for the treatment of the burning and for the defects appearing after the removal of tumour.

The organic matter present in the bio-polymers allows a smooth and proper reaction functioning of the body on the insertion of these bio-polymers in the body. Other than this bio-polymer can easily be used in medical applications because of their non-immunogenicity, and non-antigenicity to active proteins or cells (Thakur *et al.*, 2014c). Moreover the bio-polymers have another advantage as they have ability to control the cell membrane by suppressing the nonspecific uptake of nanomaterial in a cell (Thakur *et al.*, 2013a). The drug delivery through these bio-polymers has been used by the biomedical researchers for a long time. These bio-polymers are not harmful for the body and the human body also response to these materials quickly. However, it was really a difficult task for the biomedical engineers to take the drug to exactly the place where it is required. This difficulty was resolved by the introduction of magnetic biochar into the picture.

The contribution of agricultural waste material in medical science is studied for a long time (Sindhu *et al.*, 2014) and magnetic bio char in the biomechanical engineering and medicine is also growing. Magnetic drug delivery has attracted many biomedical scientists and researchers from a long time. In 1970 the idea of magnetic drug delivery was surfaced and these materials are playing a very important role in it. The main idea in magnetic drug delivery concept is to infuse the drug into the body which is bound or entrapped in a magnetically responsive compound. Once the drug along with the magnetic medium is injected into the body, it can be guided precisely to the target site by the means of external magnetic field produced by a magnetic gradient generator. In this technique, magnetically controlled drug carriers (magnetic bio char and bio-polymer combination) adsorb the medicine and other required chemicals to the selected target area very precisely and then they release the adsorbed medicine or chemical. This technique has been found to be very useful especially in the treatment of cancer (Rocher *et al.*, 2008). One other application of magnetic bio char is its utilization in the radioimmunoassay (RIA), which is a method to measure the small amount of substances in the blood including polypeptide hormones, steroids, digoxin and progesterone (Safarik *et al.*, 2012).

In another approach a magnetite micro-particles using epoxy resin and coated with activated carbon were synthesized for their utilization as adhesive employing a new method for covering the magnetic particles with a stable non-porous layer of a material and used it successfully as a carrier for the immobilization of *Saccharomyces cerevisiae* cells (Al-Hassan *et al.*, 1991).

16.6 Challenges and Future Scope of Magnetic Bio Char

Magnetic bio char with high porosity and optimized magnetic properties has gained a lot of attention in the recent past. New techniques to synthesize the magnetic bio char are tried and tested. Although magnetic bio char has successfully addressed most of the challenges faced by bio char, still, a scope of improvements is required to find new techniques that can make magnetic bio char synthesis more economic. Other than this, when the magnetic medium is doped in the bio char, the magnetic medium sometimes sits in the pores of the bio char and eats up some adsorption sites which in turn reduces the porosity and BET surface area of the magnetized bio char. Its degradability can also help in its utilization in soil improvement related applications by the sequestration of carbon. High pore size of magnetic bio char may adsorb the nutrients from the soil and may lower the rate of degradation of these nutrients from the soil resulting in the improvement in the fertility of the soil. Since magnetic bio char is a magnetic material, with properly optimized magnetic properties it can have a wide range of applications such as it can be used in bio-sensors. Many researchers are working on the magnetic bio char for its better utilization in medical science. Future research is based on the development of a new magnetic bio char materials that are more controllable and easy to guide to make the drug delivery system more efficient. Researchers are also working to develop magnetic bio char based drug carrier which, after delivering the chemical at the target area, degrade itself into the components and add into the existing chemicals in the body.

16.7 Summary

Magnetic bio char is a relatively new material which is a magnetic medium filled bio char material which is readily used in heavy metal removal, selective adsorption of chemicals and organic compounds from a solution. The beauty of the magnetic bio char lies in the fact that once the adsorption process is over, it is easy to separate it from the aqueous solution and can be re-used after some processing, thus making the adsorption process more environment friendly as well as economically viable.

Many researchers have shown their keen interest in synthesizing magnetic bio char applying different techniques. There are basically four main techniques to synthesize magnetic bio char. In first technique the magnetic medium is impregnated over the agricultural waste and then the magnetically impregnated agricultural waste is passed through pyrolysis (either microwave or fast) process. The second technique does the same thing in reverse order. The agricultural waste is first converted into bio char by pyrolysis followed by the chemical precipitation of ferrous or ferric salts on

the obtained bio char by some alkaline medium (mostly NaOH) to get the magnetic bio char. Generally iron based magnetic medium solution (FeSO_4 or FeCl_3) are used for the chemical precipitation but cobalt, copper or nickel based magnetic solutions have also been used frequently. Next technique uses the high temperature to prepare the magnetic bio char. Iron or nickel particles are impregnated over the synthesized agriculture waste bio char and this magnetic particle loaded agriculture waste bio char is heated to a high temperature in specific atmosphere. Required atmosphere and temperature depends upon the combination of the agriculture waste and the salts used in the synthesizing process. One another method to prepare magnetic bio char is the encapsulation of bio char with some magnetic particle in the presence of some suitable bio-polymer. Use of bio-polymer in the magnetic bio char opens the door for the magnetic bio char to be used in the area of biomechanical engineering and medicine. Alginate and chitosan are two most commonly used bio-polymers in the synthesis of magnetic bio char because of their excellent biocompatibility and non-toxicity.

Magnetic bio chars composite materials are also studied and discussed widely and becoming popular day by day because of their wide range of applications, due to the flexibility of optimization of their properties. Because of their variable valance of iron magnetic bio char composites exhibit excellent magnetic properties and structural stability. Spinel ferrite with chemical formula AFe_2O_4 with A being Zn, Mn, Fe, Co, Ni etc. are employed to magnetize the bio char material. Within the spinel ferrite family, cobalt ferrite (CoFe_2O_4) and nickel ferrite (NiFe_2O_4) have been investigated extensively tunable coercivity, moderate saturation magnetization and large anisotropy.

Generally the magnetic bio char offer a high value of BET surface area and total pore volume except few exceptions. Although even with the small BET surface area a moderate to high adsorption capacity have been reported which is due to the fact that magnetized bio char can adsorb more metal ions per unit surface area. Additionally, these materials imbibe water resulting in opening up of the adsorption sites. Low coercive field and remnant magnetization values are considered to be better for the magnetic bio char materials as these will lead to ease in the separation from the aqueous solution after the adsorption, and ensure the re-dispensability after the regeneration process is over, respectively. High saturation magnetization is also desirable from the magnetic bio char material. Different magnetic bio char materials have successfully synthesized satisfied these magnetic criterion.

Magnetic bio char has a tremendous scope for its utilization in water treatment. It can easily adsorb heavy metals such as Pb, As, Cd, Zn, Cr etc. from from the solution. Moreover, various organic compounds like phenol, tetracycline have also been removed using adsorption technique from magnetic bio char. Selective adsorption through magnetic char widens the domain of the applicability of magnetic bio char in chemical, textile and water purification applications. Since magnetic bio char can be regenerated and can be re-used after the adsorption, it makes the adsorption of heavy metals and different kind chemicals more environment-friendly as well as cost effective. Bio-polymer based magnetic bio char nowadays are successfully used as drug carriers in the magnetic drug delivery system in which the drug carriers adsorb the medicine or chemicals and then these magnetically controlled drug carriers take the medicine

or chemicals to the target area very accurately. These techniques are widely used in the treatment of cancer or other diseases.

Magnetic bio char is relatively a new material and researchers are working to develop more efficient and economical synthesizing techniques. Although magnetic bio char has sufficiently high adsorption capacity still reduction in the adsorption sites of bio char on doping with the magnetic particles is a challenge needed to be addressed. Magnetic bio char has more potential in medical applications where the researchers are trying to develop new magnetic bio char based drug carrier with more adsorption capacity and better control. Due to its magnetic nature magnetic bio char based material can also be synthesized (with some necessary modifications) to be used in bio-sensors.

Acknowledgement

This research is financially supported by University of Malaya, Ministry of Higher Education High Impact Research (UM.C/HIR/MOHE/ENG/20) and Exploratory Research Grant Scheme (ERGS: ER013-2013A).

References

- Achak, M., Hafidi, A., Ouazzani, N., Sayadi, S., Mandi, L. Low cost biosorbent “banana peel” for the removal of phenolic compounds from olive mill wastewater: Kinetic and equilibrium studies. *Journal of Hazardous Materials*, 166(1), 117–125, 2009.
- Adams, C., Watson, T. Treatability of s -Triazine Herbicide Metabolites Using Powdered Activated Carbon. *Journal of Environmental Engineering*, 122(4), 327–330, 1996.
- Ai, L., Huang, H., Chen, Z., Wei, X., Jiang, J. Activated carbon/CoFe₂O₄ composites: Facile synthesis, magnetic performance and their potential application for the removal of malachite green from water. *Chemical Engineering Journal*, 156(2), 243–249, 2010.
- Ai, L., Li, M., Li, L. Adsorption of Methylene Blue from Aqueous Solution with Activated Carbon/Cobalt Ferrite/Alginate Composite Beads: Kinetics, Isotherms, and Thermodynamics. *Journal of Chemical & Engineering Data*, 56(8), 3475–3483, 2011.
- Al-Dujaili, E., Forrest, G., Edwards, C., Landon, J. Evaluation and application of magnetizable charcoal for separation in radioimmunoassays. *Clinical chemistry*, 25(8), 1402–1405, 1979.
- Al-Hassan, Z., Ivanova, V., Dobрева, E., Penchev, I., Hristov, J., Rachev, R., Petrov, R. Non-porous magnetic supports for cell immobilization. *Journal of Fermentation and Bioengineering*, 71(2), 114–117, 1991.
- Ania, C.O., Menéndez, J.A., Parra, J.B., Pis, J.J. Microwave-induced regeneration of activated carbons polluted with phenol. A comparison with conventional thermal regeneration. *Carbon*, 42(7), 1383–1387, 2004.
- Ania, C.O., Parra, J.B., Menéndez, J.A., Pis, J.J. Effect of microwave and conventional regeneration on the microporous and mesoporous network and on the adsorptive capacity of activated carbons. *Microporous and Mesoporous Materials*, 85(1–2), 7–15, 2005.
- Ania, C.O., Parra, J.B., Menéndez, J.A., Pis, J.J. Microwave-assisted regeneration of activated carbons loaded with pharmaceuticals. *Water Research*, 41(15), 3299–3306, 2007.
- Annadurai, G., Juang, R.-S., Lee, D.-J. Factorial design analysis for adsorption of dye on activated carbon beads incorporated with calcium alginate. *Advances in Environmental Research*, 6(2), 191–198, 2002.

- Ao, Y., Xu, J., Fu, D., Shen, X., Yuan, C. A novel magnetically separable composite photocatalyst: Titania-coated magnetic activated carbon. *Separation and Purification Technology*, 61(3), 436–441, 2008a.
- Ao, Y., Xu, J., Fu, D., Yuan, C. Photocatalytic degradation of X-3B by titania-coated magnetic activated carbon under UV and visible irradiation. *Journal of Alloys and Compounds*, 471(1–2), 33–38, 2009.
- Ao, Y., Xu, J., Fu, D., Yuan, C. A simple route for the preparation of anatase titania-coated magnetic porous carbons with enhanced photocatalytic activity. *Carbon*, 46(4), 596–603, 2008b.
- Badillo-Almaraz, V., Trocellier, P., Dávila-Rangel, I. Adsorption of aqueous Zn(II) species on synthetic zeolites. *Nuclear Instruments and Methods in Physics Research Section B: Beam Interactions with Materials and Atoms*, 210, 424–428, 2003.
- Baig, S.A., Zhu, J., Muhammad, N., Sheng, T., Xu, X. Effect of synthesis methods on magnetic Kans grass biochar for enhanced As(III, V) adsorption from aqueous solutions. *Biomass and Bioenergy*, 71, 299–310, 2014.
- Battin, T.J., Kammer, F.v.d., Weilhartner, A., Ottofuelling, S., Hofmann, T. Nanostructured TiO₂: Transport Behavior and Effects on Aquatic Microbial Communities under Environmental Conditions. *Environmental Science & Technology*, 43(21), 8098–8104, 2009.
- Benaddi, H., Bandosz, T.J., Jagiello, J., Schwarz, J.A., Rouzaud, J.N., Legras, D., Béguin, F. Surface functionality and porosity of activated carbons obtained from chemical activation of wood. *Carbon*, 38(5), 669–674, 2000.
- Benaïssa, H., Elouchdi, M.A. Removal of copper ions from aqueous solutions by dried sunflower leaves. *Chemical Engineering and Processing: Process Intensification*, 46(7), 614–622, 2007.
- Cao, F., Yin, P., Liu, X., Liu, C., Qu, R. Mercury adsorption from fuel ethanol onto phosphonated silica gel prepared by heterogenous method. *Renewable Energy*, 71, 61–68, 2014.
- Castro, C.S., Guerreiro, M.C., Gonçalves, M., Oliveira, L.C.A., Anastácio, A.S. Activated carbon/iron oxide composites for the removal of atrazine from aqueous medium. *Journal of Hazardous Materials*, 164(2–3), 609–614, 2009.
- Chen, B., Chen, Z., Lv, S. A novel magnetic biochar efficiently sorbs organic pollutants and phosphate. *Bioresource Technology*, 102(2), 716–723, 2011.
- Dawes, C., Gardner, J. Radioimmunoassay of digoxin employing charcoal entrapped in magnetic polyacrylamide particles. *Clinica Chimica Acta*, 86(3), 353–356, 1978.
- DeLuca, T.H., MacKenzie, M.D., Gundale, M.J. *Biochar effects on soil nutrient transformations*, 2009.
- Devi, P., Saroha, A.K. Synthesis of the magnetic biochar composites for use as an adsorbent for the removal of pentachlorophenol from the effluent. *Bioresource Technology*, 169, 525–531, 2014.
- Di Natale, F., Erto, A., Lancia, A. Desorption of arsenic from exhaust activated carbons used for water purification. *Journal of Hazardous Materials*, 260, 451–458, 2013.
- Fuertes, A.B., Tartaj, P. A Facile Route for the Preparation of Superparamagnetic Porous Carbons. *Chemistry of Materials*, 18(6), 1675–1679, 2006.
- Gorria, P., Sevilla, M., Blanco, J.A., Fuertes, A.B. Synthesis of magnetically separable adsorbents through the incorporation of protected nickel nanoparticles in an activated carbon. *Carbon*, 44(10), 1954–1957, 2006.
- Gronnow, M.J., White, R.J., Clark, J.H., Macquarrie, D.J. Energy Efficiency in Chemical Reactions: A Comparative Study of Different Reaction Techniques. *Organic Process Research & Development*, 9(4), 516–518, 2005.
- Harikishore Kumar Reddy, D., Lee, S.-M. Magnetic biochar composite: Facile synthesis, characterization, and application for heavy metal removal. *Colloids and Surfaces A: Physicochemical and Engineering Aspects*, 454, 96–103, 2014.
- Huidobro, A., Pastor, A.C., Rodriguez-Reinoso, F. Preparation of activated carbon cloth from viscous rayon: Part IV. Chemical activation. *Carbon*, 39(3), 389–398, 2001.

- Ithakissios, D., Kubiawicz, D. Use of protein containing magnetic microparticles in radioassays. *Clinical chemistry*, 23(11), 2072–2079, 1977.
- Kappe, C.O. Controlled Microwave Heating in Modern Organic Synthesis. *Angewandte Chemie International Edition*, 43(46), 6250–6284, 2004.
- Kean, T., Thanou, M. Biodegradation, biodistribution and toxicity of chitosan. *Advanced Drug Delivery Reviews*, 62(1), 3–11, 2010.
- Khoramzadeh, E., Nasernejad, B., Halladj, R. Mercury biosorption from aqueous solutions by Sugarcane Bagasse. *Journal of the Taiwan Institute of Chemical Engineers*, 44(2), 266–269, 2013.
- Kondo, K., Jin, T., Miura, O. Removal of less biodegradable dissolved organic matters in water by superconducting magnetic separation with magnetic mesoporous carbon. *Physica C: Superconductivity*, 470(20), 1808–1811, 2010.
- Li, W., Peng, J., Zhang, L., Yang, K., Xia, H., Zhang, S., Guo, S.-h. Preparation of activated carbon from coconut shell chars in pilot-scale microwave heating equipment at 60 kW. *Waste Management*, 29(2), 756–760, 2009.
- Lim, S.-F., Zheng, Y.-M., Chen, J.P. Organic arsenic adsorption onto a magnetic sorbent. *Langmuir*, 25(9), 4973–4978, 2009.
- Lin, Y.-B., Fugetsu, B., Terui, N., Tanaka, S. Removal of organic compounds by alginate gel beads with entrapped activated carbon. *Journal of Hazardous Materials*, 120(1–3), 237–241, 2005.
- Liu, Q.-S., Zheng, T., Wang, P., Guo, L. Preparation and characterization of activated carbon from bamboo by microwave-induced phosphoric acid activation. *Industrial Crops and Products*, 31(2), 233–238, 2010.
- Liu, S., Zhang, L., Zhou, J., Xiang, J., Sun, J., Guan, J. Fiberlike Fe_2O_3 Macroporous Nanomaterials Fabricated by Calcinating Regenerate Cellulose Composite Fibers. *Chemistry of Materials*, 20(11), 3623–3628, 2008.
- López de Arroyabe Loyo, R., Nikitenko, S.I., Scheinost, A.C., Simonoff, M. Immobilization of selenite on Fe_3O_4 and Fe/Fe₃C ultrasmall particles. *Environmental science & technology*, 42(7), 2451–2456, 2008.
- Luo, X., Zhang, L. High effective adsorption of organic dyes on magnetic cellulose beads entrapping activated carbon. *Journal of Hazardous Materials*, 171(1–3), 340–347, 2009.
- Ma, J., Zhu, Z., Chen, B., Yang, M., Zhou, H., Li, C., Yu, F., Chen, J. One-pot, large-scale synthesis of magnetic activated carbon nanotubes and their applications for arsenic removal. *Journal of Materials Chemistry A*, 1(15), 4662–4666, 2013.
- Mahmoodi, N.M., Hayati, B., Arami, M., Lan, C. Adsorption of textile dyes on Pine Cone from colored wastewater: Kinetic, equilibrium and thermodynamic studies. *Desalination*, 268(1–3), 117–125, 2011.
- Mašek, O., Budarin, V., Gronnow, M., Crombie, K., Brownsort, P., Fitzpatrick, E., Hurst, P. Microwave and slow pyrolysis biochar—Comparison of physical and functional properties. *Journal of Analytical and Applied Pyrolysis*, 100, 41–48, 2013.
- Mohan, D., Kumar, H., Sarswat, A., Alexandre-Franco, M., Pittman Jr, C.U. Cadmium and lead remediation using magnetic oak wood and oak bark fast pyrolysis bio-chars. *Chemical Engineering Journal*, 236(0), 513–528, 2014.
- Mohan, D., Rajput, S., Singh, V.K., Steele, P.H., Pittman Jr, C.U. Modeling and evaluation of chromium remediation from water using low cost bio-char, a green adsorbent. *Journal of Hazardous Materials*, 188(1–3), 319–333, 2011.
- Mohan, D., Sharma, R., Singh, V.K., Steele, P., Pittman, C.U. Fluoride Removal from Water using Bio-Char, a Green Waste, Low-Cost Adsorbent: Equilibrium Uptake and Sorption Dynamics Modeling. *Industrial & Engineering Chemistry Research*, 51(2), 900–914, 2012.
- Mohan, D., Singh, P., Sarswat, A., Steele, P.H., Pittman Jr, C.U. Lead sorptive removal using magnetic and nonmagnetic fast pyrolysis energy cane biochars. *Journal of Colloid and Interface Science*, 448, 238–250, 2015.

- Mubarak, N.M., Alicia, R.F., Abdullah, E.C., Sahu, J.N., Haslija, A.B.A., Tan, J. Statistical optimization and kinetic studies on removal of Zn^{2+} using functionalized carbon nanotubes and magnetic biochar. *Journal of Environmental Chemical Engineering*, 1(3), 486–495, 2013.
- Mubarak, N.M., Kundu, A., Sahu, J.N., Abdullah, E.C., Jayakumar, N.S. Synthesis of palm oil empty fruit bunch magnetic pyrolytic char impregnating with FeCl_3 by microwave heating technique. *Biomass and Bioenergy*, 61, 265–275, 2014.
- Nguyen, T.D., Phan, N.H., Do, M.H., Ngo, K.T. Magnetic Fe_2MO_4 (M:Fe, Mn) activated carbons: Fabrication, characterization and heterogeneous Fenton oxidation of methyl orange. *Journal of Hazardous Materials*, 185(2–3), 653–661, 2011.
- Nizamuddin, S., Mubarak, N.M., Tiripathi, M., Jayakumar, N.S., Sahu, J.N., Ganesan, P. Chemical, dielectric and structural characterization of optimized hydrochar produced from hydrothermal carbonization of palm shell. *Fuel*, 163, 88–97, 2016.
- Oliveira, L.C.A., Rios, R.V.R.A., Fabris, J.D., Garg, V., Sapag, K., Lago, R.M. Activated carbon/iron oxide magnetic composites for the adsorption of contaminants in water. *Carbon*, 40(12), 2177–2183, 2002.
- Pappu, A., Patil, V., Jain, S., Mahindrakar, A., Haque, R., Thakur, V.K. Advances in industrial prospective of cellulosic macromolecules enriched banana biofibre resources: A review. *International Journal of Biological Macromolecules*, 79, 449–458, 2015.
- Park, H.G., Kim, T.W., Chae, M.Y., Yoo, I.-K. Activated carbon-containing alginate adsorbent for the simultaneous removal of heavy metals and toxic organics. *Process Biochemistry*, 42(10), 1371–1377, 2007.
- Rocher, V., Siaugue, J.-M., Cabuil, V., Bee, A. Removal of organic dyes by magnetic alginate beads. *Water Research*, 42(4–5), 1290–1298, 2008.
- Ruthiraan, M., Mubarak, N.M., Thines, R.K., Abdullah, E.C., Sahu, J.N., Jayakumar, N.S., Ganesan, P. Comparative kinetic study of functionalized carbon nanotubes and magnetic biochar for removal of Cd^{2+} ions from wastewater. *Korean Journal of Chemical Engineering*, 32(3), 446–457, 2015.
- Safarik, I., Horska, K., Pospiskova, K., Safarikova, M. Magnetically Responsive Activated Carbons for Bio- and Environmental Applications. *International Review of Chemical Engineering*, 4(3), 346–352, 2012.
- Safarik, I., Horska, K., Safarikova, M. Magnetically responsive biocomposites for inorganic and organic xenobiotics removal. in: *Microbial biosorption of metals*, Springer, pp. 301–320, 2011.
- Schwickardi, M., Olejnik, S., Salabas, E.-L., Schmidt, W., Schuth, F. Scalable synthesis of activated carbon with superparamagnetic properties. *Chemical Communications*(38), 3987–3989, 2006.
- Sindhu, K.A., Prasanth, R., Thakur, V.K. Medical Applications of Cellulose and its Derivatives: Present and Future. in: *Nanocellulose Polymer Nanocomposites*, John Wiley & Sons, Inc., pp. 437–477, 2014.
- Sun, P., Hui, C., Azim Khan, R., Du, J., Zhang, Q., Zhao, Y.-H. Efficient removal of crystal violet using Fe_3O_4 -coated biochar: the role of the Fe_3O_4 nanoparticles and modeling study their adsorption behavior. *Scientific Reports*, 5, 12638, 2015.
- Thakur, M.K., Gupta, R.K., Thakur, V.K. Surface modification of cellulose using silane coupling agent. *Carbohydrate Polymers*, 111, 849–855, 2014a.
- Thakur, V.K. *Green composites from natural resources*. CRC Press, 2013.
- Thakur, V.K., Grewell, D., Thunga, M., Kessler, M.R. Novel Composites from Eco-Friendly Soy Flour/SBS Triblock Copolymer. *Macromolecular Materials and Engineering*, 299(8), 953–958, 2014b.
- Thakur, V.K., Singha, A.S., Thakur, M.K. Ecofriendly Biocomposites from Natural fibers: Mechanical and Weathering study. *International Journal of Polymer Analysis and Characterization*, 18(1), 64–72, 2013a.

- Thakur, V.K., Singha, A.S., Thakur, M.K. Natural Cellulosic Polymers as Potential Reinforcement in Composites: Physicochemical and Mechanical Studies. *Advances in Polymer Technology*, 32(S1), E427–E435, 2013b.
- Thakur, V.K., Singha, A.S., Thakur, M.K. Pressure Induced Synthesis of EA Grafted Saccharum cilliare Fibers. *International Journal of Polymeric Materials and Polymeric Biomaterials*, 63(1), 17–22, 2014c.
- Thakur, V.K., Singha, A.S., Thakur, M.K. Rapid Synthesis of MMA Grafted Pine Needles Using Microwave Radiation. *Polymer-Plastics Technology and Engineering*, 51(15), 1598–1604, 2012a.
- Thakur, V.K., Singha, A.S., Thakur, M.K. Surface Modification of Natural Polymers to Impart Low Water Absorbency. *International Journal of Polymer Analysis and Characterization*, 17(2), 133–143, 2012b.
- Thakur, V.K., Singha, A.S., Thakur, M.K. Synthesis of Natural Cellulose–Based Graft Copolymers Using Methyl Methacrylate as an Efficient Monomer. *Advances in Polymer Technology*, 32(S1), E741–E748, 2013c.
- Thakur, V.K., Thakur, M.K. Processing and characterization of natural cellulose fibers/thermoset polymer composites. *Carbohydrate Polymers*, 109, 102–117, 2014.
- Thakur, V.K., Thakur, M.K. Recent advances in green hydrogels from lignin: a review. *International Journal of Biological Macromolecules*, 72, 834–847, 2015.
- Thakur, V.K., Thakur, M.K., Gupta, R.K. Development of functionalized cellulosic biopolymers by graft copolymerization. *International Journal of Biological Macromolecules*, 62, 44–51, 2013d.
- Thakur, V.K., Thakur, M.K., Gupta, R.K. Graft Copolymers from Natural Polymers Using Free Radical Polymerization. *International Journal of Polymer Analysis and Characterization*, 18(7), 495–503, 2013e.
- Thakur, V.K., Thakur, M.K., Gupta, R.K. Review: Raw Natural Fiber–Based Polymer Composites. *International Journal of Polymer Analysis and Characterization*, 19(3), 256–271, 2014d.
- Thakur, V.K., Thakur, M.K., Raghavan, P., Kessler, M.R. Progress in Green Polymer Composites from Lignin for Multifunctional Applications: A Review. *ACS Sustainable Chemistry & Engineering*, 2(5), 1072–1092, 2014e.
- Thakur, V.K., Thakur, M.K., Singha, A.S. Free Radical–Induced Graft Copolymerization onto Natural Fibers. *International Journal of Polymer Analysis and Characterization*, 18(6), 430–438, 2013f.
- Thakur, M.K., Thakur, V.K., Gupta, R.K., Pappu, A., Synthesis and Applications of Biodegradable Soy Based Graft Copolymers: A Review. *ACS Sustain. Chem. Eng.* 4, 1–17, 2016.
- Thakur, V.K., Kessler, M.R., Free radical induced graft copolymerization of ethyl acrylate onto SOY for multifunctional materials. *Mater. Today Commun.* 1, 34–41, 2014a.
- Thakur, V.K., Kessler, M.R., Synthesis and characterization of AN-g-SOY for sustainable polymer composites. *ACS Sustain. Chem. Eng.* 2, 2454–2460, 2014b.
- Tian, Y., Wu, M., Lin, X., Huang, P., Huang, Y. Synthesis of magnetic wheat straw for arsenic adsorption. *Journal of Hazardous Materials*, 193, 10–16, 2011.
- Tripathi, M., Sahu, J.N., Ganesan, P., Dey, T.K. Effect of temperature on dielectric properties and penetration depth of oil palm shell (OPS) and OPS char synthesized by microwave pyrolysis of OPS. *Fuel*, 153, 257–266, 2015a.
- Tripathi, M., Sahu, J.N., Ganesan, P., Monash, P., Dey, T.K. Effect of microwave frequency on dielectric properties of oil palm shell (OPS) and OPS char synthesized by microwave pyrolysis of OPS. *Journal of Analytical and Applied Pyrolysis*, 112, 306–312, 2015b.

- Voicu, S.I., Condruz, R.M., Mitran, V., Cimpean, A., Miculescu, F., Andronesu, C., Miculescu, M., Thakur, V.K., Sericin Covalent Immobilization onto Cellulose Acetate Membrane for Biomedical Applications. *ACS Sustain. Chem. Eng.* 4, 1765–1774, 2016.
- Wang, D.-W., Li, F., Lu, G.Q., Cheng, H.-M. Synthesis and dye separation performance of ferromagnetic hierarchical porous carbon. *Carbon*, 46(12), 1593–1599, 2008.
- Wang, S.-y., Tang, Y.-k., Chen, C., Wu, J.-t., Huang, Z., Mo, Y.-y., Zhang, K.-x., Chen, J.-b. Regeneration of magnetic biochar derived from eucalyptus leaf residue for lead(II) removal. *Bioresource Technology*, 186, 360–364, 2015a.
- Wang, S.-y., Tang, Y.-k., Li, K., Mo, Y.-y., Li, H.-f., Gu, Z.-q. Combined performance of biochar sorption and magnetic separation processes for treatment of chromium-contained electroplating wastewater. *Bioresource Technology*, 174, 67–73, 2014.
- Wang, S., Gao, B., Zimmerman, A.R., Li, Y., Ma, L., Harris, W.G., Migliaccio, K.W. Removal of arsenic by magnetic biochar prepared from pinewood and natural hematite. *Bioresource Technology*, 175, 391–395, 2015b.
- Wiatrowski, H.A., Das, S., Kukkadapu, R., Ilton, E.S., Barkay, T., Yee, N. Reduction of Hg(II) to Hg(0) by Magnetite. *Environmental Science & Technology*, 43(14), 5307–5313, 2009.
- Widder, K.J., Senyei, A.E., Scarpelli, D.G. Magnetic microspheres: a model system for site specific drug delivery *in vivo*. *Experimental Biology and Medicine*, 158(2), 141–146, 1978.
- Wu, K.H., Shin, Y.M., Yang, C.C., Wang, G.P., Horng, D.N. Preparation and characterization of bamboo charcoal/Ni_{0.5}Zn_{0.5}Fe₂O₄ composite with core-shell structure. *Materials Letters*, 60(21–22), 2707–2710, 2006.
- Wu, H., Thakur, V.K., Kessler, M.R., Novel low-cost hybrid composites from asphaltene/SBS tri-block copolymer with improved thermal and mechanical properties. *J. Mater. Sci.* 51, 2394–2403, 2016.
- Xue, Y., Gao, B., Yao, Y., Inyang, M., Zhang, M., Zimmerman, A.R., Ro, K.S. Hydrogen peroxide modification enhances the ability of biochar (hydrochar) produced from hydrothermal carbonization of peanut hull to remove aqueous heavy metals: Batch and column tests. *Chemical Engineering Journal*, 200–202, 673–680, 2012.
- Yan, L., Kong, L., Qu, Z., Li, L., Shen, G. Magnetic Biochar Decorated with ZnS Nanocrystals for Pb (II) Removal. *ACS Sustainable Chemistry & Engineering*, 3(1), 125–132, 2015.
- Yang, M., Xie, Q., Zhang, J., Liu, J., Wang, Y., Zhang, X., Zhang, Q. Effects of coal rank, Fe₃O₄ amounts and activation temperature on the preparation and characteristics of magnetic activated carbon. *Mining Science and Technology (China)*, 20(6), 872–876, 2010.
- Yang, N., Zhu, S., Zhang, D., Xu, S. Synthesis and properties of magnetic Fe₃O₄-activated carbon nanocomposite particles for dye removal. *Materials Letters*, 62(4–5), 645–647, 2008.
- Zeng, L., Li, X., Liu, J. Adsorptive removal of phosphate from aqueous solutions using iron oxide tailings. *Water Research*, 38(5), 1318–1326, 2004.
- Zhang-Steenwinkel, Y., van der Zande, L.M., Castricum, H.L., Blik, A., van den Brink, R.W., Elzinga, G.D. Microwave-assisted *in-situ* regeneration of a perovskite coated diesel soot filter. *Chemical Engineering Science*, 60(3), 797–804, 2005.
- Zhang, G., Qu, J., Liu, H., Cooper, A.T., Wu, R. CuFe₂O₄/activated carbon composite: A novel magnetic adsorbent for the removal of acid orange II and catalytic regeneration. *Chemosphere*, 68(6), 1058–1066, 2007.
- Zhang, J., Xie, Q., Liu, J., Yang, M., Yao, X. Role of Ni(NO₃)₂ in the preparation of a magnetic coal-based activated carbon. *Mining Science and Technology (China)*, 21(4), 599–603, 2011a.
- Zhang, M.-m., Liu, Y.-g., Li, T.-t., Xu, W.-h., Zheng, B.-h., Tan, X.-f., Wang, H., Guo, Y.-m., Guo, F.-y., Wang, S.-f. Chitosan modification of magnetic biochar produced from Eichhornia

- crassipes for enhanced sorption of Cr(vi) from aqueous solution. *RSC Advances*, 5(58), 46955–46964, 2015.
- Zhang, M., Gao, B., Varnoosfaderani, S., Hebard, A., Yao, Y., Inyang, M. Preparation and characterization of a novel magnetic biochar for arsenic removal. *Bioresource Technology*, 130, 457–462, 2013.
- Zhang, W., Wang, L., Sun, H. Modifications of black carbons and their influence on pyrene sorption. *Chemosphere*, 85(8), 1306–1311, 2011b.
- Zhu, Y., Zhang, L., Schappacher, F.M., Pöttgen, R., Shi, J., Kaskel, S. Synthesis of Magnetically Separable Porous Carbon Microspheres and Their Adsorption Properties of Phenol and Nitrobenzene from Aqueous Solution. *The Journal of Physical Chemistry C*, 112(23), 8623–8628, 2008.

Polyurethanes Foams from Bio-Based and Recycled Components

S.Gaidukovs^{1*}, U.Cabulis² and G.Gaidukova³

¹*Faculty of Materials Science and Applied Chemistry, Institute of Polymer Materials, Riga Technical University, Riga, Latvia*

²*Polymer Laboratory, Latvian State Institute of Wood Chemistry, Riga, Latvia*

³*Faculty of Materials Science and Applied Chemistry, Institute of Applied Chemistry, Riga Technical University, Riga, Latvia*

Abstract

The chapter deals with the preparation of polyurethanes using the polyols obtained from different vegetable oils (rapeseed oil, tall oil, etc.) and recycled component (chemical recycling of polyethylene terephthalate). Synthesis of the proposed polyols will be reported. Fabrication of coatings and foams from obtained polyurethane and polyurethane composites will be discussed. Use of nano-clays and carbon nanotubes as fillers for obtained polyurethanes will be proposed.

The preparation of polyurethane (PU) rigid foams from bio-based and recycled components is reported. Total renewable and recycle component content is 55%. The rapeseed oil (RO) and recycled polyethylene terephthalate (rPET) were used to synthesize by the transesterification reaction the polyol for PU. Additives of adipic acid (ADA) and glycerol (GL) were added to modify the chemical structure of the final polyol. Hydroxyl value, acid value, water content, and viscosity, which depend from the RO, rPET, ADA and GL initial content, were used to describe the polyols. The prepared PU foams from the obtained polyols were characterized by Fourier transform infrared spectroscopy (FT-IR), compression test and water absorption measurements. The properties of the obtained foams relate on the content of the bio-based components, recycled components and additives in the used polyol formulations. The foams cellular structure was investigated by the use of optical microscope (OM).

Keywords: Polyurethane rigid foams, polyol, rapeseed oil, recycled PET, physical–mechanical properties

17.1 Introduction

Polyurethane (PU) is one of the high consumption commodity polymers. Considering different design of their macromolecular structure, PU polymers family can include elastomers, thermoplastics, thermosets and one or two components curable compositions.

*Corresponding author: gaidukov@gmail.com

Their applications are also very broad – solid rubbers, rigid and soft foams, fibers, coatings, adhesives, sealants, etc (Ashida, 2006, Prisacariu, 2011, Szycher, 2012, Sonnenschein, 2014). PUs are characterized by urethane group (—NH—(C=O)—O—) in the backbone, but they may contain also aliphatic and aromatic hydrocarbons, esters, ethers, amides, urea and isocyanurate groups. Generally, the PU are synthesized by the use of the reactions of isocyanates with compounds containing terminal hydroxyl groups (Szycher, 2012). For example, the fabrication of the PU soft and rigid foams is connected with the use of oligomeric polyols and diisocyanates (polyisocyanates) (Ashida, 2006).

Generally, crude oil is utilized to produce the raw ingredients (polyols and isocyanates) for PU synthesis (Ionescu, 2005, Sonnenschein, 2014). Recently, natural raw components for PU fabrications have attracted considerable interest because of the green chemistry and environmental concerns (Petrovic, 2008, Lligadas *et al.*, 2010, Pfister *et al.*, 2011, Babb, 2012).

Vegetable oils can be chosen as bio-based and renewable feedstock to produce polyol components for PU materials manufacturing. The hydroxylated derivatives of the soybean (Orgilés-Calpena *et al.*, 2014), coconut (Chethana *et al.*, 2014), rapeseed (Stirna *et al.*, 2006), sunflower (Zlatanić *et al.*, 2004), palm (Lee *et al.*, 2007) and castor (Beneš *et al.*, 2012) oils can be used for the synthesis of PU materials. For example, rapeseed oil (RO) is abundant and inexpensive renewable natural compound (Meier *et al.*, 2007, Islam *et al.*, 2014). It does not contain necessary hydroxyl groups and cannot react with the isocyanate components, but it can be easily chemically converted to the polyol. The main chemical modification routes are ozonolysis (De Souza *et al.*, 2012), epoxidation (Zhang *et al.*, 2014), hydroformylation (Petrović *et al.*, 2012), esterification (Valero *et al.*, 2012) and amidization (Kirpluks *et al.*, 2013) reactions. All of the functionalization methods mentioned above involve the formation of the polyol suitable for the PU foams preparation (Petrovic, 2008, Lligadas *et al.*, 2010, Pfister *et al.*, 2011, Babb, 2012). The molecular weight and hydroxyl groups' content in the final polyol product depends from the applied modification method. Generally, the values are in the range of 500 – 4000 g/mol and 50 – 300 mg KOH/g. Kayrite *et al.* reports that RO can be utilized as an excellent starting material to synthesize the oligomeric polyols for flexible and rigid PU foams fabrications (Prociak *et al.*, 2012, Kirpluks *et al.*, 2013, Kairyte *et al.*, 2015). Butanediol, ϵ -caprolactone, glycerol and polyglycols are proposed as chain extenders to modify the functionality and molecular structure of the polyol and network structure PU materials (Yeganeh *et al.*, 2007, Lee *et al.*, 2009, Mosiewicki *et al.*, 2015).

The next trend for production of PU, which is mostly driven by the ecological sustainability concerns, is connected with the utilization of recycled polymer materials (Dutt *et al.*, 2013).

Nowadays, many investigations have been dedicated to the recycling of linear polyesters – polyethylene terephthalate (PET) waste (Awaja *et al.*, 2005, Sinha *et al.*, 2010). PET is the commodity plastic widely used for the production of different consumer products – bottles, films and fibers materials. It is conventionally produced by the polycondensation reaction of terephthalic acid (TPA) and ethylene glycol (EG) (Fakirov, 2002, Thomas *et al.*, 2011). Two principal strategies have been applied to recycle the PET waste - mechanical and chemical routes (Dutt and Soni, 2013). Zhang *et al.* and other researchers have studied the recycling possibilities of PET waste by

other processes – biodegradation and enzyme degradation (Zhang *et al.*, 2004, Zhang *et al.*, 2006, Shah *et al.*, 2014, Hermanová *et al.*, 2015).

The mechanical recycling of the post-consumer PET waste is performed by the melt extrusion and reactive extrusion processing of the polymer to bottles, packaging films and fibers (Welle, 2011). The chemical recycling of PET is the depolymerization process to the monomer and oligomer substances (Karayannidis *et al.*, 2007). It is achieved by the thermal treatment of the plastic flakes in the solution. A large variety of solvents (organic solvents, glycols, ionic liquids, supercritical liquids, etc.), chemicals (alcohols, carbonic acids, anhydrides, etc.) and catalysts (metal-organic compounds, phase transfer compounds, hydrotalcites, metal oxides, etc.) are successfully utilized for that purpose (Goto *et al.*, 2002, Karayannidis and Achilias, 2007, Imran *et al.*, 2013, Yue *et al.*, 2013, Bartolome *et al.*, 2014, Chen *et al.*, 2014). The main chemical reactions to depolymerize the PET are glycolysis, methanolysis, hydrolysis and aminolysis (Fakirov, 2002, Carta *et al.*, 2003, Nikles *et al.*, 2005). It is reported that the depolymerization process of PET can be intensified with the assistance of ultrasonic and microwave treatment (Paliwal *et al.*, 2013, Rusen *et al.*, 2013). Miscellaneous PET depolymerization products have been developed – unsaturated polyester resins, alkyd resins, and polyols for polyurethane foams and coatings (Viksne *et al.*, 2000, Patel *et al.*, 2005, Güçlü *et al.*, 2009, Vitkauskienė *et al.*, 2011).

Depolymerization products of PET can be successfully utilized in the production of aromatic polyester polyols, which may be used for manufacturing of the PU foams (Vaidya *et al.*, 1989, Saravari *et al.*, 2004, Roy *et al.*, 2013). It is reported that the presence of aromatic blocks in the backbone structure of the polyol enhance the final mechanical, thermal properties and resistance to the solvents and oils of the PU foams. Unfortunately, the aromatic polyester polyols from recycled PET are characterized with the limited compatibility with the physical foaming agents as hydrofluorocarbons and crystallization in time. Many authors convince that the use of glycerol (GL), adipic acid (ADA), ϵ -caprolactone, butanediol and polyglycols as functional additives can modify the branching and functionality of the molecular backbone structure of the polyol (Vitkauskienė *et al.*, 2011, Kathalewar *et al.*, 2013). Also, the effect of castor and palm oils additives on the structure of the polyols is reported in the literature (Saravari *et al.*, 2007, Beneš *et al.*, 2013, Cakić *et al.*, 2015). As a result of the use of the modified polyols, the final thermal and physical–mechanical properties of the PU materials have been improved.

In this chapter, we report new formulations of PU polyols, which were synthesized from building blocks of RO and depolymerized PET oligomer, and their use in the manufacturing of PU foams. In particular, the synthesis of PU polyols was carried out in three steps: (1) the transesterification of RO with triethanolamine; (2) the industrial PET waste depolymerization by the transesterification reaction with diethylene glycol (DEG) in the presence of various concentrations of functional additives ADA and GL; and, (3) sequential, synthesis of the final oligomeric polyol by the transesterification of the above mentioned intermediary components. The synthesized polyols consist from renewable and recycled components; combine the advantages of aromatic and aliphatic structure blocks in the backbone; and were used to process the PU rigid foams. The structure and mechanical properties, considering the modifying components and the chemical structure of the processed PU foams were investigated.

17.2 Experiments

17.2.1 Raw Materials

All raw components were used without any additional treatments. PET flakes of clear grade were granted from PET Baltija, Latvia. RO $I_2=117$ I2 mg/100 g) was supplied from Iecavnieks & Co, Latvia.

TEA (99.5%) from BASF, Germany; zinc acetate dehydrate (ZnAc) ($\geq 98\%$) from Sigma Aldrich, Germany, DEG (99%) from Sigma Aldrich, Germany were used without any further purifications for synthesis of PU polyols.

Polyether polyols Lupranol 3422 (BASF, Germany; OH value=490 mg KOH/g), polymeric diphenylmethane diisocyanate IsoPMDI 92140 (pMDI) (BASF, Germany; NCO group content = 31.5%), foaming agent Solkane 365/227 (Solvay, Belgium; Pentafluorobutane/Heptafluoropropane 87/13) and other reagents such as the catalyst dimethylaminopropyldipropylamine PC CAT NP-10 (Performance Chemicals Handels, Germany), silicone surfactant NIAx Silicone L6915 (Momentive Performance Materials, Germany), flame retardant trichloropropylphosphate (Lanxess, Germany) were used without further purification for preparation of PU rigid foams.

17.2.2 Polyol Synthesis

In a synthesis, the PET flakes (1 M) were slowly added to the DEG (2 M) at 190 °C in the presence of ZnAc; then heated to 240–250 °C. ADA and GL functional additives were introduced into the reaction blend. The reaction was carried out for additional 3 h at 240–250 °C. The obtained GL/ADA aromatic polyols were blended with rapeseed oil based (RO/TEA 2.9) polyol component by the weight ratio 1:1. The reaction mixture was heated to 180 °C and left at this temperature for 1 h. No catalyst was added during the transesterification reaction.

The bio-based polyol RO/TEA 2.9 was synthesized by the transesterification reaction of RO with TEA; the reaction was carried out at 170°C for 1 hour in the presence of a catalyst (0.15 wt. % of ZnAc). The molar ratio was 1 M of RO to 2.9 M of TEA. RO/TEA polyol synthesis was discussed previously by Stirna *et al.* (Stirna *et al.*, 2006).

These synthesis reactions were carried out in a three-neck 1.0 L reaction flask equipped with a mechanical stirrer, a thermometer, a condenser and an argon inlet.

Overall 14 different polyols were prepared. The final polyols were named GL/ADA and GL/ADA-RO. Their synthesis compositions are summarized in Table 17.1.

17.2.3 Characterization of Polyols

Hydroxyl numbers (OH) of the polyols were determined using acetic acetylation method according to DIN 53240. The acid values were determined according to DIN 53402.

The moisture content in polyol was tested using conventional Karl Fischer method and DIN 51777.

Viscosity measurements were carried out using Haake Viscotester 6L/R plus Rotational Viscometer (ThermoScientific, Germany) at 20 °C.

Table 17.1 The compositions of synthesized polyols from recycled PET, RO and additives.

Sample	Recycled component		Functional additives				Biobased component	
	PET, mol	DEG, mol	GL,		ADA,		RO, mol	TEA mol
			wt. %	mol	wt. %	mol		
GL/ADA 0/1	1	2	0	0.00	1	0.03	–	–
GL/ADA 1/1	1	2	1	0.04	1	0.03	–	–
GL/ADA 1/3	1	2	1	0.04	3	0.08	–	–
GL/ADA 1/6	1	2	1	0.13	6	0.08	–	–
GL/ADA 3/3	1	2	3	0.04	3	0.17	–	–
GL/ADA 3/6	1	2	3	0.13	6	0.17	–	–
GL/ADA 6/6	1	2	6	0.26	6	0.17	–	–
GL/ADA-RO 0/1	1	2	0	0.00	1	0.03	0.31	0.90
GL/ADA-RO 1/1	1	2	1	0.04	1	0.03	0.31	0.91
GL/ADA-RO 1/3	1	2	1	0.04	3	0.08	0.32	0.93
GL/ADA-RO 1/6	1	2	1	0.13	6	0.08	0.33	0.95
GL/ADA-RO 3/3	1	2	3	0.04	3	0.17	0.33	0.96
GL/ADA-RO 3/6	1	2	3	0.13	6	0.17	0.34	0.97
GL/ADA-RO 6/6	1	2	6	0.26	6	0.17	0.35	1.00

The Fourier transform infra-red spectra measurements (FTIR-ATR) were made on a Perkin-Elmer spectrometer Spectrum One FTIR Spectrometer (Germany). The FTIR-ATR spectra of polyols were collected at a resolution of 4 cm^{-1} .

17.2.4 Preparation of Polyurethane Rigid Foams

The obtained GL/ADA and GL/ADA-RO polyols were used to obtain the rigid PU foams. Formulation and foaming parameters of rigid PU foams are given in Table 17.2.

The necessary amount of pMDI was calculated according to isocyanate index 130. Foaming process was monitored by measuring the characteristic parameters: the duration of cream time, gel time and tack-free time. The cream time indicates the rise start of foam, gel time – a transition of the mix from liquid to solid state and tack-free time – when foam solidifies completely.

The PU foams were prepared on lab scale in 2-stage mixing of the components by free-rising method in a mould at room temperature. Firstly, the polyol system was mixed in a 500 mL plastic beaker. Afterwards the isocyanate was added and mixed for 15 s at a speed rate of 2000 rpm. Then the mixture was quickly poured into an open plastic mould with dimensions $30 \times 30 \times 10\text{ cm}$. The prepared PU foam blocks were conditioned at a room temperature for at least 24 h. After that the specimens for different physical–mechanical tests were cut from prepared PU foam blocks using band saw.

Table 17.2 Formulations for rigid PU foams.

Component	Part by weight					
	GL/ADA 0/1 / GL/ADA-RO 0/1	GL/ADA 1/1 / GL/ADA-RO 1/1	GL/ADA 1/3 / GL/ADA-RO 1/3	GL/ADA 1/6 / GL/ADA-RO 1/6	GL/ADA 3/3 / GL/ADA-RO 3/3	GL/ADA 3/6 / GL/ADA-RO 3/6
Corresponding polyol				70.0		GL/ADA 6/6 / GL/ADA-RO 6/6
Lupranol 3422				30.0		
Trichlorpropylphosphate				16.0		
NIAX Silicone L6915				1.5		
Water				2.2		
PC CAT NP-I0				1.6		
Solkane 365/227				16.0		
pMDI	192.2/175.6	191.0/176.7	191.0/178.1	192.3/185.6	191.0/174.6	191.0/184.4
						191.0/200.8

17.2.5 Characterization of Rigid Polyurethane Foams

Bulk density of obtained rigid PU foams was measured according to standard test method ISO 845 for apparent density of plastic foams.

PU foams specimens with dimension $5 \times 5 \times 5$ cm were cut out for water absorption measurements. It was tested according to ISO 2896 by immersing the specimens in water for 28 days. Closed cell content was measured according to ISO 4590.

The FTIR-ATR was used to study the bondings in prepared PU foams. FTIR-ATR spectra of manually compressed PU foams were collected at a resolution of 4 cm^{-1} on a Nicolet 6700 (ThermoScientific, Germany) in the region of $800\text{--}4000 \text{ cm}^{-1}$. Sixteen measurements of every specimen were performed and average spectrum is shown.

The compression strength and elasticity modulus of parallel (Z) and perpendicular (X) to foaming direction of PU foams were measured according to ISO 844 standard on testing machine Zwick Z100 (Zwick Roell, Germany).

Cells size distributions were calculated from the cellular structure images of foams cross-section, which were taken using an optical microscope Leica DMR (Leica Microsystems, Germany) at 5x magnification. Leica Image Suite™ software was applied for cells measurements.

17.3 Results and Discussion

17.3.1 Characterization of Polyols

The novel polyols containing bio-based and recycled components were synthesized in three steps.

Step 1.

RO consists of unsaturated fatty acids – oleic (56%), linoleic (26%) and linolenic acids (10%), and other, as well as saturated fatty acids – palmitic (4%) and stearic acids (2%), and other fatty acids (2%) (Petrovic, 2008). RO transesterification reaction has occurred according to Figure 17.1 (Petrovic, 2008, Kirpluks *et al.*, 2013). The obtained RO/ TEA polyol contains 1 M RO and 2.9 M TEA.

It contains saturated and unsaturated fatty acid chain blocks with alkyl chain length $C_{16}\text{--}C_{18}$. The obtained polyol was characterized with viscosity 160 mPa·s, hydroxyl value 363 mg KOH/g, acid value 2.5 mg KOH/g and the water content 0.12%.

Step 2.

Glycolysis reaction of PET waste was performed by heating the polymer flakes with a DEG in the presence of ZnAc catalyst (Chen *et al.*, 1999). Functional additives GL and ADA were added to the depolymerized blend to change the molecular chain length, branching and functionality. The final polyol formulations have contained 14 different combinations of GL/ADA ratios (Table 17.1).

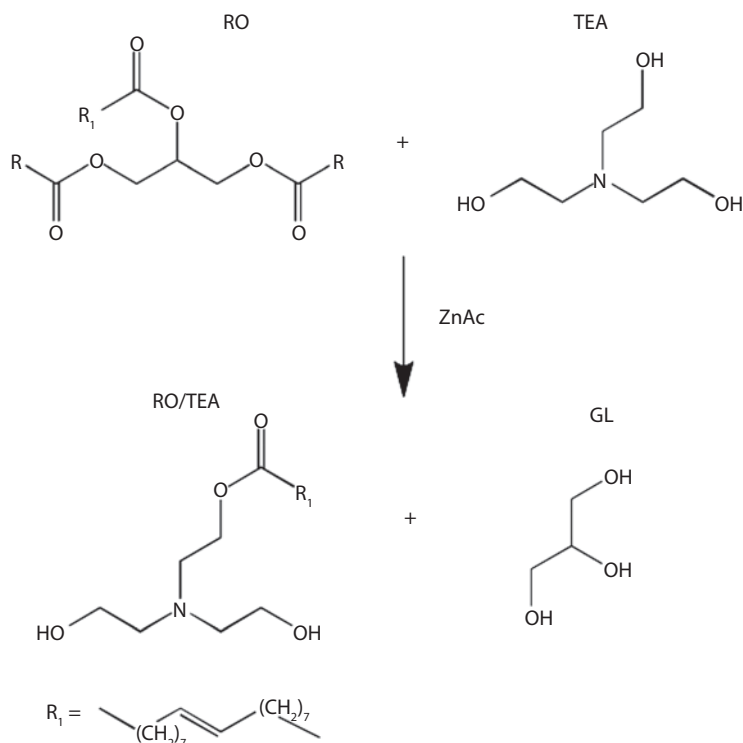


Figure 17.1 Synthesis of RO/TEA polyol.

Step 3.

The obtained GL/ADA polyols were further transesterified with bio-based RO/TEA polyol. The possible structures of obtained polyols are presented in Figure 17.2. The acid numbers, hydroxyl values, water contents and viscosities of finally obtained GL/ADA and GL/ADA-RO polyols are summarized in Table 17.3.

Polyols' viscosity is a very important processing characteristic (Ionescu, 2005). Polyols with low viscosity have many advantages. They can be easily processed to PU foams. High molecular weight polymers and branched chain cross-linked networks can be obtained. Generally, glycolysis of PET resulted in high viscosity oligomeric polyols (3130 mPa·s for GL/ADA 0/1) (Table 17.3). It can be concluded that addition of small amount (1–6 wt.%) of GL and/or ADA decreases the viscosity of polyols three times (1165 mPa·s for GL/ADA 6/6), which corresponds to low molecular weight chains. The GL/ADA-RO polyols, synthesized from GL/ADA with addition of 50 wt.% of RO, are characterized with a much lower viscosity values compared to initial GL/ADA polyols. The GL/ADA-RO polyols' viscosity was in the range from 700 to 850 mPa s at 20 °C, which is appropriate for obtaining the PU rigid foams.

By increasing the content of functional additives GL/ADA in the concentration range from 0/1 to 6/6 %, the polyols' OH values increase by 20% that is from 472 till 515 mg KOH/g. The experimental OH values are lower than the theoretically calculated OH* values due to possible some dehydration of hydroxyl groups and molecular chain branching (Ionescu, 2005, Szycher, 2012). After the transesterification reaction

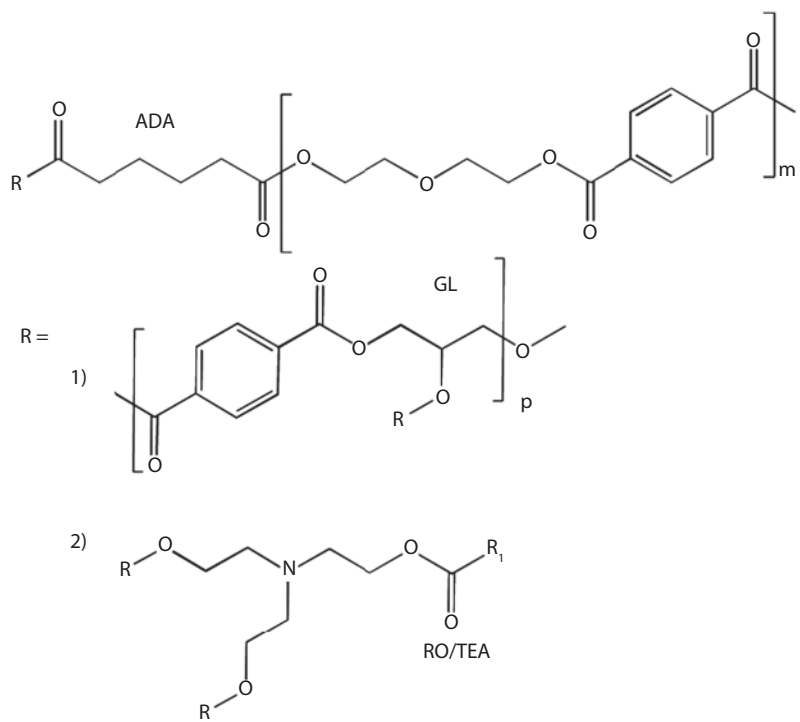


Figure 17.2 Possible structure of polyols obtained from depolymerized PET and transesterified RO, containing fragments of ADA and GL.

Table 17.3 Properties of synthesized polyols.

Polyol	OH value, mg KOH/g	OH*. theor value, mg KOH/g	Acid value, mg KOH/g	Water content, %	Viscosity at 20 °C, mPa·s
GL/ADA 0/1	472	549	3.04	0.17	3130
GL/ADA 1/1	466	562	2.88	0.18	2490
GL/ADA 1/3	466	551	2.63	0.22	2060
GL/ADA 1/6	492	575	2.66	0.18	1650
GL/ADA 3/3	531	536	1.79	0.11	1255
GL/ADA 3/6	503	559	3.2	0.11	1165
GL/ADA 6/6	515	593	1.32	0.09	1172
GL/ADA-RO 0/1	405	461	4.02	0.11	700
GL/ADA-RO 1/1	408	467	4.2	0.14	725
GL/ADA-RO 1/3	417	461	2.9	0.09	820
GL/ADA-RO 1/6	399	474	2.83	0.13	725
GL/ADA-RO 3/3	449	454	2.49	0.10	710
GL/ADA-RO 3/6	440	466	2.7	0.16	725
GL/ADA-RO 6/6	400	483	3.17	0.11	850

of GL/ADA and RO/TEA polyols, the products GL/ADA-RO are characterized with about 20% lower OH values.

All processed polyols have low acid numbers, which are less than 4.5 mg KOH/g. The received values are suitable for the production of PU rigid foams (Ionescu, 2005, Szycher, 2012). Water content in all polyols is less than 0.25% which is acceptable for obtaining the rigid foams (Ionescu, 2005, Szycher, 2012).

Table 17.4 shows data of renewable and recycled content in synthesized polyols. GL/ADA formulations of polyols do not consider any renewable component content in the structure. GL/ADA-RO polyols contain approximately 33% of renewable part (RO) and about 22% of recyclate part (rPET). Total renewable and recyclate content is about 55%, which exceeds the average values reported in the literature (Beneš *et al.*, 2012, Cakić *et al.*, 2015).

The FTIR spectra of the synthesized polyols confirmed the PET glycolysis with DEG and GL/ADA transesterification with RO/TEA. FTIR spectra GL/ADA and GL/ADA-RO of different composition polyols are very similar, regardless of the functional additives concentration used for their preparation. Hence, polyols only containing 1/1 and 6/6 of GL/ADA have been included as representatives in the Figure 17.3.

The presence of recycled PET component in the polyol is mainly indicated by the absorption band intensities of aromatic C=C vibrations at 1578, 1505 and 1410 cm^{-1} , the absorption band of bending and stretching vibrations of aromatic C-H at 875 and 730 cm^{-1} and the stretching vibration band of aromatic C=O carbonyl group at 1265 and 1120 cm^{-1} . The broad band at 3400 cm^{-1} characterizes the free hydroxyl –OH groups in all polyols.

Table 17.4 Renewable and recycled content in obtained polyols.

Polyol	Renewable content, %	Recyclate content, %	Total renewable + recyclate content, %
GL/ADA 0/1	–	46.9	46.9
GL/ADA 1/1	–	46.5	46.5
GL/ADA 1/3	–	45.6	45.6
GL/ADA 1/6	–	44.7	44.7
GL/ADA 3/3	–	44.3	44.3
GL/ADA 3/6	–	43.5	43.5
GL/ADA 6/6	–	42.3	42.3
GL/ADA-R 0/1	33.5	23.5	57.0
GL/ADA-R 1/1	33.5	23.2	56.7
GL/ADA-R 1/3	33.5	22.8	56.3
GL/ADA-R 1/6	33.5	22.4	55.9
GL/ADA-R 3/3	33.5	22.2	55.7
GL/ADA-R 3/6	33.5	21.8	55.3
GL/ADA-R 6/6	33.5	21.2	54.7

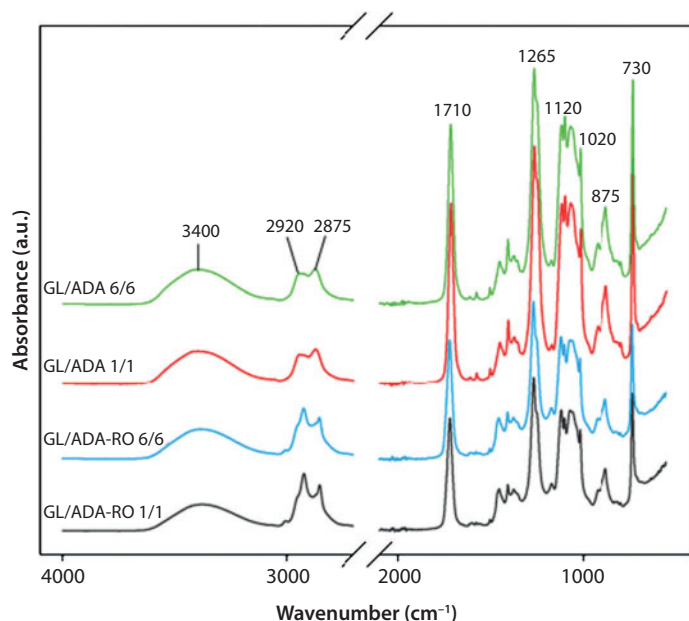


Figure 17.3 FTIR spectra of obtained polyols.

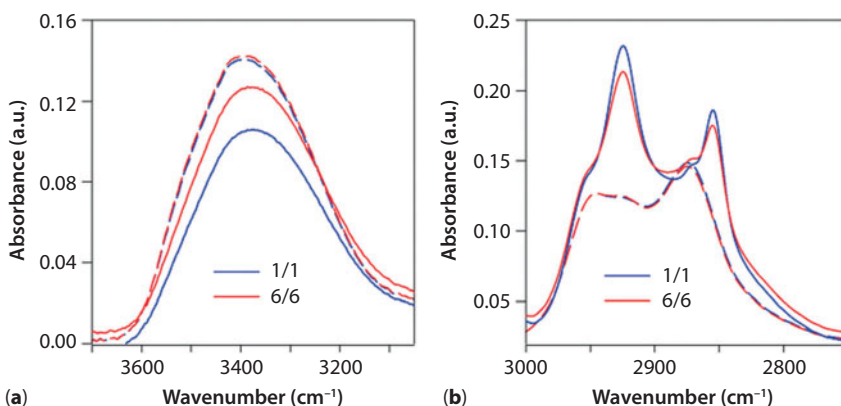


Figure 17.4 FTIR spectra of -OH (a) and -CH₂ (b) groups absorption bands for polyols; dashed line – GL/ADA, solid line – GL/ADA-RO.

There is also an important absorption band at 1710 cm⁻¹, which corresponds to the carbonyl C=O bonds in ester groups. It can also be seen that the absorption intensity decreases for GL/ADA-RO polyols, which is in agreement to the decrease in the number of ester groups due to the transesterification reaction in the third step of the synthesis.

The regions of hydroxyl, aliphatic and aromatic groups vibrations are put in detailed focus in Figures 17.4–6, because these regions provide useful information of the linkages of the polyol (Sonnenschein, 2014).

Figure 17.4a shows that absolute absorption intensity at 3400 cm⁻¹ is stronger for GL/ADA polyols, which relates to higher hydroxyl absolute values of these polyols in comparison to GL/ADA-RO polyols' series, as was reported in Table 17.3. The GL/ADA content and ratio minimally affect the absorption intensities. Due to transesterification

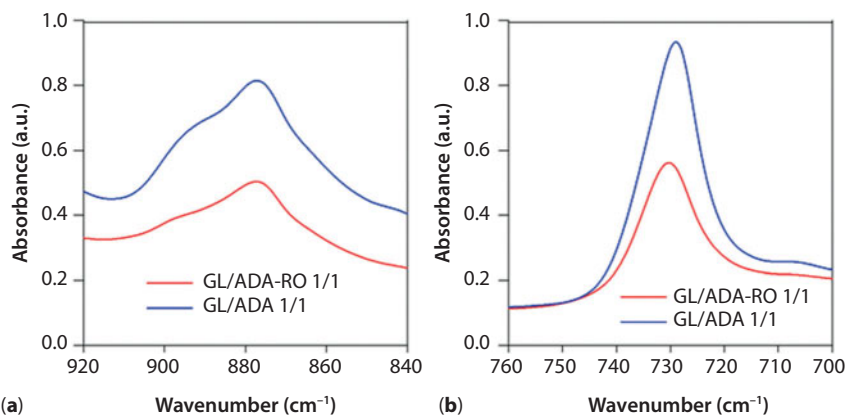


Figure 17.5 FTIR-ATR spectra of aromatic group absorption band for polyols.

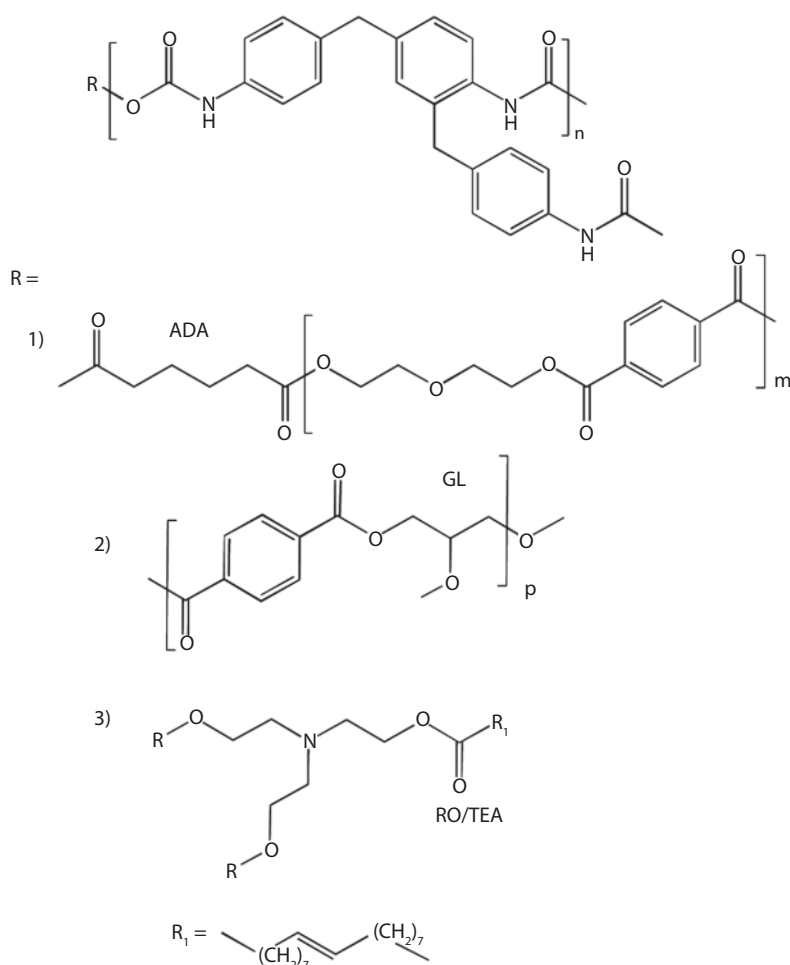


Figure 17.6 Possible structure of prepared PU, containing fragments of recycled PET and biobased RO.

reaction in the third reaction step, the hydroxyl groups are consumed, as a result the absorption intensity in this region decreases. The OH value decreases from an initial value of 515 mg KOH/g for GL/ADA 6/6 to 400 mg KOH/g for GL/ADA-RO after reaction with RO/TEA.

In the 3000-2700 cm^{-1} range (see Figure 17.4b), two intensive bands at 2920 and 2875 cm^{-1} can be observed due to stretching $-\text{CH}_2$ groups of aromatic and aliphatic structures in the chain backbone (Carta *et al.*, 2003). For all GL/ADA-RO polyols containing bio-based component, the characteristic intensities in this region are more pronounced due to the presence of long alkyl chain fragments from RO i.e. fatty acid radicals in the molecular chain backbone (see Figure 17.2).

Another significant difference is the appearance of an absorption band at 875 and 730 cm^{-1} corresponding to the aromatic groups from recycled PET oligomers (Figure 17.5). The fact that lower absorption bands' intensifies for GL/ADA-RO, complies well with the overall decrease of the recycle (aromatic component) content in the GL/ADA-RO polyols.

17.3.2 Formation of PU Rigid Foams

The main parameters, characterizing the stages of PU foam formation, are the cream time, the gel time, and the tack-free time. They are listed in Table 17.5. It was observed, that the cream time, which is measured as foam rise time due to the release of blowing gases, is approximately 30 s after mixing of the components. The gel time for all the polyols' formulations is in the range 55–65 s. The gel time and the cream time of the formulations with polyols GL/ADA-RO, containing bio-based and recycled components,

Table 17.5 Parameters of rigid PU foam formation process.

Sample	Cream time, s	Gel time, s	Tack-free time, s	Closed cell content, vol. %	Density, kg/m^3
GL/ADA 0/1	30	57	67	95	42.6
GL/ADA 1/1	31	55	67	96	42.5
GL/ADA 1/3	25	50	60	93	42.8
GL/ADA 1/6	25	50	60	97	43.1
GL/ADA 3/3	34	55	70	89	45.9
GL/ADA 3/6	32	57	71	90	45.1
GL/ADA 6/6	33	56	67	98	45.9
GL/ADA-RO 0/1	25	50	63	95	38.3
GL/ADA-RO 1/1	28	55	75	95	37.7
GL/ADA-RO 1/3	28	50	70	94	38.8
GL/ADA-RO 1/6	35	65	105	94	47.2
GL/ADA-RO 3/3	30	52	103	93	44.7
GL/ADA-RO 3/6	32	60	110	97	46.4
GL/ADA-RO 6/6	32	65	120	93	52.5

was comparable to the formulations with polyols GL/ADA, containing only recycled components. The tack-free time is measured at point when the foam solidifies completely because of chain cross-linking and macromolecular network development. It was observed, that GL/ADA concentration in the polyols GL/ADA and GL/ADA-RO shows almost no systematic changes in the values of the cream time, gel time and tack-free time of the investigated formulations foaming process.

The tack-free time of the some formulations containing polyols GL/ADA-RO, received by reaction of both bio-based and recycled components, is almost two times longer than for formulations containing GL/ADA polyols. It relates well to the lower hydroxyl values and lower chain branching of the GL/ADA-RO polyols. Longer flexible segments and higher flexible segment content in the chains after the transesterification of RO/TEA and GL/ADA polyols result in incorporation of bio-based RO radicals (fatty acid aliphatic chains fragments) into the molecular backbone for GL/ADA-RO polyols. The possible chemical structure of obtained PU molecular chain network, which was obtained with the GL/ADA-RO polyols obtained from the glycolysis of rPET with addition of functional additives (GL/ADA) and its sequential transesterification with RO/TEA is presented in Figure 17.6.

17.3.3 Cellular Structure of PU Rigid Foams

The effect of incorporation of fatty oil based aliphatic fragments (bio-based RO component) into the polyol molecular chain backbone was also confirmed in cellular structure of PU rigid foams. The PU foams from GL/ADA polyol and the PU foams from GL/ADA-RO polyol, are compared in Figure 17.7a,b. It is visible in optical microscopy images that after the addition of RO, the GL/ADA-RO formulation gives larger and more regular cell structure for PU rigid foam. This is due to the presence of aliphatic fragments in the backbone, which increase the overall flexibility of the molecular chain and decrease the viscosity of the polyol (Xu *et al.*, 2015).

The results of optical microscopy's images analysis of the cellular structure of PU rigid foams are summarized in Figure 17.8. The average cell size of PU GL/ADA foams is about 330 μm . PU GL/ADA-RO rigid foams are characterized with the average cell size 420 μm , which is approximately 30% higher than for PU GL/ADA foams. The GL/ADA content in the polyol does not show remarkable modifications in the cell size of the obtained PU rigid foams.

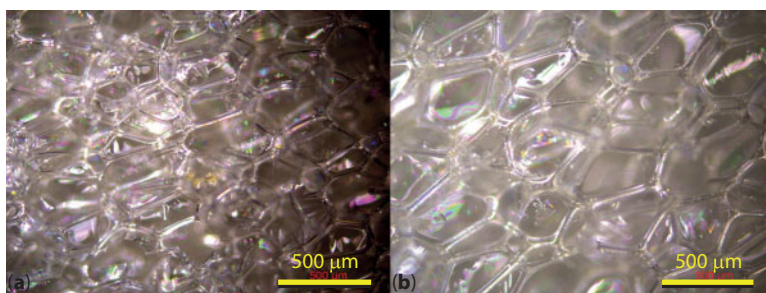


Figure 17.7 OM images of PU rigid foams prepared using polyols (a) ADA/GL 0/1 and (b) ADA/GLA-RO 0/1.

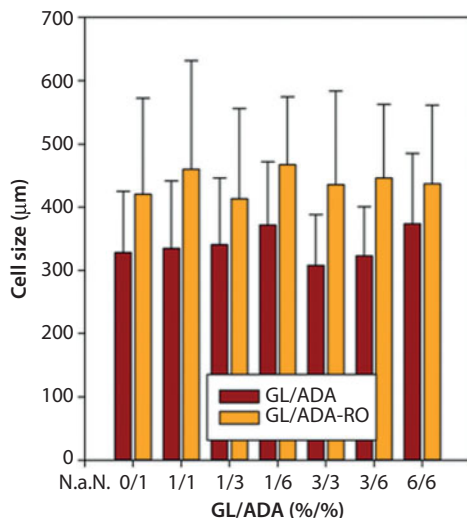


Figure 17.8 Cell size of PU rigid foams.

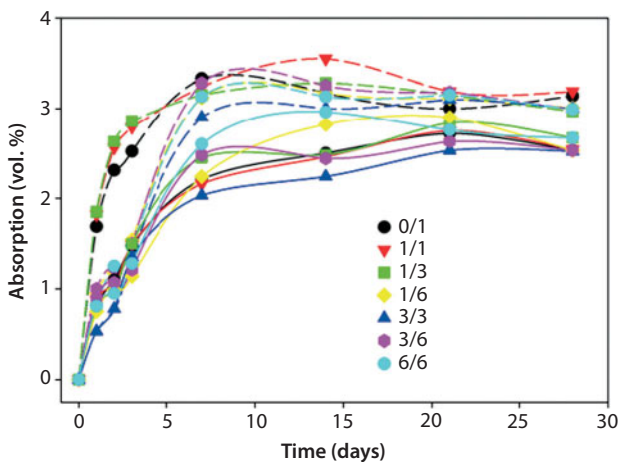


Figure 17.9 Water absorption of PU rigid foams; dashed line – GL/ADA, solid line – GL/ADA-RO.

The water absorption was tested by immersing PU foam samples in water. The water absorption kinetic curves for PU GL/ADA and PU GL/ADA-RO are shown in Figure 17.9.

The density and the calculated closed cell content for the prepared PU rigid foams are given in Table 17.5. The water absorption in absolute values are below 3 wt.%. The lower water absorption properties were observed for PU GL/ADA foams, which also relates to slightly higher closed cell content (Atta *et al.*, 2013). Closed cell content for PU GL/ADA and PU GL/ADA-RO rigid foams is in the range from 90 to 96 vol.%.

17.3.4 Compression Strength of PU Rigid Foams

The mechanical properties of PU rigid foams directly depend on polyols chemical structure, which are used in PU formulations (Ionescu, 2005, Szycher, 2012). Generally,

compression tests of the rigid foams are carried out in the foam rise direction (index z) and perpendicular (index x) to the foam rise direction (Stirna *et al.*, 2011). They were used to measure the elasticity (E) and the strength (σ) of prepared PU rigid foams (see Figure 17.10). The obtained mechanical properties of foams are dependent to the developed cell anisotropy (Hamilton *et al.*, 2013).

PU rigid foams prepared from GL/ADA polyols showed slightly higher compression strength s_x and s_z than foams prepared from GL/ADA-RO polyols. The elasticity coefficient E_x and E_z of the PU GL/ADA foams is higher than for PU GL/ADA-RO foams. Probably, the long flexible aliphatic chains (fatty acid chains C_{16} – C_{18}), which are present in PU macromolecular network of GL/ADA-RO foams, (Figure 17.6) have plasticizing effect and have endowed the viscoelasticity to the foams deformation properties (Ashida, 2006). Then, the distance between the cross-linking points in the PU network increased for GL/ADA-RO foams, correspondingly. The higher mechanical properties of PU GL/ADA foams can be also assumed due to the higher concentration of ester and aromatic groups in the polyol and developed PU chain network (Ionescu, 2005); then, possible, more efficient and stronger hydrogen bondings between the functional groups in the developed PU GL/ADA polymer network have to be assumed (Li *et al.*, 2014). In our investigation it

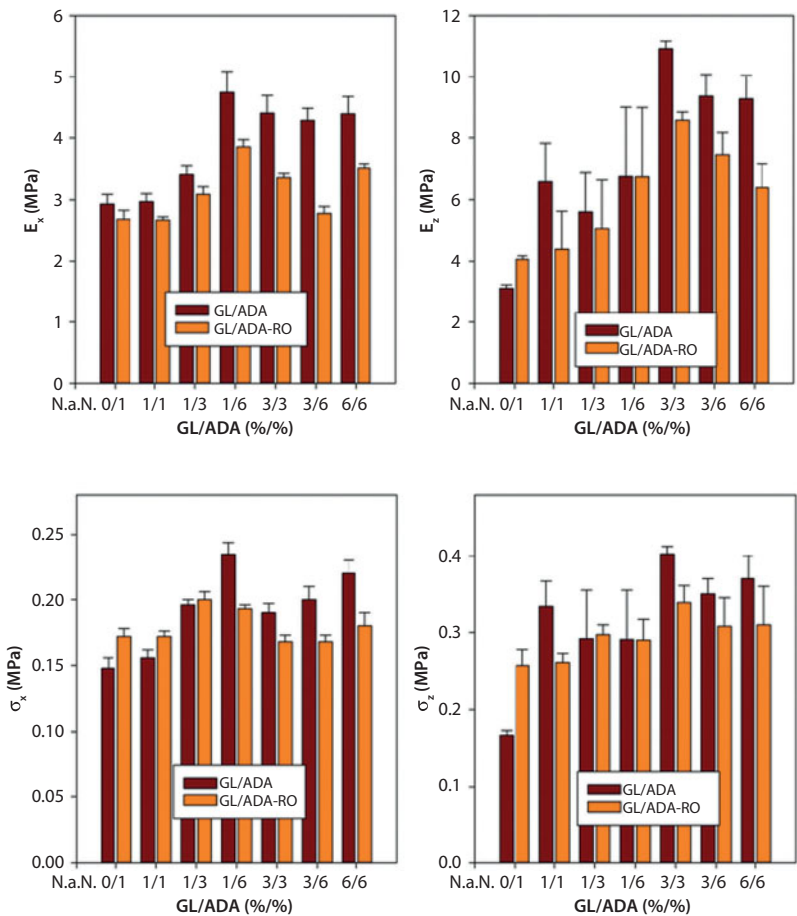


Figure 17.10 Mechanical properties of PU rigid foams.

was reflected by observed 20% decrease (only for some foams) of mechanical parameters (σ , E) of PU rigid foams prepared using GL/ADA-RO polyol formulations.

In the case of PU foams prepared with different content of functional additives GL and ADA, the E and σ parameters have tendency to increase significantly as the higher content of functional additives is introduced into the polyols (Vitkauskiene *et al.*, 2011). For example, E_z of PU rigid foam increased almost 3 times after the use of the polyol GL/ADA 6/6 in the foam manufacturing, considering the polyol GL/ADA 0/1 as reference. PU GL/ADA-RO foams have very similar influence of functional additives concentrations on the mechanical parameters of the foams.

The higher content of GL used in the polyols synthesis has resulted in branched chain structure and additional hydroxyl groups (higher OH value, Table 17.3) in the middle of the chains (Luo *et al.*, 2014). Then, polyol reaction with isocyanate has developed dense PU macromolecular network with short distance between the cross-linkings. The addition of ADA brings the extra alkyl soft segments (C_4) in the PU network (Xu *et al.*, 2015). These shorter soft segments in the PU macromolecular chain have very favourable influence on the conformational mobility and development of the dense network of hydrogen bondings (Ionescu, 2005). The assumption of strong influence of hydrogen bonding on the mechanical properties of PU also has evidences shown by Stirna *et al.* (Stirna *et al.*, 2011).

17.3.5 FTIR of PU Rigid Foams

Using FTIR spectroscopy data, the characteristic groups of PU chain network can be clarified. It is well known that the existence of hydrogen bonds in PU can be also observed by FTIR spectroscopy (Sonnenschein, 2014). Possibilities for hydrogen bond formation in PU are the ester–urethane, urethane–urethane, and urethane–amide hydrogen bonding. FTIR spectra was recorded for PU GL/ADA and PU GL/ADA-RO rigid foams. The spectra of PU, containing different amounts of functional additives of ADA and GL, are practically very similar to each other. Representative spectra in absorption mode of obtained PU rigid foams are presented in Figure 17.11.

The obtained FTIR spectra of PU corresponds well to the PU foams characteristic absorption bands available in literature (Hu *et al.*, 2002, Hatchett *et al.*, 2005, Stirna *et al.*, 2006). The bands at 3300 cm^{-1} characterize hydrogen-bonded N-H stretching, 2925 cm^{-1} for aromatic C-H stretching, 2854 cm^{-1} for aliphatic C-H stretching, 1710 cm^{-1} for C=O ester group, 1615 cm^{-1} for stretching C=O urethane group, 1511 cm^{-1} for C=O aromatic ring.

The sharp peaks at 2925 and 2854 cm^{-1} due to methylene groups' vibrations are observed only for PU GL/ADA-RO foams; they correspond to the long aliphatic fragments attributed from RO radical incorporated to polyol molecule chain backbone after the third reaction step. Contrary, PU GL/ADA polyols characterize the absence of long aliphatic segments; thus, the very broad characteristic absorption band is indicated in the same absorption region. PU rigid foams prepared with GL/ADA and PU rigid foams prepared with GL/ADA-RO exhibit the same intensity absorption bands at 1615 cm^{-1} , which can be attributed to the urethane carbonyl groups. The PU GL/ADA-RO foams showed the decreased absorption intensity at the band 1720 cm^{-1} in comparison to PU GL/ADA foams, which is attributed to lower content of ester carbonyl groups.

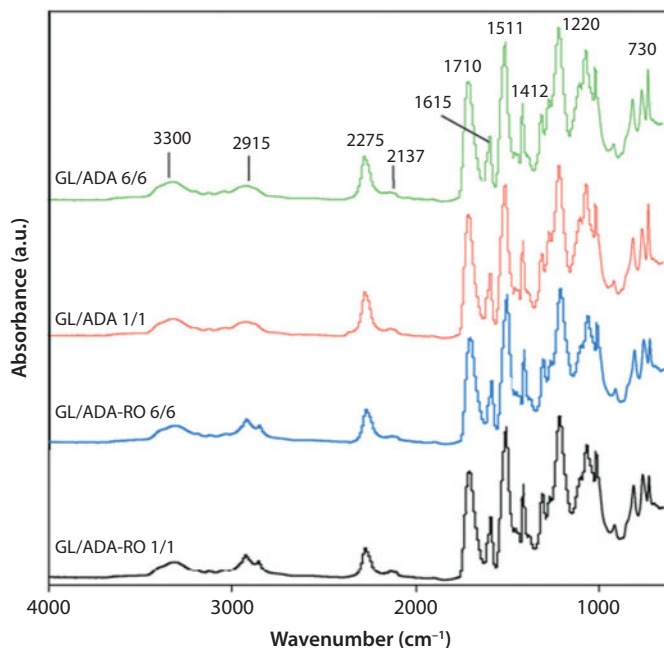


Figure 17.11 FTIR-ATR spectra of PU rigid foams.

The presence of the absorption band at 2275 cm^{-1} clearly indicates that there are free isocyanate groups remaining in all PU rigid foams (Hu *et al.*, 2002, Stirna *et al.*, 2006). Carbodiimide group $\text{RN}=\text{C}=\text{NR}$ formation is associated with the clear absorption band at 2137 cm^{-1} , the same for all the PU foams (Hu *et al.*, 2002, Hatchett *et al.*, 2005, Stirna *et al.*, 2006). The presence of aromatic structures and isocyanurate rings in the PU are indicated with the absorption bands at 1597 and 1412 cm^{-1} , respectively, which agree with the initially chosen isocyanate index 130. The formation of cross-linked polymer network with urethane and isocyanurate nature chain fragments characterize the obtained PU rigid foams (Hatchett *et al.*, 2005). The adsorption band at 1220 cm^{-1} indicates CN vibrations of urethane groups (Javni *et al.*, 2000).

17.4 Conclusions

Novel PU polyols containing bio-based and recycled components were synthesized from the rapeseed and rPET pellets, correspondingly. The final polyols contained 33% of renewable part and 22% of recycle part. Functional additives ADA and GL were used in the synthesis to control the chain structure, branching and functionality of the polyol. PU polyols were characterized using various methods.

The presented results confirmed that PU polyols synthesized from RO and rPET can be successfully applied for obtaining the PU rigid foams. The modifications of polyol with GL and ADA improved the compression strength and elasticity properties of the obtained PU foams. The presence of RO fragments in the chain network increased PU rigid foams' cell size by approximately 30%.

Finally, the FTIR spectra confirm the assumption of higher mechanical properties for PU GL/ADA foam due to the stronger hydrogen bonding and higher concentration of ester and aromatic groups. PU GL/ADA-RO was plasticized by the presence of long aliphatic chains in the backbone.

Acknowledgements

The financial support of the European Regional Development Fund project Contract No 2014/0043/2DP/2.1.1.1.0./14/APIA/VIAA/063 is gratefully acknowledged.

References

- Ashida, K., *Polyurethane and Related Foams*, CRC Press, 2006.
- Atta, A. M., Brostow, W., Datashvili, T., El-Ghazawy, R. A., Lobland, H. E. H., Hasan, A. R. M. and Perez, J. M., Porous polyurethane foams based on recycled poly(ethylene terephthalate) for oil sorption. *Polym. Int.*, 62, 116–126, 2013.
- Awaja, F. and Pavel, D., Recycling of PET. *Eur. Polym. J.*, 41, 1453–1477, 2005.
- Babb, D. *Polyurethanes from Renewable Resources. Synthetic Biodegradable Polymers*. B. Rieger, A. Kunkel, G. W. Coates *et al.*, Springer Berlin Heidelberg. 245: 315–360, 2012.
- Bartolome, L., Imran, M., Lee, K. G., Sangalang, A., Ahn, J. K. and Kim, D. H., Superparamagnetic γ -Fe₂O₃ nanoparticles as an easily recoverable catalyst for the chemical recycling of PET. *Green Chem.*, 16, 279–286, 2014.
- Beneš, H., Slabá, J., Walterová, Z. and Rais, D., Recycling of waste poly(ethylene terephthalate) with castor oil using microwave heating. *Polym. Degrad. Stab.*, 98, 2232–2243, 2013.
- Beneš, H., Vlček, T., Černá, R., Hromádková, J., Walterová, Z. and Svitáková, R., Polyurethanes with bio-based and recycled components. *European Journal of Lipid Science and Technology*, 114, 71–83, 2012.
- Cakić, S. M., Ristić, I. S., Cincović, M. M., Stojiljković, D. T., János, C. J., Miroslav, C. J. and Stamenković, J. V., Glycolized poly(ethylene terephthalate) waste and castor oil-based polyols for waterborne polyurethane adhesives containing hexamethoxymethyl melamine. *Prog. Org. Coat.*, 78, 357–368, 2015.
- Carta, D., Cao, G. and D'Angeli, C., Chemical Recycling of Poly(ethylene terephthalate) (PET) by Hydrolysis and Glycolysis. *Environmental Science and Pollution Research*, 10, 390–394, 2003.
- Chen, F., Yang, F., Wang, G. and Li, W., Calcined Zn/Al hydrotalcites as solid base catalysts for glycolysis of poly(ethylene terephthalate). *J. Appl. Polym. Sci.*, 2014.
- Chen, J.-W. and Chen, L.-W., The glycolysis of poly(ethylene terephthalate). *J. Appl. Polym. Sci.*, 73, 35–40, 1999.
- Chethana, M., Madhukar, B. S., Siddaramaiah and Somashekar, R., Structure-property relationship of biobased polyurethanes obtained from mixture of naturally occurring vegetable oils. *Adv. Polym. Technol.*, 33, 2014.
- De Souza, V. H. R., Silva, S. A., Ramos, L. P. and Zawadzki, S. F., Synthesis and characterization of polyols derived from corn oil by epoxidation and ozonolysis. *IAOCS, Journal of the American Oil Chemists' Society*, 89, 1723–1731, 2012.
- Dutt, K. and Soni, R. K., A review on synthesis of value added products from polyethylene terephthalate (PET) waste. *Polymer Science - Series B*, 55, 430–452, 2013.

- Fakirov, S., *Handbook of Thermoplastic Polyesters*, Wiley-VCH Verlag, 2002.
- Goto, M., Koyamoto, H., Kodama, A., Hirose, T. and Nagaoka, S., Depolymerization of polyethylene terephthalate in supercritical methanol. *Journal of Physics Condensed Matter*, 14, 11427–11430, 2002.
- Güçlü, G. and Orbay, M., Alkyd resins synthesized from postconsumer PET bottles. *Prog. Org. Coat.*, 65, 362–365, 2009.
- Hamilton, A. R., Thomsen, O. T., Madaleno, L. A. O., Jensen, L. R., Rauhe, J. C. M. and Pyrz, R., Evaluation of the anisotropic mechanical properties of reinforced polyurethane foams. *Composites Science and Technology*, 87, 210–217, 2013.
- Hatchett, D. W., Kodippili, G., Kinyanjui, J. M., Benincasa, F. and Sapochak, L., FTIR analysis of thermally processed PU foam. *Polymer Degradation and Stability*, 87, 555–561, 2005.
- Hermanová, S., Šmejkalová, P., Merna, J. and Zarevúcka, M., Biodegradation of waste PET based copolyesters in thermophilic anaerobic sludge. *Polym. Degrad. Stab.*, 111, 176–184, 2015.
- Hu, Y. H., Gao, Y., Wang, D. N., Hu, C. P., Zu, S., Vanoverloop, L. and Randall, D., Rigid polyurethane foam prepared from a rape seed oil based polyol. *Journal of Applied Polymer Science*, 84, 591–597, 2002.
- Imran, M., Kim, D. H., Al-Masry, W. A., Mahmood, A., Hassan, A., Haider, S. and Ramay, S. M., Manganese-, cobalt-, and zinc-based mixed-oxide spinels as novel catalysts for the chemical recycling of poly(ethylene terephthalate) via glycolysis. *Polym. Degrad. Stab.*, 98, 904–915, 2013.
- Ionescu, M., *Chemistry and Technology of Polyols for Polyurethanes*, Rapra Technology, 2005.
- Islam, M. R., Beg, M. D. H. and Jamari, S. S., Development of vegetable-oil-based polymers. *J. Appl. Polym. Sci.*, 131, 9016–9028, 2014.
- Javni, I., Petrović, Z. S., Guo, A. and Fuller, R., Thermal stability of polyurethanes based on vegetable oils. *J. Appl. Polym. Sci.*, 77, 1723–1734, 2000.
- Kairyte, A. and Vejelis, S., Evaluation of forming mixture composition impact on properties of water blown rigid polyurethane (PUR) foam from rapeseed oil polyol. *Industrial Crops and Products*, 66, 210–215, 2015.
- Karayannidis, G. P. and Achilias, D. S., Chemical recycling of poly(ethylene terephthalate). *Macromol. Mater. Eng.*, 292, 128–146, 2007.
- Kathalewar, M., Dhopalkar, N., Pacharane, B., Sabnis, A., Raut, P. and Bhawe, V., Chemical recycling of PET using neopentyl glycol: Reaction kinetics and preparation of polyurethane coatings. *Prog. Org. Coat.*, 76, 147–156, 2013.
- Kirpluks, M., Cabulis, U., Kurańska, M. and Prociak, A., Three different approaches for polyol synthesis from rapeseed oil. *Key Eng. Mater.* 559: 69–74, 2013.
- Lee, C. S., Ooi, T. L., Chuah, C. H. and Ahmad, S., Rigid polyurethane foam production from palm oil-based epoxidized diethanolamides. *IAOCS, Journal of the American Oil Chemists' Society*, 84, 1161–1167, 2007.
- Lee, N., Kwon, O. J., Chun, B. C., Cho, J. W. and Park, J. S., Characterization of castor oil/polycaprolactone polyurethane biocomposites reinforced with hemp fibers. *Fibers and Polymers*, 10, 154–160, 2009.
- Li, C., Luo, X., Li, T., Tong, X. and Li, Y., Polyurethane foams based on crude glycerol-derived biopolyols: One-pot preparation of biopolyols with branched fatty acid ester chains and its effects on foam formation and properties. *Polymer*, 55, 6529–6538, 2014.
- Lligadas, G., Ronda, J. C., Galiá, M. and Cádiz, V., Plant oils as platform chemicals for polyurethane synthesis: Current state-of-the-art. *Biomacromolecules*, 11, 2825–2835, 2010.
- Luo, X. L. and Li, Y. B., Synthesis and Characterization of Polyols and Polyurethane Foams from PET Waste and Crude Glycerol. *J. Polym. Environ.*, 22, 318–328, 2014.
- Meier, M. A. R., Metzger, J. O. and Schubert, U. S., Plant oil renewable resources as green alternatives in polymer science. *Chemical Society Reviews*, 36, 1788–1802, 2007.

- Mosiewicki, M. A., Rojek, P., Michałowski, S., Aranguren, M. I. and Prociak, A., Rapeseed oil-based polyurethane foams modified with glycerol and cellulose micro/nanocrystals. *J. Appl. Polym. Sci.*, 132, 2015.
- Nikles, D. E. and Farahat, M. S., New motivation for the depolymerization products derived from poly(ethylene terephthalate) (PET) waste: A review. *Macromol. Mater. Eng.*, 290, 13–30, 2005.
- Orgilés-Calpena, E., Arán-Aís, F., Torró-Palau, A. M. and Orgilés-Barceló, C., Synthesis and characterisation of potentially biodegradable polyurethane adhesives from soybased polyols. *Polymers from Renewable Resources*, 5, 99–114, 2014.
- Paliwal, N. R. and Mungray, A. K., Ultrasound assisted alkaline hydrolysis of poly(ethylene terephthalate) in presence of phase transfer catalyst. *Polym. Degrad. Stab.*, 98, 2094–2101, 2013.
- Patel, M. R., Patel, J. V. and Sinha, V. K., Polymeric precursors from PET waste and their application in polyurethane coatings. *Polymer Degradation and Stability*, 90, 111–115, 2005.
- Petrovic, Z. S., Polyurethanes from vegetable oils. *Polym. Rev. (Philadelphia, PA, U. S.)*, 48, 109–155, 2008.
- Petrović, Z. S., Cvetković, I., Milić, J., Hong, D. and Javni, I., Hyperbranched polyols from hydroformylated methyl soyate. *J. Appl. Polym. Sci.*, 125, 2920–2928, 2012.
- Pfister, D. P., Xia, Y. and Larock, R. C., Recent advances in vegetable oil-based polyurethanes. *ChemSusChem*, 4, 703–717, 2011.
- Prisacariu, C., *Polyurethane Elastomers*, 2, Springer Vienna, 2011.
- Prociak, A., Rojek, P. and Pawlik, H., Flexible polyurethane foams modified with natural oil based polyols. *Journal of Cellular Plastics*, 48, 489–499, 2012.
- Roy, P. K., Mathur, R., Kumar, D. and Rajagopal, C., Tertiary recycling of poly(ethylene terephthalate) wastes for production of polyurethane-polyisocyanurate foams. *Journal of Environmental Chemical Engineering*, 1, 1062–1069, 2013.
- Rusen, E., Mocanu, A., Rizea, F., Diacon, A., Calinescu, I., Mititeanu, L., Dumitrescu, D. and Popa, A. M., Post-consumer PET bottles recycling: II. PET depolymerization using microwaves. *Materiale Plastice*, 50, 201–207, 2013.
- Saravari, O., Pathomwattanasak, K. and Pimpan, V., Synthesis of urethane oils from palm oil and waste PET bottles. *Journal of Applied Polymer Science*, 105, 1802–1807, 2007.
- Saravari, O., Vessabutr, B. and Pimpan, V., Synthesis of urethane oils from waste poly(ethylene terephthalate) bottles. *J. Appl. Polym. Sci.*, 92, 3040–3045, 2004.
- Shah, A. A., Kato, S., Shintani, N., Kamini, N. R. and Nakajima-Kambe, T., Microbial degradation of aliphatic and aliphatic-aromatic co-polyesters. *Appl. Microbiol. Biotechnol.*, 98, 3437–3447, 2014.
- Sinha, V., Patel, M. R. and Patel, J. V., Pet waste management by chemical recycling: A review. *J. Polym. Environ.*, 18, 8–25, 2010.
- Sonnenschein, M. F., *Polyurethanes: Science, Technology, Markets, and Trends*, John Wiley & Sons, 2014.
- Stirna, U., Beverte, I., Yakushin, V. and Cabulis, U., Mechanical properties of rigid polyurethane foams at room and cryogenic temperatures. *Journal of Cellular Plastics*, 47, 337–355, 2011.
- Stirna, U., Sevastyanova, I., Misane, M., Cabulis, U. and Beverte, I., Structure and properties of polyurethane foams obtained from rapeseed oil polyols. *Proceedings of the Estonian Academy of Sciences*, 55, 101–110, 2006.
- Stirna, U., Sevastyanova, I., Misane, M., Cabulis, U. and Beverte, I., Structure and properties of polyurethane foams obtained from rapeseed oil polyols. *Proc. Est Acad. Sci.*, 55, 101–110, 2006.
- Szycher, M., *Szycher's Handbook of Polyurethanes*, CRC Press, 2012.

- Thomas, S. and Visakh, P. M. Engineering and Specialty Thermoplastics: Polyethers and Polyesters: State-of-the-art, New Challenges and Opportunities. *Handbook of Engineering and Speciality Thermoplastics*, John Wiley & Sons, Inc.: 1–14, 2011.
- Vaidya, U. R. and Nadkarni, V. M., Polyester polyols from glycolyzed PET waste: effect of glycol type on kinetics of polyesterification. *J. Appl. Polym. Sci.*, 38, 1179–1190, 1989.
- Valero, M. F. and Gonzalez, A., Polyurethane adhesive system from castor oil modified by a transesterification reaction. *Journal of Elastomers and Plastics*, 44, 433–442, 2012.
- Viksne, A., Kalnins, M., Rence, L. and Berzina, R., Unsaturated polyester resins based on the PET waste glycolysis products by ethylene, propylene and diethylene glycols and their mixtures. *Polymer Recycling*, 5, 15–22, 2000.
- Vitkauskienė, I., Makuska, R., Stirna, U. and Cabulis, U., Synthesis and physical-mechanical properties of polyurethane- polyisocyanurate foams based on PET-waste-derived modified polyols. *Journal of Cellular Plastics*, 47, 467–482, 2011.
- Vitkauskienė, I., Makuška, R., Stirna, U. and Cabulis, U., Thermal properties of polyurethane-polyisocyanurate foams based on poly(ethylene terephthalate) waste. *Medziagotyra*, 17, 249–253, 2011.
- Welle, F., Twenty years of PET bottle to bottle recycling - An overview. *Resources, Conservation and Recycling*, 55, 865–875, 2011.
- Xu, W., Zhou, L. P., Sun, W. F., Zhang, J. R. and Tu, W. P., Effect of Difunctional Acids on the Physicochemical, Thermal, and Mechanical Properties of Polyester Polyol-Based Polyurethane Coatings. *J. Appl. Polym. Sci.*, 132, 10, 2015.
- Yeganeh, H. and Hojati-Talemi, P., Preparation and properties of novel biodegradable polyurethane networks based on castor oil and poly(ethylene glycol). *Polym. Degrad. Stab.*, 92, 480–489, 2007.
- Yue, Q. F., Xiao, L. F., Zhang, M. L. and Bai, X. F., The glycolysis of poly(ethylene terephthalate) waste: Lewis acidic ionic liquids as high efficient catalysts. *Polymers*, 5, 1258–1271, 2013.
- Zhang, C., Ding, R. and Kessler, M. R., Reduction of epoxidized vegetable oils: A novel method to prepare bio-based polyols for polyurethanes. *Macromol. Rapid Commun.*, 35, 1068–1074, 2014.
- Zhang, J., Gong, J., Shao, G., Qin, J. and Gu, Z., Biodegradability of diethylene glycol terephthalate and poly(ethylene terephthalate) fiber by crude enzymes extracted from activated sludge. *J. Appl. Polym. Sci.*, 100, 3855–3859, 2006.
- Zhang, J., Wang, X., Gong, J. and Gu, Z., A study on the biodegradability of polyethylene terephthalate fiber and diethylene glycol terephthalate. *J. Appl. Polym. Sci.*, 93, 1089–1096, 2004.
- Zlatanić, A., Lava, C., Zhang, W. and Petrović, Z. S., Effect of Structure on Properties of Polyols and Polyurethanes Based on Different Vegetable Oils. *J. Polym. Sci., Part B: Polym. Phys.*, 42, 809–816, 2004.

Biodegradable Polymers for Protein and Peptide Therapeutics: Next Generation Delivery Systems

Sathish Dyawanapelly^{1†}, Nishant Kumar Jain^{2†}, Sindhu KR^{2†}, Maruthi Prasanna³ and Akhilesh Vikram Singh^{4*}

¹*Department of Pharmaceutical Sciences and Technology, Institute of Chemical Technology, Matunga, Mumbai, India*

²*Department of Biosciences and Bioengineering, Indian Institute of Technology Bombay, Mumbai, India*

³*Research Center for Molecular Medicine and Chronic Diseases (CIMUS), University of Santiago de Compostela (USC), Santiago de Compostela, Spain*

⁴*Department of Materials Engineering, Indian Institute of Science (IISc), Bangalore, Karnataka, India*

Abstract

Over the past decades, therapeutic use of many protein and peptides are hampered by *in vitro* and *in vivo* stability, short-half life and immunogenicity. To address an unmet need of protein therapeutics, biologists and chemists together have invented polymer-protein conjugates. These polymer-protein therapeutics have successfully developed and investigated extensively with a variety of natural and synthetic biodegradable polymers such as poly (ethylene glycol), polysialic acid, polyglycerol, polyamidoamine, poly (methyl methacrylate), poly(hydroxyethyl methacrylate), poly(N-isopropylacrylamide), poly(ethylene glycol) methyl ether acrylate, poly(N-vinylpyrrolidone), dextran, dextrin, hyaluronic acid and hydroxyethyl starch. Polymer-protein therapeutics has attracted tremendous attention in the last few years. Such strategies have the potential to develop as next generation protein therapeutics. This chapter will highlight synthesis strategies, design concepts, recent progress, clinical studies and future prospects for protein-and peptide-polymer conjugates.

Keywords: Polymer conjugation, protein delivery, hyperglycosylation, PEGylation, protein, peptide

*Corresponding author: akhileshvikram@gmail.com

†These authors contributed equally to this work.

18.1 Introduction

Proteins as therapeutic agents includes endogenous proteins (cytokines, growth factors, enzymes, coagulation factors) and their blockers/inhibitors (soluble receptors, monoclonal antibodies and engineered forms of these proteins), which are clinically approved for the treatment of various diseases including cancer, autoimmune diseases and metabolic disorders (Krejsa *et al.*, 2006). For example, asparaginase (Elspar[®]) has been approved for treatment of acute myeloid leukemia. The global market of bioengineered protein drugs is expected to increase from \$151.9 billion in 2013 to about \$222.7 billion in 2019 (Yu *et al.*, 2015).

Over the past decades, therapeutic applications of many protein and peptides are hampered due to *in vitro* and *in vivo* instability, short-half life and immunogenicity. Importantly, enzymatic degradation (proteolysis) and rapid renal clearance of proteins and peptides from the body are major limitation for therapy (Pasut & Veronese, 2012). Any therapeutic protein for clinical use should have potent activity, negligible immunogenicity and a long circulation half-life.

In recent years, biologists and chemists together have developed polymer-protein conjugate to address an unmet need of protein therapeutics (Thakur *et al.*, 2016). The various categories of polymer therapeutics that have been explored till date include, polymer-drug conjugates, polymer-protein conjugates and polymer-antigen conjugates. Polymer-drug conjugates for targeted cancer therapy briefly explained in our previous publications (Dyawanapelly *et al.*, 2015, Singh *et al.*, 2015). Polymer therapeutics also has been reported to possess significant stability, improved safety, and efficacy in comparison to their native therapeutics (Kontermann, 2011). Furthermore, modification by polymer results in increased the circulation half-life, altered bio-distribution and enhanced water solubility of an active molecule like proteins (Gokarn *et al.*, 2012). These advantages have led to the successful development and regulatory approval of therapeutics in biotech and pharmaceutical industry.

The first polyethylene glycol (PEG) conjugated protein was approved by FDA for routine clinical use in the early 1990s. PEGylated proteins conjugates has led to the development of numerous therapeutics, including PEG-asparaginase (Oncaspar[®]) for acute lymphoblastic leukemia (ALL), PEG-adenosine deaminase (Adagen[®]) for severe combined immunodeficiency disease (SCID), PEG-interferon α -2a (Pegasys[®]) for hepatitis C, PEG-interferon α -2b (PEG-Intron[®]) for hepatitis C. Moreover, PEG-granulocyte colony-stimulating factor (G-CSF) (Neulasta[®]) was developed for treatment of neutropenia during chemotherapy, and PEG-growth hormone receptor antagonist (Somavert[®]) for acromegaly (Veronese & Pasut, 2005, Larson & Ghandehari, 2012). For example, in order to improve the stability and pharmacokinetic profile of uricase, PEG-uricase conjugations are developed by linking uricase to the distal ends of linear PEGs.

18.2 Protein Therapeutics and Their Challenges

18.2.1 Asparaginase

L-asparaginase is a one of the cornerstones of multi-drug combination chemotherapy for the treatment of acute lymphoblastic leukaemia (ALL) in children and young adult

patients (van der Meer *et al.*, 2014). This asparaginase enzyme interferes with protein synthesis by delaminating asparagine and glutamine results in cell death as lymphoblasts are deficient in asparagine synthetase (Angiolillo *et al.*, 2014).

Native *Escherichia coli* (*E. coli*) L-asparaginase has a shorter half-life and is immunogenic *in vivo*. Its use has been limited by most frequent and serious hypersensitivity reaction and development of anti-asparaginase antibodies, which neutralize their activity. However, PEG-asparaginase has a longer half-life and is potentially less immunogenic and can be more feasibly administered intravenously than native L-asparaginase (Fu and Sakamoto, 2007, Angiolillo *et al.*, 2014). Moreover, deamination of asparagine into aspartic acid results in rapid and complete depletion of serum asparagine (Place *et al.*, 2015). In a recent study, Angiolillo *et al.*, have investigated pharmacokinetic and pharmacodynamic comparability studies between PEG-asparaginase (SS-PEG) and Calaspargase PEGol (SC-PEG) in patients with acute lymphoblastic leukemia (ALL) (Angiolillo *et al.*, 2014). Both SS-PEG and SC-PEG were the PEGylated forms of *Escherichia coli* L-Asparaginase with a succinimidyl succinate (SS) and succinimidyl carbamate (SC) linker, respectively. Studies indicated that SC-PEG showed 2.5 fold prolonged half-life of asparaginase compared to SS-PEG.

18.2.2 Adenosine Deaminase

Adenosine deaminase (ADA) is an important enzyme of the purine salvage pathway, which converts adenosine/deoxyadenosine into inosine/deoxy inosine and ammonia. It can be used clinically for enzyme replacement therapy in ADA deficiency. Deficiency of ADA enzyme leads to toxic accumulation of the enzyme substrates such as adenosine and deoxyadenosine in immature lymphoid cells. A result in “severe combined immunodeficiency (SCID),” the immune system of the afflicted individual is severely compromised or completely lacking (Filpula and Sapra, 2014). Furthermore, a PEGylated form of adenosine deaminase (PEG-ADA) has been developed to improve safety and efficacy of adenosine deaminase by prolonging half-life (3–6 days in human) and reducing immunogenicity compared to native enzyme (half-life = 30 min) (Davis, 2003).

18.2.3 Granulocyte Colony-Stimulating Factor

Granulocyte colony-stimulating factor (G-CSF) is an endogenous hematopoietic growth factor which enhances phagocytic activity, anti-microbial activity, antibody-dependent and cell mediated cytotoxicity. Recombinant human granulocyte colony-stimulating factor (rhG-CSF), Neupogen® (filgrastim, Amgen) have been approved for the treatment of neutropenia (low neutrophil counts) during cancer chemotherapy (Shin *et al.*, 2014). Due to rapid clearance from the body, it shows very short half-life (3.5–3.8 h). To extend the half-life of G-CSF, scientists have been developed PEGylated G-CSF (PEGfilgrastim, Neulasta®, Amgen), which increases its stability (Son *et al.*, 2012).

18.2.4 Anti-Tumor Necrosis Factor

Anti-tumor necrosis factor (anti-TNF) antibodies have been used to treat inflammatory bowel diseases. For example, Infliximab, the anti-TNF antibody has been approved

for Crohn's disease treatment (Bourne *et al.*, 2008). However, its use was limited by immunosuppression in clinical use. To overcome limitations of anti-TNF- α , PEGylated humanized anti-TNF fragment (CDP870) was developed (Choy *et al.*, 2002). It has been used in the treatment of Crohn's disease and rheumatoid arthritis.

18.2.5 Interferons

Interferons (INFs) are a class of cytokines that has an essential function in the regulation of cell growth and differentiation via activation of a cascade of intracellular pathways. These INFs possess antiviral, immunomodulatory, and antiproliferative activity, which are indicated for the treatment of melanoma, hepatitis B and C (Osborn *et al.*, 2002). The safety, pharmacokinetic and pharmacodynamic profiles, and antiviral efficacy of PEGylated INF- α 2b monotherapy was investigated in chronic hepatitis C patients ($n = 58$). Clinical results showed 10-fold greater elimination half-life (35–72 h) than that of non-PEGylated INF- α 2b (3–8h) (Glue *et al.*, 2000). Pegylated INF- α (PEG INF- α) has replaced conventional INF- α formulations in the treatment of chronic hepatitis C (Reddy, 2003). Similarly, to decrease dosing frequency and to increase the pharmacokinetic profile of INF- α was fused to human serum albumin, Albuferon (Osborn *et al.*, 2002).

Furthermore, Interferon- β has been approved for treatment of relapsing multiple sclerosis (Calabresi *et al.*, 2014). To improve the safety, tolerability and pharmacokinetics of INF- β , PEGylated INF- β -1a conjugates were developed and investigated for the potential first-line treatment of relapsing multiple sclerosis (Kieseier & Calabresi, 2012, Hu *et al.*, 2012).

18.2.6 Growth Hormone Antagonist

Clinically growth hormone antagonist (GHA) is used for the treatment of acromegaly. It acts by inhibiting hyper-secretion of growth hormone. However, therapeutic use of GHA is limited due to short half-life (15–20 min) and instability. FDA approved multi-PEGylated GHA, (Pegvisomant, Pfizer Inc., USA) that exhibited prolonged plasma half-life (~ 72 h) and decreased dosing frequency compared to native protein (Wu *et al.*, 2013).

18.2.7 Uricase

Recombinant uricases are potent hypouricaemic agents for tophaceous gout patients. To improve half-life and to reduce immunogenicity of uricase, PEGylated recombinant mammalian uricase (Puricase[®]) was developed jointly by Mountain View Pharmaceuticals, Inc., Duke University and Savient Pharmaceuticals, Inc (Sherman *et al.*, 2008). Moreover, PEGylated uricase has 6–14 days of plasma half-life and decreased immunogenicity (production of anti-uricase antibody) in human (Tsuji *et al.*, 1985). Rasburicase (recombinant fungal uricase) and pegloticase (monomethoxyl- PEGylated recombinant mammalian uricase) are approved for treatment of hyperuricemia (Yang *et al.*, 2012b). Recently, uricase was conjugated with polysialic acid (PSA) to improve the pharmacological effect of the enzyme *in vivo* (Punnappuzha *et al.*, 2014).

18.2.8 Erythropoiesis Stimulating Agent

Erythropoietin is a glycoprotein hormone, which maintains erythropoiesis and homeostasis in mammals by regulating the cell proliferation, differentiation, and survival of erythroid progenitor cells (Woodburn *et al.*, 2012). Recombinant human erythropoietin and its protein variants are clinically used for the treatment of chronic kidney disease (CKD)-associated anemia. More importantly, an erythropoiesis-stimulating agent (ESA) restores the appropriate stimulatory signal to erythroid progenitor cells located within the bone marrow, thereby treating the anemia, reducing the incidence of secondary sequelae (Woodburn *et al.*, 2012).

In one study, peginesatide, a novel PEGylated peptide-based ESA has been developed with a prolonged half-life and slow clearance rate which is used for the treatment of anemia associated with CKD (Fan *et al.*, 2006). Currently, hyperglycosylated recombinant human EPO (rHuEPO) analogues (for example, Darbepoetin alfa, AMG 114 and AMG 205) and PEGylated rHuEPO (for example, Pegzyrepoetin alfa and MK-2578) have been developed and used for the treatment of anemia associated with CKD (Sinclair, 2013).

18.3 Biodegradable Polymers for Conjugation

Biodegradable polymers have extensive applications in therapeutic or biomedical platforms (Thakur & Thakur, 2014a, b). They can be used for the delivery of therapeutics such as drugs, protein, enzymes, nucleic acids and antigens/vaccines for treating various diseases ((Voicu *et al.*, 2016; Pappu *et al.*, 2015). This polymer therapeutics can protect the active molecules from enzymatic degradation, modify the pharmacokinetic profile of therapeutics, and decrease the side effects and/or increase the *in vivo* safety and efficacy. Among all the polymers, biodegradable, biocompatible, non-toxic and non-immunogenic polymers are highly recommended for biomedical research application (Riva *et al.*, 2011).

Over the past few decades, many therapeutics have been conjugated with various biodegradable polymers such as

1. **Synthetic polymers:** Poly (ethylene glycol), N-(2-hydroxypropyl)-methacrylamide copolymers (HPMA), HPMA copolymers, poly (ethyleneimine) (PEI), poly (acryloyl morpholine) (PACM), poly (vinylpyrrolidone) (PVP), polyamidoamines, divinylethermaleic anhydride/acid copolymer (DIVEMA), poly (styrene-co-maleic acid/anhydride) (SMA), polyvinyl alcohol (PVA)
2. **Bio polymers:** Albumin, chitosan, dextran, dextrin, hyaluronic acid, pullulan, gelatin and its derivatives
3. **Pseudosynthetic polymers:** Poly glutamic acid, poly (L-lysine), poly (malic acid), poly (aspartamides), poly ((N-hydroxyethyl)- L-glutamine) (PHEG) and poly (styrene-co-maleic acid/anhydride) (SMA) (Jung and Theato, 2013, Pasut and Veronese, 2007). Among all polymers available to be used for conjugation, PEG is one of the most commonly studied polymers for polymer-protein and polymer-drug conjugations.

A variety of polymers and their interaction with proteins are discussed in the following sections: PEG, poly-sialic acid, polyglycerols (PG), PAMAM, porphyrin, hydroxy-ethyl starch, dextran, dextrin hyaluronic acid and other polymer-protein therapeutics.

18.4 PEGylated Protein Therapeutics

Protein and peptides have been explored greatly as a therapeutic agent in the treatment of several human diseases. Approximately more than 300 polypeptide drugs are undergoing in clinical trials and more than 80 drugs are marketed in the United States (Harris & Chess, 2003). The driving force for their use in pharmaco-therapy is the ability to mimic the endogenous hormones and antibodies. However, inherent instability of protein and peptides, both structurally and chemically, have hampered the development of peptide and protein drugs. One reason for instability is low bioavailability, size and hydrophilic nature of peptides. Despite of above mentioned limitations, a number of recent technological breakthrough and advances have incited major interest in their usage as a therapeutic agent. One such advancement in modifying the properties of protein and peptides is PEGylation, which has opened a new technology in developing pharmaceutical formulations (Uhlig *et al.*, 2014).

PEGylation defines the modification of a protein and peptide by linking of one or more PEG chain. The first PEGylation was described in the 1970s on albumin and catalase modification, which was an important milestone for the development of protein and peptides as a therapeutic agent. Since then, the PEGylation procedure was expanded and developed tremendously. Various commercially available polyethylene glycol-protein conjugates are listed in Table 18.1, includes PEG conjugates of adenosine deaminase, asparaginase, IFN- α 2B, IFN- α 2A, G-CSF, Anti-VEGF aptamer and GH-antagonist. It plays a very important role in drug delivery; enhancing the properties of proteins and peptides as a therapeutic agent. The polymer PEG used for PEGylation is biologically inert and non-immunogenic chemical that confers increased solubility to proteins. Although other polymers, such as dextran, had been explored to overcome the limitations of protein, PEG was preferred for protein modification as it was already approved by FDA for body-care products and as excipient in many pharmaceutical formulations (Pasut & Veronese, 2009).

18.4.1 Basic Features and Properties of PEG

PEG possesses several properties that make it suitable candidate in various biological, chemical and pharmaceutical applications (Veronese & Pasut, 2005):

- It is non-toxic and non-immunogenic, which can be attached to surfaces of the particles and conjugated to molecules without interfering with cellular functions or target immunogenicity.
- Hydrophilic-attachment of PEG to proteins, peptides and biomolecules can decrease the aggregation and increase the solubility.
- Their high flexibility can provide surface treatment or bioconjugation without any steric hindrance.

Table 18.1 Commercial polyethylene glycol-protein conjugates (Pasut and Veronese, 2012).

Parent drug	Conjugate	Commercial name	Application	Approved year	Improvements	Pharmacokinetic parameters	Pharmacodynamic parameters
Adenosine deaminase	PEGadamas	Adagen®	SCID	1990	Proteolytic protection, reduced immunogenicity	Increased half-life and sustained absorption	Improved sustained response
Asparaginase	PEGasparginase	Oncaspar®	Leukaemia	1994	Reduce immunogenicity	Increased half-life	Improved sustained response
IFN- α 2B	PEG-interferon- α 2b	PEG-INTRON®	Hepatitis C	2000	Increase size to slow renal clearance	Sustained absorption Increased half-life (from 3–8 h to 65 h) Decreased volume of distribution Decreased systemic clearance	Antitumor activity increase 18 fold Improved sustained response to chronic hepatitis
IFN- α 2A	PEG-interferon- α 2a	PEGASYS®	Hepatitis C	2001	Increase size to slow renal clearance	Sustained absorption Increased half-life (from 3–8 h to 65 h) Decreased volume of distribution Decreased systemic clearance	Improved sustained response to chronic hepatitis

(Continued)

Table 18.1 Cont.

Parent drug	Conjugate	Commercial name	Application	Approved year	Improvements	Pharmacokinetic parameters	Pharmacodynamic parameters
G-CSF	PEGfilgrastim	Neulasta®	Neutropenia	2002	Increase size to slow renal clearance	Increased half-life (1.8h–7 h)	14 fold longer effect in sustaining neutrophil count in rat
Anti- VEGF aptamer	PEGaptanib	Macugen®	Age related macular degeneration	2004	Increase size to slow renal clearance Slow diffusion away from site of action in vitreous humor	Increased half-life (0.33–9 h)	3 fold increased inhibition of VEGF induced vascular permeability in guinea pigs
GH-antagonist	PEGvisomant	Somavert®	Acromegaly	2003	Protection from proteases	Increased half-life (15 min–10 h)	Improved sustained response

PEG: Polyethyleneglycol; SCID: Severe combined immunodeficiency; IFN: Interferon; G-CSF: Granulocyte colony stimulating factor; VEGF: Vascular endothelial growth factor; GH: Growth factor.

- Polymer having specific molecular weight (low/high) with narrow polydispersity can be synthesized.
- Possess only one terminal functional group, which makes ideal for protein modification without risk of cross-linking.
- Being hydrated polymer makes it ideal to mask sites of the protein responsible for immunogenicity.

The mentioned properties of PEG enables in modifying the properties of the biomolecule. PEG attachment modifies pharmacokinetic and pharmacodynamics properties of proteins and peptides by conveying its Physico-chemical properties to the biomolecules. Conjugation of the polymer can accomplish several desirable objectives: increases the hydrodynamic volume conferred to conjugated molecules, thus reducing its renal clearance; degradation by proteolytic enzymes is reduced by preventing the approach of antibodies or antigen presenting cells (APC), modification of electro-osmotic flow, reduction of protein opsonization, increased pH and thermal stability. Therefore PEGylation is of interest in pharmaceutical technology, where many insoluble and unstable drugs or biomolecules can be more easily administered. The different aspects of PEGylation with emphasis on protein and polypeptide conjugation with specific problems encountered during PEG conjugation and their clinical aspects, which has been discussed briefly in the next section.

18.4.2 Critical Factors for Protein PEGylation: PEG Structure and Size

The choice of PEG is based on their ease to activate and conjugate with the proteins. To attain desired properties without altering the proteins biological activity, the structure and size of PEG plays a significant role in conjugation. For a long time 5kDa sized PEG end capped with a methoxy group and terminated with a hydroxyl group was in use, later conjugation was complicated due to a significant amount of diol impurities in the sample which leads to inter or intra- molecular cross-linking reactions. To overcome these shortcomings a low polydispersity, activated, very-high molecular weight polymer 30–40kDa was introduced at the end of the 1990s, which was more suitable for medical applications, as it offers better protection for protein (Veronese & Mero, 2008).

18.4.3 Chemistry and Different Sites of PEGylation

PEG derivatives are of two types. One is linear PEG chain which can effectively prolong the circulation time of PEGylated protein *in-vivo*, but enables potential alteration, when PEGylated proteins interact with their molecular targets. The second is branched methoxy PEG derivative that has one linking end but many PEG chains with free ends, which avoids unfavorable alterations when the PEGylated proteins interacts with their molecular targets (Martin & Modi, 2001). The steric hindrance is the major factor, which often reduces the bioactivity of proteins at the binding region of the molecule. Thus use of fewer PEG chains of higher molecular weight results in reduced loss of activity, as it avoids interference with amino acids that are essential for receptor binding. Further, the decreased binding increases the circulation time of conjugated protein (Chapman, 2002).

Functional group for selective PEGylation

1. **S-alkylation of thiol groups:** Maleimide and iodoacetamide are selective for S-alkylation at the linking ends under neutral conditions. Disulfides are specific for thiol groups in the linking ends.
2. **N-acylation of amino groups:** Activated carboxyl esters are essential for linking the ends under alkaline condition.
3. **N-alkylation:** Aldehyde, epoxide, Trifluoromethane sulfonate, 2, 6-dichlorotriazole are effective at the linking ends. N-alkylation is better than N-acylation when the electrostatic interaction is essential for activity and stability of the therapeutic protein.

18.4.3.1 PEGylation of Amine Group

The most common reactive group for PEGylation is α -NH₂ and ϵ -NH₂ group of lysine, since amino groups are most abundantly available on the protein surface. The PEG-polymer conjugation can be done either by acylation and alkylation. Alkylation maintains a positively charged amine, whereas acylation gives a neutral amide. The substitution of amino group with neutral side chains such as asparagine, glutamine, serine, and threonine, with lysine residues can introduce additional amino groups for PEGylation.

- i. **First-generation of PEG derivatives:** First generation PEGylation techniques generally use linear PEGs with low molecular weight (<12KDa) forming multiple PEG isomers. PEG derivatives that are involved in protein PEGylation are (a) PEG p-nitrophenyl carbonate, (b) PEG tresylate, (c) PEG succinimidyl carbonate, (d) PEG benzotriazole carbonate, (e) PEG dichlorotriazine, (f) PEG trichlorophenyl carbonate, (g) PEG carbonylimidazole and (h) PEG succinimidyl succinate. Generation of PEG diol impurities, unstable linkage, high molecular weight and lack of selectivity in the modification are the major limitations of first generation derivative. Despite these limitations several first generation PEGylated drugs such as pegylated adenosine deaminase, pegasparginase received regulatory approval and are still in use.
- ii. **Second generation of PEG derivatives:** They have been designed to overcome the shortcomings of the first generation. mPEG-propionaldehyde and mPEG-acetaldehyde are commonly used derivatives, since aldehyde having lower pK_a is largely selective for N-terminal alpha-amine. mPEG-propionaldehyde has been used for PEGylating G-CSF, TNF and IFN(Zhang *et al.*, 2012).

18.4.3.2 PEGylation of Thiol Group

As amino groups are abundantly available on the surface of therapeutic protein, creates steric hindrance from the linked PEG chains which results in the production of

modification isomers, whose purification is difficult. On the other hand, the thiol groups are rarely available on the surface and are easily PEGylated selectively via S-alkylation under neutral conditions. This approach offers an advantage of site-specific PEGylation that will minimize the loss in biological activity.

Due to their low abundance, thiol group neither masks all immunogenic sites of exogenous therapeutic protein nor increases their effective size for longer circulation. The aforementioned limitation can be circumvented by PEGylation of both amino groups and thiol groups via alkylation by controlling the modification isomers.

18.4.3.3 Disulfide Bridging PEGylation of Proteins

Most of the therapeutic proteins do not possess free cysteine for site specific conjugation; rather it has paired even numbered cysteine to form disulfides to compensate relatively lower number of hydrophobic interaction. Solvent accessible disulfide which is usually present in the small proteins can be reduced chemically to its two free cysteine sulfur atoms, without altering its tertiary structure. To reconnect the two cysteine sulfur atoms via three carbon bridges, PEGylation could be done by bis-alkylation (Brocchini *et al.*, 2008). Examples of disulfide bridging PEGylation: therapeutic proteins that have been examined for disulfide bridging include cytokines such as PEGylated interferon α -2 and G-CSF and antibody fragments.

18.4.4 Enzymatic PEGylation

The selectivity of PEGylation is increased specifically to a single or few amino acid residues in the native protein by the utilization of the properties of the enzymes such as transglutaminases (TGase) and glycosyltransferase.

TGase are a group of enzymes originating from prokaryotes or eukaryotes acting at glutamine side chain. PEG-NH₂ is linked to glutamine residues of the protein by TGase. TGase needs specific amino acid sequence and flexibility of the substrate for its activity. The modification of glutamine residue by chemical methods is difficult, it may involve labeling other residues or either degrading the protein structure. Therefore, usually only one or two out of several glutamines in a protein, possess the prerequisites for TGase catalysis. Moreover, O-(N-acetylgalactosamin)-transferase and sialyl-transferase enzymes have been used for PEGylation, the process which is known as “glycop-egylation” (Bezuglov *et al.*, 2009). These enzymes are employed to link the amino acids threonine and serine.

18.4.4.1 Proteins Modified by TGase PEGylation

- i. **Apomyoglobin:** It consists of 153 amino acid residues that have been used as a model protein by many investigators for folding and stability.
- ii. **α -lactalbumin:** It is a calcium binding protein, essential for the biosynthesis of lactose in the mammary gland. It is extensively used as a model protein for folding and stability studies.
- iii. **Human growth hormone (hCH):** It is a polypeptide hormone consisting of 191 amino acids residues possessing several biological activities

such as growth, lactation and activation of macrophages. This protein has a short half-life, requires repeated administration to maintain the plasma concentration. PEGylation of hCH showed better pharmacokinetic parameters (DeFrees *et al.*, 2006, Fontana *et al.*, 2008).

18.4.5 PEGylation of Proteins Containing Unnatural Amino Acid

Incorporation of unnatural amino acid at specific site is a versatile tool for modification of the proteins. This technique need an amber suppressor tRNA, that carry the desired unnatural amino acid that can recognize an amber stop codon (i.e. TAG triplet). Incorporation of several such unnatural amino acids into proteins was performed for different modification purpose. P-acetyl-L-phenylalanine and p-azidophenylalanine have been used for PEGylation of proteins. The former reacts selectively with hydrazine-PEGs or amine-oxyPEGs, while the latter can be coupled with alkyne-PEG. One such example of the technique is hCH. The conjugate PEG-hGH has been already tested in clinical phase I-II (Cho *et al.*, 2011, Deiters *et al.*, 2004, Pasut & Veronese, 2012).

18.4.6 Non-Covalent PEGylation

The covalent PEGylation is capable of affecting the protein activity and also requires purification step, which reduces the recovery of conjugate. The non-covalent PEGylation has been proposed to circumvent the aforementioned limitation of covalent PEGylation. The hydrophobic pockets of proteins can bind hydrophobic molecules leading to PEG/protein interaction. PEG-tryptophan and PEG-dansyl were developed to exploit these interactions and they effectively reduced the aggregation of a model peptide, salmon calcitonin (sCT), during their storage. These derivatives have been proposed for their use as new excipients and this PEG/protein interaction is unknown so far it is maintained *in vivo*, as the sCT competitive displacement might occur with serum proteins (Mero *et al.*, 2011).

18.4.7 Releasable of PEGylation

Chemically designed linkers are employed in releasable PEGylation that tether PEG to drugs. Releasable PEGylation shows controlled release mechanism via shedding of covalently attached PEG strands, which provides benefits for the small molecules that are susceptible to steric crowding. Hence linker selection plays an important role in controlling physical and structural properties. The design of a particular linker related to the preferred amino acid chain on protein. Primary amines containing lysine and N-terminal amine are most convenient nucleophile for attachment of activated linkers.

Hydrolisable linker should fulfill the criteria that, after cleavage it does not leave any moiety attached to the protein. Differently, the linked residue might trigger an immunogenic response by acting as an epitope. Furthermore, it is important to control the rate of protein release for optimizing the pharmacodynamic response.

The following are the different types of linkers

18.4.7.1 Aromatic Linkers (BE Series)

The benzyl elimination system behaves as a double prodrug, where hydrolysis results in the initial release of PEG polymer followed by BE elimination. PEG BE linkers are ideal candidates for controlled release of amino containing biological agents.

18.4.7.2 Synthetic BE Linkers

Synthetic BE linkers were synthesized as N- hydroxysuccinimidyl activated carbonates. These are designed specifically to react with an amine of alkyl terminus. The design demonstrates controlled release of the protein by reducing the rate of hydrolysis of the PEG. However, BE series of releasable linkers showed prolonged stability when stored at 4 °C.

18.4.7.3 Aliphatic Linkers (Bicin Linkers)

N-modified bis-2- hydroxyethylglycinamide (bicin) have been examined as self-immolating linkers for rPEGylation. de-PEGylation of bicin linkers takes place by cyclization after hydrolysis. The conjugates showed controlled protein release via the number of conjugated mPEG chains. Altering the structure of the ester trigger could be used to control the intrinsic rate of de-PEGylation, which would be valuable in the case of monoPEGylated bioconjugates.

18.4.7.4 B-alanine Linkers

However, rPEGylation strategy is based on a β - alanine spacer between mPEG and the protein. Partial de-PEGylation was observed by the hydrolysis of the amide bond between mPEG and the protein. For effective rPEGylation and full release of the protein, temporary protecting groups on protein amino and phenol groups are required, so that the polymer is selectively conjugated on the histidine residues (Filpula & Zhao, 2008, Gong *et al.*, 2015, Pasut & Veronese, 2012).

18.4.8 Pharmacology of PEGylation

PEGylation of protein prolongs the circulation time by two principals; reducing its clearance and increasing the protection from proteolytic degradation. The mechanisms are as follows (Fishburn, 2008).

- Kidney clearance occurs for compounds having molecular weight approximately 20kDa above which its renal filtration reduces and hepatobiliary clearance dominates. PEGylation of protein increases its molecular weight (50kDa), thereby reduces the renal clearance rates leads to the prolongation of circulation time.
- PEG provides protection from the proteases and peptidase by impairing the access for proteolytic enzymes and enables the high affinity interactions between the target receptor and protein moiety for effective biological activity.

18.4.9 Emerging PEGylated Drugs

Research groups are striving to improve the consistencies of protein drugs using PEGylation technologies, so as to target the ever-increasing range of medication (Kang *et al.*, 2009). For clinical status of currently developed polyethylene glycol-protein conjugates, see Table 18.2.

18.4.9.1 PEGylated hCH (ARX-201)

It is the leading product of growth hormone. Preclinical data showed an effective increase in the mouse body weight after a single dose of 2.1mg/kg which is equivalent to the daily dose of hCH at 03mg/kg for 8days.

18.4.9.2 PEG-G-CSF (DA-3031)

Pegfilgrastim is formed by utilizing 20-kDa linear PEG, whereas the DA-3031 is the product of 23-kDa PEG which is bound to four lysine residues of G-CSF. Pharmacokinetic data revealed that the PEG-G-CSF has 2.7 to 11 fold greater than the native G-CSF and Pegfilgrastim.

18.4.9.3 PEG-IFN- α -2a (DA-3021)

It is a product of IFN- α -2a with 43.5-kDa branched PEG. Pharmacokinetic parameters showed better half-life, T_{max} and C_{max}.

18.4.9.4 PEG-GLP-1

Glucagon- like peptide (GLP) is used in the treatment of type II diabetes, which has potent hypoglycemic efficacy, but it is degraded rapidly by dipeptidyl peptidase-IV (DPP-IV). The 2-kDa mPEG-succinimidyl propionate derivative is used to modify the Lys of GLP-1 which prolonged its half-life.

18.4.9.5 PEG-Growth Hormone Releasing Factor (PEG-GRF)

Growth hormone releasing factor, which stimulates the release of somatropin, is readily excreted by the kidneys. Trials are underway to increase its half-life by coupling PEG to Lys (21) of GRF (D'antonio *et al.*, 2004).

18.4.9.6 PEG-Salmon Calcitonin

Salmon calcitonin (sCT) is used to treat Osteoporosis and Paget's disease. Attempts have been successfully made to improve its biological activity and to find alternative routes of administration by PEGylation at Lys (18) of calcitonin.

18.4.9.7 PEG-Uricase

Numerous attempts have been made by the administration of uricase to treat gout and hyperuricemia, whereas immunogenicity was expressed in the treated group as the uricase was extracted from various sources. Attempts have been made to circumvent the

Table 18.2 Clinical status of currently developed polyethylene glycol-protein conjugates.

Polyethylene glycol (PEG) conjugate	Size o PEG moiety (kDa)	Status	Indication	Advantages	Reference
PEG-hGH/ARX-201	30	Phase III	Growth disorder	Significantly increased the body weight compared to the IGF-1	Jung Seok Kang <i>et al.</i> , 2009
PEG-G-CSF/DA-3031	23	Phase II	Neutropenia	Revealed greater half-life and AUC than pegfilgrastim	Jung Seok Kang <i>et al.</i> , 2009
PEG-IFN- α -2a/DA-3021	43.5	Phase I	Hepatitis C virus	Showed greater T_{max} , C_{max} , $t_{1/2}$ and AUC values than IFN- α -2a	Jung Seok Kang <i>et al.</i> , 2009
PEG- Uricase	20	Phase III	Gout	Higher specific enzyme activity and longer half-life than both uricase-PEG-5 and native uricase	Bomalaski JS <i>et al.</i> , 2002
PEG-GLP-1	2	–	Type II Diabetes	Improved glucose stabilization in blood	Lee SH <i>et al.</i> , 2005
PEG-arginase/BCT-100	20	Phase III	Cancer	Suppress ornithine transcarbamylase (OTC), argininosuccinate synthetase (ASS)	Cheng PN <i>et al.</i> , 2007
PEG-glutaminase	–	Phase II	Solid tumor	Increased uptake of DNA synthesis antagonist	2008
PEG- recombinant staphylokinase variant	–	Phase III	Thrombosis	Exhibited a thrombolytic effect similar to that of tissue-type plasminogen activator	2006

PEG: Polyethyleneglycol; hGh: Human growth hormone; IGF: Insulin like growth factor; G-CSF: Granulocyte colony stimulating factor; AUC: Area under the curve; IFN: Interferon; GLP: Glucagon like peptide; OTC: Ornithine transcarbamylase; ASS: Argininosuccinate synthetase.

immunogenicity by PEGylation of uricase. Uricase-PEG-20, which is under clinical trial, shows less immunogenicity and longer half-life compared with uricase-PEG-5 and native uricase (Sherman *et al.*, 2008).

18.4.9.8 PEG-arginine Deiminase (ADI)

Arginine is synthesized via interstitial-renal axis. Deficiency of arginine in tumor cells leads to death of the cells; therefore arginine degrading enzymes are reported to exhibit tumoricidal activity. Arginine deiminase is one of those arginine degrading enzymes that are more effective than L-asparaginase. PEG-20 is used for PEGylating ADI to overcome shorter half-life and *in-vivo* antigenicity. ADI-PEG-20 successfully reduced the arginine levels in hepatocellular carcinoma.

18.4.10 Limitations of PEGylation

- PEG cloud barrier suppress their interaction with cells thereby blocking the cellular uptake.
- The degradation products of PEG accumulate in the lysosomes inducing *in vivo* toxicity.
- Repeated injection of PEG based carriers induces production of anti-PEG IgM mediated complement activation that enhances the blood clearance and this phenomenon is called “accelerated blood clearance (ABC).”

18.4.11 Emerging Techniques Alternative to PEGylation

Future advances in PEGylation can be made by overcoming the limitations by increasing biodegradability and altering their high viscosity at high molecular weight. Few such studies are already been done on branched and hyper-branched PEGs for these purposes. As an alternative to PEGylation for protein conjugation, other new techniques with the polymers like hyaluronic acid, hydroxy-ethyl-starch (HESylation), polyoxazoline (POZylation), and polysialic acid (PolyXen) have been emerging other alternatives. The clinical investigation of such conjugates using similar approaches will offer the promising potentials to explore the alternative polymers (Viegas *et al.*, 2011, Gregoriadis *et al.*, 2005, Mero *et al.*, 2008).

18.5 Glycosylation of Proteins

Most of the therapeutic proteins are characterized by poor physicochemical as well as pharmacological properties which mainly include stability, shorter half-life and limited biological activity. Currently, glycoengineering is one of the most promising protein modification strategies where one or more sugar molecules are covalently bound on the polypeptide backbone. Hence, Glycoproteins represent the major share of marketed and clinical development phase therapeutic proteins. The nature of the carbohydrate (glycan) component linked to the protein plays an crucial role in guiding the

molecular stability, solubility/bioavailability, biological activity, immunogenicity, and pharmacokinetic profile of the glycoprotein (Li & d'Anjou, 2009). It is also one of the most extensively investigated and prevalent post-translational peptide modification strategies that the proteins undergo in the body (Pisal *et al.*, 2010). Protein glycosylation exhibits heterogeneous pattern regarding the position of glycan attachment as well as glycan's structure. Apart from this, the same protein may display a different number of surface glycans attached to a single glycosylation site (Sola & Griebenow, 2010). Glycoengineering of therapeutic proteins may produce neutralizing antibodies due to immune recognition of the mutated amino acid sequence (Li & d'Anjou, 2009).

18.5.1 Types of Glycosylation *In vivo*

Glycopeptide bonds can be classified based on the sugar-peptide bond present between the sugar unit and peptide molecule. It has been reported that around 13 different monosaccharides and 8 amino acid types are involved in the formation of glycopeptide bonds resulting in 41 bond combinations which are mainly grouped into either of the 5 categories, including N-linked, O-linked, C-linked, glypiation and phosphoglycosylation (Spiro, 2002).

In the process of mimicking glycosylation of endogenous proteins, several experiments have been done to hyperglycosylate the therapeutic proteins leading to prolonged circulation time and reduced immunogenicity resembling that of that of PEGylation (Pisal *et al.*, 2010).

18.5.2 Effect of Glycosylation on Proteins

Glycosylation affects the solubility, stability, plasma half-life, protein folding, surface properties, immunogenicity as well as *in vivo* therapeutic activity of conjugated protein. The polar nature of the glycans improves the solubility of the glycoprotein in the serum as well as its pharmacokinetic profile. Various instability variables include thermal, oxidative, pH and proteolytic degradation, precipitation and aggregation (Li & d'Anjou, 2009). The extent of stabilization of protein due to glycosylation depends on the number of glycans attached to the protein surface; their length and branching; and the charges of their terminal end glycans which further results in the enhanced *in vivo* potency by delivering a higher load of functional protein. With respect to circulation half-life, glycosylated proteins exhibit longer circulating life times than non-glycosylated proteins and partially glycosylated proteins. Improper glycosylated proteins displayed higher clearance rate from the circulation by specific receptor-based mechanisms. In addition to this, as the amount of glycan content increases circulating lifetimes also increases. It has been reported that the therapeutic efficacy of the protein also increases during glycosylation due to enhanced *in vivo* bioavailability, prolonged circulating levels, decreased clearance rate and prolonged period of action through the modification of their pharmacokinetic as well as pharmacodynamic properties. Negatively charged glycans are more efficient in preventing antibody proteolysis (Pisal *et al.*, 2010, Sola & Griebenow, 2010). The most widely used oligosaccharide for the modification of proteins using glycosylation is the polysialic acid, which is discussed briefly in the next section.

18.5.3 Polysialic Acid (PSA)-Protein Conjugates

Polysialic acid (PSA) is an anionic, hydrophilic, linear homopolymer of α -(2, 8) and/or α -(2, 9)-linked N-acetylneuraminic acid (Neu5Ac; sialic acid monomers). PSA is also referred as colominic acid (CA) and it is a human endogenous substance, which completely degrades in the body to non-toxic sialic acid by neuraminidase. PSAs with different chain lengths can be readily harvested from the bacterial cultures involving moderate costs. The polymer properties mainly include non-immunogenicity, biodegradability, reducing the immunogenicity and antigenicity of the protein polypeptide, escaping from phagocytes and presenting long circulation time *in vivo*. PSAs do not promote the generation of immunological memory despite their T-independent antigenic nature. However, the half-life of polysialic is mainly dependent on the chain length as well as the presence or absence of phospholipid. Modification of small molecules with PSA imparts many excellent properties that endow the conjugates with targeting, biocompatible and nontoxic characteristics besides retaining the therapeutics activity of Protein. The strong negative charge aids its modification ability to change the protein's surface charge and binding ability. In addition, prolonged survival time in the blood circulation of the constructs was seen due to inexistence of a recognized receptor in the body for Neu5Ac and reduction in potential for proteolysis thereby, improving the stability of the constructs (Gregoriadis *et al.*, 1993, Jain *et al.*, 2003, Zhang *et al.*, 2014, Lin *et al.*, 2015).

Conjugation of therapeutic molecules with PSA involves the attachment of the amino groups or the N-terminal of the protein with the activated carboxyl, aldehyde or hydroxyl groups of the PSA polymer formed by periodate oxidation. During this interaction the construct may contain variable number of PSA chains attached to each molecule. Nonetheless, care should be taken during the coupling reactions in order to preserve and protect the tertiary structure of the polymer, which could further avoid alteration in clearance mechanism (Gregoriadis *et al.*, 1993, Gregoriadis *et al.*, 2005).

It has been reported that the larger chain PSAs can be widely used to deliver smaller molecules and peptides whereas the shorter chain PSAs can be used to coat the proteins with larger molecular weight and drug carriers such as liposomes (Gregoriadis *et al.*, 1993).

PSA offers a wide range of advantages and serves as an alternative to PEG for developing various protein based conjugates. Firstly, PSA forms a hydrophilic cloudy barrier that protects the protein from interacting with the plasma proteins or macrophages, which results in decreasing the reticuloendothelial system (RES) uptake and prolonging the circulation half-life. On the other hand, PEG cloud barrier suppress their interaction with cells thereby blocking the cellular uptake. Secondly, the degradation products of PSA, which are CO₂ and water, are non-toxic, whereas the degradation products of PEG accumulate in the lysosomes inducing *in vivo* toxicity. In addition, repeated injection of PEG based carriers induces "accelerated blood clearance (ABC)." Therefore, using PSA as a non-immunogenic, non-toxic and biodegradable novel material has a lot of potential when compared to PEG in the field of developing bioconjugates (Gregoriadis *et al.*, 1993, Zhang *et al.*, 2014, Pisal *et al.*, 2010). The drawback associated with covalent attachment of protein with PSA or PEG

include the formation of inactive conjugate due to unfavorable changes in the protein conformation (Pisal *et al.*, 2010). The outcome of polysialylation on different proteins such as catalase, asparaginase, insulin, single chain Fv Fragment (scFv), cytokine, G-CSF, erythropoietin (Darbepoetin Alfa), IgG Fab fragments and monoclonal antibody H17E2, shown in Table 18.3.

18.5.3.1 *Polysialic Acid-catalase Conjugates*

Catalase was successfully coupled to Colominic Acid (CA), a low molecular weight polysialic acid which exhibited only a meager loss of enzymatic activity and enhanced stability when compared to native enzyme upon polysialylation. Polysialylated catalase displayed two fold (70%) retention of the initial activity compared to the enzyme control (29–35%) when subjected to similar conditions. Results suggested that the presence of hydrophilic, negatively charged CA molecules around the polysialylated enzymes acts as a shield and provides hydrophilic microenvironment which protects the enzyme from proteolytic degradation due to plasma proteases thereby conferring higher stability to the conjugate (Fernandes & Gregoriadis, 1996).

18.5.3.2 *Polysialic Acid-asparaginase Conjugates*

Covalent coupling of L-asparaginase to CA by reductive amination have been reported (Fernandes and Gregoriadis, 1997). The reaction was carried out using different molar ratios of the enzyme as well as CA which resulted in conjugates showing a varying number of CA per molecule of enzyme. The activity of the asparaginase in the conjugate almost remained the almost same (82–86%), while after PEG modification, its activity declined seriously. Besides this, the polysialylated asparaginase was eliminated from the blood circulation at a slower pace than the native enzyme thereby extending the half-life of asparaginase (3–4 fold) which limits wastage of proteins. In addition, they also concluded that the conjugate formed was water soluble, non-immunogenic, non-antigenic, proteolytic resistant and showed no interaction with respective receptors (Fernandes & Gregoriadis, 1997, Fernandes & Gregoriadis, 2001).

18.5.3.3 *Polysialic Acid-insulin Conjugates*

Recombinant Human Insulin was conjugated with CA via reductive amination using different molar ratios of CA and insulin (25:1 to 150:1 range). Results suggested that upon subcutaneous injection of an equivalent amount (0.3 units per mouse) of intact insulin as well as polysialylated insulin to animal groups, blood glucose levels were reduced to nadir values at 1 h in both the cases. But they differed in the time that took to reach the normal level. Intact insulin took 3 h whereas polysialylated insulin took 6 h (39 kDa CA-insulin) and 9 h (22 kDa CA-insulin). Hence, 2–3 fold increase in the duration of glucose suppression was seen in mice due to polysialylated insulin when compared to the native form. Apart from improving solubility and stability, polysialylation also prolonged the circulatory half-life which resulted in improving the therapeutic efficacy of the hormone besides reducing the immunogenicity or antigenicity as well as frequency of administration (Jain *et al.*, 2003).

Table 18.3 Polysialic acid-protein conjugates.

Polymers	Conjugate	Reaction involved	Effect of conjugation on the protein/peptide	Indication	Reference
Polysialic acid (PSA)	PSA-Catalase	PSA was oxidized by sodium periodate and subsequently coupled to catalase via reductive amination in the presence of sodium cyanoborohydride	Two fold (70%) retention of initial activity compared to enzyme controls (29–35%) Reduction in enzyme affinity towards the substrate (H_2O_2) Enhanced proteolytic stability due to steric stabilization by hydrophilic biodegradable polysialic acid	–	(Fernandes and Gregoriadis, 1996)
	PSA-Asparaginase	PSA was oxidized by sodium periodate and subsequently coupled to asparaginase via reductive amination in the presence of sodium cyanoborohydride	Formation of water soluble, non-immunogenic, non-antigenic and proteolytic resistant conjugate with extended half-life (3–4 fold) Retention in initial activity of asparaginase up to (82–86%), while after PEG modification, its activity declined seriously	Acute lymphoblastic leukemia, non-Hodgkin's lymphoma and pancreatic carcinoma	(Fernandes and Gregoriadis, 1997, Fernandes and Gregoriadis, 2001)

	PSA-Insulin	PSA was oxidized by sodium periodate and subsequently coupled to amino groups of recombinant human insulin via reductive amination in the presence of sodium cyanoborohydride	Conjugate exhibited improved solubility, stability and prolonged circulatory half-life Reduction in immunogenicity or antigenicity and frequency of administration An improved pharmacological property with increase in the duration of glucose suppression (2–3 fold) was seen in mice	Diabetes mellitus	(Jain <i>et al.</i> , 2003)
	PSA-Single chain Fv Fragment (scFv)	A. PSA was oxidized by sodium periodate and subsequently coupled to anti-carcinoembryonic antigen (CEA)-MFE-23 by two different methods. 1. Amine directed coupling involving reductive amination in the presence of sodium cyanoborohydride 2. Site specific thiol directed coupling of maleimide-PSA with reduced protein	Reduction in immunogenicity (20 folds) was observed for the conjugate formed by amine directed coupling Site specific conjugation resulted in higher tumor uptake (30-fold) besides showing improved specificity ratios compared to the conjugate prepared by amine directed coupling It also exhibited increase (5-fold) in half-life while retaining biological function	Colorectal cancer	(Constantinou <i>et al.</i> , 2009)

(Continued)

Table 18.3 Cont.

Polymer	Conjugate	Reaction involved	Effect of conjugation on the protein/peptide	Indication	Reference
		B. PSA was oxidized by sodium periodate and subsequently coupled to amino groups of anti-placental alkaline phosphatase (PLAP)-F1 via reductive amination in the presence of sodium cyanoborohydride	Increase in circulation half-life (3.4-fold) and bioavailability along with very little loss of activity was seen for PSA-F1 conjugate		
	PSA-Cytokine	Acid activated polysialic acid was added to cytokine present in phosphate buffer (pH 7.3) supplemented with 2% mannitol at room temperature	Effect of PSA-IFN α 2b and PSA-IFN β 1b complexes on Daudi cell lines was studied and found that the PSA-IFN α 2b complexes as well as PSA-IFN β 1b complexes exhibited the same activity as unmodified proteins	Regulates cell proliferation	(Bezuglov <i>et al.</i> , 2009)

	PSA-G-CSF	Acid activated polysilic acid was added to G-CSF present in sodium acetate buffer (pH 5) supplemented with 2% mannitol at room temperature	The activity of PSA-G-CSF complexes on human promyelocytic leukemia HL-60 cell lines was found to be same as native protein and the protein mobility decreased with increase in PSA content	Regulates cell proliferation	(Bezuglov <i>et al.</i> , 2009)
	PSA-Erythropoietin (Darbepoetin Alfa)	Site-directed mutagenesis of human EPO cDNA clone to change the nucleic acid sequence encoding one or more amino acids results in production of glycosylated EPO analogues with extra N-linked carbohydrate chain (4-chain analogue). The final conjugate containing 5 N-linked chain was obtained by combining the carbohydrate addition sites of 2 successfully glycosylated 4-chain analogues	Darbepoetin alpha demonstrated a threefold longer serum half-life and increased <i>in vivo</i> activity. Decreased receptor-binding activity was observed due to increased sialic acid content resulting in a prolonged and increased biological response <i>in vivo</i> . Decrease in frequency of administration to obtain the same amount of response as native protein	Anaemia associated with chronic renal failure, cancer and HIV infection	(Sinclair, 2013, Pissal <i>et al.</i> , 2010, Li and d'Anjou, 2009, Egrie and Browne, 2001)

(Continued)

Table1 8.3 Cont.

Polymer	Conjugate	Reaction involved	Effect of conjugation on the protein/peptide	Indication	Reference
	PSA-IgG Fab fragments monoclonal anti-body H17E2	PSA was oxidized by sodium periodate and subsequently coupled to amino groups of H17E2 monoclonal antibody via reductive amination in the presence of sodium cyanoborohydride	The electrophoretic mobility of the Fab fragment altered with different coupling ratios (PSA: Fab) and lengths (11kDa and 22kDa) The conjugate exhibited greater serum stability, lower immunogenicity, prolonged residence time in blood circulation and greater bioavailability The immunoreactivity of the Fab antibody towards the placental alkaline phosphatase (PLAP) antigen altered very slightly. Polysialylation increased both blood exposure (5-fold) and tumor uptake (3-fold) of the Fab fragment in a KB human tumor xenograft mouse model	Antitumor activity	(Constantinou <i>et al.</i> , 2008)

PSA: Polysialic acid, H_2O_2 ; Hydrogen peroxide, PEG; Polyethylene glycol; CEA: Carcinoembryonic antigen; PLAP: Placental alkaline phosphatase; IFN: Interferon; G-CSF: Granulocyte-colony stimulating factor; EPO: Erythropoietin; HIV: Human immunodeficiency virus; IgG: Immunoglobulin.

18.5.3.4 Polysialic Acid-single Chain Fv Fragment Conjugates

The key drawback associated with the Single-chain Fvs (scFvs) is their rapid elimination from the circulation mainly due to their smaller size. Researchers have showed that polysialylation can augment the residence time of an anti-placental alkaline phosphatase (PLAP) and anti-carcinoembryonic antigen (CEA) scFv (F1 and MFE-23, respectively). Site specific conjugation of PSA with MFE-23 via engineered C-terminal thiols resulted in entities displaying full immunoreactivity and enhanced residence time leading to greater tumor uptake (30-fold) along with bettered specificity ratios in comparison to the conjugate prepared by amine directed chemical conjugation. They concluded that the polysialylation can increase (5-fold) the residence time as well as reduce the immunogenicity (20-fold) and cross-reaction of the therapeutic protein besides preserving its biological activity. The polysialylated-F1 conjugate showed an increase in circulation half-life (3.4-fold) and bioavailability along with a very little loss of activity (Constantinou *et al.*, 2009).

18.5.3.5 Polysialic Acid-cytokine Conjugates

Natural cytokines such as interferons and G-CSF are known to regulate cell proliferation. PSA complexes with IFN α 2b and IFN β 1b were prepared and their effect was tested on a Daudi cell line, which is a widely-used model to test the antiproliferative effect of interferon-containing remedies. Both PSA-IFN α 2b and PSA-IFN β 1b complexes exhibited the same activity as unmodified protein (Bezuglov *et al.*, 2009).

18.5.3.6 Polysialic Acid-G-CSF Conjugates

G-CSF increases the neutrophil number whenever it is introduced into the organism. Complexes of G-CSF (M 19.6 kD) with PSA (M 22 kD) were prepared and it has been observed that the protein mobility decreases with an increase of PSA content. They have compared the biological effect of PSA-G-CSF complexes and standard G-CSF solution on the proliferation of promyelocytic leukemia HL-60 cell lines, differentiated in neutrophil like cells with DMSO. They concluded that the activity of PSA-G-CSF complexes was the same as native protein (Bezuglov *et al.*, 2009).

18.5.3.7 Polysialic Acid-erythropoietin Conjugates

Darbepoetin alfa, an U.S FDA approved product marketed by Amgen is the hyperglycosylated analog of recombinant human erythropoietin (rHuEPO) that showed improved pharmacokinetic and pharmacodynamic properties. It contains two more N-linked glycosylated sites resulting in a total of five N-linked glycosylated sites and five amino acid changes from rHuEPO. It has been used in the treatment of anaemia associated with cancer, kidney disease and chemotherapy. Darbepoetin alfa demonstrated increase in half-life (3 fold) as well as *in vivo* biological activity. On the other hand, higher sialic acid content resulted in decreasing the receptor-binding activity thereby prolonging the biological response *in vivo* (Sinclair, 2013, Pisal *et al.*, 2010, Li & d'Anjou, 2009, Egrie & Browne, 2001).

18.5.3.8 Polysialic Acid-IgG Fab Fragments Conjugate

Fab antibody fragments exhibit a very low half-life in comparison to intact IgG monoclonal antibodies due to lack of considerable lymphatic recycling attributed by the Fc portion of the antibody and hence they serve as ideal targets for polysialylation. CA molecules of different chain length, short (11kDa) and longer (22 kDa) were attached to the antitumor monoclonal antibody H17E2 Fab fragment. Results suggested that the electrophoretic mobility of the Fab fragment altered with different coupling ratios (PSA: Fab) and lengths (11kDa and 22kDa). But the immunoreactivity of the Fab antibody towards the placental alkaline phosphatase (PLAP) antigen altered very slightly. Polysialylation increased both blood exposure (5-fold) and tumor uptake (3-fold) of the Fab fragment in a KB human tumor xenograft mouse model. In addition, the conjugate also exhibited greater stability, lower immunogenicity, prolonged residence time in blood circulation and greater bioavailability. Hence, the results concluded that the conjugate showed improved pharmacokinetic as well as pharmacodynamics properties *in vivo* (Constantinou *et al.*, 2008).

18.6 Polyglycerols (PG)-Protein Conjugates

Dendritic Polyglycerols (PG) are hyper branched, highly flexible polymers belonging to aliphatic polyether class (Wilms *et al.*, 2009). They are stable, nontoxic, hydrophilic, biocompatible, bio-inert and biodegradable in nature. They are characterized by well-defined 3D structure with tunable end group functionalities available for surface modification with high transport capacity, multivalent charge and ligand display for targeting biological cells and tissue (Khandare & Calderon, 2015, Frey & Haag, 2002, Calderon *et al.*, 2010). They are synthesized in a controlled manner to obtain definite molecular weight and narrow molecular polydispersity using anionic ring opening multibranching polymerization (ROMBP) of glycidol with slow monomer addition and partial deprotonation of the initiator which forms the core of the molecule (Sunder *et al.*, 2000). Synthesis of very high molecular weight HPGs with low polydispersity using high monomer to initiator ratios in the presence and absence of emulsifying solvents polyether polyols was reported (Kainthan *et al.*, 2007). The initiator can be used to create polyglycerols with a controlled lipophilic-hydrophilic balance that represents a novel class of non-ionic surfactants. Despite the fact that the *in vivo* toxicity profile of PG is similar to PEG, due to its unique features of multivalent interactions and a relatively higher thermal and oxidative stability makes PG an efficient material for biomedical applications when compared to PEG (Calderon *et al.*, 2010).

18.6.1 Polyglycerol-Ovalbumin Peptide Conjugates

Shipi *et al.* have synthesized a conjugate of peptide OVA (pOVA) with Oligoglycerols (OG) and Polyglycerols (PG) via Michael addition reaction. The reaction involved the conjugation of the peptide to PG via an ester linkage (PG-E-pOVA) as well as Amide linkage (PG-A-pOVA) to study the effect of linker chemistry. They found that the PG-peptide conjugate displayed an increase in bioavailability compared to

OG-peptide conjugate and unconjugated peptide. The linker chemistry also played a crucial role in inducing responses *in vivo* whereas the *in vitro* results were irrelevant. The PG-A-pOVA conjugate showed higher TNF production, lower frequencies of Foxp3+ regulatory T-cells and induced a stronger proliferation whereas PG-E-pOVA conjugate was the most tolerogenic construct. Results suggested that conjugation of peptides with PG leads to an enhancement in bioavailability as well as efficacy of vaccination strategies (Gupta *et al.*, 2015). Effect of polyglycerol conjugates of PG-pOVA indicated in Table 18.4.

18.6.2 Polyglycerol-Arginine-Glycine-Aspartic Acid (RGD) Peptide Conjugates

Zhang *et al.* conjugated Hyperbranched Polyglycerol (HPG) with RGD peptide via divinyl sulfone (HPG-RGD). RGD peptide plays a crucial role in thrombosis by binding to platelet integrin GPIIb/IIIa and disrupting platelet-fibrinogen binding and platelet cross-linking. But, because of their shorter *in vivo* residence time and high IC₅₀ values the use of RGD peptides clinically is limited. Results showed that the conjugate was efficient in binding to GPIIb/IIIa and the molecular weight as well as the number of RGD peptides attached to the HPG-RGD conjugate determines its effectiveness. Moreover, the HPG-RGD conjugate displayed reduction in the IC₅₀ value and inhibited the platelet aggregation. Simultaneously, they found that IC₅₀ value of RGD was a function number of RGD peptides attached to each HPG in an inverse linear manner, see Table 18.4. Hence HPG-RGD conjugate can be explored as an novel antithrombotic agent.

18.7 Dendrimer-Protein Conjugates

Dendrimers are a group of hyperbranched polymers having unique 3D architecture with multivalent surface functional groups available for conjugation. They are characterized by uniform size, controlled chemical structure, high water solubility and low polydispersity index (Tomalia *et al.*, 1985, Klajnert & Bryszewska, 2000, Abbasi *et al.*, 2014). They are prepared step by step in a controlled manner either by the convergent or divergent method. The structure of dendrimer consists of a central core from which the branches of other atoms called “Dendrons,” which grow through a variety of chemical reactions (Abbasi *et al.*, 2014). They are biocompatible and their surface charge depends on the nature of the functional groups available at the surface i.e., carboxylic acid, amine etc. Different types of dendrimers based on the chemical composition includes polyamidoamine (PAMAM), polyethyleneimine (PEI), polylysine based dendrimers, phenyl acetylene dendrimers, polyaryl ether dendrimer, pentaporphyrin dendrimers, PAMAMOS (polyamidoamine-organosilicon) dendrimer, polyester based dendrimers etc (Gillies & Fréchet, 2005). Among them, PAMAM dendrimers are widely explored in the field of biomaterial applications. PAMAM dendrimers are available in different generations which differ in the size and the quantum of surface functional groups available for modification. Effect of dendrimer based protein conjugates include, trypsin, trypsin inhibitor, $\alpha 4\beta 1$ integrin binding peptide and glucose oxidase presented in Table 18.4.

Table 18.4 Polyglycerol-protein, dendrimer-protein and hydroxyl ethyl starch-protein conjugates.

Polymer	Conjugate	Reaction involved	Effect of conjugation on the protein/peptide	Indication	Reference
Polyglycerol (PG)	Polyglycerol-ovalbumin peptide (PG-pOVA)	OG and PG were coupled to the cysteine-modified model peptide OVA (pOVA) via a Michael addition reaction through site-specific conjugation. The peptide was conjugated to PG via an ester linkage (PG-E-pOVA) as well as Amide linkage (PG-A-pOVA) to study the effect of linker chemistry	The PG-peptide conjugates displayed an extended bioavailability compared to OG-peptide conjugates and unconjugated peptide The linker chemistry also played a crucial role in inducing responses <i>in vivo</i> whereas the <i>in vitro</i> results were irrelevant The PG-A-pOVA (amide) conjugate induced higher proliferation, increased TNF production and lower frequencies of Foxp3+ regulatory T-cells whereas PG-E-pOVA (ester) was the most tolerogenic conjugate All the conjugates were highly water soluble	Treatment of autoimmune diseases and allergy.	(Gupta <i>et al.</i> , 2015)
	PG-RGD Peptide	Vinyl sulfone functionalized PG was coupled to RGD peptide through cysteine coupling	The PG-RGD conjugate exhibited increased platelet inhibitory activity (2–3 fold) and the IC ₅₀ value of RGD was decreased The IC ₅₀ of RGD was a function number of RGD peptides per HPG in an inverse linear manner	Anti-thrombotic	(Zhang <i>et al.</i> , 2008)

Dendrimer	PAMAM G-4 -TRYPSIN and PAMAM G-4 -TRYPSIN Inhibitor	Conjugation of PAMAM G-4 with trypsin and trypsin inhibitors occurs via hydrophilic, H-bonding and van der Waals interactions	More stable conjugate was formed with trypsin inhibitor when compared with the trypsin The hydrophobicity of the pro- tein plays an important role in binding with the polymer as higher binding affinity was seen with more hydrophobic trypsin inhibitor	–	(Chanphai and Tajmir-Riahi, 2016)
	PAMAM- $\alpha 4\beta 1$ integrin binding peptide (LDV and EILDVPST peptide)	The peptides (LDV and EILDVPST) conjugates were synthesized on immobilized dendri- meric scaffold using standard Fmoc solid- phase peptide chemistry	Ability of the conjugates to inhibit the binding of biotinylated- EILDVPST-NH2 to integrin receptor was evaluated The LDV-dendrimer con- jugate showed little or no response when compared to EILDVPST-NH2 whereas, the EILDVPST-dendrimer conju- gate showed 12 fold increase in binding affinity	Rheumatoid arthritis and asthma	(Monaghan <i>et al.</i> , 2001)
	Dendrimer Porphyrin-Glucose Oxidase	Glucose oxidase (GOX) enzyme was immo- bilized on to the silica coated porphyrin dendrimer surface by covalently attachment	Compared to the control surface that was coated with PAA, the protein immobilized on dendrimer surface was showed higher protein loading, uniform distribution of immobilized enzyme, increased sensitivity as well as higher activity towards the target analyte (H_2O_2)	–	(Lee <i>et al.</i> , 2009)

(Continued)

Table 18.4 Cont.

Polymer	Conjugate	Reaction involved	Effect of conjugation on the protein/peptide	Indication	Reference
Hydroxyethyl starch (HES)	HES-Erythropoietin Mimetic Peptide (AGEM400(HES))	Supravalent-Maleimide-HES dissolved in phosphate buffer pH= 6.5 was added to the deprotected AGEM400 peptide solution (in phosphate buffer pH = 6.5) and vigorously stirred for 2h at 37 °C	The conjugate demonstrated excellent <i>in vitro</i> efficacy which was superior to that of the peptide alone and comparable to the efficacy of erythropoietin and darbepoietin alpha AGEM400 (HES) exhibited enhanced binding affinity and displayed functions in similar fashion as EPO AGEM400 (HES) replaced EPO from its receptor and the soluble EPO receptor inhibited the <i>in vitro</i> activity of AGEM400 (HES)	Synthetic Erythropoietin mimetic agent	(Greindl <i>et al.</i> , 2010)
	HES-Anakinra conjugate	Anakinra was conjugated to propionaldehyde-HES using reductive amination in the presence of sodium cyanoborohydride	The conjugate exhibited increase in their size as well circulation half-life The conjugate displayed an considerable increase in the stability of protein without affecting its secondary structure HESylated protein displayed high receptor binding affinity, increase in the half-life (6.5-fold) as well as AUC (45-fold) than native protein	Rheumatoid arthritis	(Liebner <i>et al.</i> , 2014)

PG: Polyglycerols; OG: Oligoglycerols; IC₅₀:50% Inhibitory concentration; RGD: Arginine-glycine-aspartic acid peptide; HPG: Hyperbranched Polyglycerol; PAMAM G4: Polyamidoamine generation-4; GOX: Glucose oxidase; PAA: Polyacrylic acid; H₂O₂: Hydrogen peroxide; EPO: Erythropoietin; HES: Hydroxyethyl starch AUC-Area under the curve.

18.7.1 PAMAM-Trypsin and Trypsin Inhibitor Conjugates

Conjugations of PAMAM G-4 to trypsin as well as trypsin inhibitor have been reported to study the binding affinity of the peptide-polymer conjugate via hydrophilic, H-bonding and vanderwaals interactions. Trypsin is a water soluble globular protein that acts as a proteolytic enzyme which breaks the peptide bonds present between the lysine and the carboxylic groups of arginine. Whereas, trypsin inhibitors are small proteins or polypeptides that inhibit the activity of trypsin results in certain disease in animals and humans. The thermodynamic and spectroscopic analysis for trypsin and trypsin inhibitor conjugates with PAMAM-G4 in aqueous solution at physiological conditions was performed. Results suggested that a more stable conjugate was formed with trypsin inhibitor when compared with the trypsin (Chanphai & Tajmir-Riahi, 2016). Apart from this, they concluded that the hydrophobicity of the protein plays a crucial role in binding with the polymer as higher binding affinity was seen with more hydrophobic trypsin inhibitor.

18.7.2 PAMAM- $\alpha 4\beta 1$ Integrin Binding Peptide Conjugates

PAMAM dendrimer was conjugated with LDV and EILDVPST peptide using solid phase synthesis to study their binding effect towards integrin protein. LDV is the minimum active peptide sequence in fibronectin whereas EILDVPST is the fuller length biotinylated peptide. The conjugates were subsequently studied for their inhibitory role on the binding of biotinylated-EILDVPST-NH₂ to the integrin receptor expressed on cancer cells using competition ELISA. The LDV-dendrimer conjugate showed little or no response when compared to EILDVPST-NH₂ whereas, the EILDVPST-dendrimer conjugate showed 12 fold increase in binding affinity (Monaghan *et al.*, 2001).

18.7.3 Porphyrin Dendrimer-Glucose Oxidase Conjugates

Ionic dendrimer porphyrin was coated on to the positively charged silica surface via electrostatic interaction followed by the immobilization of glucose oxidase (GOX) enzyme on to the dendrimer modified surface by covalent attachment and the protein activity was studied. The porphyrin core of the dendrimer exhibits fluorescence property which was exploited in quantifying the relative amounts of dendrimer and the enzyme-catalyzed reaction occurring on the surfaces. Protein immobilized on dendrimer surface showed higher protein loading and activity than the PAA coated control surface. A quantitative relationship was established between the quenching and glucose concentration which depends on the fact that the hydrogen peroxide generated from the oxidation of glucose quenches the fluorescence of porphyrin core (Lee *et al.*, 2009). Hence this group successfully synthesized a protein microarray that could exhibit high protein density with a uniform distribution of immobilized enzyme on the substrate which can further enhance the sensitivity of assay along with maintaining its activity towards the target analyte.

18.8 HESylation of Proteins

Hydroxyethyl starch (HES) is a water soluble semi-synthetic polysaccharide produced from natural starch. HES is formed by acid hydrolysis of amylopectin rich natural

starch (Maize starch or Potato starch) followed by hydroxyethylation of free 2,3 and 6 hydroxyl positions of both α -1,4- and α -1,6- linked glucose residues. Besides its use as a cryoprotectant, it is also clinically approved as plasma volume expanders (PVEs) (Besheer *et al.*, 2007). HESylation involves conjugation of proteins or drugs to biodegradable HES which increases size and hydrophilicity of the protein. Serum α -amylase degrades HES and its rate is controlled by the extent of hydroxyethylation (Liebner *et al.*, 2014). HESylation enhances the biological activity due to the increase in the circulation half-life as well as decrease in the renal clearance (Sharma *et al.*, 2014). HES are highly biocompatible and because of its structural similarity with that of glycogen (glucose storage polymer in humans) it lacks immunogenicity. Reaction time must be optimized in such a way so as to prevent the formation of cross-linked conjugates (Pasut, 2014). Fresenius Kabi, a European Pharma company has developed HESylation technology to improve the half-life of various protein drugs including G-CSF and EPO. Effect of hydroxyethyl starch conjugates of erythropoietin mimetic peptide and anakinra were shown in Table 18.4.

18.8.1 HES-Erythropoietin Mimetic Peptide (AGEM400 (HES)) Conjugate

AGEM400(HES), a novel dimeric Erythropoietin Mimetic Peptide (EMP) Conjugated to HES was developed and its efficacy was evaluated (Greindl *et al.*, 2010). The conjugate demonstrated significant *in vitro* efficacy than native peptide, erythropoietin (EPO) and Aranesp® (Darbepoietin alpha). Further, AGEM400 (HES) exhibited enhanced binding affinity whereas; Hematide (a dimeric EMP to PEG conjugate) showed a five-fold decrease in receptor binding affinity as well as decreased *in vitro* efficacy, as compared to peptide only. AGEM400 (HES) displayed functions in a similar fashion as EPO. They observed that EPO was replaced from its receptor by AGEM400 (HES) and the soluble EPO receptor inhibited the *in vitro* activity of AGEM400 (HES). Based on the results obtained, they concluded that AGEM400 (HES) can serve as a promising erythropoiesis stimulating agent for anemia's related to renal insufficiency and/or in oncological settings.

18.8.2 HES-Anakinra Conjugates

Anakinra is a recombinant human interleukin 1 receptor antagonist (rhIL-1ra) that binds to the IL-1 receptor approved for adult patients with rheumatic arthritis. The crucial drawback associated with anakinra is its shorter half-life (108 min) because of which it has to be administrated daily. In a study, HES was conjugated to anakinra using reductive amination which engendered an increase in their size as well circulation half-life. Moreover, the conjugate displayed a considerable enhancement in protein stability without affecting its secondary structure. Furthermore, the HESylated protein exhibited higher receptor binding affinity, increase in the half-life (6.5-fold) as well as AUC (45-fold) than native protein (Liebner *et al.*, 2014). Researchers concluded that HESylation can significantly improve the pharmacokinetic parameters of anakinra without affecting its structure or binding affinity.

18.8.3 HES-G-CSF Conjugates

Octapharma Biopharmaceuticals GmbH, a German based pharmaceutical company has developed HES- G-CSF conjugate based on the HESylation technology of Fresenius Kabi Deutschland GmbH. The formation of a conjugate with HES resulted in increasing the size of the molecule which prevented its fast elimination and thereby increasing its plasma half-life and duration of action. The HES-G-CSF project is about to complete the preclinical phase with preparations ongoing for entering into first clinical phase (<http://www.octapharma-biopharmaceuticals.com>).

18.9 Dextran-Protein Conjugates

Dextran is a biocompatible polymer of α -D-glucose held together predominantly by α -1,6-linkages belonging to polysaccharide family. This polymer offers a wide range of advantages which includes higher water solubility, biodegradability, uncharged nature, low toxicity and its high coupling capacity. However, toxicity depends on the molecular weight of the dextran used. Large molecular size is associated with toxicity and a high incidence of allergic reactions. Partially hydrolyzed and size-fractionated linear dextrans can be produced from *Leuconostoc mesenteroides* (Wileman, 1991). Various research groups have shown that the attachment of soluble dextrans to proteins can drastically increase the circulation half-life of the protein. Lower molecular weight dextrans (<15kDa) can be excreted freely through glomerulus whereas the higher molecular weight dextrans (50kDa) are rarely excreted in humans due to restricted passage. In contrast, higher molecular weight dextrans undergo uptake by the liver with a continuous and rapid elimination from the parenchymal cells taking place. Dextran is susceptible to RES uptake and has also shown RES-blocking capacity when given as a PVE. It has also been demonstrated to be resistant to lysosomal digestion in kidney tubules (Melton *et al.*, 1987). See Table 18.5, effect of dextran conjugation on asparaginase, carboxypeptidase G₂, uricase, insulin and hemoglobin.

18.9.1 Dextran-Asparaginase Conjugates

The major drawbacks associated with asparaginase are its low half-life and development of immune reactions upon repeated injections of the enzyme. In a study, soluble dextran-asparaginase conjugates were formed which showed an increase in circulatory persistence and marked reduction in antigen reactivity. Moreover, the steric barrier formed by dextran around asparaginase protects the enzyme from *in vivo* degradation as well as slows down its inactivation by the immune system. Besides extending the plasma half-life to a great extent, it also improved the stability of the enzyme (Wileman, 1991). The conjugates retained 50% its enzymatic activity besides being well tolerated upon repeated injections. Moreover, it also exhibited significant resistance to proteolysis by trypsin and chymotrypsin and inactivation by the asparaginase-specific antibody (Wileman *et al.*, 1986).

18.9.2 Dextran-Carboxypeptidase G₂ Conjugates

Both soluble and cyanogen bromide (CNBr) activated dextrans were conjugated with carboxypeptidase G₂ (CPG₂) and further studied for *in vivo* clearance fate in the mouse.

Study results suggested that the native form does not show any tissue uptake whereas, the dextran conjugates were retained in the liver with both the components of conjugate degrading at different rates (Melton *et al.*, 1987). The protein part of the conjugate gets excreted upon liberation from the dextran in the liver. Whereas, the dextran part of the conjugate is degrades at a slower rate. Increased half-lives of dextran conjugates were noticed when RES blockade was carried out by administering colloidal carbon to mice. Results indicated that RES was involved in the clearance of the developed conjugates reducing their clearance rate by half. In contrast, the degradation and clearance rate of native CPG₂ occurs due to the parenchymal cells of the liver but not the RES as it showed same clearance rate. It resulted in the availability of the conjugate at the tumor site for prolonged period resulting in higher cytotoxicity.

18.9.3 Dextran-Uricase Conjugates

Uricase (UC) was coupled with dextran derivatives i.e. neutral dextran, cationic diethylaminoethyl-dextran (DEAED) and anionic carboxymethyl-dextran (CMD) by periodate oxidation. The disposition characteristics of UC and its conjugates were studied in mice. Results suggested that the disappearance rate of UC was accelerated with neutral dextran which otherwise has a considerably long plasma half-life in mice. In case of conjugate with DEAED, decrease in the plasma half-life was observed apart from its enhanced hepatic up-take and urinary excretion. On the other hand, increase in plasma half-life was observed in comparison to the native enzyme when conjugated with CMD whereas the uptake by the liver was restricted (Takuya *et al.*, 1990). Hence the results suggested that the physicochemical properties of dextran derivatives play a crucial role in controlling the biopharmaceutical properties of peptide drugs.

18.9.4 Dextran-Insulin Conjugates

The GlyA1 insulin amino group was site specifically conjugated to activated carboxyl groups of carboxymethyl dextran (CMD). An average of 3–4 molecules of insulin was grafted to each linear chain of CMD. The bioactivity of conjugated insulin was 2.6 times lesser than that of native insulin. However, the CMD-insulin conjugate displayed similar insulin receptor binding constant and mitogenic activity to that of native insulin. In addition, the CMD-insulin conjugate showed prolonged plasma half-life (114.1 min) when compared to that of soluble Zn-insulin (12.4 min). *In vivo* pharmacokinetic results of the conjugate demonstrated that the mean residence time (MRT) was prolonged (103.5 min) when compared to that of soluble Zn-insulin (40.5 min) upon subcutaneous administration. Whereas the pharmacodynamic results of Zn-insulin were reflected to same upon subcutaneous administration of conjugate. The time required to attain minimum glucose concentration was found to be 95.7 min, which was considerably longer than that of insulin (62 min). Hence they concluded that the conjugation of insulin to CMD leads to delayed pharmacodynamic profile of bioactive conjugate showing prolonged response (Baudyš *et al.*, 1998). Another group of researchers have studied the effects of insulin-dextran conjugate and native insulin on the adipose tissue metabolism (Sakamoto *et al.*, 1977). They observed that the conjugates formed were

Table 18.5 Dextran-protein and dextrin-protein conjugates.

Polymer	Conjugate	Reaction involved	Effect of conjugation on the protein/ peptide	Indication	Reference
Dextran	Dextran-Asparaginase	Reaction occurs between the lysine residues of the enzyme and electrophilic groups (imidocarbonate or dialdehyde) introduced into dextran in aqueous buffer at alkaline pH 9	<p>The conjugate formed was soluble, stable and displayed extended plasma half-life as well as marked reduction in antigen reactivity.</p> <p>The steric barrier formed by dextrin around asparaginase protects the enzyme from <i>in vivo</i> degradation as well as slows down its inactivation by the immune system.</p> <p>The conjugates retained 50% of its enzymatic activity besides being well tolerated, upon repeated injections.</p> <p>It also displayed resistance to proteolysis by trypsin and chymotrypsin and inactivation by asparaginase-specific antibody</p>	Acute lymphoblastic leukemia, non-Hodgkin's lymphoma and pancreatic carcinoma	(Wileman <i>et al.</i> , 1986) and (Wileman, 1991)
	Dextran-Carboxypeptidase G ₂	The activated dextran was conjugated to enzyme	<p>The native form does not showed any tissue uptake whereas, the dextran conjugates were retained in liver with both the components of the conjugate degrading at different rates</p> <p>Increased half-life due to reticuloendothelial system (RES) blockage which resulted in enhanced cytotoxicity due to availability of the conjugate at the tumor site for prolonged period</p>	Anticancer	(Melton <i>et al.</i> , 1987)

(Continued)

Table 18.5 Cont.

Polymer	Conjugate	Reaction involved	Effect of conjugation on the protein/ peptide	Indication	Reference
	Dextran-Uricase	Three types of dextran, neutral dextran and its derivatives, cationic diethyl-aminoethyl-dextran (DEAED), or anionic carboxymethyl-dextran (CMD), were oxidized by sodium periodate followed by reaction with uricase (UC) via reductive amination in presence of sodium borohydride	Conjugation with neutral dextran resulted in accelerating the disappearance of UC which otherwise has a relatively high plasma half-life in mice. Conjugation with diethylaminoethyl dextran (DEAED) resulted in an conjugate with very low plasma half-life and enhanced hepatic up-take and urinary excretion Conjugation with carboxy methyl dextran (CMD) resulted in increasing the plasma half-life in comparison to that of the native enzyme whereas the uptake by the liver was restricted	Gout and hyperuricemia associated with nephropathy Or hematological malignancies	(Takuya <i>et al.</i> , 1990)
	Dextran-Insulin	Site-specific attachment of activated carboxyl groups of carboxymethyl dextran (CMD) attached to the amino group of GlyA1 present in insulin	The CMD-insulin conjugate exhibited a decrease in bioactivity (2.6-fold) with a prolonged plasma elimination half-life of 114.1 min and <i>in vivo</i> mean residence time (MRT) of 103.5 min The CMD-insulin conjugate displayed similar insulin receptor binding constant and mitogenic activity to that of native insulin The time required to attain minimal glucose concentration was 95.7 min, which was significantly longer than that of insulin (62 min)	Diabetes mellitus	(Baudyš <i>et al.</i> , 1998) and (Sakamoto <i>et al.</i> , 1977)

			<p>Conjugation of insulin to CMD leads to delayed pharmacodynamic profile of bioactive conjugate showing prolonged response</p> <p>The conjugates formed were stable and no release of the free insulin was seen after incubation with adipose tissue besides mimicking the effect of native insulin on metabolism of adipose tissue</p>		
	Dextran-Hemoglobin	<p>Hemoglobin was conjugated to dextran by two different methods</p> <ol style="list-style-type: none"> 1. Alkylation: Hemoglobin reacts with bromoacetyl group incorporated into dextran by alkylation (80% yield) 2. Periodate oxidation: Hemoglobin reacts with dialdehyde group incorporated into dextran by periodate oxidation (60% yield) 	<p>Conjugate formation resulted in prevention of massive hemoglobinuria and prolonged functional life span</p> <p>Both soluble conjugates could bind and release oxygen reversibly</p> <p>The oxygen-binding curves of both the conjugates showed shift towards the left relative to that of free hemoglobin</p> <p>The conjugates were excreted by kidneys and showed slower circulation clearance rate than free hemoglobin in rabbit</p>	Blood substitute	(Tam <i>et al.</i> , 1976)
Dextrin	Dextrin-rhEGF	<p>Succinoylated dextrin was conjugated to lysine residues present within the rhEGF molecule forming a stable amide bonds via EDC/sulfo-NHS coupling reaction</p>	<p>The conjugate formation protected rhEGF degradation by proteinases</p> <p>The release of rhEGF from dextrin-rhEGF conjugate in the presence of α-amylase resulted in the <i>in vitro</i> stimulation of proliferation and migration of normal dermal fibroblasts</p>	Acute or chronic wound treatment	(Hardwicke <i>et al.</i> , 2010) and (Hardwicke <i>et al.</i> , 2011)

(Continued)

Table 18.5 Cont.

Polymer	Conjugate	Reaction involved	Effect of conjugation on the protein/ peptide	Indication	Reference
			Chronic wound fibroblasts and keratinocytes, provides the evidence to support the viability of the PUMPT approach <i>In vivo</i> results obtained at macroscopic level suggested that the dextrin–rhEGF conjugate considerably enhanced the wound closure and neo-dermal tissue formation whereas histological results showed significant increase in granulation tissue deposition and angiogenesis upon topically application		
	Dextrin-Trypsin	Succinoylated dextrin was conjugated to trypsin forming a stable amide bonds via EDC/sulfo-NHS coupling reaction	Reduction in activity of the conjugated enzyme (34–69%) was observed depending on the degree of succinoylation (9–32 mol %) of dextrin and its molecular mass (7700 and 47200 g/mol) However, the activity of enzyme (92–115%) was restored in presence of α -amylase providing a proof to explore the viability of the PUMPT approach	–	(Duncan <i>et al.</i> , 2008)
	Dextrin- melanocyte stimulating hormone (MSH)	Succinoylated dextrin was conjugated to MSH forming a stable amide bonds via EDC/sulfo-NHS coupling reaction	For melanocyte stimulating hormone (MSH) intermediate molecular dextrin (47200 g/mol) was used to form dextrin-MSH conjugate with 37 wt % of MSH content	–	(Duncan <i>et al.</i> , 2008)

			<p>Reduction in biological activity of the conjugate in the form of decreased melanin production to 11% in murine melanoma (B16F10) cells was observed</p> <p>The activity of conjugate was restored to 33% of the control value in the presence of α-amylase providing evidence to support the viability of the PUMPT approach</p>	Anticancer	(Ferguson <i>et al.</i> , 2010b)
Dextrin-Phospholipase A2	Dextrin was conjugated to PLA2 forming a stable amide bonds via EDC/sulfo-NHS coupling reaction	<p>Reduced PLA2 toxicity and enhanced tumor targeting by the EPR-mediated effect</p> <p>The conjugate showed decreased PLA2 bioactivity which was fully restored in the presence of α-amylase</p> <p>The conjugate displayed enhanced cytotoxicity, higher internalization via endocytosis as well as reduced hemolytic activity <i>in vitro</i></p> <p>Reduction in cytotoxicity of both PLA2 and dextrin-PLA2 was observed when the cells were co-incubated with TKI inhibitor, gefitinib suggesting a TK mediated PLA2 mechanism of action</p> <p>The conjugate showed enhanced cytotoxicity in the presence of doxorubicin suggesting its potential for development of combination therapy</p>			

RES: Reticuloendothelial system; DEAE-Diethyl-aminoethyl-dextran; CMD: Carboxymethyl-dextran; UC: Uricase; MRT: Mean residence time; rhEGF: Human recombinant epidermal growth factor; EDC: 1-Ethyl-3-(3-dimethylaminopropyl) carbodiimide; NHS: N-Hydroxysuccinimide; PUMPT: Polymer-masking-unmasking-protein therapy; MSH: Melanocyte stimulating hormone; EPR: Enhanced permeation and retention; PLA2: Phospholipase A2; TKI: Tyrosine kinase inhibitor; TK-Tyrosine kinase.

stable and no release of the free insulin was seen after incubation with adipose tissue besides mimicking the effect of native insulin on the metabolism of adipose tissue.

18.9.5 Dextran-Hemoglobin Conjugates

The present study highlights the formation of a conjugate between soluble dextran and human hemoglobin synthesized by two different methods namely alkylation and dialdehyde method (Tam *et al.*, 1976). Both the methods differed in terms of yield of the conjugate with the former showing 80% and latter about 60% in terms of hemoglobin. Conjugate formation resulted in the prolonging the life span by preventing substantial hemoglobinuria. The oxygen-binding curves of both the conjugates showed a shift towards the left relative to that of free hemoglobin but they could bind and release oxygen reversibly. However, the conjugates were excreted by kidneys and showed slower circulation clearance rate than free hemoglobin in the rabbit. Hence, the resulting conjugate minimizes the disadvantage associated with native form thereby serving as a potential blood substitute.

18.10 Dextrin-Protein Conjugates

Dextrin is a biocompatible polymer consisting of D-glucose units which are held together by α -1,4-glucosidic linkages forming a linear polymer. It is non-toxic, hydrophilic and biodegradable polymer which is produced from the starch by its controlled hydrolysis. The *in vivo* degradation of the polymer occurs in the extracellular fluid in the presence of α -amylase. It can be attached to succinic acid via hydroxyl groups of dextrin resulting in carboxyl group which can aid in its conjugation to proteins. Dextrin molecules with variable degree of succinylation and molecular weight ranges can be obtained (Pasut, 2014). Recent studies have reported its potential for a novel concept of polymer-masking-unmasking-protein therapy (PUMPT) where the protein activity is transiently masked temporarily resulting in stabilization or inactivation of the protein during transit. Protein unmasking occurs at the target site in the presence of an enzyme which triggers polymer degradation and subsequently restores bioactivity of a protein (Hardwicke *et al.*, 2010, Ferguson *et al.*, 2010b). See Table 18.5, effect of dextrin conjugation on rhEGF, trypsin, melanocyte stimulating hormone (MSH) and phospholipase A2.

18.10.1 Dextrin-rhEGF Conjugates

Researchers have synthesized a bioresponsive dextrin-recombinant human epidermal growth factor (rhEGF) conjugate which can be used to promote tissue repair with PUMPT concept. It was found that formation dextrin- rhEGF conjugate resulted in protecting rhEGF degradation by proteinases and restoration of bioactivity for a prolonged period in the presence of physiological concentrations of α -amylase. The ability of the conjugate to release rhEGF in chronic wound fluid in the presence of α -amylase was also evaluated (Hardwicke *et al.*, 2010). Results highlighted the presence of EGF in acute, but not in chronic wound fluid. Whereas, higher concentrations of α -Amylase

was observed in acute wound fluid (188 IU/L) compared to chronic wound fluid (52 IU/L). Despite the absence of elastase in acute wound fluid, it was detected in chronic wound fluid (2.1 ± 1.2 RFU/min). They observed that the incubation of Dextrin-rhEGF in chronic wound fluid resulted in the release of rhEGF (ELISA) mediated through endogenous α -amylase which reached to peak level at 48 h. *In vitro* results obtained by scratch wound assay suggested that both the free rhEGF and dextrin-rhEGF conjugate resulted in enhancement in cell migration (HaCaT keratinocytes and human fibroblasts) in comparison to the controls. Furthermore, increased proliferation of fibroblasts (normal dermal fibroblasts ~160%; chronic wound fibroblasts ~140%) was seen after 72 h of incubation with dextrin-rhEGF conjugate when subjected to physiological levels of α -amylase (93 IU/L).

In vivo preclinical evaluation of conjugate was carried out in the db/db diabetic mouse model to determine its pharmacokinetics and whether the liberation of rhEGF into such a complex and aggressive environment can still lead to bioactivity by the same research group in their subsequent work (Hardwicke *et al.*, 2011). They assessed the wound healing in terms of initiation of neo-dermal tissue deposition and wound closure, over a 16 day period. Histological examination was also carried by using tissues harvested at day 16. Results obtained at the macroscopic level suggested that topically-applied dextrin-rhEGF significantly accelerated wound closure and neo-dermal tissue formation whereas histological results showed a significant increase in granulation tissue deposition and angiogenesis, relative to untreated, succinylated dextrin and rhEGF alone controls.

18.10.2 Dextrin-Trypsin and Melanocyte Stimulating Hormone (MSH) Conjugates

Dextrin was conjugated with trypsin to study the effect of degree of succinylation (9–32 mol %) as well as dextrin molecular mass (7700 and 47200 g/mol) on its ability to mask/unmask trypsin activity. Reduction in the activity of conjugated enzyme (34–69%) was observed based on the degree of succinylation and molecular mass of dextrin used. Moreover, the activity of the enzyme (92–115%) was restored in the presence of α -amylase. On the other hand, for melanocyte stimulating hormone (MSH) intermediate molecular dextrin (47200 g/mol) was used to form a dextrin-MSH conjugate with 37 wt % of MSH content. The biological activity of conjugate was assessed in presence and absence of α -amylase by measuring melanin production by murine melanoma (B16F10) cells. Results displayed a reduction in melanin production to 11% after conjugation. Whereas, the activity of conjugate was restored to 33% of the control value in the presence of α -amylase (Duncan *et al.*, 2008).

18.10.3 Dextrin-Phospholipase A2

A novel bio-responsive, biodegradable anticancer therapeutic polymer conjugate of dextrin-phospholipase A2 (PLA2) was developed using PUMPT concept with an aim to reduce the toxicity associated with the PLA2 as well as to increase its tumor targeting by the EPR-mediated effect (Ferguson *et al.*, 2010b). The effect of combination with tyrosine kinase inhibitors (TKI) and/or chemotherapy was also evaluated *in vivo*. The

conjugate showed decreased PLA2 bioactivity which was fully restored in the presence of α -amylase. The conjugate displayed enhanced cytotoxicity, higher internalization via endocytosis as well as reduced hemolytic activity *in vitro*. Reduction in cytotoxicity of both PLA2 and dextrin-PLA2 was observed when the cells were co-incubated with TKI inhibitor, gefitinib suggesting a TK mediated PLA2 mechanism of action. Apart from this, the conjugate showed enhanced cytotoxicity in the presence of doxorubicin suggesting its potential for development of combination therapy.

18.11 Hyaluronic Acid (HA)-Protein Conjugates

Hyaluronic acid (or hyaluronan) (HA) is a naturally occurring polysaccharide polymer containing two alternating units of D-glucuronic acid and N-acetyl D-glucosamine with a molecular weight of $10^5 - 10^7$ Da. HA is a linear, negatively charged, hydrophilic, non-immunogenic, biocompatible and biodegradable polymer. HA is involved in performing various functions within the extracellular matrix such as cell growth, differentiation, and migration. It may also be involved in the progression of some malignant tumor (Jaracz *et al.*, 2005). Conjugation of biological molecules to HA can be carried out in an aqueous medium mainly by two methods. The first method involves the activation of the carboxyl groups present in the HA whereas the second method involves the oxidation of HA backbone in the presence of periodate to form aldehyde groups. The major drawback associated with these methods, especially for the first one, is the production of conjugates with low homogeneity and batch to batch variation due to random coupling (Mero & Campisi, 2014).

18.11.1 Hyaluronic Acid-Interferon α Conjugate

Interferon alpha (IFN α) consists of 165 amino acids and has been extensively used in the treatment of chronic HCV infection and melanoma. Various drug delivery systems which could decrease the injection frequency in order to improve the patient compliance of IFN α have been recently developed. In this current work, hyaluronic acid was conjugated with interferon alpha (HA-IFN α) to produce a target specific long-acting derivative for the treatment of HCV infection (Yang *et al.*, 2011). The number of IFN α molecules attached to HA can be controlled in the range of 2–9 molecules per single HA chain by changing the amount of IFN α in the feed with bioconjugation efficiency higher than 95%. *In vitro* anti-proliferative activity of the conjugate was evaluated in Daudi cells and it was found to be lower than that of native IFN α , but comparable to that of PEG-Intron. Near-infrared fluorescence (NIRF) dye labelled HA-IFN α conjugate demonstrated site specific delivery to the liver in mice. Moreover, the pharmacokinetic data revealed that the HA-IFN α conjugate exhibit enhanced residence time up to 5 days depending on the extent of HA modification. The antiviral activity of the HA-IFN α conjugate was confirmed *in vivo* by higher expression of 2',5'-oligoadenylate synthetase 1 (OAS 1)) in the liver tissues than the results obtained with IFN α and PEG-Intron. Effect of hyaluronic acid conjugation on interferon α , human growth hormone, insulin, trypsin, EGF, Exendin-4, anti-Flt1 peptide and superoxide dismutase, indicated in Table 18.6.

Table 18.6 Hyaluronic acid-protein conjugates.

Polymer	Conjugate	Reaction involved	Effect of conjugation on the protein/peptide	Indication	Reference
Hyaluronic Acid (HA)	HA-Interferon α (HA-IFN α)	HA-IFN α conjugate was synthesized by coupling reaction between aldehyde modified HA and the N-terminal group of IFN α	<i>In vitro</i> anti-proliferatory activity of the conjugate was found to be lower than that of native IFN α in Daudi cells Near-infrared fluorescence (NIRF) dye labelled HA-IFN α conjugate demonstrated site specific delivery to the liver in mice HA-IFN α conjugate exhibit enhanced resistance time up to 5 days depending on the degree of HA modification <i>In vivo</i> antiviral activity of the HA-IFN α conjugate was confirmed by higher expression of 2', 5'-oligoadenylate synthetase 1 (OAS 1) in the liver tissues	Hepatitis C virus infection (HCV)	(Yang <i>et al.</i> , 2011)
	HA-Human growth hormone (HA-hGH)	The aldehyde modified HA obtained via sodium periodate oxidation was coupled with the N-terminal primary amine group of hGH in presence of sodium cyanoborohydride	HA-hGH conjugate displayed receptor mediated transdermal delivery of hGH <i>In vivo</i> expression of elevated levels of phosphorylated Janus kinase 2 (p-JAK2) in the fibroblast of Detroit 551 cell through hGH-receptor mediated signaling pathway. Topical treatment of HA-hGH conjugate exhibited higher AUC (10-fold) and bio-availability (16-fold) compared to hGH delivered topically	Cosmetic and tissue engineering applications	(Yang <i>et al.</i> , 2012a)

(Continued)

Table 18.6 Cont.

Polymer	Conjugate	Reaction involved	Effect of conjugation on the protein/ peptide	Indication	Reference
	HA- Insulin HA-INS	The aldehyde derivative of hyaluronic obtained by addition of 1, 1'-carbonyldiimidazole and 4-aminobutyraldehyde diethyl acetal was coupled by N-terminal site-selective conjugation with insulin in the presence of sodium cyanoborohydride	Insulin (INS) was conjugated with HA differing in the degree of acetal substitution (4% and 21%) resulting in HA-INS 1 and HA-INS 2, respectively The two conjugates HA-INS 1 and HA-INS 2 exhibited a different peptide loading (17% and 32%, w/w respectively) which was attributed to differences in steric hindrance between the polypeptide chains Both the conjugates were non-hemolytic in the concentration used for <i>in-vivo</i> studies The HA-INS 1 conjugate showed a lowering effect on blood glucose level for up to 6 h, while free insulin exhausted its action after 1 h HA-INS 2 showed no significant effect on glucose titer which was attributed to steric entanglement affecting the receptor/protein recognition	Diabetes mellitus	(Mero <i>et al.</i> , 2013)
	HA- Trypsin	The HA was conjugated to trypsin via EDC/Sulfo-NHS coupling reaction	The HA-Trypsin conjugates exhibited a trypsin content of 2.2–2.7% (w/w) with a small amount of free trypsin (<5%) Increase in the activity (1.5-fold) of conjugate was observed in the presence of Hyaluronidase (HAase) HA-trypsin demonstrated enhanced stability to proteolytic degradation by elastase, non-masking of enzyme activity upon HA conjugation and enhanced trypsin activity in the presence of HAase	-	(Ferguson <i>et al.</i> , 2010a)

	HA-EGF	The HA was conjugated to EGF via EDC/Sulfo-NHS coupling reaction	<p>The HA-EGF conjugate displayed an EGF content of 0.91–1.05% (w/w) with absence of free EGF (<1%)</p> <p>HA conjugation reduced the proliferative effects of EGF <i>in vitro</i> with HEP2 cells</p> <p>The HA-EGF conjugates failed to restore their cell proliferation activity even in the presence of HAase due to inhibition of receptor binding</p> <p>HA-EGF conjugate does not displayed typical masking/unmasking behavior</p>	Tissue repair	(Ferguson <i>et al.</i> , 2010a)
	HA- Exendin 4	The vinyl sulfone modified HA (HA-VS) was coupled to thiolated exendin 4 via Michael addition	<p>Conjugation improved <i>in vitro</i> serum stability of exendin 4 by 20-fold without any loss of bioactivity</p> <p><i>In vivo</i> studies of HA – exendin 4 conjugates in type 2 db/db mice demonstrated improved insulinotropic activity as well excellent glucose-lowering capabilities up to 3 days after a single subcutaneous injection while the effect of free exendin-4 exhausted within a day</p> <p>The conjugation of exendin 4 with HA has increased its residence time in blood thereby reducing the frequency of administration</p>	Type 2 diabetes mellitus	(Kong <i>et al.</i> , 2010)

(Continued)

Table 18.6 Cont.

Polymer	Conjugate	Reaction involved	Effect of conjugation on the protein/peptide	Indication	Reference
	HA- anti-Flt1 peptide	The Tetra-n-butyl ammonium hydroxide modified HA (HA-TBA) was coupled to anti-Flt1 peptide in the presence of benzotriazol-1-yloxy-tris(dimethyl-amino) phosphonium hexafluorophosphate (BOP) resulting in amide bond formation between carboxyl groups of HA and N-terminal amine groups of peptide	HA increased the aqueous solubility of the peptide Conjugate retained its activity and significantly reduced the binding of Flt1-Fc to VEGF ₁₆₅ coated on the well Inhibitory effect on corneal neovascularization as well as on retinal choroidal neovascularization (CNV) Reduction in retinal vascular permeability as well as deformation of retinal vascular structure was seen in diabetic retinopathy Reduction in the expression of VEGF receptor 2, increase in residence time up to 2 weeks	Corneal neovascularization, retinal neovascularization and diabetic retinopathy	(Oh <i>et al.</i> , 2011, Oh <i>et al.</i> , 2009)
	HA- Superoxide Dismutase (HA-SOD)	Amino groups of SOD were conjugated with carboxyl groups in the hyaluronic acid using EDC coupling reaction	<i>In vitro</i> results demonstrated that the conjugate retained 70% of the activity of free SOD <i>In vivo</i> studies of the conjugate exhibited much higher anti-inflammatory activities than either HA or SOD alone in inflammatory disease models The immunoreactivity of SOD in mice was also reduced after conjugation with HA	Anti-inflammatory agent	(Sakurai <i>et al.</i> , 1997)

HA: Hyaluronic acid; IFN: Interferon NIREF: Near-infrared fluorescence; HCV: Hepatitis C virus; OAS1: 2', 5'-oligoadenylate synthetase 1; hGH: Human growth factor; p-JAK2: Phosphorylated Janus kinase 2; AUC: Area under the curve; INS: Insulin; HAase: Hyaluronidase; EDC: 1-Ethyl-3-(3-dimethylaminopropyl) carbodiimide; NHS: N-Hydroxysuccinimide; EGF: Endothelial growth factor; VS: Vinyl sulfone; TBA: Tetra-n-butyl ammonium hydroxide; BOP: Benzotriazol-1-yloxy-tris(dimethyl-amino) phosphonium hexafluorophosphate; CNV: Retinal choroidal neovascularization; VEGF: Vascular endothelial growth factor; SOD: Superoxide dismutase.

18.11.2 Hyaluronic Acid-hGH Conjugate

Human growth hormone (hGH) has been extensively used in the treatment of short stature as it plays an important role for cell proliferation, mitosis, and differentiation. hGH promotes the synthesis of insulin-like growth factor I (IGF-1) in fibroblast and the released IGF-1 can enhance the proliferation of keratinocyte. In a study, HA-hGH conjugate was synthesized for receptor mediated transdermal delivery of hGH (Yang *et al.*, 2012a). The number of hGH molecules attached to HA in the conjugate could be controlled in the range from 1–9 by varying the amount of hGH in the feed with a bioconjugation efficiency higher than 95%. *In vivo* biological activity of HA-hGH conjugate was confirmed by the elevated expression level of phosphorylated Janus kinase 2 (p-JAK2) in the fibroblast of Detroit 551 cell through hGH-receptor mediated signaling pathway. Results of the pharmacokinetic studies demonstrated that the HA-hGH conjugate exhibited higher AUC (10-fold-) and bioavailability (16-fold-) compared to hGH upon topical treatment.

18.11.3 Hyaluronic Acid-Insulin Conjugate

Insulin (INS) was conjugated with HA resulting in conjugates HA-INS 1 and HA-INS 2 which differed in their degree of acetal substitution as 4% and 21% respectively. The effect of conjugation on protein loading was investigated (Mero *et al.*, 2013). The conjugates HA-INS 1 and HA-INS 2 exhibited a peptide loading of 17% and 32%, w/w respectively. The difference in their peptide loading was attributed to the steric hindrance variation present between the polypeptide chains. The yield of the conjugates for HA-INS 1 and HA-INS 2 was found to be 9.6% w/w and 18% w/w respectively. Results of blood compatibility studies suggested that both the conjugates were non-hemolytic in the concentration used for *in vivo* studies. *In vivo* studies were carried out in Sprague-Dawley rats in which Type I diabetes was induced with streptozotocin. The activity of lowering blood glucose level extended up to 6 h for HA-INS 1 conjugate whereas the free insulin was active only up to 1 h. In contrast, HA-INS 2 displayed no prominent effect on glucose titer which was attributed to steric entanglement affecting the receptor/protein recognition.

18.11.4 Hyaluronic Acid-Trypsin

The HA fragments ($M_w \sim 90,000$ g/mol) were coupled to model enzyme, trypsin to evaluate the potential of PUMPT concept. The HA-Trypsin conjugates exhibited a trypsin content of 2.2–2.7% (w/w) with a small amount of free trypsin (<5%). Conjugation of HA with trypsin did not alter the enzyme activity significantly but increase in the activity (1.5-fold) was observed in the presence of Hyaluronidase (HAase). In addition, HA-trypsin conjugates displayed ~52% greater stability in the physiological concentration of human leukocyte elastase (0.45 U/mL) compared to free trypsin (Ferguson *et al.*, 2010a). Hence, they concluded that HA-trypsin demonstrated increase in stability to proteolytic degradation by elastase, non-masking of enzyme activity upon HA conjugation and enhanced trypsin activity in the presence of hyaluronidase.

18.11.5 Hyaluronic Acid-EGF Conjugate

The HA fragments ($M_w \sim 90,000$ g/mol) were conjugated to EGF as a model growth factor to evaluate the potential of PUMPT concept. The HA-EGF conjugate displayed an EGF content of 0.91–1.05% (w/w) with the absence of free EGF (<1%). They observed that the HA conjugation decreased the *in vitro* proliferative effects of EGF with HEP2 cells. However, the HA-EGF conjugates failed to restore their cell proliferation activity even in the presence of HAase. They proposed that the HA binds to the lysine residue present at K48 which is present very close to EGF's receptor binding domain since K28 is buried within the tertiary structure of EGF. Hence, no proliferative activity was observed with HA-EGF conjugate due to inhibition of receptor binding suggesting that the conjugate does not exhibit typical masking/unmasking behavior (Ferguson *et al.*, 2010a).

18.11.6 Hyaluronic Acid-Exendin 4 Conjugates

Exendin 4 (exenatide) is an incretin mimetic that exhibits gluco-regulatory activities containing 39-amino acid peptide similar to glucagon-like peptide-1 (GLP-1) observed in mammals. It is used in the treatment of type 2 diabetes (db)s. By virtue of its shorter half-life (60–90 min) it required twice a day injection and hence its use is limited. Conjugation of exendin 4 with HA was developed using Michael addition (Kong *et al.*, 2010). They found that the number of exendin 4 molecules attached per single HA chain could be controlled in the range of 5–30 molecules with a bioconjugation efficiency of >90%. Moreover, conjugation enhanced the *in vitro* serum stability of exendin 4 by 20-fold without any loss of bioactivity. *In vivo* studies of HA – exendin 4 conjugates in type 2 db/db mice demonstrated better insulinotropic activity as well excellent glucose-lowering capabilities up to 3 days after a single subcutaneous injection while the effect of free exendin-4 exhausted within a day. Hence, they concluded that the conjugation of exendin 4 with HA has increased its residence time in the blood thereby reducing the frequency of administration. Furthermore, HA-Exendin 4 conjugate has a potential to be used as twice a week dosage form for the treatment of type II diabetes.

18.11.7 Hyaluronic Acid-anti-Flt1 Peptide Conjugates

Anti-Flt1 peptide of GNQWFI is a short antagonistic water insoluble hexapeptide for vascular endothelial growth factor receptor 1 (VEGFR1) inhibiting VEGFR1 mediated endothelial cell migration and tube formation. The anti-Flt1 peptide was coupled to hyaluronate (HA) ($RMM > 106$ kDa) and evaluated for its potential use in the treatment of corneal/retinal neovascularization as well as diabetic retinopathy. Overexpression of VEGF occurs in the retina in these pathologies, leading to angiogenesis and hyper-permeability. HA was chosen because of its hydrophilic nature which can increase the aqueous solubility of the peptide. The properties of the polymer such as viscoelasticity and mucoadhesive nature can further improve the outcome of the therapy for this specific application. The average content of peptide attached per single HA chain was in the range of 3–30 molecules which can be controlled by changing the feeding amount of peptide. *In vitro* results suggest that the HA-anti-Flt1 peptide conjugate retained

its activity and considerable reduction in the binding of Flt1-Fc to VEGF₁₆₅ coated on the well was observed when compared to the equivalent amount of free peptide (28 and 35%, respectively). Moreover, the inhibitory effect of the conjugate on the corneal neovascularization was confirmed *in vivo* in animal model. Reduction in retinal vascular permeability, as well as deformation of retinal vascular structure, was seen in diabetic retinopathy model rats after treatment with HA–Anti-Flt1 conjugate. Moreover, Reduction in the expression of VEGF receptor 2 was also seen after treatment with anti-Flt1 peptide–HA conjugate. The residence time of the conjugate was also increased up to 2 weeks. The solubility of the anti-Flt1 peptide–HA conjugate in water further potentiates its use in anti-angiogenic therapeutics (Oh *et al.*, 2011, Oh *et al.*, 2009).

18.11.8 Hyaluronic Acid-Superoxide Dismutase Conjugates

Superoxide dismutase (SOD) catalyzes the dismutation of highly reactive superoxide anion to molecular oxygen and hydrogen peroxide. Its potential as a therapeutic agent for adverse inflammatory reactions mediated by superoxide anion has been tested. Because of its high clearance rate as well as immunogenicity the clinical application of this enzyme has been limited. HA was conjugated with SOD obtained from bovine erythrocytes and evaluated for its potential as a novel anti-inflammatory agent (Sakurai *et al.*, 1997). The conjugate displayed an average of 1.5 molecules of SOD attached per each molecule of hyaluronate. *In vitro* results demonstrated that 70% of SOD activity was retained in the conjugate. Whereas *in vivo* studies of the conjugate displayed much higher anti-inflammatory activities than either HA or SOD alone in inflammatory disease models. The immunoreactivity of SOD in mice was also reduced after conjugation with HA and hence it can be safely injected into patients with RA without immunological side effects.

18.12 Some Other Polymer-Protein Conjugates

In one study, to enhance antitumor activity and stability of cytokine, TNF- α is conjugated with polyvinylpyrrolidone (PVP-TNF- α) and investigated on solid tumors mice model. This novel PVP-TNF- α conjugate fraction 3 showed >200- and >2- fold higher antitumor effect when compared to that of native TNF- α and MPEG-TNF- α respectively. Moreover, the PVP-TNF- α fraction 3 (360 min) showed 80- fold increase in the plasma half-life than native TNF- α (4.6 min) and 3- fold increase with respect to MPEG-TNF- α (122 min) (Kamada *et al.*, 2000). In recent, styrene-maleic acid-copolymer conjugated zinc protoporphyrin developed as a candidate drug for tumor-targeted therapy and imaging (Fang *et al.*, 2015).

18.13 PASylation

A biological polymer have been developed using unstructured polypeptide chains comprising of small residues of Pro, Ala and Ser (PAS). The properties of this polymer were found to be similar to PEG and hence PAS role in prolonging the plasma half-lives of

therapeutic proteins was studied. PAS sequences are hydrophilic, uncharged, non-toxic, non-immunogenic as well as biodegradable thereby preventing organ accumulation (Schlappschy *et al.*, 2013). However, PASylation avoids *in vitro* coupling or modification steps as the production of active protein occurs at the genetic level in *Escherichia coli*. Researchers demonstrated that PASylation can enhance the circulation half-life as well as *in vivo* bioactivity of therapeutic proteins such as growth hormone, interferon or Fab fragments. Moreover, its circulation half-life in mice was directly proportional to the polypeptide lengths (200, 400 and 600 A) used for fusion. The fused proteins displayed homogeneity with respect to molecular size, stability in the blood circulation, biodegradability, non-toxicity as well as absence of immunogenicity. However, PASylation does not serve as a potential strategy for delivering the proteins exhibiting high immunogenicity as it does not fully shield the protein surfaces, as that occurs during polymer conjugation.

18.14 Conclusion and Future Perspectives

Being fascinated, chemists are making efforts to scale up and improve the efficacy of proteins by conjugating with polymers, either by chemical or biological strategies. The PEGylated proteins were clinically used very often in the 1990s. The trend is changing due to the clinical development of polymer-drug conjugates and polymer combinations; also interest in the fields of 'nanomedicines and nanodiagnostics' is creating demand to all classes of polymer therapeutics. Nevertheless, there are many challenges to be addressed to ensure their safe and rapid translation into routine clinical use. Obviously, polymer-protein/peptide conjugates are complex and diverse. To address this, knowledge in the field of computation and simulation are critical. This enables the basic understanding of hybrid biomaterials. This can aid the hybrid biomaterials like polymer-protein/peptide conjugates to reach their full potential. In fact, as organ specific targeting of conjugates still remained an unsolved problem. To address these problems, efforts are being made by incorporating a wide range of functionalities, such as amino acids bearing different side-chain functional groups into the resulting structures. This may open a path to new protein/peptide conjugates with exciting new properties or functions; which may serve as an alternative to PEGylation to modify the protein properties to enhance their efficacy, targeting and clearance, thereby promoting them clinically.

Abbreviations

IC ₅₀	50% Inhibitory concentration
ABC	Accelerated blood clearance
ADA	Adenosine deaminase
AFM	Atomic Force Microscopy
AIDS	Acquired immune deficiency syndrome
ALL	Acute lymphoblastic leukemia

Anti-TNF	Anti-Tumor necrosis factor
Anti-VEGF	Anti- Vascular endothelial growth factor
APC	Antigen presenting cells
AUC	Area under curve
BE	Benzyl elimination system
Bicin	N-modified bis-2- hydroxyethylglycinamide
CA	Colominic acid
CEA	Carcinoembryonic antigen
CKD	Chronic kidney disease
CMD	Carboxymethyl-dextran
CNBr	Cyanogen bromide
CNV	Choroidal neovascularization
CPG ₂	Carboxypeptidase G ₂
DEAED	Diethylaminoethyl-dextran
DIVEMA	Divinylethermaleic anhydride/acid
DMARDs	Disease modifying anti-rheumatic drugs
DMSO	Dimethylsulfoxide
DPP-IV	Dipeptidyl peptidase-IV
EGF	Endothelial growth factor
ELISA	Enzyme-linked immunosorbent assay
EMP	Erythropoietin mimetic peptide
EPO	Erythropoietin
EPR	Enhanced permeation and retention
ESA	Erythropoiesis stimulating agent
FDA	Food and Drug Abbreviations
FITC	Fluorescein isothiocyanate
G-CSF	Granulocyte colony stimulating Factor
GHA	Growth hormone antagonist
GLP	Glucagon like peptide
GOX	Glucose oxidase
GRF	Growth hormone releasing factor
HA	Hyaluronic acid
HAase	Hyaluronidase
hCH	Human growth hormone
HCV	Hepatitis C
HES	Hydroxyl ethyl starch
HIV	Human Immunodeficiency Virus

HPG	Hyperbranched Polyglycerol
HPMA	N-(2-hydroxypropyl)-methacrylamide
IFN	Interferon
IGF-1	Insulin-like growth factor I
INS	Insulin
L-BAPNA	N-benzoyl-L-arginine-p-nitroanilide
MHCII	Major histocompatibility complex II
MRT	Mean residence time
MSH	Melanocyte stimulating hormone
Neu5Ac	N-acetylneuraminic acid
NIRF	Near-infrared fluorescence
OAS 1	2',5'-oligoadenylate synthetase 1
OG	Oligoglycerols
PAA	Polyacrylic acid
PACM	Poly(acroloylmorpholine)
PAMAM	Polyamidoamine
PAMAM-G4	Polyamidoamine generation 4
PAMAMOS	Polyamidoamine-organosilicon
PAS	Proline, Alanine and Serine
Pd	pharmacodynamic
PEG	Polyethylene glycol
PEG-ADA	PEGylated adenosine deaminase
PEI	Poly(ethyleneimine)
PG	Polyglycerols
PHEG	Poly((N-hydroxyethyl)- L-glutamine)
p-JAK2	Phosphorylated Janus kinase 2
Pk	Pharmacokinetic
PLA2	Phospholipase A2
PLAP	Placental alkaline phosphatases
pOVA	Ovalbumin peptide
POZ	Polyoxazoline
PSA	Polysialic acid
PUMPT	Polymer-masking-unmasking-protein therapy
PVA	Polyvinyl alcohol
PVE	Plasma volume expanders
PVP	Poly(vinylpyrrolidone)
RA	Rheumatoid arthritis

RES	Reticuloendothelial system
RGD	Arginine-glycine-aspartic acid) peptide
rhG-CSF	Recombinant human G-CSF
rHuEPO	Hyperglycosylated recombinant human EPO
RMM	Relative molecular mass
ROMBP	Ring opening multibranching polymerization
SC	Succinimidyl Carbamate
Sc-Fvs	Single-chain Fvs
SCID	Severe Combined Immunodeficiency Disease
SC-PEG	Calaspargase PEGol
sCT	Salmon Calcitonin
SMA	Styrene-co-maleic acid/anhydride
SOD	Superoxide dismutase
SS	Succinimidyl Succinate
SS-PEG	PEG-aspargase
TCR	T-cell receptor
TGase	Transglutaminase
TK	Tyrosine kinase
TKI	Tyrosine kinase inhibitors
TNF	Tumor necrosis factor
UC	Uricase
VEGF	Vascular endothelial growth factor
VEGFR	Vascular endothelial growth factor receptor
VEGFR 1	Vascular endothelial growth factor receptor 1

References

- Abbasi, E., Aval, S. F., Akbarzadeh, A., Milani, M., Nasrabadi, H. T., Joo, S. W., Hanifehpour, Y., Nejati-Koshki, K. & Pashaei-Asl, R. Dendrimers: synthesis, applications, and properties. *Nanoscale Research Letters*, 9, 1, 2014.
- Angiolillo, A. L., Schore, R. J., Devidas, M., Borowitz, M. J., Carroll, A. J., Gastier-Foster, J. M., Heerema, N. A., Keilani, T., Lane, A. R. & Loh, M. L. Pharmacokinetic and Pharmacodynamic Properties of Calaspargase Pegol Escherichia coli L-Asparaginase in the Treatment of Patients With Acute Lymphoblastic Leukemia: Results From Children's Oncology Group Study AALL07P4. *Journal of Clinical Oncology*, 55, 5763, 2014.
- Baudyś, M., Letourneur, D., Liu, F., Mix, D., Jozefonvicz, J. & Kim, S. W. Extending insulin action *in vivo* by conjugation to carboxymethyl dextran. *Bioconjugate Chemistry*, 9, 176, 1998.
- Besheer, A., Hause, G., Kressler, J. & Mäder, K. Hydrophobically modified hydroxyethyl starch: synthesis, characterization, and aqueous self-assembly into nano-sized polymeric micelles and vesicles. *Biomacromolecules*, 8, 359, 2007.

- Bezuglov, V. V., Gretskeya, N. M., Klinov, D. V., Bobrov, M. Y., Shibanova, E. D., Akimov, M. G., Fomina-Ageeva, E. V., Zinchenko, G. N., Bairamashvili, D. I. & Miroshnikov, A. I. Nanocomplexes of recombinant proteins and polysialic acid: Preparation, characteristics, and biological activity. *Russian Journal of Bioorganic Chemistry*, 35, 320, 2009.
- Bourne, T., Fossati, G. & Nesbitt, A. A PEGylated Fab-Fragment against Tumor Necrosis Factor for the Treatment of Crohn Disease. *BioDrugs*, 22, 331, 2008.
- Brocchini, S., Godwin, A., Balan, S., Choi, J.-W., Zloh, M. & Shaunak, S. Disulfide bridge based PEGylation of proteins. *Advanced Drug Delivery Reviews*, 60, 3, 2008.
- Calabresi, P. A., Kieseier, B. C., Arnold, D. L., Balcer, L. J., Boyko, A., Pelletier, J., Liu, S., Zhu, Y., Seddighzadeh, A. & Hung, S. Pegylated interferon beta-1a for relapsing-remitting multiple sclerosis (ADVANCE): a randomised, phase 3, double-blind study. *The Lancet Neurology*, 13, 657, 2014.
- Calderon, M., Quadir, M. A., Sharma, S. K. & Haag, R. Dendritic polyglycerols for biomedical applications. *Adv Mater*, 22, 190, 2010.
- Chanphai, P. & Tajmir-Riahi, H. A. Trypsin and trypsin inhibitor bind PAMAM nanoparticles: Effect of hydrophobicity on protein-polymer conjugation. *J. Colloid Interface Sci.*, 461, 419, 2016.
- Chapman, A. P. PEGylated antibodies and antibody fragments for improved therapy: a review. *Advanced drug delivery reviews*, 54, 531, 2002.
- Cho, H., Daniel, T., Buechler, Y. J., Litzinger, D. C., Maio, Z., Putnam, A.-M. H., Kraynov, V. S., Sim, B.-C., Bussell, S. & Javahishvili, T. Optimized clinical performance of growth hormone with an expanded genetic code. *Proceedings of the National Academy of Sciences*, 108, 9060, 2011.
- Choy, E. H. S., Hazleman, B., Smith, M., Moss, K., Lisi, L., Scott, D. G. I., Patel, J., Sopwith, M. & Isenberg, D. A. Efficacy of a novel PEGylated humanized anti-TNF fragment (CDP870) in patients with rheumatoid arthritis: a phase II double-blinded, randomized, dose-escalating trial. *Rheumatology*, 41, 1133, 2002.
- Constantinou, A., Epenetos, A., Hreczuk-Hirst, D., Jain, S., Wright, M., Chester, K. & Deonarain, M. Site-specific polysialylation of an antitumor single-chain Fv fragment. *Bioconjugate Chemistry*, 20, 924, 2009.
- Constantinou, A., Epenetos, A. A., Hreczuk-Hirst, D., Jain, S. & Deonarain, M. P. Modulation of antibody pharmacokinetics by chemical polysialylation. *Bioconjugate Chemistry*, 19, 643, 2008.
- D'antonio, M., Louveau, I., Esposito, P., Bertolino, M. & Canali, S. Pharmacodynamic evaluation of a PEGylated analogue of human growth hormone releasing factor in rats and pigs. *Growth Hormone & IGF Research*, 14, 226, 2004.
- Davis, F. F. PEG-adenosine deaminase and PEG-asparaginase. *Polymer Drugs in the Clinical Stage*. Springer, 2003.
- DeFrees, S., Wang, Z.-G., Xing, R., Scott, A. E., Wang, J., Zopf, D., Gouty, D. L., Sjoberg, E. R., Panneerselvam, K. & Brinkman-Van der Linden, E. C. GlycoPEGylation of recombinant therapeutic proteins produced in *Escherichia coli*. *Glycobiology*, 16, 833, 2006.
- Deiters, A., Cropp, T. A., Summerer, D., Mukherji, M. & Schultz, P. G. Site-specific PEGylation of proteins containing unnatural amino acids. *Bioorganic & Medicinal Chemistry Letters*, 14, 5743, 2004.
- Duncan, R., Gilbert, H. R., Carbajo, R. J. & Vicent, M. J. Polymer Masked– Unmasked Protein Therapy. 1. Bioresponsive Dextrin– Trypsin and– Melanocyte Stimulating Hormone Conjugates Designed for α -Amylase Activation. *Biomacromolecules*, 9, 1146, 2008.
- Dyawanapelly, S., Junnuthula, V. R. & Singh, A. V. The Holy Grail of Polymer Therapeutics for Cancer Therapy: An Overview on the Pharmacokinetics and Bio Distribution. *Current Drug Metabolism*, 16, 522, 2015.

- Egrie, J. C. & Browne, J. K. Development and characterization of novel erythropoiesis stimulating protein (NESP). *Nephrology Dialysis Transplantation*, 16, 3, 2001.
- Fan, Q., Leuther, K. K., Holmes, C. P., Fong, K.-l., Zhang, J., Velkovska, S., Chen, M.-j., Mortensen, R. B., Leu, K. & Green, J. M. Preclinical evaluation of Hematide, a novel erythropoiesis stimulating agent, for the treatment of anemia. *Experimental Hematology*, 34, 1303, 2006.
- Fang, J., Tsukigawa, K., Liao, L., Yin, H., Eguchi, K. & Maeda, H. Styrene-maleic acid-copolymer conjugated zinc protoporphyrin as a candidate drug for tumor-targeted therapy and imaging. *Journal of Drug Targeting*, 1, 2015.
- Ferguson, E. L., Alshame, A. M. & Thomas, D. W. Evaluation of hyaluronic acid-protein conjugates for polymer masked-unmasked protein therapy. *Int. J. Pharm.*, 402, 95, 2010a.
- Ferguson, E. L., Richardson, S. C. & Duncan, R. Studies on the Mechanism of Action of Dextrin- Phospholipase A2 and Its Suitability for Use in Combination Therapy. *Molecular Pharmaceutics*, 7, 510, 2010b.
- Fernandes, A. I. & Gregoriadis, G. Synthesis, characterization and properties of sialylated catalase. *Biochimica et Biophysica Acta (BBA)-Protein Structure and Molecular Enzymology*, 1293, 90, 1996.
- Fernandes, A. I. & Gregoriadis, G. Polysialylated asparaginase: preparation, activity and pharmacokinetics. *Biochimica et Biophysica Acta (BBA)-Protein Structure and Molecular Enzymology*, 1341, 26, 1997.
- Fernandes, A. I. & Gregoriadis, G. The effect of polysialylation on the immunogenicity and antigenicity of asparaginase: implication in its pharmacokinetics. *International Journal of Pharmaceutics*, 217, 215, 2001.
- Filpula, D. & Zhao, H. Releasable PEGylation of proteins with customized linkers. *Advanced Drug Delivery Reviews*, 60, 29, 2008.
- Filpula, D. R. & Sapra, P. Adenosine deaminase anticancer therapy. U.S. Patent No. 8,741,283, 2014.
- Fishburn, C. S. The pharmacology of PEGylation: balancing PD with PK to generate novel therapeutics. *Journal of Pharmaceutical Sciences*, 97, 4167, 2008.
- Fontana, A., Spolaore, B., Mero, A. & Veronese, F. M. Site-specific modification and PEGylation of pharmaceutical proteins mediated by transglutaminase. *Advanced Drug Delivery Reviews*, 60, 13, 2008.
- Frey, H. & Haag, R. Dendritic polyglycerol: a new versatile biocompatible material. *Reviews in Molecular Biotechnology*, 90, 257, 2002.
- Fu, C. H. & Sakamoto, K. M. PEG-asparaginase. *Expert Opinion on Pharmacotherapy*, 8, 1977, 2007.
- Gillies, E. R. & Fréchet, J. M. J. Dendrimers and dendritic polymers in drug delivery. *Drug Discovery Today*, 10, 35, 2005.
- Glue, P., Fang, J. W. S., Rouzier-Panis, R., Raffanel, C., Sabo, R., Gupta, S. K., Salfi, M. & Jacobs, S. Pegylated interferon- α 2b: Pharmacokinetics, pharmacodynamics, safety, and preliminary efficacy data. *Clinical Pharmacology & Therapeutics*, 68, 556, 2000.
- Gokarn, Y. R., McLean, M. & Laue, T. M. Effect of PEGylation on protein hydrodynamics. *Molecular Pharmaceutics*, 9, 762, 2012.
- Gong, Y., Leroux, J.-C. & Gauthier, M. A. Releasable conjugation of polymers to proteins. *Bioconjugate Chemistry*, 26, 1172, 2015.
- Gregoriadis, G., Jain, S., Papaioannou, I. & Laing, P. Improving the therapeutic efficacy of peptides and proteins: a role for polysialic acids. *International Journal of Pharmaceutics*, 300, 125, 2005.
- Gregoriadis, G., McCormack, B., Wang, Z. & Lively, R. Polysialic acids: potential in drug delivery. *FEBS Letters*, 315, 271, 1993.
- Greindl, A., Kessler, C., Breuer, B., Haberl, U., Rybka, A., Emgenbroich, M., Pötgens, A. J. & Frank, H.-G. AGEM400 (HES), a novel erythropoietin mimetic peptide conjugated to hydroxyethyl starch with excellent *in vitro* efficacy. *Open Hematology Journal*, 4, 1, 2010.

- Gupta, S., Pfeil, J., Kumar, S., Poulsen, C., Lauer, U., Hamann, A., Hoffmann, U. & Haag, R. Tolerogenic Modulation of the Immune Response by Oligoglycerol-and Polyglycerol-Peptide Conjugates. *Bioconjugate Chemistry*, 26, 669, 2015.
- Hardwicke, J., Moseley, R., Stephens, P., Harding, K., Duncan, R. & Thomas, D. W. Bioresponsive dextrin– rhEGF conjugates: *In vitro* evaluation in models relevant to its proposed use as a treatment for chronic wounds. *Molecular pharmaceuticals*, 7, 699, 2010.
- Hardwicke, J. T., Hart, J., Bell, A., Duncan, R., Thomas, D. W. & Moseley, R. The effect of dextrin–rhEGF on the healing of full-thickness, excisional wounds in the (db/db) diabetic mouse. *J. Control Release*, 152, 411, 2011.
- Harris, J. M. & Chess, R. B. Effect of pegylation on pharmaceuticals. *Nature Reviews Drug Discovery*, 2, 214, 2003.
- <http://www.octapharma-biopharmaceuticals.com> <http://www.octapharma-biopharmaceuticals.com/en/research-development/projects.html>, Accessed on 06/12/2015.
- Hu, X., Miller, L., Richman, S., Hitchman, S., Glick, G., Liu, S., Zhu, Y., Crossman, M., Nestorov, I. & Gronke, R. S. A Novel PEGylated Interferon Beta-1a for Multiple Sclerosis: Safety, Pharmacology, and Biology. *The Journal of Clinical Pharmacology*, 52, 798, 2012.
- Jain, S., Hreczuk-Hirst, D. H., McCormack, B., Mital, M., Epenetos, A., Laing, P. & Gregoriadis, G. Polysialylated insulin: synthesis, characterization and biological activity *in vivo*. *Biochimica et Biophysica Acta (BBA) - General Subjects*, 1622, 42, 2003.
- Jaracz, S., Chen, J., Kuznetsova, L. V. & Ojima, I. Recent advances in tumor-targeting anticancer drug conjugates. *Bioorganic & Medicinal Chemistry*, 13, 5043, 2005.
- Jung, B. & Theato, P. Chemical strategies for the synthesis of protein-polymer conjugates. *Bio-synthetic Polymer Conjugates*. Springer, 2013.
- Kainthan, R. K., Hester, S. R., Levin, E., Devine, D. V. & Brooks, D. E. *In vitro* biological evaluation of high molecular weight hyperbranched polyglycerols. *Biomaterials*, 28, 4581, 2007.
- Kamada, H., Tsutsumi, Y., Yamamoto, Y., Kihira, T., Kaneda, Y., Mu, Y., Kodaira, H., Tsunoda, S.-I., Nakagawa, S. & Mayumi, T. Antitumor activity of tumor necrosis factor- α conjugated with polyvinylpyrrolidone on solid tumors in mice. *Cancer Research*, 60, 6416, 2000.
- Kang, J. S., DeLuca, P. P. & Lee, K. C. Emerging PEGylated drugs. *Expert Opinion on Emerging Drugs*, 14, 363, 2009.
- Khandare, J. & Calderon, M. Dendritic polymers for smart drug delivery applications. *Nanoscale*, 7, 3806, 2015.
- Kieseier, B. C. & Calabresi, P. A. PEGylation of Interferon- β -1a. *CNS Drugs*, 26, 205, 2012.
- Klajnert, B. & Bryszewska, M. Dendrimers: properties and applications. *Acta biochimica polonica*, 48, 199, 2000.
- Kong, J. H., Oh, E. J., Chae, S. Y., Lee, K. C. & Hahn, S. K. Long acting hyaluronate--exendin 4 conjugate for the treatment of type 2 diabetes. *Biomaterials*, 31, 4121, 2010.
- Kontermann, R. E. Strategies for extended serum half-life of protein therapeutics. *Current opinion in biotechnology*, 22, 868, 2011.
- Krejsa, C., Rogge, M. & Sadee, W. Protein therapeutics: new applications for pharmacogenetics. *Nature Reviews Drug Discovery*, 5, 507, 2006.
- Larson, N. & Ghandehari, H. Polymeric conjugates for drug delivery. *Chemistry of Materials*, 24, 840, 2012.
- Lee, Y., Kim, J., Kim, S., Jang, W.-D., Park, S. & Koh, W.-G. Protein-conjugated, glucose-sensitive surface using fluorescent dendrimer porphyrin. *J. Mater. Chem.*, 19, 5643, 2009.
- Li, H. & d'Anjou, M. Pharmacological significance of glycosylation in therapeutic proteins. *Curr. Opin. Biotechnol.*, 20, 678, 2009.
- Liebner, R., Mathaes, R., Meyer, M., Hey, T., Winter, G. & Besheer, A. Protein HESylation for half-life extension: synthesis, characterization and pharmacokinetics of HESylated anakinra. *Eur. J. Pharm. Biopharm.*, 87, 378, 2014.

- Lin, B. X., Qiao, Y., Shi, B. & Tao, Y. Polysialic acid biosynthesis and production in *Escherichia coli*: current state and perspectives. *Appl. Microbiol. Biotechnol.*, 1, 2015.
- Martin, N. & Modi, M. Pegylation: a novel process for modifying pharmacokinetics. *Clin. Pharmacokinet.*, 40, 539, 2001.
- Melton, R., Wiblin, C., Baskerville, A., Foster, R. & Sherwood, R. Covalent linkage of carboxypeptidase-G2 to soluble dextrans. 2. *In vivo* distribution and fate of conjugates. *Biochemical Pharmacology*, 36, 113, 1987.
- Mero, A. & Campisi, M. Hyaluronic acid bioconjugates for the delivery of bioactive molecules. *Polymers*, 6, 346, 2014.
- Mero, A., Ishino, T., Chaiken, I., Veronese, F. M. & Pasut, G. Multivalent and flexible PEG-nitrilotriacetic acid derivatives for non-covalent protein pegylation. *Pharmaceutical Research*, 28, 2412, 2011.
- Mero, A., Pasqualin, M., Campisi, M., Renier, D. & Pasut, G. Conjugation of hyaluronan to proteins. *Carbohydr. Polym.*, 92, 2163, 2013.
- Mero, A., Pasut, G., Dalla Via, L., Fijten, M. W., Schubert, U. S., Hoogenboom, R. & Veronese, F. M. Synthesis and characterization of poly (2-ethyl 2-oxazoline)-conjugates with proteins and drugs: Suitable alternatives to PEG-conjugates? *Journal of Controlled Release*, 125, 87, 2008.
- Monaghan, S., Griffith-Johnson, D., Matthews, I. & Bradley, M. Solid-phase synthesis of peptide-dendrimer conjugates for an investigation of integrin binding. *Arkivoc*, 10, 46, 2001.
- Oh, E. J., Choi, J. S., Kim, H., Joo, C. K. & Hahn, S. K. Anti-Flt1 peptide - hyaluronate conjugate for the treatment of retinal neovascularization and diabetic retinopathy. *Biomaterials*, 32, 3115, 2011.
- Oh, E. J., Park, K., Choi, J. S., Joo, C. K. & Hahn, S. K. Synthesis, characterization, and preliminary assessment of anti-Flt1 peptide-hyaluronate conjugate for the treatment of corneal neovascularization. *Biomaterials*, 30, 6026, 2009.
- Osborn, B. L., Olsen, H. S., Nardelli, B., Murray, J. H., Zhou, J. X. H., Garcia, A., Moody, G., Zaritskaya, L. S. & Sung, C. Pharmacokinetic and pharmacodynamic studies of a human serum albumin-interferon- α fusion protein in cynomolgus monkeys. *Journal of Pharmacology and Experimental Therapeutics*, 303, 540, 2002.
- Pasut, G. Polymers for Protein Conjugation. *Polymers*, 6, 160, 2014.
- Pasut, G. & Veronese, F. M. Polymer-drug conjugation, recent achievements and general strategies. *Progress in Polymer Science*, 32, 933, 2007.
- Pasut, G. & Veronese, F. M. PEG conjugates in clinical development or use as anticancer agents: an overview. *Advanced Drug Delivery Reviews*, 61, 1177, 2009.
- Pasut, G. & Veronese, F. M. State of the art in PEGylation: the great versatility achieved after forty years of research. *Journal of Controlled Release*, 161, 461, 2012.
- Pappu, A., Patil, V., Jain, S., Mahindrakar, A., Haque, R., Thakur, V.K., Advances in industrial prospective of cellulosic macromolecules enriched banana biofibre resources: A review. *Int. J. Biol. Macromol.*, 79, 449, 2015.
- Pisal, D. S., Kosloski, M. P. & Balu-Iyer, S. V. Delivery of therapeutic proteins. *J. Pharm. Sci.*, 99, 2557, 2010.
- Place, A. E., Stevenson, K. E., Vrooman, L. M., Harris, M. H., Hunt, S. K., O'Brien, J. E., Supko J. G., Asselin, B. L., Athale, U. H. & Clavell, L. A. Intravenous pegylated asparaginase versus intramuscular native *Escherichia coli*-asparaginase in newly diagnosed childhood acute lymphoblastic leukaemia (DFCI 05-001): a randomised, open-label phase 3 trial. *The Lancet Oncology*, 16, 1677, 2015.
- Punnappuzha, A., Ponnannettiappan, J., Nishith, R. S., Hadigal, S. & Pai, P. G. Synthesis and Characterization of Polysialic Acid-Uricase Conjugates for the Treatment of Hyperuricemia. *International Journal of Peptide Research and Therapeutics*, 20, 465, 2014.
- Reddy, K. R. Development and pharmacokinetics and pharmacodynamics of pegylated interferon alfa-2a (40 kD). *Seminars in Liver Disease*, 2003.

- Riva, R., Ragelle, H., des Rieux, A., Duhem, N., Jérôme, C. & Préat, V. Chitosan and chitosan derivatives in drug delivery and tissue engineering. *Chitosan for Biomaterials II*. Springer, 2011.
- Sakamoto, Y., Akanuma, Y., Kosaka, K. & Jeanrenaud, B. Comparative effects of narative insulin and insulin-dextran complexes on the metabolism of adipose tissue. *Biochimica et Biophysica Acta (BBA)-General Subjects*, 498, 102, 1977.
- Sakurai, K., Miyazaki, K., Kodera, Y., Nishimura, H., Shingu, M. & Inada, Y. Anti-inflammatory activity of superoxide dismutase conjugated with sodium hyaluronate. *Glycoconjugate Journal*, 14, 723, 1997.
- Schlapschy, M., Binder, U., Borger, C., Theobald, I., Wachinger, K., Kisling, S., Haller, D. & Skerra, A. PASylation: a biological alternative to PEGylation for extending the plasma half-life of pharmaceutically active proteins. *Protein Eng. Des. Sel.*, 26, 489, 2013.
- Sharma, A. R., Kundu, S. K., Nam, J. S., Sharma, G., Priya Doss, C. G., Lee, S. S. & Chakraborty, C. Next generation delivery system for proteins and genes of therapeutic purpose: why and how? *Biomed. Res. Int.*, 2014, 327950, 2014.
- Sherman, M. R., Saifer, M. G. P. & Perez-Ruiz, F. PEG-uricase in the management of treatment-resistant gout and hyperuricemia. *Advanced Drug Delivery Reviews*, 60, 59, 2008.
- Shin, K.-H., Lim, K. S., Lee, H., Jang, I.-J. & Yu, K.-S. An assessment of the pharmacokinetics, pharmacodynamics, and tolerability of GCPGC, a novel pegylated granulocyte colony-stimulating factor (G-CSF), in healthy subjects. *Investigational New Drugs*, 32, 636, 2014.
- Sinclair, A. M. Erythropoiesis stimulating agents: approaches to modulate activity. *Biologics: Targets & Therapy*, 7, 161, 2013.
- Singh, A. V., Raichur, A. M. & Dyawanapelly, S. *Encyclopedia of Biomedical Polymers and Polymeric Biomaterials*, 2015. CRC Press, New York, USA.
- Sola, R. J. & Griebenow, K. 2010. Glycosylation of therapeutic proteins: an effective strategy to optimize efficacy. *BioDrugs*, 24, 9, 2015.
- Son, J. P., Jun, S.-W., Choi, Y.-K., Park, H. S., Son, M. K., Lee, M. Y., Kang, S. H., Kang, J. S. & Park, Y. I. Structural identification and biological activity of positional isomers of long-acting and mono-PEGylated recombinant human granulocyte colony-stimulating factor with trimeric-structured methoxy polyethylene glycol N-hydroxysuccinimidyl functional group. *Analytical Biochemistry*, 423, 286, 2012.
- Spiro, R. G. Protein glycosylation: nature, distribution, enzymatic formation, and disease implications of glycopeptide bonds. *Glycobiology*, 12, 43R, 2002.
- Sunder, A., Mülhaupt, R. & Frey, H. Hyperbranched polyether-polyols based on polyglycerol: polarity design by block copolymerization with propylene oxide. *Macromolecules*, 33, 309, 2000.
- Takuya, F., Yoshihisa, Y., Yoshinobu, T., Mitsuru, H. & Hitoshi, S. Alteration of biopharmaceutical properties of drugs by their conjugation with water-soluble macromolecules: uricase-dextran conjugate. *Journal of Controlled Release*, 11, 149, 1990.
- Tam, S.-C., Blumenstein, J. & Wong, J. Soluble dextran-hemoglobin complex as a potential blood substitute. *Proceedings of the National Academy of Sciences*, 73, 2128, 1976.
- Thakur, M.K., Thakur, V.K., Gupta, R.K., Pappu, A., Synthesis and Applications of Biodegradable Soy Based Graft Copolymers: A Review. *ACS Sustain. Chem. Eng.* 4, 1–17, 2016.
- Thakur, V.K., Thakur, M.K., Recent Advances in Graft Copolymerization and Applications of Chitosan: A Review. *ACS Sustain. Chem. Eng.* 2, 2637, 2014a.
- Thakur, V.K., Thakur, M.K., Recent trends in hydrogels based on psyllium polysaccharide: a review. *J. Clean. Prod.* 82, 1, 2014b.
- Tomalia, D. A., Baker, H., Dewald, J., Hall, M., Kallos, G., Martin, S., Roeck, J., Ryder, J. & Smith, P. A new class of polymers: starburst-dendritic macromolecules. *Polymer Journal*, 17, 117, 1985.
- Tsuji, J.-I., Hirose, K., Kasahara, E., Naitoh, M. & Yamamoto, I. Studies on antigenicity of the polyethylene glycol (PEG)-modified uricase. *International Journal of Immunopharmacology*, 7, 725, 1985.

- Uhlig, T., Kyprianou, T., Martinelli, F. G., Oppici, C. A., Heiligers, D., Hills, D., Calvo, X. R. & Verhaert, P. The emergence of peptides in the pharmaceutical business: From exploration to exploitation. *EuPA Open Proteomics*, 4, 58, 2014.
- van der Meer, L. T., Terry, S. Y. A., van Ingen-Schenau, D. S., Andree, K. C., Hoogerbrugge, P. M., Boerman, O. C. & van Leeuwen, F. N. The Therapeutic Protein Asparaginase Is Efficiently Cleared By Bone Marrow and Spleen Resident Macrophages. *Blood*, 124, 3630, 2014.
- Veronese, F. M. & Mero, A. The impact of PEGylation on biological therapies. *BioDrugs*, 22, 315, 2008.
- Veronese, F. M. & Pasut, G. PEGylation, successful approach to drug delivery. *Drug Discovery Today*, 10, 1451, 2005.
- Viegas, T. X., Bentley, M. D., Harris, J. M., Fang, Z., Yoon, K., Dizman, B., Weimer, R., Mero, A., Pasut, G. & Veronese, F. M. Polyoxazoline: chemistry, properties, and applications in drug delivery. *Bioconjugate Chemistry*, 22, 976, 2011.
- Voicu, S.I., Condruz, R.M., Mitran, V., Cimpean, A., Miculescu, F., Andronescu, C., Miculescu, M., Thakur, V.K., Sericin Covalent Immobilization onto Cellulose Acetate Membrane for Biomedical Applications. *ACS Sustain. Chem. Eng.* 4, 1765, 2016.
- Wileman, T. E. Properties of asparaginase-dextran conjugates. *Advanced Drug Delivery Reviews*, 6, 167, 1991.
- Wileman, T. E., Foster, R. L. & Elliott, P. N. Soluble asparaginase-dextran conjugates show increased circulatory persistence and lowered antigen reactivity. *Journal of Pharmacy and Pharmacology*, 38, 264, 1986.
- Wilms, D., Stiriba, S.-E. & Frey, H. Hyperbranched polyglycerols: from the controlled synthesis of biocompatible polyether polyols to multipurpose applications. *Accounts of Chemical Research*, 43, 129, 2009.
- Woodburn, K. W., Holmes, C. P., Wilson, S. D., Fong, K.-L., Press, R. J., Moriya, Y. & Tagawa, Y. Absorption, distribution, metabolism and excretion of peginesatide, a novel erythropoiesis-stimulating agent, in rats. *Xenobiotica*, 42, 660, 2012.
- Wu, L., Ho, S. V., Wang, W., Gao, J., Zhang, G., Su, Z. & Hu, T. N-terminal mono-PEGylation of growth hormone antagonist: Correlation of PEG size and pharmacodynamic behavior. *International Journal of Pharmaceutics*, 453, 533, 2013.
- Yang, J. A., Kim, E. S., Kwon, J. H., Kim, H., Shin, J. H., Yun, S. H., Choi, K. Y. & Hahn, S. K. Transdermal delivery of hyaluronic acid -- human growth hormone conjugate. *Biomaterials*, 33, 5947, 2012a.
- Yang, J. A., Park, K., Jung, H., Kim, H., Hong, S. W., Yoon, S. K. & Hahn, S. K. Target specific hyaluronic acid-interferon alpha conjugate for the treatment of hepatitis C virus infection. *Biomaterials*, 32, 8722, 2011.
- Yang, X., Yuan, Y., Zhan, C.-G. & Liao, F. Uricases as therapeutic agents to treat refractory gout: current states and future directions. *Drug Development Research*, 73, 66, 2012b.
- Yu, M., Wu, J., Shi, J. & Farokhzad, O. C. Nanotechnology for protein delivery: Overview and perspectives. *Journal of Controlled Release*, 2015.
- Zhang, C., Yang, X.-L., Yuan, Y.-h., Pu, J. & Liao, F. Site-specific PEGylation of therapeutic proteins via optimization of both accessible reactive amino acid residues and PEG derivatives. *BioDrugs*, 26, 209, 2012.
- Zhang, J., Krajden, O., Kainthan, R., Kizhakkedathu, J., Constantinescu, I., Brooks, D. & Gyongyossy-Issa, M. Conjugation to hyperbranched polyglycerols improves RGD-mediated inhibition of platelet function *in vitro*. *Bioconjugate chemistry*, 19, 1241, 2008.
- Zhang, T., She, Z., Huang, Z., Li, J., Luo, X. & Deng, Y. Application of sialic acid/polysialic acid in the drug delivery systems. *Asian Journal of Pharmaceutical Sciences*, 9, 75, 2014.

Index

- 5-hydroxymethylfurfural, 158
- 3,4-dihydroxyphenylalanine (DOPA), 134
- Absorber, 94–95
- Abundance, 244, 257
- Acetylation, 246, 248
- Acid hydrolysis, 66–70, 85, 250, 257, 259
- Acoustic, 244
- Acrodur®, 303–304
- Acrylic resin, 289, 304
- Acrylonitril butadiene rubber (NBR), 299–300
- Activated carbon, 409–410
- Acyclic diene metathesis (ADMET), 110, 112, 118, 119
- Additive, 94, 99–101
- Adenosine deaminase, 485
- Adhesives, 129–132, 135, 167, 169, 172, 177
- Aerospace, 243, 261–262
- AFM, atomic force microscopy, 74
- Agave, 28–33, 35–36, 52–54
- Agricultural waste, 244
- Agro-based, 245
- Albumin, 315, 320–321, 326–328, 331
- Algal biomass, 136–137
- ALGLUE biomass, 137–142
- Aliphatic linkers (bicin linkers), 495
- Alkali, 246, 248, 256, 261
- Amorphous domains, 64, 66, 75
- Anhydrides, 154, 166, 167
- Annealing, 25, 29, 51–55
- Antimicrobials, 339, 344–346, 349–351, 354, 357, 358
- Antioxidants, 337–342, 353, 354, 357, 358
- Anti-tumor necrosis factor, 485
- Apatite, 311, 325–327
- Applications of magnetic bio char, 450
- Aromatic, 95, 97
- Aromatic linkers (BE series), 495
- Asparaginase, 484
- Aspect ratio, 255, 257
- Automotive, 243, 261–262
- Azetidine cation, 172
- Bamboo, 31
- Banana, 32–33, 35
- Barrier properties, 27, 338–340, 348, 358
- Basic features and properties of PEG, 488
- Bioactive glass ceramics, 310
- Bioactive glasses, 310, 312, 320–321, 331, 398–400
- Bioactivity, 310–311, 325–326
- Bio-based CF, 15
- Bio-based polymers, 273
- Biocompatibility, 278, 279, 320–321, 325
- Biocompatible, 245
- Biocomposites, 77, 84, 244, 246, 250, 255, 257, 259–261, 276, 277
- Biodegradability, 279, 280, 309
- Biodegradable, 61, 80, 82, 243–244, 246, 255–256, 262
- Biodegradable polymers for conjugation, 487
- Bio-derived polymers, 273
- Biodiesel, 152
- Bio-fillers, 244, 249, 254–255, 265
- Bioglass®, 311–312
- Biomacromolecules, 388–394
- Biomass, 67, 254
- Biomass cross-linking and blocking (BCB technology), 137
- Biomaterials, 309
- Biomedical and biotechnological applications, 280
- Bio-mimetic adhesives, 134

- Bio-oil, 161
- Biopolymers, 81, 85, 243, 254–256, 262, 273
 - Category 1, 273
 - Category 2, 273
 - Category 3, 273
- Bio-resin, 257
- Biosensors, 282, 283
- Bisphenol A, 154
- Blends, 1, 9, 12
- Blood albumen glues, 131
- Blowing agent, 93–94, 96–99, 101
- Bombyx mori, 195–200
 - chemistry, 195–198
 - physical properties, 198–200
 - structures, 195–198
- Brown liquor, 110
- Building insulation, 93
- Calcium carbonate, 396–397
- California air resources board (CARB), 130
- Cambond biomass
 - greener process, 145
 - insulation and interior decoration, 142–143
 - MDF, PB and OSB, 143–144
 - particle boards, 144–145
 - straw beam, 142
- Canola, 171
- Carbon black, 289, 298–300
- Carbon nanotubes, 410–417
- Carbonization, 1, 2, 9, 10, 13
- Carboxymethylation, 379
- Catalyst, 93, 96–98, 101
- Cellulose, 28–29, 31–32, 35–36, 39–41, 43–46, 51, 53, 62–80, 83, 85, 112, 120, 127, 128, 243–246, 249–250, 254–255, 257, 259, 264
 - MCC, microcrystalline, 61, 63, 66–85
 - nanofibrils, 78
 - nanowhiskers, 78
- Cellulose derivatization, 167–168
 - grafting, 167
 - oxidation, 167, 169
- Cellulose nanocrystals, 250
- Cellulose nanofibers, 252
- Cellulose nanofibrils, 250
- Cellulose nanowhiskers, 244–245, 249–250, 257
- CF precursors, 2–4, 12–14
- CF production, 2, 4–6, 9, 12
- Characteristics of magnetic bio char, 447
 - magnetic characteristics, 449
 - surface area characteristics, 448
- Characterization, 61, 72, 85
- Characterization of polysaccharide,
 - organoleptic evaluation, 224, 231
 - preliminary phytochemical evaluation, 225, 231
- Chemical composition, 85
- Chemical extraction, 250
- Chemical structure, 61, 65, 72, 73
- Chemical treatments, 246, 248, 250
- Chemistry and different sites of PEGylation, 492
- Chitin, 41–42, 249
- Chitosan, 114, 116, 117, 120, 122, 126, 127, 169, 249, 371–434
- Chondroitin sulfate, 374–376
- Classification of biopolymers, 273
- Coconut husk, 244
- Coir, 28–33, 35–36, 52–54
- Collagen, 372–373
- Collection of tubers, 224
- Colloidal MCC, 67, 71
- Colocasia esculenta, 222, 223
- Composites, 61–63, 66, 71, 77–85, 243–244, 246–248, 250, 254–257, 259–262, 265
- Compression molding, 255–256, 261
- Conductivity, 93, 101
- Construction, 261–262
- Cordenka, 32–33
- Core layer, 93, 97
- Corn, 26, 29, 31–32
- Cotton, 33
- Cotton stalk, 244
- Coupling agents, 246, 249
- Critical factors for protein PEGylation: PEG structure and size, 491
- Crystalline domains, 63, 64, 75
- Crystallinity, 25, 29, 31–32, 38–41, 44, 47–48, 50–52, 54–55, 61, 63, 66, 67, 70, 71, 75–77, 85
- Crystallization, 27, 29–31, 41, 44, 47, 51
- Debonding, 262
- Decomposition, 75–77
- Degradation, 27, 37, 44, 47, 51, 55, 260
- Degree of crystallinity, 75

- Degree of polymerization, 63, 70, 71, 74–76
- Dendrimer-protein conjugates, 509
- Density, 30, 37–49
- Depolymerization, 463, 469
- Depolymerization process, 70
- Dextran-asparaginase conjugates, 515
- Dextran-carboxypeptidase G2 conjugates, 515
- Dextran-hemoglobin conjugates, 522
- Dextran-insulin conjugates, 516
- Dextran-protein conjugates, 515
- Dextran-uricase conjugates, 516
- Dextrin-Phospholipase A2, 523
- Dextrin-protein conjugates, 522
- Dextrin-rhEGF conjugates, 522
- Dextrin-Trypsin and melanocyte stimulating hormone (MSH) conjugates, 523
- Differential scanning calorimeter (DSC), 228, 232, 233
- DIGLUE biomass, 137–142
- Dispersion, 251, 257
- Disulfide bridging PEGylation of proteins, 493
- Distiller's dry grain and solubles (DDGS), 135–136, 144
- DNA, 388–390

- Eco-efficiency, 243, 264
- Eco-friendly, 243, 255
- Effect of glycosylation on proteins, 499
- Electron energy dispersive X-ray spectroscopy, 319
- Emerging PEGylated drugs, 496
- Emerging techniques alternative to PEGylation, 498
- Enzymatic oxidation, 162
- Enzymatic PEGylation, 493
- Epichlorohydrin, 164, 165
- Epoxidation, 164, 167, 175–176
- Epoxidized soybean oil (ESO), 134
- Epoxy, 164, 175–176
- Epoxy resins, 80
- Erythropoiesis stimulating agent, 487
- Estimation of total sugar content, 229, 232
- Eugenol, 108, 110, 119, 120, 126, 127
- Europe-Middle East-Africa (EMEA), 131
- Extraction, 250, 257
- Extrusion, 37, 39, 42–46, 51, 55, 67, 69, 81, 82

- Fe_3O_4 , 400–404
- Feather protein-based resins, 135
- Fiber extraction method
 - hand scraping, 293
 - machine decortication, 293
 - mechanical grinding, 293
 - water retting, 293
- Fiber modification, 246, 249
- Fibers natural, 159
- Fibrinogen, 315, 320–321, 323, 325–327, 329–331
- Flax, 30, 32–35, 47–48, 51
- Flexural, 256
- Flexural modulus, 256
- Foams, 36–39, 41–51, 55, 158–159, 164
- Formaldehyde-based adhesives, 129–130
- FT-IR imaging, 316, 326
- FT-IR spectroscopy, 315–316, 327, 331
- FTIR, Fourier transform infrared spectrometer, 72, 73
- Furfural, 159
- Furfuryl alcohol, 93, 95–97, 101

- Gelatin, 374
- Gene therapy, 388
- Glucomannan, 378–380
- Glutaraldehyde, 323
- Glycerol, 152–156
- Glycerol carbonates, 152–153
- Glycerol esters, 155
- Glycolysis, 467, 468
- Glycosylation of proteins, 498
- Glyoxal, 157
- Glyoxylic acid, 108–110
- Gold nanoparticles, 404–407
- Granulocyte colony-stimulating factor, 485
- Graphene, 417–420
- Graphene oxide, 417–420
- Graphitization, 2, 9, 13–15
- Green chemistry, 243, 265
- Green composites, 243, 265
- Groundnut shell, 244
- Growth hormone antagonist, 486
- Guaiacol, 108–110, 120, 124, 127

- Hardener, 96–97
- Heat distortion temperature (HDT), 301–302
- Hemicellulose, 64, 65, 67, 73, 77, 244, 246, 254–255
- Hemoglobin, 315, 320–321, 324, 331

- Hemp, 31–32, 36, 161
 Hemp fiber, 248
 Heparin, 378
 HES-anakinra conjugates, 514
 HES-erythropoietin mimetic peptide (AGEM400 (HES)) conjugate, 514
 HES-G-CSF conjugates, 515
 HESylation of proteins, 513
 Hexamine, 158
 Homogeneity, 94, 97–101
 Hot melts, 155, 166
 Hyaluronic acid, 376–378
 Hyaluronic acid - insulin conjugate, 525
 Hyaluronic acid - interferon α conjugate, 524
 Hyaluronic acid (HA)-protein conjugates, 524
 Hyaluronic acid-anti-Flt1 peptide conjugates, 526
 Hyaluronic acid-EGF conjugate, 526
 Hyaluronic acid-exendin 4 conjugates, 526
 Hyaluronic acid-hGH conjugate, 525
 Hyaluronic acid-Superoxide dismutase conjugates, 531
 Hyaluronic acid-Trypsin, 525
 Hybrid reinforcement, 289, 299–300
 Hydrophilic, 71, 78, 80, 246–248
 Hydrophobic, 78, 80
 Hydroxyapatite, 395–396
 Hydroxyl group, 246
 Hyperbranched, 154–156

 Identification of gum components by thin layer chromatography, 229, 234
 Impact, 27, 34–35, 46, 48, 50, 54
 Industrial ecology, 265
 Industrial waste, 3, 8, 15
 Injection molding, 31, 37, 46–49, 51, 55
In-situ Polymerization, 81, 83
 Interaction, 66, 82
 Interface, 28, 30, 36, 40, 43, 52
 Interfacial adhesion, 249
 Interfacial bonding, 257
 Interferons, 486
 Internal bond (IB), 138, 140, 142
 Investigation of structure of polysaccharide, 230, 234–236
 Isolation, 61, 64, 67
 Isolation of polysaccharide, 224
 Iso-PhoroneDi-Amine (IPDA), 120

 Jute, 29, 34–36

 Kenaf, 161
 Keratin-based biomaterials, 276

 Laccase, 162
 Leptotes bicolor, 109
 Light weight, 254, 257, 264
 Lignin, 28, 32, 36, 64, 65, 67, 73, 77, 108, 109, 111, 112, 121, 122, 125–128, 132, 159–165, 243–244, 248–250, 254–255, 259–261, 264
 Lignin foam, 98
 Lignin functionalization, 163
 Lignin-based CF, 10–12
 Lignocellulosic, 244, 246, 250, 257
 Lignocellulosic fibers, 246, 250
 Lignosulfonates, 159–165
 Limitations of PEGylation, 498
 Liposomes, 393–394
 Liquefied wood, 167
 Liquefied woody biomass, 134–135
 Low cost, 243, 264
 L-phenylalanine, 110

 Macroalgae/crops, 136
 Magnetic bio char, 437–438
 Maize, 171
 Maleic anhydride, 28, 34, 41
 Maple, 29–30, 33, 35, 52
 Marine adhesive proteins (MAPs), 134
 Mechanical fibrillation, 257
 Mechanical grinding, 252
 Mechanical properties, 25, 27–28, 32, 34, 37, 40, 46–48, 54–55, 85, 245–246, 249–250, 256–257, 259–262, 337–342, 345, 346, 348, 349, 351, 353, 354, 357, 358
 Mechanical treatment, 250
 Medium density fibreboard (MDF), 130, 143–144
 Melt derived glasses, 312–313
 Melt mixing, 261
 Methacrylated vanillin–glyceroldimethacrylate (MVGDM), 121
 Microalgae, 136–137
 Microfibrillated cellulose, 250
 Mimosa, 97–98
 Modulus, 27, 33–34, 36, 39–40, 42, 48–50, 52–54, 250, 254, 257, 259–261

- Modulus of elasticity (MOE), 138, 141
- Modulus of rupture (MOR), 138, 140
- Moisture absorption, 246, 260–261
- Moisture sorption, 246
- Molecular weight, 61, 67, 74, 75
- Molybdenum, 321–322
- Morphological properties, 260–261
- Morphology, 61, 63, 70, 73, 74, 78, 81, 85

- Nanocellulose, 250, 259
- Nanocomposites, 66, 250, 257, 259
- Nanofibrillated cellulose, 250
- Nanopapers, 252, 254
- Natural fibers, 78, 135, 243–244, 247, 249–250, 256, 257, 262, 264
- Natural resources, 1, 2, 3, 6, 15
- Non-covalent PEGylation, 494
- Non-viral vectors, 388
- Nucleating agent, 27, 31, 47
- Nucleation, 30–31, 37, 40–43, 45–47, 49
- Nylon 6, 80, 81

- Occurrence and physicochemical properties of keratin, 274–276
- Oils, 175–177
- Organosilanes, 323
- Orientation
 - crystalline, 302
 - fiber, 298, 301
- Oriented strand boards (OSB), 130, 143–144

- Packaging, 25–27, 55, 243, 256, 261
- Palm, 32
- PAMAM-trypsin and trypsin inhibitor conjugates, 513
- PAMAM- $\alpha 4\beta 1$ integrin binding peptide conjugates, 513
- PAN-based CF, 12, 13
- Particle size, 67, 70, 71, 73
- Particleboards (PB), 130, 143–144, 158, 163, 172
- PASylation, 531
- PEG- Growth hormone releasing factor (PEG-GRF), 496
- PEG-arginine deaminase (ADI), 498
- PEG-G-CSF (DA-3031), 496
- PEG-GLP-1, 496
- PEG-IFN- α -2a (DA-3021), 496
- PEG-Salmon calcitonin, 496
- PEG-Uricase, 496
- PEGylated hCH (ARX-201), 496
- PEGylated protein therapeutics, 488
- PEGylation of amine group, 492
- PEGylation of proteins containing unnatural amino acid, 494
- PEGylation of thiol group, 492
- Peptides, 391–392
- Performance, 249, 256–257, 261–262, 265
- Peroxidase, 162
- Petrochemical-based adhesives, 129–130
- Pharmacology of PEGylation, 495
- Phenol-formaldehyde (PF), 134
- Phthalic anhydride, 155
- Physico-chemical evaluation
 - loss on drying (LOD), 227, 231
 - pH, 227, 231
 - powder flow characteristics, 226, 231
 - solubility, 225, 231
 - specific gravity, 227, 231
 - swelling capacity, 227, 231
 - viscosity, 228, 231
- Physical properties, 250
- Pine, 28–33, 35–36, 52–54
- Pineapple leaf fiber (PALF)
 - applications, 298
 - characteristic, 295
 - composition, 297
 - extraction, 293, 296–297
 - nonwoven mat, 289, 294–295, 303–304
 - properties, 291
 - structure, 292
- Pitch-based CF, 1, 15
- Plasticizer, 27, 35
- Plywood, 158, 172
- Poly (butylenes succinate), 81
- Poly (lactic acid), 81, 82, 383–384
- Poly (vinyl alcohol), 81, 82
- Poly vinyl alcohol (PVA), 120, 123, 126
- Poly(3-hydroxybutyrate), 256
- Poly(butylene succinate), 256
- Poly(ethylene glycol), 27
- Poly(ethylene oxide), 256
- Poly(furfuryl alcohol), 257
- Poly(γ -glutamic acid), 386–387
- Polyaniline, 80, 81, 84
- Polycaprolactone, 26, 80, 164, 181, 256
- Polyesters, 155, 165, 181
- Polyethylene, 27–28, 54, 79, 80
- Polyethylene chloride, 255

- Polyethylene oxide, 255
- Polyethylene terephthalate, 462, 464
- Polyethylene terephthalate (PET), 113
- Polyethyleneimine, 162, 173
- Polyglycerol-arginine-glycine-aspartic acid (RGD) peptide conjugates, 509
- Polyglycerol-ovalbumin peptide conjugates, 508
- Polyglycerols, 153
- Polyglycerols (PG)-protein conjugates, 508
- Polyhedral oligomeric silsesquioxanes (POSS), 120
- Polyhydroxyalkonates, 177–179
- Polyhydroxybutyrate, 26–27, 164
- Polylactic acid (PLA), 25–55, 179–182, 256
- Polylactic acid esters, 181
- Polymer, 95–99, 244, 246–247, 249, 251, 255–257, 259, 261
- Polymer matrices, 244, 246, 255–257
- Polymorphs, 64
- Polyols, 164, 166–167, 175, 463, 464, 468
- Polyoxymethylene (POM), 113
- Polypropylene (PP), 28, 51, 54, 79–82, 255, 289, 301–302
- Polysaccharides, 165–170
- Polysialic acid (PSA)-protein conjugates, 500
- Polysialic acid-asparaginase conjugates, 501
- Polysialic acid-catalase conjugates, 501
- Polysialic acid-cytokine conjugates, 507
- Polysialic acid-erythropoietin conjugates, 507
- Polysialic acid-G-CSF Conjugates, 507
- Polysialic acid-IgG Fab fragments conjugate, 508
- Polysialic acid-insulin conjugates, 501
- Polysialic acid-single chain Fv fragment conjugates, 507
- Polyurethane, 82, 83, 163, 175, 255, 461
- Polyurethanes, 380–383
- Polyvinyl alcohol, 255, 384–386
- Porphyrin dendrimer-glucose oxidase conjugates, 513
- Potential applications, 281
- Powdered MCC, 71
- Preliminary particle board preparation method compositions, 137–138 programmed board pressing process, 138
- Process, 93, 96–100
- Processing methods, 260
- Processing techniques, 256, 265
- Properties of bio-composites for bio-medical applications, 278
- Protein adsorption, 309–310, 315, 319–321, 327
- Protein crosslinking, 172
- Protein secondary structure, 314, 318–319, 321
- Protein therapeutics and their challenges, 484
- Proteins, 171–174
- Proteins modified by TGase PEGylation, 493
- Pulping, 250
- Purification of polysaccharide, 224
- Pyrolysis, 161
- Ramie, 34, 36
- Recyclable materials, 243
- Regenerated cellulose, 6, 7, 12, 13
- Reinforcement, 61, 62, 66, 71, 78, 79, 81–83, 85
- Reinforcing, 244, 247, 250, 257, 259, 262
- Releasables of PEGylation, 494
- Renewable, 243–244, 249, 254, 256–257, 259, 262
- Renewable materials, 260
- Rheological study, 230, 234, 236, 237
- Rice husk, 243–255, 260, 261
- Rigid foams, 466, 473
- Sandwich panel, 93–94, 97, 100, 102
- Santoprene, 302
- Scanning electron microscopy, 319, 331
- SEC, size exclusion chromatography, 75
- SEM, scanning electron microscopy, 74
- Shellac, 249
- Silane, 246, 248–249, 256, 261
- Silica, 289, 299–300
- Silicon dioxide, 397–398
- Silk, 211
 - biocomposites, 205–211
 - biomedical, 205
 - cellulose, 210
 - degumming, 203–205
 - films, 210
 - nanotubes (carbon), 210
 - spectroscopy, 200–201
 - textiles, 205
 - water interactions, 201–203

- Silver, 321, 328
- Silver nanoparticles, 407–409
- SiRNA, 388, 390
- Sisal, 33–35, 51, 161
- Sol-gel derived glasses, 312–313
- Solution casting, 81
- Some other polymer-protein conjugates, 531
- Soy, 171–172
- Soya protein-based wood adhesives, 133–134
- Spider silk, 189–195
 - computational research, 192–193
 - properties, 189–192
 - recombinant, 193–195
 - structures, 189–192
 - types, 189–192
- Spinning, 1–3, 6, 9–11, 13
- Stability, 245–246, 254, 260, 261
- Starch, 26, 79–82, 112, 165, 174, 181
- Starch-based adhesive, 132
- Starch-based nanocomposites, 338–339
 - starch based nanocomposites with natural antioxidant, 338, 339–342
 - starch-based nanocomposites with bactericidal fillers, 342–343
 - starch-based nanocomposites with natural filler and bactericidal fillers, 352–355
- Stiffness, 256–257, 259, 261–262
- Straw, 161
- Strength, 25–27, 32–36, 40, 45–46, 48–50, 54, 243–246, 252, 254, 256–257, 259–262, 264
- Structural properties, 345, 346, 348, 351
- Structure, 61, 63–65, 67, 70–75, 77, 78
- Sugarcane bagasse, 244–245, 257
- Supermasscolloider, 252, 257
- Surface chemistry, 78
- Surface modification, 247, 249, 261
- Surface soundness (SS), 138, 140
- Sustainability, 243–244, 261–262, 265
- Sustainable, 243–244, 247, 249, 255, 257, 259–262
- Sustainable materials, 243, 255, 257
- Sustainable products, 243
- Synthesis of magnetic bio char, 438
 - chemical precipitation, 440
 - composites, 446
 - encapsulation using bio-polymer, 442
 - high temperature treatment of agriculture waste char/activated carbon, 442
 - microwave heating, 444
 - pyrolysis of agriculture waste, 439
- Synthetic BE linkers, 495
- Synthetic fibers, 244, 246
- Synthetic fillers, 243–244, 259
- Synthetic Polymers, 380–387
- Tannin condensation, 157
- Tannin foam
 - black, 93, 95
 - composite, 93, 100, 102
 - density, 95, 98–99, 101
 - fire-resistance, 93, 100–101
 - formaldehyde-free, 94, 97, 100–102
 - industrial, 93–94, 99, 102
 - insulation, 93–96, 100
 - lightweight, 93, 100
 - open-pores, 95
 - orthotropic, 95
 - porous, 93, 95
 - rigid, 94–95, 99
 - structure, 95, 97
 - thermal, 93–96, 98–99
 - water resistance, 96
- Tannin-furanic, 95, 99
- Tannins, 133, 156–159
- t-cinnamic acid, 110
- TEM, transmission electron microscopy, 70, 74
- Temperature, 67, 72, 75–78, 82
- Tensile modulus, 252, 254, 259
- Tensile strength, 244, 252, 254, 256, 259, 260
- Thermal extrusion, 1, 9, 11
- Thermal insulator, 244
- Thermal Stability, 63, 75, 77, 83
- Thermoplastics, 164, 167, 259
- Thermosets, 256, 259
- Thermosetting, 96
- Thickness swelling (TS), 138–139, 142
- Tissue engineering, 281, 282
- Toluene, 113
- Triglycerides, 112
- Types of glycosylation in vivo, 499
- Uniaxial reinforcement, 298, 302, 304
- Unsaturated polyester, 289

- Uricase, 486
- Urotropine, 158

- Vanilla planifolia, 109
- Vanillin, 107–128
- Vanillin azo coumarin (VAC), 123
- Vegetable oils, 152, 166, 175–177, 462, 464
 - cellular structure, 474
 - compression strength, 475
 - elasticity modulus, 476
 - FTIR, 471, 477
 - optical microscopy, 474
 - Water absorption, 475
- Viscometry, 75
- Viscosity, 37, 40–42, 44, 46–47, 49, 51, 55

- Water absorption capacity (WAC), 138–139, 142
- Waste management, 244, 260
- Waste wood, 8, 14
- Water absorption, 260
- Wheat, 171
- Wheat straw, 244–245
- Wood, 28–29, 34–39, 42–43, 48–53
- Wood composite, 129–130
- Wood panel process, 129–145
- Wound healing, 281

- X-ray powder diffraction (XRD), 229, 232

- B-alanine linkers, 495
- β -D-glucoside, 109

Also of Interest

Check out these published related titles from Scrivener Publishing

Journal of Renewable Materials

Editors: Alessandro Gandini and Ramaswamy Nagarajan
www.scrivenerpublishing.com

Biobased and Environmentally Benign Coatings

Edited by Atul Tiwari, Anthony Galanis, and Mark D. Soucek
Published 2016. ISBN: 978-1-119-18492-8

Lignocellulosic Fibers and Wood Handbook

Edited by Mohamed Naceur Belgacem and Antonio Pizzi
Published 2016. ISBN: 978-1-118-77352-9

Biodegradable and Biobased Polymers for Environmental and Biomedical Applications

Edited by Susheel Kalia and Luc Avérous
Published 2016. ISBN: 978-1-119-11733-9

Advanced Composites Materials

Edited by Ashutosh Tiwari, Mohammad Rabia Alenzi and Seong Chan Jun
Published 2016. ISBN: 9781119242536

Fundamentals of Conjugated Polymer Blends, Copolymers and Composites Synthesis, Properties, and Applications

Edited by Parveen Saini
Published 2015. ISBN: 978-1-118-54949-0

Lignocellulosic Polymer Composites Processing, Characterization, and Properties

Edited by Vijay Kumar Thakur
Published 2014. ISBN 978-1-118-77357-4

Nanocellulose Polymer Nanocomposites Fundamentals and Applications

Edited by Vijay Kumar Thakur
Published 2014. ISBN 978-1-118-87190-4

Handbook of Cellulosic Ethanol

By Ananda S. Amarasekara
Published 2014. ISBN 978-1-118-23300-9

The Chemistry of Bio-based Polymers

By Johannes Karl Fink

Published 2014. ISBN 978-1-118-83725-2

Biofuels Production

Edited by Vikash Babu, Ashish Thapliyal and Girijesh Kumar Patel

Published 2014. ISBN 978-1-118-63450-9

Handbook of Bioplastics and Biocomposites Engineering Applications

Edited by Srikanth Pilla

Published 2011. ISBN 978-0-470-62607-8

Renewable Polymers: Synthesis, Processing, and Technology

Edited by Vikas Mittal

Published 2011. ISBN 978-0-470-93877-5

Plastics Sustainability

Towards a Peaceful Coexistence between Bio-based and Fossil Fuel-Based Plastics

Michael Tolinski

Published 2011. ISBN 978-0-470-93878-2

Green Chemistry for Environmental Remediation

Edited by Rashmi Sanghi and Vandana Singh

Published 2011 ISBN 978-0-470-94308-3

WILEY END USER LICENSE AGREEMENT

Go to www.wiley.com/go/eula to access Wiley's ebook EULA.